



This is a digital copy of a book that was preserved for generations on library shelves before it was carefully scanned by Google as part of a project to make the world's books discoverable online.

It has survived long enough for the copyright to expire and the book to enter the public domain. A public domain book is one that was never subject to copyright or whose legal copyright term has expired. Whether a book is in the public domain may vary country to country. Public domain books are our gateways to the past, representing a wealth of history, culture and knowledge that's often difficult to discover.

Marks, notations and other marginalia present in the original volume will appear in this file - a reminder of this book's long journey from the publisher to a library and finally to you.

### Usage guidelines

Google is proud to partner with libraries to digitize public domain materials and make them widely accessible. Public domain books belong to the public and we are merely their custodians. Nevertheless, this work is expensive, so in order to keep providing this resource, we have taken steps to prevent abuse by commercial parties, including placing technical restrictions on automated querying.

We also ask that you:

- + *Make non-commercial use of the files* We designed Google Book Search for use by individuals, and we request that you use these files for personal, non-commercial purposes.
- + *Refrain from automated querying* Do not send automated queries of any sort to Google's system: If you are conducting research on machine translation, optical character recognition or other areas where access to a large amount of text is helpful, please contact us. We encourage the use of public domain materials for these purposes and may be able to help.
- + *Maintain attribution* The Google "watermark" you see on each file is essential for informing people about this project and helping them find additional materials through Google Book Search. Please do not remove it.
- + *Keep it legal* Whatever your use, remember that you are responsible for ensuring that what you are doing is legal. Do not assume that just because we believe a book is in the public domain for users in the United States, that the work is also in the public domain for users in other countries. Whether a book is still in copyright varies from country to country, and we can't offer guidance on whether any specific use of any specific book is allowed. Please do not assume that a book's appearance in Google Book Search means it can be used in any manner anywhere in the world. Copyright infringement liability can be quite severe.

### About Google Book Search

Google's mission is to organize the world's information and to make it universally accessible and useful. Google Book Search helps readers discover the world's books while helping authors and publishers reach new audiences. You can search through the full text of this book on the web at <http://books.google.com/>







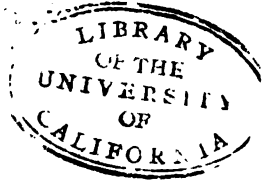






Oct. 1920

DEPARTMENT OF COMMERCE



# SCIENTIFIC PAPERS

OF THE

# BUREAU OF STANDARDS

S. W. STRATTON, DIRECTOR

(Continuing the Bulletin of the Bureau of Standards)

VOLUME 15  
1919-20



WASHINGTON  
GOVERNMENT PRINTING OFFICE  
1920

70 1000  
1000000

71  
1004  
v. 15



# INDEX TO VOLUME 15

## A

- Acetylene flame, Spectrum of, 639.
- Acid Bessemer steels, oxygen content, 259.
- Adler, L., J. R. Cain and*, Equilibrium conditions in the system carbon, iron oxide, and hydrogen in relation to the Ledebur method for determining oxygen in steel, 353.
- Air, Combustible gas in, 47.
- Airplane antenna constants, 199.
- Alloy steel, Transformations in, 91.
- Aluminum and its light alloys, 105.
- Aluminum, Some alloys of, with magnesium and with zinc, 653.
- Analysis, water, Turbidity standard of, 693.
- Annealing and characteristics of glass, 537.
- Antenna and coil aeriads in radio transmission and reception, 435.
- Antenna constants, Airplane, 199.

## B

- Boiling point of sulphur, 163.
- Buckingham, E., and J. D. Edwards*, Efflux of gases through small orifices, 573.
- Burgess, H. A., E. F. Mueller and*, Standardization of the sulphur boiling point, 163.

## C

- Cain, J. R., and L. Adler*, Equilibrium conditions in the system carbon, iron oxide, and hydrogen in relation to the Ledebur method for determining oxygen in steel, 353.
- , and *E. Pettijohn*, Oxygen content by the Ledebur method of acid Bessemer steels deoxidized in various ways, 259.
- Calcium vapors, electrons in, 723.
- Carbon, iron oxide, and hydrogen, system, equilibrium conditions, 353.
- Characteristics of glass, 537.
- Cheney, W. L.*, Magnetic testing of straight rods in in intense fields, 625.
- Coblentz, W. W.*, Constants of radiation of a uniformly heated inclosure, 529.
- , Distribution of energy in the spectrum of an acetylene flame, 639.
- , Methods for computing and intercomparing radiation data, 617.
- , and *H. Kahler*, Reflecting power of stellite and lacquered silver, 215.
- , —, Some optical and photoelectric properties of molybdenite, 121.
- , —, Spectral photoelectric sensitivity of silver sulphide and several other substances, 231.
- , *M. B. Long, and H. Kahler*, Decrease in ultra-violet and total radiation with usage of quartz mercury vapor lamps, 1.

- Coblentz, W. W., R. G. Wallenberg and*, Preparation and reflective properties of some alloys of aluminum with magnesium and with zinc, 653.
- Computing and intercomparing radiation data, 617.
- Concerning the annealing and characteristics of glass, 537.
- Constants, Airplane antenna, 199.
- Constants of radiation of a uniformly heated inclosure, 529.
- Constitution and metallography of aluminum and its light alloys with copper and with magnesium, 105.
- Contrast sensibility of the eye, 679.
- Combustible gas in the air, instruments for showing, 47.
- Cork, J. M.*, Airplane antenna constants, 199.

## D

- Decrease in ultra-violet and total radiation with usage of quartz mercury vapor lamps, 1.
- Dallinger, J. H.*, Principles of radio transmission and reception with antenna and coil aeriads, 435.
- Deoxidized acid Bessemer steels, oxygen content, 259.
- Dependence of the input impedance of a three-electrode vacuum tube upon the load in the plate circuit, 367.
- Derivatives of physical quantities, 21.
- Determination of the output characteristics of electron tube generators, 497.
- Determination of thermal expansion of molybdenum, 31.
- Dilatometer, a new interferential, 669.
- Direction of propagation of long electromagnetic waves, 419.
- Distribution of energy in the spectrum of an acetylene flame, 639.
- Dry cells, voltage of, 659.
- Duralumin, Heat treatment of, 271.

## E

- Edwards, J. D., E. Buckingham and*, Efflux of gases through small orifices, 573.
- Effect of rate of temperature change on the transformations in an alloy steel, 91.
- Efflux of gases through small orifices, 573.
- Electromagnetic waves, long, 419.
- Electrons in vapors of lead and calcium, 723.
- Electron tube generators, output characteristics, 497.
- Energy, Distribution of, in the spectrum of an acetylene flame, 639.
- Equilibrium conditions in the system carbon, iron oxide, and hydrogen in relation to the Ledebur method for determining oxygen in steel, 353.
- Expansion of molybdenum, thermal, 31.
- Expansion, thermal, of insulating materials, 387.
- Eye, Contrast sensibility of, 679.



## F

- Finkelstein, J. L., R. M. Wilhelm and*, A standardized method for the determination of solidification points, especially of naphthalene and paraffin, 185.  
 Flame, acetylene, spectrum of, 639.  
 Flaws in rifle-barrel steel, 219.  
*Foote, P. D., F. L. Mohler, and H. F. Stimson*, Ionization and resonance potentials for electrons in vapors of lead and calcium, 723.  
*Freeman, J. R., jr., P. D. Merica, R. G. Wallenberg and*, Constitution and metallography of aluminum and its light alloys with copper and with magnesium, 105.  
 —, *H. Scott and*, Use of a modified Rosenhain furnace for thermal analysis, 317.

## G

- Gases, Efflux through small orifices, 573.  
 Generators, electron tube, output characteristics of, 497.  
 Glass, annealing and characteristics of, 537.  
*Gibson, K. S.*, Photoelectric spectrophotometry by the null method, 325.

## H

- Heat treatment of duralumin, 271.  
*Hersey, M. D.*, A relation connecting the derivatives of physical quantities, 21.  
*Hidnerl, P., L. W. Schad and*, Preliminary determination of the thermal expansion of molybdenum, 31.  
 —, *W. H. Souder and*, Thermal expansion of insulating materials, 387.  
*Holler, H. D., and L. M. Rückie*, Relation of voltage of dry cells to hydrogen-ion concentration, 659.  
*Hull, L. M.*, Determination of the output characteristics of electron tube generators, 497.  
 Hydrogen-ion concentration, Relation to voltage of dry cells, 659.

## I

- Inclosure, Constants of radiation in, 529.  
 Input impedance of a three-electrode vacuum tube, 367.  
 Instruments for showing the presence and amount of combustible gas in the air, 47.  
 Insulating materials, Thermal expansion of, 387.  
 Intense fields, Magnetic testing of straight rods in, 625.  
 Interferential dilatometer, 669.  
 Inverse-rate method for thermal analysis, 101.  
 Ionization and resonance potentials for electrons in vapors of lead and calcium, 723.  
 Iron and mild steel, Microstructure, 519.

## K

- Kahler, H., W. W. Coblenz and*, Reflecting power of stellite and lacquered silver, 215.  
 —, —, Some optical and photoelectric properties of molybdenite, 121.  
 —, —, Spectral photoelectric sensitivity of silver sulphide and several other substances, 231.  
 —, —, *M. B. Long and*, Decrease in ultra-violet and total radiation with usage of quartz mercury vapor lamps, 1.

- Kahler, H., and E. P. T. Tyndall*, Contrast sensibility of the eye, 679.  
*Kouwenhoven, W. B., R. L. Sanford and*, Location of flaws in rifle-barrel steel by magnetic analysis, 219.  
 Krypton spectrum, wave lengths, 251.

## L

- Lacquered silver, Reflecting power, 215.  
 Lead and calcium vapors, electrons in, 723.  
 Ledebur method, 259, 353.  
 Light alloys of aluminium, 105.  
 Load in the plate circuit, 367.  
 Location of flaws in rifle-barrel steel by magnetic analysis, 219.  
 Long electromagnetic waves, 419.  
*Long, M. B., W. W. Coblenz, and H. Kahler*, Decrease in ultraviolet and total radiation with usage of quartz mercury vapor lamps, 1.

## M

- Magnetic analysis to locate flaws in rifle-barrel steel, 219.  
 Magnetic testing of straight rods in intense fields, 625.  
 Measurements of wave lengths in the spectra of krypton and xenon, 251.  
*Merica, P. D.*, A simplification of the inverse-rate method for thermal analysis, 101.  
 —, *R. G. Wallenberg, and J. R. Freeman, jr.*, Constitution and metallography of aluminum and its light alloys with copper and with magnesium, 105.  
 —, —, *and H. Scott*, Heat treatment of duralumin, 271.  
*Merrill, P. W.*, Measurements of wave lengths in the spectra of krypton and xenon, 251.  
 Metallography of aluminum and its light alloys, 105.  
 Methods for computing and intercomparing radiation data, 617.  
*Michelson, A. A.*, Optical conditions accompanying the striae which appear as imperfections in optical glass, 41.  
 Microstructure of iron and mild steel at high temperatures, 519.  
 Mild steel, microstructure, 519.  
*Miller, J. M.*, Dependence of the input impedance of a three-electrode vacuum tube upon the load in the plate circuit, 367.  
*Mohler, F. L., P. D. Foote, and H. F. Stimson*, Ionization and resonance potentials for electrons in vapors of lead and calcium, 723.  
 Molybdenite, optical and photoelectric properties, 121.  
 Molybdenum, thermal expansion of, 31.  
*Mueller, B. F., and H. A. Burgess*, Standardization of the sulphur boiling point, 163.

## N

- Naphthalene and paraffin, solidification points, 185.  
 New forms of instruments for showing the presence and amount of combustible gas in the air, 47.  
 New interferential dilatometer, 669.  
 Null method in photoelectric spectrophotometry, 325.

## O

- Optical and photoelectric properties of molybdenite, 121.  
 Optical conditions accompanying the striae which appear as imperfections in optical glass, 41.  
 Optical glass, striae in, 41.  
 Orifices, small, Efflux of gases through, 573.  
 Output characteristics of electron tube generators, 497.  
 Oxygen content by the Ledebur method of acid Bessemer steels deoxidized in various ways, 259.  
 Oxygen in steel by Ledebur method, 353.

## P

- Paraffin and naphthalene, solidification points, 185.  
*Pettijohn, E., J. R. Cain and*, Oxygen content by the Ledebur method of acid Bessemer steels deoxidized in various ways, 259.  
 Photoelectric properties of molybdenite, 121.  
 Photoelectric spectrophotometry by the null method, 325.  
 Physical quantities, derivatives of, 21.  
 Plate circuit, load in the, 367.  
 Potentials, Ionization and resonance, 723.  
 Preliminary determination of the thermal expansion of molybdenum, 31.  
 Preparation and reflective properties of some alloys of aluminum with magnesium and with zinc, 653.  
*Priest, I. G.,* A new interferential dilatometer, 669.  
 Principles of radio transmission and reception with antenna and coil aeriels, 435.

## R

- Radiation, Constants of, 529.  
 Radiation data, computing and intercomparing, 617.  
 Radiation in quartz lamps, 1.  
 Radio transmission and reception, Principles of, 435.  
*Rawdon, H. S., and H. Scott,* Microstructure of iron and mild steel at high temperatures, 519.  
 Reflecting power of stellite and lacquered silver, 215.  
 Reflective properties of some alloys of aluminum, 653.  
 Relation connecting the derivatives of physical quantities, 21.  
 Relation of voltage of dry cells to hydrogen-ion concentration, 659.  
 Resonance potentials for electrons, 723.  
 Rifle-barrel steel, Location of flaws, 219.  
*Ritchie, L. M., H. D. Holler and*, Relation of voltage of dry cells to hydrogen-ion concentration, 659.  
 Rods, straight, in intense fields, 625.  
 Rosenhain furnace, modified, for thermal analysis, 317.

## S

- Sanford, R. L., and W. B. Kowbenhoven,* Location of flaws in rifle-barrel steel by magnetic analysis, 219.  
*Schad, L. W., and P. Hidaert,* Preliminary determination of the thermal expansion of molybdenum, 31.  
*Scott, H.,* Effect of rate of temperature change on the transformations in an alloy steel, 91.  
 —, and *J. R. Freeman, jr.,* Use of a modified Rosenhain furnace for thermal analysis, 317.

- Scott, H., P. D. Merica, R. G. Wallenberg and,* Heat treatment of duralumin, 271.  
 —, *H. S. Rawdon and,* Microstructure of iron and mild steel at high temperatures, 519.  
 Sensibility of the eye, 679.  
 Silver sulphide, Spectral photoelectric sensitivity, 231.  
 Simplification of the inverse-rate method for thermal analysis, 91.  
 Solidification points, method for determination of, 185.  
 Some optical and photoelectric properties of molybdenite, 121.  
*Souder, W. H., and P. Hidnert,* Thermal expansion of insulating materials, 387.  
 Spectral photoelectric sensitivity of silver sulphide and several other substances, 231.  
 Spectra of krypton and xenon, 251.  
 Spectrophotometry, Photoelectric, 325.  
 Spectrum of an acetylene flame, 639.  
 Standardization of the boiling point of sulphur, 163.  
 Standardized method for determination of solidification points, especially of naphthalene and paraffin, 185.  
 Standard, Turbidity, of water analysis, 693.  
 Steel, rifle-barrel, Location of flaws, 219.  
 Stellite and lacquered silver, Reflecting power, 215.  
*Stimson, H. F., F. L. Mohler, and P. D. Foote,* Ionization and resonance potentials for electrons in vapors of lead and calcium, 723.  
 Striae in optical glass, 41.  
 Sulphur boiling point, 163.  
 System carbon, iron oxide, and hydrogen, Equilibrium conditions, 353.

## T

- Taylor, A. H.,* Variations in direction of propagation of long electromagnetic waves, 419.  
 Temperature change, Effect on the transformation in an alloy steel, 91.  
 Testing, Magnetic, of straight rods, 625.  
 Thermal analysis, inverse-rate method, 101.  
 Thermal analysis with modified Rosenhain furnace, 317.  
 Thermal expansion of insulating materials, 387.  
 Thermal expansion of molybdenum, 31.  
*Tool, A. Q., and J. Valasek,* Concerning the annealing and characteristics of glass, 537.  
 Transformations in an alloy steel, 91.  
 Turbidity standard of water analysis, 693.  
*Tyndall, E. P. T., E. Karrer and,* Contrast sensibility of the eye, 679.

## U

- Uniformly heated inclosure, Constants of radiation in, 529.  
 Use of a modified Rosenhain furnace for thermal analysis, 317.

## V

- Vacuum tube, Input impedance of, 367.  
*Valasek, J., A. Q. Tool and,* Concerning the annealing and characteristics of glass, 537.  
 Vapor lamps, quartz mercury, 1.  
 Vapors of lead and calcium, Electrons in, 723.  
 Variation in direction of propagation of long electromagnetic waves, 419.  
 Voltage of dry cells, 659.

## W

Wallenberg, R. G., and W. W. Coblenz, Preparation and reflective properties of some alloys of aluminum with magnesium and with zinc, 653.

—, P. D. Merica, and J. R. Freeman, Constitution and metallography of aluminum and its light alloys with copper and with magnesium, 105.

—, —, and H. Scott, Heat treatment of duralumin, 271.

Water analysis by turbidity standard, 693.

Wave lengths in the spectra of krypton and xenon, 251.

Weaver, E. R., and E. E. Weibel, New forms of instruments for showing the presence and amount of combustible gas in the air, 47.

Weibel, E. E., E. R. Weaver and, New forms of instruments for showing the presence and amount of combustible gas in the air, 47.

Wells, P. V., Turbidity standards of water analysis, 693.

Wilhelm, R. M., and J. L. Finkelstein, A standardized method for the determination of solidification points, especially of naphthalene and paraffin, 185.

## X

Xenon spectrum, wave lengths, 251.

## CONTENTS OF VOLUME 15

	Page
330. DECREASE IN ULTRA-VIOLET AND TOTAL RADIATION WITH USAGE OF QUARTZ MERCURY VAPOR LAMPS.....	
<i>W. W. Coblents, M. B. Long, and H. Kahler</i>	1
331. A RELATION CONNECTING THE DERIVATIVES OF PHYSICAL QUANTITIES....	
<i>M. D. Hersey</i>	21
332. PRELIMINARY DETERMINATION OF THE THERMAL EXPANSION OF MOLYBDENUM.....	
<i>L. W. Schad and P. Hidnert</i>	31
333. OPTICAL CONDITIONS ACCOMPANYING THE STRIAE WHICH APPEAR AS IMPERFECTIONS IN OPTICAL GLASS.....	
<i>Lieut. Commander A. A. Michelson, U. S. N. R. F.</i>	41
334. NEW FORMS OF INSTRUMENTS FOR SHOWING THE PRESENCE AND AMOUNT OF COMBUSTIBLE GAS IN THE AIR....	
<i>E. R. Weaver and E. E. Weibel</i>	47
335. EFFECT OF RATE OF TEMPERATURE CHANGE ON THE TRANSFORMATIONS IN AN ALLOY STEEL.....	
<i>Howard Scott</i>	91
336. A SIMPLIFICATION OF THE INVERSE-RATE METHOD FOR THERMAL ANALYSIS.....	
<i>P. D. Merica</i>	101
337. CONSTITUTION AND METALLOGRAPHY OF ALUMINUM AND ITS LIGHT ALLOYS WITH COPPER AND WITH MAGNESIUM.....	
<i>P. D. Merica, R. G. Wallenberg, and J. R. Freeman, jr.</i>	105
338. SOME OPTICAL AND PHOTOELECTRIC PROPERTIES OF MOLYBDENITE.....	
<i>W. W. Coblents and H. Kahler</i>	121
339. STANDARDIZATION OF THE SULPHUR BOILING POINT.....	
<i>E. F. Mueller and H. A. Burgess</i>	163
340. A STANDARDIZED METHOD FOR THE DETERMINATION OF SOLIDIFICATION POINTS, ESPECIALLY OF NAPHTHALENE AND PARAFFIN.....	
<i>R. M. Wilhelm and J. L. Finkelstein</i>	185
341. AIRPLANE ANTENNA CONSTANTS.....	
<i>J. M. Cork</i>	199
342. REFLECTING POWER OF STELLITE AND LACQUERED SILVER.....	
<i>W. W. Coblents and H. Kahler</i>	215
343. LOCATION OF FLAWS IN RIFLE-BARREL STEEL BY MAGNETIC ANALYSIS..	
<i>R. L. Sanford and Wm. B. Kouwenhoven</i>	219
344. SPECTRAL PHOTOELECTRIC SENSITIVITY OF SILVER SULPHIDE AND SEVERAL OTHER SUBSTANCES.....	
<i>W. W. Coblents and H. Kahler</i>	231
345. MEASUREMENTS OF WAVE LENGTHS IN THE SPECTRA OF KRYPTON AND XENON.....	
<i>Paul W. Merrill</i>	251
346. OXYGEN CONTENT BY THE LEDEBUR METHOD OF ACID BESSEMER STEELS DEOXIDIZED IN VARIOUS WAYS.....	
<i>J. R. Cain and Earl Pettijohn</i>	259
347. HEAT TREATMENT OF DURALUMIN.....	
<i>P. D. Merica, R. G. Wallenberg, and H. Scott</i>	271
348. USE OF A MODIFIED ROSENHAIN FURNACE FOR THERMAL ANALYSIS.....	
<i>H. Scott and J. R. Freeman, jr.</i>	317
349. PHOTOELECTRIC SPECTROPHOTOMETRY BY THE NULL METHOD..	
<i>K. S. Gibson</i>	325
350. EQUILIBRIUM CONDITIONS IN THE SYSTEM CARBON, IRON OXIDE, AND HYDROGEN IN RELATION TO THE LEDEBUR METHOD FOR DETERMINING OXYGEN IN STEEL.....	
<i>J. R. Cain and Leon Adler</i>	353
351. DEPENDENCE OF THE INPUT IMPEDENCE OF A THREE-ELECTRODE VACUUM TUBE UPON THE LOAD IN THE PLATE CIRCUIT.....	
<i>John M. Miller</i>	367

	Page
352. THERMAL EXPANSION OF INSULATING MATERIALS.....	
<i>Wilmer H. Souder and Peter Hidnert</i>	387
353. VARIATION IN DIRECTION OF PROPAGATION OF LONG ELECTROMAGNETIC WAVES.....	
<i>Lieut. Commander A. H. Taylor, U. S. N. R. F.</i>	419
354. PRINCIPLES OF RADIO TRANSMISSION AND RECEPTION WITH ANTENNA AND COIL AERIALS.....	
<i>J. H. Dellinger</i>	435
355. DETERMINATION OF THE OUTPUT CHARACTERISTICS OF ELECTRON TUBE GENERATORS.....	
<i>Lewis M. Hull</i>	497
356. MICROSTRUCTURE OF IRON AND MILD STEEL AT HIGH TEMPERATURES....	
<i>Henry S. Rawdon and Howard Scott</i>	519
357. CONSTANTS OF RADIATION OF A UNIFORMLY HEATED INCLOSURE.....	
<i>W. W. Coblenz</i>	529
358. CONCERNING THE ANNEALING AND CHARACTERISTICS OF GLASS.....	
<i>A. Q. Tool and J. Valasek</i>	537
359. EFFLUX OF GASES THROUGH SMALL ORIFICES.....	
<i>Edgar Buckingham and Junius David Edwards</i>	573
360. METHODS FOR COMPUTING AND INTERCOMPARING RADIATION DATA.....	
<i>W. W. Coblenz</i>	617
361. MAGNETIC TESTING OF STRAIGHT RODS IN INTENSE FIELDS.....	
<i>W. L. Cheney</i>	625
362. DISTRIBUTION OF ENERGY IN THE SPECTRUM OF AN ACETYLENE FLAME..	
<i>W. W. Coblenz</i>	639
363. PREPARATION AND REFLECTIVE PROPERTIES OF SOME ALLOYS OF ALUMINUM WITH MAGNESIUM AND WITH ZINC.....	
<i>R. G. Wallenberg and W. W. Coblenz</i>	653
364. RELATION OF VOLTAGE OF DRY CELLS TO HYDROGEN-ION CONCENTRATION.....	
<i>H. D. Holler and L. M. Ritchie</i>	659
365. A NEW INTERFERENTIAL DILATOMETER.....	
<i>Irwin G. Priest</i>	669
366. CONTRAST SENSIBILITY OF THE EYE..	
<i>Enoch Karrer and E. P. T. Tyndall</i>	679
367. TURBIDITY STANDARD OF WATER ANALYSIS.....	
<i>P. V. Wells</i>	693
368. IONIZATION AND RESONANCE POTENTIALS FOR ELECTRONS IN VAPORS OF LEAD AND CALCIUM..	
<i>F. L. Mohler, Paul D. Foote, and H. F. Stimson</i>	723
INDEX TO VOLUME 15.....	737







DEPARTMENT OF COMMERCE

# SCIENTIFIC PAPERS

OF THE

# BUREAU OF STANDARDS

S. W. STRATTON, DIRECTOR

No. 330

## THE DECREASE IN ULTRA-VIOLET AND TOTAL RADIATION WITH USAGE OF QUARTZ MERCURY VAPOR LAMPS

BY

W. W. COBLENTZ, Associate Physicist

M. B. LONG, Assistant Physicist

and

H. KAHLER, Laboratory Assistant

*Bureau of Standards*

ISSUED NOVEMBER 12, 1918



PRICE, 5 CENTS

Sold only by the Superintendent of Documents, Government Printing Office,  
Washington, D. C.

WASHINGTON  
GOVERNMENT PRINTING OFFICE  
1918

70 1941  
ABSORBED

# THE DECREASE IN ULTRA-VIOLET AND TOTAL RADIATION WITH USAGE OF QUARTZ MERCURY VAPOR LAMPS

By W. W. Coblentz, M. B. Long, and H. Kahler

## CONTENTS

	Page
I. Introductory statement.....	1
II. Instruments and methods.....	2
III. Experimental data.....	8
1. Variation in emissivity with power input.....	9
2. Variation of irradiation parallel with axis of lamp.....	10
3. Decrease in ultra-violet radiation with usage of lamp.....	11
4. Decrease in total radiation with distance from lamp.....	12
5. Decrease in total radiation with usage of lamp.....	13
6. Total radiation and operating efficiency of quartz mercury vapor lamps.....	17
7. Comparative data of various sources of radiation.....	18
Radiometric measurements on a dye-fading carbon arc lamp..	18
IV. Summary.....	19

## I. INTRODUCTORY STATEMENT

The radiations from quartz mercury vapor lamps are being used extensively in accelerating photochemical actions, as a bactericide in sterilizing water, as a therapeutic agent, in dye-fading tests, etc.

The violet and ultra-violet rays, as distinguished from the infra-red rays, appear to have a marked effect in accelerating chemical action, and there has arisen among manufacturers of paper, dyes, cloth, rubber goods, paints, etc., a distinct need for a source of ultra-violet radiation of high intensity which does not decrease with usage.

It is well known that the intensity of the radiation (especially the ultra-violet component) from quartz mercury vapor lamps decreases greatly with usage. This decrease in intensity with usage has been determined qualitatively by several experiments,<sup>1</sup> using physical, chemical, and biological tests. But no exact quantitative data appear to be available showing how rapidly

<sup>1</sup> Vaillant, *Compt. Rend.*, 142, p. 81; 1906; Bordier, *Arch. d'Elect. Medicale*, 18, p. 390, 1910; Courmont and Nogier, *Compt. Rend.*, 162, p. 1746; 1911.

and how much the intensity decreases with time of operation of the lamp.

Some months ago the problem was presented, first, to devise methods for determining quantitatively this decrease in intensity of emission with usage, and, second, to make preliminary measurements on radiant power-life tests of quartz mercury vapor lamps.

## II. INSTRUMENTS AND METHODS

In considering various methods for observing the radiations emitted by quartz mercury vapor lamps it was apparent that photography would not give reproducible quantitative results,

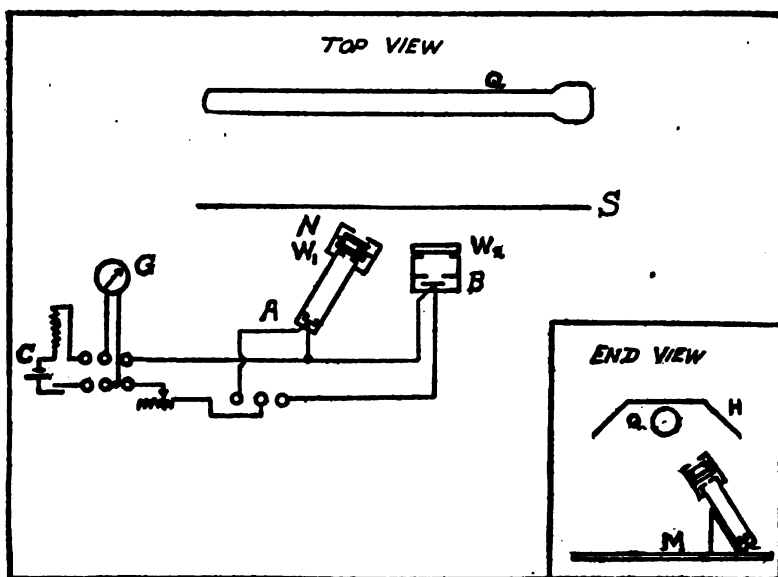


FIG. 1.—Arrangement of apparatus for measuring the radiation from quartz mercury vapor lamps

while photometric methods are not sufficiently comprehensive to take into consideration the decrease in intensity of the ultra-violet component of the radiations from the lamp.

The logical method of procedure is to measure the intensity of the radiations in absolute units by using a nonselective radiometer (e. g., thermopile) which can be calibrated by means of a standard of radiation.<sup>2</sup> This method was employed throughout the present investigation.

<sup>2</sup> This Bulletin, 11, p. 87; 1914.

The radiometer used was a thermopile of bismuth-silver,<sup>3</sup> which was covered with a quartz window ( $t=0.15$  mm) to prevent unsteadiness caused by air currents. The thermopile was placed in a mounting, *M*, Fig. 1, which could be secured in a fixed position, facing the lamp. When not in use, this radiometer outfit was removed to a secure place free from dust and likelihood of injury.

The general arrangement of the apparatus is shown in Fig. 1, in which *Q* is the quartz mercury lamp, with its protecting hood *H*. The shutter *S* permits the radiations from the lamp to fall upon the thermopiles *A* and *B*. The absorption cells of water are at *W*<sub>1</sub> and *W*<sub>2</sub>. The Noviol absorption glass is mounted at *N*.

The electric current which was generated by the thermopile was measured by means of an iron-clad Thomson galvanometer,<sup>4</sup> *G*, Fig. 1; though for most of the work a sensitive d'Arsonval galvanometer would have served the purpose.

Apparatus (*C*, Fig. 1) was provided for testing the current sensitivity of the galvanometer, which varied from day to day. The radiation sensitivity, in absolute units (gram-calories), of the thermopile-galvanometer combination was determined at frequent intervals by exposing the thermopile to the standard of radiation just mentioned. The sensitivity of the radiometric apparatus was such that for the standard galvanometer current sensitivity of  $i=5 \times 10^{-10}$  ampere, a deflection of 1 cm (caused by radiation from the standard lamp) represented an energy flux of 2.21 microwatt per square centimeter. Multiplying the observed galvanometer deflection by this factor, and knowing the distance intervening between the lamp and the thermopile, it was an easy matter to specify the intensity of the energy (the radiant flux) incident at the point where the measurement was made. This distance was 40 cm from the axis of the lamp and equidistant from the effective ends of the quartz glass tube.

Under normal operation the quartz glass tube of a mercury vapor lamp becomes heated to a dull red, thus emitting considerable infra-red radiation of wave lengths greater than  $2\mu$  ( $\mu=0.001$  mm). On the other hand, the emission spectrum of the mercury vapor consists of strong lines which abound in the ultra-violet, visible, and the infra-red spectrum, extending to about  $1.6\mu$ , as shown in Fig. 2, in which the ultra-violet measurements were taken from

<sup>3</sup> This Bulletin, 11, p. 137; 1914.

<sup>4</sup> This Bulletin, 13, p. 423; 1916.

a paper by Souder.<sup>5</sup> The visible and infra-red measurements were obtained from a paper by Coblenz,<sup>6</sup> corrections having been made for slit widths and for power input such as used in the lamps employed in the present work. The three crosses (xxx) show the distribution of intensities on a lower power input, under which condition the green mercury line is more intense than the yellow lines. There is, of course, considerable energy radiated in the form of a continuous spectrum, which would affect the relative proportions in the visible and in the ultra-violet and which is not indicated in these measurements. The emission lines, of wave lengths greater than  $1.6\mu$ , contribute but little to the total radiation emitted by the mercury vapor.

A cell, 1 cm in thickness, having thin (1.5 mm) windows of quartz and containing distilled water (which is opaque to radiations greater than  $1.4\mu$ ) was placed over the thermopile to absorb the

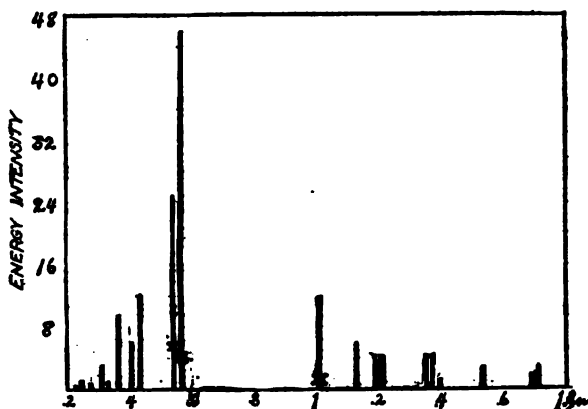


FIG. 2.—Energy distribution in the spectral lines emitted by quartz mercury vapor lamps

radiations emitted by the quartz glass tube. This cell is transparent to ultra-violet rays and its use increases the accuracy of the observations by absorbing infra-red radiations emitted by the electrodes and the quartz tube, which vary greatly in temperature, depending upon the temperature of the surrounding air, etc.

As already stated, the energy radiated by a quartz mercury vapor lamp suffers depletion of the ultra-violet component with usage of the lamp. This is attributable to discoloration (blackening) and devitrification of the bulb which absorbs the ultra-violet more strongly than the visible rays.<sup>7</sup>

<sup>5</sup> Souder, *Phys. Rev.*, **8**, p. 316; 1916.

<sup>6</sup> The *Bulletin*, **9**, p. 96; 1912. The wave lengths are from Paschen, *Ann. der Phys.*, **27**, p. 558; 1908.

<sup>7</sup> Quartz-glass changes into crystalline quartz (tridymite) when heated to about 900°.

From the experimental data at hand, it would appear that (at the expense of decreasing somewhat the total energy radiated) there would be a marked increase in the useful life and luminous efficiency by operating the lamp at a lower temperature. This would decrease the vaporization of the tungsten electrodes and, hence, the blackening of the walls of the lamp.

It is well known that with increase in energy input the luminous efficiency of a mercury vapor lamp increases and passes through a maximum value.<sup>8</sup>

As was shown in a previous investigation<sup>9</sup> this phenomenon is attributable to the more rapid increase in infra-red energy emission (with increase in energy input) as compared with the emission of visible and ultra-violet rays.

For high values of energy input the ultra-violet and visible emission lines are relatively less intense than the infra-red lines, while for a low-energy input the reverse condition is true, viz, the visible and ultra-violet rays are relatively the more intense, as illustrated by the crosses (xxx) in Fig. 2.

Hence in measuring the decrease in intensity of the ultra violet as compared with the visible radiations, with usage of the lamp, it was necessary to resort to some expedient which would avoid the above-mentioned change in relative intensities of the visible and ultra-violet with change in energy input. For, at the beginning of the investigation, it was not known what changes with usage the lamps might undergo in their volt-ampere characteristics, in their evacuation, etc.

The simplest method of measuring the decrease in the violet component with usage of the lamp would be to use a screen (1) which transmits all the ultra-violet and absorbs all the visible and infra-red rays, or (2) which absorbs all the ultra-violet and transmits all the visible and the infra-red. No such ideal screen is known, but a deep-yellow glass (Corning Noviol, shade B) which absorbs all the ultra-violet rays shorter than  $\lambda = 0.4\mu$  was found to answer the purpose.<sup>10</sup>

In a preliminary investigation of the transmission of the radiations from the quartz mercury vapor lamps through glasses of various colors, with variation in energy input into the lamps (see Table 1), it was found that this sample of yellow glass was

<sup>8</sup> Klich and Retachinsky, *Ann. der Phys.*, (4) 20, p. 563; 1906.

<sup>9</sup> This Bulletin, 9, p. 96; 1912.

<sup>10</sup> The transmission of this glass is given in this Bureau's Technologic Paper No. 93, 2d ed., p. 17, Fig. 12. See also this Bulletin, 14, p. 653; 1918.



unique in having, within the errors of observation, the same transmission for a variation in energy input of 100 to 200 watts. This simplified the experimental work, for it was then unnecessary to operate the lamp at the same energy input when making the transmission measurements from time to time, and any change in the transmission of this glass with usage of the lamp would be attributable to a change in the quality of the radiations emitted by (transmitted through the walls of) the lamp. A progressive decrease in the ultra-violet radiation, with usage of the lamp, would cause a progressive increase in the percentage of the total radiation which can pass through the yellow glass.

TABLE 1.—Transmission of the Radiations of Wave Lengths Less than  $1.4\mu$  from R. U. V. Quartz Mercury Vapor Lamp Through Glasses of Various Colors, with Variation in Energy Input

[A. O. C.—American Optical Co.; C. G. W.—Corning Glass Works]

Color of glass	Trade name	Source	Energy input in watts					
			100	200	260	400	540	615
Colorless.....	Lab. No. 58.....	A.O.C.	51.5	48.0	.....	44.6	43.4	44.2
Red.....	Selenium.....	C.G.W.	4.9	5.2	.....	6.2	7.3	8.2
Orange.....	634.....	C.G.W.	11.2	12.5	.....	14.7	16.4	17.2
Amber.....	.....	B.S.	13.2	12.7	.....	13.5	13.6	14.5
Blue-green.....	Lab. No. 59.....	A.O.C.	23.4	20.7	.....	19.8	18.8	18.5
Purple.....	G55 A62.....	C.G.W.	14.3	16.0	.....	17.9	18.1	17.7
Yellow.....	Noviol, shade B.....	C.G.W.	31.2	31.1	.....	30.9	32.5	32.2
Do. a.....	.....	.....	.....	.....	28.7	.....	.....	29.0

a Using a new lamp

This is so because, in passing out through the walls of the lamp, the ultra-violet radiations suffer a proportionately greater reduction in intensity than the (visible) radiations which are not absorbed by the yellow glass. A determination of the transmission consists in noting the galvanometer deflections when the plate of yellow glass intervenes between the thermopile and the lamp and when no glass intervenes. The ratio of these two deflections is a measure of the transmission, which increases with decrease in the ultra-violet rays.

The decrease of the ultra-violet component was determined by making transmission observations upon the radiations emitted from a length of about 5 cm of the central part of the quartz lamp tube, in order to avoid the radiations from the incandescent electrodes. For this purpose a bismuth-silver thermopile, having a circular receiver<sup>11</sup> 5 mm in diameter, was mounted in a

<sup>11</sup> This Bulletin, 11, p. 168, Fig. 3, No. 3.

suitable brass tube, *A*, Fig. 1, which admitted radiations coming only from the central part of the lamp. A 1 cm cell, *W*<sub>1</sub>, Fig. 1, having thin quartz windows (20 mm opening) and containing distilled water, absorbed most of the radiations from the hot quartz tube, but transmitted the ultra-violet rays. The Noviol and other glasses used in the transmission tests were placed in front of the water cell (at *N*, Fig. 1) and any change in the transmission with age of the lamp would be ascribable to a decrease in the ultra-violet component of the radiations passing through the walls of the lamp.

The decrease in total radiation with usage was determined by measuring the radiations emanating from the whole lamp, including radiations unavoidably reflected from the hood, *H*, Fig. 1, which was used over the lamp. For this measurement a bismuth-silver thermopile, *B*, Fig. 1, having a linear receiver, 2 by 15 mm, long axis at right angles with the long axis of the lamp, was used. No water cells with quartz windows of suitable size being available at the time when the work was undertaken, a 1 cm cell, with crown-glass windows, *W*<sub>2</sub> (35 mm opening), was used to absorb the infra-red rays. This second radiometric outfit gave a partial check on the observations made with the Noviol absorption glass. Of course the total radiation was observed also on the 5 cm length of the lamp, but no record was kept of the energy input of the lamp, the galvanometer sensitivity, the distance of the thermopile from the lamp, etc., which data would be required in reducing the data obtained with the thermopile (with circular receiver) used in measuring the ultra-violet component.

The lamps under investigation were mounted in a light-tight inclosure, which was kept thoroughly ventilated, without producing a strong draft over the lamps.

In order to protect the eyes from injury when adjusting the thermopiles for making radiometric measurements, the attendants wore deep amber-colored glasses, Corning Noviweld, shade 6<sup>12</sup>. As a further precaution against injury from reflected light, the inside of the inclosure and the mountings were painted black. This is a precaution which should be observed in dye-fading and similar tests involving the use of quartz mercury vapor lamps. The injurious effects of ultra-violet light are usually not felt until some hours have elapsed after exposure to these rays.

---

<sup>12</sup> See this Bureau's Technologic Paper No. 93, on glasses for protecting the eyes from injurious radiations.

### III. EXPERIMENTAL DATA

The data discussed under this caption were obtained on lamps purchased from the Cooper-Hewitt Electric Co. and from the R. U. V. Co.<sup>18</sup>

In the discussion of the data these two types of lamps are referred to as C. H. and R. U. V. Of the former, 110-volt and 220-volt lamps were available. Of the latter type only 220-volt lamps were obtainable.

These lamps, with their auxiliary ballast resistances were operated on the specified voltage and currents. A watt-hour meter was connected in the circuit of each lamp, and, on the days when the radiation measurements were made, a wattmeter, an ammeter, and sometimes a voltmeter were used to obtain data on the electrical characteristics of the lamp. The electrical characteristics of the lamp vary somewhat with the temperature of the surroundings.

The R. U. V. lamp is operated at a very high temperature, and the voltage-current relation is rather unstable. Because of this great fluctuation in power input it was necessary to watch the wattmeter and make radiometric measurements when the wattmeter indicated a certain value, say 615 watts. The C. H. lamps did not fluctuate in energy input, other than that which resulted from fluctuation in the line voltage.

The lamps were not operated continuously and some ceased to function after 800 to 1200 hours of actual usage, owing to leakage of air into the bulb.

On continuous operation quartz mercury lamps are known to depreciate less rapidly—i. e., have a longer life—than when operated intermittently. The present data are, therefore, not to be considered as a "life test," as measured in the total number of hours a lamp may be operated. These lamps were in operation extending over a period of three and one-half months. As in the case of incandescent lamps, the question will probably arise as to what constitutes the useful life of a quartz mercury vapor lamp. In the present case the lamps were used in dye-fading experiments (the radiometric measurements in all cases being incidental), and the use of one lamp was discontinued after its total radiation intensity had decreased to one-third its original value, although mechanically the burner appeared to be in good condition.

---

<sup>18</sup> Cooper-Hewitt Electric Co., Hoboken, N. J. The R. U. V. Co., 150 Broadway, N. Y.

## 1. VARIATION IN EMISSIVITY WITH POWER INPUT

The lamps being operated on the city power circuit were subject to fluctuations in power input. The total radiation from the lamp (through the water cell) with variation in power input was, therefore, determined at the start by operating it on a storage battery. The data so obtained (see Fig. 3) were used in reducing the observations of the total radiation, with usage, to a standard power input, say 400 watts for the C. H. lamps and 600 watts for the R. U. V. lamps. For this purpose the experimental curves

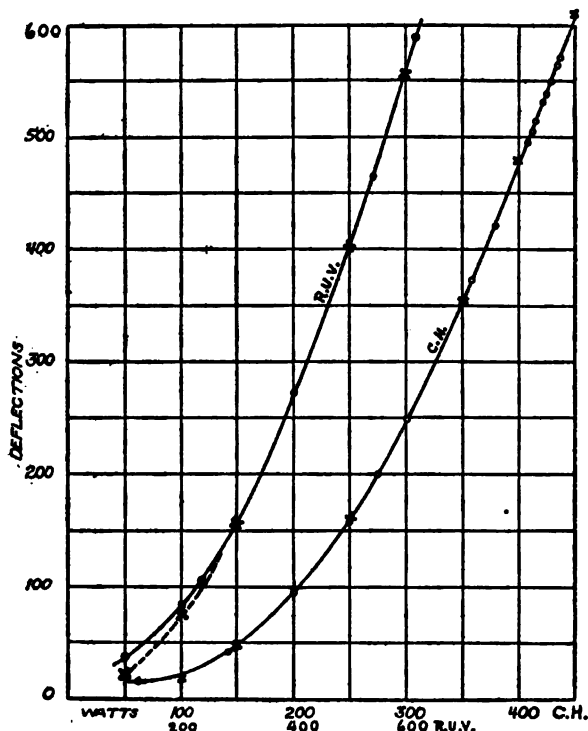


FIG. 3.—Variation in total radiation emitted with variation in power input

illustrated in Fig. 3 are closely represented by the formula  $E = KW^x$  where  $E$  is the energy of wave lengths less than  $1.4\mu$  emitted by the quartz mercury vapor,  $K$  is a constant, and  $W$  is the power input in watts.

For one of the R. U. V. quartz mercury lamps studied (upper curve Fig. 3), the formula  $E = 0.00462 W^{1.88}$  was found to fit the observations to within less than 1 per cent over a range of power input from 300 to 600 watts. As shown by the crosses in Fig. 3, for a power input of 200 watts or less the computed values differ considerably from the observed.

For the C. H. lamp (lower curve, Fig. 3) the formula  $E = 0.000457 W^{2.314}$  was found to fit the observations to within 1 per cent over a range of 150 to 400 watts of power input, giving values which are 2 per cent low at 100 watts and 2 per cent high at 450 watts, as shown by the crosses in the lower curve, Fig. 3.

## 2. VARIATION OF IRRADIATION PARALLEL WITH AXIS OF THE LAMP

In connection with the dye-fading tests, it was of interest to determine the intensity of the irradiation along a line parallel with and at a distance of 40 cm from the axis of the lamp.

The present measurements were made with a linear thermopile of special design, in which the receiver was not inclosed in the protecting tube usually provided, and no water cell was used. In

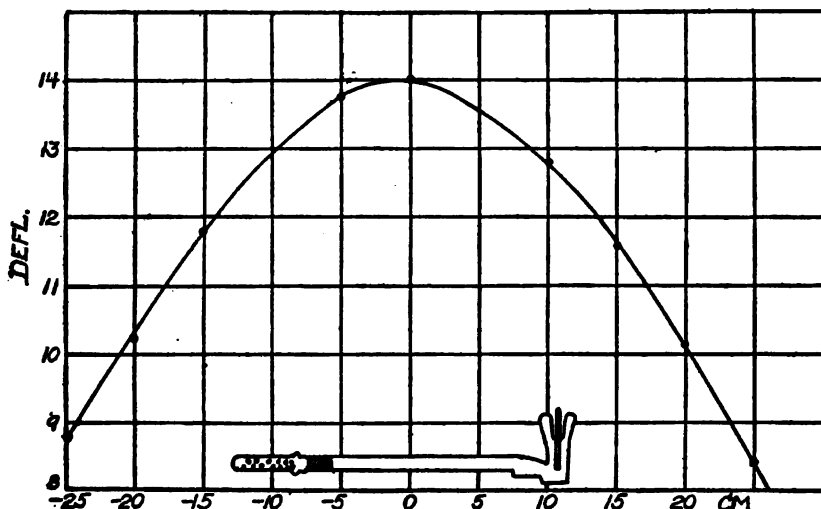


FIG. 4.—Variation of illumination parallel with axis of tube of quartz mercury vapor lamp; also illustration of lamp

this manner radiations, incident over a very wide angle, could fall upon the receiver, which moved in ways, which were placed parallel with the axis of the lamp.

The radiometric observations were made upon an R. U. V. lamp, length about 15 cm, illustrated in the lower part of Fig. 4. Measurements were made of the radiation intensity at what was judged to be the optical center of the lamp and at intervals of 5 cm to the right and left of this point. These measurements are illustrated in Fig. 4, in which the ordinates represent the intensities (the galvanometer deflections) observed at various points along the axis of the lamp. From this it appears that, for a

length of about 10 cm, which constitutes the light-giving portion of the lamp, the intensity is fairly uniform.

### 3. DECREASE IN ULTRA-VIOLET RADIATION WITH USAGE OF LAMP

As already mentioned, the decrease in the ultra-violet radiation emitted by quartz mercury vapor lamps was determined by observing the transmission of these radiations (of wave lengths less than  $1.4\mu$ ) through a sample of Noviol glass,<sup>14</sup> shade B, with usage of the lamp. These data are given in the next to the last column in Tables 3, 4, and 5, which are published to illustrate the behavior of some of the lamps examined.

The transmission of this yellow glass is of the order of 29 to 30 per cent for a new lamp, and increases to 35 to 45 per cent, depending upon the usage of the lamp.

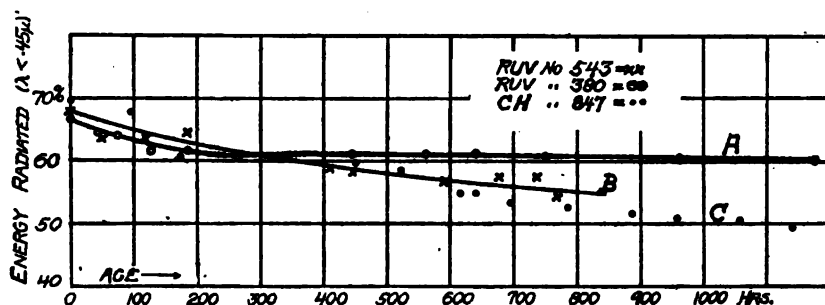


Fig. 5.—Decrease in ultra-violet radiation with usage of quartz mercury vapor lamps

The last column in Tables 3, 4, and 5 gives the per cent of ultra-violet radiation of wave lengths less than  $0.45\mu$  in the total radiation (of wave lengths less than  $1.4\mu$ ) emitted, with usage of the lamp. It is obtained from the transmission data (in the preceding column)

on the basis that the ultra-violet =  $100 - \frac{Tr}{0.9}$ . The factor 0.9 is

introduced to correct for absorption and reflection losses in the glass. In Fig. 5 is illustrated the decrease in ultra-violet radiation with usage of several quartz mercury vapor lamps. During the first 500 to 700 hours usage there was no marked difference in the per cent of ultra-violet emitted by these lamps. (See Table 6.)

It may be observed that the ultra-violet component of wave lengths less than  $0.45\mu$  amounts to about 67 per cent of the total radiation (of wave lengths less than  $1.4\mu$ ) emitted by the mercury vapor when using a new lamp, and decreases to 60 per cent or less after operating the lamp for some time.

<sup>14</sup> From the Corning Glass Works, Corning, N. Y.

In the case of the C. H. lamp, Table 5, the quartz tube had become tinged a faint brown, which seems to obstruct the ultra-violet rays. The R. U. V. lamps become discolored with a dark substance which is no doubt vaporized from the tungsten electrodes. This does not seem to obstruct the ultra-violet quite so much as the brown deposit, but tests on a larger number of lamps would be required to establish these observations as true in general.

As already mentioned, there is considerable infra-red radiation present as the result of heating of the electrodes and the supports of the lamp. The ultra-violet component is only about 20 per cent of the total radiation (of all wave lengths) emanating from the whole lamp.

#### 4. DECREASE IN TOTAL RADIATION WITH DISTANCE FROM LAMP

In order to determine the decrease in intensity of emission with usage, it is necessary to operate the radiometer at a fixed distance (this setting could be made accurate to 1 mm) or to know the variation of intensity with variation in distance from the lamp.

Measurements of the intensity of radiations (transmitted by the 1 cm water cell) at various distances from the lamp indicated that the increase in intensity with decrease in distance is more rapid than the inverse square law of the distance. This is illustrated in Table 2, in which column 2 gives the observed intensities and column 3 gives the computed intensities (using the distance 40 cm as the comparison point) on the basis of the inverse square law, which of course applies only to a point source. In this test the lamp, in its hood, was moved vertically over the thermopile, which had its receiver horizontal (the long axis being at right angles with) and at equal distances from the ends of the lamp.

TABLE 2.—Decrease in Intensity of total Radiation of Wave Lengths Less than  $1.4\mu$  with Distance from a 220-Volt C. H. Lamp

[Extrapolated values are in parentheses]

Distance in millimeters	Intensity		Distance in millimeters	Intensity	
	Observed	Calculated		Observed	Calculated
280.....		284	407.....	134.5	
300.....	(240)	248	400.....	(139)	139
338.....	190.5	195	459.....	105.5	
360.....	(171)	171.6	500.....	89.5	89.0



## 5. DECREASE IN TOTAL RADIATION WITH USAGE OF LAMP

The decrease in the radiation of wave lengths less than  $1.4\mu$  emitted by quartz mercury vapor lamps was determined by means of a linear thermopile and 1-cm water cell, placed at a distance of 40 cm from the lamp, as described on a preceding page.

Observational data for two R. U. V. lamps and one C. H. lamp (all of the 220-volt type) are illustrated in Fig. 6.

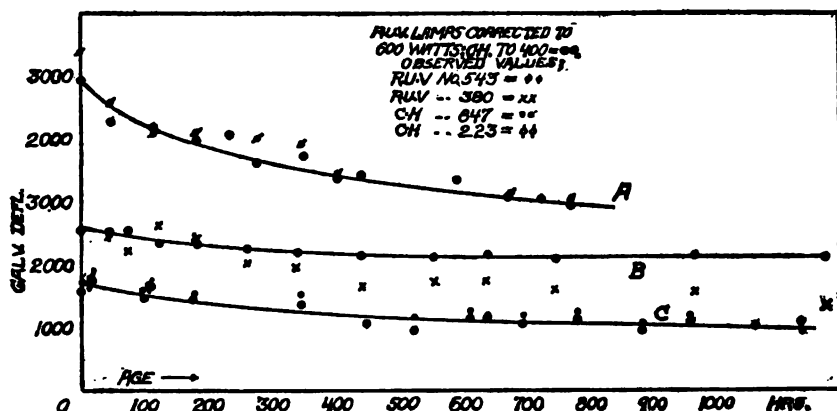


FIG. 6.—Decrease in radiation from quartz mercury vapor lamps with usage, as observed through a 1 cm cell of water, with glass windows

In the R. U. V. lamps tested, the end containing the positive electrode (tungsten target) became blackened over a length of 2 to 3 cm during the first 100 to 200 hours' operation. As a result there was at first a rather rapid decrease in the total radiation emitted, after which the total radiation continued slowly to decrease in intensity throughout the 1200 to 1500 hours during which the lamps were under observation, although the power input remained constant.

In one R. U. V. lamp (No. 380, Fig. 6) the power input as well as the total radiation continued to decrease with usage, and during the first 200 hours the ballast resistance was kept adjusted so that the lamp operated on 600 watts.

After 300 hours no further adjustments were made to the ballast resistance. This accounts for the large difference between the observed curve (crosses xx, B, Fig. 6) and the observations to be expected for a power input of 600 watts. These data are given in column 5 of Table 3 which gives the observed galvanometer deflections (intensity) and column 6 which gives these same deflections reduced to a power input of 600 watts. This lamp

did not blacken rapidly with usage, and, if it had continued to operate on 600 watts, it would appear that, after 500 hours' usage, the total energy radiated, as well as the ultra-violet radiation, would have decreased very slowly with usage.

TABLE 3.—Radiant Power Life Test of Quartz Mercury Vapor Lamp, R. U. V. No. 380, 220 Volt

Age of lamp in hours	Power input			Energy radiated		Operating efficiency	Transmission through Noviol glass	Ultra-violet radiation $\lambda$ less than $0.45 \mu$
	Amperes	Volts	Watt-meter	Observed galvanometer deflection	Observed galvanometer deflection reduced to 600 watt input			
				cm	cm		Per cent	Per cent
1.4.....	3.5	.....	600	2572	2572	11.2	30.2	66.4
44.....	3.5	175	585	2485	2576	11.15	32.1	64.4
74.7.....	3.8	176	555	2279	2568	11.7	32.4	64.0
124.3.....	3.7	171	660	2690	2395	9.65	34.5	61.7
185.4.....	3.5	178	615	2450	2375	10.0	34.8	61.3
263.8.....	3.2	178	552	2040	2280	10.3	35.4	60.7
342.8.....	3.1	177	540	1917	2220	9.8	35.5	60.6
445.....	3.0	170	495	1650	2180	10.0	35.1	61.0
561.....	3.0	176	510	1736	2170	9.76	35.0	61.0
641.....	3.0	175	510	1750	2180	9.64	35.1	61.0
749.1.....	3.0	169	507	1658	2098	9.02	35.6	60.4
968.....	2.7	178	480	1556	2140	9.66	35.9	60.1
1178.....	3.0	168	540	1858	2120	8.14	35.9	60.2

TABLE 4.—Radiant-Power Life Test of Quartz Mercury Lamp, R. U. V. No. 543, 220 Volt

Age of lamp in hours	Power input			Energy radiated		Operating efficiency	Transmission through Noviol glass	Ultra-violet radiation $\lambda$ less than $0.45 \mu$
	Amperes	Volts	Watt-meter	Observed galvanometer deflection	Observed galvanometer deflection reduced to 600 watt input			
				cm	cm		Per cent	Per cent
0.....	3.8	170	638	3446	2966	9.05	29.0	67.8
50.....	3.9	165	636	2645	2296	.....	32.8	63.6
117.....	3.9	160	613	2109	2208	.....	32.7	63.7
185.....	3.6	170	618	2158	2015	.....	32.2	64.2
236.....	3.6	165	594	2032	2076	.....	.....	.....
280.....	4.5	145	652	2000	1620	.....	.....	.....
352.....	4.1	155	632	1960	1730	6.97	.....	.....
409.....	.....	.....	607	1486	1448	.....	37.0	58.9
446.....	.....	.....	602	1491	1480	.....	37.7	58.1
593.....	.....	.....	595	1301	1325	.....	39.0	56.7
678.....	.....	.....	618	1188	1100	.....	38.4	57.3
724.....	4.2	.....	622	1098	1046	.....	.....	.....
739.....	4.7	.....	641	1170	994	.....	38.4	57.3
765.....	4.2	.....	617	1062	996	3.07	40.8	54.6

Another R. U. V. lamp (curve A, Fig. 6 and Table 4) continued to operate on a fairly uniform energy input, but, in the course of 800 hours' operation, the energy emitted (galvanometer deflections) decreased to about one-third its original intensity.

In the C. H. lamps the constricted (negative) end becomes discolored with a brown deposit which reduces the intensity of the radiation rather rapidly during the first 200 hours. This deposit extends to the main part of the tube, with usage, and absorbs considerable ultra-violet radiation in spite of the fact that the coating is so thin that it imparts only a faint yellowish tinge to the lamp. This is illustrated in the lower curves, C, in Figs. 5 and 6. Column 5 of Table 5 gives the observed galvanometer deflections (intensity) reduced to the same galvanometer sensitivity and column 6 gives these same deflections reduced to a uniform power input of 400 watts.

TABLE 5.—Radiant Power Life Test of Quartz Mercury Vapor Lamp, Cooper Hewitt No. 847, 220 Volt

Age of lamp in hours	Power input			Energy radiated		Operating efficiency	Transmission through Noval glass	Ultra-violet radiation $\lambda$ less than $0.45 \mu$
	Amperes	Volts	Watt-meter	Observed galvanometer deflection	Observed galvanometer deflection reduced to 400 watt input			
				cm	cm		Per cent	Per cent
0.....	3.0	.....	413	1735	1611	8.24	27.5	69.4
97.....	.....	.....	413	1612	1497	.....	29.0	67.8
177.....	.....	.....	401	1511	1503	.....	35.6	60.4
343.....	.....	.....	416	1513	1380	.....	35.6	60.4
450.....	.....	.....	401	1041	1033	.....	36.1	39.9
522.....	3.3	.....	439	1158	910	.....	38.0	58.2
615.....	2.8	.....	420	1282	1141	.....	40.6	34.9
640.....	3	142	413	1189	1104	4.87	40.6	54.9
696.3.....	3.05	138	416	1136	1036	.....	42.1	53.2
783.....	2.9	144	416	1214	1107	4.93	43.0	52.3
886.....	2.8	143	422	1052	925	.....	43.8	51.2
959.....	2.8	.....	397	1052	1069	.....	44.3	50.8
1064.....	2.9	.....	405	1054	1025	4.20	44.5	50.5
1140.....	2.75	.....	386	960	1034	.....	45.8	49.1

The radiometric data on radiant-power life tests of several quartz mercury vapor lamps are summarized in Table 6. For some lamps, the tests are incomplete. However, from the data presented herewith, it is evident that the total radiation as well as the ultra-violet component decreases markedly with usage of quartz mercury vapor lamps. While the number of lamps are too

few to form conclusions as to the general behavior of such lamps, the above-mentioned data indicate a decrease in intensity of one-half to one-third the initial value in the course of 1000 to 1200 hours' operation.

**TABLE 6.**—Summary of Radiant-Power Life Tests of Quartz Mercury Vapor Lamps Giving the Decrease in Radiation from 0 to 1.4 $\mu$  and in the Per Cent of Ultra-Violet Radiation with Age of Lamp; also the Power Input and Operating Efficiency

[Tests incomplete on several lamps]

Age in hours	Radiant energy, g cal/cm <sup>2</sup> sec $\times 10^{-3}$						Ultra violet (per cent)					
	R. U. V., 220 volts		C. H., 220 volts			C. H., 110 volts	R. U. V., 220 volts		C. H., 220 volts			C. H., 110 volts
	543	380	836	223	847	813	543	380	836	223	847	813
0.....	31.1	27.4	20.1	17.9	16.6	7.3	67	66	70	69	69	66
100.....	22.5	24.9	17.0	16.7	14.5	5.3	64	63	.....	66	66	.....
200.....	19.5	23.3	13.9	.....	13.1	.....	62	61	.....	.....	63	* 54
300.....	17.0	22.1	.....	.....	12.1	.....	60	61	.....	.....	61	.....
400.....	15.0	21.1	.....	.....	11.3	.....	59	61	.....	.....	59	.....
500.....	13.1	20.3	.....	.....	10.7	.....	57	61	.....	.....	57	.....
600.....	11.3	19.6	.....	.....	10.1	.....	56	61	.....	.....	56	.....
700.....	9.6	19.0	.....	.....	9.6	.....	55	61	.....	.....	54	.....
800.....	7.9	18.4	.....	.....	9.2	.....	55	61	.....	.....	53	.....
900.....	.....	17.8	.....	.....	8.8	.....	.....	60	.....	.....	52	.....
1,000.....	.....	17.3	.....	.....	8.4	.....	.....	60	.....	.....	51	.....
1,100.....	.....	16.7	.....	.....	8.1	.....	.....	60	.....	.....	50	.....
1,200.....	.....	16.2	.....	.....	7.8	.....	.....	60	.....	.....	49	.....

Lamp	Serial No.	Power input in watts		Operating efficiency $\times 10^{-3}$	
		Lamp	Lamp plus ballast resistance	Age, 0 hours	Age, 800 hours
R. U. V., 220 volts.....	543	600	1,025	12.1	3.3
R. U. V., 220 volts.....	380	600	770	13.4	10.8
C. H., 220 volts.....	836	400	928	8.4	.....
C. H., 220 volts.....	223	400	690	10.9	.....
C. H., 220 volts.....	847	400	690	9.9	5.9
C. H., 110 volts.....	813	250	360	8.6	.....

\* Estimated age; actual time of operation of this lamp is unknown.

As already mentioned, the lamps (especially the R. U. V. type, which originally was designed for an entirely different purpose from the one mentioned in this paper) are operated at too high a temperature to obtain a fairly constant performance. As a result the useful life of the lamps, now obtainable, does not appear

to be much greater than 1000 to 1500 hours. Of course, the lamps are sometimes usable for several thousand hours, especially when operated continuously. However, the average laboratory lamp is not operated continuously.

By dispensing with the high intensity which is obtained on the rated normal operation, these lamps will not discolor nor devitrify so rapidly and their useful life can be greatly prolonged, without much loss in time in making the aforementioned tests.

#### 6. TOTAL RADIATION AND OPERATING EFFICIENCY OF QUARTZ MERCURY VAPOR LAMPS

It is of interest to record, in absolute value, the total radiation of all wave lengths; also the radiation of wave lengths less than  $1.4\mu$ , emitted by quartz-mercury vapor lamps.

The data given in column 6 of Tables 3, 4, and 5 may be reduced to energy in absolute value by multiplying the observed galvanometer deflections by the factor  $1 \text{ cm defl.} = 2.21 \times 10^{-6} \text{ watt} = 5.29 \times 10^{-7} \text{ g-cal. per cm}^2 \text{ per sec.}$

The total radiation of all wave lengths from quartz-mercury vapor lamps is rather indefinite owing to the presence of the hood and other surroundings which become heated and emit radiations of long wave lengths. It was found that the  $1 \text{ cm}$  water cell, with glass windows, transmitted from 14 to 15 per cent of the total radiation from these two types of lamps. From this, and from direct measurements, it was found that the total radiation of all wave lengths is about 7 times that indicated by the measurements given in column 6 of Tables 3, 4, and 5 or about  $0.01 \text{ g-cal. per cm}^2 \text{ per sec.}$  at  $40 \text{ cm}$  from the center of a new R. U. V. lamp. The 220-volt R. U. V. lamps, including ballast resistance, were operated on a power input which was about 15 per cent greater than that used on the 220-volt C. H. lamps.

In order to determine the energy flux of wave lengths less than  $1.4\mu$  incident at a point  $40 \text{ cm}$  from the lamp (and equidistant from the ends as already described) it is necessary to correct the observations for absorption by the glass water cell. It was found that the  $1 \text{ cm}$  water cell with quartz windows transmitted 1.6 times (1.3 for an old lamp) as much mercury vapor radiation as did the  $1 \text{ cm}$  water cell having glass windows. Moreover, it was found that a  $1 \text{ cm}$  water cell having quartz windows transmitted 84 per cent of the mercury vapor radiations which had passed through a similar  $1 \text{ cm}$  water cell having quartz windows. From

this it would appear that the total radiation intensity of wave lengths less than  $1.4\mu$ , incident at 40 cm from these quartz mercury vapor lamps, when new, is  $(1.6 \div 0.84 =)$  1.9 times that indicated in column 6 of Tables 3, 4, and 5. For lamps, operated 1000 hours, this factor would be  $(1.3 \div 0.84 =)$  1.55 instead of 1.9. For intermediate intervals this decrease is taken to be uniform. Using these factors and the one for reducing the galvanometer deflections to gram-calories, the data in column 6 of Tables 3, 4, and 5 are given (for even intervals of 100 hours) in Table 6.

The energy of wave lengths less than  $1.4\mu$  radiated by the R. U. V. lamps was probably 40 to 60 per cent greater (depending upon usage, etc., see Fig. 6 and Table 6) than that of the C. H. lamp. In the latter about 40 per cent of the applied energy is used in the ballast. This reduces the operating efficiency (ratio of energy radiated to energy input) as shown in the lower part of Table 6.

At the high energy input used, the voltage-current characteristics of the R. U. V. lamp is rather unstable so that there was constantly a great fluctuation in energy input. This caused great difficulty in making radiant energy measurements. This difficulty was not experienced with the C. H. lamp.

#### 7. COMPARATIVE DATA OF VARIOUS SOURCES OF RADIATION

In view of the frequent inquiries for sources of ultra-violet radiation and the relative proportions of ultra-violet and visible radiations in various well-known sources of light, it is of interest to include comparative data in this paper.

Some years ago Bell<sup>18</sup> determined the ultra-violet component of the radiations emitted by various artificial sources. It is of interest to note that he found that a Cooper-Hewitt glass mercury vapor lamp emits only about one-sixth as much ultra-violet as is found in a quartz mercury vapor lamp.

In Table 7 is given a comparison of the solar radiation for average air mass (2.7 for a 10-hour day) with the intensity at 40 cm from the axis and equidistant from the ends of the new 220-volt C. H. quartz mercury vapor lamp; also the average total radiation of two new 220 volts R. U. V. lamps.

*Radiometric Measurements On a Dye-Fading Carbon Arc Lamp.*—Tests were made also on a 220-volt arc lamp<sup>19</sup> with "violet flame" carbon electrodes, used in dye-fading tests. The power input was about 4000 watts.

<sup>18</sup> Bell, Amer. Acad. Arts and Sci., 48, p. 1; 1912.

<sup>19</sup> Made by the Atlas Electric Co., Chicago, Ill.

TABLE 7.—Comparison of Solar Radiation with that of Quartz Mercury Vapor Lamp,  
C. H. 223

Wave length	Solar radiation		Quartz mercury vapor radiation	
	Gram-calorie per square centimeter per second	Per cent of total	Gram-calorie per square centimeter per second	Per cent of total
0 to $0.45\mu$ .....	0.0008	5	0.0011	20
0 to $1.4\mu$ .....	.0129	.....	.0017	30
$0.45$ to $1.4\mu$ .....	.0121	78	.0006	11
$1.4\mu$ to $\infty$ .....	.0026	17	.0039	70
0 to $\infty$ .....	.0155	100	.0056	100
0 to $\infty$ .....	.....	.....	.01	.....

DYE-FADING CARBON ARC				
0 to $1.4\mu$ .....	.....	.....	0.0051	.....

\* R. U. V. lamp.

The total radiation intensity (of wave lengths less than  $1.4\mu$ ) at a distance of 40 cm from the arc with the glass globe in place was about  $5.1 \times 10^{-8}$  g-cal. per  $\text{cm}^2$  per sec. The ultra-violet component of wave lengths less than  $0.45\mu$  (determined by means of the Noviol glass previously described) is about 59 per cent of the above-mentioned total radiation.

From this it appears that the ultra-violet component is practically the same as that of the quartz-mercury vapor lamp, while its total radiation is two to three times that of the mercury vapor lamps.

The power input is about five times that of the mercury vapor lamps. However, the increase in useful area surrounding the carbon arc, having approximately equal illumination, is about two and a half times that of the mercury arc. This increase in useful area compensates for the increased power input, so that the operating efficiency is practically the same for these two types of lamps. If a quartz mercury vapor lamp can be constructed so that it can be used in a vertical position, the operating efficiency can be more than doubled by utilizing the space entirely surrounding the axis of the burner.

#### IV. SUMMARY

The object of the present investigation was, first, to devise methods for determining, quantitatively, the decrease in intensity of emission with usage and, second, to make preliminary measurements on radiant-power life tests of quartz mercury vapor lamps.

The lamps used were made by the Cooper-Hewitt Electric Co. and by the R. U. V. Co. (Inc.).

This paper gives experimental data on the decrease in intensity of the ultra-violet and of the total radiation with usage of quartz mercury vapor lamps.

The intensities were measured radiometrically by means of a bismuth-silver thermopile and auxiliary galvanometer. A water cell 1 cm in thickness with quartz windows was used in front of the thermopile to absorb the infra-red rays of long wave length, which are emitted by the electrodes and surroundings.

The decrease in ultra-violet rays was determined by observing the change in transmission of a yellow (Corning Noviol, shade B) glass, with usage of the lamps.

It was found that the transmission of this glass did not vary appreciably with the power put into the lamp. Hence, any change in transmission of this glass with usage of the lamp was ascribable to variations (decrease) in emission of ultra-violet rays caused by absorption in passing through the quartz glass tube, which becomes discolored with usage. By this means it was established that the ultra-violet rays, emitted from quartz mercury vapor lamps, decrease from an initial value of about 70 per cent (of the total radiation of wave lengths less than  $1.4\mu$ ) when the lamp is new to about 50 per cent after 1000 to 1500 hours' usage.

During the first 500 hours' usage no marked difference was observed in the per cent of ultra-violet emitted by these two types of lamps.

It was observed that the total radiation from these lamps decreased in intensity by one-half to one-third the initial value in the course of 1000 to 1200 hours.

Data are given (1) on the variation of the total radiation emitted by quartz mercury vapor lamps with variation in energy input, (2) on the variation of the intensity of the irradiation parallel with the axis of the lamp, and (3) on the variation of the intensity of the total radiation with distance from the lamp.

Comparative data are given on the ultra-violet component in the radiations from the sun, from quartz mercury vapor lamps, and also from a carbon arc lamp which is used in dye-fading tests.

WASHINGTON, June 8, 1918.



1919

DEPARTMENT OF COMMERCE  
BUREAU OF STANDARDS

S. W. STRATTON, Director

SCIENTIFIC PAPERS OF THE BUREAU OF STANDARDS, No. 331

[Issued December 30, 1918]

A RELATION CONNECTING THE DERIVATIVES  
OF PHYSICAL QUANTITIES<sup>1</sup>

By Mayo D. Hency, Associate Physicist

CONTENTS

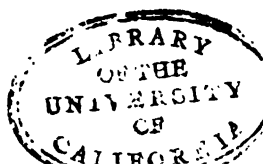
	Page.
I. INTRODUCTION.....	21
1. Scope of the paper.....	21
2. Statement of the problem.....	22
3. Other classes of relations among derivatives.....	22
II. THEORETICAL DISCUSSION.....	23
1. Derivation of the new relation.....	23
2. Extension to higher derivatives.....	25
3. Integral form of the relation.....	25
4. Discussion of the constant-product restriction.....	26
III. SOME ILLUSTRATIVE EXAMPLES.....	27
1. Variation of journal friction with size of bearing.....	27
2. Effect of gravity on a rolling-ball viscosimeter.....	28
3. Effect of high pressure on accuracy of a rolling-ball viscosimeter..	29

I. INTRODUCTION

1. *Scope of the Paper.*—In this paper it is shown how the theory of dimensions may be used in a differential form; a procedure which appears fruitful particularly in investigating the effect of given sources of error on the performance of measuring instruments.

The examples which led to the necessity for developing this method are discussed at the end of the paper and illustrated by experimental data.

<sup>1</sup> This work was done at the Jefferson Physical Laboratory, Harvard University, in 1916, and presented as an interesting application of Buckingham's II theorem during a series of four lectures on Dimensional Reasoning given at the Friday evening conferences.



2. *Statement of the Problem.*—Given the fact that some relation of unknown form

$$Q_0 = f(Q_1, Q_2, \dots, Q_{N-1}) \quad (1)$$

subsists between  $N$  physical quantities  $Q_0, Q_1, Q_2, \dots, Q_{N-1}$ , no others being involved, it is required to deduce a relation of known form

$$\frac{\partial Q_0}{\partial Q_1} = F\left(\frac{\partial Q_0}{\partial Q_2}, Q_0, Q_1, Q_2, \dots, Q_{N-1}\right) \quad (2)$$

such that at any point whose generalized coordinates,  $Q_0, Q_1, Q_2$ , etc., are given, the value of any one of the  $N - 1$  partial derivatives of  $Q_0$  can be computed from some other one. Thus, it is required to calculate one of the component slopes of the generalized surface (1) from a knowledge of another, although the equation of the surface is not available. The interest of the problem to the physicist lies in the fact that he may wish to learn the value of a derivative not readily accessible to experiment, in a case where some other derivative of the same quantity can easily be observed. It will be shown that a definite solution can always be obtained, provided certain dimensionless products of the  $N$  quantities are held constant.

3. *Other Classes of Relations Among Derivatives.*—The proposition, that relations may be found connecting the derivatives of quantities in the absence of a primitive equation, is not new. There are two other classes of such relations. One consists of mathematical identities, applicable to any set of related quantities, whether physical or not. To this class belongs the identity

$$\frac{\partial}{\partial Q_1} \frac{\partial Q_0}{\partial Q_2} = \frac{\partial}{\partial Q_2} \frac{\partial Q_0}{\partial Q_1} \quad (3)$$

as well as the triple product relation

$$\frac{\partial Q_0}{\partial Q_1} \cdot \frac{\partial Q_1}{\partial Q_2} \cdot \frac{\partial Q_2}{\partial Q_0} = -1 \quad (4)$$

The other class comprises relations requiring the explicit use of physical laws, such as the two laws of thermodynamics, or Hamilton's principle. To this class belong Maxwell's four thermodynamic relations, and the reciprocal relations of generalized dynamics.<sup>2</sup> The relations to be presented here are of a nature

<sup>2</sup> J. J. Thomson, *Applications of dynamics to physics and chemistry*, Chap. 5.

intermediate between the other two classes, in that they require a knowledge only of the dimensions of the quantities.

## II. THEORETICAL DISCUSSION.

1. *Derivation of the New Relation.*—The present result depends upon and is a corollary to Buckingham's  $\Pi$ -theorem,<sup>3</sup> according to which any complete physical equation is reducible to the form

$$\text{funct. } (\Pi_1, \Pi_2, \dots, \Pi_i) = 0 \quad (5)$$

in which the  $\Pi$ 's are all the independent dimensionless products which can be built up by combining in any way the  $N$  physical quantities involved. Further, the total number of such products, or dimensionless arguments, will always be the same, no matter how the quantities are grouped. This number will be

$$i = N - k \quad (6)$$

if  $k$  is the number of fundamental units needed for measuring the  $N$  quantities.<sup>4</sup>

Let  $\Pi_0$  and  $\Pi$  designate any two of the  $i$  products in (5) which contain between them the three quantities  $Q_0, Q_1$ , and  $Q_2$  in which we are interested. Let  $Q_0$  appear to the first power in  $\Pi_0$  and not at all in any other product, which can always be done, for Buckingham has shown that a certain standard arrangement is possible in which each product contains to the first power some one quantity of type  $P$  which occurs nowhere else.<sup>5</sup> We shall then have

$$\Pi_0 = Q_1^{\alpha_1} Q_2^{\alpha_2} \dots Q_k^{\alpha_k} \cdot Q_0 \quad (7)$$

and

$$\Pi = Q_1^{\beta_1} Q_2^{\beta_2} \dots Q_k^{\beta_k} \cdot Q_{k+1} \quad (8)$$

The exponents are abstract numbers fixed by the dimensions of the  $N$  quantities; in any particular problem some of them may be zero. If we now agree to keep the remaining  $i-2$  products constant, (5) becomes

$$\Pi_0 = \phi(\Pi) \quad (9)$$

in which the form of  $\phi$  is unknown. The restriction to constant

<sup>3</sup> Journal Wash. Acad. Sci., 4, pp. 347-353, 1914; Phys. Rev., 4, pp. 345-376, 1914; Trans. Am. Soc. Mech. Engs., 87, pp. 263-296; 1915. Anyone who can sufficiently visualize the meaning of the  $\Pi$ -theorem will be able to treat each concrete problem by itself, dispensing with the formulas of the present paper save as a check.

<sup>4</sup> The question of the number of fundamental units needed has been discussed by Riabouchinsky, Rayleigh, and Buckingham; see Nature, 90, pp. 396-397; 1915.

<sup>5</sup> Trans. Am. Soc. Mech. Engs., 87, pp. 291-292; note equation (11) and its discussion.

products can always be fulfilled in theory, but it may lead to difficulties in practice; it will be discussed in a later section. Differentiating (9) and then (8) gives in succession

$$\frac{\partial \Pi_0}{\partial Q_1} = \frac{d\phi}{d\Pi} \cdot \frac{\partial \Pi}{\partial Q_1} = \frac{d\phi}{d\Pi} \frac{\alpha \Pi}{Q_1} \quad (10)$$

From (7)

$$\frac{\partial \Pi_0}{\partial Q_1} = \frac{\partial Q_0}{\partial Q_1} \frac{\Pi_0}{Q_0} + \frac{\alpha_0 \Pi_0}{Q_1} \quad (11)$$

Comparing (10) and (11)

$$\Pi \frac{d\phi}{d\Pi} = \frac{Q_1 \Pi_0}{\alpha} \left( \frac{1}{Q_0} \frac{\partial Q_0}{\partial Q_1} + \frac{\alpha_0}{Q_1} \right) \quad (12)$$

Similarly

$$\Pi \frac{d\phi}{d\Pi} = \frac{Q_2 \Pi_0}{\beta} \left( \frac{1}{Q_0} \frac{\partial Q_0}{\partial Q_2} + \frac{\beta_0}{Q_2} \right) \quad (13)$$

Comparing (12) and (13)

$$\frac{\partial Q_0}{\partial Q_1} = \left( \frac{\alpha}{\beta} \beta_0 - \alpha_0 \right) \frac{Q_0}{Q_1} + \frac{\alpha}{\beta} \frac{Q_2}{Q_1} \frac{\partial Q_0}{\partial Q_2} \quad (14)$$

Hence the desired relation (2) has the linear form

$$\frac{\partial Q_0}{\partial Q_1} = a + b \frac{\partial Q_0}{\partial Q_2} \quad (15)$$

in which the coefficients

$$a = \left( \frac{\alpha}{\beta} \beta_0 - \alpha_0 \right) \frac{Q_0}{Q_1} \quad (16)$$

and

$$b = \frac{\alpha}{\beta} \frac{Q_2}{Q_1} \quad (17)$$

involve none of the  $N$  quantities save  $Q_0$ ,  $Q_1$ , and  $Q_2$ .

Evidently (14) can be written also

$$\frac{\partial \log Q_0}{\partial \log Q_1} = \left( \frac{\alpha}{\beta} \beta_0 - \alpha_0 \right) + \frac{\alpha}{\beta} \frac{\partial \log Q_0}{\partial \log Q_2} \quad (18)$$

in which the coefficients are independent of the coordinates. Thus the relation connecting the logarithmic derivatives is the same all over the generalized surface.

If no two independent products can be found which do contain between them the three quantities  $Q_0$ ,  $Q_1$ , and  $Q_2$ , either  $\alpha$  or  $\beta$

will vanish, showing that the derivatives are independent. Thus, while it is always possible to find a relation connecting any derivative with some other, it is not always possible to find a relation connecting a given derivative with any other desired.

2. *Extension to Higher Derivatives.*—Differentiating (14) with respect to  $Q_1$  and using the identity (3) gives

$$\frac{\partial^2 Q_0}{\partial Q_1^2} = A + B \frac{\partial Q_0}{\partial Q_2} + C \frac{\partial^2 Q_0}{\partial Q_2^2} \quad (19)$$

in which the coefficients are

$$A = \frac{Q_0}{Q_1^2} \left( \frac{\alpha}{\beta} \beta_0 - \alpha_0 \right) \left( \frac{\alpha}{\beta} \beta_0 - \alpha_0 - 1 \right) \quad (20)$$

$$B = \frac{Q_2}{Q_1^2} \frac{\alpha}{\beta} \left( \frac{\alpha}{\beta} - 1 \right) (1 + 2\alpha_0) \quad (21)$$

and

$$C = \left( \frac{Q_2 \alpha}{Q_1 \beta} \right)^2 \quad (22)$$

Thus the curvature with respect to  $Q_1$  can be calculated from the slope and the curvature with respect to  $Q_2$ .

3. *Integral Form of the Relation.*<sup>4</sup>—Integrating (14) at the point ( $Q_0 = q_0$ ,  $Q_1 = q_1$ ,  $Q_2 = q_2$ ) over an interval so short that  $\frac{\partial Q_0}{\partial Q_2}$  may be treated as constant, and denoting its value by the symbol  $\frac{\partial q_0}{\partial q_2}$ , gives for the primitive equation of an element of the surface

$$\frac{Q_0}{q_0} = \left( \frac{Q_1}{q_1} \right)^h \quad (23)$$

in which

$$h = \frac{\alpha}{\beta} \left( \frac{q_2}{q_0} \frac{\partial q_0}{\partial q_2} + \beta_0 \right) - \alpha_0 \quad (24)$$

The use of (23) would permit a direct comparison of any new results obtained by the present method with empirical results previously published in one-term, constant-exponent formulas.

<sup>4</sup> If instead of an isolated value of  $\frac{\partial Q_0}{\partial Q_2}$  we were furnished with the entire curve  $Q_0 = f_1(Q_2)$ , the direct use of the II-theorem would be preferable, and would give the whole curve  $Q_0 = f_1(Q_2)$ . If successively furnished with additional curves,  $Q_0 = f_2(Q_2)$  and so on, we could gradually build up generalized cross sections of the surface ( $x$ ) until, when  $N-k$  independent curves had been given, we should have the whole of it. The problem of developing empirical equations synthetically has not been treated in the available papers. That problem is a general one, of which the problem of the present paper is a special case; this situation is illustrated by the fact that our final result (23) applies only to an infinitesimal piece of the curve  $Q_0 = f_1(Q_2)$ .

4. *Discussion of the Constant-Product Restriction.*—Let  $\Pi_0$  denote any one of the  $i-2$  arguments which we have agreed to hold constant, and let  $Q$  stand for either  $Q_1$  or  $Q_2$ . Then, unless  $\Pi_0$  can be so chosen that it does not contain  $Q$ , it must be so chosen that it will contain some additional quantity  $Q_0$  not occurring in any other product. The rule for keeping  $\Pi_0$  constant will then be: Vary  $Q_0$  simultaneously in such a manner as to compensate the changes due to  $Q$ .

If  $Q$  enters  $\Pi_0$  to the  $n^{\text{th}}$  power and  $Q_0$  enters it to the first, the derivatives in (15) and elsewhere are subject to one or more conditions of the type  $Q_0 \propto Q^{-n}$ . For such a derivative let us adopt from now on the notation  $\left(\frac{\partial Q_0}{\partial Q}\right)_{Q_0 \propto Q^{-n}}$ . There are two experimentally independent methods for getting its numerical value: First, by directly observing the change in  $Q_0$  with  $Q$  while simultaneously changing  $Q_0$  in the prescribed manner; second, by calculating it from separate observations on the change in  $Q_0$  with  $Q$  at constant  $Q_0$ , and the change in  $Q_0$  with  $Q_0$  at constant  $Q$ . Expanding the conditioned derivative into the form  $\left(\frac{\partial Q_0}{\partial Q}\right)_{Q_0} + \left(\frac{\partial Q_0}{\partial Q_0}\right)_Q \frac{dQ_0}{dQ}$  and taking account of the fixed relation between  $Q_0$  and  $Q$  leads to the working formula

$$\left(\frac{\partial Q_0}{\partial Q}\right)_{Q_0 \propto Q^{-n}} = \left(\frac{\partial Q_0}{\partial Q}\right)_Q - n \frac{Q_0}{Q} \left(\frac{\partial Q_0}{\partial Q_0}\right)_Q \quad (25)$$

for the second method. In the most general case where there are  $i-2$  arguments to be kept constant, the second term on the right of (25) will be replaced by  $-\frac{1}{Q}$  times the summation of  $i-2$  terms of the type  $nQ_0 \left(\frac{\partial Q_0}{\partial Q_0}\right)_Q$ .

While the procedure outlined in this section is always possible and sufficient, it is not always necessary or even desirable. For example: if the number of quantities,  $N$ , does not exceed the number of fundamental units,  $k$ , by more than 2, there will be no other arguments than  $\Pi_0$  and  $\Pi$ ; again, if the remaining  $i-2$  arguments do not involve  $Q$  (i. e.,  $Q_1$  or  $Q_2$ ), their constancy will not be disturbed at all by the fact that  $Q_1$  and  $Q_2$  do vary. Further expedients for simplifying the work will suggest themselves upon examining each particular case by itself.

### III. SOME ILLUSTRATIVE EXAMPLES

For reference in solving problems it is convenient to rewrite (5) in the form

$$Q_1^{\alpha} Q_2^{\beta} \cdots Q_k^{\gamma} \cdot Q_0 = \text{funct.} (Q_1^{\alpha} Q_2^{\beta} \cdots Q_k^{\gamma} \cdot Q_{k+1}, \text{ and other } \Pi\text{'s}) \quad (26)$$

The values of  $\alpha$ ,  $\beta$ , etc., can now be read off directly by identifying them with the corresponding numerical exponents in the equation, of type (26), afforded by the particular example in hand.

1. *Variation of Journal Friction with Size of Bearing.*—In the case of a journal bearing, under certain restrictions, we may expect a relation of type (1) to connect the coefficient of friction  $f$ , with the viscosity of the lubricant  $\mu$ , the revolutions per unit time  $n$ , the bearing pressure  $p$ , the journal diameter  $D$ , and the volume of oil  $V$  forced through the bearing in unit time. Let it be required to calculate the effect of altering the size of the machine from a test in which nothing is varied but the rate of pumping oil through the bearing. It may be shown by the  $\Pi$ -theorem that

$$f = \text{funct.} \left( \frac{D^3 n}{V}, \frac{\mu n}{p}, \text{shape} \right) \quad (27)$$

Let now  $f$ ,  $D$ , and  $V$  serve, respectively, as  $Q_0$ ,  $Q_1$ , and  $Q_2$ . Comparing (27) with (26),  $\alpha_0 = 0$ ,  $\beta_0 = 0$ ,  $\alpha = 3$ ,  $\beta = -1$ ; hence, by (16) and (17),  $a = 0$  and  $b = -3\frac{V}{D}$ , or

$$\frac{\partial f}{\partial D} = -3\frac{V}{D} \frac{\partial f}{\partial V} \quad (28)$$

Also, by (20) and (22),  $A = 0$ ,  $B = 12\frac{V}{D^3}$ , and  $C = 9\left(\frac{V}{D}\right)^2$ ; therefore

$$\frac{\partial^2 f}{\partial D^2} = 12\frac{V}{D^3} \frac{\partial f}{\partial V} + 9\left(\frac{V}{D}\right)^2 \frac{\partial^2 f}{\partial V^2} \quad (29)$$

Equations (28) and (29) enable us to predict the bearing losses of any slightly larger or smaller machine in the same geometrically similar series. This requirement of geometrical similarity is an instance of the constant-product restriction. The products in this case are the length ratios fixing the shape. The first of the two results in this example, namely, equation (28), follows readily enough from equation (27) without calling in the aid of the present theorem at all. For in differentiating  $f$  first with

respect to  $D$  and then with respect to  $V$  the *same* unknown occurs both times and can be eliminated, leaving the desired relation between  $\frac{\partial f}{\partial D}$  and  $\frac{\partial f}{\partial V}$ . The contemplation of this example, which can be solved by inspection because the left-hand member of equation (27) has only one quantity in it, reveals instructively the meaning of the theorem and shows that it is simple when understood.

2. *Effect of Gravity on a Rolling-Ball Viscosimeter.*—Let it be required to find the effect of gravity on a rolling-ball viscosimeter in terms of the effect produced by changing the size of the instrument. Let  $D$ ,  $l$ , and  $\theta$  denote, respectively, the diameter and length of the tube and its angle of inclination to the horizontal,  $d$  and  $\rho_0$  the diameter and density of the ball,  $\rho$  and  $\mu$  the density and viscosity of the liquid, and  $t$  the roll-time<sup>7</sup> in a locality<sup>8</sup> of gravity  $g$ . Assuming that a complete relation does subsist among these quantities, the  $\Pi$ -theorem shows that any equation describing that relation, whether obtained theoretically or experimentally, must be reducible to the form

$$\frac{\mu}{\rho D^2} t = \text{funct.} \left( \frac{\rho_0}{\rho}, \frac{g \rho^2 D^4}{\mu^2}, \text{shape} \right) \quad (30)$$

the shape, in turn, being fixed by the arguments  $\frac{d}{D}$ ,  $\frac{l}{D}$ , and  $\theta$ .

Taking  $t$ ,  $g$ , and  $D$ , respectively, for  $Q_0$ ,  $Q_1$ , and  $Q_2$  gives  $\alpha_0 = 0$ ,  $\beta_0 = -2$ ,  $\alpha = 1$ , and  $\beta = 3$ ; so that by (18)

$$\frac{g}{t} \frac{\partial t}{\partial g} = -\frac{2}{3} + \frac{1}{3} \frac{D}{t} \frac{\partial t}{\partial D} \quad (31)$$

An interesting check on (31) is afforded by differentiating the empirical equation for such an instrument.<sup>9</sup> The equation has been presented in the form  $y = a + bx$ , in which  $x$  denotes

$\tau \sqrt{Dg \left( \frac{\rho_0}{\rho} - 1 \right)}$  and  $y$  denotes  $\nu \sqrt{D^3 g \left( \frac{\rho_0}{\rho} - 1 \right)}$ ,  $\tau$  being the roll-time per unit length  $\frac{t}{l}$ ,  $\nu$  the kinematic viscosity  $\frac{\mu}{\rho}$ , and  $a$  and

<sup>7</sup> That is, the time required for the ball to roll down. This instrument, proposed by Flowers (Proc. Am. Soc. Test. Mat., 14, pp. 565; 1914), is further discussed by the writer in Journal Wash. Acad. Sci., 6, pp. 527; 1916.

<sup>8</sup> Having set up such a viscosimeter in Cambridge, the question arose whether there would be any sensible change upon taking it to Washington, where gravity is 0.3 per cent less. The conclusion is that the roll-time in a very viscous liquid will be 0.3 per cent greater in Washington; and that the effect of gravity diminishes when the fluidity of the liquid increases, falling to 0.2 per cent for water.

<sup>9</sup> Journal Wash. Acad. Sci., 6, pp. 528, eq. (6); 1916.



$b$  particular numerical values fixed by a particular choice of  $\frac{d}{D}$  and  $\theta$ . Recast in the form (30), it becomes

$$\frac{\mu}{\rho D^3} t = \frac{1}{b} \cdot \frac{1}{\frac{\rho_0}{\rho} - 1} \left( 1 - a \sqrt{\frac{\rho_0}{\rho} - 1} \sqrt{\frac{g \rho^3 D^3}{\mu^2}} \right) \frac{\mu^2}{g \rho^3 D^3} \cdot \frac{l}{D} \quad (32)$$

or

$$t = \frac{A}{gD} (1 + B \sqrt{gD^3}) \quad (33)$$

in which  $A$  and  $B$  (both intrinsically positive) do not involve  $g$  at all, nor  $D$  except in a shape factor. The values of  $\frac{g}{t} \frac{\partial t}{\partial g}$  and  $\frac{D}{t} \frac{\partial t}{\partial D}$  found by differentiating (33) do satisfy (31).

3. *Effect of High Pressure on Accuracy of a Rolling-Ball Viscosimeter.*—Without knowing the empirical equation let it be required to predict the change in roll-time due to any small change in liquid density, such as would occur upon using the tube under pressure, by reference to an observation on the effect of changing the ball density. Since an expression for  $\frac{\partial t}{\partial \rho}$  in terms of  $\frac{\partial t}{\partial \rho_0}$  is sought,  $t$ ,  $\rho$ , and  $\rho_0$  are selected for  $Q_0$ ,  $Q_1$ , and  $Q_2$ , respectively. If (30) were to be used as it stands, there would be a restriction on the derivative  $\frac{\partial t}{\partial \rho}$ , which is hardly to be desired. An equivalent result in a more convenient form can evidently be obtained by confining  $\rho$  to a smaller number of arguments. This is done by replacing (30) by one of the alternative forms provided by the  $\pi$ -theorem, such as

$$\sqrt{-\frac{g^2}{D}} t = \text{funct.} \left( \frac{\rho_0}{\rho}, \frac{g \rho_0^3 D^3}{\mu^2}, \text{shape} \right) \quad (34)$$

Comparing this with (26),  $\alpha_0 = 0$ ,  $\beta_0 = 0$ ,  $\alpha = 1$ ,  $\beta = -1$ ; hence by (14)

$$\frac{\partial t}{\partial \rho} = -\frac{\rho_0}{\rho} \left( \frac{\partial t}{\partial \rho_0} \right)_{\mu \propto \rho_0} \quad (35)$$

or by (25)

$$\frac{\partial t}{\partial \rho} = -\frac{1}{\rho} \left( \rho_0 \frac{\partial t}{\partial \rho_0} + \mu \frac{\partial t}{\partial \mu} \right) \quad (36)$$

In the last transformation  $\mu$  took the part of  $Q_0$  and  $\rho_0$  of  $Q$ , while  $n$  had the value  $-1$ .

The following observations afford an experimental illustration of (36). They were made with a tube 59 cm long and 1 cm in diameter, containing a one-fourth inch (0.635 cm) ball, ordinarily of steel ( $\rho_0 = 7.7$  g/cm<sup>3</sup>). The tube was filled with lard oil ( $\mu = 0.74$  cgs units,  $\rho = 0.92$  g/cm<sup>3</sup>). The slope  $\frac{\partial t}{\partial \mu}$  was found to be 31 cgs units. Substituting now a brass ball ( $\rho_0 = 8.6$  g/cm<sup>3</sup>) for the steel one, the roll-time dropped from 27.9 to 24.7 seconds, making  $\frac{\partial t}{\partial \rho_0}$  equal to  $-3.6$  cgs units. From these data, in conjunction with (36), the value  $\frac{\partial t}{\partial \rho} = 5.2$  cgs units would be predicted. From (32), the actual value is found to be 5.7 cgs units. Since  $\frac{\partial t}{\partial \rho}$  is itself a correction term, the agreement is sufficient.

WASHINGTON, September 23, 1918.



---

PRICE, 5 CENTS.

Sold only by the Superintendent of Documents, Government Printing Office, Washington, D. C.

DEPARTMENT OF COMMERCE

# SCIENTIFIC PAPERS OF THE BUREAU OF STANDARDS

S. W. STRATTON, DIRECTOR

No. 331

## A RELATION CONNECTING THE DERIVATIVES OF PHYSICAL QUANTITIES

BY

MAYO D. HERSEY, Physicist

*Bureau of Standards*

ISSUED SEPTEMBER 25, 1919



PRICE, 5 CENTS

Sold only by the Superintendent of Documents, Government Printing Office  
Washington, D. C.

WASHINGTON  
GOVERNMENT PRINTING OFFICE  
1919



# A RELATION CONNECTING THE DERIVATIVES OF PHYSICAL QUANTITIES<sup>1</sup>

By Mayo D. Hersey

## CONTENTS

	Page
I. Introduction.....	21
1. Scope of the paper.....	21
2. Statement of the problem.....	22
3. Other classes of relations among derivatives.....	22
II. Theoretical discussion.....	23
1. Derivation of the new relation.....	23
2. Extension to higher derivatives.....	25
3. Integral form of the relation.....	25
4. Discussion of the constant-product restriction.....	26
III. Some illustrative examples.....	27
1. Variation of journal friction with size of bearing.....	27
2. Effect of gravity on a rolling-ball viscosimeter.....	28
3. Effect of high pressure on accuracy of a rolling-ball viscosimeter..	29

## I. INTRODUCTION

1. *Scope of the Paper.*—In this paper it is shown how the theory of dimensions may be used in a differential form; a procedure which appears fruitful particularly in investigating the effect of given sources of error on the performance of measuring instruments.

The examples which led to the necessity for developing this method are discussed at the end of the paper and illustrated by experimental data.

2. *Statement of the Problem.*—Given the fact that some relation of unknown form

$$Q_0 = f(Q_1, Q_2, \dots, Q_{N-1}) \quad (1)$$

subsists between  $N$  physical quantities  $Q_0, Q_1, Q_2, \dots, Q_{N-1}$ , no others being involved, it is required to deduce a relation of known form

$$\frac{\partial Q_0}{\partial Q_1} = F\left(\frac{\partial Q_0}{\partial Q_2}, Q_0, Q_1, Q_2, \dots, Q_{N-1}\right) \quad (2)$$

<sup>1</sup> This work was done at the Jefferson Physical Laboratory, Harvard University, in 1916, and presented as an interesting application of Buckingham's II theorem during a series of four lectures on Dimensional Reasoning given at the Friday evening conferences. It was first published in the *Journal Wash. Acad. Sci.*, 6, pp. 620-629, 1916, and is reprinted here to provide the mathematical basis for a forthcoming paper on the effect of temperature on bodies of constant shape.

## EVALUATION OF CONSTANTS

From the observations of the heating curve (observation numbers 8 to 19, inclusive) the following empirical equation was computed by the method of least squares:

$$\Delta L^* = 4.090(t + 142.5)10^{-6} + 0.00226(t + 142.5)^2 10^{-6}$$

where  $t$  is any temperature between  $-142$  and  $+305^\circ \text{C}$ .

The following table gives a comparison of the observed values with those computed from this empirical formula:

TABLE 2

Temperature in degrees centigrade	Observed $\Delta L^*$	Computed $\Delta L$	Residuals	Squares of residuals
-142.5	$0 \times 10^{-6}$	$0 \times 10^{-6}$	$0 \times 10^{-6}$	$0 \times 10^{-12}$
-123.1	76	80	-4	16
-77.2	249	277	-28	784
-24.4	502	515	-13	169
+18.7	713	718	-5	25
49.2	867	867	0	0
101.6	1146	1133	+13	169
151.0	1404	1395	9	81
198.6	1664	1658	6	36
249.1	1957	1948	9	81
305.2	2273	2284	-11	121
305.3	2280	2285	-5	25
				$1507 \times 10^{-12}$

The sum of the squares of the residuals is  $1507 \times 10^{-12}$  and hence

$r = 0.6745 \sqrt{\frac{1507 \times 10^{-12}}{12 - 2}} = \pm 8.3 \times 10^{-6}$  per unit length is the probable error of a single computed value if the observations be regarded as exact, or the probable error of an observation if the law expressed in the empirical formula be regarded as exact.

From a consideration of the performance of the apparatus it is believed that the maximum error of observation does not exceed  $\pm 5 \times 10^{-6}$ , and therefore the experimental probable error of a single observation is less than  $\pm 5 \times 10^{-6}$ . The authors are therefore led to believe that a part of the probable error,  $\pm 8.3 \times 10^{-6}$ , represents the amount by which the expansion fails to follow the quadratic law as expressed in the above equation.

The value obtained for the probable error is affected by the departure of the expansion curve from the parabolic law. That this departure exists is witnessed by the continuity of the signs of the residuals in Table 2.

\* $\Delta L$  represents the change per unit length from the length at the lowest temperature  $-142.5^\circ \text{C}$ . The values of Table 2 are obtained by adding 709.6 to observations 8 to 19 of Table 1.

Table 3 shows the deviations of the observed values (observation numbers 19 to 23, inclusive) of the cooling curve from this empirical equation representing the heating curve.

TABLE 3

Temperature in degrees centigrade	Observed $\Delta L^*$	Computed $\Delta L$	Deviations
305.3	$2280 \times 10^{-6}$	$2285 \times 10^{-6}$	$-5 \times 10^{-6}$
223.9	1805	1802	+3
141.5	1335	1344	-9
83.4	1046	1039	+7
22.4	732	736	-4

The average deviation of the cooling curve from the computed heating curve is  $\pm 5.6 \times 10^{-6}$ .

From inspection of the residuals in Table 2, it is apparent that the previous second degree equation does not satisfy with sufficient accuracy all the observations over the whole temperature range. It was found necessary to obtain two equations, one for the range from  $-142^\circ$  to room temperature and another for the range above room temperature.

The following equation, computed from observation numbers 1 to 12, inclusive,

$$\Delta L^* = 3.522(t + 142.5)10^{-6} + 0.00570(t + 142.5)^2 10^{-6}$$

satisfies the observations below room temperature. A comparison of all the observed values below room temperature with those computed from this equation is given in the following table:

TABLE 4

Temperature in degrees centigrade	Observed $\Delta L^*$	Computed $\Delta L$	Residuals
17.8	$710 \times 10^{-6}$	$711 \times 10^{-6}$	$-1 \times 10^{-6}$
17.8	711	711	0
0.2	621	619	+2
-23.5	502	500	+2
-50.0	373	375	-2
-75.2	259	263	-4
-99.8	162	161	+1
-142.5	0	0	0
-123.1	76	70	+6
-77.2	249	254	-5
-24.4	502	495	+7
+18.7	713	716	-3

\* $\Delta L$  represents the change per unit length from the length at the temperature  $-142.5^\circ \text{C}$ .

The probable error of a single observation is  $\pm 2.6 \times 10^{-6}$ .

From the observations of the heating curve (room temperature to  $+305^{\circ}\text{C}$ ), the following empirical equation was computed:

$$\Delta L^* = 5.088(t - 18.7)10^{-6} + 0.00126(t - 18.7)^2 10^{-6}$$

where  $t$  is any temperature between 19 and  $305^{\circ}\text{C}$ .

The following table gives a comparison of the observed values with those computed from this empirical formula:

TABLE 5

Temperature in degrees centigrade	Observed $\Delta L^*$	Computed $\Delta L$	Residuals
18.7	$0 \times 10^{-6}$	$0 \times 10^{-6}$	$0 \times 10^{-6}$
49.2	154	156	-2
101.6	432	430	+2
151.0	691	695	-4
198.6	951	956	-5
249.1	1243	1239	+4
305.2	1560	1561	-1
305.3	1566	1562	+4

The probable error of a single observation is  $\pm 2.5 \times 10^{-6}$ .

Table 6 shows the deviations of the observed values (observation numbers 19 to 23, inclusive) of the cooling curve from this empirical equation representing the heating curve.

TABLE 6

Temperature in degrees centigrade	Observed $\Delta L^*$	Computed $\Delta L$	Deviations
305.3	$1566 \times 10^{-6}$	$1562 \times 10^{-6}$	$+4 \times 10^{-6}$
223.9	1091	1097	-6
141.5	622	644	-22
83.4	332	334	-2
22.4	18	19	-1

The average deviation of the cooling curve from the computed heating curve is  $7.0 \times 10^{-6}$ . From these deviations it is apparent that the cooling curve lies slightly below the heating curve.

The two equations of expansion expressed in terms of  $L_0$ , the length of the material at  $0^{\circ}\text{C}$ , are

$$L_t = L_0(1 + 5.15t \times 10^{-6} + 0.00570t^2 \times 10^{-6}) \text{ and}$$

$$L_t = L_0(1 + 5.04t \times 10^{-6} + 0.00126t^2 \times 10^{-6})$$

where  $L_t$  is the length of the specimen at any temperature  $t$  within the proper range; in the first case 19 to  $-142^{\circ}\text{C}$  and in the second case 19 to  $+305^{\circ}\text{C}$ .

\*  $\Delta L$  represents the change per unit length from the length at the temperature  $18.7^{\circ}\text{C}$ .



## RESULTS OF TEST 2

Several days later observations were taken from room temperature to 304°C. The results obtained on the second test of the same specimen are shown in Table 7 and Fig. 2.

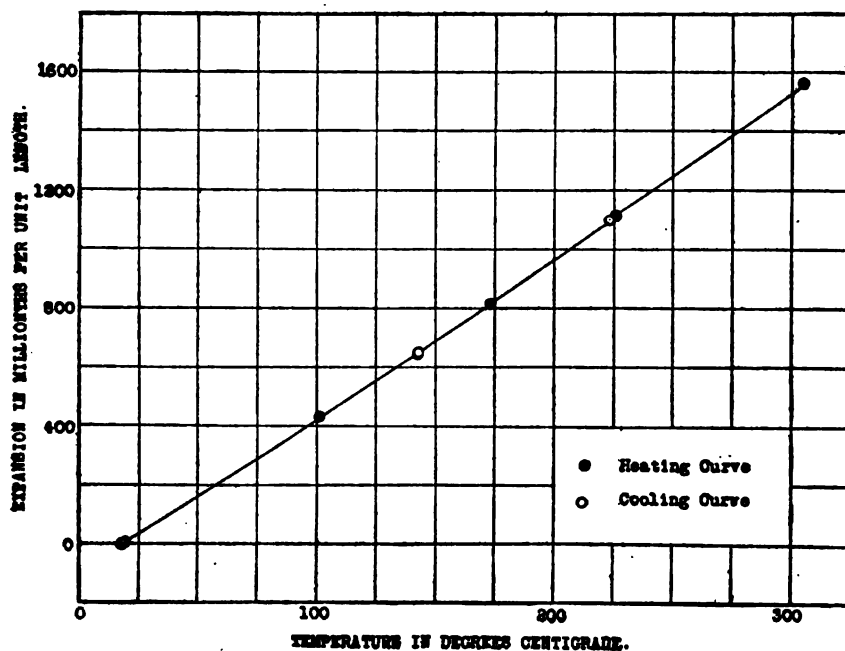


FIG. 2.—Linear expansion of molybdenum as a function of temperature (Test 2, Table 7)

TABLE 7

Observation number	Date	Time	Temperature	$\Delta L$ *
	1917		° C	
1-a	Oct. 22	10.19 a. m.	18.0	$0 \times 10^{-3}$
2-a	Oct. 22	11.15 a. m.	101.9	430
3-a	Oct. 22	11.51 a. m.	173.2	816
4-a	Oct. 22	12.35 p. m.	225.8	1115
5-a	Oct. 22	1.42 p. m.	304.5	1565
6-a	Oct. 22	2.43 p. m.	223.2	1099
7-a	Oct. 22	3.35 p. m.	143.1	648
8-a	Oct. 22	3.53 p. m.	142.8	643
9-a	Oct. 23	10.46 a. m.	19.8	4

\*  $\Delta L$  represents the change per unit length from the length at the initial temperature 18° C.

## EVALUATION OF CONSTANTS

From the observations (numbers 1-a to 5-a, inclusive) of the heating curve the following empirical equation was computed by the method of least squares:

$$\Delta L = 5.038(t - 18.0)10^{-6} + 0.00149(t - 18.0)^2 10^{-6}$$

where  $\Delta L$  is the same as in the previous table, and  $t$  is any temperature between 18 and 304° C.

The following table gives a comparison of the observed values with those computed from this empirical formula:

TABLE 8

Temperature in degrees centigrade	Observed $\Delta L^*$	Computed $\Delta L$	Residuals
18.0	$0 \times 10^{-6}$	$0 \times 10^{-6}$	$0 \times 10^{-6}$
101.3	430	430	0
173.2	816	818	-2
225.8	1115	1111	+4
304.5	1565	1566	-1

The probable error of a single observation is  $\pm 1.8 \times 10^{-6}$ .

Table 9 gives a comparison of the observed values (observation numbers 5-a to 9-a, inclusive) of the cooling curve with those computed from this same empirical formula for the heating curve.

TABLE 9

Temperature in degrees centigrade	Observed $\Delta L^*$	Computed $\Delta L$	Deviations
304.5	$1565 \times 10^{-6}$	$1566 \times 10^{-6}$	$-1 \times 10^{-6}$
223.2	1099	1097	+2
143.1	648	654	-6
142.8	643	652	-9
19.8	4	9	-5

The average deviation of the cooling curve from the computed heating curve is  $4.6 \times 10^{-6}$  per unit length.

On the second heating the length at any temperature between 18 and 304° C may be represented by the following empirical equation:

$$L_t = L_0(1 + 4.98t \times 10^{-6} + 0.00149t^2 \times 10^{-6})$$

---

\* $\Delta L$  represents the change per unit length from the length at the initial temperature 18° C.

## COMPARISON OF TESTS

From the observations of the two tests two quadratic equations were obtained which satisfy the observations above room temperature. These equations are

$$L_t = L_0(1 + 5.04t \times 10^{-6} + 0.00126t^2 \times 10^{-6}). \text{ First test.}$$

$$L_t = L_0(1 + 4.98t \times 10^{-6} + 0.00149t^2 \times 10^{-6}). \text{ Second test.}$$

A comparison of these equations will show a very close agreement. The coefficient of  $t$  in the first equation is slightly larger than that in the second equation, but the reverse is true of the coefficient of  $t^2$ . The lengths determined from these equations do not differ by more than  $4 \times 10^{-6}$  per unit length. Since this approaches the limit of accuracy of the apparatus, the following average equation

$$L_t = L_0(1 + 5.01t \times 10^{-6} + 0.00138t^2 \times 10^{-6})$$

is given as the most probable second-degree equation for the expansion of this specimen of molybdenum from room temperature to  $305^\circ \text{C}$ .

The instantaneous coefficients computed for every  $50^\circ$  from  $-100$  to  $+300^\circ \text{C}$  are given in the following table. The instantaneous coefficient or rate of expansion at any temperature is the tangent to the expansion curve at that temperature.

TABLE 10

Temperature in degrees centigrade	Instantaneous coefficients
-100	$4.0 \times 10^{-6}$
- 50	4.6
0	5.1
+ 50	5.1
100	5.3
150	5.4
200	5.6
250	5.7
300	5.8

The work is being continued to secure values over a greater temperature range.

## SUMMARY

1. The thermal expansion of molybdenum has been determined between  $-142$  and  $+305^\circ \text{C}$ .
2. It is impossible to secure a second-degree equation which adequately represents the behavior of the material throughout this temperature range.

3. The most probable equation applicable between  $-142$  and  $+19^{\circ}\text{C}$  is

$$L_t = L_0(1 + 5.15t \times 10^{-6} + 0.00570t^2 \times 10^{-6})$$

4. The most probable equation applicable between  $19$  and  $+305^{\circ}\text{C}$  is

$$L_t = L_0(1 + 5.01t \times 10^{-6} + 0.00138t^2 \times 10^{-6})$$

5. The instantaneous coefficient or rate of expansion increases with temperature.

We are greatly indebted to Roger W. Eisinger for his aid in the computations; also to Dr. W. H. Souder for his valuable suggestions.

WASHINGTON, JUNE 17, 1918.

---

ADDITIONAL COPIES  
OF THIS PUBLICATION MAY BE PROCURED FROM  
THE SUPERINTENDENT OF DOCUMENTS  
GOVERNMENT PRINTING OFFICE  
WASHINGTON, D. C.  
AT  
5 CENTS PER COPY  
V

DEPARTMENT OF COMMERCE  
BUREAU OF STANDARDS

S. W. STRATTON, Director

SCIENTIFIC PAPERS OF THE BUREAU OF STANDARDS, No. 333

[Issued March 20, 1919]

OPTICAL CONDITIONS ACCOMPANYING THE STRIAE  
WHICH APPEAR AS IMPERFECTIONS IN OPTICAL  
GLASS

By Lieut. Commander A. A. Michelson, U. S. N., R. F.

Striae in optical glass may conveniently be divided into two classes: First, those which appear under proper conditions as isolated bright streaks on a dark background and, second, those in which such bright streaks are very numerous and run into one another, forming bright but irregularly continuous bands.

Even a superficial examination of the two kinds shows that the optical qualities of the former type are practically unaffected by the striae, while the latter specimens are *in general* unfitted for use in optical instruments.

For the investigation of the former class a specimen containing a single approximately plane and very narrow stria—resembling a crack in the glass—was ground and polished so that the stria was approximately perpendicular to the polished plane parallel surfaces.

This specimen shows "total reflection" at the stria when the "grazing" angle is sufficiently small (from zero to about 20 degrees) and equally on either surface of the stria.

At greater angles there is an abrupt drop in the intensity to nearly zero.

If it be admitted that these peculiarities are caused by a layer of smaller index of refraction than the remaining portion of the specimen, the maximum change in index may be readily calculated from the "grazing angle." This was found to be from  $3^{\circ}$  to  $6^{\circ}$  for this specimen (corresponding to an exterior angle of  $4.5^{\circ}$  to  $9^{\circ}$ ). From this it follows that the ratio of indices is approximately from 0.995 to 0.9975, or the difference in refractive index at the stria is from 0.005 to 0.0025.

(It may be noted that if the stria was in reality a crack, which it so strongly resembles, the exterior grazing angle should be so

large that total reflection under the conditions of the experiment would occur at all incidences.)

Again if the intensities be plotted with  $\frac{\partial n}{n} = -0.005$  and  $\frac{\partial n}{n} = +0.005$ , the corresponding graphs drawn in the figure show

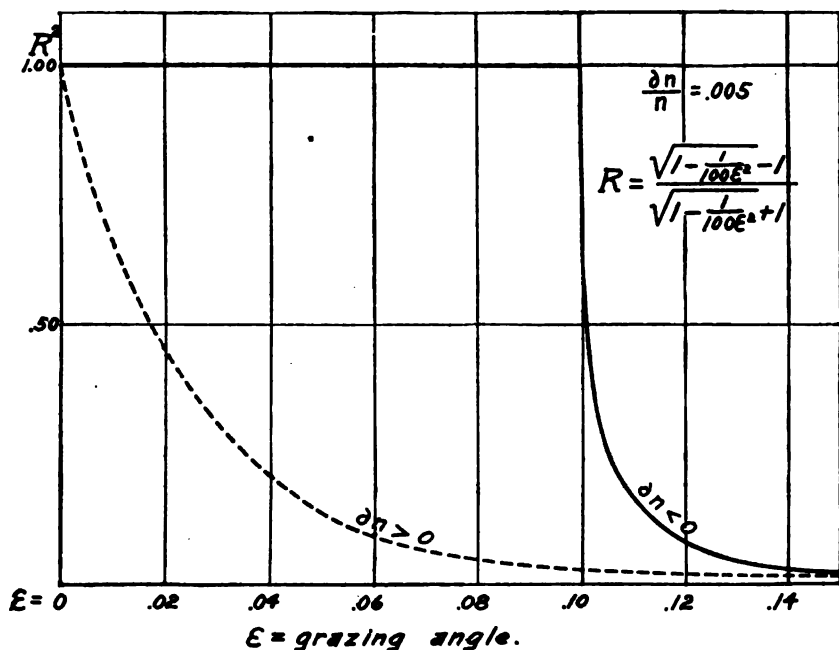


FIG. 1

in the former case (smaller index at stria)  $\delta$  the sudden drop in intensity at "grazing angle"  $\epsilon = 0.1$ , while in the other case (larger index at stria) there is a steady diminution from  $\epsilon = 0$  to  $\epsilon = 90^\circ$ .

This shows conclusively that this stria is caused by a film of smaller index of refraction than the remainder of the glass.

It was hoped that the following experiment would give the law of change of index as the stria is approached from either side:

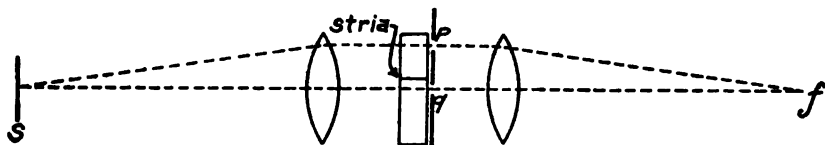


FIG. 2

The image of a tungsten filament was concentrated on the slit  $s$  of a collimator, and the parallel rays fell on the specimen. Thence two pencils passed through the apertures  $p$  and  $q$  in a screen to the

objective of the observing telescope at the focus of which at  $f$ , interference fringes are observed. The position of these was noted as the aperture  $q$  was moved past the stria, and careful observation showed no appreciable movement of the fringes until the aperture was exactly over the stria, when the fringes disappeared.

A motion of one-tenth the distance between the fringes is clearly measurable, and with a thickness of the specimen corresponding to 16 000 light waves it follows from the formula

$$\partial N = \frac{t}{\lambda}(n_1 - n_2) < 0.1$$

$$n_1 - n_2 < \frac{1}{160\,000}$$

which shows that, within the limit of errors of observation, there is no change in index of refraction until the stria itself is reached.

The thickness of the stria was found to be something less than a fourth of a millimeter. In order to get a somewhat more accurate estimate, however, another specimen was cut with a face inclined at an angle of about  $1/30$  to the plane of the stria. The total reflection at  $K$  gave an edge whose width was of the order

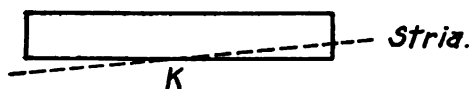


FIG. 3

of  $1/4$  mm or less, so that the corresponding width of the stria must have been less than  $1/120$  mm.

A still more convincing confirmation of the preceding results is furnished by the following interferometer test:

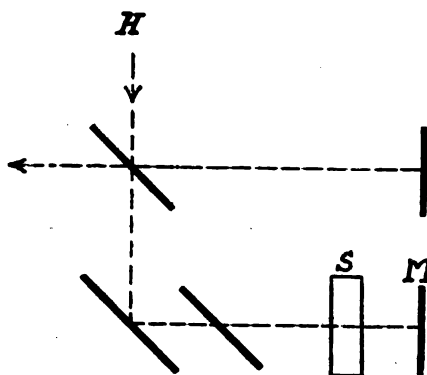


FIG. 4

The interferometer arranged as shown diagrammatically in the figure receives light from a helium tube  $H$ , which traverses in one of the branches the specimen  $S$ , containing the vertical stria.

The interference fringes are arranged to appear as horizontal bands coinciding with the surface of the mirror  $M$ . These appear entirely straight, except at the stria, where they merge abruptly into the narrow dark line which is formed by the projection of the stria.

If the specimen be inclined so that the exterior angle of incidence is  $i_0$ , it may be shown that  $\Delta = \frac{2t}{\lambda} \left[ 1 - \sqrt{1 - \frac{2n\partial n}{\sin^2 i_0}} \right]$  in which  $n$  is the index of refraction of the glass and  $\partial n$  the excess of this index over that of the stria.

For values of  $i_0$  not too small  $\Delta = \frac{2t}{\lambda} \frac{n\partial n}{\sin^2 i_0}$

The limiting value for real values of  $\Delta$  is given by  $\sin^2 i_0 = 2n\partial n$  and as this is approximately  $\sin i = 0.05$  the corresponding value of  $2n\partial n$  is 0.0025 whence  $\Delta = \frac{2t \cdot 0.0025}{\lambda \sin^2 i_0}$

Taking a moderate value of  $i_0$ , say, corresponding to  $\sin i_0 = 0.2$  the corresponding observed value of  $\Delta$  is 0.45, which gives  $t = 18\lambda$  which corresponds to a thickness of about one one-hundredth of a millimeter.

It results from the foregoing that isolated striae are of no more importance than are the bubbles found in some of the best telescope objectives.

In the case of striae of the second class this is not true in general, so that it is not desirable to attempt to utilize such glass for optical purposes where a high resolving power is required.

Nevertheless, it is important to add that for many purposes, such as for binoculars, gun-sight telescopes, periscopes, etc., such glass may give excellent results if the planes of striation are *perpendicular to the line of sight*.<sup>1</sup> Such glass should not be used for prisms.

In this report there is no attempt to account for the presence of striae of either class, but with all due reserve it may be surmised that they are possibly due to different causes, the former (single isolated striae) possibly resulting from material of different

<sup>1</sup> A specimen of glass exceptionally badly striated when viewed end on was placed between collimator and observing telescope of the spectroscope (aperture 2'') which gives admirable definition. When the specimen was introduced with the striations perpendicular to the line of sight, no deterioration of the definition was observed. Hence a lens of such glass would perform quite as well as if the striation were not present.



index (which may be melted from the stirrer itself or from other material which follows the stirrer). The second class of striae are more likely due to variations in the mass of the material and have no immediate connection with the stirrer.

In the absence of knowledge of the technique of glass production it would be presumptuous to hazard advice concerning the possibility of eliminating striae. But it seems clear that original homogeneity of materials and as high a temperature as the material will bear are desirable.

WASHINGTON, November, 1918.











DEPARTMENT OF COMMERCE

---

# SCIENTIFIC PAPERS

OF THE

# BUREAU OF STANDARDS

S. W. STRATTON, DIRECTOR

---

No. 334

NEW FORMS OF INSTRUMENTS FOR SHOWING THE  
PRESENCE AND AMOUNT OF COMBUSTIBLE GAS  
IN THE AIR

BY

E. R. WEAVER, Associate Chemist

and

E. E. WEIBEL, Associate Physicist

*Bureau of Standards*

---

ISSUED JUNE 23, 1919



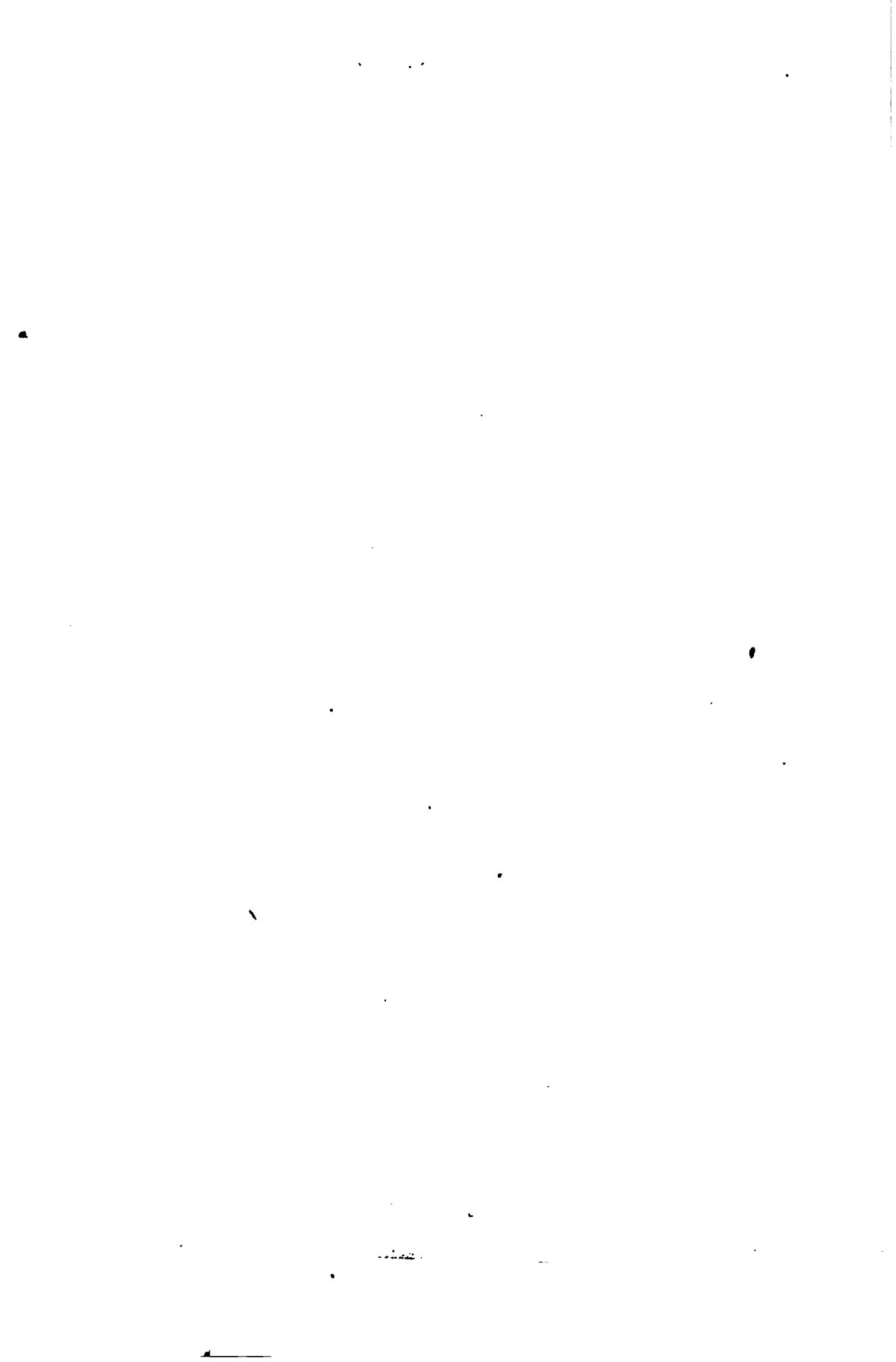
PRICE, 15 CENTS

Sold only by the Superintendent of Documents, Government Printing Office  
Washington, D. C.

---

WASHINGTON  
GOVERNMENT PRINTING OFFICE

1919





# NEW FORMS OF INSTRUMENTS FOR SHOWING THE PRESENCE AND AMOUNT OF COMBUSTIBLE GAS IN THE AIR

By E. R. Weaver and E. E. Weibel

## CONTENTS

	Page
Introduction.....	47
I. General description of instruments.....	48
1. Principles of operation of new devices.....	48
2. Compensated-bridge indicator.....	49
3. Glowing-wire indicator.....	51
4. Bimetallic detector.....	52
II. Investigation of principles involved.....	53
1. Combustion at the surface of a heated wire.....	53
(a) Purpose and methods of experiments.....	53
(b) Results of experiments.....	58
2. Compensated bridge indicator.....	64
(a) Principles.....	64
(b) Design of parts.....	69
(c) Description and tests.....	72
3. Glowing-wire indicator.....	77
4. Bimetallic detector.....	78
III. Specifications for the construction and calibration of instruments.....	81
1. Compensated bridge indicator.....	81
(a) Construction of apparatus.....	81
2. Glowing-wire indicator.....	88
3. Bimetallic detector.....	89

## INTRODUCTION

The detection and automatic indication of the presence of combustible gases in the air is a problem of great importance in many industries both for controlling certain processes and for safeguarding life and property wherever there is danger of fire or explosions due to the presence of such mixtures. In the spring of 1916, an investigation of some of the forms of gas detectors in use was begun by the Bureau of Standards.

None of the existing forms of apparatus was found suitable for all purposes, and the investigation has led to the design of several new forms which are more reliable than the old ones or better adapted to certain specific uses. These new forms of ap-

paratus are the subject of the present paper. The experimental work described was completed about April 1, 1917, but for various reasons it has not been published until the present time.

A paper describing the older forms of detectors, at least in principle, and some of the experimental work done upon them, is in preparation.

After the work on the compensated bridge indicator was completed a United States patent was granted to Messrs. Philip and Steele<sup>1</sup> covering many of the features of this type of instrument as developed at the Bureau of Standards. The date of application for their patent shows that Messrs. Philip and Steele's work far antedates our own. The forms of the two instruments, the conditions under which they were designed to be used, and the methods of using them are so different, however, that a description of the Bureau of Standards form of instrument seems well worth while. In addition, the large amount of experimental work relating to gaseous combustion at the surface of heated wires is of general application to any instrument depending for its action upon this phenomenon.

For convenience the report on this work has been divided into the following parts:

Section I contains a brief description of the new devices, the principles upon which they operate, the results of tests showing their accuracy and reliability, and a brief discussion of their application.

Section II is a detailed account of the theory involved in the design of the instruments and of the experimental work concerned with the features of design, together with a description of the tests to which the completed instruments have been subjected.

Section III contains drawings and specifications for the construction and installation of the instruments and accessory apparatus.

## I. GENERAL DESCRIPTION OF INSTRUMENTS

### 1. PRINCIPLES OF OPERATION OF NEW DEVICES

All of the new devices described in this paper depend upon the combustion at the surface of an electrically heated platinum wire of the gas contained in the surrounding atmosphere. This surface combustion takes place at a temperature much below the normal ignition temperature of the gas in air or at the surface of another

---

<sup>1</sup> U. S. Patent No. 1224321, May 1, 1917.

material which does not exert a catalytic effect. The resulting rise in temperature of the wire depends upon the quantity of the combustible gas which is present. The measurement of temperature rise is made in various ways, each of which is better suited to certain particular purposes than is any of the others. For some purposes an indicator is required—i. e., an instrument which will indicate, either continuously or when desired, the amount of the combustible gas present. For other purposes only a detector is required—i. e., an instrument which sounds an alarm or otherwise shows the presence of a dangerous amount of the combustible gas. The following devices which have been developed are suited to various uses:

1. The "compensated bridge indicator," depending for its operation upon the change in electrical resistance of the wire, gives a continuous indication of the amount of combustible gas at the point at which the resistance element, called the "detector bridge," is placed. When the percentage of gas reaches a predetermined limit, a circuit is closed, actuating an alarm or other protective device.

2. The "glowing-wire indicator" is a portable device with which an observer may quickly determine the amount of combustible gas at any accessible place. This is done by adjusting the current through an active wire to such a value that the wire just shows a visible glow. The current required decreases with increase in the amount of gas present.

3. The "bimetallic detector" is an automatic device in which the heat of combustion of the gas at the surface of the wire causes the bending of an adjacent bimetallic strip, which in turn closes an alarm circuit.

## 2. COMPENSATED BRIDGE INDICATOR

*Description.*—The resistance element or detector bridge of the compensated bridge indicator consists of a balanced Wheatstone bridge made up of four platinum wires, two of which, on opposite sides of the bridge, are rendered inactive by a thin coating of some substance which does not readily cause surface combustion. The bridge wires are heated by an electrical current to a temperature high enough to cause combustion of the gas at the surface of the uncoated or "active" wires. When no combustible gas is present, the active and inactive wires are about equally affected by changes of electrical current, room temperature, and air currents. Consequently, the bridge remains balanced in spite of

changes in surrounding conditions; but in the presence of a combustible gas combustion takes place at the surface of the active wires, increasing their temperature and resistance, while no change occurs in the inactive wires. Consequently, the bridge becomes unbalanced by an amount depending upon the quantity of combustible gas present. A voltmeter with scale graduated to show the percentage of the combustible gas to be indicated (e. g., hydrogen in electrolytic oxygen or carbon monoxide about gas producers) is connected across the bridge and serves to show at all times the percentage of gas present. A contact-making attachment causes an alarm to ring when the amount of gas reaches the limit for which the contact has been set. A diagram of a compensated bridge indicator is given in Fig. 17.

*Tests.*—Several instruments of this type have been made and tested at the Bureau of Standards. The indicators show smaller changes in hydrogen concentration than can be detected by ordinary volumetric analysis, but their operation over a long period of time usually results in a change of balance which makes it necessary to rebalance. The absolute accuracy of the readings can not, of course, be greater at any time than the volumetric analyses by which the instruments were calibrated. The tests upon one instrument, which was in constant use for several months in a battery compartment, show that the instrument is capable of giving good results over a considerable period of time if operated under the most favorable conditions. These conditions include the maintenance of a constant current, freedom from excessive vibration, and the requirement that the instrument be not exposed to a high concentration of combustible gas for a very long period of time. All of these requirements depend upon the low elastic limit of platinum at high temperatures and the consequent slow stretching of the wires, even under their own weight.

The suitability of the instrument for indicating methane is doubtful on account of the high temperature required. For a short period of time, it will give reliable indications of this gas; but it is improbable that permanent changes in the wires at so high a temperature could be long avoided.

*Application.*—The device is suited to the continuous indication of the presence of hydrogen, carbon monoxide, illuminating gas, methane, and the vapors of some combustible liquids in air. It is especially suitable for use in determining the composition of gas in inaccessible places and for indicating at some central station the condition of the atmosphere in all parts of an industrial plant.

*Merits of the Compensated Bridge Indicator.*—The experience with the apparatus up to the present time apparently fully justifies the following statements as to the merits of the compensated bridge indicator:

1. The apparatus is of simple construction, readily made up from ordinary materials by any competent instrument maker.
2. The detector bridge can be made small, and, since it requires no attention, can be located at any desired point even though somewhat inaccessible.
3. The indicating instrument can be located at a distance from the resistance element and the alarm, if desired, at a distance from either.
4. The apparatus requires little attention in operation.
5. No supplies are required except direct current of the voltage ordinarily used on lighting circuits. The apparatus is readily adapted for use on a circuit of any voltage above 5 volts.
6. The usual variation of the voltage of the electrical supply does not affect materially the operation of the instrument unless excessively high or low voltages are long continued.
7. The apparatus, when once properly calibrated, will indicate changes of concentration of hydrogen smaller than can be detected by the methods of gas analysis commonly used in commercial practice.
8. The apparatus operates an alarm at any desired percentage of combustible gas.
9. The indications of the apparatus are not affected by changes in temperature at the point of location of the detector bridge.
10. The apparatus responds promptly to changes in the amount of combustible gas present, for the time lag is not more than 10 seconds for a properly constructed instrument.
11. The most important and delicate parts of the apparatus are made of some of the materials most resistant to chemical action, namely, platinum and glass.
12. The initial cost of construction of the apparatus is not great, the most expensive part being a voltmeter of ordinary commercial form.

### 3. GLOWING-WIRE INDICATOR

The glowing-wire indicator consists of two short lengths of fine platinum wire, the currents through which are supplied by a dry battery and controlled by two small rheostats. A wiring diagram is shown in Fig. 21. The whole is arranged in a convenient

form for carrying in the hand or the pocket. One wire is active; the other inactive. By adjusting the two rheostats the two wires may be made to glow with the same intensity. One rheostat determines the ratio of the currents in the wires which changes with percentage of gas present. This rheostat can therefore be graduated to read percentage directly. The other rheostat serves to regulate the total current through both wires. This device is practically independent of the illumination at the place of use and entirely independent of the voltage of the battery used.

The glowing-wire indicator is, of course, designed for the purpose of directly observing the atmospheric condition at a point at which no permanent detector is located. It should be of value in looking for leaks in gas mains and examining spaces, such as coal bunkers, or gas-making machinery opened for repairs in which the presence of a dangerous amount of combustible gas is suspected.

The apparatus is considerably more complicated and somewhat more expensive than the detecting bridge of the bridge indicator, but no additional electrical instrument or alarm is required, and the apparatus as a whole should not cost more than one-half as much as a complete bridge indicator.

#### 4. BIMETALLIC DETECTOR

The bimetallic detector, which is intended only to actuate an alarm or other mechanism when the amount of combustible gas in the atmosphere reaches the limit for which the device is set, is a simple and inexpensive instrument, the principle of which was first used by Alderson and Holmes,<sup>2</sup> who specify a detector substantially like the one designed at this Bureau. The Bureau instrument consists of two bimetallic strips with one end of each rigidly fixed to an insulating support. A millimeter or two below the strips are stretched platinum wires, one active, the other inactive, which serve to heat the bimetallic strips. When equally heated these strips bend equally, but when unequally heated they indicate by a relative movement of their free ends the difference in temperature.

The platinum wires are connected in series to any convenient source of electrical current, direct or alternating. The free ends of the bimetallic strips bear contact points which, when the strips come together, short circuit the platinum wires through an alarm, as is shown by the wiring diagram in Fig. 16. In an atmosphere

---

<sup>2</sup> British Patent No. 24371 of 1909.

free from combustible gas the two bimetallic strips are equally heated by the currents through the platinum wires and bend alike whatever the amount of heat from the electrical current or other source which affects the two strips alike. But in the presence of a combustible gas, combustion at the surface of the active wire causes the adjacent strip to be heated to a higher temperature. This results in a movement of this strip which closes the alarm circuit if gas is present in excess of the predetermined quantity for which the apparatus is set. One of the contacts is adjustable, permitting the instrument to be set for various percentages of combustible gas.

The device has been tried out and found to operate satisfactorily. It may be made very sensitive to the presence of a combustible gas. The instrument tried out at the Bureau could be readily adjusted to sound the alarm at less than 0.1 per cent of hydrogen.

The bimetallic detector is especially adapted for use in any place in which a sensitive device for alarm only is desired. It can be located wherever the detector bridge of a bridge indicator could be placed, and its low cost makes it available for use in many positions in which the cost of installing a bridge indicator would not be justified. The instrument may be made small, the one constructed at this Bureau having the dimensions 3 by 5 by 10 centimeters, equal to about  $1\frac{1}{4}$  inches by 2 inches by 4 inches. It is even less subject than the bridge indicator to drafts, changes of current, and other possible disturbing influences. The fact that it will use alternating as well as direct current makes the instrument available for use on any power supply.

## II. INVESTIGATION OF PRINCIPLES INVOLVED

### 1. COMBUSTION AT THE SURFACE OF A HEATED WIRE

#### (a) PURPOSE AND METHODS OF EXPERIMENTS

In order to design intelligently any of the instruments described in the first part of this paper, it was necessary to determine with some accuracy the most suitable materials for the active and inactive wires; the temperature required to cause combustion at the surface of the active wire; the relations between the resistance, temperature, current, diameter, length, and arrangement of wires in the apparatus; and the amount of heat produced by combustion in atmospheres containing various amounts of combustible gas with each arrangement.

*Methods of Study.*—Owing to the large number and variety of experiments made upon combustion at the surface of heated wires, it would be confusing to endeavor to present all the methods employed independently of a discussion of the immediate objects of the experiments and the results obtained. The basic experiments should be, however, briefly described before giving in detail the results obtained. Wires of various materials and sizes were heated electrically in air and in various gas mixtures. In each experiment the heating current,  $I$ , and the resistance,  $R$ , of the wires were measured. The mean temperatures,  $t$ , of the platinum

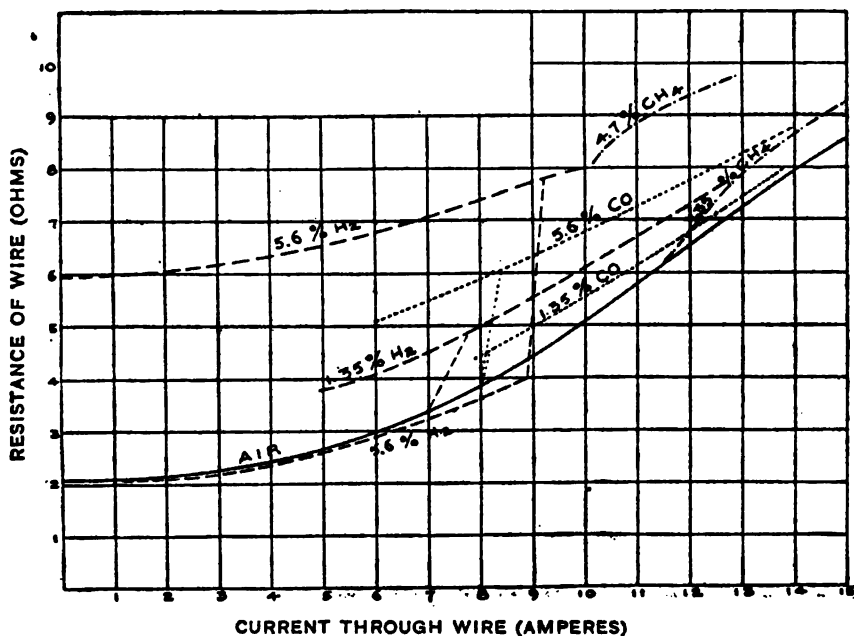


FIG. 1.—Representative observations of combustion at the surface of a heated wire

wires were determined from their resistance by using the known relation between temperature and resistance  $R = R_0(1 + At - Bt^2)$ . In the few cases when it was necessary to know the temperatures of wires of other metals, these were determined approximately by assuming the temperature equal to that of a platinum wire of the same diameter heated by the same amount of power. The rate of dissipation of energy from the wire was, of course, equal to the sum of the input of electrical power,  $RI^2$ , and the rate of production of heat by combustion, called  $H$ . If we assume that the rate of dissipation of energy from the wire was independent of small changes in the composition of the surrounding atmosphere, then



the difference in electrical power input required to maintain the wire at the temperature  $t$  with and without combustion taking place is equal to the power input from combustion,  $H$ .

A group of characteristic curves representing the observation upon a particular wire is given in Fig. 1, while Table 1 presents the numerical data for one gas mixture, together with some of the quantities of interest which are computed from the observation. The discontinuity of the curves in Fig. 1 is caused by the fact that the wire may be heated by a fairly large current without combustion taking place, but when combustion is once started it will continue in some cases even when the current is reduced to zero. The application of the results of these experiments to the problems of design will appear when the results are described in detail.

TABLE 1.—Representative Data on Combustion of Carbon Monoxide at the Surface of a Platinum Wire 0.097 mm in Diameter and 14 cm long (amount of carbon monoxide in air entering bottle 5.6 per cent)

Current observed, $I$	Resistance observed, $R$	Electrical power, $RI^2$	Temperature, $t$	Heat loss in air, $L$	Power from combustion, $L - RI^2$
Amperes	Ohms	Watts	°C	Watts	Watts
0.5	2.67	0.67	115	0.67	0.00
0.6	5.09	1.83	526	5.09	3.26
0.7	5.47	2.68	596	6.07	3.39
0.8	5.88	3.76	669	7.20	3.44
0.9	6.31	5.11	750	8.60	3.49
1.0	6.78	6.78	840	10.20	3.42
1.1	7.28	8.22	950	12.19	3.37
1.2	7.79	11.22	1065	15.76	4.54
1.3	8.28	14.00	1182	17.58	3.58
1.4	8.79	17.23	1313	21.04	3.81

*Apparatus Used.*—The apparatus used in the experiments just outlined is shown diagrammatically in Fig. 2. The test wire was placed in a bottle 28 cm in diameter and 40 cm high. It was connected by copper leads about 4 mm in diameter to the standard resistances connected to form a Wheatstone bridge as shown. A steady stream of gas of constant composition was passed through the test chamber. A gas mixture of constant composition was obtained by gearing together two calibrated wet meters, one of which measured the air, the other the combustible gas, and passing the mixture from the meters into a mixing bottle to reduce fluctuations in composition. The composition of the mixture entering the test bottle was checked from time to time by gas analysis. When suitable precautions were used, this method was found quite

satisfactory, the composition of the mixture remaining very constant and agreeing well with the values calculated from the meter calibrations. In the final experiments, samples of gas were also taken through a capillary tube from a point very near the wires. Gas analyses were made by an ordinary combustion method, using a 100 cc burette graduated to 0.1 cc and a Levy combustion capillary of fused quartz containing a glowing platinum wire.

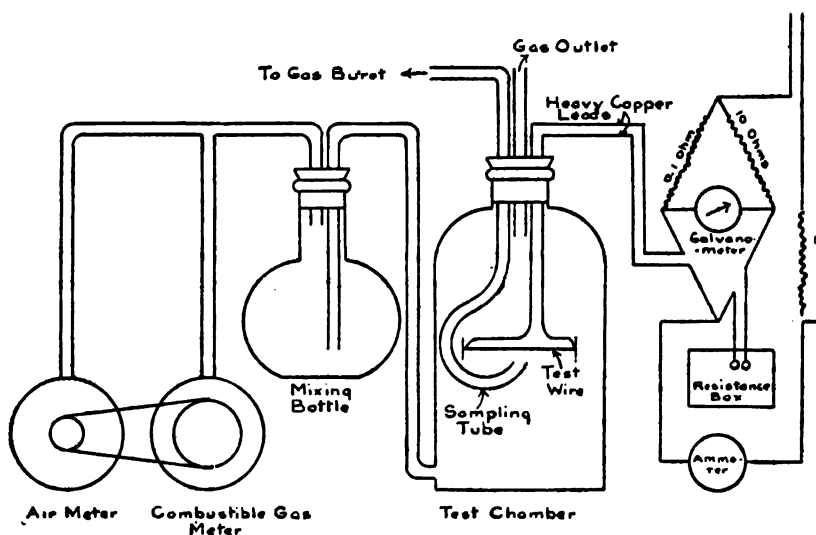


FIG. 2.—Apparatus for determining combustion at the surface of heated wires

*Wires Used in Investigation.*—Table 2 gives the sizes and some of the constants of the wires used in this investigation.

TABLE 2

Designation	Material	Diameter in millimeters	Resistivity at 0° C, microhm per cm <sup>2</sup>	Temperature coefficients		Remarks
				A	B	
A.....	Platinum.....	0.012	11.6	0.0036	0.0000058	Wollaston wire.
B.....	do.....	.053	13.8	.00278	.0000058	Commercial wire.
C.....	do.....	.097	10.35	.00367	.0000058	
D.....	do.....	.226	9.8	.00382	.0000058	
	Palladium.....	.226	11.1			
	Gold.....	.226	2.15			
	Silver.....	.226	1.52			
	Nickel.....	.226	10.0			

*Accuracy of Observations.*—The accuracy of the standard resistances and the sensitiveness of the galvanometer used were greater than the general accuracy demanded in the investigation. The

resistances of the leads were measured and taken into account whenever of any importance, but in most of the experiments this correction was entirely negligible. The currents used were never large enough to cause appreciable errors due to the heating of the measuring resistances. The only appreciable source of error in the electrical measurements was in the observation of the current. Several instruments of standard make and appropriate range were used for this purpose in the different experiments, and corrections were always made for the portion of the current, seldom more than 1 per cent, which passed through the ammeter but not through the test wire. When different ammeters were used for experiments made under the same conditions, the corrected results were always concordant.

Without doubt the most important source of error was that involved in determining the amount of combustible gas present. It was the object of the experiments to determine how much power from combustion was available for the detection of the combustible gases. It would have been desirable to reproduce the conditions which would exist if a heated wire were exposed to the atmosphere of a large chamber containing a uniform amount of combustible gas and free from air currents other than those caused by the hot wire. However, because a considerable amount of the combustible gas is burned out of a space the size of the bottle used, the composition of the gas in the bottle is never the same as that of the gas at the inlet. Passing gas into the bottle at an accelerated rate makes the composition of the gas throughout the bottle more uniform, but causes strong air currents which may affect the condition of the wire to a considerable extent. Analyzing a sample of gas from a point near the wire does not entirely solve the problem, since it is uncertain to what distance the operation of the wire in an open room would affect the composition of the atmosphere.

Another approximation is involved in the calculation of the temperature of the wire, the heat from combustion per unit length, etc., from the average resistance per unit length. There is always a cooling effect due to conduction through the leads. This source of error has, in most cases, been neglected, on account of its small magnitude, the difficulty of correcting for it, and because it occurs to about the same extent in the complete instruments as in the test wires, and failure to consider it has little or no effect upon the design of the instruments.

## (b) RESULTS OF EXPERIMENTS

*Temperature Coefficient of Resistance.*—Before proceeding to a detailed study of combustion at the surface of a wire, it is first necessary to know the relation between resistance and temperature for the wires used. The temperature coefficient of resistance was determined over the interval from 0 to 100° C for the wires used in all the more important experiments, and the resistance-temperature curve plotted to 1200° C using the formula  $R=R_0(1+At-Bt^2)$ , assuming a value of  $B$  equal to that for pure plati-

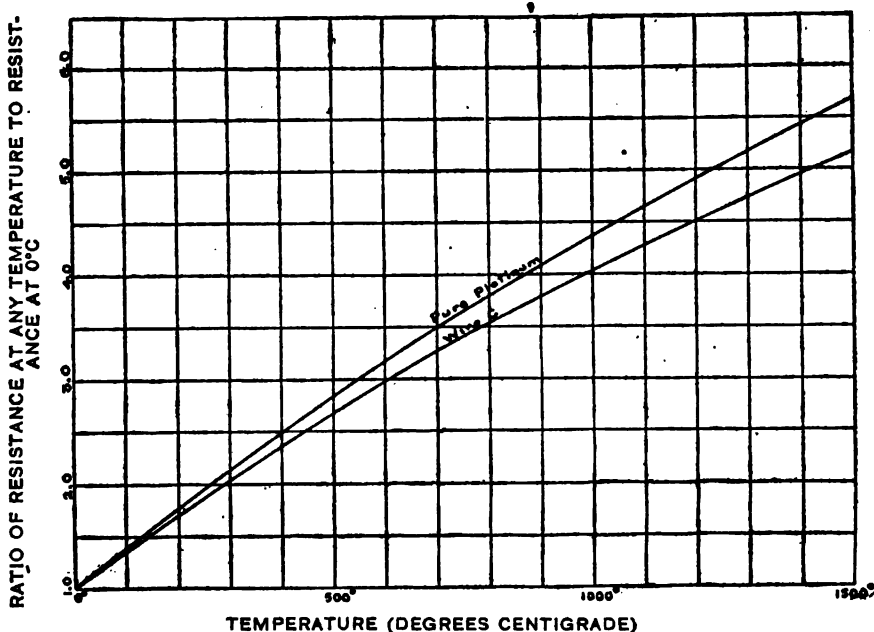


FIG. 3.—Temperature-resistance curve for platinum.

num. Above 1200° the curve was continued as a straight line.<sup>3</sup> The temperature-resistance curves for pure platinum and for wire C, which was most used in these experiments, are given in Fig. 3.

*Heat Loss from Wires in Air.*—The loss of heat from wires in air has been made the object of study by numerous observers who have proposed formulas for expressing the observed values. The most generally accepted formulas are those due to Langmuir<sup>4</sup> and to Lorenz.<sup>5</sup>

In Fig. 4 are plotted the observed average heat loss per centimeter from 3.8, 14, and 31 cm lengths of wire C and an 11 cm length of wire A. As checks upon these observations the heat

<sup>3</sup> Langmuir, Jour. Amer. Chem. Soc. 28, p. 1357, 1906.

<sup>5</sup> Ann. Phys., 18, p. 582.

<sup>4</sup> Physical Review, 34, p. 401.

loss from the larger wire calculated from Lorenz's formula, and the heat loss for both wires calculated from Langmuir's formula are plotted. The constants in the Lorenz formula were calculated from the observed heat loss at  $400^{\circ}\text{C}$ . In calculating for both curves the heat loss due to radiation, the values used for the emissivity of platinum at various temperatures were taken from Langmuir's paper.

The observed heat loss for the larger wire lies between the values calculated from the formulas of Lorenz and of Langmuir.

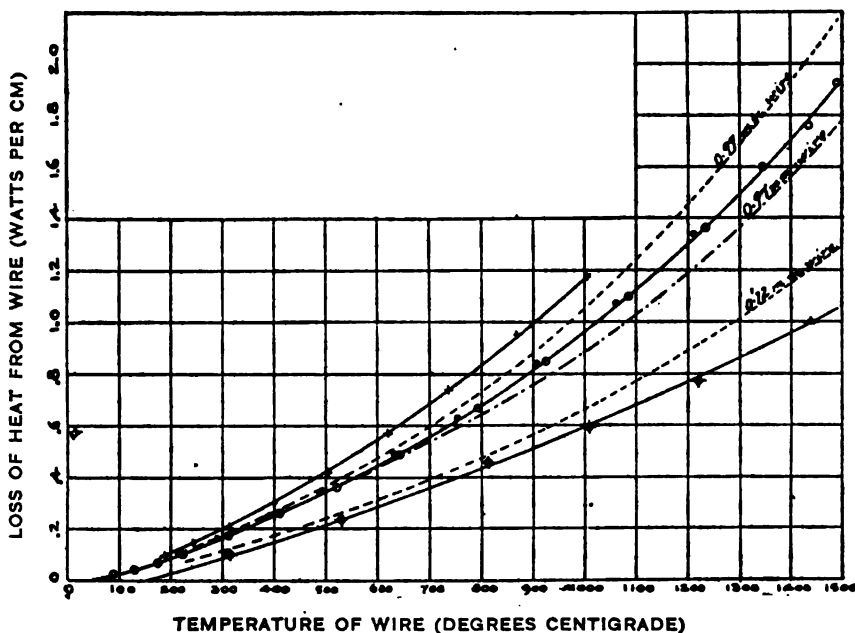


FIG. 4.—Loss of heat from wires in air

Curves in order from top represent: (1) Observed loss from 14 cm length of 0.097 mm wire; (2) loss from infinite length of same wire calculated from Langmuir's equation; (3) observed loss from 14 and 31 cm lengths of same wire; (4) loss from infinite length of same wire calculated from Lorenz's equation; (5) loss from infinite length of 0.015 mm wire calculated from Langmuir's equation; (6) observed loss from 0.015 mm wire.

It is apparent that for reasonable lengths of wire the difference between the observed average heat loss at a given temperature and the true heat loss is negligible for our purposes.

The distribution of heat due to combustion is probably nearly the same as that due to the electrical current. If this is true, no serious error due to lead conduction is involved in the values for power from combustion per unit length.

*Metal Used.*—In order to determine what metals were most suitable for the detector wires, platinum, palladium, gold, silver, and nickel wires were heated in mixtures of air with amounts of

hydrogen varying from a few tenths of a per cent up to and beyond the explosive limit. A few of the observations on wires 0.226 mm in diameter are plotted in Fig. 5. It was found that all the metals behave similarly until a temperature of about  $175^{\circ}\text{C}$  is reached. Above this temperature combustion takes place at the surface of both the platinum and palladium, and the amount of combustion increases at first very rapidly with rise of temperature and then becomes nearly constant. Since, when combustion begins, the rise of temperature due to combustion itself raises the temperature of the wire considerably, the resistance-

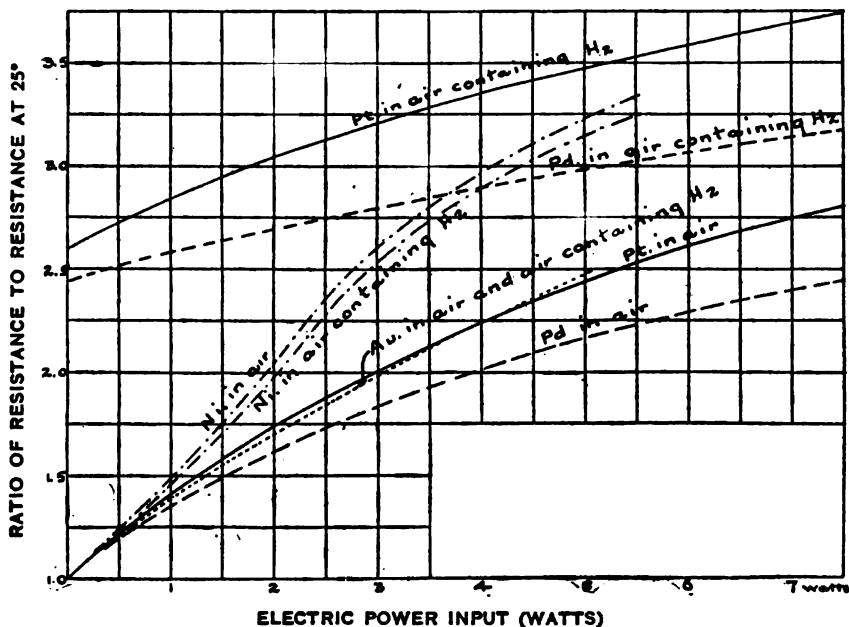


FIG. 5.—Change of resistance of heated wires of same size but of different metals in air and in air containing 5 per cent hydrogen

current curve shows a decided break when the temperature reaches a value such that the rate of increase of power from combustion becomes greater than the rate of increase of heat loss. This temperature is for convenience called the "ignition temperature," although it should be understood that some combustion takes place below this temperature and that combustion is not necessarily complete even at higher temperatures. In Fig. 5, the curves for platinum and palladium in air containing hydrogen represent the data obtained after heating to the ignition temperature. Gold, silver, and nickel show no such definite ignition temperature; indeed, the effect of the presence of hydro-

gen is only to cool these metals until a temperature of at least six or seven hundred degrees is reached.

These experiments with various metals show that there is no inherent advantage in the use of palladium over platinum for the combustion even of hydrogen, and that none of the other metals tried can be used for active wires. On the other hand, platinum has several advantages over palladium; it has a higher temperature coefficient of resistance causing a greater increment of resistance for the same amount of combustion, it has a higher melting point and is therefore less likely to be accidentally burned out, it is much more resistant to chemical action, and it is somewhat easier to obtain commercially. Platinum has, therefore, been used exclusively for the apparatus recommended.

*Ignition Temperatures.*—The temperature to which a detector wire must be heated is determined by the so-called "ignition temperature" defined in the preceding section. It was, consequently, of considerable importance to determine the ignition temperature of platinum in the various gases. Direct observations for this purpose were made with three wires, samples A, B, and C, which contained different amounts of impurity, as shown by their temperature coefficients given in Table 2.

The Wollaston wire (sample A) was used immediately after dissolving the silver in nitric acid and without previous heating.

The method of observation was as follows: By very slowly increasing the current through the wire, it was gradually heated in an atmosphere containing the gas, the percentage of which was found to make no difference in the ignition temperature. The Wheatstone bridge was kept balanced at all times. As soon as the resistance of the wire began to increase without increase of current, the resistance reading was recorded and the corresponding temperature was called the ignition temperature. The values found for hydrogen are given in Table 3.

These observations served to confirm previous results, which indicated that a wire becomes more active after being heated in hydrogen and that its activity gradually declines when the wire is left unheated for a long time. New wires must be glowd to remove the film of grease or other inactive material covering the metal. No wire which had once been active was observed to require a temperature higher than  $330^{\circ}\text{C}$  to ignite hydrogen. The ignition temperature for carbon monoxide and for illuminating gas was found to be practically the same as that for hydrogen.

If any difference exists, the lower temperature is required for carbon monoxide. Methane behaves somewhat differently. Combustion first begins at a temperature of about  $700^{\circ}\text{C}$  and increases so gradually with increase of temperature that it is impossible to assign any definite ignition temperature.

TABLE 3.—“Ignition Temperatures” of Hydrogen at the Surface of Platinum Wires

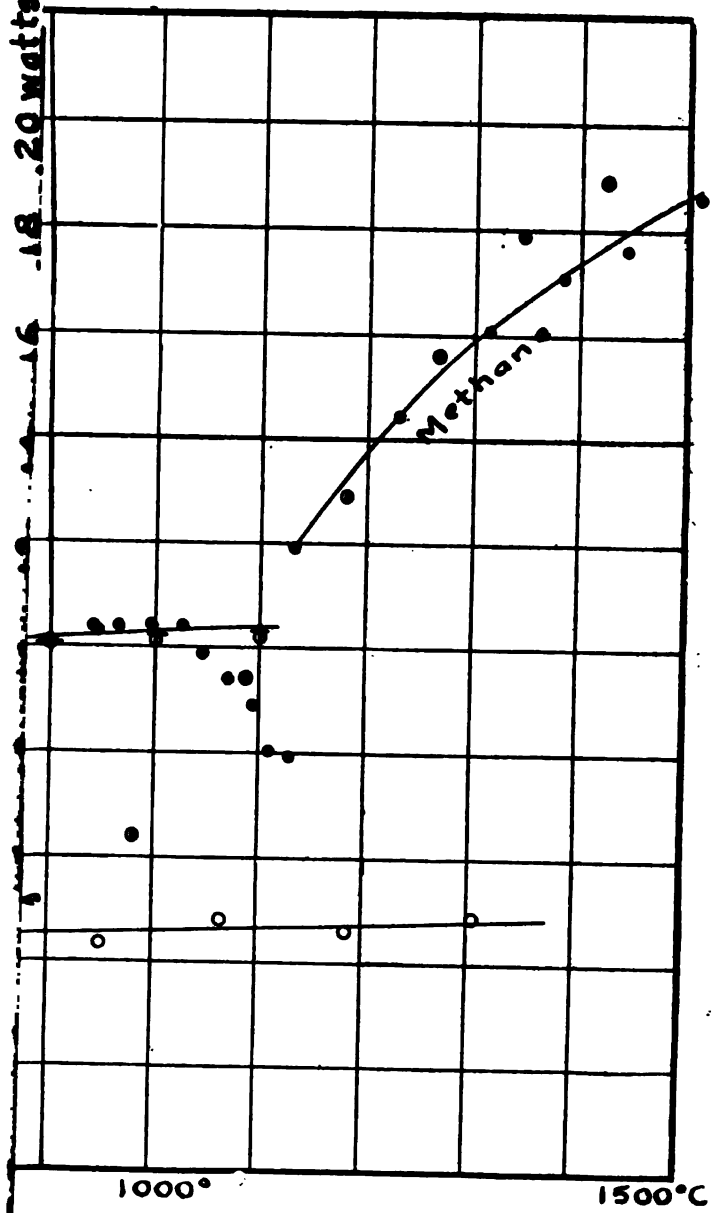
Diameter of wire	Ignition temperature	Remarks
0.097 mm, sample C.....	174	
	175	
	192	Observed 17 hours after previous heating
	108	Observed 1 minute after previous heating
	171	
	170	
0.053 mm, sample B.....	175	
	142	
	165	
	168	
	170	
	175	
0.012, sample A.....	730	Wire not previously heated
	190	
	191	
	185	
	265	Observed 2 hours after previous heating
	157	

*Heat of Combustion.*—The total amount of heat from combustion at the surface of a wire was determined in the manner described and illustrated under the heading “Method of study.” The amount of heat from combustion per unit length of wire C for each per cent of gas entering the test bottle is plotted in Fig. 6. The data represented by the curve for hydrogen include the results of over 100 observations upon seven concentrations of hydrogen in the gas mixture. The individual observations upon three concentrations are given in order to show the agreement of results. The heating effect upon the wire of the 8.2 per cent mixture falls off at temperatures above  $1000^{\circ}\text{C}$ . This is no doubt caused by the fact that combustion takes place at some distance from the wire, and the supply of hydrogen to the surface of the wire is thereby reduced. It will be seen that the amount of carbon monoxide burned is almost independent of temperature, while the amount of methane burned increases rapidly with increase of temperature.

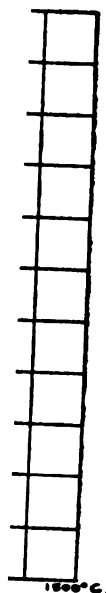


POWER FROM COMBUSTION (WATTS PER CENTIMETER OF WIRE FOR EACH PER CENT OF COMBUSTIBLE GAS IN GAS ENTERING TEST CHAMBER)

16 18 20 watts



shown  
les of  
e side  
alysis  
tering  
repre-  
by an  
latter  
tector  
essive



1000°  
CENTIGRADE)

1500°C

1 observations are represented as follows: Hydrogen, O, 2.2 per cent; +, 5.6 per cent; ., 1.35 per cent; O, 4.7 per cent.

ig the

on of  
suffi-  
e are  
cible.  
count  
of the

If an  
bon  
busti  
so gr  
assig

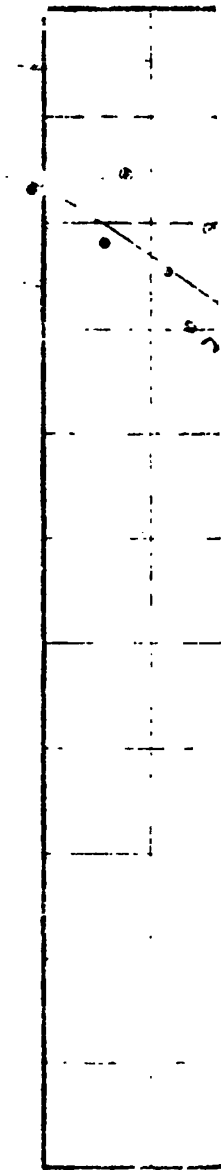
TABLE

0.097 m

0.053 m

0.012, m

He  
tion :  
scribe  
The s  
each  
The d  
of ov  
in the  
centr  
The h  
off at  
the fa  
wire,  
therel  
oxide  
amou  
temp



0.002

Fig. 7 shows the results of tests exactly similar to those shown in Fig. 6, except that different wires were used and that samples of gas drawn from a point about 2 centimeters below and to one side of the wire were analyzed and the percentage found by analysis was used in computing results instead of the percentage entering the bottle. It is probable that the results shown in Fig. 7 represent more closely the amount of gas which would be burned by an exposed wire in a large room than do those of Fig. 6. This latter figure may, however, better represent the performance of a detector partially inclosed to protect it from mechanical injury, excessive

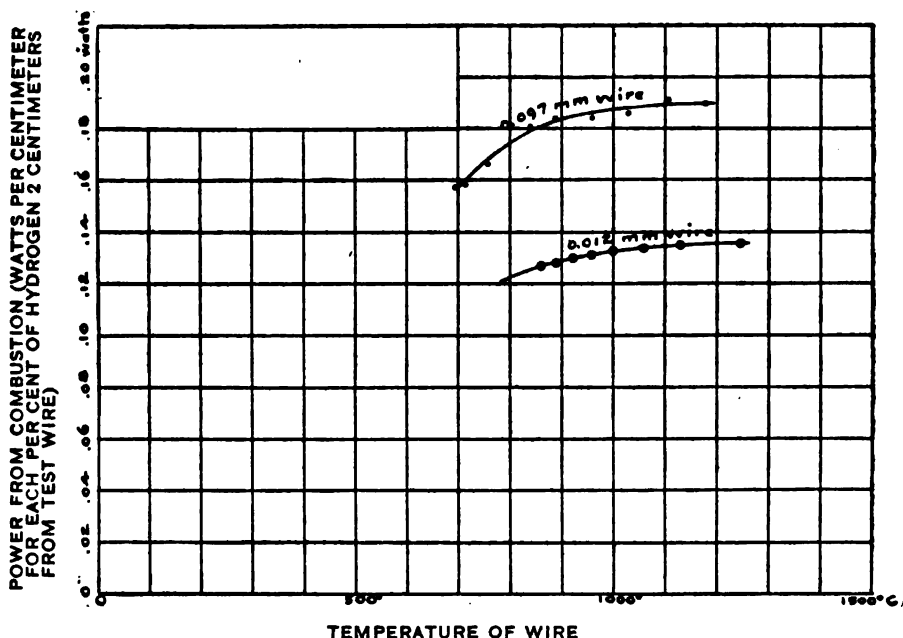


FIG. 7.—Observed power from combustion at the surfaces of different wires

drafts, or to prevent the hot wires igniting the gas surrounding the detector.

The above experiments lead to the following conclusions:

1. The power from combustion depends upon the condition of the surface of the wire to some extent, but when heated to a sufficiently high temperature the differences due to this cause are slight and the amount of power from combustion is reproducible.
2. The power from combustion is proportional to the amount of gas in the surrounding atmosphere until the composition of the mixture approaches the explosive limit.

3. The power from combustion increases with the temperature of the wire, most rapidly in the case of methane.

4. Any observed differences in the power from combustion which could be ascribed to differences in the sizes of wires were of the same order of magnitude as the differences in total heat loss per second due to the same cause.

*Temperature of Wires.*—Since neither the heat loss in air nor the power from combustion varies rapidly with size of wire, it is to be expected that the temperature rise produced by combustion, which is a function of the ratio of the other two properties, will not depend greatly upon size. Indeed, the process of diffusion by which the combustible gas reaches the wire and the process of conduction by which most of the heat is removed are sometimes regarded as a single phenomenon. Convection plays the same part in both processes, and the effect of radiation from wires of the sizes and temperatures with which we are concerned is not great. A consideration of these facts leads to the conclusion that the temperature rise due to combustion must be practically independent of the diameter of the wire. A considerable number of experiments verify this conclusion. The temperature rise for the two wires A and C, differing in diameter by a factor of 8, showed a difference in temperature rise for each per cent of hydrogen of less than 2 per cent, and this difference is believed to have been due to the small amount of platinum black left when the silver was removed from the Wollaston wire.

## 2. COMPENSATED BRIDGE INDICATOR

### (a) PRINCIPLES

A single wire whose resistance is measured by means of a Wheatstone bridge may be used to determine the amount of combustible gas in the atmosphere, but is not suitable for use in an automatic instrument, because its resistance is affected by changes in the current used to heat the wire and in the temperature and movements of the atmosphere surrounding it.

In order to overcome this difficulty the compensated bridge indicator was developed. This instrument consists of an equal arm Wheatstone bridge in which one pair of opposite arms is active, while the other pair is inactive. Then if the resistances of all the arms are equally affected by changes in the conditions of operation, the balance of the bridge will not be affected by such changes. In the presence of a combustible gas, however, the combustion heats the active wires, increasing their resistance and

unbalancing the bridge. The operation of a Wheatstone bridge of this kind can be deduced from Kirchhoff's laws, and shows how the unbalanced current, which causes the voltmeter to deflect, depends upon the resistance and sensitivity of the wires, the total current, the resistance of the voltmeter, etc.

If  $r_1$  is the resistance of an active wire and  $r_2$  that of an inactive wire, Kirchhoff's laws give for the galvanometer or voltmeter current

$$i = \frac{\frac{1}{2}(r_1 - r_2)I'}{r + \frac{1}{2}(r_1 + r_2)}$$

where  $I'$  is the total current and  $r$  is the voltmeter resistance. The resistances of the wires change with current and per cent of combustible gas in approximately the following manner:

$$r_1 = R \left( 1 + SX + C_1 \frac{I_1 - \frac{1}{2}I}{\frac{1}{2}I} \right)$$

$$r_2 = R \left( 1 + C_2 \frac{I_2 - \frac{1}{2}I}{\frac{1}{2}I} \right)$$

Where—

$R$  is the resistance of one wire of the bridge when the normal operating current  $I$  flows through the bridge as a whole, when no combustion is taking place, and when the bridge is balanced.

$S$  is the "sensitivity" of the active wires, defined as the proportional change in resistance with change in percentage of combustible gas  $x$ , so that  $S$  is identical with  $dR/Rdx$ .

$I_1$  and  $I_2$  are the currents in the active and inactive wires, respectively.

$C_1$  and  $C_2$  are the coefficients, respectively, for the active and inactive wire of proportional change of resistance with proportional change of current, i. e.,  $C$  is defined as  $\frac{dR}{R}$  divided by  $\frac{dI}{I}$ .

Substituting these values in the equation for the voltmeter current and remembering that  $I_1 = \frac{1}{2}(I' - i)$  and  $I_2 = \frac{1}{2}(I + i)$  one finds:

$$i = \frac{\frac{1}{2}RI' \left[ SX + (C_1 - C_2) \frac{(I' - I)}{I} \right]}{r + R + \frac{1}{2}SRX + \frac{1}{2}(C_1 + C_2) \frac{RI'}{I}}$$

It is seen from this that one can consider the unbalanced voltage

$$e = \frac{1}{2}RI' \left[ SX + (C_1 - C_2) \frac{(I' - I)}{I} \right]$$

to act on the complete voltmeter circuit, which has a resistance equal to

$$r + R + \frac{(C_1 + C_2) I' R}{2I} + \frac{RSx}{2},$$

where  $\frac{(C_1 + C_2) I' R}{2I}$  is an "apparent heating resistance," and  $\frac{RSx}{2}$  is the increase in bridge resistance due to the presence of the gas.

When  $C_1$  equals  $C_2$  the unbalanced voltage is simply  $\frac{RI'Sx}{2}$  and the resistance is  $r + R + \frac{CI'R}{I} + \frac{RSx}{2}$ .

Usually  $\frac{RSx}{2}$  and  $\frac{CI'R}{I}$  are only small parts of the resistance, so that the voltmeter current, and hence the reading, is proportional

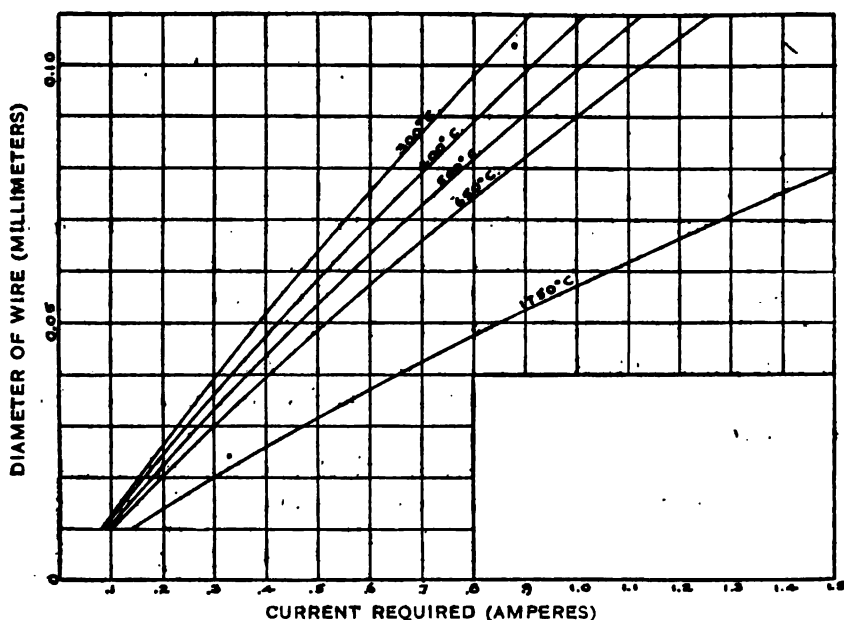


FIG. 8.—Current required to heat platinum wires of small diameter to various temperatures in air

to the sensitivity of the wires and the voltage across the bridge and inversely proportional to the resistance in the voltmeter circuit.

The sensitivity of a wire, unless very short and large, is practically independent of its length, but varies with the temperature, as shown by the curves of Fig. 9. These curves have been plotted from the direct observations on the resistance change in the various

gases of platinum wires whose diameters varied from 0.012 mm to 0.226 mm. There is some increase in sensitivity with diminution in the diameter of the wire, but the curves will give values sufficiently accurate for use in the design of compensated bridge indicators or any other devices using the resistance change as a measure of the amount of combustible gas in the atmosphere.

The sensitivity to other gases and vapors has not been accurately measured, but for illuminating gas, alcohol vapor, gasoline vapor, and some other compounds it is comparable with that for

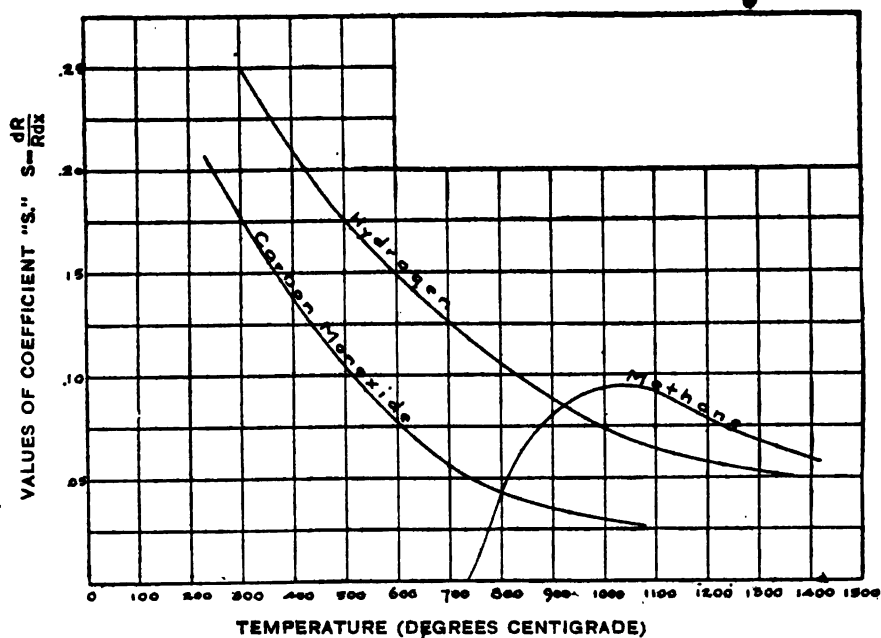


FIG. 9.—Coefficient of sensitivity of platinum wires

hydrogen. It is believed that there is ample sensitivity for the detection of any combustible mixtures before an explosive condition is reached.

The coefficient  $C$  of proportional resistance change with change of current is practically independent of the length and diameter of the wire, unless this is very short and large, but varies with the temperature, as shown by the curve in Fig. 10, which has been plotted from direct observations of the resistance change with change in current with the wires in air. This furnishes a means of determining the value of the coefficient  $C$  which the inactive compensating wires must have if the bridge is to be compensated. The apparent heating resistance  $CR$  can be readily calculated.

Although it is possible to make  $C_1$  and  $C_2$  exactly equal by proper choice of active and inactive wires, in practice it is better to have a slight difference. When  $C_1$  is not equal to  $C_2$ , the additional unbalanced voltage, i. e.,

$$\frac{RI'}{2} \frac{(C_1 - C_2)(I' - I)}{I}$$

causes a deflection when the current is above or below the normal operating current. The magnitude of this effect is proportional

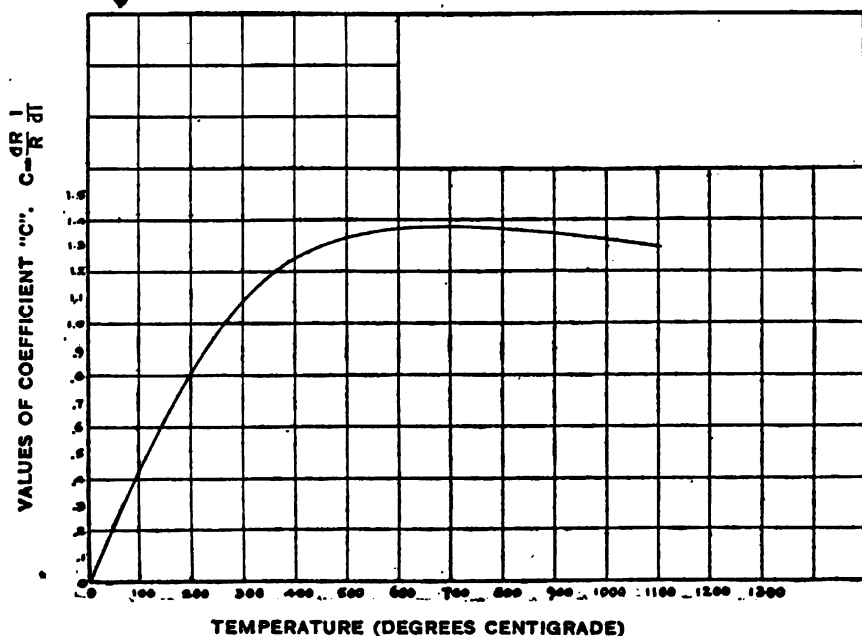


FIG. 10.—Coefficient of resistance change of small platinum wires with change of current at any temperature

to the difference in the coefficients  $C_1$  and  $C_2$ . If instead of choosing a compensating wire whose coefficient is exactly equal to that of the active wire a wire is chosen which has a slightly different coefficient, it is possible to make the indications independent of (instead of proportional to) the total current for a given percentage reading. This will, however, only hold for this percentage, and the deflection for percentages above and below this will vary from the correct values in opposite directions with variation in the current. The variation in the readings due to change in current is, however, less than it would be with wires having the same coefficients.



It can be easily shown that to produce absolute compensation at the percentage  $x'$  requires that

$$C_1 - C_2 = Sx'.$$

The coefficient of proportional resistance change with change of current is found to change with the temperature and therefore with the current in such a manner that it is usually possible to select as the value of the operating current one which will give absolute compensation in the percentage range of special interest.

(b) DESIGN OF PARTS.

In the design of a compensated bridge indicator to measure a particular range of percentages of a certain gas the best procedure is as follows:

1. Choose a convenient diameter  $d$  of wire (0.025 to 0.1 mm).
2. From the curves in Fig. 8 determine the current required to raise the wires to the following temperatures: For hydrogen, carbon monoxide, illuminating gas, and alcohol vapor,  $500^\circ\text{C}$ ; for gasolene vapor,  $700^\circ\text{C}$ ; and for methane and acetylene,  $900^\circ\text{C}$ . The current given in the curves is one-half the operating current.
3. From the curves in Fig. 9 determine the sensitivity  $S$ .
4. From the curves in Fig. 10 determine the coefficient  $C$ .
5. Choose a convenient length  $L$  (not less than 1000 times the diameter).
6. Compute the resistance  $R$  from the following formula:

$$R = 1.25 \times 10^{-4} \frac{L}{D^2} Z$$

where  $Z$  is the ratio of the resistance of pure platinum at the operating temperature to the resistance at  $0^\circ\text{C}$  obtained from Fig. 3, and  $L$  is the length and  $D$  the diameter of the wire in centimeters.

7. Compute the unbalanced voltage  $e$  from the maximum percentage to be indicated by using the formula

$$e = \frac{RISx}{2}$$

8. Compute the bridge resistance  $r$  by using formula

$$r = R + CR + \frac{RSx}{2}$$

9. Select a voltmeter which will give full scale deflection on the unbalanced voltage computed in 7 above when in series with a resistance greater than that computed in 8 above.

The effect of variations in the design of the instrument may be determined in any particular case from the formulas and directions just given. The following general statements may, however, be useful:

Increasing the diameter of the detector wires diminishes the sensitiveness of the instrument and increases the operating current. It is consequently an advantage to use wires as small as is consistent with mechanical strength and the difficulty of covering with an inactive coating.

Increasing the operating temperature of the wires increases the current required and increases the sensitiveness of the instrument. This is limited by the temperature at which the inactive wire becomes active and by the stretching of the active wire in a high percentage of combustible gas. Decreasing the operating temperature decreases the current required and decreases the sensitiveness very rapidly, especially for methane.

When the bridge resistance is small compared with the voltmeter resistance, the sensitiveness increases nearly in proportion to the length of the bridge wires.

For compensating wires one may use any wires which continue inactive, which have the same resistance as the active wires, and which have nearly the same coefficients of change of resistance with change of current. As has already been stated, the compensating wires are most easily prepared by coating platinum with a substance which will render it inactive.

Gold, nickel, and glass have been used for this purpose, but the metal coatings were found to be less satisfactory than glass for the three following reasons:

1. The metal coatings are not permanent; volatilization or alloying or both take place slowly until the protective coating practically disappears. This may take several months of continuous service, but is sure to occur in the end. No such change has yet been observed with glass-covered wires.

2. The metal-plated wires are at the same temperature as the active wires and cause combustion if the temperature is raised sufficiently. With such difficultly combustible gases as methane and acetylene the temperature range within which the gas will burn at the surface of platinum and not at the surface of gold or nickel is rather small. The glass-covered wires, on the other hand, are not heated to such high temperatures in operation as are the active wires, and they remain inactive at higher temperatures than do the gold or nickel surfaces.

3. The difference in coefficient  $C$  between the glass-covered and the bare platinum wires enables us to choose an operating condition such that the indications of the instrument will be independent of temperature at the percentage of gas of most interest. Fig. 11 shows the differences in behavior of a heavily glass-coated and a bare platinum wire when heated in air. It will be observed that practically perfect compensation for changes of current over the range 0.45 to 0.75 ampere can be obtained by making the compensating wires about 20 per cent longer than the active wires.

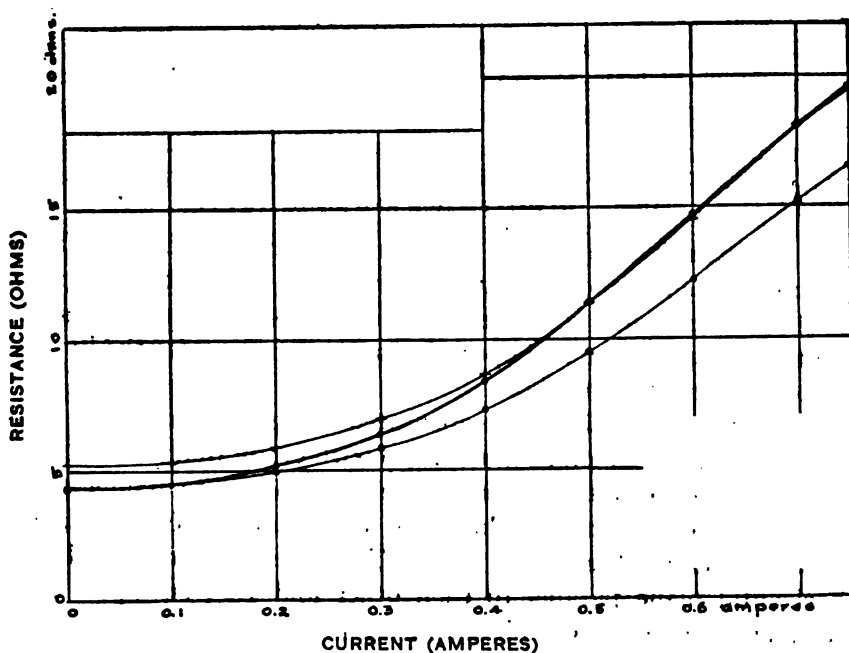


FIG. 11.—Observed resistance in air of bare and glass-covered platinum wire

Upper curve, 9.5 cm glass-covered wire; middle (heavy) curve, 8 cm bare wire; lower curve, 8 cm glass-covered wire.

For compensating the instrument to give readings independent of current in the presence of a considerable amount of combustible gas, the difference in length need not be so great as this.

If the compensated bridge indicator is to be used under conditions in which there is a possibility of the gas mixture reaching the explosive proportions, metal protective gauzes should be placed between the wires and the outside atmosphere. Double copper gauzes 24 meshes per cm (60 meshes per inch) have been found to be satisfactory even in hydrogen-air mixtures of maximum explosibility. When gauzes are used or when the wires are inclosed in any manner which obstructs the passage of the gas, the

sensitiveness is thereby reduced somewhat. This need not be serious and seldom exceeds a reduction of 50 per cent.

The wires of the indicator must be so arranged as to be equally affected by motion of air caused by drafts or convection currents. The effect of drafts which may affect the wires unequally can be diminished sufficiently for most work by the use of properly placed baffle plates. Such baffle plates will not affect the sensitiveness of the instrument greatly. The combined effect of the baffle plates and the protective gauzes on the instrument specified in Section III is to diminish the total reading of the instrument by a little less than 50 per cent. This is of no consequence for the purpose for which the instrument is intended, since the sensitiveness of the type of voltmeter employed is so great that a series resistance has to be introduced to increase its range, expressed as percentage of hydrogen.

#### (c) DESCRIPTION AND TESTS

A considerable number of compensated bridge indicators have been constructed and tested. However, the following description of three instruments with the results of tests should suffice to show that the construction and operation are satisfactory for the limited period covered by the tests.

*Indicator A.*—A simple compensated bridge indicator was constructed using four platinum wires 0.0026 cm in diameter and 5.6 cm long. Two of these wires were gold plated to render them inactive, the gold plating being so thin that the change in resistance was less than 1 per cent. The wires were mounted in a horizontal plane parallel to each other and 1.25 cm apart in a rectangular case 2.5 cm high, the top and bottom of which were open, so that the wires were freely exposed to the surrounding atmosphere. A Weston miniature voltmeter having 3 and 15 volt ranges, with resistances of 220 and 1100 ohms, respectively, was used as the indicating instrument.

By adjusting one wire the bridge was balanced. The detector bridge was then placed in a box supplied with a steady stream of air containing, in any experiment, a constant and known percentage of hydrogen. Fig. 12 shows how the reading changes with change in the percentage of hydrogen in the air entering the box. It is observed that concentrations as low as 0.07 per cent give an indication, and that the proportionality between reading and percentage falls off only slightly at the higher percentages.

The effect upon the readings of protecting the instrument with double gauzes and baffle plates is also shown. The gauzes com-



Bulletin Bureau of Standards, Vol. 15

FIG. 13.—Indicator "B" with connections

pletely covered the openings at the top and bottom of the rectangular case and the baffle plates were parallel to these and 0.75 cm outside. The gauze was of iron wire 0.035 cm (0.014 inch) in diameter with 11 meshes per cm (28 meshes per inch).

The reading of this instrument for a given percentage was found to be practically proportional to the total current, which is in accordance with the theory of the compensated bridge in which the two coefficients,  $C$ , are equal.

This indicator was also tried out with carbon monoxide and with illuminating gas. The indications for any percentage of

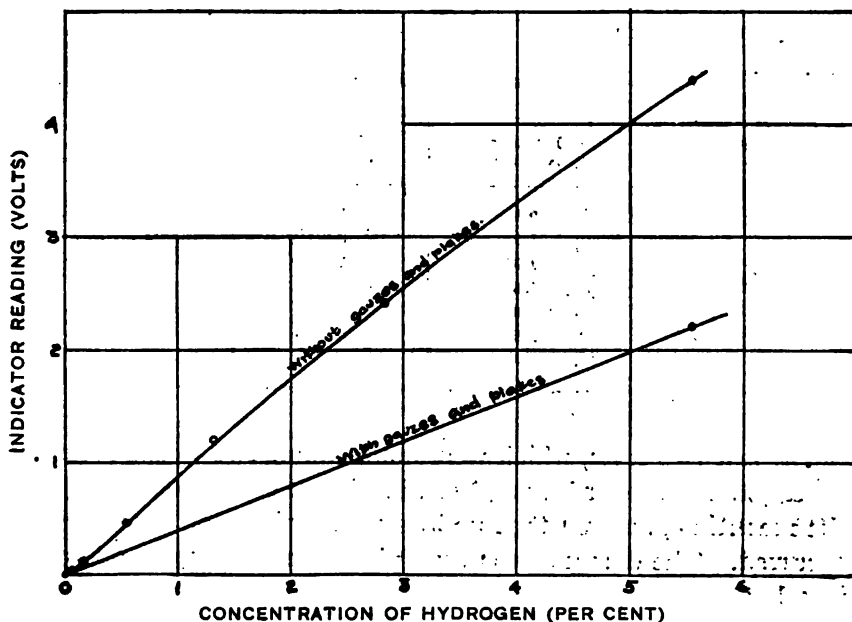


FIG. 12.—Calibration curves for indicator "A"

carbon monoxide was found to be about one-half that for the same percentage of hydrogen, while illuminating gas produced an indication slightly greater than that for the same percentage of hydrogen.

*Indicator B.*—Fig. 13 shows a complete compensated bridge indicator which was designed to indicate the percentage of hydrogen and to sound an alarm when this percentage had reached any predetermined value. The essential parts of this indicator are similar to those just described. The bridge was made of platinum wires, two of them gold plated, 0.053 mm in diameter and 6 cm long, supported in a hard-rubber case fitted with double gauzes and baffle plates. The indicating instrument is a Weston millivolt-

meter, the scale of which was calibrated to read the percentage of hydrogen directly and to which a contact-making device had been attached. The lamp shows when the detector bridge current is flowing. The alarm bell is mounted on the back of the board and is operated through the contact-making device on the voltmeter from the main direct current supply.

The detector was calibrated and subjected to a large number and variety of tests during a period of two months. Table 4 shows some of the results of placing the detector bridge in a testing chamber supplied with a continuous stream of hydrogen-air mixture and comparing the indicator reading and the results of analysis of samples taken near the bridge.

TABLE 4.—Calibration of Indicator B by Gas Analysis

Per cent by analysis	Indicator Reading	Per cent by analysis	Indicator Reading
(*)	0.0	1.7	1.7
1.1	1.0	2.0	2.0
1.85	1.9	1.15	1.2
1.85	1.8	2.1	2.1
2.05	2.0	2.2	2.2
2.5	2.5	2.2	2.2
3.7	4.0		

\* No hydrogen.

The last two tests, which were made about two weeks after the others, the indicator having been in almost continuous service in the meantime, showed that no loss of sensitivity or accuracy had occurred. The detector was then placed in continuous operation in a battery compartment where it gave an indication of hydrogen in about the same quantity every time the battery was charged. After about two months continuous service, however, the indications of the instrument dropped off to about one-half the amount shown by analysis, and it was found that the change was due to the compensating wires having become active. The very thin gold plating (the change of resistance of the wire after plating indicated a coating less than 2 by  $10^{-8}$  mm thick) was found to have disappeared by volatilization or alloying, although the fact that the instrument still showed one-half its original sensitivity was proof that some gold still remained. The ultimate activation of the gold-plated wires, which was the only observed cause of change in calibration in the earlier instruments, has been entirely overcome by the use of the glass-covered wires.



Several indicators have been made using glass-covered wires and have, throughout all tests, given consistent results, and no change in calibration has been observed with any of them in which fair-sized wire was used and was not placed under tension.

The tests made on only a single instrument with glass-covered wires will be described. This instrument is designated as indicator C.

*Indicator C.*—The bridge of indicator C was made up of four wires of commercial platinum 0.053 mm in diameter and 6 cm

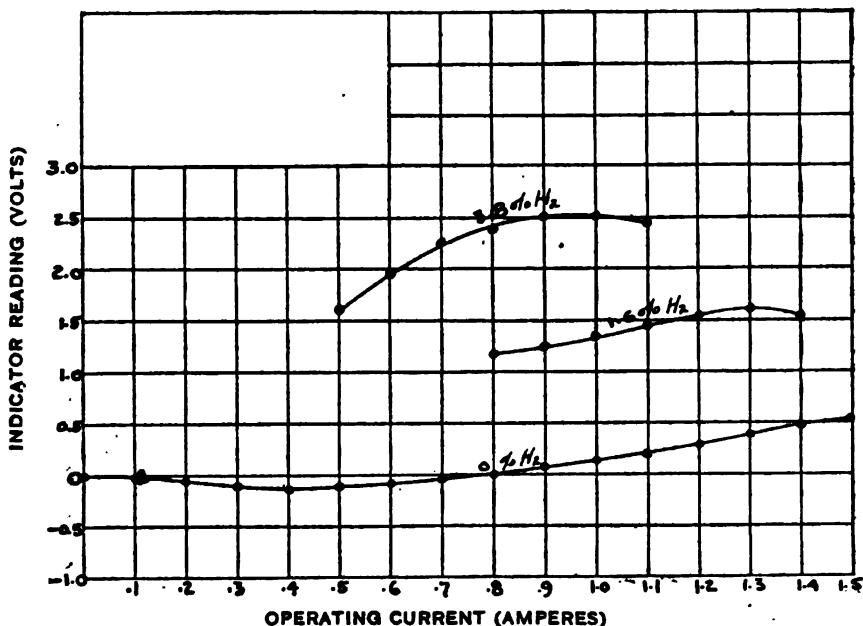


FIG. 14.—Operation of indicator "C" with currents of different strengths

long, two of them coated with glass in the manner described on page 83. The bridge was used with and without protective gauzes and baffle plates. It was found that the use of the protection cut down the reading for a given concentration of hydrogen to one-half the value given by the unprotected instrument. Using the unprotected bridge, and measuring the unbalanced voltage with a Weston portable millivoltmeter of 9 ohms resistance in series with 191 ohms additional, the readings shown in Fig. 14 were obtained. The concentration of hydrogen was determined by analysis of samples of gas drawn from a point just beside the bridge frame. The figure shows how the unbalanced voltage changes with the percentage of hydrogen and with changes in the

operating current. The effect of the difference in the coefficients  $C$  and the variation of this difference with percentage and current—i. e., with temperature—is clearly observable. The unbalanced voltage, calculated from the formulas and curves given under "Principles," for the normal operating current of 1 ampere, agreed with the observed value within 3 per cent.

*Use for Detecting Other Gases.*—The same indicator was used with certain necessary variations in the temperature of operation and resistance of voltmeter circuit, for testing for other gases. The voltmeter deflection for 1 per cent of each of the different gases was compared with the deflection caused by 1 per cent of hydrogen arbitrarily called 100, with the following results:

	Relative deflection caused by equal percentage of gas
Hydrogen.....	100
Illuminating gas.....	86
Methane.....	106
Carbon monoxide.....	61
Benzene vapor.....	400
Ethyl-alcohol vapor.....	360
Gasoline vapor.....	1140
Acetone vapor.....	438

The general applicability of the detector is thus evident.

In some of these experiments explosive mixtures were formed inside the detector case, but the flame never penetrated the gauzes to the surrounding atmosphere. The reading of the detector when the explosive mixture was formed was of especial interest, since it represented the greatest deflection obtainable in the presence of the particular gas. Again referring the results to hydrogen, the relative deflections caused by the explosive mixtures were as follows:

	Relative deflection caused by explosive mixture
Hydrogen.....	100
Gasoline.....	139
Ether.....	146
Benzene.....	132
Acetone.....	133
Carbon monoxide.....	100

These results, while not of great accuracy, show that *the indication given by the explosive mixture of a gas in air is of the same order of magnitude whatever the gas may be.*

## 3. GLOWING-WIRE INDICATOR

The temperature at which a platinum wire shows a visible glow, while depending somewhat upon the conditions of observation, can be judged quite accurately under any ordinary conditions of illumination. Six observations were made upon a 31 cm length of wire C by the following method: The wire was stretched horizontally in an ordinarily well-lighted room, but in a position in which the light from the windows did not fall directly upon it. It was then heated by a current which was slowly increased until

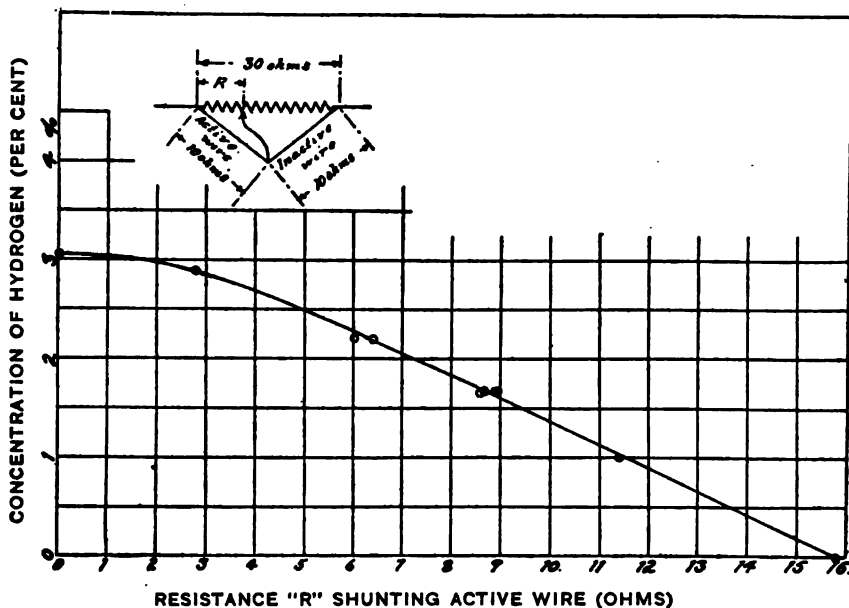


FIG. 15.—Diagram of connections and curve showing performance of glowing-wire indicator

the reflected light was no longer noticed in comparison with the radiated light. The resistance was then measured and the temperature calculated, with the following results for the six observations: 675°, 684°, 684°, 680°, 688°, 690° C. The precision with which the temperature at the first visible glow can be determined is thus evident.

It has been shown by Lummer and Kurlbaum \* that, at this temperature a change of 1 per cent in the absolute temperature causes a change of about 30 per cent in the light emitted. Taking data from Figs. 4, 7, and 10, it is found that at this temperature 1 per cent change in current causes a change of about 1.3 per cent

\* Verh. d. Deutsch. Phys. Ges., II, p. 89; 1900.

in the absolute temperature, or 40 per cent in the light emitted; whereas the presence of one-tenth of 1 per cent of hydrogen in the atmosphere about the wire causes a temperature change of 2 per cent in the absolute temperature or 60 per cent in the light emitted. It is apparent from these facts that the absolute temperature can be easily determined from the luminosity of the wire to within 2 per cent. Consequently one should be able to determine the amount of hydrogen present in the atmosphere about the wire to a tenth of 1 per cent by observing the current required to make the wire glow.

An apparatus using this principle for determining the amount of combustible gas is very simply made, consisting merely of a platinum wire, an ammeter, and a source of current. The apparatus can be calibrated by observing the current required to make the wire glow in atmospheres containing various percentages of combustible gas. If a concentration of gas greater than that required to keep the wire at visibility without electrical heating is to be measured, the amount of air reaching the wire must be limited by inclosing in gauzes or by otherwise restricting the air flow.

The necessity for using an ammeter is eliminated in the portable glowing-wire indicator shown in Fig. 21. An inactive wire is mounted beside the active wire and is used as a standard for brightness. The 15-ohm rheostat shown determines the ratio of the currents in the active and inactive wires, and the 10-ohm rheostat varies the total current. Since the ratio of currents required to make the two wires glow with equal brightness will decrease with the percentage of gas present, the 15-ohm rheostat can be calibrated in terms of the percentage of gas.

The relation between the readings of a glowing-wire indicator having somewhat different electrical resistances than those above specified, with analyses of the gas taken from a point a few centimeters from the wire, together with a diagram of connections, are shown in Fig. 15. It will be seen that the greatest deviation from the calibration curve of any single observation is only 0.1 per cent of hydrogen, while the average deviation is only a few hundredths of a per cent.

#### 4. BIMETALLIC DETECTOR

The action of a bimetallic detector depends upon the temperature change in a bimetallic strip caused by temperature changes in a near-by wire. It would be difficult to predict the temperature

change of a strip produced by a given temperature change of the wire, and even if this were known, the movement of the strip would be difficult to compute since it is a function of the length and of the thickness, coefficient of expansion, and elastic modulus of each of the metals of which the strip is composed. Fortunately, the use of an adjustable contact permits so wide a range of adjustment that it is unnecessary to design the instrument to give any predetermined deflection.

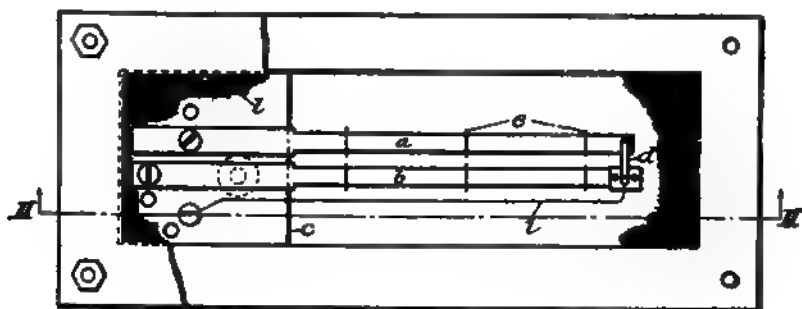
Fig. 16 shows one of these instruments made at this Bureau. The bimetallic strips used in it were made up from brass 0.23 mm thick and a nickel-steel alloy of the same thickness. The two bimetallic strips *a* and *b* are each attached at one end to an insulating support *c* in such a position that the free ends of the strips will bend in the same direction (downward in the drawings) when heated. One of the strips, *b*, bears an insulated contact piece, *d*, which makes contact with the free end of *a* when the free ends of the two strips are in a certain relative position. By means of perforated mica disks *e* wires *f* and *g* are suspended a short distance below strips *a* and *b*. One end of each wire is attached to the connecting piece *h*. Wire *f* is a platinum wire 0.05 mm in diameter coated with glass, and *g* is a piece of the same wire without coating. A copper wire *i* connects the contact piece *d* to a binding post and thence to one terminal of an electric bell *j*, the other terminal of which is connected to *b*. The screw *k* serves to adjust the position of *b*, and thus the distance between the contact points on *a* and *d*. As in the case of the other types of instruments, the hot wires are inclosed by gauzes, which permit circulation of air, but protect the instrument from mechanical injury, and serve to prevent the ignition of gas in the surrounding atmosphere.

When an electrical current is passed through the instrument, the two strips *a* and *b* are equally affected by heat from the wires; hence there is no relative movement of their free ends. But when a combustible gas is present, it burns at the surface of the wire *g*; the heat from combustion is transmitted to the adjacent strip *b*, which bends downward and closes the contact between *d* and *a*. The wires *f* and *g*, which have a rather high resistance, are then short-circuited through *j*, and the alarm rings.

This instrument has been tried out and found to work satisfactorily. It is easily adjusted to make contact in the presence of 0.2 per cent of hydrogen. With this adjustment it does not make contact at any current when no combustible gas is present.

In order to test the relative sensitivity of the apparatus with different currents flowing, the detector was placed in a box having a volume of 0.2 cubic foot. A stream of air containing 2.5 per cent

7.



2.

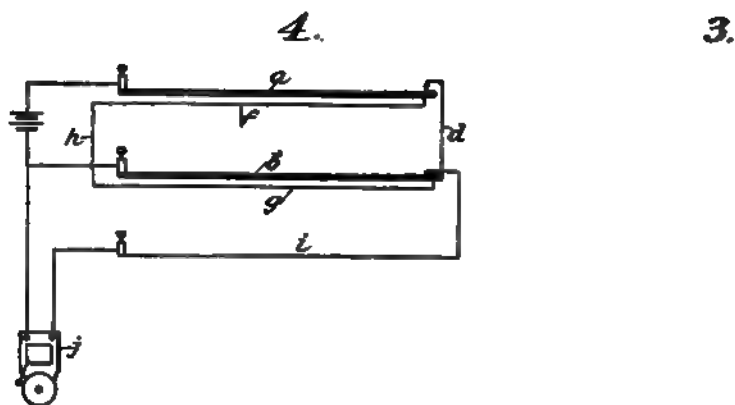


FIG. 16.—The bimetallic detector

of hydrogen was introduced into the box at the rate of 0.1 cubic foot per minute, and the time from starting the gas until the alarm rang was observed when currents of 0.4, 0.5, and 0.6 ampere

were passed through the apparatus. With 0.4 ampere the times were 8, 10, and 11 seconds; with 0.5 ampere, from 9 to 12 seconds, averaging  $10\frac{1}{2}$  seconds, and with 0.6 ampere 13 to 14 seconds. These results indicate greater sensitivity when only a small current is used to operate the instrument, but there is little difference in this respect.

The sensitiveness of the instrument can be increased by increasing the length or reducing the thickness of the bimetallic strips.

### III. SPECIFICATIONS FOR THE CONSTRUCTION AND CALIBRATION OF INSTRUMENTS

#### 1. COMPENSATED BRIDGE INDICATOR

##### (a) CONSTRUCTION OF APPARATUS

The following specifications apply to the compensated bridge indicator believed to be best for general use. The form is one which has successfully met every test to which it has been subjected in the laboratories of the Bureau of Standards. The complete equipment (see Figs. 13 and 17) consists of as many detector bridges as are desired, a contact-making voltmeter and a cut-out switch for each detector, a main control switch, an indicating lamp, one ballast resistance, one alarm bell, and the cables connecting the detectors with the switchboard apparatus. The apparatus may, of course, be connected in a different manner than that shown in Fig. 20.

*Detector Bridge.*—The details of a detector bridge are shown to half size in Fig. 19. The four wires making up the bridge are fused to short pieces of copper wire of much larger diameter and the latter are soldered to four metal pieces (*a*) screwed to the insulating piece (*b*). This constitutes the detector element (*A*). The base part (*B*) consists of a metal plate (*c*), the cover plate (*d*) having a square opening covered with double gauzes and the insulating piece (*e*). The parts are all fastened together and the four screws (*g*) extend downward and serve to hold the detector element (*A*) and the cover (*c*) in place. Four rubber-covered wires are lead-soldered to the four metal pieces (*a*) and pass out through one side of the insulating piece (*b*). The lower part consists of the cover plate (*h*) with double gauzes and the baffle plate (*i*). The parts *h* and *i* are similar to *d* and *c*, respectively.

To assemble the detector, the detector element (*A*) is slipped on the four projecting screws (*g*) and fits nicely against the insulating piece (*e*); the cover (*c*) is then slipped on and the outside nuts placed on the screws (*g*). The four wires are then connected to the cable.

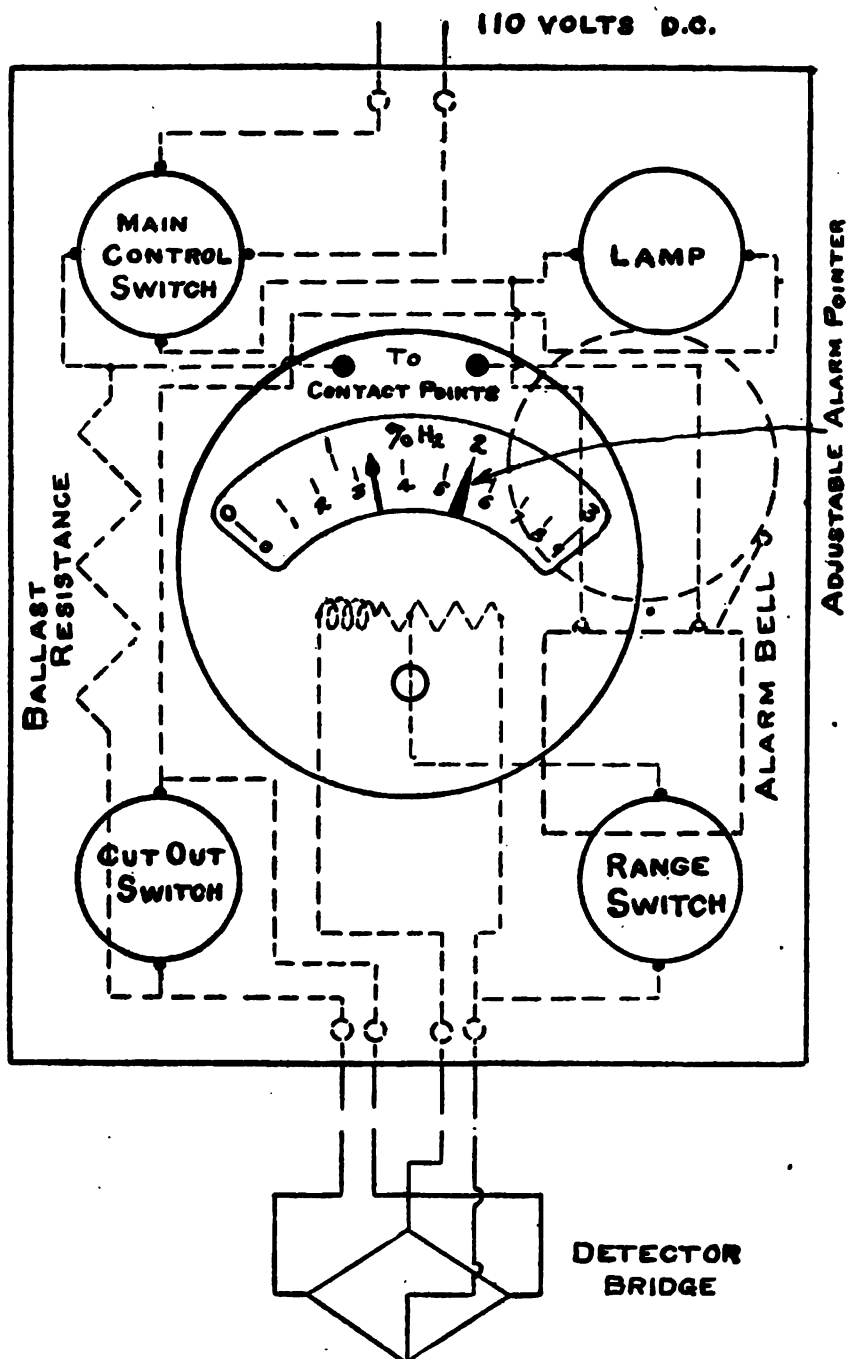


FIG. 17.—Diagram of connections of indicator "A"



The detector wires are to be of pure platinum 0.05 mm or 2 mils in diameter. Two of the wires (as marked) are to be covered with a thin coating of "sealing in" glass as described in the next section.

In fusing the glass-coated wires to the copper leads, the greatest care must be taken not to reduce the glass at the point of fusion. The copper must be melted in the reducing flame a few millimeters from the glass-coated wire, the two ends brought quickly together, and immediately removed from the flame. The wires should be straight when soldered into place.

When intended for use in battery compartments, the other metal parts of the detector, including the gauzes, are to be lead-

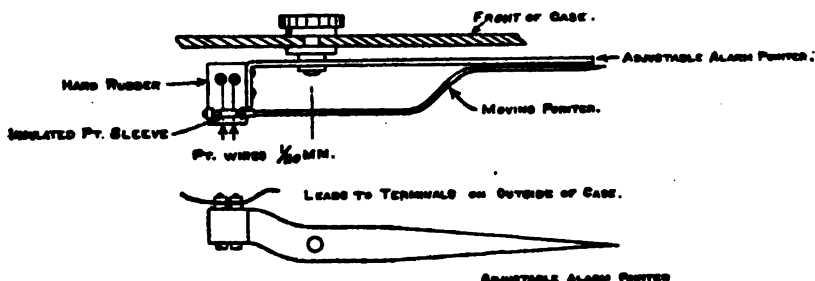


FIG. 18.—Contact-making arrangement for voltmeter used with indicator "A"

coated in order to protect against corrosion by sulphuric-acid fumes.

The insulating pieces (b) and (e) are to be of hard rubber or Bakelite or any material known to give good service under the conditions of use of the detector.

*Preparation of Glass-coated Wire.*—A platinum wire is most quickly coated by melting a bead of sealing-in glass in the oxidizing flame of a fine-tipped blowpipe and allowing it to flow along the wire three or four times. The coating so formed should be quite smooth and not thicker than the diameter of the wire.

A better method is as follows: Make a hole twice the diameter of the wire or larger through a piece of platinum foil, thread one end of the wire through the hole from above, lay a small piece of sealing-in glass on the foil over the hole, heat with the tip of the oxidizing flame of the blowpipe until the glass is melted, and then draw the wire slowly through the melted glass and the hole in the strip. The wire comes out with a rather thick coating of glass, which incloses air between the glass and the platinum at many points and does not adhere very well. Now make a smaller hole through the strip about 1.5 times the diameter of the wire. Thread the end of the wire through, heat, and draw as before, but

without adding any more glass. This second operation removes most of the air from the glass and makes the coating adhere much better. Finally anneal the coating by running the wire slowly through the very tip of a blowpipe flame, even beyond the point at which the flame is visible. The wire should now be difficult to distinguish from the uncoated wire without the aid of a magnifying glass. The coating should adhere perfectly, even when the wire is bent through a rather short radius. Sealing-in glass must never be heated except in a strongly oxidizing flame, since it contains lead which is easily reduced to the metallic form and will alloy with the platinum. Even a very small amount of lead will change the properties of the wire in such a way as to make it useless.

*Indicating Instrument.*—A contact-making voltmeter is to be provided for each detector bridge. This voltmeter should give full scale deflection on 0.5 volt when in series with 25 ohms. The instrument should be of rugged construction, capable of being mounted on a switchboard at the observing point. The voltmeter is to be provided with a contact-making attachment which closes an independent circuit when the pointer reaches a certain position, fixed by an extra adjustable pointer, which indicates the percentage at which the alarm is sounded. The contact-making attachment shown in Fig. 18 could be attached to a standard instrument if desired.

*Accessory Apparatus.*—The indicating and control apparatus for all the detectors is to be mounted on a switchboard. On the front of the board are one main switch, one indicating lamp, the contact-making voltmeters, and one cut-out switch for each of the latter. The ballast resistance and the alarm bell can be placed on the back of the switchboard.

The indicating lamp serves to show when the detectors are in operation. A 6-volt, 10-watt tungsten lamp is suitable for this purpose.

The ballast resistance should be made similar to any of the reliable resistance units in common use. The total resistance is to be determined by the number of indicators and the voltage of the supply circuit, and should be such that 1 ampere will flow through the circuit when all the detectors, the indicating lamp, and the ballast resistance are connected in series.

The switches are to be capable of handling 1 ampere at 110 volts under the conditions of use. Ordinary snap switches will usually serve the purpose.

SUPPORTING BASE ~ B

SECTION THRU  
ASSEMBLED APPARATUS  
AT X-X.

DETECTOR ELEMENT ~ A.

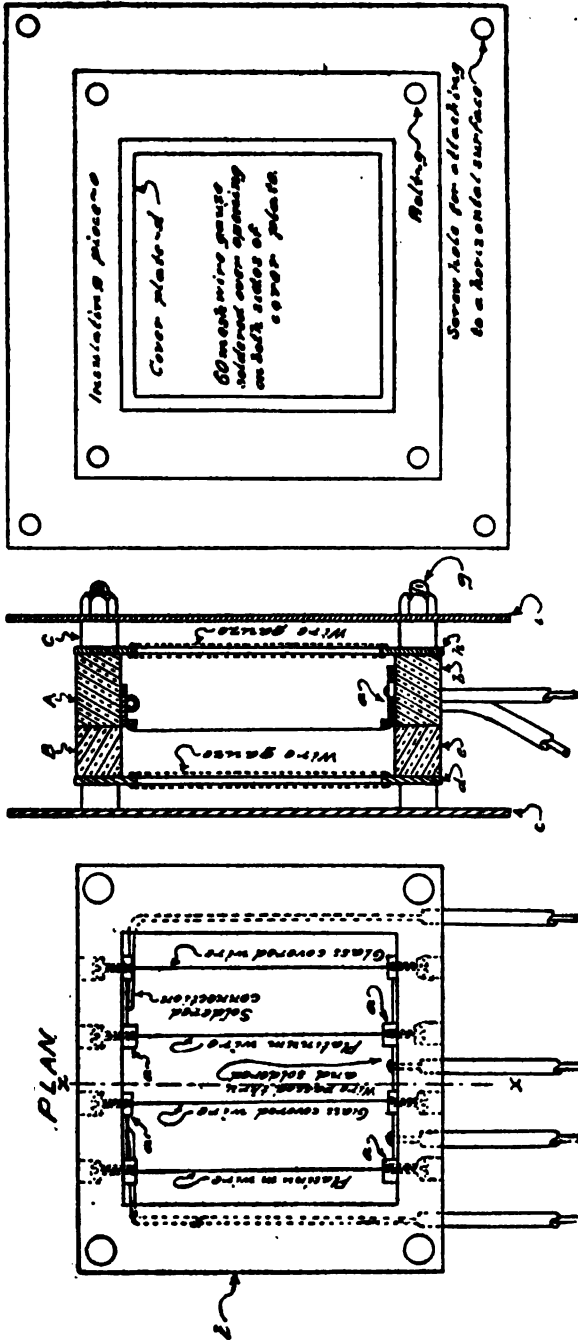


FIG. 19.—Construction of detector bridge

The alarm bell can be of any approved type, operating at the voltage of the supply circuit, or a relay may be connected in place of the bell and used to operate any mechanism desired.

*Connections.*—The apparatus for a four-station equipment may be connected as shown in Fig. 20. If more or less than four stations are installed together, the method of wiring would be similar. The bridges may, of course, be connected in parallel and a separate alarm may be used with each if desired.

The connections between the parts of the apparatus are made with conductors not smaller than 0.8 mm (or No. 20 American

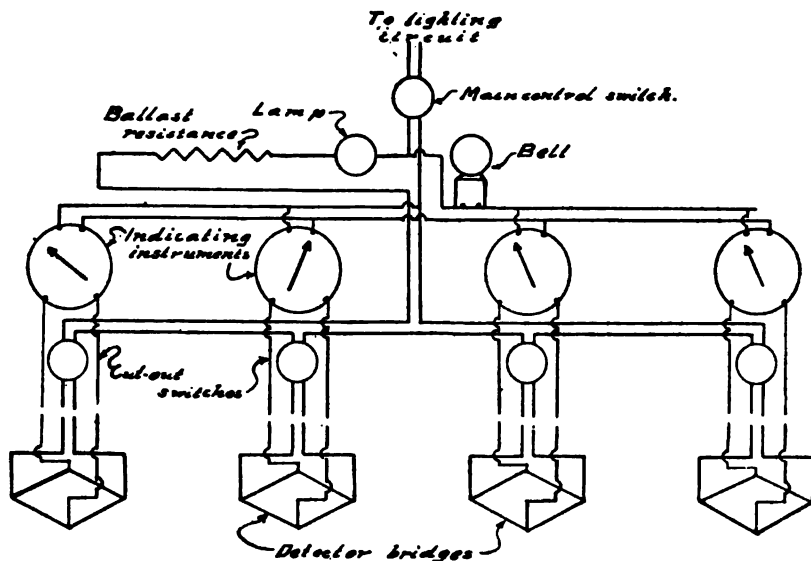


FIG. 20.—Diagram of connections for 4-station installation of bridge indicators

wire gage) copper wire. A four-conductor cable is used to connect each detector to the switchboard apparatus. The connections between the cable and the wires from the detector must be well made, suitably insulated, and protected from mechanical injury.

*Calibration.*—The detector bridge is balanced for a current of 1 ampere when in air containing no combustible gas. This may require a slight adjustment of the length of one or more of the detector wires.

The scale of the indicating instrument is calibrated by comparison with gas analyses. This is accomplished by operating the detector in a chamber of convenient size, through which a stream of air containing a constant percentage of combustible gas

is passed at a constant rate until the reading of the indicator is constant. A sample of air is then drawn from a point near the detector case and analyzed by any reliable method. Since the detector reading is very nearly proportional to the amount of gas present, it is often sufficient to determine one point in the scale, and it will never be necessary to determine more than two or three points.

If the instrument is to be used only to indicate danger from explosion, the following method of calibration is easy and should be sufficiently accurate: Divide the scale of the indicating instrument into equal parts, reading from 0 to the explosive limit of the gas, place the detector in an atmosphere containing a known percentage of the gas equal to about three-fourths the explosive percentage, and adjust the resistance in series with the voltmeter until the reading is correct.

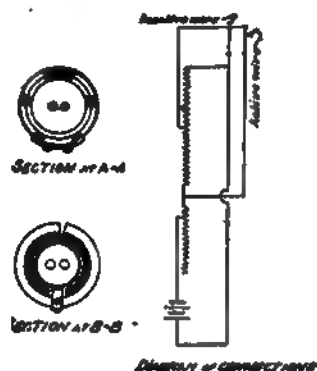
A continuous stream of gas mixture of known and uniform composition can be obtained by the use of geared meters, as shown in Fig. 2. To use this method successfully, it is best to have meters, one of which passes only about one-tenth the volume of gas per revolution that is passed by the other. The gas pressure on the meter passing the smaller volume of gas should be governed very accurately (within a few millimeters of water pressure) and the governor should pass a considerable volume of gas without any appreciable change in pressure. The connections from the meters through the mixing and testing chambers to the outlet should be large enough so that there will be no considerable back pressure upon the meters at the rate of flow used.

*Operation.*—When connected up as directed, it is only necessary to close the main switch to put the indicators in operation. As long as the indicator lamp is lighted and the bridges are balanced there is no probability that anything is wrong with the instruments. If the indicator lamp goes out, the cut-out switch for each instrument should be closed in turn. If the lamp lights up, the bridge then "cut out" is at fault and should be repaired, the other instruments remaining in service until this is accomplished. If, for any reason, it is suspected that oil or other impurity may have reached the active wires and rendered them inactive, they should be heated to a high temperature for a minute or two by increasing the current through the instruments to 1.5 amperes. This current will not injure the detector and will remove any probable impurity which would render the wires inactive. When the bridge is first used, the wires must always be "glowed" in this manner.

## 2. GLOWING-WIRE INDICATOR

Fig. 21 shows the details of construction and a diagram of connections for a portable glowing-wire indicator of the form believed to be most suitable for general use. The following specifications apply to this instrument:

*Wires.*—The active and inactive wires are to be of pure platinum 0.05 mm (2 mils) in diameter and 2 cm long. One wire is made inactive by coating with "sealing-in" glass.



LONGITUDINAL SECTION

FRONT ELEVATION

FIG. 21.—Portable glowing-wire indicator

*Cap.*—A cylindrical cap covered with double protective gauzes with 25 meshes per cm or 60 meshes per inch and containing a glass or mica observing window is to be provided as shown. The portion of the cap opposite the window is to be blackened to afford a dark background for observing the wires. The cap is to be held in position by the end plug, which can be removed to allow access to the wires.

*Rheostats.*—The rheostats are to be made by winding resistance wire of constantan or other equally good resistance material on the

insulating core. Bakelite is a suitable material for the core. The sliding contacts must make good electrical connections between the rheostat wires and the outside brass tube.

*Battery.*—The battery should be capable of furnishing, at some position of the series rheostat, 0.9 ampere total current. From five to nine small cells, such as are used with pocket flash lights, should be satisfactory. Provision should be made for readily opening the battery case for renewing the battery.

*Calibration.*—The portable glowing-wire indicator should be calibrated in the following manner:

1. With the indicator in a gas-free atmosphere and shaded from any very bright light, adjust the two rheostats so that the two wires are equally bright. Mark the position of the slide of the 15-ohm rheostat as 0.0. In making this and all other settings, the brightness at which the most consistent settings can be made should be used. This will be when the radiated light from the wires is just distinctly visible.

2. With the indicator in atmospheres containing known percentages of the gas to be tested for, adjust the positions of the rheostats until both wires show the same brightness as before. Mark the positions of the slide on the 15-ohm rheostat with the known percentage of gas. Unless great accuracy is desired, it will be unnecessary to determine more than three points on the scale. One of these is the position corresponding to no combustible gas present; one the position and percentage corresponding to no current through the active wire. The concentration for the third point should be equal to about 80 per cent of that required to keep the active wire glowing without electrical heat.

3. A scale should be marked on the brass tube, using the observed positions as reference marks and making the divisions between reference marks equal.

### 3. BIMETALLIC DETECTOR

Specifications are given below for a bimetallic detector believed to be suitable for operating an alarm at small percentages of all combustible gases. Fig. 16 shows details of construction and a diagram of connections.

*Wires.*—The active and inactive wires are to be of pure platinum 0.05 mm (2 mils) in diameter, and about 15 cm long. The one wire is to be rendered inactive by means of a thin coating of "sealing-in" glass. The wires are to be supported 1 mm below

the bimetallic strips by means of small perforated mica pieces spaced about 2.5 cm apart.

A small flexible wire is to be provided to make connection between the insulated contact block mounted at the end of one strip and the binding screw to which one terminal of the alarm is to be connected.

*Bimetallic Strips.*—The length and width of the bimetallic strips should be as shown in the figure. The thickness depends upon the material used, which should be such that the end of a piece 10 cm long will move 5 mm when the temperature of the strip is changed 50° C. A bimetallic strip made from brass 0.25 mm thick firmly fastened to a strip of a nickel-steel alloy 0.25 mm thick operated satisfactorily.

*Other Details.*—An adjusting screw is to be provided equivalent to the form shown, for varying the distance between the contacting points in order to vary the percentage at which the alarm will operate.


A case is to be provided with openings covered with double gauzes of 25 meshes per cm (60 meshes per inch).

The detector is to be so arranged that electrical connections to the source of current and to the alarm can be readily made.

*Calibration.*—The operating current is to be 0.5 ampere if hydrogen, carbon monoxide, illuminating gas, or the vapor of most organic liquids is to be detected, but 0.7 ampere if methane is to be detected.

The screw should be adjusted so that contact is not made when the normal operating current is flowing and no combustible gas is present, but so that it just operates when the device is placed in an atmosphere containing the percentage of the gas which it is desired to detect.

WASHINGTON, April 18, 1918.









DEPARTMENT OF COMMERCE

---

**SCIENTIFIC PAPERS**  
OF THE  
**BUREAU OF STANDARDS**

S. W. STRATTON, DIRECTOR

---

No. 335

**EFFECT OF RATE OF TEMPERATURE CHANGE  
ON THE TRANSFORMATIONS IN AN  
ALLOY STEEL**

BY

HOWARD SCOTT, Assistant Physicist  
*Bureau of Standards*

---

ISSUED JULY 10, 1919



**PRICE, 5 CENTS**

Sold only by the Superintendent of Documents, Government Printing Office  
Washington, D. C.

---

WASHINGTON  
GOVERNMENT PRINTING OFFICE  
1919



# EFFECT OF RATE OF TEMPERATURE CHANGE ON THE TRANSFORMATIONS IN AN ALLOY STEEL

By Howard Scott

## CONTENTS

	Page
I. Introduction.....	91
II. Previous investigations.....	92
III. Experimental method.....	93
IV. Thermal curves.....	93
V. Effect of cooling rate.....	96
1. Microstructure.....	96
2. Relation of $Ar'$ to $Ar''$ .....	97
3. Suppression of $Ar'$ .....	97
VI. Transformations on heating.....	98
1. Transformation $Acr$ .....	98
2. Effect of previous cooling rate on $Acr-3$ .....	99
VII. Summary.....	100

## I. INTRODUCTION

Since Böhler discovered in 1903, on cooling certain alloy steels, the phenomenon of a new and lower temperature transformation than the usual  $Ar_{3-2-1}$  obtained by increasing the maximum temperature ( $T_{max}$ ) to which the material was heated, a considerable amount of work has been published,<sup>1</sup> connecting this phenomenon with a large number of dissimilar steels of high alloy content. From the fact that the transformation divides itself, taking place at two widely separated temperatures, it has been called a split transformation. The significant facts established by recent investigators<sup>2</sup> are (a) that when the transformation occurs at the higher temperature,  $Ar'$ , troostite or a decomposition product is formed and (b) that when the transformation occurs at the lower temperature,  $Ar''$ , the resulting structure is martensite. The terminology  $Ar'$  and  $Ar''$ , adopted here, is that of Portevin.<sup>3</sup>

<sup>1</sup> Yatskevitch, *Rev. de Met.*, 15, p. 65; 1918, Bibliography to 1915.

<sup>2</sup> Dejean, *Rev. de Met.*, 14, p. 641; 1917. Portevin, *ibid.*, 14, p. 707; 1917. Edwards, *J. Iron and Steel Inst.*, 98, p. 114; 1916.

<sup>3</sup> Portevin, *loc. cit.*

## II. PREVIOUS INVESTIGATIONS

Reviewing the work on this subject <sup>4</sup> published in a recent issue of *Revue de Metallurgie* and referring in particular to his statement that martensite is a solution of carbide in alpha iron, H. Le Chatelier says:

How then can a theory already 20 years old demand new investigations? The reason for it is that we have not succeeded in proving directly the real presence of the transformation of iron during the very short duration of the quenching. The fall of temperature takes place at the rate of several hundred degrees per second and the observation of phenomena so rapid requires particularly sensitive methods of recording. I have attempted without success to observe the moment of the reappearance of the magnetic property during the quenching of bars 15 mm square, but the inequalities of temperature from one point to another in the mass conceal the phenomenon. M. Chevenard <sup>5</sup>, in working on wires of a diameter 100 times smaller and using as a characteristic of the transformation of iron the change of length instead of the variation of magnetism, has surmounted for the first time the difficulties which seemed at first view insurmountable, and he has done it with an extreme precision. The thermal measurements of Portevin and Garvin <sup>6</sup> and of Dejean <sup>7</sup> lead to the same conclusions, although in a fashion less direct.

The results presented here add further confirmation of the theory of Le Chatelier, though in a less direct manner than those of Chevenard. Thermal and microscopic data are brought forward here to establish the effect of rate of temperature change on the temperature and nature of the transformations in a steel of the composition C, 1.75; Mn, 0.26; Co, 2.90; Cr, 15.0.

Similar work has been done by Edwards <sup>8</sup> on a steel of the composition C, 0.63; Cr, 6.15; Si, 0.07; Mn, 0.17.

However, he arrives at the conclusion that—

The maximum hardness was obtained when the thermal transformation had been entirely prevented, and when this was accomplished the steel was purely martensitic in structure.

The present work fails to confirm this statement, as does that of the investigators already referred to. Edwards was unable to observe the transformation  $Ar''$  with the formation of martensite, probably for the reasons given by Rosenhain <sup>9</sup> in his discussion of Edwards' paper.

Yatsevitch, <sup>10</sup> Dejean <sup>11</sup>, and Honda <sup>12</sup> have used two or three cooling rates in their experiments with varying  $T_{max.}$ , and their results show, as do Edwards's that the transformation split occurs for lower values of  $T_{max.}$  with faster cooling rates.

<sup>4</sup> Le Chatelier, *Rev. de Met.*, 14, p. 602; 1917.

<sup>5</sup> Chevenard, *Rev. de Met.*, 14, p. 610; 1917.

<sup>6</sup> Portevin and Garvin, *Rev. de Met.*, 14, p. 607; 1917.

<sup>7</sup> Dejean, *Rev. de Met.*, 14, p. 641; 1917.

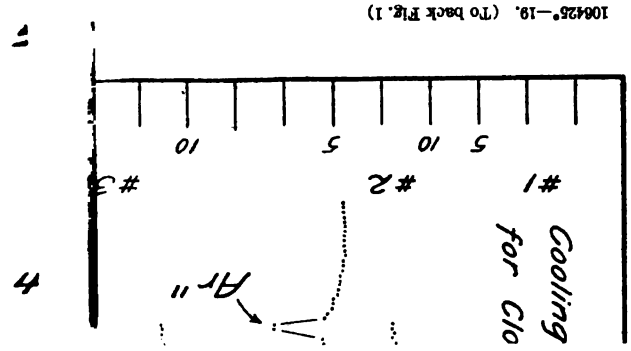
<sup>8</sup> Edwards, loc. cit.

<sup>9</sup> Rosenhain, *J. Iron and Steel Inst.*, 98, p. 247; 1916.

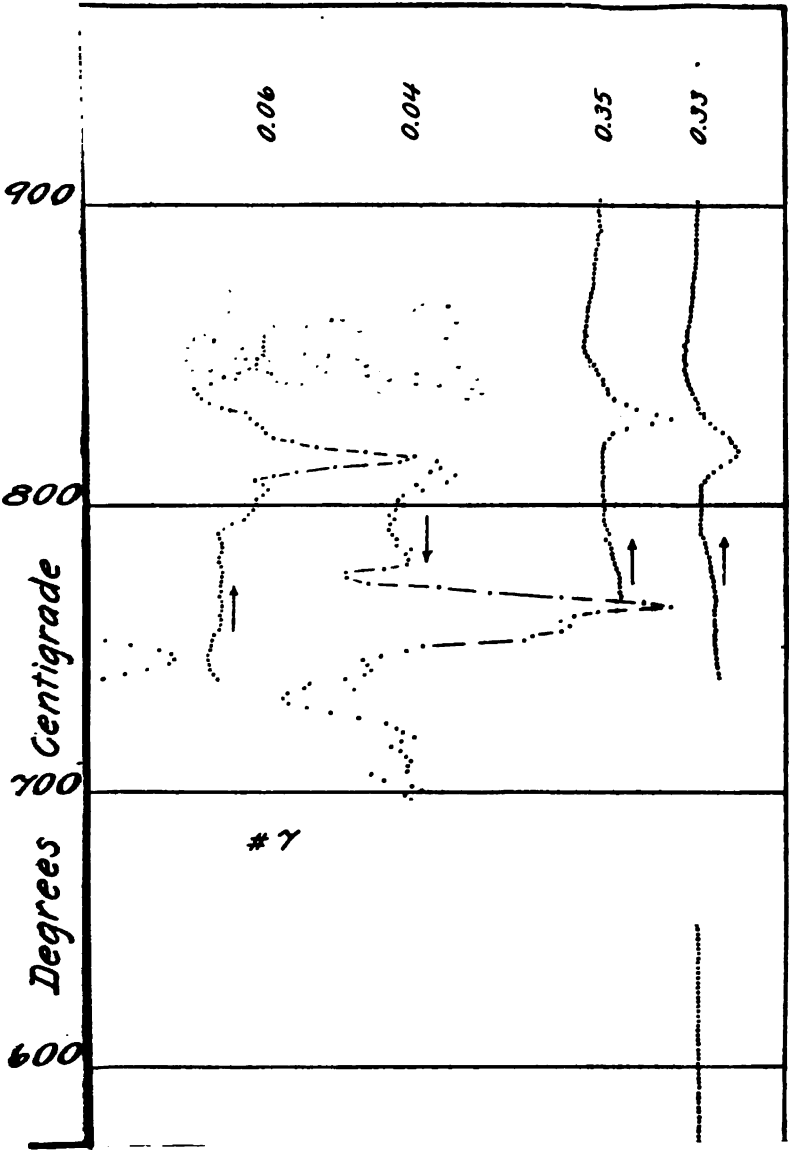
<sup>10</sup> Yatsevitch, loc. cit.

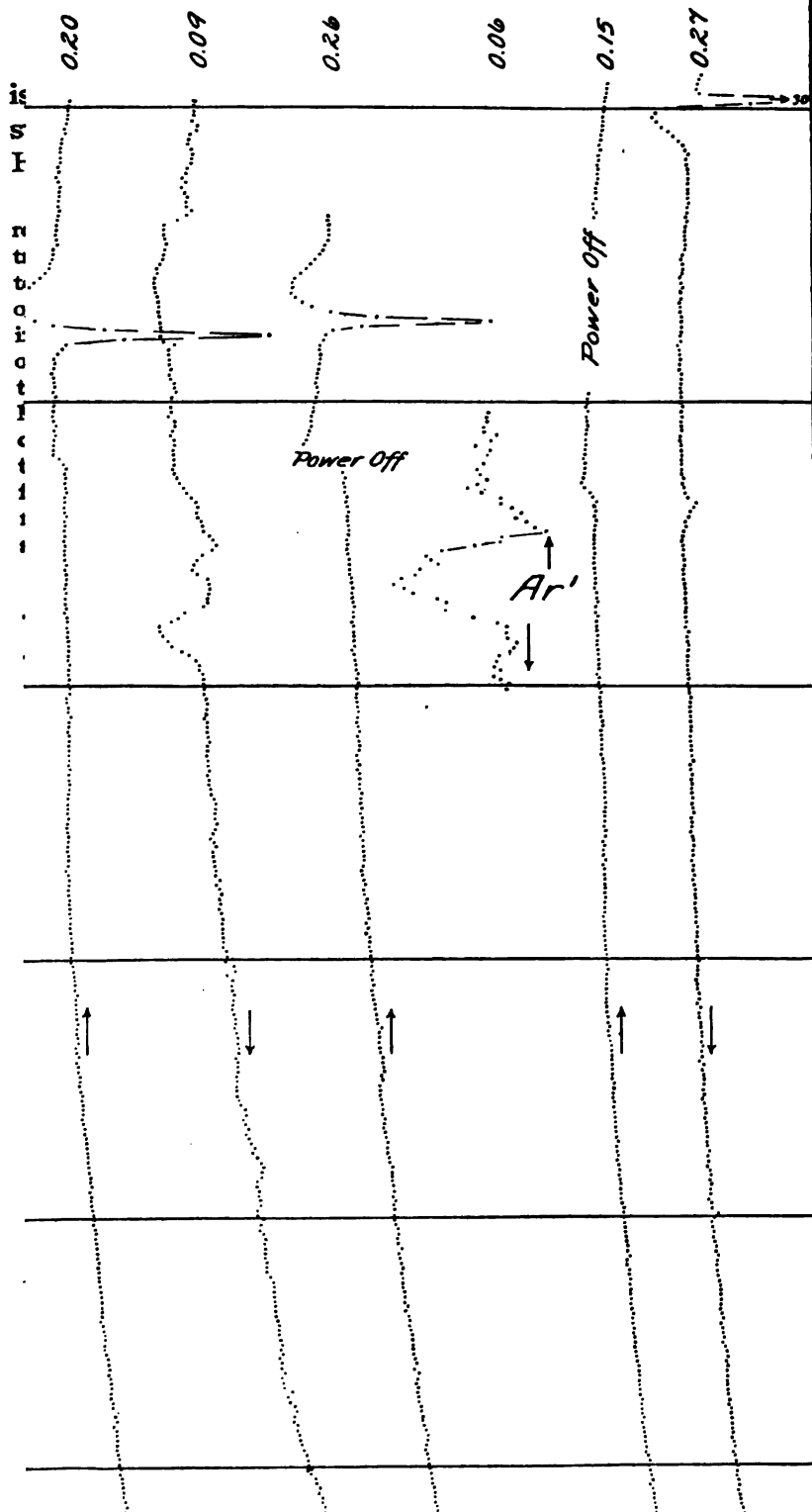
<sup>11</sup> Dejean, loc. cit.

<sup>12</sup> Honda and Murakami, *Sci. Rep. Tohoku Imp. Univ.*, 6, p. 235; 1918.



106426-19. (To back Fig. 1)







The previous investigators in this field have laid particular stress on the variation of  $T_{\max.}$ , the rate remaining constant, while the variation of rate,  $T_{\max.}$  remaining constant, has received little attention. The present work attempts to apply the latter method to the investigation of an alloy steel with the object in view of correlating the results of that method with those of the former and to establish the relationship between the several phenomena observed.

### III. EXPERIMENTAL METHOD

The method employed for obtaining the thermal curves was to heat the samples, attached to the hot junction of a 0.5 mm diameter platinum, 90 platinum-10 rhodium thermocouple, in an electric vacuum furnace, taking potential measurements on a dial potentiometer and measuring the time interval on a chronograph, as described in the Bureau of Standards Scientific Paper 213. The furnace, however, was one recently built at the Bureau, a modified form of the one described by Rosenhain<sup>18</sup> and in use at the National Physical Laboratory. This furnace, which will be described at a later date, was admirable for the purpose at hand, as extreme rates of temperature change can be obtained with smooth curves over long ranges.

### IV. THERMAL CURVES

The curves of Figs. 1 and 2 were plotted by the inverse rate method from readings taken every 0.02 millivolt (approximately 2° C) except for several extremely fast runs, which, however, are plotted on that basis.

The curves of Fig. 1 are a preliminary series taken on sample A of about 10 g mass to locate the transformation ranges and without fully knowing the characteristics of the material. The data for the curves of Fig. 2 were taken on sample B, mass 0.81 g, keeping  $T_{\max.}$  constant and extending the observations to lower temperatures than for sample A. The values given for rate of temperature change were reduced from the inverse rate curve observations taken on heating just before  $Ac_1-3$  and on cooling midway between  $Ar'$  and  $Ar''$ .

The transformations as designated on the curves of Figs. 1 and 2 are  $Act$ , an evolution of heat on heating a sample previously cooled at a rate that gave  $Ar''$ ;  $Ac_2$ , the magnetic transformation;  $Ac_1-3$ , the transformations  $Ac_1$  and  $Ac_3$  merged or nearly superimposed;  $Ar'$ , the upper transformation of the split  $Ar$  transformations; and  $Ar''$ , the lower transformation. The temperature values of these transformations are collected in Table 1.

<sup>18</sup> Rosenhain, *Inst. of Metals*, 18, p. 164; 1915.

TABLE 1.—Temperature Ranges of Transformations in Degrees Centigrade

SAMPLE A

Run	Rate of heating °C. per second	Ac <sub>1</sub>		Ac <sub>2</sub>	Ac <sub>1-3</sub>			Ar'		Ar''		T. max.
		Begin- ning	Maxi- mum		Begin- ning	Maxi- mum	End	Begin- ning	Maxi- mum	Begin- ning	Maxi- mum	
First.....	0.20	.....	.....	781	825	834	856	787	785	.....	.....	1050
Second.....	.30	.....	.....	781	819	829	855	742	715	446	414	985
Third.....	.06	.....	.....	780	.....	816	841	.....	760	740	.....	1110
Fourth.....	1.09	.....	.....	782	.....	836	.....	.....	.....	.....	.....	970
Fifth.....	.25	.....	.....	781	804	816	847	755	.....	422	396	925
Sixth.....	.08	.....	.....	780	794	809	836	772	748	714	.....	880
Seventh.....	.06	.....	.....	780	809	817	841	776	766	734	.....	870
Eighth.....	.35	.....	.....	778	821	831	854	.....	.....	.....	.....	925
Ninth.....	.33	.....	.....	.....	809	819	847	.....	.....	401	385	925

SAMPLE B

Run	Rate of heating °C. per second	Ac <sub>1</sub>		Ac <sub>2</sub>	Ac <sub>1-3</sub>			Rate of cooling °C. per second	Ar'		Ar''		T. max.
		Begin- ning	Maxi- mum		Begin- ning	Maxi- mum	End		Begin- ning	Maxi- mum	Begin- ning	Maxi- mum	
First.....	0.27	592	637	780	808	818	840	3.40	( <sup>a</sup> )	.....	381	373	920
Second.....	.31	578	634	780	809	816	832	1.20	.....	.....	429	[409] [394]	920
Third.....	.31	544	601	779	808	816	832	.60	748 <sup>a</sup>	706	442	[429] [405]	920
Fourth.....	.33	518	621 <sup>a</sup>	778	813	818	835	.50	740	711	442	[430] [410]	920
Fifth.....	.20	564	601 <sup>a</sup>	778	807	818	829	.43	748	[719] [694]	449	[430] [410]	920
Sixth.....	.20	.....	.....	778	814	824	835	.17	759	[743] [719]	.....	.....	920
Seventh.....	.20	.....	.....	778	814	824	835	.09	775	[731] [756]	.....	.....	920
Eighth.....	.26	.....	.....	.....	821	829	842	.06	770	756	.....	.....	920

<sup>a</sup> Rate of cooling too fast for close observations.

The appropriateness of the transformation notation  $Ac1-3$  and  $Ar1$  will be seen from the discussion of those transformations.

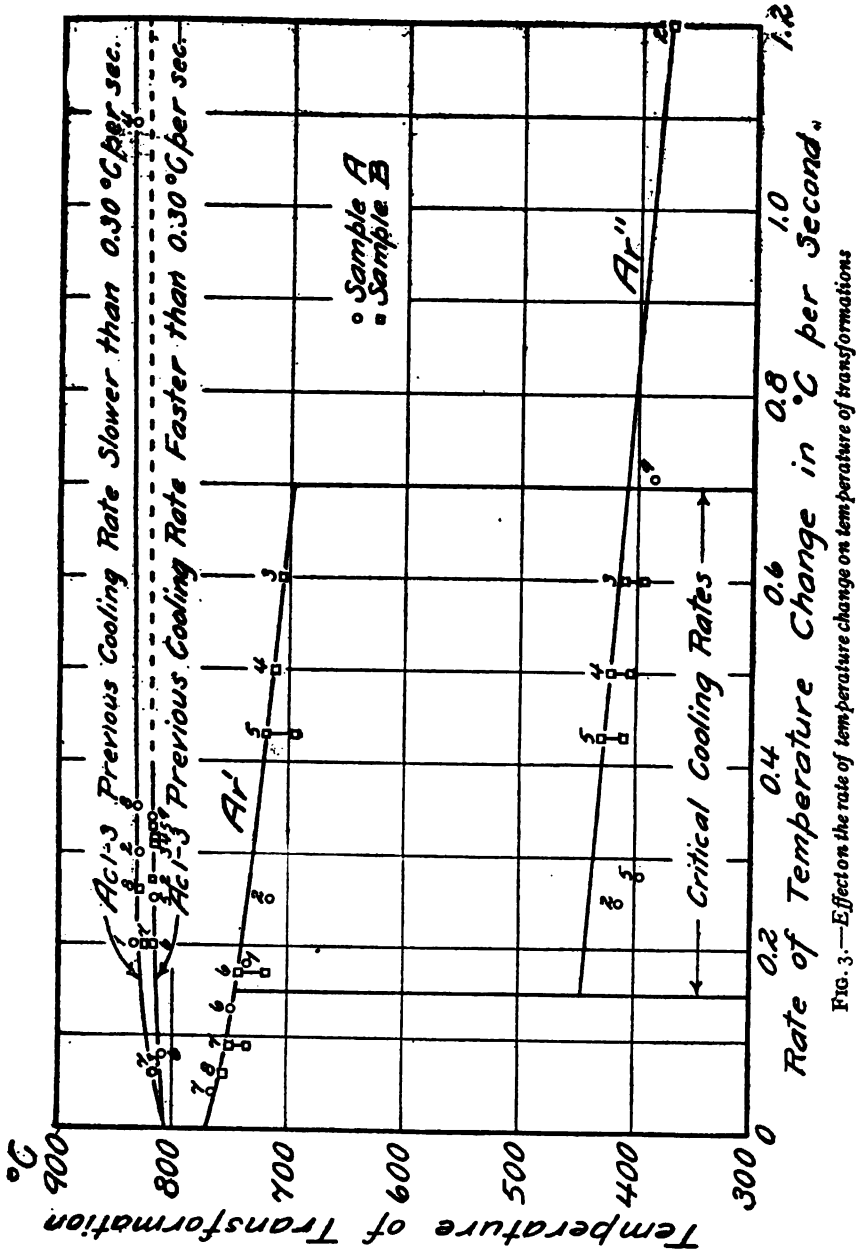


FIG. 3.—Effect on the rate of temperature change on temperature of transformations

Two values for the maximum transformation temperature indicate a double peak. In Fig. 3 the temperature values of  $Ac1-3$ ,  $Ar1$ , and  $Ar2$  given in Table I are plotted against rate of temperature

change in degrees centigrade per second. No attempt is made to interpret the double peaks, and the lines representing  $Ar'$  and  $Ar''$  in Fig. 3 are rather arbitrarily drawn through the higher values.

## V. EFFECT OF COOLING RATE

An inspection of the cooling curves of Figs. 1 and 2 shows that  $Ar'$  is the normal  $Ar_{3-2-1}$  of slow cooling rates, but that it gradually dies off in intensity with increasing rate. While  $Ar'$  is falling off in intensity, the transformation  $Ar''$  comes into existence and gains in intensity, being a maximum for rates that do not show  $Ar'$ .

This region over which both  $Ar'$  and  $Ar''$  occur, as shown in Fig. 3, will be called the critical cooling range. Its limits were roughly determined as 0.15 and 0.70° C per second, by plotting a measure of the transformation intensities, obtained by a method to be described in a subsequent section, against rate and extending a straight line through the values back to zero.

The remarkable change in properties caused by this very slight change in rate is represented, when the same phenomenon is observed on varying  $T_{max.}$ , by the considerable temperature variation of approximately 300° C for some high-speed steels.<sup>14</sup>

The fact that the split transformation occurs with a constant value of  $T_{max.}$  shows that it is unnecessary to hypothecate a dissociation of the carbide (or carbides) to explain this phenomenon.

### 1. MICROSTRUCTURE<sup>15</sup>

To establish the structural difference between the material cooled at a rate that gave  $Ar'$  and one that gave  $Ar''$  and the analogy to the phenomena obtained by varying  $T_{max.}$  for this steel, micrographs were taken of samples cooled at several definite rates of cooling. The micrograph, Fig. 4, taken after cooling at a rate of 0.01° C per second,  $Ar'$  only occurring, shows an irregular mass of fine carbide particles, corresponding to pearlite in carbon steels and distinct from the coarse particles of free carbide, in a ferrite matrix. Figs. 5 and 6, micrographs, taken of samples cooled at rates of 0.30 and 0.33° C per second, respectively, show characteristic black troostite patches on a background of martensite. With those cooling rates the transformations  $Ar'$  and  $Ar''$  were both obtained. Fig. 7, which is of sample A following a cooling rate of 0.71° C per second, shows a martensitic structure although the

<sup>14</sup> Honda and Murakami, loc. cit.; Carpenter, loc. cit.

<sup>15</sup> Micrographs by H. S. Rawdon.

FIG. 4.—*Cooling rate, 0.01° C per second. Transformation  $A\gamma'$*   
Magnification 1000x. Etched in 2 per cent  $\text{HNO}_3$  in alcohol

FIG. 5.—*Cooling rate, 0.30° C per second. Transformation  $A\gamma'$  and  $A\gamma''$*   
Magnification 1000x. Etched in 2 per cent  $\text{HNO}_3$  in alcohol

FIG. 6.—Cooling rate,  $0.33^{\circ}$  C per second. Transformation  $Ar'$  and  $Ar''$   
Magnification 2000x. Etched in 2 per cent  $HNO_3$  in alcohol

FIG. 7.—Cooling rate,  $0.71^{\circ}$  C per second. Transformation  $Ar''$   
Magnification 2000x. Etched in 2 per cent  $HNO_3$  in alcohol

needlelike markings, characteristic of high-carbon steels, are only slightly evident.

The conclusions to be drawn from the preceding microscopic evidence are that troostite or a decomposition product forms with the transformation  $Ar'$  and martensite with the transformation  $Ar''$ , precisely what obtains when the same transformations are observed in other alloy steels with varying  $T_{max}$ .

## 2. RELATION OF " $Ar'$ " TO " $Ar''$ "

The radical structural difference between the material showing  $Ar'$  and that showing  $Ar''$  presumes a similar radical difference in the transformations  $Ar'$  and  $Ar''$ . To demonstrate the possibility of this difference, the intensities of the transformations  $Ac1-3$ ,  $Ac2$ ,  $Ar'$ , and  $Ar''$  have been estimated by means of a planimeter measuring the area of the positive departure of the thermal curves from the assumed neutral body curves through the respective transformation ranges. The results given in Table 2 show a well-marked loss in intensity of the sum of the areas of  $Ar'$  and  $Ar''$  at the cooling rate  $1.20^\circ \text{C}$  per second, which gives  $Ar''$  above. On the assumption that  $Ar''$  is no new transformation other than  $Ar_3$ ,  $2$ , or  $1$ , the conclusion is that some one or more of the transformations  $Ar_3$ ,  $2$ , and  $1$  constituting  $Ar'$  is suppressed.

TABLE 2.—Areas of Thermal Curves in Square Millimeters Corresponding to Heat Effects of Transformations in Sample B

Run	$Ac1-3$	$Ac2$	$Ac1-3 +$ transformation $Ac2$	Cooling rate, de- grees per second	$Ar'$	$Ar''$	$Ar'$ trans- forma- tion + $Ar''$
First.....				3.40			
Second.....	36	74	110	1.20		84	84
Third.....	40	66	106	.60	26	72	98
Fourth.....	40	68	108	.50	38	60	98
Fifth.....	64	64	128	.43	56	48	104
Sixth.....	60	64	124	.17	100		100
Seventh.....	72	72	144	.09	120		120
Eighth.....	72			.06	116		116
Average.....		68	120				

## 3. SUPPRESSION OF " $Ar_1$ "

The preceding conclusion agrees with the generally accepted conception that martensite is a solid solution of cementite in some form of iron. This means that  $Ar_1$  is suppressed with the formation of martensite and further evidence is not wanting. The transformation intensities indicate that a heat effect of the mag-

nitude of  $Ar_1$  is missing at  $Ar''$ . The work of Honda on the magnetic properties of tungsten steels in a paper before the September meeting of the Journal of the Iron and Steel Institute, however, shows that the carbide is retained in solution at  $Ar''$  for the carbide in solution does not undergo the transformation  $A_0$ . The transformations  $Act$  and  $Ac_{1-3}$  offer still further substantiation to which attention will be called in their discussion.

There still remains the possibility that one of the other transformations,  $Ar_3$  or 2, is suppressed. This, however, is manifestly impossible, for  $A_3$  and  $A_2$  coincide when  $A_3$  is depressed below the normal temperature of  $A_2$ <sup>16</sup> and martensite is magnetic. The magnetic curves of Honda and Murakami<sup>17</sup>, taken on a number of tungsten steels showing a split transformation with increasing  $T_{max}$ , also indicate the occurrence of  $A_2$  at  $Ar''$ .

The conclusion that must therefore be adopted is that  $Ar_1$  is suppressed with the formation of martensite, or that  $Ar''$  constitutes the transformations  $Ar_3$  and 2.

## VI. TRANSFORMATIONS ON HEATING

The thermal curves of Figs. 1 and 2 show two transformations  $Ac_{1-3}$  and  $Ac_2$  occurring uniformly within narrow temperature limits and a transformation  $Act$  occurring only following certain cooling rates. The identity of  $Ac_2$  is established by its markedly characteristic shape and its uniform occurrence at about  $780^\circ\text{C}$  which is in close proximity to its maximum,  $768^\circ$ , in pure iron. This phenomenon of  $Ac_1$  occurring above  $Ac_2$  in alloy steels is not new and has been well established by Moore<sup>18</sup> for a chromium steel. The transformation  $Ac_{1-3}$  hardly needs identification, although attention should be called to its sluggish ending which indicates that the transformations concerned do not completely coincide. This is further illustrated by the change in area of the peak, which is evidently  $Ac_1$  from the effect of previous cooling rate on its position, with the temperature of its occurrence.

### 1. TRANSFORMATION " $Act$ "

The transformation  $Act$  is indicated by an inflection to the left which denotes an evolution of heat on the heating curve and occurs over a considerable temperature range. It is a maximum following cooling rates that give  $Ar''$  alone, and loses in intensity following decreasing rates through the critical cooling range, becom-

<sup>16</sup> Honda and Takagi, *Sci. Rep. Tohoku Imp. Univ.*, 6, p. 324; 1918.

<sup>17</sup> Honda and Murakami, *loc. cit.*

<sup>18</sup> Moore, *J. Iron and Steel Inst.*, 81, p. 268; 1910.



ing zero when  $Ar'$  alone occurs. It is therefore roughly proportional in intensity to  $Ar''$  or the amount of martensite present. By its analogy to tempering the conclusion may be drawn that  $AcI$  represents the precipitation of the carbide in solution to form at first troostite and as it progresses the coarsening of the carbide.

This phenomenon of a heat evolution on heating steels that show  $Ar''$  was observed by Carpenter<sup>19</sup> on differential thermal curves with which  $T$  max. was varied and connected with tempering.

The nature of  $AcI$ , a gradual building up of the heat evolution over a long temperature range, may throw some light on the spontaneous heat evolution and also the change in other physical properties of quenched steels as observed by Hadfield and Brush<sup>20</sup>, by Matsushita<sup>21</sup>, and by Campbell<sup>22</sup>. The indications are that the transformation starts to a minute degree at very low temperatures, possibly at ordinary temperatures, particularly in carbon-steels which temper at lower temperatures than alloy steels.

The existence of  $AcI$  as an evolution of heat following cooling rates that give  $Ar''$  is further confirmation of the suppression of  $ArI$  with the formation of martensite.

## 2. EFFECT OF PREVIOUS COOLING RATE ON " $AcI-3$ "

It will be seen on examining Fig. 3 that practically all the temperature values for the maximum of  $AcI-3$  lie on two smooth curves. The data of Table 1 show that the runs which correspond to the numbers on the upper curve were obtained following cooling rates that gave  $Ar'$  predominant and those on the lower curve following cooling rates that gave  $Ar''$  predominant. The temperature interval,  $10^{\circ}$  to  $15^{\circ}$  C, between those two curves may therefore be attributed to the state of division of the carbide resulting from the previous heat treatment.

The phenomenon noted in the preceding paragraph offers still further substantiation of the suppression of  $Ar'$  with the formation of martensite.

It may be of interest to note that the curves of Fig. 3 drawn through the temperature values of  $AcI-3$  and  $Ar'$  do not point toward a common equilibrium temperature  $AeI$ .

<sup>19</sup> Carpenter, *J. Iron and Steel Inst.*, **67**, p. 433; 1905.

<sup>20</sup> Hadfield and Brush, *Proc. Royal Soc.*, **88**, p. 188; 1917.

<sup>21</sup> Matsushita, *Sci. Rep. Tohoku Imp. Univ.*, **7**, p. 43; 1918.

<sup>22</sup> Campbell, *Reprint J. Iron and Steel Inst.*, **98**, p. 421; 1912.

## VII. SUMMARY

The results of previous investigators have been taken to show that with the occurrence of a split transformation on cooling alloy steels from increasingly higher temperatures (a) that when the higher temperature transformation  $Ar'$  is observed with low values of  $T_{max}$ , troostite or a decomposition product results and (b) that when the lower temperature transformation  $Ar''$  is observed with high values of  $T_{max}$ , martensite is the resulting product.

The present investigation has shown for a certain alloy steel that on varying the rate of cooling, the maximum temperature remaining constant, a strictly analogous phenomenon is observed, increasing rate of cooling having the same effect as increasing  $T_{max}$ .

Conclusions are drawn to the effect that—

(a) The transformation  $Ar'$  consists of the transformations  $Ar_3$ , 2, and 1.

(b) The transformation  $Ar''$  consists of the transformations  $Ar_3$  and 2.

(c) The transformation  $Ar_1$ , suppressed when  $Ar''$  is observed, occurs on heating as  $Ac_1$  with an evolution of heat and the formation of troostite or a coarser condition of the carbide.

(d) The maximum of the transformation  $Ac_1-3$  occurs at a higher temperature when the previous cooling rate gave  $Ar'$  than when it gave  $Ar''$ .

The author desires to express his indebtedness to H. S. Rawdon for the micrographic work and to Miss P. L. Thompson for her skillful assistance in preparing the experimental data.

WASHINGTON, December 23, 1918.



AUG 13 1919

DEPARTMENT OF COMMERCE

BUREAU OF STANDARDS

S. W. STRATTON, Director



SCIENTIFIC PAPERS OF THE BUREAU OF STANDARDS NO. 336

[ISSUED JUNE 11, 1919]

A SIMPLIFICATION OF THE INVERSE-RATE METHOD  
FOR THERMAL ANALYSIS

By P. D. Merica, Physicist

One of the most useful and at the same time least commonly used methods of thermal analysis for the determination of transformations in metals and alloys consists in the recording of the time intervals required for successive increments of temperature change during heating or cooling, the temperature of the furnace which contains the specimen being altered at a uniform rate. The curve obtained by plotting these time intervals as a function of the mean temperature of the specimen during the interval is called the inverse-rate curve. It is probably due to the fact that no simple and convenient method has apparently been available for the measurement of the successive time intervals that this method has not been so generally used as, for example, the differential method, for which, in addition, several types of automatic or semiautomatic apparatus have been designed.

Whenever this method has been used the intervals have usually been measured with the use of a chronograph. Its operation as practiced at the Bureau of Standards<sup>1</sup> is as follows: The temperature of the specimen is measured by thermocouple and dial potentiometer; the operator sets the potentiometer at successive values of the emf, differing by equal increments, usually 0.02 millivolt, and records the exact instant on the chronograph, by pressing a contact key, at which the galvanometer coil passes through its null position. Two-second intervals are also recorded

<sup>1</sup>G. K. Burgess and J. J. Crowe, Critical Ranges,  $A_2$  and  $A_3$  of Pure Iron, this Bulletin, 10 (Scientific Paper No. 213); 1913.

on the same chronograph record, and the number of seconds elapsing between successive signals is afterwards counted from the record and plotted as a function of the emf, or of the temperature.

This method is an admirable one, and by it most minute thermal arrests may be detected, but it requires the use of a good chronograph, which is generally difficult to obtain, and the time of one operator during the recording and subsequently to read the intervals from the record. The latter operation often takes from one to two hours. There is here suggested a simple, convenient, and, it is believed, equally accurate method of recording the successive time intervals by which the expense of chronograph and the time of one operator in counting the chronograph record may be eliminated. The remainder of the apparatus, consisting of furnace, thermocouple, and potentiometer, is used exactly as in the former method.

Two stop watches are used, which may conveniently be mounted in a small frame to be held in one hand, a finger being placed on each stem. During the "run" the operator sets the potentiometer and marks the instant at which the galvanometer is at zero by pressing the stems of both watches simultaneously, stopping one at the end of the interval which it has measured and starting the other upon its measurement of the next. The interval is read and recorded upon a suitable blank sheet, the hand of this watch returned to its zero position, and the potentiometer set at the next value. The operation is repeated for each successive interval. The intervals so recorded are afterwards plotted directly as a function of the emf.

Fig. 1 shows the inverse-rate curves for two complete "runs," including the heating and the cooling curve, made on pure iron. Both A<sub>3</sub> and A<sub>2</sub> are indicated on the first set of curves, only A<sub>2</sub> on the second set. In each case the intervals were recorded both with the stop watches and with the chronograph in the usual manner; the curves marked *c* were taken with chronograph, those marked *w* with stop watches. It is evident that there is little difference in the smoothness of the two sets of curves or in the accuracy or precision of measurement of the time interval.

A general consideration of the accuracy of the stop watch also indicates that the precision of measurement by stop watch is sufficient for the purposes of thermal analysis. It is only rarely, perhaps once in a hundred times, that a stop watch is not accu-

rate to within one-fifth of a second, and its maximum error is two-fifths of a second. It is found that the variation of successive intervals of time measured in the inverse-rate method, due to actual non-uniform rate of cooling or heating of the furnace, or to inaccuracy of the operator in signaling the moment when the potentiometer is balanced is of approximately the same value; that is, one-fifth of a second. It is therefore not necessary to

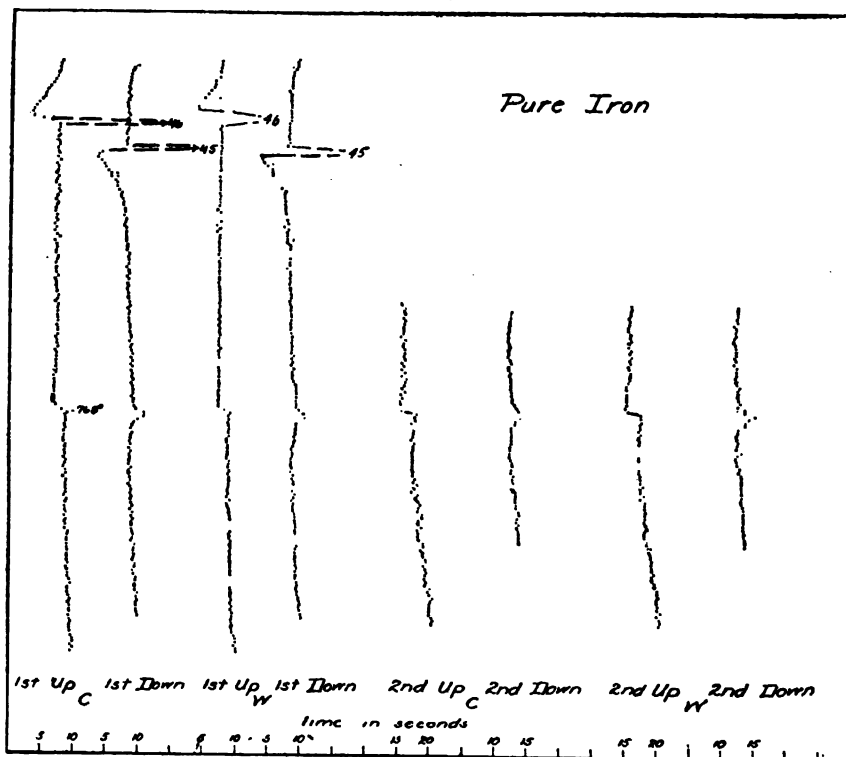


FIG. 1.—Heating and cooling inverse-rate curves of pure iron taken (C) with chronograph, and (W) with stop-watch

obtain the greater precision of time measurement which is unquestionably possible by the use of the chronograph.

When the ordinary dial type of precision potentiometer is used, the operator has sufficient time for all of the operations necessary: setting the potentiometer, reading and recording the time interval from the watch, within an average interval of 15 seconds. This is recommended for usual conditions.

The curves recorded above were taken with a cheap variety of stop watch, costing about \$10. It does not appear that a more

expensive watch is necessary. It is, however, not advisable to use the type of stop watch which has also the usual hour and second hands, as the presence of so many indicating hands will only confuse the operator, who is obliged to read quickly and can not take much time in recognizing the stop hand.

The author acknowledges the assistance of Miss H. G. Movius in obtaining the curves described above.

WASHINGTON, March 12, 1919.

---

ADDITIONAL COPIES  
OF THIS PUBLICATION MAY BE PROCURED FROM  
THE SUPERINTENDENT OF DOCUMENTS  
GOVERNMENT PRINTING OFFICE  
WASHINGTON, D. C.  
AT  
5 CENTS PER COPY  
V



TO WHOM  
IT MAY CONCERN



# CONSTITUTION AND METALLOGRAPHY OF ALUMINUM AND ITS LIGHT ALLOYS WITH COPPER AND WITH MAGNESIUM

By P. D. Merica, R. G. Waltenberg, and J. R. Freeman, jr.

## CONTENTS

	Page
I. Introduction.....	105
II. Constitution of commercial aluminum.....	106
III. Solubility of $\text{CuAl}_2$ in aluminum at different temperatures.....	111
Effect of magnesium on the solubility of $\text{CuAl}_2$ in aluminum.....	115
IV. Solubility of $\text{Mg}_2\text{Al}_3$ in aluminum at different temperatures.....	115
V. Solubility of metals and metal compounds in aluminum.....	118
VI. Summary and conclusions.....	118

## I. INTRODUCTION

Aluminum and its alloys have been the subject of much investigation <sup>1</sup> during recent years, in the course of which the principal features of the constitution of most of the binary alloy systems with aluminum have been determined.

Except in the case of a few metals—silicon, bismuth, cadmium, lead, zinc, and tin—an aluminum-rich compound is formed in each binary system, which forms a eutectic with the aluminum or its solid solution with this compound. Thus, such compounds as  $\text{FeAl}_3$ ,  $\text{CuAl}_2$ ,  $\text{Mg}_2\text{Al}_3$ , and  $\text{NiAl}_3$  are formed, which are found in aluminum-rich alloys of their respective series as eutectics with the aluminum solid solution. These compounds are in all cases hard and brittle and their presence affects profoundly the physical properties of the alloys in which they occur. Within the zinc-aluminum system a compound,  $\text{Al}_7\text{Zn}_{12}$ , is formed which decomposes at lower temperatures.

Silicon and tin each form a simple eutectiferous series with aluminum. Bismuth, lead, and cadmium are only partially miscible in the liquid state with aluminum.

<sup>1</sup> Discussion and bibliography of the literature dealing with aluminum and its alloys will be found in Circular of the Bureau of Standards, No. 76; 1929.

The extent of the solubility in aluminum in solid solution of these compounds or of the elements themselves in the case of those series in which compounds are not formed is of the greatest importance in considering the effect of these compounds or elements upon the physical properties of aluminum-rich alloys. Whether the compound,  $\text{CuAl}_2$ , is dissolved in the aluminum in an aluminum-rich alloy or is in the form of a hard and brittle constituent distributed throughout the mass must be a question of primary importance in a consideration of the mechanical properties of the alloy.

Reference to the equilibrium diagrams of the binary aluminum alloys as they are established to-day shows that with a few exceptions the solubilities of these compounds either have not been determined with any exactness or not at all. Only the solubility of zinc and that of  $\text{CuAl}_2$  in aluminum have received any attention, the former at two, the latter at only one temperature; reference is made to these determinations below. In many other cases an estimate, at best unsatisfactory, has been made from thermal analysis of the position of the end of the eutectic horizontal line or arrest.

The authors have undertaken to determine the solubilities of a number of these compounds at different temperatures and thus to establish the missing solubility-temperature curve of these compounds in the equilibrium diagram. This paper deals with the solubility-temperature curves of  $\text{CuAl}_2$  and of  $\text{Mg}_2\text{Al}_3$ , and incidentally with the solubility of  $\text{FeAl}_3$  and the condition and solubility of silicon in aluminum; later determinations will be reported on the curves for  $\text{MnAl}_2$  and  $\text{NiAl}_2$ .

## II. CONSTITUTION OF COMMERCIAL ALUMINUM

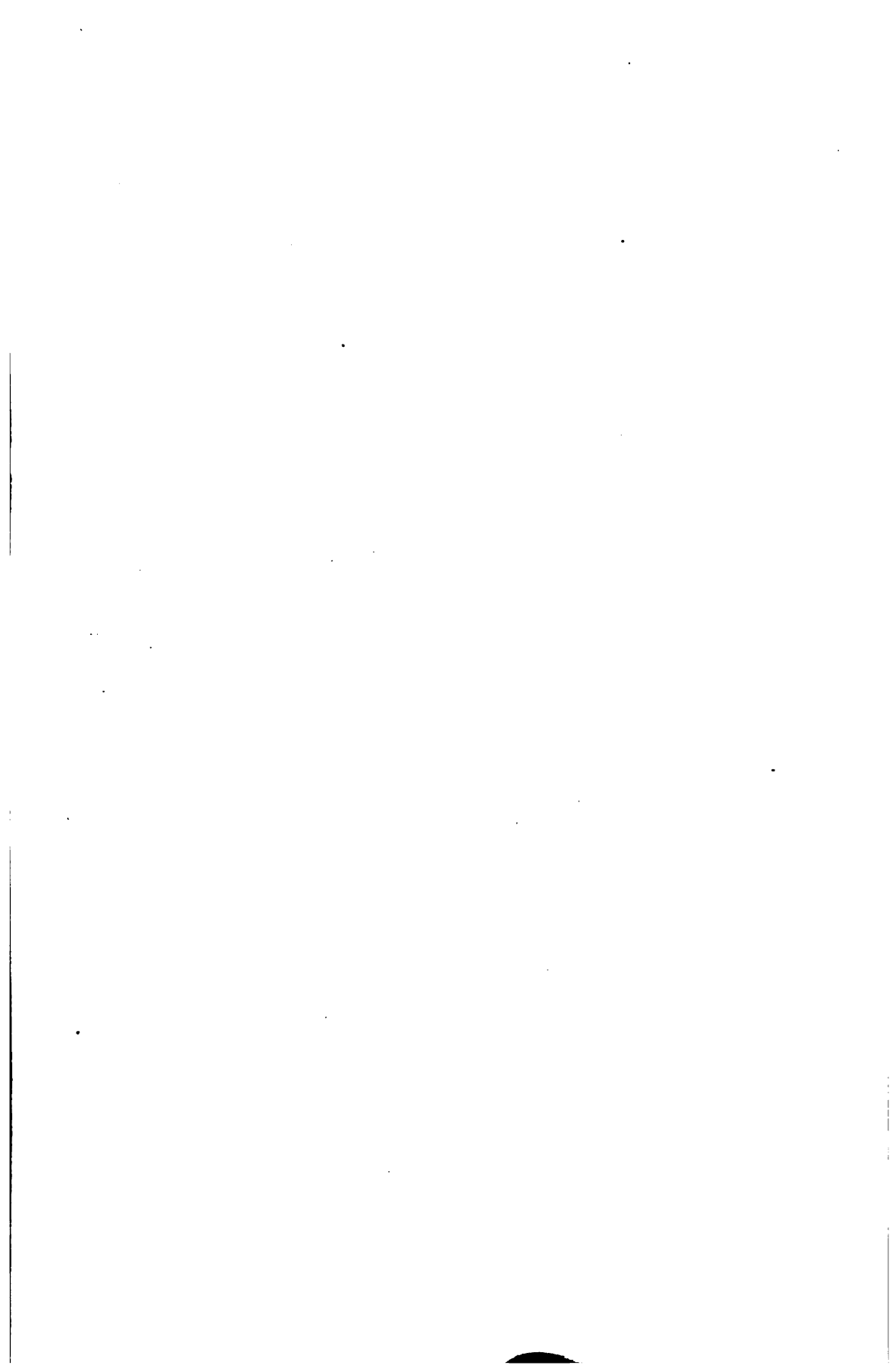
Commercial ingot aluminum contains from 0.2 to 0.5 per cent each of iron and of silicon as impurities, which are at least partially visible under the microscope. Figs. 1 and 2 show the microstructures of two compositions of aluminum ingot at a low magnification; the grains of aluminum are partly surrounded by particles of other constituents, the amount of which is greater in a composition having higher content of total impurities. In Figs. 3, 4, and 5 are shown microstructures of the same materials at higher magnification.

The microstructure of aluminum and of its light alloys is best developed by careful grinding and polishing, followed by etching with a dilute solution of sodium hydroxide; the authors prefer one

FIG. 1.—*Pure aluminum (Al-5) containing Fe, 0.24 per cent; Si, 0.14 per cent (etched with 0.1 per cent NaOH).  $\times 100$*

FIG. 2.—*Commercial ingot aluminum (Al-2) containing Fe, 0.5 per cent; Si, 0.2 per cent (etched with 0.1 per cent NaOH).  $\times 100$*

FIG. 3.—*Pure aluminum ingot containing Fe, 0.15 per cent; Si, 0.12 per cent, showing fine particles, probably of constituent X.  $\times 1500$*



of 0.1 per cent, with the addition of approximately 10 per cent alcohol. Such a solution does not etch deeply enough to develop the grain boundaries but it does bring out quite well the various other constituents found in aluminum and its light alloys which are often in such fine distribution that they are obliterated by heavier etching with more concentrated solutions of sodium hydroxide or of hydrofluoric acid which are more commonly used. As much care must be used in the grinding and polishing of the metal as in its etching in order to secure the best results, the grinding with the finer grades of emery paper must be done with the aid of some lubricant such as paraffin, oil, or simply alcohol, and best results are obtained by polishing with alumina on suitable cloth moistened with alcohol. The subject of the preparation of aluminum for microscopic examination is discussed in two papers by R. J. Anderson.<sup>2</sup>

The constitution of the binary alloys of iron with aluminum has been investigated by Gwyer.<sup>3</sup> The compound  $\text{FeAl}_3$  forms a eutectic with aluminum at  $649^\circ \text{C}$ ; its composition is unknown, but it contains undoubtedly a low percentage of iron—1 to 2 per cent. Gwyer did not determine the solubility of  $\text{FeAl}_3$  in aluminum, but noted that it was very slight.

The most complete investigations of the equilibrium of binary alloys of silicon and aluminum were made by Fränkel<sup>4</sup> and Roberts;<sup>5</sup> the latter investigation confirming the first one in practically all respects. According to these investigations no compound is formed in this series; the two elements form a eutectic at about 15 per cent silicon and  $576^\circ \text{C}$ ; the solubility of silicon in aluminum is given as less than 0.5 per cent.

It was necessary for the authors' work on the solubility of  $\text{CuAl}$ , and  $\text{Mg}_2\text{Al}_3$ , that they first be able to identify the various constituents which would be present in alloys of aluminum with these metals. On comparing the microstructures, therefore, of several different compositions of aluminum in the light of these investigations of the equilibrium between aluminum and iron and aluminum and silicon it was possible to identify a light bluish constituent occurring in all compositions as  $\text{FeAl}_3$ ; this is shown in Fig. 4. In compositions having less than about 0.2 per cent

<sup>2</sup> R. J. Anderson, *The Metallography of Aluminum*, Chem. and Met. Engineering, 18, p. 172, 1918; and *Journal of the Franklin Institute*, 187, p. 1, 1919.

<sup>3</sup> A. Gwyer, *Constitution of Binary Alloys of Aluminum with Iron, Copper, Nickel, Cobalt, Lead, and Cadmium*, Zeit. anorg. Chem., 57, p. 113; 1908.

<sup>4</sup> W. Fränkel, *Silicon-Aluminum Alloys*, Zeit. anorg. Chem., 58, p. 154; 1908.

<sup>5</sup> C. E. Roberts, *Silicon-Aluminum Alloys*, Trans. Chem. Soc., 106, p. 1383; 1914.

of silicon no other constituent was noticed in the eutectic islands; in those having this amount or more of silicon a second constituent, slightly darker than the  $\text{FeAl}_3$ , was noticed. This is shown, together with the  $\text{FeAl}_3$ , in Fig. 5. In order to be more certain of the identity of these two constituents of the eutectic islands, samples were prepared from a relatively pure aluminum, called Al-1, containing:

	Per cent
Iron .....	0.15
Silicon .....	.12
Copper .....	.02

With the addition of more silicon and of more iron the microstructure of these samples showed that as the silicon was increased the darker constituent increased in amount, whereas as the iron increased the amount of the lighter one increased in amount. Fig. 6 shows the two constituents in a sample containing 2 per cent each of iron and silicon. It was at first assumed that this darker constituent was crystallized silicon, in accordance with the equilibrium diagram. However, the results of thermal analyses made on 30 g samples of different compositions of aluminum did not bear this conception out.

Cooling curves of the inverse-rate type on four different compositions of aluminum are shown in Fig. 7. The temperature of the  $\text{FeAl}_3$ -aluminum eutectic arrest is indicated clearly on each; it is lower with increasing silicon content. The sample Al-1, containing only 0.12 per cent of silicon, showed no other arrest between this temperature and ordinary temperature; this specimen contained only the one eutectic; that is, that with the constituent identified as  $\text{FeAl}_3$ . The other compositions of higher silicon content show a lower arrest at  $610^\circ\text{C}$ , quite constant in temperature; the intensity of the arrest increases with the increase in silicon content. None of these compositions showed an arrest at  $576^\circ\text{C}$ . The appearance of the arrest at  $610^\circ\text{C}$  corresponds with the appearance of the darker constituent in the eutectic in small amounts. With higher amounts of silicon, therefore, a thermal arrest is found at about  $576^\circ\text{C}$ , corresponding to the silicon-aluminum eutectic (and this was confirmed by the authors), which is not found in aluminum of low silicon content; in place of the  $576^\circ\text{C}$  arrest is found one at  $610^\circ\text{C}$ .

The evidence seems to point to the fact that the second and darker constituent found in the eutectic islands in aluminum is not silicon, but a compound of unknown composition, either of

FIG. 4.—Commercial aluminum (Al-2), showing eutectics of  $FeAl_3$  and of constituent X.  $\times 1000$

FIG. 5.—Commercial aluminum (Al-2), showing eutectics of  $FeAl_3$  and of constituent X.  $\times 1000$

FIG. 6.—Alloy containing 2 per cent each of iron and silicon. The two constituents, Si (dark) and the  $FeAl$  (light) are readily distinguished.  $\times 1000$





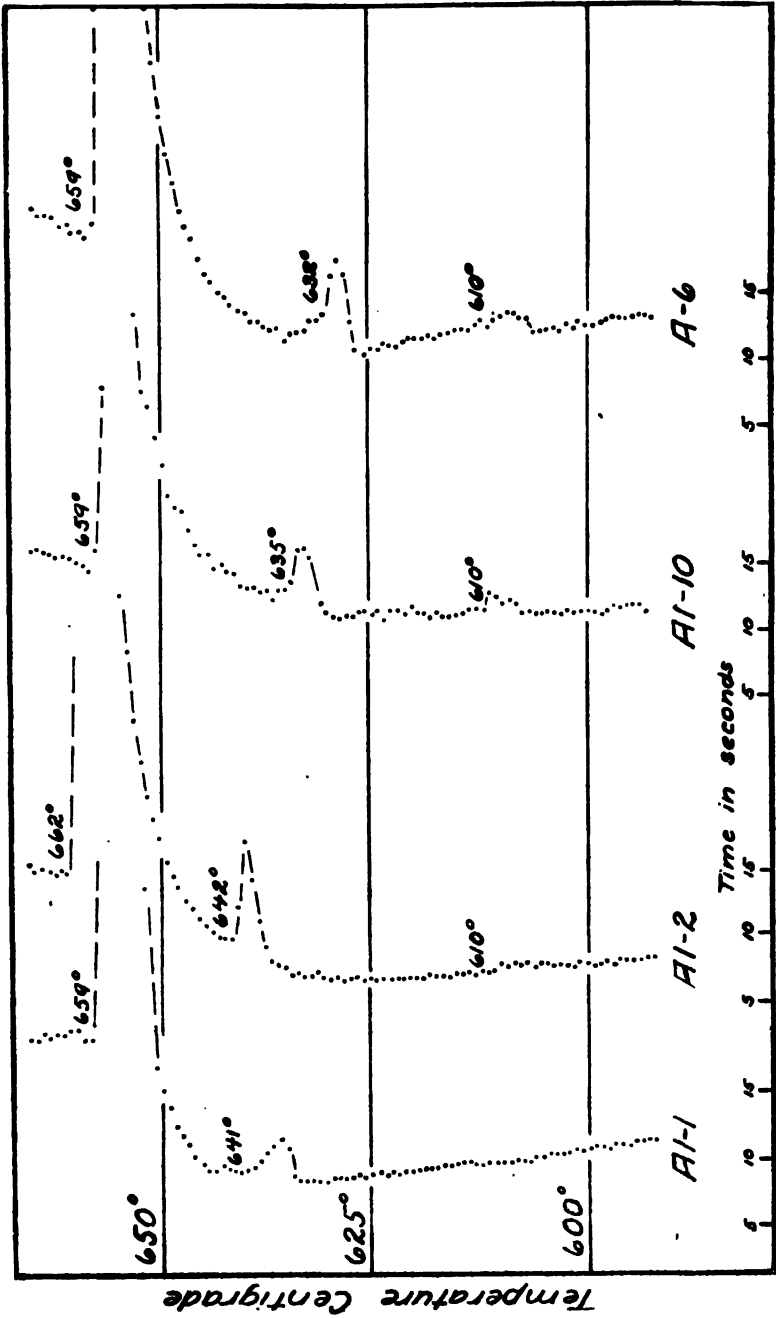


FIG. 7.—Inverse rate cooling curves of aluminum with different amounts of silicon; Al-1, 0.12 per cent Si; Al-2, 0.2 per cent Si; Al-10, 0.24 per cent Si; A-6, 0.3 per cent Si

iron and silicon alone, or of these with aluminum; it will henceforth be referred to as  $X$  ( $AlFeSi$ ). The ternary liquidus surfaces must have somewhat the form shown in Fig. 8. Within the area

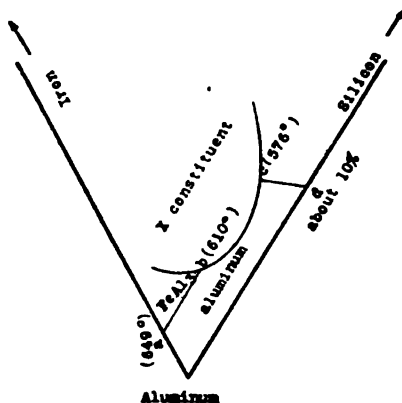


FIG. 8.—Suggested form of liquidus surfaces of ternary system aluminum-iron-silicon near aluminum end

$Al-abcd$  aluminum separates from the liquid; along the line  $ab$  eutectic of  $FeAl_3$  and aluminum; along the line  $dc$  eutectic of silicon and aluminum; along the line  $bc$  the eutectic of aluminum and the compound  $X$ ; at the points  $b$  and  $c$  of invariant equilibrium two binary eutectics. This view, of course, remains to be confirmed by a necessarily much more extensive study of the ternary equilibrium; it appears at present, however, to be the only consistent interpretation of the facts.

Another feature of the structure of commercial aluminum is of the greatest interest. In Figs. 3, 4, and 5 there will be noticed, besides the grains of aluminum and the eutectic islands, a number of quite fine particles of some constituent scattered throughout the grains of aluminum. These are apparently particles of the constituent  $X$ , and possibly also of  $FeAl_3$ , which have separated from solid solution in aluminum at temperatures below the eutectic one. It was noted above that there is a slight solubility of the constituent  $X$  in aluminum, since it is not found as a part of the eutectic when the amount of silicon is only 0.12 per cent, nor is an arrest found at  $610^\circ C$ . At  $610^\circ C$ , therefore, approximately 0.12 to 0.20 per cent of silicon as  $X$  dissolves in aluminum; at lower temperatures its solubility diminishes and it precipitates again in much finer particles.

Little can be said as yet about the solubility of  $\text{FeAl}_3$  in aluminum, as in the purest aluminum yet prepared and examined,  $\text{FeAl}_3$  has been found in quite appreciable quantities; this sample, Al-1, contained 0.15 per cent of iron. Iron, as  $\text{FeAl}_3$ , is therefore not completely soluble in aluminum in this amount. It may be mentioned also that although no attempts were made to discover whether by annealing this amount of iron could be made to dissolve in commercial aluminum, in the course of the work described below it was noted that in alloys containing besides this amount of iron about 0.5 per cent copper, no solution of the  $\text{FeAl}_3$  occurred upon annealing for 20 hours at  $500^\circ \text{C}$ .

In the course of the examination and investigation of aluminum no evidence has been found of any transformation of silicon from one form into another, nor of the existence of the so-called graphitoidal silicon. This latter term originated with the analyst of aluminum and its light alloys, who finds under certain conditions that there is a residue left from the action of the concentrated acids used in dissolving the sample, which is insoluble in hydrofluoric acid. It is suggested that the occurrence of the silicon in the various forms, (1) of eutectic particles of constituent X, (2) of eutectic particles of silicon, (3) of segregate particles of X, and (4) of a solid solution in aluminum, possibly explains the phenomena experienced in the analysis of the metal. Thus, the silicon existing in solid solution in aluminum would undoubtedly dissolve readily in the concentrated acids to give  $\text{SiO}_2$ , whereas the particles of X or of crystallized silicon would be much less soluble.

### III. SOLUBILITY OF $\text{CuAl}$ , IN ALUMINUM AT DIFFERENT TEMPERATURES.

The equilibrium of copper-aluminum alloys has been investigated by Gwyer (see footnote 3, p. 107), Carpenter and Edwards<sup>8</sup>, Curry<sup>7</sup>, Guillet<sup>8</sup>, Campbell and Matthews,<sup>9</sup> and others. Gwyer finds that 4 per cent of copper dissolves in aluminum as  $\text{CuAl}_2$ . Carpenter and Edwards place the solubility at 4 per cent, Curry at 11 per cent, and Campbell and Matthews at 2 per cent. These values hold for the eutectic temperature  $540^\circ \text{C}$ .

<sup>6</sup> Proc. Inst. Mech. Eng., p. 57; 1907.

<sup>7</sup> Journ. Phys. Chem., 11, p. 425; 1907.

112675°—19—2

<sup>8</sup> C. R. 141, p. 464; 1905.

<sup>9</sup> Journ. Am. Chem. Soc., 24, p. 253; 1902.

Annealing experiments were undertaken to ascertain the course of the solubility temperature curve. For these determinations 100 g melts of different compositions of copper-aluminum alloys, varying from 0.5 to 5 per cent of copper, were made in a small gas furnace; the purest aluminum available was used, namely, Al-1, of which the composition is given on page 108. The resulting alloys were cast in chill molds, one-half inch in diameter. Figs. 9 and 10 show the typical structures of these alloys as chill cast in this form. Free  $\text{CuAl}_2$  was observed even in the cast specimen C-20 containing 0.5 per cent copper.

The  $\text{CuAl}_2$  can readily be distinguished from the  $\text{FeAl}_2$  particles by the fact that they are much whiter in natural color and that they do not turn brown upon etching for several minutes with 0.1 per cent  $\text{NaOH}$  as does  $\text{FeAl}_2$ .

The compositions of the cast alloys are given in Table 1.

Specimens of these alloys were annealed for 20 hours at 525, 500, 400, and 300° C, quenched in water from these temperatures and examined microscopically for the presence of free  $\text{CuAl}_2$ . The results of these examinations are also given in Table 1. A series of photomicrographs, Figs. 11 to 14, show the microstructures of alloys C24-B to C27-B after annealing at 500° C and quenching.  $\text{CuAl}_2$  is found in C27-B (3.8 per cent Cu) and C26-B (3.6 per cent Cu) but not in C25-B (3.1 per cent Cu) and C24-B (2.5 per cent Cu).

TABLE 1.—The Microscopic Examination for the Presence of Free  $\text{CuAl}_2$  in Annealed Chill Cast Copper-Aluminum Alloys

[All specimens were quenched in water after annealing]

Number of alloy	Per cent of copper	Results of microscopic examination to determine whether free $\text{CuAl}_2$ was present after annealing			
		Annealed at 525° C, marked G	Annealed at 500° C, marked B	Annealed at 400° C, marked A	Annealed at 300° C, marked C
	Per cent				
C-20.....	0.5	No $\text{CuAl}_2$ .....	No $\text{CuAl}_2$ .....	No $\text{CuAl}_2$ .....	No $\text{CuAl}_2$
C-21.....	1.1	.....do.....	.....do.....	.....do.....	Do.
C-22.....	1.6	.....do.....	.....do.....	.....do.....	Small amount
C-23.....	2.1	.....do.....	.....do.....	Small amount.....	Much $\text{CuAl}_2$
C-24.....	2.5	.....do.....	.....do.....	Much $\text{CuAl}_2$ .....	Do.
C-25.....	3.1	.....do.....	.....do.....	.....do.....	Do.
C-26.....	3.6	.....do.....	Small amount.....	.....do.....	Do.
C-27.....	3.8	One or two particles only.	Much $\text{CuAl}_2$ .....	.....do.....	Do.
C-28.....	4.5	Small amount.....	.....do.....	.....do.....	Do.
C-29.....	5.1	Much $\text{CuAl}_2$ .....	.....do.....	.....do.....	Do.



FIG. 9.—Alloy C20 as cast, showing eutectic of  $\text{CuAl}_2$ —aluminum;  
Cu, 0.5 per cent.  $\times 100$

FIG. 10.—Alloy C29 as cast, showing eutectic of  $\text{CuAl}_2$ —aluminum;  
Cu, 5.1 per cent.  $\times 100$

FIG. 11.—Alloy C27B; Cu, 3.8 per cent.  
X<sub>300</sub>

FIG. 12.—Alloy C26B; Cu, 3.6 per cent.  
X<sub>300</sub>

FIG. 13.—Alloy C25B; Cu, 3.1 per cent.  
X<sub>300</sub>

FIG. 14.—Alloy C24B; Cu, 2.5 per cent.  
X<sub>300</sub>

*The structure of alloys C24 to 27B, annealed and quenched from 500° C*

To observe whether 20 hours' annealing was really sufficient to bring about equilibrium within these alloys, specimens of C20 to C25 (and marked H) were annealed 10 days at 400° C and quenched. The results of examination showed that C23-H contained a small amount of CuAl<sub>2</sub>, C22-H, none, in exact agreement with observations after 20 hours' annealing at the same temperature.

A curious fact was noticed in the annealing of these alloys. Once the CuAl<sub>2</sub> has dissolved in the aluminum it precipitates again from supersaturated solutions only with difficulty; or, perhaps more accurately stated, it apparently precipitates from such solutions, but in particles of very high dispersion or small size, and these particles coalesce into larger ones only with difficulty. Specimens of the C20 to C29-B series, which had been annealed 20 hours at 500° C and quenched, were reannealed and quenched from lower temperatures as follows: C20 to C29-B-1, at 320° C for 45 hours; C20 to C29-B-2, at 400° C for 20 hours. Reannealing caused apparently no change in the structure of any of the alloys; at least no particles of CuAl<sub>2</sub> of a size comparable with the original eutectic generation reappeared in those samples to correspond with the diminution of solubility at the lower temperatures. Fig. 15 shows the structure of C25-B-1, which may be compared with Figs. 11 to 14.

Only upon very slow cooling through the temperature range 500 to 300° C do segregate or precipitated particles of CuAl<sub>2</sub> coalesce to such an extent that they may readily be identified as such. Specimens of C25-B and of E13-B which had been annealed at 500° C were reheated to 500° C and cooled from that temperature very slowly to room temperature. The furnace cooled from 500 to 345° C in 15 hours. Areas were marked off on both specimens before this final treatment and examined before and after heating and cooling. As annealed and quenched no CuAl<sub>2</sub>, corresponding to the equilibrium solubility, was found in either of the specimens; after heating to 500° C and cooling at this slow rate CuAl<sub>2</sub> particles of fairly large size were found in both specimens in profusion. Figs. 16 and 17 show an area of C25-B before and after heating and slow cooling, respectively.

Samples of alloys E9 to E11 were annealed for various periods of time at 400° C to determine what period was necessary to produce equilibrium between the CuAl<sub>2</sub> and solid solution. The results of these experiments are given in Table 2. At 400° C equilibrium was attained in these small chill-cast specimens after 30 minutes; after that period no further change took place.

TABLE 2.—Microscopic Examination for the Presence of Free  $\text{CuAl}_2$  in Samples of Chill-Cast Copper-Aluminum Alloys Annealed at  $400^\circ \text{C}$  and Quenched

Number of sample	Per cent copper	Period of annealing	Temperature of annealing	Examination for the presence of free $\text{CuAl}_2$
		Hours	$^\circ\text{C}$	
E9-A.....	1.0	$\frac{1}{2}$	400	Small amount of $\text{CuAl}_2$ .
E10-A.....	1.5	$\frac{1}{2}$	400	Considerable $\text{CuAl}_2$ .
E9-B.....	1.0	$\frac{1}{2}$	400	No $\text{CuAl}_2$ .
E10-B.....	1.5	$\frac{1}{2}$	400	Very small amount of $\text{CuAl}_2$ .
E11-B.....	1.9	$\frac{1}{2}$	400	Much $\text{CuAl}_2$ .
E10-C.....	1.5	1	400	No $\text{CuAl}_2$ .
E11-C.....	1.9	1	400	Small amount of $\text{CuAl}_2$ .
E10-E.....	1.5	13	400	No $\text{CuAl}_2$ .
E11-E.....	1.9	13	400	Small amount of $\text{CuAl}_2$ .

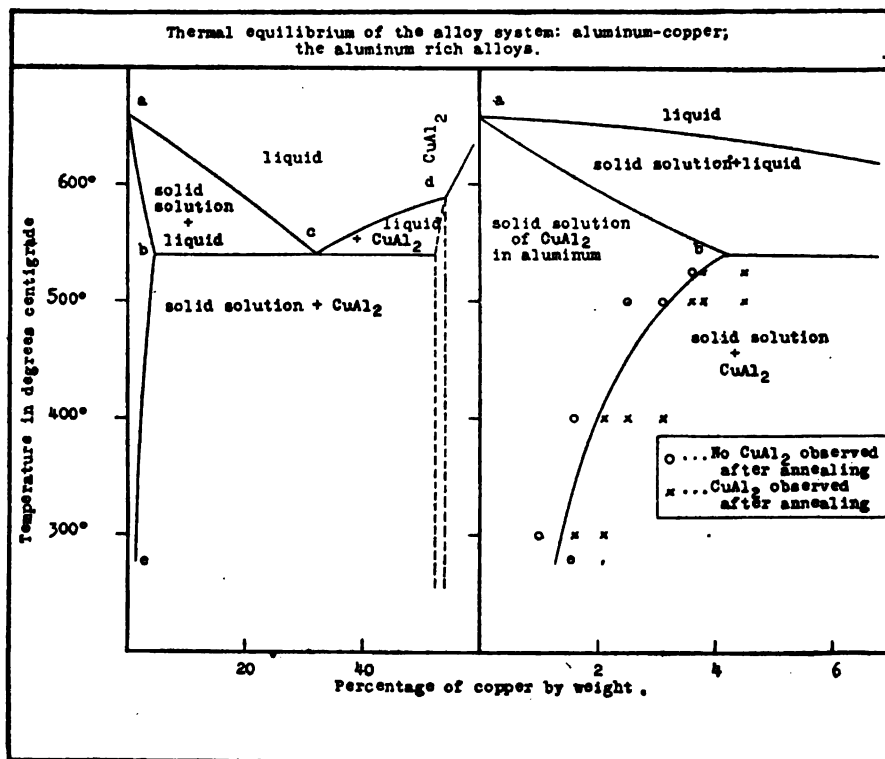


FIG. 18

In Fig. 18 are shown the results of these solubility determinations. There is given the aluminum side of the equilibrium diagram of copper and aluminum, of which the portion, *be*, has been determined by the above experiments; the remainder is taken



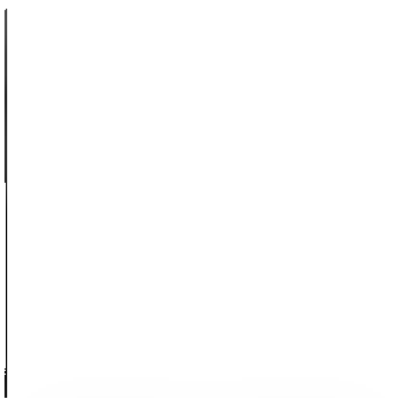


FIG. 15.—Alloy C25B-1, annealed 20 hours at 500° C, quenched, reannealed 45 hours at 320° C, and quenched. No particles of  $\text{CuAl}_2$  are visible at this magnification; Cu, 3.1 per cent.  $\times 300$

FIG. 16.—Specimen C25B, annealed at 500° C and quenched; Cu, 3.1 per cent.  $\times 300$

FIG. 17.—Same area of C25B as shown in Fig. 16 but after reheating to 500° C and slowly cooling.  $\text{CuAl}_2$  has precipitated and coalesced.  $\times 300$

FIG. 19.—Magnesium-aluminum alloy  
A38, as chill cast; Mg, 17.8 per cent  
(etched with 5 per cent NaOH).  $\times 300$

FIG. 20.—A37-400; Mg, 17.1 per cent.  
 $\times 300$

FIG. 21.—A27-400; Mg, 13.2 per cent.  
 $\times 300$

FIG. 22.—A36-400; Mg, 11.7 per cent.  
 $\times 300$

Figs. 20, 21, and 22 show structure of magnesium-aluminum alloys, annealed 20 hours  
at 400° C and quenched (etched with 5 per cent NaOH)

from the results of previous investigations. The solubility of  $\text{CuAl}_2$  decreases with decreasing temperature from about 4 per cent at  $525^\circ \text{C}$  to about 1 per cent at  $300^\circ \text{C}$ , and is apparently still diminishing at lower temperatures.

#### EFFECT OF MAGNESIUM UPON THE SOLUBILITY OF $\text{CuAl}_2$ IN ALUMINUM

In seeking an explanation for the effect of magnesium upon the physical properties of heat-treated duralumin (see footnote 14, p. 118) the question presented itself whether the solubility-temperature curve of  $\text{CuAl}_2$  in aluminum was displaced by the presence of the usual small amounts of magnesium.

Specimens were chill cast containing the following constituents:

	Copper	Magnesium
	Per cent	Per cent
C30.....	1	0.5
C31.....	2	.5
C32.....	3	.5
C33.....	4	.5
C34.....	1	1.0
C35.....	2	1.0
C36.....	3	1.0
C37.....	4	1.0

These were examined after annealing 20 hours at  $500^\circ \text{C}$ , followed by quenching. Specimens C32 and C36 contained after this annealing no free  $\text{CuAl}_2$ , whereas specimens C33 and C37 did. Apparently as much as 1 per cent of magnesium does not affect appreciably the temperature-solubility curve of  $\text{CuAl}_2$  in aluminum.

#### IV. SOLUBILITY OF $\text{Mg}_2\text{Al}_3$ IN ALUMINUM AT DIFFERENT TEMPERATURES

The equilibrium of magnesium-aluminum alloys has been studied by Schirmeister,<sup>10</sup> Wilm,<sup>11</sup> and Grube.<sup>12</sup> Schirmeister finds no eutectic arrest for the eutectic of  $\text{Mg}_2\text{Al}_3$  aluminum at 1 per cent magnesium; Grube makes no comment on the amount of  $\text{Mg}_2\text{Al}_3$  which may be soluble in aluminum.

For the authors' determinations, samples of magnesium-aluminum alloys were prepared in the same manner as were those for the previous series. Table 3 gives the compositions of the alloys so prepared and Fig. 19 shows the typical duplex structure of one of the chill cast alloys, No. A-38.

<sup>10</sup> Metall u. Erz., 2, p. 528; 1924.

<sup>11</sup> Metallurgie, 8, p. 225; 1921.

<sup>12</sup> Zeit anorg. Chem., 45, p. 225; 1905.

Specimens of the alloys were annealed for 20 hours at 450, 400, and 300° C and then quenched. The microstructure was developed by etching with 5 per cent NaOH solution and the specimens were examined for the presence of free  $Mg_2Al_3$ . Table 3 also gives the results of these determinations. Figs. 20 to 22 show typical microstructures for a series annealed at 400° C.

TABLE 3.—Microscopic Examination for the Presence of Free  $Mg_2Al_3$  in Annealed Chill-Cast Magnesium-Aluminum Alloys

[All specimens were quenched in water after annealing]

Number of alloy	Per cent of magnesium	Results of microscopic examination whether free $Mg_2Al_3$ was present after annealing		
		Annealed at 450° C, marked -45	Annealed at 400° C, marked -4	Annealed at 300° C, marked -3
A-31	5.9	No $Mg_2Al_3$ .....	No $Mg_2Al_3$ .....	Small amount $Mg_2Al_3$
A-32	6.9	.....do.....	.....do.....	Much $Mg_2Al_3$
A-34	9.1	.....do.....	.....do.....	Do.
A-36	11.7	.....do.....	.....do.....	Do.
A-35	12.2	.....do.....	.....do.....	Do.
A-27	13.2	Small amount $Mg_2Al_3$ .....	Small amount $Mg_2Al_3$ .....	Do.
A-37	17.1	Much $Mg_2Al_3$ .....	Much $Mg_2Al_3$ .....	Do.
A-38	17.8	.....do.....	.....do.....	

The solubility of  $Mg_2Al_3$  in aluminum decreases with lowering of the temperature exactly as in the case of  $CuAl_2$ . Specimens of A35-450 and of A36-450 annealed 20 hours at 450° C and quenched were reheated to 420° C and allowed to cool very slowly in the furnace. The furnace cooled from 420° to 260° C in 24 hours. In these specimens, previously free from  $Mg_2Al_3$ , this second heat treatment caused a copious precipitate of this constituent. Figs. 23 and 24 show the structure of A35-450 before and after slow cooling, respectively.

The results of these determinations are shown in Fig. 27, in which is reproduced a portion of the equilibrium diagram as determined by Grube for the magnesium-aluminum alloys, and in which is inserted the portion, *be*, determined by the above experiments.

In aluminum-rich alloys of magnesium with commercial aluminum besides the two constituents, or phases, aluminum solid solution and  $Mg_2Al_3$ , another constituent is invariably found, the amount of which seems to increase slowly, if at all, with increase of magnesium content beyond about 1 per cent. It has a deep blue color and is easily distinguished from the other two constituents mentioned, and from the  $FeAl_3$ , which is also present. It is

FIG. 23.—A35-450; Mg, 12.2 per cent  
(quenched).  $\times 300$

FIG. 24.—A35-450A; Mg, 12.2 per cent  
(slowly cooled).  $\times 300$

Magnesium-aluminum alloy A35-450, which contains no  $Mg_2Al_3$  after annealing at  $450^\circ\text{C}$  and quenching (Fig. 23), but in which  $Mg_2Al_3$  precipitates upon reheating to  $420^\circ\text{C}$  and slowly cooling (Fig. 24)

FIG. 25.—A35-300; Mg, 12.2 per cent.  
 $\times 500$

FIG. 26.—A37-300; Mg, 17.1 per cent.  
 $\times 500$

Magnesium-aluminum alloys annealed at  $300^\circ\text{C}$ , showing the deep-blue constituent (dark in the photograph)

**FIG. 28** — Alloy N28, containing: Cu, 4.98 per cent; Mg, 2.41 per cent; Fe, 0.62 per cent; and Si, 0.32 per cent, and showing deep-blue constituent characteristic of aluminum-rich alloys containing magnesium  
X1000

shown in Figs. 25 and 26. This constituent occurs in alloys also containing both copper and magnesium. Fig. 28 shows an island of  $\text{CuAl}_2$  in such an alloy in which is embedded a particle of this blue constituent.

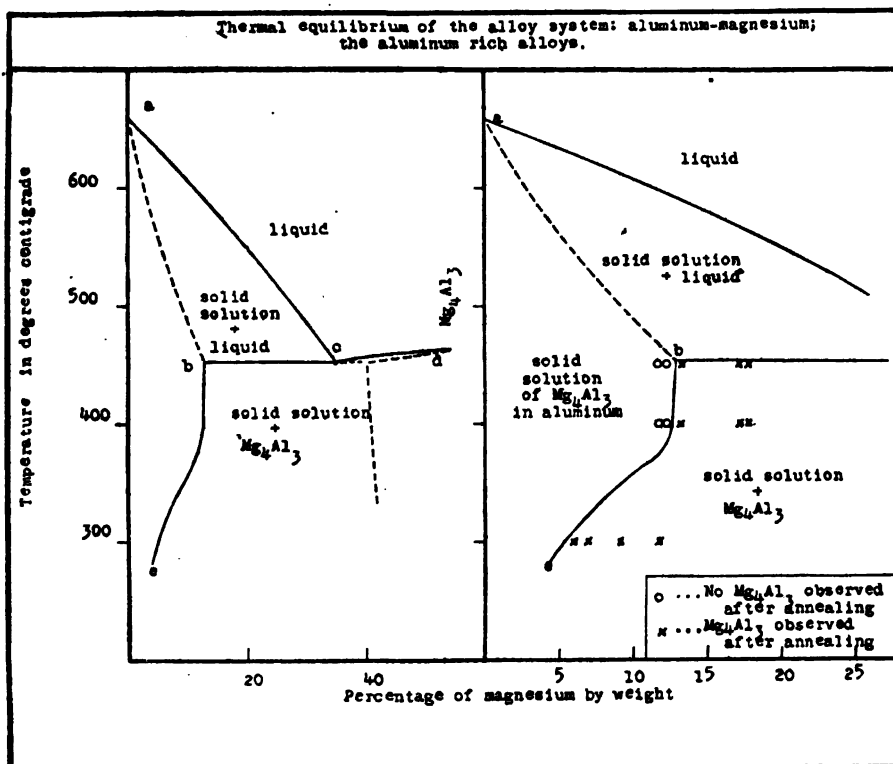


FIG. 27

This is believed to be  $\text{Mg}_2\text{Si}$ , although the authors have no direct evidence for this belief. Vogel<sup>18</sup> found a very marked and definite compound,  $\text{Mg}_2\text{Si}$ , in his study of the binary series, magnesium-silicon, which was of a deep blue color, much resembling the constituent described above. It is unlikely that this constituent is a compound of iron and magnesium since these two metals unite only with much difficulty and probably do not form a compound. The only other possibility therefore is that the constituent is a silicate or a ternary or quaternary compound containing magnesium, silicon, iron, or aluminum.

The occurrence of this constituent in light alloys of aluminum containing magnesium is believed to be of the greatest significance in connection with the effect of magnesium upon the mechanical

<sup>18</sup> Vogel, Magnesium-silicon alloys, *Zeit., anorg. Chem.*, 61, p. 46; 1909.

and other physical properties of these alloys. This question is, however, discussed at greater length in another article.<sup>14</sup>

## V. SOLUBILITY OF METALS AND METAL COMPOUNDS IN ALUMINUM

A review of the results obtained above and of those obtained by Rosenhain and Archbutt<sup>15</sup> and of Bauer and Vogel<sup>16</sup> on the solubility of zinc in aluminum shows that a decreasing solubility in aluminum with decreasing temperature of that constituent in immediate equilibrium with the aluminum is characteristic of the metal. Thus the solubility of zinc in aluminum at 443° C is about 40 per cent, whereas at 256° C it is only about 25 per cent.

This form of the solubility curve is, of course, not unusual; yet we find in the case of equilibrium of metals many cases in which the solubility of a constituent increases with decreasing temperature. Thus in the zinc-copper series the solubility of the beta constituent in the alpha one decreases with increasing temperature. In another article (see footnote 14) the significance of the form of solubility curve characteristic of aluminum is discussed.

## VI. SUMMARY AND CONCLUSIONS

The temperature-solubility curves of  $\text{CuAl}_2$  and of  $\text{Mg}_2\text{Al}_3$  in aluminum were determined by the method of annealing and microscopic examination. Aluminum dissolves about 4.2 per cent of copper as  $\text{CuAl}_2$  at 525° C and about 12.5 per cent of magnesium as  $\text{Mg}_2\text{Al}_3$  at 450° C.

The solubility of both compounds decreases with decreasing temperature. At 300° C aluminum dissolves only 1 per cent of copper as  $\text{CuAl}_2$  and slightly less than 5.9 per cent of magnesium as  $\text{Mg}_2\text{Al}_3$ .

The structural identification of the various constituents,  $\text{FeAl}_3$ ,  $\text{CuAl}_2$ ,  $\text{Mg}_2\text{Al}_3$ , found in alloys with magnesium and with copper is described, and a constituent is noted in all light aluminum alloys containing magnesium which is believed to be  $\text{Mg}_2\text{Si}$ .

The solubility of iron as  $\text{FeAl}_3$  in aluminum is at all temperatures less than 0.15 per cent.

<sup>14</sup> Merica, Waltenberg and Scott, Heat-treatment of Duralumin, this Bulletin, 15, 1919.

<sup>15</sup> Phil. Trans., 211, p. 315; 1911.

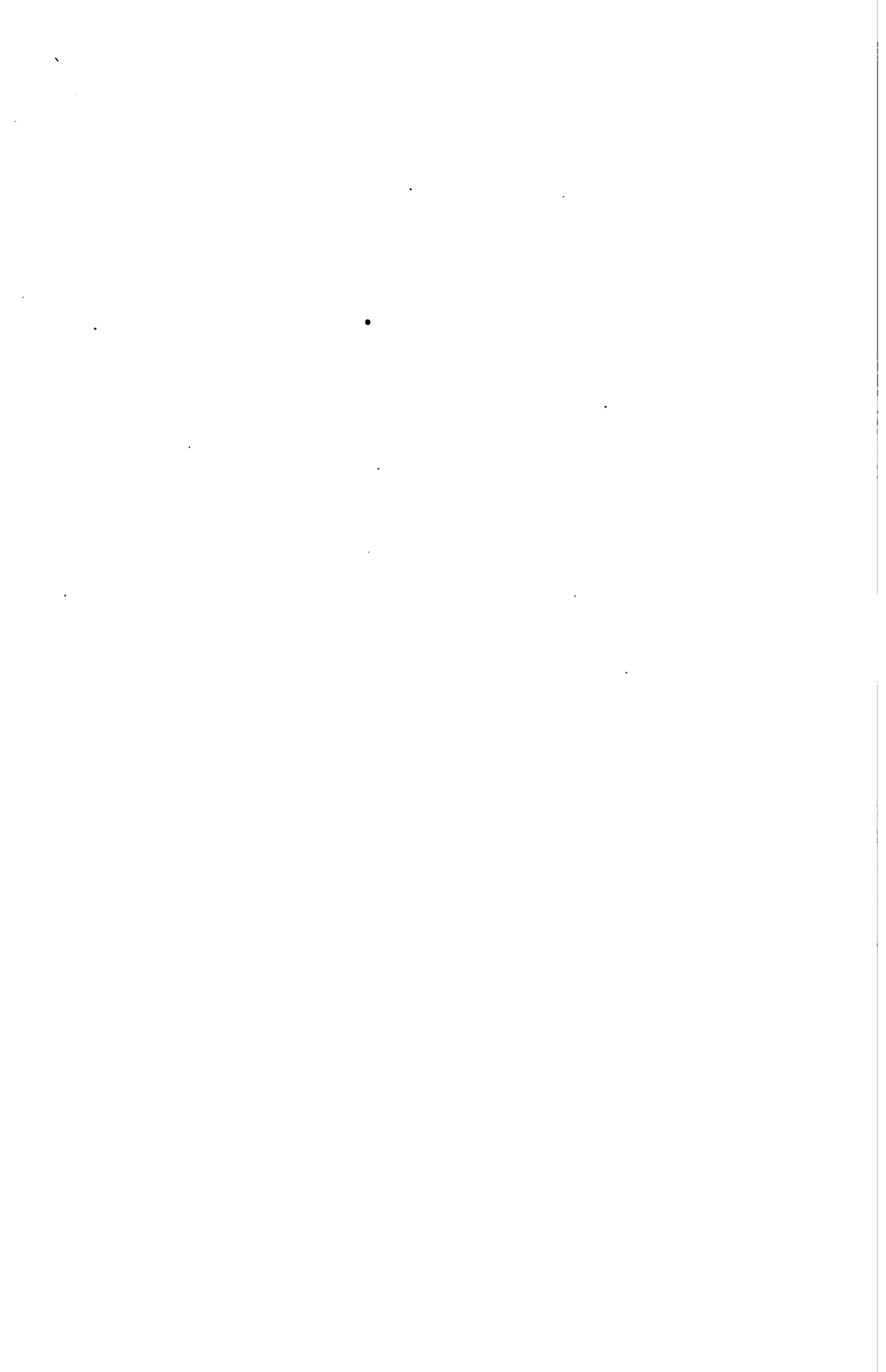
<sup>16</sup> Int. Zeit. Metallographie, 8, p. 101; 1916.



Small amounts of silicon up to from 0.12 to 0.20 per cent are dissolved by aluminum at the eutectic temperature, but are reprecipitated upon cooling corresponding to the diminished solubility for silicon of aluminum at lower temperatures.

Silicon in the usual commercial amounts is probably present as a compound of iron and silicon, together with some aluminum. The composition of this compound is not known but it separates out with aluminum and  $\text{FeAl}_3$  at an invariant point at  $610^\circ \text{C}$ .

WASHINGTON, February 2, 1919.







DEPARTMENT OF COMMERCE

---

**SCIENTIFIC PAPERS**  
OF THE  
**BUREAU OF STANDARDS**

S. W. STRATTON, DIRECTOR

---

No. 338

**SOME OPTICAL AND PHOTOELECTRIC  
PROPERTIES OF MOLYBDENITE**

BY

W. W. COBLENTZ, Associate Physicist  
and  
H. KAHLER, Laboratory Assistant  
*Bureau of Standards*

---

ISSUED AUGUST 16, 1919



PRICE, 10 CENTS

Sold only by the Superintendent of Documents, Government Printing Office  
Washington, D. C.

---

WASHINGTON  
GOVERNMENT PRINTING OFFICE  
1919



# SOME OPTICAL AND PHOTOELECTRIC PROPERTIES OF MOLYBDENITE

By W. W. Coblenz and H. Kahler

## CONTENTS

	Page
I. Introductory statement.....	121
II. Summary of previous work.....	122
III. Apparatus and methods.....	123
1. Diffuse-light tests.....	125
2. Sources of material examined.....	126
IV. Transmitting and reflecting power of molybdenite.....	126
1. Transmission measurements.....	127
2. Reflectivity measurements.....	128
V. Variation of photoelectric current with time of exposure.....	132
VI. Spectral range of photoelectric sensitivity.....	134
VII. Experimental data on various samples.....	136
VIII. Effect of intensity of radiation upon electrical conductivity.....	141
IX. Effect of temperature upon photoelectric sensitivity.....	146
X. Effect of humidity, vacuum, and mechanical working.....	151
XI. Photoelectric sensitivity versus current rectification.....	153
1. Exudation of a dark-blue liquid.....	155
XII. Theoretical applications.....	156
XIII. Summary.....	159
APPENDICES:	
Appendix 1.—Photoelectric activity induced in unilluminated parts of a crystal.....	161
Appendix 2.—Polarization by reflection from molybdenite.....	161

## I. INTRODUCTORY STATEMENT

In previous communications<sup>1</sup> data were given on the photoelectric sensitivity of various minerals, using heterochromatic light. As it frequently happens, while this preliminary investigation was in progress, the results of a similar survey were published.<sup>2</sup> This method of attack was therefore discontinued and the detailed investigation of the spectral photoelectric sensitivity of various substances was resumed.<sup>3</sup>

<sup>1</sup> Proc. Phil. Soc. Wash., Feb. 3, 1917; Jour. Wash. Acad. Sci., 7, p. 525, 1917; this Bulletin, 14, p. 592, 1918.

<sup>2</sup> Case, Phys. Rev. (2), 9, p. 305, April, 1917.

<sup>3</sup> Data on selenium, potassium, etc., are given in this Bulletin, 14, p. 507, 1918. Preliminary data on molybdenite were obtained with the assistance of M. B. Long and published under joint authorship in the Phys. Rev., 11, p. 497, 1918, and 13, p. 140, 1919. The latter gives data presented at the Pittsburgh meeting, Dec. 27, 1917.

The present paper gives data on the spectral photoelectric sensitivity of molybdenite, under various conditions of operation. Molybdenite was selected for detailed examination because it is one of the few minerals available which is sufficiently homogeneous to determine various optical and electrical properties, all of which data may prove useful in arriving at an explanation of the phenomenon of change in electrical resistance of certain substances when exposed to thermal radiation.

## II. SUMMARY OF PREVIOUS WORK

Prior to January, 1917, but few solid substances were known which exhibited the property of changing in electrical resistance when exposed to thermal radiant energy, especially visible and ultra-violet rays. Among the substances examined were selenium, stibnite, cuprous oxide, and the halide salts of silver.

*Selenium.*—It is beyond the scope of this paper to attempt to summarize all the investigations made on this substance. Selenium has a very prominent maximum of photoelectric sensitivity at about  $0.7 \mu$  ( $\mu = 0.001 \text{ mm}$ ) and a less intense wide band of sensitivity throughout the visible spectrum. The recent investigations of Dietrich<sup>4</sup> show that the character of the wavelength sensitivity curve can be controlled by heat treatment. Annealing the cell at  $200^\circ \text{C}$  produces a maximum sensitivity in the extreme red, while annealing it at  $150^\circ \text{C}$  shifts the maximum sensitivity to  $0.55 \mu$ .

Elliot<sup>5</sup> examined the photoelectrical sensitivity of selenium at room temperature, also at liquid-air temperature. His results show that the  $0.7 \mu$  band shifts toward the short wave lengths ( $0.6 \mu$ ) at low temperatures. Furthermore, there is an appreciable increase in sensitivity in the infra-red producing a wide band with a maximum sensitivity at about  $1.2 \mu$ .

Further tests (see Fig. 1) were made in the present investigation, using a Giltay selenium cell, and a fluorite prism to determine conclusively that, at room temperatures, selenium is practically insensitive throughout the infra-red spectrum to  $4 \mu$ .

*Stibnite.*—The light sensitivity of stibnite ( $\text{Sb}_2\text{S}_3$ ) as affected by temperature has been studied by Elliot.<sup>6</sup> At  $20^\circ \text{C}$  the light-sensitivity curve of stibnite is somewhat similar to the selenium curve shown in Fig. 1, excepting that the maximum sensitivity occurs at about  $0.75 \mu$ . Lowering the temperature to  $-190^\circ \text{C}$  (?)

<sup>4</sup> Dietrich, *Phys. Rev.* (2), p. 467, 1914; 8, p. 191, 1916.

<sup>5</sup> Elliot, *Phys. Rev.* (2), 5, p. 59, 1915.

<sup>6</sup> Elliot, *Phys. Rev.* (2), 5, p. 53, 1915.



causes this maximum to shift to about  $0.68 \mu$ , and increases somewhat the sensitivity throughout the infra-red to about  $2 \mu$ . That stibnite is sensitive to infra-red rays even at room temperature was shown by Martin<sup>7</sup> who observed a strong photoelectric effect produced by infra-red rays transmitted by a plate of ebonite 2 mm in thickness.

**Cuprous Oxide.**—The photoelectric sensitivity of cuprous oxide ( $\text{Cu}_2\text{O}$ ) was studied by Pfund.<sup>8</sup> He found the region of greatest light sensitivity to be in the ultra-violet, near  $\lambda = 0.28 \mu$ . A smaller maximum was observed at about  $0.625 \mu$ . Lowering the temperature from  $19^\circ \text{C}$  to  $-127^\circ \text{C}$  shifted this latter band toward the shorter wave lengths,  $-0.6 \mu$ . Using the same mate-

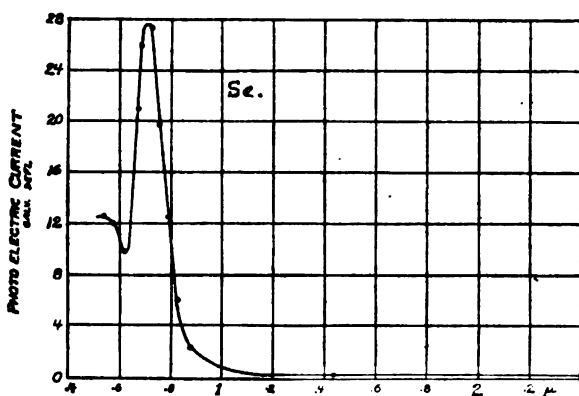


FIG. 1.—Spectral photoelectric sensitivity of selenium

rial, the light-sensitivity curve depends upon the design of the cell. A further observation of importance was that the change in conductivity in cuprous oxide is limited to the portions penetrated by radiation.

### III. APPARATUS AND METHODS

The spectroradiometric apparatus used consisted of a mirror spectrometer, a fluorite prism, and a vacuum bismuth-silver thermopile, described in previous papers.<sup>9</sup>

The source of radiation consisted of a 500-watt, gas-filled tungsten lamp securely mounted in front of the slit of the spectrometer. Using a vacuum thermopile and an accurately calibrated ammeter, the lamp was calibrated to emit equal energies throughout the spectrum. Starting in the blue-green, the lamp

<sup>7</sup> Martin, *Phys. Zeit.*, 12, p. 47, 1911.

<sup>8</sup> Pfund, *Phys. Rev. (2)*, 7, p. 289, 1916.

<sup>9</sup> This Bulletin, 10, p. 7, 1913; 11, p. 132, 1914.

was operated at normal current (4-ampere) and the galvanometer deflection noted. This deflection was taken as a standard and for the remainder of the spectrum the current was varied so as to give the same deflection throughout the spectrum to  $4\ \mu$ . These ammeter readings (which were as low as 1.5 amperes at about  $1.6\ \mu$ ) were then plotted upon coordinate paper. Several subsequent calibrations, made during the course of this investigation, showed no appreciable change in the original calibration curve.

The arrangement of the apparatus for projecting the monochromatic radiation upon the photoelectric substance is shown in Fig. 2. The radiations from the tungsten lamp, after being dispersed into a spectrum, pass through the exit slit *S* (size 0.5 by 10 mm), and, after reflection from a 50 cm focal length, silvered-

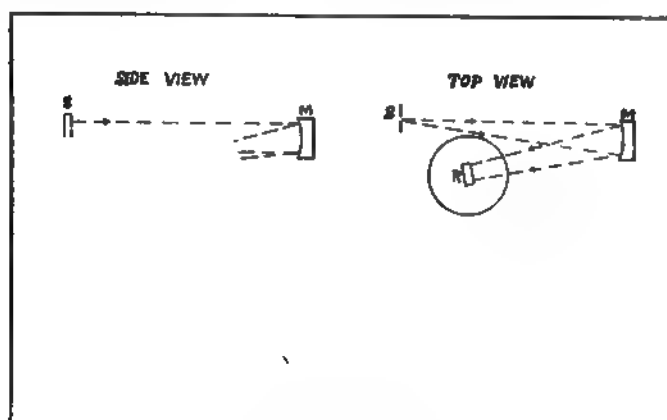


FIG. 2.—Arrangement of apparatus

glass mirror and a right-angled glass prism, are brought to focus upon the substance *P*, which is under investigation. In this manner radiations of different wave lengths, and of equal energy value ( $=1.1 \times 10^{-6}$  watt, as determined by measurement with the thermopile placed at *P*) could be projected upon the molybdenite.

The crystal of molybdenite was soldered to copper electrodes (illustrated in the rectangular diagrams, in Figs. 10 and 11), usually mounted upon a fiber support,<sup>10</sup> which was attached (by wire) to a heavy metal base, *P*, Fig. 2. The whole was mounted in a glass vessel *G*, about 25 cm in length and 5 cm in diameter. The copper-constantan thermocouple and the current wires leading to the molybdenite are shown diagrammatically at *T*. The

<sup>10</sup> Shown in No. 4 of Fig. 3, this Bulletin, 11, p. 254, 1924.

glass container rested upon a flexible-metal support in a Dewar flask, containing liquid air, ice, or water which was heated to a definite temperature by passing an electric current through a thin strip of manganin immersed in the water.

The liquid air was replenished by means of a cardboard funnel attached to the Dewar flask, which was surrounded with cotton batting in order to maintain constant temperature conditions. After making the initial adjustments, small quantities of liquid air could be introduced into the flask without disturbing the adjustments. For most of the observations the glass vessel was evacuated. In this manner various temperatures could be obtained, which could be easily maintained constant to  $0.1^{\circ}$  C. This is an important item in view of the fact that a change in temperature causes a change in the conductivity, and hence a change in the "dark current" through the crystal. The scale reading of the galvanometer is greatly affected by variations in the dark current.

The resistivity of molybdenite is high. The crystal was therefore operated directly in circuit with a d'Arsonval galvanometer and an electric battery of suitable voltage, which varied from 2 to 4 volts when the crystal was at room temperature to 120 volts, at liquid-air temperature.

The sample under investigation was usually covered with a piece of thick, white cardboard, perforated by a slit (0.5 by 10 mm.) which enabled the observer to expose a definite part of the crystal to radiation.

The method of observation consisted in setting the spectrometer circle, so as to permit radiation of a given wave length to pass out through the slit *S*, and from thence to the crystal *P*. The ammeter was set to the proper value as determined by the calibration curve. The shutter was then raised and the crystal exposed to the radiation stimulus for an unlimited time, which varied from 5 seconds for visible radiations to 6 to 12 minutes for infra-red rays.

#### 1. DIFFUSE-LIGHT TESTS

The novelty of finding bands of photoelectric sensitivity far beyond the range heretofore observed in the infra-red raised the question whether this might be owing to scattered radiations. Tests were therefore made using glass screens<sup>11</sup> (e. g., Corning G585), which absorbed all radiations except those at  $1\ \mu$ . By

means of the thermopile the lamp was calibrated to emit the same energy with and without the glass screen in place before the spectrometer slit. Repeated tests showed that within less than 1 per cent the scattered light had no effect on the shape and position of the bands of photoelectric sensitivity observed at 1 to 1.2  $\mu$ . The observations were therefore made without employing additional screens for absorbing scattered light.

## 2. SOURCES OF MATERIAL EXAMINED

The majority of the samples examined, 18 in all, were obtained from the United States National Museum. Some were obtained from mineral dealers. The localities from which they had been obtained were Alaska, Australia, Canada, Japan; and in the United States, California, Colorado, Maine, Montana, Vermont, and Washington. From preliminary sensitivity tests, made with a photophone consisting of a rotating sector, telephone, and an audion amplifier, using high intensities, it was found that all the material was of low resistance and low or uncertain photoelectric sensitivity, except certain samples obtained from Yorkes Peninsula, South Australia. Projecting an image of a point source of light upon the samples showed that the photoelectric sensitivity was usually localized in spots as shown in Figs. 10 and 11, and as previously found in bismuthinite.<sup>12</sup>

## IV. TRANSMITTING AND REFLECTING POWER OF MOLYBDENITE

As already mentioned, molybdenite is unusually well adapted for investigating the bearing of various physical properties upon photoelectrical sensitivity. It was therefore of interest to determine whether there is any close relation between the optical and photoelectrical properties of this substance. For this purpose the spectral transmission and reflection of several samples were determined by means of the spectroradiometric apparatus used in the photoelectric work.

On the supposition that photoelectric activity is a resonance phenomenon, Pfund<sup>13</sup> sought a relation between thermal radiant energy absorbed and change in electrical conductivity. On this basis he should have found the greatest photoelectrical activity of selenium in the blue, where the absorption was the greatest. This deduction was not verified by experiment, which showed

<sup>12</sup> This Bulletin, 14, p. 591; 1918.

<sup>13</sup> Pfund, *Phys. Rev.*, 28, p. 324; 1909.

that the maximum photoelectric sensitivity of selenium is in the red.

Previous investigations<sup>14</sup> show that molybdenite has a low transmission in the visible spectrum, followed by great transparency and high reflectivity in the infra-red. A decrease in temperature to boiling liquid air greatly increases the transparency of molybdenite. Crandall quotes observations, made by Trowbridge, showing that a sample of molybdenite which was transparent down to  $0.702\ \mu$ , at room temperature, became transparent down to  $0.666\ \mu$ , at  $-190^\circ\text{C}$ . This is of interest in connection with the observations of a shift of the position of maximum

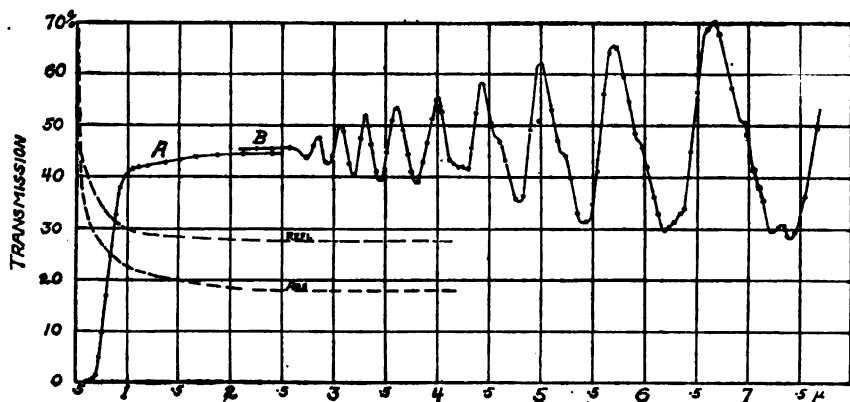


FIG. 3.—Transmission of molybdenite

photoelectric activity toward the short wave lengths with decrease in temperature.

### 1. TRANSMISSION MEASUREMENTS

The transmission of a sample of molybdenite ( $0.007\text{ mm}$  in thickness<sup>15</sup>) is given in Fig. 3. This sample transmitted only the red end of the visible spectrum. Beyond  $1\ \mu$  the transmission is uniform, as previously observed. The data published by Crandall,<sup>16</sup> who eliminated the losses by reflection by making measurements on two samples of different thickness, show that beyond  $1\ \mu$  the absorption decreases abruptly to a low, uniform value. (See Fig. 3.) As will be noticed presently, the greatest photo-

<sup>14</sup> Coblentz, Publication No. 97, Carnegie Institute, Washington, pp. 13 and 41, 1908; Crandall, *Phys. Rev.* (2), 2, p. 343, 1913.

<sup>15</sup> The transmissivity observations were obtained with the assistance of M. B. Long, and published in this Bulletin, 14, p. 653; 1918. The thickness was determined by L. V. Judson of the weights and measures division, using an end comparator. The specimen was pressed on a Johansson block by means of a plunger having an optically flat contact surface  $2\text{ mm}$  in diameter, the pressure being 200 g.

<sup>16</sup> Crandall, *Phys. Rev.* (2), 2, p. 343; 1913.

electric activity of molybdenite occurs in the region of the spectrum where the absorption is changing rapidly, from which it would appear that, as previously had been observed to a more limited extent, the connection between optical absorption and photoelectrical activity is rather intricate.

The wavy character of the transmission curve beyond  $2.5\mu$  is the result of interference bands. It is of interest in showing the resolving power of the apparatus. Curves of this type are of interest to students in physical optics in connection with the question of interference and the conservation of energy. The reflectivity curve of a somewhat thinner sample was published

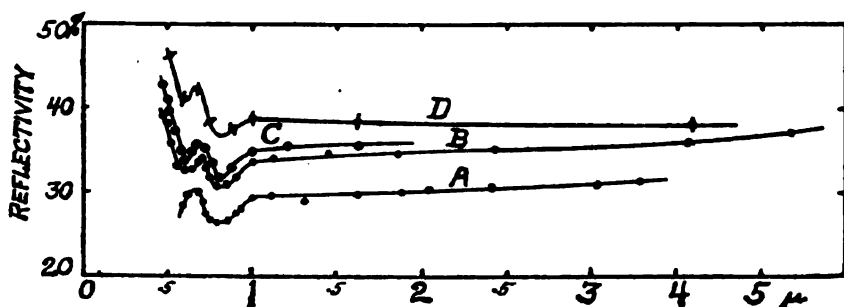


FIG. 4.—Reflectivity of molybdenite

by Crandall<sup>17</sup> who has calculated the optical constants of this mineral.

## 2. REFLECTIVITY MEASUREMENTS

In the present experiments the reflecting power of molybdenite was determined by comparison with a silver-on-glass mirror, correction being applied for absorption in the silver. The material examined was National Museum sample No. 53046, from Wakefield, Canada. The mirrors were made by pressing thin laminae of molybdenite upon plate glass. This produced smooth surfaces quite free from indentations.

In Fig. 4, curve A gives the reflecting power of a sample 0.1 mm in thickness. Curve B gives the reflectivity of a sample 0.3 mm in thickness, having a higher polish. In order to establish more thoroughly the indentations in the reflectivity curve at  $\lambda = 0.54\mu$  and  $\lambda = 0.63\mu$ , as well as the higher reflecting power in the violet, the silver mirror was replaced by a right-angled glass prism<sup>18</sup> which is nonselective in its reflection. The data obtained on this same sample, using the glass-prism reflector, are illustrated in curve C.

<sup>17</sup> Crandall, *Phys. Rev.* (2), 2, p. 356; 1913.

<sup>18</sup> This Bulletin, 14, p. 307; 1917.

On removing this sample from its mounting a thin, flat lamina adhered to the glass. The polish of this cleavage surface was higher than one could obtain by rubbing the surface, and the reflecting power is probably as near to the true value as can be attained.

These observations show that the reflecting power of molybdenite is highly selective in the visible spectrum, decreasing from 46 per cent at  $0.5\mu$  to a much lower value at  $1\mu$ , beyond which point the reflectivity is fairly uniform, as previously observed. This selective reflection is easily demonstrated by pressing a thin plate of molybdenite into a V-shaped cavity, which appears a brilliant indigo-blue when viewed in daylight.

The previous measurements<sup>19</sup> of reflecting power were made on a massive sample 2 to 3 cm in thickness. The polish was not as high as in the present work. For long waves, however, the question of polish is not a serious matter. The data then obtained indicate a reflectivity of 20 to 22 per cent, which is considerably lower than observed in the present measurements. The observations at long wave lengths where scattering is low indicate that the true reflectivity of this sample could not be very much higher than the observed value. The sample was of sufficient thickness to prevent augmentation of the reflected light by internal reflection. On the other hand, the samples used by Crandall, as well as the samples used in the present investigation, are so thin and the absorption is so low that radiations which enter the sample are reflected at the second surface, and returning (without great diminution in intensity) emerge and cause the observed reflectivity value to be higher than the true value. That this really occurs is shown in Table 1 and in the dotted curves *Refl* and *Abs*, in Fig. 3; also curve *D*, Fig. 4. These two samples had their natural cleavage surfaces untouched; hence their reflection is closely the same. Assuming five internal reflections for computing the reflectivity and four internal reflections for computing the transmitted radiations, and using the values given in Table 1 (where *A* = the per cent absorption in traversing once through the layer; say *A* = 20.5 per cent and *r* = 28.8 per cent at  $\lambda = 1.3\mu$ ) it is found that the observed transmission and reflection data are accurately reproduced. At  $0.5\mu$  there is complete opacity and the observed reflecting power (*R* = 46 per cent) is the true value. On the basis of this computation the true reflecting power, *r* (Table 1),

<sup>19</sup> Publication No. 97, Carnegie Institution of Washington; 1908.

of molybdenite is illustrated by the dotted curve *Refl* in Fig. 3, which is more nearly in agreement with the previous observations. The absorption produced in traversing once through the layer is illustrated in the curve marked *Abs* in Fig. 3; complete absorption occurred at wave lengths less than  $0.5\mu$ . These calculations indicate that the true reflecting power is of the order of 28 to 30 per cent instead of 38 to 40 per cent, as observed.

TABLE 1.—Transmission, Reflection, and Refractive Index of Molybdenite

[Key to symbols: *A*—the assumed per cent of entering light absorbed in traversing the thickness of the layer; *r*—the assumed per cent of incident light reflected at the first surface; *E*—summation of returning light; *T*—summation of transmitted light;  $n = \frac{1}{1-r} (1+r \pm \sqrt{4r})$ .]

	$\lambda = 1\mu$	$1.3\mu$	$2.2\mu$	$4\mu$
<i>A</i> .....	22.3	20.5	18.1	18.1
<i>r</i> .....	29.8	28.8	27.8	27.8
<i>E</i> (observed) .....	39.0	38.5	38.1	38.0
<i>E</i> (computed) .....	39.1	38.5	38.0	38.0
<i>T</i> (observed) .....	40.5	42.5	45.0	45.0
<i>T</i> (computed) .....	40.5	42.5	45.0	45.0
<i>n</i> .....	3.40	3.30	3.23	3.23

Using the values of *r* illustrated in Fig. 3, and neglecting the extinction coefficient, the refractive index *n* is computed on the basis of  $r = \left(\frac{n-1}{n+1}\right)^2$ . These values of *n* are given in Table 1. They are somewhat larger than similar data computed from the interference bands shown in Fig. 3, employing the formula

$$n = \frac{N\lambda_1\lambda_2}{2t(\lambda_2 - \lambda_1)}$$

in which *N* is the number of bands between  $\lambda_1$  and  $\lambda_2$  (see column 3, Table 2), and using the observed thickness of  $t = 0.007$  mm. Using  $t = 0.006$  mm gives values of *n* which are 12 per cent larger, corresponding more nearly with the values given in Table 1.

Computations of *n* are given also, utilizing single maxima or minima, and remembering that the difference in optical length of path for interference in transmission is  $2nt$  or about  $42\mu$ . Following the method of computation given by Crandall, using the formula  $2n_1t = N_1\lambda_1$ , and taking the values of  $N_1$  given in Table 2, the corresponding values of  $n_1$  were obtained. (See columns 5 and 9 of Table 2.)



In making these computations it is assumed that the small indentations (e. g.,  $4.6\mu$ ,  $5.2\mu$ ) are a second series of interference bands, the origin of which is undetermined. Only the bands given in columns 2 and 6 of Table 2 were used.

**TABLE 2.**—Refractive Indices of Molybdenite Computed by Formulas Given in Text, Using Transmission Minima or Maxima

Minima					Maxima			
$\lambda$	$\lambda_1$	$n$	$N_1$	$n_1$	$\lambda_1$	$n$	$N_1$	$n_1$
2.72	2.72	.....	14.5	2.82	2.85	.....	14	2.85
2.94	2.94	2.64	13.5	2.83	3.07	2.98	13	2.83
3.19	3.19	2.89	12.5	2.85	3.30	2.98	12	2.83
3.44	3.44	2.88	11.5	2.83	.....	.....	.....	.....
3.66 $\alpha$	.....	.....	.....	.....	3.60	2.70	11	2.83
3.80	3.80	2.66	10.5	2.85	.....	.....	.....	.....
4.07	.....	.....	.....	.....	4.00	2.77	10	2.85
4.30	4.22	2.59	9.5	2.86	4.42	2.88	9	2.84
4.53	.....	.....	.....	.....	.....	.....	.....	.....
4.77	4.79	2.74	8.5	2.91	.....	.....	.....	.....
4.96 $\alpha$	.....	.....	.....	.....	4.99	2.81	8	2.85
5.20	.....	.....	.....	.....	.....	.....	.....	.....
5.44	5.41	2.85	7.5	2.90	.....	.....	.....	.....
5.68 $\alpha$	.....	.....	.....	.....	5.70	2.88	7	2.85
5.94	.....	.....	.....	.....	.....	.....	.....	.....
6.18	.....	.....	.....	.....	.....	.....	.....	.....
6.40	6.30	2.93	6.5	2.92	.....	.....	.....	.....
6.65	.....	.....	.....	.....	6.65	.....	6	2.85
6.93	.....	.....	.....	.....	.....	.....	.....	.....
7.20	.....	.....	.....	.....	.....	.....	.....	.....
7.45	7.35	.....	5.5	2.89	.....	.....	.....	.....

$\alpha$ —Missing.

Using consecutive bands gives values of  $n$  which increase in value to  $n=14$  at  $\lambda=7\mu$ . This is inconsistent in view of the constancy of the absorption and reflection data. The region of anomalous dispersion is at  $0.5\mu$ , beyond which point the refractive index should decrease.

These data are somewhat different from those published by Crandall.<sup>20</sup> It is to be noticed that, comparing data obtained on samples having practically the same thickness, twice as many interference bands were observed in the present examination. The common difference between these bands is about  $0.23\mu$ , whereas Crandall's curves show bands separated by about  $0.45\mu$  to  $0.5\mu$  or multiples of this number.

<sup>20</sup> Crandall, *Phys. Rev. (s)*, **2**, p. 356; 1913.

## V. VARIATION OF PHOTOELECTRIC CURRENT WITH TIME OF EXPOSURE

It is well known that the photoelectric response of selenium lags considerably more for infra-red rays than for visual rays. Molybdenite is much quicker than selenium in its photoelectric response (change in electrical conductivity) when exposed to radiation, irrespective of wave length.

In view of the far greater range of sensitivity in the infra-red than heretofore observed, it is of interest to give the response-time curves of molybdenite for various wave lengths.

Fig. 14, curve A, gives the spectral photoelectric sensitivity of molybdenite when exposed for 10 seconds, while curve B gives

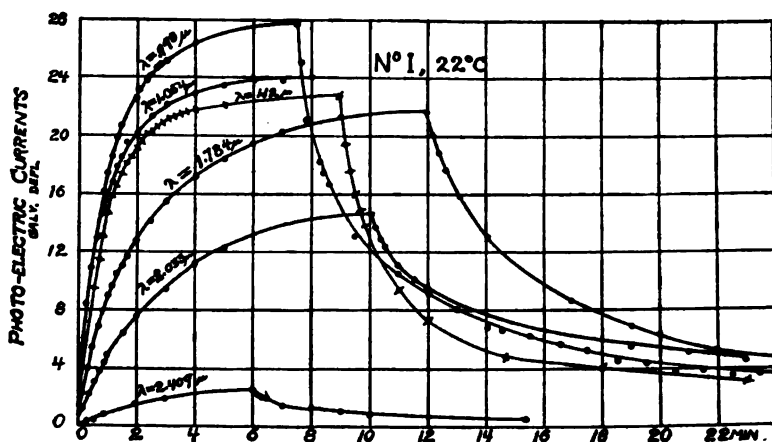


FIG. 5.—Variation of photoelectric current with time of exposure to radiation

the corresponding curve for unlimited exposure; that is, exposure until there is no further increase in the galvanometer deflection.

At  $\lambda = 0.76\mu$  the difference in photoelectric current (galvanometer deflection) for limited exposure and for unlimited exposure (which at this point was about 30 seconds) was very small. On the other hand, beyond  $\lambda = 1.4\mu$  the response is so slow that, on a 10-second exposure, the photoelectric sensitivity appears to be inappreciable.

In Fig. 5 a series of response-time curves are given, showing the variation in conductivity (photoelectric current) with time of exposure to the radiation stimulus and the rate of recovery of the sample to its original resistance. The data show that in the yellow part of the spectrum equilibrium in electrical conductivity is attained after 5 to 10 seconds exposure. This exposure

time increases very rapidly after passing beyond  $\lambda = 0.75\mu$  where an exposure of about 30 seconds is required. The time for recovery is prolonged to about two times the exposure time for equilibrium. In making the observations, twice the exposure time was therefore allowed for recovery of the original conductivity.

Experiments<sup>21</sup> show that at low temperatures the increase in conductivity of selenium when exposed to light, and the recovery after exposure, is markedly slower than at ordinary temperatures. It is of interest, therefore, to notice the behavior of molybdenite at low temperatures. As shown in Fig. 6, lowering the temperature has no marked influence upon the rate of response (conductivity) of molybdenite when exposed to radiation; nor is the time of recovery markedly different from that observed at room temperature. By a marked difference in response and recovery is meant a factor of two or three times the time (8 to 12 minutes) indicated in Fig. 5. A delay of one to three minutes for recovery at liquid-air temperatures, as compared with room temperatures, is not to be considered in view of the very rapid change in dark current (zero shift of scale reading) owing to a slight change in temperature, which could not be maintained constant closer than about  $0.03^\circ\text{C}$ .

From a casual inspection of Fig. 5 it might be inferred that it required a longer time of exposure to radiations of wave length  $\lambda = 1.784\mu$  than for  $\lambda = 2.033\mu$  in order to obtain conductivity equilibrium. In reality the upward trend of the curve for  $\lambda = 2.033\mu$  shows that equilibrium had not yet been attained after 10 minutes exposure, and that a longer exposure should have been made. However, for practical purposes it was better to terminate the exposure at this point in view of the possibility of losing by zero shift (temperature change) what might have been gained in conductivity change by further exposure of the sample to radiation.

In Fig. 6 the scale of galvanometer deflections for  $\lambda = 1.357\mu$  is magnified four times.

In practice it was the custom to allow twice the exposure time for recovery. The fact that in making a series of observations there was no continuous zero shift in one direction would indicate that allowing twice the exposure time for recombination was sufficient for complete recovery to the original dark resistance.

<sup>21</sup> McDowell, *Phys. Rev.*, **22**, p. 524, 1910.

## VI. SPECTRAL RANGE OF PHOTOELECTRIC SENSITIVITY

The first tests of photoelectric sensitivity of molybdenite were made by using wide bands of spectral energy obtained by using glass screens,<sup>22</sup> residual rays, etc. By this means it was possible to obtain radiant energy stimuli of wave lengths ranging from  $\lambda = 0.365 \mu$  in the ultra-violet to  $\lambda = 9 \mu$  in the remote infra-red.

When using the transmission glasses the source of light was either a Nernst glower or a quartz mercury vapor lamp. The energy was measured by means of a thermopile.

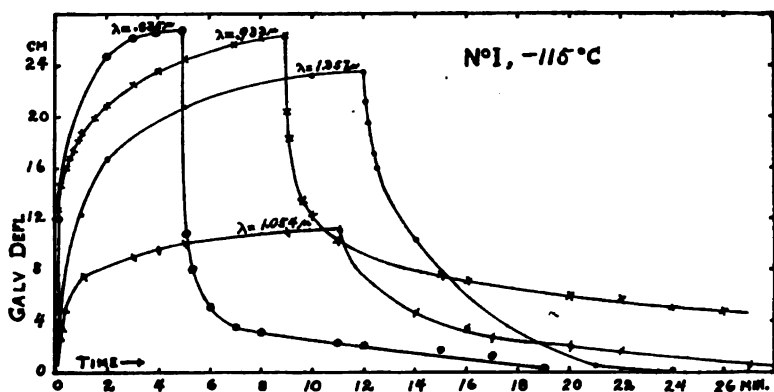


FIG. 6.—Variation of photoelectric current with time of exposure to radiation

For making this examination the following regions of the spectrum were utilized:

1. That part of the spectrum transmitted through a 5 per cent solution<sup>23</sup> of cupric chloride in a cell 2 cm in thickness and a plate of Corning glass, G55, A62 (new number G586). The maximum of the transmitted energy lies in the ultra-violet at about  $\lambda = 0.36 \mu$ . Insertion of a piece of red glass showed that all of the observed photoelectrical activity was caused by the ultra-violet rays from the mercury vapor lamp. A subsequent test showed conclusively that molybdenite at room temperature, at least, is less sensitive in the ultra-violet ( $\lambda = 0.36 \mu$ ) than in the visible spectrum, as shown in Fig. 14.

2. By using a 2 cm cell of water and Crookes's sage-green (ferrous No. 30) glass, a fairly monochromatic band is obtained, having its maximum intensity at  $\lambda = 0.53 \mu$ .

<sup>22</sup> This Bulletin, 14, p. 653, 1918. Some of the photoelectric data obtained by this method were given at the Pittsburgh meeting, Amer. Assn. Adv. Sci., Dec., 1917 (see Phys. Rev., 13, p. 140, 1919).

<sup>23</sup> Bulletin, 7, p. 619, 1911; 9, p. 110, 1912.

3. Using a Corning Noviweld glass "shade 30 per cent," a 2 cm water cell, and a Nernst glower, regulated to give equal energies throughout the spectrum, the maximum intensity of the light stimulus was at about  $\lambda = 0.56 \mu$ .

4. Using Corning purple glass, G55, A62, Schott's red glass, 2745, and a 2 cm cell of water, gave a transmission band having its maximum intensity at  $\lambda = 0.77 \mu$ .

5. Using Corning blue-purple glass G585, Schott's red glass, 2745, and a 2 cm cell of water (when using the Nernst glower below normal operation) gave a band of maximum transmission at about  $\lambda = 0.85 \mu$ .

6. Using three sheets of electric-smoke glass gave a wide band of spectral energy with a maximum at about  $2.2 \mu$ .

7. The radiation from a Bunsen flame gave an emission band with maximum at  $4.4 \mu$ .

8. The residual rays obtained by reflection from two surfaces of quartz, using a Nernst glower as a source, gave two intense bands of selective reflection,  $8.5 \mu$  and  $9.05 \mu$ , respectively, the mean value being about  $\lambda = 8.8 \mu$ .

Using equal energies, the data obtained by this method showed that molybdenite is somewhat photoelectrically sensitive in the violet, and has a maximum of sensitivity at about  $1 \mu$  in the infra-red. An indentation in the curve indicated a possible maximum (No. 1 was used, see Fig. 7) at  $\lambda = 0.75 \mu$ , as was demonstrated conclusively in a later examination. A fairly high sensitivity was indicated at  $2.2 \mu$ . The Bunsen flame caused a small change in electrical conductivity. This was probably produced by radiations of wave length  $1.8 \mu$  and  $2.7 \mu$ . A subsequent examination using the spectrometer showed no sensitivity at 3 to  $4 \mu$ .

As indicated elsewhere,<sup>24</sup> the most important contribution to be made by this test was to establish to what extent this decrease in electrical resistance is caused by rise in temperature when exposed to radiation. The measurements, using radiations dominating at  $\lambda = 8$  to  $9 \mu$  are useful in settling this question. Since the reflection and absorption of molybdenite is uniform throughout the spectrum the application of equal energies of different wave lengths should produce approximately the same thermal change, irrespective of the wave length.

Using radiations of wave length  $\lambda = 8$  to  $9 \mu$ , the photoelectric effect produced a galvanometer deflection of 15.5 to 16 mm. On

<sup>24</sup> This Bulletin, 14, p. 603, 1918.

inserting a plate of clear glass, which is opaque to radiations of wave length greater than  $4\ \mu$ , the deflection was 14.5 mm, indicating that the photoelectric effect is produced by scattered radiations of wave length less than  $4\ \mu$ . Moreover, it is caused entirely by the energy of wave lengths less than  $4\ \mu$ . For, correcting for losses by reflection and absorption which amount to 8 to 9 per cent in the glass plate, the deflection is increased from 14.5 to 15.8 mm, which is in agreement with the observations made without the glass.

The conclusions to be drawn from these experiments are that molybdenite is not photoelectrically sensitive to infra-red rays of wave lengths  $\lambda = 8$  to  $9\ \mu$ , and that the observations at the shorter

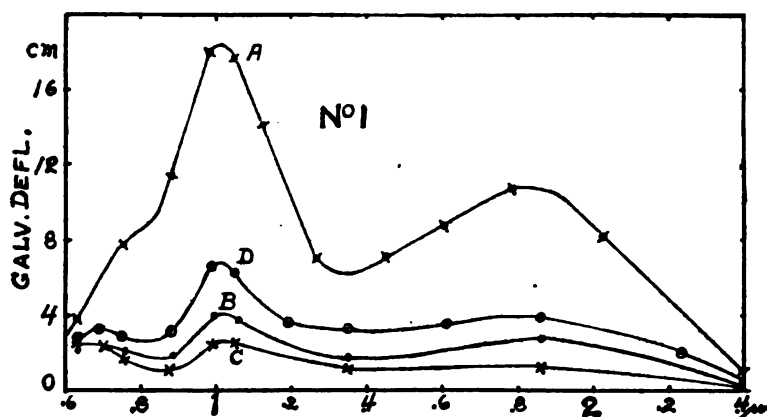


FIG. 7.—Spectral photoelectric sensitivity of different parts of a crystal of molybdenite

wave lengths were not affected by the purely thermal changes produced on exposure to radiation.

## VII. EXPERIMENTAL DATA ON VARIOUS SAMPLES

Unless otherwise stated, the samples examined were selected from material obtained from Yorke Peninsula, South Australia. They were numbered consecutively as investigated. Their dimensions and resistances are given in Table 3. Under the present caption are given additional particulars and comments relative to the behavior of these samples.

In all these illustrations, unless otherwise stated, the samples were exposed in the glass container *P*, shown in Fig. 2.

In these illustrations the ordinates represent the observed galvanometer deflections, which are proportional to the change in electrical conductivity caused by the energy stimulus.

TABLE 3.—Dark Resistance of Molybdenite Samples Against Direction of Current

[Key to symbols: *L*—Length; *W*—width; *T*—thickness in centimeters; *SP. R*— $\frac{\text{Resistance}}{\text{CM}^2}$ ; *R* and *R'*—ohmic resistance in opposite directions. Source.—A—Australia; Al—Alaska; C—Canada; J—Japan; Col—Colorado.]

No.	Source.	<i>R</i>	<i>R'</i>	<i>R</i> − <i>R'</i>	$\frac{R-R'}{R}$	<i>L</i>	<i>W</i>	<i>T</i>	<i>SP. R</i>	<i>SP. R'</i>
1.....	A.....	640 000	625 000	15 000	2.3	0.6	0.4	.....	.....	.....
2.....	A.....	1 340 000	1 135 000	205 000	15.3	.8	.4	0.004	2680	2270
4.....	A.....	457 000	443 000	14 000	3.1	.8	.2	.011	1255	1215
5.....	A.....	600 000	590 000	10 000	1.7	.....	.....	.....	.....	.....
6.....	A.....	590 000	515 000	75 000	12.7	.7	.4	.008	2690	2350
7.....	A.....	1 670 000	1 640 000	30 000	1.8	.....	.....	.....	.....	.....
8.....	A.....	100 000	92 000	8 000	8	.6	.5	.006	500	460
9.....	A.....	448 000	440 000	8 000	1.8	.7	.4	.003	758	751
10.....	A.....	4 000 000	3 900 000	100 000	2.5	.6	.35	.006	14 000	13 700
11.....	A.....	3 300 000	2 100 000	1 200 000	36.4	.8	.5	.008	16 500	10 500
12.....	A.....	540 000	463 000	77 000	14.3	.6	.5	.....	.....	.....
13.....	A.....	334 000	329 000	5 000	1.5	.7	.3	.....	.....	.....
14.....	A.....	675 000	570 000	105 000	15.6	.8	.3	.....	.....	.....
15.....	A.....	1 050 000	1 000 000	50 000	4.8	.8	.35	.007	3220	3060
16.....	A.....	9 900 000	5 000 000	4 900 000	49.5	.5	.3	.....	.....	.....
17.....	A.....	820 000	790 000	30 000	3.7	.8	.4	.....	.....	.....
18.....	Al.....	54 000	16 400	37 600	69.6	.8	.3	.005	101	30.7
19.....	Al.....	8 500	4 300	4 200	49.4	1.1	.3	.005	11.6	5.86
20 <sup>a</sup> .....	C.....	1 760	1 760	0	0	1.2	.3	.006	2.6	2.6
21 <sup>a</sup> .....	C.....	9 470	9 470	0	0	1.5	.5	.005	15.8	15.8
22 <sup>a</sup> .....	J.....	2 875	2 875	0	0	.68	.35	.006	8.9	8.9
23 <sup>a</sup> .....	C.....	69 800	69 800	0	0	.9	.12	.001	10	10
24 <sup>a</sup> .....	C.....	20 900	20 900	300	1.4	.85	.17	.002	8.5	8.5
25 <sup>a</sup> .....	Col.....	17 210	16 980	230	1.3	.87	.12	.004	9.5	9.4

<sup>a</sup>—non-sensitive.

*Sample No. 1.*—In Fig. 7 curve *A* gives the spectral photo-electric sensitivity when this sample was mounted directly in front of the spectrometer slit *S*, Fig. 2, and hence observed at a somewhat higher intensity than curve *D*, which was observed when the sample was in the glass container.

The mounting of this specimen happened to be perforated, permitting irradiation of the rear surface of the molybdenite. Curves *B* and *C* show the change in electrical conductivity when an edge and central portion of the rear side were exposed to radiation.

As will be noticed in subsequent tests of other samples, the position of the maxima and their relative intensities as well as their absolute intensities depend upon the part of the crystal exposed. This sample has maxima at wave lengths  $\lambda=0.72\mu$ ,  $1.02\mu$ , and  $1.78\mu$ .

The effect of temperature and of intensity upon these maxima is illustrated in Figs. 14 to 17.

*Sample No. 2.*—Curves *A* and *B*, Fig. 8, show the photoelectric sensitivity of two regions of this sample. A small maximum appears at  $\lambda=0.85\mu$  and two maxima of about equal intensity at wave lengths  $\lambda=0.99\mu$  and  $1.85\mu$ , respectively.

*Sample No. 3.*—Curves *C* and *D*, Fig. 8, illustrate the photoelectric behavior of two positions on this sample which appears similar to sample No. 1. There are maxima at wave lengths  $\lambda=0.73\mu$ ,  $1.03\mu$ , and  $1.82\mu$ , respectively.

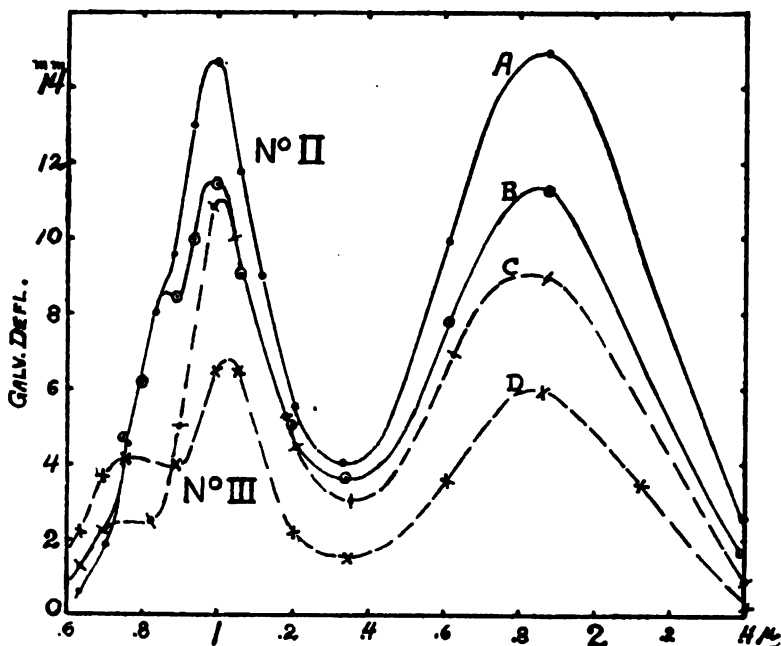


FIG. 8.—Photoelectric sensitivity of different parts of a crystal; also of different crystals

*Sample No. 4.*—This is the most remarkable sample examined in that at room temperature it has but one maximum, occurring at about  $\lambda=0.85\mu$ ; Fig. 9, curves *D* and *E*, show the photoelectric behavior for two positions. The photoelectric sensitivity seemed to be confined to one small spot (see Fig. 19) for its behavior at low temperatures.

*Sample No. 5.*—Curves *A*, *B*, *C*, Fig. 9, illustrate the photoelectrical behavior of different parts of the surface. This sample is conspicuous for the absence of the first band usually observed at  $\lambda=0.7\mu$  to  $0.8\mu$  and for the greater intensity of the  $1.85\mu$  band as compared with the one at  $1\mu$ .



*Sample No. 6.*—In Fig. 10 the lower curve shows the behavior of sample No. 6, which is similar to No. 5, with a possible small band at  $\lambda = 0.8\mu$ . The other maxima are at  $1.02\mu$  and  $1.85\mu$ .

The inserted diagram shows the important spots (indicated by shaded areas) of photoelectric sensitivity. The black dots represent points giving high rectification of current, which will be discussed presently.

*Sample No. 7.*—In Fig. 10 curve A illustrates the spectral photoelectric response of the central portion of sample No. 7. In

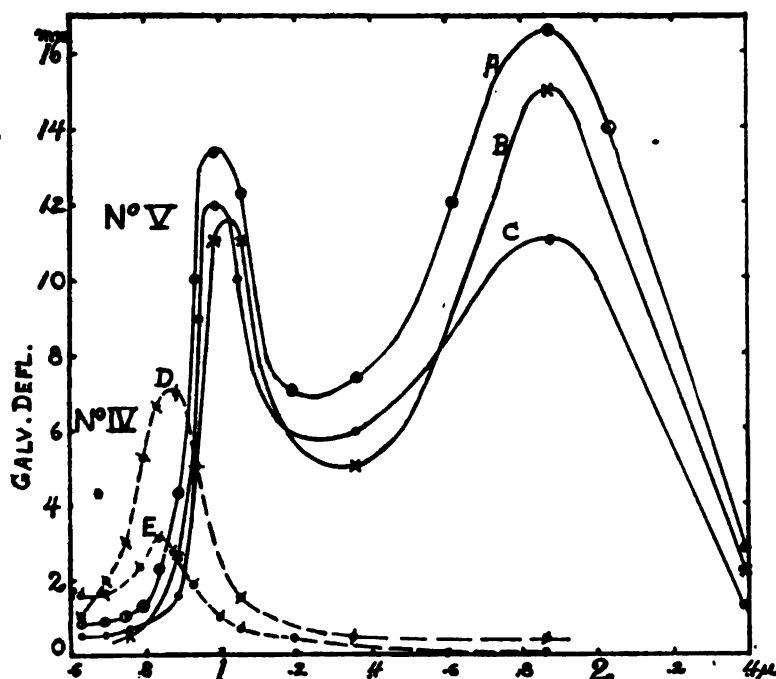


FIG. 9.—Photoelectric sensitivity of different parts of a crystal; also of different crystals

the upper rectangular diagram the shaded area represents the portion of the crystal which was photoelectrically sensitive, while the black dots represent points which showed high-current rectification. There are maxima at wave lengths  $\lambda = 0.85\mu$ ,  $1.02\mu$ , and  $1.85\mu$ .

*Sample No. 8.*—In Fig. 11 the shaded portion of the rectangular diagram, marked  $\text{MoS}_2$ , represents the portion of the sample which was photoelectrically sensitive as determined with a photophone, the energy stimulus being about 1 mm in diameter. The

image of the spectrometer slit (0.5 by 10 mm) was projected lengthwise, at the points marked *A*, *B*, *C*, *D*, and *E* upon the crystal. The corresponding sensitivity curves are given in Figs. 11 and 12. These curves (*C* is incomplete) are interesting in that they show the gradual development of a maximum at wave length  $\lambda = 0.85\mu$ , belonging to a crystal aggregation in the center of the sample, which differs from the sensitive material along the lower edge of the crystal, curve *E*. The material along the lower edge of the crystal produced but two maxima, at wave lengths  $\lambda = 1.02\mu$  and  $1.85\mu$ , respectively, as found in sample No. 5.

*Sample No. 9.*—In Fig. 13 is given the spectral sensitivity curve of sample No. 9, which is conspicuous for its two maxima of equal

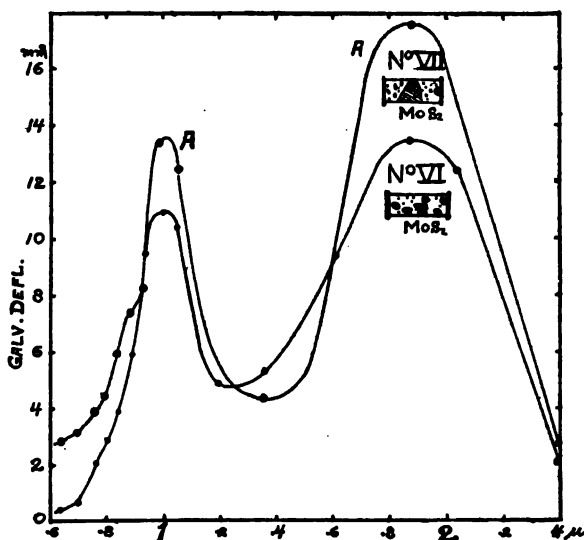


FIG. 10.—Photoelectric sensitivity of various crystals of molybdenite

intensity at wave lengths  $\lambda = 1.02\mu$  and  $1.85\mu$ , and a small maxima at  $\lambda = 0.85\mu$ .

*Sample No. 10.*—This sample was quite insensitive. However, an examination of two positions, curves *A* and *B*, Fig. 13, shows a maximum sensitivity at wave length  $\lambda = 0.86\mu$ . It is sensitive also in the region of  $\lambda = 1.85\mu$ , as observed in other samples, especially No. 4.

*Sample No. 11.*—The dotted curve in Fig. 12 gives the sensitivity curve of sample No. 11, which, like No. 5, is conspicuous for the absence of the band usually found at about  $0.8\mu$ . The maxima of sensitivity are at wave lengths  $\lambda = 1.02\mu$  and  $1.85\mu$ , respectively.

*Samples No. 18, 20, and 22.*—These samples were tested for sensitivity at the temperature of boiling liquid air where, as shown in Fig. 21, they show sensitivity in the region of  $\lambda = 0.85\mu$ .

At room temperatures sample No. 18 showed slight sensitivity (1 to 2 mm deflection) in the spectrum from  $0.6\mu$  to  $1\mu$ . Samples No. 20 and 22 were not sensitive even when exposed to radiation of much higher intensity.

The foregoing results show that at room temperatures the sensitivity maxima, at wave lengths  $\lambda = 1.02\mu$  and  $1.80\mu$ , respectively, always occur together. Some samples show an additional

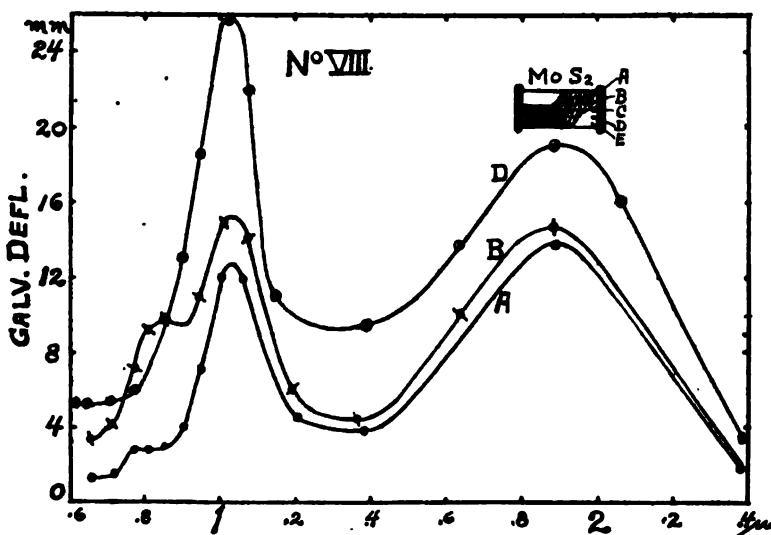


FIG. 11.—Photoelectric sensitivity of different parts of molybdenite sample No. 8. (See also Fig. 12.)

maximum at  $\lambda = 0.7\mu$  to  $0.85\mu$ . Other samples show only a single band of sensitivity at wave length  $\lambda = 0.85\mu$ .

## VIII. EFFECT OF INTENSITY OF RADIATION UPON ELECTRICAL CONDUCTIVITY

Attempts have been made to formulate laws connecting the intensity (energy  $E$ ) of the exciting light and the resulting change (galvanometer deflection) in conductivity of the selenium cell. In an investigation of the application of selenium to photometry Pfund<sup>25</sup> points out that the final law will depend upon the character of the cell, time of exposure, and the absolute intensity of the exciting light. He made no attempt to establish a law for

<sup>25</sup> Pfund, *Phys. Rev.*, **34**, p. 375, 1912.

very intense or very weak illuminations. Using exposures of 12.5 seconds, he found that the law connecting  $d$  and  $E$  to be approximately of the form  $d = K E^\beta$  where  $K$  and  $\beta$  are constant as long as the wave length of the exciting light remains unchanged. The value of  $\beta$  was approximately 0.5, or the conductivity is approximately proportional to the square root of the energy stimulus.

In a subsequent investigation of the selenium cell, Nicholson,<sup>26</sup> using unlimited exposures, found the square-root law to be only approximately true; that instead of the value of  $\beta$  being

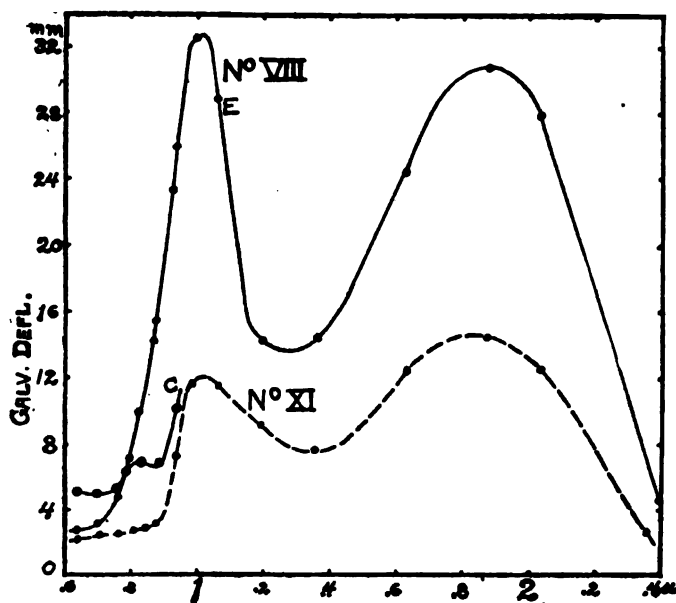


FIG. 12.—Photoelectric sensitivity of different parts of a crystal

constant there is an appreciable minimum at  $\lambda = 0.6\mu$  where  $\beta = 0.4$ . Spectral purity does not explain this disagreement.

Using exposures of 10 seconds, Elliot<sup>27</sup> investigated the law connecting the energy of the exciting light and the change in conductivity induced in stibnite. He assumed the square-root law to hold, and found that the values of  $\beta$  did not prove the law. He argues that if unlimited exposures had been used it would be safe to say that the square-root law would hold for stibnite, and then concludes that stibnite obeys the law, with  $\beta = 0.5$ , approximately. The conclusion to be drawn from the foregoing citation is that the experimental data do not indicate a simple

<sup>26</sup> Nicholson, Phys. Rev. (2), 8, p. 9, 1914.

<sup>27</sup> Elliot, Phys. Rev. (2), 8, p. 59, 1915.

square-root law, though for very rough calculations one might assume the law to obtain.

In view of the uncertainty of the experimental data just cited it was of interest to make similar tests of the effect of intensity of the exciting light upon the electrical conductivity of molybdenite at 22° C.

For this purpose sample No. 1 was securely mounted in front of the spectrometer slit *S*, Fig. 2. The observations are illustrated in Fig. 14, in which curve *B* gives the sensitivity for an intensity  $E = 20$ , while curve *C* shows the change in conductivity produced by an intensity  $E = 1$ . The latter intensity was obtained by covering the prism with a piece of black cardboard with a

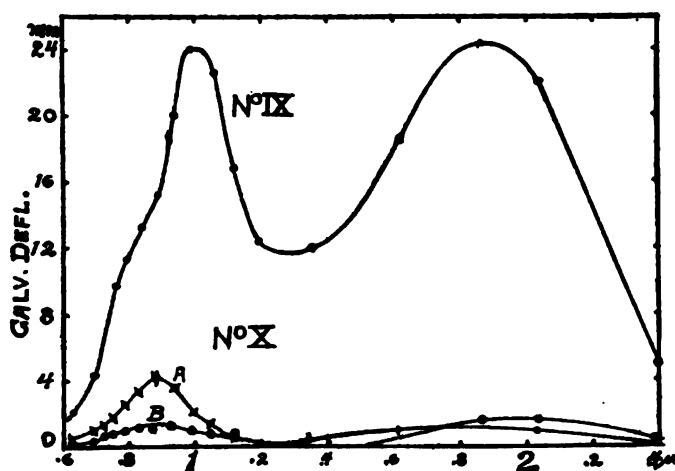


FIG. 13.—Photoelectric sensitivity of different crystals of molybdenite

slit in it, which happened to transmit almost exactly one-twentieth of the initial intensity. The results show that on increasing the intensity 20 times the spectral photoelectric responses are increased about 10 times in the region up to  $0.75\mu$ , 11 times at  $1.05\mu$ , and 20 times at  $1.8\mu$ . In other words, on increasing the intensity 20 times the change in conductivity produced by energy of wave lengths  $\lambda = 1.8\mu$  is twice as great as observed at  $\lambda = 0.75\mu$ . These energy stimuli are indicated by  $E = 1$  and  $E = 20$  in Fig. 15, which gives a series of isochromatic response curves for various wave lengths and for much higher intensities (40 times greater) than used in the investigation of the various samples just described.

In Fig. 14 curve *A* is for limited exposure and curve *B* for exposure until a steady state is attained, as already described.

Using the data illustrated in Fig. 15, which are for unlimited exposure (and are considered more accurate than those illustrated in Fig. 14), computations were made to test the validity of the square-root law. The computations show that (see Table 4) the induced change in electrical conductivity is not, as a general rule, proportional to the square root of the intensity (energy) of the radiation stimulus.

For example, selecting wave length  $\lambda = 0.6252\mu$ , using  $E = 2$  and  $E = 8$  (square root of ratio = 2), the corresponding galvanometer deflections,  $d$ , are 4.4 and 9.8, or a ratio of 2.23 instead

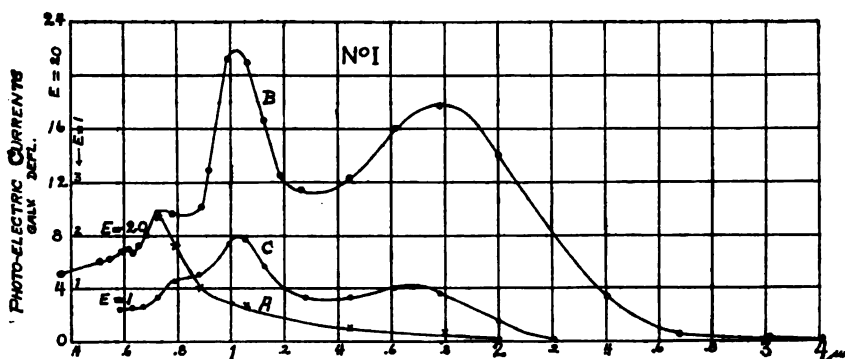


FIG. 14.—Effect of intensity of radiation upon spectral photoelectric sensitivity

of 2.0, as would be expected on the basis of the alleged square-root law.

TABLE 4.—Showing the Relation Between the Intensity  $E$  of the Exciting Light and the Resulting Change in Conductivity, Galvanometer Deflection,  $d$ ;  $d = kE^s$

$\frac{1}{\beta} \sqrt{\frac{E_y}{E_x}} - 2$		$\frac{\lambda = 0.5876\mu}{\lambda = 0.625\mu}$			$\lambda = 0.6975$			$\lambda = 0.725$			$\lambda = 0.882$			$\lambda = 1.44$			$\lambda = 2.033$		
$E_y$	$E_x$	$d_y$	$d_x$	$\frac{d_y}{d_x}$	$d_y$	$d_x$	$\frac{d_y}{d_x}$	$d_y$	$d_x$	$\frac{d_y}{d_x}$	$d_y$	$d_x$	$\frac{d_y}{d_x}$	$d_y$	$d_x$	$\frac{d_y}{d_x}$	$d_y$	$d_x$	$\frac{d_y}{d_x}$
4	.....	6.6	.....	2.44	—	.....	—	8.5	.....	3.15	9.7	.....	2.77	12.4	.....	2.48	14.1	.....	2.35
.....	1	2.7	.....	.....	—	.....	—	2.7	.....	3.5	.....	.....	.....	5	.....	.....	6	.....	.....
8	.....	9.8	.....	2.22	12.1	.....	2.42	13.1	.....	2.54	14.9	.....	2.44	17.6	.....	2.67	19.7	.....	1.97
.....	2	4.4	.....	.....	5	.....	.....	5.1	.....	.....	6.1	.....	.....	6.6	.....	.....	10	.....	.....
10	.....	11.1	.....	2.21	13.7	.....	2.40	15	.....	2.46	15.0	.....	2.14	20	.....	2.08	22.1	.....	1.98
.....	2.5	5.0	.....	.....	5.7	.....	.....	6.1	.....	.....	7.0	.....	.....	9.6	.....	.....	11.2	.....	.....
12	.....	12.5	.....	2.27	15.1	.....	2.32	16.7	.....	2.39	19.1	.....	2.38	22.1	.....	2.06	24.4	.....	2.02
.....	3.0	5.5	.....	.....	6.5	.....	.....	7.0	.....	.....	8.0	.....	.....	10.7	.....	.....	12.1	.....	.....
16	.....	—	.....	.....	17.9	.....	2.24	19.8	.....	2.34	23.1	.....	2.38	—	.....	.....	—	.....	.....
.....	4	—	.....	.....	8	.....	.....	8.5	.....	.....	9.7	.....	.....	—	.....	.....	—	.....	.....

From the intensities used and the spectral range examined, it appears that at low intensities of the exciting radiation the change in electrical conductivity induced in molybdenite is much greater than for higher intensities. For rough calculations the value of  $\beta = 0.43$  may be used.

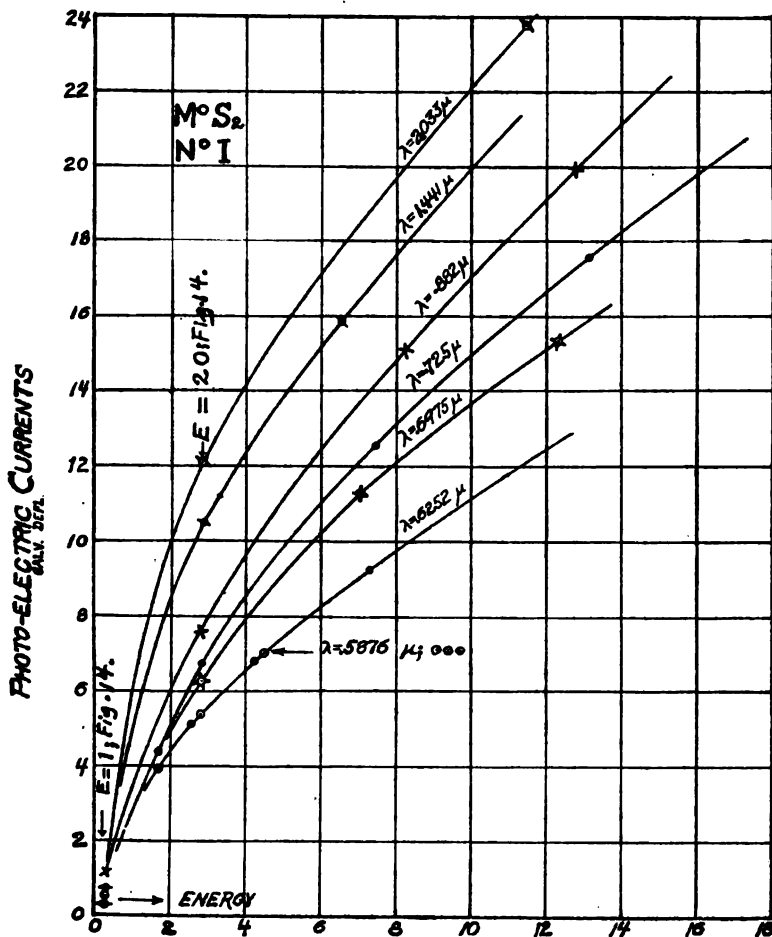


FIG. 15.—Effect of intensity of radiation upon photoelectric response

The data in Table 4 were obtained from Fig. 15, in which the abscissa represents the energy,  $E$ , to which the molybdenite was exposed. Using even values of  $E$  and four times its value (e. g.,  $E=4$  and  $E=16$ ) the ratio of the corresponding galvanometer deflections,  $d_{16} \div d_4$  should equal the whole number 2 if the square-root law holds. An inspection of these columns of ratios  $\left(\frac{d_y}{d_x}\right)$  for different wave lengths shows that the value  $\beta$  depends upon the wave length as well as the intensity of the exciting radiations.

## IX. EFFECT OF TEMPERATURE ON PHOTOELECTRIC SENSITIVITY

An interesting part of this investigation was the determination of the effect of temperature on photoelectrical conductivity. The electrical conductivity of molybdenite decreases rapidly with decrease in temperature, so that at a temperature of  $-140^{\circ}$  to  $-178^{\circ}$  C (attained by cooling with liquid air) the resistance is 150 to 2000 times as great as at room temperature. On the other hand, at this low temperature the change in conductivity

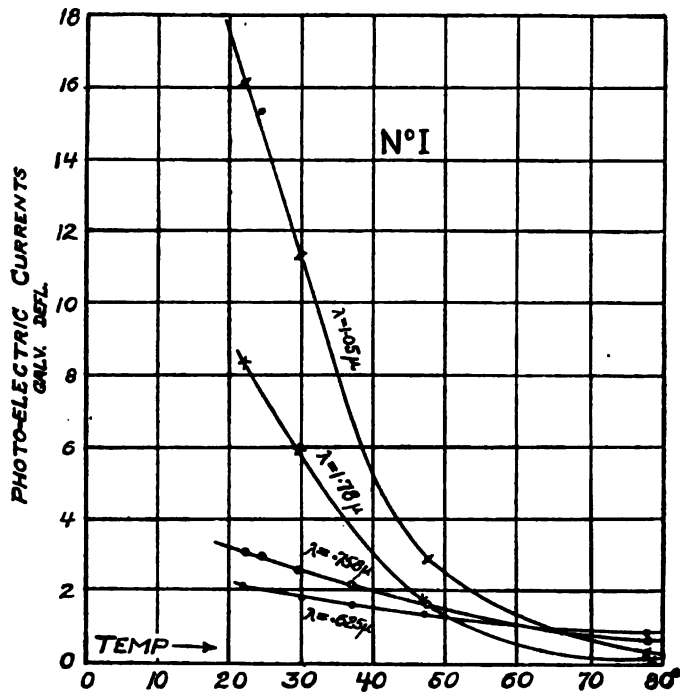


FIG 16.—Effect of temperature upon photoelectric sensitivity

induced in some samples of molybdenite, when exposed to radiation of certain wave lengths, is from 50 to 200 times as great as at room temperatures. This comparison was obtained by increasing the voltage applied to the sample, at liquid-air temperature, to produce practically the same dark current (galvanometer deflection of 60 to 85 cm) as obtained when the sample was operated at room temperature. In practice the samples were operated on 2 to 4 volts at room temperature and on 40 to 133 volts (dry cells) at liquid-air temperatures. The dark currents were noted and a factor was applied to indicate the deflection that



would have been obtained if the sample had shown the same dark current at these two temperatures. This does not affect the relative spectral sensitivity curves, but merely gives the reader some idea of the size of the deflections that would be expected when the crystal was examined under comparable conditions.

*Sample No. 1.*—In one test the molybdenite sample No. 1 was mounted in a small wooden box containing a thermometer and a thin strip of platinum heated by a storage battery. A rock-salt window permitted exposure to radiation. The sample was mounted at the exit spectrometer slit. As shown in Fig. 16, using

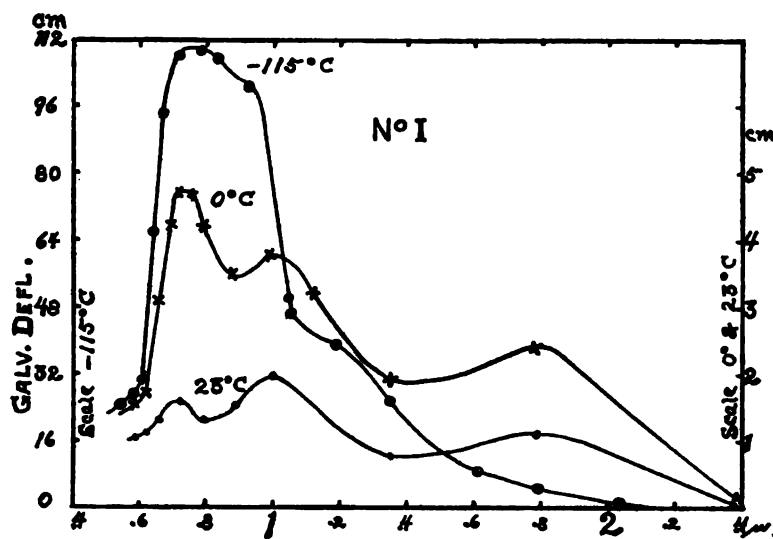


FIG. 17.—Effect of temperature upon spectral photoelectric sensitivity

the same intensity (applied voltage, 2 volts) and varying the temperature of the sample, it was found that the maxima at  $\lambda = 1.5\mu$  and  $1.78\mu$  decreased very rapidly in intensity, so that at  $80^\circ\text{C}$  the photoelectric action produced by radiations of these wave lengths had practically disappeared, whereas the radiations of short-wave lengths still produced a change in electrical conductivity.

In the following tests the sample was mounted in the glass receptacle illustrated in Fig. 2 and the temperature changed as already described. In Fig. 17 is illustrated the change in photoelectric sensitivity of sample No. 1 when operated at  $23^\circ\text{C}$ ,  $0^\circ\text{C}$ , and  $-115^\circ\text{C}$ . For the latter temperature the observed galvanometer deflections (maximum = 16 cm) were multiplied

by the factor 8, in order to show the approximate sizes of the deflection to be expected for the same dark current. The potential actually applied was 10 volts.

At  $0^{\circ}\text{C}$ , sample No. 1 on 2 volts gave a (dark-current) galvanometer deflection of 43 cm and on 4 volts a deflection of 86 cm. Using radiations of  $\lambda = 0.724\mu$ , the corresponding (photoelectric) galvanometer deflections were 23.5 and 47 mm, respectively, indicating a close proportionality between the dark current and the photoelectric current.

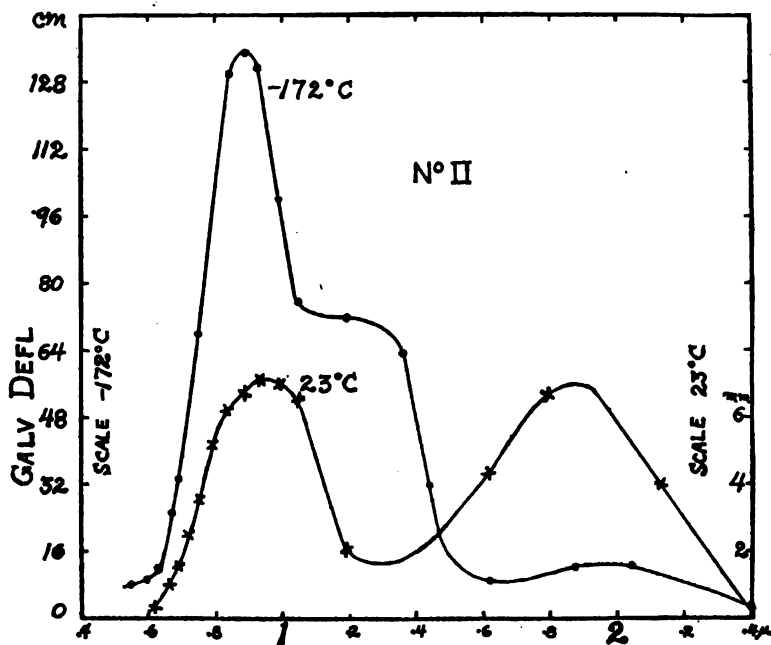


FIG. 18.—Effect of temperature upon spectral photoelectric sensitivity

These curves show that as the temperature decreases the radiations of short-wave lengths produce a greater change in electrical conductivity than do the long-wave lengths. As a result, the maximum of the sensitivity curve is shifted from  $\lambda = 1.02\mu$  to  $\lambda = 0.75\mu$ . A new band occurs at  $\lambda = 1.2\mu$ .

*Sample No. 2.*—In Fig. 18 are given the photoelectric sensitivity curves of sample No. 2 at  $23^{\circ}\text{C}$  and  $-172^{\circ}\text{C}$ , respectively. In the latter the scale of deflections is magnified 8 times, to represent equal dark-current conditions. The voltage applied at  $-172^{\circ}\text{C}$  was 133 volts. The maximum of the sensitivity curve is shifted to the short wave lengths, the maxima being at  $\lambda = 0.88\mu$ ,  $1.20\mu$ , and  $1.9\mu$ , respectively.

*Sample No. 4.*—The effect of temperature upon the photoelectric conductivity of sample No. 4 is shown in Fig. 19. The observations at 25° C confirm the measurements made some months earlier, curves *D* and *E*, Fig. 9. At -178° C the maximum appears to be shifted slightly to the longer wave lengths,  $\lambda = 0.89\mu$ , and a second band appears at  $\lambda = 1.23\mu$ . The observed galvanometer deflections (2 cm at  $\lambda = 1.23\mu$ ) are multiplied by the factor 25, to indicate the deflections to be expected for the same dark current, at these two temperatures. The deflections being so small it is uncertain whether the  $1.23\mu$  band is present at room temperature. At -178° C this sample was practically nonconducting, and 133 volts were applied in making the examination, as against 2 volts at room temperature.

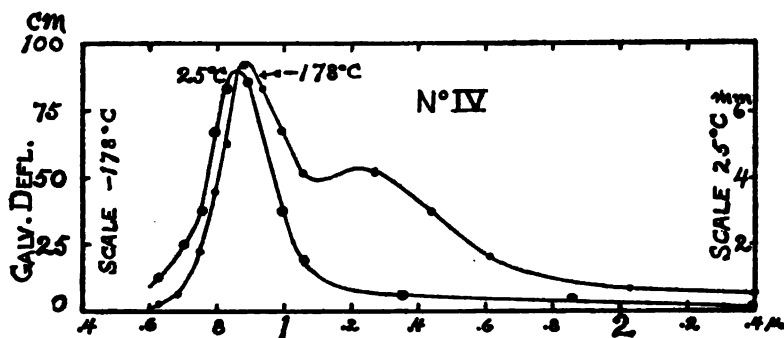


FIG. 19.—Effect of temperature upon spectral photoelectric sensitivity

*Sample No. 5.*—In Fig. 20 are given a series of photoelectric conductivity curves of sample No. 5, which was mounted as shown in Fig. 2 and observed under similar conditions. The temperature points 38° C, 26° C, 0° C, and -142° C were obtained by means of hot water, ice, and liquid air, as already explained. The potentials applied were 2 volts at 38° C and 26° C, 4 volts at 0° C, and 40 volts at 142° C. The observed galvanometer deflections are given in Fig. 20. In order to make the observations comparable (for the same dark current), the galvanometer deflections for 0° C would be 17 times greater than plotted in Fig. 20.

These data are of interest in showing the rapid shift of the maximum sensitivity toward the short wave lengths, with decrease in temperature. At -142° C there are maxima at  $\lambda = 0.88\mu$ ,  $1.35\mu$ , and  $1.9\mu$ , respectively, as compared with two maxima at  $\lambda = 1.02\mu$  and  $1.9\mu$ , respectively, at room temperatures.

In view of the long time required in order to obtain the data at  $1.8\mu$ , the irregularities in the relative intensities and in the position of the maximum are probably to be attributed to experimental errors.

*Sample No. 18.*—National Museum specimen No. 61448, from Shirakawa Hidi, Japan. This material had a low resistance and a low photoelectrical conductivity at room temperatures. At liquid-air temperatures,  $-178^{\circ}\text{C}$ , this sample shows a band of

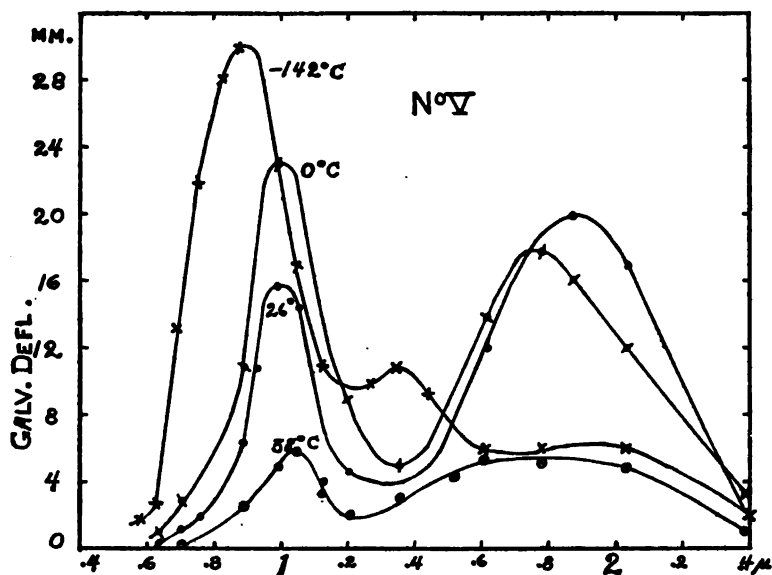


FIG. 20.—Effect of temperature upon spectral photoelectric sensitivity

photoelectrical sensitivity with a maximum at  $\lambda = 0.85\mu$ . (See Fig. 21.)

*Sample No. 20.*—National Museum specimen No. 53046, from Wakefield, Canada. Transmission and reflection measurements were also made on this material, which has a low photoelectric conductivity even at low temperatures, at  $-177^{\circ}\text{C}$ . There is a single maximum at wave length  $\lambda = 0.85\mu$  (lower curve of Fig. 21).

*Sample No. 22.*—National Museum specimen No. 86194, from near Chilcoot Pass, Alaska. This material has a low resistance and low photoelectric sensitivity at room temperatures. At  $-178^{\circ}\text{C}$  this material shows a wide band of spectral photoelectric sensitivity, with a maximum at wave length  $\lambda = 0.85\mu$ . (Fig. 21).

A general survey of these curves shows that samples of molybdenite which show but small photoelectrical sensitivity at room temperatures exhibit considerable photoelectrical conductivity at

the temperature of boiling liquid air. This, of course, is to be expected in view of what was observed on samples which are quite sensitive at ordinary temperatures. The comparison is one of magnitude of photoelectrical sensitivity rather than one of quality. For at low temperatures, where all samples exhibit sufficient photoelectrical sensitivity to make the tests trustworthy, the maximum photoelectrical conductivity of samples from different localities is produced by radiations of wave lengths in the spectrum at  $\lambda = 0.85\mu$ . As already mentioned, Crandall<sup>22</sup> records observations made by Trowbridge which show that the transparency of molybdenite is considerably increased in the visible

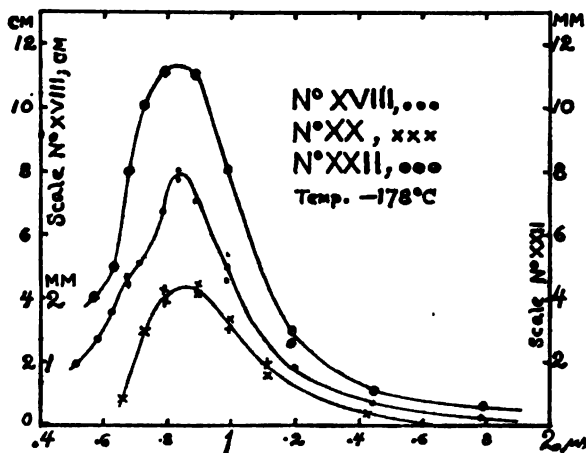


FIG. 21.—Effect of temperature upon spectral photoelectric sensitivity

spectrum when the material is cooled to liquid-air temperature. Just what this has to do with a similar shift of the maximum of the photo electric sensitivity curve toward the visible spectrum is not known. That such a shift occurs appears to be an established fact. That the greatest photoelectrical activity occurs where the absorption is low, and that this region of maximum activity shifts toward the region of maximum absorption, is worthy of notice even though no explanation is offered to account for the observations.

## X. EFFECT OF HUMIDITY, VACUUM, AND MECHANICAL WORKING

In the early part of this investigation the question arose as to the effect of humidity on the photoelectrical conductivity of molybdenite. The test was made in an air-tight glass receptacle

<sup>22</sup> Crandall, *Phys. Rev.* (2), 2, p. 343; 1913.

which replaced the glass tube G, Fig. 2. Provision was made to introduce phosphorus pentoxide into the vessel and sealing it without disturbing the adjustments. An interval of four hours elapsed after introducing the dehydrating material. The observations were made at 25° C with the humidity of the surrounding air amounting to 81 per cent or 12.1 g per cubic meter.

The results obtained show that this amount of moisture had no observable effect upon the photoelectrical conductivity.

Observations of the effect of air upon photoelectrical change in conductivity were made, using the sample in the glass receptacle G, Fig. 2. Keeping the temperature constant, the results obtained with the molybdenite in air and a vacuum show that the spectral photoelectric sensitivity curve was not affected by the surrounding air. Recent experiments of Tisdale<sup>29</sup> indicate that the photoelectric conductivity of selenium is affected by gases and metallic vapors.

The conclusion arrived at is that the photoelectrical conductivity observed in molybdenite is inherent in the crystal, and that this property is not affected by the ordinary changes in humidity and gas pressure.

One line of investigation which requires further attention is the effect produced upon the photoelectrical sensitivity when the surface of the molybdenite sample is worked mechanically.

In a previous investigation<sup>30</sup> it was found that silver sulphide which had been prepared in the laboratory and subjected to rolling and hammering was not very sensitive photo-electrically. On the other hand, a sample of the natural mineral, acanthite  $\text{Ag}_2\text{S}$ , was rendered photoelectrically insensitive by hammering the crystals into a flat plate. Furthermore, in this preliminary work there was evidence that samples of molybdenite were photoelectrically less sensitive after rubbing and polishing the lamina.

In the present tests the sample was soldered to No. 26 copper-wire electrodes (see Fig. 10) and a sensitive spot was located by means of the radiophone. This photoelectrically sensitive spot was then pressed and rubbed with a smooth, flat, wooden toothpick. On reexamination (using a radiophone), the spot was found less sensitive photoelectrically than it was before subjecting it to pressure. No material having been removed in the process of rubbing and smoothing the surface, it would appear that destruction of crystal structure may have something to do with the change

<sup>29</sup> Tisdale, *Phys. Rev. (2)*, 12, p. 325; 1918.

<sup>30</sup> This Bulletin, 14, p. 591; 1918.

in photoelectric sensitivity. Sometimes laminae of molybdenite are found which contain pockets of fine crystalline material, and it is not unreasonable to suppose that crystals of microscopic size are included in the regular lamina.

## XI. PHOTOELECTRIC SENSITIVITY VERSUS CURRENT RECTIFICATION

In the course of this investigation it was observed, as already mentioned, that samples of molybdenite which are photoelectrically sensitive have a considerably higher electrical resistance (see Table 3) than samples which are not sensitive to light. Moreover, the conductivity of the insensitive samples was found to be quite independent of the direction in which the current passed (lengthwise) through the crystal.

On the other hand, samples of molybdenite which are sensitive photoelectrically were found to possess a much higher conductivity when the electric current (from a 4-volt battery) was passed in one direction than when it was passed in the opposite direction through the crystal. As shown in Table 3, this difference in current leakage (dark current), as dependent upon the direction of the current through the crystal, varied from 10 to 30 per cent for different crystals. In observing the foregoing sensitivity curves, the photoelectric current was therefore proportionately increased by connecting the crystal into the battery circuit in the proper direction to obtain the maximum change in photoelectric conductivity.

In view of these observations it was of interest to determine whether there is any connection between photoelectric sensitivity and the rectifying action which occurs when the crystal is placed in a high frequency oscillating circuit.<sup>21</sup>

For this purpose crystals (size 10 by 4 by 0.1 mm) were selected which showed one or two small photoelectrically sensitive spots, but which were quite insensitive throughout the remainder of the surface of the crystal.

These sensitive spots were mapped by projecting a spot of light upon the sample, the change in conductivity being detected by means of the radiophonic apparatus described elsewhere in this paper. In Figs. 10 and 11 the rectangular areas represent the sample soldered to copper-wire electrodes. The photoelectrically sensitive spots are represented by the cross-hatched areas.

<sup>21</sup> These data were obtained in collaboration with Dr. Louise S. McDowell and reported upon at the meeting of the American Phys. Soc., December, 1918; Phys. Rev., 18, p. 154, 1919.

The rectification tests were made by means of an ordinary-tuned buzzer circuit. The telephone and detector, in series, were placed in parallel with the condenser of the secondary circuit. The coupling was adjusted to produce strong oscillations in the secondary circuit.

The molybdenite crystal was explored for rectification by touching the surface by means of a fine metal point. In Figs. 10 and 11 the dark points in the rectangular areas represent spots showing current rectification, the size of the spot representing the magnitude of the effect observed.

The results of these tests show that the low-resistance, photoelectrically insensitive samples of molybdenite are far more efficient rectifiers than the high-resistance light-sensitive specimens. One specimen which showed no photoelectric sensitivity whatever, as determined by a sensitive galvanometer, produced decided rectification over almost its entire surface. In fact, it was difficult to find a spot which produced no rectification. On the other hand, the samples of molybdenite having a high resistance exhibited the rectifying action only in spots, which usually did not coincide with the photoelectrically sensitive spots. These radioelectrically sensitive spots were widely scattered over the surface, but sometimes comparatively large areas were found which showed no electrical rectification, as indicated by the telephone. Only the most sensitive spots of the high-resistance material produced a rectification approaching that of the specimens having a low resistance.

In two instances especially electrically sensitive spots were found upon the light-sensitive areas (see Fig. 10, *No. VII*), but other equally sensitive spots occurred in the areas which were photoelectrically insensitive. This test alone would seem to be sufficient to prove that the two phenomena are not intimately connected.

The conclusions to be drawn are, therefore, that (1) the low-resistance, photoelectrically insensitive molybdenite exhibits much greater rectifying action than the high-resistance photoelectrically sensitive specimens; (2) there is no apparent relation between the electrical rectification and the photoelectric change in conductivity observed in molybdenite.



## 1. EXUDATION OF A DARK-BLUE LIQUID

One of the numerous questions requiring further investigation is the exudation of a dark-blue liquid from some samples of molybdenite. At the beginning of this investigation it was found that some samples became a black amorphous mass in spots when electric current was passed through them. The behavior of one sample deserves description. In making the preliminary sensitivity tests this sample was clamped between heavy brass electrodes and tested for local sensitivity, using an audion amplifier and telephone receiver. It was found that one end of this sample, close to the electrode, was unusually sensitive, causing a loud note to be emitted by the telephone receiver. On examination a bubble of liquid was found in violent ebullition. Exposure of this bubble to light produced a change in electric current and hence a sound in the telephone receiver. Other samples were found which became dark masses in spots which did not appear to be markedly sensitive photoelectrically.

The presence of a dark-blue liquid (probably the "blue oxide" described by Guichard<sup>22</sup>) on a surface of a molybdenite detector is mentioned by Huizinga<sup>23</sup>. According to Guichard the blue oxide of molybdenum is a colloid which is extremely soluble in water.

In view of the foregoing experiments, further tests were made on the production and the photoelectric sensitivity of this dark substance. In order to produce this dark substance, the end of a thin platinum wire was placed in contact with the surface of a sample of molybdenite, and this combination was joined in series with a dry battery of 10 to 75 volts and an audion amplifier. It was found that a black viscous mass was formed on the high-resistance, photoelectrically sensitive samples, but no blackening of the surface occurred at the point of contact of the platinum wire with the surface of samples of molybdenite which had a low resistance. This black substance, which indicated an acid reaction when tested with litmus paper, was formed irrespective of the direction of the electric current. Tested with an iron-constantan thermocouple of fine wires, the temperature rise at the point of contact of the platinum wire with the molybdenite was the higher for the low-resistance material. It would, therefore, seem that this is not a phenomenon resulting alone from a high tempera-

<sup>22</sup> Guichard, *Ann. Chimie et Physique* (7), **28**, p. 519, 1901; Huizinga, *Proc. K. Akad. Amsterdam*, **19**, p. 512, 1917.

ture. This blue substance becomes hard and brittle on breaking the electric circuit and is easily removed by touching the surface with a bit of cotton moistened with water.

For the photoelectric test a spot of thin, dark substance, about 3 mm in diameter, was formed surrounding the point of contact of the platinum point with the surface of a sample of molybdenite of average photoelectric sensitivity. Light of high intensity passing through the rotating sector disk was projected upon this viscous, bubbling substance. Sensitivity tests were made before the formation of this substance, also during its formation, and again after its removal. The results showed that, if anything, the presence of this substance decreased the photoelectric sensitivity of the sample. In other words, this blue oxide does not appear to be sensitive photoelectrically.

A further observation worth mentioning is that the bunsen-flame spectrum of molybdenite shows more sodium in the photoelectrically sensitive samples than in the nonsensitive material. Evidently this whole subject needs further investigation.

## XII. THEORETICAL APPLICATIONS

It is of interest to notice the bearing of the foregoing data upon theories of photoelectrical conduction. Pfund<sup>23</sup> has proposed a theory based on electronic conduction, the electrons being set free by the incident radiations. Among others, he has sought a connection between optical absorption and photoelectrical activity. He avoids the apparent inconsistency of greatest photoelectrical activity in the region of the spectrum where the absorption is the least by assuming a critical thickness at which change of resistance sets in. In the region of greatest absorption the rays do not penetrate deeply and the current-carrying layer is less than this critical thickness. In the more transparent regions of the spectrum the depth of penetration is greater; the current-carrying layer becomes greater than the critical thickness and hence a greater change in conductivity is possible. It is assumed that the light is effective in producing changes in resistance only until the amplitude has decreased to a certain minimum value, below which its effectiveness is lost. This agrees with the resonance theory, since no electrons are expelled from the atom until the amplitude due to resonance exceeds a definite minimum value.

---

<sup>23</sup> Pfund, *Phys. Rev.*, **28**, p. 324, 1909.

On the basis that the maximum of sensitivity depends upon the depth of penetration of light, increasing the intensity, and therefore the penetration, should cause a shift of the maximum toward the shorter wave lengths. Pfund's tests seemed to show this, though in a subsequent investigation<sup>34</sup> he publishes a series of curves, which might be interpreted to show, as found in the present investigation, that with increase in intensity the region of maximum photoelectrical activity shifts toward the infra-red and the sharp bands increase most rapidly on the long wavelength side, with increase in intensity.

Another theory is based upon evidence<sup>35</sup> that there are several forms of material (selenium) differing widely in resistivity, and that the action of radiation is to transform the less conducting material into one having greater conductivity. For selenium, Brown<sup>36</sup> assumes the existence of three forms, and in subsequent investigations has formed a large number of crystals by sublimation of the material in an electrically heated oven.<sup>37</sup>

In the present paper no attempt is made to harmonize the observations with these theories. In this connection, however, it is of interest to note that there are several sulphur compounds of molybdenum,  $\text{Mo}_2\text{S}_3$ ,  $\text{MoS}_4$ ,  $\text{MoS}_3$ , and  $\text{MoS}_2$ ,<sup>38</sup> which have been made artificially. The question naturally arises as to whether these observed bands of spectral photoelectrical sensitivity are connected with small inclusions of some of these sulphur compounds. The experimental data might lead one to infer that there are several forms present, causing characteristic bands of photoelectric sensitivity. For example, the bands of photoelectric sensitivity at  $\lambda = 1.02\mu$  and  $1.85\mu$  always occur together. Some samples of molybdenite show an additional maximum at  $\lambda = 0.75\mu$  or  $0.85\mu$ , while another sample, No. 4, shows only a single band at  $\lambda = 0.85\mu$ . It is planned, therefore, to test the spectral photoelectrical sensitivity of artificial sulphur-compounds of molybdenum.

The observation of a series of maxima of photoelectric sensitivity is so novel, and the data at hand are so meager, that it is rather hazardous to attempt to discuss their theoretical bearing. If we had plotted frequencies, instead of wave lengths, it would be evident that these maxima are separated by equal intervals. This

<sup>34</sup> Pfund, *Phys. Rev.*, **24**, p. 370; 1912.

<sup>35</sup> Marc. *Die Phys. and Chem. Eigensch. Metallisches Selen*, 1909; Ulljanin, *Wied. Ann.*, **34**, p. 241, 1888.

<sup>36</sup> Brown, *Phys. Rev.*, **32**, pp. 237 and 252; **33**, p. 1, 1911.

<sup>37</sup> Brown, *Phys. Rev.* (2), **4**, p. 85, 1914.

<sup>38</sup> Guichard, *Ann. Chim. et Physique* (7), **28**, p. 498, 1901.

is illustrated in Fig. 22, where the data given in Fig. 17 are plotted, the abscissae being the reciprocals of the wave lengths

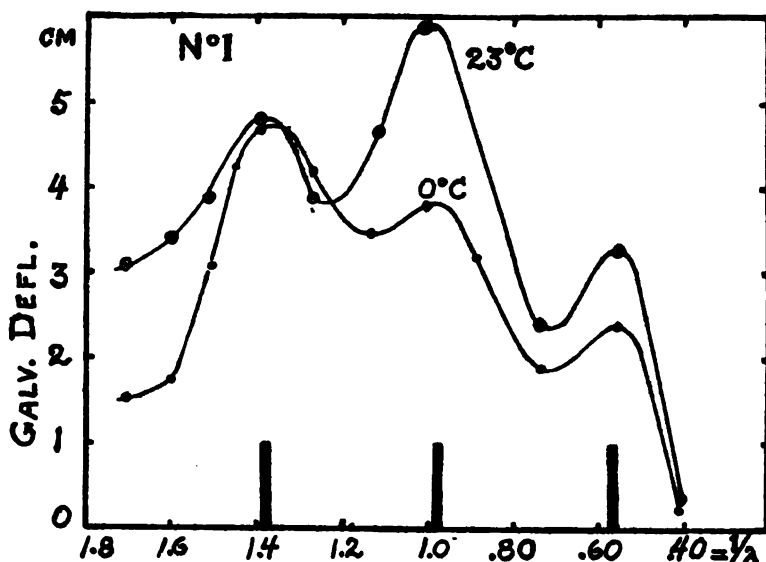


FIG 22.—Spectral photoelectric sensitivity plotted against frequency instead of wave length of the radiation stimulus

(in  $\mu = 0.001$  mm). The ordinates of the curve for  $23^{\circ}$  C are magnified three times, in order to facilitate comparison.

TABLE 5.—Maxima of Photoelectric Sensitivity and the Wave Number,  $n$ , or Common Difference Between the Reciprocals of these Wave Lengths

Sample—	Sample—
<p>No. 1:</p> <p><math>23^{\circ}</math> C.....<math>\left\{ \begin{array}{l} \lambda = 0.72\mu &gt; n = 41 \\ \lambda = 1.02\mu &gt; n = 42 \\ \lambda = 1.78\mu &gt; n = 42 \end{array} \right.</math></p> <p><math>0^{\circ}</math> C.....<math>\left\{ \begin{array}{l} \lambda = 0.73\mu &gt; n = 40 \\ \lambda = 1.04\mu &gt; n = 40 \\ \lambda = 1.78\mu &gt; n = 40 \end{array} \right.</math></p> <p><math>-115^{\circ}</math> C.....<math>\left\{ \begin{array}{l} \lambda = 0.75\mu &gt; n = 26 \\ \lambda = 0.93\mu &gt; n = 26 \\ \lambda = 1.2\mu &gt; n = 26 \end{array} \right.</math></p>	<p>No. 2:</p> <p><math>-172^{\circ}</math> C.....<math>\left\{ \begin{array}{l} \lambda = 0.88\mu &gt; n = 30 \\ \lambda = 1.20\mu &gt; n = 31 \\ \lambda = 1.90\mu &gt; n = 31 \end{array} \right.</math></p> <p>No. 3:</p> <p><math>22^{\circ}</math> C.....<math>\left\{ \begin{array}{l} \lambda = 0.73\mu &gt; n = 40 \\ \lambda = 1.03\mu &gt; n = 40 \\ \lambda = 1.62\mu &gt; n = 42 \end{array} \right.</math></p> <p>No. 4:</p> <p><math>-178^{\circ}</math> C.....<math>\left\{ \begin{array}{l} \lambda = 0.89\mu &gt; n = 31 \\ \lambda = 1.23\mu &gt; n = 30(?) \\ \lambda = 2(?) &gt; n = 30(?) \end{array} \right.</math></p>

As shown in Table 5, the difference in the frequency maxima or wave number is  $n = 40$  for room temperature; while at low temperatures it is  $n = 25$  in some cases and  $n = 30$ , just as though there were several kinds of crystals present. The data on samples No. 2 and

No. 4 would seem to indicate, as already noted, that the great variation in photoelectric sensitivity seems to be one of degree of sensitivity and not one of quality.

It is to be noted that the spectral lines represent an emission of thermal radiation as the result of (electrical) excitation of gas ions or electrons, whereas in the present case thermal radiations of certain frequencies produce marked changes in the electrical conductivity of the substance. On the resonance theory one would be led to expect fundamental and harmonic frequencies which are capable of producing marked changes in electrical conductivity. On this basis one would expect to find additional harmonic bands, which for sample No. 1 should occur at  $\lambda = 0.56\mu$  and  $\lambda = 6.5\mu$ . As a matter of fact this sample is quite sensitive in the visible spectrum (see Fig. 14), but this question was not foreseen and the energy calibration was not sufficiently accurate to establish a maximum at this wave length.

Before discussing the data more closely, it will be desirable to make a further examination of these samples, using a very much larger dispersion, which will give greater purity of the radiation stimulus in the region of  $0.6\mu$  to  $1.2\mu$ . As matters now stand, it is not apparent, in some cases, why the band at  $0.72\mu$  is absent if it is harmonic with the bands at  $1.02\mu$  and  $1.78\mu$ .

### XIII. SUMMARY

The present paper gives data on the change in the electrical conductivity of molybdenite when exposed to thermal radiations of wave lengths extending from wave length  $\lambda = 0.36\mu$  in the ultra-violet to beyond  $\lambda = 9\mu$  in the infra-red.

The radiations of wave lengths extending from the ultra-violet to about  $3\mu$  produce a change in the electrical conductivity of molybdenite. The effect of temperature, humidity, intensity of the exciting light, etc., upon the photoelectrical sensitivity of molybdenite was investigated. Atmospheric humidity does not appear to affect the shape of the spectral photoelectric sensitivity curve.

The effect of increasing the intensity of the exciting radiations appears to be to produce a more rapid response in the long wave lengths than in the short wave lengths, with a resultant shift of the spectral photoelectric sensitivity curve toward the long wave lengths.

There is no simple law governing the variation in the photoelectric response in molybdenite, with variation in intensity of the radiation stimulus.

At room temperatures there are maxima of sensitivity in the region of  $\lambda = 0.7\mu$ ,  $0.85\mu$ ,  $1.02\mu$ , and  $1.8\mu$ . Beyond  $2.5\mu$  the photoelectric sensitivity is practically nil.

Raising the temperature causes a rapid decrease in the spectral photoelectric sensitivity, especially in the regions of  $1.02\mu$  to  $1.8\mu$ . At  $80^\circ\text{C}$ . the spectral photoelectric sensitivity has practically disappeared, only slight indications being observed for radiations of wave lengths  $\lambda = 0.6\mu$  to  $0.8\mu$ .

The effect produced by lowering the temperature is to greatly increase the sensitivity curve throughout the whole spectrum from the ultra-violet to  $2.5\mu$  in the infra-red. This increase in sensitivity is greatest in the region of  $0.8\mu$  to  $0.9\mu$ , so that at the temperature of boiling liquid air the maximum sensitivity occurs at about  $0.85\mu$ , with a new band at  $1.25\mu$  to  $1.35\mu$ . Samples of molybdenite which are quite insensitive at room temperatures become fairly sensitive, photoelectrically, at  $-178^\circ\text{C}$ . At low temperatures the spectral photoelectric sensitivity curves of all samples are quite similar, with a maximum in the region of  $0.8\mu$  to  $0.9\mu$ . From this it would appear that this photoelectric property is one of degree rather than one of quality. The fact that the bands at  $1.02\mu$  and  $1.8\mu$  occur together, and that the  $0.85\mu$  band may occur alone suggests the possibility that they are characteristic bands of spectral photoelectric sensitivity of different sulphur compounds of molybdenum.

Using frequency instead of wave length to indicate the spectral position of the radiations which cause the maximum change in electrical conductivity, it is found that in some instances there is a constant difference of the wave numbers analogous to the series relations of spectral lines.

The time required for recovery of equilibrium in electrical conductivity is close to twice the time of exposure.

Mechanical working of the material appears to lower the photoelectric sensitivity.

There appears to be no close connection between photoelectric sensitivity and current rectification in molybdenite.

Measurements of reflecting power show that molybdenite has a high reflectivity in the violet, which decreases to a uniform value beyond  $1\mu$ . Similarly, the transmission is high and uniform beyond  $1\mu$  in the infra-red. Using these data refractive indices were computed, indicating a value of  $n = 3$  for wave lengths greater than  $1\mu$ .

The greatest photoelectrical activity occurs in the region of the spectrum, where there is a rapid decrease in spectral absorption.

## APPENDIX

### Appendix 1.—PHOTOELECTRIC ACTIVITY INDUCED IN UNILLUMINATED PARTS OF A CRYSTAL

It was shown by Brown and Sieg<sup>39</sup> that light falling upon one part of a crystal of selenium produced a change in conductivity throughout the crystal. In one sample this effect was produced by illuminating the crystal at a distance of 8 to 10 mm from the point of contact of the electrodes. Subsequent tests by Brown<sup>40</sup> did not disclose whether this light action is transmitted as a result of change in crystalline structure, elastic vibration, or merely by diffusion.

This observation of a change in conductivity in portions of a crystal not directly illuminated has been tested also on cuprous oxide, by Pfund.<sup>41</sup> He found that if cuprous oxide shows this transmitted effect at all, it is infinitesimal in comparison with that observed in selenium.

It was of interest, therefore, to determine whether one part of a crystal of molybdenite undergoes a change in conductivity when another part of this same crystal is exposed to radiation. This test is best performed by illuminating a portion of the crystal which extends beyond the point of contact of the electrodes. In one test a platinum wire touching the surface of the molybdenite was used for one of the electrodes. When this platinum point was placed so that the exciting light fell between the two electrodes, the sample of molybdenite changed in conductivity, as indicated by the sound in the radiophone. On placing this platinum point so that the exciting light fell outside of these two electrodes no sound was produced in the radiophone. Various tests showed that illuminating one portion of a sensitive sample of molybdenite does not induce a change in conductivity in an unilluminated (but equally sensitive) portion of this same crystal. In other words, no change in conductivity appears to be produced by diffusion, internal reflection, etc., in molybdenite.

### Appendix 2.—POLARIZATION BY REFLECTION FROM MOLYBDENITE

Pfund<sup>42</sup> has shown that a selenium mirror provides an excellent means for producing polarized radiations. In view of the fact that molybdenite has a higher reflecting power than selenium, it was of interest to determine its polarizing properties. For this purpose two thin plates of molybdenite were mounted upon glass plates, as already described in the reflectivity measurements. The one was used as a polarizer and the other as an analyzer. These two mirrors were placed in an apparatus which permitted rotation of the analyzer. The source of (undispersed) radiation was a Nernst glower. The intensities were measured with a thermopile and galvanometer.

The galvanometer deflections were noted (1) when the planes of the polarizer and analyzer were parallel and (2) when they were crossed. Using mirrors of selenium, the ratio of the galvanometer deflections for these two positions (parallel: crossed) was of the order of 800:1; for maximum polarization.

<sup>39</sup> Brown and Sieg, *Phil. Mag.* (6), 28, p. 497; 1914.

<sup>40</sup> Brown, *Phys. Rev.* (2), 5, p. 404; 1915.

<sup>41</sup> Pfund, *Phys. Rev.* (2), 7, p. 296; 1916.

<sup>42</sup> Pfund, *Astrophys. Jr.*, 24, p. 19; 1906.

Using mirrors of molybdenite for maximum polarization, the ratio of the galvanometer deflections for these two positions (parallel: crossed) was only about 8:1. Evidently molybdenite is not suitable for producing plane polarized light.

In view of the high reflecting power of molybdenite it was of interest to determine whether it transforms plane into elliptically polarized light, as is true of a metal. The test was made with plane polarized radiations from a selenium mirror, which were reflected from the molybdenite mirror in the manner described by Pfund.

Preliminary tests with radiations transmitted by red glass showed that, for the spectral region from 1 to  $4\mu$ , calcite reflects vitreously (i. e., does not transform plane into elliptically polarized light), as previously observed.

Similar tests on molybdenite,  $\text{MoS}_2$ , showed that plane polarized radiations ( $\lambda=1\mu$  to  $4\mu$ ) are elliptically polarized, the ellipticity (ratio of axes) being about 3:1. Similarly, a very flat cleavage surface of stibnite,  $\text{Sb}_2\text{S}_3$ , produced an ellipticity of about 12:1.

These ratios are of course not very accurate, but they are consistent in that molybdenite is more metallic (judged by its elliptic polarization) than stibnite; also in having a higher reflecting power and especially a higher absorption coefficient. An investigation of the optical properties of substances like the above, which lie on the borderland between metals and nonmetals, would no doubt prove profitable.

WASHINGTON, December 18, 1918.







DEPARTMENT OF COMMERCE

---

# SCIENTIFIC PAPERS OF THE BUREAU OF STANDARDS

S. W. STRATTON, DIRECTOR

---

No. 339

---

## STANDARDIZATION OF THE SULPHUR BOILING POINT

BY

E. F. MUELLER, Associate Physicist

and

H. A. BURGESS, Laboratory Assistant

*Bureau of Standards*

---

ISSUED OCTOBER 4, 1919



PRICE, 5 CENTS

Sold only by the Superintendent of Documents, Government Printing Office,  
Washington, D. C.

---

WASHINGTON  
GOVERNMENT PRINTING OFFICE  
1919



# STANDARDIZATION OF THE SULPHUR BOILING POINT

By E. F. Mueller and H. A. Burgess

## CONTENTS

	Page
I. Introduction.....	163
II. Apparatus used.....	166
III. Description of experiments.....	168
1. Comparison of radiation shields.....	168
2. Influence of type of sulphur boiling apparatus.....	177
3. Purity of sulphur.....	179
4. The relation between the vapor pressure of sulphur and temperature.....	180
IV. Summary.....	181
Appendix.—Proposed standardization of the sulphur boiling point.....	183

## I. INTRODUCTION

The sulphur boiling point occupies a position of unusual importance among the thermometric fixed points on account of the care and accuracy with which its temperature has been determined, the precision with which this temperature may be reproduced, but most of all on account of the very general practice of using it to determine one of the fundamental calibration constants of the platinum resistance thermometer, which serves as the most precise and convenient means now available for defining the temperature scale in the range  $-50^{\circ}$  to  $+500^{\circ}$  C. The best measurements available are insufficient to show that the scale so defined differs from the thermodynamic scale in any part of this range.

The results of the best determinations of the temperature of the sulphur boiling point on the thermodynamic scale are summarized in Table 1 which, with the exception of the last entry, is abbreviated from that given by Day and Sosman.<sup>1</sup>

<sup>1</sup> Am. Jour. of Science IV, 88, p. 530; 1912. Also Jour. Wash. Acad. of Sciences, 2, p. 174; 1912. Also Ann. d. Physik IV, 88, p. 865; 1912.

TABLE 1.—Determinations of the Temperature of the Sulphur Boiling Point

Date	Author	Temperature, thermo- dynamic scale
		° C
1890	Callendar and Griffiths.....	444.91
1902	Chappuis and Harker.....	444.80
1908	Eumerlopoulos.....	444.93
1911	Holborn and Hemming.....	444.51
1912	Day and Sosman.....	444.55
1914	Eumerlopoulos <sup>a</sup> .....	444.61

<sup>a</sup> Proc. Roy. Soc. London, A, 80, p. 189; 1914.

From the data of Table 1 it appears that any value which may be selected as representing the temperature of the sulphur boiling point may be in error by  $0.1^{\circ}$  or even  $0.2^{\circ}$ , and that fixing this point to a few hundredths of a degree, which is the precision attainable with a resistance thermometer, is at present a matter of definition. On the grounds that greater weight should be given to the newer determinations, but that the value is not known better than  $0.1^{\circ}$ , there is a choice as to whether  $444.5^{\circ}$  or  $444.6^{\circ}$  shall be selected. As none of the values is as low as  $444.5^{\circ}$  and all the older values are decidedly above this, the Bureau has adopted the value  $444.6^{\circ}$ . For the purpose of defining the scale of the platinum resistance thermometer, the temperature of the sulphur boiling point under standard atmospheric pressure is taken by definition as  $444.60^{\circ}$ .

An analogous procedure has been found useful in defining the electric units for practical use. Thus the ohm for practical use is defined as the resistance of a column of mercury the length of which is specified to an accuracy of 1 part in 100 000, while it is known that the ohm so defined may differ from the cgs unit by perhaps 1 part in 3000.

Having decided upon the value to be used for the temperature of the sulphur boiling point, it is necessary to define the experimental conditions so as to make the temperature reproducible with the highest attainable precision in order that the temperature scale defined by the platinum resistance thermometer may also be as definite and reproducible as possible.

The effect of the experimental conditions, particularly as regards shielding of the thermometer, had been investigated by Callendar and Griffiths,<sup>2</sup> Waidner and G. K. Burgess,<sup>3</sup> and by

<sup>2</sup> Phil. Trans., A, 189, p. 143; 1891.

<sup>3</sup> Bull. Bureau of Standards, 6, p. 189; 1910 (B. S. Scientific Paper No. 124).

others. More recently Meissner<sup>4</sup> reported further experiments which showed that the temperature assumed by a resistance thermometer in the sulphur vapor depended upon the reflecting power of the interior of the shield. His work raised some doubt as to the adequacy of the older work, but was incomplete in some respects. It did not indicate, for example, to what extent the effectiveness of a given shield depended upon the nature of the material used for the protecting tube of the thermometer. Waidner and Burgess had also investigated the temperatures in various types of boiling apparatus. Apparently there has been no investigation of the effect of impurities in the sulphur upon the observed boiling point. The variation of temperature with pressure has been experimentally investigated by Holborn and Henning,<sup>5</sup> and by Harker and Sexton.<sup>6</sup>

As the result of these investigations the method of using the sulphur boiling point has, to a certain extent, become standardized. It has become the common practice to use a boiling tube of glass or like material about 5 cm in diameter. Also it is generally recognized that the source and manner of heating should be so controlled as not to superheat the vapor, and that the thermometer must be suitably protected from the effect of loss of heat by radiation or otherwise, as without such protection the observed value may be a degree or more in error.

The manner of observing these avowedly necessary precautions has differed considerably with different experimenters, apparently depending upon convenience or personal preferences. None but glass or similar boiling tubes have been used since Regnault's time. Both gas and electricity have been used for heating, and of either type of apparatus there have been numerous designs. The greatest variation has, however, occurred in the type of radiation shield employed on the thermometer, whether gas, mercurial, or electrical thermometers were used. These shields have been of many shapes and sizes, and have been constructed of glass and platinum, iron, asbestos, and aluminum. The tubes incasing the platinum thermometers have been either glass, quartz, or porcelain.

It is the purpose of this paper to present further evidence on the effect of these experimental conditions with the object of making this evidence sufficiently complete to serve as a basis for

<sup>4</sup> *Annalen d Physik* IV, **89**, p. 1230; 1912.

<sup>5</sup> *Annalen d Physik* IV, **26**, p. 859, 1908; IV, **85**, p. 772, 1911.

<sup>6</sup> *Report British Association*, p. 621, 1908.

standard specifications for the use of the sulphur boiling point as a calibration temperature. The work was therefore planned so as to supplement and complete, in so far as possible, the work of previous investigators.

## II. APPARATUS USED

The greater part of the work was done with a gas-heated apparatus shown in Fig. 1. This apparatus is a development of the gas-heated apparatus which has been used regularly at the Bureau for some years.<sup>7</sup> The improvements are mainly in certain details which give greater ease and convenience in manipulation. The new apparatus was made to accommodate two lengths of boiling tubes of about 45 cm and 70 cm, respectively, both of which were used, and the insulating jacket was made in two sections to suit the two lengths. The source of heat was a Méker blast burner, the flame of which played against a heavy ribbed iron casting containing a well about 7 cm deep in which the lower end of the boiling tube rested. The liquid sulphur surface was kept about 5 cm above the top of this casting to prevent superheating of the vapor. The thermometer was held in a specially designed clamp which could be opened or closed quickly by one motion and which when once set in position held the thermometer always in alignment and concentric with the boiling tube. This clamp was carried on a rack and pinion carriage which moved up and down on the main vertical supporting rod of the apparatus, which was equipped with a scale for reading directly the position of the thermometer coil inside the boiling tube. The heat insulation was very efficient and the sulphur could be brought to boiling sufficiently for an observation in less than an hour after starting.

Both glass and fused quartz tubes were used, the latter provided with a narrow fused-in window of transparent quartz near the top through which the line of condensation could be observed. Ample opening was left in the cover of the boiling tube for equalization of pressure inside and outside the tube.

The apparatus is so arranged that the ribbed casting and the burner can be removed and an electric heater substituted. This heater consists of a porcelain tube, 15 cm long, having an inside diameter 5 to 10 mm larger than that of the boiling tubes used. The heating coil is of nichrome tape wound on the porcelain. The

---

<sup>7</sup> Waidner and Burgess, *loc. cit.*, p. 187.



FIG. 1.—*Gas-heated sulphur boiling apparatus*



top of this porcelain tube occupies the same position as the top of the ribbed casting, and the heating coil covers the upper 8 cm of it. The boiling tube extends into this tube about 7 cm, resting on a cushion of soft asbestos.

A heater of this type had been improvised for some special experiments and proved so satisfactory that the heater described above was built and has superseded the gas heater.

The resistance thermometers used were made in the usual form with cylindrical coils and were inclosed in glass or porcelain tubes. Some of the thermometers were provided with interchangeable glass and porcelain tubes. The coils were of the strain-free type<sup>8</sup> and the leads were so fastened to the supporting mica strips that any strain on the leads could not be communicated to the coil. The connections were of the potential terminal type. Resistances were measured with a mercury contact Wheatstone bridge together with a commutator according to the method previously described.<sup>9</sup>

The constants of the thermometers as determined at various times are given in Table 2 where  $R_0$  is the resistance in melting ice, and  $F$  the increase in resistance on heating from  $0^\circ$  to  $100^\circ$  C. The measuring currents used in thermometers  $C_{26}$ ,  $C_{27}$ , and  $C_{28}$  were 4 milliamperes and the current used in  $C_{22}$  was 2 milliamperes.

The heating effect of the measuring current used for  $C_{26}$ ,  $C_{27}$ , and  $C_{28}$  was about  $0^\circ.003$ , and for  $C_{22}$  was about  $0^\circ.002$  in both ice and steam. It is known from the work of Waidner and Burgess and of Smith<sup>10</sup> that for thermometers of this type the heating effect of the measuring current, maintained constant, is of the same order of magnitude at  $450^\circ$  as at  $0^\circ$  and at  $100^\circ$ .

The coils of  $C_{26}$ ,  $C_{27}$ , and  $C_{28}$  are about 4.5 cm long and the protecting tubes are 5 mm internal and 7 mm external diameter. The coil of  $C_{22}$  is about 8 cm long and the protecting tube is 8 mm internal and 10 mm external diameter.

A Fuess siphon-type barometer, which could be read to an accuracy of 0.02 to 0.04 mm, was used for the measurements of atmospheric pressure. All pressures were expressed in the equivalent millimeters of mercury at  $0^\circ$  and under standard gravity ( $g = 980.665$ ).

<sup>8</sup> Waidner and Burgess, loc. cit., p. 115.

<sup>9</sup> Mueller, this Bulletin, 18, p. 547; 1916 (B. S. Scientific Paper No. 288).

<sup>10</sup> F. E. Smith, Phil. Mag., VI, 24, p. 545; 1912.

TABLE 2.—Resistances at 0 °C ( $R_0$ ) and Fundamental Intervals ( $F$ ) of Thermometers Used

Date	$C_{20}$		$C_{27}$		$C_{28}$		$C_{29}$	
	$R_0$	$F$	$R_0$	$F$	$R$	$F$	$R_0$	$F$
	Ohms	Ohm	Ohms	Ohm	Ohms	Ohm	Ohms	Ohms
July 19, 1915..					2. 53727	0. 9936 <sub>4</sub>		
Oct. 23, 1915..	2. 53788	0. 9924 <sub>9</sub>	2. 54871	0. 9983 <sub>1</sub>				
Nov. 2, 1915..	2. 53785							
Nov. 4, 1915..			2. 54867		2. 53725			
Nov. 12, 1915..			2. 54869					
Nov. 23, 1915..			2. 54871					
Jan. 4, 1916..			2. 54869					
Jan. 24, 1916..	2. 53785	. 9924 <sub>9</sub>	2. 54870	. 9983 <sub>1</sub>	2. 53725	. 9936 <sub>2</sub>		
Feb. 28, 1916..							25. 5472	9. 987 <sub>8</sub>
Mar. 9, 1916..			2. 54870		2. 53726			
Mar. 28, 1916..							25. 5476	9. 987 <sub>8</sub>
Apr. 5, 1916..							25. 5476	9. 987 <sub>8</sub>
May 11, 1916..			2. 54870					
May 12, 1916..					2. 53724			
May 19, 1916..							25. 5461	
May 26, 1916..			2. 54869					
June 20, 1916..			2. 54868					
June 23, 1916..							25. 5499	

\* The comparatively large changes noted in this thermometer were not satisfactorily explained. Fortunately, they were without effect on any of the results obtained with it in this investigation.

### III. DESCRIPTION OF EXPERIMENTS

#### 1. COMPARISON OF RADIATION SHIELDS

Some of the shields used are illustrated in Fig. 2. The openings at the tops of the shields were made to fit the thermometer tubes closely. All the shields were made so that any openings in the shields were at least 2 cm above or below the coils of the thermometers.

For the comparative tests a thermometer, inclosed in its shield, was inserted into the sulphur vapor, and the resistance and corresponding barometric pressure were observed for four different depths of immersion of the thermometer, with its attached shield, these positions being such that the bottom of the shield was 6, 8, 10, and 12 cm, respectively, above the surface of the liquid sulphur. Time was allowed for the establishment of equilibrium before each reading. In most of the experiments the changes of temperature observed accompanying the above displacements were, after changes in barometric pressure had been allowed for, within the limits of observational error (less than 0.02°), and this constancy was a valuable indication of suitable experimental conditions.

Where such constancy was not observed the fact is noted in the tables. In all cases the result given in the tables is the one obtained from the readings at the 8 cm height.

The temperature of the vapor was deduced from the barometric pressure by use of the formula,

$$t = 444.^\circ 6 + 0.0910 (p - 760) - 0.000049 (p - 760)^2$$

which is based on data given later in this paper.

The comparison of the temperatures as observed with the resistance thermometer is made most conveniently by computing for

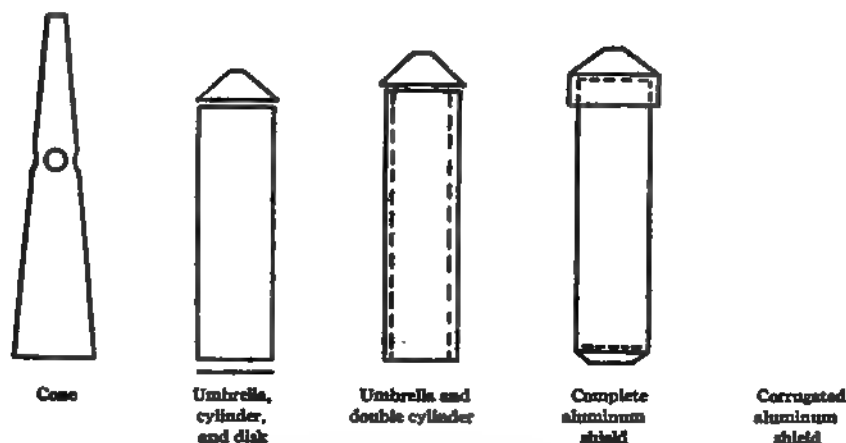


FIG. 2.—Types of radiation shields

each observation the platinum temperature, designated  $pt_{760}$ , corresponding to standard barometric pressure.

By differentiating the Callendar formula

$$t - pt = \delta \left( \frac{t}{100} - 1 \right) \frac{t}{100} \text{ where } pt = \left( \frac{R_t - R_0}{F} \right)_{100}$$

a relation

$$dpt = \left( 1 + \frac{\delta}{100} - \frac{2\delta t}{100^2} \right) dt$$

is found, which for values of  $\delta = 1.495$  and  $t = 444^\circ$  becomes

$$\Delta pt = 0.882 \Delta t$$

This equation is applicable for the entire range of barometric pressures and for all the values of  $\delta$  occurring in this series of experiments.

The comparative data for various shields, all obtained in the gas-heated boiling apparatus, are assembled in Table 3, classified according to kind of shield used. The table shows the date of the observation, the number of the thermometer, the material of the thermometer protecting tube, the type of shield used, the platinum temperature corresponding to standard barometric pressure as calculated from each observation, and the amount by which this is *lower* than the average platinum temperature found with all the shields which were adequate.

The experimental work was planned and carried out so that all results could be referred to a standard type of shield—that is, during each day's observations an iron cone or an iron cylinder with umbrella was used at least once—and it would have been possible to present the data in this comparative form. On assembling the results it appeared that it would be simpler to give the results in the form shown in Table 3 with the further advantage of eliminating accidental errors in the individual observations made with the standard shields.

Fortunately, the facts brought out in Table 3 can be very briefly summarized. It will be noted that all the iron shields, either with or without the lower disk, gave practically the same value of  $pt_{760}$  for any one thermometer, and the mean of all the values obtained with these shields may be considered the standard value. Since it is evident that no shield can cause the thermometer to assume a temperature higher than that of the vapor, it follows that low values of  $pt_{760}$  indicate inadequate shielding. All of the data substantiate Meissner's view that a shield, the inner surface of which is a good reflector, will be ineffective. This is now shown to be true whether the thermometer is inclosed in glass or in porcelain. Thus the iron shields, the Callendar Griffiths shield, graphite cylinder, asbestos cone, an aluminum shield, blackened inside, are all effective. Even an aluminum cylinder, with the walls sharply corrugated, forming a series of wedges, and which is therefore a good radiator, was as effective as the other shields.

A complete aluminum shield was nearly realized in a cylindrical shield with overhanging umbrella and the lower edge of the cylinder extending below the lower disk and curving inward, so that all direct radiation from the platinum coil in any direction met the shield, while a free circulation of vapor was possible. With this shield the thermometer read  $0.02^\circ$  or  $0.03^\circ$  lower than when inclosed in the adequate shields previously mentioned.

TABLE 3.—Comparisons of Shields in Gas-Heated Apparatus

## (a) IRON SHIELDS

Date	Observation number	Thermometer number	Tube inclosing thermometer	Description of shield	$P_{700}$	Lowering of $P_{700}$	Remarks
					Degrees	Degrees	
Nov. 2, 1915	1	C <sub>28</sub>	Porcelain	Cone.....	421.65	0.00	Average for C <sub>28</sub> , 421.65
Nov. 8, 1915	2	C <sub>27</sub>	...do.....	Umbrella and cone..	421.72	.00	
Nov. 9, 1915	3	C <sub>27</sub>	Glass.....	...do.....	421.73	-.01	
Nov. 23, 1915	4	C <sub>27</sub>	...do.....	...do.....	421.70	+.02	
Jan. 4, 1916	5	C <sub>27</sub>	...do.....	...do.....	421.69	+.03	
Mar. 9, 1916	6	C <sub>27</sub>	Porcelain	...do.....	421.72	.00	Reading unsteady.
Apr. 24, 1916	7	C <sub>28</sub>	...do.....	...do.....	421.73	+.01	
May 1, 1916	8	C <sub>27</sub>	...do.....	...do.....	421.73	+.01	
Nov. 9, 1915	9	C <sub>27</sub>	Glass.....	Umbrella, cone, and disk.	421.69	+.03	
Nov. 10, 1915	10	C <sub>27</sub>	...do.....	Umbrella and cylinder.	421.72	.00	
Nov. 12, 1915	11	C <sub>27</sub>	...do.....	...do.....	421.72	.00	Do
Do.....	12	C <sub>27</sub>	...do.....	...do.....	421.75	-.03	
May 26, 1916	13	C <sub>27</sub>	Porcelain	...do.....	421.73	-.01	
June 20, 1916	14	C <sub>27</sub>	...do.....	...do.....	421.73	-.01	
Jan. 5, 1916	15	C <sub>27</sub>	Glass.....	Umbrella and smaller cylinder, 23mm diameter.	421.71	+.01	
Nov. 12, 1915	16	C <sub>27</sub>	...do.....	Umbrella, cylinder, and disk.	421.73	-.01	Average for C <sub>27</sub> , 421.72
Nov. 16, 1915	17	C <sub>27</sub>	...do.....	...do.....	421.69	+.03	
Jan. 5, 1916	18	C <sub>27</sub>	...do.....	Umbrella and double cylinder.	421.74	-.02	
Nov. 4, 1915	19	C <sub>28</sub>	...do.....	Cone.....	421.67	.00	
Nov. 5, 1915	20	C <sub>28</sub>	...do.....	Umbrella and cone..	421.68	-.01	
May 20, 1916	21	C <sub>28</sub>	...do.....	Umbrella and double cylinder.	421.68	-.01	Average for C <sub>28</sub> , 421.67
Mar. 9, 1916	22	C <sub>28</sub>	...do.....	Umbrella and cylinder.	421.66	+.01	
Do.....	23	C <sub>28</sub>	...do.....	...do.....	421.67	.00	
May 12, 1916	24	C <sub>28</sub>	...do.....	Umbrella and small cylinder, 23mm diameter.	421.65	+.02	
May 20, 1916	25	C <sub>28</sub>	...do.....	...do.....	421.66	+.01	
May 12, 1916	26	C <sub>28</sub>	...do.....	Umbrella and cylinder, 30mm diameter.	421.66	+.01	Average for C <sub>28</sub> , 421.67
Do.....	27	C <sub>28</sub>	...do.....	Umbrella and cylinder, 33mm diameter.	421.68	-.01	
May 20, 1916	28	C <sub>28</sub>	...do.....	Umbrella and cylinder, 32mm diameter.	421.68	-.01	

TABLE 3—Continued

## (b) MODIFIED ALUMINUM SHIELDS

Date	Observation number	Thermometer number	Tube inclosing thermometer	Description of shield	Pt 700	Lowering of Pt 700	Remarks
Nov. 9, 1915	29	C <sub>27</sub>	Glass.....	Double cone and disk	Degrees 421.70	Degrees +.02	
Nov. 10, 1915	30	C <sub>27</sub>	...do.....	Umbrella and cylinder, blackened inside.	421.72	.00	
Do.....	31	C <sub>27</sub>	...do.....	Umbrella and cylinder, blackened inside, and disk.	421.72	.00	
Do.....	32	C <sub>27</sub>	...do.....	do.....	421.72	.00	
Nov. 23, 1915	33	C <sub>27</sub>	...do.....	do.....	421.73	-.01	
Jan. 4, 1916	34	C <sub>27</sub>	...do.....	do.....	421.70	+.02	
Nov. 16, 1915	35	C <sub>27</sub>	...do.....	Umbrella and corrugated cylinder.	421.71	+.01	
Do.....	36	C <sub>27</sub>	...do.....	Umbrella, corrugated cylinder, and disk.	421.72	.00	

## (c) MISCELLANEOUS SHIELDS

Nov. 10, 1915	37	C <sub>27</sub>	Glass.....	Graphite umbrella and cylinder.	421.73	-.01	
Nov. 16, 1915	38	C <sub>27</sub>	...do.....	Asbestos cone.....	421.71	+.01	
Do.....	39	C <sub>27</sub>	...do.....	Asbestos cone and disk.	421.71	+.01	
Jan. 3, 1916	40	C <sub>27</sub>	...do.....	Callendar Griffiths..	421.73	-.01	

## (d) BRIGHT ALUMINUM SHIELDS (INADEQUATE SHIELDING)

Nov. 2, 1915	41	C <sub>28</sub>	Porcelain.	Cone.....	421.58	+.07	
Nov. 6, 1915	42	C <sub>27</sub>	...do.....	Umbrella, cone, and disk.	421.70	+.02	
Nov. 8, 1915	43	C <sub>27</sub>	...do.....	Cone and disk.....	421.68	+.04	
Jan. 4, 1916	44	C <sub>27</sub>	Glass.....	Umbrella and cylinder.	421.51	+.21	
Nov. 8, 1915	45	C <sub>27</sub>	Porcelain.	Umbrella, cylinder, and disk.	421.66	+.06	Old, dull shield.
Jan. 5, 1916	46	C <sub>27</sub>	...do.....	do.....	421.60	+.12	New bright shield.
Nov. 23, 1915	47	C <sub>27</sub>	Glass.....	do.....	421.62	+.10	Unsteady.
Jan. 4, 1916	48	C <sub>27</sub>	...do.....	do.....	421.60	+.12	
Nov. 23, 1915	49	C <sub>27</sub>	...do.....	Complete shield....	421.70	+.02	
Jan. 4, 1916	50	C <sub>27</sub>	...do.....	do.....	421.69	+.03	
Nov. 4, 1915	51	C <sub>28</sub>	...do.....	Cone.....	421.48	+.19	
Nov. 5, 1915	52	C <sub>28</sub>	...do.....	Umbrella and cone..	421.49	+.18	
Do.....	53	C <sub>28</sub>	...do.....	Umbrella, cone, and disk.	421.60	+.07	

The data for the other aluminum shields, with bright inside surfaces, show that the temperature attained by a thermometer inclosed in such a shield depends upon the form of the shield,



primarily upon the extent to which the shield forms a complete inclosure, upon the extent to which the interior of the shield has become dull or blackened, and also upon the material (transparency) of the protecting tube of the thermometer. The readings obtained range from  $0.2^{\circ}$  low, taken with a simple cone on a glass-inclosed thermometer, to  $0.02^{\circ}$  low, taken with a nearly closed shield on a porcelain-inclosed thermometer. The extreme lowerings found were  $0.2^{\circ}$  for a glass-inclosed thermometer and  $0.1^{\circ}$  for a porcelain-inclosed thermometer.

Inadequate shielding is also usually accompanied by considerable variations in temperature, sometimes amounting to  $0.1^{\circ}$ , when the thermometer is displaced vertically, but the absence of such variation is not necessarily proof of adequate shielding. It may also be remarked in passing that the absence of such variations does not prove that there is no superheating of the vapor, as in one instance constant temperatures were observed with a displacement of 4 cm where, owing to insufficient depth of liquid sulphur in the tube, the vapor was superheated about  $0.5^{\circ}$ .

These results are in the main in agreement with those of Meissner, in so far as they cover the same field. They differ from his in regard to the effectiveness of nearly closed aluminum shields, which, according to our results, are more effective than Meissner found them to be. However, there is agreement on the essential point that no bright aluminum shield is completely effective.

*Tight-Fitting Umbrella not Necessary.*—In most of the shields used, the hole in the center of the umbrella was made to fit the thermometer tube rather closely. Some observers have recommended using asbestos string tied around the thermometer tube just above the umbrella. This was also tried and found to be unnecessary and on account of its inconvenience is regarded as undesirable. Even entirely omitting the umbrella and using only a cylindrical iron shield open at both ends around the coil produced a lowering of only about  $0.05^{\circ}$ .

*Diameter of Cylindrical Shields.*—Two thermometers,  $C_{28}$  and  $C_{29}$ , were used, both inclosed in glass tubes having diameters of 7 and 10 mm, respectively, with shields varying in diameter from 1.5 cm greater than the diameter of the thermometer tube to the largest that the boiling tube would conveniently admit. Two series of observations with  $C_{28}$  on different days point to a slightly higher reading with increasing diameter, while observations with  $C_{29}$  point to an opposite tendency. The observed effect is, how-

ever, too small to be of significance, if the diameter of the shield is not more than about 2.5 cm greater than that of the thermometer tube, and the thermometer is reasonably concentric with the shield. The fact that good results are obtained with conical shields also indicates that the diameter is of minor importance. It appears, therefore, that shields from 1.5 to 2.5 cm greater in diameter than the diameter of the thermometer tube are preferable.

*Effect of Lower Disk.*—An effect which Meissner attributed to the presence of the lower disk, namely, a variable reading during which the resistance varies slowly up and down with apparently various stationary values was noted and investigated. It is true that this effect was noticed most often when the lower disk was present. In order to determine, if possible, whether there existed a critical distance for the disk from the shield edge to give maximum unsteadiness, an iron shield was equipped with a movable disk, the position of which could be controlled from outside the boiling tube. On one day this shield gave perfectly steady readings for all apertures possible; that is, from 2 mm distance to 11 mm between the disk and the edge of the shield. A few days later the use of this same shield at an aperture of 5 mm was accompanied by fluctuations amounting to  $0.01^{\circ}$ . In any case, only under extreme conditions, such as raising the thermometer until the top of the shield reached the line of condensation, were fluctuations of  $0.05^{\circ}$  noted. When the sulphur was boiling vigorously with a high and sharp condensation line, shields with lower disks gave as steady readings as when the disks were absent. Also continued boiling sometimes caused waverings to disappear and the readings to become steady, as noted by Meissner.

It might be supposed that fluctuations amounting to  $0.01^{\circ}$  or  $0.02^{\circ}$  are of no serious consequence, and that the reliability of the results is limited only by the accuracy with which the resistance can be determined. Several observations, however, substantiate the conclusion that the reading when unsteady to the extent of  $0.01^{\circ}$  only is probably considerably too low, as shown by comparing the steady readings numbered 3 and 16 in Table 3 with unsteady readings numbered 9 and 17 which were obtained, respectively, with the same shields. The lower disk was abandoned on iron shields since there is a tendency for unsteady, and hence uncertain, readings.

*Effect of Omitting Shield.*—A thermometer protected only by an umbrella above the coil, assumed temperatures from  $0.5^{\circ}$  to  $3^{\circ}$  below the temperature assumed by a shielded thermometer, the

lowering depending upon the height of the coil above the liquid sulphur. The results of similar experiments previously reported indicate that the thermometer under such circumstances reads low by a fairly definite amount, although it might be expected that the temperature assumed by the thermometer would depend upon a large number of factors, such as depth of immersion in the vapor, temperature to which the insulation of the bath has become heated, etc.

*Temperature of Shield.*—Apart from the effect of the shield upon the temperature assumed by the thermometer, it is of some interest to determine the temperature of the shield itself. If the thermometer be inclosed in a long, close-fitting, closed-end metal tube, the thermometer coil should assume the temperature of the tube, and the tube although differing in form perhaps assumes a temperature not differing much from the temperature assumed by a shield. In this way an iron tube with umbrella above was found to have a temperature about  $0.15^{\circ}$  lower than that assumed by an adequately shielded thermometer, while an aluminum tube assumed a temperature only about  $0.01^{\circ}$  lower. Without the umbrella the iron tube had a temperature about  $0.3^{\circ}$  lower and the aluminum shield a temperature about  $0.04^{\circ}$  lower than that assumed by a shielded thermometer.

The higher temperature assumed by the externally polished aluminum shield might have been predicted from theoretical considerations, since the aluminum is a poor radiator. It would appear that the best single shield would have a polished exterior and blackened interior, but we have not recommended the adoption of such a shield to the exclusion of other forms because of the difficulty of preparing such shields, and because observation of the temperature of the thermometer inclosed in such a shield shows that the advantage is purely a theoretical one.

*Preferred Type of Shield.*—From the result of the experimental work described we have come to the conclusion that, in general, the best type of shield is a simple sheet-iron cylinder from 1.5 to 2.5 cm larger in diameter than the thermometer tube and 4 cm or more longer than the coil, open below and with an umbrella above. This umbrella should fit the thermometer tube closely and extend beyond the edge of the cylinder, leaving a space 5 mm to 1 cm high between umbrella and cylinder for circulation of the vapor. For the material of the shield sheet iron is preferred in general. The main objection to the iron shield seems to be that the sulphur attacks the iron and forms considerable scale, as a

result of which the iron is consumed and the bath discolored, although without affecting the temperature of the boiling point. Practically all the loose scale is formed when the shield is withdrawn from the bath, however, when the sulphur takes fire spontaneously, so that only a small amount of scale need be left in the boiling tube if care is taken. The life of the iron shield is longer than might be expected. One in particular that had been used a dozen times did not appear appreciably thinner than when first made. This objection to the iron shield is not a serious matter in view of the high and consistent readings obtained with it.

It is possible that the slightly higher temperature ( $0.01^{\circ}$  or at most  $0.02^{\circ}$ ) obtained with the double iron shields may not be attributable entirely to experimental error, and that the use of a single shield will result in slightly low readings. The difference is so small, however, that it seems desirable to standardize the single shield for use in the sulphur boiling point apparatus, in the interest of simplicity. It should be noted that in the electrically heated apparatus this difference was not found. (See Table 4.)

In cases where the iron is objectionable, aluminum, blackened on the inside, may be substituted, and in case it is desirable to introduce nothing but aluminum into the bath, a corrugated aluminum shield is satisfactory, although it requires more time to make. Once made, it is perhaps the most satisfactory of any. Any of the three shields mentioned have been shown to satisfy sufficiently well the following criteria of effective shielding:

(1) The reading must not change more than  $0.02^{\circ}$  upon moving the thermometer with the shield up and down in the vapor column for at least 6 cm; for example, from 6 to 12 cm above the liquid surface.

(2) The reading must be steady; if fluctuations amounting to even  $0.01^{\circ}$  are present, a readjustment should be made.

(3) The readings should be capable of being repeated from day to day to within  $0.03^{\circ}$ .

(4) The use of the shield should lead to the same value of  $Pt_{760}$  for a given thermometer regardless of the thermometer protecting tube.

(5) The use of the shield must not lead to different readings with age or repeated use.

(6) Doubling the shield—that is, putting a shield within a similar one—should not change the indications of the thermometer.

(7) The use of the shield should lead to as high a reading as would be obtained by using any other form of shield.

## 2. INFLUENCE OF TYPE OF SULPHUR BOILING APPARATUS

To test for possible effects of differences in methods of heating, in dimensions and in the heat insulation around the tube, several types of boiling apparatus were constructed and experiments were made to determine the effects of various types of insulation around the boiling tube.

An electrically heated boiling apparatus was built along the lines of the one used by Meissner and described in his paper, the main difference being that the heating coil did not extend under the boiling tube but was wound on an outer porcelain tube, the coil extending upward from a point about on a level with the bottom of the sulphur-containing tube for a distance of about 6 cm. The bottom of the porcelain tube which extended somewhat below the heating coil was closed with asbestos board. An auxiliary heating coil was wound on the upper part of the porcelain tube to hasten the boiling, but was disconnected at least half an hour before observing. The porcelain tube was 30 cm long, the inner diameter being about 4 mm greater than the outer diameter of the boiling tube, and thus a small air space was left between the two similar to that shown in Meissner's drawing. This apparatus proved very effective in heating up quickly on about 400 watts, and readings taken on different days were about as consistent as those observed with the gas-heated apparatus.

Nine observations were taken in this apparatus with two thermometers,  $C_{27}$  and  $C_{28}$ , the former having a glazed porcelain tube and the latter a glass tube. Comparing these observations which are shown in Table 4 with those made in the gas-heated apparatus, using adequate shields in both cases,  $C_{27}$  gives a value for electric heating  $0.01^\circ$  higher than for gas heating, and  $C_{28}$  gives a value for electric heating  $0.03^\circ$  higher than for gas heating. The readings were remarkably constant for displacements of the thermometers up and down for a distance of more than 10 cm, the usual variation not exceeding  $0.01^\circ$ . In this type of boiling apparatus there is a possibility that the vapor may be superheated owing to conduction up the porcelain tube, or to convection of highly heated air in the space between the porcelain tube and the boiling tube.

Through the kindness of Messrs. Day and Sosman, the electrically heated apparatus was made available in which their direct determination of the sulphur boiling point by the gas thermometer was carried out. The boiling tube of this apparatus is 71 mm internal

diameter, while that of the specially constructed apparatus above described is 42 mm. A direct comparison of the two was made by interchanging thermometer  $C_{28}$  from one to the other, resulting in a value for the large tube about  $0.03^\circ$  lower than for the small tube. The temperature observed in the large tube was therefore the same as that observed in the gas-heated apparatus previously described.

TABLE 4.—Observations with Electrically Heated Sulphur Boiling Apparatus

## (a) MEISSNER TYPE

Date	Thermometer number	Tube inclosing thermometer	Type of shield	$P_{H_2O}$	Remarks
Mar. 4, 1916	$C_{27}$	Porcelain	Umbrella and iron cone.....	421.72	Average for $C_{27}$ 421.73. <sup>a</sup>
Mar. 9, 1916	$C_{27}$	...do.....	...do.....	421.75	
Do .....	$C_{27}$	...do.....	...do.....	421.73	
Mar. 4, 1916	$C_{27}$	...do.....	Calendar Orbits	421.73	
June 2, 1916	$C_{27}$	...do.....	Umbrella and iron cylinder...	421.72	
Mar. 9, 1916	$C_{28}$	Glass.....	...do.....	421.70	Average for $C_{28}$ 421.70. <sup>b</sup>
Do .....	$C_{28}$	...do.....	...do.....	421.69	
Mar. 20, 1916	$C_{28}$	...do.....	...do.....	421.70	
Mar. 6, 1916	$C_{28}$	...do.....	Umbrella and double iron cylinder.	421.70	

## (b) DAY AND SOGMAN BOILING TUBE

Mar. 20, 1916	$C_{28}$	Glass.....	Umbrella and iron cylinder...	421.67	
---------------	----------	------------	-------------------------------	--------	--

<sup>a</sup> Average for gas-heated apparatus is 421.73.<sup>b</sup> Average for gas-heated apparatus is 421.67.

A tube of small diameter (25 mm internal) was also used as a boiling tube. It was heated with a gas burner and insulated with sheet asbestos. Measurements in this tube indicated superheating of the vapor and considerable differences of temperature at different heights in the tube.

*Effect of Surroundings of Tube.*—In order to determine to what extent the heat insulation and the character of the surface next to the boiling tube, whether this surface be a good or a poor reflector, might influence the reading of the thermometer, a 70 cm boiling tube was used in a short jacket, leaving about 30 cm of the tube extending out into the air. By using a very large flame, it was possible to raise the condensation line high enough to obtain a boiling-point observation in that portion of the tube surrounded only by the air. Boiling-point observations were made under this condition and with the tube surrounded with sheet iron, nickel foil, and thin sheet asbestos. The results are given in Table 5.

**TABLE 5.—Effect of Surroundings of Boiling Tube Upon Indications of Thermometer  $C_{27}$  with Porcelain Inclosing Tube Shielded with Iron Umbrella and Cylinder**

Material surrounding boiling tube	$P_{H_2S}$
Air.....	421. 64
Sheet iron.....	421. 68
Nickel foil.....	421. 71
Thin asbestos.....	421. 72
Thick insulation.....	421. 72

From the two sets of experiments last described it appears that it would be well to set a lower limit, say 4 cm, to the diameter of the tube in the standard form of boiling apparatus. While it is necessary to provide some insulation for the tube it is evident that a very small amount is sufficient and that the amount used will be dictated by considerations of efficiency.

### 3. PURITY OF SULPHUR

Small known quantities of arsenic and selenium were added to boiling pure sulphur and the boiling point observed in the usual way after each such addition. These materials were selected as being the most probable impurities occurring in ordinary sulphur and which might be expected to affect the boiling point. The results are given in Table 6.

**TABLE 6.—Effect of Added Impurities on the Boiling Point of Sulphur**

Condition of sulphur	Observed $P_{H_2S}$
Pure.....	421. 73
With 0.05 per cent arsenic added.....	421. 73
With 0.1 per cent arsenic added.....	421. 75
With 0.05 per cent selenium added (plus the 0.1 per cent arsenic).....	421. 81
With 0.1 per cent selenium added (plus the 0.1 per cent arsenic).....	421. 82

It is evident that selenium, even in small amounts, would be objectionable. All previous experience indicates, however, that such impurities are not likely to be found in purified sulphur. This is further confirmed by the fact that the boiling point of a sample of crude sulphur, from Louisiana, was found to be not over  $0.01^{\circ}$  higher than that of the purified sulphur used regularly. The crude sulphur was part of a specimen exhibited in the local office of the Southern Railway Co. and was supplied through the courtesy of their local representative.

#### 4. THE RELATION BETWEEN THE VAPOR PRESSURE OF SULPHUR AND TEMPERATURE

The excellent agreement between the results obtained by Holborn and Henning and by Harker and Sexton might be taken to indicate that any repetition of their work would be superfluous. However, in the present investigation an extended comparison of shields was made during a considerable time interval which involved a range of barometric pressure of 747 to 763 mm, and an equation was necessary which would represent the pressure-temperature relation of sulphur vapor to an accuracy of the order of  $0.01^{\circ}$ . An examination of Holborn and Henning's data indicated that the excellent agreement of the two sets of observations might have been to some extent, at least, fortuitous, and this, together with the fact that Harker and Sexton's data could not be obtained at all, made it appear desirable to redetermine the relation. The present work gave results in agreement with the older formulas, but a considerably higher degree of precision was attained in the measurements.

The pressure-control apparatus is shown in Fig. 3. The boiling tube was closed by a rubber stopper protected from the heat and from contact with the sulphur vapor by a disk of asbestos. Connection was made with 8 mm internal diameter tubing through a trap of 2 liters' capacity to the water manometer and to the pressure regulator. The manometer was made of 11 mm internal diameter glass tubing and was equipped with mirror and millimeter scale for reading menisci. The pressure regulator was an ordinary 5 cubic foot meter prover with water seal. This proved admirable for pressure control, since it took up any fluctuations of pressure. By means of levers and weights any desired pressure in the given range could be easily produced and maintained regardless of changes in temperature, etc. Simultaneous readings were made of the thermometer, manometer, and barometer.

In each series of observations readings were first taken at one or two pressures very near to 760 mm, then the pressure was increased (or decreased) step by step to the highest (or lowest) attainable with the apparatus, then changed step by step to obtain points intermediate between these previously observed, until the pressure of 760 mm was again obtained. Further observations at pressures below (or above) 760 mm were then made. In computing the pressures account was taken of the density of the water in the manometer, the expansion of the manometer scale, and of the



FIG. 3.—*Apparatus for varying and measuring pressure of boiling sulphur*



differences in level between the thermometer in the sulphur vapor, the water menisci, and the barometer, in addition to the usual barometric corrections. From the considerable number of observations at pressures near 760 mm a value of  $\delta$  was computed, and in this way the curve was made to pass through the point  $t=444.6$   $p=760$  mm. This method of computation might involve the use of a value of  $\delta$  differing by one or two units in the third decimal place from the best value of  $\delta$  for that thermometer, but insured the agreement of observed and calculated values for normal pressure.

Three series of observations were made and two thermometers were used. All of the observed points are reproduced in Fig. 4, in

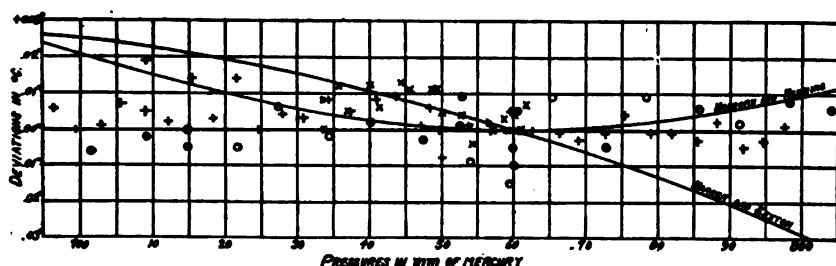


FIG. 4.—Observed minus calculated values of temperatures plotted against pressure

× Observations with thermometer C<sub>1</sub>, May 26, 1916.

+ Observations with thermometer C<sub>1</sub>, June 20, 1916.

○ Observations with thermometer C<sub>2</sub>, June 23, 1916.

Positive ordinates indicate higher temperatures than those calculated from the equation.

$$t = 444.60 + 0.0910(p - 760) - 0.000049(p - 760)^2 \text{ (Mueller and Burgess).}$$

Other equations:

$$t = 444.60 + 0.0910(p - 760) - 0.000043(p - 760)^2 \text{ (Holborn and Henning).}$$

$$t = 444.60 + 0.0904(p - 760) - 0.000051(p - 760)^2 \text{ (Harker and Sexton).}$$

which the deviations of the observed temperatures from those calculated by means of the equation

$$t = t_{760} + 0.0910(p - 760) - 0.000049(p - 760)^2$$

which was found to represent the observations, are plotted against the pressure. The deviations of Holborn and Henning's equation and of Harper and Sexton's equation from the above equation are also shown in Fig. 4.

#### IV. SUMMARY

The importance of the sulphur boiling point as defining a standard temperature and the necessity of obtaining further evidence upon certain questions concerning the effect of experimental conditions upon the results obtained in its use, are considered.

The work of Meissner, which showed that the reflecting power of the inner surface of a radiation shield may have a considerable effect upon the temperature assumed by a resistance thermometer in the sulphur boiling apparatus has been confirmed and extended. A number of types of shields were found to be satisfactory.

The influence of the type of boiling apparatus upon the observed temperature was found to be very small.

The effect of certain impurities in the sulphur upon the observed boiling point was investigated.

The change of vapor pressure with temperature over the range of pressures from 700 to 800 mm was redetermined.

## APPENDIX

### PROPOSED STANDARDIZATION OF THE SULPHUR BOILING POINT

All experimental work published has been drawn upon in preparation of these specifications. The specifications relate to apparatus and procedure suitable for the standardization primarily of resistance thermometers and thermocouples, and it was therefore considered permissible to limit the type of apparatus somewhat closely. The aim has been to impose conditions which are sufficient to insure that the thermometer shall assume a definite temperature, dependent only upon the pressure, when placed in the apparatus, and the question as to whether these conditions are really necessary has received only secondary consideration. Thus the question as to the temperature attained in tubes larger or smaller than those specified need not be considered. It may further be supposed that the thermometer or couple will be mounted in a protecting tube or sheath, and that the diameter of such a tube or width of the sheath will be less than 2 cm.

The specifications relate to the following matters: (1) Boiling apparatus, (2) purity of sulphur, (3) radiation shield, (4) procedure, and (5) computations.

(1) *Boiling Apparatus*.—The boiling tube is of glass, fused silica or similar material, and has an internal diameter of not less than 4 nor more than 6 cm. The length must be such that the length of the vapor column measured from the surface of the liquid sulphur to the level of the top of the insulating material surrounding the tube shall exceed the length of the thermometer coil by at least 20 cm.<sup>11</sup> Heating is by any suitable heater at the bottom of the tube, and the arrangement must be such that the heating element, and all conducting material in contact with it, terminate at least 4 cm below the level of the liquid sulphur. If a flame is allowed to impinge directly on the tube, the heat insulation must extend at least 4 cm below the level of the liquid sulphur. There should be a ring of insulating material above the heater, fitting the tube closely, to prevent superheating of the vapor by convection currents outside the tube. Above the heater the tube is surrounded with insulating material, not necessarily in contact with it, and of such character as to provide heat insulation equivalent to a thickness of not less than 1 cm of asbestos. The length of this insulation has already been specified. Any device used to close the top of the boiling tube must allow a free opening for equalization of pressure.

(2) *Purity of Sulphur*.—The sulphur should contain not over 0.02 per cent of impurities. It should be tested to determine whether selenium is present.

(3) *Radiation Shield*.—The radiation shield consists of a cylinder open at both ends and provided with a conical umbrella above. The cylindrical part is to be 1.5 to 2.5 cm larger in diameter than the protecting tube of the thermometer, and at least 1 cm smaller than the inside diameter of the boiling tube. The cylinder should extend 1.5 cm or more beyond the coil at each end. The umbrella should fit the thermometer tube closely, should overhang the cylinder, and be separated from the latter by a space 0.5 to 1 cm high. The inner surface of the cylinder must be a poor reflector, such as sheet iron, blackened aluminum, asbestos, or a deeply corrugated surface.

<sup>11</sup> This length was arrived at as follows: The minimum distance from the liquid surface to the bottom of the shield was taken as 6 cm, excess of length of shield over length of thermometer coil 6 cm, distance available for displacing thermometer 6 cm, and minimum distance from top of shield to level of top of insulation 2 cm.

(4) *Procedure*.—The sulphur is brought to boiling <sup>12</sup> and the heating is so regulated that the condensation line is sharply defined and is 1 cm or more above the level of the top of the insulating material. The thermometer, inclosed in its shield, is inserted into the vapor, taking care to have the thermometer coil properly located with respect to the shield, and the thermometer and shield centered in the boiling tube. After putting the thermometer into the vapor time must be allowed for the line of condensation again to reach its proper level. Simultaneous readings of the temperature and barometric pressure are then made. In all cases care should be taken to prove that the temperature is not affected by displacing the thermometer 2 or 3 cm either up or down from its usual position.

(5) *Computations*.—Temperatures are calculated from the pressure by use of the formula,

$$T = 444.60 + 0.0910 (p - 760) - 0.000049 (p - 760)^2$$

If necessary, account should be taken of any difference in pressure between the levels at which the thermometer bulb and the open end of the barometer, respectively, are located. Pressures are to be expressed in the equivalent millimeters of mercury at 0° and under standard gravity ( $g = 980.665$ ).

---

<sup>12</sup> If the sulphur has been allowed to solidify in the bottom of the tube, it must be melted from the top downward to avoid breaking the tube. A better procedure is that recommended by Rothe (*Z. S. für Instrk.*, 23, p. 366, 1903), viz, on completing work with the apparatus it is turned so that the tube makes an angle of 30° or less with the horizontal, so that the sulphur on solidifying extends along the sides of the tube, in which position it may be melted down with less danger of breaking the tube. Even when the procedure recommended is followed, breakage of tubes may be reduced by carefully melting the sulphur from the top downward over a bunsen burner before applying heat to it in the apparatus.

WASHINGTON, January 22, 1919.

OCT 25 1919

DEPARTMENT OF COMMERCE

# SCIENTIFIC PAPERS

OF THE

# BUREAU OF STANDARDS

S. W. STRATTON, DIRECTOR

No. 340

A STANDARDIZED METHOD FOR THE DETERMINATION OF SOLIDIFICATION POINTS, ESPECIALLY OF NAPHTHALENE AND PARAFFIN

BY

R. M. WILHELM, Assistant Physicist

and

J. L. FINKELSTEIN, Assistant Physicist

*Bureau of Standards*

ISSUED SEPTEMBER 12, 1919



PRICE, 5 CENTS

Sold only by the Superintendent of Documents, Government Printing Office  
Washington, D. C.

WASHINGTON  
GOVERNMENT PRINTING OFFICE  
1919





# A STANDARDIZED METHOD FOR THE DETERMINATION OF SOLIDIFICATION POINTS, ESPECIALLY OF NAPHTHALENE AND PARAFFIN

By R. M. Wilhelm and J. L. Finkelstein

## CONTENTS

	Page
I. Introduction.....	185
II. Principles underlying the constant-temperature method.....	186
III. The capillary-tube methods.....	187
IV. Preliminary experimental work.....	187
V. Description of standardized apparatus and method.....	189
VI. Solidification point of paraffin.....	194
VII. Summary.....	197

## I. INTRODUCTION

Inquiries which the Bureau has received from time to time concerning a standard method for making freezing-point determinations of substances such as naphthalene and paraffin have made it evident that there is little uniformity in the methods used for such work in the industries. This conclusion has been confirmed by an inspection of Treasury Decisions,<sup>1</sup> in which one finds disputes arising out of a failure of industrial laboratories to agree among themselves or with the customs laboratories as to the methods that should be used in obtaining solidification-point determinations of naphthalene, which under a law of 1916 will be admitted free of duty if its solidification point is below 79° C. Naphthalene solidifying at or above this temperature is classified as refined.

The need for such a standard method and apparatus resulted in the calling of a conference of officials of the Customs Service at

<sup>1</sup> Treasury Decisions, 85, Oct. 24, 1918; No. 7 (T. D. 37790-G. H. 8197), p. 5.

the Bureau of Standards to discuss this question. This conference,<sup>3</sup> held in December, 1917, at the Bureau, made certain recommendations in regard to a standard method for obtaining the freezing point of naphthalene. The conference recommended a method which has long been in use in physical-chemical work, namely, the constant-temperature method. The details of the method as applied to determinations of the solidification point of naphthalene and other substances will be described later.

## II. PRINCIPLES UNDERLYING THE CONSTANT-TEMPERATURE METHOD

In general, an impure substance does not have a definite freezing point. For a pure substance the melting and freezing points are identical and either may be defined as the temperature at which crystals and liquid will exist in contact and in equilibrium at standard atmospheric pressure. If a pure liquid is allowed to cool slowly enough, the temperature will be observed to become constant as soon as crystals begin to separate out and will remain constant until all or a considerable part of the substance has solidified.

This constant temperature is often preceded by undercooling, but as soon as crystals form the temperature rises sharply to the freezing point, which may thus be accurately observed. The amount of undercooling which takes place may be greatly diminished by stirring the liquid.

The experimental determination of the freezing point is, therefore, relatively simple if a sufficient quantity of the material is used so that the temperature can be measured by means of a thermometer inserted into it. Melting-point determinations by this method are much more difficult and uncertain than those of freezing point, especially for solids of low thermal conductivity.

If an impure liquid is allowed to cool slowly, the crystals which separate out are, in general, of higher purity than the original

---

<sup>3</sup> Those attending this conference were T. D. Simons, Baltimore; D. L. Coburn, Boston; C. C. Roberts, Philadelphia; J. H. Hines, Chicago; E. R. Pickrell, New York; and H. L. Barrick, Washington, from the Treasury Department; and C. E. Waters, E. F. Mueller, R. M. Wilhelm, and J. L. Finkelstein from the Bureau of Standards, Washington.

material, so that the impurities are concentrated in the liquid, which results in a continued lowering of the freezing point as the freezing progresses. If the freezing point of an impure liquid is determined, the temperature will, therefore, not remain constant at any time, but will fall slowly after freezing has begun. It will be noted that the initial freezing point—that is, the temperature observed just after crystals are beginning to form or immediately after undercooling ceases—bears a definite relation to the amount of impurity present. When the freezing point is used as a criterion of purity, the initial freezing temperature is, therefore, the one which is of interest and is by definition called the “freezing” or “solidification” point. In dealing with more or less indefinite mixtures, such as paraffin, the initial freezing point is also by definition taken as the actual freezing point of the substance.

### III. THE CAPILLARY-TUBE METHODS

Among the various methods used to determine freezing or melting points those which make use of a capillary tube of some form are very common. Experiments made here and in other laboratories have demonstrated that the capillary-tube melting-point method will not usually give so consistent nor so accurate results as the constant-temperature method. In special cases, however, when only a small quantity of material is available or when speed rather than accuracy is desired, it may be more satisfactory, or even necessary, to use this less-accurate method.

### IV. PRELIMINARY EXPERIMENTAL WORK

The freezing-point method which will be described was adopted as the result of experimental work done at several of the customs laboratories and at the Bureau of Standards during November and December, 1917, on various types of apparatus and methods which had been used previous to that time in customs laboratories.

In the main, three types of freezing-point apparatus were investigated at this Bureau, and determinations were made, under various conditions, of the solidification point of pure naphthalene,

pure naphthalene to which other substances had been added, and impure samples which had been submitted to the Bureau.

The three types of apparatus which were designated as Nos. 1, 2, and 3 may be briefly described as follows:

No. 1 was practically the same as the apparatus which will be described later in this paper.

No. 2 consisted of a cylindrical Dewar or vacuum container, 20 cm in depth and 3 cm in internal diameter, in which the test sample was allowed to cool while its solidification point was being observed.

No. 3 consisted of a  $\frac{3}{8}$ -inch test tube containing the sample immersed in a beaker of water which was heated sufficiently to melt the naphthalene and then allowed to cool while the solidification point was being observed.

Comparative measurements made with the three types of apparatus, using pure naphthalene, showed that consistent and accurate results could be obtained with any of them if proper precautions were taken. The results of the comparison are given in Table 1.

**TABLE 1.—Averages of Solidification Points Found for a Sample of Pure Naphthalene with Three Types of Apparatus and with Resistance and Mercurial Thermometers.**

Apparatus	Platinum resistance thermometer	Mercurial thermometer
	° C	° C
No. 1.....	80.10	80.08
No. 2.....	80.10	80.10
No. 3.....	80.12	80.10

The choice of the apparatus can, from the above results, be seen to depend largely upon the factors of simplicity, convenience, availability, and speed.

Apparatus No. 1 seemed to possess advantages in the above respects sufficient to warrant its adoption.

In the experimental work a platinum resistance thermometer, a mercurial thermometer graduated from 0 to 100° C in 0.2° intervals, and a mercurial thermometer graduated from 70 to 110° C

in 0.1° intervals were used. With the long mercurial thermometers the stem correction was large, and for this reason the short thermometer, graduated according to specifications which will be given later, was preferred. Thermometers graduated for partial immersion did not seem desirable.

The effect of adding moisture to the pure sample is given below:

	°C
Pure sample naphthalene, solidification point.....	80.13
3 per cent distilled water added, solidification point.....	79.78
Heated one hour at 110°, solidification point.....	80.10

This experiment shows very clearly the importance of designing whether or not the sample shall be dried previous to making the solidification point determination if consistent results are to be obtained.

A dry sample exposed to an atmosphere saturated with moisture in a closed vessel for three days showed no change in the freezing point.

## V. DESCRIPTION OF STANDARDIZED APPARATUS AND METHOD

The following is a description of the apparatus and method finally adopted and used at this Bureau for the determination of the solidification point of naphthalene and recommended in the report of the previously mentioned conference. As will be shown later, the method can be used satisfactorily for obtaining the freezing points of paraffins and many other substances.

*Apparatus.*—The form of the apparatus shown in Fig. 1 consists of a 7/8-inch test tube, 7 inches long (a stock size) surrounded by an air jacket which may be formed by a bottle. The bottle is closed by a stopper which supports the test tube. The test tube carries a stopper about 7/8 inch thick, with suitable perforations for thermometer and stirrer. The stirrer consists of a loop of glass, with a glass stem, the loop surrounding the thermometer. The test tube, with its jacket, is placed in a water bath. The level of the water in the water bath should be at least as high as the level of the melted naphthalene. A stirrer in the water bath is not necessary.

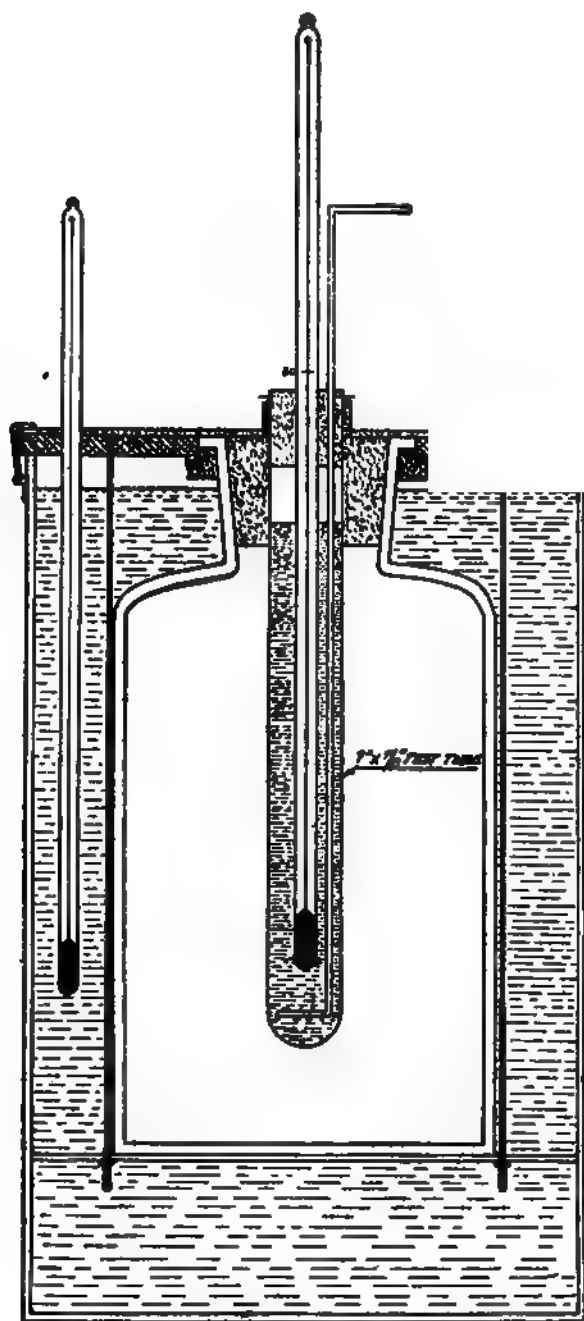


FIG. 1.—Apparatus for determining solidification points

**Thermometers.**—The thermometer used is to be made according to the following specifications. The use of other suitable thermometers—that is, thermometers similar to this but having no ice point—is permissible.

The general appearance of the thermometer is shown in Fig. 2. It is graduated from  $-1^{\circ}$  to  $+1^{\circ}$  and from 74 to  $102^{\circ}$  in  $0.1$  intervals.

The required dimensions are: Total length, 33 to 35 cm; diameter of stem, 5.5 to 6.5 mm; length of  $28^{\circ}$  interval from 74 to  $102^{\circ}$ , not less than 18 cm; bulb same diameter as stem, or smaller, length not over 4 cm; and the  $80^{\circ}$  mark not less than 14 cm nor more than 16 cm above bottom of bulb.

The bulb should be made of suitable thermometric glass, and the stem of enamel-backed thermometer tubing.

The graduation lines should be clear and sharp, and their thickness should be not more than 0.1 of the length of a graduation interval. The longer lines should preferably extend equally to the right and left of the shorter ones. The numbers should be placed as shown in the drawing. The bulb should be thoroughly annealed to prevent change of indications with time.

The manufacturer's name or trade-mark and a serial number should be engraved on the thermometer.

A suitable case, preferably of brass, with a slip or screw cap, should be provided for the thermometer.

The correction at any point of the scale should not exceed  $0.15^{\circ}$  C, nor should the change in the corrections over any interval exceed 0.5 per cent of that interval. These

FIG. 2.—Thermometer used in determining solidification point of naphthalene

requirements apply provided the thermometer is used with bulb and mercury column at the same temperature.

*Procedure.*—(a) Take care to get a representative portion of the sample, break up lumps or moth balls, and mix thoroughly, but avoid loss of volatile matter as much as possible.<sup>a</sup>

(b) Melt the naphthalene by immersing the test tube in water heated to not over 90° C. The level of the melted naphthalene should be about 2 inches below the top of the tube in which it is contained. If a large number of determinations are to be made, a water bath maintained at about 90°, and provided with a suitable support for a number of test tubes, will be found convenient. The naphthalene should not be heated above 90° nor longer than necessary, and the tubes should be kept closed in order to avoid loss of volatile material.

(c) Transfer the naphthalene to the apparatus described above. The temperature of the water bath should be between 70 and 75° and need not be raised during the determination. Insert thermometer and stirrer, which may have been previously warmed. This will raise the level of the melted naphthalene about  $\frac{1}{2}$  inch, and the level should then be about  $\frac{1}{2}$  inch below the stopper (limits of  $\frac{1}{4}$  inch to  $\frac{3}{4}$  inch permissible).

The bottom of the thermometer bulb should be at least  $\frac{1}{2}$  inch above the bottom of the test tube. After the temperature of the naphthalene reaches 81°, take readings every half minute, stirring the naphthalene continuously but not violently. In making the readings estimate to the nearest 0.1 division (0.01°) and take the usual precautions to avoid parallax. Readings may be more easily made with the aid of a magnifying glass; but this is not necessary. The solidifying point corresponds to the first series of five or more readings, during which the temperature remains constant (change not over 0.02°). Usually undercooling will occur, in which case the constant temperature should be observed immediately after the undercooling ceases. If the five readings are not identical, take the average of the five readings. Apply the scale and stem corrections. The stem correction for the thermometer specified and the type

<sup>a</sup> In view of the effect of the presence of water in the sample and of the fact that the water can be easily removed without special refining methods, the conference recommended that the sample be freed from moisture before making the determination, provided such procedure were permissible under the law. In a recent supplement to the Manual of Methods for the Port of New York directions are given for drying the naphthalene previous to the solidification-point determination.



of apparatus used will be small (about  $0.03^{\circ}$ ) and may therefore be determined once for all according to the following formula:

Stem correction equals  $0.00016 N(T-t)$  (centigrade temperatures).

$N$  = number of degrees of mercury column emergent.

$T$  = temperature of bulb.

$t$  = average temperature of emergent mercury column.

(d) Repeat the determination with a fresh portion of the sample. The two determinations should agree within  $0.05^{\circ}$ ; and if they do not, make a third determination. Average the results.

It is to be noted that in the above procedure there has been incorporated what is virtually a definition of the solidification point, namely, the temperature at which solidification begins. This definition was adopted by the conference because the determination of the solidification point is essentially a criterion of purity, and it is the depression of the initial freezing point below that of the pure substance which is a measure of the amount of impurity present.

Recommendations substantially the same as the above were submitted to six customs laboratories in various cities, and a cooperative test was made by these laboratories and the Bureau on three samples of naphthalene.

The original samples were received at this Bureau, and subsamples were carefully taken from each. These subsamples were then sent to the different laboratories along with thermometers made according to the specifications previously noted. These thermometers were tested at the Bureau for scale errors before sending to the various offices.

The solidification points obtained at the various laboratories and at this Bureau are given in Table 2.

TABLE 2.—Solidification Points of Three Samples of Naphthalene as Measured at Six Customs Laboratories and at the Bureau of Standards

Sample number	Bureau of Standards	I	II	III	IV	V	VI
	$^{\circ}\text{C}$	$^{\circ}\text{C}$	$^{\circ}\text{C}$	$^{\circ}\text{C}$	$^{\circ}\text{C}$	$^{\circ}\text{C}$	$^{\circ}\text{C}$
D 867.....	79.80	79.70	79.83	79.78	79.87	79.81	(a)
D 723.....	79.51	79.34	79.52	79.53	79.58	79.51	79.60
D 460.....	79.24	79.00	(a)	79.30	79.33	79.38	79.30

a No sample supplied.

It can be seen that the results obtained at the various laboratories and at the Bureau are in good agreement except those reported for laboratory No. I. The low results of No. I may be explained by the fact that a smaller amount of naphthalene than that required in the specifications was used. This laboratory failed to receive a copy of the conference report and used a method which differed in some essential details from that specified.

The agreement of the various laboratories would indicate that determinations of the solidification point of naphthalene in the neighborhood of  $79^{\circ}\text{C}$  are reproducible by this method to  $0.1$  or  $0.2^{\circ}\text{C}$ . The experiments of the Bureau have shown that for naphthalene of higher purity the freezing points of samples can be repeated to  $0.05^{\circ}$  or better.

## VI. SOLIDIFICATION POINT OF PARAFFIN

This same method and apparatus with slight modifications of thermometer and temperature of outer bath were used for paraffin freezing-point determinations. The results are given in Table 3.

TABLE 3.—Determinations of Solidification Points of Three Samples of Paraffin

Designation	Temperature outer bath	Readings	Correction	Solidification point
	$^{\circ}\text{C}$	$^{\circ}\text{C}$	$^{\circ}\text{C}$	$^{\circ}\text{C}$
Sample 1.....	40	54.5	+0.8	55.3
	40	54.5	+ .8	55.3
	40	54.6	+ .8	55.4
	38	54.6	+ .8	55.4
				55.35
Sample 2.....	47	53.8	+ .8	54.6
	46	53.8	+ .8	54.6
	43	53.8	+ .8	54.6
	43	53.8	+ .8	54.6
				54.6
Sample 3.....	36	48.2	+ .8	49.0
	36	48.3	+ .8	49.1
	35	48.2	+ .8	49.0
	35	48.3	+ .8	49.1
				49.05

<sup>a</sup> The average reading over a period of about two minutes, during which temperature remained constant to  $0.1^{\circ}$ .

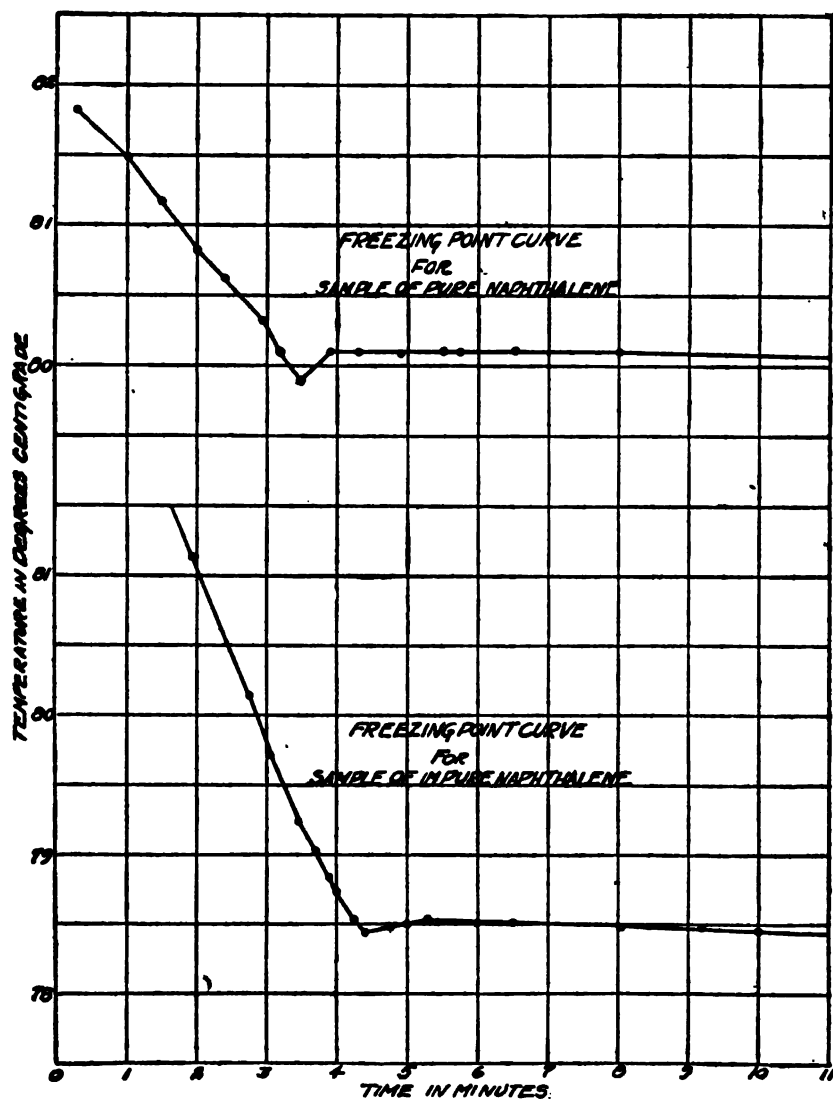


FIG. 3.—Solidification curves for naphthalene

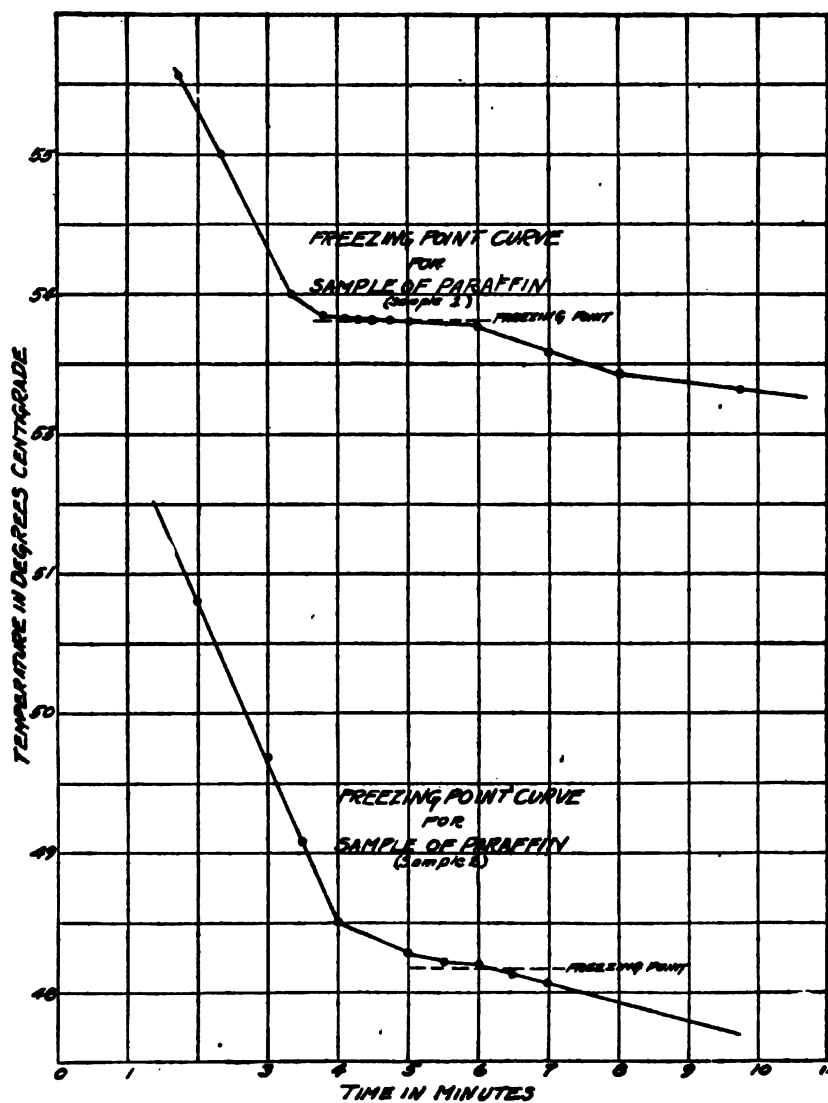


FIG. 4.—Solidification curves for paraffin

The above results indicate that the determination of the solidification point of paraffin may be obtained with the apparatus described to an accuracy of about  $0.1^{\circ}$  or better.

The most desirable thermometer for paraffin freezing-point determinations would be one graduated from  $40$  to  $70^{\circ}\text{C}$  or higher in  $0.1$  or  $0.2^{\circ}$  intervals.

If such a special thermometer is not available, consistent and accurate results can be obtained with other suitable thermometers, provided allowance is made for scale error and error due to the emergent mercury column.

In paraffin the undercooling preceding solidification is scarcely observable. The constant-temperature phenomenon is also not as marked as in naphthalene, since paraffin is a mixture and the composition of the liquid changes as solidification proceeds. These experiments, however, have shown that, in general, the temperature will stay constant to within  $0.1^{\circ}$  for about two minutes if the apparatus described is used.

Some typical freezing-point curves of naphthalene and paraffin are shown in Figs. 3 and 4.

This method has been applied in the laboratory to the determination of the solidification points of benzoic acid and also of antifreezing solutions, brines, fire-extinguishing liquids, etc., by the substitution of a cold bath, maintained at a suitable temperature, for the heated water bath.

## VII. SUMMARY

After a brief treatment of the definitions of melting and freezing points, both of pure substances and of mixtures, a method of making solidification-point determinations is described. This method, which is an adaptation of a well-known one, was recommended at a conference of Bureau of Standards and United States customs officials and was adopted by the U. S. Customs Service for the determination of the solidification point of naphthalene. The method has been applied to the determination of the freezing points of many other substances.

WASHINGTON, February 14, 1919.



OCT 25 1919

DEPARTMENT OF COMMERCE

---

**SCIENTIFIC PAPERS**  
OF THE  
**BUREAU OF STANDARDS**

S. W. STRATTON, DIRECTOR

---

No. 341

**AIRPLANE ANTENNA CONSTANTS**

BY

J. M. CORK, Assistant Physicist

*Bureau of Standards*

---

ISSUED SEPTEMBER 17, 1919



PRICE, 5 CENTS

Sold only by the Superintendent of Documents, Government Printing Office  
Washington, D. C.

---

WASHINGTON  
GOVERNMENT PRINTING OFFICE  
1919





# AIRPLANE ANTENNA CONSTANTS<sup>1</sup>

By J. M. Cork

## CONTENTS

	Page
I. Purpose.....	199
II. Capacity and resistance measurements.....	199
1. Apparatus.....	199
2. Manipulation.....	200
3. Theory.....	201
4. Results.....	204
(a) Fixed antennas.....	204
(b) Trailing antennas.....	207
III. Directional effect.....	211

## I. PURPOSE

The purpose of this work was to obtain general information regarding the effective capacity, effective resistance, true capacity, true inductance, and wave length, as well as the transmitting directional effect of various types of airplane antennas. In addition to trailing antennas of one, two, and four wires, the constants of various fixed antennas were measured in an attempt to find a satisfactory substitute for the trailing wire at short wave lengths.

## II. CAPACITY AND RESISTANCE MEASUREMENTS

### 1. APPARATUS

All measurements were made in flight, using a continuous wave oscillator feeding directly into the antenna. A measurement of the effective resistance and effective capacity of each antenna was made at several different wave lengths, from which resistance wave-length and capacity wave-length curves were drawn. A wiring diagram of the test set used is shown in Fig. 1. It may be observed that this is the familiar Colpitts circuit, in which the antenna takes the place of the regular coupling condenser. By changing  $K_1$  from  $A$  to  $B$  a dummy antenna is substituted for the

<sup>1</sup> The data given in this paper were obtained by the writer while an officer in the Signal Corps, United States Army, and is published with the consent of this organization.

one under test. This consisted of a calibrated straight wire resistance variable in steps of 0.1 ohm, and a variable condenser calibrated for both capacity and resistance at various wave lengths and angular settings. The oscillator and dummy antenna, together with a wave meter of suitable range, were mounted on the bakelite panel of a set box which fitted in the front of the cockpit, convenient for reading condensers and ammeters. By switch  $K_2$  the wave meter could be open circuited and thus absorb no energy. All condensers were shielded by grounded copper cases. For measurements at short wave lengths the inductance was made by winding No. 14 wire on a wooden toroidal core, having taps every three turns for various wave lengths. This

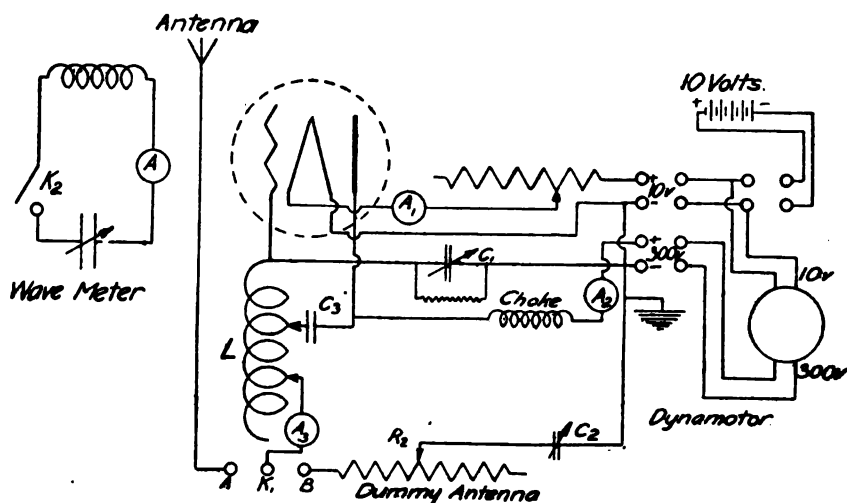


FIG. 1.—Wiring diagram of airplane antenna test set

eliminated to a large degree all stray magnetic fields. Power was supplied by a 10-volt storage battery and a 300-volt dynamotor, battery driven.  $A_1$ ,  $A_2$ ,  $A_3$  are ammeters in filament, dynamotor, and oscillating circuits, respectively. A grid leak of 50 000 ohms shunted the variable grid condenser. All leads carrying oscillations were made as short as possible to avoid stray capacities.

## 2. MANIPULATION

The effective capacity was determined by adjusting the inductance taps and grid condenser for good oscillation at approximately the desired wave length, with the antenna in circuit, then setting the wave meter at resonance. The switch  $K_1$  is next turned to

$B$  and the dummy condenser adjusted until the wave meter is again in resonance. From the condenser calibration the capacity at this wave length may be obtained. To find the effective resistance, having set capacities as above, the wave meter is open circuited by opening  $K_1$  and the reading of  $A$ , noted with  $K_1$  at  $A$ ; now turning  $K_1$  to  $B$ ,  $R_2$  is adjusted until the  $A$ , reading is duplicated. From the calibration of  $R_2$ , the effective resistance is obtained. This furnishes a very accurate and sensitive means for the determination of effective antenna resistance. By varying the grid condenser the range of critical sensitivity may be set at any

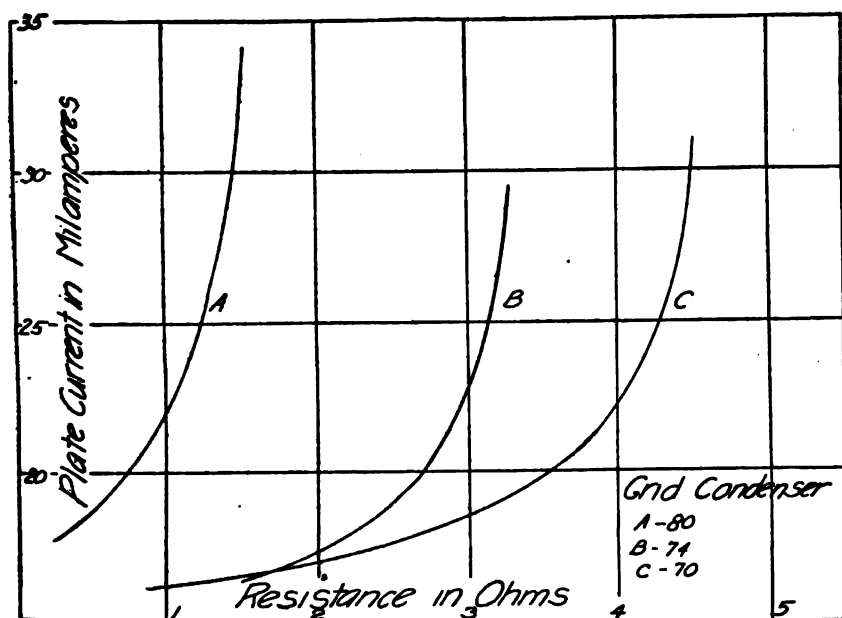


FIG. 2.—Sensitivity of test set for changes in the resistance of the oscillating circuit

resistance value desired. Fig. 2 shows the effect of changing the grid condenser setting, giving at the critical range a change of more than 1 milliampere for 0.1 ohm change in resistance. Thus if the resistance be first found approximately, the grid condenser may be set so as to make the point fall at a sensitive position.

### 3. THEORY

Fig. 3 shows typical wave-length capacity and wave-length resistance curves. At longer wave lengths the effective capacity becomes asymptotic to a value which is the natural or true capacity  $C_0$ . Therefore, since at the natural wave length the

total reactance of the antenna is zero (i. e., for an infinitesimal applied voltage a large current flows in the antenna),  $\frac{I}{\omega C}$  effective is zero. But the effective capacitance at all times equals the difference between the natural capacitance and natural inductive reactance, or

$$\frac{I}{\omega C} \text{ effective} = \frac{I}{\omega C_0} - L_0 \omega$$

or,

$$L_0 = \frac{I}{\omega^2} \left( \frac{I}{C_0} - \frac{I}{C} \text{ effective} \right)$$

and

$$\lambda_0 = 2\pi \sqrt{L_0 C_0}$$

The natural wave length may be approximated graphically by noting the ordinate to which either the resistance or effective

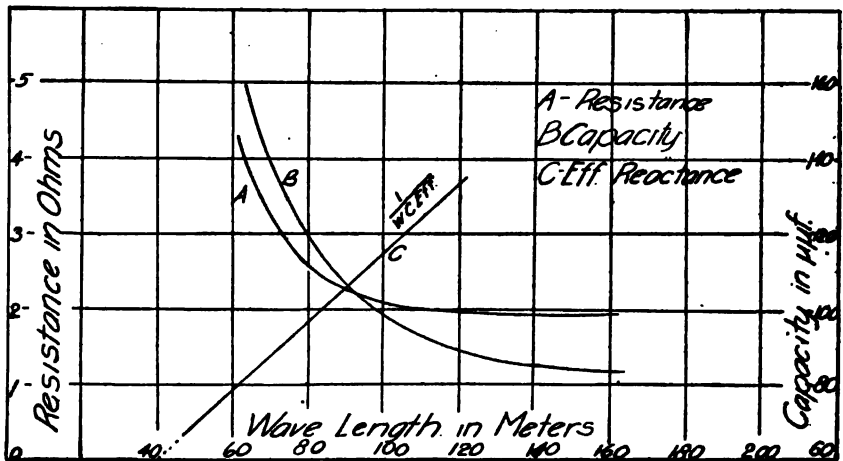


FIG. 3.—Constants of a typical fixed airplane antenna

capacity curves are asymptotic; or, better still, since at wave lengths above the fundamental the capacity reactance predominates, by plotting an effective capacitance wave-length curve as shown in C, Fig. 3, practically a straight line is obtained. This may be extended to intersect the wave-length axis, thus giving the natural wave length. Instead of the effective capacitance  $\frac{I}{\omega C}$  effective,  $\frac{\lambda}{C}$  effective may be used as well, since not actual reactance values but only the intersection of the line with the axis is desired.

The curve shown in B, Fig. 3, gives effective antenna resistance. This, of course, is the resultant of several components. Fig. 4

shows the manner in which the components might be expected theoretically to change with increasing wave length;  $b$  represents the pure ohmic resistance due to the metallic conductors. At long wave lengths this is practically a constant, but increases slightly at short wave lengths due to skin effect, shown by  $b'$ . If  $R^1$  denotes the sum of the direct-current resistance  $R$ , plus the

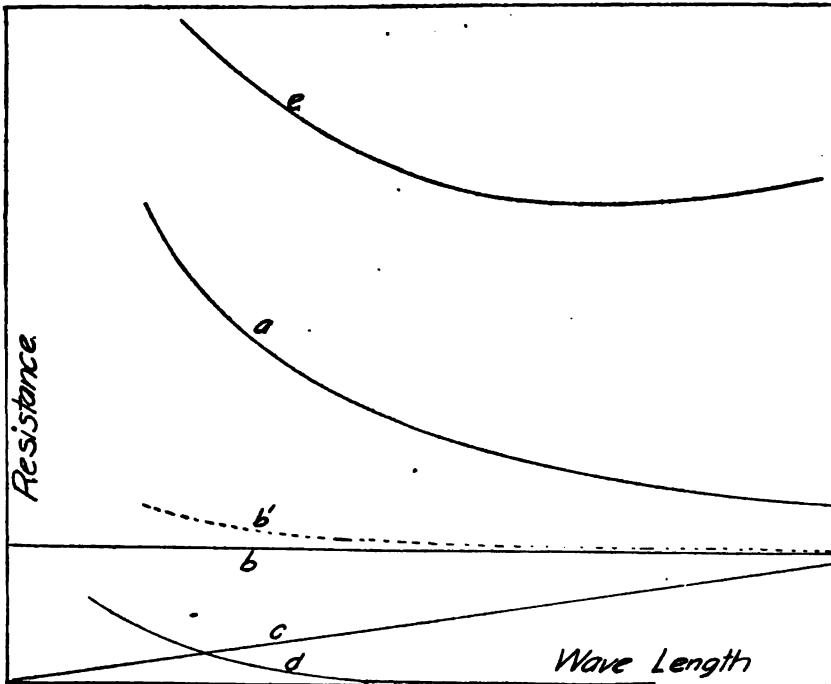


FIG. 4.—Components of antenna resistance

additional resistance due to skin effect, at very short wave lengths an approximate formula for the variation of  $R^1$  is

$$R^1 = R \frac{K}{\lambda^{1/2}}$$

But as  $\lambda$  increases, the approximate formula <sup>2</sup> becomes

$$R^1 = R \left( 1 + \frac{K}{\lambda^2} - \frac{K^2}{\lambda^4} + \dots \right)$$

Curve  $c$  represents resistance due to dielectric loss. In this respect an antenna like a condenser has a phase angle, and may

<sup>2</sup> Fleming, Principles of Elec. Wave Telegraphy, p. 137.

be considered as a resistance and a pure capacity in series, the resistance increasing as the first power of the wave length. The location of the dielectric producing the loss has been the subject of considerable investigation. Dr. J. M. Miller<sup>3</sup> has shown that the earth, as was commonly assumed, is rarely the cause, but rather dielectrics in the proximity of the antenna. It is of interest to observe that this effect was not noted in any of the airplane measurements made.

Curve *d* represents any eddy current or hysteresis losses that might occur. It would be difficult to separate these from the radiation resistance, but they are perhaps both entirely negligible. They would increase approximately with the frequency. Curve *a* represents that part of the resistance due to electromagnetic radiation. It is this factor which it is desirable to have as large as possible. By considering a grounded antenna as one-half of a Hertz oscillator, it has been shown that

$$R_a = 160\pi^2 \left( \frac{ah}{\lambda} \right)^2 \text{ ohms approximately.}$$

Where *h* is the length of wire,  $\lambda$  the wave length and *a* represents the form factor or approximately the ratio of the average current along the antenna length to the value at the base. For an antenna oscillating at its natural wave length this has the value  $\frac{2}{\pi}$ , but for a loaded antenna as is common in practice the current distribution curve is practically a straight line and  $a = \frac{1}{2}$ . Then for an airplane antenna of length, say, 200 feet, transmitting at a wave length of 400 meters,  $R_a = 6$  ohms approximately, and at 1000 meters  $R_a = 1$  ohm approximately.

#### 4. RESULTS

(a) *Fixed Antennas*.—Measurements were made upon fixed antennas over a range in wave length from 60 to 160 meters. In all cases the airplane wires bonded together were used as ground.

Fig. 5 shows some of the arrangements of wires measured. Most of these were first measured close to the plane, then raised on 2-foot and then 4-foot masts. The change from close to plane to 2-foot mast produced a much larger decrease in natural capacity than the change from 2 to 4 foot masts. The raise in height,

<sup>3</sup> Bur. of Standards Scientific Paper No. 356.

however, is accompanied by an increase in radiation resistance. Typical wave-length capacity and wave-length resistance curves of the fixed antennas are shown in Fig. 3. This is for an antenna

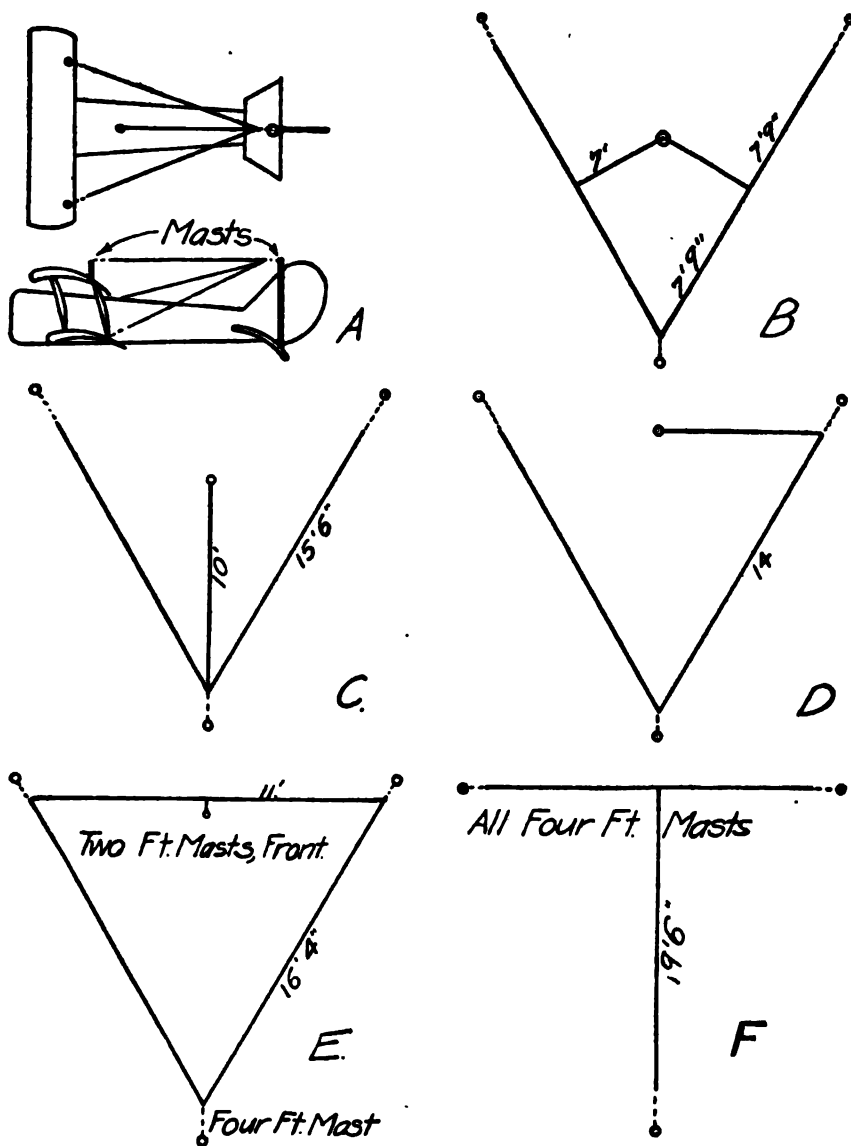


FIG. 5.—Types of fixed airplane antennas

of the form D shown in Fig. 5 raised on masts 2 feet high. The height of mast used is determined by the maximum wind resistance allowable, as well as by the electrical characteristics. Antenna

form D, Fig. 3, is about equivalent in characteristics to a single 45-foot trailing wire except that it is not so directional in trans-

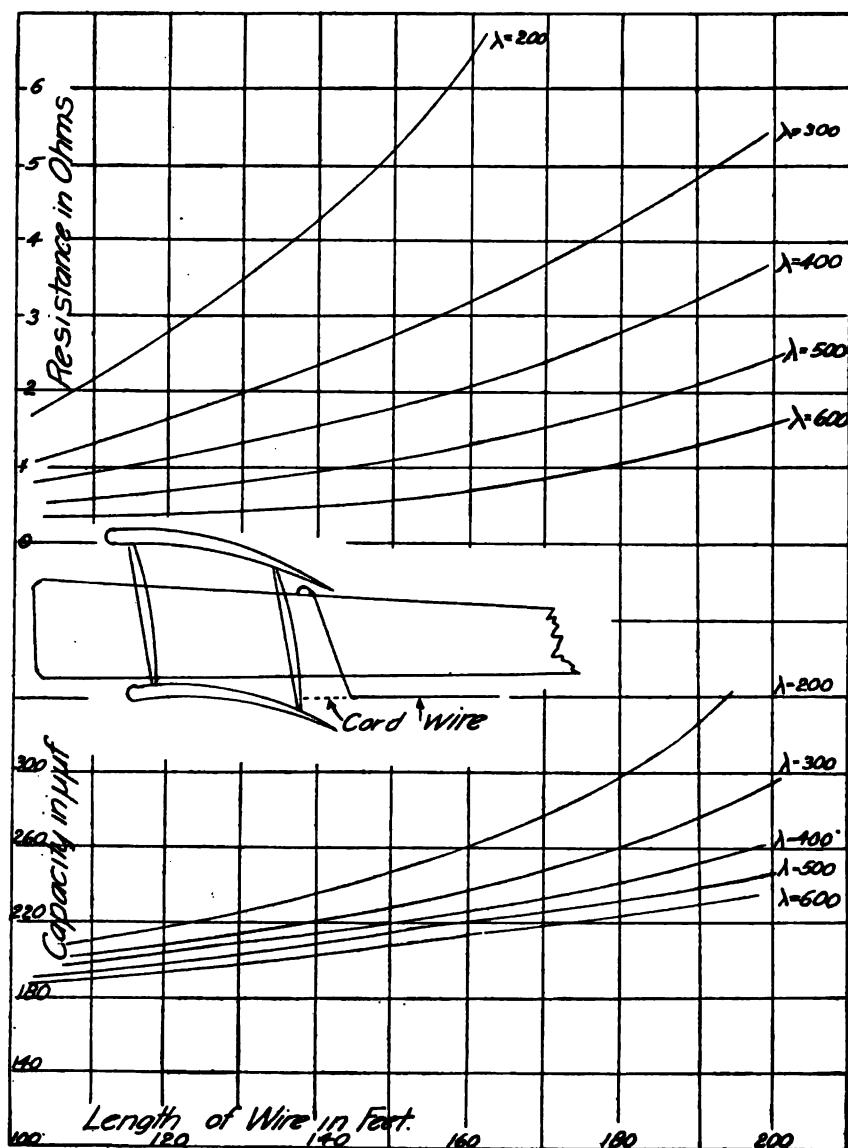


FIG. 6.—Summary of the constants for various lengths of single-wire antennas

mitting. Using this antenna and a single tube oscillator, voice signals have been heard at a distance of 15 miles from plane to ground, using a three-tube receiver.



(b) *Trailing Antennas.*—Measurements were made upon trailing wires over a wave-length range from 100 to 600 meters. The single-wire antenna was attached by an insulator and 40-inch

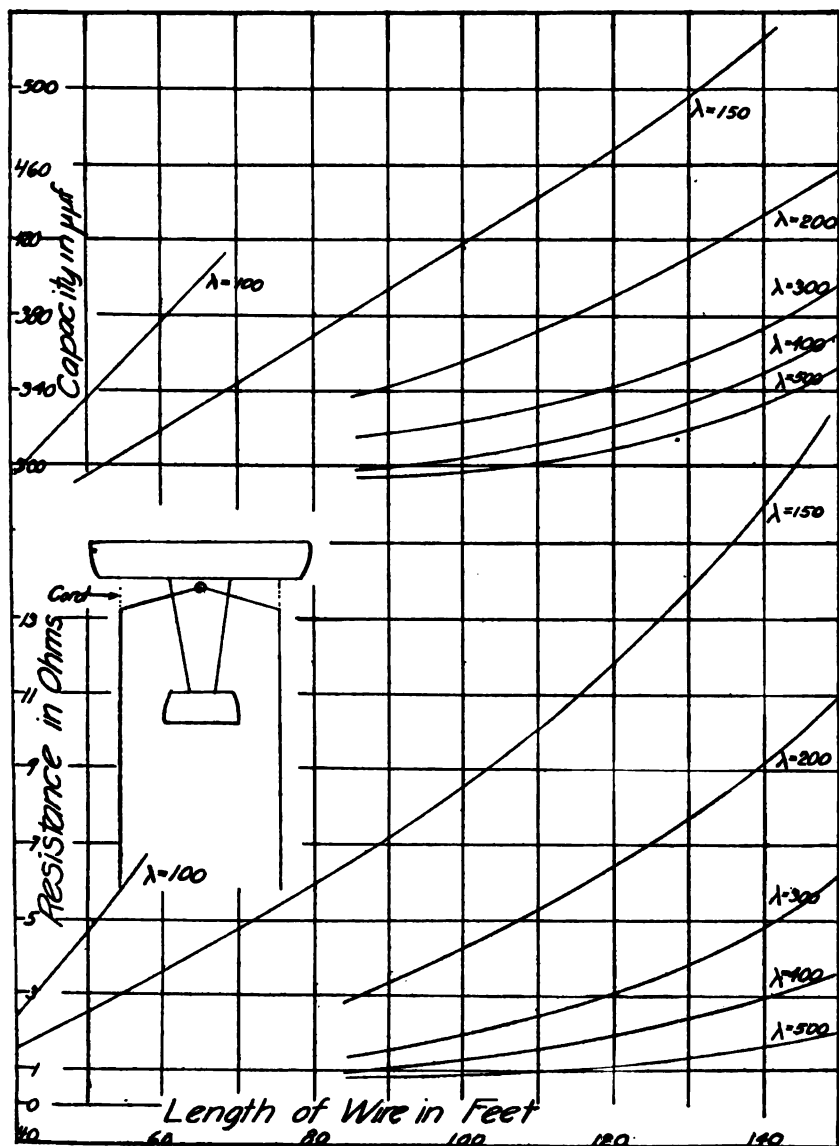


FIG. 7.—Summary of the constants for various lengths of two-wire antennas

string to the inside strut of the plane. The position of the lead in wire is quite an important factor in determining the total capacity of the antenna and should be kept as far as possible from

the wire network of the machine. Various lengths of wire were thus used, and in Fig. 6 the results are summarized by plotting capacity length of wire and resistance length of wire curves at

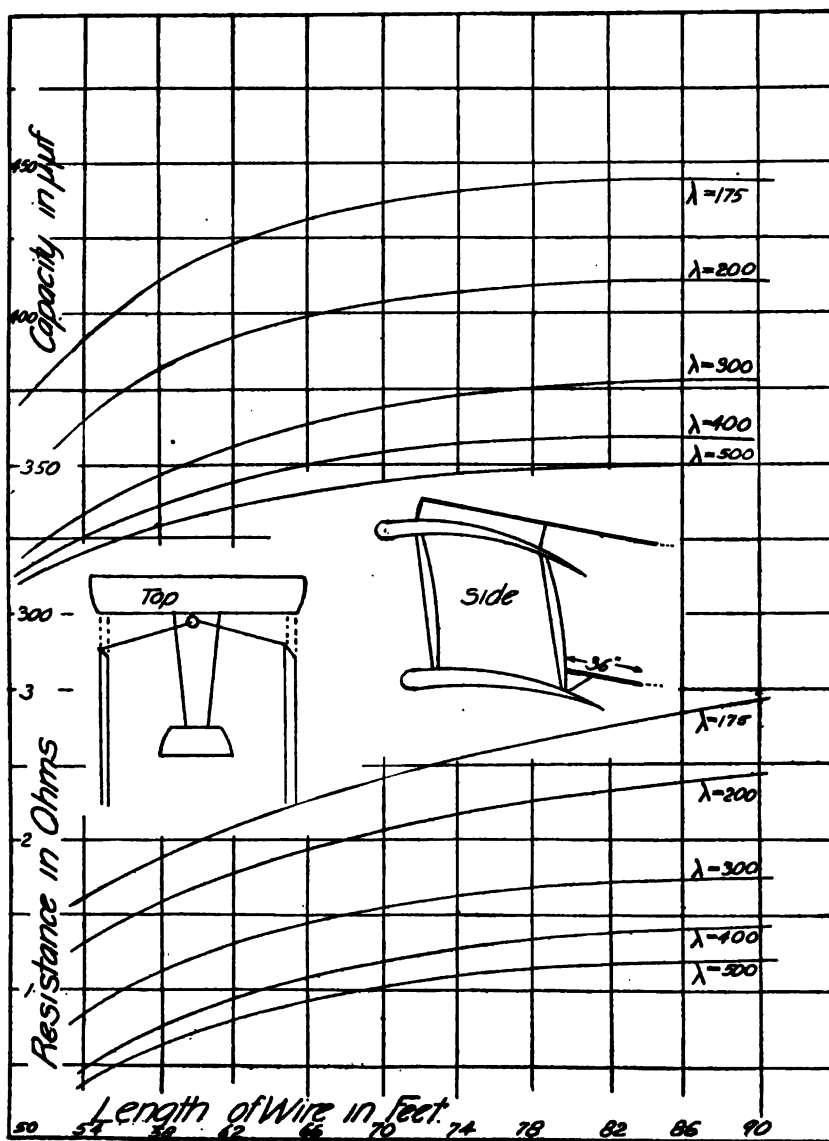


FIG. 8.—Summary of the constants for various lengths of four-wire antennas

various wave lengths. Thus the characteristics for any wire length may be obtained by taking the ordinates of the various wave-length curves at that abscissa. Fig. 7 shows a like sum-

mary for a two-wire antenna attached as shown in the figure, using the wires in parallel against airplane wires as ground. Data were also obtained using one wire as the ground and the

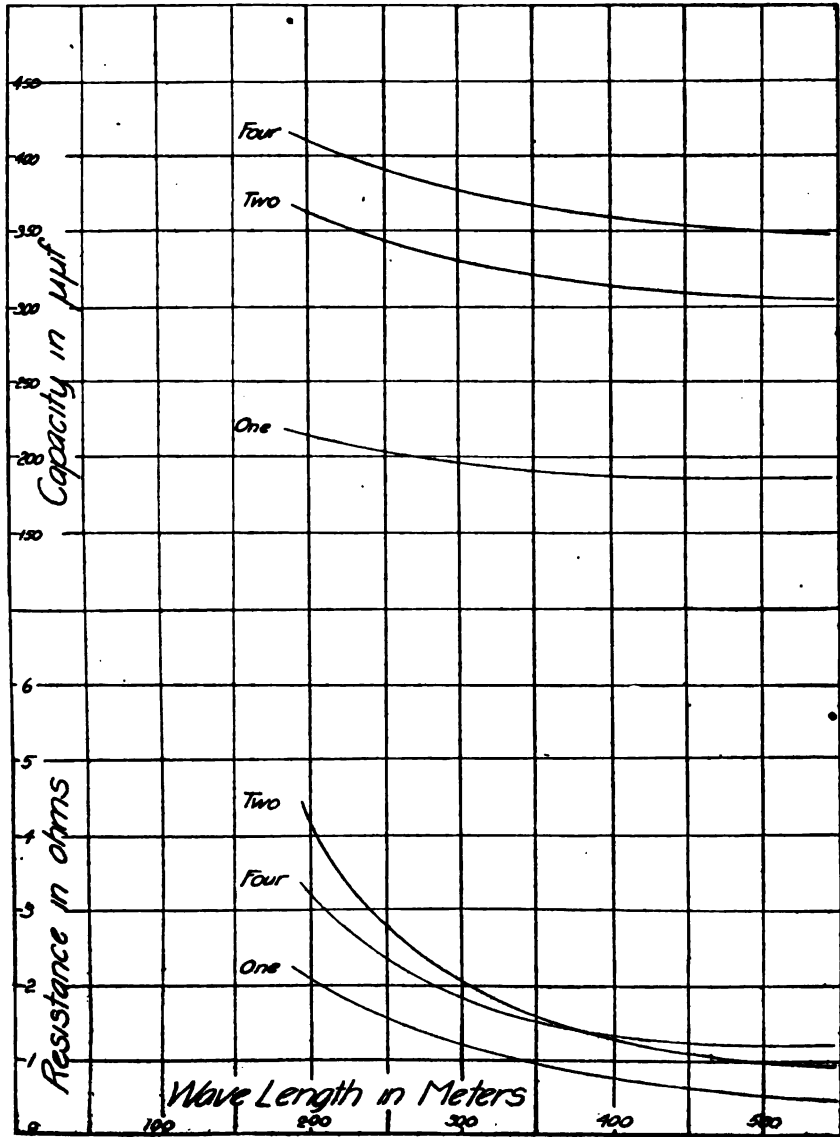


FIG. 9—Comparison of the constants of a 100-foot trailing antenna of one, two, and four wires

other as antenna. The capacity in this case is very greatly reduced, and the radiation resistance is also less. Fig. 8 shows a summary of a four-wire antenna, using machine as ground. This

antenna has a very large capacity, as would be expected. Fig 9 shows a comparison of the characteristics of a 100-foot single, two, and four wire antenna. The resistance could in no case be observed to increase at longer wave lengths due to dielectric losses.

The effect of the same antenna on different planes was also tried. Fig. 10 shows a typical trailing wire antenna on  $A_1$ , a DeHaviland plane,  $A_2$ , a Curtiss training plane,  $A_3$ , a Curtiss plane with a fine network of wires in wings placed there to improve the

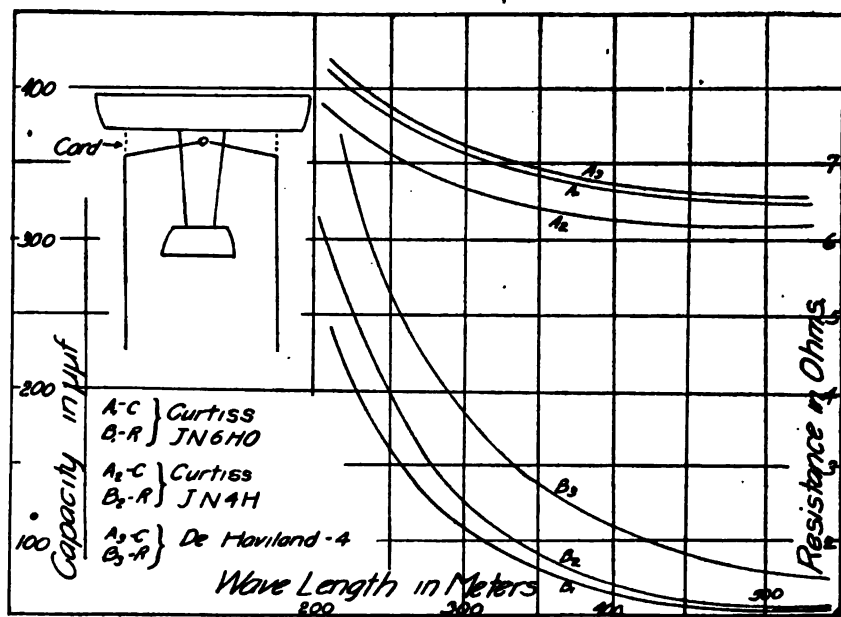


FIG. 10.—A comparison of the constants of the same antenna on different types of airplanes

plane for radio purposes. While the capacity of  $A_1$  was larger than  $A_2$ , its radiation resistance appeared less and results indicated that the unmetallized plane should actually be a better transmitter than  $A_1$ . While the final demonstration of this was interrupted, preliminary results with actual sets in use seemed to indicate it.

The capacity values mentioned herewith are perhaps accurate to within 10 micro-microfarads, as repeat tests did not differ by this amount. The resistance values, however, may be in error by 20 per cent, especially at the longer wave-length values.

### III. DIRECTIONAL EFFECT

In order to determine the directional transmitting effect of the various antennas, a receiving set, as shown in Fig. 11, was connected to a symmetrical vertical wire antenna. The receiving set consisted of a detector tube with grid at positive potential and a three-stage audio-amplifier with tubes having a negative grid potential. In the plate circuit of the last tube was placed the primary circuit of a transformer with secondary connected to the heater of a thermocouple. The output emf of the thermocouple was connected to a sensitive Paul microammeter. Then

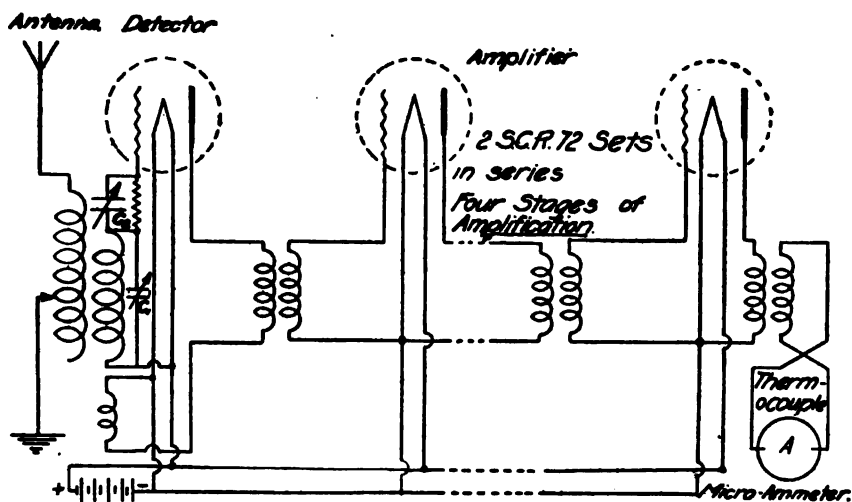


FIG. 11.—Wiring diagram of receiving set

with a modulated undamped transmitter the plane flew over a marked distant point in the different directions of the compass. When directly over the point the operator shut off the transmitter, and at the receiving station the microammeter reading just before dropping to zero was recorded.

As it would be very difficult to compute mathematically the exact relation between microammeter reading and received energy, since it would necessitate knowing just where on its characteristic curve each tube was being worked, the following test was made. The current in the transmitting antenna was set at various known values, as  $I_1$  and  $I_2$ , and the corresponding micro-ammeter readings,  $C_1$  and  $C_2$  taken, wave length and direction remaining the same; the constants should remain almost the

same if the amplitude of the incoming wave did not vary greatly. Thus, assume—

$$I_1 = K C_1^a$$

and,

$$I_2 = K C_2^a$$

then

$$a = \frac{\log I_1 - \log I_2}{\log C_1 - \log C_2}$$

This means then that if the microammeter readings are to be proportional to transmitted currents, they must be raised to the  $a$  power, or, if proportional to energy to the  $2a$  power.

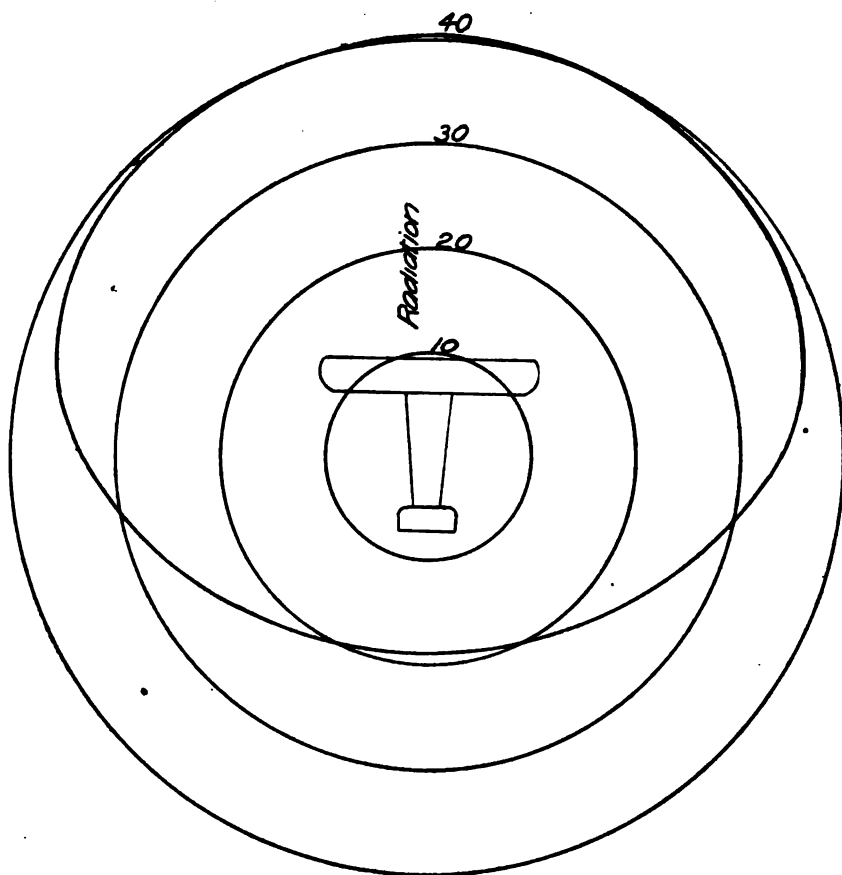


FIG. 12.—Directional effect of a two trailing wire airplane antenna

Making this correction in the data, the trailing wire antenna is found to be quite directional, giving about twice the radiation in the direction of motion that it does in the reverse direction, as

shown by Fig. 12. The fixed antennas are not decidedly directional.

The directional effect is probably a function of the relation between the antenna length and the wave length. A theoretical explanation of this effect is quite difficult. The electrostatic component of the electromagnetic field at a distance  $r$  from a radiator having a length component perpendicular to  $r$  of  $h \sin \alpha$  and a current of  $I_0$  is <sup>4</sup>

$$E_1 = 2 \pi V_2 \frac{h \sin \alpha I_0}{\lambda r} \text{ where } V_2 = 3 \times 10^{10}$$

and the magnetic component at right angles and in the same phase

$$M_1 = 2 \pi \frac{h \sin \alpha I_0}{\lambda r}$$

From these equations currents parallel with the antenna wire should have no effect upon the energy received at points directly in line with the wire, forward or backward. This energy must, then, be due to radiation from perpendicular currents. It may be, however, that the inclination of the antenna with the horizontal line of flight presents a perpendicular radiating component to a point forward, which would be less or entirely lacking to a point in the rear. In general, any explanation of the directive effect of the Marconi bent antenna when used over sea water would apply to the airplane antenna.

This opportunity is taken to express thanks to A. A. Oswald, of the Western Electric Co., for valuable suggestions given, and to those officers and enlisted men of the Signal Corps by whose authority and assistance this work was made possible.

WASHINGTON, February 21, 1919.

---

<sup>4</sup> J. Zenneck, *Wireless Telegraphy*, p. 35; Feb. 21, 1919.





OCT 25 1919

DEPARTMENT OF COMMERCE

---

# SCIENTIFIC PAPERS

OF THE

# BUREAU OF STANDARDS

S. W. STRATTON, DIRECTOR

---

No. 342

## REFLECTING POWER OF STELLITE AND LACQUERED SILVER

BY

W. W. COBLENTZ, Associate Physicist  
and

H. KAHLER, Laboratory Assistant

---

ISSUED SEPTEMBER 11, 1919



PRICE, 5 CENTS

Sold only by the Superintendent of Documents, Government Printing Office  
Washington, D. C.

---

WASHINGTON  
GOVERNMENT PRINTING OFFICE

1919



# REFLECTING POWER OF STELLITE AND LACQUERED SILVER

By W. W. Coblenz and H. Kahler

## I. REFLECTIVITY OF STELLITE

In a previous communication<sup>1</sup> data were published on the reflecting power of stellite which is reported to be an alloy principally of chromium, cobalt, and molybdenum.<sup>2</sup>

The apparatus used was a mirror spectrometer, fluorite prism, and a vacuum thermopile of bismuth silver, as described in previous papers. The source of radiation was a Nernst glower. The reflectivity data were obtained by comparison with silver. In order to determine the absolute reflecting power, the observed data were corrected for absorption by the silver mirror.

TABLE 1.—Reflecting Power of Stellite

Wave length $\mu=0.001$ mm	Reflectivity	
	No. 1	No. 2
$\mu$	Per cent	Per cent
0.45	62.0	64.0
.50	63.6	66.0
.55	64.5	69.5
.60	65.2	71.0
.65	65.8	72.2
.70	66.5	72.5
.80	67.5	73.0
.90	68.3	73.5
1.00	68.9	74.0
1.20	70.1	74.5
1.40	71.2	75.0
1.50	71.9	75.3
1.75	73.3	76.0
2.00	74.7	76.8
2.50	77.1	78.6
3.00	79.2	80.0
3.50	81.0	81.4
4.00	82.5	82.8

The sample examined (No. 1 in Table 1) was plane, quite highly polished, but it was not of uniform homogeneity. The new data presented herewith were obtained on a very homogeneous, highly

<sup>1</sup> This Bulletin, 14, p. 315; 1917.

<sup>2</sup> Obtainable from the Haynes Stellite Co., Kokomo, Ind.

polished plane mirror (sample No. 2, Table 1), about 3 cm. in diameter. Its optical properties differ from those of the preceding sample in that the reflecting power is considerably higher in the blue and yellow part of the spectrum. Beyond  $3\ \mu$  in the infra-red the reflecting power of these two samples is practically the same.

Evidently the reflecting power will be greatly affected by the composition of the alloy and, hence, in exact work where stellite mirrors are used, the reflecting power of new samples should be determined. However, the present data give one some idea of what is to be expected in comparing the reflecting power of this material with that of other metals used for reflecting mirrors.

## II. REFLECTIVITY OF LACQUERED MIRRORS

Theoretically a lacquered silver mirror should reflect almost as much light as does an unlacquered surface. In practice, however, the reflecting power was found to vary greatly with the homogeneity of the lacquered surface.

For making these tests, various water-white silver lacquers such as "Albaline," "Zapon," etc., were diluted, filtered, and poured upon freshly polished silver-on-glass mirrors. The excess material was allowed to drain off and the mirror placed in a level position to dry.

A newly lacquered silver mirror was found to reflect from 70 to 75 per cent of the incident yellow light. In the red end of the spectrum it reflected from 80 to 85 per cent, as against 90 to 95 per cent for unlacquered silver. No doubt by using an especially prepared lacquer, which has been thoroughly filtered to remove the discrete particles of nitrocellulose, a higher reflecting power can be obtained.

In the near infra-red where nitrocellulose is free from absorption bands the reflecting power increased gradually to about 95 per cent, but beyond  $3\ \mu$  the reflectivity curve shows deep indentations owing to selective absorption of the lacquer.

*Effect of Ultra-Violet Light.*—Lacquered silver mirrors can not be used near sources of ultra-violet light owing to photochemical action which occurs in the lacquer. As a result the silver under the lacquer is turned brown in color, following exposure to a carbon arc or a quartz mercury vapor lamp.

For example, after six hours' exposure at a distance of 0.5 meter from a small (15 amp.) carbon arc, it was found that a lacquered silver-on-glass mirror had changed to a brownish color, which

greatly increased the absorption in the violet. This is well illustrated in the last column of Table 2.

From these data it is evident that, in a powerful searchlight, such a lacquered silver mirror would be injured in a few hours. A bare nickel-plated glass mirror would be just as efficient. A gold-plated mirror would be more satisfactory.

TABLE 2.—Reflecting Power of a Lacquered Silver Mirror Before and After Exposure to Ultra-Violet Light

Wave length in $\mu=0.001$ mm	Reflectivity	
	Before exposure	After exposure
$\mu$	Per cent	Per cent
0.55	68.6	62.0
.60	73.5	68.7
.65	77.0	73.8
.70	79.8	77.5
.75	81.9	80.5
1.00	87.8	....
1.25	90.8	....
1.50	93.2	....
2.00	95.0	....

### III. SUMMARY

The object of the present paper is to give data on the reflecting power of the latest production of stellite and also of lacquered silver mirrors. It is shown that the reflectivity of stellite varies somewhat in the visible spectrum depending upon the homogeneity and no doubt upon the exact composition of the alloy.

Data are given on the reflecting power of lacquered silver mirrors, before and after exposure to ultra-violet light. It is shown that owing to photochemical action in the lacquer the silver is turned brown in color, thus reducing its reflecting power.

WASHINGTON, April 4, 1919.



DEC 20 1919



DEPARTMENT OF COMMERCE

# SCIENTIFIC PAPERS OF THE BUREAU OF STANDARDS

S. W. STRATTON, DIRECTOR

No. 343

## LOCATION OF FLAWS IN RIFLE-BARREL STEEL BY MAGNETIC ANALYSIS

BY

R. L. SANFORD, Associate Physicist

and

WM. B. KOUWENHOVEN, Consulting Engineer

*Bureau of Standards*

ISSUED OCTOBER 3, 1919



PRICE, 5 CENTS

Sold only by the Superintendent of Documents, Government Printing Office  
Washington, D. C.

WASHINGTON  
GOVERNMENT PRINTING OFFICE

1919





# LOCATION OF FLAWS IN RIFLE-BARREL STEEL BY MAGNETIC ANALYSIS

By R. L. Sanford and Wm. B. Kouwenhoven

## CONTENTS

	Page
I. Introduction.....	219
II. Theory.....	219
III. Description of apparatus and procedure.....	221
IV. Preliminary study and adjustment.....	223
V. Experimental results.....	225
VI. Summary.....	228

## I. INTRODUCTION

One of the practical applications of magnetic analysis consists of the detection of flaws in bar stock used in the manufacture of steel products. At the request of the Ordnance Department of the Army and the Winchester Repeating Arms Co., an investigation was undertaken during the war with the end in view of applying this method of magnetic analysis to the testing of rifle-barrel steel.

In view of the fact that flaws, generally consisting of pipes or slag inclusions, interfere with the drilling of the barrels or may possibly affect their strength, it was considered that a nondestructive test which would detect and locate such flaws before further work had been done on the barrels would prove to be of great value. Such a method of inspection would make possible not only the rejection of faulty material, but also the acceptance of all the satisfactory bars in a given shipment and thus effect a great saving both of material and labor. It is the object of this paper to describe the apparatus used in the investigation and to present the results thus far obtained.

## II. THEORY

The method employed was that of the determination of the degree of magnetic uniformity along the length of the bars, based upon the theory that if a bar is uniform magnetically along its

length, it is also uniform mechanically. A number of barrel forgings were first tested by a point-by-point method originally used for the examination of bars intended for magnetic standards and which has already been described.<sup>1</sup> Fig. 1 shows a specimen curve obtained by this method, and Fig. 2 is a photograph showing

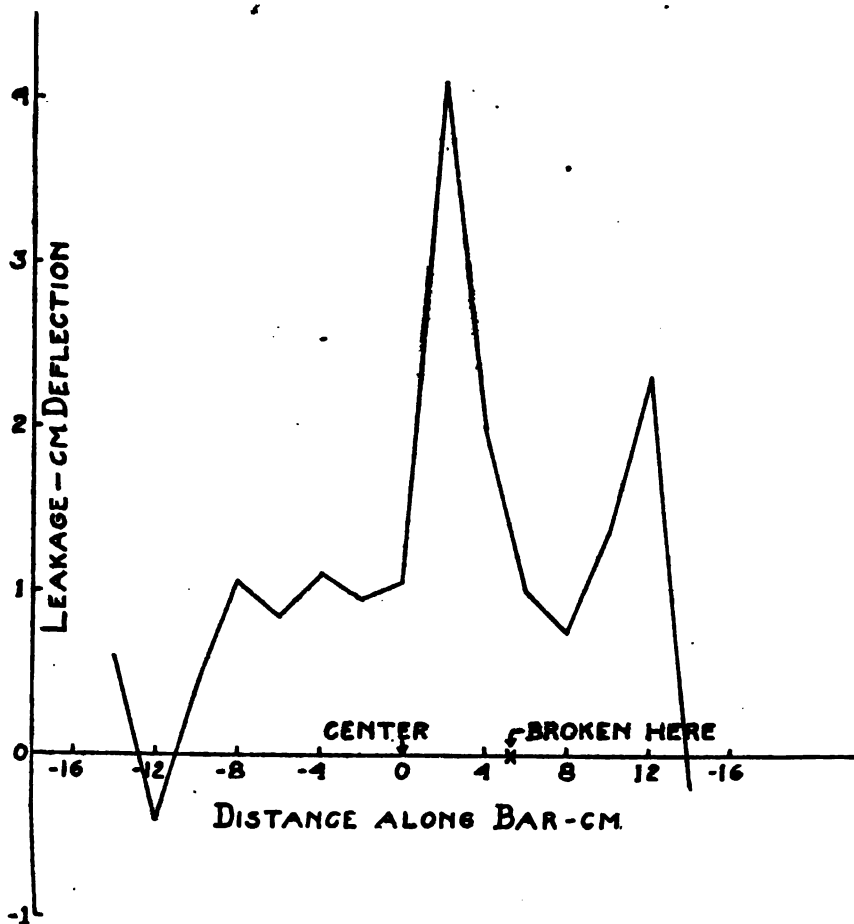


FIG. 1.—Magnetic uniformity curve. Piped sample

the flaw which was indicated by this curve. Since this method is not adapted to the examination of very long bars, and is too time-consuming for a commercial test, it was decided to use a somewhat different method, substantially similar to that used by Burrows<sup>2</sup> for the examination of steel rails. In this method the magnetizing

<sup>1</sup> Sanford, The Determination of the Degree of Uniformity of Bars for Magnetic Standards, Bureau of Standards Scientific Papers No. 295.

<sup>2</sup> Burrows, Correlation of the Magnetic and Mechanical Properties of Steel, Bureau of Standards Scientific Papers No. 272, p. 203.

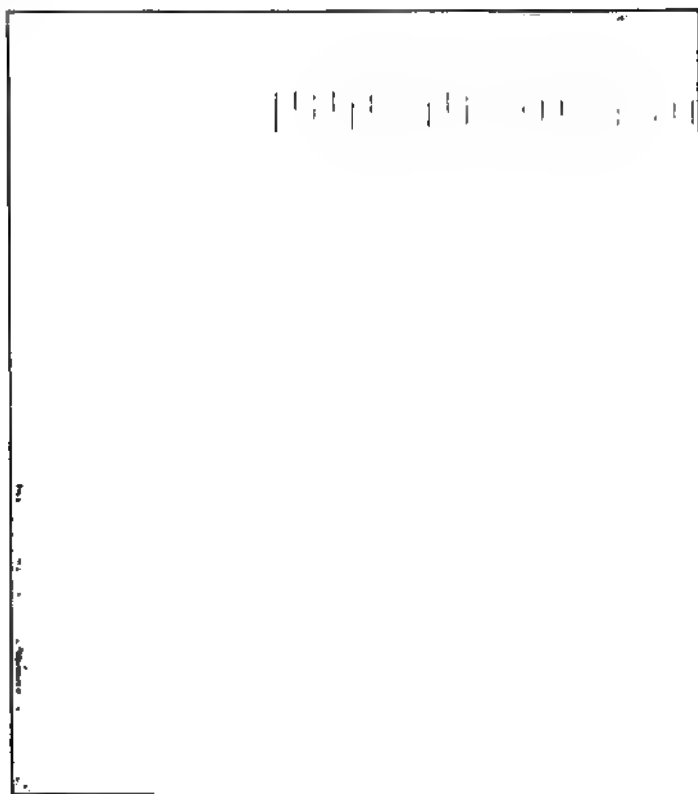


FIG. 2.—*Photograph of the flaw indicated in the curve of Fig. 1*

Scientific Papers of the Bureau of Standards, Vol. 15

FIG. 3.—*Apparatus assembled at the Bureau of Standards*

force is applied by means of a solenoid which surrounds the bar and travels along its length. Mounted within this magnetizing solenoid is a test coil by means of which variations in magnetic flux within the bar can be measured. If the bar is magnetically uniform along its length its permeability is constant for a given magnetizing force and the magnetic flux at each point as the solenoid is moving along is constant. If this is the case, there will be no electromotive force induced in the test coil as the solenoid travels the length of the bar. If, on the other hand, the permeability is not constant, the flux will vary and a corresponding electromotive force will be induced in the test coil which, if the coils are moved at a constant speed along the bar, is proportional to the change in flux. If, instead of using a single test coil in the manner just described, we use two test coils connected in series opposition we obtain a result that is practically not affected by slight variations in the magnetizing current during a run, as any variations in flux linked with one coil is neutralized by corresponding changes in the other.

### III. DESCRIPTION OF APPARATUS AND PROCEDURE

Fig. 3 is a photograph of the apparatus as set up at the Bureau of Standards for preliminary experiments before it was taken to the Winchester plant at New Haven for test under factory conditions. The bar to be examined is clamped at the centers of two triangular end plates of cast iron. These end plates are supported by three wrought-iron pipes which also constitute the return circuit for the magnetic flux induced in the test bar. The magnetizing solenoid, which is shown in more detail in Fig. 4, is supported between the pipes by means of cords running over pulleys and carrying counterweights which hang inside the supporting pipes. One of these cords is continuous and runs over a drum mounted on the shaft of a small electric motor. By means of this arrangement the coils can be run up and down along the length of the bar. Magnetizing current is supplied to the solenoid by means of a storage battery and regulated by means of sliding rheostats. The guiding rollers shown in Fig. 4 were later arranged to bear on the test bar instead of on the iron pipes, as it was found that many of the bars were not straight. The test coils are mounted on a separate tube and their position is adjustable. These test coils have 500 turns each, and are connected through suitable resistances to the galvanometer shown at the right of the

apparatus in the photograph. Deflections of the galvanometer are observed by means of a spot of light reflected from its mirror onto a ground-glass scale. Permanent records of these deflections are made by means of a photographic arrangement which consists of a long light-tight box upon one end of which is mounted an ordinary oscillograph drum which carries the photographic film. This drum is rotated at the proper speed by means of a belt connected to the driving motor of the apparatus. By means of contacts located at 1-foot intervals on the driving cord, a light is flashed inside the box which makes a record on the film for each foot of travel, and thus affords a means for locating the position

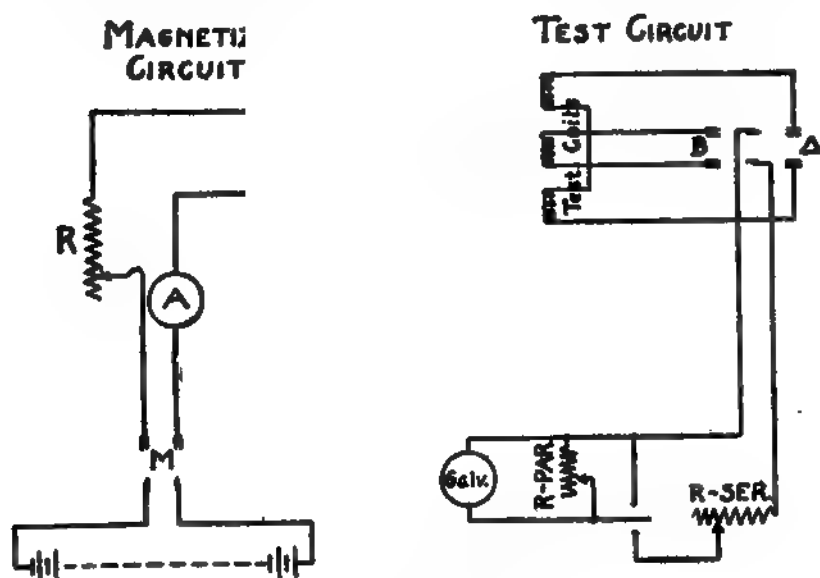


FIG. 5.—Diagram of electrical connections

on the bar of any observed nonuniformity. A diagram of the electrical connections is given in Fig. 5.

When a photographic record indicating the magnetic uniformity of a bar is to be made, the procedure is as follows: The bar is clamped in the apparatus, the galvanometer circuit is then closed, and the drum carrying the photographic film is given one complete revolution. The spot of light reflected from the galvanometer mirror thereby traces a straight line which serves as the reference axis. The spot of light is then closed and the magnetizing current is adjusted to the proper value by means of the regulating rheostat *R*. With the galvanometer connected either to the single test coil or the differential coils as desired, the driving motor is

FIG. 4.—*Magnetizing solenoid and test coils*





then started and the coil is run the length of the specimen with the film holder rotating at a uniform speed. Most of the records have been made by running the coils in one direction with the galvanometer connected to the single test coil, and in the other

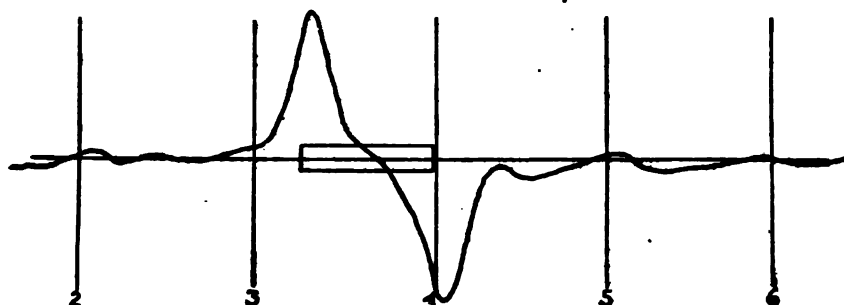


FIG. 6.—Record with single test coil

direction with the galvanometer connected to the differential coils. Fig. 6 shows a record taken by the use of the single coil, and Fig. 7 shows the corresponding record taken with the differential coils. A rectangle is drawn on each of these records to show the position and extent of a strip of transformer iron which was attached to the bar in order to give the effect of a flaw.

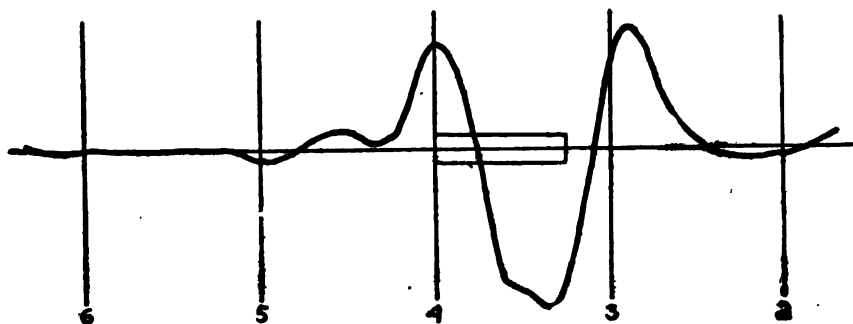


FIG. 7.—Record with differential test coil

#### IV. PRELIMINARY STUDY AND ADJUSTMENT

After the apparatus was completed and set up in the laboratory, it was necessary to consider a number of points in connection with its operation and to decide upon the proper adjustment of the test coils. The points to be considered included the proper flux density,  $B$ , in the specimen, the proper speed for the moving coils, the period of the galvanometer and, as just mentioned, the best location of the test coils. As a result of observations taken under a

great variety of conditions, it was found that a flux density of approximately 15 000 gauss gives the best results. The speed of travel finally adopted was approximately  $\frac{1}{2}$  foot per second. It is necessary in order to insure that the record gives a true indication of the condition of the specimens that the galvanometer have a fairly short period. If the period is too long, the galvanometer does not follow closely the changes in the induced electromotive force. A period of approximately one second was found to be satisfactory. The photograph of the test coils shows only two coils in position. For convenience, however, a third coil was made,

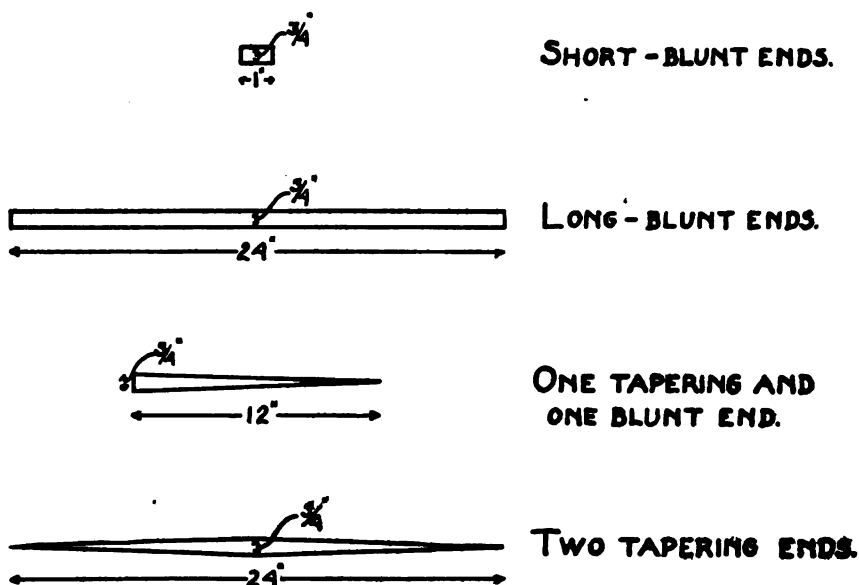


FIG. 8.—Dimensions of added strips

and the differential coils were located 10 cm. apart and equidistant from the single coil which was located at the middle of the magnetizing solenoid. With this symmetrical arrangement, records could be duplicated by running the coils in either direction.

A preliminary exploration to determine the flux distribution along the specimen for different positions of the magnetizing solenoid was made by a point-by-point method, using the single test coil connected to a ballistic galvanometer. Readings were taken upon reversal of the magnetizing current. The result of this exploration showed that, for a given magnetizing current, the flux is constant at different points along a uniform bar except for the regions very near the ends.

In order to study the effect of flaws varying in extent and kind, a number of records were made on a bar previously found to be uniform, to which were attached strips of transformer steel of various shapes and sizes. This procedure was necessary, because of the difficulty of producing longitudinal flaws by artificial means. Fig. 8 shows the shapes and dimensions of the strips thus used. Figs. 9 to 12, inclusive, are records obtained in this way. The location and shape of the added strip is indicated in each case upon the record. The figures show records taken both by means of the single test coil and by means of the differential coils. Figs. 13 and 14 show the effect of various treatments on a bar originally uniform. The treatments given, and the locations, are indicated in the figures. It was at first feared that, due to the sensitiveness of the method, spurious indications would be obtained for bars which had been slightly bent during shipment and handling at the factory. The result of this last test, however, indicates that such is not the case.

After the preliminary experiments just described, the apparatus was shipped to the plant of the Winchester Repeating Arms Co., at New Haven, and there set up for final trial.

## V. EXPERIMENTAL RESULTS

The greatest difficulty in this line of investigation lies in the interpretation of the results. This is due to the fact that there are many causes which may produce magnetic inhomogeneity and it is difficult to differentiate between them. The work at New Haven was done with the end in view of obtaining data which would establish the amount of variation and the type of curve which accompanies a pipe. The procedure was to make records of bars which in a preliminary test showed large variations. These bars were chosen from lots of steel which had previously been rejected as the result of tests in the drilling shop. It is an interesting fact that even though this lot of steel had previously been rejected on account of pipes, not a single pipe was discovered in the drilling tests on samples for which records of the magnetic uniformity had been obtained. This is true of all the steel examined up to March 31, 1919.

Figs. 15 and 16 show records of the degree of magnetic homogeneity of four bars of steel. These records were made with the differential test coils and with a fairly low sensitivity of the galvanometer. The portions of these bars from which barrel

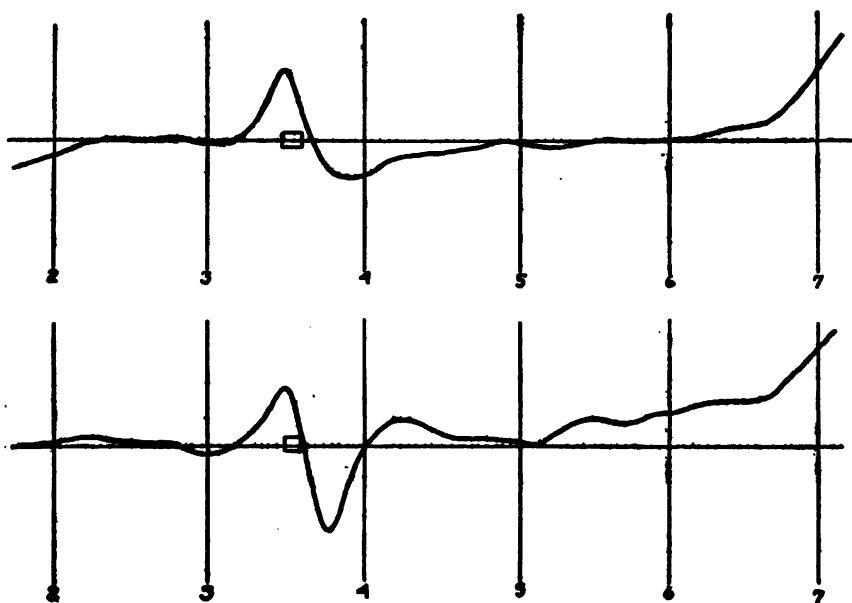


FIG. 9

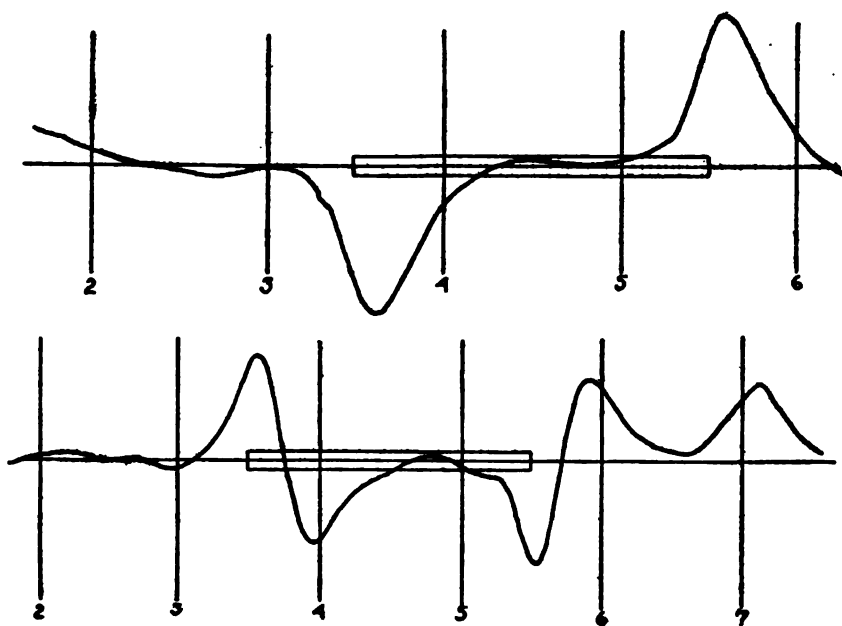


FIG. 10

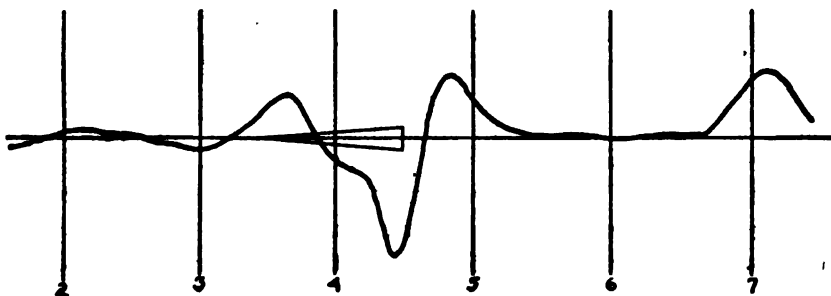
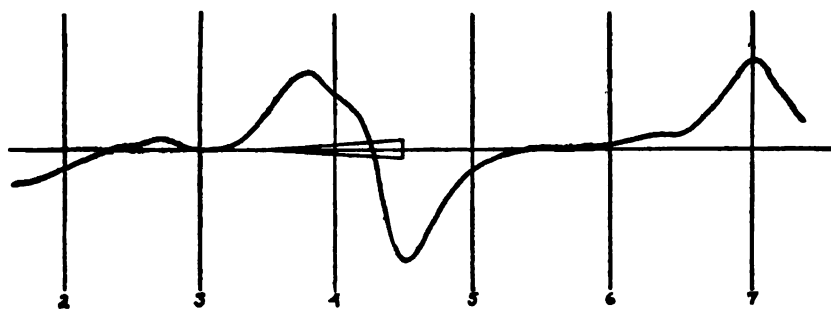


FIG. 11

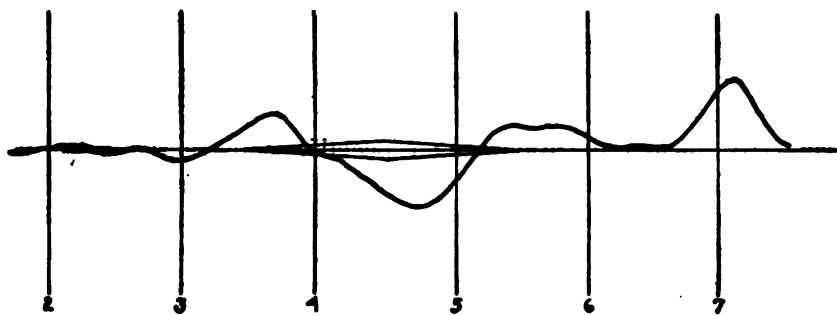
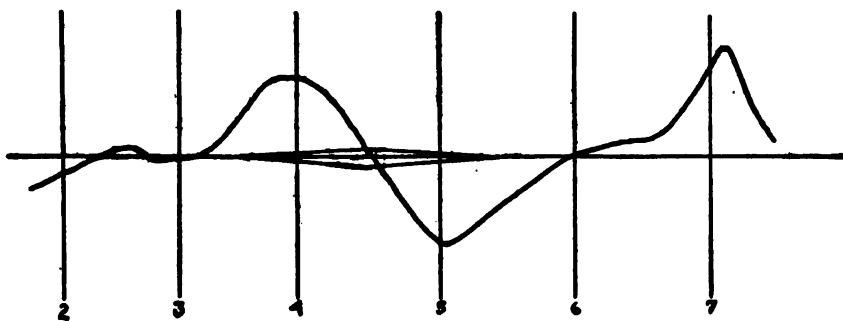


FIG. 12

lengths were cut are indicated in the figure. Barrels A, B, C, and D, cut from bars 1 and 9 and those cut from the entire length of bars 2 and 4 were sent to the shop for drilling tests. Barrels B and D gave trouble in drilling and each destroyed the edge of

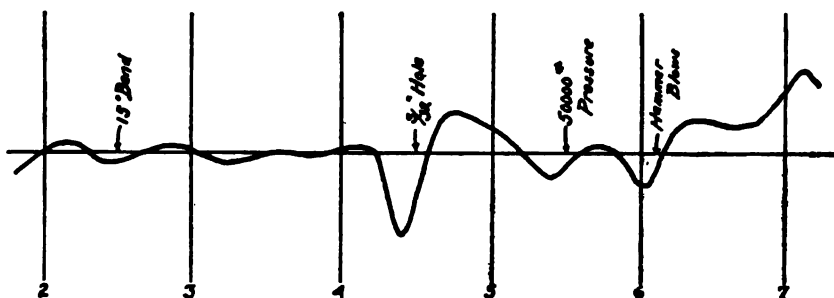


FIG. 13

a drill, thus necessitating the use of a new drill to finish the bore. None of the other barrels gave trouble and the inside surfaces of all were smooth and bright. In view of the fact that additional data are necessary in order to draw satisfactory conclusions, the Winchester Repeating Arms Co. is continuing the investigation.

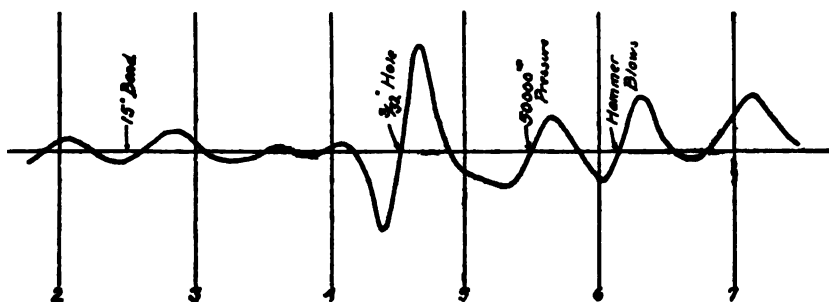


FIG. 14

## VI. SUMMARY

This paper describes an investigation which was undertaken for the purpose of determining whether an application of magnetic analysis was practicable for the detection of flaws in rifle-barrel steel. By means of apparatus especially constructed for the purpose a large number of bars were explored for magnetic uniformity along their length. In spite of the fact that these bars were taken from material which had previously been rejected as the result of drilling tests, not one was found which contained a pipe. The results obtained, however, demonstrated that the

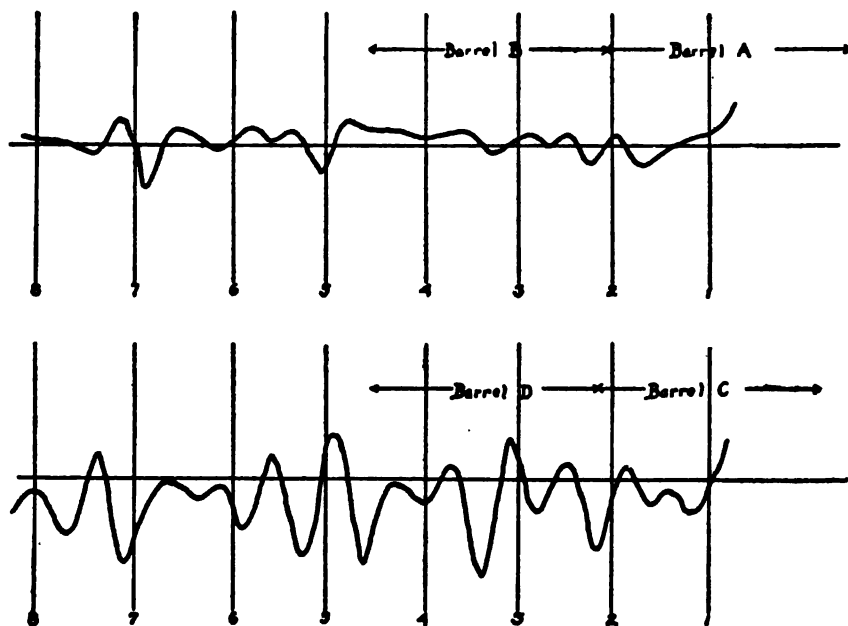


FIG. 15

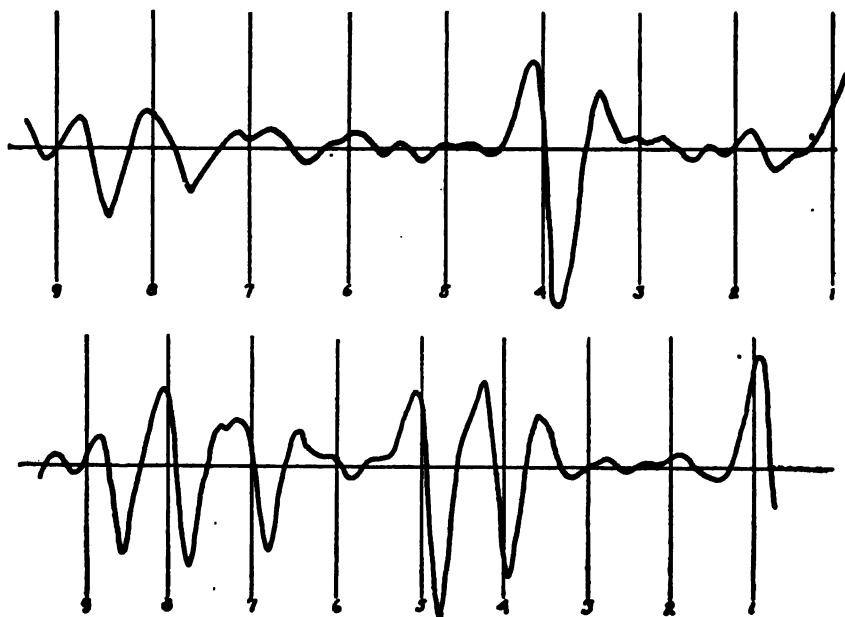


FIG. 16

method is amply sensitive to detect and locate flaws. Further study is necessary to determine to what degree the sensitivity of the apparatus should be reduced in order not to cause the rejection of material which is satisfactory for all practical purposes, and also to determine the type and magnitude of the effect which will be produced by a pipe. For this reason the work is being continued by the Winchester Repeating Arms Co., who cooperated in the investigation and at whose plant the apparatus has been installed.

The authors wish to take this opportunity to acknowledge their indebtedness to J. S. Gravely, M. F. Fischer, and J. S. Becker for their valuable assistance in carrying out this investigation.

WASHINGTON, April 14, 1919.







DEPARTMENT OF COMMERCE

---

# SCIENTIFIC PAPERS

OF THE

# BUREAU OF STANDARDS

S. W. STRATTON, DIRECTOR

---

No. 344

## SPECTRAL PHOTOELECTRIC SENSITIVITY OF SILVER SULPHIDE AND SEVERAL OTHER SUBSTANCES

BY

W. W. COBLENTZ, Associate Physicist

H. KAHLER, Laboratory Assistant

*Bureau of Standards*

---

ISSUED SEPTEMBER 19, 1919



PRICE, 5 CENTS

Sold only by the Superintendent of Documents, Government Printing Office  
Washington, D. C.

---

WASHINGTON  
GOVERNMENT PRINTING OFFICE  
1919



# SPECTRAL PHOTOELECTRIC SENSITIVITY OF SILVER SULPHIDE AND SEVERAL OTHER SUBSTANCES

By W. W. Coblenz and H. Kahler

## CONTENTS

	Page
I. Introductory statement.....	231
II. Apparatus and methods.....	232
III. Photoelectrical sensitivity of silver sulphide.....	234
1. Electrical polarization tests.....	234
2. Transmission measurements.....	235
3. Variation of photoelectric current with time of exposure.....	236
4. Effect of intensity of radiation upon electrical conductivity.....	237
5. Photoelectrical sensitivity of different parts of a crystal.....	238
6. Effect of temperature upon photoelectrical sensitivity.....	241
7. Effect of mechanical working upon spectral photoelectric sensitivity.....	243
IV. Photoelectrical sensitivity of bismuthinite.....	245
V. Photoelectrical sensitivity tests of various substances.....	246
1. Galena.....	247
2. Cyndrite.....	247
3. Pyrites.....	247
4. Jamesonite.....	248
VI. Summary.....	248

## I. INTRODUCTORY STATEMENT

The preceding paper<sup>1</sup> on this subject dealt with the spectral photoelectric sensitivity of molybdenite, under various conditions of operation, such as change in intensity of irradiation, change in temperature, etc. The present paper gives data of a similar investigation of various minerals, some of which had previously been tested<sup>2</sup> for photoelectrical sensitivity using heterogeneous thermal radiations. Further investigations should include a more detailed examination of some of the phenomena described in these foregoing papers.

As is well known, some substances exhibit luminescence only at low temperatures. It was, therefore, of interest to determine whether, similarly, some substances (for example, electrically conducting sulphides) might exhibit the phenomenon of photo-

<sup>1</sup> This Bulletin, 15, p. 120: 1919.

<sup>2</sup> This Bulletin, 14, p. 591: 1918.

electrical sensitivity at low temperatures. In the preceding investigation of molybdenite, samples, which were quite insensitive photoelectrically at room temperatures, became fairly sensitive when cooled to low temperatures.

## II. APPARATUS AND METHODS

The spectroradiometric apparatus was essentially the same as that used in a similar investigation of the photoelectrical sensitivity of molybdenite to which reference should be made for a description of the general experimental procedure.<sup>3</sup> Several minor changes in experimentation had to be introduced in view

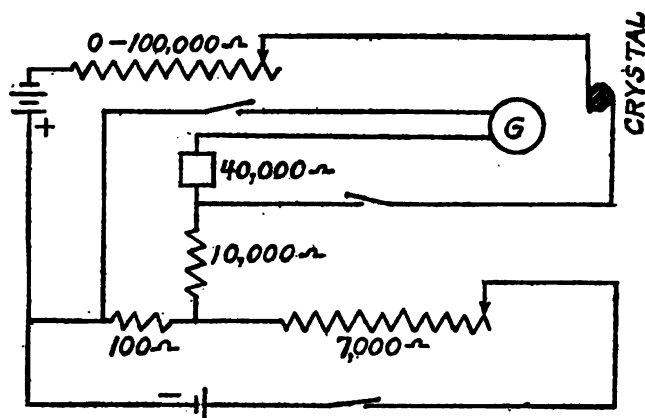


FIG. 1.—Arrangement of electrical connections

of the low electrical resistance and the low photoelectrical sensitivity of the material examined.

In order to balance the large dark current which obtained in these minerals, at room temperature, current from an auxiliary battery was passed in the opposite direction through the galvanometer, *G*, as shown in Fig. 1. The preliminary electrical adjustments were made by using a d'Arsonval galvanometer, which was then replaced by an ironclad Thomson galvanometer.<sup>4</sup> This was necessary in order to be able to measure the small photoelectric currents induced in most of the crystals. This appears to be the first time that a sensitive Thomson galvanometer has been used in this type of photoelectric work. Usually the photoelectric currents were sufficiently large so that a resistance of 10 000 to 20 000 ohms was kept in series with the galvanometer.

<sup>3</sup> This Bulletin, 15, p. 120, Fig. 2: 1919.

<sup>4</sup> This Bulletin, 15, p. 423: 1916.

At low temperatures the dark current through the sample under examination was usually so low that it was unnecessary to balance its effect by means of the auxiliary battery.

The material examined was (1) the natural crystalline mineral, Acanthite, and (2) a laboratory preparation, made by G. W. Vinal<sup>6</sup>, and hammered into a thin (0.05 mm) homogeneous flexible strip. This is sample No. IV in the present investigation. The crystalline material, Acanthite,  $\text{Ag}_2\text{S}$  was obtained from the United States National Museum. Samples Nos. I and II came from Freiberg, Saxony. Samples Nos. III and V (U. S. Nat. Mus. No. 85162) came from Zastecas, Mexico. Their dimensions ranged from 12 to 18 mm in length and from 2 to 4 mm in width. Their ends were filed flat and clamped securely between copper washers by means of small brass screws. This provided excellent electrodes. This combination was then mounted securely upon a fiber block and the crystal was covered with cardboard with a slit cut into it to admit radiation upon a certain part of the sample under examination.

In the first tests the copper lead wires were attached by heating the wires to their melting point, and then touching them to the acanthite crystal. "This made a good juncture, which, however, deteriorated very rapidly after passing electric current for a short time. This did not have any effect upon the spectral photoelectric sensitivity curve, as found by actual observation; but the method had to be abandoned because of the gradual increase in resistance as a result of electrolytic action at the juncture. In one case this difficulty did not manifest itself until the following day, although the crystal had not been attached to the battery for more than a half hour on the preceding day.

The preliminary observations were always extended to about  $3\mu$ . However, none of the substances examined were photoelectrically sensitive beyond  $2\mu$ . Because of the low intrinsic photoelectrical sensitivity of silver sulphide, the intensity of the radiation stimulus used throughout this investigation was nine times that used in the investigation of molybdenite. At this intensity the equal energy spectrum—that is, the photoelectrical observations—began at  $0.75\mu$  (see Fig. 6,  $E=9$ ). But tests made with the intensity  $E=1$ , which was used on molybdenite, showed that the spectral photoelectric sensitivity of silver sulphide is much less in the yellow than in the red, and in succeeding parts of the spectrum.

<sup>6</sup> Vinal, this Bulletin, 14, p. 331: 1917.

### III. PHOTOELECTRICAL SENSITIVITY OF SILVER SULPHIDE

In the beginning of this investigation it was observed that silver sulphide had unusual properties not possessed by the substances previously examined. It was observed that the maximum galvanometer deflection was attained in a few seconds, after which the photoelectrical activity decreased to perhaps only one-fourth its original effect. There seemed to be a large "fatigue,"\* though previous writers have not described the phenomenon very clearly, if at all.

Aside from this "fatigue," considerable difficulty was experienced in making observations at room temperature. After a

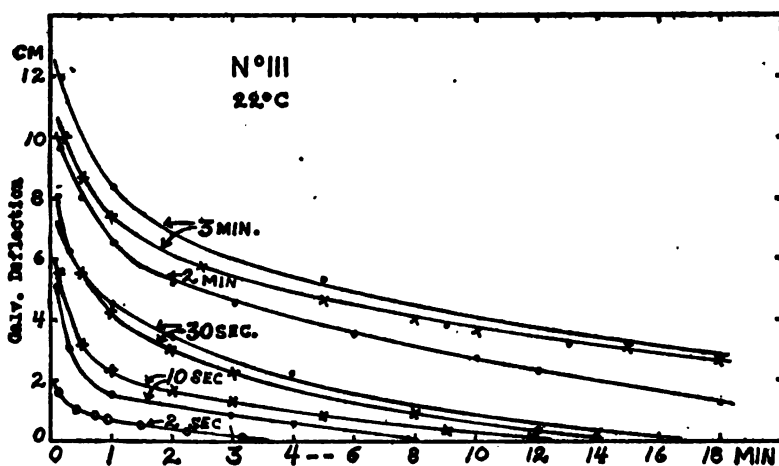


FIG. 2.—Decrease in polarization current with time

short time the galvanometer would become very unsteady, though on reversing the current through the crystal this unsteadiness would sometimes be eliminated for a short time. Evidently electrolytic action was present and one of the first tests made was on the electrolytic action induced in the crystal.

In order to reduce this unsteadiness it was, therefore, necessary to pass current through the crystal only when making observations. In order to diminish the effect of fatigue the maximum throw of the galvanometer, which was attained in about three seconds, was observed.

#### 1. ELECTRICAL POLARIZATION TESTS

The electrolytic polarization voltage developed in the crystal was tested very simply by means of the Thomson galvanometer having a single swing of about 2.5 seconds. By means of a double-

\* Case, *Phys. Rev. (a)*, 9, p. 305, 1917, mentions a large fatigue.



throw switch, the crystal was connected for a short time (two seconds to three minutes) with a 2-volt storage battery, then quickly joined to the galvanometer. This would produce a large deflection, which would gradually return to the zero reading. As shown in Fig. 2, passing current through the crystal for two seconds, and then connecting to the galvanometer, would produce a deflection of 2 cm, while passing the current for three minutes would produce a deflection of about 12 cm. In other words, as shown in Fig. 3 (which gives the maximum deflection, from Fig. 2) the polarization voltage increases very rapidly during the first few seconds, then gradually assumes a constant value.

Observations were made of the polarization produced when the crystal was kept in the dark (Fig. 2, dots, • • •) and when it

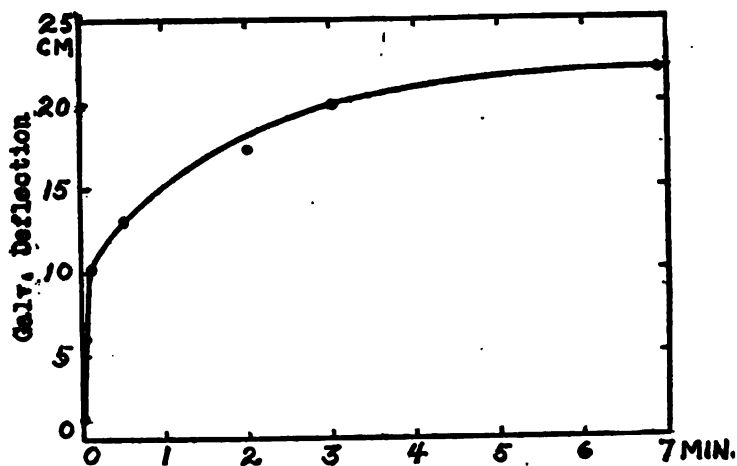


FIG. 3.—Rise of polarization voltage with time

was illuminated (Fig. 2, crosses,  $\times \times \times$ ). The results show that with this rather crude method of observation no marked difference was observed in the polarization current.

## 2. TRANSMISSION MEASUREMENTS

In view of the interest in the question whether there is any connection between absorption and photoelectrical sensitivity, transmission measurements were made on a thin sample of silver sulphide prepared by Mr. Vinal. The sample examined was a thin flexible plate about 15 by 8 by 0.05 mm. Several examinations were made, the final test being made with the plate of silver sulphide placed directly over the spectrometer slit. The examination extended from  $0.6\mu$  to  $4\mu$ . Throughout this region of the spectrum the sample appeared to be entirely opaque.

### 3. VARIATION OF PHOTOELECTRIC CURRENT WITH TIME OF EXPOSURE

In the paper on molybdenite it was shown that for wave lengths greater than  $0.75\mu$  the time of exposure for equilibrium varies from 30 seconds to several minutes and that the time for recovery is twice the exposure time.

At room temperature silver sulphide behaves in an entirely different manner. As shown in curve A, Fig. 4, on exposing the crystal to radiation, the maximum galvanometer deflection is attained in 3 to 5 seconds after which the photoelectric current gradually decreases, so that after 15 minutes' exposure the deflection is perhaps only one-seventh its maximum value. If the light stimulus is then removed, the galvanometer gives a deflec-

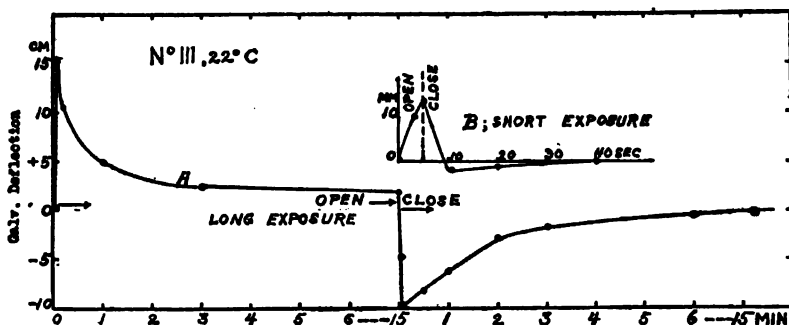


FIG. 4.—Variation of photoelectric current with time of exposure at room temperature

tion in the opposite direction and finally returns to zero. It was, therefore, not possible to subject the crystal to unlimited exposure (at room temperature) as was done with molybdenite. The system of observation adopted for all the herein recorded measurements, at room temperature, was to expose the crystal for about 5 seconds, read the maximum throw, and then close the shutter. The galvanometer deflection then returned to its zero position, as shown in curve B of Fig. 4. It is therefore quite probable that, if unlimited exposure could have been used, the sensitivity maxima would occur at slightly longer wave lengths than here recorded. At low temperatures this electrolytic action disappears, and the time-response curves, as shown in Fig. 5, are somewhat similar to those observed on molybdenite with this difference, that the time for recovery is the same as the time of response.

#### 4. EFFECT OF INTENSITY OF RADIATION UPON ELECTRICAL CONDUCTIVITY

The effect produced upon the spectral photoelectric sensitivity of silver sulphide (Acanthite, sample No. I) on varying the intensity of the exciting radiation is shown in Fig. 6. Increasing the intensity nine times has a marked effect in increasing the

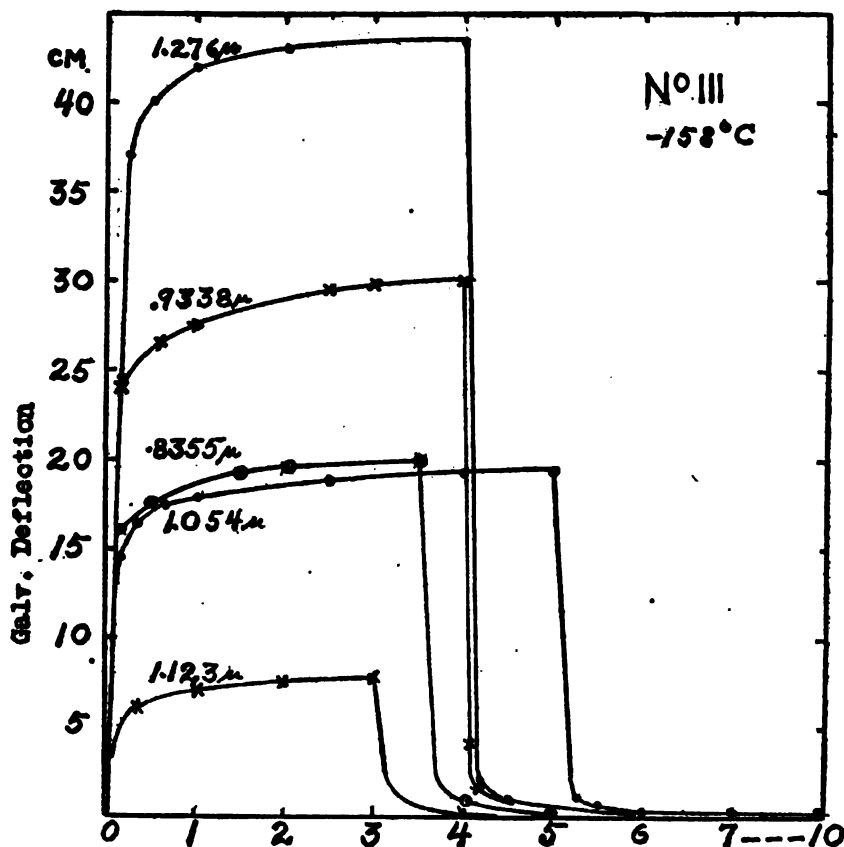


FIG. 5.—Variation of photoelectric current in silver sulphide with time of exposure, at low temperatures

photoelectrical sensitivity in the long wave lengths, as previously observed in molybdenite.

In Fig. 7, a series of isochromatic curves are given, showing the effect of intensity as well as temperature upon the photoelectric response. At  $-158^{\circ}\text{C}$ . the effect of electrolytic action is absent and it was possible to expose the sample to radiation until photoelectric equilibrium was attained. The response curves for wave lengths  $\lambda = 1.054\ \mu$  and  $1.357\ \mu$  are entirely different from those

obtained at room temperature. But they verify the observations at room temperature showing that with increasing intensity the photoelectrical sensitivity shifts toward the long wave lengths. For example, the ratio of galvanometer deflections at  $\lambda = 1.054 \mu$ , for  $E = 5$  and  $E = 20$  (square root of the ratio of these intensities = 2) is 3 while for  $\lambda = 1.357 \mu$  this ratio is 6. Furthermore, the

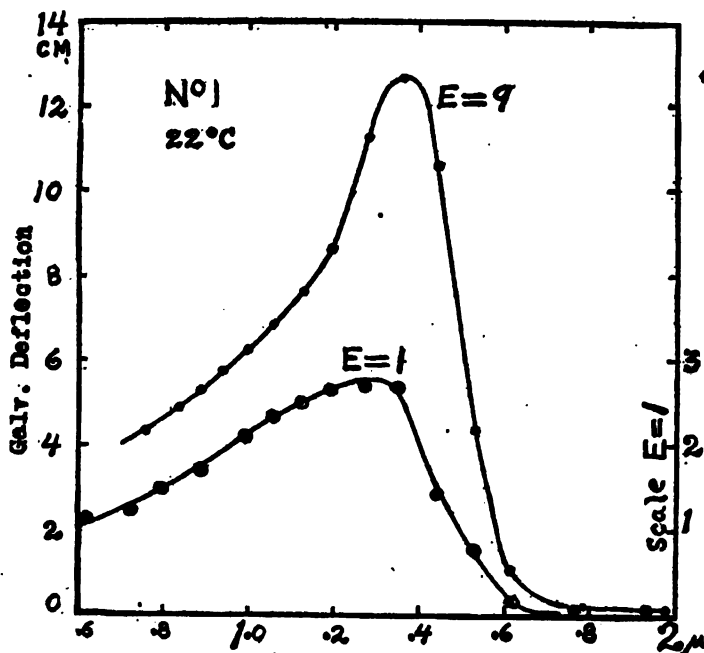


FIG. 6.—Effect of intensity of energy stimulus upon the spectral photoelectric sensitivity of acanthite

much discussed "square root law" does not hold, as was observed in molybdenite.

##### 5. PHOTOELECTRICAL SENSITIVITY OF DIFFERENT PARTS OF A CRYSTAL

In the preceding paper it was shown that different parts of a sample of molybdenite exhibit markedly different photoelectrical sensitivity curves, and attention was called to the possibility of this phenomenon being ascribable to the presence of different kinds of sulphides of molybdenum.

The spectral photoelectric sensitivity curve of acanthite ( $\text{Ag}_2\text{S}$ ) at room temperature is not unlike that of selenium except that its maximum occurs much farther in the infra-red; at  $\lambda = 1.35 \mu$ . There is a region of high sensitivity at  $0.6 \mu$  to  $1 \mu$  (see Fig. 6)

similar to the high sensitivity of selenium, in the visible spectrum. The sensitivity in this region, relative to that at the maximum, varies somewhat for different parts of the crystal, but it is not very conspicuous in comparison with the observations on molybdenite.

In Fig. 8 curve *A* gives the photoelectrical sensitivity of the front (smooth) side of sample No. I, while curve *B* illustrates the

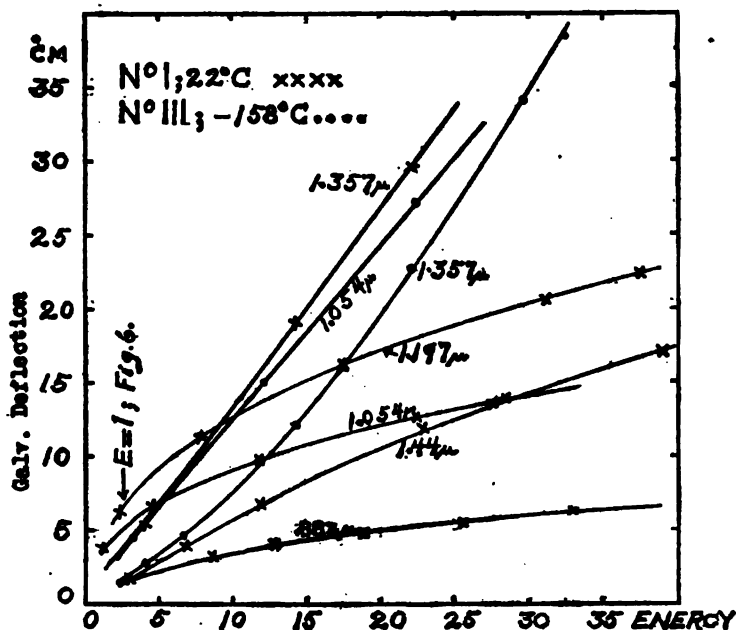


FIG. 7.—Effect of intensity of energy stimulus upon the spectral photoelectric response of acanthite

sensitivity of the opposite side of this crystal which side was rough and uneven. Similarly, curves *A* and *B*, Fig. 9, illustrate the spectral photoelectric sensitivity respectively of the front and rear side of sample No. II. In Fig. 10 curve *A* illustrates the photoelectrical sensitivity of the smooth (front) side, and curve *B* the rear (rough) side of sample No. III, which came from Zastecas, Mexico. Curve *A* in Fig. 13 illustrates the sensitivity of a similar sample, No. V. With the exception of the latter, all these spectral photoelectrical sensitivity curves are very similar, considering the fact that in all cases the observations are somewhat affected by the electrolytic action. The observations at low temperatures confirm these data, showing a marked similarity in the spectral photoelectric sensitivity curves of the natural (unworked) crystal of acanthite.

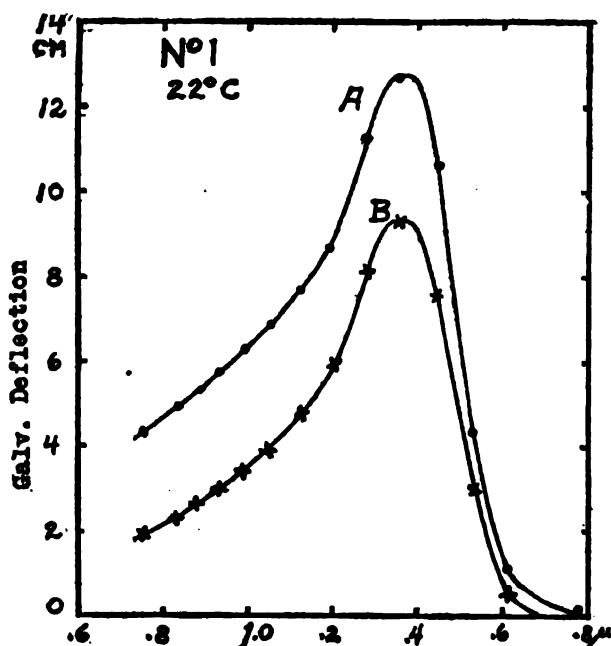


FIG. 8.—Spectral photoelectric sensitivity of different parts of a crystal of acanthite

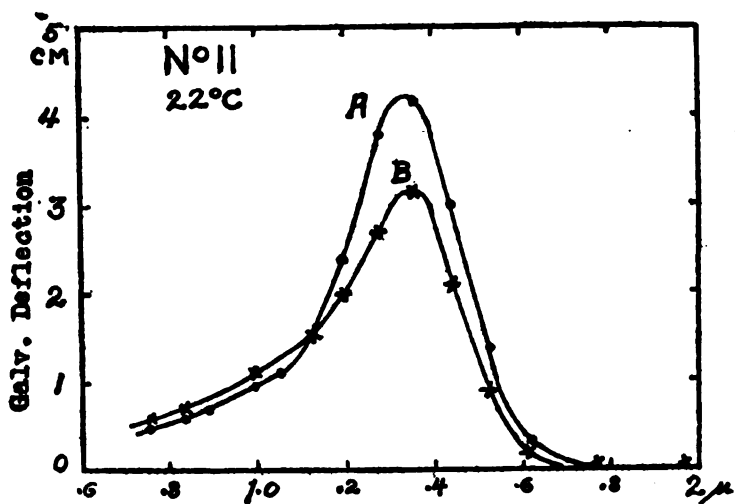


FIG. 9.—Photoelectrical sensitivity of different parts of a crystal of acanthite

## 6. EFFECT OF TEMPERATURE UPON PHOTOELECTRICAL SENSITIVITY

As already mentioned, disturbances from electrolytic action ceases at low temperatures, and it is possible to obtain spectral photoelectric sensitivity curves for unlimited time exposures.

The effect of lowering the temperature to  $-158^{\circ}\text{C}$  is to produce a sharp symmetrical band of spectral photoelectric sensitivity with a single maximum at  $1.2\mu$ . This is illustrated in Figs. 11, 12, and 13, for samples Nos. II, III, and V. The intrinsic sensitivity is greatly increased at low temperatures, but no attempt was made to obtain a comparison of the sensitivity at these two temperatures as was done with molybdenite.

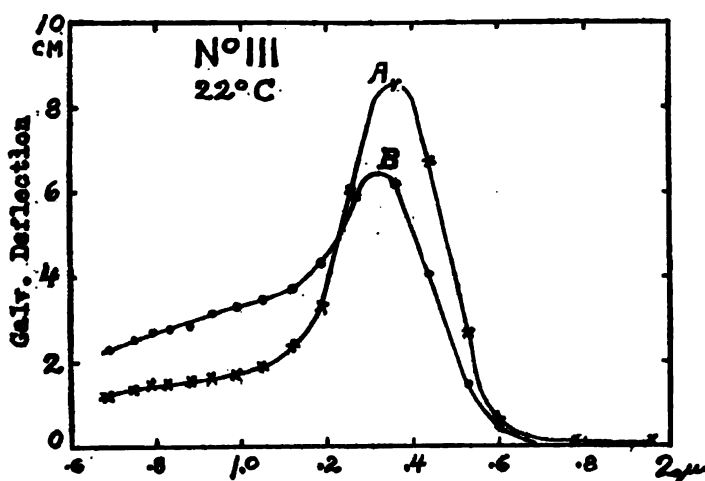


FIG. 10.—Photoelectrical sensitivity of different parts of a crystal of silver sulphide (acanthite)

In Fig. 11 the deflections for  $-158^{\circ}\text{C}$  were four times the scale indicated. In Figs. 12 and 13 the observations at room temperatures were one-tenth the scale indicated.

It is of interest to record that the temperature coefficient of resistance of silver sulphide is high, so that at  $-158^{\circ}\text{C}$  the hammered material is practically an insulator, and it is possible to connect a sensitive ( $i = 3 \times 10^{-10}$  ampere) Thomson galvanometer directly through a crystal and a battery of several volts. For example, sample No. IV (Fig. 16), which had a resistance of 3 ohms at  $22^{\circ}\text{C}$ , was joined directly through the galvanometer and 2 volts, causing a deflection of only 15 mm. The resistance was increased about 100 000 000 times that at room temperature. Similarly, sample No. I, after rehammering, was joined through

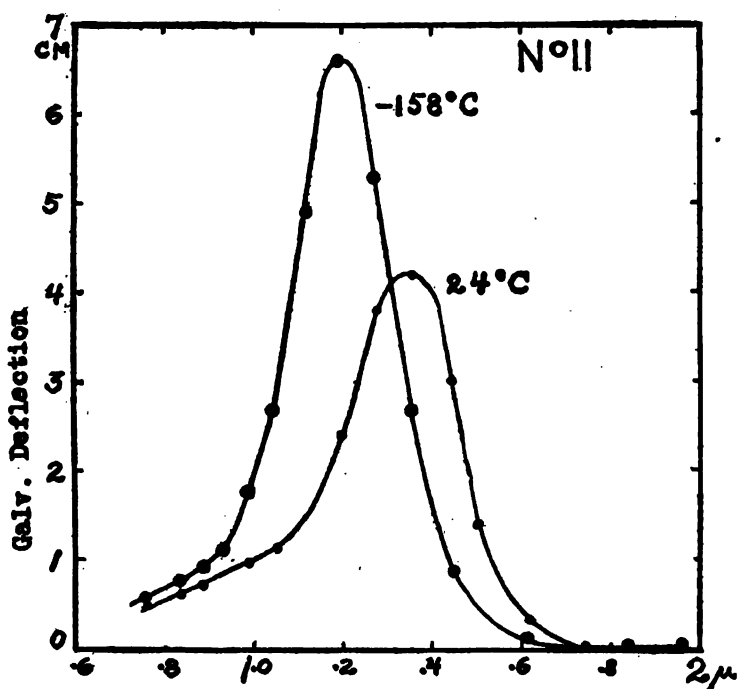


FIG. 11.—Effect of temperature upon the photoelectrical sensitivity of acanthite

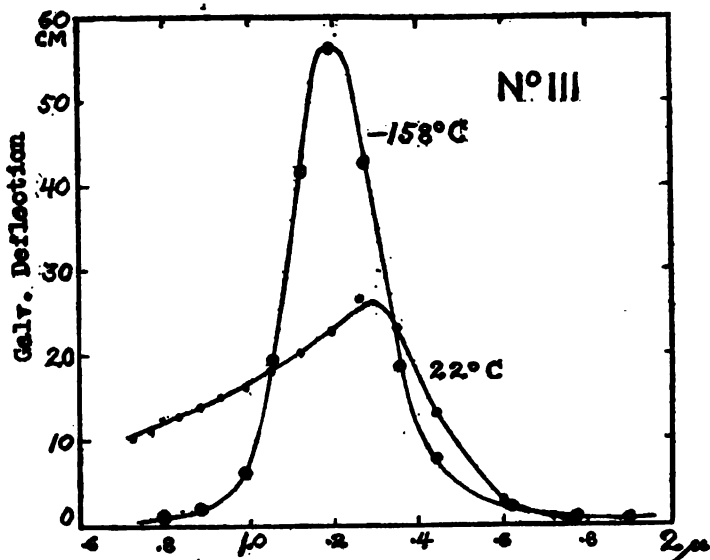


FIG. 12.—Effect of temperature upon the spectral photoelectric sensitivity of acanthite



19.6 volts to the galvanometer, causing a (dark current) deflection of only 17 mm. In other words, its resistance was several hundred meg-ohms. That this is not a result of poor contact at the electrodes was shown by increase in resistance with hammering; that is, decrease in thickness of the material.

#### 7. EFFECT OF MECHANICAL WORKING UPON SPECTRAL PHOTOELECTRIC SENSITIVITY

In previous communications<sup>7</sup> attention was called to observations on a change in spectral photoelectric sensitivity as a result of hammering and otherwise mechanically working the crystal. The hammered material is less sensitive photoelectrically

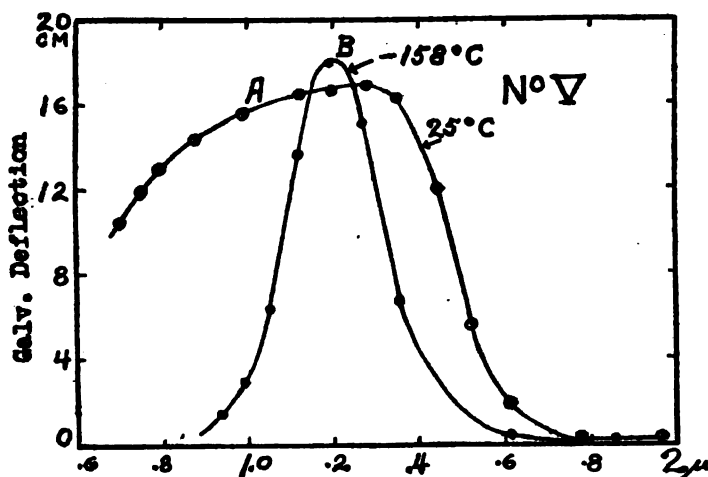


FIG. 13.—Effect of temperature upon the photoelectric sensitivity of acanthite

cally than the crystalline material. For this reason, as well as difficulties in observing at room temperature, the photoelectrical measurements were made at low temperatures,  $-158^{\circ}\text{C}$ . Through an oversight the sensitivity of sample No. I was not determined before hammering. However, judging from the similarity in behavior of all the other samples (see Figs. 11, 12, and 13), it is not unreasonable to suppose that the maximum of the unhammered sample occurs at  $1.2\mu$ . After subjecting this crystal to hammering, the spectral photoelectric sensitivity curve appears complex with maxima at  $0.95\mu$  and  $1.12\mu$ , as illustrated in curve A, Fig. 14. On further hammering the crystal it was reduced to a thin, pliable, noncrystalline lamina (about 0.2 mm in thickness) having a highly metallic luster. As shown

<sup>7</sup> This Bulletin, 15, p. 120; 1919. Physical Review (2), 18, p. 163; 1919.

in curve *B*, Fig. 14, the sensitivity curve is quite symmetrical with a maximum at  $1.23\mu$ , which is somewhat greater than the maximum  $1.20\mu$ , observed in the crystalline state (see Figs. 11, 12, and 13.)

In curve *A*, Fig. 15, is illustrated the sensitivity curve of sample No. III, which before hammering has a maximum at  $1.19\mu$ . After hammering, curve *B*, the maximum sensitivity appears slightly shifted, to about  $1.2\mu$ . This sample was very

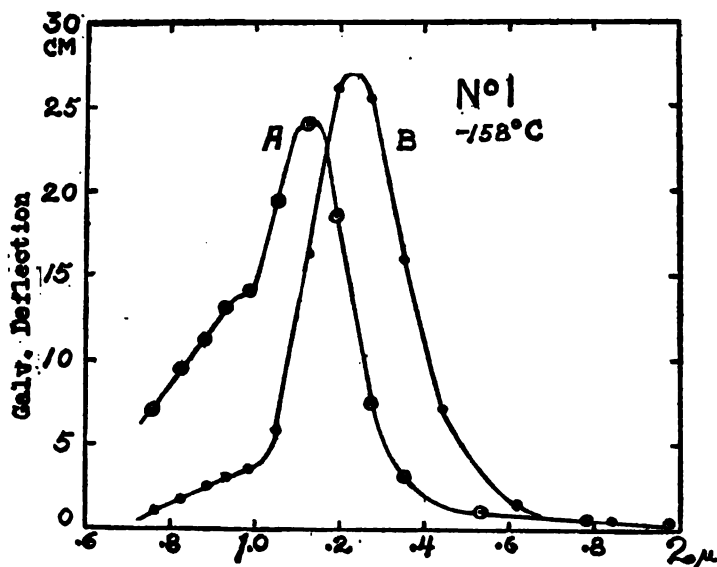


FIG. 14.—Effect of mechanical working upon the photoelectrical sensitivity of acanthite

brittle, which condition did not permit hammering the material into a pliable noncrystalline plate.

In Fig. 16 is shown the spectral photoelectric sensitivity curve of a laboratory preparation of silver sulphide by G. W. Vinal.<sup>8</sup> It consisted of a thin, flexible, noncrystalline plate, size about 15 by 3 by 0.05 mm.

As shown in the lower curve of Fig. 16, at  $25^{\circ}\text{C}$ , this material did not show photoelectrical sensitivity for the spectral radiation intensities applied. However, for these same intensities, applied at  $-158^{\circ}\text{C}$ , the intrinsic sensitivity is high, and the spectral photoelectric sensitivity curve is quite symmetrical, with a maximum at  $1.05\mu$ . This maximum is at a much shorter wave length than observed in the natural mineral acanthite.

<sup>8</sup> Vinal, this Bulletin, 14, p. 331; 1917.

From the data herewith presented, it appears that the spectral photoelectrical sensitivity curve of silver sulphide is influenced by the physical condition of the mineral. It appears profitable to continue this investigation of the natural mineral as well as the artificial product after subjecting it to heat treatment, mechanical working, etc.

#### IV. PHOTOELECTRICAL SENSITIVITY OF BISMUTHINITE

In a previous investigation<sup>9</sup> it was shown that crystals of bismuthinite,  $\text{Bi}_2\text{S}_3$ , are sensitive in spots, often localized at the intergrowth of two bundles of acicular crystals. The sample (U. S. Nat. Mus. No. 14046, from Cornwall, England) used in the

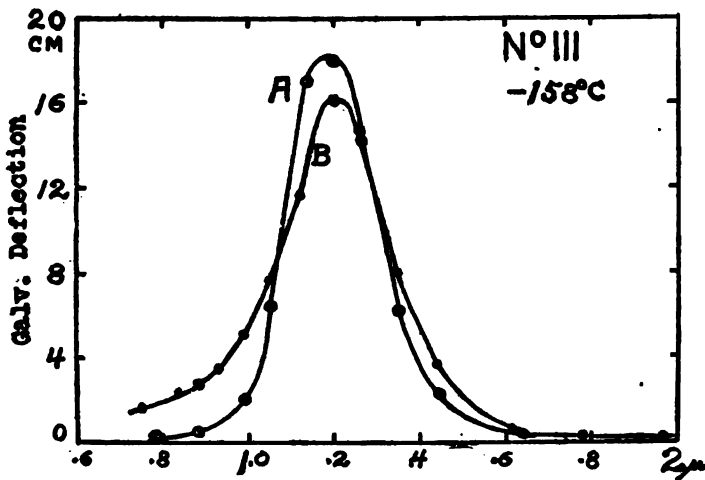


FIG. 15.—Effect of mechanical working upon the spectral photoelectric sensitivity of acanthite

present examination was a straight rod of fibrous material about 10 by 1.5 by 0.7 mm. The electrodes, which were of No. 30 copper, were attached to the crystal by means of solder. As described in the paper, just cited, the solder on cooling and solidifying holds the crystals very securely to the copper wires. Tests were made showing that dental amalgam is an excellent means for attaching wires to substances that will not take solder, but this research was terminated before this procedure was adopted as a general method of making electrical connections.

Tests made at room temperatures showed that the highest spectral intensities attainable were not sufficient to obtain a reliable photoelectrical sensitivity curve. Measurements were there-

<sup>9</sup> This Bulletin, 14, p. 599: 1918.

fore made only when the bismuthinite was at low temperatures,  $-166^{\circ}\text{C}$ . But even at this temperature the galvanometer was very unsteady, owing to lack of proper temperature control of the sample, the resistance of which changes rapidly with temperature. A change of a hundredth of a degree in temperature is sufficient to cause a drift in the galvanometer reading. To eliminate the effect of drift in the galvanometer reading, the ballistic throw was used. In this manner the spectral photoelectric sensitivity curve, *B*, Fig. 17, was obtained. It represents the average of a great many readings, and shows that there are two sensitivity maxima, at about  $0.64\mu$  and  $1.08\mu$ , respectively. Curve *A* illus-

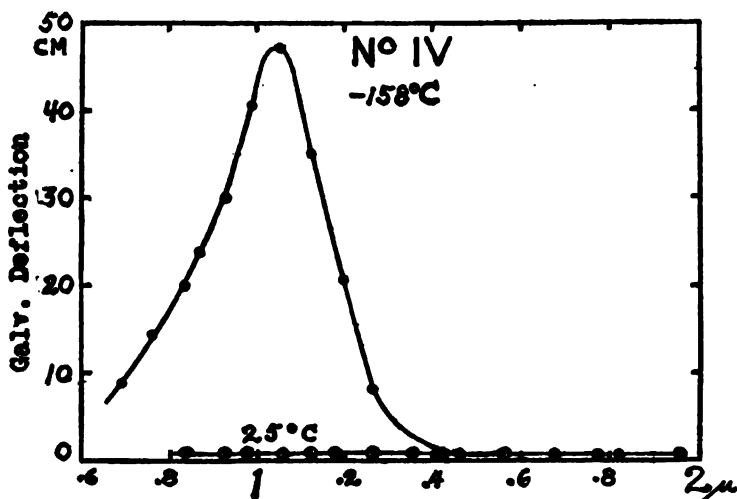


FIG. 16.—Photoelectrical sensitivity of an amorphous plate of a laboratory preparation of silver sulphide

trates a set of observations obtained by using unlimited exposure, which was from one to two minutes. The galvanometer deflections (amounting to about 5 cm at the maximum) are three times the scale indicated in Fig. 17.

## V. PHOTOELECTRICAL SENSITIVITY TESTS OF VARIOUS SUBSTANCES

As already mentioned, it was of interest to determine whether substances which are quite insensitive, photoelectrically, become markedly sensitive at low temperatures. Spectral photoelectric sensitivity tests were made on galena, pyrites, jamesonite, and cylindrite. Previous tests<sup>10</sup> showed that for high intensities

<sup>10</sup> This Bulletin, 14, pp. 593-595: 1918.

cylindrite appeared photoelectrically sensitive. Case,<sup>11</sup> using an arc light focussed upon the samples under test, found that galena and jamesonite were fairly sensitive to light.

### 1. GALENA (PbS)

The sample examined was a beautiful regular prism 12 by 3 by 3 mm. The electrodes were of thin copper wire heated to the melting point, and quickly touched to the galena, which is melted, forming a strong juncture. Using the highest obtainable spectral

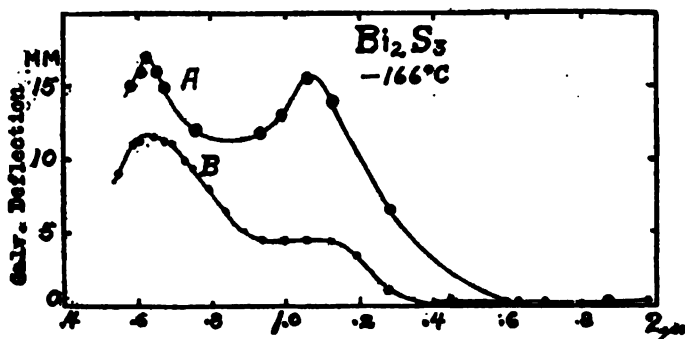


FIG. 17.—Spectral photoelectric sensitivity of bismuthinite

intensities, this sample of galena gave no indications of photo-electrical sensitivity either at 22° C or at -160° C.

### 2. CYLINDRITE

This is a lead-antimony tin mineral which occurs in cylindrical form. The sample examined was a beautiful cylinder about 2.5 mm in diameter and 12 mm long. The copper lead wires were attached by heating them as was done with galena.

For the intensities obtainable this sample showed no photo-electrical sensitivity at -160° C.

### 3. PYRITES (FeS<sub>2</sub>)

The sample examined was a homogeneous fragment of a crystal about 9 by 3 by 3 mm. The electrodes were fine, No. 36 copper wire wound in grooves filed around the ends of the crystal. No photoelectrical sensitivity was observed at -160° C. Previous tests, using high intensities, showed that this mineral is not sensitive at room temperatures.

<sup>11</sup> Case, Phys. Rev. (2), 9, p. 305: 1917.

4. JAMESONITE (2 Pb S.  $\text{Sb}_2\text{S}_3$ , SMITHSONIAN COLLECTION NO. 12 500, FROM CORNWALL, ENGLAND)

The sample examined was a bundle of acicular crystals, 10 by 2.5 by 2 mm. The electrodes were No. 36 copper wire tightly wound in grooves filed close to the ends of the crystal. This outfit was mounted securely upon a fiber base.

In the previous examination, using heterogeneous light, this mineral was found to be only slightly sensitive photoelectrically. The present tests were disappointing in that for the highest spectral intensities obtainable no evidence of photoelectrical sensitivity was found at  $-160^\circ\text{C}$ .

## VI. SUMMARY

This paper gives data on the change in the electrical resistance of the sulphides of silver and of bismuth, when exposed to radiations of wave lengths extending from  $0.6\mu$  in the visible spectrum to about  $3\mu$  in the infra-red. Measurements were made also upon galena, cylindrite, pyrites, and jamesonite, which, however, did not show photoelectrical sensitivity for the highest spectral radiation intensities available.

In the sulphides of silver and of bismuth the radiations extending from  $0.6\mu$  to about  $1.8\mu$  produce a noticeable change in electrical conductivity.

The effect of temperature, of intensity of the exciting radiation, and of mechanical working upon photoelectrical sensitivity of silver sulphide, was investigated.

Both the natural mineral, acanthite and a laboratory preparation were examined. The latter material, which was hammered into a thin flexible plate, was found insensitive photoelectrically at room temperature. But at  $-157^\circ\text{C}$  a sharp maximum of photoelectrical sensitivity was observed for radiations of wave length  $\lambda = 1.05\mu$ .

At room temperatures the natural crystalline material differs from other photoelectrically sensitive substances studied in that the photoelectric response becomes fatigued and, after an exposure of two to three seconds to light, the positive resistance change (galvanometer deflection) begins to be effective. For unlimited exposure the galvanometer deflection returns to about one-fifth of its maximum deflection. On removing the light stimulus the galvanometer gives a negative deflection, which in the course of a few minutes returns to the original zero scale reading. In other words, the change in resistance of the crystal, when exposed to

radiation, is first negative and then positive, the resultant change being negative and roughly one-fifth the original change. At low temperatures,  $-158^{\circ}\text{C}$ , this polarization phenomenon disappears, and the response to radiation is the same as that of other substances, for example, selenium and molybdenite. The spectral photoelectric sensitivity curve of crystalline silver sulphide, acanthite, at room temperature is conspicuous for its high sensitivity in the region of the spectrum extending from  $0.6\mu$  to  $1.2\mu$  followed by a maximum at about  $1.35\mu$ . Lowering the temperature to  $-158^{\circ}\text{C}$  greatly increases the photoelectrical sensitivity of acanthite throughout the spectrum examined. The sensitivity curve is quite symmetrical with a maximum at  $1.2\mu$ .

Increasing the intensity of the exciting radiations produces a more rapid response in the long wave lengths than in the short wave lengths, with a consequent shift of the maximum of the photoelectrical sensitivity curve toward the long wave lengths.

There is no simple law governing the variation in the photoelectric response in silver sulphide with variation in intensity of the radiation stimulus.

Mechanical working (hammering into a thin plate) appears to lower the intrinsic photoelectrical sensitivity of acanthite and changes the position of the maximum of spectral sensitivity.

A spectral photoelectric sensitivity curve of bismuthinite,  $\text{Bi}_2\text{S}_3$ , was obtained at  $-166^{\circ}\text{C}$ . There are maxima of sensitivity at  $0.64\mu$  and  $1.08\mu$ , respectively.

WASHINGTON, March 4, 1919.





DEC 20 1919

DEPARTMENT OF COMMERCE



# SCIENTIFIC PAPERS OF THE BUREAU OF STANDARDS

S. W. STRATTON, DIRECTOR

No. 345

MEASUREMENTS OF WAVE LENGTHS IN THE  
SPECTRA OF KRYPTON AND XENON

BY

PAUL W. MERRILL, Associate Physicist  
*Bureau of Standards*

ISSUED OCTOBER 3, 1919



PRICE, 5 CENTS

Sold only by the Superintendent of Documents, Government Printing Office  
Washington, D. C.

WASHINGTON  
GOVERNMENT PRINTING OFFICE

1919



# MEASUREMENTS OF WAVE LENGTHS IN THE SPECTRA OF KRYPTON AND XENON

By Paul W. Merrill

## CONTENTS

	Page
I. Introduction.....	251
II. Method of measurement.....	252
III. Results.....	252
1. Krypton.....	252
2. Xenon.....	254
IV. Discussion.....	256
V. Summary.....	257

## I. INTRODUCTION

The purpose of this paper is to record measurements of the wave lengths of lines in the red and infra-red spectral regions of krypton and xenon. The present measurements were made in continuation of considerable work upon the spectra of the rare gases already done by the Bureau of Standards.<sup>1</sup>

The rare gases are as follows:

	Atomic weight
Helium.....	4.0
Neon.....	20.2
Argon.....	39.9
Krypton.....	82.9
Xenon.....	130.2

<sup>1</sup> This Bulletin, 14, pp. 159 and 765; 1918, (Scientific Papers Nos. 302 and 309).  
121191°—19

Published tables of wave lengths contain no xenon lines in the infra-red region and only two krypton lines. Thus these spectra have been practically unknown beyond the limits 6456 Å for krypton and 6198 Å for xenon. Thanks to Baly,<sup>2</sup> the spectra are quite well observed throughout shorter wave lengths. The other rare gases have been more thoroughly investigated. Since all of these elements are of particular interest to the spectroscopist it is desirable to complete our knowledge of them as rapidly as possible. Not only are their spectral lines suitable for working standards for wave length determinations of high accuracy, but they are important for theoretical reasons on account of the relative simplicity of their spectra, and because of certain very interesting numerical relations already discovered.

## II. METHODS OF MEASUREMENT

The spectra were obtained with a concave grating giving a dispersion of 10 angstroms per millimeter. The second order iron comparison spectrum gave the nearly normal dispersion curve from which the rare-gas wave lengths were interpolated. Owing to the long exposures and to the fact that there was no means of introducing the comparison spectrum during the exposure, several of the plates showed small systematic shifts. The resulting wave lengths, therefore, are not of a very high order of accuracy; the values based on three or more determinations should be within 0.02 or 0.03 Å of the truth. In the tables which follow, those lines for which the uncertainty appears to be more than this are indicated by raising or omitting the second decimal figure.

## III. RESULTS

### 1. KRYPTON

Table 1 shows the krypton lines of longer wave length measured in the first order. The two strongest lines in this region, 7587.40 Å and 7601.55 Å, appear in Kayser's *Handbuch* as the two longest lines of the spectrum. In reality they are the beginning of a group of lines extending toward longer wave lengths, the krypton spectrum being analogous in this respect to that of argon and neon.

---

<sup>2</sup> Baly, *Phil. Trans., A* 202, pp. 183-242; 1904.

TABLE 1.—Kr Lines Measured in First Order

Intensity	L. A.	Number of exposures	Baly	Intensity	L. A.	Number of exposures	Runge
3	6421.1	1	6421.11	0	7635.1	1	.....
5	6456.3 <sup>a</sup>	1	6456.44	7	7685.22	5	.....
1	6576.4 <sup>a</sup>	1	.....	8	7694.53	5	.....
2	6652.2 <sup>a</sup>	1	.....	0	7741.3	1	.....
3	6699.1 <sup>a</sup>	1	.....	2	7746.81	3	.....
0	6739.9	1	.....	0	7776.2	1	.....
3	6813.0 <sup>a</sup>	1	.....	1	7806.5 <sup>a</sup>	1	.....
0	6846.4	1	.....	7	7854.79	5	.....
1	6869.0 <sup>a</sup>	1	.....	2	7913.38	3	.....
5	6904.6 <sup>a</sup>	1	.....	2	7928.5 <sup>a</sup>	3	.....
2	7224.0 <sup>a</sup>	3	.....	0	7982.4	1	.....
2	7287.27	4	.....	4	8059.47	5	.....
2	7425.52	4	.....	7	8104.33	5	.....
3	7486.85	5	.....	10	8112.87	5	.....
1	7493.6	1	.....	6	8190.02	5	.....
1	7494.1	1	.....	4	8263.22	5	.....
0	7503.9	1	.....	3	8281.02	5	.....
0	7514.7	1	Range	6	8298.07	5	.....
15	7587.40	6	7587.20	2	8506.85	5	.....
20	7601.55	6	7601.19	3	8776.73	5	.....
				1	8928.72	5	.....

The krypton tubes, which were furnished by Sir William Ramsey, contained krypton of a high degree of purity. Two argon lines are doubtfully present in the spectrum, while the strongest line of the xenon spectrum, 8231.62 Å, shows faintly.

For the purpose of comparing the gas in these tubes with that observed by Baly, one or two short exposures were made in the blue, using the second order spectrum. The few lines obtained correspond with the strongest lines observed by Baly<sup>3</sup> and Runge,<sup>4</sup> while no extraneous lines appear. The results are given in Table 2.

TABLE 2.—Kr Lines Measured in Second Order

Intensity	L. A.	Baly	Runge
1	4273.95	4273.99	4273.93
0	4318.6 <sup>a</sup>	4318.58	4318.54
1	4319.57	4319.60	4319.60
1	4376.11	4376.16	4376.07
0	4463.7 <sup>a</sup>	4463.71	4463.65

<sup>a</sup> Baly, loc. cit.<sup>4</sup> Runge, *Astroph. J.*, 10, p. 73; 1899.

A very brief inspection of the wave lengths for numerical regularities has shown three new pairs of constant frequency differences of the type discovered by Paulson.<sup>6</sup> The data for all eight of these pairs are given in Table 3.

TABLE 3.—Frequency Differences in Krypton Spectrum

L. A.	$\Delta \lambda$ vacuum	L. A.	$\Delta \lambda$ vacuum
4273.99	945.04	5570.28	944.99
4453.95		5879.84	
4283.01	944.95	7601.55	944.97
4463.71		8190.02	
4318.58	945.06	7694.53	945.00
4502.39		8298.07	
5562.23	944.96	8104.33	945.06
5870.90		8776.73	

The mean value of the frequency difference is 945.00. The greatest divergence from this value is 0.06, which is one part in 200 000 of the frequency. This is probably not outside the errors of measurement, especially if we assume the error of a difference to be 1.4 times that of an individual line. It would be of great interest to measure these lines with a much higher accuracy to see whether the differences remain constant to a part in several million, as has been found to be the case with neon.

## 2. XENON

The xenon as supplied by the laboratories of Sir William Ramsey was very pure. In the regions shown by the tables to overlap with Baly's measurements, the spectrum corresponds to that observed by him. Some plates taken by F. M. Walters, jr., with a 1-prism spectrograph covering a long range of the shorter wave lengths, also show a reasonable correspondence with Baly's spectra. The grating measurements are contained in Tables 4 and 5.

<sup>6</sup> *Anna lender Physik*, 45, p. 428; 1914.

TABLE 4.—Xe Lines Measured in First Order

Intensity	I. A.	Number of exposures	Baly	Intensity	I. A.	Number of exposures	Baly
1	5823.9 <sup>a</sup>	1	5823.86	0	7266.4	1	.....
0	5824.9	1	5824.76	1	7283.9 <sup>a</sup>	2	.....
1	5875.0 <sup>a</sup>	1	5875.08	3	7285.3 <sup>a</sup>	2	.....
1	5895.0 <sup>a</sup>	1	5894.98	2	7316.3 <sup>a</sup>	2	.....
0	5931.2	1	.....	2	7321.4 <sup>a</sup>	2	.....
1	5934.2 <sup>a</sup>	1	.....	2	7336.4 <sup>a</sup>	2	.....
0	6163.8	1	6164.09	1	7355.6 <sup>a</sup>	2	.....
1	6178.3 <sup>a</sup>	1	6178.59	2	7385.9 <sup>a</sup>	2	.....
0	6179.6	1	6179.95	3	7393.8 <sup>a</sup>	2	.....
2	6182.4 <sup>a</sup>	1	6182.71	1	7400.4 <sup>a</sup>	2	.....
1	6198.3 <sup>a</sup>	1	6198.49	0	7424.0 <sup>a</sup>	2	.....
3	6318.0 <sup>a</sup>	1	.....	1	7472.0 <sup>a</sup>	2	.....
3	6469.7 <sup>a</sup>	1	.....	0	7473.9 <sup>a</sup>	2	.....
1	6472.8 <sup>a</sup>	1	.....	0	7559.7	2	.....
1	6487.7 <sup>a</sup>	1	.....	2	7584.6 <sup>a</sup>	4	.....
0	6498.7	1	.....	4	7642.04	5	.....
0	6504.1	1	.....	1	7643.8 <sup>a</sup>	4	.....
1	6595.5 <sup>a</sup>	1	.....	0	7664.3	1	.....
0	6666.8	2	.....	1	7802.7 <sup>a</sup>	3	.....
2	6668.8 <sup>a</sup>	2	.....	3	7887.4 <sup>a</sup>	4	.....
3	6727.9 <sup>a</sup>	2	.....	2	7967.34	4	.....
1	6827.1 <sup>a</sup>	1	.....	1	8057.2 <sup>a</sup>	3	.....
0	6866.6	1	.....	1	8061.3 <sup>a</sup>	3	.....
1	6872.0 <sup>a</sup>	1	.....	2	8206.30	4	.....
3	6882.0 <sup>a</sup>	2	.....	15	8231.62	6	.....
0	6976.1	1	.....	1	8266.5 <sup>a</sup>	3	.....
0	7047.2	1	.....	12	8280.08	6	.....
2	7119.5 <sup>a</sup>	3	.....	3	8346.76	4	.....
1	7257.9 <sup>a</sup>	1	.....	4	8409.17	4	.....
0	7262.6	1	.....	6	8819.38	4	.....
				1	8952.25	4	.....
				1	9045.44	3	.....
				0	9162.7 <sup>a</sup>	2	.....

TABLE 5.—Xe Lines Measured in Second Order

Intensity	I. A.	Number of exposures	Baly	Intensity	I. A.	Number of exposures	Baly
0	<sup>a</sup> (3967.6)	1	3967.59	10	4671.22 <sup>a</sup>	3	4671.24
3	4500.98	2	4500.96	3	4671.56	2	.....
1	4524.70	2	4524.65	1	4697.02	2	4696.99
6	4624.27 <sup>a</sup>	3	4624.28	2	4734.18	2	4734.12
0	4624.58	2	.....	1	4807.06	2	4807.01
				0	4807.6 <sup>a</sup>	1	.....

<sup>a</sup> Position estimated.

By far the strongest lines in the region 5823–9162 are 8231.62 and 8280.08. These two lines seem to correspond to the strong lines which stand at the short wave length end of groups of lines of the other rare gases. They are certainly among the most important lines in the whole spectrum, possibly being those by which traces of the elements could be most easily identified. The line 8231 was measured three times on the krypton photographs, yielding a value of 8231.62, in exact agreement with the wave length from the xenon tube.

Attention is called to the close companions to the lines 4624, 4671, and 4807. These may have been lost in the over-exposed images of the strong lines on Baly's plates.

#### IV. DISCUSSION

Although all the principal lines of the helium spectrum have been shown to fall unmistakably into six series, no important series relationships have as yet been found among the stronger lines of the other rare gases. While it would be rash to say they do not exist, a different type of regularity is predominant in present data—namely, that of constant difference pairs. The four gases of greater atomic weight possess another feature in common which is apparently not partaken of by the helium spectrum. That is the tendency of the lines to form groups, the position of which apparently has some relation to the atomic weight. Observations upon neon and argon had previously shown that each spectrum possessed a group of very strong lines in the red, with the further characteristic that the shortest lines of the group were especially strong, and that in the direction of the violet from these lines lay a region containing only weak lines. As has already been remarked in this paper, the krypton spectrum exhibits somewhat the same phenomena. This is probably also the case with xenon, the very strong lines 8231 and 8280 beginning a group of strong lines, which, however, is not very conspicuous or greatly extended owing to the rapidly decreasing efficiency of the photographic plate in this portion of the spectrum.

Moreover, strong lines or groups of the different gases show a regular displacement from one spectrum to another in the order of the atomic weights. To exhibit this the writer photographed the four rare gases side by side upon the same plate with a very small dispersion spectrograph. The similarity of the spectra and the progression in the position of two groups of lines is shown by Fig. 1,



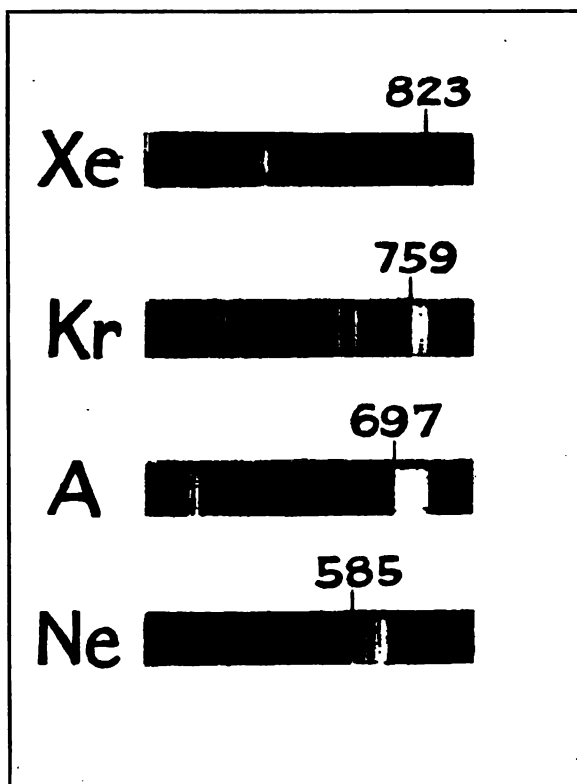


FIG. 1.—Spectra of the four rare gases showing similarity and progression in the group position



which is a copy of this photograph. Bearing in mind that the long wave-length group in xenon is much weakened by photographic effects, and that the short wave-length group of neon fails to appear on account of the absorption of the prism used, the correspondence is rather striking. The correspondence between individual lines is not clear. No extended search for individual relationships has as yet been made. A few simple functions of atomic weight and number have been tried to represent the position of the lines. The writer is not convinced that the apparent success in a few cases indicates anything of importance, as it may be due to a few coincidences. At any event no complete system has been evolved and it remains to be seen whether such relationships exist.

F. M. Walters made the photographs to check the character of the krypton and xenon spectra in the violet and ultra-violet and assisted in some of the wave-length reductions.

#### V. SUMMARY

This paper records photographic measurements of wave lengths in the spectra of krypton and xenon, principally in the red and infra-red. In krypton 37 new lines were measured between 6576 Å and 8928 Å; in xenon 52 new lines between 6318 Å and 9162 Å. In this region there are numerous strong lines which are probably among the most important in the spectra of these elements. The xenon lines at 8231 Å and 8280 Å are especially notable. These and other lines may be of value as wave-length standards in the infra-red.

Attention is called to a probable analogy between the spectra of the rare gases neon, argon, krypton, and xenon which this investigation has brought to light.

WASHINGTON, April 28, 1919.



JAN 3 1920

DEPARTMENT OF COMMERCE



# SCIENTIFIC PAPERS

OF THE

# BUREAU OF STANDARDS

S. W. STRATTON, DIRECTOR

No. 346

**OXYGEN CONTENT BY THE LEDEBUR METHOD OF  
ACID BESSEMER STEELS DEOXIDIZED  
IN VARIOUS WAYS**

BY

J. R. CAIN, Chemist

and

EARL PETTIJOHN, Assistant Chemist

*Bureau of Standards*

ISSUED NOVEMBER 11, 1919



PRICE, 5 CENTS

Sold by the Superintendent of Documents, Government Printing Office  
Washington, D. C.

WASHINGTON  
GOVERNMENT PRINTING OFFICE  
1919



# OXYGEN CONTENT BY THE LEDEBUR METHOD OF ACID BESSEMER STEELS DEOXIDIZED IN VARIOUS WAYS

By J. R. Cain and Earl Pettijohn

## CONTENTS

	Page
I. Introduction.....	259
II. Deoxidation tests made at Watertown Arsenal.....	260
III. Deoxidation tests made at the Bethlehem Steel Co. plant at Sparrows Point, Md.....	263
IV. General discussion.....	267
V. Summary.....	270

## I. INTRODUCTION

The present work is an attempt to throw some light on the relationship, if any, which exists between the method of deoxidation of a steel and the oxygen content as determined by the Ledebur method when carried out as described by Cain and Pettijohn.<sup>1</sup> Incidentally, some other data related to deoxidation problems are given. The work is incomplete, in the sense that it is not, and does not purport to be, a systematic study of this question, since it represents only (1) modified commercial practice at one plant for the production of acid Bessemer steel, and (2) an experimental deoxidation practice developed for the study of this particular phase of steel manufacture. In view of the great variations in commercial deoxidation practice at different works and with different processes of steel manufacture, this present investigation should be regarded as no more than introductory to the subject.

The data in this paper relate to two sets of steel ingots, the one made during deoxidation tests carried out at the Watertown Arsenal in 1915 and the other made during a cooperative investigation between this Bureau and the Bethlehem Steel Co.'s plant at Sparrows Point, Md., in 1917. The first-named investigation was described by Boylston<sup>2</sup> and the original paper should be consulted. Only so much of the data from Boylston's paper is included here as is considered necessary for correlation with data obtained in the present investigation.

<sup>1</sup> Bureau of Standards Technologic Paper No. 118.

<sup>2</sup> Investigation of the Relative Merits of Various Agents for the Deoxidation of Steel. Carnegie Scholarship Memoirs, 7, pp. 102-131, 131-171, 1916.

## II. DEOXIDATION TESTS MADE AT WATERTOWN ARSENAL

Boylston's work was carried out in two phases. The first part was a preliminary investigation made by adding to Tropenas converter steel varying proportions of the deoxidizers tested, namely, commercial grades of ferrosilicon, ferromanganese, aluminum, ferrotitanium, and ferrocobalt titanium. The additions were made in a preheated ladle, the metal held for a short time in the ladle after the addition, and then poured into ingot molds which were made of sand. The object of these preliminary experiments was to ascertain the best proportion of deoxidizer under each set of the conditions described in the original paper. The criterion used in judging the effect of the deoxidizer was the relative density of the ingots, which was roughly determined for the whole ingot (these were 20 inches long by 6 inches diameter) by weighing first in air and then in water.

The best proportions of each deoxidizer as fixed by the preliminary experiments were then used in deoxidizing a heat of steel made in a Tropenas converter and having the composition shown in the fourth horizontal column of Table 2.

Table 1 gives the principal details of metallurgical interest concerning this heat, and Table 2 the analysis of the materials used in making it.

TABLE 1.—Details of Heat No. 4458 Made at Watertown Arsenal

	Time of operations		
	Hours	Minutes	Seconds
Metal into converter .....	2	9	0
	2	12	0
Started to blow .....	2	12	30
Blow ended (7 seconds overblown) .....	2	48	40
Converter to 2-ton ladle .....	3	0	0
Materials			Pounds
Weight of cupola metal added to metal in converter .....			425
Weight of ferromanganese added (77 per cent Mn) .....			45
Weight of ferrosilicon added (56 per cent Si) .....			7
Weight of converter metal .....			5092
Weight of steel and additions .....			5569



TABLE 2.—Chemical Composition of Raw Materials and Steel Used at Watertown Arsenal

Material	C	Mn	Si	S	P
	Per cent	Per cent	Per cent	Per cent	Per cent
Cupola iron.....	3.40	0.47	1.650	0.047	0.035
Converter metal.....	.08	Trace	.016	.....	.....
Converter metal plus additions (calculated).....	.387	.68	.218	.054	.040
Same, by analysis.....	.37	.51	.186	.057	.037
Ferromanganese.....	6.55	77.00	.908	.024	.185
Ferrosilicon.....	.16	.....	56.000	.....	.....

Table 3 gives the compositions of the various deoxidizers used in the investigation and the manner of using these is shown in Table 4.

TABLE 3.—Chemical Composition of Deoxidizers Used at Watertown Arsenal

Deoxidizer	C	Mn	Si	S	P	Al	Ti	Fe
	Per cent	Per cent	Per cent	Per cent	Per cent	Per cent	Per cent	Per cent
Ferromanganese.....	6.55	77.00	0.908	0.024	0.185	.....	.....	.....
Ferrosilicon.....	.16	.....	56.00	.....	.....	.....	.....	.....
Ferrocabon titanium.....	5.92	.....	2.10	.....	.....	None	14.32	.....
Ferrotitanium C-free.....	.....	.....	1.30	.....	.....	7.61	24.00	.....
Aluminum.....	.....	.....	.87	.....	.....	99.08	.....	0.05

<sup>a</sup> By difference.

TABLE 4.—Time of Pouring Ingots and Details as to Use of Deoxidizers

	Ingot			Ingot			Ingot			Ingot			Ingot		
	1, 2, 3			6, 5, 4			7, 8, 9			12, 11, 10			13, 14, 15		
	h.	m.	s.	h.	m.	s.	h.	m.	s.	h.	m.	s.	h.	m.	s.
Metal into ladle.....	3	5	50	3	16	55	3	7	30	3	14	48	3	8	55
Deoxidizer added.....	3	5	56	3	16	56	3	7	30	3	14	48	3	9	00
Finished pouring into ladle.....	3	6	25	3	17	00	3	7	57	3	15	10	3	9	05
Metal poured into first ingot.....	3	09	20	3	19	45	3	10	25	3	17	14	3	11	35
Third ingot finished.....	3	10	56	3	21	20	3	11	34	3	18	31	3	13	00
Deoxidizer held in ladle.....	0	2	55	0	2	45	0	2	28	0	2	04	0	2	30
Weight of deoxidizer added (pounds).....	6.98			6.275			4.16			7.15			2.02		
Weight of steel in ladle (pounds).....	1054			1015			1067			1000			1395		
Per cent of deoxidizing element added.....	0.095			0.492			0.093			0.40			0.144		
Kind of deoxidizer added.....	Fe-C-Ti			Fe-Mn			<sup>a</sup> Fe-Ti			Fe-Si			Al		
Per cent of active element in deoxidizer.....	14.32			79.65			24.0			56.0			98.0		
Ounces of deoxidizer (calculated) per ton of steel.....	212			198			125			229			46		
Ounces of deoxidizer element (calculated) per ton of steel.....	30.4			157.7			30.0			128			45.6		

NOTE.—The additions were all made in small preheated ladles each of which had the approximate capacity of the ingot molds used; the steel after addition of the deoxidizer was held in the ladles for the times shown in Table 4, before pouring into sand molds.

<sup>a</sup> Carbon free.

Table 5 gives the determinations by the present authors of the Ledebur oxygen content of the ingots (two missing) described in Table 4.

TABLE 5.—Oxygen Determinations on Steels Made at Watertown Arsenal

Deoxidizer	Ingot	Oxygen
		Per cent
Ferrocabon titanium.....	1	0.012
	2	.013
	3	.017
Ferromanganese.....	4	Missing
	5	.014
	6	.017
Carbon-free ferrotitanium.....	7	.014
	8	.009
	9	.011
Ferro-silicon.....	10	Missing
	11	.010
	12	.016
Aluminum.....	13	.012
	14	.018
	15	.016

Table 6 gives mechanical tests of annealed test pieces taken from these ingots.

TABLE 6.—Tensile Tests of Annealed Forged Steel Specimens (Made at Watertown Arsenal)<sup>a</sup>

Ingot	Deoxidizer	Elastic limit	Tensile strength	Elongation in 2 inches	Contraction of area
		Lbs./in. <sup>2</sup>	Lbs./in. <sup>2</sup>	Per cent	Per cent
1F	Ferrocabon titanium.....	47 500	82 500	27.5	49.1
2F		52 000	82 000	29.0	51.9
3F		51 000	81 500	28.5	51.9
5F	Ferromanganese.....	48 000	83 500	25.5	46.2
6F		49 000	79 000	30.5	54.6
7F		46 000	77 000	31.0	57.2
8F	Carbon-free ferrotitanium.....	48 500	78 000	31.5	57.2
9F		50 500	84 000	26.5	46.2
11F		52 500	82 500	29.0	54.6
12F	Ferro-silicon.....	53 500	84 500	28.5	51.9
13F		47 000	78 500	29.5	57.2
14F	Aluminum.....	48 500	78 000	31.0	54.6
15F		44 500	79 500	29.5	51.9

<sup>a</sup> The test bars were prepared from pieces about 2 inches square by 7 inches long cut from the top of each forged ingot (forged to 2 inches round) after a 3-inch top discard. They were annealed by heating at 850° in a Semi-Muffle furnace for one hour and cooled in air; they were then reheated at 850° for one-half hour and cooled in air; finally, they were heated a third time at 850° for one-half hour and cooled in air.

From an inspection of Tables 5 and 6 it is evident that the marked variations in deoxidation treatment of the same steel, as detailed in text and tables, has had but little effect on the oxygen content of the various ingots as determined by the Ledebur method; some difference in mechanical properties is evident, but not so marked as to be considered highly important, except possibly with reference to the determinations of elastic limit.

FIG. 1.—Ladle test ingots from heat 15600, deoxidized with spiegel. (Bottom ingot is blown metal)

FIG. 2.—*Ladle test ingots from heat 16602, deoxidized with ferrosilicon. (Bottom ingot is blown metal)*

FIG. 3.—Ladle test ingots from heat 16657, deoxidized in the ladle with aluminum.  
(Bottom ingot is blown metal)

FIG. 4.—*Ladle test ingots from heat 16661, deoxidized with ferrocobon titanium.  
(Bottom ingot is blown metal)*

### III. DEOXIDATION TESTS MADE AT THE BETHLEHEM STEEL CO. PLANT AT SPARROWS POINT, MD.

The tests at Sparrows Point were made at the Bessemer (acid) plant by certain variations in the regular commercial practice used here for making Bessemer steel. This practice consists essentially in charging into the converter molten pig iron taken from a mixer, together with a certain proportion of scrap, blowing the mixture in the converter until carbon, manganese, and silicon are removed practically completely; then deoxidizing, recarburizing, and adjusting residual manganese content by the addition of molten spiegel. The details concerning the various heats used in making these tests, so far as available, are given in Tables 7 and 8.

TABLE 7.—Analytical Details of Experiments Made at Bethlehem Steel Co.

Heat	Mixture blown in converter		Deoxidizer		Blown metal		Ladle test of heat					Ladle tests of individual ingots		
	Si	Mn	Si	Mn	C	Mn	C	Mn	Si	P	S		C	Mn
	P. ct.	P. ct.	P. ct.	P. ct.	P. ct.	P. ct.	P. ct.	P. ct.	P. ct.	P. ct.	P. ct.	P. ct.	P. ct.	P. ct.
16600	0.77	1.44	1.37 <sup>a</sup>	14.58	0.056	Nil	0.36	0.75	0.05	0.044	0.024	1	0.356	0.75
												2	.858	.75
												3	.858	.75
												4	.372	.75
												5	.362	.75
												6	.366	.76
16602	1.25	.93	a 1.50	a 14.64	.038	Nil	.38	.72	.05	.086	.042	1	.372	.72
			b 50.00	-----	-----	-----	-----	-----	-----	-----	-----	2	.374	.73
												3	.382	.72
												4	.380	.71
												5	.392	.70
												6	.376	.73
16637	.43	.62	a 1.39	a 15.50	.064	Nil	.39	.99	.09	.060	.046	1	.404	1.01
			c .99	-----	-----	-----	-----	-----	-----	-----	-----	2	.398	1.00
												3	.390	.97
												4	.392	.98
												5	.410	.97
												6	.380	.98
16661	1.55	1.68	a 1.39	a 15.38	.092	.08	.45	.95	.05	.092	.016	1	.432	.80
			d 15.50	-----	-----	-----	-----	-----	-----	-----	-----	2	.434	.81
												3	.468	.85
												4	.448	.82
												5	.466	.74
												6	.444	.76

<sup>a</sup> Spiegel.

<sup>b</sup> Ferrosilicon.

<sup>c</sup> Aluminum.

<sup>d</sup> Ferrotitanium.

TABLE 8.—Metallurgical Details of Heats Made at Bethlehem Steel Co.

Heat	Weight			Time held after adding deoxidizer	Time of heating ingots before rolling
	Spiegel	Mixer metal	Scrap		
	Pounds	Pounds	Pounds	m.	h. m.
16600.....	3170	37 000	3500	0	1 45
16602.....	3600	42 000	3500	2	1 55
16657.....	3560	37 000	3000	2	1 45
16661.....	3560	38 000	3500	-2	1 50

NOTE.—Size of ingots 21 by 23 by 64 inches; weight of ingots 6800 pounds.

Heat 16600 was made as usual, being deoxidized with spiegel; to each ingot of this heat 5 ounces of stick aluminum was added as the metal flowed into the mold. Heat 16602 was deoxidized with ferrosilicon added in the ladle after the spiegel addition; heat 16657 with aluminum in the ladle after the spiegel; and heat 16661 with ferrocobalt titanium (15.5 per cent Ti) in the ladle after the spiegel. Every other ingot of the last three heats received aluminum treatment in the mold in the manner described for heat 16600.

All the ingots were rolled into rails after 10 per cent top and 3 per cent bottom discard and the Bureau was supplied with the

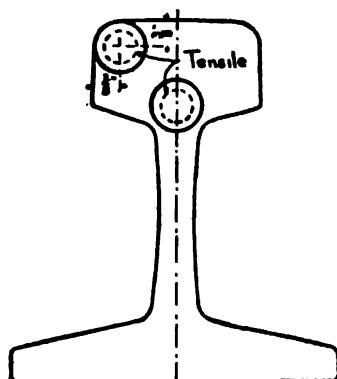


FIG. 5.—Diagram showing positions 1, 2, 3, and 4 of test bars in rail ends.

front ends of the first rail from each ingot; one ladle-test ingot per large ingot was also taken at the time when each large ingot was one-half poured; these test ingots were poured from a small spoon which was filled by holding it beneath the stream of metal flowing from the ladle when the stopper was nearly closed. Photographs of the faces of the test ingots on the medial longitudinal plane are shown in Figs.

For making the oxygen determinations chips were milled under oil (as described in the cited paper by Cain and Pettijohn) from each split-test ingot and from some of the corresponding rail ends. Oxygen was also determined in the blown metal for each heat. For additional information test bars were machined from the rail ends and their mechanical properties determined. This series of experiments was expected to yield information, (1) as to variation



of Ledebur oxygen content corresponding to the different deoxidizers used under comparable conditions; (2) the effect on Ledebur oxygen content of further aluminum treatment in the molds; (3) the combined effect, if any, of preheating for rolling and of rolling on Ledebur oxygen content; (4) the physical properties corresponding to the different methods of deoxidation, other factors being approximately the same; and (5) the change in these physical properties caused by the aluminum treatment in the molds.

Table 8 gives the Ledebur oxygen determinations on these samples and some nitrogen determinations. Table 9 gives the physical properties of the test bars. Before machining the test bars all the rail ends were put into the same physical condition by heating for three-fourths hour at 800° in a muffle furnace and cooling in the furnace.\*

---

\* Some slight change in oxygen content may have been caused by this treatment. However, it would be the same for all the rails and does not affect the comparison of deoxidizers which this study involves.

TABLE 9.—Determination of Nitrogen and Oxygen in Steels Made by the Bethlehem Steel Co.

Heat	Deoxidizer used	Ingot (order in which poured)	Treatment in mold	Oxygen—		Nitrogen <sup>a</sup>
				In ladle-test ingot	In corresponding rail	
				Per cent	Per cent	Per cent
16600	Spiegel.....	1.....	5 ounces Al added...	0.021	0.018	.....
		2.....	do.....	.028	.019	0.0135
		3.....	do.....	.008	.017	.0135
		4.....	do.....	.020	.....	.0128
		5.....	do.....	.006	.....	.0145
		6.....	do.....	.016	.019	.0127
		Blown metal.....	No Al added.....	.023	.....	.....
16602	Ferrosilicon.....	1.....	5 ounces Al added...	.009	.....	.....
		2.....	No Al added.....	.017	.016	.....
		3.....	5 ounces Al added...	.011	.....	.0117
		4.....	No Al added.....	.004	.012	.0097
		5.....	5 ounces Al added...	.010	.....	.....
		6.....	No Al added.....	.011	.010	.....
		Blown metal.....	do.....	.024	.....	.....
16657	Aluminum.....	1.....	5 ounces Al added...	.017	.....	.0128
		2.....	No Al added.....	.015	.018	.0104
		3.....	5 ounces Al added...	.014	.015	.....
		4.....	No Al added.....	.....	.016	.....
		5.....	5 ounces Al added...	.013	.016	.....
		6.....	No Al added.....	.014	.015	.....
		Blown metal.....	do.....	.027	.....	.....
16661	Ferrotitanium.....	1.....	5 ounces Al added...	.018	.017	.....
		2.....	No Al added.....	.015	.011	.....
		3.....	5 ounces Al added...	.012	.018	.0151
		4.....	No Al added.....	.006	(b)	.0127
		5.....	5 ounces Al added...	.009	.012	.....
		6.....	No Al added.....	.004	.....	.....
		Blown metal.....	do.....	.014	.....	.....

<sup>a</sup> The nitrogen determinations were made by Louis Jordan, of this Bureau, using Allen's method (Jour. Iron and Steel Inst., 1880, p. 181), with modifications, which will be described in a subsequent paper. This method gives "combined" nitrogen; i. e., that present as nitride. The nature of the particular nitride or nitrides usually present in steel is being investigated at the Bureau.

<sup>b</sup> Not determined.

#### IV. GENERAL DISCUSSION

A study of the results given in Tables 5 and 9 discloses no relationship between the Ledebur oxygen content and (1) the various methods of deoxidation used in the ladle; (2) the aluminum treatment in the molds; and (3) the effect of reheating for rolling and of rolling. Nevertheless, the steels in each case had physical characteristics varying somewhat with the deoxidation method, as shown in Tables 6 and 10. These differences are not completely accounted for by other factors, such as heat treatment (which was identical for the steels of each test) or by chemical composition, which was identical for all the ingots made at Watertown, but only approximately so for the steels made at Sparrows Point. Evidently, then, the Ledebur method does not measure anything which indicates efficiency of deoxidation in such steels. Some of the reasons for this are described by the authors in their paper on the Ledebur method (*loc. cit.*). A probable explanation is that the slags produced during deoxidation (e. g., ferrous silicates, ferrous aluminates, ferrous manganous silicates, ferrous titanates, etc.) and not separated from the steel before solidification are responsible for some of the differences in physical properties shown; such slags, in general, do not yield their oxygen to the Ledebur method, and in this regard the method fails. As shown in the cited paper by the present authors, the Ledebur method can give but little information on the gas content of steel after deoxidation, and in this respect, also, it affords no help in studying the efficiency of deoxidizers, which are really degasifiers.

TABLE 10.—Mechanical Tests of Rail Ends

[The (a) and (b) refer to the position in the rail from which the test bars were taken, as shown in Fig. 5]

Deoxidizer; treatment of ingots	Yield point	Ultimate strength	Elongation in 2 inches	Reduction in area
Heat No. 16600 (spiegel):	Lbs./in. <sup>2</sup>	Lbs./in. <sup>2</sup>	Per cent	Per cent
5 ounces Al in mold.....	(a) 56 500	97 000	24.5	46.5
	(b) 57 200	97 700	.....	46.7
Do.....	(a) 58 000	97 000	26.0	45.0
	(b) 59 800	98 500	23.5	44.2
Do.....	(a) 56 500	96 500	26.0	47.5
	(b) 58 000	98 750	24.0	42.5
Heat No. 16602 (ferrosilicon):				
5 ounces Al in mold.....	(a) 60 000	103 000	23.5	45.0
	(b) 61 500	102 750	25.0	45.5
No Al in mold.....	(a) 61 250	100 250	23.0	44.5
	(b) 58 250	100 250	23.5	45.5
5 ounces Al in mold.....	(a) 57 500	100 250	25.0	45.5
	(b) 61 200	100 200	26.0	45.9
No Al in mold.....	(a) 58 250	98 000	23.0	43.5
	(b) 61 300	100 800	22.5	41.2
Heat No. 16657:				
Aluminum in ladle.....	(a) 61 500	103 750	24.0	44.5
No Al in mold.....	(b) 59 000	102 500	25.5	45.0
5 ounces Al in mold.....	(a) 59 250	102 500	23.0	43.0
	(b) 58 500	102 000	23.0	43.5
No Al in mold.....	(a) 58 500	106 750	23.5	41.5
	(b) 61 000	106 500	23.0	42.0
5 ounces Al in mold.....	(a) 58 250	102 750	24.0	43.5
	(b) 61 800	103 600	23.5	43.2
Heat No. 16661 (ferrotitanium):				
5 ounces Al in mold.....	(a) 61 750	113 500	18.0	36.0
	(b) 61 900	113 500	19.5	36.3
No Al in mold.....	(a) .....	108 800	16.5	29.6
	(b) 64 750	122 500	16.5	27.5
5 ounces Al in mold.....	(a) 59 500	107 500	12.0	15.5
	(b) 62 250	112 000	18.5	37.0
No Al in mold.....	(a) 60 000	105 750	7.5	10.0
	(b) 59 250	108 250	18.5	35.5
Averages:				
16600.....	57 600	97 800	24.8	45.1
16602.....	59 900	100 700	23.9	44.5
16657.....	59 700	103 800	23.7	43.3
16661.....	61 300	111 500	15.9	28.5

The slight variations in the results for oxygen on the various successive ladle-test ingots of a heat are probably due to segregation; the most unsound test ingots (Figs. 1 and 4) representing heats deoxidized with spiegel and ferrotitanium, respectively, are the worst in this regard; whereas the soundest ones (Figs. 2 and 3), deoxidized, respectively, with ferrosilicon and aluminum, show the least oxygen variation in the successive ladle-test ingots.

The peculiar results obtained by the use of ferrotitanium in the Bethlehem Steel Co. steels are of particular interest. They indicate segregation of some kind, yet the analyses of successive ingots of this heat (see Table 7) for constituents other than oxygen do not show excessive segregation, although they are not nearly so uniform as the ingots of the other heats. In this connection it is interesting that the successive ingots of the heat deoxidized at Watertown with ferrocobalt titanium were quite uniform as regards physical properties, as shown by the data in Boylston's paper. Only 0.003 per cent of residual titanium was found in the ladle-test ingots of heat 16661, so that none of the properties of this steel can be attributed to titanium alloyed with it.

The results communicated by Boylston for gas content (*loc. cit.*) of the various ingots made during the test at Watertown could not be used by him to throw any light on the efficiency of the various deoxidizers. These results, however, did not represent the total gas content obtained by melting the metal, evacuating and measuring the released gases; instead they were obtained by heating the steel samples to 1000° for 30 hours in vacuo. Just what proportion of the total gas present was obtained in this way is not brought out in the paper, and hence the interpretation of the results is difficult. Work is now in progress at this Bureau on methods for determining gas in steel by melting in vacuo.

The nitrogen determinations shown in the last column of Table 9 are given in this paper for three reasons: First, to supplement the determinations of gases in these steels made by Boylston, which determinations are reported in his paper. The nitrogen shown in Table 9 is undoubtedly to be added to Boylston's results, since the method he used would probably not determine this. Second, to throw some light on the special properties claimed for titanium as a remover of nitrogen in steels. As far as the evidence of this paper goes—and it must be regarded as very incomplete—no more nitrogen is removed by titanium than by the other deoxidizers. Third, to ascertain whether or not aluminum, by the formation of aluminum nitrides, facilitates removal of nitrogen. The results here, also, are negative, but again the same caution should be exercised in interpretation of data.

The authors acknowledge the courtesy of officials of the Watertown Arsenal and of Prof. Boylston for opportunity to cooperate in their investigation; and of the Bethlehem Steel Co., and particularly F. F. Lines, who made many helpful suggestions and facilitated the work in every way possible. They are indebted to the division of engineering and structural materials of the Bureau for the results of Table 10.

## V. SUMMARY

1. The Ledebur method for oxygen did not indicate significant differences in oxygen content in steels with nearly identical chemical composition and heat treatment but having different deoxidation treatments.

2. No differences in nitride nitrogen were shown for such steels.

3. The work of Boylston cited in this paper showed no distinctive differences in the gas content of such steels as obtained by heating in vacuo to 1000° for 30 hours.

4. Judged by the evidence of this paper and that of Boylston, the three chemical methods just named—being those much used heretofore—are inadequate for the study of deoxidation.

5. Mechanical tests show some differences in quality of the steels according to deoxidation treatment, but these differences are not marked and are masked somewhat by other factors.

WASHINGTON, December 23, 1918.







DEPARTMENT OF COMMERCE

---

# SCIENTIFIC PAPERS

OF THE

# BUREAU OF STANDARDS

S. W. STRATTON, DIRECTOR

---

No. 347

## HEAT TREATMENT OF DURALUMIN

BY

P. D. MERICA, Physicist

R. G. WALTENBERG, Assistant Physicist

H. SCOTT, Assistant Physicist

*Bureau of Standards*

---

ISSUED NOVEMBER 15, 1919



PRICE, 10 CENTS

Sold only by the Superintendent of Documents, Government Printing Office  
Washington, D. C.

---

WASHINGTON  
GOVERNMENT PRINTING OFFICE

1919



# HEAT TREATMENT OF DURALUMIN

By P. D. Merica, R. G. Waltenberg, and H. Scott

## CONTENTS

	Page
I. Introduction.....	271
II. Composition and preparation of alloys.....	273
III. Heat treatment and aging.....	273
1. Effect of quenching temperature.....	278
2. Effect of aging temperature.....	281
3. Effect of temperature of quenching bath.....	285
4. Effect of prior heating at quenching temperature.....	293
5. Effect of preheating to 515° C before quenching from lower temperatures.....	293
IV. Miscellaneous tests.....	293
1. Density and dilatation.....	296
2. Electrical resistivity.....	297
V. Mechanism of hardening during aging after rapid cooling.....	299
1. Structure of duralumin.....	306
2. Analogy between the hardening of duralumin and that of steel...	310
3. Eutectic structure and influence of magnesium.....	311
VI. Conclusions relative to the manufacture and heat treatment of duralumin.....	314
VII. Summary and conclusions.....	315

## I. INTRODUCTION

The remarkable phenomena exhibited by the aluminum alloy known as duralumin were discovered during the years 1903-1911 by A. Wilm<sup>1,2</sup> and have been described by him and others.<sup>3,4,5,6</sup>

The unusual feature of this alloy is the fact, as was shown by Wilm, that it can be hardened quite appreciably by quenching from temperatures below its melting point followed by aging at ordinary temperatures, which consists merely of allowing the material to stand at these temperatures. The hardness is not produced by the quenching alone, but increases during the period

<sup>1</sup> A. Wilm, Physical-Metallurgical investigations of aluminum alloys containing magnesium, *Metallurgie* 8, p. 225; 1911.

<sup>2</sup> A. Wilm, The hardening of light aluminum alloys, *Metallurgie*, 8, p. 650.

<sup>3</sup> L. M. Cohn, Duralumin, *Verh. Z. Beforderung des Gewerbefortschritts*, 89, p. 643; 1910.

<sup>4</sup> L. M. Cohn, Changes in the physical properties of aluminum and its alloys, with special reference to duralumin, *Elektrotechnik u. Maschinenbau*, 81, p. 430; 1913.

<sup>5</sup> L. M. Cohn, Duralumin, *Elektrotechnik u. Maschinenbau*, 80, pp. 809, 829; 1912.

<sup>6</sup> P. D. Merica, Aluminum and its light alloys, Circular 76 of the Bureau of Standards, 1918, also *Chem. and Met. Eng.*, 19, pp. 135, 200, 329, 587, 635, 729, 780; 1918.

of aging, which may be from one to three days. Cohn (see notes 3 and 5, p. 271) gives data showing the increase of hardness of duralumin during aging, after quenching in water from about 450° C. Upon annealing the alloy so hardened by aging, it is softened exactly as is hardened steel.

The composition of this alloy usually varies within the following limits:

	Per cent
Copper.....	3 —4.5
Magnesium.....	0.4—1.0
Manganese.....	0 —0.7
Aluminum.....	Balance
Iron (as impurities).....	0.4—1
Silicon (as impurities).....	0.3—0.6

Its density is about 2.8. It is used only in the forged or rolled condition.

This alloy has been produced for some years commercially and is in demand for the fabrication of parts for which both lightness and strength are required, such as for aircraft. Its tensile strength will average 50 000 to 60 000 pounds per square inch after appropriate heat treatment, such as that described by Wilm.

With the purpose of ascertaining whether the heat treatment described by him actually developed the best mechanical properties possible for duralumin, the authors undertook a study of the effect of variation in heat-treatment conditions, that is, quenching temperature, aging temperature, etc., upon these properties and, in connection with another investigation,<sup>7</sup> a study of the effect of chemical composition upon them.

E. Blough had already called the attention of one of the authors to the fact that the amount of hardening produced by heat treatment was influenced quite markedly by the temperature from which the material was quenched, a most interesting fact which was not brought out by Wilm's published investigations, which mentioned merely the effect of aging after quenching from one temperature, in the neighborhood of 450° C.

An explanation was sought also for the mechanism of hardening during aging of this alloy, and additional data were obtained bearing upon this phase of the matter.

The experiments here described were carried out partly in the laboratories of the Bureau of Standards and partly in cooperation

<sup>7</sup> P. D. Merica, R. G. Waltenberg, and A. N. Finn, The tensile properties and resistance to corrosion of rolled light alloys of aluminum and magnesium with copper, with nickel, and with manganese, *Technology Paper No. 132* of the Bureau of Standards, 1919.

with the Aluminum Company of America in its laboratories at New Kensington. The alloys used were prepared at the New Kensington plant of this company, and the authors wish to express their appreciation of the assistance and cooperation which has been given throughout by this company through E. Blough, chief chemist. H. H. Beatty of Mr. Blough's staff was active in assisting this work.

## II. COMPOSITION AND PREPARATION OF ALLOYS

In Table 1 are given the chemical compositions of the alloys of the aluminum-copper-magnesium series which were used in these experiments. The ingots, 12 by 24 by 3½ inches, were rolled hot at about 410° C to ¼ inch thick and thereupon cold rolled to 0.081 inch (12 B. & S. gage), annealed at about 425° C, rolled cold to 0.051 inch (16 B. & S. gage), annealed again and cold rolled to 0.032 inch (20 B. & S. gage). The casting and rolling was done at the New Kensington plant of the United States Aluminum Co.

TABLE 1.—Chemical Composition of Alloys <sup>a</sup>

Number	Aluminum	Magnesium	Copper	Iron	Silicon
C1.....	97.27	1.16	0.72	0.56	0.29
C2.....	96.69	2.37	.04	.62	.28
C3.....	97.15	None	2.15	.36	.34
C4.....	96.65	2.84	.04	.27	.20
C5.....	96.11	None	3.19	.40	.30
C6.....	96.72	2.03	.72	.30	.23
C7.....	96.62	1.00	1.80	.35	.23
C8.....	96.68	1.07	1.67	.33	.23
C9.....	95.98	3.50	.08	.26	.18
C10.....	95.83	2.95	.74	.27	.21
C11.....	95.51	1.26	2.58	.41	.22
C12.....	95.74	.46	3.18	.34	.24
A1-12.....	95.48	.64	3.22	.39	.27
E3.....	96.80	1.06	1.56	.32	.26
M4.....	94.36	1.08	3.74	.52	.30
E4.....	94.47	1.06	3.68	.50	.29

<sup>a</sup> Aluminum by difference.

## III. HEAT TREATMENT AND AGING

Tensile tests and scleroscope measurements were made upon specimens taken (1) from the sheets as rolled, (2) from the rolled sheets, annealed, and (3) from the rolled sheets after heat treatment consisting of heating to various temperatures in a gas or

electric furnace, quenching in water, and aging at room or other temperatures for different periods. The results of these tests are given in Table 2.

**TABLE 2.**—The Tensile Properties and Scleroscope Hardness of Rolled, of Annealed, and of Heat-treated Aluminum-Copper-Magnesium Alloys

Number	As rolled			After annealing at 422° C		
	Sclero- scope hardness magnifying hammer	Tensile strength	Elonga- tion in 2 inches	Sclero- scope hardness magnifying hammer	Tensile strength	Elonga- tion in 2 inches
		Lbs./in. <sup>2</sup>	Per cent		Lbs./in. <sup>2</sup>	Per cent
C1 .....	42	49 000	2.0	15.5	33 000	.....
		48 400	2.5		33 100	15.0
		48 600	2.5		32 700	14.0
		49 600	2.5		.....	.....
C2 .....	19	25 800	4.0	7.5	16 600	35.0
		23 600	3.0		15 900	35.0
		23 600	3.5		16 100	33.0
		34 900	2.5		21 600	31.0
C3 .....	35	35 700	.....	7.0	21 800	33.0
		34 000	1.5		22 000	33.5
		38 400	.....		29 200	18.0
C4 .....	37	38 600	1.5	10.5	29 200	18.0
		37 200	1.5		29 400	21.0
		35 900	.....		23 000	30.0
C5 .....	34	37 500	2.5	8.0	22 400	28.5
		37 700	2.0		22 800	32.5
		35 300	1.0		30 500	.....
C6 .....	38	38 500	0.5	13.0	29 900	18.5
		38 100	1.5		30 800	16.0
		44 200	2.0		35 300	26.0
C7 .....	44	45 500	2.0	17.0	34 600	25.5
		45 300	.....		34 800	25.0
		38 100	1.5		28 500	18.5
C8 .....	38	38 100	.....	12.5	29 100	18.5
		41 200	1.5		31 600	17.5
		43 200	1.5		31 200	17.5
C9 .....	38	41 200	1.5	12.0	30 500	.....
		44 800	1.5		30 600	19.0
		44 600	1.5		30 200	19.0
C10 .....	45	47 500	1.5	12.0	30 200	17.0
		56 700	2.0		34 900	20.5
		52 900	1.5		36 000	24.0
C11 .....	50	58 400	2.0	15.5	.....	.....
		38 900	5.0		23 100	24.0
		38 600	5.0		23 000	24.0

**TABLE 2.—The Tensile Properties and Scleroscope Hardness of Rolled, of Annealed, and of Heat-treated Aluminum-Copper-Magnesium Alloys—Continued**

Number	After heat treatment consisting of quenching in water and aging									
	Quenched from 478° C					Quenched from 510° C				
	Aging		Scleroscope hardness magnifying hammer	Tensile strength	Elongation in 2 inches	Aging		Scleroscope hardness magnifying hammer	Tensile strength	Elongation in 2 inches
	Aged at 110°	Aged at 20°				Aged at 110°	Aged at 20°			
	Days	Days		Lbs./in. <sup>2</sup>	P. ct.	Days	Days		Lbs./in. <sup>2</sup>	P. ct.
C1		11	20	36 870	18.5		11	17	38 030	17.0
		11		37 080	17.0		11		37 220	16.5
		11		36 260	14.0	3	8		48 120	16.0
C2		11	8			3	8	8	47 210	18.5
		11		16 830	39.0		11		16 670	34.0
		11		16 510	38.5		11		16 670	33.0
C3		11	11	16 510	38.5	3	8	13	16 510	28.0
		11				3	8		16 510	33.0
		11		28 020	15.5		11		26 350	19.0
C4		11	14	25 810	25.0		11	11	27 690	11.5
		11		25 440	25.0	3	8		29 420	20.0
		11				3	8		27 790	19.5
C5		11	15	29 300	20.0		11	14	30 060	23.0
		11		28 910	20.0		11		29 700	16.5
		11		30 280	22.0	3	8		31 590	19.0
C6		11	15			3	8	14	31 350	20.0
		11				3	8		31 960	15.5
		11		33 220	15.0		11		30 500	14.0
C7		11	14	32 580	18.5		11	15	30 910	19.0
		11		31 930	16.0	3	8		33 970	
		11				3	8		38 370	17.0
C8		11	23.5	31 050	20.0		11	26	33 950	23.5
		11		33 790	19.0		11		43 190	18.5
		11		31 640	17.5	3	8		43 560	18.0
C9		11	26			3	8	24	45 650	18.5
		11		42 350	21.0		11		45 740	19.5
		11		42 530	21.0	3	8		53 970	20.0
C10		11	28.5	42 350	21.0		11	22	52 250	
		11				3	8		44 130	24.5
		11		46 400	19.5		11		44 910	23.0
C11	7	6	31	47 030			11	32	49 680	19.5
	7	6		48 900	20.0	3	8		51 530	17.0
		11		47 650	22.0	3	8		29 120	21.0
C12		11	15	31 790	21.5		11	13	29 500	22.0
		11		30 450	18.0		11		30 270	23.0
		11		30 070	14.0	3	8		30 270	22.0
C13		11	14			3	8	14	37 430	24.5
		11		38 030	26.0		11		37 630	21.5
		11		37 630	25.0		11		47 690	21.5
C14		11	28	38 430	22.5	3	8	26	47 690	22.5
		11				3	8		51 520	21.0
		13		50 450			11		50 870	24.0
C15		13	31	48 950	22.0		11	34	54 740	23.0
	7	6		51 740	22.0	3	8		55 590	20.0
	7	6		50 880	22.0	3	8		42 370	14.5
C16		11	19-23	38 330	14.0		11	25-28	39 340	16.5
		11		38 730	13.5		11		49 230	26.5
		11		35 910	12.5	3	8		49 830	25.5

TABLE 2.—The Tensile Properties and Scleroscope Hardness of Rolled, of Annealed, and of Heat-treated Aluminum-Copper-Magnesium Alloys—Continued

Number	After heat treatment consisting of quenching in water and aging—Continued								
	Quenched from 520° C				Quenched from 525° C				
	Aged at 20°	Scleroscope hardness magnifying hammer	Tensile strength	Elongation in 2 inches	Aging		Scleroscope hardness magnifying hammer	Tensile strength	Elongation in 2 inches
					Aged at 110°	Aged at 20°			
	Days		Lbs./in. <sup>2</sup>	P. ct.	Days	Days		Lbs./in. <sup>2</sup>	P. ct.
C1.....	11	18.5	36 870	18.5		11	16	37 220	14.0
	11		36 910	19.0		11		38 130	17.0
					3	8		50 140	17.0
					3	8		49 930	17.5
C2.....	11	8	13 970	37.0		11	8	16 350	
	11		14 290	35.0		11		16 870	35.0
					3	8		16 980	31.0
					3	8		17 340	30.0
C3.....	11	13	24 700	18.5		11	13	28 550	23.0
	11		25 440	21.0		11		28 640	
					3	8		26 800	17.5
					3	8		26 980	20.0
C4.....	11	12	27 540	22.0		11	12	29 600	20.5
	11		27 150	20.0		11		29 100	22.0
					3	8		34 850	17.0
					3	8		35 350	16.5
C5.....	11	14	29 150	13.0		11	10.5	29 540	19.0
	11		29 580	16.0		11		32 490	16.5
					3	8		28 170	23.0
					3	8		27 960	26.0
C6.....	11	17	36 140	21.5		11	15	34 980	17.5
	11		33 990	19.5		11		35 470	18.0
					3	8		47 580	20.5
					3	8		45 840	16.5
C7.....	11	25	42 530	22.5		11	16	46 850	20.5
	11		42 160	22.5		11		46 760	19.5
					3	8		54 170	21.0
					3	8		56 110	19.0
C8.....	11	25.5	45 160	26.0		11	25	46 520	23.0
	11		44 720	25.0		11		46 030	25.5
	11		44 720	21.0	3	8		53 440	21.0
	11		44 070	22.0	3	8		53 000	19.0
C9.....	11	13	29 500	22.5		11	13	33 790	21.0
	11		30 070	19.5		11		32 510	17.5
					3	8		34 800	17.5
					3	8		34 890	18.0
C10.....	11	14.5	37 430	23.0		11	15	35 160	22.5
	11		38 230	22.0		11		35 430	22.0
					3	8		44 260	19.9
					3	8		46 450	20.0
C11.....									
C12.....						11	22	42 660	14.0
						11		36 500	19.9
					3	8		50 890	23.0



All of the alloys except those containing no copper (Nos. C2 C4, and C9) show an increase of hardness of the heat-treated specimens over that of the annealed samples. The increase of hardness in those alloys containing copper, but no magnesium, is smaller than that in those containing both, but is quite definite. This is shown in the following table:

Number of alloy	Increase of tensile strength of heat-treated alloy (510° C) over annealed alloy
<b>Alloys containing no copper:</b>	<b>Per cent</b>
C2.....	+ 2
C4.....	+ 3
C9.....	- 4
<b>Alloys containing copper but no magnesium:</b>	
C3.....	+30
C5.....	+36
<b>Alloys containing both copper and magnesium:</b>	
C1.....	45
C11.....	56
C12.....	110

It is noticed that the best mechanical properties are produced by quenching from the higher temperatures (500 to 525° C). This is shown in Table 3, giving further data on two alloys, C8 and C11, and will be shown more clearly below.

TABLE 3.—Effect of Quenching Temperature on Tensile Properties

Quenching temperature	Alloy C8					Alloy C11				
	Aging		Mechanical properties			Aging		Mechanical properties		
	20° C	110° C	Sclero-scope hard-ness	Ultimate tensile strength	Elonga-tion in 2 inches	20° C	110° C	Sclero-scope hard-ness	Ultimate tensile strength	Elonga-tion in 2 inches
	Days	Days		Lbs./in. <sup>2</sup>	Per ct.	Days	Days		Lbs./in. <sup>2</sup>	Per ct.
371° C.....	13	.....	11	27 260	16.0	13	.....	18	35 900	19.0
	13	.....		26 220	18.0	13	.....		36 550	17.0
	7	6	12	29 130	18.5	7	6	17	35 020	21.0
	7	6		29 130	20.0	7	6		35 020	21.0
422° C.....	13	.....	23	39 540	12.0	13	.....	25	43 790	15.5
	13	.....		40 160	13.5	13	.....		43 360	18.5
	7	6	23	41 200	17.0	7	6	24	44 010	23.5
	7	6		41 200	22.0	7	6		43 580	24.0
478° C.....	13	.....	26	46 400	19.5	13	.....	28	50 450	.....
	13	.....		47 030	.....	13	.....		48 950	22.0
	7	6	28.5	48 900	20.0	7	6	31	51 740	22.0
	7	6		47 650	22.0	7	6		50 880	22.0
500° C.....	11	.....	27	47 230	18.5	11	.....	28	52 990	20.5
	11	.....		47 860	20.5	11	.....		52 990	21.0
	11	.....	22	44 130	24.5	11	.....	29.5	51 520	21.0
	11	.....		44 910	23.0	11	.....		50 870	24.0
510° C.....	8	3	32	49 680	19.5	8	3	34	54 740	23.0
	8	3		51 530	17.0	8	3		55 590	20.0
520° C.....	11	.....	25.5	45 160	26.0	.....	.....	.....	.....	.....
	11	.....		44 720	25.0	.....	.....	.....	.....	.....
	11	.....		44 720	21.0	.....	.....	.....	.....	.....
	11	.....		44 070	22.0	.....	.....	.....	.....	.....
525° C.....	11	.....	25	46 520	23.0	.....	.....	.....	.....	.....
	11	.....		46 030	25.5	.....	.....	.....	.....	.....
	8	3	31	53 440	21.0	.....	.....	.....	.....	.....
	8	3		53 000	19.0	.....	.....	.....	.....	.....
533° C.....	13	.....	30-35	34 960	5.0	13	.....	33	48 370	9.5
	13	.....		40 570	9.0	13	.....		47 060	10.0

Not only does the hardness increase after heat treatment, but so also does the ductility, as evidenced by the elongation in the tensile test. This is shown in Tables 2 and 3.

### 1. EFFECT OF QUENCHING TEMPERATURE

In Fig. 1 are shown the scleroscope hardness values of C11 quenched in water (20° C) from different temperatures and aged at room temperature for periods of time from a few hours to 30 days. The form of these aging curves is similar to that shown by Cohn (see notes 3 and 5 on p. 271); that is, the hardness increases after quenching, at first rapidly and then more slowly. It is fur-

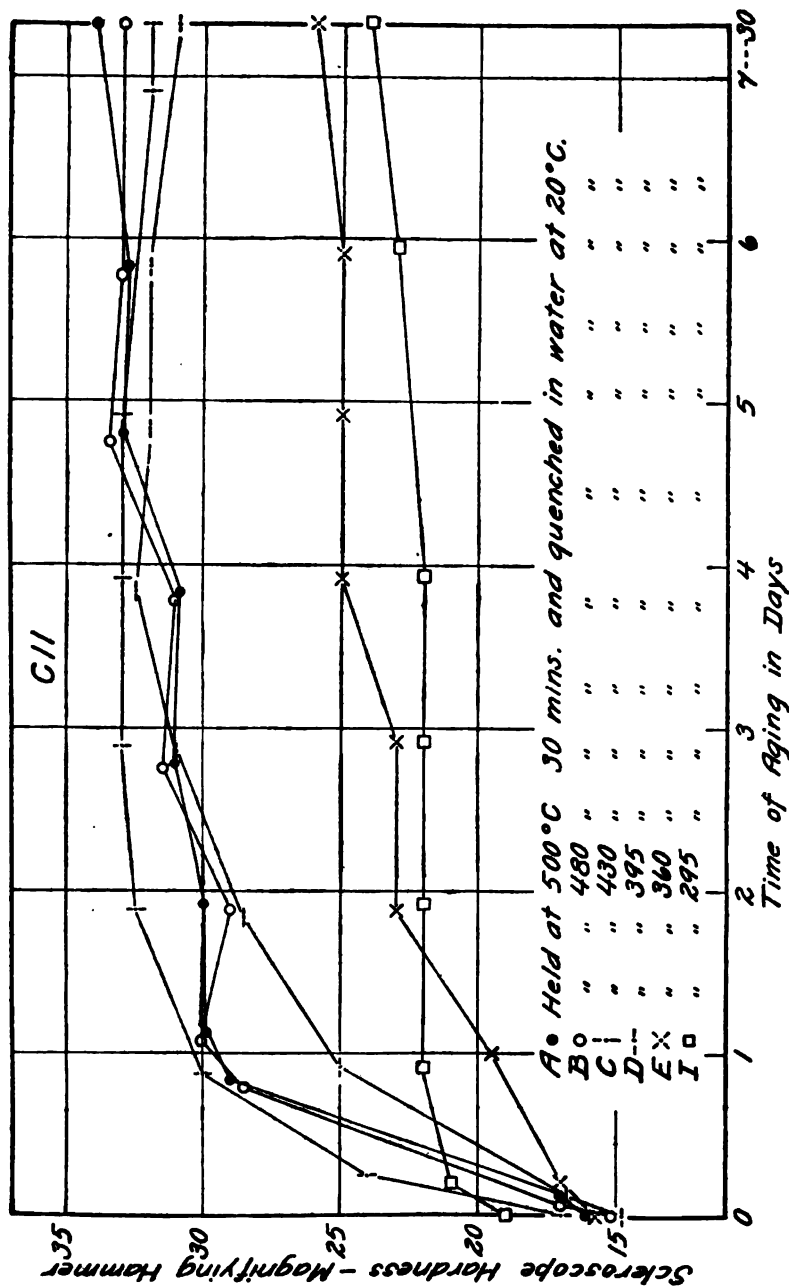


FIG. 1.—Effect of quenching temperature on the scleroscope hardness during aging of quenched specimens of C-11

ther evident that the maximum hardness attained increases with the temperature up to approximately  $520^{\circ}\text{C}$ .

The effect of quenching temperature is also shown very nicely in an experiment of which the results are shown in Fig. 2. Two strips of 0.087-inch sheet of alloy N34 were used. The strip was placed in the furnace for heating in such a manner that a nearly linear temperature gradient existed between the two ends, as

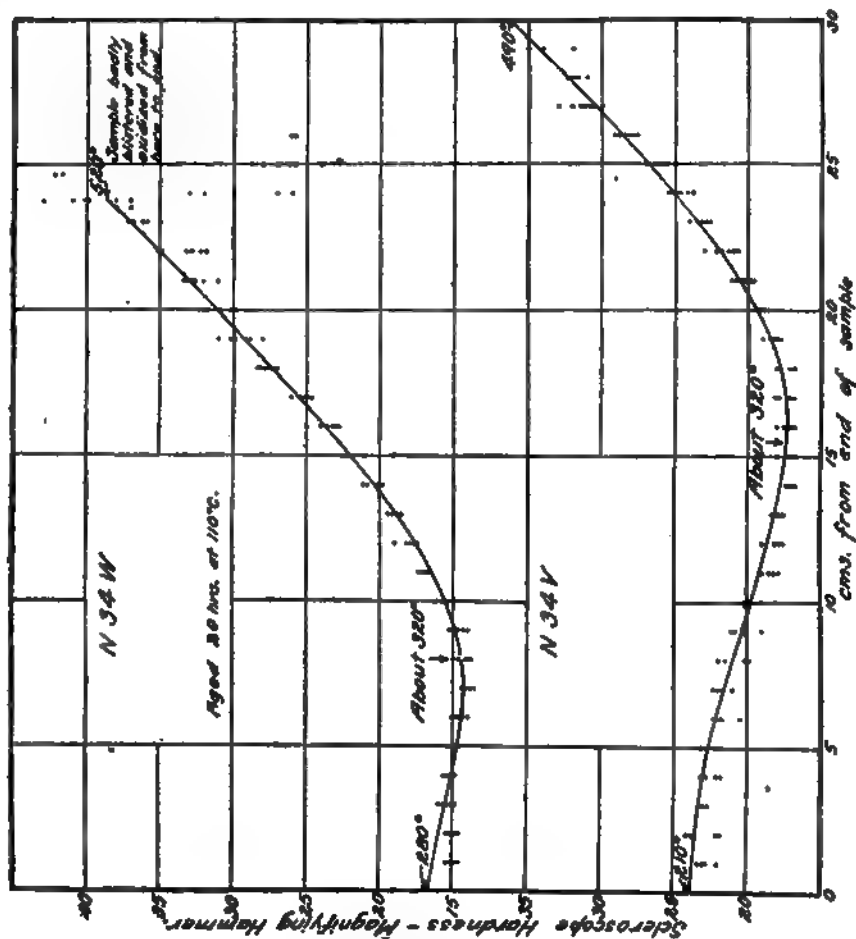


FIG. 2.—Effect of quenching temperature on scleroscope hardness. (Alloy N-34)

shown by thermocouples placed along the strip. Upon attaining the desired range of temperatures, the strip was quenched in boiling water and aged 20 hours at  $110^{\circ}\text{C}$ . The scleroscope hardness was then determined along the axis of the strip, and is shown in Fig. 2 as a function of the distance from one end of the sample. The distance may be regarded as a rough temperature

scale, the outside temperature limits having been determined and marked on the curve. One strip was quenched when the two ends were at 520 and 280° C, respectively; the other, when the ends were at 490 and 210° C, respectively. Beginning at about 300° C, the effect of increased quenching temperature, other factors remaining alike, is to increase the hardness after aging until a temperature of about 520° C is reached. Beyond that temperature the hardness again decreases; the material becomes covered with a dark gray oxide coating and generally also with blisters, marking the temperature of eutectic melting. The effect of heating to temperatures around 300° C is chiefly to anneal the specimen and to give lower values of the hardness (minimum on the curve) than is given by heating at lower temperatures.

## 2. EFFECT OF AGING TEMPERATURE

In Table 4 are given results of tests showing the effect of temperature of quenching bath and of aging carried out in the bath. The samples used were strips of A1-12 quenched from 520° C. The increase of strength with time of aging is evident.



A more complete picture of the phenomenon of hardening by aging at different temperatures is obtained from Figs. 3, 4, and 5, based upon data obtained on specimens of N34. The scleroscope values of Fig. 3 were obtained upon samples quenched in boiling water from two temperatures, 515 and 525° C, and aged at different temperatures. The same figures are replotted in Fig. 4 in different form.

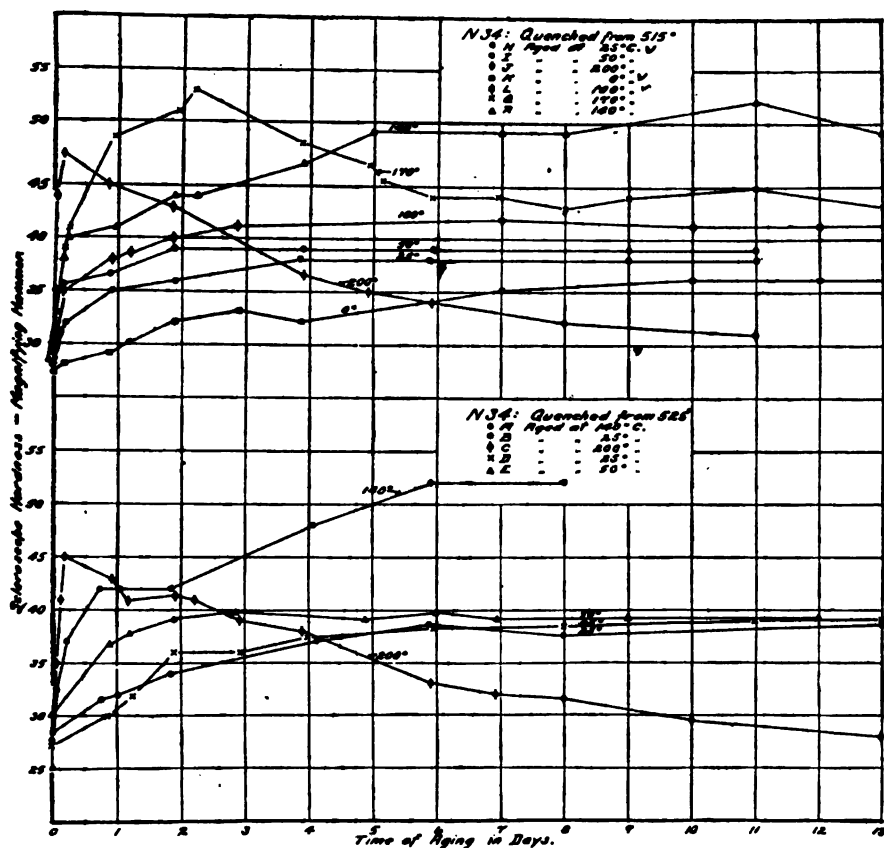


FIG. 3.—Effect of aging at different temperatures on the scleroscope hardness of samples quenched from 515°C and 525°C. (Alloy N-34)

It is noted (1) that the rate of hardening increases as the temperature of aging increases, (2) that the maximum hardness is obtained by aging at temperatures above 100° C, and (3) that at aging temperatures above 140° C the hardness eventually drops after reaching its maximum.

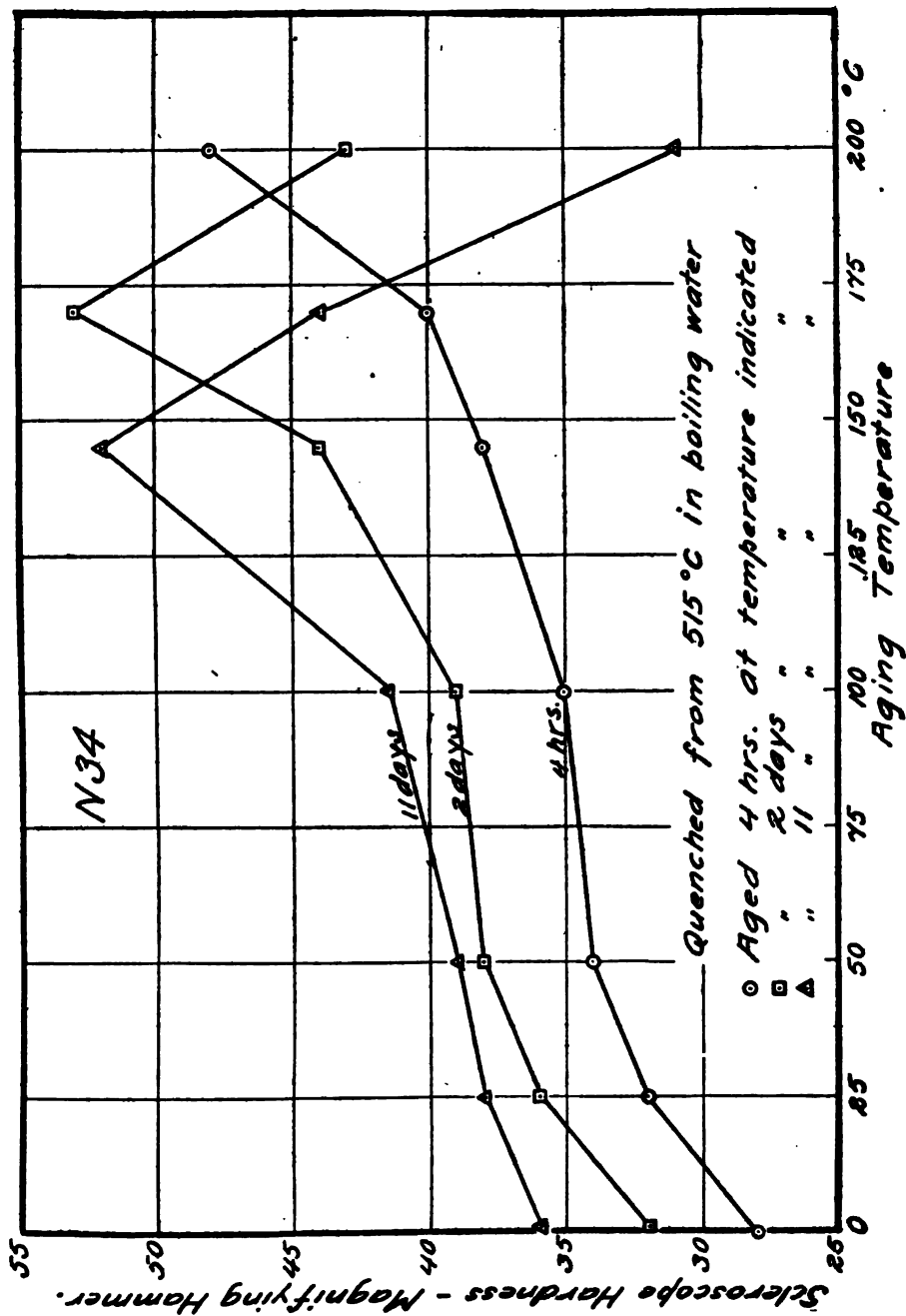


FIG. 4.—Effect of temperature of aging on scleroscope hardness. (Alloy N-34)



Fig. 5 shows the results of an experiment similar to that of Fig. 2. The strips were quenched from  $515^{\circ}\text{C}$  in boiling water and aged for 20 hours thereafter in a furnace giving a temperature gradient from one end to the other of the sample. For a time of aging of 20 hours the hardness first increases with the temperature to a maximum at about  $180^{\circ}\text{C}$  and then decreases. Above this temperature annealing sets in.

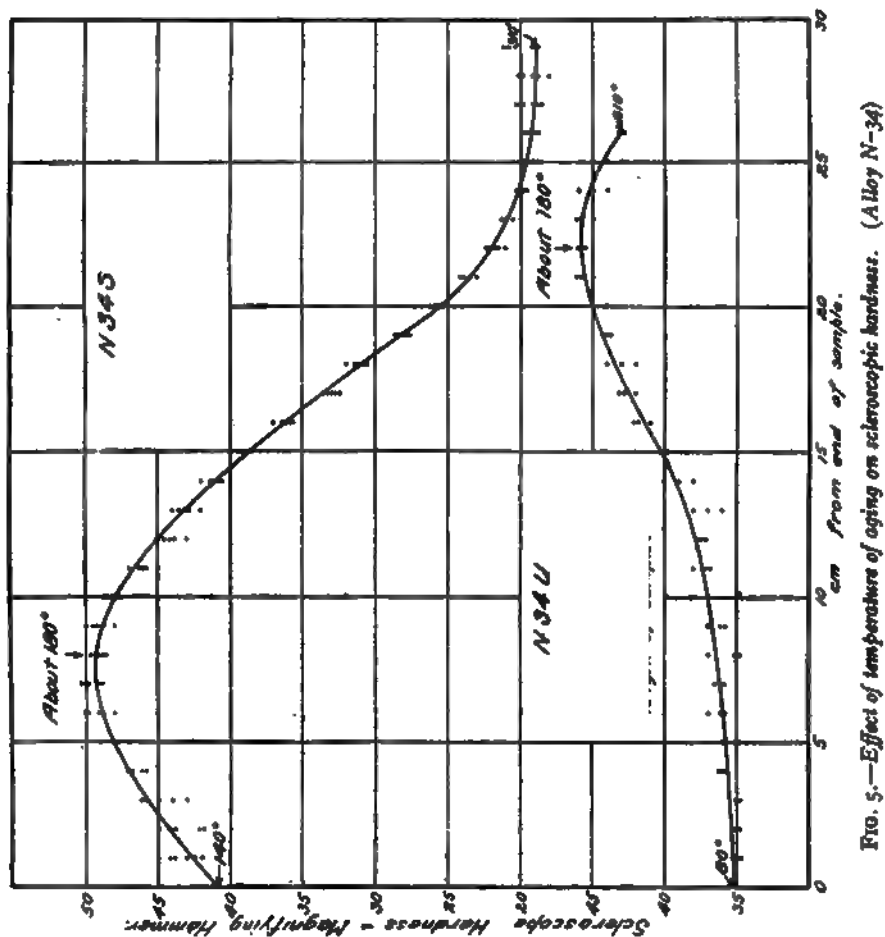


FIG. 5.—Effect of temperature of aging on scleroscopic hardness. (Alloy N-34)

### 3. EFFECT OF TEMPERATURE OF QUENCHING BATH

Table 5 shows the effect of temperature of the quenching bath upon samples of A1-12 quenched from  $520^{\circ}\text{C}$ .

It is noticed that the tensile strength of the alloys, as well as the elongation, increases with the time of aging. There is no marked

effect of the temperature of the quenching bath indicated in these results. Those samples quenched to  $150^{\circ}\text{C}$  gave practically the same results as those quenched to  $230^{\circ}\text{C}$ , although there is a slight improvement in the tensile properties of those quenched to  $150^{\circ}\text{C}$  over those quenched to  $100^{\circ}\text{C}$ .

In Table 6 are shown results of tests to determine the effect of aging at room temperature after aging at the temperature of the quenching bath. It will be noted that there is only a slight increase in the strength of the alloy produced by aging at  $20^{\circ}\text{C}$  after aging at the temperature of the quenching bath.

TABLE 5.—Effect of Quenching in Baths at Different Temperatures, Followed by Aging at Room Temperature (20° C)

[Specimen of alloy Al-12 quenched to room temperature from 540° C]

Hours aged	Quenched to 100° C; aged at 20° C				Quenched to 150° C; aged at 20° C				Quenched to 200° C; aged at 20° C				Quenched to 230° C; aged at 20° C			
	Tensile strength		Elongation in 2 inches		Tensile strength		Elongation in 2 inches		Tensile strength		Elongation in 2 inches		Tensile strength		Elongation in 2 inches	
	Lbs./in. <sup>2</sup>	Per cent	Per cent	Scleroscope hardness	Lbs./in. <sup>2</sup>	Per cent	Per cent	Scleroscope hardness	Lbs./in. <sup>2</sup>	Per cent	Per cent	Scleroscope hardness	Lbs./in. <sup>2</sup>	Per cent	Per cent	Scleroscope hardness
0	41 800	27.0	20	20	43 250	23.5	23.5	23	42 950	20.5	23.5	23	41 950	23.5	24	24
0	41 250	22.0	21	21	43 550	23.0	23.0	23	43 600	19.5	23.0	23	42 500	26.0	24.5	24.5
1/4									49 300	15.5		39-40	45 500	21.5	25	25
1/2									50 450	14.0		39	44 900	26.0	25	25
1	45 750	21.5	25	25	44 500	26.0	26.0	25.5	49 750	15.0	15.0	37-39	44 100	22.5	25-28	25-28
1	45 025	22.0	24	24	44 050			25	48 550	15.0		36-37	45 000	22.0	26	26
1 1/2	44 900	19.0	24	24												
1 1/2	44 450	23.0	24	24												
2	44 550	23.0	24	24												
2																
3					43 850			24	50 100	16.0		37	44 850		25	25
3					44 600	27.0	27.0	23.5	49 000	11.5	11.5	37	43 700	23.0	22-25	22-25
3									49 100	16.5	16.5	37				
19	44 700	24.5	25	25					50 950	16.0	16.0	37-39				
19	47 100	24.5	27	27					48 850	16.0	16.0	37				
48	45 950	25.5	26	26					48 950	12.5	12.5	38				
48	47 000	22.0	26	26					49 250	16.0	16.0					
96	47 000	22.0	26	26					48 950	14.0	14.0					
96	48 250	22.0	26	26	51 500	20.0	20.0	31					51 600	25.0	30	30
96					52 500			30					50 400	24.0	30	30

TABLE 6.—Effect of Aging at Room Temperature (20° C) After Aging at Temperature of Bath

[Specimens of alloy Ar-12 quenched from 550° C]

## AGED ¼ HOUR AT QUENCHING TEMPERATURE

Hours aged at 20° C	Quenched to 100° C; aged at 20° C			Quenched to 150° C; aged at 20° C			Quenched to 200° C; aged at 20° C			Quenched to 230° C; aged at 20° C		
	Tensile strength	Elongation in 2 inches	Scleroscope hardness	Tensile strength	Elongation in 2 inches	Scleroscope hardness	Tensile strength	Elongation in 2 inches	Scleroscope hardness	Tensile strength	Elongation in 2 inches	Scleroscope hardness
	Lbs./in. <sup>2</sup>	Per cent		Lbs./in. <sup>2</sup>	Per cent		Lbs./in. <sup>2</sup>	Per cent		Lbs./in. <sup>2</sup>	Per cent	
¼	.....	.....	.....	.....	.....	.....	.....	.....	.....	.....	.....	.....
¼	.....	.....	.....	.....	.....	.....	.....	.....	.....	.....	.....	.....
1	.....	.....	.....	49 100	26.0	31	.....	.....	.....	45 150	10.0	35
1	.....	.....	.....	50 500	23.0	31	.....	.....	.....	46 250	10.0	37
2	.....	.....	.....	49 500	25.5	28	.....	.....	.....	42 850	12.0	32
2	.....	.....	.....	49 600	26.0	28-30	.....	.....	.....	42 600	10.5	35
3	.....	.....	.....	.....	.....	.....	.....	.....	.....	45 750	9.0	36
3	.....	.....	.....	.....	.....	.....	.....	.....	.....	46 100	10.5	36
96	.....	.....	.....	a 50 800	.....	a 31	.....	.....	.....	.....	.....	.....
96	.....	.....	.....	a 52 000	a 25.5	a 31	53 200	10.0	40	48 500	10.0	34
96	.....	.....	.....	.....	.....	.....	51 700	12.0	41	46 450	8.5	34

## AGED 1 HOUR AT QUENCHING TEMPERATURE

Hours aged at 20° C	Quenched to 100° C; aged at 20° C			Quenched to 150° C; aged at 20° C			Quenched to 200° C; aged at 20° C			Quenched to 230° C; aged at 20° C		
	Tensile strength	Elongation in 2 inches	Scleroscope hardness	Tensile strength	Elongation in 2 inches	Scleroscope hardness	Tensile strength	Elongation in 2 inches	Scleroscope hardness	Tensile strength	Elongation in 2 inches	Scleroscope hardness
	Lbs./in. <sup>2</sup>	Per cent		Lbs./in. <sup>2</sup>	Per cent		Lbs./in. <sup>2</sup>	Per cent		Lbs./in. <sup>2</sup>	Per cent	
2	.....	.....	.....	49 250	25.5	31	.....	.....	.....	b 47 050	b 9.5	b 38-41
2	.....	.....	.....	50 600	25.0	31	.....	.....	.....	b 47 300	b 9.5	b 36-39
96	.....	.....	.....	a 52 900	.....	a 31	50 600	9.0	43	48 600	.....	87
96	.....	.....	.....	a 52 500	.....	a 31	49 400	7.0	41	48 550	.....	89

AGED 3 HOURS AT QUENCHING TEMPERATURE

2	.....	.....	.....	51 450	24.5	33	.....	.....	b 47 600	b 9.0	b 37
2	.....	.....	.....	48 500	23.0	33	.....	.....	b 47 100	b 9.0	b 37
96	48 900	24.5	28	a 54 600	a 24.0	a 32	53 150	44	50 400	8.5	38
96	47 450	.....	27	a 53 850	a 22.5	a 32	53 550	11.0	50 750	.....	41

AGED 3 HOURS AT QUENCHING TEMPERATURE

2	.....	.....	.....	52 450	22.0	34	.....	.....	.....	.....	.....
2	.....	.....	.....	49 900	23.0	34	.....	.....	.....	.....	.....
96	.....	.....	.....	.....	.....	.....	54 950	43	.....	.....	.....
96	.....	.....	.....	a 56 250	a 19.5	a 32.5	54 550	10.0	.....	.....	.....

AGED 19 HOURS AT QUENCHING TEMPERATURE

96	51 000	24.5	.....	.....	.....	.....	.....	.....	.....	.....	.....
96	51 550	.....	.....	.....	.....	.....	.....	.....	.....	.....	.....

AGED 48 HOURS AT QUENCHING TEMPERATURE

96	52 000	20.5	.....	.....	.....	.....	.....	.....	.....	.....	.....
96	51 600	23.5	.....	.....	.....	.....	.....	.....	.....	.....	.....

a These specimens were aged at 20° C for 120 hours.

b Aged ½ hour at 20° C.

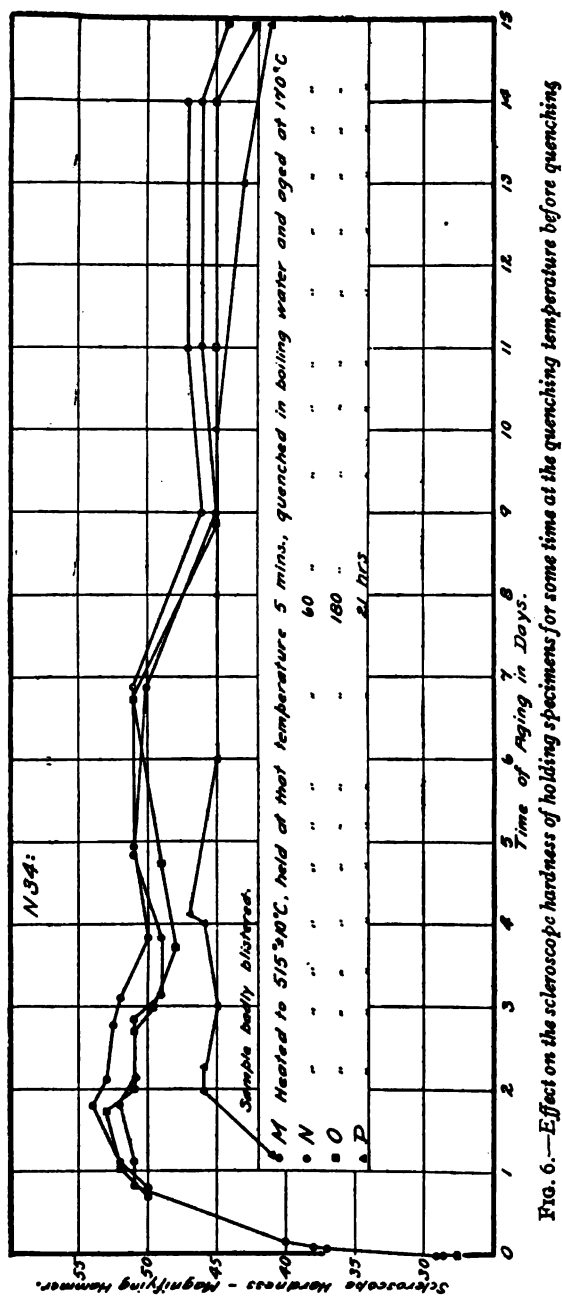


FIG. 6.—Effect on the scleroscope hardness of holding specimens for some time at the quenching temperature before quenching

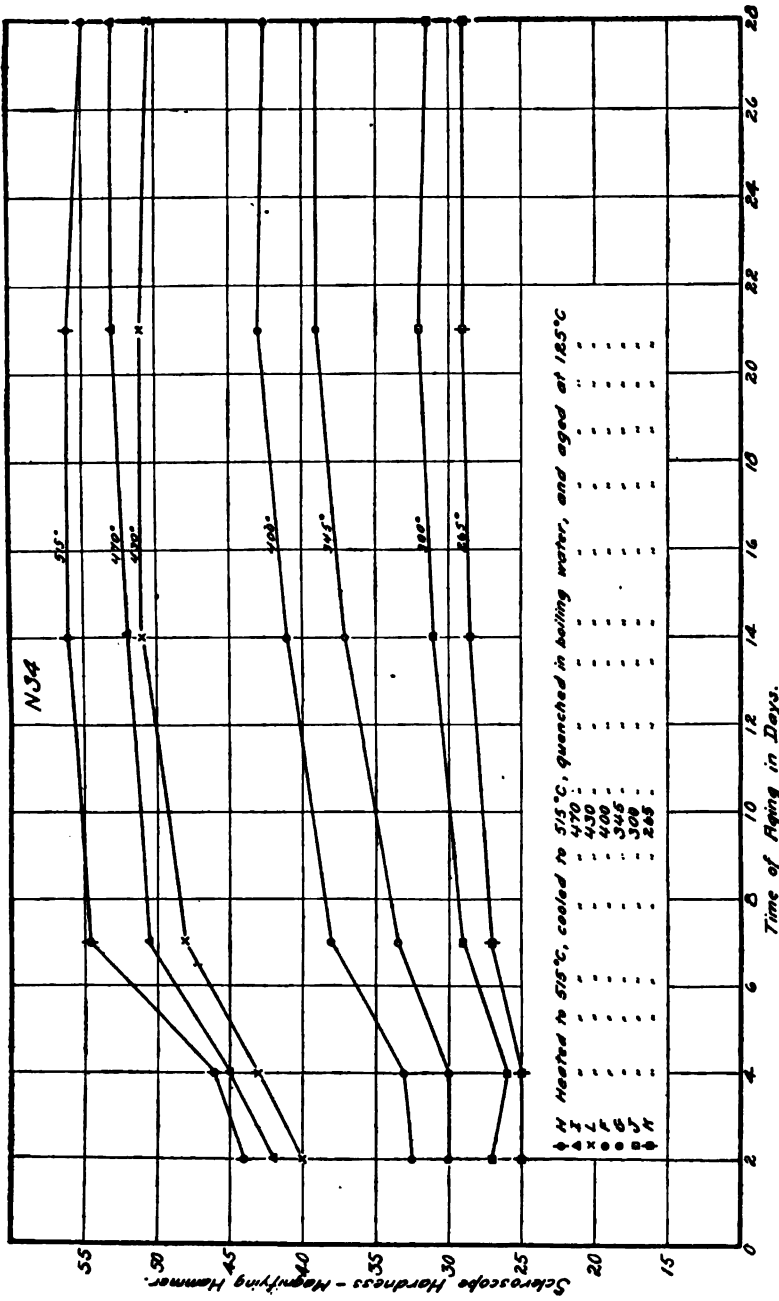


FIG. 7.—Effect on scleroscope hardness of preheating specimens higher than the quenching temperature, cooling to the latter, then quenching and aging

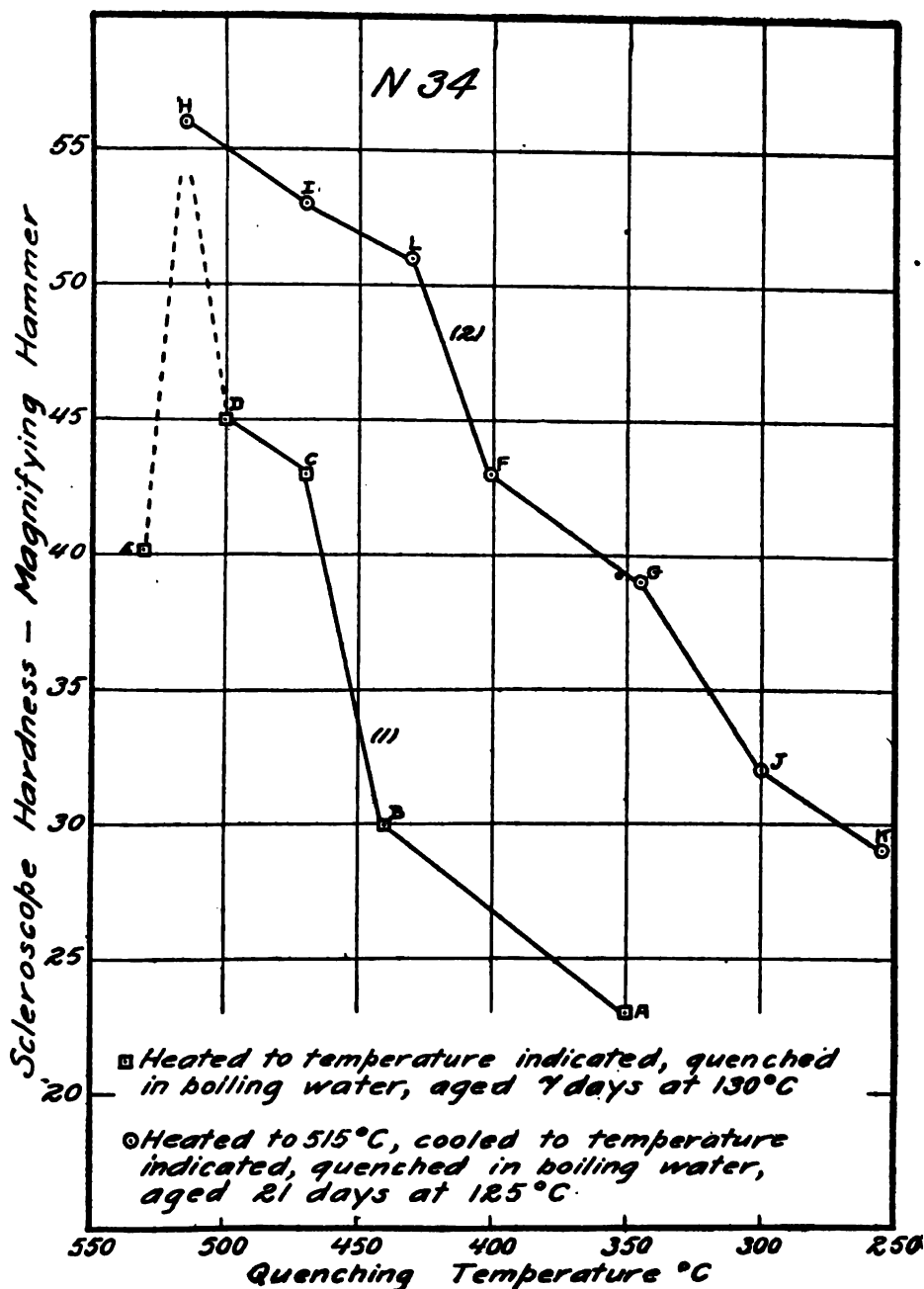


FIG. 8.—Comparison of scleroscope hardness of specimens of Alloy N-34, (1) heated to quenching temperature, quenched and aged 7 days at 130° C, and (2) heated to 515° C, cooled to quenching temperature, quenched and aged 21 days at 125° C



#### 4. EFFECT OF PRIOR HEATING AT THE QUENCHING TEMPERATURE

Fig. 6 shows the results of hardness measurements on samples held at the quenching temperature for varying periods of time quenched and aged at  $170^{\circ}\text{C}$ . The samples held from 5 to 180 minutes at the quenching temperature give values of the hardness differing by less than the probable error of measurement. The low values found on the sample held 21 hours are due probably to the blistering which was noticed in the sample.

#### 5. EFFECT OF PREHEATING TO $515^{\circ}\text{C}$ BEFORE QUENCHING FROM LOWER TEMPERATURES

In Figs. 7 and 8 are shown the results of experiments to determine whether preheating to a temperature higher than the quenching one before quenching gave a different hardness than by heating merely to the quenching temperature.

Although owing to a slight difference in the aging conditions the comparison is not quite definite, it is obvious (1) that the hardness obtained by heating to  $515^{\circ}\text{C}$ , cooling to a temperature,  $t$  (when  $t < 515^{\circ}\text{C}$ ), and quenching is always greater than that obtained by quenching from  $t^{\circ}$ , and (2) that whether the specimen is preheated or not to a higher temperature before quenching from some lower temperature the hardness obtained increases with higher quenching temperatures.

### IV. MISCELLANEOUS TESTS

In Table 7 are shown the results of a number of tests of alloy N34, including determinations of the proportional limit of several heat-treated samples.

TABLE 7.—Effect of Varying Aging Temperature and Time of Aging on the Tensile Properties of Aluminum Alloy Sheet <sup>a</sup> (Alloy N34)

No.	Thick- ness of sheet	Heat treatment quenched from—	Aged at—	Aged	Sclero- scope hard- ness magnify- ing ham- mer	Ultimate strength	Propor- tional limit	Elen- gation in 2 inches	Remarks
	Inch	° C	° C	Days		Lbs./in. <sup>2</sup>	Lbs./in. <sup>2</sup>	Per ct.	
14	0.034	515	.....	0	26	.....	17 000	5	Broke at extensometer contact.
15	.034	515	.....	0	26	38 200	17 000	6	Do.
24	.034	515	105	2	39	52 900	27 000	7	Do.
25	.034	515	105	2	39	54 900	29 000	7	Do.
26	.034	515	105	4	39	55 500	27 000	9	Do.
27	.034	515	105	4	39	55 200	26 000	8.5	Do.
28	.034	515	105	7	38	63 200	.....	23	No extension measurements.
29	.034	515	105	7	38	56 200	29 000	9	Broke at extensometer contact.
30	.034	515	105	9	42	61 200	30 000	16	Extensometer attached to flat sur- faces. Broke at gage point.
31	.034	515	105	9	41	60 600	29 000	14.5	Do.
32	.034	515	105	14	40	62 200	31 000	21	Extensometer attached to flat sur- faces.
33	.034	515	105	14	41	61 600	33 000	23	Do.
16	.034	515	125	2	41-46	49 500	27 000	2.5	Broke at extensometer contact.
17	.034	515	125	2	42-50	54 500	32 000	3	Do.
18	.034	515	125	4	45-50	58 200	30 000	3	Do.
19	.034	515	125	4	45-50	58 500	33 000	4	Do.
20	.034	515	125	7	44-47	60 000	39 000	4.5	Do.
21	.034	515	125	7	42-48	58 000	37 000	4	Do.
34	.067	515	125	7	46-50	61 200	32 000	18	Extensometer attached to flat sur- face.
35	.067	515	125	7	47-52	62 000	31 000	18	Do.
22	.034	515	125	14	47-52	64 900	37 000	11	Do.
23	.034	515	125	14	47-54	61 500	35 000	3	Extensometer attached to flat sur- face. Fractured at blister.
2	.034	515	150	2	50	51 110	.....	16	No extension measurements.
3	.034	515	150	2	49	50 940	.....	16.5	Do.
4	.034	515	150	4	50	59 800	.....	11.5	Do.
5	.034	515	150	4	50	61 500	41 000	6	Broke at extensometer contact.
6	.034	515	150	6	50	63 800	.....	6	No extensometer measurements.
7	.034	515	150	6	50	62 200	43 000	6.5	Broke at extensometer contact.
1	.067	515	170	2	50	63 900	.....	10	No extension measurements.
8	.034	515	170	2	51.5	51 420	.....	10.5	Do.
9	.034	515	170	2	51.5	51 850	.....	10	Do.
10	.034	515	170	2	51.5	50 760	.....	9.5	Do.
11	.034	515	170	4	44	58 200	.....	9.5	Do.
12	.034	515	170	4	44	55 500	.....	5	Do.
13	.034	515	170	4	.....	57 300	34 000	6	Broke at extensometer contact.

<sup>a</sup> Where two values of the hardness are given the lower one shows the hardness of the end near the door of the furnace in which the sample was heated for quenching, and the other value is the hardness of the opposite end, the difference in hardness being the result of a temperature gradient in the furnace. The specimens in this condition all broke at the soft end and hence their tensile properties are hardly as high as can be expected of the material.



## 1. DENSITY AND DILATATION

The density was determined of samples of N<sub>34</sub> in different conditions, and Table 8 gives the results of these tests. In some cases one dimension of the specimen was determined also, and its changes recorded in column 4 of the same table. The changes in density are quite small as the material undergoes heat treatment or annealing, except when the temperature exceeds from 520 to 530° C, the temperature of eutectic melting, when a marked increase in length is noted.

TABLE 8.—The Density and Length Changes in Duralumin (N<sub>34</sub>)

Sample	Treatment	Density	Length
			Inches
N34 D1.....	Quenched; not aged.....	2.762	.....
N34 D1.....	Same as above, after aging at 150° C.....	2.762	.....
N34 D2.....	Annealed, after rolling, at 515° C.....	2.759	.....
N34 D3.....	As rolled, 0.033 inch thick.....	2.754	12.014
N34 D3-a.....	Same after annealing at 500° C.....	2.742	12.024
N34 D3-a.....	Annealed at 530° C.....	.....	12.0477
N34 D4.....	As rolled, 0.068 inch thick.....	2.750	11.982
N34 D4-a.....	Same after annealing at 500° C.....	2.747	11.982
N34 D4-a.....	Annealed at 530° C.....	.....	11.9973
N34 D5.....	As rolled, 0.25 inch thick.....	2.764	11.9954
N34 D5-a.....	Same after annealing at 500° C.....	2.762	11.9963
N34 D5-a.....	Annealed at 530° C.....	.....	12.0019

The linear expansion up to 520° C was determined on two bars of N34, one as rolled, the other after heat treatment, consisting of quenching from 520° C and aging two days at 120° C. The expansion curves are given in Fig. 10 and show irregularities in the neighborhood of 300° C.

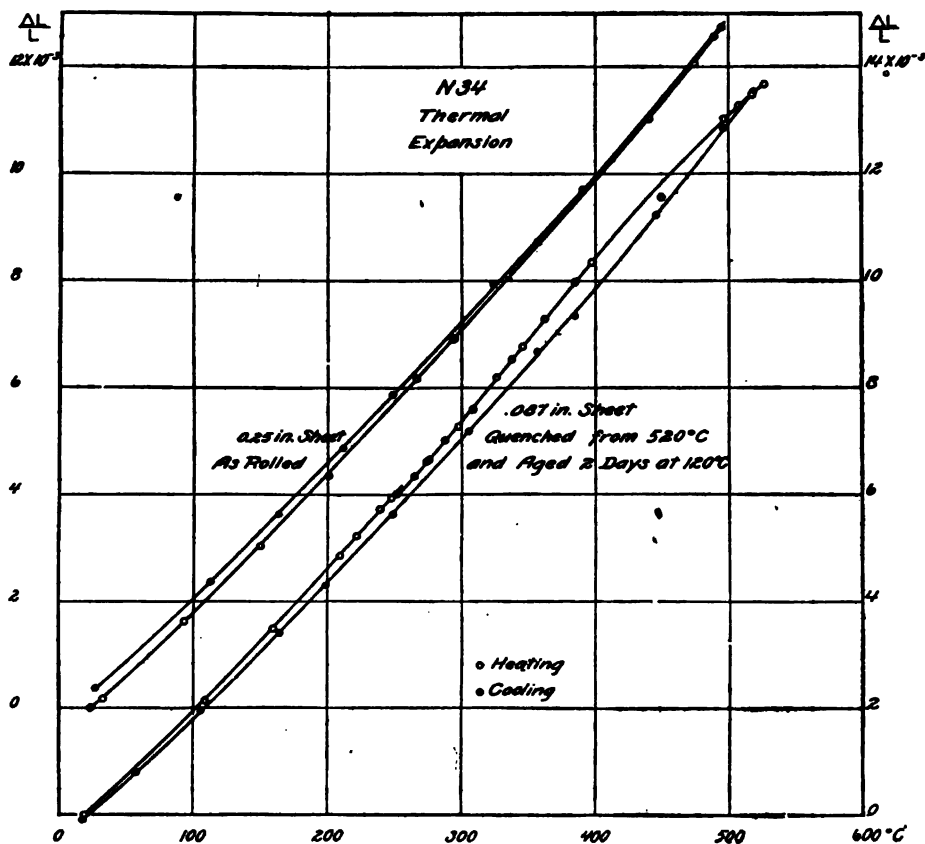


FIG. 10.—Linear expansion of N-34, 0 to 500° C

## 2. THE ELECTRICAL RESISTIVITY

Electrical resistivity measurements were made in vacuo over the temperature range 0 to 530° C by the method described by Burgess and Kellberg<sup>8</sup> on 0.25 mm wire drawn from a cylinder cut from 1/4-inch sheet of C11. It was necessary, however, to bring both of the aluminum-alloy leads out of the thermometer, as it was impossible to weld them to platinum. The data obtained

<sup>8</sup> Scientific Paper of the Bureau of Standards, No. 136; 1924.

from the first run are plotted as resistance of aluminum alloy against temperature in Fig. 11.

The change in direction of the resistivity curve at about  $300^{\circ}\text{C}$  is quite evident and indicates a change in the constitution of the alloy. It is evident both on heating and cooling, although a

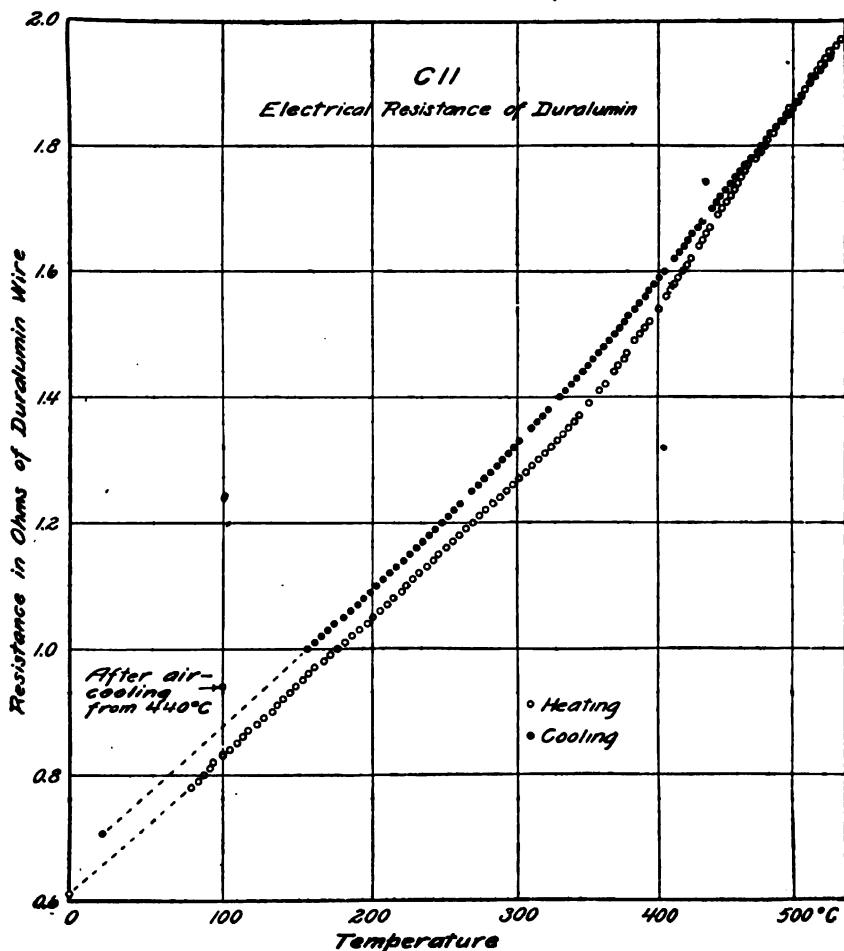


FIG. 11.—Electrical resistivity of C-11, 0 to  $520^{\circ}\text{C}$

change in resistivity at room temperature has taken place, resulting from the annealing produced during the series of measurements.

Following this run the material was heated to  $440^{\circ}\text{C}$  in its tube and cooled in air. The cooling was fairly rapid, as the outside diameter of the quartz tube was only 8 mm. The tube was then

put in a steam bath and resistance measurements taken, as shown in the table below:

Time in steam bath	Pt re- sistance	Al re- sistance	Time in steam bath	Pt re- sistance	Al re- sistance
	Ohms.	Ohms.		Ohms.	Ohms.
0 hour.....	1.7302	0.9035	4½ hours.....	1.7300	0.9063
½ hour.....	1.7303	.9047	6 hours.....	1.7301	.9069
1 hour.....	1.7302	.9051	7 hours.....	1.7301	.9068
2 hours.....	1.7297	.9054	11 hour.....	1.7298	.9069
3 hours.....	1.7301	.9060			

The specific resistance of this alloy was determined on a wire drawn to 2.54 mm diameter and annealed at 400° C. It was found to be 3.35 microhms per centimeter cube.

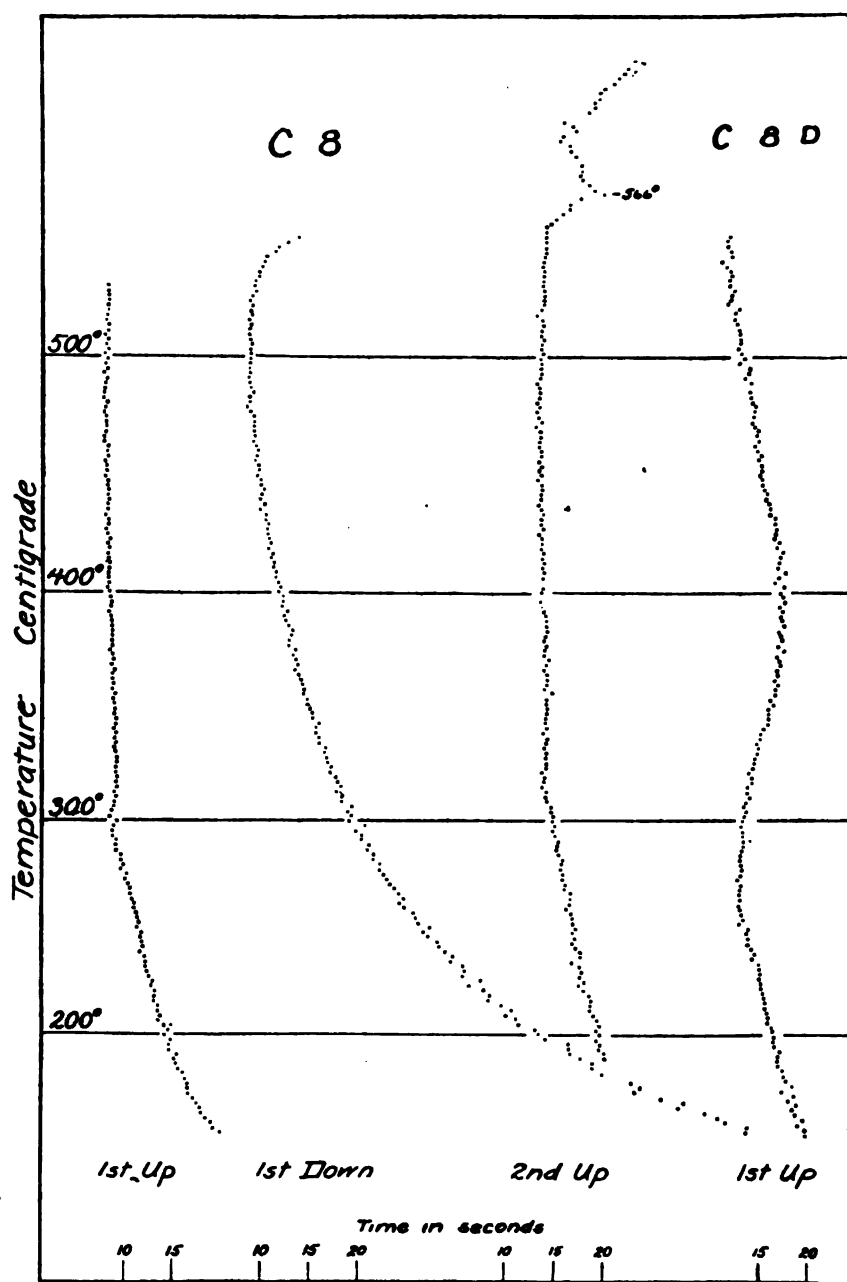
## V. MECHANISM OF HARDENING DURING AGING AFTER RAPID COOLING

Apparently no attempt has ever been made to develop an explanation for the changes in the physical, particularly mechanical, properties of this alloy during aging after rapid cooling. The changes which take place are quite marked and definite and must correspond to some quite as definite changes in the structure and constitution of the alloy, or at least to profound molecular changes. If we are not able to show that actual phase changes take place during aging, we must then ascribe these changes in physical properties to alterations in the atomic or molecular structure.

All of the evidence which the authors have been able to find or to accumulate seems to indicate that the hardening during aging is actually accompanied by a phase change within the alloy. In so far as it can be said then that this phase change causes the hardening, for the reason that it accompanies it, this phase change may be regarded as its active cause.

Elsewhere<sup>9</sup> the authors have determined the solubility at different temperatures in aluminum of  $\text{CuAl}_3$  and of  $\text{Mg}_2\text{Al}_3$ , the aluminum-rich compounds of the copper-aluminum and magnesium-aluminum binary alloy series, respectively. The solubility-temperature curves of these compounds are reproduced in Figs. 12 and 13; the solubility of both compounds diminishes rapidly with lowered temperature.

<sup>9</sup> P. D. Merica, R. G. Waltenberg, and J. R. Freeman, jr., The Constitution and Metallography of Aluminum and its Light Alloys with Copper and with Magnesium, Scientific Paper of the Bureau of Standards, No. 337, 1919; also Bull. A. I. M. E. No. 151, p. 1031, 1919.



### Inverse Rate Curves

FIG. 14.—Heating and cooling curves of C-8. First run up showing arrest at 300° C was taken three hours after quenching. C-8-D is a curve obtained on a quenched sample after aging 18 months at 20°C



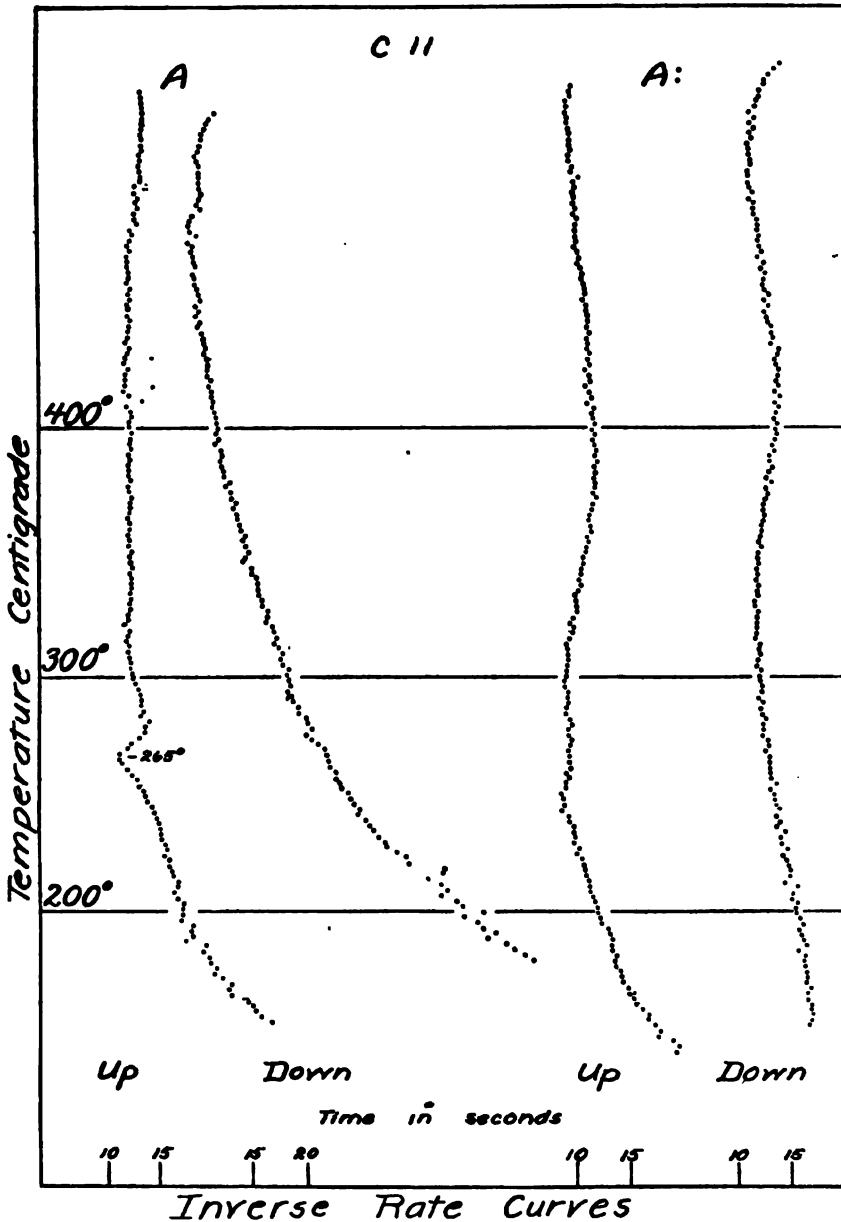


FIG. 15.—Heating and cooling curves of C-II. First run up on C-II-A shows an arrest at 265° C in a sample which had been quenched and then aged 12 days at 20° C. Second run up, marked C-II-A, shows no arrest in a sample which had been quenched into boiling water and aged 10 days at 120° C

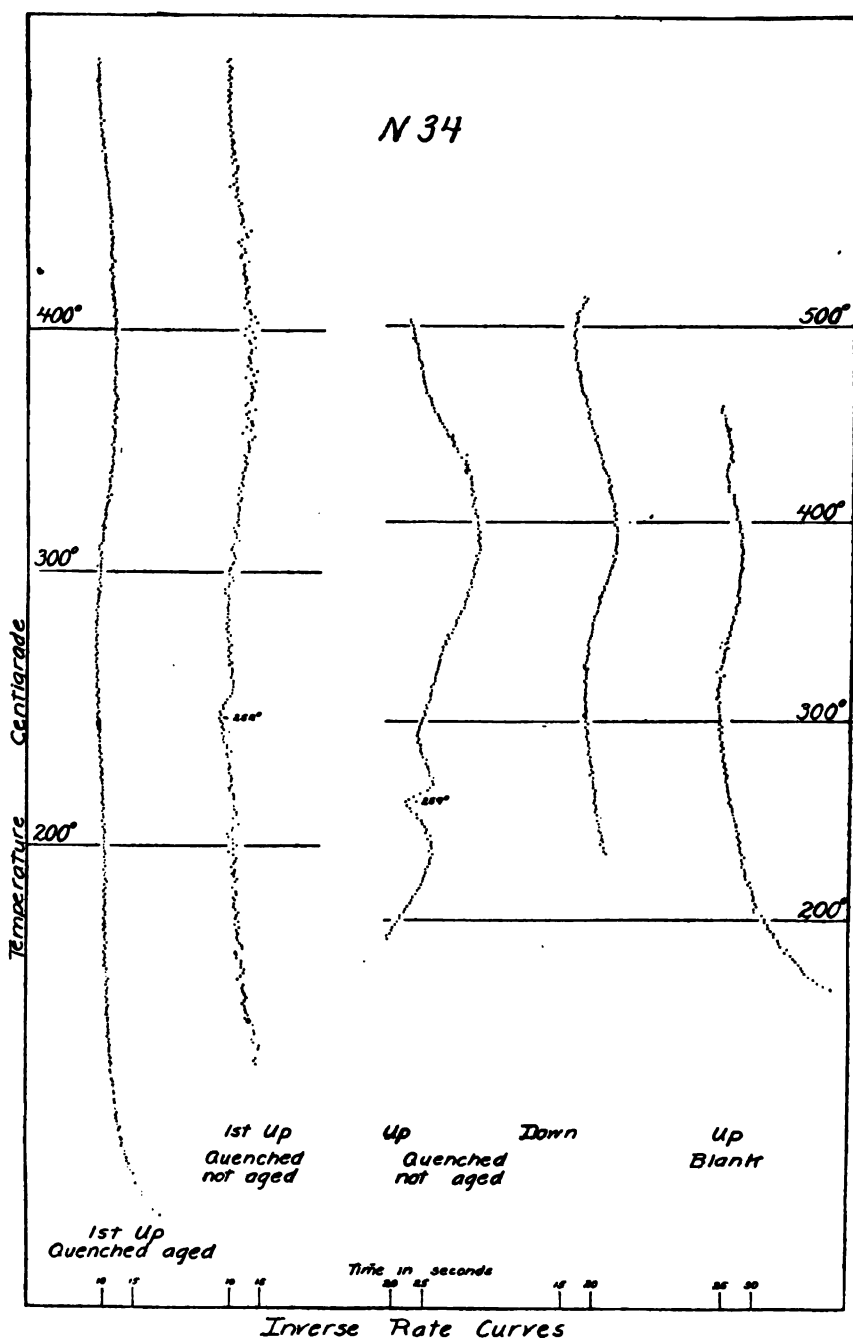


FIG. 16.—Heating and cooling curves of N-34 showing inverse arrest in quenched samples which had not been aged but no arrest in samples which had been aged after quenching

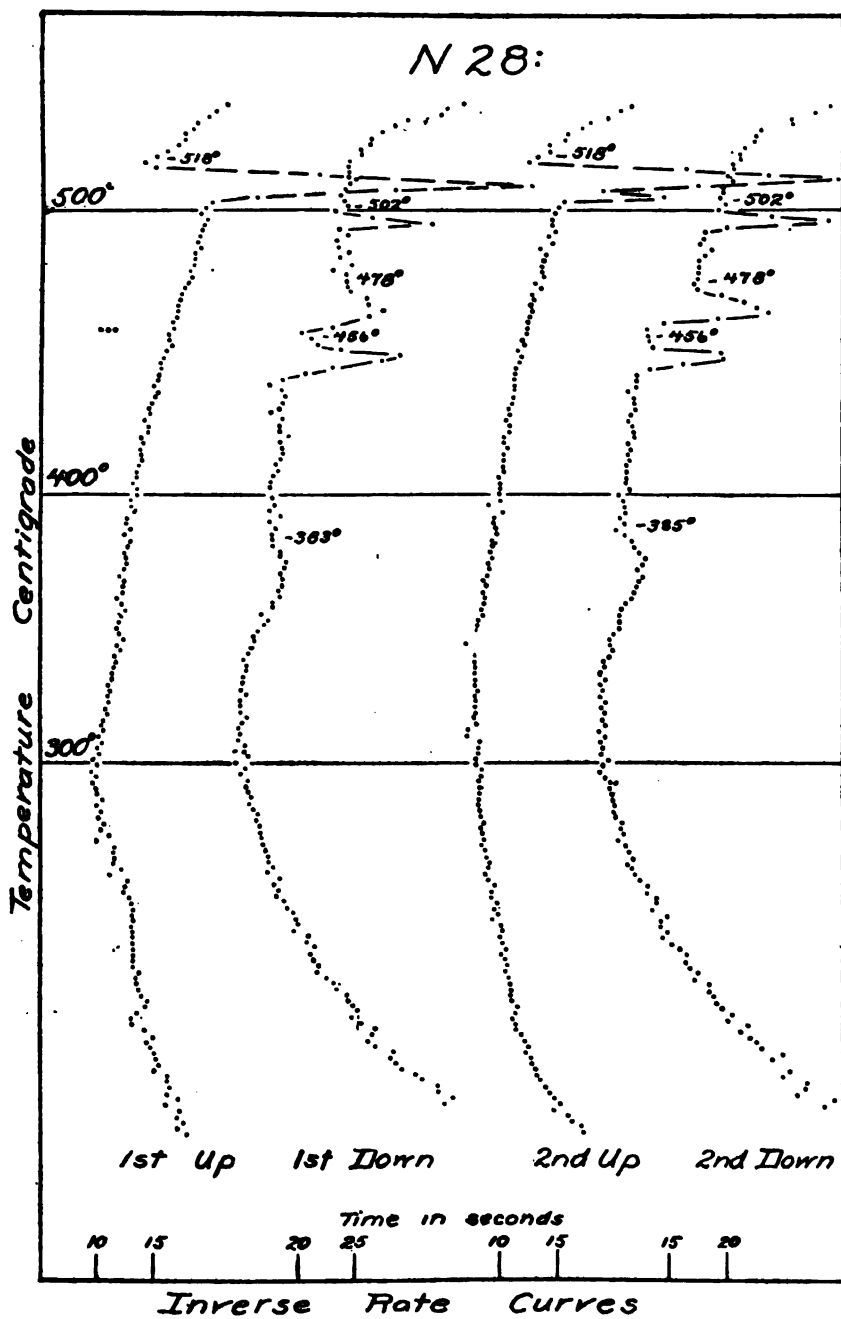


FIG. 17.—Heating and cooling curve of N-28. (Cu 4.08 per cent, Mg. 2.41 per cent)

This chemical reaction can hardly be other than the precipitation of  $\text{CuAl}_3$  from its supersaturated solution in aluminum, although direct visual evidence bearing on this question is also lacking. In describing the attempt which was made to recognize microscopically the phase change during aging just predicated a digression must be made in order to discuss the general features of the microstructure of duralumin, which has apparently not been done before.

### 1. STRUCTURE OF DURALUMIN

This microstructure may be developed either by etching in a relatively concentrated solution of sodium hydroxide,  $\text{NaOH}$ , a dilute solution of hydrofluoric acid,  $\text{HF}$ , or in a dilute solution of  $\text{NaOH}$ . The grain structure of the alloy is best developed by the two former solutions; 10 per cent  $\text{NaOH}$  and 5 per cent  $\text{HF}$  are generally used for this purpose. For the identification and study of the different microscopic constituents of the alloy a 0.1 per cent solution of  $\text{NaOH}$  has, however, shown itself much superior to the former ones, and this solution has been used in most of the authors' investigations.

Duralumin after rolling shows a structure similar to that in Fig. 18, which is quite typical. Fig. 19 shows the same alloy at a higher magnification. Grains of aluminum (in which are dissolved  $\text{Si}$ ,  $\text{CuAl}_3$ , and  $\text{Mg}_2\text{Al}_3$ ) are surrounded by strings of islands of eutectic ( $\text{CuAl}_3$ , aluminum,  $\text{FeAl}_3$ , aluminum, and possibly others), which are white in Fig. 18. Upon examination under a higher power the eutectic is seen to consist of two constituents, one of a brownish color, the other white. These two constituents are evident in Fig. 19. In another article by the authors (see note 9, on p. —) these two constituents have been identified as  $\text{FeAl}_3$  (brown) and  $\text{CuAl}_3$  (white), respectively. Quite often, but not always, the  $\text{FeAl}_3$  surrounds the  $\text{CuAl}_3$ , as is shown in the figure.

Besides these two constituents a third, of pronounced bluish color, is visible. This is readily distinguished under the microscope; not always so readily in a photograph. It is seen within an island of  $\text{CuAl}_3$  in Fig. 20. In the same article the authors have expressed the opinion that this is  $\text{Mg}_2\text{Si}$ ; it only occurs in alloys containing magnesium.

Upon still closer observation the grains of aluminum solid solution are seen to contain minute particles of a constituent. These are shown in Figs. 21 to 25. These particles are so small that it is impossible to identify them with certainty. Inasmuch as they

FIG. 18.—Rolled duralumin, *N* 34. Etched with 0.1 per cent  
NaOH.  $\times 100$

FIG. 19.—Rolled duralumin, *N* 34 (*E4*). Etched with 0.1 per cent  
NaOH.  $\times 1000$

FIG. 20.—Specimen of N 28 containing Cu and Mg, showing island of  $Mg_2Si$  (dark) within one of  $CuAl_2$  (white).  $\times 1000$

FIG. 21.—Sample of duralumin, E 3, showing  $FeAl_3$  and  $CuAl_2$  eutectic, and fine particles throughout ground mass.  $\times 1000$

FIG. 22.—Sample of E 3, same as Fig. 21.  $\times 2000$

FIG. 23.—Sample of duralumin E 3-F, after annealing 20 hours at  $500^{\circ}\text{C}$ ., quenching and aging at room temperature.  $\times 1000$

FIG. 24.—*Same material as in Fig. 23.  $\times 1000$*

FIG. 25.—*Sample of duralumin, E 4-F, after annealing 20 hours at 500° C., quenching and aging at room temperature.  $\times 1000$*



occur also in aluminum itself, they must consist in part, at least, of the compound X (of iron, silicon, and probably also aluminum; see note 9, on p. 299) and possibly  $\text{FeAl}_3$ ; probably  $\text{CuAl}_2$  is also present in this form. All of this generation of particles have undoubtedly separated during cooling from a solid solution in aluminum at higher temperatures.

The visible structure of duralumin changes but slightly upon heat treatment. Rolled duralumin consists of elongated grains. Upon heating such material to  $500^\circ\text{C}$  recrystallization of the aluminum solid solution grains first occurs, and the fine grains so formed increase in size. This growth is naturally interrupted by quenching. Immediately after quenching, therefore, the grains may be either larger or smaller than the original ones, depending upon the period of heating at  $500^\circ\text{C}$  and the rate of heating to that temperature. During subsequent aging the grains do not change in size. Heating to  $500^\circ\text{C}$  also results in the solution of some or all of the  $\text{CuAl}_2$  eutectic grains seen in the rolled material to correspond to equilibrium. The  $\text{FeAl}_3$  does not dissolve.

If there occurs during the aging of duralumin after quenching a gradual precipitation of  $\text{CuAl}_2$  particles to correspond to its diminished solubility at the lower temperatures, one would expect to be able to observe some difference between the microstructure of the quenched unaged specimen and that of the quenched one after thorough aging. The particles of  $\text{CuAl}_2$  may quite well be too small to be resolvable microscopically, but the presence of a large number of such colloidal particles might be expected to accelerate the etching of the specimen; at least troostite etches much more readily than martensite or sorbite, and it is considered quite generally to consist of a colloidal solution of  $\text{Fe}_3\text{C}$  in alpha iron. Samples of N<sub>34</sub>, some of which had been heated at  $500^\circ\text{C}$ , quenched in water and immediately etched, and some of which had been subsequently aged at  $130^\circ\text{C}$  after identical treatment to develop maximum hardness, were carefully compared in their appearance after etching in the same solution (0.1 per cent NaOH) and for the same periods of time. No difference was observed in the structure nor in the general shades of the etched surfaces of these two groups of specimens.

The authors have to date, therefore, no direct structural evidence of the precipitation of  $\text{CuAl}_2$  during aging of duralumin.

A difference in the rate of etching of quenched unaged and of quenched and aged may quite possibly be obscured by the pres-

ence of other constituents in fine dispersion, present in both cases. It was noted above that there are always present a number of fine particles of the X constituents. A structural study of duralumin made with pure aluminum free from iron and silicon might yield more positive results.

It is interesting to note that although the velocity of nuclear formation of  $\text{CuAl}_2$  at temperatures from 20° to 400° C seems to be quite normal, judging by thermal analysis, the velocity of crystallization or of coalescence of the nuclei is evidently quite remarkably small. Thus it was found (see note 9 on p. 299) that there was no visible precipitation of  $\text{CuAl}_2$  in an alloy containing 3 per cent of copper upon annealing at 300° C for 20 hours after obtaining all of the  $\text{CuAl}_2$  in solution by annealing at 500° C. Only by very slow cooling from 500 to 20° C could a visible precipitate of  $\text{CuAl}_2$  be produced. Slow velocities of crystallization seem to be characteristic both of  $\text{CuAl}_2$  and of aluminum.

Although it can not be directly proved that the thermal arrest at about 250° C, noticed upon heating a quenched unaged specimen of duralumin, is due to the precipitation of  $\text{CuAl}_2$ , no evidence directly contradicts this assumption, which is in entire accord with our knowledge of the equilibrium within the alloy, and this arrest can not be assigned to any other phase change.

It has been shown by many previous investigations and confirmed by the authors that aluminum undergoes no transformation in the solid state between ordinary temperatures and its melting point. No other phase changes could occur in the main mass of duralumin, the grains of solid solution, therefore, except those of solution or precipitation of  $\text{FeAl}_3$ , of the X compound, of  $\text{CuAl}_2$ , of  $\text{Mg}_2\text{Al}_3$ , or of  $\text{Mg}_2\text{Si}$  within the grains. Aluminum, which contains the same amounts of  $\text{FeAl}_3$  and of the X compound as does duralumin, is not altered by heat treatment as is duralumin, nor does it show a reverse heat effect upon heating as does the latter. This heat effect must therefore be due to the precipitation either of  $\text{CuAl}_2$ ,  $\text{Mg}_2\text{Al}_3$ , or  $\text{Mg}_2\text{Si}$ . But the alloys containing only magnesium in amounts up to 3 per cent also do not harden upon aging. There remains only the precipitation of  $\text{CuAl}_2$  with which to explain this heat effect.

The theory outlined above of the mechanism of the hardening of duralumin during aging most readily explains the interesting fact discovered by Mr. Blough, and confirmed by the authors, that the amount of hardening during aging increases as the temperature of quenching increases. At higher quenching tempera-

tures more and more  $\text{CuAl}_2$  is dissolved in solid solution. After quenching the  $\text{CuAl}_2$  is in excess of its solubility; the higher the quenching temperature the greater is the excess, and this is precipitated during aging. The hardening is in proportion to the amount of the highly dispersed  $\text{CuAl}_2$  formed.

If this theory is accepted for the moment, it is interesting to consider the effect of degree of dispersion upon hardness in the case of a solid solution, in this case of  $\text{CuAl}_2$  in aluminum. Duralumin immediately after quenching is generally softer than it is in the annealed condition. Thus, alloy C11 in the form of sheet gave the following values of hardness: Scleroscope hardness (magnifying hammer): Annealed at  $300^\circ$ , 17; quenched, but not aged, 16; quenched and aged 8 days, 35. This is probably due to the fact that a specimen as ordinarily cooled after annealing still contains some dissolved  $\text{CuAl}_2$  in excess of its solubility; the material hardens slightly during cooling. Specimens cooled extremely slowly give a scleroscope hardness of from 7 to 10, much lower than that of the quenched unaged ones.

Upon aging a quenched specimen at  $200^\circ \text{C}$ , for example, the hardness first increases to a maximum and afterward decreases. During that aging there has been first a formation of fine nuclei of  $\text{CuAl}_2$  followed by coalescence of these particles into ones of larger size. There is, therefore, a certain average size of particle of  $\text{CuAl}_2$ , for which the hardness of the material is a maximum; atomic dispersion of the solute,  $\text{CuAl}_2$ , is not the dispersion that produces the maximum hardness, but some intermediate one between it and that at which the particles become visible by ordinary means.

It is interesting to observe that the properties of other light alloys of aluminum are influenced by heat treatment and aging. Thus Rosenhain and Archbutt<sup>10</sup> have found that the tensile strength of sand-cast aluminum-zinc alloys increases upon aging. In another article (see note 7, on p. 272) by two of the authors it has been shown that whereas alloys of aluminum-magnesium, aluminum-manganese, aluminum-manganese-magnesium, and aluminum-nickel do not harden upon quenching and aging; those of aluminum-magnesium-nickel do. The solubility of zinc in aluminum decreases from 40 per cent at the eutectic temperature to about 25 per cent at  $256^\circ \text{C}$  and is probably much less at still lower temperatures. As in the case of the copper-aluminum alloys

<sup>10</sup> Report to the Alloys Research Committee, Proc. Inst. Mech. Eng., p. 319; 1912.

decreasing solubility at lower temperatures of the constituent,  $\text{CuAl}$ , or zinc, is accompanied by the possibility of hardening by quenching and aging.

Inasmuch as the aluminum-nickel-magnesium alloys also harden by aging, we may expect an appreciable solubility of  $\text{NiAl}$ , in solid aluminum at higher temperatures. The solubility of  $\text{MnAl}$ , is undoubtedly quite low.

## 2. ANALOGY BETWEEN THE HARDENING OF DURALUMIN AND THAT OF STEEL

The hardening of duralumin upon the basis of this hypothesis presents an interesting analogy with that of steel. The hardening of steel is due to the partial or entire suppression of the eutectoid transformation. Most recent thought regards it as due more directly to the suppression of the cementite precipitation (as pearlite), the transformation of  $\gamma$  into  $\alpha$  iron having taken place at least in part. The partial suppression, therefore, of the precipitation of a compound from a solid solution is common both to rapidly cooled steel and to duralumin.

A sample of steel which has been hardened, but not tempered, shows an evolution of heat upon heating<sup>11</sup> through its tempering range exactly as does duralumin. This is due to the precipitation of  $\text{Fe}_3\text{C}$  in finely divided form in the case of steel exactly as it seems to be due to that of  $\text{CuAl}$ , in duralumin.

During the tempering or aging of steel at from 100 to 300° C the hardness usually decreases immediately; that is, the maximum hardness of steel is obtained by quenching alone, whereas that of duralumin is produced after aging. In the case of some high-carbon steels (from 0.9 to 1.7 per cent C), however, the hardness increases during tempering after quenching exactly as in the case of duralumin.<sup>12</sup> The maximum hardness in hardened steel increases with the carbon content, as it does in duralumin with the copper content.

It has been found that tool steel containing tungsten undergoes an increase of hardness during tempering at from 400 to 650° C after quenching from 1350° C.<sup>13</sup>

<sup>11</sup> H. Scott, Effect of Rate of Temperature Change on Transformations in Alloy Steel, *Scientific Paper* No. 335, of the Bureau of Standards, 1919; also *Bull. A. I. M. E.* No. 146, p. 157; 1919.

<sup>12</sup> E. Maurer, Härten und Anlassen von Eisen und Stahl, *Metallurgie*, 6, p. 33; 1909.

<sup>13</sup> Edwards and Kikkawa, *Journ. Iron and Steel Institute*, 92, p. 6; 1914.

### 3. EUTECTIC STRUCTURE AND INFLUENCE OF MAGNESIUM

There is one fact which is not readily explained by the author's hypothesis. Although alloys containing only magnesium and no copper do not harden and alloys containing only copper with no magnesium do harden, those containing both copper and magnesium undergo a much greater hardening than do those with copper alone. Magnesium, therefore, exerts no effect by itself in this direction, and is not essential to the hardening power, but it materially increases the effect of the copper. The hypothesis developed above does not indicate any reason for this effect.

The authors are of the opinion that the influence of the magnesium is of a secondary nature. Thus it seems probable that some magnesium unites with the silicon present to form  $Mg_2Si$ , the blue constituent always found in alloys containing magnesium. The removal of the silicon in this manner may be the direct cause of the resultant increase of hardening effect. This would agree with the observed fact that with usual silicon content 0.5 per cent magnesium is enough to fully develop the partially latent hardening power of the copper-aluminum alloys. The addition of more magnesium produces a somewhat harder alloy in all conditions, but does not materially increase the hardening effect. This is shown by the following comparison:

Alloy	Copper	Magnesium	Tensile strength		Increase in tensile strength upon hardening
			Annealed	Hardened	
	Per cent	Per cent	Lbs./in. <sup>2</sup>	Lbs./in. <sup>2</sup>	Per cent
C11.....	2.6	1.3	35 000	56 000	60
C12.....	3.2	0.5	23 000	49 000	110

Consideration of the test results of Table 2 shows that magnesium hardens the aluminum matrix considerably even in the annealed condition. It is probable that the alteration of this matrix affects markedly the dispersion of the precipitation of  $CuAl$ , during aging and consequently the mechanical properties obtained.

There is another feature of the structure of duralumin which is of great importance and in which may be found some part of the explanation for the effect of magnesium. This is the manner in which the  $FeAl$ , and the  $CuAl$ , eutectics crystallize.

There are several possible binary eutectics in duralumin, namely, the following:

Eutectic	Eutectic temperature
	° C
FeAl <sub>3</sub> +aluminum solid solution.....	640-650
Si (cryst)+aluminum solid solution.....	570-580
X compound+aluminum solid solution.....	610
CuAl <sub>2</sub> +aluminum solid solution.....	520-540
Mg <sub>2</sub> Al <sub>3</sub> +aluminum solid solution.....	450
Mg <sub>2</sub> Si+aluminum solid solution.....	440 (?)

The amounts, by volume, of the eutectics with FeAl<sub>3</sub> and with CuAl<sub>2</sub> in ordinary duralumin are fairly large and about equal, that with Mg<sub>2</sub>Si somewhat less, that with X and with Mg<sub>2</sub>Al<sub>3</sub> usually almost nil. The approximate temperatures of eutectic solidification are given above; they represent in all cases the temperatures observed in the presence of both the FeAl<sub>3</sub> and the X eutectic. The presence of CuAl<sub>2</sub> or Mg<sub>2</sub>Si lowers the eutectic temperatures of the other binary eutectics. Thus, in the presence of Mg<sub>2</sub>Si, the eutectic temperature of CuAl<sub>2</sub>-aluminum is reduced from 540 to 520-530° C, and this is always obtained as a thermal arrest in heating or cooling duralumin.

The order of solidification of these binary eutectics in aluminum-rich alloys is a matter of the greatest importance. Fig. 26 shows the probable form of the equilibrium at the aluminum end of the ternary system, Al-Cu-Fe. An alloy containing about 0.5 per cent Fe and 3 per cent Cu (at *g* in the figure) would follow the line *gf-fc* upon solidification. A solid solution of aluminum with CuAl<sub>2</sub> (FeAl<sub>3</sub> is almost insoluble in aluminum) first crystallizes, and the composition of the liquid changes along the curve *gf* with lowering of temperature. At *f* the binary eutectic FeAl<sub>3</sub>-aluminum solid solution crystallizes, and also along *fc*. The liquid remaining at *f* is contained in the interstices between the solid grains of aluminum solid solution, and the FeAl<sub>3</sub> crystallizes upon these grains at the boundary between solid and liquid. At *c* the binary eutectic CuAl<sub>2</sub>-aluminum solid solution also crystallizes with the remainder of the first eutectic. The resultant structure is shown in Figs. 19, 20, 21, 22, 23, and 24. The FeAl<sub>3</sub> often entirely surrounds and isolates the CuAl<sub>2</sub> crystals.

When a specimen having such a structure is heated to 500° C for quenching, much of the CuAl<sub>2</sub> may be separated from the

aluminum by this layer of insoluble  $\text{FeAl}_3$ , and is effectually prevented from dissolving. Thus E<sub>3</sub>-F, containing only 1.56 per cent Cu, heated 20 hours at 500° C and quenched, still contains free  $\text{CuAl}_2$ , although its solubility at that temperature was about 3 per cent. Its structure is shown in Fig. 23. The undissolved  $\text{CuAl}_2$  (light) is surrounded by  $\text{FeAl}_3$  (dark). (The other light islands are  $\text{Mg}_2\text{Si}$ , which are distinguishable under the microscope as of bluish color, but photograph light.)

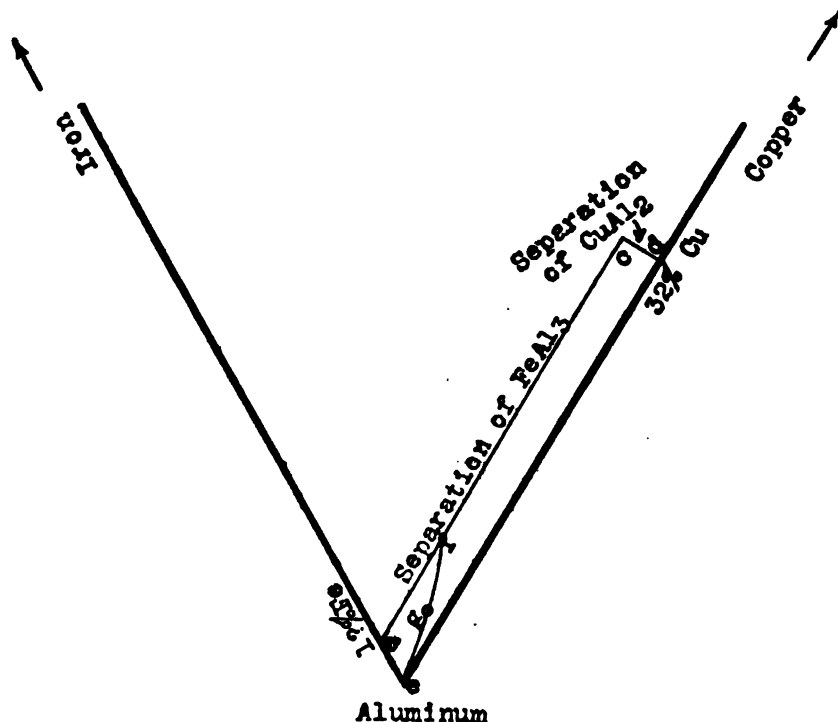


FIG. 26.—Suggested form of liquidus surfaces of ternary system aluminum-iron-copper near aluminum end

This inclosure of the compound of one binary eutectic by that of another seems to be characteristic of light aluminum alloys.

Fig. 20 shows an island of  $\text{CuAl}_2$  inclosing one of  $\text{Mg}_2\text{Si}$ . Such a structure explains probably the confusing heating and cooling thermal curves often obtained with copper-aluminum-magnesium alloys. In Fig. 16 was shown several normal heating and cooling curves for N<sub>34</sub> containing both copper and magnesium. The inverse heat effect in the quenched alloy at about 260° C and the eutectic arrest at 510° C are both visible. In Fig. 17 are shown the heating and cooling curve of N<sub>28</sub> containing Cu 4.98 per

cent and Mg 2.41 per cent. On the up curve the usual  $520^{\circ}\text{C}$  arrest is noticed; upon cooling, however, instead of one, three arrests are noticed, at  $502^{\circ}\text{C}$ , at  $478^{\circ}\text{C}$ , and at  $456^{\circ}\text{C}$ . This cycle will repeat itself indefinitely not only in this alloy but in others containing copper and magnesium, particularly when of rather high copper and magnesium content.

The structure of Fig. 20 was obtained in N28 after the thermal analysis was completed and is characteristic; practically all of the  $\text{Mg}_2\text{Si}$  is surrounded completely by  $\text{CuAl}_2$ . Upon cooling,  $\text{CuAl}_2$  separates at the first arrest ( $500^{\circ}\text{C}$ ), at the second and third  $\text{Mg}_2\text{Si}$  and possibly some traces of  $\text{MgAl}_2$ . These crystallize inside of the  $\text{CuAl}_2$ ; the aluminum particles of the respective eutectics coalesce with the aluminum grains. Upon reheating this alloy the surface of contact between  $\text{Mg}_2\text{Si}$  and aluminum is so slight that the melting of the eutectic, which should normally occur at the two lower cooling arrests, proceeds too slowly to give an arrest, and not until the protecting sheath of  $\text{CuAl}_2$  melts as eutectic at the higher ( $520^{\circ}\text{C}$ ) arrest does the  $\text{Mg}_2\text{Si}$  melt also.

These thermal arrests obtained around  $500^{\circ}\text{C}$  are related to the formation of the various eutectics and do not have anything to do with the hardening of duralumin.

## **VI. CONCLUSIONS RELATIVE TO THE MANUFACTURE AND HEAT TREATMENT OF DURALUMIN**

It has been shown that when duralumin is rapidly cooled by quenching from temperatures between  $250$  and  $520^{\circ}\text{C}$ , and aged thereupon at temperatures from  $0$  to  $200^{\circ}\text{C}$ , the hardness and, at least at lower aging temperatures, the ductility increase. The actual values of hardness and ductility thus obtained depend upon the quenching temperatures; they increase with that temperature up to about  $520^{\circ}\text{C}$ , corresponding to the increase of  $\text{CuAl}_2$  in solid solution. At this temperature any free  $\text{CuAl}_2$  melts as a eutectic and the material is spoiled; this eutectic temperature therefore marks the upper limit of the useful quenching temperature range.

In order to develop the best mechanical properties by heat treatment, a quenching temperature should be used as near this as is possible without running risk of burning the metal by the melting of this eutectic. In practice it should be possible to quench from temperatures between  $510$  and  $515^{\circ}\text{C}$ .

The period of time at which sheet material should profitably be held at the quenching temperature lies between  $10$  and  $20$  minutes. Heavier sections such as bars might require more time at this



temperature, as the structure of such sections would be coarser and would require somewhat more time for the complete solution of the  $\text{CuAl}_2$ .

Quenching is best and most conveniently carried out in boiling water. The mechanical properties are better after quenching in hot than after quenching in cold water, and there is less danger of cracking due to cooling stresses.

The best temperature for subsequent aging depends upon the mechanical properties that are desired. For most purposes it will be found best to age at  $100^\circ\text{C}$  for about 5 to 6 days. The greater portion of the hardening effect takes place within this period. Such a treatment develops both high strength and high ductility. If a material having a higher proportional limit but lower ductility is desired, the material may be aged at higher temperatures up to  $150^\circ\text{C}$  for from 2 to 4 days.

The authors' experience has not led them to recommend a different composition for duralumin than that in current use; that is, Cu, 3 to 4.5 per cent; Mg, 0.4 to 1.0 per cent; Mn, 0 to 0.7 per cent; 99 per cent Al (remainder).

It is believed that it would be of advantage to preheat the ingots for hot rolling to a somewhat higher temperature than is sometimes used. It would be desirable to preheat to  $500^\circ\text{C}$  or as near to that temperature as the temperature uniformity of the furnace permitted; the free  $\text{CuAl}_2$  would have better opportunity of going into solution at this temperature than at lower ones. Rolling, however, can not be done at this temperature, due to the eutectic of the  $\text{Mg}_2\text{Si}$  melting at  $450^\circ\text{C}$  and consequent hot shortness of the material. It might therefore be advisable to preheat to  $500^\circ\text{C}$ , but to roll at about  $450^\circ\text{C}$ .

## VII. SUMMARY AND CONCLUSIONS

The heat treatment of alloys of the type, duralumin, was investigated and the effect observed of variations in the heat-treating conditions, such as quenching temperature, temperature of quenching bath, and of aging or tempering, and time of aging upon the mechanical properties.

Conclusions are drawn relative to the best conditions for commercial heat-treating practice for this alloy. The temperature of quenching should not be above that of the  $\text{CuAl}_2$  aluminum eutectic, which is usually about  $520^\circ\text{C}$ , but should be as near to this as possible without danger of eutectic melting. The pieces should be held at this temperature from 10 to 20 minutes and

quenched preferably in boiling water. The hardening may for most purposes best be produced by aging for about 5 days at 100° C.

A theory of the mechanism of hardening of duralumin during aging, after quenching from higher temperatures, was developed which is based upon the decreasing solubility of the compound  $\text{CuAl}$ , in solid solution in aluminum with decreasing temperatures from 520° C to ordinary temperatures. It is believed that the precipitation of excess  $\text{CuAl}$ , which is suppressed by quenching proceeds during aging, the precipitation taking place in very highly dispersed form. The hardening is due to the formation of this highly dispersed precipitate.

According to this theory the hardening of duralumin during aging or tempering after quenching presents a very close analogy with that of steel, and the evidence in support of the theory is of the same nature and of approximately the same competence as that in support of the prevailing theory of the hardening of steel.

WASHINGTON, February 27, 1919.

DEPARTMENT OF COMMERCE



# SCIENTIFIC PAPERS OF THE BUREAU OF STANDARDS

S. W. STRATTON, DIRECTOR

No. 348

## USE OF A MODIFIED ROSENHAIN FURNACE FOR THERMAL ANALYSIS

BY

H. SCOTT and J. R. FREEMAN, Jr., Assistant Physicists

*Bureau of Standards*

ISSUED OCTOBER 24, 1919



PRICE, 5 CENTS

Sold only by the Superintendent of Documents, Government Printing Office  
Washington, D. C.

WASHINGTON  
GOVERNMENT PRINTING OFFICE

1919



# USE OF A MODIFIED ROSENHAIN FURNACE FOR THERMAL ANALYSIS

By H. Scott, and J. R. Freeman, jr.

## CONTENTS

	Page
I. Introduction.....	317
II. Description of furnace.....	318
III. Description of the elevating mechanism.....	318
IV. Details of operation.....	321
V. Summary.....	323

## I. INTRODUCTION

In a paper presented before the Institute of Metals entitled "Some Appliances for Metallographic Research," Rosenhain<sup>1</sup> described a new type of furnace designed primarily for the thermal analysis of metals by the inverse-rate method and used by him with considerable success in the metallurgical department of the National Physical Laboratory. In his discussion of this type of furnace Rosenhain pointed out certain difficulties met with in its operation, such as uniformity of rate of heating or cooling being inadequate for the degree of accuracy desired. To overcome this difficulty, he suggested in place of motor propulsion a gravity drive controlled by a "hydraulic cylinder with a relief valve whose width of opening can be regulated to allow of any desired rate of motion." The authors in constructing a thermal-analysis furnace of Rosenhain's type have, therefore, followed his suggestion and also added certain features which increase somewhat the convenience and simplicity of its operation. Requests for information regarding this furnace and the highly satisfactory results obtained from its use justify, it is believed, describing its construction and operation in sufficient detail to make possible its duplication or improvement.

---

<sup>1</sup> Rosenhain, J., *Inst. of Metals*, 18, p. 160; 1915.

## II. DESCRIPTION OF FURNACE

The details of the furnace construction are shown in Fig. 1, which is drawn to scale. The heating tube is of  $\frac{1}{4}$ -inch wall "alundum," heated at the upper end by 17 turns of 0.52-mm platinum wire, which is coated with alundum cement supplied for this purpose. The cement coating is essential when a temperature over  $1000^{\circ}\text{C}$  is required, as it prevents hot spots with the resulting burning out of the heater. This platinum-wire winding, unlike "nichrome," is entirely satisfactory for temperatures of at least  $1000^{\circ}\text{C}$ . It has been maintained at that temperature continuously for two months and shows no signs of deterioration. This temperature is maintained by a current of 5 amperes drawn from 30 volts potential; so its necessarily continuous operation is quite economical.

The furnace is heated at the top, as is Rosenhain's, to avoid convection currents, but the sample in its containing tube is introduced from the bottom, or cold end, thereby avoiding the disadvantages of his method, which consist of inconvenience in position of the sample and control apparatus and the heating of some portion of the sample tube at all times to the maximum temperature of the furnace. The latter disadvantage may prove serious in the event of slight inhomogeneities in the thermocouple wire.

## III. DESCRIPTION OF THE ELEVATING MECHANISM

The details of the rate-control mechanism are shown in Fig. 2. The weights *K* (total weight, 15 pounds), operating over pulleys, lift the elevator *B*, and the weight *J* (weight, 2 pounds) lowers it. The rate of motion of the tube *C*, clamped on the elevator, is controlled by the flow of oil from one end of the cylinder *L* to the other through the needle valve *M*. The oil cylinder is kept open to the air and filled with a good grade of engine oil, care being taken that the oil is free from dirt and air bubbles, which might easily cause variations in the rate of motion of the plunger. The sample tube *C* is held and centered with three set screws in a sleeve *D*, which fits into a receptacle on the elevator, facilitating rapid changing of the sample. A guide rod *E* prevents rotation of the elevator and steadies its motion.

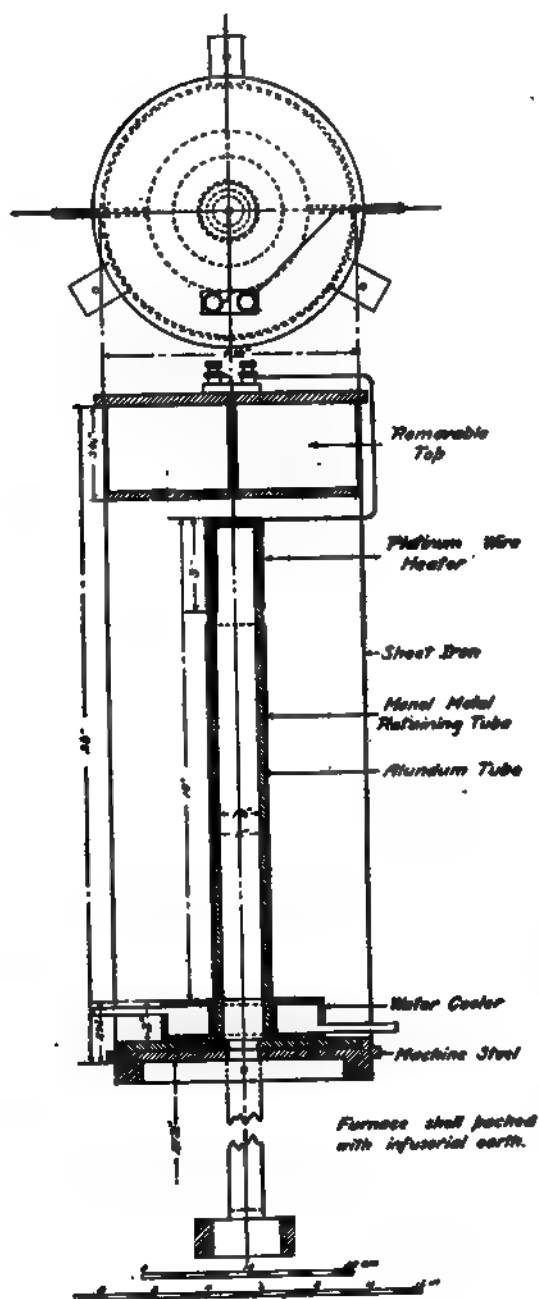


FIG. 1.—Diagram of furnace

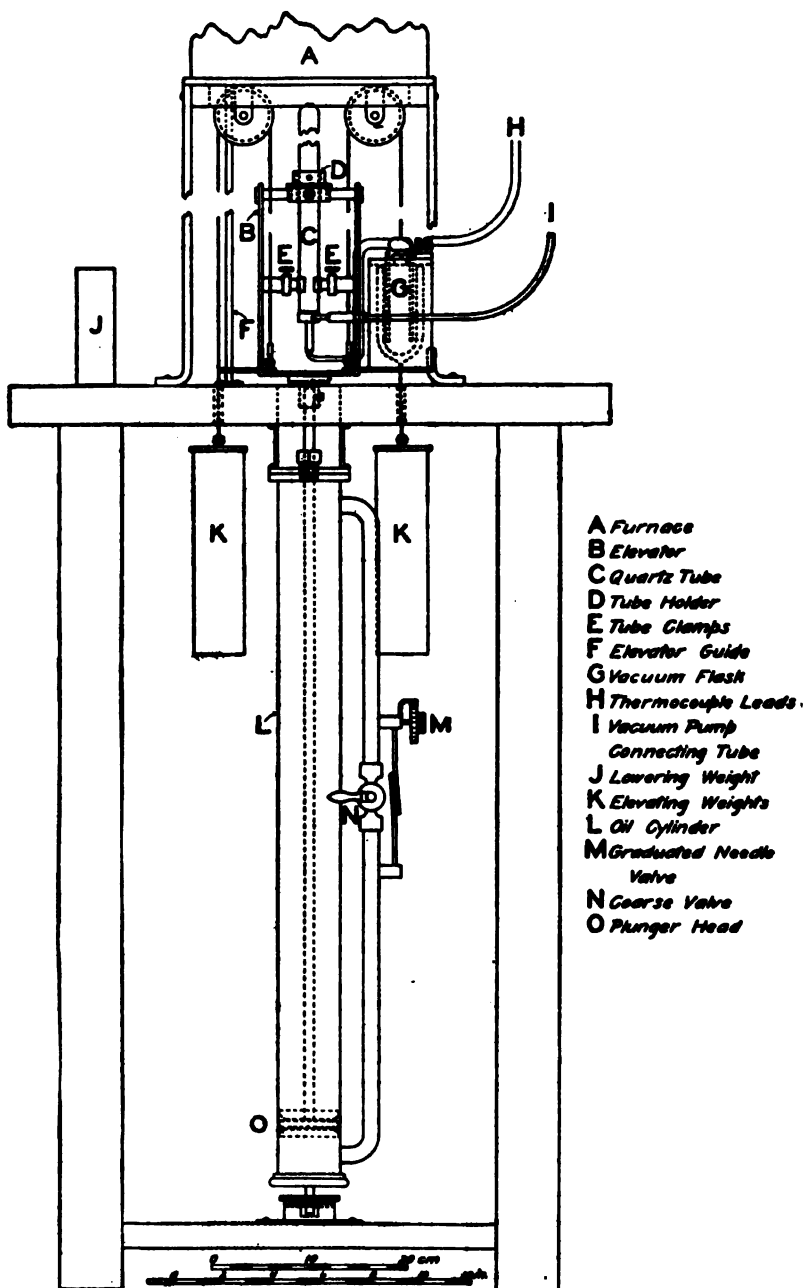


FIG. 2.—Diagram of elevating mechanism



## IV. DETAILS OF OPERATION

The differential method of obtaining curves may be used with this furnace, but the experience of the authors has been that more valuable and satisfactory results are obtained by use of the inverse-rate method, and this has accordingly been used almost

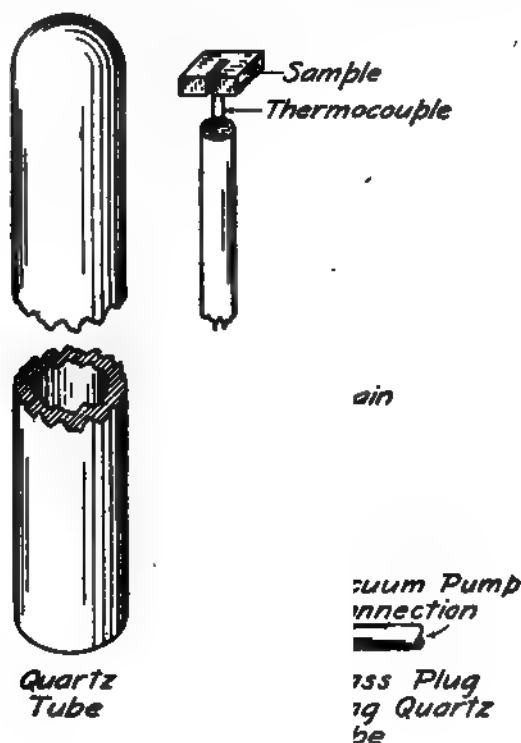


FIG. 3.—Sample mounting

exclusively. The adoption of the inverse-rate method limits the pyrometric requirements to a single thermocouple and potentiometer. This permits of the use of a somewhat novel method of mounting samples first used by Burgess and Crowe<sup>2</sup> in their researches on pure iron.

The aforementioned method of mounting is illustrated in Fig. 3. The operations involved consist simply of cutting a 0.5-mm slot in the sample with a small hack saw and riveting in this slot the

<sup>2</sup> Burgess and Crowe, The Critical Ranges  $A_2$  and  $A_3$  of Pure Iron, Bureau of Standards Scientific Paper No. 212.

flattened head at the hot junction of a platinum—90 platinum—10 rhodium thermocouple in the form of 0.5-mm-diameter wire. The mounted sample is sealed in the quartz tube and a vacuum maintained through the brass-plug connection.

This method of mounting has the advantages of good thermal contact between the sample and the thermocouple, use of small samples (usually  $\frac{1}{8}$  by  $\frac{1}{4}$  by  $\frac{3}{8}$  inch) weighing about 1.7 g), with the consequent elimination of detectable thermal gradients, and ease of preparation of samples. Its chief disadvantage is the slight contamination of the thermocouple resulting from close contact with the sample at high temperatures. This source of error is easily avoided by using a homogeneous thermocouple and frequently removing the short length subject to contamination. A check can be had on the accuracy and sensitivity of the apparatus under actual operating conditions by taking curves on pure iron, the A<sub>2</sub> transformation of which has a maximum heat effect very constant at 768° C,<sup>3</sup> independent of rate of temperature change.

The temperature measurements are made with a dial potentiometer and the time interval recorded on a drum-type chronograph, which instruments have already been described.<sup>4</sup> The assembled apparatus is shown in Fig. 4.

A heating and cooling curve, characteristic of the furnace, taken on a transformationless (28 per cent nickel) steel over the temperature range of from 50 to 1000° C, is shown in Fig. 5, each curve being divided into two sections for convenience in reproduction. Curves of a steel showing several critical points of small intensity and taken with this apparatus are available in the work of one of the present authors.<sup>5</sup> It may be noted from Fig. 5 that the rate of temperature change is somewhat slower at the lower temperatures than at the higher, as would be expected, but that the change is not sufficient to obscure a transformation occurring anywhere between 100 and 1000° C. This change in rate is emphasized at the lower temperatures on the thermal curves of Fig. 5, due to the parabolic form of the relation between temperature and emf of the platinum couple, for the curves are plotted with time of unit emf change as abscissæ as a matter of

<sup>3</sup> Burgess and Crowe, loc. cit.

<sup>4</sup> Burgess and Crowe, loc. cit. Dr. P. D. Merica has substituted a pair of stop watches for the costly chronograph with good results, providing the time interval is greater than 15 seconds. Bull. A. I. M. & M. E. 151 p. 1027.

<sup>5</sup> Scott, H., Bureau of Standards Scientific Paper No. 335.

FIG. 4.—*Assembled furnace and auxiliary apparatus*

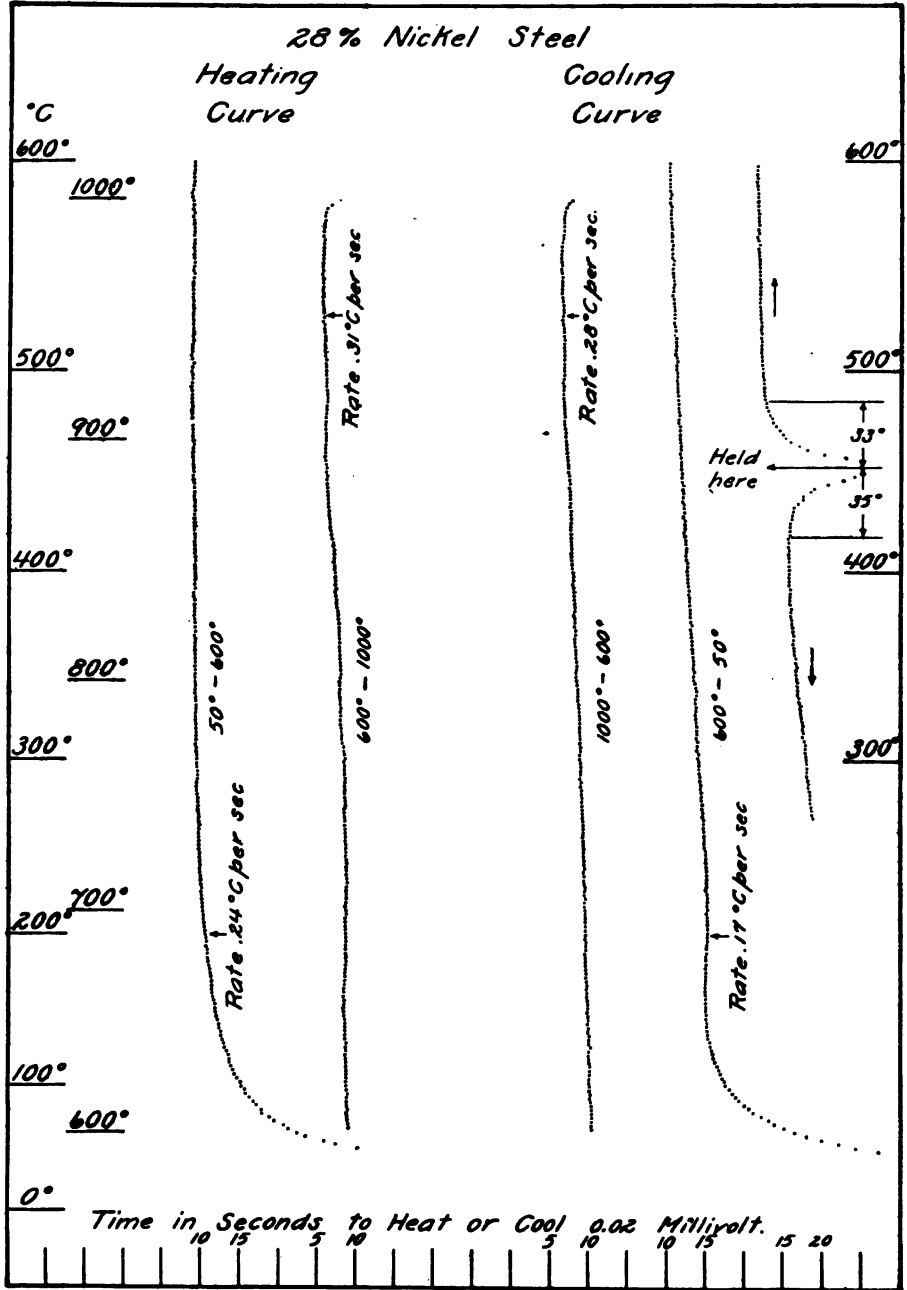


FIG. 5.—Thermal curves of 28 per cent nickel steel

convenience. The actual rate change can be reduced, and probably eliminated for a given rate; by using a metal cylinder or alundun tube tapered to increase the heat conduction at the lower temperatures.

It might be apprehended that the gravity drive would impart an extended acceleration to the elevator instead of a uniform velocity, but that the time required for the rate to become uniform is slight is shown by the short curves on the right-hand side of Fig. 4, obtained by bringing the sample to the constant temperature designated and then taking readings from the time of opening the valve. The time required for the rate to become normal for that valve setting is only  $6\frac{1}{2}$  minutes on heating and  $4\frac{1}{2}$  minutes on cooling, while the corresponding temperature interval is only  $33^{\circ}$  and  $35^{\circ}$  C. This is an extremely useful characteristic of the furnace, as it enables the separation of one transformation superimposed on the end of another by holding the sample at a temperature at which the first transformation will complete itself and then starting. It also facilitates the study of the effect of time of holding in the proximity of the transformation temperature on its position; that is, determining the limits of the transformation temperature at what amounts to zero rate of temperature change.

## V. SUMMARY

A description is given of a thermal-analysis furnace constructed on the principle of Rosenhain's furnace, the chief departures from his design being: (1) Use of a gravity-drive rate control and (2) introduction of the sample through the bottom and cold end of the furnace. The advantages and faults of these modifications are mentioned.

The methods of operation developed and adopted for use with this furnace are described and discussed, the principal variation from the usual practice being the mounting of the sample in direct thermal contact with the thermocouple.

F. E. Mann contributed skill in the construction of this furnace and Miss H. G. Movius and H. A. Wadsworth assisted in its successful development.

WASHINGTON, D. C., May 28, 1919.









DEPARTMENT OF COMMERCE

---

# SCIENTIFIC PAPERS OF THE BUREAU OF STANDARDS

S. W. STRATTON, DIRECTOR

---

No. 349

---

## PHOTOELECTRIC SPECTROPHOTOMETRY BY THE NULL METHOD

BY

K. S. GIBSON, Associate Physicist  
*Bureau of Standards*

---

ISSUED OCTOBER 11, 1919



PRICE, 5 CENTS

Sold only by the Superintendent of Documents, Government Printing Office  
Washington, D. C.

---

WASHINGTON  
GOVERNMENT PRINTING OFFICE

1919



# PHOTOELECTRIC SPECTROPHOTOMETRY BY THE NULL METHOD<sup>1</sup>

By K. S. Gibson

## CONTENTS

	Page
I. Introduction.....	325
II. Spectral transmission.....	329
1. Apparatus.....	329
2. Method.....	333
3. Errors and accuracy.....	337
III. Diffuse spectral reflection.....	348
IV. Other applications.....	350
V. Summary.....	352

## I. INTRODUCTION

Anyone who has had experience in trying to make spectrophotometric measurements of transmission or reflection in the blue and violet parts of the spectrum is well aware of the difficulty of obtaining reliable determinations in this region. Nearly all methods have relatively low sensitivity, or else are inaccurate for other reasons, from wave lengths 400 to 500 millimicrons ( $m\mu$ ). Radiometric methods, which are so suitable for infra-red work and which have been used also in the visible and even in the ultra-violet, are, nevertheless, not of the highest accuracy in these latter regions because of the relatively low radiant power of all sources used for this kind of work, the radiant power decreasing continuously with the wave length. It is very difficult to obtain accurate determinations below 500  $m\mu$  by the usual radiometric methods. Any visual method is limited in the blue and violet because of the combined low visibility of the human eye and the low radiant power of the sources used, except at the few wave lengths where monochromatic light of great intensity can be obtained, as from the mercury arc. The Hilger sector photometer method, which is the only photographic method of speed and reliability, also has its limitations for this region. Being such a

<sup>1</sup> An abstract of this paper was presented to the Optical Society of America at the Baltimore meeting, Dec., 27, 1918.

practicable method for the ultra-violet, it is always used in connection with a quartz spectrograph, and the low dispersion thus obtained in the violet and blue makes it difficult to obtain reproducible values at these wave lengths. Moreover, it is to a certain extent unreliable at high transmissions. In a recent paper<sup>2</sup> some examples are given of the kind of agreements and disagreements obtained from 400 to 500  $m\mu$  when the transmissions of good specimens were measured by visual (König-Martens and Lummer-Brodhun spectrophotometers and Martens photometer with monochromatic light) and photographic (Hilger sector photometer) methods.

However, because of their extreme sensitivity to the blue and violet, as well as to the ultra-violet, certain kinds of photoelectric cells offer possibilities of devising a method for obtaining as accurate spectrophotometric measurements from 400 to 500  $m\mu$ , and beyond this range, as are obtained at any other wave lengths by any other method. The potassium-hydride cell now on the market, when used with an incandescent lamp and a glass dispersing prism, gives a maximum response usually near 460  $m\mu$ ; and the photoelectric method, under these conditions, admirably supplements the visual and photographic methods, being best where they become poor and becoming poor only after they have become reliable.

In connection with the color-standardization work of the National Bureau of Standards,<sup>3</sup> it is desired to have available a number of independent methods of making spectrophotometric determinations, especially in the visible part of the spectrum; for it is generally admitted that the fundamental basis of color specification is spectrophotometry. To supplement the other methods at present in use at the Bureau, and especially to overcome the previously mentioned uncertainty of measurements made in the blue and violet, the writer in 1917 was given the problem of developing a method for accurate and convenient photoelectric spectrophotometry suitable for routine determinations. A null method was decided upon for reasons which will be explained later, an electrometer serving merely as an indicator of equality between two photoelectric currents. The making and assembling of apparatus was completed in April, 1918; and since that time it has been in continual use, being very satisfactory as

<sup>2</sup> Gibson and McNicholas, *The Ultra-Violet and Visible Transmission of Eye-Protective Glasses*, Bureau of Standards Tech. Paper, No. 119, June, 1919.

<sup>3</sup> I. G. Priest, *The Work of the National Bureau of Standards on the Establishment of Color Standards and Methods of Color Specifications*, Trans. I. E. S., XIII, p. 38; 1918.

to speed of operation, ease of keeping in working condition, and reliability of measurement.

In a recent paper by Coblenz<sup>4</sup> is given a brief summary of some of the characteristics and methods of use of the photoelectric cell, together with references to most of the papers on the subject, and no general discussion will be given herein except as serves the needs of this paper. Hitherto, whenever the photoelectric cell has been used in measuring spectral transmission or reflection, and, in fact, in practically all kinds of work, some form of deflection method has been used. Any deflection method, except a method of equal deflections, is almost valueless for accurate work unless the relation between the photoelectric current and the exciting radiant power is accurately known for all values of wave length and radiant power to be used. It has been a much-discussed question whether or not this relation takes the form of a straight-line curve for any or all photoelectric cells. Suffice it here to say that it has been concluded by the majority of investigators in this field that it is not safe to assume for any photoelectric cell a direct proportionality between photoelectric current and exciting radiant power. Any cell which is to be used in a deflection method (with the exception just noted) must first be carefully tested (and calibrated if any deviation from the straight-line relationship is detected), and should be repeatedly retested to make sure that conditions have not changed and that things are always in proper working order.

Another source of trouble in most deflection methods has been the difficulty of eliminating the so-called dark current; i. e., the current through the cell when not irradiated.<sup>5</sup> When this has not been completely eliminated or balanced, its magnitude has usually been measured and corrections made in the computations. Gradually, however, the technique of making photoelectric cells has been improved, until now most of the cells made on the "black-body" principle are found to obey very nearly the straight-line relationship, and the dark current can be much more easily suppressed.

Nevertheless, a method which eliminates any possible errors and the necessity of any tests, calibrations, or corrections due to these two factors is of much greater value and reliability than is any method into which these factors may enter.

<sup>4</sup> Instruments and Methods Used in Radiometry, III, Bureau of Standards Scientific Paper, No. 379-1913.

<sup>5</sup> The terms irradiate and irradiation, as emphasized by H. E. Ives (*Astro. Journ.*, XLV, p. 39; 1917), should be used analogously to the terms illuminate and illumination when radiant energy rather than light is discussed.

Either the galvanometer or the electrometer may be used with the photoelectric cell in spectrophotometry. If the radiant powers used are sufficiently great, then, of course, the galvanometer is quicker and more convenient than the electrometer. The advantage of the electrometer over the galvanometer, however, is the greater sensitivity that can be attained, which enables measurements to be made over a greater range of wave lengths and, at least for low values of transmission, with much greater accuracy. The use of the electrometer in any deflection method, however, requires considerable time and skill if accurate results are to be obtained. A strict proportionality between deflections of the disk, as read by means of the mirror and scale, and the potential acquired by the quadrants must be proved by test or a calibration made. The use of the rate-of-drift method or the total-deflection or ballistic-throw (in a given interval of time) method necessitates the use of timing devices, with their inconvenience and possible introduction of further errors. If the electrometer is shunted around a high resistance and the steady deflections read, the sensitivity is lowered.

The only means by which the questions of the current-irradiation relationship and the dark current may be avoided and their possible errors eliminated, while retaining the extreme sensitivity of the unshunted electrometer, is by the proper use of a null method, where the electrometer serves simply as an indicator of certain desired conditions.

The photoelectric null method has not heretofore been used in the measurement of spectral transmission or reflection, indeed in scarcely any kind of quantitative work. Its possibilities were first brought out by Richtmyer,<sup>6</sup> who used two photoelectric cells and batteries in a sort of Wheatstone bridge arrangement, the electrometer serving merely as an indicator of equality between the currents through the two photoelectric cells. These currents were excited by the undispersed radiant energy from two incandescent lamps. By varying the distances of the lamps from the cells, data were obtained which showed that the cells obeyed exactly the same current-irradiation law. He pointed out that, besides eliminating all errors due to dark currents, this method makes possible, for certain kinds of work, a precision of measurement not otherwise available.

The arrangement of apparatus for the null method herein described is essentially the same as that used by Richtmyer, but

---

<sup>6</sup> Phys. Rev. (2), VI, p. 66; 1915.

adapted to the needs of spectrophotometry. It has so far been used for two purposes, the measurement of spectral transmission and the measurement of diffuse spectral reflection relative to that of a second substance, such as magnesium carbonate, as a standard. Other applications will be pointed out later. Inasmuch as by far the greater part of the work for which the apparatus was needed was the measurement of spectral transmission, the method was designed and the apparatus installed with this primarily in mind.

## II. SPECTRAL TRANSMISSION

### 1. APPARATUS

The essential parts of the apparatus<sup>1</sup> are outlined in Fig. 1, which, in connection with the key on the page opposite the figure, is practically self-explanatory. In addition the following points might be noted:

In order to eliminate so far as possible all vibrations which might affect the sensitive electrometer disk, the apparatus was set up in the basement on the ground floor, an absolutely rigid support being furnished by the concrete piers, slate slab, and cast-iron base. This arrangement has been entirely satisfactory, the electrometer being unaffected by vibrations of any kind.

The aluminum box (aluminum being used because of its light weight) with the iron base serves three purposes:

1. Being grounded, it gives complete protection to the electrometer, the photoelectric cells, and the connecting wires from all extraneous electrical disturbances.

2. It prevents any radiant energy to which the photoelectric cells are sensitive from reaching them, except what comes through the windows  $W_1$  or  $W_2$ . The inside walls, including the partitions  $N$ , are painted a dull black.

3. It makes it possible to dry out thoroughly the air around the electrometer, the photoelectric cells, and the insulating materials—an absolute necessity for success. Concentrated sulphuric acid in open dishes in each one of the three compartments has been very efficient as a drying agent. Melted paraffin was poured into the lower brass channels to make them air-tight, but it has not been necessary to seal in the cover

The electrometer is adjusted so that the reading of the spot of light is about the same when the disk is charged to +150 volts as

<sup>1</sup> The aluminum inclosure, the electrometer, the bilateral slits, the carrier arrangement, the lamp inclosures, and many other minor pieces of the apparatus were constructed in the Bureau instrument shop by J. A. Johannessen.

## KEY TO FIG. 1

[Apparatus drawn to scale shown in diagram except for batteries and a few other minor details.]

FFFF—Slate slab supported by two concrete pillars resting on basement floor.

IIII—Cast-iron base 3.5 cm thick resting upon slate slab.

JJJJ—Aluminum box 50 cm high, divided into three compartments by partitions *N* and fitting into brass channels on iron base. Has aluminum cover fitting into brass channels at top of box.

E—Dolezalek quadrant electrometer, resting on iron base, with aluminum disk *E'* suspended by platinized quartz fiber.

*P<sub>1</sub>P<sub>2</sub>*—Kunz potassium-hydride photoelectric cells supported by tripods resting on iron base.

AAA—Pieces of polished amber with brass rods through centers.

GG'—Ground-wire connections to water pipe. Cast-iron base, aluminum box, electrometer case, and one pair of quadrants permanently grounded.

U—U tube filled with mercury into which dips a pointed amalgamated copper wire. Used for make-and-break ground connection for second pair of electrometer quadrants, controlled from *X*, *X'*, or *X''*

WW<sub>1</sub>W<sub>2</sub>—Windows.

H—Hilger constant-deviation spectrometer, resting on slate slab, with glass prism and accurately adjustable bilateral slits *S<sub>1</sub>* and *S<sub>2</sub>*.

T—Track of iron Scimatco optical bench resting on ground floor.

*L<sub>1</sub>*—Mazda C moving-picture lamp rated at 600 watts (30 volts, 20 amperes), filament in one plane about 1 cm square, completely inclosed except for concealed ventilating openings and openings 3 cm in diameter in front and back of filament. *L<sub>2</sub>* is carried by a three-wheeled car moving along photometer track and carrying a marker directly beneath filament by which its distance from slit *S<sub>1</sub>* may be read on scale shown in diagram.

Z—Black felt screens, supported on T, enabling measurements to be made with other lights in the room.

Y—Leeds and Northrup rotating sector and motor *Y'*, supported on T, used to test inverse-square law for *L<sub>2</sub>* and to increase range of measurements.

C—Sliding carrier, supported on T, containing specimen *B*, whose transmission is to be measured. Carrier slides back and forth from C to C'.

Q—Container for selective ray filters.

*L<sub>1</sub>*—Mazda C automobile headlight lamp rated at 14 watts (7 volts, 2 amperes), inclosure similar to that for *L<sub>2</sub>*, supported by iron base. *L<sub>1</sub>* and *L<sub>2</sub>* are run in parallel with suitable adjustable resistances on a 60-volt storage battery.

*S<sub>1</sub>*—Accurately adjustable bilateral slit, supported on iron base, identical with *S<sub>2</sub>* and *S<sub>3</sub>*.

Q'—White opal glass screen.

V—Battery of Eveready cells, usually about +150 volts, by which electrometer disk may be charged through conducting suspension.

*V<sub>1</sub>V<sub>2</sub>*—Battery of Eveready cells, usually about 40 and 80 volts, respectively, of such value that the dark currents through *P<sub>1</sub>* and *P<sub>2</sub>* are approximately equal.

R—Adjustable high resistance.

KK<sub>1</sub>K<sub>2</sub>—Knife switches.

L—25-watt vacuum tungsten lamp. Light from filament is reflected and focused by small mirror on electrometer disk to give image on 50 cm ground-glass scale at D.

X—Approximate position of observer when scale is at D.

*X'D', X''D''*—Other positions of observer and ground-glass scale under conditions explained in paper. In these cases light from L is reflected to *D'* or *D''* by a mirror *M'* or *M''*.



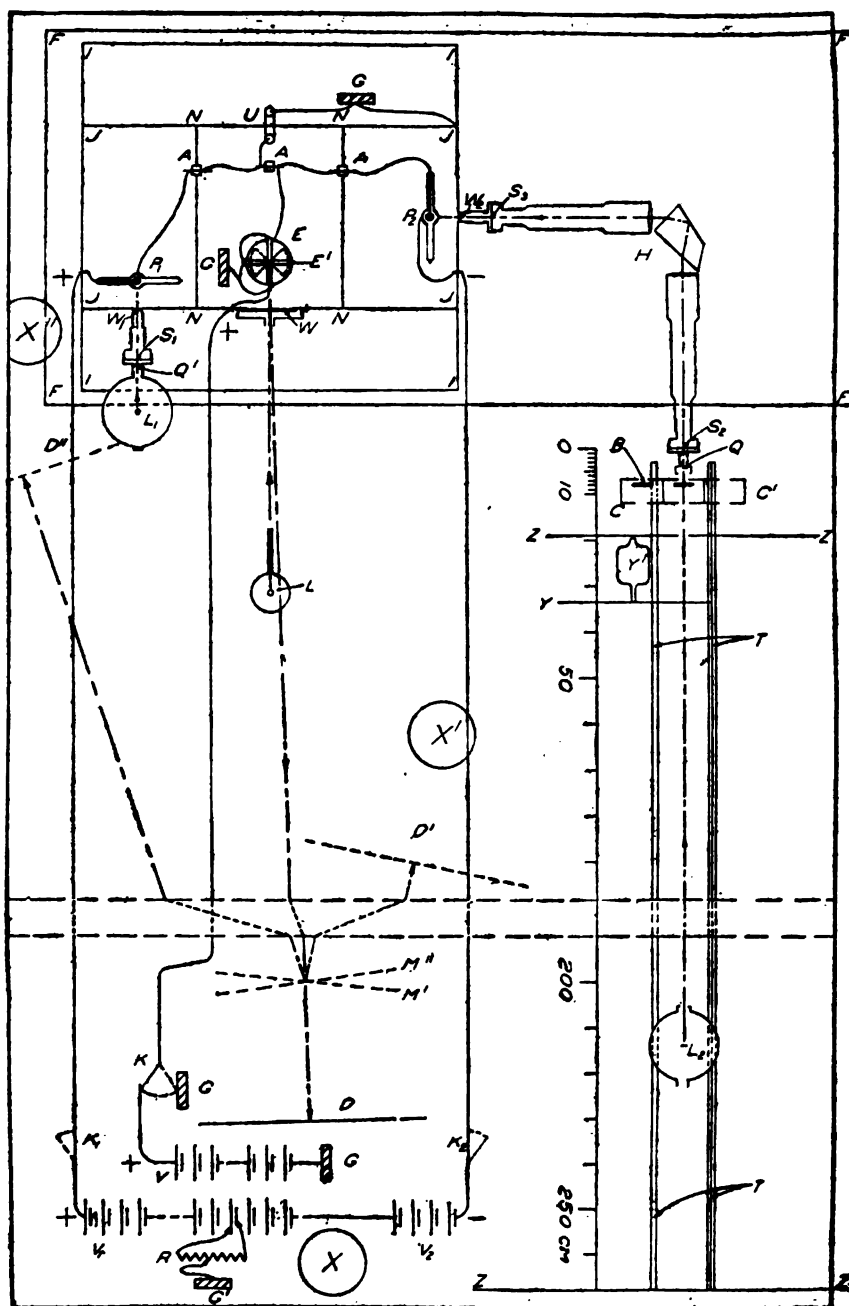


FIG. 1.—Diagram of apparatus. For explanation, see opposite page  
117366°—19—2

when it is uncharged. However, the position of the "charged zero," which varies with the charge, has no effect on the measurements. The charging battery  $V$  is kept somewhere between +125 and +175 volts. When charged to +150 volts and with the scale at 2.5 m, the sensitivity is about 3000 mm deflection for a difference of potential between the quadrants of 1 volt.

The prism and lenses of the Hilger constant-deviation spectrometer are completely inclosed by many thicknesses of black felt, and absolutely no stray visible or ultra-violet radiant energy can get into the spectrometer except what comes through the slit  $S_2$ . Even this has been to a great extent eliminated by specially made diaphragms placed in the collimators, and what still remains can be easily taken care of by selective ray filters placed in  $Q$ . The calibration was carefully checked and such adjustments made as to bring the 436 mercury line into focus at the slit  $S_2$  without parallax. The slits were very carefully made and are accurately graduated to hundredths of millimeters. As shown in the diagram, they are stopped down by means of caps fitting over them, so that slit  $S_2$  is in effect but 1.0 cm and  $S_1$  but 2.0 cm in height.  $S_2$  and  $S_1$  are always kept at the same width, usually 0.20 mm.

The carrier  $C$  contains two hard-rubber holders, one of which holds the specimen  $B$ , whose transmission is to be studied, while the other may hold a comparison specimen or be simply a blank, as desired. The whole carrier arrangement is very substantially made and keeps the specimen securely in position, enabling it to be brought back always to exactly the same place.

The arrangement of  $L_1$ ,  $S_1$ , and  $Q'$  is such that the amount of radiant energy falling on the photoelectric cell  $P_1$  will be accurately proportional to the width of  $S_1$ .

The distance of  $L_2$  from  $S_2$  can never be made less than 46 cm because of the other apparatus on the bench, such as the sector, carrier, etc. This, combined with the fact that the filament of  $L_2$  is in a plane only 1 cm square, enables the inverse-square law to be assumed; that is, the amount of radiant energy entering the slit  $S_2$  varies inversely as the square of the distance of  $L_2$  from  $S_2$ . The rotating sector serves as a means of checking this inverse-square law and also as a means of making sure that the apparatus keeps in perfect working condition from day to day. The length of the photometer bench enables  $L_2$  to be moved back to 255 cm from the slit. Therefore, the range of transmission possible with the 10 per cent sector is from 1.00 to approximately

0.004. The distance of  $L_2$  from the slit  $S_2$  is varied by means of a cord fastened to the ends of the car carrying  $L_2$  and passing over pulleys at the ends of the photometer bench, and is controlled by the observer at  $X$  or  $X'$ .

By operating  $L_1$  and  $L_2$  in parallel, errors due to any fluctuating voltage are partially eliminated. These currents through  $L_1$  and  $L_2$  are read by ammeters and controlled by rheostats operated from the position  $X'$ . When an observer works alone, he takes the position  $X'$  (the scale being at  $D'$  and the mirror at  $M'$ ), where he can watch the currents through  $L_1$  and  $L_2$ , observe the spot of light on  $D'$ , and adjust the distance of  $L_2$ , and where it is convenient for him to change the wave-length scale of  $H$  and to shift the carrier  $C$  back and forth. If he has an assistant, the observer takes the position  $X$ , where he can adjust the distance of  $L_2$  and observe the spot of light on  $D$ . In this case, the assistant is at  $X'$ , where he can watch the currents, adjust the wave length, and operate the carrier.

The switches  $K_1$  and  $K_2$  are usually kept closed even when the apparatus is not in use; and inasmuch as the dark currents do not need to be exactly balanced for transmission measurements, the values of  $V_1$  and  $V_2$  are very seldom changed. The value of the ratio  $V_2/V_1$  necessary to balance the dark currents through  $P_1$  and  $P_2$  is approximately two, though this varies somewhat from time to time. The switch  $K$  is used to charge the electrometer disk or to ground it when not in use. Every few weeks the batteries are tested, and those found depreciating are replaced by new ones. Otherwise  $V$ ,  $V_1$ , and  $V_2$  need no attention. Under actual operating conditions the various quantities have so far usually had the following values, these being such as to give the desired sensitivity and balance with the lamp  $L_2$  well back on the track:

$V = +150$  volts, approximately.

$V_1 = +40$  volts, approximately.

$V_2 = -80$  volts, approximately.

$S_1 = 1.00$  mm.

$S_2 = S_1 = 0.20$  mm.

$i_1 = 1.25-1.85$  amperes = current through  $L_1$ .

$i_2 = 17.0-19.5$  amperes = current through  $L_2$ .

## 2. METHOD

The theory upon which the whole method is based is very simple, indeed. When the ground connection is made at  $U$ , both pairs of quadrants are at zero potential. Under this condition the

charged electrometer disk will be at rest. Let the voltage applied to  $P_1$  be  $V_1$  and that applied to  $P_2$  be  $V_2$ , and let the total resistances (mainly that of the photoelectric cells) between  $U$  and  $G'$  be  $R_1$  by way of  $P_1$  and  $R_2$  by way of  $P_2$ . Then through  $P_1$  a current will flow of magnitude  $I_1 = V_1/R_1$  and through  $P_2$  of magnitude  $I_2 = V_2/R_2$ . No radiant energy to which the photoelectric cells are sensitive is considered as falling on them,  $I_1$  and  $I_2$  being what are ordinarily called the dark currents.

If the ground connection at  $U$  is broken, the electrometer disk will be deflected (shown by the drift of the spot of light) unless  $I_1$  is exactly equal to  $I_2$ . If they are not equal, they may be made so by changing the relative values of  $V_1$  and  $V_2$ . This is done by varying the point of ground connection at  $G'$ .

Now let  $P_1$  and  $P_2$  be irradiated by  $L_1$  and  $L_2$ . This will bring about a great increase in the photoelectric currents  $I_1$  and  $I_2$ , and the irradiations may be so adjusted (by varying the currents  $i_1$  or  $i_2$ , the width of  $S_1$ , or the distance of  $L_2$ ) as to make  $I_1$  again exactly equal to  $I_2$ , as shown by the zero motion of the electrometer disk when the ground connection at  $U$  is broken. Now let the irradiation of  $P_2$  from  $L_2$  be reduced by interposing the specimen  $B$ . Then  $I_2$  will be less than  $I_1$ , and, with  $U$  broken, the spot of light will be deflected. Two methods may be employed to make  $I_1$  and  $I_2$  again equal, a means of obtaining a measure of the transmission of  $B$  being thus possible: (1) The amount of radiant energy falling on  $P_1$  may be decreased by narrowing  $S_1$  until  $I_1$  becomes equal to  $I_2$ , the ratio of the slit widths in the two cases being a measure of the transmission; or (2) the amount of radiant energy falling on  $P_2$  may be increased by moving  $L_2$  nearer the slit  $S_2$  until  $I_2$  again becomes equal to  $I_1$ , the inverse ratio of the squares of the distances in the two cases giving the transmission.

The value of the transmission obtained by the two methods will be the same only in case the dark currents are exactly equal and in case the two photoelectric cells obey exactly the same irradiation-current law. In case either of these conditions is not fulfilled, the value of the transmission obtained by the first method will be in error, but by the second method the accuracy of the value of the transmission will be unimpaired though either or both of these conditions are not fulfilled. Therefore, as is illustrated below, the transmission is measured by merely varying the distance of  $L_2$  from the slit  $S_2$ , this distance being the only variable in the operation; for the width of the slit  $S_1$ , the amount and quality of the radiant energy falling on  $P_1$  and  $P_2$ , the photo-

electric currents  $I_1$  and  $I_2$ , and the currents through  $L_1$  and  $L_2$ , are unchanged, whether the specimen is in or out.

The following is the procedure used in measuring the transmission of the specimen  $B$ : At the start the electrometer disk is charged by throwing the switch  $K$ , and the equality of the dark currents through  $P_1$  and  $P_2$  tested by breaking the ground connection of the electrometer quadrants at  $U$ . Then the lamps  $L_1$  and  $L_2$  are lighted and the currents adjusted to obtain the desired balance when the carrier is in the position  $C$ —"specimen out." This exact balance of photoelectric currents is obtained by bringing the light on the scale  $D$  to rest, not necessarily at the zero position but in a *position of no motion*, which indicates that the electrometer quadrants are receiving no further charge; that is,  $I_1 = I_2$ . Let this distance of  $L_2$  from  $S_2$  with the specimen out be  $d_A$ . Then the carrier is moved to position  $C'$ , bringing the specimen into position in the path of the radiant energy from  $L_2$ —"specimen in"—and, *with  $S_1$  and all other factors unchanged,  $L_2$  is moved forward until a balance is again obtained*, as indicated by the zero motion of the spot of light from the electrometer. Let this distance of  $L_2$  from  $S_2$  with the specimen in be  $d_B$ . As a check, the specimen is again taken out (carrier back to  $C$ ) and  $L_2$  moved back till a balance is again obtained. This third reading  $d_A$  should check the first. It usually agrees to within a few millimeters, and the average is used. If, as is seldom the case, it differs by two centimeters or more, the readings are usually repeated. This depends on the accuracy desirable. Thus three readings are taken at each wave length, one with the specimen in and two with the specimen out, the transmission being equal to  $(d_B/d_A)^2$ . At low transmissions, since it is desirable to make sure that  $d_B$  can be obtained, the readings are usually taken in the order  $d_B$ ,  $d_A$ ,  $d_B$ , the rotating sector being started if it is impossible to obtain  $d_A$  otherwise. For values of transmission of about 0.05 or less, the value of  $d_A$  is always obtained with the sector rotating, the ratio  $(d_B/d_A)^2$  being multiplied by the proper factor to obtain the transmission. More readings can, of course, be taken if extreme accuracy is desired, but the above set of three, comprising a single determination, gives sufficient accuracy for nearly all kinds of work. The average time for a set of three readings is from 2 to 5 minutes, and the first set can usually be obtained within 10 minutes after entering the room.

The operating current of  $L_2$  is practically always within the range 17.0–19.5 amperes, 19.5 being set as the upper limit

in order to prolong the life of the lamp (rated at 20 amperes). The current  $i_2$  (through  $L_2$ ) might be kept at 19.5 amperes at all wave lengths and  $i_1$  (the current through  $L_1$ ) varied until the desired balance is obtained. However, this results in the blue in a sensitivity greater than is necessary. Therefore, it has been found practicable to make  $i_2$  about 17.0 amperes at 460  $m\mu$ , making  $i_1$  of such value as to bring about the desired balance. For wave lengths greater or less than 460  $m\mu$ , the value of  $i_1$  is kept constant and  $i_2$  increased until, at about 410 and 540  $m\mu$ ,  $i_2$  is made equal to 19.5 amperes. When measurements are made at wave lengths greater or less than these values,  $i_2$  is kept at

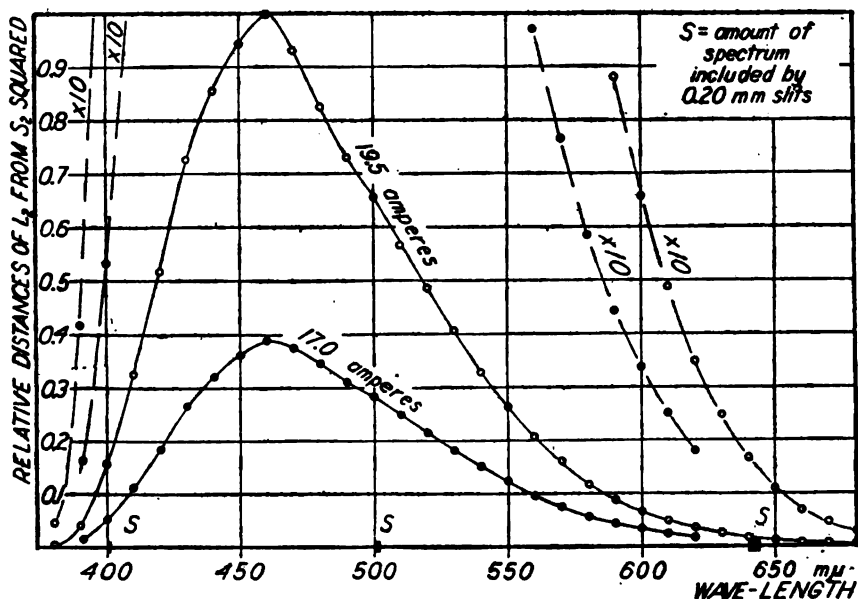


FIG. 2.—Curves showing spectral response of cell  $P_2$ , for currents of 19.5 and 17.0 amperes through  $L_2$ , under conditions of apparatus shown in Fig. 1

19.5 amperes and  $i_1$  lowered to get the desired balance. For low transmissions, higher values of the ratio  $i_2/i_1$  become necessary. Thus a constant sensitivity is usually used for all wave lengths between 410 and 540  $m\mu$ , but at wave lengths greater or less than these limits a lowered sensitivity becomes necessary. However, lowered sensitivity means not entirely a decrease in the accuracy of the measurements, but, in part, merely an increase in the time required to obtain them.

In Fig. 2 are shown what might be called the spectral response curves of cell  $P_2$ , for currents of 19.5 and 17.0 amperes through  $L_2$ , under the particular conditions obtaining with this apparatus;

that is, they are as actually obtained, uncorrected in any way, for the variable absorption or dispersion of the prism or the variable spectral distribution of radiant power from  $L_1$ . The ordinates are proportional to the squares of the distances of  $L_2$  from  $S_2$ , necessary to obtain a balance,  $i_1$  and  $S_1$  being kept constant. The curves are doubtless a little high at the extremities, due to stray radiant energy from the blue or green regions. Stray ultra-violet radiant energy is effectually excluded by the absorption of the large glass prism, to which is also mainly due the sharp decrease in the response from 460 to 380 m $\mu$ .

### 3. ERRORS AND ACCURACY

As already stated, certain errors ordinarily met with when the photoelectric cell and electrometer are used to measure spectral transmission are eliminated by the null method herein described. These are:

1. Errors due to the photoelectric current not being strictly proportional to the radiant power incident on the cell. No calibrations of the cells are necessary, and it makes no difference what the relation is between radiant power and photoelectric current.

2. Errors due to what is ordinarily known as the dark current. It makes no difference whether or not it is eliminated. Nor do the dark currents through the two cells have to be the same, though approximately this condition is desirable for convenience' sake. It is necessary merely that conditions be steady over a period of from two to five minutes, the time usually required for a set of readings. Actually, conditions seem to be practically steady and unchanging for days, even weeks, at a time. In spite of this, any slight continuous change in conditions would tend to be nullified by the procedure of taking the first and third readings with the specimen removed and using the average.

3. Errors due to the use of the electrometer as a deflection instrument. Such errors may be those due to the deflections of the electrometer disk as given by the spot of light on the scale not being strictly proportional to the charge or potential acquired by the quadrants, those due to leakage of charges because of imperfect insulation or moist air, or those connected with the use of timing devices.

The errors which may be present can be put into two classes, those resulting from this method and apparatus and those to

which all methods of spectrophotometry are liable. The errors resulting from this method and apparatus are of three kinds:

1. Those due to slight variations in the currents through the two lamps. In spite of the use of storage batteries, there are often small variations in the currents of one or both lamps, usually the large one, due probably to variations in the contact resistances by which the currents are regulated. If the first and third readings of a set disagree by more than 2 cm, it is nearly always found to be due to one current or the other having varied and for the moment escaped observation. However, by means of the ammeters the currents are kept as nearly constant as it is possible to judge by the eye, and usually the third reading will check the first to 1 cm or better. And as already noted, the method of averaging the first and third readings tends to eliminate any errors due to gradually changing conditions.

2. Those due to the inverse-square law not being exactly obeyed by  $L_1$ . This would be expected to be very small because of the filament occupying an area of only 1 cm<sup>2</sup> and because it is not possible to move the filament closer to the slit than 46 cm. It has been tested by means of the rotating sector. Other investigators<sup>8</sup> have found that Talbot's law holds for the photoelectric cell; and a great number of observations at different times and at many wave lengths on the apparatus herein described prove that the inverse-square law is obeyed, assuming Talbot's law to hold, or that Talbot's law is obeyed, assuming the inverse-square law to hold. Actually, the error due to any failure of  $L_1$  to obey the inverse-square law is too small to be detected over the range of distances used. It might be noted here that when the transmission of thick specimens is measured, correction is made to the value of  $d_s$  as read on the scale, this reading being larger than the true optical distance of  $L_1$  from  $S_1$ .

3. Errors of observation, mainly those due to a natural tendency to hurry and not wait for the spot of light to come absolutely to rest. Two classes of work might be distinguished in this connection; first, measurements where only ordinary accuracy is desired, as in most tests and in other work where information as to the spectral transmission merely is desired; and secondly, measurements of a higher accuracy, where fine specimens are being standardized or where different methods are being com-

<sup>8</sup> H. E. Ives, *Astro. Journ.*, 48, p. 24; 1916. J. Kunz, *Astro. Journ.*, 45, p. 69; 1917.



pared by means of standard specimens or a rotating sector. The difference in the two cases is partly that of the time used in making the observation, higher accuracy being reached by waiting a longer time to see if the spot of light is truly at rest, and partly that of the number of readings in a set, more readings being taken for greater accuracy; e. g., the first, third, fifth, and seventh with the specimen out, the second, fourth, and sixth with it in, averages being used in computing the transmission.

The errors to which all methods of spectrophotometry are liable are those connected with the dispersion apparatus. These may be due to:

1. Stray radiant energy. As already mentioned, special diaphragms and, when needed, selective ray filters eliminate this error so far as can be detected.

2. Inaccurate wave-length calibration. The scale of the Hilger constant-deviation spectrometer is already calibrated in wave lengths with considerable accuracy. This calibration was very carefully checked visually from 390 to 600  $m\mu$  by means of the Fraunhofer lines and a curve of corrections plotted, which is used in making wave-length settings. This correction does not amount to more than 0.7  $m\mu$  over this range. It was rechecked photoelectrically by means of the mercury lines after the spectrometer was set in place. Errors in the wave-length settings are believed to be not greater than 0.2  $m\mu$  in the blue and 0.5  $m\mu$  in the red.

3. The use of finite slit widths in the spectrometer. Errors introduced for this reason are minimized by making the two slits  $S_1$  and  $S_2$  equal and constant for any set of readings. The amount of the spectrum included at different wave lengths by slit widths equal to 0.20 mm is indicated in Fig. 2. Higher accuracy might be reached by reducing the slit widths from 0.20 to 0.10 mm, but with the present voltages on the cells this would, except in the blue, necessitate lowering the sensitivity, and would thus decrease the accuracy, as well as the range, at which it is possible to make measurements. Except for very narrow bands, this error due to finite slit widths is considered negligible for constant values of 0.20 mm or less. By raising the voltages on  $P_1$  and  $P_2$ , keeping the proper value of the ratio  $V_2/V_1$ , the sensitivity would be increased, and it is probable that, with sufficiently higher voltages, the slits  $S_1$  and  $S_2$  could be reduced to 0.10 mm with a resulting sensitivity as great as at present used. However, it is not desirable to get

too near the critical voltage of the cells, and so far it has not seemed necessary to use voltages higher than those given. Further study of this question is planned.

The accuracy of the transmission measurements obtainable by this method and apparatus has been tested mainly in two ways:

1. By measuring the transmission of rotating sectors of known aperture.
2. By measuring the transmission of standard samples and other good specimens whose transmission has also been obtained by other methods, visual and photographic.

Further confidence in the method has been obtained as follows:

1. By measuring the transmission of two standard samples and using each of these in turn as a known comparison sample for obtaining the transmission of a third sample.
2. By measuring samples of different thicknesses and comparing observed with computed results, assuming Lambert's law.
3. By repeating measurements on the same specimen.
4. By the smoothness of transmission curves obtained.

So far as the errors resulting from this method are concerned—viz, those due to possible variations in the currents through the lamps, those due to failure of  $L_2$  to obey the inverse-square law, and those classed as errors of observation—their combined effect may be tested by means of measurements made on the rotating sectors. Tests have so far been made on sectors rated at 80, 50, and 10 per cent transmission, the true transmissions having been determined by the photometric section of the Bureau as 0.800, 0.500, and 0.102. Out of 12 measurements made on the 0.800 sector 8 were within 0.003 of this value, the greatest deviation being 0.007. Out of 21 measurements made on the 0.500 sector 16 were within 0.002 of this value, the greatest deviation being 0.008. Out of 10 measurements made on the 0.102 sector 6 were within 0.0015 of this value, the greatest deviation being 0.003. These measurements comprise all that have been made since the sectors were received, with the exception of those made on one lamp which did not stand vertically in the socket and which gave values from 0.005 to 0.015 too low. They have been obtained at a number of different times, on different lamps, by different observers, at wave lengths from 400 to 600  $\mu$ , and with  $L_2$  at distances from  $S_2$  varying from 250 cm to 50 cm. Not many of them are precision measurements, the majority being taken with the same ordinary care used in most transmission measurements.

There is no consistent deviation from the inverse-square law when  $L_s$  is anywhere from 50 to 250 cm from  $S_s$ . Conversely, as already noted, the above measurements add considerable proof that Talbot's law of the rotating sector is valid when applied to the photoelectric cell. The speed of rotation seems to make no difference.

However, the tests by means of the rotating sectors give no clue to the uncertainties or errors which are liable to be present in all methods of spectrophotometry; viz, those due to stray light, finite slit widths, etc. In fact, the only final test for any method is its agreement with other methods, due regard being paid to all the known factors of accuracy or error. Inasmuch as an investigation now being made into the agreements between the different methods at present used in the color-standardization work of the Bureau has not yet been completed, comparison is made in this paper only with results obtained visually on the Martens polarization photometer<sup>9</sup> at those wave lengths where monochromatic light can be obtained. The mercury arc has been used as a source, the violet, blue, green, and yellow lines being isolated by suitable color screens, giving practically monochromatic light at 406, 436, 546, and 578  $m\mu$ . Inasmuch as all questions of stray light and slit widths are avoided in this instrument, it is a valuable means of comparison. However, if steep transmission curves happen to be encountered at 406 or 578  $m\mu$ , then, of course, uncertainty enters, since there are in reality two lines close together at approximately these wave lengths. It should be noted also that, since the transmission is equal to  $\tan \theta_1 \cot \theta_2$ , there results at low transmissions much greater accuracy in terms of the transmission unit than at high transmissions. For example, the range of angle giving transmissions from 0.50 to 1.00 is about  $35^\circ$ – $45^\circ$  for  $\theta_1$  and  $45^\circ$ – $55^\circ$  for  $\theta_2$ , but for transmissions from 0.00 to 0.50 the range is  $0^\circ$ – $35^\circ$  and  $55^\circ$ – $90^\circ$ , respectively. This makes little difference for green and yellow light, to which the eye is very sensitive; but for the blue and especially the violet mercury lines the uncertainty of measurement for high transmissions is considerable. It is thought, therefore, that discrepancies occurring at 436 and 406  $m\mu$  are mainly due to errors on the Martens

<sup>9</sup> Phys. Zeit. I, p. 299; 1900. In this instrument two beams of light from the same source are polarized mutually perpendicular by means of a Wollaston prism and brought together to form the two halves of a photometric field. This field is viewed through a nicol prism, and the adjustment is such that the two halves of the field are brought to equality by the analyzing nicol at about  $45^\circ$  on the scale. The specimen was placed first in one beam and then in the other and the analyzing nicol rotated in each case until a photometric match was obtained. The tangent of the angle in one case multiplied by the cotangent in the other gives the transmission of the specimen; that is,  $T = \tan \theta_1 \cot \theta_2$ .

photometer. It is at 546 and 578  $m\mu$ , if the curves are not too steep at this latter wave length, that the most valuable checking can be done, for here the visual method is of great precision, while the photoelectric method is not at its best from the standpoint of either sensitivity or dispersion. Whatever accuracy and reliability, then, is found for the photoelectric method at these wave lengths should be equaled or surpassed throughout the whole range from these wave lengths to and including 410  $m\mu$ .

A number of transmission<sup>10</sup> curves are shown in Figs. 3 to 9. The Jena specimens whose curves are shown in Figs. 3 to 7, with some

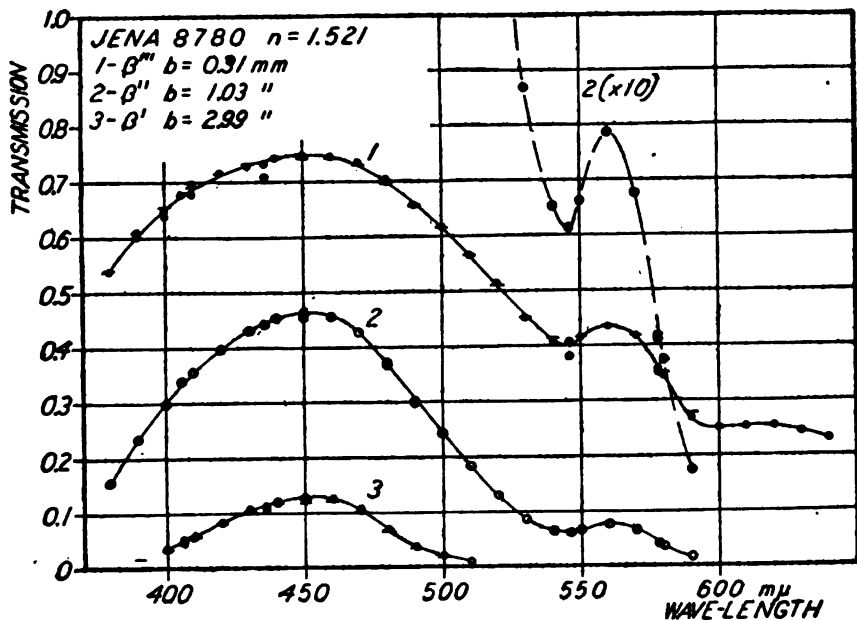


FIG. 3.—Transmission curves illustrating agreements between photoelectric and visual methods. For explanation see p. 24

346

red samples whose curves are not shown, comprise a set of standard precision glasses kept on file at the Bureau. These glasses, so far as can be detected, are free from all defects such as striæ, bubbles, etc., and have been finished with great care, the surfaces being highly polished and made parallel to within 0.01 mm. They were prepared and are used mainly for a comparison of different methods in order that any discrepancies found may be laid entirely to the methods and not to the specimens. The other samples, Figs. 8 and 9, are considered as fairly good specimens, but were not

<sup>10</sup> The transmission of a specimen (distance between surfaces =  $b$ ) is defined as that fraction of radiant power incident on the first surface which gets through the second surface.

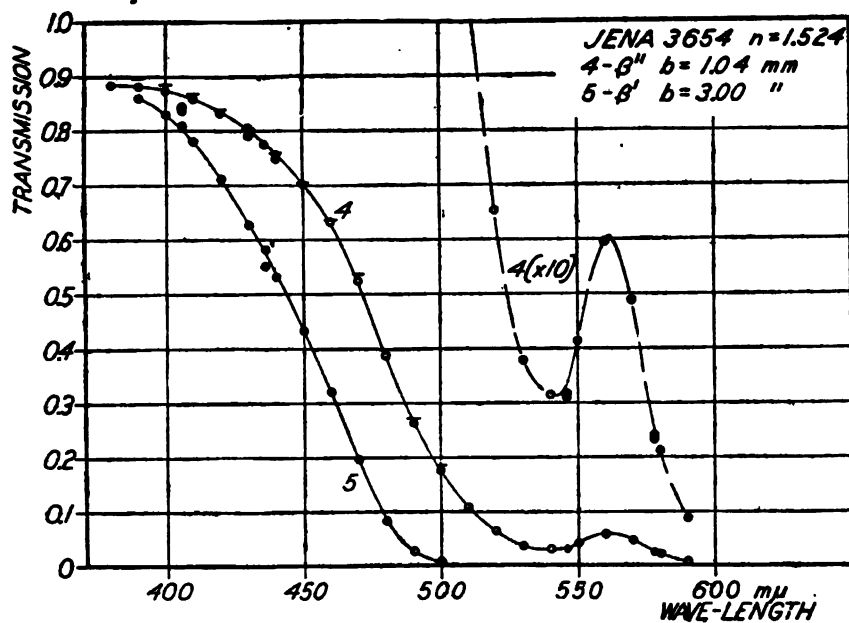


FIG. 4.—Transmission curves illustrating agreements between photoelectric and visual methods. For explanation see p. 24 **346**

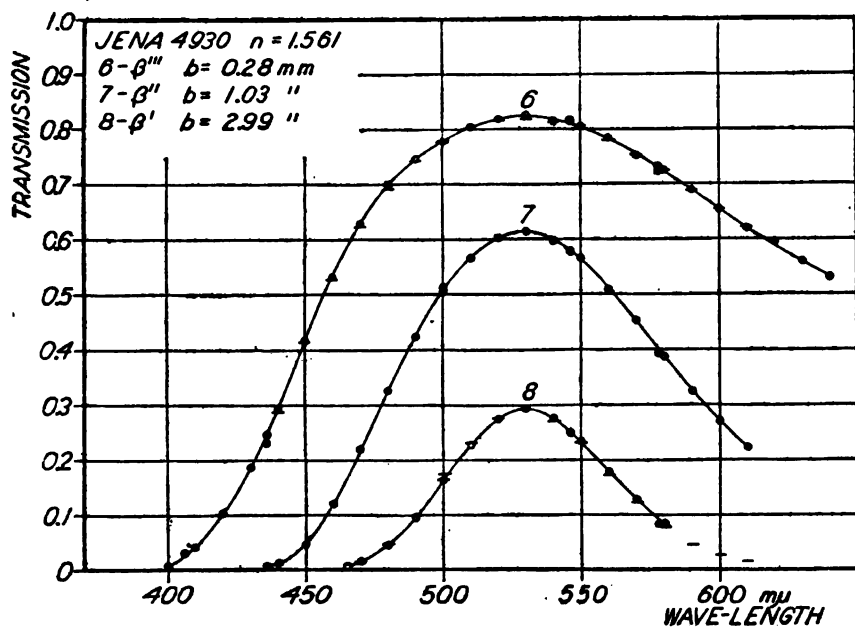


FIG. 5.—Transmission curves illustrating agreements between photoelectric and visual methods. For explanation see p. 24 **346**

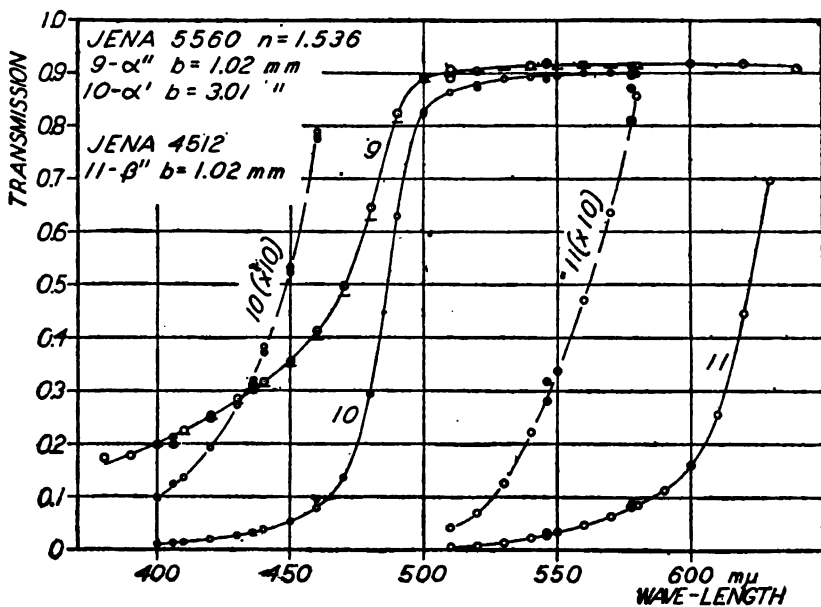


FIG. 6.—Transmission curves illustrating agreements between photoelectric and visual methods. For explanation see p. 24. **346**

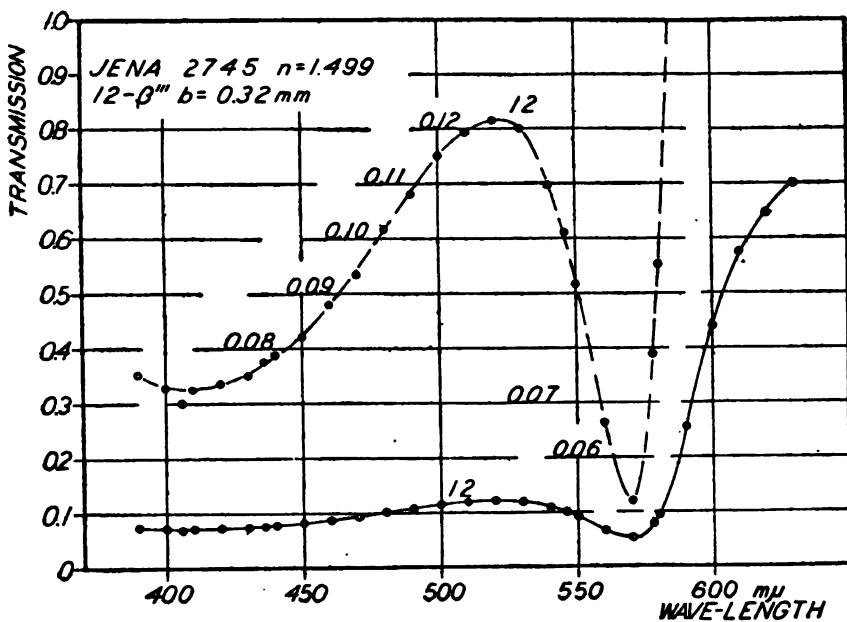


FIG. 7.—Transmission curves illustrating agreements between photoelectric and visual methods. For explanation see p. 24. **346**

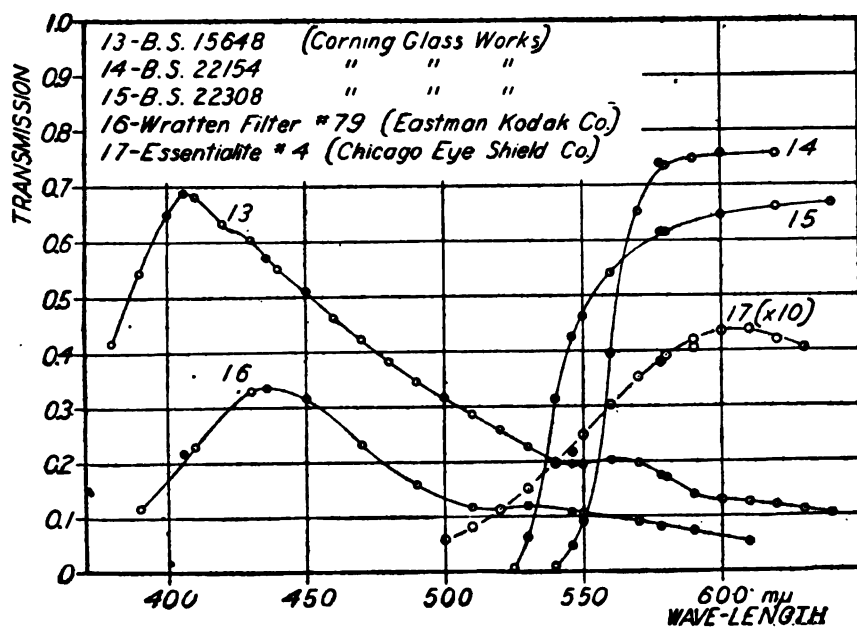


FIG. 8.—Transmission curves illustrating agreements between photoelectric and visual methods. For explanation see p. 24.

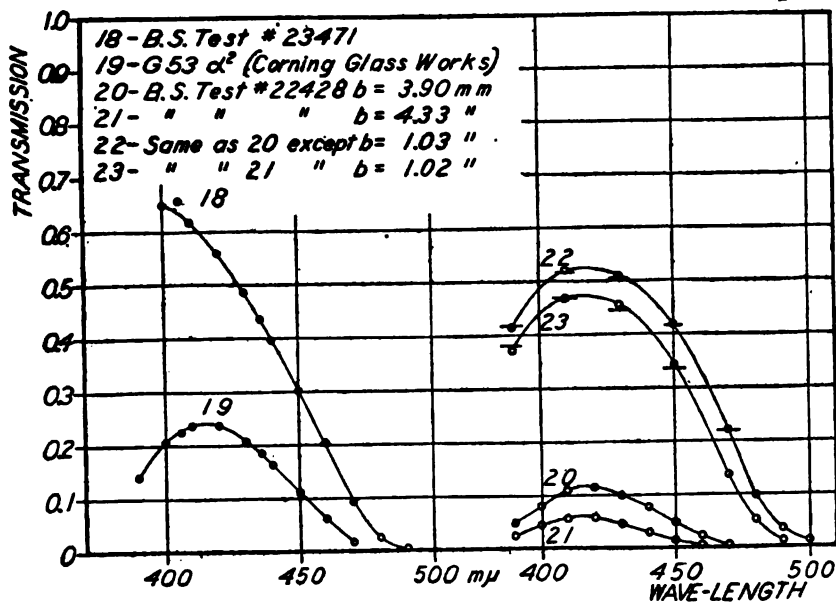


FIG. 9.—Transmission curves illustrating agreements between photoelectric and visual methods. For explanation see p. 24.

prepared with such care as the Jena standards. "B. S." numbers and Greek letters are Bureau of Standards, not makers', designations.

Values obtained photoelectrically are shown by the white-centered circles; those visually on the Martens photometer by black circles. Values of transmission below 0.10 (or 0.12, Fig. 7) are usually plotted to a scale magnified 10 times in order to bring out various points better. This is indicated on the curves by the dotted lines. Where possible, values of transmission have been measured at different thicknesses in order to compare observed with computed results, assuming Lambert's law. Such computed values are shown by short horizontal black lines. In the case of the Jena specimens this computation could be very accurately carried out, for the index of refraction  $n$  for each kind of Jena glass had been carefully measured.

In a study of these curves, attention is called to the following points:

1. Curves are shown for all specimens which have ever been tested by both methods, with the exception of some blue glasses which have the same types of curves and which show the same sort of agreements or disagreements at 436 and 406  $m\mu$  as the blue glasses herein shown.

2. Most of the photoelectric determinations have been made by the writer, most of the visual determinations by other observers.

3. No values have been omitted which were obtained between 380 and 640  $m\mu$ , inclusive, by either method.

4. The values plotted are in all cases single determinations; no averages have been used. By a single determination is meant a value obtained at any one wave length before going to another wave length. On the photoelectric apparatus this single determination consists usually of three readings—two with the specimen out and one with it in, or vice versa. In but very few cases were more than these three readings taken in a single determination. On the Martens photometer a single determination consists of from 2 to 10 readings for both  $\theta_1$  and  $\theta_2$ .

5. The values plotted fall almost uniformly on a smooth curve, even to 380 and 640  $m\mu$ . This is also shown by the curves in Fig. 2, in which the values plotted are single determinations.

6. The values obtained on the Martens photometer seldom fall off this smooth curve by as much as 0.01. Different determinations of the transmission obtained on this instrument show that even at 546 and 578  $m\mu$  a discrepancy between methods is not



entirely due to error in the photoelectric method. Discrepancies occurring at 406 and 436  $m\mu$  are considered mainly due to error in the visual method.

7. Values below 0.15, when plotted to a magnified scale, show the same smoothness of curve and a discrepancy between methods seldom more than 0.0015.

8. Beyond 600  $m\mu$  an increasing error is often noticed in the photoelectric method (shown by comparison with a visual method, König-Martens spectrophotometer, of known reliability in this region) amounting in some cases to as much as 0.05 at 650  $m\mu$ . A careful study of conditions beyond 600  $m\mu$  has not been made.

9. Discrepancies between observed and computed results are of interest as a test of Lambert's law, but, in general, should not be considered as a test of the accuracy of a method.

In addition to the data given in the figures, values of transmission at 546  $m\mu$  have been measured by each method on a number of fairly good specimens. The results were no different from those illustrated by the curves.

Besides the data herein given showing the kind of agreements obtained by these two methods, many other data are on file which have been obtained by other methods, visual and photographic, and which will in time be published. By a comparison with all these methods and after nearly a year's continual use, it is believed that the following statements of the accuracy obtainable by the photoelectric null method herein described are true:

1. Between wave lengths 410 and 550  $m\mu$ , inclusive, the uncertainty of measurements is not greater than 0.01 for values of transmission between 0.00 and 1.00, and not greater than 0.003 between 0.00 and 0.10.<sup>11</sup>

2. Beyond this range as far as 390 and 600  $m\mu$ , inclusive, the uncertainty is not greatly increased, being at these wave lengths not more than twice as great as throughout the better range.

3. To state it in another way, the percentage uncertainty from wave lengths 410 to 550  $m\mu$ , inclusive, varies from not more than 1 per cent at high transmissions to not more than 10 per cent for values of transmission equal to 0.01 or less, with slightly increasing uncertainty beyond these wave lengths as far as 390 and 600  $m\mu$ , inclusive.

---

<sup>11</sup> To illustrate: If transmission values equal to 0.793 or 0.0396 be obtained, it is believed that the true values can be guaranteed to be within the values 0.783 to 0.803 or 0.0366 to 0.0426, respectively. This method of stating the uncertainty is followed throughout the paper, except in paragraph 3 on this page.

### III. DIFFUSE SPECTRAL REFLECTION

The diffuse spectral reflection of substances is measured relative to that of some "white" substance, such as magnesium carbonate, taken as a standard and given the value of 1.00 for the reflection at all wave lengths. The changes necessary in transforming the apparatus to the measurement of reflection instead of transmission may be explained by means of Fig. 10. The lamp  $L_2$  (Fig. 1), which for its minimum distance from the slit  $S_2$  is in the position of  $L_2$  (Fig. 10) for transmission measure-

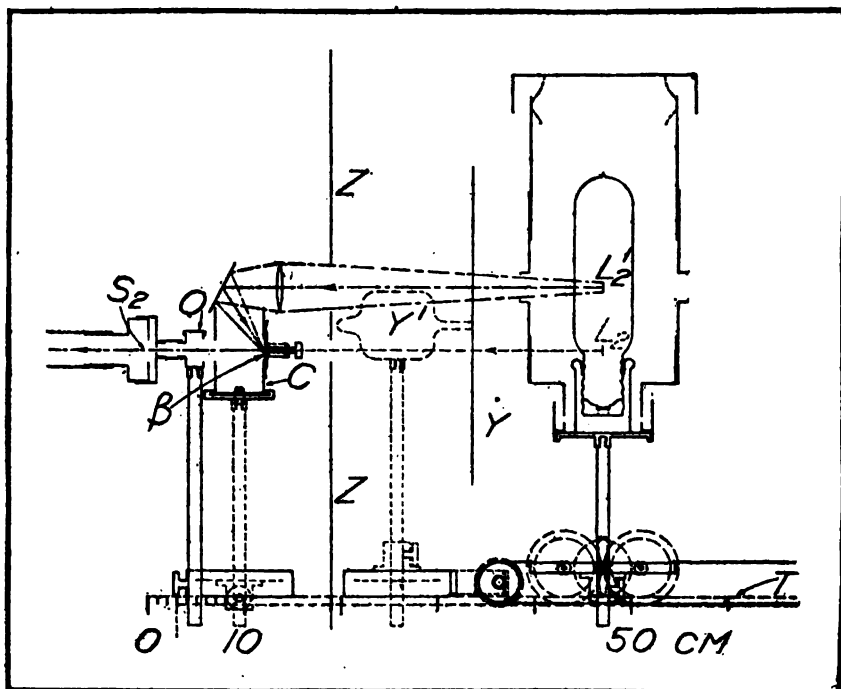


FIG. 10.—Illustrating changes in apparatus necessary for measuring diffuse spectral reflection

ments, is raised to the position of  $L_2'$  and kept in that position without further change. The hard-rubber holders which keep the specimen  $B$  (Fig. 1) in position are removed from the carrier  $C$ . The material whose reflection is to be studied is held firmly in position over one of the openings in  $C$  as indicated at  $\beta$  (Fig. 10), being pressed firmly and uniformly against the outside of  $C$  by means of a suitable clamp fastened to  $C$ . The comparison substance is clamped in position over the outside of the other opening in  $C$  (not shown in Fig. 10). By means of a

lens and mirror, as shown, the radiant energy from  $L_1'$  is brought to a focus on the surface of the reflecting substance at  $\beta$ , in front of  $S_2$ . In short, the arrangement is such that either the standard substance or that whose reflection is to be measured may be brought, by moving the carrier  $C$  back and forth, into position in exactly the same place in the focus of the radiant energy from  $L_1'$  and directly in front of the slit  $S_2$ . The diffuse reflection in the direction of  $S_2$  enters the spectrometer and reaches the cell  $P_2$  as before, the photoelectric current thus excited being balanced by the current from  $P_1$  due to  $L_1$ . The observer takes the position  $X''$  (Fig. 1), where he can vary the width of  $S_1$  while watching the spot of light, the mirror and scale being at  $M''$  and  $D''$ . As before, an assistant is at  $X'$ , where he can watch the currents, manipulate the carrier  $C$ , and adjust the wavelength scale of  $H$ .

To obtain the value of the diffuse reflection, the following readings are taken: First, the standard magnesium-carbonate surface is brought into position before  $S_2$  in the focus of the radiant energy from  $L_1'$ , and  $S_1$  varied to obtain a balance. Then the sample whose reflection is to be measured is brought into position by moving the carrier  $C$ , and  $S_1$  varied to get a new balance. Finally, a check value of  $S_1$  is taken with the standard back in position, and the ratio of the value of  $S_1$  with the sample in position to the average of the values of  $S_1$  when the standard is in position is taken as the reflection of the sample relative to that of the standard.

As so far used, the slits  $S_1$  and  $S_2$  have usually been made 0.25 or 0.30 mm wide, although for values of reflection below 0.05, as well as at 390  $m\mu$ , they are usually made 0.40 or 0.50 mm; and at 460  $m\mu$ , when the magnesium-carbonate surface is before  $S_2$ , the value of  $S_1$  necessary for a balance is from 1.50 to 2.00 mm, the currents through the lamps being the same as before. Under these conditions the sensitivity is thus approximately the same as that used in measuring transmission. There is this difference, however. In the method used for transmission measurements a constant sensitivity is used throughout a single determination—that is, whether the specimen is in or out—but in the method just described for reflection the sensitivity depends on the reflection, and thus varies in a single determination. This is unimportant except at very low reflections.

This is still a null method and avoids all errors connected with electrometer deflection methods. But, as already mentioned,

errors will be introduced in this use of the null method if the two photoelectric cells do not obey the same current-irradiation law and if the two dark currents through  $P_1$  and  $P_2$  are not exactly balanced. As previously explained, the dark currents may be balanced by adjusting the ground connection  $G'$  (Fig. 1) until the ratio  $V_2/V_1$  is of the proper value. That the two photoelectric cells obey practically the same current-irradiation law has been proved at different times, with the apparatus as in Fig. 1, by testing the relation between values of the squares of the distances of  $L_2$  from  $S_2$  and the corresponding values of the width of  $S_1$  necessary to obtain a balance as shown by the electrometer. The results show that for a balanced condition the width of the slit  $S_1$  is directly proportional to the squares of the distances of  $L_2$  from  $S_2$ ; that is, there is a straight-line relation. When plotted, the values of  $S_1$  show no consistent deviation from this straight line, being never more than 0.01 mm from it for values between 0.30 and 2.00 mm. At 0.20 mm and below, this deviation is occasionally, though not always, as much as 0.02 mm. Above 2.00 mm, it has not been tried.

The method has not been as thoroughly tested as that for transmission measurements. A few tests have been made, however, on various substances, and a comparison with other methods, visual and photographic, has been thus possible. It is believed that the following statements are true in regard to the reflection of completely diffusing substances relative to that of some second completely diffusing material like magnesium carbonate:

1. Between 410 and 550  $m\mu$ , inclusive, the uncertainty of values obtained is not greater than 0.02 for values of relative reflection between 0.00 and 1.00, and not greater than 0.01 between 0.00 and 0.20.

2. This uncertainty increases somewhat as wave lengths 390 and 600  $m\mu$  are reached, being perhaps twice as great as throughout the better range.

#### IV. OTHER APPLICATIONS

The apparatus as herein described is well adapted for the comparison of the spectral distribution of radiant power of two sources over the same range of wave lengths as used in transmission and reflection measurements. If the two sources are such that they obey the inverse-square law, the method of varying their distances from  $S_2$  could be used,  $S_1$  being kept constant. If the inverse-square law were not obeyed by either source, the other

method could be used, their distances from  $S_2$  being kept constant and  $S_1$  varied to obtain a balance. The accuracy would be the same, respectively, as that already stated for the measurement of transmission or reflection. For greatest accuracy a device should be made by which first one and then the other source could be moved into position, check readings being taken on one source before and after the reading on the other. For lack of such a device, curves similar to those of Fig. 2 for each source could be obtained by varying the distance of the source from  $S_2$  or by varying the width of  $S_1$ , and the ratio of the ordinates of the two curves, wave length by wave length, would give the relative spectral distribution of radiant power. If one of the two lamps is a standard whose radiant power curve is known, then, of course, the actual distribution curve for the other lamp could be computed.

Another use to which this apparatus could be put would be the measurement of fluorescence. If a curve similar to that of Fig. 2 were obtained for a source whose spectral distribution of radiant power is known, this curve could be reduced to that for a source emitting equal amounts of energy at all wave lengths. With the apparatus arranged as in Fig. 10, the fluorescent material could be held in the position of the reflecting surface  $\beta$ , and the exciting radiant energy, which, of course, must be of constant intensity and of wave length different from that of the fluorescence, focused upon it. The values of  $S_1$  necessary for a balance could then be obtained at each wave length; and if these values were divided by the values for the equal-energy source, the result would be the amount of energy emitted by the fluorescent substance at each wave length.

As already mentioned, the sudden decrease of the sensitivity as wave lengths shorter than  $460\text{ m}\mu$  are encountered is largely due to the absorption of the large glass prism in the Hilger constant-deviation spectrometer, the potassium-hydride surface being very sensitive to the ultra-violet. There is, of course, nothing about the method which would prevent its extension into the ultra-violet, if a spectrometer with quartz prism and lenses were used in place of the present instrument. The windows  $W_1$  and  $W_2$  (Fig. 1) are made of quartz, and photoelectric cells can be obtained made entirely of quartz or with quartz windows. For wave lengths shorter than about  $300\text{ m}\mu$ , a different source would have to be used because of the absorption in the thin glass bulb.

## V. SUMMARY

Reliable determinations of spectral transmission throughout the green, blue, and violet have been made by means of the photoelectric null method as herein described.

This apparatus has been in continual use since April, 1918, and has proved very satisfactory as regards speed of operation, ease of keeping in proper working condition, and accuracy of measurement.

All errors have been eliminated, as well as the necessity of any tests, calibrations, or corrections, in connection with the current-irradiation law or the dark currents of the photoelectric cells, or with electrometer deflection methods.

The only variable in the process of making a determination of the transmission at any wave length is the accurately measurable distance of a small light source from the slit of the spectrometer.

Because of the higher sensitivity of the electrometer, it has been possible to make measurements over a greater range and, at least for low values of transmission, with greater accuracy than could be made if a galvanometer were used.

The accuracy has been tested by measuring the transmission of rotating sectors of known aperture and the transmission of standard glasses which have been measured by other methods, visual and photographic. It is believed the following statements are true:

1. Between wave lengths 410 and 550  $m\mu$ , inclusive, the uncertainty of measurements is not greater than 0.01 for values of transmission between 0.00 and 1.00, and not greater than 0.003 for values between 0.00 and 0.10.

2. Beyond this range as far as 390 and 600  $m\mu$  the uncertainty is slightly greater, being at these wave lengths perhaps twice as great as throughout the better range.

Measurements of diffuse spectral reflection relative to that of magnesium carbonate have been made, comparison with other methods indicating an uncertainty, between wave lengths 410 and 550  $m\mu$ , inclusive, not greater than 0.02 for values of relative reflection between 0.00 and 1.00, and not greater than 0.01 for values between 0.00 and 0.20, this uncertainty becoming perhaps twice as great as wave lengths 390 and 600  $m\mu$  are reached.

The method is also applicable to the measurement of the relative radiant power of two sources and to the measurement of fluorescence, and could be extended into the ultra-violet if quartz parts were used instead of glass.

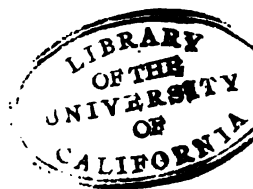
WASHINGTON, February 12, 1919.







JAN 6 1920



DEPARTMENT OF COMMERCE

# SCIENTIFIC PAPERS OF THE BUREAU OF STANDARDS

S. W. STRATTON, DIRECTOR

No. 350

**EQUILIBRIUM CONDITIONS IN THE SYSTEM  
CARBON, IRON OXIDE, AND HYDROGEN IN RELATION  
TO THE LEDEBUR METHOD FOR  
DETERMINING OXYGEN IN STEEL**

BY

J. R. CAIN, Chemist

and

LEON ADLER, Assistant Chemist

*Bureau of Standards*

ISSUED NOVEMBER 10, 1919



PRICE, 5 CENTS

Sold only by the Superintendent of Documents, Government Printing Office  
Washington, D. C.

WASHINGTON  
GOVERNMENT PRINTING OFFICE

1919



# EQUILIBRIUM CONDITIONS IN THE SYSTEM CARBON, IRON OXIDE, AND HYDROGEN IN RELATION TO THE LEDEBUR METHOD FOR DETERMINING OXYGEN IN STEEL

By J. R. Cain and Leon Adler

## CONTENTS

	Page
I. Introduction.....	353
II. Experimental study.....	355
1. Apparatus.....	357
2. Procedure.....	357
3. Materials used.....	358
4. Reduction experiments with mixtures of iron oxide and graphite— Constant rate of passing hydrogen.....	359
5. Reduction experiments with mixtures of iron oxide and iron con- taining iron carbide—(combined carbon)—Constant rate of passing hydrogen.....	359
6. Reduction experiments with mixtures of iron oxide and chilled cast iron, partially annealed and unannealed—Constant rate of passing hydrogen.....	360
7. Reduction experiments with mixtures of unannealed cast iron and iron oxide—Rate of passing hydrogen varied.....	361
8. Investigations concerning the oxygen not evolved as water in the preceding experiments.....	362
9. Oxygen determinations by the Ledebur method on the same steels with varying rates of hydrogen.....	365
III. General discussion.....	365
IV. Conclusions.....	366

## I. INTRODUCTION

Ledebur's method<sup>1</sup> for determining oxygen in steel and iron is carried out by heating chips of the metal to 900° in a current of hydrogen and weighing the water formed by the (type) reaction (1)  $\text{FeO} + \text{H}_2 = \text{Fe} + \text{H}_2\text{O}$ . If oxides of other metals are present these may or may not be affected.<sup>2</sup>

In order that the results shall be accurate, it is essential that (1) the reduction shall be performed only by hydrogen, and not by the carbon present in the steel; (2) the water vapor formed shall not be decomposed by secondary reactions before it is weighed;

<sup>1</sup> Ledebur, *Leitfaden für Eisenhütten Laboratorien*, 9th Aufl., p. 154.

<sup>2</sup> Cain and Pettijohn, Bureau of Standards Technical Paper No. 118; 1919.

(3) conditions must be chosen so that the equilibrium of reaction (1) is shifted as far as possible toward the right.

How complicated reaction (1) may be when applied to steel—i. e., an iron-carbon system instead of iron only—can be seen by inspection of equations 2 to 9 inclusive, which describe various interreactions that are possible in the gaseous phase or between gaseous and solid phases in the system iron, iron oxide, carbon, and hydrogen at 900°.

Reactions:

- (2)  $\text{FeO} + \text{C} \rightleftharpoons \text{Fe} + \text{CO}$
- (3)  $\text{FeO} + \text{CO} \rightleftharpoons \text{Fe} + \text{CO}_2$
- (4)  $2\text{CO} \rightleftharpoons \text{CO}_2 + \text{C}$
- (5)  $\text{Fe} + \text{YCO} = \text{FeC}_Y + \text{XCO}_2$   
( $\text{Fe}_3\text{C}$ ?)
- (6)  $\text{CO}_2 + \text{H}_2 \rightleftharpoons \text{CO} + \text{H}_2\text{O}$
- (7)  $\text{CO} + \text{YH}_2 \rightleftharpoons \text{H}_2\text{O} + \text{XCH}_Y$
- (8)  $\text{C} + \text{H}_2\text{O} \rightleftharpoons \text{CO} + \text{H}_2$
- (9)  $\text{C} + \text{H}_2 = \text{XCH}_Y$
- (10)  $2\text{H}_2\text{O} \rightleftharpoons 2\text{H}_2 + \text{O}_2$

Ledebur seems to have overlooked or disregarded these reactions when he devised his method, and the present work was undertaken to give information as to their effect on the results obtainable by the Ledebur method when certain variables are introduced into it. These reactions have been studied from different angles by many workers, but usually the conditions of their investigations are so different from those described herein that not many conclusions can be drawn from the previous work. However, certain deductions can be made with a reasonable degree of certainty.

Langmuir's work <sup>3</sup> shows that the thermal dissociation of water into hydrogen and oxygen (equation 10) is negligible at 900° to 1000°.

Reaction (2) was investigated by Schenk and Heller <sup>4</sup> with regard to the specific effect of different forms of carbon. They found that amorphous carbon was more active than graphite in reducing iron oxide. Falcke <sup>5</sup> states that reactions (2) and (3) proceed together and begin at 500° to 600°.

Reaction (4) has been investigated by Rhead and Wheeler <sup>6</sup>, Fay and Seeker,<sup>7</sup> and others. The study of this reaction is usually

<sup>3</sup> Irving Langmuir, *J. Am. Chem. Soc.*, **28**, p. 1357; 1906.

<sup>4</sup> *Ber.*, **38**, p. 2139; 1905.

<sup>5</sup> Falcke, *Z. Electrochemie*, **21**, pp. 37-50, 1915; **22**, pp. 121-133; 1916; *Ber.*, **46**, pp. 743-750.

<sup>6</sup> Rhead and Wheeler, *J. Chem. Soc.*, **97**, p. 2178, 1910; **99**, p. 1140, 1911; **101**, p. 831, 1912.

<sup>7</sup> Fay and Seeker, *J. Am. Chem. Soc.*, **25**, p. 640; 1903.

connected with investigations of reactions (2) and (3), since reduced metals and their oxides catalyze these reactions in one direction or the other.

The principal results of these researches that concern the present investigation are (1) that reaction (4) takes place toward the right only at temperatures below  $1000^{\circ}$ ; (2) that the speed of the reaction is greatly affected by temperature; for instance at  $850^{\circ}$  it is 66 times as fast as the reverse reaction (Rhead and Wheeler loc. cit.); (3) that the reduced iron and unreduced oxide both catalyze the reverse reaction; (4) that the speed of the gas current through the apparatus or over the catalyzers is of great importance.

Reaction (5) has been investigated by Giolitti<sup>9</sup> in connection with casehardening experiments. His book on casehardening gives many other references. This reaction proceeds rapidly above  $810^{\circ}\text{C}$ .

Reaction (6) has been studied by O. Hahn<sup>10</sup> and by Boudouard;<sup>10</sup> reaction (8) has also been studied by O. Hahn.<sup>11</sup> The reduction of carbon monoxide by hydrogen, where water is the only reaction product instead of hydrocarbons, as indicated in reaction (7), has been studied by Gautier. The reduction of carbon dioxide by hydrogen takes place at temperatures as low as  $400^{\circ}$ .

Reaction (8) has been frequently investigated in connection with gas-producer studies; the reduction of water vapor by carbon begins at about  $600^{\circ}$  and is very rapid at  $1100^{\circ}$ .

The formation of hydrocarbons from interaction of carbon and hydrogen (reaction 9) has been studied by the authors and mentioned by others. Such reactions are easily possible under the conditions prescribed by Ledebur, and they took place in some of the experiments described later in this paper.

## II. EXPERIMENTAL STUDY

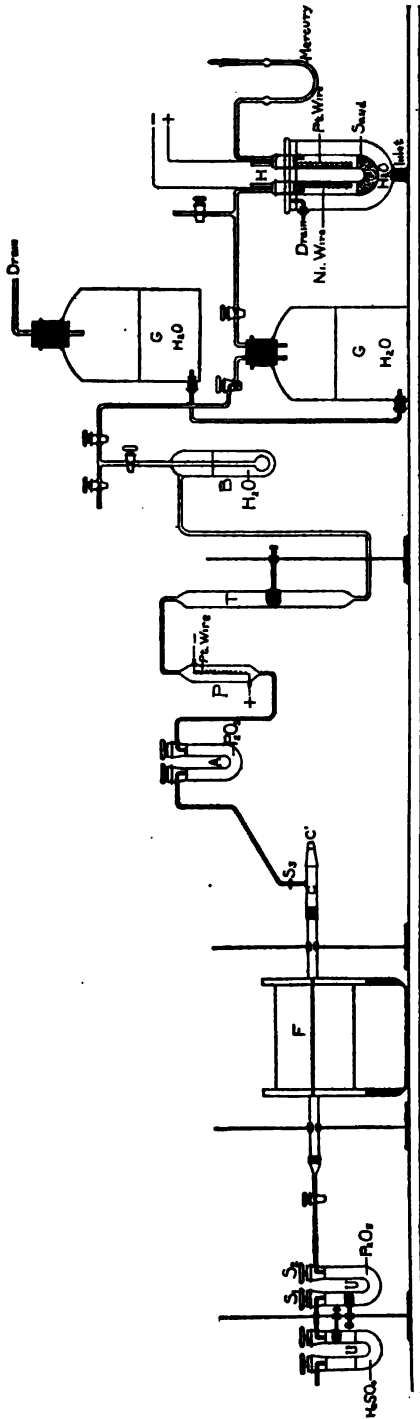
To study the relation of these reactions to the Ledebur method, a series of experiments was made in which mixtures of iron oxide and iron containing iron carbide or of iron and various forms of carbon were heated to  $900^{\circ}$  in pure hydrogen. The proportions of the mixtures and the rates of passage of the hydrogen were varied in a systematic way, and the reaction products were collected and studied.

<sup>9</sup> Giolitti, F., *Cementation of Iron and Steel* (translated by Richards and Roniller), Graw-Hill Book Co., N. Y.; 1915.

<sup>10</sup> O. Hahn, *Z. Physik. Chem.*, **42**, p. 705, 1903; **44**, p. 513, 1903; **48**, p. 735; 1904.

<sup>11</sup> M. Boudouard, *Bul. Soc. Chim.*, 3d series, **25**, 484; 1901.

<sup>12</sup> Loc. cit.



## 1. APPARATUS

The apparatus used is shown in Fig. 1. It consists of the electrolytic hydrogen generator (*H*) with reservoirs *G*, followed by bubble counter *B* and calcium chloride lower *T*, the preheater *P* and its absorber (*A*) ( $P_2O_5$ ) for removing traces of oxygen from the hydrogen, the furnace and combustion tube (*F*) for heating the mixtures (which are contained in quartz boats), phosphorous pentoxide tubes (*U*) for collecting the water formed, and sulphuric acid guard tube *U'*. When carbon dioxide was to be determined, a Meyer tube containing barium hydroxide was used to collect it; the precipitated barium carbonate was filtered off and titrated. The apparatus for determining carbon monoxide followed. This is described in detail later in this paper. The electrolytic hydrogen generator and its purifying apparatus, and also the special electric furnace, are illustrated and described elsewhere.<sup>12</sup>

The glass tube (*C*) was cemented on the porcelain combustion tube with De Khotinsky cement; the ground-glass cap (*C'*) could be removed and a boat introduced without removing *C*. With a little care in lubrication of (*C'*) this device was found very satisfactory. By suitable manipulation of the stopcocks at either end of the combustion tube, it could be freed of air by alternately evacuating (an efficient water aspirator was found very satisfactory) and filling with hydrogen. Two evacuations and replacements with hydrogen reduced the residual oxygen (from air) to less than 0.000022 g, provided the aspiration reduced the pressure to 20 mm mercury. Any good aspirator will do this at moderate room temperatures; at higher temperatures prevailing in summer a vacuum of 30 mm mercury is obtained. This would leave 0.00009 g oxygen in the tube after two evacuations. The effect of such quantities of oxygen is negligible in the present work. The temperature of the furnace was determined every few days with a thermocouple and held at 900° by maintaining a constant current.

## 2. PROCEDURE

The boat containing the mixture being tested was placed in the furnace and the residual oxygen and water vapor removed as described. The current was then turned on the furnace and the purified hydrogen admitted; the rate of passage of this current was kept constant and was calculated from the total volume used (determined from the change of height of the water in *G*) divided

---

<sup>12</sup> Cain and Pettijohn, loc. cit.

by the time it was passed. The heating of the tube to  $900^{\circ}$  from room temperature required about 20 minutes. The average time required for an operation was  $1\frac{1}{2}$  hours. At the conclusion of an experiment the current was shut off from the furnace and cocks  $S_1$  and  $S_2$  were closed; the phosphorous pentoxide tube was disconnected and weighed after standing in the balance one-half hour. Many experiments were made with the different types of reduction described later, in order to be certain that all reduction products had been removed from the furnace in the allotted time; these tests were made by connecting a second phosphorous pentoxide tube and aspirating during another half hour. In all cases, except a group of experiments where very low rates of hydrogen were used, the gain in weight of the second tube was negligible (0.01 to 0.02 mg). The difficulty just mentioned in the case of low rates of hydrogen passage was met by removing the vapor by exhausting the whole system back to cock  $S_3$ . This was done with a water aspirator and was so effective that all the water from a reaction was absorbed by the phosphorous pentoxide tube in 10 minutes. This tube was inclosed in an outer vessel (a vacuum desiccator), also evacuated, so as to prevent collapse of its thin walls. A number of blank determinations made according to the procedure above described, but with no substance in the boat, showed them to be negligible (less than 0.1 mg). These blank determinations were made at frequent intervals and the results were always below the limit stated except with very high rates of hydrogen admission. This was probably because the catalyzer had insufficient capacity to completely remove the oxygen impurity at these rates. However, the correction necessary even in such cases was very small (about 1 per cent of the total water weighed).

### 3. MATERIALS USED

(a) *Magnetite Ore, Bureau of Standards Analyzed Sample No. 29.*—Certificate analysis FeO 28.78 per cent,  $\text{Fe}_2\text{O}_3$  52.2 per cent; the rest was  $\text{SiO}_2$ ,  $\text{TiO}_2$ ,  $\text{Al}_2\text{O}_3$ ,  $\text{V}_2\text{O}_5$ , MnO, CaO, MgO,  $\text{K}_2\text{O}$ ,  $\text{Na}_2\text{O}$ , and  $\text{P}_2\text{O}_5$ . With the exception of the  $\text{V}_2\text{O}_5$ , which is reduced to  $\text{V}_2\text{O}_3$ , these are all substances not reduced by hydrogen under the conditions used in these investigations. (See Cain and Pettijohn, loc. cit.) Water calculated as equivalent to 1 g of ore = 0.2390 g.

(b) *Sibley Iron Ore, Bureau of Standards Analyzed Sample No. 27.*—Certificate analysis Fe 69.2 per cent; P 0.037 per cent;  $\text{SiO}_2$ ,



0.77. Assuming all the Fe to be present as  $\text{Fe}_2\text{O}_3$ , the water calculated as equivalent to 1 g of ore = 0.3345 g.

(c) *Acheson Graphite, Powdered*.—This contained about 99.5 per cent carbon.

(d) *White Cast Iron*.—Total carbon 3.98 per cent graphitic carbon 0.02 per cent; combined carbon (by difference) 3.96 per cent.

#### 4. REDUCTION EXPERIMENTS WITH MIXTURES OF IRON OXIDE AND GRAPHITE—CONSTANT RATE OF PASSING HYDROGEN

Mixtures of the magnetite and Sibley ores with graphite, as shown in Table 1, were reduced at  $900^\circ$ , passing hydrogen at the rate of 2 liters per hour. The reaction was studied by determining the amounts of water formed.

TABLE 1.—Reduction of Mixtures of Iron Oxide and Graphite

[Amount of  $\text{H}_2$  constant]

Ore used	Weight of ore	Carbon in mixture	Water calculated	Water found	Water recovered
	g	Per cent	g	g	Per cent
Magnetite, B. S. No. 29.....	0.3002	0.00	0.0718	0.0722	100.4
Do .....	.0984	.00	.0235	.0232	98.4
Sibley ore, B. S. No. 27.....	.1011	.00	.0338	.0335	99.2
Magnetite, B. S. No. 29.....	.1007	3.70	.0232	.0234	100.8
Do.....	.1001	26.00	.0231	.0232	100.3
Do.....	.1007	63.00	.0232	.0232	100.0

These results show that graphite under these conditions exerts no reducing action on the iron oxide, all the reduction being performed by the hydrogen.

#### 5. REDUCTION EXPERIMENTS WITH MIXTURES OF IRON OXIDE AND IRON CONTAINING IRON CARBIDE (COMBINED CARBON)—CONSTANT RATE OF PASSING HYDROGEN

A mixture of 4 g of the Sibley ore with 1 g of graphite was heated for 20 hours at  $900^\circ$  with hydrogen passing until the escaping gas no longer gave a test for water; the mixture was cooled in the furnace under hydrogen and then pulverized. This operation gave an iron high in combined carbon.

Mixtures of this substance with the magnetite ore in the proportions shown in Table 2 were prepared, reduced as described in section 4, and the amounts of water formed in each experiment noted.

TABLE 2.—Reduction of Mixtures of Iron Oxide and "Cemented" Iron  
[Amount of  $H_2$  constant]

Weight of magnetite ore	Weight of cemented material	Water calculated	Water recovered	Water recovered
g	g	g	g	Per cent
0.1004	0.1400	0.0240	0.0232	96.6
.1006	.1450	.0241	.0230	95.5
.1005	.2015	.0240	.0226	94.2
.1002	.3504	.0240	.0176	73.4
.1004	.4911	.0240	.0157	65.5

The results of Table 2 show that the amount of water decreases as the proportion of "cemented iron" increases in the mixtures, which show that the carbon in the mixture has partially reduced the iron oxide.

#### 6. REDUCTION EXPERIMENTS WITH MIXTURES OF IRON OXIDE AND CHILLED CAST IRON, PARTIALLY ANNEALED AND UNANNEALED—CONSTANT RATE OF PASSING HYDROGEN

Mixtures of the annealed and unannealed iron (crushed to 80 mesh) and magnetite ore as shown in Table 3 were prepared and reduced in hydrogen at  $900^\circ$ , the water being collected and weighed. The rate of passage of the hydrogen in the experiments described in Table 3 was the same—about 1 liter per hour. The cast iron was a convenient material to use for these experiments, since it contained a known large amount of combined carbon.

TABLE 3.—Reduction Experiments with Mixtures of Iron Oxide and Cast Iron  
[Amount of  $H_2$  constant]

##### A. PARTIALLY ANNEALED IRON<sup>a</sup>

Weight of ore	Weight of cast iron	Water calculated	Water recovered	Water recovered
g	g	g	g	Per cent
0.1007	0.2652	0.0241	0.0194	80.5
.1000	.4496	.0239	.0163	68.2
.1000	.4725	.0239	.0108	45.2
.1006	.4727	.0240	.0109	45.4
.1005	.5880	.0240	.0092	38.0

##### B. UNANNEALED IRON

Weight of ore	Weight of cast iron	Water calculated	Water recovered	Water recovered
g	g	g	g	Per cent
0.1002	0.2007	0.0239	0.0107	44.9
.1001	.4006	.0239	.0093	38.9
.1000	.5020	.0239	.0057	23.8

<sup>a</sup> The oxygen content of the iron before annealing was 0.034 per cent. This iron was only partially annealed, which explains the A and B results of the above table.

These results show that the yield of water diminishes as the proportion of cast iron in the mixtures increases and that the specific effect of unannealed iron is greater than that of the annealed iron. The carbides in the iron seem to be responsible for the disturbance of the reaction.

#### 7. REDUCTION EXPERIMENTS WITH MIXTURES OF UNANNEALED CAST IRON AND IRON OXIDE—RATE OF PASSAGE OF HYDROGEN VARIED

The details of these experiments are shown in Table 4 and in Fig. 2. The amounts of water recovered increased with all mix-

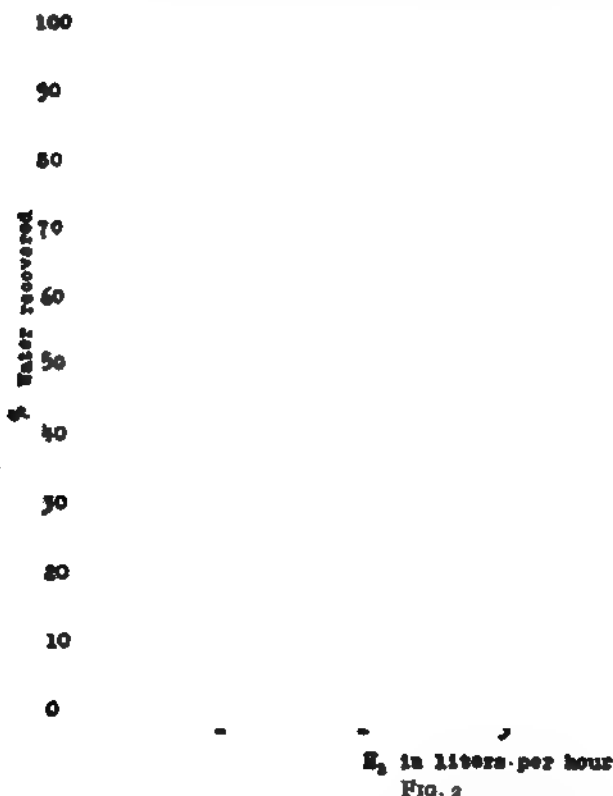


FIG. 2

tures as the rate of passing hydrogen increased and approached a maximum limit at the rate of 3 liters per hour. As shown by Fig. 2, it would be impossible to recover more than 75 per cent of the water when the ratio of ferrous oxide to carbon (combined) is 1 to 5. In any steel the proportion of carbon relative to ferrous oxide is much greater than this, hence it seems very probable from these experiments that the Ledebur method can not determine more than 75 per cent of the oxygen in steels and that the actual recovery will be much less if hydrogen is passed too slowly.

TABLE 4.—Reduction of a Mixture of Iron Oxide and Unannealed Chilled Iron

[Amount of hydrogen varied]

Weight of ore (B. S. No. 29)	Weight of cast iron	Speed	Water cal- culated	Water re- covered	Water re- covered
g	g	Liter/hour	g	g	Per cent
0.2002	1.0010	0.30	0.0478	0.0102	21.3
.2007	1.0010	.45	.0480	.0116	24.2
.2001	1.0050	.85	.0478	.0173	36.2
.2005	1.0004	1.20	.0480	.0194	40.4
.2003	1.0000	1.40	.0479	.0223	46.6
.2001	1.0000	1.50	.0478	.0254	53.2
.2000	1.0006	1.70	.0478	.0268	55.0
.2000	1.0007	1.90	.0478	.0276	57.8
.2000	1.0002	2.40	.0480	.0313	65.4
.2002	1.0000	3.10	.0480	.0319	66.5
.2000	1.0000	3.30	.0480	.0339	70.7
.2004	1.0000	4.70	.0482	.0349	72.5
.2007	1.0000	6.30	.0482	.0352	73.0

#### 8. INVESTIGATIONS CONCERNING THE OXYGEN NOT EVOLVED AS WATER IN THE PRECEDING EXPERIMENTS

Since the experiments described in the preceding sections had shown such a large deficit under certain conditions in the yield of water to be expected, it was decided to determine the form and amounts of some of the compounds other than water which were carried out of the furnace by the escaping hydrogen. The probable constituents in this mixture were carbon monoxide, carbon dioxide, saturated hydrocarbons, and unsaturated hydrocarbons.

Nesmjelow<sup>12</sup> has shown that carbon monoxide can be determined in the presence of saturated hydrocarbons and hydrogen by passing oxygen and the gaseous mixture several times over copper oxide heated to 250°. Unsaturated hydrocarbons interfere to some extent in this determination, but the conditions of these experiments seemed unfavorable for the production of any considerable proportion of such compounds, and this part of the work was carried out on this assumption. The total amount of saturated hydrocarbons (which was accurately determined, see later paragraphs), as shown in Table 5, was very small; hence the assumption that the per cent of unsaturated hydrocarbons was still smaller seems justified.

Preliminary tests of Nesmjelow's method confirmed his results, and this method was accordingly adopted for the study. The apparatus for these determinations followed the phosphorus

<sup>12</sup> Nesmjelow, Z., *Analy. Chem.*, 48, p. 232; 1909.

pentoxide tube shown at *U* in Fig. 1, and consisted of (1) a Meyer tube filled with barium hydroxide to absorb the carbon dioxide, (2) an electrically heated, hard-glass combustion tube filled with copper oxide maintained at a temperature of  $250^{\circ}$ , (3) a Meyer tube filled with barium hydroxide solution for absorbing the carbon dioxide produced in the copper oxide tube, (4) a porcelain-combustion tube heated to  $850^{\circ}$  for oxidizing the saturated hydrocarbons, and (5) a Meyer tube filled with barium hydroxide solution for collecting the carbon dioxide generated in this furnace. The barium carbonate in the various Meyer tubes was determined by the titration method.<sup>14</sup> The results are shown in Table 6, which is arranged to show the total recovery of the carbon in the solid gaseous phases. This was done by determining the carbon left in the solid substance after each experiment and adding to it the carbon found in the gaseous phase. The results are also shown graphically in Fig. 2.

These experiments show that the greater proportion of the missing oxygen escapes as carbon monoxide, and that this effect is minimized by increasing the rate at which the hydrogen passes. If the carbon monoxide and carbon dioxide curves are extrapolated they intersect the horizontal axis at about 5; in other words, if hydrogen were passed at the rate of 5 liters per hour, or faster, no carbon monoxide or dioxide would be produced. It is doubtful, however, whether such extrapolation is justified.

#### 9. OXYGEN DETERMINATIONS BY THE LEDEBUR METHOD ON THE SAME STEELS WITH VARYING RATES OF HYDROGEN

In order to show the specific application of the preceding work to the determination of oxygen in steels by Ledebur's method, determinations were made on several steels when hydrogen was passed at rates varying from 0.7 to 5.3 liters per hour. The samples were prepared by cutting under oil and with the other precautions described by Cain and Pettijohn (*loc. cit.*). The results are shown in Table 7 and bring out quite clearly the necessity for a rapid current of hydrogen.

---

<sup>14</sup> J. R. Cain, Bureau of Standards Technical Paper No. 33; 1914.

TABLE 6.—Summary of Reductions by  $H_2$  of Iron Oxide and Cast-Iron Mixtures With Analyses of Escaping Gases

No.	Weight of—		H <sub>2</sub> speed Liters/hour	H <sub>2</sub> O calcu- lated	H <sub>2</sub> O recovered as H <sub>2</sub> O		H <sub>2</sub> O equivalent to CO <sub>2</sub>		H <sub>2</sub> O equivalent to CO		Total H <sub>2</sub> O accounted for		Orig- inal carbon in solid	Carbon in CO and CO <sub>2</sub>	Carbon in solu- tion hydro- carbons	Carbon recovered		
	Ore (B. S. No. 28)	White iron			g	g	Per cent	g	Per cent	g	Per cent	g				g	In gas	All forms
1.....	0.2007	1.0010	0.45	0.0480	0.0116	24.2	0.0028	5.8	0.0267	55.6	0.0411	85.6	.....	.....	.....	.....	.....	
2.....	.2001	1.0005	.85	.0478	.0173	36.2	.0036	7.5	.0269	56.4	.0478	100.0	.....	.....	.....	.....	.....	
3.....	.2005	1.0004	1.2	.0480	.0194	40.4	.0025	5.2	.0207	43.2	.0426	88.8	0.0175	0.0191	.....	(e)	0.0366	
4.....	.2003	1.0000	1.4	.0479	.0223	46.6	.0026	5.4	.0211	44.1	.0460	96.1	.....	.....	.....	.....	.....	
5.....	.2001	1.0000	1.5	.0478	.0254	53.2	.0026	5.4	.0185	38.8	.0465	97.4	.....	.....	.....	(e)	.0327	
6.....	.2003	1.0002	1.5	.0479	.0236	49.4	.0023	4.8	.0196	41.0	.0455	95.2	.0213	.0138	0.0031	0.0031	.0382	
7.....	.2000	1.0006	1.7	.0478	.0263	55.0	.0017	3.6	.0195	40.9	.0475	99.5	.0234	.0135	.0026	.0026	.0395	
8.....	.2000	1.0007	1.9	.0478	.0276	57.8	.0021	4.4	.0183	38.3	.0480	100.5	.0235	.0128	.0031	.0031	.0394	
9.....	.2000	1.0002	2.4	.0480	.0313	65.4	.0021	4.4	.0162	33.8	.0496	103.6	.0250	.0115	.0024	.0024	.0399	
Average.....	.....	.....	.....	.....	.....	.....	.....	.....	.....	.....	.....	997.5	.....	.....	.....	.....	998.1	

<sup>a</sup> Not determined.<sup>b</sup> Not including 1 and 3 where the  $CO$  is known to be low.<sup>c</sup> Not including 3 and 5 where the hydrocarbons were not determined because of explosions.

TABLE 7.—Oxygen Determinations on Steels; Variable Amounts of Hydrogen Used

Steel used *	Speed of hydrogen	Oxygen
	Liters/hour	Per cent
Acid open hearth, 0.2 per cent C; B. S., No. 19a.....	1.5	0.017
	5.3	.023
Basic open hearth, 0.2 per cent C; B. S., No. 11a.....	.7	.025
	1.0	.030
	1.4	.033
	4.0	.038
Acid open hearth, 0.8 per cent C; B. S., No. 34.....	1.1	.015
	4.7	.023
Basic open hearth, 1.0 per cent C; B. S., No. 16a.....	1.1	.020
	4.6	.030

\* All were Bureau of Standards analyzed samples.

## III. GENERAL DISCUSSION

Considering the experimental results of this paper in relation to some of the reactions given in the introductory section, it is evident that the rate of hydrogen passage affects certain of the reactions and has no effect, or only minor effect, on others. Reactions (2),  $\text{FeO} + \text{C} \rightleftharpoons \text{Fe} + \text{CO}$ , and (3),  $\text{FeO} + \text{CO} \rightleftharpoons \text{Fe} + \text{CO}_2$ , would tend to produce larger amounts of carbon monoxide with increase in hydrogen rate, which is contrary to the experimental results obtained. Hence under the experimental conditions herein described these reactions are not much affected. The equilibrium of reaction (4),  $2\text{CO} \rightleftharpoons \text{CO}_2 + \text{C}$  (i. e., thermal dissociation of carbon monoxide), would be shifted toward the left with rapid hydrogen passage, a result in conformity with what was found. Reaction (6),  $\text{CO}_2 + \text{H}_2 \rightleftharpoons \text{CO} + \text{H}_2\text{O}$ , tends to proceed toward the right in the  $900^\circ$  zone of the furnace; hence a rapid current of hydrogen would have the effect of suppressing production of carbon monoxide by this reaction since the reacting substances would thus be carried away rapidly from the reaction zone. This expectation is also borne out by the results of this paper. Reactions (7),  $\text{CO} + \text{H}_2 = \text{H}_2\text{O} + \text{C}_x\text{H}_y$ , and (9),  $\text{C} + \text{H}_2 = \text{C}_x'\text{H}_y'$ , do not seem to be greatly affected, as shown in experiments 6, 7, 8, and 9 of Table 6, by variation of the hydrogen rate. No conclusions regarding these reactions could be drawn, however, without further work.

Reaction (8),  $\text{C} + \text{H}_2\text{O} \rightleftharpoons \text{CO} + \text{H}_2$ , is the one most affected by the amount of hydrogen passed, its shift being toward the left, in conformity with theory. As shown in Table 4, the equilibrium for this equation under conditions described in Section VI permits no

more than 75 per cent of the reduction of the ferrous oxide to be affected by hydrogen in the reaction  $\text{FeO} + \text{C} + \text{H}_2 \rightleftharpoons \text{Fe} + \text{H}_2\text{O} + \text{CO}$ . One particular experimental condition of Section VI just referred to, namely, a ratio of carbon to ferrous oxide of 5 to 1, was chosen to simulate to some extent the ratio of carbon to ferrous oxide that might be expected in steels. Hence it seems safe to say that in determining oxygen in steels by the Ledebur method not over 75 per cent of that present as ferrous oxide will be shown. Actually, if analyses hitherto reported by other workers are correct and if the oxygen in steels reported by them was really present as ferrous oxide, the ratio of carbon to oxide in steels is much greater than 5 to 1, and hence the proportion of oxygen determined in steels by the Ledebur method is probably still less.

#### IV. CONCLUSIONS

1. Graphite does not reduce ferrous oxide or water vapor at 900° if hydrogen is passing at the rate of 2 liters or more per hour.
2. Combined carbon in iron reduces ferrous oxide (with formation of carbon monoxide) under the conditions given in conclusion 1, to an extent varying with the proportion of carbide present.
3. The percentage of ferrous oxide reduced by hydrogen from a mixture of iron carbide with ferrous oxide is a function of the rate of passage of the hydrogen, and, as shown by experiments in this paper, reaches a maximum of 75 per cent reduction when hydrogen passes at about 3 liters per hour. The remaining oxygen is evolved principally as carbon monoxide and partly as carbon dioxide.
4. The Ledebur method under most favorable conditions probably can not account for more than 75 per cent of the oxygen present in a steel as ferrous oxide.

WASHINGTON, January 18, 1919.







DEPARTMENT OF COMMERCE

---

# SCIENTIFIC PAPERS OF THE BUREAU OF STANDARDS

S. W. STRATTON, DIRECTOR

---

No. 351

DEPENDENCE OF THE INPUT IMPEDANCE OF A  
THREE-ELECTRODE VACUUM TUBE UPON  
THE LOAD IN THE PLATE CIRCUIT

BY

JOHN M. MILLER, Physicist  
*Bureau of Standards*

---

ISSUED NOVEMBER 21, 1919



PRICE, 5 CENTS

Sold only by the Superintendent of Documents, Government Printing Office  
Washington, D. C.

---

WASHINGTON  
GOVERNMENT PRINTING OFFICE

1919



# DEPENDENCE OF THE INPUT IMPEDANCE OF A THREE-ELECTRODE VACUUM TUBE UPON THE LOAD IN THE PLATE CIRCUIT

By John M. Miller

## CONTENTS

	Page
I. Introduction.....	367
II. General theory of the dependence of the input impedance upon the load in the plate circuit.....	369
III. Input impedance for the case of a pure resistance load in the plate circuit.....	373
IV. Experimental determinations with a pure resistance load in the plate circuit.....	375
1. Determination of $k$ , $r_p$ , and $\frac{k R_p}{R_p + r_p}$ .....	375
2. Determination of $C_1$ , $C_2$ , and $C_3$ .....	375
3. Determination of $c_g$ .....	377
4. Comparison of observed and computed results.....	377
V. Input impedance for the case of an inductive load in the plate circuit..	379
VI. Experimental determinations with an inductive load.....	383
1. Determination of the tube constants.....	383
2. Measurement of the oscillatory circuit resistance.....	384
3. Comparison of observed and computed results.....	384
VII. Input impedance for the case of a capacity load in the plate circuit.....	385
VIII. Summary of results.....	385

## 1. INTRODUCTION

In a previous paper<sup>1</sup> was treated the theory of the use of a three-electrode vacuum tube as an amplifier, showing the importance of the amplification constant as determining the voltage amplification of the tube and the internal resistance of the tube in the plate or output circuit as determining the alternating current flowing in that circuit. A dynamic method was given for determining these important quantities directly.

The present paper is an extension of the theory and is concerned with the characteristics of the grid or input circuit. The input impedance of the tube is of importance in determining the input power and the voltage supplied to the input terminals of the tube by the apparatus in the input circuit.

<sup>1</sup> Miller, Proc. I. R. E., 6, 242, 1918.

If the grid of the tube is positive with respect to the filament, there will be a flow of electrons between the filament and grid. If distortion is neglected and the frequency is so low that capacity effects are negligible, the internal input circuit is under these conditions characterized by a pure resistance and an emf in series. The value of the resistance is determined by the reciprocal of the slope of the grid-current—grid-voltage characteristic corresponding to the operating voltages. This is analagous to the internal or output resistance of the plate circuit. The internal emf which acts in the grid circuit is determined by the product of the ratio of the slopes of the grid-current—plate-voltage and grid-current—grid-voltage characteristics with the alternating voltage of the plate relative to the filament which occurs as the result of a load in the plate circuit. This again is analagous to the way in which the amplification constant and impressed alternating voltage on the grid determine the voltage acting in the plate circuit of the tube. All of these facts are implicitly contained in the equations (5) derived by M. Latour<sup>2</sup> in his paper on the "Theoretical Discussion of the Audion."

If the grid of the tube is negative with respect to the filament so that no appreciable electron flow takes place between these electrodes, it would appear offhand that the input impedance of the tube would be rather unimportant in determining the voltage received from the apparatus in the external circuit. In very many cases in practice, however, this is not true, and as a consequence of the capacities between the tube electrodes and connecting wires, the internal characteristics of the plate circuit of the tube and the external load in the plate circuit, the character of the input impedance of the tube markedly affects its behavior as an amplifier. The following treatment will be concerned solely with the character of the input impedance of the tube when the grid is negative with respect to the filament.

It will be shown that when the load in the plate circuit is a resistance or capacity the input impedance can be represented as a positive resistance and capacity in series. Thus the tube is not a pure voltage device, but absorbs power.

When the load is inductive the input impedance can, in many cases, be represented as a negative resistance and capacity in series. This represents regeneration through the tube itself, and is of importance in the regenerative effects and oscillations in amplifiers.

---

<sup>2</sup> M. Latour, "Electrician," 78, p. 280; 1916.

## II. GENERAL THEORY OF THE DEPENDENCE OF THE INPUT IMPEDANCE UPON THE LOAD IN THE PLATE CIRCUIT

A three-electrode vacuum tube and associated circuits may be represented diagrammatically as in Fig. 1, where the continuous lines represent the circuits outside of the tube, while the dotted lines show the internal electrical characteristics of the tube. The points *F*, *G*, and *P* represent the three electrodes, filament, grid, and plate. The filament, grid, and plate batteries are not shown. Between filament and grid in the external circuit is applied the input emf which is an alternating voltage  $E_g$ . In the external circuit between filament and plate is inserted apparatus, such as phones, or the primary winding of a transformer, and this is designated in the figure as any impedance  $Z_p = R_p + jX_p$  where

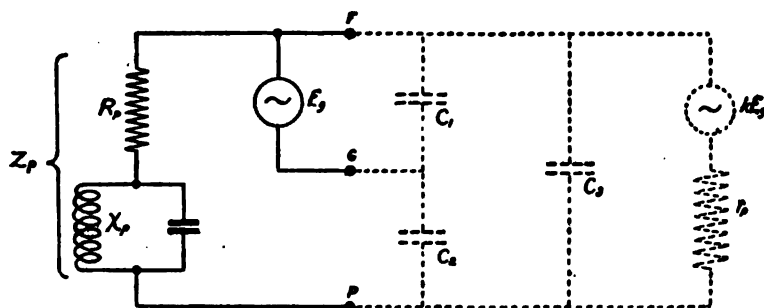


FIG. 1.—Diagrammatic representation of a vacuum tube and external circuits

$R_p$  is the resistance component and  $X_p$  the reactance component. The latter may be positive or negative, according as to whether it is inductive or capacitive. Within the tube the capacities between the three electrodes are represented by  $C_1$ ,  $C_2$ , and  $C_3$ . In general, the capacities between the leads to these elements are not negligible and will be assumed to be lumped in correct manner with the intraelectrode capacities. Further, as shown in the earlier paper cited above, the impressed emf  $E_g$  gives rise to an internal emf  $kE_g$  ( $k$  = amplification constant) which, acting in series with the internal output resistance  $r_p$ , is impressed between the filament and plate of the tube. In this diagrammatic representation of the tube it is assumed for simplicity that the capacities between the tube electrodes and appropriate leads are free from dielectric absorption and that the grid is maintained sufficiently negative with respect to the filament, and the insulation and vacuum are such that there is no appreciable conductive flow

between the grid and filament as a result of the impressed emf  $E_g$ . Otherwise it would be necessary to assume resistances in series or in parallel with the capacities  $C_1$ ,  $C_2$ , and  $C_3$  to represent dielectric losses and an emf and series resistance in parallel with  $C_1$ , as discussed above.

The problem, then, of finding the input impedance of the tube  $Z_g$  is that of determining the current  $I_g$  which flows in the external input circuit as a result of the voltage  $E_g$ . In Fig. 2 the circuit is redrawn and the currents represented as  $I_g$ ,  $I_1$ ,  $I_2$ ,  $I_3$ , etc.

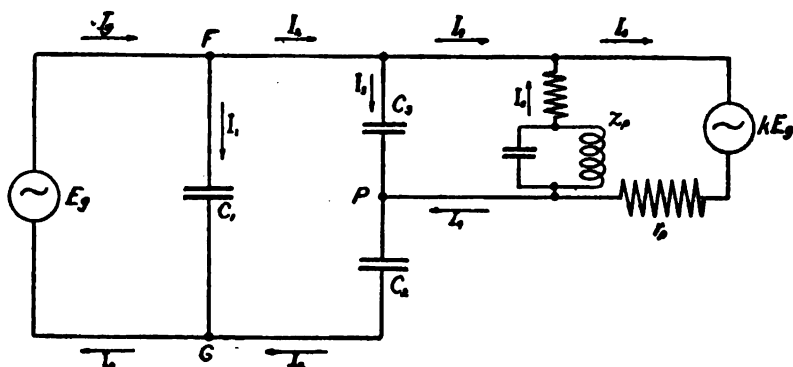


FIG. 2.—Vacuum tube and external circuits as an electrical network

By Kirchhoff's laws we have the following seven equations connecting the seven unknown currents, which permit us to determine  $I_g$  in terms of the quantities  $E_g$ ,  $k$ ,  $Z_p$ ,  $r_p$ ,  $C_1$ ,  $C_2$ , and  $C_3$ .

Thus,

$$k E_g = I_5 r_p + I_6 Z_p \quad (1)$$

$$I_g = I_1 + I_2 \quad (2)$$

$$0 = I_2 Z_p + \frac{I_3}{j \omega C_3} \quad (3)$$

$$I_3 = I_5 + I_4 \quad (4)$$

$$0 = \frac{I_2}{j \omega C_2} + \frac{I_3}{j \omega C_2} - \frac{I_1}{j \omega C_1} \quad (5)$$

$$I_g = I_1 + I_2 \quad (6)$$

$$E_g = \frac{I_1}{j \omega C_1} \quad (7)$$

Eliminating  $I_1$ ,  $I_2$ ,  $I_3$ ,  $I_4$ ,  $I_5$ , and  $I_6$  between these equations and



writing  $z_g = \frac{E_g}{I_g}$  we obtain the following expression for the input impedance:

$$z_g = \frac{r_p (C_2 + C_3) - \frac{j}{\omega} - \frac{j}{\omega} \frac{r_p}{Z_p}}{k C_2 + C_1 + C_2 + \frac{r_p}{Z_p} (C_1 + C_2) + j \omega r_p (C_1 C_2 + C_1 C_3 + C_2 C_3)} \quad (8)$$

$$\text{Substituting } Z_p = R_p + j X_p \quad (9)$$

in (8) we obtain the equation

$$z_g = \frac{a + j b}{c + j d} \quad (10)$$

where

$$\begin{aligned} a &= R_p (C_2 + C_3) + \frac{X_p}{\omega r_p} \\ b &= X_p (C_2 + C_3) - \frac{R_p}{\omega r_p} - \frac{1}{\omega} \\ c &= \frac{R_p}{r_p} (k C_2 + C_1 + C_2) + C_1 + C_2 - \omega X_p (C_1 C_2 + C_1 C_3 + C_2 C_3) \\ d &= \frac{X_p}{r_p} (k C_2 + C_1 + C_2) + \omega R_p (C_1 C_2 + C_1 C_3 + C_2 C_3) \end{aligned} \quad (11)$$

And if  $z_g$  is separated into resistance and reactance components  $r_g$  and  $x_g$ , we have

$$z_g = r_g + j x_g \quad (12)$$

$$r_g = \frac{a c + b d}{c^2 + d^2} \quad (13)$$

$$x_g = \frac{b c - a d}{(c^2 + d^2)} \quad (14)$$

If  $X_p$  is negative, corresponding to a capacity reactance in the plate circuit, we have the following terms in the numerator of  $r_g$ :

Positive terms	Negative terms
$\omega X_p R_p (C_2 + C_3) (C_1 C_2 + C_1 C_3 + C_2 C_3)$	$\omega X_p R_p (C_2 + C_3) (C_1 C_2 + C_1 C_3 + C_2 C_3)$
$\frac{X_p^2}{r_p} (C_2 + C_3) (k C_2 + C_1 + C_2)$	$\frac{X_p^2}{r_p} (C_1 C_2 + C_1 C_3 + C_2 C_3)$
$\frac{R_p X_p}{\omega r_p^2} (k C_2 + C_1 + C_2)$	$\frac{R_p X_p}{\omega r_p^2} (k C_2 + C_1 + C_2)$

Positive terms	Negative terms
$\frac{X_p}{\omega r_p} (kC_2 + C_1 + C_2)$	$\frac{X_p}{\omega r_p} (C_1 + C_2)$
$\frac{R_p^2}{r_p} (C_2 + C_2) (kC_2 + C_1 + C_2)$	$\frac{R_p^2}{r_p} (C_1C_2 + C_1C_2 + C_2C_2)$
$R_p (C_2 + C_2) (C_1 + C_2)$	$R_p (C_1C_2 + C_1C_2 + C_2C_2)$

It is evident from inspection that the positive terms will exceed numerically the negative terms when  $X_p \geq 0$ , and since the denominator of  $r_g$  is always positive,  $r_g$  must always be positive.

The resistance component of the input impedance of a three-electrode vacuum tube is always positive, and hence the input absorbs power if the load in the plate circuit is capacitive or a pure resistance even when the grid is negative with respect to the filament.

In the succeeding treatment it will be shown that the input impedance of the tube may be equivalent to a considerable capacity with a high resistance in series, in which case the absorption of power in the input of the tube becomes very large.

If, however, the load is inductive ( $X_p > 0$ ), the terms above which contain  $X_p$  will change sign. The numerator of  $r_g$  will then become

$$R_p C_2^2 + \frac{R_p^2}{r_p} (kC_2^2 + C_2^2 + kC_2 C_2) + \frac{X_p^2}{r_p} (kC_2^2 + C_2^2 + kC_2 C_2) - \frac{X_p}{\omega r_p} (kC_2).$$

Hence  $r_g$  will be negative if

$$\frac{kX_p}{\omega r_p} > \frac{X_p^2}{r_p} (kC_2 + C_2 + kC_2) + \frac{R_p^2}{r_p} (kC_2 + C_2 + kC_2) + R_p C_2. \quad (15)$$

The resistance component of the input impedance of a three-electrode vacuum tube can be negative and the tube will supply power to the external input circuit; i. e., regenerate, if the load in the plate circuit is inductive.

This explains the regenerative effect of an inductive load previously noted by Armstrong,<sup>3</sup> and also the regenerative effects and oscillations in amplifiers, which can occur even when there is no electrostatic or electromagnetic coupling between the input and output circuits other than through the tube itself.

The dependence of the regenerative action upon the inductive load in the plate circuit will be treated theoretically and experimentally in a succeeding section.

<sup>3</sup> Armstrong, E. H., *Proc. I. R. E.*, 3, p. 215, 1915; in particular Fig. 10, on p. 220.

### III. INPUT IMPEDANCE FOR THE CASE OF A PURE RESISTANCE LOAD IN THE PLATE CIRCUIT

We will first consider the case where the load in the plate circuit is a pure resistance; that is,  $Z_p = R_p$ . Equation (8) then becomes

$$z_g = \frac{r_p(C_2 + C_3) - \frac{j}{\omega} \left(1 + \frac{r_p}{R_p}\right)}{kC_2 + \left(1 + \frac{r_p}{R_p}\right)(C_1 + C_2) + j\omega r_p (C_1 C_2 + C_1 C_3 + C_2 C_3)} \quad (16)$$

If we let  $a = r_p (C_2 + C_3)$

$$b = \left(1 + \frac{r_p}{R_p}\right) \quad (17)$$

$$c = kC_2 + \left(1 + \frac{r_p}{R_p}\right)(C_1 + C_2)$$

$$d = r_p (C_1 C_2 + C_1 C_3 + C_2 C_3)$$

$$\text{Then } z_g = \frac{\left(a - \frac{j b}{\omega}\right)(c - j\omega d)}{c^2 + \omega^2 d^2} = \frac{ac + bd}{c^2 + \omega^2 d^2} + \frac{1}{j\omega \frac{(c^2 + \omega^2 d^2)}{(bc + a\omega^2 d)}}$$

If the input impedance is represented by an apparent resistance  $r_g$  in series with an apparent capacity  $c_g$ , the values of these quantities are given by

$$\begin{aligned} r_g &= \frac{ac + bd}{c^2 + \omega^2 d^2} \\ c_g &= \frac{c^2 + \omega^2 d^2}{bc + a\omega^2 d} \end{aligned} \quad (18)$$

The relative importance of the quantities involved may be expressed by  $b \gg a, c \gg d$ . Hence at low frequencies (in general for  $\omega < 10^6$ )

$$\begin{aligned} r_g &= \frac{ac + bd}{c^2} \\ c_g &= \frac{c}{b} \end{aligned} \quad (19)$$

For  $R_p = 0; r_g = 0; c_g = C_1 + C_2$ . Under these conditions the plate circuit constitutes a short circuit between filament and plate, eliminating the capacity  $C_2$  and putting  $C_1$  and  $C_3$  in parallel between grid and filament.

As  $R_p$  increases relative to  $r_p$ , both  $r_g$  and  $c_g$  increase.  $r_g$  can increase to nearly the order of  $r_p$ . The variation in  $c_g$  can be expressed by the equation

$$c_g = C_1 + C_2 + C_3 \left( \frac{k R_p}{r_p + R_p} \right) \quad (20)$$

From this it appears that the capacity  $C_3$  between grid and filament is important in increasing the apparent input capacity. The maximum increase (for  $R_p \gg r_p$ ) is  $k C_3$ . It is of interest to note that the quantity  $\frac{k R_p}{r_p + R_p}$  is, under the assumed frequency conditions, the ratio of the voltage across  $R_p$  to the input

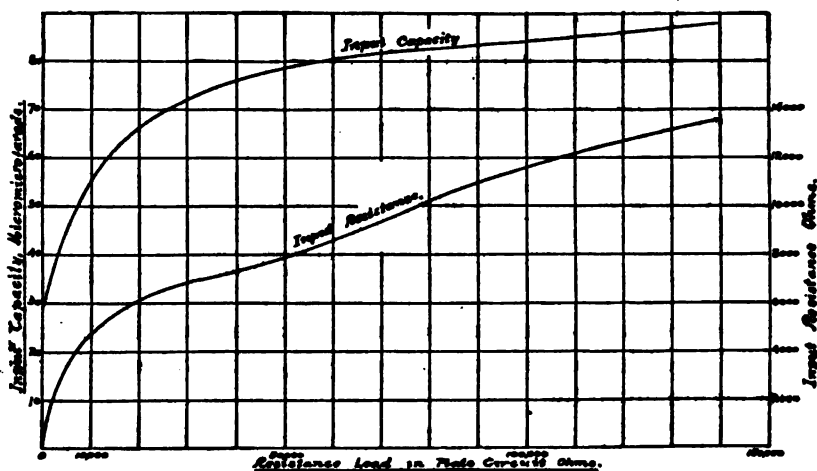


FIG. 3.—Variation of input characteristics with resistance load in the plate circuit

voltage  $E_g$  and hence determines the voltage amplification per stage of a resistance coupled amplifier. Thus the apparent input capacity can become a number of times greater than the actual capacities between the tube electrodes, and since the apparent input resistance can also become very high, the dissipation of power in the input circuit of the tube may be considerable, even when the grid is negative with respect to the filament.

When the frequency is so high that the terms containing  $\omega^2$  become important, these resistance and capacity effects become less marked. For very high frequencies

$$r_g = 0$$

$$c_g = \frac{C_1 C_2 + C_1 C_3 + C_2 C_3}{C_2 + C_3}$$

This latter is the capacity of  $C_2$  and  $C_3$  in series and paralleled

by  $C_1$ —i. e., the capacity between filament and grid with the plate circuit open. At these frequencies, however, the voltage across the resistance  $R_p$  is reduced, because of capacity effects and approaches zero with increasing frequency. Fig. 3 shows the variation of  $r_g$  and  $c_g$  with the load  $R_p$  for a particular tube of the J or VT-1 type for wave lengths longer than about 2000 m.

#### IV. EXPERIMENTAL DETERMINATIONS WITH A PURE RESISTANCE LOAD IN THE PLATE CIRCUIT

##### 1. DETERMINATION OF $k$ , $r_p$ , AND $\frac{k R_p}{R_p + r_p}$

A dynamic method for determining  $k$  and  $r_p$ , which was described in an earlier paper,<sup>4</sup> was utilized in these measurements. Since with a constant plate battery the actual voltage on the tube is reduced as a result of the drop in voltage across  $R_p$ , the determinations were so made that values of  $k$ ,  $r_p$ , and  $\frac{k R_p}{R_p + r_p}$  could be obtained which corresponded to the actual voltage on the plate for a given  $R_p$ . This was effected by obtaining curves for  $k$  and  $r_p$  for varying plate voltages, and then, with a constant plate battery, the actual voltage on the tube was determined for different values of  $R_p$  by making readings of the plate current and computing the voltage drop.

Two of the tubes used in the experiments and the electrical data of their use are described in Table 1.

TABLE 1

Type.	Plate voltage	Filament current	Grid voltage
J or VT-1.....	40	1.1	-1.5
VT-3.....	40	0.2	-1.5

Figs. 4 and 5 give the curves showing the dependence of  $k$ ,  $r_p$ , and  $\frac{k R_p}{R_p + r_p}$  upon the load  $R_p$  for these two tubes.

##### 2. DETERMINATION OF $C_1$ , $C_2$ , AND $C_3$

A series-resistance capacity bridge was used to measure the tube capacities, using an amplifier and phones as a balance indicator. A ground connection was put on a third arm of the bridge, and this was adjusted so as to bring the detecting arm of the bridge

<sup>4</sup>See reference 1.

at ground potential. The measurements were made at about 1000 cycles with a few tenths of a volt impressed on the bridge. Under these conditions the bridge was sensitive to one-tenth

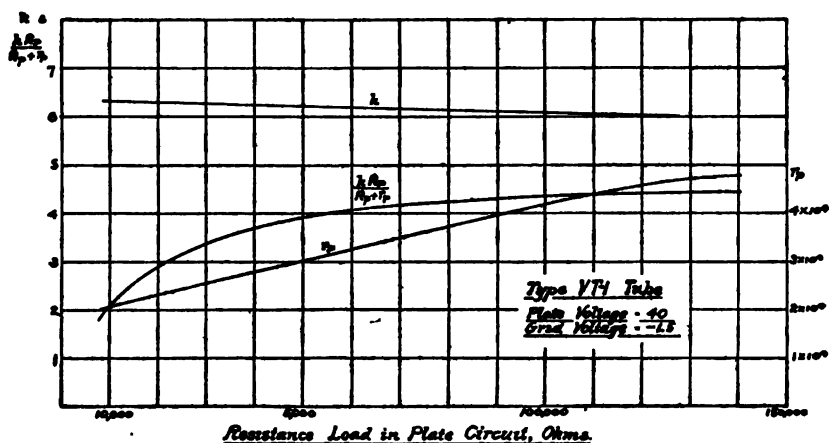


FIG. 4.—Amplification constant, voltage amplification and internal plate circuit resistance with varying resistance load. VT-1 tube

micromicrofarad. One arm of the bridge contained a variable air condenser of 250 micromicrofarads capacity, across which the capacities to be measured were connected and determined by the necessary change in the variable to maintain the bridge balance.

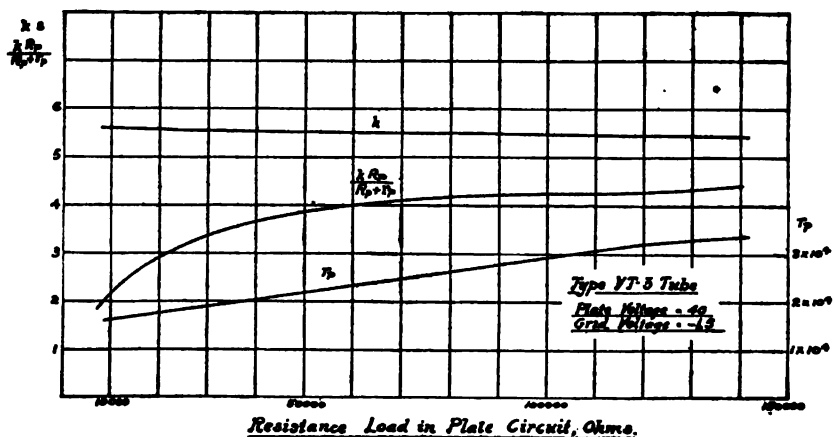


FIG. 5.—Amplification constant, voltage amplification and internal plate circuit resistance with varying resistance load. VT-3 tube

The filament, plate, and grid batteries were connected directly to the negative filament terminal, and this point was likewise connected to the ground potential part of the bridge. Those

portions of the connecting leads to the tube electrodes which followed the potentials of the electrodes themselves were considered as part of the electrodes and included in the capacity measurements. The tube socket was a Signal Corps receiving-tube socket and its capacities were also included.

The capacities  $C_1$ ,  $C_2$ , and  $C_3$  were separately determined in the following manner:

(a) Connect  $G$  and  $P$  together and measure capacity to  $F$ . This short-circuits  $C_2$  and gives  $C_1 + C_3$ .

(b) Connect  $G$  and  $F$  and measure to  $P$ . This gives  $C_2 + C_3$ .

(c) Connect  $F$  and  $P$  (i. e.  $R_p = 0$ ) and measure to  $G$ . This gives  $C_1 + C_2$ .

From these observations, then

$$2C_1 = (a) + (c) - (b)$$

$$2C_2 = (b) + (c) - (a)$$

$$2C_3 = (a) + (b) - (c)$$

The values of the capacities in micromicrofarads as measured for the two tubes mentioned previously were found to be as shown in Table 2.

TABLE 2

Type	$C_1 + C_3$	$C_2 + C_3$	$C_1 + C_2$	$C_1$	$C_2$	$C_3$
VT-1.....	28.2	26.6	27.9	14.7	13.1	13.4
VT-3.....	24.1	18.8	18.9	12.1	6.8	12.0

These capacity values are considerably increased because of the tube socket and leads used in the experiments.

### 3. DETERMINATION OF $c_g$

The apparent input capacity  $c_g$  for different resistance loads was determined in the same way as  $C_1 + C_3$  in (2) above, excepting that the resistance  $R_p$  was inserted in the plate circuit of the tube.

### 4. COMPARISON OF OBSERVED AND COMPUTED RESULTS

In Tables 3 and 4 the various resistance loads which were inserted in the plate circuit are given in the first column and in the other columns the calculated and experimentally observed values of the input capacity  $c_g$  are given in micromicrofarads.

TABLE 3.—VT-1 Tube

$R_p$ , ohms	Input capacity	
	Computed	Observed
0	-----	27.9
8000	51.4	49.0
16 000	64.5	61.5
49 400	78.9	76.1
97 000	84.2	84.3
139 000	86.1	87.6

TABLE 4.—VT-3 Tube

$R_p$ , ohms	Input capacity	
	Computed	Observed
0	-----	18.9
8200	31.8	32.4
18 500	38.1	40.1
49 800	45.1	46.9
98 500	47.5	51.2
140 500	49.0	53.1

To show the importance of the capacity  $C_2$  in determining  $c_g$  a separate series of measurements were carried out in which the capacity  $C_2$  was increased by connecting a small condenser between the grid and plate. A different tube of the VT-1 type was used in these measurements and the resistance  $R_p$  was 30 000 ohms throughout, leading to a value of  $\frac{k R_p}{R_p + r_p}$  of 3.29. Measurements of the apparent input capacity were made with  $C_2$  increased by zero, 17.5, and 34.3 micromicrofarads. The values of  $C_2$  were, then, 11.8, 29.3, and 46.1 micromicrofarads, the value of  $C_1$  was 12.2 micromicrofarads, the values of  $C_1 + C_2$  were 24.0, 41.5, and 58.3 micromicrofarads. The values of  $c_g$  as calculated from the formula  $c_g = C_1 + C_2 + C_2 \frac{k R_p}{r_p + R_p}$  for the three cases were 62.8, 137.9, and 210.0 micromicrofarads. The experimentally observed values were 64.3, 138.6, and 205.4 micromicrofarads, showing an agreement of about 2 per cent.

It was found to be impossible to check the values of  $r_g$  experimentally at the frequencies used in the bridge measurements because of dielectric absorption in the tube capacities. At these low frequencies the dielectric losses introduce effective resistances



which are many times greater than those given by the expression for  $r_g$ , which does not take dielectric losses into account. The measurements can no doubt be made at radio frequencies, but are rendered somewhat difficult because of the limited input voltage which can be applied to the tube if the grid is to remain at all times negative with respect to the filament. The dielectric losses in the tube capacities are doubtless important in the use of tubes at long waves, and should be taken into account in the design of tube bases and sockets.

## V. INPUT IMPEDANCE FOR THE CASE OF AN INDUCTIVE LOAD IN THE PLATE CIRCUIT

In case the load in the plate circuit is an inductance  $L_p$  and resistance  $R_p$  and the input impedance of the tube is represented by a series resistance  $r_g$  and capacity  $c_g$ , we obtain from equations (11), (13), and (14) the following:

$$r_g = \frac{a c + b d}{c^2 + d^2} \quad (21)$$

$$c_g = \frac{(c^2 + d^2)}{\omega(ad - bc)} \quad (22)$$

where

$$\begin{aligned} a &= R_p(C_2 + C_3) + \frac{L_p}{r_p} \\ b &= \omega L_p(C_2 + C_3) - \frac{R_p}{\omega r_p} - \frac{1}{\omega} \\ c &= \frac{R_p}{r_p} (kC_2 + C_1 + C_3) + C_1 + C_3 - \omega^2 L_p (C_1 C_2 + C_1 C_3 + C_2 C_3) \\ d &= \frac{\omega L_p}{r_p} (kC_2 + C_1 + C_3) + \omega R_p (C_1 C_2 + C_1 C_3 + C_2 C_3) \end{aligned} \quad (23)$$

As already pointed out above in expression (15), the numerator of  $r_g$ , and hence  $r_g$  itself, will be zero or negative when

$$\frac{kL_p}{r_p} \geq \frac{\omega^2 L_p^2}{r_p} (kC_2 + C_1 + kC_3) + \frac{R_p^2}{r_p} (kC_2 + C_1 + kC_3) + R_p C_2 \quad (24)$$

The equality sign determines the values of  $L_p$ , for which the input resistance is zero. If  $R_p$  is large, the solutions for  $L_p$  at a given frequency may be imaginary, in which case no inductive load can make the input resistance negative.

Curves showing the variation in the input resistance and input capacity with the inductance in the plate circuit are given in

Figs. 6 and 7 for various values of  $R_p$ . These were computed, using formulas (21), (22), and (23) for a frequency given by  $\omega = 2 \times 10^6$ , and assuming the constants  $k = 6$ ,  $C_1 = C_2 = C_3 = 10^{-11}$  and  $r_p = 2 \times 10^4$ , which are approximately those of a VT-1 tube.

If we assume that the resistance in the plate circuit is so low compared to the reactance of  $L_p$  that the terms containing  $R_p$  are negligible, the inequality of (24) reduces to

$$\omega^2 L_p \left( C_2 + C_3 + \frac{C_2}{k} \right) < 1 \quad (25)$$

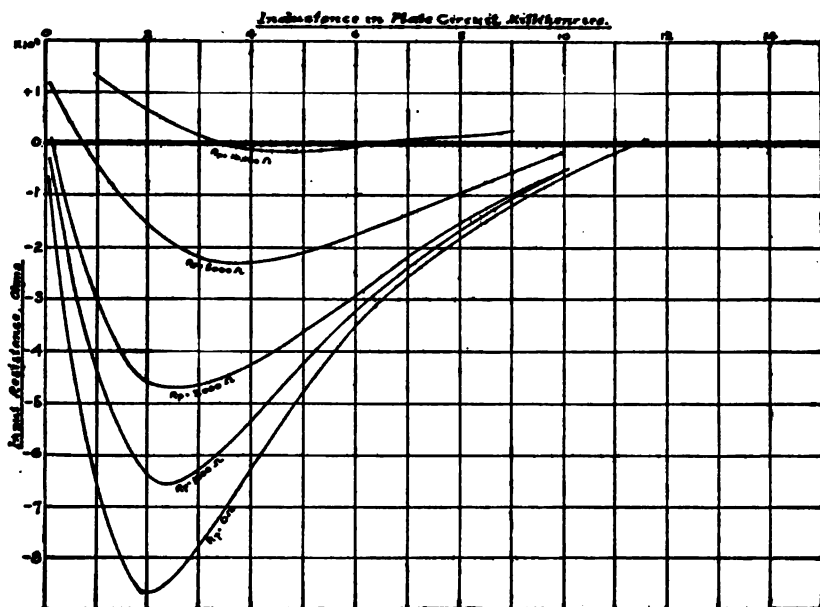


FIG. 6.—Negative input resistance caused by inductive load in plate circuit

This shows that the combination of inductive load plus the tube capacities must still be an inductive reactance in order to have regeneration, and determines the highest frequency with a given inductance  $L_p$  or the highest value of  $L_p$  at a given frequency at which regeneration can occur. At low values of  $L_p$ , or at low frequencies where  $\omega^2 L_p (C_1, C_2, \text{ or } C_3)$  is small compared to unity, and assuming  $R_p$  is small compared to  $r_p$  or  $\omega L_p$ , the only term in the numerator of  $r_g$  which is of importance is  $-\frac{L_p}{r_p} (k C_2)$ . From (21) and (23) it is seen that the denominator of  $r_g$  reduced to  $(C_1 + C_2)^2$ . Hence the value of the input resistance is given by

$$r_g = -\frac{L_p}{r_p} \frac{(k C_2)}{(C_1 + C_2)^2} \quad (26)$$

From (22) and (23) it can be seen that under the above assumptions the input capacity is given by

$$c_g = C_1 + C_2 \quad (27)$$

Under these conditions, therefore, the input impedance of a tube consists of a negative resistance proportional to the inductance in the plate circuit in series with a constant capacity. This corresponds to the portion of the curves of Figs. 6 and 7 for  $R_p = 0$  and low  $L_p$ .

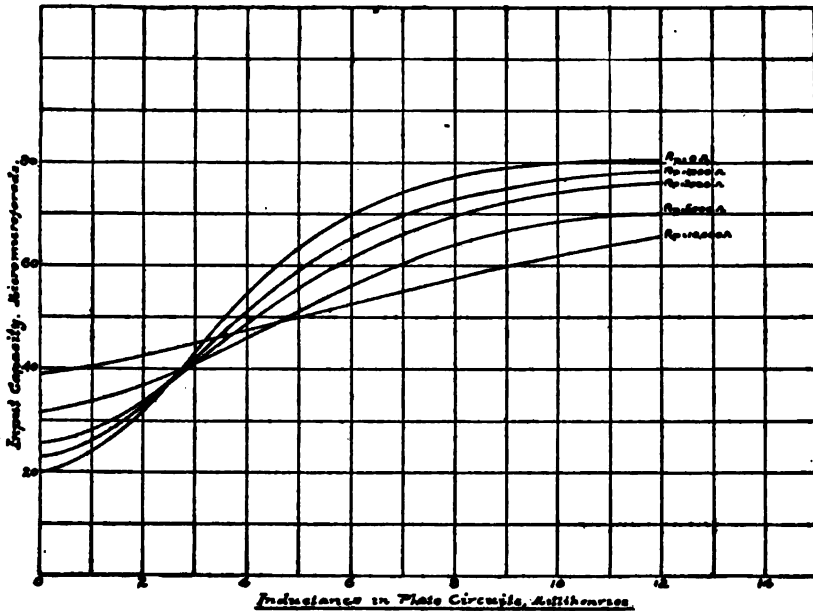


FIG. 7.—Variation in input capacity with inductive load

The magnitude of the regenerative effect produced by the negative input resistance will depend upon the constants of the external input circuit. The effect will be to reduce or neutralize the positive resistance of the external circuit. In general an oscillatory circuit is connected to the input of the tube and the apparent resistance of this circuit is reduced as a result of the regenerative action. When  $r_g$  and  $c_g$  are such as completely to neutralize the resistance of that circuit, oscillations will take place.

In the case of an amplifier this input circuit may be a transformer. The complete input circuit will be as shown in Fig. 8, where  $L$  and  $C$  represent the coil and condenser of the oscillatory

circuit, of which the resistance is  $R$ . The input characteristics of the tube are represented by  $r_g$  and  $c_g$ . The reduction in the resistance of the oscillatory circuit which results when  $r_g$  is negative, can be calculated as follows.

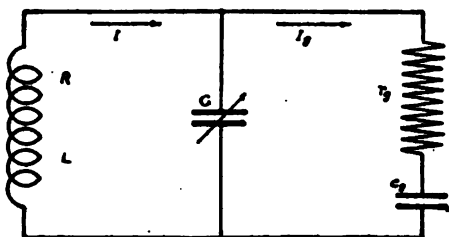


FIG. 8.—External grid circuit and input impedance of tube

Since the reactance of  $c_g$  is ordinarily very large compared to the numerical value of  $r_g$ , the current  $I$  in the oscillatory circuit will divide between  $C$  and the parallel branch containing  $c_g$  in proportion to the capacities  $C$  and  $c_g$ . Hence the current

$I_g$  flowing into the grid of the tube and through the resistance  $r_g$  is given by

$$I_g = I \frac{c_g}{C + c_g} \quad (28)$$

The power dissipated in  $r_g$  will be  $P_g = I_g^2 r_g = I^2 \left( \frac{c_g}{C + c_g} \right)^2 r_g$  (29)

This will be negative when  $r_g$  is negative, thus representing a generation of power. The power dissipated in the resistance  $R$  is

$$P_R = I^2 R \quad (30)$$

and the total power

$$P = P_R + P_g = I^2 \left[ R + \left( \frac{c_g}{C + c_g} \right)^2 r_g \right] \quad (31)$$

Thus when  $r_g$  is negative the reduction in the circuit resistance will be given by

$$\Delta R = \left( \frac{c_g}{C + c_g} \right)^2 r_g \quad (32)$$

In Fig. 9 are plotted curves of received signal against the inductance in the plate circuit, assuming the same tube constants and frequency as in Figs. 6 and 7, that the resistance in the plate circuit is negligible ( $R_p = 0$ ) and that the capacity  $C$  of Fig. 8 is 0.0015 microfarad. Three curves are shown corresponding to circuits of 7, 9, and 10 ohms resistance. The received signal is taken to be proportional to the reciprocal of the circuit resistance as reduced by the regenerative effect. The curves for the 7 ohm circuit run to infinity, indicating complete neutralization of the

circuit resistance and hence oscillations. The curves for the 9 and 10 ohm circuits are quite similar to that given by Armstrong.<sup>3</sup>

For low values of  $L_p$  we find by substituting the values of  $r_g$  and  $C_g$  from (26) and (27) in (32)

$$\Delta R = \frac{k L_p C_2}{r_p (C + C_1 + C_2)^2} \quad (33)$$

The regenerative effects are increased by increasing  $L_p$ , decreasing  $C$ , or by connecting a condenser between grid and plate so as to increase  $C_2$  when  $C_2$  is small compared to  $C$ .

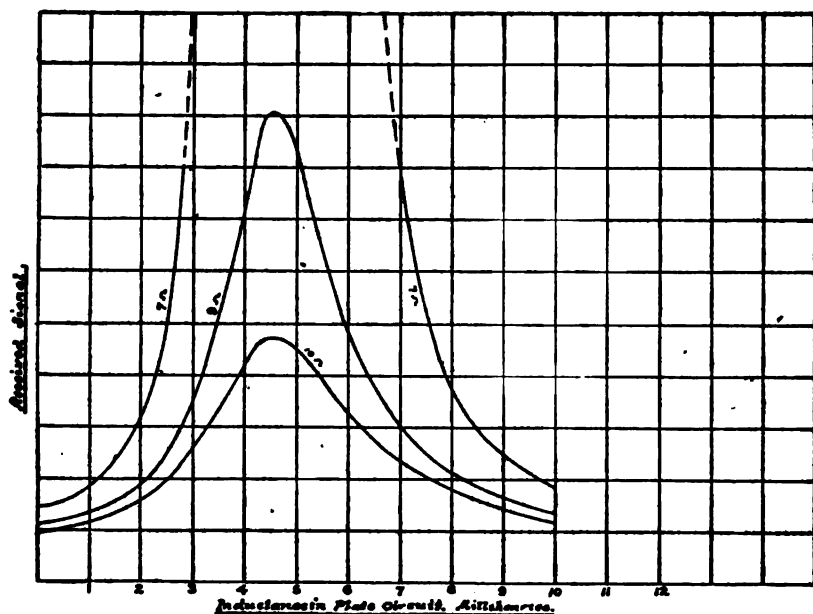


FIG. 9.—Variation of received signal with inductive load in the plate circuit

## VI. EXPERIMENTAL DETERMINATIONS WITH AN INDUCTIVE LOAD

Expression (33) was checked by measuring at radio frequencies the reduction in resistance of an oscillatory circuit connected to the input terminals of the tube when different inductances of known value were inserted in the plate circuit.

### 1. DETERMINATION OF THE TUBE CONSTANTS

A type J or VT-1 tube was used with 40 volts on the plate, -1.5 on the grid, and a filament current of 1.1 amperes. The

<sup>3</sup> Armstrong, loc. cit.

tube constants were measured, as outlined in Section IV above, and were found to be as follows for the tube used:  $k=7.2$ ,  $r_p=29\,300$ ,  $C_2=12.2$ , and  $C_1+C_2=25.7$  micromicrofarads.

## 2. MEASUREMENT OF THE OSCILLATORY CIRCUIT RESISTANCE

The oscillatory circuit was coupled to a driving circuit, and its resistance was measured at 900 m. wave length by the resistance variation method. The capacity  $C$  was 1675 micromicrofarads. The current indications were obtained with a vacuum thermocouple of 4.8 ohms resistance and a sensitive wall galvanometer. With this value of the capacity and frequency sufficient measuring current was obtained without impressing more than one volt across the condenser or on the input of the tube. Measurements made with the tube disconnected from the condenser  $C$ , and then connected, but with no inserted inductance in the plate circuit, showed that the dielectric losses in the tube capacities were not appreciable at this frequency. The resistance of the oscillatory circuit was then determined with 254 and 680 microhenries inductance in the plate circuit.

## 3. COMPARISON OF OBSERVED AND COMPUTED RESULTS

The theoretical reduction in the circuit resistance was computed from formula (33); the value of the factor  $\frac{k C_2}{r_p (C + C_1 + C_2)^2}$  as calculated from the tube constants and capacity  $C$  being  $1.037 \times 10^8$ . The results are compared in Table 5. In the first column are given the values of the inductive load in microhenries, in the second column the corresponding observed circuit resistances, in the third column the observed reduction in the circuit resistance, and in the fourth column the reduction in circuit resistance as computed by formula (33).

TABLE 5

Inductance, microhenries	Circuit resistance, ohms	Reduction in circuit resistance	
		Observed	Computed
0	6.58	-----	-----
234	6.32	0.26	0.26
680	5.88	.70	.70

## VII. INPUT IMPEDANCE FOR THE CASE OF A CAPACITY LOAD IN THE PLATE CIRCUIT

The equations of the input impedance for a capacity load can likewise be derived readily from equations (11), (13), and (14). In this case the input resistance will always be positive, so that the input absorbs power. Thus the presence of phones in the plate circuit of a tube may cause a dissipation of power in the input, because of the phones having a capacity reactance at high frequencies.

## VIII. SUMMARY OF RESULTS

1. Because of the capacities between the elements of a three-electrode vacuum tube, the input impedance of the tube depends upon the nature of the load in the plate circuit of the tube.

2. Even when the grid of the tube is negative with respect to the filament, the input impedance can be such as to absorb considerable power from the input circuit. This occurs when the load in the plate circuit is a resistance or capacity reactance.

3. When the load in the plate circuit is inductive, the input impedance can be characterized by a negative resistance, in which case regeneration or oscillations can occur as a result of coupling through the tube itself.

In conclusion the author desires to express his indebtedness to the Signal Corps, who requested and supported this investigation, and to Miss Dora E. Wells, of the Bureau of Standards, who performed most of the experimental work. The above results were communicated to the Signal Corps in reports dated April 8 and April 30, 1919, and are published with their approval.

WASHINGTON, June 11, 1919.









# THERMAL EXPANSION OF INSULATING MATERIALS

By Wilmer H. Souder and Peter Hidner

## CONTENTS

	Page
I. Introduction.....	387
II. Previous work on porcelain.....	388
III. Previous work on marble.....	388
IV. Apparatus and specimens.....	390
V. Porcelain.....	391
VI. Phenol condensation products, etc.....	399
VII. Marble and limestone.....	411
VIII. Summary.....	416

## I. INTRODUCTION

The material here presented is selected from the mass of data accumulated during thermal expansivity tests, and is of importance where insulating materials are subjected to temperature variations. The range of expansion coefficients is rather large, extending from a value of  $1.6 \times 10^{-6}$  for certain porcelains to  $109 \times 10^{-6}$  for a specimen of celluloid.

In addition to the wide range in coefficients it has also been found that practically all of the molded materials, such as bakelite, condensite, hard rubber, and celluloid, take up a permanent length change when carried through a temperature cycle, especially if temperatures above  $60^{\circ}$  C are reached. This length change, always a shrinkage, may work to advantage in cases where a slight shrinkage tends to compress and retain metallic electrodes or inserts. On the other hand, these changes become very serious in precision apparatus depending upon accurate dimensions.

The following materials have been investigated and are included in this report: Porcelain, bakelite, condensite, formica, celluloid, hard rubber, marble, and limestone.

## II. PREVIOUS WORK ON PORCELAIN

Some of the results of previous experimental determinations of the thermal expansion of porcelain are summarized in the following table. The values given for  $a$  and  $b$  are to be substituted in the general quadratic equation

$$L_t = L_0 (1 + at + bt^2)$$

where  $L_0$  is the length of the material at  $0^\circ \text{C}$  and  $L_t$  the length at  $t^\circ \text{C}$  within the proper temperature range.

TABLE 1

Kind of porcelain	Observer	Temperature range	Coefficients	
			$a$	$b$
Bayeux.....	Tutton <sup>a</sup> .....	$^\circ\text{C}$ 0-120	$2.922 \times 10^{-4}$	$7.43 \times 10^{-3}$
Do.....	Bedford.....	0-600	3.425	1.07
Do.....	Chappuis.....	0-83	2.824	6.17
Berlin.....	Halbema and Day <sup>b</sup> .....	250-625	2.954	1.125

<sup>a</sup> Proc. Phys. Soc. of Lond., 18, p. 182; 1901-1903.

<sup>b</sup> Ann. der Phys. und Chem., 8, p. 505; 1900.

Tutton agrees with Chappuis that the thermal expansion of Bayeux or Berlin porcelains can not be represented by a quadratic equation throughout a temperature range exceeding a very few hundred degrees.

Brundige<sup>1</sup> is of the opinion that expansion effects cause the major part of insulator deterioration. However, he points out that there are other investigators who believe that practically all insulator deterioration is attributed to porosity.

## III. PREVIOUS WORK ON MARBLE

Roiti's Physics (vol. 1, sec. 399, Hungarian translation, p. 457), gives as the average coefficient of expansion for  $1^\circ \text{C}$  between  $0^\circ$  and  $100^\circ \text{C}$ , the following values:

White marble.....	0.0000849 (Destigny)
Do.....	.00001072 (Dunn and Sang)

Fröhlich<sup>2</sup> found it necessary to know the coefficient of expansion of a large ring (standard of inductance) made from Carrara marble in order to determine the dimensions at a given temperature. From observations at room temperature and at  $100^\circ \text{C}$  (steam)

<sup>1</sup> Trans. Amer. Inst. Elec. Eng., 86, p. 535; 1917.

<sup>2</sup> Wiedemann Annalen der Physik und Chemie, 61, p. 206; 1907.

on a 30 cm specimen cut from the same block of marble used for the ring, he obtained 0.000012 for the average coefficient of expansion between 15 and 100° C. However, he does not state whether the specimen returned to its original dimensions after cooling.

Kaye and Laby (Physical and Chemical Constants, etc., 1911) of the National Physical Laboratory give  $1.4 \times 10^{-6}$  to  $3.5 \times 10^{-6}$  for the coefficient of expansion of marble at 15° C.

Grüneisen<sup>3</sup> gives  $4.3 \times 10^{-6}$  as the coefficient between 14 and 24°, and  $10.5 \times 10^{-6}$  between 18 and 100° C. After keeping a specimen at a constant temperature of 100° C, he found the value  $2.2 \times 10^{-6}$  for the coefficient of expansion between 14 and 24° C.

Hallock<sup>4</sup> determined the expansion of several marbles by comparing them with brass, and gives the following values from room temperature to 100° C:

A marble from Rutland, Vt.....	0.00000659
	661
A marble from Knoxville, Tenn.....	0.00000495
	525
A marble, "Keowa," from Georgia.....	0.00000348
	309
A marble, "Creole," from Georgia.....	0.0000110
A marble, "Cherokee," from Georgia.....	0.00000740
	786
	855

The duplicate values are from different bars of the same marble.

He observed the phenomenon of permanent growth after heating, especially with the Vermont and Tennessee specimens. "Being heated for the first time to 100° C and allowed to cool, they did not contract to their original length, and the next two or three heatings resulted in continued but ever diminishing increments of length at ordinary temperatures; finally a permanent condition was reached." He also found that a Vermont marble when kept at constant temperature, contracted on drying and expanded on soaking in water.

In 1832, W. H. C. Bartlett<sup>5</sup> made determinations on the expansion of some stones at ordinary temperatures (range about 100° F). He gives for the coefficient of expansion of marble, 0.000005668 =

$\frac{1}{176\,429}$  per degree Fahrenheit. He reached the conclusion that the fractures of the stones at Fort Adams, Newport Harbor, were due to ordinary changes of temperature.

<sup>3</sup> Recueil de Constantes Physiques, p. 188; 1913.

<sup>4</sup> Amer. Jour. of Science, 1st series, 22, p. 136.

<sup>5</sup> U. S. Geol. Survey Bull., No. 77, p. 109; 1891.

T. M. Reade<sup>6</sup> also determined the expansion of several rocks, and gives as the coefficient of expansion of marbles the value  $\frac{1}{184\,797}$  per degree Fahrenheit. (Temperature range not indicated.)

N. E. Wheeler<sup>7</sup> investigated a specimen of white marble from Carrara, Italy. He obtained the following values for the coefficients of expansion per degree centigrade at intervals of 100° C:

Temperature	Coefficients of expansion	
	First heating	Fifth heating
100° C.....	82.3 $\times 10^{-7}$	28.9 $\times 10^{-7}$
200° C.....	181	92.3
300° C.....	239	127.3
400° C.....	276	179.2

Nisi<sup>8</sup> used an Abbe and Pulfrich interferometer over a range extending from 0° to 40° C. He found that the thermal expansion of white Carrara marble is different in different directions, and that the rate of expansion increases with temperature. He failed to obtain a marked permanent set, on account of his very limited temperature range. The coefficients of linear expansion for differently oriented specimens at temperatures between 0° and 40° C varied from  $-0.77 \times 10^{-6}$  to  $+11.24 \times 10^{-6}$ .

Nisi states that marble is by no means an homogeneous mass, and that the anomalous behavior of marble as regards thermal expansion is closely connected with the cleavage planes.

#### IV. APPARATUS AND SPECIMENS

Each specimen was in the form of a straight rod or bar of uniform cross section. The length was about 30 cm and the cross section about 1 cm square. Both ends were cylindrical in shape.

Two kinds of apparatus<sup>9</sup> were used in making the thermal expansion tests—an oil bath<sup>10</sup> and air furnaces.

In the furnaces the specimen was supported horizontally and a 2-mil platinum wire, which was previously annealed, hung

<sup>6</sup> The Origin of Mountain Ranges; 1886.

<sup>7</sup> Trans. Royal Soc. of Canada, 3d series, 4, p. 19; 1910-11.

<sup>8</sup> Tokyo Math.-Phys. Soc. Proc., 3d series, 7, p. 97; 1913-14.

<sup>9</sup> This consists essentially of the apparatus designed and installed by A. W. Gray and L. W. Schad, formerly of this Bureau.

<sup>10</sup> For short description, see Preliminary Determination of the Thermal Expansion of Molybdenum, Scientific Papers, No. 332, p. 31.



FIG. 1.—*Farnace and traveling microscopes*



over each end. Each wire, hanging through a hollow tube below the end of the specimen and extending downward through and below the furnace, had at its lower end a vane (or weight) immersed in oil in order to dampen the vibrations. Heating was effected by electric resistance coils (outside, inside, and end coils). With careful manipulation it was possible to adjust the circuits so that during an observation the specimen was at a uniform temperature within one-tenth degree centigrade, from end to end.

The length changes were determined with a comparator consisting of two microscopes rigidly clamped on an invar bar at a distance from each other equal to the length of the specimen (30 cm.). The microscopes were so arranged that they could first be sighted on a standard-length bar kept at constant temperature, and then on the vertically suspended wires which were in contact with the ends of the specimen.

The apparatus shown in Fig. 1 was used for part of this research and portrays the essential method of making observations on materials. The furnace is shown with the top lifted. The traveling microscopes, which are sighted (simultaneously) on the two vertical wires hung from the specimen, are displaced to the right in order to show the construction of the tube protecting the vertical or drop wires. The left oil pot is removed to show the weight attached to the wire.

The temperatures in the oil bath and furnaces were determined by means of a copper-constantan and a platinum-platinum rhodium thermocouple, respectively.

## V. PORCELAIN

Data on the thermal expansion of 40 samples of various kinds of porcelain are presented in this paper.

The coefficients of expansion of these materials vary over a wide range, as may be seen from the accompanying curves and the following table. It is remarkable that the various kinds of porcelain, when heated to high temperatures and then cooled to room temperature, returned to their approximate initial lengths, as is evident from the last column in the table; that is, there is no marked set or permanent change in dimension due to the heat treatment.

The expansion curves of porcelain may be divided into three classes: Straight-line, concave, and convex curves. In the straight-line curve, the rate of expansion is constant. (See S494

in Table 2.) The concave expansion curve shows that the rate of expansion increases with temperature, but the convex curve indicates that the rate of expansion decreases with temperature. Examples of concave curves are shown by S472, S476, S496, and S500; and examples of convex curves by S436, S480, and S501.

TABLE 2

Bureau of Standards No.	Composition.							Average coefficients $\times 10^6$				Change in length after test (per cent)
	Per cent clay	Per cent feldspar	Per cent flint	Per cent whitening	Per cent calcine No. 14 <sup>a</sup>	Per cent sillimanite <sup>c</sup>	Per cent $Al_2O_3$	Room temperature to 200° C	200 to 400° C	400 to 540° C	400 to 600° C	
S391								4.4	5.4		5.8	0.00
S392								4.6	5.4		6.0	.00
S393								3.7	5.0		5.4	+ .01
S399								5.8	4.7		7.8	+ .01
S400								5.2	5.6	6.8		+ .02
S401								4.8	5.9	8.8		+ .04
S402								4.3	6.1		7.9	+ .01
S405								2.9	3.7		3.8	- .01
S416								5.2	4.4		4.9	.00
S417								5.3	4.4		4.8	+ .01
S436 <sup>a</sup>	50		20					19.4	9.4	5.5		- .02
S437	50 <sup>b</sup>		30		20			19.6	11.1	8.1		+ .03
S438	50		20		30			10.4	5.4	4.5		- .01
S442 <sup>b</sup>	50		30					7.3	6.1	4.7		.00
S443 <sup>c</sup>	50		20					8.9	4.4	4.1		.00
S444	50		20		30			10.8	5.5	4.4		.00
S445	40				20	40		3.4	4.2	4.8		.00
S472 <sup>d</sup>	50		15					1.6	3.0	3.6		- .01
S476								5.7	6.7	8.4		.00
S477								5.8	6.8	8.8		.00
S478	48				18	34		10.4	5.6	4.4		- .01
S479	40				16	44		10.9	6.6	7.8		+ .06
S480	45				15	40		8.9	5.0	5.1		- .01
S485	71.5	15.6	2.4	1.4			9.1	2.9	4.0			- .02
S486	50	16	32.5	1.5				6.2	4.6			.00
S487	77	12.5		1.45			9.05	3.4	3.9			- .01
S488	80.1	9.5		1.43			8.97	3.1	3.8			- .01
S489	85	13.5		1.5				3.2	3.5			- .01
S490	80	18.5		1.5				2.9	4.0			- .01
S491	80	13.5	5	1.5				3.3	3.2			- .01
S492	75	23.5		1.5				3.5	4.5			+ .01
S493	75	18.5	5	1.5				3.2	3.7			- .01
S494	75	10	13.5	1.5				4.1	4.1			- .01
S495	70	23.5	5	1.5				3.7				- .09
S496	70	19	9.5	1.5				3.3	4.0			.00
S497	70	15	13.5	1.5				3.4	3.6			.00
S499	80	10	8.5	1.5				4.7	4.6			.00
S500	75	13.5	10	1.5				3.7	4.3			- .01
S501	70	10	18.5	1.5				6.1	5.1		4.5	- .02
S502	50	16	34					4.7	4.6			.00

<sup>a</sup> Calcine No. 8A—30 per cent. (See Table 1.)

<sup>b</sup> Calcine No. 13—20 per cent. (See Table 1.)

<sup>c</sup> Calcine No. 13—30 per cent.

<sup>d</sup> Beryl—35 per cent.

<sup>e</sup> See Table 1.

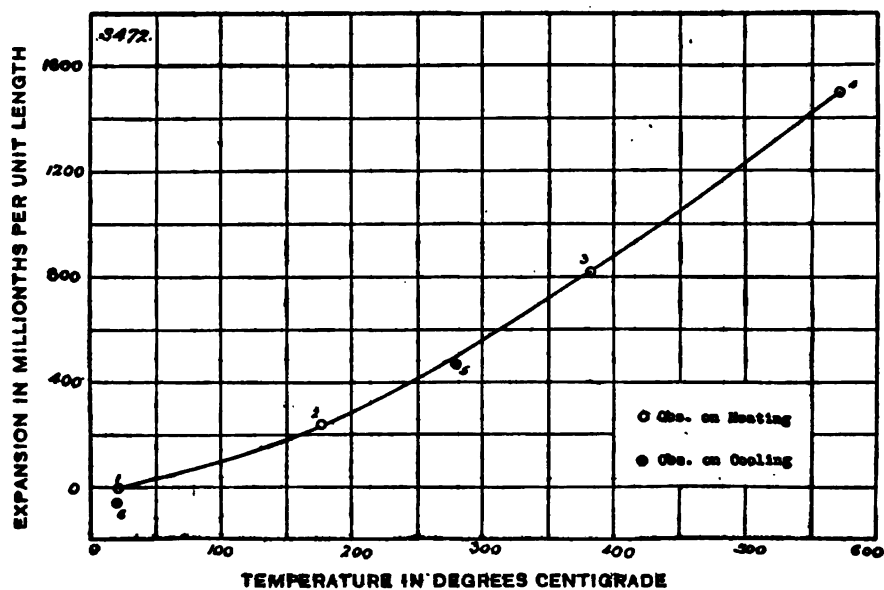


FIG. 2.—Expansion of porcelain (S 472)

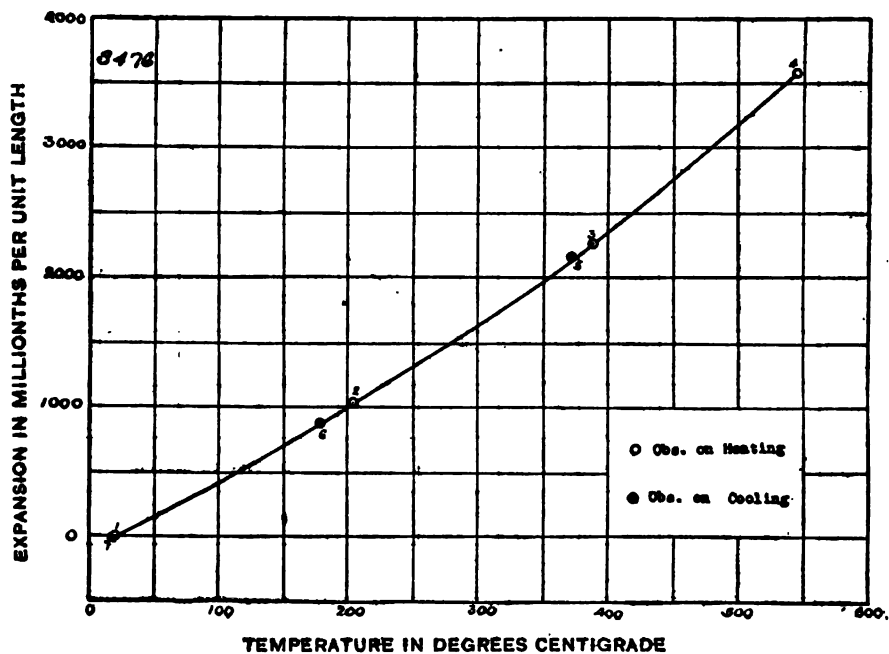


FIG. 3.—Expansion of porcelain (S 476)

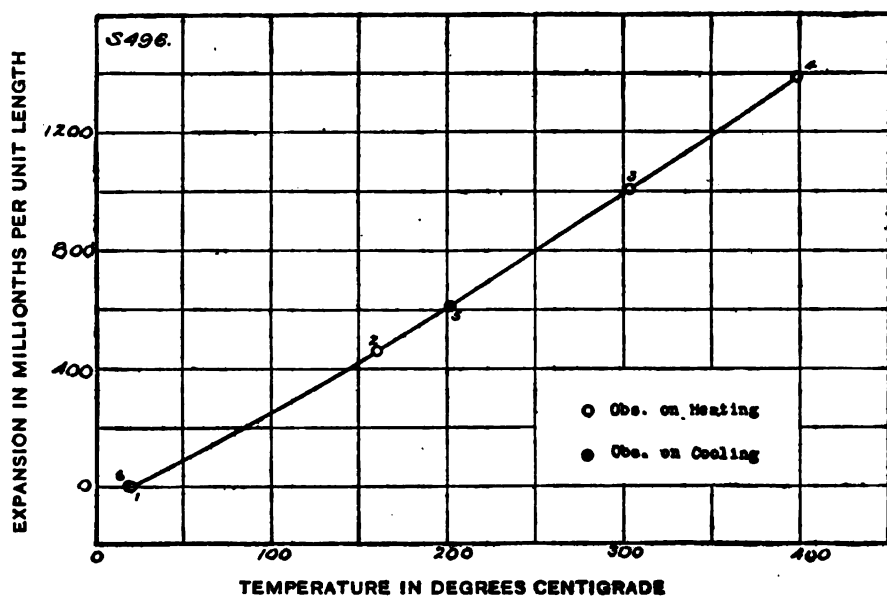


FIG. 4.—Expansion of porcelain (S 496)

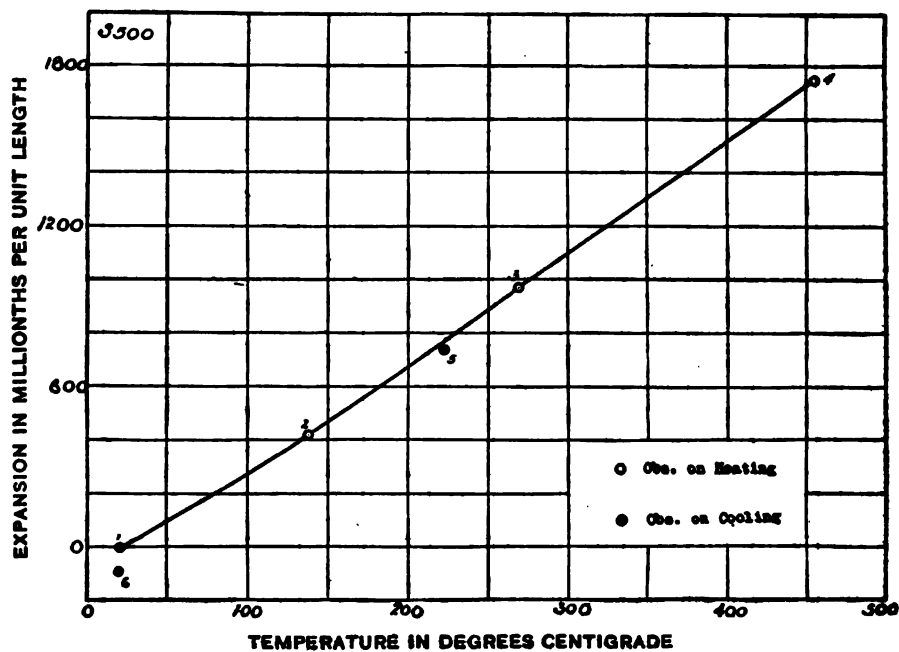


FIG. 5.—Expansion of porcelain (S 500)

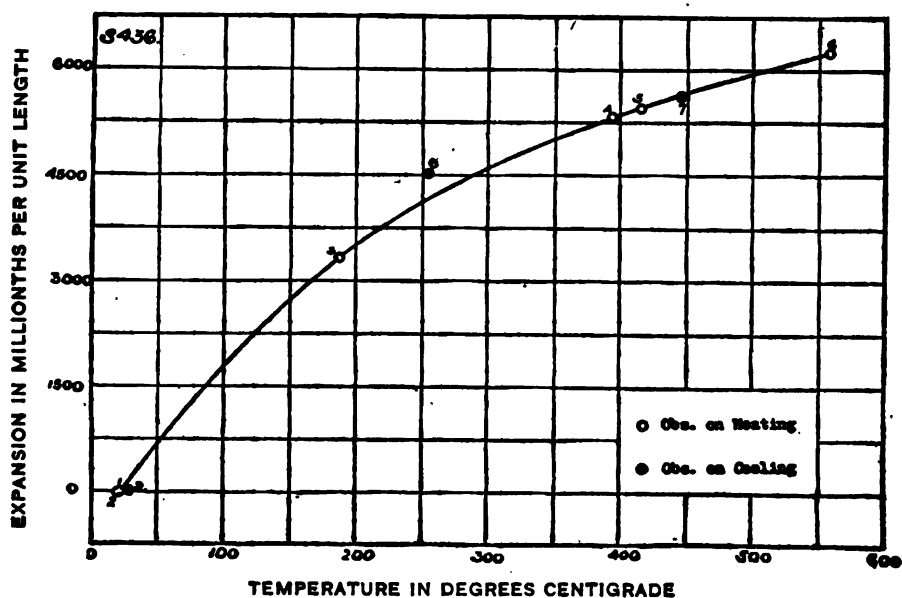


FIG. 6.—Expansion of porcelain (S 436)

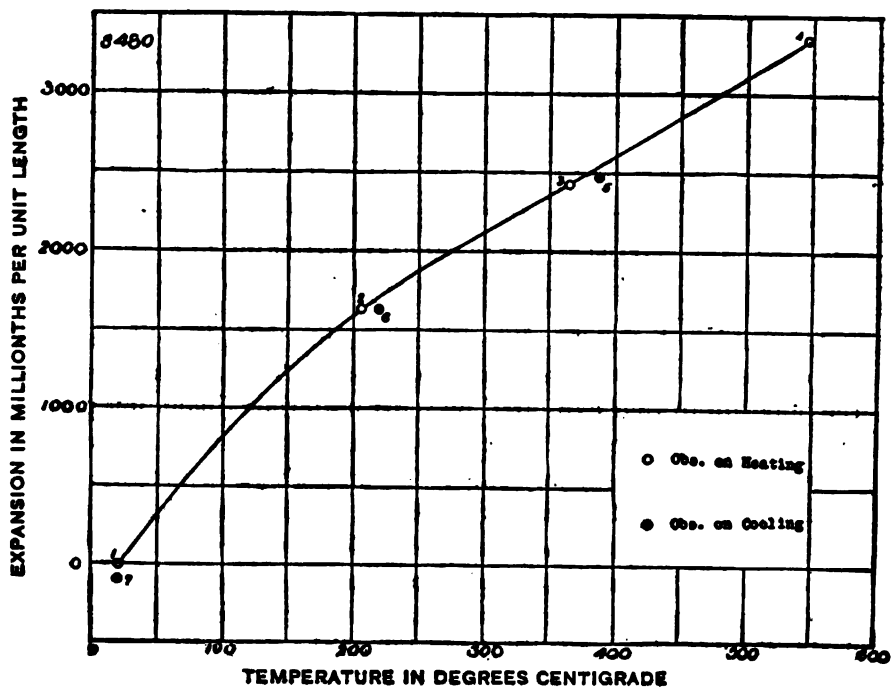


FIG. 7.—Expansion of porcelain (S 480)

The constituents of the calcines are given in the accompanying table.

TABLE 3

Composites	Clay	MgCO <sub>3</sub>	Flint	Baric acid	Al <sub>2</sub> O <sub>3</sub>
Calcline No. 8A.....	44.30	14.40	41.30	.....	.....
Calcline No. 13.....	76.15	23.85	.....	.....	.....
Calcline No. 14.....	56.00	18.20	25.00	.....	.....
Sillimanite.....	70.20	.....	.....	2.00	27.80

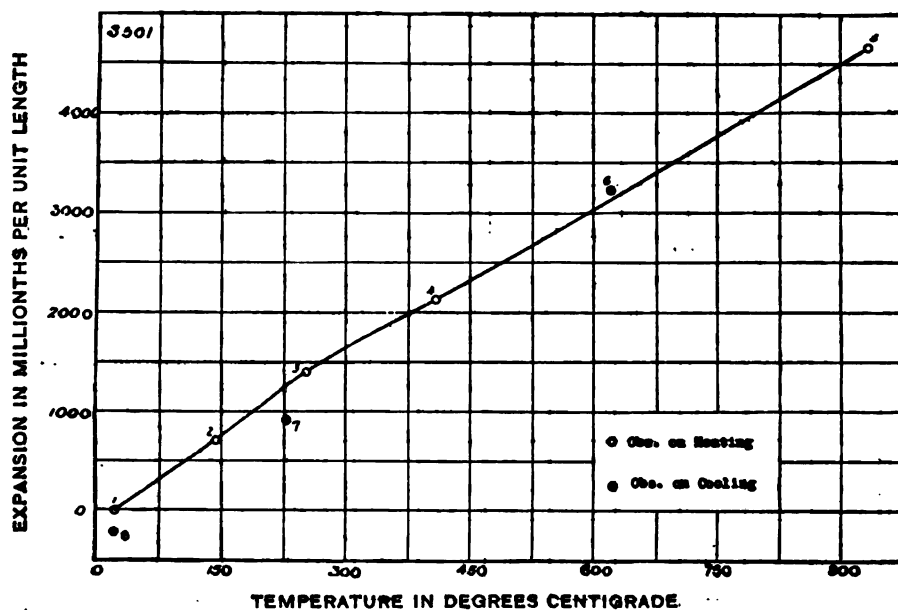


FIG. 8.—Expansion of porcelain (S 501)

Attention is directed to the curve applying to S436, which shows the convexity found in a number of cases. This characteristic is the opposite to that exhibited by most materials (including porcelain in general), especially metals which are used as electrodes or clamps. The expansion curves of metals are usually concave, and give positive values for the  $b$  in the expansion formula:

$$L_t = L_0 (1 + at + bt^2)$$

where  $L_t$  is the length at any temperature  $t$  and  $L_0$  the length at  $0^\circ$  C, whereas in the case of porcelain S436 this coefficient  $b$  is decidedly negative, causing the value of the rate of expansion to decrease with temperature. In the former case, however, the instantaneous coefficient or rate of expansion increases with temperature.

The fact that the average coefficient of S436 between room temperature and 550° C is about the same as that of certain steels does not mean that these steels may be used as perfect matches for expansion (in spark plugs, for example). The rate of expansion of this porcelain decreases rapidly with temperature (see curve S436 and Table 2), while the rate of expansion of steel increases. Serious cracking of the porcelain may occur when the differential expansion approaches a maximum.

Porcelains having low coefficients of expansion have been found to exhibit marked resistance to sudden temperature changes. Plunging cold specimens into the blast flame did not cause checking or cracking.

The large number of varying constituents in the porcelains makes it difficult to obtain an exact relationship between the composition and the coefficients of expansion. However, some relations have been deduced.

The coefficients of porcelains having the same amounts of clay, flint, and calcines depend on the kind of calcines contained. Porcelains containing calcines No. 8A, No. 14, and No. 13 have relatively large, intermediate, and small coefficients of expansion, respectively. For example, the following comparison shows the variations in the coefficients of S436, S438, and S443, which contain 50 per cent clay, 20 per cent flint, and 30 per cent calcine. (The kind of calcine is different in each case.)

Bureau of Stand- ards No.	Kind of calcine	Average coefficients		
		Room tem- perature to 200° C	200 to 400° C	400 to 540° C
S436	No. 8A.....	$19.4 \times 10^{-6}$	$9.4 \times 10^{-6}$	$5.5 \times 10^{-6}$
S438	No. 14.....	10.4	5.4	4.5
S443	No. 13.....	8.9	4.4	4.1

All porcelains containing 50 per cent clay, 20 or 30 per cent flint, and the remainder calcine (No. 8A, 13, or 14) have convex expansion curves. (See S436, S437, S438, S442, S443, and S444.)

The porcelain (S472) containing 35 per cent beryl, in addition to 50 per cent clay and 15 per cent flint, gave the lowest coefficient of expansion. Beryl is probably the constituent causing the small thermal expansion.

In a porcelain containing 40 per cent clay, an increase of 4 per cent in sillimanite and a corresponding decrease in calcine No. 14,

caused a marked increase in the coefficients, as shown by the following values:

Bureau of Standards No.	Sillimanite, per cent	Calcline No. 14, per cent	Average coefficients		
			Room tem- perature to 200° C	200 to 400° C	400 to 540° C
S445.....	40	20	$3.4 \times 10^{-6}$	$4.2 \times 10^{-6}$	$4.8 \times 10^{-6}$
S479.....	44	16	10.9	6.6	7.8

In a porcelain containing 40 per cent sillimanite, an increase of 5 per cent in clay and a corresponding decrease in calcline No. 14, caused an increase in the coefficients, as shown by the following values:

Bureau of Standards No.	Clay, per cent	Calcline No. 14, per cent	Average coefficients		
			Room tem- perature to 200° C	200 to 400° C	400 to 540° C
S445.....	40	20	$3.4 \times 10^{-6}$	$4.2 \times 10^{-6}$	$4.8 \times 10^{-6}$
S480.....	45	15	8.9	5.0	5.1

Three specimens, S485, S487, and S488, containing from 71.5 to 80.1 per cent clay and about 9 per cent  $\text{Al}_2\text{O}_3$  had low coefficients of expansion ( $2.9$  to  $3.4 \times 10^{-6}$  between room temperature and  $200^\circ\text{C}$ , and  $3.8$  to  $4.0 \times 10^{-6}$  between  $200$  and  $400^\circ\text{C}$ ).

The porcelains, S489 to S501, inclusive, containing from 70 to 85 per cent clay, in addition to feldspar (10 to 23.5 per cent), flint (0 to 18.5 per cent), and Whiting (1.5 per cent), have low coefficients of expansion, which vary from  $2.9$  to  $6.1 \times 10^{-6}$  and from  $3.2$  to  $5.1 \times 10^{-6}$  for the ranges extending from room temperature to  $200^\circ\text{C}$  and from  $200^\circ$  to  $400^\circ\text{C}$ , respectively.

Most of the porcelains described above are products of this Bureau's Pittsburgh laboratory, from which additional information<sup>11</sup> relating to composition, baking, etc., may be secured.

<sup>11</sup> Bleining and Riddle, J. Am. Ceram. Soc., 2, 564; 1919.



## VI. PHENOL CONDENSATION PRODUCTS, ETC.

An extended study was made of these materials with a view to determining their applicability for use in instruments of high precision which may be subjected to temperature variations.

The accompanying representative figures are self-explanatory, and in general show the tendency of contraction at constant tem-

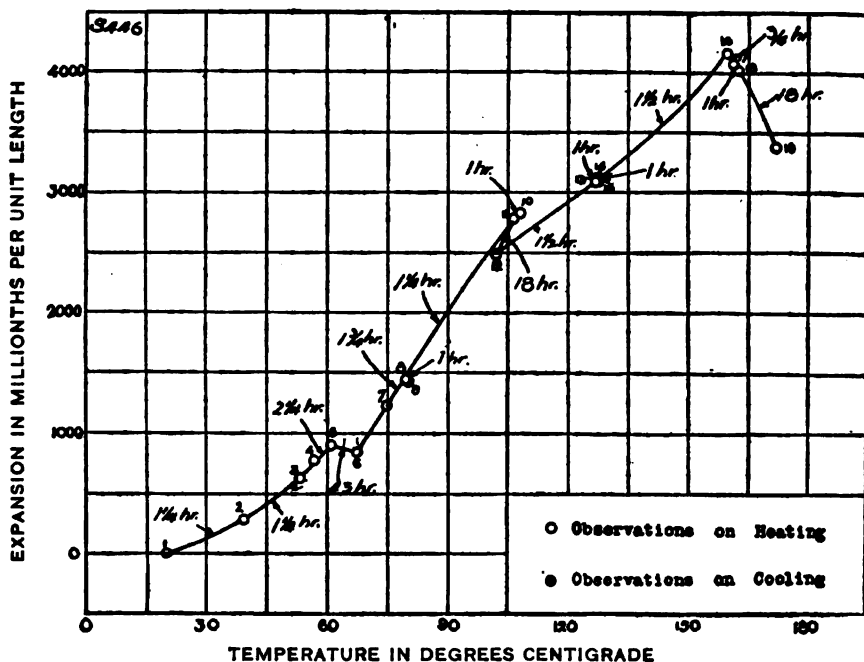


FIG. 9.—Expansion of bakelite-dilecto (black) S 446

perature (above 60° C). In most cases, after cooling to room temperature, these materials show a marked diminution in length. The numbers near the circles represent the order of the observations. The time elapsing between consecutive observations is indicated. When the time is less than one hour (except at critical temperatures) it is not indicated.

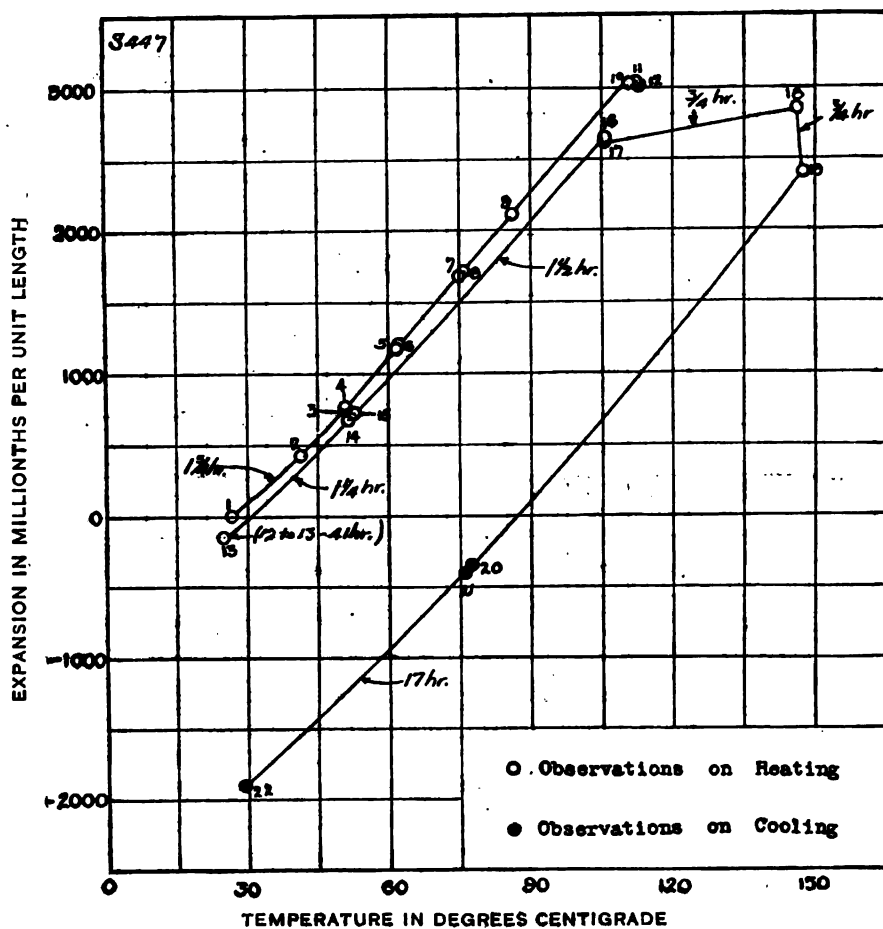


FIG. 10.—Expansion of bakelite-dilecto (black) S 447

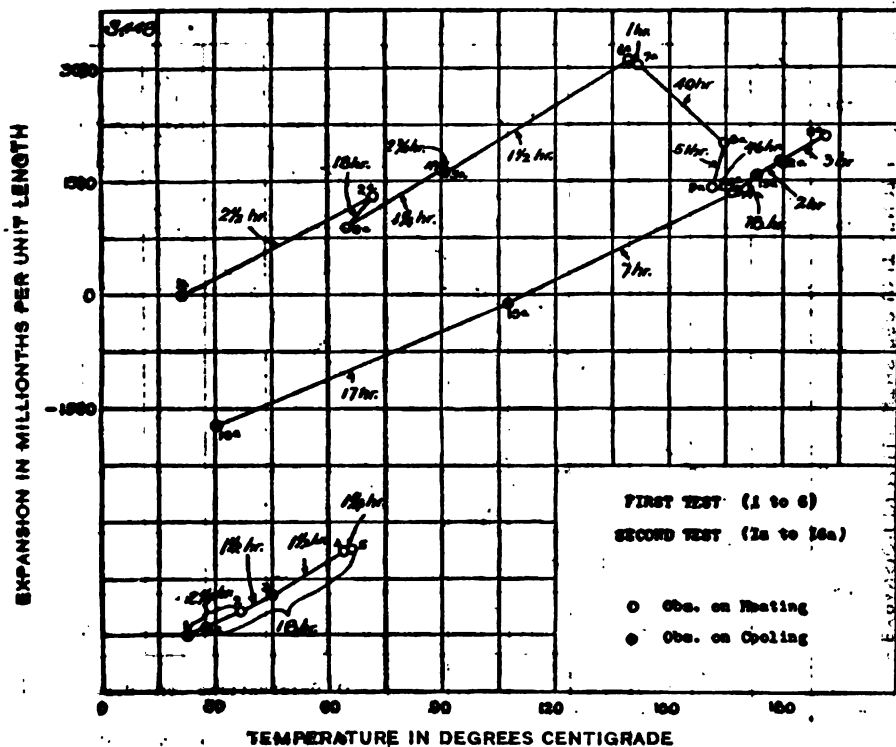


FIG. 11.—Expansion of bakelite-dielcto (natural XX grade) S 448

133855°—10—3

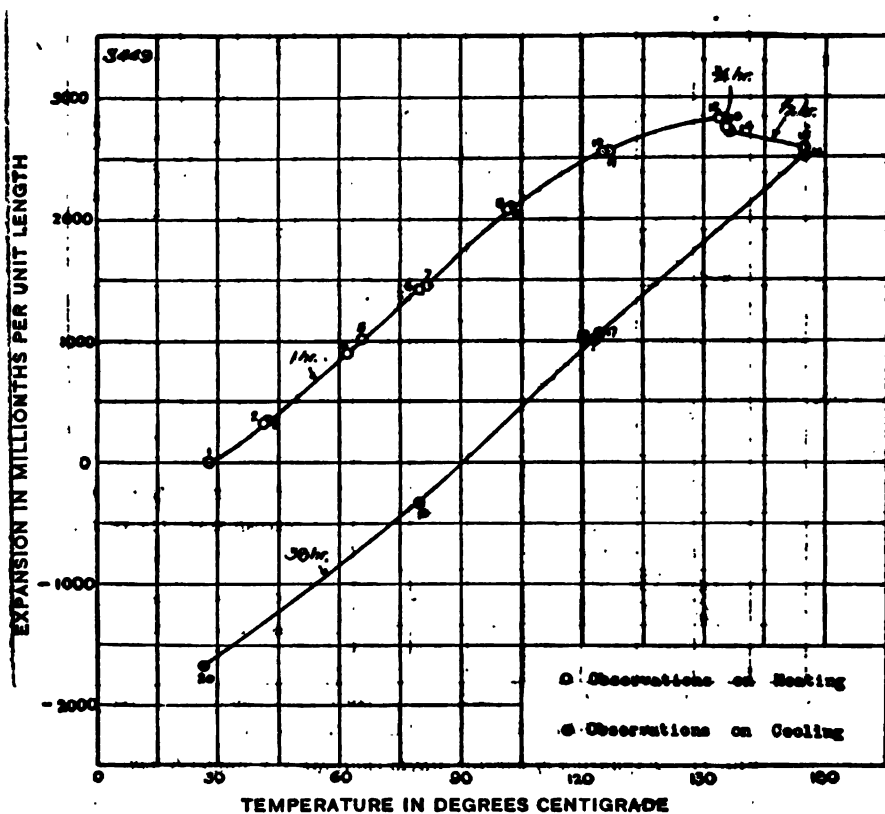


FIG. 12.—Expansion of bakelite-dilecto (natural XX grade) S 449

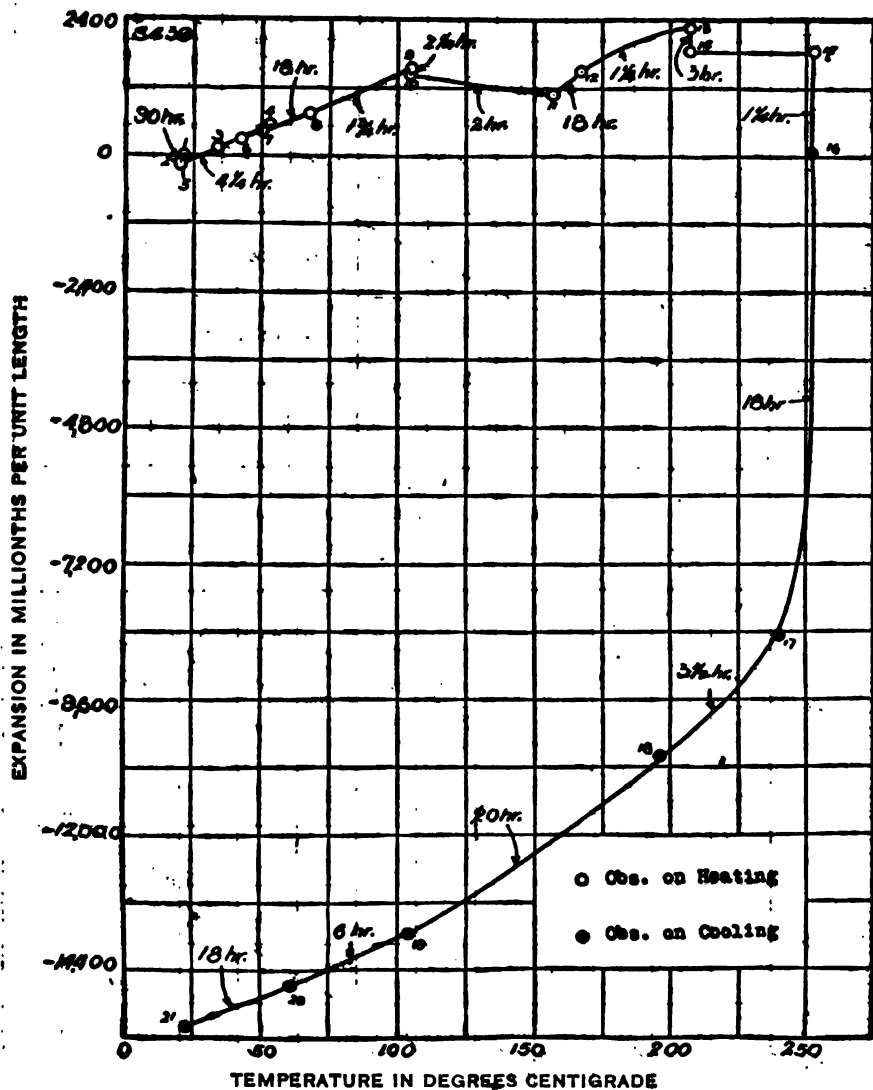


FIG. 13.—Expansion of bakelite-dielcto (XX grade) S 439

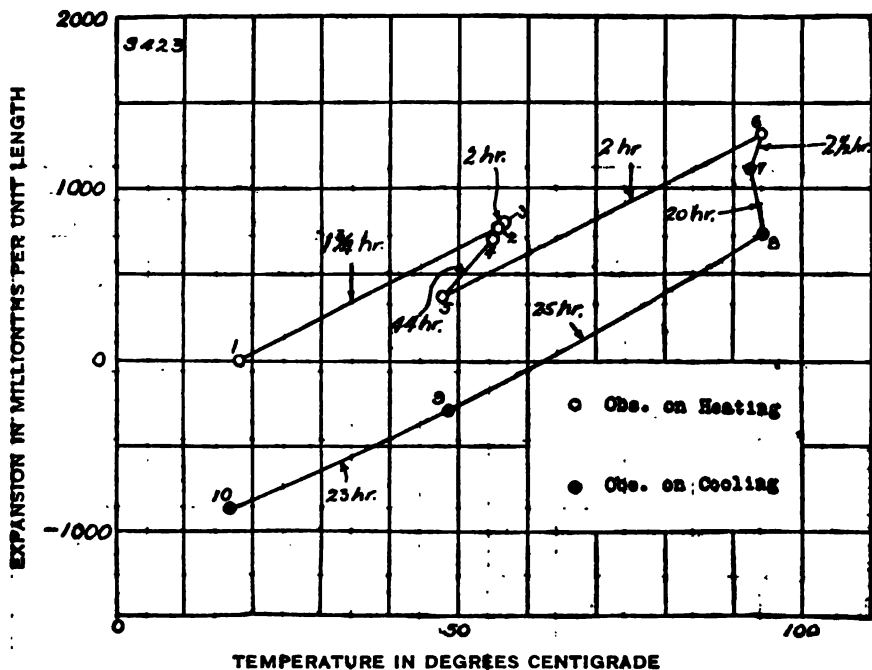


FIG. 14.—Expansion of condensite (No. 128) S 423, first test

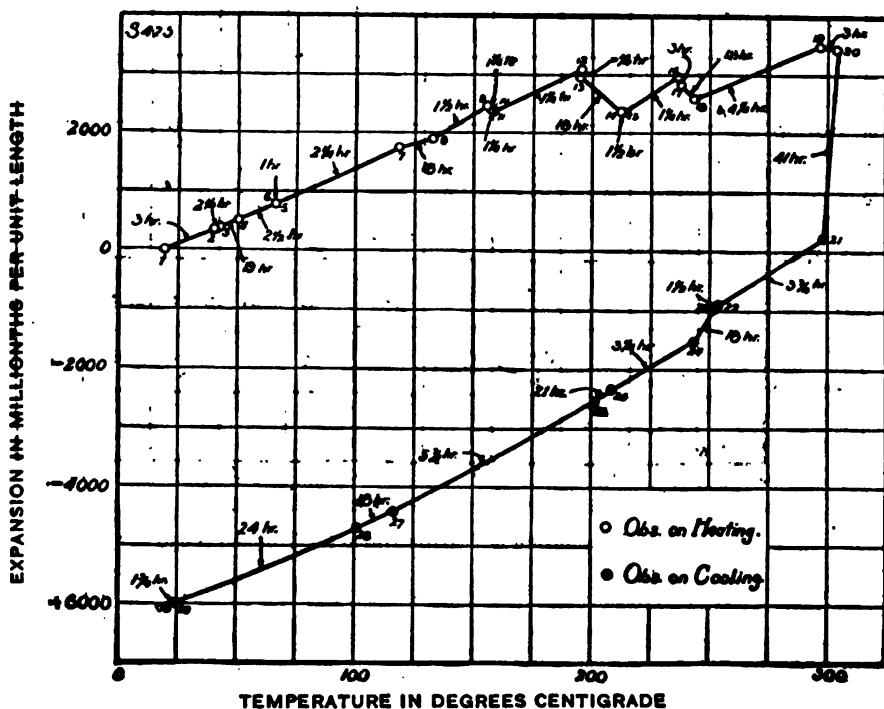


FIG. 15.—Expansion of condensite (No. 128) S 423, second test

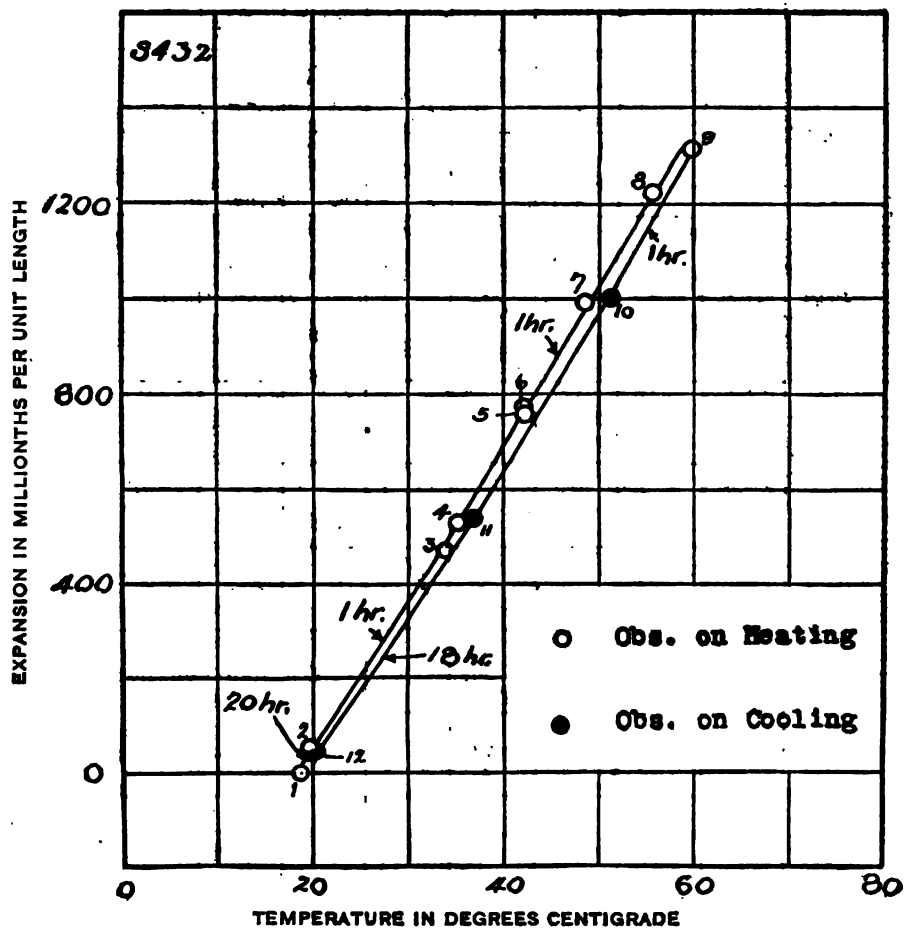


FIG. 16.—Expansion of formica (grade M) S 432

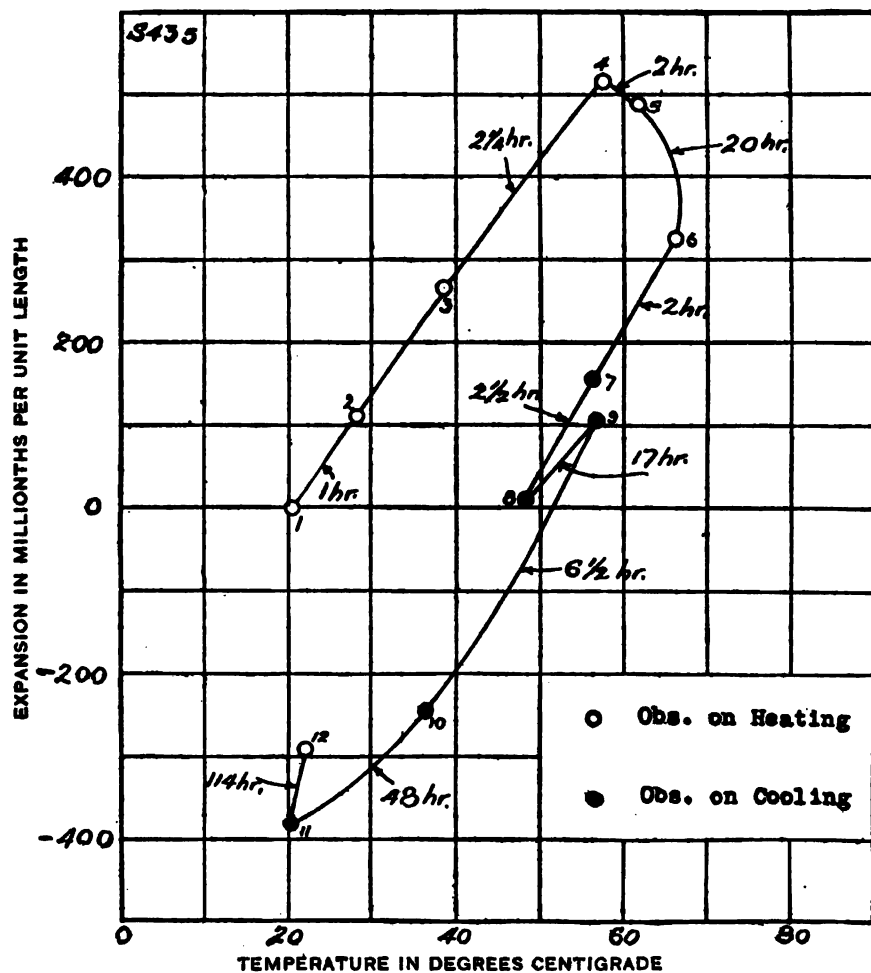


FIG. 17.—Expansion of formica (grade M) S 435



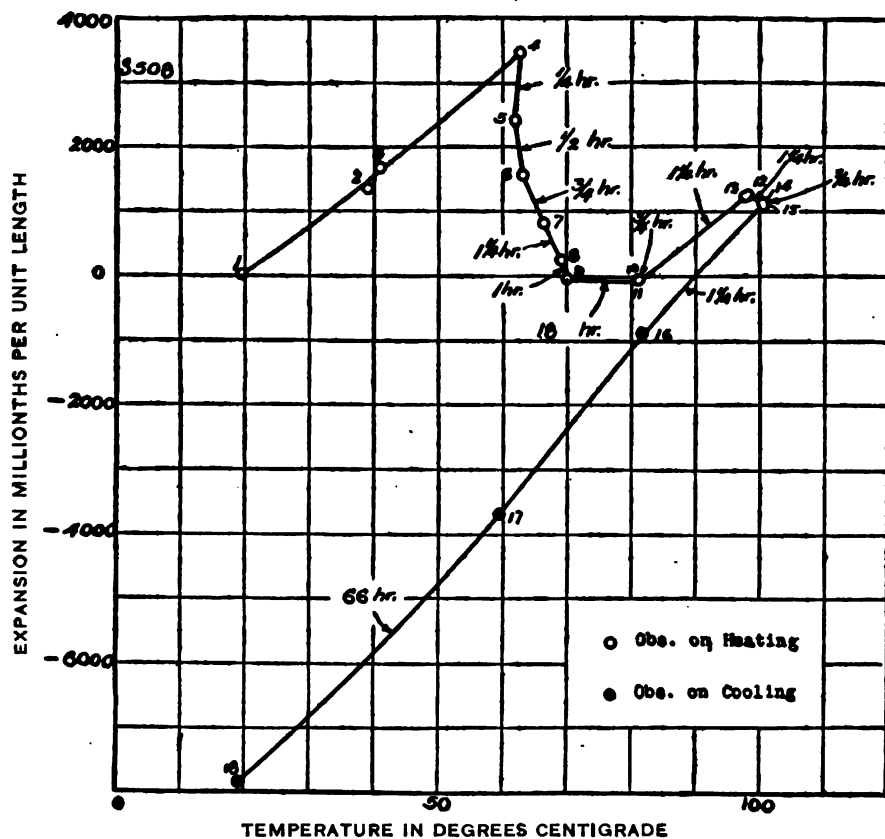


FIG. 18.—Expansion of hard rubber (S 508)

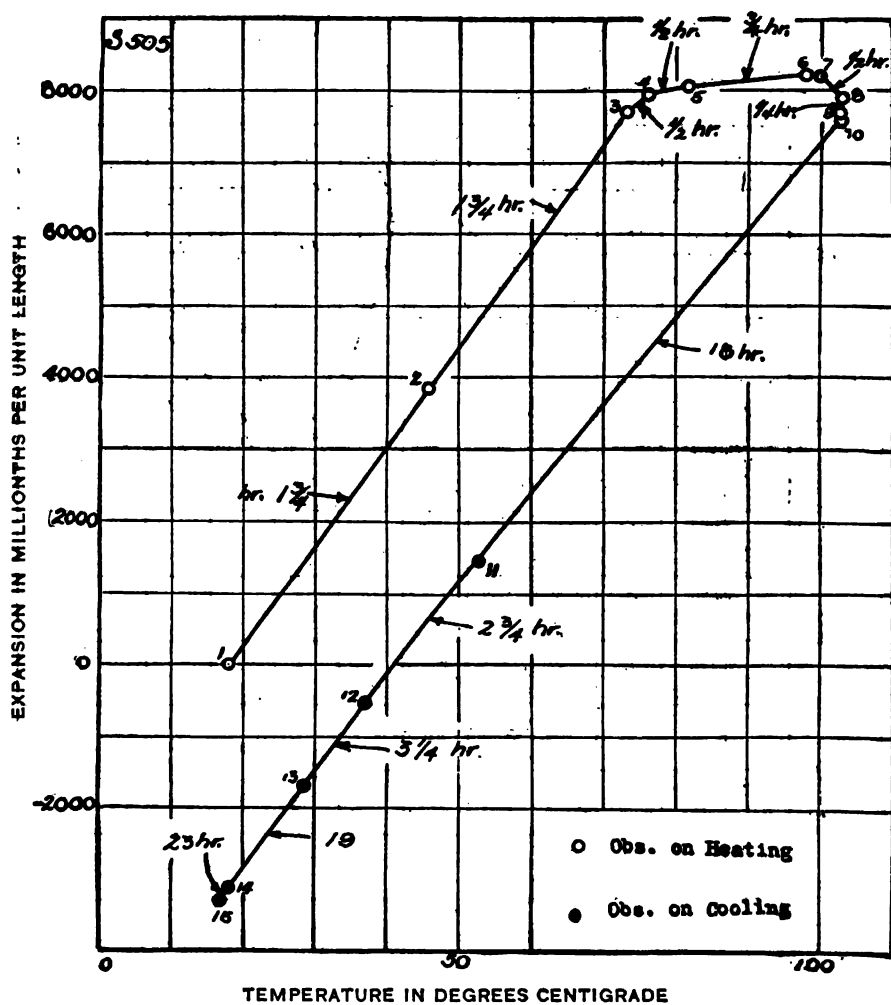


FIG. 19.—Expansion of celluloid (S 505) second heating

The coefficients of expansion obtained on various samples of these materials are summarized in the following table:

TABLE 4

Bureau of Standards No.	Material	Sample heated in—	Average coefficients $\times 10^6$
S446	Bakelite-difecto (black).....	Air furnace...	22 bet. 20 and 60° C
S447	.....do.....	Oil bath.....	36 bet. 30 and 100° C
S448	Bakelite-difecto (natural XX grade).....	Air furnace...	26 bet. 25 and 60° C
S449	.....do.....	Oil bath.....	28 bet. 30 and 100° C
S439	Bakelite-difecto (XX grade).....	Air furnace...	21 bet. 25 and 50° C
S440	Bakelite Micarta (32K grade).....	do.....	33 bet. 25 and 50° C
S441	Bakelite Micarta (323 grade).....	do.....	29 bet. 25 and 50° C
S451	Continental bakelite (bakelized canvas).....	do.....	(a)
S450	.....do.....	Oil bath.....	31 bet. 25 and 60° C
S422	Condensite (No. 100):		
	First test.....	Air furnace...	44 bet. 16 and 79° C
	Second test.....	do.....	40 bet. 20 and 60° C
S423	Condensite (No. 128):		
	First test.....	do.....	20 bet. 18 and 56° C
	Second test.....	do.....	17 bet. 20 and 100°
S424	Condensite (No. 5033E).....	do.....	27 bet. 20 and 80° C
S432	Formica (grade M) <sup>b</sup> .....	Oil bath.....	33 bet. 20 and 60° C
S438	.....do.....	Air furnace...	30 bet. 20 and 60° C
S434	.....do.....	Oil bath.....	20 bet. 20 and 60° C
S435	.....do.....	Air furnace...	14 bet. 20 and 60° C
S508	Hard rubber (red).....	do.....	80 bet. 20 and 60° C
S505	Celluloid (red).....	do.....	109 bet. 20 and 70° C
S481	Celluloid (slide rule).....	do.....	74 bet. 20 and 40° C

<sup>a</sup> Expansion very irregular.

<sup>b</sup> Nos. S432 and S433 were cut perpendicular to Nos. S434 and S435.

Most of these materials when kept at some constant temperature above 60° C shrink in length and lose weight (give off vapors). When the temperature of the material increases it expands, but when kept at a constant temperature above 60° C it contracts.

The following table gives the maximum temperatures to which the specimens were heated and the changes in weight and in length after the test. The plus (+) sign indicates a gain in weight or length and the minus (−) sign a diminution in weight or length

TABLE 5

Bureau of Standards No.	Material	Sample heated in—	Maximum temperature	Change in weight after test	Change in length after test
			° C	Per cent	Per cent
S446	Bakelite-dilecto (black) .....	Air furnace .....	172	- 6.3	-0.4
S447	.....do.....	Oil bath .....	147	- .1	- .2
S448	Bakelite-dilecto (natural XX grade) .....	Air furnace .....	191	- 2.8	- .2
S449	.....do.....	Oil bath .....	175	- .3	- .2
S439	Bakelite-dilecto (XX grade) <sup>a</sup> .....	Air furnace .....	253	-20.4	-1.5
S440	Bakelite Micarta (32X grade) .....	do .....	195	- 2.7	- .4
S441	Bakelite Micarta (323 grade) <sup>a</sup> .....	do .....	246	-27.6	-4.0
S451	Continental bakelite (bakelized canvas) .....	do .....	170	- 2.0	- .1
S450	.....do.....	Oil bath .....	160	+ .1	- .2
S422	Condensite (No. 100):				
	First test .....	Air furnace .....	79	.....	- .2
	Second test <sup>b</sup> .....	do .....	288	.....	-4.3
S423	Condensite (No. 128):				
	First test <sup>c</sup> .....	do .....	94	- .5	- .1
	Second test .....	do .....	304	- 4.0	- .6
S424	Condensite (No. 5053H) .....	do .....	124	- 2.3	- .3
S432	Formica (grade M) .....	Oil bath .....	60	+ .2	- .01
S433	.....do.....	Air furnace .....	79	- .6	- .14
S434	.....do.....	Oil bath .....	61	+ .2	.00
S435	.....do.....	Air furnace .....	66	- .3	- .03
S508	Hard rubber .....	do .....	100	- .1	- .8
S505	Celluloid (2 heatings) .....	do .....	108	- 1.1	-1.4

<sup>a</sup> After test, specimen was found warped, cracked on sides, and blistered on upper and lower surfaces.

<sup>b</sup> At 288°, specimen was contracting so rapidly that one end left support of the apparatus.

<sup>c</sup> After test 1, specimen kept in oven at 100° C. for several days. It showed a change in weight and in length of -0.6 per cent and -0.1 per cent, respectively.

From a study of the work on these materials it is evident that the length is a function of the temperature, medium in which the material is heated (air or oil), time, rapidity of heating or cooling, etc

From these experiments the conclusion may be drawn that delicate apparatus made from these materials or containing these materials as essential parts should not be heated above 60° C (140° F), if loss in weight and shrinkage or warpage are to be avoided.

The Bureau takes this opportunity of thanking the manufacturers of the above products for their cooperation in this research. Practically all of the above samples were given the Bureau by the respective manufacturers.

## VII. MARBLE AND LIMESTONE

This research<sup>12</sup> includes 10 grades of marble<sup>13</sup> selected from the quarries of Vermont, Tennessee, and Georgia, and one specimen of Indiana limestone. After heating, it was found that each showed an increase in length. This growth is roughly proportional to the maximum temperature, as is shown by S209 (Florentine blue), which was heated to 100° C, cooled to room temperature, then heated to 150°, and cooled to room temperature, and so on. Each cycle of increased temperature caused an additional increase in length. The dotted line represents how the material would have behaved if it had been heated directly to 300° C. (See S207.) Then after being cooled, it would have returned approximately to point 11, which represents a growth of more than 0.3 per cent. In other words, the growth is approximately the same, whether the specimen is heated by cycles or heated directly to the maximum temperature.

S198 (Pittsford Italian) and S285 (Appalachian gray) show the changes in length on two heatings and two coolings. It will be noticed that the growth after the second heating is less than that after the first heating. Repeated heatings tend to bring the marble to a constant or permanent state. The Vermont marble shows a larger growth than the Tennessee.

S296 (Silver gray) shows the changes in length at low temperatures. On cooling below room temperature, it is seen that the specimen expands, contrary to the usual behavior of most materials. The coefficient of expansion of this specimen on the first cooling was numerically (but opposite in sign) about the same as that of steel at room temperature. For the other marbles tested, however, the coefficients of expansion on cooling are quite small, as may be seen from Table 7. The peculiar phenomenon of minimum length is common to all the specimens tested. This point of minimum length is not constant for the different kinds of marble, and usually occurs below room temperature, in some instances as low as -20° C. Attention is directed to the slight permanent lengthening of specimens when passed through the cooling cycle.

<sup>12</sup> Parts of these data on marble were taken under the direction of L. W. Schad, formerly of this Bureau.

<sup>13</sup> Selected by D. W. Kessler, of this Bureau. For additional physical and chemical properties see Bureau of Standards Technologic Paper No. 123.

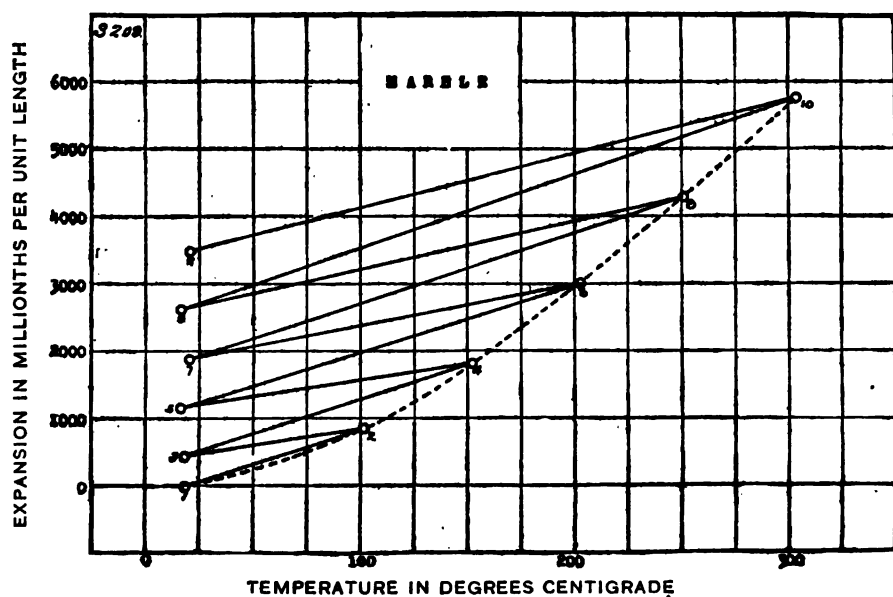


FIG. 20.—Expansion and growth of marble (S 209)

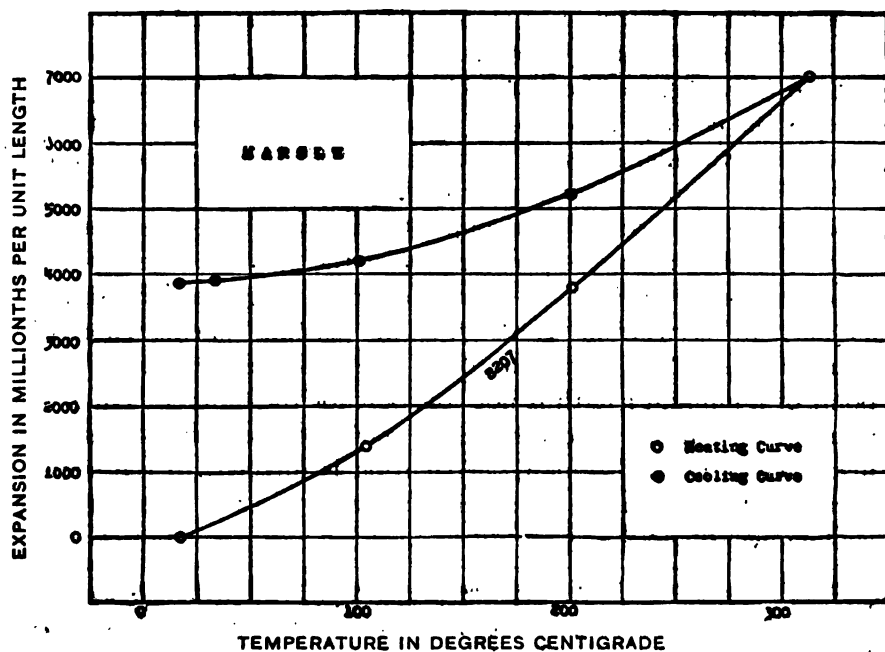


FIG. 21.—Expansion of marble. (S 207)

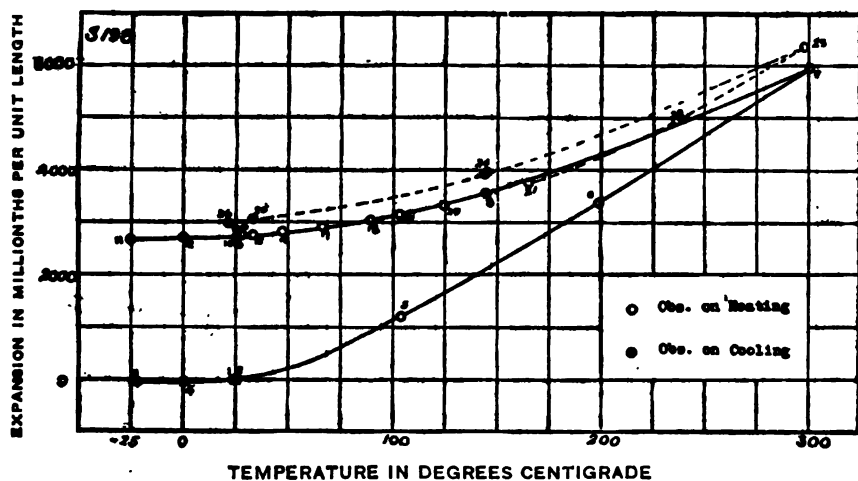


FIG. 22.—Expansion of marble (S 198)

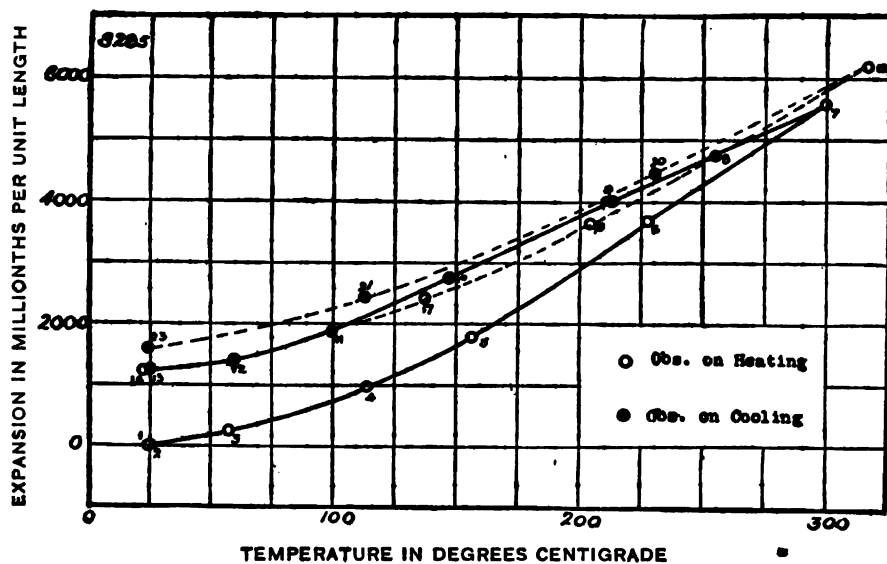


FIG. 23.—Expansion of marble (S 285)

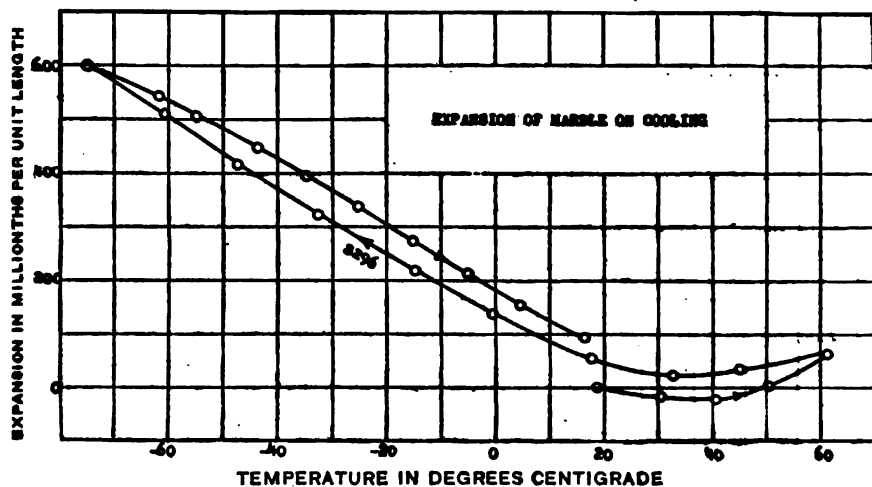


FIG. 24.—Expansion of marble at low temperature (S 206)

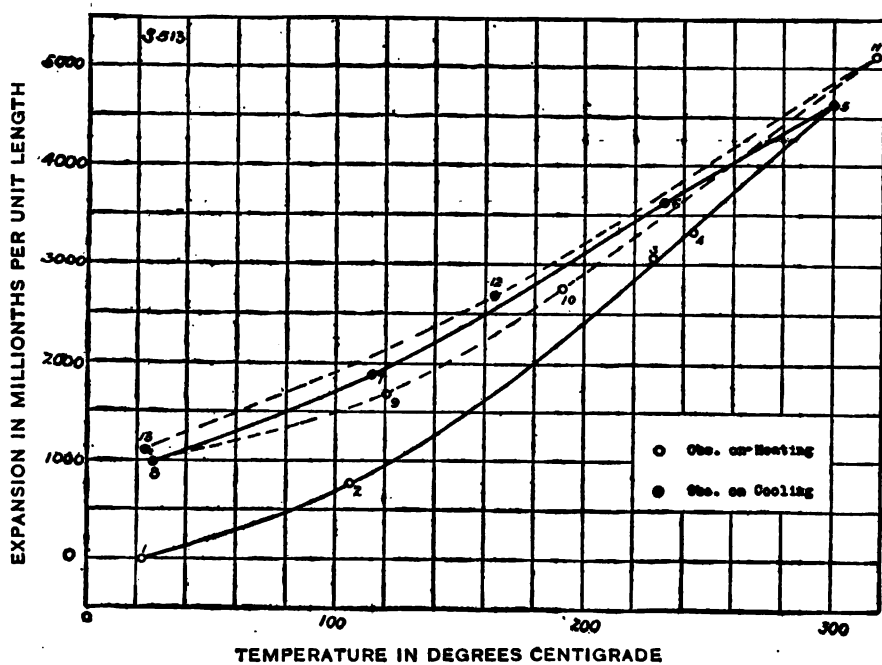


FIG. 25.—Expansion of limestone (S 513)



TABLE 6.—Average Coefficients Above Room Temperature

## HEATING

Num- ber	Name	Heated in—	20 to 65° C	25 to 100° C	100 to 200° C	200 to 300° C
S198	Pittsford Italian, 1 (Pittsford, Vt.)	Oil.....	.....	$14 \times 10^{-6}$	$23 \times 10^{-6}$	$25 \times 10^{-6}$
S207	Rutland blue, 1 (Rutland, Vt.)	do.....	.....	16	25	29
S208	Dorset gray (Dorset, Vt.)	do.....	$10 \times 10^{-6}$	.....	.....	.....
S209	Florentine blue, 1 (Florence, Vt.)	do.....	.....	10	.....	.....
S210	Riverside, 1 (Proctor, Vt.)	do.....	.....	13	.....	.....
S245	Appalachian gray, 1	Air.....	.....	10	22	27
S286	Appalachian gray, 1 (Asbury, Tenn.)	do.....	.....	10	20	27
S310	Rutland blue, 1 (Rutland, Vt.)	do.....	.....	15	23	28
S296	Silver gray, 1 (Tate, Ga.)	.....	$\alpha 1$	.....	.....	.....
S514	Hollister 1 (Florence, Vt.)	Air.....	.....	5	13	15
S513	Indiana limestone	do.....	.....	9	17	22

## COOLING

Num- ber.	Name	Heated in—	300 to 200° C	200 to 100° C	100 to 25° C	65 to 20° C
S198	Pittsford Italian, 1 (Pittsford, Vt.)	Oil.....	$17 \times 10^{-6}$	$11 \times 10^{-6}$	$6 \times 10^{-6}$	.....
S207	Rutland blue, 1 (Rutland, Vt.)	do.....	16	10	4	.....
S208	Dorset gray (Dorset, Vt.)	do.....	.....	.....	.....	$7 \times 10^{-6}$
S245	Appalachian gray, 1	Air.....	19	18	9	.....
S286	Appalachian gray, 1 (Asbury, Tenn.)	do.....	18	17	10	.....
S310	Rutland blue, 1 (Rutland, Vt.)	do.....	15	9	4	.....
S296	Silver gray, 1 (Tate, Ga.)	.....	.....	.....	.....	$\alpha 0.5$
S514	Vermont, 1	Air.....	7	3	0	.....
S513	Indiana limestone	do.....	15	14	10	.....

\* After cooling test.

TABLE 7.—Average Coefficients on Cooling Below Room Temperature

No.	Name	25 to 0° C	0 to -20° C	-20 to -40° C	-40 to -60° C	-60 to -80° C	-80 to -95° C
S283	Victoria pink 1 (Knoxville, Tenn.):						
	First test.....	$4 \times 10^{-6}$	$1 \times 10^{-6}$	.....	.....	.....	.....
	Second test.....	3	1	$-4 \times 10^{-6}$	$-4 \times 10^{-6}$	$-2 \times 10^{-6}$	.....
S287	Cumberland pink 1 (Meadow, Tenn.):						
	First test.....	4	1	- 3	- 3	- 2	$-1 \times 10^{-6}$
	Second test.....	2	0	- 2	- 2	.....	.....
S286	Silver gray, 1 (Tate, Ga.):						
	First test.....	-13	-10	-10	-10	-13	.....
	Second test.....	-4	- 6	- 6	- 7	.....	.....

Tables 6 and 7 give the coefficients of expansion of the various samples. The former table gives the values on the first heating; and the latter, on cooling below room temperature. The coefficients are higher on the first heating than on any subsequent heating. The symbols  $\perp$  and  $\parallel$  are used in the table to indicate the direction of the grain, the former representing specimens cut perpendicular to the bed and the latter parallel to the bed. Little, if any, difference in expansion can be detected; e. g., S285 and S286 are from the same block of marble, but cut in opposite directions to the grain.

The following table gives the principal constituents of the marbles investigated:

TABLE 8.—Chemical Analysis

Number <sup>a</sup>	CaO	CO <sub>2</sub>	MgO	Al <sub>2</sub> O <sub>3</sub>	Fe <sub>2</sub> O <sub>3</sub>	Loss on ignition	Insoluble in HCl
S198.....	54.49	43.65	1.33	0.20	0.05	43.81	0.44
S207.....	55.90	43.80	.27	.06	.02	43.90	.34
S208.....	55.49	43.46	.35	.06	.04	43.78	.70
S209.....	55.60	43.94	.44	.07	.01	43.86	.30
S210 <sup>b</sup> .....	55.40	43.76	.35	.10	.01	43.70	.24
S285.....	55.60	43.58	.07	.26	.06	43.89	.15
S286.....	55.60	43.58	.07	.26	.06	43.89	.15
S310.....	55.90	43.80	.27	.06	.02	43.90	.34
S296.....	55.00	43.18	.41	.09	.04	43.37	1.10
S514.....	55.54	43.75	.46	.09	.03	43.81	.24
S283.....	55.38	43.52	Trace	.14	.06	43.95	.08
S287.....	55.80	42.65	.06	.45	.16	43.68	.54

<sup>a</sup> Trace of SiO<sub>2</sub> in all samples except S514.

<sup>b</sup> SiO<sub>2</sub>=0.86.

The difference in the coefficients of the various marbles when compared with each other or the difference of some marbles when compared with certain metals, raises a question of the advisability of assembling these in structures, subject to large temperature variations, where close or accurate relative dimensions are to be maintained unless proper compensating facilities are provided.

Length measurements made two years after these tests indicate that the growth of marble after heating is permanent.

### VIII. SUMMARY

The present paper gives data on the thermal expansion of some of the more important insulating materials.

A short description of the method employed in making the observations is given. A photograph of one of the furnaces and the microscopes is shown in Fig. 1.

The dimensional changes incident to temperature variations have been measured. In most cases the expansions are too irregular to justify the use of the general quadratic equations.

The coefficients of 40 samples of various kinds of porcelain were found to vary over a wide range, from 1.6 to 19.6 millionths per unit length per degree centigrade. The coefficients of expansion are given in Table 2. The expansion curves of most materials are concave; but with porcelain three kinds of curves were found, namely, straight-line, concave, and convex curves. No marked set or permanent change in dimension due to the heat treatment was observed. Porcelains having low coefficients exhibited marked resistance to sudden temperature changes.

To understand the work done on the phenol condensation products (bakelite, condensite, formica, etc.), it is necessary to refer to the representative figures. (See p. 399.) The most striking peculiarity is the shrinkage and the loss in weight of most of these materials when subjected to temperatures above 60° C. A summary of the values obtained is given in Tables 4 and 5.

Marble and limestone showed a permanent growth when subjected to heat treatment. On cooling below room temperature, it was found that marble has a negative coefficient of expansion. The coefficients of expansion are given in Tables 6 and 7.

A knowledge of the thermal behavior of these materials is essential before assembling them in certain types of apparatus subjected to wide temperature variations.

We are indebted to John O. Eisinger for assistance in computing, etc.

WASHINGTON, June 30, 1919.





FEB 2 1920

DEPARTMENT OF COMMERCE



# SCIENTIFIC PAPERS

OF THE

# BUREAU OF STANDARDS

S. W. STRATTON, DIRECTOR

No. 353

## VARIATION IN DIRECTION OF PROPAGATION OF LONG ELECTRO-MAGNETIC WAVES

BY

Lieut. Commander A. HOYT TAYLOR, U. S. N. R. F.

*U. S. Naval Aircraft Radio Laboratory  
Bureau of Standards*

ISSUED NOVEMBER 29, 1919



PRICE, 5 CENTS

Sold only by the Superintendent of Documents, Government Printing Office  
Washington, D. C.

WASHINGTON  
GOVERNMENT PRINTING OFFICE

1919



# VARIATION IN DIRECTION OF PROPAGATION OF LONG ELECTROMAGNETIC WAVES

By Lieut. Commander A. Hoyt Taylor, U. S. N. R. F.

## CONTENTS

	Page
I. Introduction.....	419
II. Method of getting absolute minimum with direction finders.....	420
III. Comparison of maximum and minimum methods.....	421
IV. Variations in observed direction.....	424
V. Possible causes of the variation of apparent bearing.....	426
VI. Explanation of variations.....	427
VII. Conclusions.....	432

## I. INTRODUCTION

The investigation herein reported was an outcome of a study of the properties of an extremely long-wave direction-finder coil, with a view to determining the feasibility of using such long-wave direction finders on large aircraft on long flights, such as, for instance, a trans-Atlantic flight. The use of direction finders for aircraft having been carried to such a very satisfactory conclusion at the Naval Air Station, Hampton Roads, Va., on a wave length of 2500 m, it seemed highly desirable to ascertain if it might be possible to utilize for airplane direction-finder work existing high-power stations in Europe in case of extremely long flights. Since all of the trans-Atlantic stations which may be considered to be really high-power stations operate on continuous waves of lengths between 8000 and 20 000 m, it was decided to build a direction-finder coil at the Naval Aircraft Radio Laboratory, Bureau of Standards, of suitable dimensions for installation in a type F-5-L, type H-16, or type NC flying boat.

In the process of this study, comparison was made of the relative accuracy of settings obtainable with the two-coil maximum method and the usual single-coil minimum method. It was noticed that there were very considerable variations in the apparent bearing of the Naval Radio Station at New Brunswick, N. J.,

transmitting on 13 600 m, and a series of observations were undertaken with a view to determining whether these apparent variations of bearing were of local origin or not.

## II. METHOD OF GETTING ABSOLUTE MINIMUM WITH DIRECTION FINDERS

When a direction-finder coil is placed with its plane at right angles to the direction of propagation of electromagnetic waves, the resulting signal is not exactly zero, owing to the antenna effect in the coil and to other effects of less importance. This is because the antenna effect is approximately  $90^\circ$  out of phase with the true direction-finder effect. Settings of the coil are, therefore, not as sharp as they would be if an absolute minimum existed. In con-

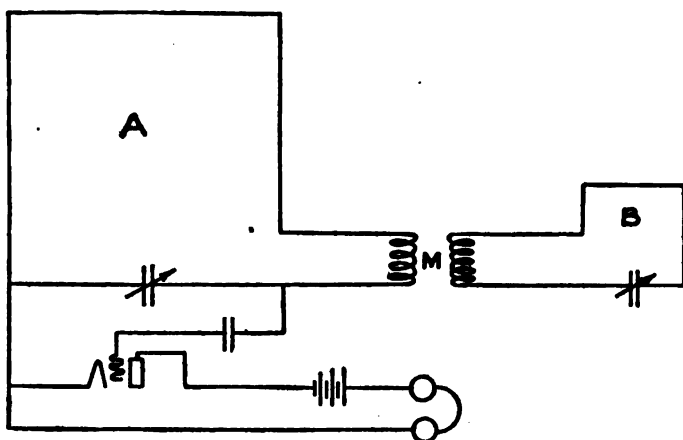


FIG. 1

nection with the long-wave direction-finder work undertaken at this laboratory, it has been found possible to produce an absolute minimum by introducing a small component of signal differing  $180^\circ$  in phase from the undesirable effect, by the method indicated below, to which Fig. 1 refers.

The apparatus consists of a long-wave direction finder, dimensions 35 by 30 inches, with three layers of litzendraht wire, each layer containing 40 turns, spaced three-sixteenths inch, represented by *A* in Fig. 1. A standard receiving circuit, without coupling, was used with two stages of amplification (not shown in Fig. 1). A small auxiliary coil *B* was very loosely coupled at *M* with the main coil and tuned to very nearly the same wave length. The method of operation is as follows: The auxiliary coil *B* is detuned, the coupling *M* made approximately zero, and the coil *A* rotated



to a minimum. It is found that upon New Brunswick and Annapolis on 13 600 and 16 700 m, respectively, the strength of signal varies between 600 and 2000, according to the degree of amplification used, and the best minimum which is obtainable without compensation is, roughly, 1 per cent of the maximum. When the best minimum has been obtained with coil *A*, coil *B* is placed at approximately right angles to *A*, so that it has no coupling with *A*. Coil *B* is then tuned to the same wave and the coupling at *M* is adjusted. Exact opposition in phase is obtained by a very slight detuning of the coil *B*. The operation is very simple and quickly made, a suitable adjustment of the coupling *M* making it possible to obtain an absolute minimum with coil *A*.

This method of obtaining an absolute minimum was reported to the direction-finder experts of the Philadelphia Navy Yard with the suggestion that they try it out on short-wave spark stations. Expert Radio Aid Stuart Ballentine made this matter the subject of a lengthy report, in which he concluded that while the method was accurate and capable of application at all wave lengths, it was not practicable on 600-m waves on account of the precision of adjustment required. The writer concurs fully with the Ballentine report. There are other methods more suitable for short-wave work.

### III. COMPARISON OF MAXIMUM AND MINIMUM METHODS

A telescope and scale were arranged in connection with a mirror on coil *A*, the distance between the mirror and scale being such that 3.5 cm on the scale equaled  $1^\circ$ . The accuracy with which settings may be duplicated is shown by the following table. Readings were taken on Annapolis on a very clear day. The readings extended over a period of about one and one-half hours. It was found best to choose the pitch of the signal rather high.

Readings in centimeters	Deviation from average in centimeters	Deviation from average in degrees
71.0	-0.1	-0.03
71.5	+ .4	+ .12
71.2	+ .1	+ .03
70.9	- .2	- .06
71.0	- .1	- .03
71.0	- .1	- .03
71.2	+ .1	+ .03
—		
Av. 71.1		

The following table is taken on the compensation wave of Annapolis:

Readings in centimeters	Deviation from average in centimeters	Deviation from average in degrees
70.5	+0.1	+0.29
69.5	.0	.0
69.1	— .04	— .12
68.6	— .09	— .26
70.3	+ .08	+ .23
69.4	— .01	— .03
69.0	— .05	— .14
69.7	+ .02	+ .06
69.5	.0	.0
69.5	.0	.0
—		
Av. 69.5		

It will be noted that the general average on the compensation wave differs by 1.6 cm, or 0.46°, from the general average on the main wave. This difference might have been due to a greater accuracy, which is evident on the settings of a higher-pitched note, the compensation wave being of lower pitch. On the other hand, it was suspected that the set was not quite as accurately compensated for minimum on the last series. The set was therefore thrown completely out of adjustment and the minimum balanced out, with special attention to the compensation wave of Annapolis and the following readings, in centimeters, obtained: 71.0, 71.0, 71.0, 71.0, and 70.9. The error here is too small to be calculable and the readings agree with those obtained upon the main wave.

In order to test the relative accuracy of the maximum method as used in airplanes with the ordinary minimum method, the following two series of readings were obtained on New Brunswick's 13 600 m wave.

#### MAXIMUM METHOD

Readings in centimeters	Deviation from average in centimeters	Deviation from average in degrees
20.5	+1.2	+0.34
17.0	— 2.3	— .66
20.0	+ .07	+ .20
19.8	+ .05	+ .14
—		
Av. 19.3		

## MINIMUM METHOD

18.0	-0.15	-0.43
20.6	+ .11	+ .31
21.0	+ .15	+ .43
17.8	- .22	- .68
20.5	+ .10	+ .29
—		
Av. 19.5		

It is evident that the accuracy of the setting that may be obtained with the maximum method is not much inferior to that obtained with the ordinary minimum method. It is known, however, that the maximum method requires a far higher degree of experience on the part of the operator, as is shown by the following table taken with the maximum method by another observer of less experience:

## MAXIMUM METHOD

Readings in centimeters	Deviation from average in centimeters	Deviation from average in degrees
22.0	+0.50	+0.14
25.0	+4.5	+1.29
20.0	-1.5	- .43
19.0	-2.5	- .71
—		
Av. 21.5		

## MINIMUM METHOD

21.5	-0.4	-0.11
22.5	+ .6	+ .17
23.0	+1.1	+ .31
20.5	-1.4	- .40
—		
Av. 21.9		

Undoubtedly when the compass is swung the use of the method of compensation of minimum herein outlined will give slightly different distortion curves than those obtained without compensation, but this should not involve any new difficulty as long as the distortion curve is known. It makes no difference what its shape is, provided none of the distortions are large.

The relative precision of the minimum method as compared with the maximum method depends largely on the character of disturbing interference and strays. In general, when the strays are very heavy and coming with nearly equal intensity from all points of the compass, the maximum method gives better results

than the minimum, because the minimum is badly obscured by the strays. But in the case of interfering signals this may not be true, as the interfering signal may come from such a direction that the reversal of the cross coil used in the maximum method may cause enormous difference in the intensity of the interference signal, thereby obscuring the setting obtainable with the maximum method in a manner even more detrimental to the results than the obscuration which would be obtained with the minimum method.

The maximum method was originated in England, and is called the Robinson method. It consists of the use of two direction-finder coils wound at right angles to each other and fixed on a common support so that they can be rotated together. One coil, known as the *A* coil, lies roughly in the plane of propagation of the observed signal, and the other coil, known as the *B* coil, is therefore roughly at right angles to it. If the *B* coil is exactly at right angles to the signal, reversal of the *B* coil will not change the strength of the received signal, which remains equal to the maximum signal obtainable with the *A* coil alone. The method of operation is to keep reversing the *B* coil until the signal seems to have the same intensity in either position of the reversing switch. The advantage of the maximum method lies in the fact that a loud signal can be heard at all times, and therefore the device can be used in an airplane where the minimum method would be impossible on account of engine noise. A device is usually provided whereby the *A* coil can be used alone in order to determine the general direction of the signal, said device consisting merely of suitable inductance or capacity to bring the tuning of the circuit to the same point where the *A* coil is cut in or cut out.

#### IV. VARIATIONS IN OBSERVED DIRECTION

Observations of the same character as those included in the preceding paragraph were then made from day to day for long periods of time during the day, and it was noticed that on signals from Annapolis, on 16 700 m, distant only 35 miles, the settings could be repeated from day to day and from hour to hour with fair accuracy, but that readings taken near the sunset hour and at night showed variations of a number of degrees. When observations were made on New Brunswick's wave of 13 600 m (distance from Washington to New Brunswick about 175 miles), very large deviations were frequently observed, as the following table, which constituted only a small share of the observations

actually taken, will show. A direct reading scale in degrees was attached to the rotating coil, as the deviations were so large that it was not necessary to use the mirror and scale to determine them. The degrees in the table are not true bearing, but rather of a purely arbitrary scale. Two days upon which the observations were taken were very foggy, being January 22 and 23, 1919.

ANNAPOLIS		ANNAPOLIS		NEW BRUNSWICK	
Time	Degrees direction- finder setting	Time	Degrees direction- finder setting	Time	Degrees direction- finder setting
Jan. 22:		7.35 p. m. ....	24.0	Jan. 22:	
12.00 m. ....	20.5	7.36 p. m. ....	23.0	11.27 a. m. ....	75.8
1.48 p. m. ....	23.9	7.40 p. m. ....	<sup>a</sup> 23.0	11.28 a. m. ....	75.8
1.49 p. m. ....	21.7	7.42 p. m. ....	24.0	11.30 a. m. ....	75.9
1.50 p. m. ....	21.5	7.43 p. m. ....	26.0	11.40 a. m. ....	75.9
1.53 p. m. ....	20.0	7.45 p. m. ....	27.0	12.01 p. m. ....	79.5
1.56 p. m. ....	21.0	7.46 p. m. ....	26.5	12.05 p. m. ....	80.0
1.57 p. m. ....	19.5	9.07 p. m. ....	25.5	12.10 p. m. ....	75.8
1.58 p. m. ....	19.0	9.10 p. m. ....	25.5	3.10 p. m. ....	70.9
2.00 p. m. ....	18.8	9.12 p. m. ....	23.5	3.12 p. m. ....	70.2
2.02 p. m. ....	19.5	9.13 p. m. ....	23.5	3.45 p. m. ....	75.0
2.26 p. m. ....	20.5	9.15 p. m. ....	23.5	4.47 p. m. ....	62.0
2.30 p. m. ....	20.0	9.25 p. m. ....	<sup>a</sup> 23.0	5.19 p. m. ....	66.9
2.46 p. m. ....	20.8	9.50 p. m. ....	<sup>a</sup> 26.0	7.05 p. m. ....	<sup>(b)</sup>
3.02 p. m. ....	23.0	9.54 p. m. ....	25.5	7.51 p. m. ....	66.5
3.04 p. m. ....	21.5	9.55 p. m. ....	25.5	7.55 p. m. ....	67.0
3.05 p. m. ....	21.0	Jan. 23:		7.57 p. m. ....	<sup>a</sup> 64.0
3.47 p. m. ....	20.0	2.07 p. m. ....	21.5	8.52 p. m. ....	68.0
3.52 p. m. ....	20.0	2.44 p. m. ....	19.7	8.55 p. m. ....	69.0
4.46 p. m. ....	24.6	2.52 p. m. ....	20.5	8.57 p. m. ....	72.0
5.04 p. m. ....	22.0	3.01 p. m. ....	20.2	8.58 p. m. ....	73.0
5.06 p. m. ....	21.5	3.07 p. m. ....	20.0	8.59 p. m. ....	72.0
5.07 p. m. ....	20.5	3.08 p. m. ....	19.5	9.00 p. m. ....	71.0
5.17 p. m. ....	20.0	3.08½ p. m. ....	20.5	9.01 p. m. ....	71.2
7.22 p. m. ....	26.0	3.09 p. m. ....	19.8	9.08 p. m. ....	71.5
7.25 p. m. ....	26.0	3.10 p. m. ....	19.7	Jan. 23:	
7.26 p. m. ....	26.2			3.41 p. m. ....	74.0
7.27 p. m. ....	26.5			4.14 p. m. ....	75.0
7.30 p. m. ....	<sup>a</sup> 26.5			4.26 p. m. ....	72.5
7.32 p. m. ....	27.0			5.02 p. m. ....	73.5
7.34 p. m. ....	25.0			5.03 p. m. ....	74.0

<sup>a</sup> Minimum very broad, unable to compensate.

<sup>b</sup> Minimum too broad for observation.

It will be seen that the maximum observed variation of the apparent direction of Annapolis is  $8.2^\circ$  and in the case of New Brunswick  $18^\circ$ . The maximum observed rate of change of apparent bearing in the case of Annapolis was  $2.2^\circ$  per minute and occurred at 1.48 p. m. on January 22. A number of cases occur where the variation on Annapolis is in the neighborhood of  $2^\circ$  per minute. In the case of New Brunswick the maximum observed

rate of change of bearing was  $1.5^{\circ}$  per minute, which was noted at 7.55 p. m. and 8.57 p. m. on January 22. Observations have, however, been made on New Brunswick showing much larger rates of change than those appearing in this table. Many of these early observations were discredited, as the results seemed to be so totally at variance with results obtained by the Navy Department on short-wave work that the whole matter was thought to be due to some peculiarity of the installation at this laboratory.

## V. POSSIBLE CAUSES OF THE VARIATION OF APPARENT BEARING

It having been suggested that the variation was due to some peculiarity of the method of compensated minimum outlined in this paper, a large number of observations were taken with the ordinary minimum method, and variations of exactly the same order of magnitude were discovered, although the accuracy of the settings was naturally not so great. The method of compensated minimum is not, therefore, responsible for any of these variations, but merely enables them to be detected more readily. A creeping variation may often be detected in the course of a few seconds, since the accuracy of settings with the new method is of the order of one-tenth of  $1^{\circ}$ .

The possibility of reradiation from local circuits and other antennas at the Bureau of Standards causing a shift in the apparent bearing was then considered. A number of observations were taken on four different evenings between 10 and 12 o'clock, between the 10th and 20th of December. An investigation showed that no antennae were being used at that time and that all electrical circuits were practically constant in this neighborhood. Even greater variations than those reported in this series were observed. Finally the antenna at the Naval Radio Aircraft Laboratory which terminates within 20 feet of the direction-finder coil was tuned to the wave length under observation. The following table shows the data obtained on Annapolis taken on January 23:

	Time	Setting
Without aerial tuned in .....	2.44 p. m. ....	19.7
With aerial .....	2.51 p. m. ....	19.5
Without aerial tuned in .....	2.52 p. m. ....	20.5
With aerial .....	2.53 p. m. ....	21.0
With aerial lead brought within 8 inches of coil .....	3.00 p. m. ....	24.0
Without aerial tuned in .....	3.01 p. m. ....	20.2

This table shows conclusively that the tuning in of the aerial produces no effect unless a lead from the aerial is brought within a few inches of the coil, and even with this greatly exaggerated case of reradiation it was only possible to rotate the apparent bearing through  $3.8^\circ$ . The change between 2.44 p. m. and 2.53 p. m. from 19.7 to 21.0 is merely what might be called the normal drift of the apparent bearing and can not be ascribed to the tuning in of the aerial.

## VI. EXPLANATION OF VARIATIONS

These severe tests of the effect of reradiation from antennas and other accidentally tuned circuits show that the changes dealt with in this paper are of an order of magnitude which can not be ascribed to local conditions at the Bureau of Standards. The writer has information that variations of this sort as high as  $20^\circ$  have been noted by British observers. The variations must therefore be ascribed to reflection and refraction effects and it is believed that they are fully in accord with the most modern notions of the manner of propagation of electromagnetic waves over the surface of the earth. These observations are therefore merely a confirmation of an already fairly well-known phenomena of reflection and refraction of electromagnetic waves from or through banks of more or less ionized layers of the atmosphere, clouds, fogs, etc. The result is that the receiving rectangle is influenced not only by the main wave which we may think of as coming in a straight line from the sending station, but by the numerous other waves coming by longer paths and converging on the receiving rectangle by virtue of their having suffered either partial reflection at various surfaces of different electrical constants or having passed through regions of such electrical constants as to produce what may be described, roughly, as prism or lens action.

It is evident that these reflected and refracted portions will arrive at the receiving rectangle from various directions and in various phases. They may be resolved into two component parts—those which have an electric vector in the plane of the receiving rectangle and those which have an electric vector at right angles to that plane. The latter will produce no effect, but the former may be still further subdivided into two electrical components—one in phase with the electric vector of the main wave and the other  $90^\circ$  out of phase with it. The latter is completely balanced out by the method of compensation employed.

Its effect is to produce a very broad minimum and in some cases was so great that it could not be fully compensated out with the degree of coupling available at the point *M* shown in Fig. 1. It will be noted from the observations taken after dark that such very broad minima were quite frequently encountered. The other component of the electric vector in plane with the coil and in phase with the main wave may be compensated by slightly rotating the coil so as to oppose their action on that of the main wave. These components are the ones that produce the shift in the apparent bearing. The fact that this shift is less noticeable on a near-by station like Annapolis than it is on a more distant station like New Brunswick is due to the main wave of a near-by station being so much stronger than these reflected and refracted components and also to the fact that over a short distance there are less opportunities for such reflection and refraction to occur.

It may be confidently expected that with greater distances more marked deviation of the apparent bearing will appear. At the same time an average of a large number of observations will probably give settings which will check up well enough with the true bearing. From what is already known of the erratic behavior of transmission in a fog, it is not surprising that abnormal variations were obtained on the two foggy days of January 22 and 23. Neither is it surprising that greater variations are experienced in the sunset period and after dark than are found on a clear day, since it is well known that all signals vary enormously in intensity during these periods. The following sunset series was obtained on February 8 on New Brunswick. It will be noted that at 5.30 p. m. it was impossible to tell from what direction New Brunswick's signals were coming and that between 5.22 and 5.38 p. m. a variation of 68° occurred.

## NEW BRUNSWICK

Time	Degrees direction- finder setting	Time	Degrees direction- finder setting
Feb. 8:		Feb. 8:	
5.18 p. m. ....	27.5	5.42 p. m. ....	67.0
5.20 p. m. ....	15.0	5.49 p. m. ....	84.0
5.22 p. m. ....		5.52 p. m. ....	83.2
5.30 p. m. ....	(a)	5.58 p. m. ....	77.8
5.38 p. m. ....	68.0		

a No minimum.



Observations taken during the same period on Annapolis showed the fluctuations indicated in the following table:

ANNAPOLIS

Time	Degrees direction- finder setting	Time	Degrees direction- finder setting
Feb. 8:		Feb. 8:	
4.08 p. m.....	19.9	5.35 p. m.....	23.8
4.10 p. m.....	19.5	5.37 p. m.....	23.8
4.18 p. m.....	21.5	5.44 p. m.....	21.0
5.06 p. m.....	25.3	5.45 p. m.....	21.0
5.14 p. m.....	25.0	5.55 p. m.....	19.0
5.24 p. m.....	18.0	5.56 p. m.....	18.8

A large number of observations have been taken on wave lengths of 4000, 9200, 9800, 10 000, 13 600, and 16 700 m. It was soon discovered that very large variations in bearing

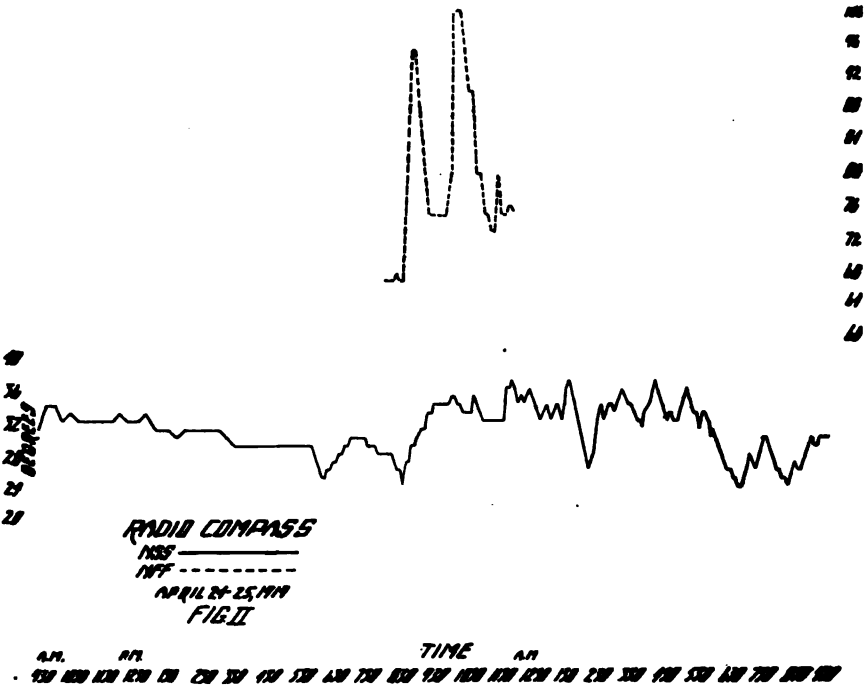
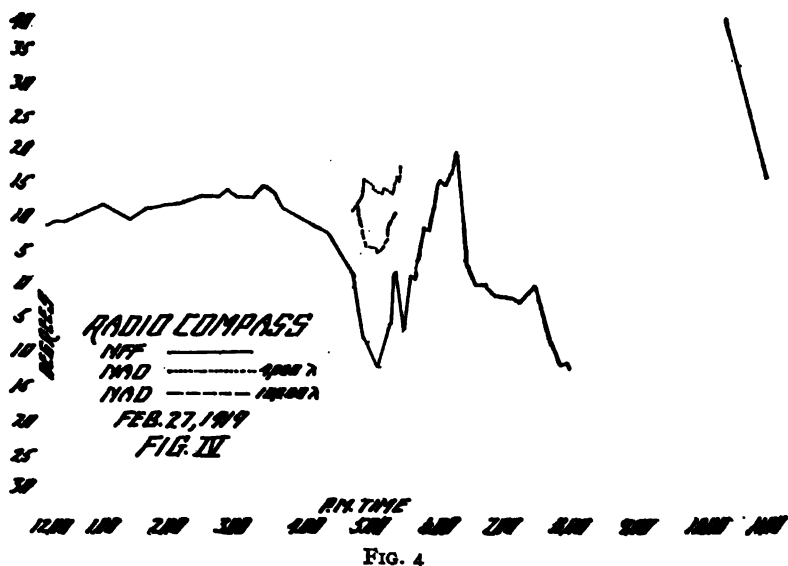
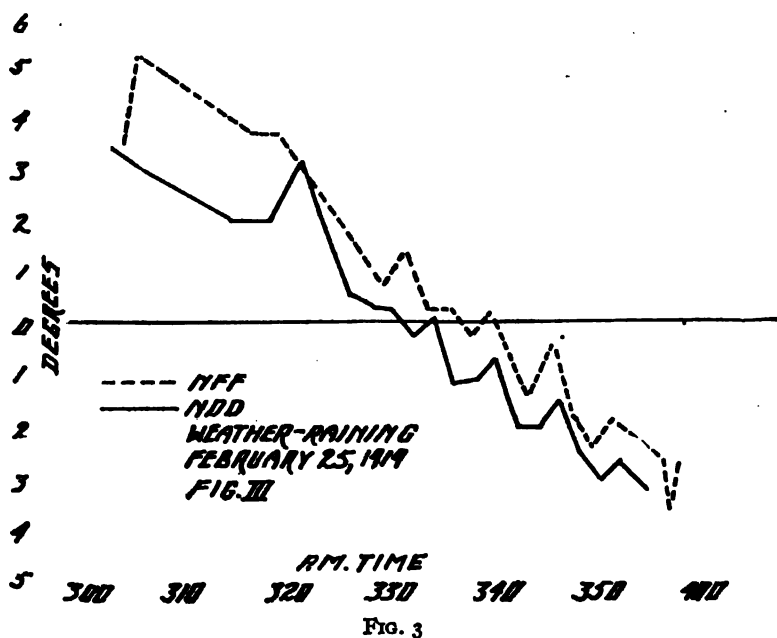


FIG. 2

occurred at night and that the variations, in general, were much worse on the long waves, the one exception to this being Annapolis on 16 700 m. This station is only 35 miles distant, which probably accounts for the small variations. Fig. 2 shows a typical variation

on Annapolis over 24-hour period. For purposes of comparison, some observations on New Brunswick on 13 600 m are shown on the same sheet. Unfortunately New Brunswick did not transmit



throughout the whole of this period. Fig. 3 shows the comparative variation during the afternoon of February 25, 1919, on New Brunswick on 13 600 m and Sayville on 9800 m. Fig. 4

shows comparative variations on New Brunswick on 13 600 m. and Boston during the sunset period on 10 000 and 4000 m. The shorter wave seemed to give the least variation. Fig. 5 shows a typical 24-hour series on New Brunswick. It will be noted that between 3 and 4 a. m. the bearing suffered a rotation of nearly  $90^\circ$ . A number of other observations have been taken on 4000 m, some of them showing very bad variations, but in general less than those obtained on longer waves. Work on continuous waves shorter than 4000 m is under way.

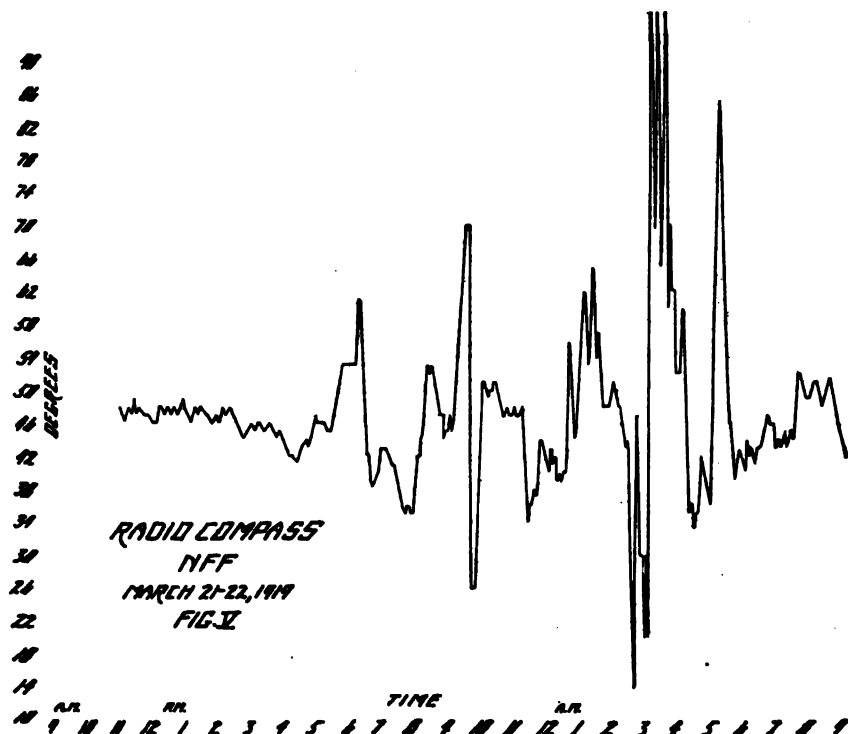


FIG. 5

Considerable work has also been done on spark signals, with particular attention to the wave lengths of 952, 1200, and 1512 m.

So far no serious variations have been observed on these waves, with the exception of a few series on Brooklyn and New York. Some of the Brooklyn observations at 1512 m taken on his press schedule between 9 and 9.40 p. m. have shown a shift as large as  $30^\circ$ . The variation of the observations on New York at 9.52 m is partly accounted for by the fact that several stations are operated under the same call letter. On the other hand, their angular

separation is only  $12^\circ$ , whereas the variations in bearing so far observed are more than double that amount.

Variations on short-spark waves are evidently quite rare and not nearly of as great magnitude as on the longer continuous waves. Results obtained at short-wave direction finder stations do not indicate variations of the order of magnitude herein described. This also is entirely understandable on the basis of the reflection and refraction idea. Short waves commonly used for direction-finding work between ship and shore are emitted by spark stations and have a considerable decrement. The wave train not being sustained, definite and persistent interference phenomena are no longer possible. Broadening of the minimum may, of course, be expected and in fact is noted in all direction-finder work. It has hitherto always been ascribed to what is called the antenna effect in the coil, but reflection and refraction may also be responsible for a considerable share of the broadening of the minimum. Moreover, with shorter waves the path differences from sender to receiver by the direct route as compared with routes via reflecting and refracting media will correspond to a much larger number of wave lengths. If the principal reflecting surfaces should prove to be the so-called Heaviside layer at very high altitudes, it is evident that there could be no definite arrangement of interference at the receiver as the latter end of one wave train might arrive at the same time as the beginning of the main wave train. The problem would, therefore, be much complicated by the fact that the wave train is not continuous and it is very difficult to see how any definite shift of wave front could result. The writer has no available data on continuous short wave stations, but ventures to suggest that there is far more likelihood of serious deviations in the apparent bearings of such stations occurring than in the cases of spark stations on similar wave lengths.

## VII. CONCLUSIONS

A method of compensating the minimum and increasing the accuracy of direction-finder settings has been worked out for long waves. It has been shown that deviations of the order of  $90^\circ$  may occur in the line of propagation of the resultant wave front in the case of very long continuous waves. The facts are fully in accord with the theory of propagation of such waves and the often expressed belief in the existence of media in the various layers of the earth's atmosphere which are capable of reflecting and refracting these waves.

The value of long continuous waves for direction-finder work is, in view of these results, very doubtful. It is, of course, possible that observations taken over a more uniform surface like the sea would not show such marked variations. Observations on long continuous waves would be of value only if the observations cover a considerable period of time and show no very wide fluctuations.

It has been indicated that these results do not cast doubt upon the accuracy of direction-finder observations carried out on short wave spark stations, since consecutive interference according to a definite plan would not be as likely to occur when a damped wave train is used. The few cases of variations of bearing on spark signals so far observed seem to be accompanied by marked fading effects, as would be expected if they are an interference phenomena. Also the minimum was broadened very considerably in many cases, but in a few cases a very bad fluctuation in bearing was accompanied by a sharpening rather than a broadening of the minimum.

No attempt in any of this work has been made to compensate local deflections so as to get the true bearing, as the writer was interested solely in time variations and not with local distortions.

It must be concluded that it would be very dangerous to use long continuous waves for direction-finder work at sea until it has been definitely proven that these variations do not occur when transmission is not partly or wholly overland. It is also very likely that even with spark stations it would not be wise to use longer waves than 1500 m until it has been definitely shown that such waves do not vary in overseas transmission as they occasionally do in overland transmission.

WASHINGTON, July 15, 1919.





DEPARTMENT OF COMMERCE

# SCIENTIFIC PAPERS

OF THE

# BUREAU OF STANDARDS

S. W. STRATTON, DIRECTOR

No. 354

## PRINCIPLES OF RADIO TRANSMISSION AND RECEPTION WITH ANTENNA AND COIL AERIALS

BY

J. H. DELLINGER, Physicist  
*Bureau of Standards*

ISSUED DECEMBER 11, 1919



PRICE, 10 CENTS

Sold only by the Superintendent of Documents, Government Printing Office  
Washington, D. C.

WASHINGTON  
GOVERNMENT PRINTING OFFICE  
1919





DEPARTMENT OF COMMERCE

---

**SCIENTIFIC PAPERS**  
OF THE  
**BUREAU OF STANDARDS**

S. W. STRATTON, DIRECTOR

---

No. 354

**PRINCIPLES OF RADIO TRANSMISSION  
AND RECEPTION WITH ANTENNA  
AND COIL AERIALS**

BY

J. H. DELLINGER, Physicist  
*Bureau of Standards*

---

ISSUED DECEMBER 11, 1919



PRICE, 10 CENTS

Sold only by the Superintendent of Documents, Government Printing Office  
Washington, D. C.

---

WASHINGTON  
GOVERNMENT PRINTING OFFICE  
1919



# PRINCIPLES OF RADIO TRANSMISSION AND RECEPTION WITH ANTENNA AND COIL AERIALS

By J. H. Dellinger

## CONTENTS

	Page
I. Introduction.....	435
II. Derivations of theoretical formulas.....	439
1. Radiation from an antenna.....	439
2. Radiation from a coil.....	443
3. Received current in an antenna.....	446
4. Received current in a coil.....	448
III. Discussion of theory of radiation and reception.....	452
1. Distinction between induction and radiation.....	452
2. Is radiation limited to high frequencies?.....	453
3. Equivalence of electrostatic and magnetic fields in a wave.....	454
4. What radiation is.....	455
IV. Comparison formulas.....	456
1. Derivation from theoretical formulas.....	456
2. Examples of comparison of coil and antenna.....	458
3. The condenser aerial.....	459
V. Transmission formulas.....	463
1. Statement of formulas.....	463
2. Discussion of transmission formulas.....	464
VI. Experimental verification of formulas.....	467
1. Principles of measurement of received current and voltage, with applications to design.....	467
2. Examples of measurements.....	477
3. Discussion of experiments.....	481
VII. Practical conclusions.....	488
1. Relative effectiveness of antennas and coil aerials.....	488
2. Principal formulas.....	489
3. Future research needed.....	492
VIII. Summary.....	493

## I. INTRODUCTION

In a radio transmitting or receiving set, either the condenser or the inductance coil is made of large dimensions. It is then called the aerial, and effects the transfer of power between the radio circuits and the ether. The coil aerial has the inherent advantage of serving as a direction finder and interference preventer, but is less effective quantitatively as a transmitting or

receiving device than the condenser type of aerial, commonly called the antenna. Both kinds of aerial are very simple in construction, consisting merely of one or more wires. An antenna consists of a wire or set of wires connected in parallel and constituting one plate of a condenser, the other plate being the ground beneath. The coil aerial is one or more turns of wire constituting a simple coil or loop. When an antenna is used its circuit is completed, in general, by placing an inductance coil in series with it and the ground; and when a coil aerial is used its circuit is completed by connecting a condenser across its terminals. The typical connections are shown in Figs. 1 and 2. The coil aerial requires no connection to ground at all.

The antenna is used when it is desired to communicate over as great a range as possible or to reduce the power required in the

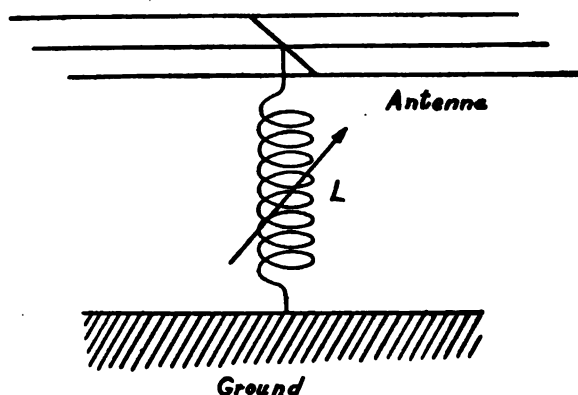


FIG. 1.—Simple antenna circuit

transmitting apparatus as much as possible. The coil is used when directional properties are particularly important. The coil radiates and receives electric waves better in the direction of its plane than in the direction of its axis, whereas the performance of an antenna is much more nearly independent of the direction of the waves. By arranging a coil so that it can be rotated it makes an excellent direction finder. When thus used on a ship or an airplane a coil aerial is sometimes called a radio compass. It has also been called a radio goniometer. By turning it so that its axis is parallel to the direction of propagation of the wave from some particular station, that wave is not received while waves from other directions are received. The coil may thus serve as an interference preventer. It is possible to attain some slight reduction of the effects of strays, commonly called static,

by using combinations of coil aerials. Submarine communication is more successful with coil aerials than with antennas, because the coil can be protected from the short-circuiting effect of the water while an antenna can not. The numerous advantages of the coil aerial make it highly important to know the relative sensitiveness or power of transmission of the device in comparison with the antenna. This publication provides the answer to this

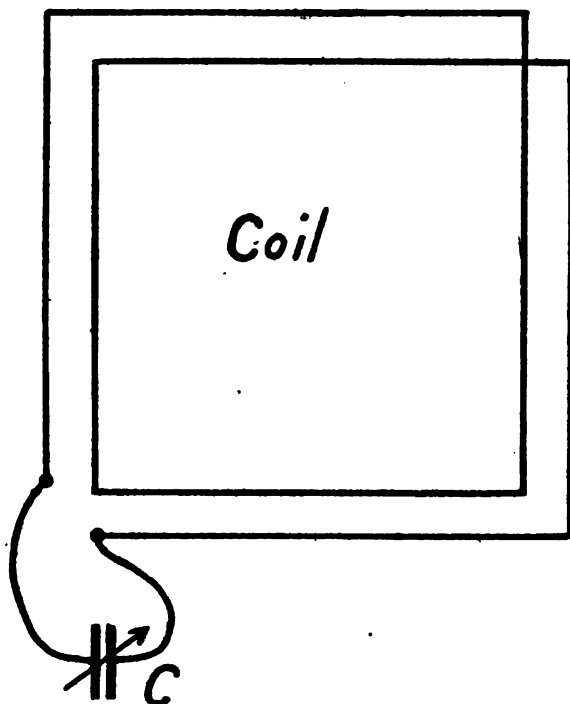


FIG. 2.—Simple coil aerial circuit

question and sets forth the theory of radiation and reception and the action of antenna and coil aerials. The relative effectiveness of any coil and antenna is given by formulas (32) to (36) in Section IV, 1, below. The uses of the coil as a direction finder, interference preventer, reducer of strays, and submarine aerial, are not treated in this article.

The most important question considered is the practical one: How far can communication be maintained by the use of any specified antennas or coil aerials? Formulas are developed by which the current received in an antenna or coil is calculated in terms of the current in a transmitting antenna or coil, resistance of receiving aerial circuit, the distance, wave length, and

dimensions of the aerials. The formulas have been found to be useful in the design of aerials and in the selection of an aerial for a particular kind of communication. They were worked out before there was any experimental information available to answer the question of the comparative quantitative value of the two kinds of aerials. Not much information on this has been obtained from experiment even yet (1919), but such experiments as have been made have substantiated the formulas. The work described in this paper was done in 1916 and 1917. The results were given in "Radio Transmission Formulas," a confidential paper of July, 1917, which was circulated in the Signal Corps and Navy. Publication was withheld during the war at the request of the Signal Corps. The formulas have also been given by the writer of the present paper on page 234 of "The Principles Underlying Radio Communication," 1918, Signal Corps Pamphlet No. 40, a book which can be purchased from the Superintendent of Documents, Government Printing Office, Washington, D. C.

*Historical.*—The coil aerial and the condenser type of aerial (antenna) both date back to the first experimenter with the electric waves that make radio telegraphy possible. H. Hertz, in 1888, used an open oscillator, which was the forerunner of the antenna, as his transmitting apparatus. For receiving he used a circle of wire, which was the first loop or coil aerial, and observed its directional properties.

The possibility of a loop or coil aerial as a transmitting device was discussed from the theoretical standpoint by G. F. Fitzgerald and later by J. A. Fleming (*Electrician*, vol. 59, pp. 936, 976, 1016; 1907). Fleming derived expressions for the radiated fields, using a curious theory in which the four sides of the coil were replaced by Hertzian doublets.

The use of a large loop or single-turn coil as an aerial in practical radio communication was described by G. Pickard (*Proceedings of the Wireless Institute of America*, vol. 1, May, 1, 1909). He discussed its properties both as a radiating and receiving aerial. He described its use as a direction finder, stating that he had determined directions with it to better than 1 degree.

In spite of this work and proposals by others, the antenna was used almost exclusively as the transmitting and receiving device until 1913. The use of the coil aerial received a great impetus by the publication of an article by F. Braun (*Jahrbuch der drahtlosen Telegraphie und Telephonie*, vol. 8, p. 1; 1914), on the Use

of Closed Circuits in Place of Open in Radio Telegraphy. He discussed the advantages of a coil aerial as a receiver and transmitter, both from the theoretical and the experimental standpoint.

Since 1913 there has been a great deal of development work done on coil aerials and they were extensively used in the war. The development of the coil aerial as a practical direction finder and receiving device was begun at the Bureau of Standards in 1915. Using electron tubes as the detecting apparatus, trans-Atlantic signals were received on a coil inside a room. Experiments with the coil as a transmitting device were carried out at the Bureau in 1917. Among the very few published treatments of development and use of the coil aerial are those in Bucher's textbook "Practical Wireless Telegraphy," 1917, p. 256; and "Radio Direction-Finding Apparatus," by A. S. Blatterman (Elec. World, vol. 73, p. 464; 1919). Most of the descriptions to date have been confidential reports of the military services of various countries.

The theoretical discussions by Fleming and Braun are cumbersome and needlessly complicated and the results are not well adapted to practical use. The present paper presents an original treatment that is relatively very simple, but none the less exact, and leads to conclusions that apply directly to practical work. This paper also points out a number of misconceptions that have existed, and endeavors to clear up some of the controversial points on the radiation of waves and the functioning of aerials.

## II. DERIVATIONS OF THEORETICAL FORMULAS

### 1. RADIATION FROM AN ANTENNA

Formula (8) below, giving the radiated magnetic field at a distance from an antenna, is a well-known formula. It has been given by various writers, and is the only one presented in this paper that requires any deep consideration of fundamental electromagnetic theory. The result is in fact implicit in Maxwell's classical treatise, "Electricity and Magnetism." The derivation given here is much more direct and brief than the others the author has seen, and is given only for that reason. The derivations of formula (10) and following ones are still simpler, and will be of more interest to most readers.

The units used in this paper are international electric units, the ordinary electric units based on the ohm, ampere, centimeter, and second. (See paper by the author on "International System

of Electric and Magnetic Units," Scientific Paper of the Bureau of Standards No. 292.) The unit of magnetic field intensity is the gilbert per cm, often called the cgs unit. The only exception to the use of units of the international system is in certain of the practical formulas where lengths are expressed in meters or miles where so stated.

In the following discussion is calculated the magnetic field intensity produced by a flat-top antenna, having electric current of uniform value throughout the length of the vertical portion. Most antennas in practice approximate closely this condition. The symbols used are:

$i$  = instantaneous current.

$I_0$  = maximum value of current.

$I$  = effective value of current.

$H_t$  = instantaneous value of magnetic field intensity.

$H_0$  = maximum value of magnetic field intensity.

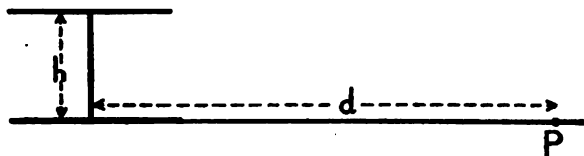


FIG. 3.—Calculation of magnetic field at a distance from an antenna

$H$  = effective value of magnetic field intensity.

$h$  = height of aerial.

$d$  = distance from sending aerial.

$\omega = 2\pi$  times frequency of the current.

$t$  = time.

$\lambda$  = wave length.

$c$  = velocity of electric waves =  $3 \times 10^{10}$  cm per second.

Subscripts (:) s = sending, r = receiving, a = antenna, c = coil.

In Fig. 3 the upper heavy line represents the flat top of the antenna and the lower heavy line the grounding area. Suppose a current is flowing having the instantaneous value  $i$  in the vertical portion. The magnetic field intensity at any point due to a varying current is different from that due to a steady current. Consequently the field can not be calculated in the same way that the magnetic field intensity of a straight wire is ordinarily calculated. When the current is varying, the magnetic field intensity is calculated by the aid of a quantity called the vector potential in such a way that the variation with time is taken into account. The instantaneous value of the vector potential of current in the



vertical conductor at a distance  $d$  in a plane perpendicular to the conductor, is

$$A = \frac{[i]h}{d} \quad (1)$$

where  $[i]$  indicates that for any time  $t$  the value of  $i$  is taken for the instant  $\left(t - \frac{d}{c}\right)$ .

Suppose the current in the antenna is a sine-wave alternating current,

$$i = I_0 \sin \omega t \quad (2)$$

$$\therefore [i] = I_0 \sin \omega \left(t - \frac{d}{c}\right)$$

$$A = \frac{h[i]}{d} = \frac{hI_0}{d} \sin \omega \left(t - \frac{d}{c}\right) \quad (3)$$

The magnetic field intensity is calculated from the vector potential by the general relation  $H_t = 0.1 \text{ curl } A$ , which for this simple case of a straight conductor becomes

$$H_t = \frac{1}{10} \frac{\partial A}{\partial d}, \quad (4)$$

the direction of  $H_t$  being perpendicular to the plane of  $h$  and  $d$ . From equation (3),

$$H_t = -\frac{h\omega I_0}{10cd} \cos \omega \left(t - \frac{d}{c}\right) - \frac{hI_0}{10d^2} \sin \omega \left(t - \frac{d}{c}\right) \quad (5)$$

This equation gives the magnetic field intensity at any point  $P$  at a distance  $d$  from the antenna. The second term represents the ordinary induction field associated with the current, while the first term is the radiation field. At a considerable distance the second term is negligible, because the second power of  $d$  occurs in the denominator. The first term then represents the magnetic field radiated from an antenna at the distance  $d$  from the antenna. The distance  $d$  is measured along the earth's surface, because the waves follow the curvature of the earth's surface instead of proceeding straight out into space. For a considerable distance from the antenna the maximum value of the magnetic field intensity during a cycle is therefore

$$H_0 = \frac{h\omega I_0}{10cd}$$

Expressing in terms of effective values,

$$H = \frac{h\omega I}{10cd} \quad (6)$$

Henceforth  $H$  means the radiated field, unless it is specifically stated to be the total field. The last equation may be expressed in terms of wave length instead of  $\omega$  by the relation

$$\frac{\omega}{c} = \frac{2\pi}{\lambda} \quad (7)$$

$$\therefore H = \frac{2\pi hI}{10\lambda d}$$

Using the subscript  $s$  to indicate that it is the sending rather than the receiving antenna which is considered,

$$H = \frac{2\pi h_s I_s}{10\lambda d} \quad (8)$$

This derivation follows the conceptions presented in the early pages of Lorentz, "The Theory of Electrons." It is equivalent to Hertz's intricate proof, but is more direct. The way in which the result is expressed here accords more closely with the physical ideas and with actual practice, being expressed in terms of current rather than electric charge, since it is current that is actually measured in an antenna, and the current, furthermore, is generally uniform in the vertical portion of the antenna.

Formula (8) gives the radiated magnetic field from a sending antenna at a distance  $d$  along the earth's surface. The units are the gilbert per cm for  $H$ , the ampere for  $I$ , and the centimeter for all lengths, as previously stated.

Undamped alternating current in the antenna was assumed. The same result, however, is obtained if the current is damped.

At very great distances from the sending aerial, the magnetic field is less than that calculated by formula (8), because of absorption of the power of the wave in the ground as it travels along. This may be taken into account by multiplying the right-hand member of (8) by a correction factor  $F_1$ . The value of this factor for daytime transmission over the ocean, derived from the experiments of L. W. Austin, Scientific Paper of the Bureau of Standards No. 159; 1911, is

$$F_1 = e^{-0.000047 \frac{d}{\sqrt{\lambda}}} \quad (9)$$

for  $d$  and  $\lambda$  both in meters. This correction ordinarily needs to be applied only when the distance is greater than 100 kilometers.

## 2. RADIATION FROM A COIL

It was formerly the belief that a coil could not radiate, because the current up one side of the coil (Fig. 4) produces a field equal and opposite to that down the other side of the coil. This is erroneous because the two equal fields are not exactly opposite. The phase between the two departs from  $180^\circ$  because of the finite time required for the field to be propagated from one side of the coil to the other. It is only along the axis of the coil that the calculated radiation is zero. The actual resultant field radiated from the coil may be deduced in either of two very simple ways, both of which are interesting from the physical

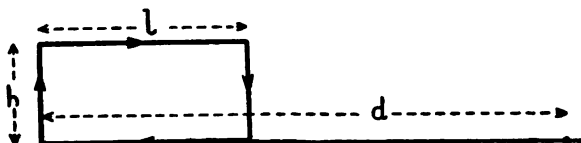


FIG. 4.—Calculation of magnetic field radiated from a coil

standpoint. The first deals with the instantaneous values of the magnetic field, and the second with the effective values.

The following additional symbols are used:

$l$  = horizontal length of coil aerial.

$N$  = number of turns of wire of coil aerial.

$\theta$  = phase angle between values of field intensity a distance  $l$  apart in the wave.

**First Deduction.**—Consider a rectangular coil of height  $h$  and horizontal length  $l$ . The magnetic field at a point  $P$  in the  $d$  direction is the resultant of the fields arising from current in the two vertical sides of the coil. The two horizontal sides contribute nothing, because a point at great distance  $d$  is practically equidistant from these two sides. The magnetic field due to any one of the vertical wires of the coil is calculated from equation (5) above. Neglecting the second term, because  $d$  is large, the instantaneous values of the magnetic field (Fig. 4) at the distances  $d$  and  $(d-l)$ , respectively, from the two vertical sides are

$$H_d = -\frac{hN\omega I_0}{10cd} \cos \omega \left( t - \frac{d}{c} \right)$$

$$H_{d-l} = +\frac{hN\omega I_0}{10c(d-l)} \cos \omega \left( t - \frac{d-l}{c} \right)$$

The resultant field  $H_t$  is the algebraic sum of these two, which becomes, since  $(d-l)$  is very nearly  $d$  when  $d$  is large,

$$H_t = -\frac{hN\omega I_0}{10\,cd} 2 \sin \omega \left( t - \frac{d-l}{c} \right) \sin \frac{\omega l}{2c}$$

The effective value of the resultant field is

$$H = \frac{2}{10} \frac{hN\omega I}{cd} \sin \frac{\omega l}{2c}$$

Using the relations

$$\frac{\omega}{c} = \frac{2\pi}{\lambda}$$

$$\text{and } \sin \frac{\omega l}{2c} = \frac{\omega l}{2c}$$

the latter holding when the angle is small; that is,  $l$  small compared with the wave length,

$$H = \frac{4\pi^2}{10} \frac{h_s l_s N_s I_s}{\lambda^2 d} \quad (10)$$

This is the radiated magnetic field from a sending coil aerial at a distance  $d$  along the earth's surface, the direction of  $d$  being the plane of the coil. The units are international units as stated under equation (8). The deduction assumes that the ground below the coil is not so good a conductor as to form an image of the coil. Thus the formula applies to a radiating coil in an airplane as well as to one at a ground or ship station.

The formula applies for either damped or undamped current  $I_s$  in the sending antenna. For very great distances the right-hand side of the formula must be multiplied by the distance correction factor  $F_1$  given in (9), the same as for a radiating antenna.

*Second Deduction.*—The radiated magnetic field due to one of the sides of the coil is  $N_s H_1$ , and from formula (8),

$$H_1 = \frac{2\pi}{10} \frac{h_s I_s}{\lambda d} \quad (11)$$

If the two vertical sides of the coil coincide, their magnetic fields would be equal and opposite, as shown by the lines  $OA$  and  $OB$ , Fig. 5. But since the two vertical sides are separated by the distance  $l$ , at any instant the field a distance  $d$  (Fig. 4) from the left side of the coil has traveled a distance  $l$  farther than the field from the right side. If then  $N_s H_1$  is the field due to the right side, the field at the same point due to the left side is shifted in phase from the position  $OB$  to  $OC$  in Fig. 5, where the angle  $\theta$  between them is the phase angle between the values of the field a distance  $l$  apart in the waves.

The distance  $l$  is the same fraction of the wave length that the angle  $\theta$  is of a complete cycle,  $2\pi$ . That is,

$$\frac{\theta}{2\pi} = \frac{l}{\lambda}$$

or 
$$\theta = 2\pi \frac{l}{\lambda} \quad (12)$$

The resultant of  $OA$  and  $OC$  is their vector sum,

$$H = N_s H_1 \sqrt{2(1 - \cos \theta)} \quad (13)$$

When  $\theta$  is small, i. e.,  $l$  small compared with the wave length,

$$\frac{H}{N_s H_1} = \sin \theta = \theta$$

$$\therefore H = N_s H_1 \theta \quad (14)$$

Thus the radiated magnetic field from a coil is equal to the field from one side of the coil multiplied by the phase angle  $\theta$  corresponding to the distance  $l$  between the sides of the coil.

From (14) and (11),

$$H = \frac{2\pi}{10} \frac{h_s N_s I_s}{\lambda d} \theta \quad (15)$$

This equation, together with (12), gives identically formula (10) obtained by the first deduction.

It was assumed in these deductions that the current was uniform throughout the coil. If the distributed capacity of the coil is appreciable the current in the coil will be different at different points. Thus the current in the middle may be greater than at the ends. This also may give rise to radiation from the coil, but is an entirely separate phenomenon from the phase angle between

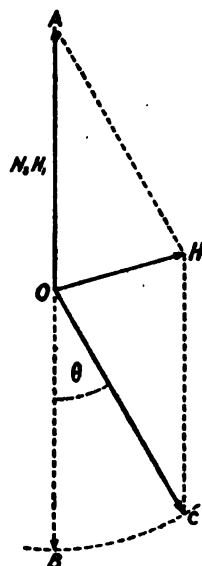


FIG. 5.—Phase relations of magnetic fields radiated from a coil

the two sides of the coil which has been discussed. This question of distributed capacity requires consideration particularly when coils are used having dimensions comparable with the wave length. The phenomenon is discussed further under "Antenna effect" in section VI, 3, below.

### 3. RECEIVED CURRENT IN AN ANTENNA

The current flowing in the receiving aerial circuit when the field intensity of the wave traversing the aerial is known can be calculated in several ways. An electromagnetic wave in space has both an electric and a magnetic field intensity which are at right angles to each other and to the direction of propagation of the wave. The two field intensities are related to each other by

$$\mathcal{E} = 300.H \quad (16)$$

where  $\mathcal{E}$  is in volts per cm and  $H$  in gilberts per cm.

The following additional symbols are used in this and the following section:

$\mathcal{E}$  = electric field intensity.

$E$  = electromotive force in receiving aerial.

$R$  = resistance of receiving aerial circuit.

$\phi$  = magnetic flux.

*First Deduction.*—The electromotive force, and thence the current, produced in an antenna may be calculated from the principle that relative motion of a magnetic field and a conductor create an electromotive force in the conductor whose value is

$$E = 10^{-9} h_r H c \quad (17)$$

when the directions of the field, the motion, and the conductor are mutually perpendicular,  $h_r$  being the length of the conductor and  $c$  the velocity of relative motion. This then gives the emf in an antenna of height  $h_r$ , produced by an electromagnetic wave having magnetic field intensity  $H$  and traveling with the velocity  $c$ .

In ordinary practice, the reactance in series with the antenna is varied to produce resonance to the frequency of the incoming wave, so that

$$I_r = \frac{E}{R} \quad (18)$$

Inserting for  $c$  its value,  $3 \times 10^{10}$  in equation (17),

$$I_r = 300. \frac{h_r H}{R} \quad (19)$$

This is the current in amperes received in a flat-top antenna, using the centimeter as the unit of length, with resistance of circuit in ohms, and the magnetic field intensity in gilberts per cm.

The received current is less than that given by the formula if the wave is damped, since an undamped alternating field was assumed in the discussion. For a damped field the emf acting on the aerial is similarly damped and equation (18) does not hold. Correct results are obtained by multiplying the right-hand side of formula (19) by the correction factor  $F$ , obtained as follows:

If the magnetic field intensity, and hence the emf, has the decrement  $\delta'$ , the effective current is not  $I_r$ , defined by (18), but another value which we shall call  $I_p$ . The value of  $I_p$  may be found by the aid of the generalized definition of decrement given in the author's paper, "The Measurement of Radio-Frequency Resistance, Phase Difference, and Decrement" (Proc. I. R. E., vol. 7, p. 27; Feb., 1919).

For decrements smaller than about 0.2, the logarithmic decrement is one-half the ratio of the average energy dissipated per cycle to the average energy associated with the current at the maximum of the cycle.

Taking the average power as  $\frac{E^2}{R}$ , the average energy dissipated per cycle  $= \frac{E^2}{fR}$ . The average energy associated with the current at the maximum of each cycle  $= L I_p^2$ . The energy-ratio definition of decrement just given applies to the sum of the decrements acting, viz, the decrement  $\delta'$  of the emf and the decrement  $\delta$  of the aerial circuit. The value of  $\delta$  is  $\frac{R}{2fL}$ . Applying the decrement definition:

$$\begin{aligned}\delta' + \delta &= \frac{\frac{E^2}{fR}}{2LI_p^2} \\ &= \frac{E^2 R}{2fLR^2 I_p^2} \\ &= \frac{E^2 \delta}{R^2 I_p^2} \\ I_p^2 &= \frac{E^2 \delta}{R^2 \delta' + \delta}\end{aligned}$$

From the relation,  $\frac{E^2}{R^2} = I_r^2$ ,

$$I_r = I_r \sqrt{\frac{\delta}{\delta' + \delta}} = I_r \sqrt{\frac{1}{1 + \frac{600 \cdot L \cdot \delta'}{R\lambda}}}$$

where  $L$  is in microhenries and  $\lambda$  is in meters.

This reduces to  $I_r = I_r$  when  $\delta'$  is small compared with  $\delta$ . Thus in the particular case of an undamped wave, where  $\delta' = 0$ , no correction is needed.

Correct results are obtained from equation (19) for any damped wave by multiplying its right-hand member by the correction factor  $F_2$ , given by

$$F_2 = \sqrt{\frac{1}{1 + \frac{600 \cdot L \cdot \delta'}{R\lambda}}} \quad (20)$$

where  $L$  is the inductance of the receiving aerial circuit in microhenries and  $\lambda$  is wave length in meters, and  $\delta'$  is the logarithmic decrement of the damped wave that is being received.

*Second Deduction.*—The same formula may be derived from entirely independent consideration of the electric field associated with the wave. The emf between two points in space is the product of the distance between them by the electric field intensity along the line joining them. Thus the emf produced in a flat-top antenna is  $\mathcal{E}$  times the height, the direction of  $\mathcal{E}$  being assumed to be vertical.

$$E = h_r \mathcal{E} \quad (21)$$

Inserting the value of  $\mathcal{E}$  from (16) and dividing by the resistance,

$$I_r = 300 \cdot \frac{h_r H}{R} \quad (22)$$

This is identically the same formula obtained above from consideration of the magnetic field.

#### 4. RECEIVED CURRENT IN A COIL

The current in a receiving coil aerial can be calculated in a number of different ways, all very simple and all giving the same result. The first conception which will be presented is simply that an emf is produced in the circuit by the time variation of magnetic flux through it.

The other modes of calculation involve the phase angle between the two vertical sides of the coil. The emf's acting in the two



vertical sides are exactly equal and oppose each other in producing a current around the circuit when the plane of the coil is perpendicular to the direction of propagation of the wave. When the coil is turned in any other direction, however, the emf's in the two sides are not exactly opposite in phase, because of the difference in time required for the field to be propagated to one side of the coil and to the other. The emf can be calculated either from the electric or the magnetic field, as in the discussion of received current in an antenna. The resultant emf can be found either from the algebraic sum of the instantaneous emf's in the two vertical sides or the vector sum of the effective emf's. These two methods are used in the second and third deductions, respectively, below.

The phase angle between the two sides of the coil is a very different thing from the phenomenon caused by the distributed capacity of the coil. It is assumed in the deductions given here that the current is uniform in all parts of the coil, which is not true when the distributed capacity is appreciable. Such capacity is large in coils of dimensions comparable with the wave length, and in such cases consideration must be given to the separate and additional phenomenon of distributed capacity.

*First Deduction.*—Assuming that the dimensions of the coil are small compared with the wave length, the magnetic field intensity is practically uniform throughout the coil. When the plane of the coil is parallel to the direction of propagation of the wave, the emf induced in the coil is

$$E = 10^{-8} \omega \phi$$

Now,

$$\phi = \mu h_r l_r N_r H$$

Since the permeability  $\mu = 1$ , and  $I_r = \frac{E}{R}$  because in ordinary practice the condenser in series with the coil aerial is adjusted to produce resonance with the frequency of the incoming wave,

$$\begin{aligned} I_r &= 10^{-8} \frac{\omega \phi}{R} = 10^{-8} \frac{\omega h_r l_r N_r H}{R} \\ &= 2\pi c 10^{-8} \frac{h_r l_r N_r H}{R \lambda} \\ I_r &= 600. \pi \frac{h_r l_r N_r H}{R \lambda} \end{aligned} \quad (23)$$

This is the current received in a rectangular coil aerial of  $N$  turns, with its plane parallel to the direction of propagation of the wave. The units are international units, as stated under formula (19). No image is assumed in the ground, so the formula applies not only to a receiving coil at a ground or ship station, but also to an airplane direction finder, provided the airplane is not flying at so great a height that the field of the wave is appreciably different from its value at the ground.

There are two correction factors that may need to be applied to this formula, both of which make the result smaller. If the wave is damped, the right-hand side of the formula should be multiplied by the decrement correction factor  $F_2$ , given by (20), the same as for a receiving antenna.

When the plane of coil is in some direction other than parallel to the direction of propagation of the wave, the right-hand side of formula (23) must be multiplied by the direction correction factor  $F_3$ , given by

$$F_3 = \cos \alpha \quad (24)$$

where  $\alpha$  is the angle between the direction of propagation of the wave and the plane of the coil.

*Second Deduction.*—The emf produced in any one of the vertical wires of the coil is given by either equation (17) or (21) above, deduced from considerations of the action of the magnetic and the electric field intensity, respectively. Each of these equations reduces to

$$E_1 = 300.h_r.H \quad (25)$$

The instantaneous emf in either of the two vertical sides of the coil is therefore

$$e' = 300.h_r.N_r.H_o \cos \omega t$$

The instantaneous emf in the other side of the coil is produced by the magnetic field existing in the wave a distance  $l$  away, when the plane of the coil is parallel to the direction of propagation of the wave. This emf  $e''$  has the same direction in space, but the opposite direction as far as producing current around the circuit is concerned.

$$e'' = -300.h_r.N_r.H_o \cos \omega \left( t - \frac{l}{c} \right)$$

The resultant emf in the circuit is the algebraic sum of these two,

$$e = 300.h_r.N_r.H_o 2 \sin \omega \left( t - \frac{l}{2c} \right) \sin \frac{\omega l}{2c}$$

The effective value of the resultant emf is

$$E = 600.h_r N_r H \sin \frac{\omega l}{2c}$$

Since when the angle is small, that is, when  $l$  is small compared with the wave length,

$$\sin \frac{\omega l}{2c} = \frac{\omega l}{2c} = \pi \frac{l}{\lambda}$$

$$E = 600.\pi \frac{h_r l N_r H}{\lambda} \quad (26)$$

Dividing by  $R$ , this gives the identical value of  $I_r$  obtained in (23) by the first mode of deduction.

*Third Deduction.*—The emf produced in one of the sides of the coil is  $N_r E_1$ , where from either equation (17) or (21) above; that is, from consideration of either the magnetic or the electric field intensity, respectively,

$$E_1 = 300.h_r H \quad (25)$$

If the two vertical sides of the coil coincided, the emf's produced in them would be equal and exactly neutralize each other, as shown by the lines  $OA$  and  $OB$ , Fig. 6. But since the two vertical sides are separated by the distance  $l$ , at any instant the field acting on one side of the coil has traveled a distance  $l$  farther than that acting on the other side. If, then,  $N_r E_1$  is the emf in one side of the coil, the emf in the other side is shifted in phase from the position  $OB$  to the position  $OC$  in Fig. 6, where the angle  $\phi$  between them is the phase angle between the values of the field a distance  $l$  apart in the wave.

The distance  $l$  is the same fraction of the wave length that the angle  $\theta$  is of a complete cycle,  $2\pi$ ; that is,

$$\frac{\theta}{2\pi} = \frac{l_r}{\lambda} \quad (27)$$

The resultant of  $OA$  and  $OC$  is their vector sum

$$E = N_r E_1 \sqrt{2(1 - \cos \theta)}. \quad (28)$$

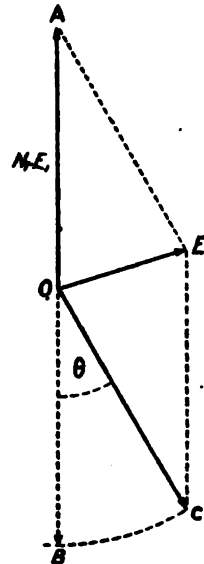


FIG. 6.—Phase relations of electromotive forces in receiving coil

When  $\theta$  is small; i. e.,  $l$  small compared with  $\lambda$

$$\frac{E}{N_r E_1} = \sin \theta \approx \theta$$

$$\therefore E = N_r E_1 \theta \quad (29)$$

From (25),

$$E = 300 \cdot h_r N_r H \theta \quad (30)$$

Thus the emf acting in the coil is equal to the emf in one side of the coil multiplied by the phase angle  $\theta$  corresponding to the distance  $l$  between the sides of the coil.

Equations (27) and (30) combined give (26), and by dividing by  $R$  formula (23) is obtained.

### III. DISCUSSION OF THEORY OF RADIATION AND RECEPTION

#### 1. DISTINCTION BETWEEN INDUCTION AND RADIATION

Certain fallacies which have appeared in textbooks and discussions arise from insufficient understanding of the difference between an induction field and a radiation field. Such fallacies are:

(a) An "open" circuit can radiate, while a "closed" circuit can not.

(b) There is no radiation from a circuit at low frequencies.

(c) Induction and radiation are the same phenomenon.

(d) The action of an antenna differs from that of a coil aerial in that the former is due to electrostatic fields and the latter to magnetic fields.

These fallacies will now be discussed. Fallacy *c* has led to the supposition that the radiation and reception of electric waves can be taught in terms of transformer action. It should not be difficult to separate the two ideas, for there is a definite and clear distinction between the field due to induction and that due to radiation. The total magnetic field at a distance  $d$  from a radiating antenna is, from equation (5)

$$H = \frac{2\pi}{10} \frac{h_r I_a}{\lambda d} + \frac{j}{10} \frac{h_r I_a}{d^2} \quad (31)$$

where  $j$  indicates that the two terms differ in phase by  $90^\circ$ . The first term represents the radiation field and the second term the induction field. The fact that one contains  $\lambda d$  in the denominator

while the other contains  $d^2$  makes them radically different in nature. This gives the mathematical distinction between induction and radiation. The physical difference is discussed in section 3 below. It should be noted that the word "induction" here means not the production of an emf, but the magnetic induction, or flux per  $\text{cm}^2$ , associated with a circuit.

The radiation field becomes relatively more important than the induction field as the distance  $d$  is increased or as the wave length is diminished (i. e., the frequency increased). The question whether radiation or induction predominates in any given case can be settled by calculation from the formula. Thus, the two fields are equal at a distance

$$d = \frac{\lambda}{2\pi}.$$

For points closer to the antenna than this the induction field predominates. For points farther away the radiation field predominates and the induction field falls off rapidly with distance and becomes negligible.

Certain early experiments in wireless signalling used true induction, e. g., the induction telegraphy of Preece and of Dolbear. When higher frequencies were used by later experimenters, signals of appreciable strength were received at distances of several wave lengths. These were genuine radiation signals, now commonly called radio.

## 2. IS RADIATION LIMITED TO HIGH FREQUENCIES?

The answer to this should be obvious from formulas (8) and (10). The radiated field does not become zero, no matter how great  $\lambda$  is. For alternating current of any frequency, no matter how low, radiation takes place from the circuit. To be sure, the radiation is greater the higher the frequency, so that high-frequency circuits are better radiators than low-frequency ones, and this is all the basis there is for the mistaken idea that only high-frequency circuits radiate.

This applies to radiation from a coil as well as from an antenna. It has sometimes been stated that a coil will not radiate, the statement being put in the form that only "open" circuits radiate. The statement is doubly faulty since electricity can flow only in closed circuits. The meaning intended by "open" circuit is a circuit containing a condenser of open form; that is, with two plates well separated. There are two misconceptions at the base of the belief that a "closed" circuit or one not containing a con-

denser would not radiate. In the first place, some have doubtless thought that waves would be started in the ether only by an electrostatic disturbance and thus could not be produced by a metallic closed circuit. Or, supposing it was understood that a magnetic disturbance in the ether would send out a wave just as readily as an electrostatic disturbance, it may have been thought that the radiation from one side of the circuit would be neutralized from that from the opposite side. As has already been shown in this paper the two disturbances do not exactly neutralize each other, on account of the finite time of propagation from one side of the circuit to the other, and the resultant is what gives rise to the radiation from a metallic closed circuit.

### 3. EQUIVALENCE OF ELECTROSTATIC AND MAGNETIC FIELDS IN A WAVE

The physical distinctions between radiation and induction are (a) the latter can be fixed in space and the former moves through space with the velocity of light, and (b) in the case of radiation the magnetic field is always accompanied by an electrostatic field of value

$$E = 300. H \quad (16)$$

and vice versa, whereas in the case of induction there is no fixed relation. It is of course true that whenever magnetic induction varies an electrostatic field is produced, and similarly whenever electrostatic induction varies a magnetic field is produced. But it is only in a radiated wave that these variations take place in such a way that one can be calculated from the other by the fixed relation (16). When there is a fixed electrostatic field associated with a circuit which does not vary, the magnetic field associated with this electrostatic field is zero, and vice versa.

In a radiated wave, then, the electrostatic and magnetic field are no longer independent phenomena but are strictly equivalent. Indeed, they are but two aspects of the same thing. Perhaps this will be clearer from the analogy of a sound wave. In a mechanical apparatus, elastic action and inertia act independently in various parts of the apparatus. In a sound wave, however, the effects of elastic action and inertia are mutual parts of a single phenomenon, the sound wave.

It is possible to separate the electrostatic and magnetic induction fields associated with a circuit by an arrangement of magnetic shields, but the electrostatic and magnetic fields in a radiated wave can not be separated. (This should not be confused with the sepa-

ration of antenna effect and coil effect discussed in Sec. VI, 3, below, under "Antenna Effect.")

In considering any effect of the electromagnetic wave, it is equally permissible to consider the electrostatic or the magnetic field associated with the wave. They are equivalent and lead to the same result. This has been amply demonstrated above in this paper. The current received in an antenna, calculated from the electrostatic field, was exactly the same as calculated from the magnetic field. The same agreement was found for the coil aerial. This disposes of the question whether the current produced in an antenna or a coil aerial is caused by the electrostatic or the magnetic field present in the wave or both.

Complete discussions of electromagnetic waves are given in such treatises as Maxwell, "Electricity and Magnetism," 1873; Jeans, "Electricity and Magnetism," 1907; Lorentz, "The Theory of Electrons," 1909.

#### 4. WHAT RADIATION IS

It has been shown that radiation differs from induction by a definitely calculable amount, that either kind of circuit radiates at any frequency, that there are both an electrostatic and a magnetic field present in every wave, having a constant ratio, and that any effect of the wave may be considered as due either to the electrostatic or the magnetic field of the wave.

Radiation is the moving disturbance of the ether, the energy associated with which does not return to the radiator.

This conception leads to more correct ideas than are current on the mechanism of radiation from an antenna and permits explanation of the radiation from a coil aerial, which is not covered at all by the usual explanations of radiation in textbooks. Such explanations have led to the impression that the radiation largely depends on the form of the electrostatic lines of force which are present at the edges of the radiator. It might thus be supposed that in a flat-top antenna or a condenser aerial the current in the central portions of the condenser was not effective in causing radiation while only that which spread into the surrounding space from the edges was effective. This appears incorrect. If it were correct, the builders of long flat-top antennas must have wasted a great deal of wire. All of the dielectric current sends a moving disturbance out into the ether. The portion of the energy associated with this disturbance that does not return to the radiator is that connected with the first term of equation (31). In this

term the total antenna current appears. The radiation is the moving disturbance caused by the whole of the current which the antenna makes flow in the dielectric.

The ordinary treatment of the mechanism of radiation from an antenna is misleading also, because it deals with radiation at the fundamental wave length. In practice antennas are usually loaded. The radiation depends in no degree whatsoever on the value or location of any of the field lines attached to the aerial, but only on the variation of the lines. And *all* the lines when varying give rise to radiation. Thus the stationary field is given by the second term of formula (31), the first is the radiation term, and they are independent.

#### IV. COMPARISON FORMULAS

##### 1. DERIVATION FROM THEORETICAL FORMULAS

Formulas are here derived to answer the practical question of how far a given coil will send or receive in comparison with a given antenna. The formulas also answer such questions as the length of a coil aerial required to give a particular ratio of performance of coil and antenna.

The ratio of the magnetic field radiated from a coil to that from an antenna, for a given sending current, distance, wave length, and height, is obtained from equation (13). The ratio of the distance from a coil to that from an antenna, at which a given magnetic field is produced, is the same as the ratio of the magnetic field produced by a coil to that produced by an antenna at a given distance. Either ratio is, therefore, given by the following expression, which assumes the same current  $I_s$ , wave length  $\lambda$ , and height  $h_s$ , for the coil and the antenna.

$$\frac{d_o}{d_a} = N_s \sqrt{2 (1 - \cos \theta)}$$

Inserting the value of  $\theta$  and neglecting the subscript  $s$ ,

$$\frac{d_o}{d_a} = N \sqrt{2 \left( 1 - \cos 2\pi \frac{l}{\lambda} \right)} \quad (32)$$

When the length of the coil  $l$  is small compared to  $\lambda$  (i. e., for most practical purposes, less than  $0.1 \lambda$ ), this simplifies to

$$\frac{d_o}{d_a} = 6.28 N \frac{l}{\lambda} \quad (33)$$



This could have been deduced directly from (8) and (10). The expression is similarly deduced for comparison of the distances obtained with a coil and an antenna of different heights,

$$\frac{d_o}{d_a} = 6.28 N \frac{l}{\lambda} \frac{h_o}{h_a} \quad (34)$$

The length of a coil required to give a particular ratio of performance to an antenna is given by solving these formulas for  $l$ . From (32),

$$l = \frac{\lambda}{2\pi} \cos^{-1} \left( 1 - \frac{1}{2N^2} \left[ \frac{d_o}{d_a} \right]^2 \right) \quad (35)$$

When the length of the coil is small compared to  $\lambda$ , the simpler formula suffices,

$$l = 0.16 \frac{\lambda}{N} \frac{d_o}{d_a} \quad (36)$$

The relative distances at which an antenna or a coil will receive a given wave are given by the same identical expressions that have just been deduced for sending aerials. Thus formula (32) may be deduced from (28) and (33) from (19) and (23). They give the ratio of the distance from the source at which a given emf will be produced in a coil aerial to that in an antenna, assuming the same height  $h_r$  and wave length  $\lambda$  for the coil and the antenna. They also give the ratio of the emf produced in a coil to that in an antenna for a given value of magnetic field intensity, or the ratio of currents when the resistances and other quantities are the same in coil and antenna. Equations (34), (35), and (36) similarly hold for receiving as well as sending aerials. For comparison of current in a coil and an antenna of different resistances as well as different heights

$$\frac{d_o}{d_a} = 6.28 N \frac{l}{\lambda} \frac{h_o}{h_a} \frac{R_a}{R_o} \quad (37)$$

The relative distances of transmission between two coil aerials and between two antennas, for a given sending current, is similarly found from equations (8), (10), (19), and (23). The ratio of received current for coils and antennas the same distance apart is given by the same formula, which assumes the same sending current  $I_s$  and wave length  $\lambda$  for the pair of coils as for the pair of antennas.

$$\frac{d_{oc}}{d_{ac}} = 39.5 \frac{I_{s,r} N_s N_r}{\lambda^2} \frac{(h_s h_r)_o}{(h_s h_r)_a} \frac{R_a}{R_o} \quad (38)$$

All of these formulas assume that the decrement correction factor  $F_d$  is the same for coil and antenna in all cases. If waves of differing decrement are used, apply the factor  $F_d$  as stated in connection with (20). If the plane of the coil considered is not parallel to the direction of propagation of the wave, apply the factor,  $\cos \alpha$ , as stated in connection with (24).

## 2. EXAMPLES OF COMPARISON OF COIL AND ANTENNA

What is the length of the coil, either as sender or receiver, equivalent to an antenna of the same height? The answer is given by (36). For  $\frac{d_o}{d_a} = 1$ ,

$$l = 0.160 \frac{\lambda}{N} \quad (39)$$

This is the correct length except for a single-turn coil. When  $N = 1$  the more exact formula (35) must be used. This gives, for the equivalent coil,

$$l = \frac{1}{6} \lambda$$

Thus a single-turn coil of length  $\frac{1}{6}$  the wave length is equivalent to an antenna of the same height. For a coil of 8 turns, however, the length of the coil equivalent to an antenna of the same height is, from (39), 0.02 of the wave length.

When the length of the coil is small compared with the wave length—that is, as already stated, when  $l$  is less than about  $0.1 \lambda$ —the performance ratio is given by (33). For a length greater than  $0.1 \lambda$ , however, the more accurate formula (32) must be used. Thus, when the length is exactly  $\frac{1}{6}$  of a wave length, from (32),

$$\frac{d_o}{d_a} = N$$

Thus any coil of length  $\frac{1}{6}$  the wave length is equivalent to an antenna of  $N$  times the height of the coil. When the length of the coil is one-quarter wave length, similarly

$$\frac{d_o}{d_a} = \sqrt{2} N$$

For a coil of length equal to one-half the wave length,

$$\frac{d_o}{d_a} = 2 N$$

This is the maximum or best performance for a coil aerial. If the length is increased beyond one-half wave length, the performance ratio decreases, and at  $l = \lambda$  it is equal to 0 just the same as for  $l = 0$ .

These values of the performance ratio of a coil aerial are obvious from Fig. 5 or 6.

These comparisons all apply to either transmitting or receiving aerials. They assume, however, in the case of a transmitting antenna or coil, that the same current flows, and, when applied to receiving aerials, that the resistance is the same, in either coil or antenna. As a matter of fact, however, it is easy to secure a considerably lower resistance in a coil aerial circuit than in an antenna circuit. This is taken account of by the factor  $\frac{R_a}{R_c}$  as in (37) and (38). The difference in current in a transmitting coil and antenna is taken account of by multiplying the right-hand members of (32) and (33) by the ratio of the sending currents  $\frac{I_o}{I_a}$ . On this account a coil is sometimes a more effective radiating or receiving device than an antenna of considerably greater dimensions.

The comparison formulas and conclusions drawn from them are subject to the same errors as the transmission formulas, as discussed in Section V, 2, below.

### 3. THE CONDENSER AERIAL

Since the dimensions of a coil aerial which would give the same performance as a given antenna are a length equal to  $\frac{0.16}{N}$  times the wave length and a height equal to the antenna height, rather large structures are required. For example, a flat-top antenna 30 m above the ground operating on a 600 m wave is equivalent to a 4-turn coil 24 m long by 30 m high. The dimensions of the equivalent coil are thus of the same order as the dimensions of the antenna.

It is possible to escape from the apparent necessity of large structures for effective radio transmission and reception in two ways. First, the coil aerial can easily be made to have a lower resistance than the antennas ordinarily used, and its size reduced in proportion to the reduction of resistance. This is mainly because the condenser used in the coil aerial circuit can be one having

practically no resistance while the condenser consisting of antenna and ground has a large resistance. Thus by due attention to the minimizing of resistance in its circuit, the coil aerial may be of small dimensions and yet highly effective. The size may, of course, be reduced also in proportion as the number of turns is increased.

It is equally possible to avoid an aerial of large dimensions without having recourse to a coil aerial. The alternative is to use the antenna principle, but use a special construction of much lower height. At first sight it would appear that this would make a poorer antenna, since the effectiveness is proportional to the height, according to either (8) or (19). And this is true if the antenna is merely lowered a moderate amount. Such lowering increases the capacity only very slightly, not nearly in proportion to the decrease in height. In order to secure an appreciable gain it is necessary to have the height very small and use a special construction to reduce the resistance as much as possible. A good method is to replace the ordinary antenna-ground structure in which the antenna is one plate of a condenser and the ground the other plate, by an aerial consisting of two horizontal metal condenser plates. This may be called a "condenser aerial." The formulas derived for antennas apply to it.

Such an aerial has lower conductor resistance than the ordinary antenna, and since it has greater capacity a smaller inductance will be used in series with it which will also have smaller resistance and thus reduce the resistance of the circuit. Furthermore, the resistance of an antenna largely arises from the imperfect dielectrics, such as vegetation, buildings, and poor insulators, present in its field (as shown in Scientific Paper of the Bureau of Standards, No. 269, by J. M. Miller), and the resistance from the grounding wires to ground. These can be eliminated in a condenser aerial. Finally, then, the resistance of the aerial circuit can be reduced to more than compensate for the reduction in height. This will result in a larger current  $I_r$  in formula (19), or in a larger  $H$  in formula (8), because of the increase of the sending current.

The advantage of the very low antenna has been observed in the experiments of Kiebitz<sup>1</sup> and others on so-called earth antennas. It is probable that still greater advantages would be obtained by the condenser aerial as here described. The special construction required to eliminate dielectric loss would involve making the lower plate considerably wider and longer than the

---

<sup>1</sup> Earthed antennas, Kiebitz, *Ann.*, **82**, p. 94, 1910; *Elec.* **68**, p. 868, 1912.

upper plate, or else having both plates a considerable distance above the ground, and keeping the space between the plates free from poor dielectrics. An aerial consisting of a pair of metal plates elevated from the ground was used, described by Oliver Lodge in 1897, and again by Lodge and Muirhead (*Proc. Royal Soc.*, vol. 82, p. 227, 1909), who found that it worked best without being grounded. The author is informed that the same sort of an aerial has recently been tried on airplanes, using the upper and lower planes as the condenser plates. Such an aerial would be ideal for airplanes if the space between could be kept free from poor dielectrics. If the plates of the condenser aerial have their length and width approximately equal, the aerial radiates in all directions. If a long narrow condenser is used it would probably be very directional, both as a transmitting and receiving device. Such a condenser might consist of a pair of parallel wires, which would be a considerable improvement on the ground antenna.

An example will make clear how the size of the condenser aerial compares with other aerials. It was found above that an antenna 30 m high was equivalent to a 4-turn coil 24 m long by 30 m high, both operating on a 600 m wave and with circuits of the same resistance. For the same wave length and with an inductance of 100 microhenries, in series, the capacity of a condenser aerial would need to be 0.00102 microfarad, which would be given by a pair of square plates 1 m apart and 10.7 m on a side. The height is thus reduced in the ratio of about 25 to 1, and the horizontal dimensions 3 to 1 in comparison with the coil aerial.

The aerial can be made as small as desired. If a given coil is to be used in series, the capacity of the aerial is maintained constant by reducing the distance between the plates when the area of the plates is reduced. The author made some interesting experiments with a small condenser aerial as a receiving device, used inside the laboratory with no ground connection. The plates consisted of copper netting. The top plate was 250 cm square and the distance between them was 15 cm. The signals received, with either a crystal detector or electron tube, were roughly of the same intensity as those received with a simple coil aerial of the type and size ordinarily used as a direction finder.

The indication of absolute direction of propagation of the waves as well as the line of propagation, which has been developed by workers in France and elsewhere, using combinations of ordinary

antenna and coil aerials, was observed in the experiments on the condenser aerial. An inductance coil of rather large dimensions used in series with the condenser acted as a receiving aerial. As this coil was rotated the signal varied from maximum in one angular position to zero in a position  $180^\circ$  from the first position; whereas the angular positions corresponding to maximum signal and to zero signal would be  $90^\circ$  apart in the case of a coil aerial independent of any antenna action. Apparently the action of the condenser aerial reinforced that of the coil in one position and neutralized it in the opposite position. When the connections to the coil were interchanged, the effect shifted  $180^\circ$ . Reversing the connections of the coil reverses the emf in the coil,  $E$ , in Fig. 6, just as a reversal of the direction of the wave would do, whereas the direction of the emf in the antenna or condenser aerial is unchanged. The reason why the condenser emf can neutralize the coil emf is probably that the capacity of the coil introduces different values of reactance to the two emf's. Thus when the circuit is tuned for one of these emf's the currents due to the two differ  $90^\circ$  in phase. This phase angle may be shifted  $180^\circ$  by a very slight variation of the reactance of the circuit. Because of this, systems for determining the absolute direction of radio waves require very delicate adjustment.

The ordinary laboratory type of condenser used in radio circuits does not function as a condenser aerial. This is because the interleaving of the plates results in the current in each portion of the dielectric being balanced by the current in a neighboring portion. This is discussed further below in Section VI, 3, and illustrated in Fig. 17.

## V. TRANSMISSION FORMULAS

## 1. STATEMENT OF FORMULAS

The current received in any aerial may be calculated in terms of the current in any transmitting aerial, either antenna or coil, by the following four formulas. They are derived by combining equations (8), (10), (19), and (23). The symbols are as previously given, also stated in the Appendix below.

Antenna to antenna:

$$I_r = \frac{188. \ h_a h_r I_s}{R \lambda d} \quad (40)$$

Antenna to coil:

$$I_r = \frac{1184. \ h_a h_r I_s N_r I_s}{R \lambda^2 d} \quad (41)$$

Coil to antenna:

$$I_r = \frac{1184. \ h_a I_s h_r N_a I_s}{R \lambda^2 d} \quad (42)$$

Coil to coil:

$$I_r = \frac{7450. \ h_a I_s h_r I_s N_a N_r I_s}{R \lambda^2 d} \quad (43)$$

The formula (40) has existed heretofore in various forms. The formulas here given generalize the antenna-to-antenna formula, so that calculations can be made for any kinds of aerials.

The lengths in these formulas may be in any units, provided the same unit is used for all the lengths. The meter is usually the most convenient unit. If the heights and wave length are in meters and the distance  $d$  in miles, the four constants in the four formulas become, respectively, 0.117, 0.736, 0.736, and 4.63.

To calculate the distance at which a given current will be received, as when a particular receiving arrangement is specified, the formulas may be stated explicitly for  $d$ .  $I_r$  and  $d$  are interchanged in each formula. For example, the formula for antenna-to-coil (41) becomes

$$d = \frac{1184. \ h_a h_r I_r N_r I_s}{R \lambda^2 I_r} \quad (44)$$

All of these transmission formulas are for daytime transmission. Greater values are obtained at night, probably because the waves are reinforced by reflection from ionized layers of the upper atmosphere, which are broken up by sunlight in the daytime. The formulas are all subject to correction factors for distance and for decrement. If the distance is very great (in ordinary cases, over 100 kilometers), the right-hand side of the formula should be multiplied by the correction factor  $F_1$ . The value given below for  $F_1$  is for transmission over sea water. Its value for transmission over land would be greater. If damped waves are used, the correction factor  $F_2$  should be similarly applied. Furthermore, if the plane of the receiving coil is not parallel to the direction of propagation of the wave, the correction factor  $F_3$  must be similarly applied to formulas (41) and (43) and related formulas, such as (44). In formulas (42) and (43) the direction of the wave is taken to be that of the plane of the transmitting coil. The three correction factors are:

$$F_1 = e^{-0.000047 \frac{d}{\sqrt{\lambda}}} \quad (9)$$

$$F_2 = \sqrt{\frac{1}{1 + \frac{600 \cdot L \delta'}{R \lambda}}} \quad (20)$$

$$F_3 = \cos \alpha \quad (24)$$

All of the correction factors make the resultant numerical values smaller.

## 2. DISCUSSION OF TRANSMISSION FORMULAS

The power in which the wave length appears in the denominator is different in the several formulas. Thus when a coil aerial is used for both transmitter and receiver the received current is inversely proportional to the cube of the wave length. Thus transmission between coils is better the shorter the wave length. This advantage of coils at short wave lengths applies only for short-distance transmission. When the distance is hundreds or thousands of kilometers, the increased absorption of the waves makes the correction factor  $F_1$  so great that short waves are impractical. So for long distances the comparison favors the antenna rather than the coil. The coil compares most favorably with the antenna, then, for transmission over short distances with very short waves. This is subject to the proviso that current of the same order of



magnitude can be put into a transmitting coil aerial as into an antenna, or that the resistance of a receiving coil is the same as that of a receiving antenna. Neither of these assumptions is wholly fulfilled, in practice, with the result that the difference of applicability of the two kinds of aerials at long and short wave lengths is less marked. (For additional comparisons of antennas and coils and further discussion, see Section IV above.)

*Limitations of Formulas.*—The formulas can not be expected to give results of great accuracy, certainly not better than a few per cent, because of the ideal conditions assumed in their derivation. Thus it is assumed that no image of the aerial exists in the ground beneath it; that is, the ground is not perfect as a conductor. As a matter of fact, the ground varies greatly in conductivity, and while in most cases the currents induced in the ground below a transmitting or receiving aerial probably have very little effect, these currents may be appreciable in some cases. This is discussed further below under "Height of Aerial."

On account of the uncertainty introduced by the ground, the formulas may apply better to airplane aerials than to those on ships or on land. It is well known, however, that radio signals are fainter on an airplane than on the ground. It is not known to what extent this is due to (1) the diminution of intensity vertically of waves sliding along the ground, (2) electrical disturbances from the ignition system of the engine, and (3) the unavoidable noises on an airplane.

In transmission over great distances, particularly at night, radio waves are reinforced by reflection from the upper conducting strata of the atmosphere. This tends to increase the current in a receiving aerial. The theory of this effect is treated in an article by G. N. Watson (Proc. Royal Soc., vol. 95, p. 546; 1919).

There are other sources of uncertainty in the application of these formulas. An antenna does not form a flat-plate condenser with the ground of such form that the curving of the field at the edges can be neglected. The simple method of calculating the radiated field is thus in doubt. Similarly, in the case of a radiating coil, the field from the top and bottom of the coil may have some effect at a distance, which has not here been taken into account. It is not certain with how great propriety the earth's surface can be taken to be equivalent to the equatorial plane of the radiating aerial. Frequently radio waves have a wave front that is tilted and not perpendicular to the earth's surface, as

- assumed in the calculation of received current. Furthermore, the formulas assumed uniform current throughout the aerial, which sometimes does not hold, because the antenna may have a vertical portion of appreciable capacity or the coil may have rather large distributed capacity. Calculations involving coil aeri-als are subject to the additional uncertainty arising from the capacity of the coil to ground or the surroundings so that it acts like an antenna as well as a coil. This is discussed under "Antenna Effect" in Section VI, 3. Another difficulty discussed in the same section is the effects of surrounding objects.

With these departures in the action of the aeri-als and the behavior of the waves from the conditions assumed, it is impossible to calculate received currents with great accuracy. It is almost surprising that the experimental results check the formulas as closely as shown in Section VI, 2, below.

*Height of Aerial.*—The value used for  $h$  is the length of the vertical side of a coil aerial, the distance from the surface of the ground to the flat top of an antenna, or the vertical distance between the two flat plates of a condenser aerial. In previous discussions it has been assumed that the ground beneath an antenna was a perfect conductor and thus the height of the radiator was twice the value of the  $h$  defined here. Experiment, however, corroborates the view here taken, which assumes that the radiating structure is independent of the earth, the waves becoming attached to the earth soon after leaving the antenna. In the present state of our knowledge the most satisfactory conception is that the radiating structure is the actual structure above the ground level. (Questions of the conductivity of the ground, presence of earth currents, etc., near the radiating aerial, are expressly not considered.)

Austin's empirical formula<sup>2</sup> for antenna-to-antenna transmission is equation (40) with a constant twice as great, and quantities  $h_1$  and  $h_2$  used instead of  $h_s$  and  $h_r$ . These quantities  $h_1$  and  $h_2$  are the "height to the center of capacity" of the transmitting and receiving antenna, respectively. This height is not defined, but its value for any particular antenna is the value that is required to make experimental results fit the formula. Now, as has been stated, such experiments as have been performed agree in general with formula (40). For instance, see the first two examples in Section VI, 2, below. It must follow, since the

---

<sup>2</sup>Scientific Paper of the Bureau of Standards, No. 226, equation (5).

constant in Austin's formula is twice as great as the constant in (40), that

$$h_1 h_2 = \frac{1}{2} h_a h_r$$

This may be satisfied by various values of  $h_1$  and  $h_2$ . One set of values would be

$$\begin{aligned} h_1 &= 0.5 h_a \\ h_2 &= 1.0 h_r \end{aligned}$$

Another would be

$$\begin{aligned} h_1 &= 0.707 h_a \\ h_2 &= 0.707 h_r \end{aligned}$$

Austin's values for the height of various antennas, thus deduced in such a way as to make them fit the experimental values observed, do in fact vary from one-half to full value of the actual antenna heights, and average around 0.7 the actual heights. It is much simpler and more direct to use the formula and the interpretation presented in this paper, bearing in mind that it is subject to the uncertainties introduced by the varying character of the ground.

The idea that the ground is not a good enough conductor to form an image of a transmitting aerial, and that the waves become attached to the ground after leaving the aerial, is in harmony with the ideas of Lodge and Muirhead, already referred to. They found that they got better transmission by using what amounted to a condenser aerial, elevated from ground, with no ground connection. This conception conflicts with the commonly accepted view that Marconi's achievement was the connection of a radiating system to the ground. What then was Marconi's achievement? The best answer to this may be one stated to the author by Prof. A. E. Kennelly, viz, the use of a large radiating system, arranged vertically.

## VI. EXPERIMENTAL VERIFICATION OF FORMULAS

### 1. PRINCIPLES OF MEASUREMENT OF RECEIVED CURRENT AND VOLTAGE, WITH APPLICATIONS TO DESIGN

The formulas presented in this paper not only make it possible to calculate approximately the field intensity produced or current received with given aerials, but also give the basis for determining what constants to select for the circuit of a particular aerial to secure the maximum effect. In other words, these formulas fur-

nish the principles of design of aerial circuits. There are a great many points not obvious from mere inspection of the formulas, which are of importance equally in design and in the measurement of received signals. These will now be considered. While this discussion is limited to what takes place in receiving aerials, the same principles and treatment can readily be applied to transmitting aerials.

The received current or voltage can be measured in a number of different ways. It is important to know just what quantity is being considered or measured. Suppose an indicating instrument  $G$ , which may be a galvanometer or a telephone receiver, is connected to a rectifying device  $D$  in parallel with the condenser of the receiving circuit, as in Fig. 7, where either  $L$  is a coil aerial,

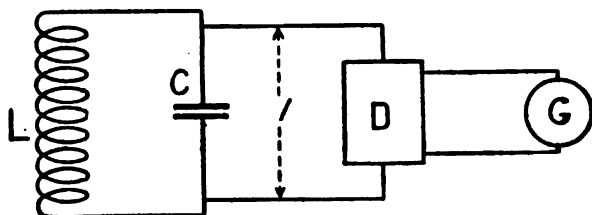


FIG. 7.—Aerial circuit with detecting apparatus across the condenser

or else  $C$  is an antenna or condenser aerial. Does the indication of the instrument measure directly (a) the emf which the wave causes to act on the circuit  $CL$ , (b) the current in the circuit, or (c) the voltage across the condenser? The answer is, of course, none of these things. The system can, however, conveniently be calibrated in terms of the voltage across the condenser. This voltage  $V$  is related to the received current  $I_r$  by the relation

$$V = \frac{I_r}{\omega C} \quad (45)$$

and since  $I_r$  is related to the emf acting by

$$I_r = \frac{E}{R} \quad (46)$$

the relation of  $V$  to  $E$  is

$$V = \frac{E}{R\omega C} \quad (47)$$

When a detecting apparatus like that of Fig. 7 is used, in which the deflections or signals depend directly on the voltage across the condenser, the results obtained with various receiving circuits will be entirely different from those obtained when the current in the circuit is directly measured, as in Fig. 8. Equations (46) and (47) show at once that the effects of varying the constants of the receiving circuit will be different, depending on whether it is  $E$ ,  $I_r$ , or  $V$  that is being measured. These three quantities for a receiving antenna are, from equations (17), (46), and (47), for unit magnetic field intensity,

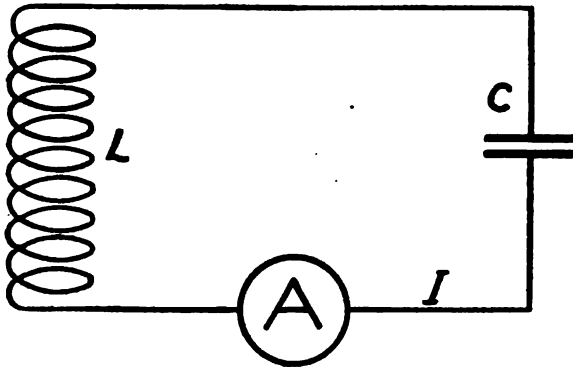


FIG. 8.—Aerial circuit with current-measuring instrument in circuit

$$E_a = 300 \cdot h_r \quad (48)$$

$$I_a = 300 \frac{h_r}{R} \quad (49)$$

$$V_a = 300 \frac{h_r}{R\omega C} \quad (50)$$

The quantity  $h_r$  may be called the “emf reception factor” for an antenna; the emf in the receiving circuit is proportional to it. Similarly  $\frac{h_r}{R}$  may be called the “current reception factor” since it determines the received current. And  $\frac{h_r}{R\omega C}$  or the equivalent  $\frac{h_r L}{R\lambda}$  may be called the “voltage reception factor” of an antenna since it determines the voltage across the antenna.

The most favorable or optimum value of any of the variables that determine the antenna emf, current, or voltage, can be determined either by direct experimental measurement of their values when actually receiving or by calculation from the reception

factors. It is desired to learn simply what will produce the maximum  $E_a$ ,  $I_a$ , or  $V_a$ . For example, it is obvious that  $E_a$  increases indefinitely as  $h_r$  increases, but more careful consideration is required to determine what will be the effect on the received current of increasing  $h_r$ . The reception factors furnish an alternative to direct reception measurements, requiring instead measurements upon the constants of the aerial circuit.

*Coil Aerial Reception Factors.*—The emf applied by the passing wave to a coil aerial, the current in the circuit, and the voltage across the condenser are, from equations (26), (46), and (47), for unit magnetic field intensity,

$$E = 600.\pi \frac{a^2 N}{\lambda} = \frac{1}{10^8} \frac{a^2 N}{\sqrt{CL}} \quad (51)$$

$$I = 600.\pi \frac{a^2 N}{R\lambda} = \frac{1}{10^8} \frac{a^2 N}{R\sqrt{CL}} \quad (52)$$

$$V = 36.\pi^2 10^{12} \frac{a^2 NL}{R\lambda^2} = \frac{1}{10^8} \frac{a^2 N}{RC} \quad (53)$$

These equations assume the coil to be square, having both height and length =  $a$ . For a coil that is not square, the formulas apply, replacing  $a$  by  $\sqrt{h_r l}$ . Two values are given for each reception factor; the first of the two is the more useful, since it is more common to consider the dependence of the reception on  $\lambda$  than on  $C$ .

$$\text{Emf reception factor} = \frac{a^2 N}{\lambda} \quad (51)$$

$$\text{Current reception factor} = \frac{a^2 N}{R\lambda} \quad (52)$$

$$\text{Voltage reception factor} = \frac{a^2 NL}{R\lambda^2} \quad (53)$$

*Design of Receiving Coil Aerials.*—The response produced in a coil aerial circuit may be measured in a great variety of ways. In the first place, it may be considered either from the viewpoint of the emf acting, the current, or the voltage across the condenser. The first of these, the emf  $E$ , may be determined for any particular case from the emf reception factor (51). The current  $I$  or voltage  $V$  may each be determined in four different ways: (1) by direct measurement with a suitable instrument, (2) by measurement of the quantities which make up the appropriate reception factor, (3) by measurement of signal strength in some such device as

sketched in Fig. 7, which has been calibrated in  $I$  or  $V$ , (4) from a "signal intensity reception factor," which can be calculated for any signal-measuring device when the law connecting the signal intensity with either  $I$  or  $V$  is known.

The design of a receiving coil requires knowledge of the dependence of the current or voltage upon the dimensions, etc., of the coil. Measurements made in all of the ways just enumerated give results in agreement with one another, provided due care is given to the avoidance of errors. The sources of error are numerous, as discussed in Section 3 below.

While direct measurement of the received current or voltage can be replaced by calculation from the reception factors, the fact remains that the design of an aerial requires experiments. This is because the quantity  $R$  in the reception factors can not be obtained by calculation. It must be obtained by measurement for the particular coil and mode of connections employed.

Measurements upon receiving aerials to determine their constants and the best design for given conditions constitute a most interesting study. In later publications from this laboratory the results of experiments will be published giving such data for typical coil aerials.

The capacity  $C$  in the formulas is the total capacity of the circuit, including the capacity of the coil,  $L$  is the pure inductance of the coil, and  $R$  is the actual resistance of the circuit.  $R$  includes the resistance of the conductors, effective resistance of the condenser and of the coil capacity, effective resistance of the detecting apparatus, and radiation resistance. All of these vary with frequency, and thus measurements of  $R$  at the frequency concerned is necessary. On account of the complexity of the quantities entering into the total  $R$ , its measurement is no easy matter. The capacity of the coil and other stray capacities may easily vitiate the measurement of  $R$ ,  $C$ , or  $L$ . The effect of the detecting apparatus always requires most careful consideration. Even if  $D$  in Fig. 7 is an electron tube, it is necessary to consider the resistance which it introduces into the aerial circuit.

*Dependence of Received Current and Voltage on Dimensions of Coil and Wave Length.*—Let  $R_o$  = resistance of coil and  $R_x$  = resistance external to coil;

$$R = R_x + R_o$$

$$I \propto \text{Current reception factor} = \frac{a^2 N}{(R_x + R_o) \lambda} \quad (54)$$

The variation of received current with number of turns, wave length, and size of coil is readily found by considering the variation of the quantities in (54). In the following discussions the spacing between turns of wire, which affects resistance and inductance, is assumed constant.

(a) Varying  $N$ , with  $\lambda$  and  $a$  constant. When  $R_x$  is large compared to  $R_o$ , we see from (54)

$$I \propto N$$

When  $R_o$  is large compared to  $R_x$ , since  $R_o \propto N$ , roughly,

$$I \propto \text{constant}$$

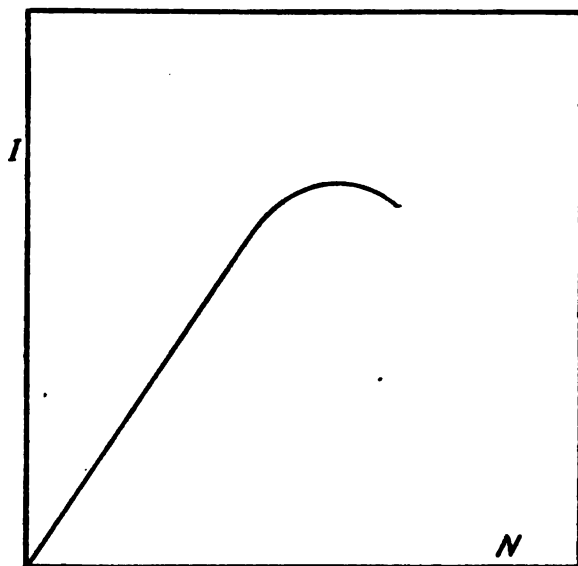


FIG. 9.—Dependence of received current on number of turns

However  $R_o$  increases somewhat faster than proportional to  $N$  as  $N$  is increased, because of the proximity of the added turns, and hence  $I$  decreases somewhat as  $N$  increases instead of being strictly constant.

$R_x$  is likely to be large compared with  $R_o$  when  $N$  is very small, and hence for small  $N$ , the variation of  $I$  with  $N$  will be a straight line, as shown in Fig. 9. As  $N$  increases,  $R_o$  becomes large compared to  $R_x$  and the tendency of  $I$  to increase with  $N$  is reversed. As a result the curve of  $I$  has a maximum. The value of  $N$  at this point may be called the "optimum number of turns." Its value will be greater the greater the external resistance.



(b) Varying  $\lambda$  with  $N$  and  $a$  constant. When  $R_x$  is large compared to  $R_o$  and does not vary appreciably with wave length

$$I \propto \frac{1}{\lambda}$$

This variation is shown in Fig. 10. When  $R_o$  is large compared to  $R_x$ , however, since  $R_o \propto \frac{1}{\sqrt{\lambda}}$ , roughly,

$$I \propto \frac{1}{\sqrt{\lambda}}$$

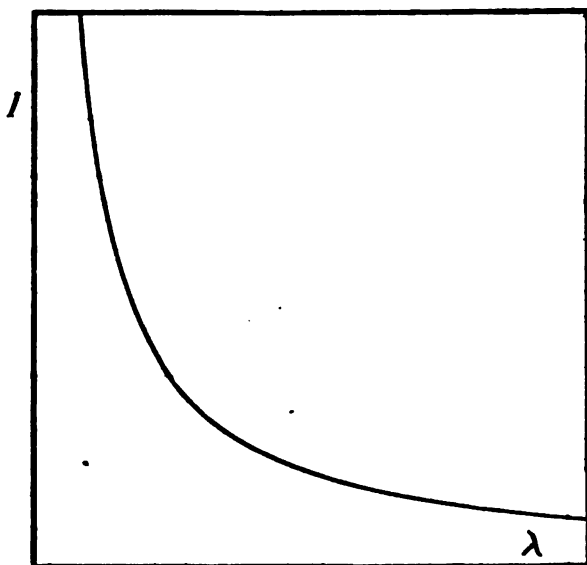


FIG. 10.—Dependence of received current on wave length when external resistance is large

However the effect of the adjacent turns increases  $R_o$  faster than stated, as  $\lambda$  is diminished, and hence  $I$  tends to approach a constant value for short wave lengths, as shown in Fig. 11. These conclusions may, however, be vitiated by the variation of  $R_x$  with  $\lambda$ .

(c) Varying  $a$ , with  $N$  and  $\lambda$  constant. When  $R_x$  is large compared to  $R_o$ ,

$$I \propto a^2$$

This is shown in Fig. 12. When  $R_o$  is large compared to  $R_x$ , since  $R_o \propto a$ ,

$$I \propto a,$$

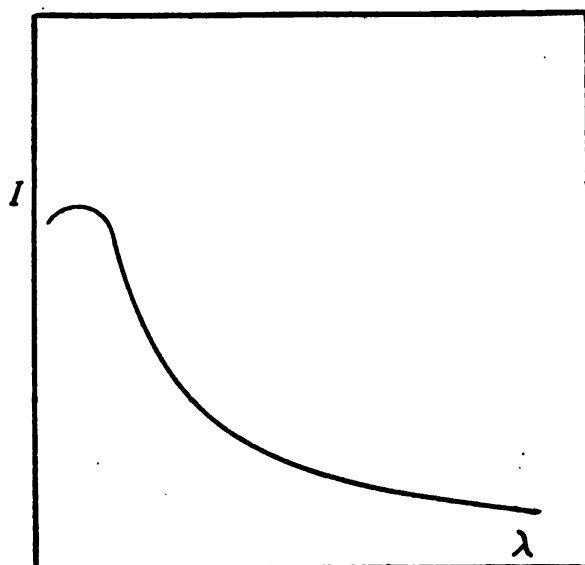


FIG. 11.—Dependence of received current on wave length when coil resistance is large

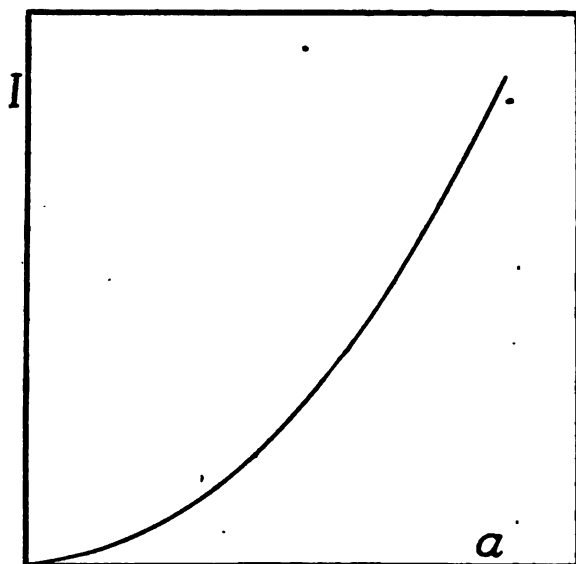


FIG. 12.—Dependence of received current on size of coil when external resistance is large

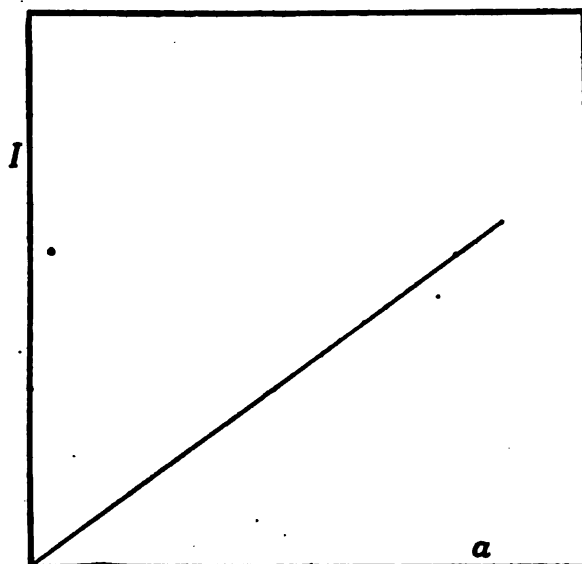


FIG. 13.—Dependence of received current on size of coil when coil resistance is large

giving the straight line in Fig. 13. From these two extreme cases it follows that an actual curve is likely to have a form that is a combination of these two, as shown in Fig. 14.

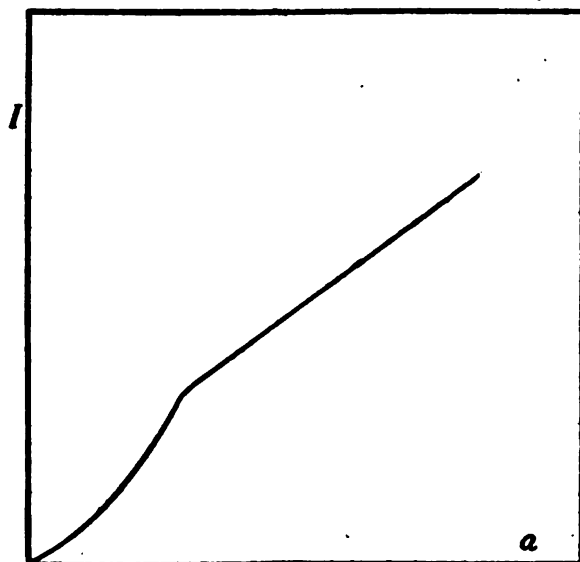


FIG. 14.—Dependence of received current on size of coil in typical case

(d) Varying  $a$ , with  $\lambda$  constant, allowing  $N$  to vary in such a way that length of wire is constant. The condition is that  $N \propto \frac{1}{a}$ . When  $R_x$  is large compared to  $R_0$ ,

$$I \propto a.$$

The curve of  $I$  is thus a straight line. When  $R_0$  is large compared to  $R_x$ , the same conclusion holds, but only roughly.  $R_0$  increases slightly as  $a$  is decreased because of the proximity of the added turns, hence  $I$  increases a little faster than proportional to  $a$ . This is shown in Fig. 15.

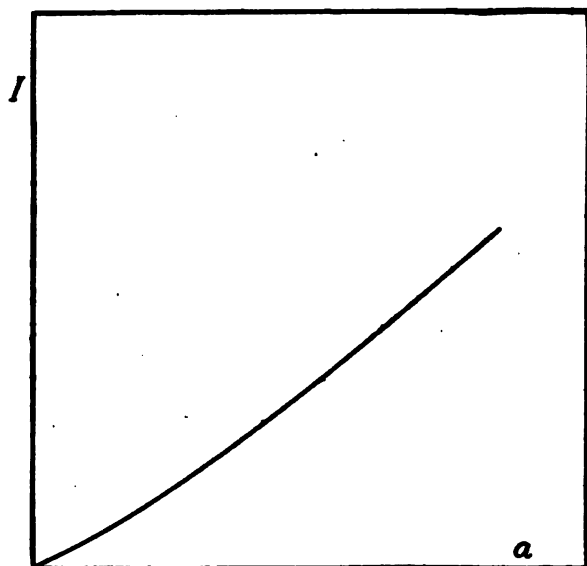


FIG. 15.—Dependence of received current on size of coil when length of wire is kept constant

The voltage reception factor differs from the current reception factor by  $\frac{L}{\lambda}$ .

Thus,

$$V \propto \text{Voltage reception factor} = \frac{a^2 N L}{(R_x + R_0) \lambda^2} \quad (55)$$

It is thus a more complex problem to determine the variation of voltage with  $N$ ,  $\lambda$ , and  $a$ , because the variation of  $L$  must be considered in addition. This may be done in each case, just as was done above for current, taking into account the relations:

$$L \propto N^{2-}$$

$$L \propto \lambda^{0-}$$

$$L \propto a^{1+}$$

$$R_o \propto N^{1+}$$

$$R_o \propto \frac{1}{\lambda^{1+}}$$

$$R_o \propto a^1$$

where the + or - sign after the exponent indicates that the actual power is slightly greater or less than that given.

The relations obtained for voltage are similar to those obtained for current. There are some characteristic differences, as, e. g., with varying  $N$  the optimum number of turns comes out greater than for received current. Thus, when the detecting apparatus depends essentially on the current, the size of the coil should be as large as possible, whereas when it depends essentially on the voltage across the condenser the number of turns should be as large as possible.

On the whole, the received current or voltage or signal intensity is increased by increasing the dimensions ( $N$  and  $a$ ) and by decreasing the wave length. These conclusions are subject to the limitation, discovered by French experimenters, and qualitatively obvious from the known increase of  $R$  near the natural wave length  $\lambda_o$  of a circuit, that poor results are obtained if  $\lambda_o > \frac{1}{3}\lambda$ . Thus, the dimensions of the coil can not be increased, or the wave length decreased, indefinitely. Beyond the limit mentioned, in fact, better results are obtained by decreasing the dimensions of the coil.

It is an interesting fact that these discussions apply not only to the design of a coil aerial for receiving signals, but that they also solve the problem of design of wave meters. The choice of constants of a wave-meter coil for any particular case is settled by the formulas and ideas here presented. The considerations given for received current and voltage apply, respectively, to the design of wave meters for measurements upon undamped or damped waves; that is, to the securing of minimum resistance and minimum decrement, respectively.

## 2. EXAMPLES OF MEASUREMENTS

Measurements having as their object the verification of the transmission formulas were discussed in the preceding section. Any experiments which verify the transmission formulas may also be considered as checking the "theoretical formulas" and

"comparison formulas." In fact experimental tests of the transmission formulas are the most rigorous test of the theory presented in this paper. All of the limitations and errors discussed in Section V, 2, affect the transmission formulas, while only a portion of them affect the theoretical and comparison formulas.

The complicated practical conditions of any experiment, the tilting of the wave front, the combination of antenna and coil effects, discussed in the next section below, and other uncertainties, make close agreement between theory and experiment unlikely. Agreement to 30 per cent should be considered as highly satisfactory verification of the essential correctness of the theory. On account of its field being more definitely localized, experiments with a coil aerial may be expected to yield greater accuracy than experiments with an antenna. The same advantage appertains to a condenser aerial. No quantitative data have been obtained with condenser aerials, to the author's knowledge; such experiments would be very desirable.

Experimental data obtained at the Bureau of Standards on radio transmission and reception are presented below. The agreement between the received current observed and the values calculated from the transmission formulas can be considered as very satisfactory. The author is informed that experiments made by the Signal Corps have led to a similar verification. In some of the Signal Corps experiments it was thought at one time that wide departures from the transmission formulas for coil aerials were observed, the received current for very short waves being much less than the transmission formulas indicated. When, however, the actual values of the resistance at the wave lengths used were determined, the agreement was very good. Particular care must be given to proper measurement of the resistance of the receiving aerial circuit.

*Antenna to Antenna.*—Experiments which supply a check on formula (40) have been published by Dr. Austin, chief of the Naval Radio telegraphic laboratory located at the Bureau of Standards.

For transmission between two antennas located on ships (Jour. Wash. Acad. Sciences, vol. 1, p. 275; 1911),  $h_s = 29.2$ ,  $h_r = 29.2$ ,  $I_s = 30.$ ,  $R = 25.$ ,  $\lambda = 1000.$ ,  $d = 1000.$  The lengths given in all these examples are in meters. Calculating from (40),

$$I_r \text{ calculated} = 0.19$$

$$I_r \text{ observed} = 0.21$$

For the Washington Navy Yard antenna transmitting to an antenna at the Bureau of Standards (Bull. Bureau of Standards, vol. 11, p. 74; 1914),  $h_s = 36.$ ,  $h_r = 30.$ ,  $I_s = 7.0$ ,  $R = 70.$ ,  $\lambda = 2800.$ ,  $d = 10\ 000.$  Calculating from (40) and (20)

$$I_r \text{ calculated} = 0.53 \times 10^{-3}$$

$$I_r \text{ observed} = 0.55 \times 10^{-3}$$

As already pointed out, the agreement of observed values with the transmission formulas indicates that it is proper to take as the antenna height the actual height from the ground to the flat top.

*Antenna to Coil.*—A number of experiments to check the antenna-to-coil transmission formulas have been made at the Bureau of Standards radio laboratory since early in 1917. The first ones did not involve quantitative measurements, but served to give a rough check on the formulas. The calculated value of current was compared with the current as estimated from the loudness of signal in a telephone receiver connected to various types of detecting devices. These signals were interpreted on the assumption that a fairly audible response is given by the currents indicated with the several types of detector.

$10^{-4}$  to  $10^{-5}$  ampere, crystal detector.

$10^{-5}$  to  $10^{-6}$  ampere, simple audion.

$10^{-6}$  ampere, oscillating audion.

For the Arlington antenna received on a coil aerial at the Bureau of Standards,  $h_s = 122.$ ,  $h_r = 4.$ ,  $l_r = 4.$ ,  $N_r = 22.$ ,  $I_s = 102.$ ,  $R = 25.$ ,  $\lambda = 3800.$ ,  $d = 7800.$  The received current calculated from (41) is 0.0018 ampere. The observed signal using crystal detector and telephone, was very loud, thus checking in a qualitative way the result calculated.

Two similar qualitative experiments were made, transmitting from an antenna at the Bureau of Standards and receiving on a portable coil aerial. In one experiment,  $h_s = 36.$ ,  $h_r = l_r = 1.07$ ,  $N_r = 11.$ ,  $I_s = 0.5$ ,  $R = 2.$ ,  $\lambda = 850.$ ,  $d = 16\ 000.$ , whence calculated  $I_r = 11. \times 10^{-6}$ . In the other,  $h_s = 12.$ ,  $h_r = l_r = 1.07$ ,  $N_r = 11.$ ,  $I_s = 0.25$ ,  $R = 2$ ,  $\lambda = 600.$ ,  $d = 11\ 000$ , whence calculated  $I_r = 5.7 \times 10^{-6}$ . In both cases the observed signal was loud with a simple audion, again giving a qualitative check on the formula.

A number of experiments have been made by Dr. Austin during 1918 and 1919, who has kindly placed the results at my disposal. A couple of typical ones will be given. For the Arlington antenna transmitting to a coil aerial at the Bureau of Standards,  $h_s = 122.$ ,  $h_r = 1.82$ ,  $l_r = 1.29$ ,  $N_r = 56.$ ,  $I_s = 100.$ ,  $R = 50.$ ,  $\lambda = 6000$ ,  $d = 7800$ .

$$I_r \text{ calculated} = 1.4 \times 10^{-4}$$

$$I_r \text{ observed} = 2.1 \times 10^{-4}$$

For the same antenna transmitting to a large coil suspended from masts outdoors,  $h_s = 122.$ ,  $h_r = 21.6$ ,  $l_r = 24.4$ ,  $N_r = 7.$ ,  $I_s = 100.$ ,  $R = 50.$ ,  $\lambda = 10\,000$ ,  $d = 7800$ ,  $\alpha = 42^\circ$ . From (41) and (24),

$$I_r \text{ calculated} = 1.0 \times 10^{-3}$$

$$I_r \text{ observed} = 1.2 \times 10^{-3}$$

A large number of transmission experiments from antennas to coils have been made by the radio laboratory of this Bureau in the early part of 1919. In a typical case, where  $h_s = 21.$ ,  $h_r = l_r = 1.44$ ,  $N_r = 8.$ ,  $I_s = 3.$ ,  $R = 7.7$ ,  $\lambda = 700.$ ,  $d = 4800.$ ,  $\delta' = 0.1$ ,  $L = 541.$ , microhenries. From (41) and (20),

$$I_r \text{ calculated} = 24. \times 10^{-6}$$

$$I_r \text{ observed} = 28. \times 10^{-6}$$

The fact that the observed current is larger than the calculated, in these and other cases, is probably due to the antenna effect, discussed in the next section. The coil structure has capacity, which makes it receive the wave by antenna action in addition to the coil action, thus increasing the current actually received.

*Coil to Antenna.*—In an experiment made by Dr. Austin, with a large coil at the Bureau of Standards transmitting to the Arlington antenna,  $h_s = 21.6$ ,  $l_s = 24.4$ ,  $h_r = 122.$ ,  $N_s = 7.$ ,  $I_s = 1.$ ,  $R = 50.$ ,  $\lambda = 2800.$ ,  $d = 7800$ ,  $\alpha = 42^\circ$ . From formula (42),

$$I_r \text{ calculated} = 1.3 \times 10^{-4}$$

$$I_r \text{ observed} = 1.5 \times 10^{-4}$$

*Coil to Coil.*—The only data available to the author on the use of the coil aerial for both transmitting and receiving are from experiments made in 1917 by Messrs. Kolster, Willoughby, and Lowell, and these are only qualitative. For transmission from a coil at the Bureau of Standards to a portable coil 40. km away,  $h_s = l_s = 3.$ ,  $h_r = l_r = 1.$ ,  $N_s = 4.$ ,  $N_r = 15.$ ,  $I_s = 10.$ ,  $R = 1.$ ,  $\lambda = 600.$ ,  $d = 40\,000$ . The received current calculated from formula (43) is  $4.6 \times 10^{-6}$ . The observed signal was loud with a simple audion.



For transmission from a coil located at a lighthouse to a coil on a ship 48. km. away,  $h_s = l_s = 3.05$ ,  $h_r = l_r = 1.22$ ,  $N_s = 3$ ,  $N_r = 10$ ,  $I_s = 10$ ,  $R = 2$ ,  $\lambda = 550$ ,  $d = 48\ 000$ . The calculated  $I_r$  is  $1.6 \times 10^{-2}$ . The observed signal was audible on a simple audion. Comparing with the current sensibility of an audion stated above, it is seen that both of these results furnish a rough check on the formula.

### 3. DISCUSSION OF EXPERIMENTS

The agreement of the experiments with the theory is highly satisfactory in view of the simple conditions assumed in the theory. The complex practical conditions preclude the likelihood of agreement within a few per cent. The various limitations of the formulas arising from actual experimental conditions are discussed above in Section V, 2.

One characteristic of the experiments with coil aerials is that the observed value of received current is in every case greater than the calculated value. This strongly suggests that the action of the coil structure involves something additional to the pure action as a coil. This would be expected also from theoretical considerations. The inevitable capacities between parts of the aerial circuit must introduce an action analogous to that of an antenna. When it is borne in mind that the coil action is really a second-order effect in comparison with the action of a system of antenna nature, it appears extremely likely that the stray capacities of any coil aerial circuit would introduce an antenna effect which would have to be considered in addition to the pure coil effect. Besides the reasons thus given by theory and by the excessive values of current observed in experiments with coil aerials, there are two other lines of evidence that the antenna effect is not negligible in coil aerials.

One of these additional lines of evidence is furnished by measurements of current in different parts of a coil aerial or the circuit thereof. If the capacities between parts are appreciable, some of the current must leave the conductors and flow off into the dielectric; the current observed with an ammeter must, therefore, be different in different parts of the circuit. These differences are actually found. The fourth kind of evidence that the antenna effect is appreciable in coil aerials is furnished by considerations of radiation resistance, which will now be discussed. Following that, the antenna effect will be considered in more detail.

*Radiation Resistance.*—It is possible to determine whether in a given system the antenna effect or coil effect predominates by

measurements of radiation resistance. The radiation resistance has different values and follows different laws for antenna and coil.

Radiation resistance in general is defined by

$$P = RI^2 \quad (56)$$

in which  $I$  is the current in the aerial used as a transmitting device,  $P$  is the power radiated, and  $R$  the radiation resistance. The study of radiation resistance is an important means of facilitating work on aerials. This may be seen from the simple fact that the magnitude of the radiation resistance gives at once the power radiated, and hence the effectiveness of a transmitting aerial or the range of communication can be judged without making transmission experiments. Field tests are thus in large part replaced by laboratory measurements. In addition to this, it is possible to discriminate between the antenna and coil effects.

The magnitude of the radiation resistance of a flat-top antenna, at wave lengths considerably greater than the fundamental, is given by the well-known expression

$$R_a = \left( 39.7 \frac{h}{\lambda} \right)^2 \quad (57)$$

An approximate expression for the radiation resistance of a coil can be derived very simply, as follows: When a radiated field exists in any part of space, the relation of the power  $P'$  radiated through that portion of space to the magnetic field intensity there existing is

$$P' \propto H^2 \quad (58)$$

for any given distance from the source, whatever the source may be. The total power radiated is proportional to the integral of  $P'$  over any surface entirely surrounding the source. This integral will be of the same form for  $H_o$ , the field due to a coil, as for  $H_a$ , the field due to an antenna, except for the effect of the variation of  $H_o$  in a plane around the radiating coil, which varies from zero to the value given in (10) for any given distance from the source. As a first approximation, this variation may be considered to make the integrated value of  $H_o$  one-half as great as it would be if  $H_o$  had the value given in (10) in all directions around the radiating coil.

$$\therefore \frac{P_o}{P_a} = \frac{1}{2} \frac{H_o^2}{H_a^2} \quad (59)$$

From (8) and (10), for a given distance from the source and a coil and antenna of same height with same current,

$$\frac{H_o}{H_a} = 2\pi \frac{lN}{\lambda} \quad (60)$$

From (56),

$$\frac{R_o}{R_a} = \frac{P}{P_a}$$

Hence from (59) and (60),

$$\frac{R_o}{R_a} = 2\pi \frac{l^2 N^2}{\lambda^2}$$

Inserting the value of  $R_a$  from (57),

$$R_o = 31100 \cdot \frac{h^2 l^2 N^2}{\lambda^4}$$

If the coil is a square one with  $h = l = a$ ,

$$R_o = \left(13.3 \frac{a}{\lambda}\right)^4 N^2 \quad (61)$$

This approximate expression for radiation resistance of a coil gives at once the variation with size, number of turns, and wave length. For example, for a set of coils of varying size, in which the length of wire is kept constant,  $R_o \propto \frac{1}{N^2}$ . It shows that for a given ratio of size to wave length,  $R_o \propto N^2$ . The principal point of interest is that  $R_o$  is inversely proportional to the fourth power of wave length.

Since the radiation resistance of an antenna is inversely proportional to the second power of wave length, and that of a coil inversely proportional to the fourth power, the radiation resistance furnishes a means of determining whether a given structure functions as a coil or as an antenna. Rough determinations of radiation resistance which were made upon a particular coil aerial showed a variation of observed radiation resistance inversely as the third power of the wave length, thus verifying the idea that the action is a combination of coil and antenna effect. The observed values, however, were all higher than the sum of the theoretical  $R_a$  and  $R_o$ . The measurement of radiation resistance is an extremely difficult operation, and satisfactory methods can not be said to have been developed as yet.

*Antenna Effect.*—Since there are differences of potential between various parts of a coil, acting either as a transmitting or receiving aerial, there must be some dielectric current through the space around the coil and between the coil and ground. It follows that there must be some antenna action, proportional to the amount of this dielectric current and the length of path over which it flows, and this will produce a current additional to that produced by the coil action unless the coil structure happens to

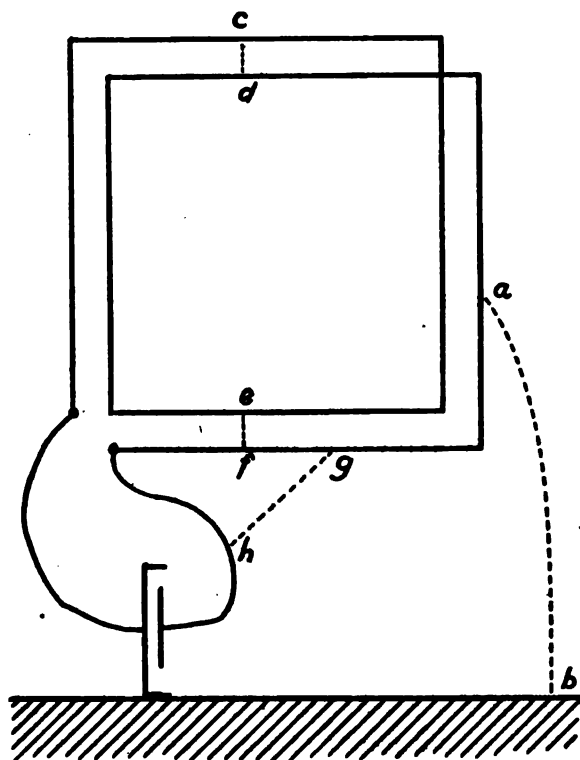


FIG. 16.—Paths of dielectric currents which cause antenna effect in coil aerial

have an exact symmetry which causes the antenna effect in each part of the coil to be balanced by an antenna effect in some other part.

Fig. 16 shows the origin of the antenna effect. As in ordinary practice, the leads cause some part of the apparatus to be practically at ground potential, the shield of the condenser is shown connected to ground. An appreciable dielectric current flows from various parts of the conducting circuit to other parts and to

ground. Typical paths of this dielectric current are shown by the dotted lines. The line *a b* suggests the dielectric current from the coil structure to ground, the lines *c d* and *e f* the dielectric current between turns of the coil, and the line *g h* the dielectric current between coil and leads. The flow of dielectric current between turns of the coil is in a horizontal direction when the coil is of prismatic form with the turns separated and all of the same area. This part of the antenna effect arises in a receiving coil of this form only when the wave front is more or less tilted from the vertical.

On account of the flow of current off through the dielectric from various parts of the circuit, ammeters placed at different places in the circuit would show different values of current to be flowing. In radio circuits it can not be assumed that the current is the same at all points around the conducting circuit, as was shown by the author in his investigation of high-frequency current measurement described in Bureau of Standards Scientific Paper No. 206; 1913.

To the extent that these dielectric currents flow, the conductors of the circuit may be considered as an antenna system. Perhaps only the current typified by the line *a b* might be thought of as giving rise to an "antenna" effect, since the others do not flow to ground; still this part of the dielectric current does not differ from the others in nature or effect, and hence it seems advisable to use the suggestive term "antenna effect" to indicate all of the effect arising from the presence of currents in the dielectric.

It might be supposed that the same sort of an effect would be caused by the flow of dielectric current in the condenser of the coil aerial circuit. This is not true ordinarily, because a condenser of the laboratory type is used in which the condenser plates are interleaved. As shown in Fig. 17, the current in one direction in the dielectric is balanced by a current in the opposite direction in the neighboring part of the condenser. This is a nonradiating condenser and is the analog of a noninductive coil, which is also nonradiating. A condenser consisting of a single pair of plates would radiate, but is not ordinarily used, because it would be much bulkier than the laboratory type of condenser. The condenser consisting of a single pair of plates would be, in fact, the "condenser aerial," which has been recommended by the author in Section IV, 3, as worthy of serious consideration in radio practice.

The effect of the distributed capacities of the aerial circuit must not be confused in any way with the phase angle between the fields existing at the two vertical sides of the coil aerial. The phase angle referred to is the seat of the action of the coil aerial as such. The dielectric currents flowing in the distributed or stray capacities of the circuit, however, give rise to the direct action as an antenna, not depending in any way on the separation between the two vertical sides of the coil. All of these remarks apply both to transmission and reception.

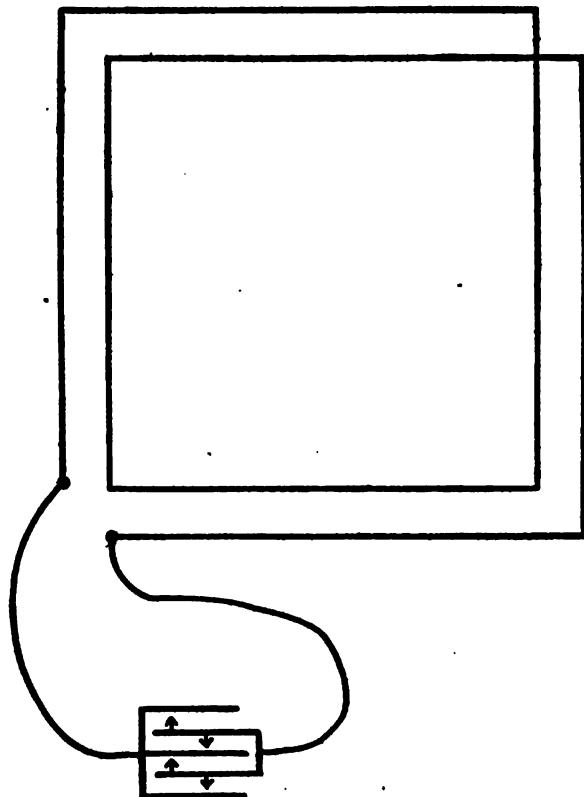


FIG. 17.—Directions of flow of dielectric currents in laboratory type of condenser

It is rather difficult to determine what fraction of the effect of a coil aerial is due to antenna action and what part to coil action. In many cases, doubtless, the antenna action predominates. It is possible, however, to separate the effects in any particular case by the several different methods. The antenna effect may be calculated, at least for parts of the circuit, by the aid of careful ammeter readings, which show what amount of the current has flowed off into the dielectric. The antenna effect may be elimi-

nated, thus leaving only the coil effect, by a carefully-arranged system of shields and grounds; or, by a symmetrical arrangement of the coil structure which causes the antenna effect in each part to be balanced by the antenna effect in some other part. The coil effect may be eliminated, on the other hand, in the case of a receiving coil, by taking advantage of the fact that the coil effect depends on the direction of orientation, while the antenna effect (at least the major part of it) does not; that is, by turning the coil so its plane is parallel to the wave front. A method which eliminates the coil effect and retains a part of the antenna effect is to open one of the coil leads, thus leaving the coil aerial connected to the circuit at one point, placing in series with it an inductance coil of very small dimensions, but of the same inductance, the circuit being completed by the capacity of the coil aerial to ground.

*Effects of surroundings.*—Currents are induced in metal and other objects near a transmitting aerial, and sometimes are powerful enough to affect the radiation appreciably. The objects near a receiving aerial have currents produced in them by the passing wave. These currents in nearby objects, which may include the ground, induce emf's in the receiving aerial. It is to be noted that this effect of neighboring objects is caused by induction and not radiation from them, which would be comparatively feeble.

The emf thus induced in a coil aerial from the surroundings is of the same or opposite phase as that caused by the wave. It differs in this respect from the emf due to the antenna effect discussed above. The antenna effect ordinarily produces an emf which is  $90^\circ$  out of phase with the coil effect and does not vary with the orientation of the coil. The antenna effect can thus never balance out the coil effect, and it is impossible to reduce the received current to zero, no matter how the coil is turned. The emf induced by the surroundings, however, depends upon the orientation of the coil. This emf will be reduced to zero by turning the coil at a different orientation from that at which the emf due to the wave is zero unless the line between distorting object and the coil aerial is the direction of propagation of the wave. The result of this is that the total emf is reduced to zero at some orientation other than that obtained when the wave alone acts on the coil aerial. There is thus a distortion in the apparent direction of the wave, caused by objects surrounding the coil aerial.

Corrections can be made for this effect upon the indications of a direction finder. The errors for various directions of wave are determined, and this gives a calibration by which subsequent observations at the same wave length are corrected.

## VII. PRACTICAL CONCLUSIONS

### 1. RELATIVE EFFECTIVENESS OF ANTENNAS AND COIL AERIALS

(a) Generally speaking a coil aerial is as powerful a transmitting or receiving device as an antenna only when its dimensions approach those of the antenna.

(b) It is easy to make the resistance of a coil aerial circuit much smaller than the resistance of the ordinary antenna circuit and thus make a small coil as effective as a large antenna. A small aerial as effective as a large antenna can, however, also be secured by the use of the antenna-like aerial called the "condenser aerial."

Heeding these principles and using amplifiers in receiving, radio aerials can in the future be much smaller than heretofore.

(c) The relative effectiveness of a coil and antenna, in terms of the wave length, number of turns, etc., is given by formula (33) and the related formulas.

(d) A coil aerial exhibits antenna action as well as coil action, because of capacities between its parts and surroundings. The antenna action sometimes overbalances the coil action.

(e) The advantage of the coil aerial is greatest for short wave lengths. It is consequently likely to be well suited to airplane communication. The increasing advantage of the coil as a transmitting aerial as the wave length is decreased is subject to the proviso that the same current can be gotten into a coil as into an antenna. In fact, the whole practical problem is to get as much current as possible in the aerial.

(f) The use of coil aerials at both receiving and transmitting ends of the communication is particularly suitable for short waves, since the received current in such a system is inversely proportional to the cube of the wave length.



## 2. PRINCIPAL FORMULAS

The units used are international electric units, the ordinary electric units based on the ohm, ampere, centimeter, and second, except where otherwise stated. The principal symbols are the following:

## Symbols

$i$  = instantaneous current.

$I_0$  = maximum value of current.

$I$  = effective value of current.

$H_t$  = instantaneous value of magnetic field intensity.

$H_0$  = maximum value of magnetic field intensity.

$H$  = effective value of magnetic field intensity.

$h$  = height of aerial

$d$  = distance along earth's surface from sending aerial.

$\omega$  =  $2\pi$  times frequency of the current.

$t$  = time.

$\lambda$  = wave length.

$c$  = velocity of electric waves =  $3 \times 10^{10}$  cm per second.

$l$  = horizontal length of coil aerial.

$N$  = number of turns of wire of coil aerial.

$a$  = length of side of square coil.

$\theta$  = phase angle between values of field intensity a distance  $l$  apart in the wave.

$\mathcal{E}$  = electric field intensity.

$E$  = electromotive force in receiving aerial.

$\delta'$  = logarithmic decrement of  $H$  or  $E$ .

$\phi$  = magnetic flux.

$R$  = resistance of receiving aerial circuit.

$C$  = capacity of receiving aerial circuit.

$L$  = inductance of receiving aerial circuit.

$\alpha$  = angle between direction of propagation of wave and plane of coil.

Subscripts:  $s$  = sending,  $r$  = receiving,  $a$  = antenna,  $c$  = coil.

The following are the principal formulas presented in this paper:  
Radiated magnetic field intensity from an antenna or condenser aerial:

$$H = \frac{2\pi}{10} \frac{h_s I_s}{\lambda d} \quad (8)$$

Radiated magnetic field intensity from a coil:

$$H = \frac{4\pi^2}{10} \frac{h_s I_s N_s I_s}{\lambda^2 d} \quad (10)$$

Received current in an antenna or condenser aerial:

$$I_r = 300. \frac{h_r H}{R} \quad (19)$$

Received current in a coil:

$$I_r = 600. \pi \frac{h_r I_r N_r H}{R \lambda} \quad (23)$$

Distance correction factor:

$$F_1 = e^{-0.000047 \frac{d}{\sqrt{\lambda}}} \quad (9)$$

Decrement correction factor:

$$F_2 = \sqrt{\frac{1}{1 + \frac{600. L \delta'}{R \lambda}}} \quad (20)$$

Direction correction factor:

$$F_3 = \cos \alpha \quad (24)$$

Antenna to antenna transmission:

$$I_r = \frac{188. h_a h_r I_a}{R \lambda d} \quad (40)$$

Antenna to coil transmission:

$$I_r = \frac{1184. h_a h_r I_a N_r}{R \lambda^2 d} \quad (41)$$

Coil to antenna transmission:

$$I_r = \frac{1184. h_a I_a h_r N_a}{R \lambda^2 d} \quad (42)$$

Coil to coil transmission:

$$I_r = \frac{7450. h_a I_a h_r N_a N_r}{R \lambda^3 d} \quad (43)$$

The lengths in the four preceding formulas may be in any units. Meters are commonly used. Any of these formulas may be expressed in terms of  $d$ . For example,

Distance at which a given current is received in a coil for a given transmitting current in an antenna :

$$d = \frac{1184 \cdot h_a h_r I_r N_r I_s}{R \lambda^2 I_r} \quad (44)$$

Total magnetic field from an antenna, including radiation and induction:

$$H = \frac{2\pi}{10} \frac{h_a I_s}{\lambda d} + \frac{j}{10} \frac{h_a I_s}{d^2} \quad (31)$$

Relative effectiveness of coil and antenna for same height and wave length:

$$\frac{d_o}{d_a} = N \sqrt{2 \left( 1 - \cos 2\pi \frac{l}{\lambda} \right)} \quad (32)$$

Ditto,  $l$  small compared to  $\lambda$ :

$$\frac{d_o}{d_a} = 6.28 N \frac{l}{\lambda} \quad (33)$$

Length of coil aerial equivalent to antenna of the same height.

$$l = 0.16 \frac{\lambda}{N} \quad (39)$$

Current in aerial circuit:

$$I_r = \frac{E}{R} \quad (46)$$

Voltage across condenser in aerial circuit:

$$V = \frac{E}{R\omega C} \quad (47)$$

Coil aerial reception factors:

$$\text{Emf reception factor} = \frac{a^2 N}{\lambda} \quad (51)$$

$$\text{Current reception factor} = \frac{a^2 N}{R\lambda} \quad (52)$$

$$\text{Voltage reception factor} = \frac{a^2 N L}{R\lambda^2} \quad (53)$$

Radiation resistance:

$$R_a = \left( 39.7 \frac{h}{\lambda} \right)^2 \quad (57)$$

$$R_o = \left( 13.3 \frac{a}{\lambda} \right)^4 N^2 \quad (61)$$

### 3. FUTURE RESEARCH NEEDED

The subject of research on electric waves can be considered as barely begun. The study presented in this article has revealed vast and most interesting problems awaiting solution, which can be solved. The functioning of aerials, both in transmitting and receiving, can now be considered as roughly understood. Recent advances in radio measurements and technique open the way to experiments and progress which will bring about far-reaching control of electric waves. A few of the detailed problems which border on the subject matter of this paper and await solution will now be mentioned.

*Theoretical Problems.*—(a) Develop a simple and straightforward derivation of the radiated field from a coil, directly and without considering the action of the sides separately as antennas.

(b) Work up an explanation of the mechanism of radiation that brings out clearly the relation of the radiation to the induction field and shows that all of the dielectric current is effective in causing radiation, which shall take the place of the usual explanation in terms of the snapping off of lines of force.

(c) Determine the effects of the phase angle between different parts of the dielectric field in an antenna or condenser aerial, especially the long, low types.

(d) Develop methods of measuring radiation resistance.

(e) Work out laws of variation of voltage reception factor of coil aerials, and laws of variation of both current and voltage reception factors of antenna and condenser aerials. Similarly, develop accurate and useful transmission factors.

*Experimental Problems.*—(a) Determine the relative effectiveness, over a very wide range of sizes, wave lengths, etc., of the various types of aerials. Do this by (1) direct measurements to verify transmission formulas, (2) measurements of the factors that enter into the reception factors, (3) measurements of radiation resistance.

(b) Make transmission experiments at very great distances over typical kinds of land, to obtain distance absorption factors.

(c) Try out condenser aerials, comparing performance with transmission formulas. Build such aerials with minimum resistance. Demonstrate the nonradiating nature of the laboratory type of condenser, comparing it with condenser aerials.

(d) Compare trailing wire, condenser aerial, and coil aerial, on airplanes.

(e) Find out how directive as transmitting devices coil and condenser aerials and "earth antennas" are; measure magnitude and direction of field at various distances from the aerial, at numerous wave lengths, etc.

(f) Determine relative magnitudes of induction and radiation close to transmitting aerials. Determine also directions of fields, to secure complete knowledge of phenomena near radiating systems.

(g) Measure currents in ground as well as the fields above the ground, to determine how wave attaches itself to the ground.

(h) Study distributed capacities in coil aerial circuits by measuring current at different points in circuit.

(i) Determine values of antenna effect, and develop means of controlling or eliminating it by shielding systems, etc.

(j) Make quantitative investigation of receiving systems combining antenna and coil aerial. Measure phases of currents. Determine under what circumstances the indication of absolute direction is reversed when the tuning is slightly varied.

(k) Determine effects of surrounding objects on currents in transmitting and receiving aerials. Measure magnitude and phase of currents in typical cases.

(l) Develop methods of connecting generating apparatus to various types of aerials to get maximum current into the aerial, especially at short wave lengths.

## VIII. SUMMARY

The advantages of the coil aerial as a direction finder, interference preventer, reducer of strays, and submarine aerial make it important to know how effective the coil aerial is, in comparison with the ordinary antenna, as a transmitting and receiving device. This article gives the answer. Simple formulas are worked out from fundamental electromagnetic theory, by which the performance of any aerial can be calculated. Experiments have verified the formulas, and show that they are a valuable aid in the choice and design of an aerial to fit any particular requirement.

The principal formulas are of three kinds: (1) theoretical formulas, giving the magnetic field intensity at any distance from either kind of aerial and the current produced by a given field intensity in either kind of aerial; (2) comparison formulas, giving the ratio of performance of antenna and coil aerial under various conditions; (3) and transmission formulas, giving the current in any receiving aerial in terms of the current in the distant transmitting aerial.

The theory and nature of radiation are discussed, and applied to the elucidation of some current fallacies. There has been a vast haziness of ideas on these points. The distinction between induction fields and radiation fields is presented. It is shown that the receiving action in any kind of an aerial may be considered as arising either from the electrostatic or the magnetic field present in the wave. Such questions are discussed as the distinction between "open" and "closed" circuits. It is shown that a metallically closed circuit can radiate, and that radiation takes place at all frequencies, the amount of radiation being greater the higher the frequency.

The ratio of the range of communication obtainable with a coil aerial to that with an antenna is proportional to the number of turns and horizontal length of the coil and is inversely proportional to the wave length. The coil aerial is hence particularly suited to communication on short wave lengths. A coil aerial is quantitatively as powerful as an antenna only when its dimensions approach those of the antenna. However, it is easy to make the resistance of a coil aerial circuit much smaller than the resistance of the ordinary antenna circuit and thus make a small coil as effective as a large antenna.

A small aerial as effective as the ordinary antenna may be secured without recourse to the coil principle by using an aerial consisting of a condenser having two large parallel plates, arranged so that the dielectric of the condenser includes no ground. The circuit of such an aerial may be made to have a very low resistance. It appears likely that, with the use of either condenser or coil aeriels together with sensitive amplifiers, radio aeriels will in the future be much smaller than heretofore. These principles apply with particular advantage to airplane aeriels.

A coil aerial usually functions by a combination of the pure coil action and antenna action. The latter arises from the stray capacities and capacities to ground which are inevitably present.

The existence of these capacities may be shown by differences in ammeter readings at different points of the circuit. The antenna effect makes the actual received current in experiments with coil aerials larger than the values calculated from the transmission formulas. The observed values are also affected by currents in neighboring objects.

A formula for the radiation resistance of coil aerials is worked out. Comparison of experiment with this formula supplies additional evidence that the coil aerial operates by a combination of antenna and coil effects.

The fundamental principles of design of aerials are given. The various modes of measuring received current and voltage across the condenser are discussed. The relations of these two quantities to the electromotive force acting in the aerial must be carefully observed in calculations or design. Reception factors are derived, to which the received current or voltage are proportional. Experimental data on the functioning of aerials may be secured either from actual transmission experiments or from measurements of the quantities which enter into the reception factor.

This investigation has opened up a large and most interesting field for further research. Progress in the control and utilization of electric waves depends on the investigation of such theoretical and experimental problems as have been suggested in Section VII, 3, herein.

WASHINGTON, June 18, 1919.











# DETERMINATION OF THE OUTPUT CHARACTERISTICS OF ELECTRON TUBE GENERATORS

By Lewis M. Hull

## CONTENTS

	Page
I. Introduction.....	497
II. Oscillating tube.....	498
III. Derived characteristic.....	501
IV. Power output.....	503
V. Current output.....	507

## I. INTRODUCTION

Within the last three years the experimental development of the three-electrode electron tube as a generator of alternating currents has been carried out to such an extent that the device is at present the standard source of supply for radio telephone and telegraph circuits in all cases where extremely high power is not required. At the same time no adequate methods have been evolved whereby the efficiency and power output of such a generator can be stated with any degree of accuracy in terms of the electrical constants of the tube itself. Several analyses of the general operation of electron tube generators are now available.<sup>1</sup> But none of these are accurate enough and at the same time comprehensive enough to allow a quantitative prediction from the two important factors in power-tube operation—plate voltage and filament emission—of the alternating-current power which can be developed in a radio-frequency circuit of known resistance, inductance, and capacity. Power tubes are rated in watts output and watts input from empirical data upon circuits adjusted to particular settings, experimentally determined, for maximum power or maximum efficiency. Such ratings give no intimation of the power which will be developed by the tube if any constant of the output circuit be changed.

<sup>1</sup> J. Bethenod, *Lum. Elect.*, Dec. 9, 1916.

G. Vallauri, *L'Elettrotecnica*: IV, No. 3, pp. 18, 19; 1917.

L. A. Hazeltine, *Proc. I. R. E.*, April, 1918.

T. Kikuchi, *Proc. Physico-Mathematical Society of Japan*, February, 1919.

In this paper a method of analysis will be presented by means of which it is possible to design a circuit to obtain maximum output from a given tube, or, conversely, to select a tube which will furnish with reasonable efficiency its maximum power to a particular output circuit.

## II. OSCILLATING TUBE

The explanation of the phenomena taking place in connection with the oscillations generated by an electron tube can well be illustrated by the diagrammatic sketch in Fig. 1. This represents the

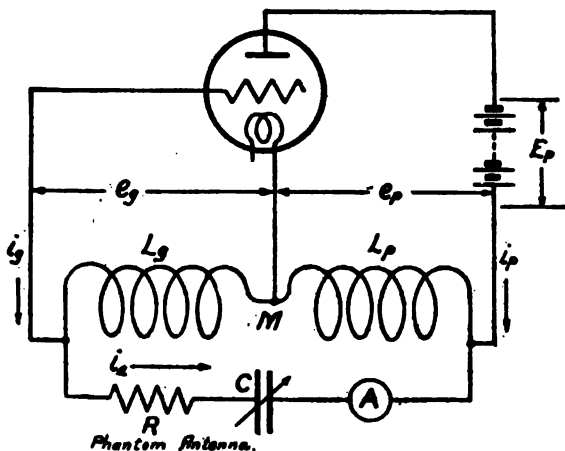


FIG. 1.—Direct-coupled generating circuit

so-called Hartley circuit which is typical of the circuits used for the purpose of generating oscillations. The grid and filament of the tube in this particular circuit are connected to the branched circuit containing inductance and capacity, constituting the oscillatory circuit, in such a manner as to include a portion of the inductance of that circuit, that is the coil  $L_g$ . Likewise between the plate and filament of the tube is included the coil  $L_p$ .

Suppose, first, that the tube is not generating oscillations. Under the action of the plate battery a steady current will flow from the plate to the filament inside of the tube and from filament to plate through the coil  $L_p$  in the external circuit. The magnitude of this current will vary with the voltage of the grid; it can become zero when the grid is highly negative but can not reverse in direction. Also there can be a flow from grid to filament inside the tube, the current returning from filament to grid through the coil  $L_g$  in the external circuit. This latter current is appreciable only when the grid is positive with respect to the

filament. Except for effects which are extraneous to this treatment, this current is also unidirectional.

When the tube is in the oscillating condition these currents will not be steady, but will become pulsating. The pulsating currents generated by the tube enter the circuit from the filament and leave it through the plate and grid connections; they are pulsating, and not alternating, on account of the unidirectional conductivity between filament and plate and filament and grid. The circuit  $L_g L_p C$  is resonant to the fundamental constituents of these pulsating currents, and an oscillatory current is generated which circulates around this branched circuit, flowing in series through the condenser  $C$  and the coils  $L_p$  and  $L_g$ . This current, which will be called the output current, can be many times greater in amplitude than either of the pulsating currents. The pulsations in the steady current, which flows during the static condition from the filament to the plate, are caused by periodic variations in the potential of the grid with respect to the filament; these variations in grid potential are induced in the grid coil  $L_g$  by the output current. There is a similar voltage induced by the output current across the plate coil  $L_p$ . It is true of this circuit, and typical of any circuit for generating oscillations, that during that portion of the cycle of the output current when the grid is positive with respect to the filament as a result of the voltage induced in the coil  $L_g$ , the voltage drop between the plate and filament connections (across the coil  $L_p$ ) is such as to oppose the voltage of the plate battery and hence to reduce the voltage acting between filament and plate in the tube. During the other part of the cycle, when the grid is negative with respect to the filament, the voltage acting between plate and filament is increased above that of the steady voltage of the plate battery. During the portion of the cycle when the grid is positive with respect to the filament current flows within the tube between the grid and filament, and this current increases as the grid becomes more positive. The direction of the current flow is in the direction of the emf, that is, from grid to filament inside the tube and from filament to grid outside of the tube. Further, as the grid becomes positive with respect to the filament, there is a resultant increase in the current flow between the plate and filament of the tube, even though the plate voltage on the tube is being reduced. This increase is limited, when the stable oscillating condition has been reached, by the saturation effect, which may occur at lower

values of plate current than that corresponding to the total filament emission, owing to the loss of electrons to the grid.

As has been stated, the plate current wave is distorted at the other extreme of the cycle—that is, when the grid is negative—by rectification effects; moreover, the grid current is always pulsating, and is zero for a considerable part of a cycle, while the grid is negative. Consequently the waves of current supplied to the circuit between *F* and *P* and *F* and *G* (Fig. 2) are each composed of a direct or average constituent, a fundamental constituent corresponding in frequency to that of the output current, and a number of higher frequency or harmonic constituents.

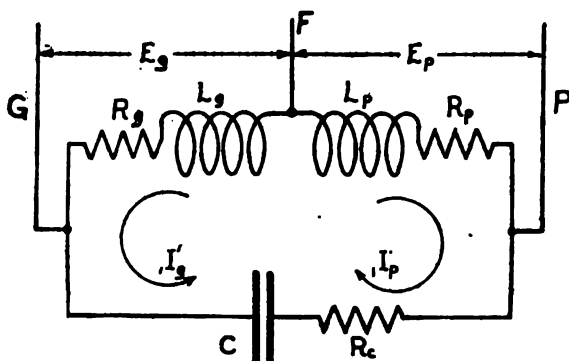


FIG. 2.—Output circuit

The useful oscillating output current depends neither upon the direct or average values of the plate and grid currents nor upon the multiple frequency constituents; it is determined solely by the fundamental constituents of these currents, to which the same considerations as regards direction and phase relations apply as have been roughly stated with regard to the distorted current waves.

Thus, speaking only in terms of the useful current constituents, a sinusoidal, alternating current flows in the grid circuit in phase with the alternating voltage across the coil  $L_g$ , and therefore represents a withdrawal of power from the output circuit, which power is expended within the tube. On the other hand, a sinusoidal, alternating constituent of plate current flows in opposition to the voltage across the coil  $L_p$ ; this means that power is being supplied to the output circuit from the plate circuit of the tube. As will appear later, the impedance of the output circuit to all frequencies that are harmonic multiples of the fundamental is very great;

hence there are no appreciable multiple frequency constituents of current circulating in the output circuit, and the alternating voltages across the coils  $L_p$  and  $L_g$  are in all cases practically sinusoidal. Consequently the useful power supplied by the tube can be determined in terms of the alternating voltage across  $L_p$  and the fundamental constituent of plate current. If we could neglect the grid current, this would be the power available for dissipation in the resistances. As the output current increases the amplitudes of the alternating voltages across the plate and grid coils increase proportionately. The alternating grid current increases more and more rapidly, as the amplitude of the plate voltage becomes larger. On this account the power loss to the grid increases. The power supplied by the plate increases with increasing plate voltage, but as the grid voltage increases, the effective saturation current is reached when the grid is positive, and the plate current becomes zero for an appreciable part of the cycle when the grid is negative; consequently a continued increase in the amplitude of the output current results chiefly in an increase in the harmonic constituents of plate current without greatly increasing the fundamental. Obviously, then, a condition of stability ensues when the power supplied by the fundamental of plate current minus the power dissipated by the fundamental of grid current is just equal to the power dissipated by the output current in  $R_g$ ,  $R_p$ , and  $R_o$ .

### III. DERIVED CHARACTERISTIC

The first quantitative measurements that must be made upon a tube are measurements of the plate and grid currents which flow when different plate and grid voltages are applied to the tube. It is evident from the arrangement of the output circuit, Fig. 2, that  $e_p$  and  $e_g$ , the instantaneous values of the voltage induced by the output current in the plate and grid coils, are not only opposite in sign with respect to the neutral filament, but are at all times in the same ratio of magnitudes as the ratio of inductance of the plate and grid coils. If we define  $n = L_p/L_g$ , then at any instant during a cycle of output current  $e_p = n e_g$ , assuming these voltages to be caused entirely by the output current. Thus it is possible to apply steady voltages to a tube, to vary these voltages step by step maintaining the same ratio as during an actual oscillation and to measure the instantaneous values which the plate and grid currents will assume during an oscillation.

Curves showing the plate and grid currents as explicit functions of the grid voltage, taking account of the simultaneous changes in plate voltage which would occur if these currents supplied an output circuit having a given ratio of coupling reactances are called the derived characteristic of a tube. This term was proposed by Hazeltine,<sup>2</sup> who also originated the idea of a constant ratio of plate and grid voltages while a tube is in oscillation. According to his method the characteristic is plotted by making successive changes in a steady value of  $e_s$ , the voltage applied to

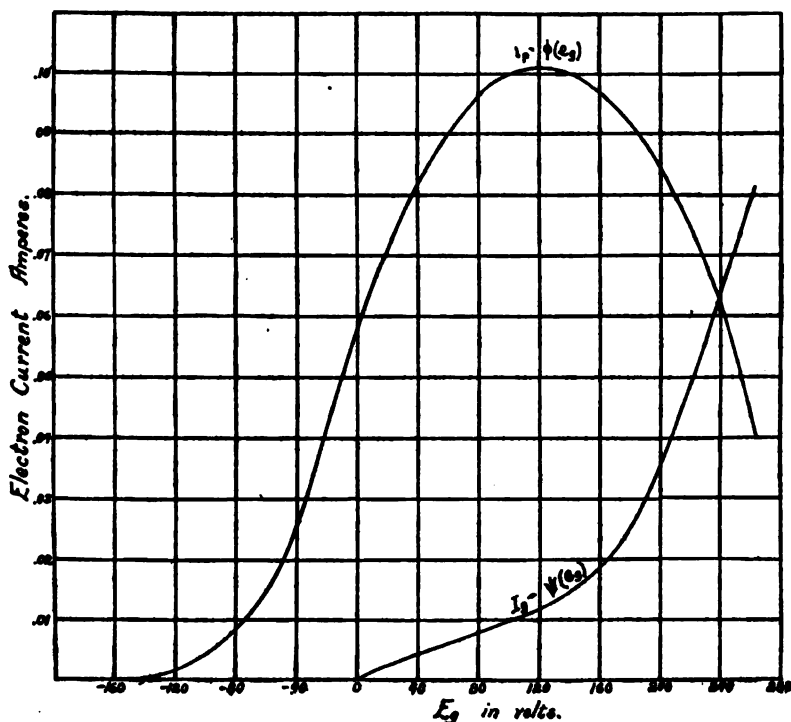


FIG. 3.—Derived characteristic

the grid of the tube, at the same time making changes in  $e_p$ , the voltage applied to the plate, opposite in direction and equal in magnitude to  $n e_s$ , and by measuring the resulting values of  $i_g$  and  $i_p$ . Such a derived characteristic is shown in Fig. 3, plotted for a type VT-16 tungsten-filament tube starting from the operating point determined by a steady plate voltage of 300 and grid voltage of zero. A battery of small resistance was connected between filament and grid, and with each increase in the potential of

<sup>2</sup> L. A. Hazeltine, loc. cit.



the grid above that of the filament the voltage of the plate battery was decreased by an equal amount, while for each reduction in the grid voltage below that of the filament the plate-battery voltage was increased. Hence this characteristic is applicable to any circuit in which  $n = 1$ .

The value of a derived characteristic obtained in this manner as an indication of the grid and plate currents during an actual oscillation depends upon (1) the equality of the output current through the two branches of the output circuit from filament to plate; and (2) the constancy with which a phase difference of  $180^\circ$  is maintained between voltages of plate and grid with respect to the filament.

In the subsequent sections the following points will be discussed:

1. A method for obtaining from the Hazeltine derived characteristic the power characteristics of the tube.
2. The application of these power characteristics in determining the current output in a circuit of known capacity and resistance.
3. Experimental results upon an oscillating circuit justifying both the Hazeltine characteristic and the application thereof.

#### IV. POWER OUTPUT

In the circuit shown in Fig. 1  $i_p$ ,  $i_g$ , and  $i_a$  are the instantaneous values of the plate, grid, and antenna or output currents, respectively, while  $E_b$  is the steady voltage of the plate battery and  $e_g$  and  $e_p$  are the instantaneous values of the alternating voltages across the grid and plate coupling coils.  $R_p$  and  $R_g$ , the resistances of the coupling coils, are small compared with the reactances of these coils, so the alternating plate and grid voltages can be considered as due only to the reactances of these coils, justifying the definition of  $n$  by the ratio  $L_p/L_g$ .

Let a derived characteristic of the tube be plotted for this value of  $n$ . Then  $i_p$  and  $i_g$  are known as explicit functions of  $e_g$ .

$$\begin{aligned} i_p &= \phi(e_g) \\ i_g &= \psi(e_g) \end{aligned} \quad (1)$$

Make the assumption, which will be justified later, that  $i_a$  is undistorted and hence  $e_g$  is a pure sinusoid, of the form:

$$\begin{aligned} e_g &= E_g \sin \omega t \\ \text{Then } i_p &= \phi(E_g \sin \omega t) \\ \text{and } i_g &= \psi(E_g \sin \omega t) \end{aligned}$$

Whatever the form of the  $\phi$  and  $\psi$  functions, the wave forms of  $i_p$  and  $i_g$  will be symmetrical with respect to  $\pi/2$  from  $\omega t = 0$  to  $\omega t = \pi$ , and also with respect to  $3\pi/2$  from  $\omega t = \pi$  to  $\omega t = 2\pi$ . This indicates that the phase angles of all harmonic constituents of  $i_p$  and  $i_g$  are alternately 0 and  $90^\circ$  with respect to the fundamental, the frequency of which is that of the grid voltage,  $\omega$ . That is:

$$\begin{aligned} i_p = & {}_0I_p + {}_1I_p \sin \omega t + {}_2I_p \cos 2\omega t + \cdots + {}_{2k-1}I_p \sin (2k-1)\omega t + \\ & {}_{2k}I_p \cos 2k\omega t - - \\ i_g = & {}_0I_g + {}_1I_g \sin \omega t + {}_2I_g \cos 2\omega t + \cdots + {}_{2k-1}I_g \sin (2k-1)\omega t + \\ & {}_{2k}I_g \cos 2k\omega t - - \end{aligned} \quad (3)$$

The current in the output circuit will be of the form:

$$i_a = {}_1I_a \sin \omega t + {}_2I_a \cos 2\omega t + \cdots + {}_{2k-1}I_a \sin (2k-1)\omega t + {}_{2k}I_a \cos 2k\omega t - - \quad (4)$$

In order for  $i_g$  to be approximately sinusoidal the amplitude of any harmonic constituent,  ${}_kI_a$ , must be small compared with the amplitude of the fundamental  ${}_1I_a$ . It is found in practice that the instantaneous values of  $i_p$ , given by  $i_p = \bar{\phi}(L_g \omega {}_1I_1 \sin \omega t)$  differ from those given by  $i_p = \phi[L_g \omega ({}_1I_a \sin \omega t + {}_2I_a \cos 2\omega t - \cdots)]$  by an amount less than the experimental errors introduced in plotting the derived characteristic which determines the  $\phi$  function. (Equation 1.)

The amplitude of any constituent of the output current,  ${}_kI_a$ , can be calculated in terms of the amplitude of the same constituent of the plate and grid currents,  ${}_kI_p$  and  ${}_kI_g$ , by consideration of the impedance of the output circuit to that frequency,  $k\omega$ . For the present, however, we shall consider only the constituents which determine the input and the useful output. These constituents are  ${}_0I_p$ ,  ${}_1I_p$ , and  ${}_1I_g$ , the direct component of the plate current, the sinusoidal fundamental constituent of the plate current, and the fundamental constituent of the grid current, respectively. Assuming sinusoidal plate and grid voltages, these constituents can be calculated directly from the derived characteristic by any method of approximate harmonic analysis. Fig. 4 shows  ${}_1I_p$ ,  ${}_0I_p$ , and  ${}_1I_g$  as functions of  ${}_1E_g$ , the amplitude of the grid voltage. The points on these curves were obtained for a given value of  ${}_1E_g$  by calculation from a number of measured ordinates of the characteristic, Fig. 3, equally spaced throughout a cycle which  $i_g$  and  $i_p$  would pass as  ${}_1E_g \sin \omega t$  traverses a complete cycle. It is not necessary to plot the actual current waves in order to space these ordinates equally. If 18 ordinates be

used, they can be measured directly upon the characteristics at values of  $e_g$  given by  ${}_1E_g \sin \pi/9$ ,  ${}_1E_g \sin 2\pi/9$ ,  ${}_1E_g \sin \pi/3$ , etc.

The curves of Fig. 4 are sufficient to indicate the power output and efficiency which can be obtained from this tube in any output circuit for which  $n=1$ , the tube being operated at 300 volts steady plate potential and 1.35-ampere filament current.

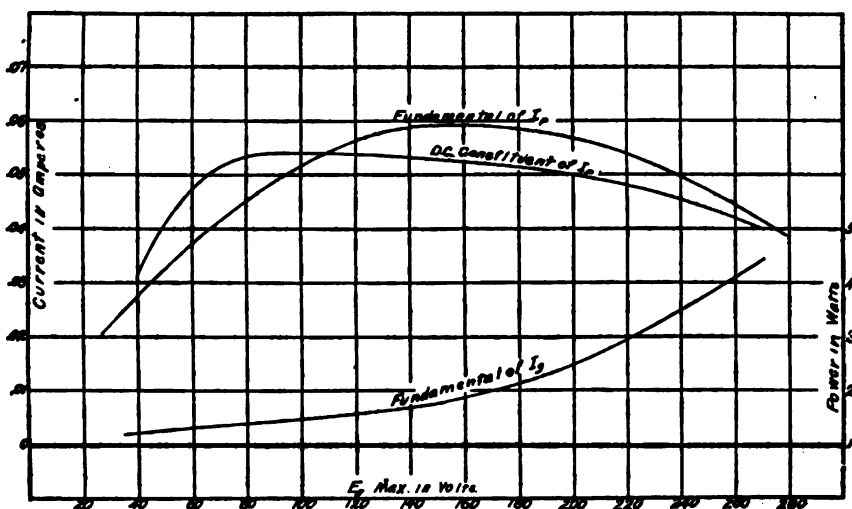


FIG. 4.—Fundamental current amplitudes

The effective power supplied by the plate battery is  $E_b \times {}_0I_p$ .  ${}_0I_p$  is actually the reading of a d. c. ammeter connected in series with the plate battery, since all of the alternating constituents are pure sinusoids, symmetrical with respect to  ${}_0I_p$ . The power output from the tube can be determined either in terms of the output current and the resistance  $R=R_p+R_g+R_o$ , or in terms of the alternating plate and grid voltages associated with the fundamental constituent of the plate and grid currents.

In terms of the plate and grid voltage the effective power output is

$$P_o = \frac{1}{2} ({}_1E_p I_p - {}_1E_g I_g)$$

Substituting  ${}_1E_p = n {}_1E_g$ :

$$P_o = \frac{{}_1E_p}{2} \left( I_p - \frac{1}{n} I_g \right) = \frac{n {}_1E_g}{9} \left( I_p - \frac{1}{n} I_g \right) \quad (5)$$

The power drawn from the plate battery is

$$P_i = E_b \times {}_0I_p \quad (6)$$

Hence the efficiency, for any inductively coupled output circuit, is

$$\eta = 0.5 \frac{E_p}{E_b} \left( \frac{I_p - I_g/n}{I_p} \right) = 0.5 \frac{E_g}{E_b} \left( \frac{n I_p - I_g}{I_p} \right) \quad (7)$$

It might be supposed that the maximum possible power is obtained from the tube when the plate voltage is reduced to zero at each oscillation; that is, when  $E_p = E_b$ . If  $I_g$  could be neglected, this would be the criterion for maximum output. However, it is characteristic of electron tubes employing a pure electron discharge that the factor  $(I_p - I/n)$  decreases more rapidly than  $nE_g$  increases, for any value of  $n$ , as  $E_p$  approaches  $E_b$  in amplitude.

It is possible to get 50 per cent efficiency from a tube if  $n$  be so chosen that  $(I_p - I_g/n) = I_p$  when  $E_g = E_b/n$ . Physically this implies that the fundamental constituent of the plate current must be greater by an amount  $I_g/n$  than the direct-current constituent; that is, the plate current wave must be flattened at both extremes of the alternation. It is a familiar experimental fact that a highly distorted or flattened wave of plate current leads to high efficiency, though not necessarily to high output. The ultimate criterion of the output is given by equation (5), and it is impossible to make any accurate generalizations concerning maximum output without analytical expressions for the characteristic surfaces of both plate and grid currents. It is conceivable that with values of  $n$  greater than 1, with a high plate-battery voltage, and with a negative potential applied to the grid, an efficiency greater than 50 per cent might be obtained.

By reference again to Fig. 4 it can be seen that for this particular tube, working at a plate voltage of 300 and supplying any output circuit for which  $n = 1$ , maximum output will be obtained at plate and grid voltages considerably smaller than  $E_b$ . The maximum value of the function  $\frac{n_1 E_g}{2} (I_p - I_g/n)$  occurs at  $E_g = 190$ , when  $P_o = 4.37$  watts. The maximum efficiency occurs at approximately the same point and is 29.5 per cent. It does not follow from this that the maximum efficiency occurs at the point of maximum output for any other value of  $n$  or of  $E_b$ . Without changing  $E_b$  the tube could be operated more efficiently with a higher value of  $n$ . In general, it is found that a tube operated at high plate voltages yields a large fundamental of plate current relative to the direct constituent, owing to the increased flattening of the wave form due to saturation and rectification effects.

Hence operation at higher voltage on the plate of this tube would give increased output, owing to the decrease in  ${}_1I_g$  which accompanies high values of  $E_b$ , and increased efficiency, due both to this and to the saturation effect.

## V. CURRENT OUTPUT

The current characteristics of the generator, such as are shown on Fig. 4, are entirely adequate for the prediction of the maximum power and efficiency that a tube is capable of delivering. In order to determine what constants of the output circuit will give the maximum output, an analysis of this output circuit is necessary. The plate and grid voltages depend upon the fundamental constituent of the output current  ${}_1I_a$ , which, in turn, depends upon  ${}_1I_p$ , the fundamental constituent of the plate circuit. In order to calculate the actual current in the output circuit which will dissipate the power furnished by the tube, this circuit must be correlated with the tube circuit so as to express the output characteristic, using as a parameter a variable of the output circuit instead of one of the exciting voltages. Thus we can derive from the general output characteristic of the tube a particular supply characteristic for the output circuit.

Consider the circuit shown in Fig. 2, which is merely the output circuit of the inductively coupled system shown in Fig. 1. Speaking again only in terms of the sinusoidal fundamental constituents  ${}_1I_p$  enters the circuit at  $P$ , divides between the path  $L_p R_p$  on one side and the path  $R_o C R_g L_g$  on the other side, leaving the circuit at  $F$ . Similarly,  ${}_1I_g$  enters the circuit at  $G$ , divides between  $R_g L_g$  and  $C, R_o, R_p, L_p$ , leaving the circuit at  $F$ . The fundamental of plate current,  ${}_1I_p$ , maintains a circulating current in the output circuit,  ${}_1I_p'$ , in comparison with which  ${}_1I_p$  itself may be negligibly small, if the series resistance,  $R = R_g + R_p + R_o$ , be small compared with the effective resistance of the divided circuit between  $F$  and  $P$ . If the current distribution in the circuit be determined only by the reactances—that is, if the resistance of each branch of the circuit be small compared with the reactance of that branch—the current  ${}_1I_p'$  will be equal in all parts of the circuit. Similarly, the fundamental of grid current maintains in the parallel circuit between  $G$  and  $F$  a circulating current  ${}_1I_g'$ , which opposes  ${}_1I_p'$  in all branches of the circuit. The useful output current can be thought of as the difference between these

$${}_1I_a = {}_1I_p' - {}_1I_g'$$

A convenient method of calculating the output current is the loss method, which was employed by Hazeltine<sup>3</sup> in considering briefly the entire distorted plate current wave. The net power supplied to the circuit, taking account of the grid losses, expressed above by the opposition of  ${}_1I_g'$  to  ${}_1I_p'$ , is given by equation (5):

$$P_o = \frac{n_1 E_g}{2} ({}_1I_p - I_g/n)$$

$P_o$  can be obtained graphically as a function of  $E_g$  from the current characteristic (such as Fig. 4).

$$P_o = f({}_1E_g) \quad (8)$$

But

$$\begin{aligned} {}_1E_g &= L_g \omega {}_1I_a \\ &= \frac{L_g}{\sqrt{(L_g + L_p + 2M)C}} {}_1I_a \end{aligned} \quad (9)$$

Moreover,

$$P_o = {}_1I_a^2 R. \quad (10)$$

where  $R = R_p + R_g + R_o$ . Eliminating  ${}_1I_a$  by substitution from (10) in (9).

$${}_1E_g = L_g \sqrt{\frac{P_o}{R C (L_p + L_g + 2M)}} \quad (11)$$

also

$$P_o = f({}_1E_g) \quad (8)$$

A simultaneous graphical solution of these two equations gives  $P_o$ , the power output, as a function either of the resistance or of the capacity in the output circuit.

$$\begin{aligned} P_o &= f'(C), R = \text{const.} \\ P_o &= f''(R), C = \text{const.} \end{aligned}$$

Since  ${}_1I_a = \sqrt{\frac{P_o}{R}}$  the output current follows immediately as a function of the variables of the output circuit.

In making a numerical proof of the foregoing theory for the tube described by the characteristics of Fig. 4 a slightly different method of attack was used in order to facilitate the calculation of the various harmonic constituents of the output current. The principal harmonics have been calculated and measured in order to indicate the insignificance of the error involved in assuming sinusoidal plate and grid voltages for a determination of the output characteristics.

<sup>3</sup>Loc. cit.

In the circuit of Fig. 2 let  $L_p = L_g$ ; then  $n = 1$  and Fig. 4 leads to an expression of the power which the tube will develop in this circuit. As a further simplification make  $M = 0$ , the mutual between  $L_p$  and  $L_g$ . Then the equation for the power output reduces to

$$P_o = \frac{1}{2} \frac{E_g}{2} ({}_1I_p - {}_1I_g),$$

and we can consider this circuit as being driven by an effective supply current,  ${}_1I_e$ , which is the difference between the fundamental of plate current and the fundamental of grid current.

$${}_1I_e = {}_1I_p - {}_1I_g.$$

Similarly, for any harmonic constituents of the plate and grid currents, the effective current is

$${}_kI_e = {}_kI_p - {}_kI_g.$$

Any constituent of the circulating output current can be found as the high-amplitude components of  ${}_kI_e$ , which flow through either branch of the divided circuit between  $F$  and  $P$  (Fig. 2). Obviously if  $\sqrt{R_p^2 + L_p^2 \omega^2} = \sqrt{R_g^2 + L_g^2 \omega^2}$  the effective supply current can be treated as if applied to the output circuit between  $F$  and  $G$  or between  $F$  and  $P$ . In either case, if we assume that the resistances of the separate branches are small compared with the reactances, a consideration of the relative impedances of the inductance branch and the inductance-capacity branch of the output circuit leads to the equality of any individual constituent of the output current in all parts of the output circuit, a fact mentioned previously in connection with the fundamental alone. If  ${}_kI_a$  be the  $k$ th frequency constituent of the output current flowing through the capacity branch of the circuit, then  ${}_kI_a$  is related to the  $k$ th constituent of the effective supply current by the relation

$$\frac{{}_kI_a}{{}_kI_e} = \frac{kL\omega}{\sqrt{R^2 + \left(2kL\omega - \frac{1}{kC\omega}\right)^2}} \quad (12)$$

assuming that the total impedance of either of the coupling coils is  $kL\omega$ . This is justifiable even when  $k = 1$ . Substituting  $\omega = \frac{1}{\sqrt{2LC}}$  this reduces to

$$\frac{{}_kI_a}{{}_kI_e} = \frac{k}{\sqrt{\left(k - \frac{1}{k}\right)^2 + \left(\frac{R}{2Lk\omega}\right)^2}}$$

For all harmonic constituents  $\left(\frac{R}{2Lk\omega}\right)^2$  is insignificant compared with  $\left(k - \frac{1}{k}\right)^2$  and this reduces to

$${}_k I_a = \frac{k^2}{2(k^2 - 1)} {}_1 I_o \quad (13)$$

For the fundamental constituent  $k=1$ ,  $\frac{R}{2L\omega}$  becomes important, and the output current is given by

$$\begin{aligned} {}_1 I_a &= \frac{2L\omega}{R} {}_1 I_o \\ &= \frac{1}{R} \sqrt{\frac{2L}{C}} {}_1 I_o \end{aligned} \quad (14)$$

An immediate deduction from these expressions is that the ratio of the fundamental in the antenna to any harmonic is practically inversely proportional to the antenna resistance. In other words, the impedance of the output circuit to the fundamental constituent of the supply current is merely the resistance of the circuit, while the resistance forms an insignificant part of its impedance to all harmonics. A small change in  $R$  thus makes a large change in the fundamental constituent relative to the corresponding change in the harmonic.

${}_1 I_o$  is known empirically from the curves of Fig. 4 as a function of the grid voltage amplitude:  ${}_1 I_o = f({}_1 E_g)$ . But  ${}_1 E_g = L\omega {}_1 I_a$ .  
 $= \sqrt{\frac{L}{2C}} {}_1 I_a$ . Eliminating  ${}_1 I_a$  between this and equation (14):

$$\begin{cases} {}_1 I_o = \frac{2RC}{L} {}_1 E_g \end{cases} \quad (15)a$$

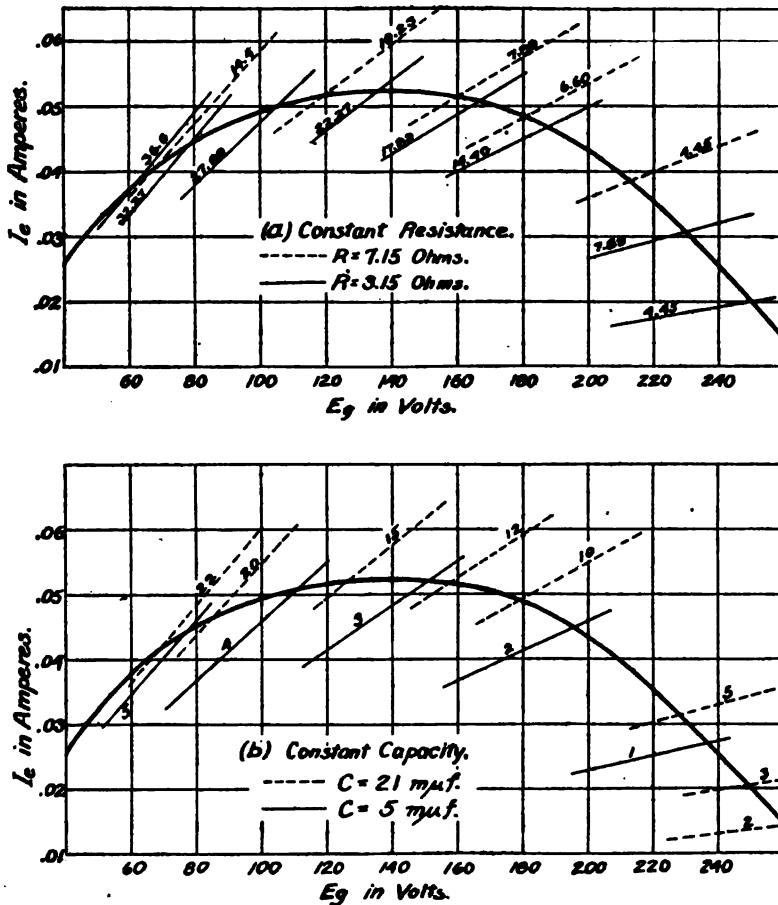
also—

$$\begin{cases} {}_1 I_o = f({}_1 E_g) \end{cases} \quad (15)b$$

Voltage characteristics of the output circuit showing  $E_g$  and  $E_p$  as functions of the resistance and capacity are furnished by graphical solutions of these equations. Fig. 5a shows such solutions for constant resistance and variable capacity and Fig. 5b, for constant capacity and variable resistance, for a circuit in which  $L=0.365$  millihenries,  $R=2.20$  ohms, and  $C=5.35$  millimicrofarads. These inductance and capacity values give a range of fundamental wave lengths of 3000 to 10 000 meters, which are large enough to make the capacitive reactance of the plate and grid coils insignificant compared with their inductive reactance. The



graphical solutions are accomplished by plotting equation (15b) from the output characteristic of Fig. 4, by direct subtraction of  ${}_1I_g$  from  ${}_1I_p$  and by plotting equation (15a) for a number of values of  $C$ , at a constant value of  $R$ , and for a number of values of  $R$  at a constant value of  $C$ . The points of intersection of these straight lines with the empirical function (15b) give  $E_g$  as a func-



output characteristics of the generator (Fig. 4) which are applicable to any output circuit. The current supply characteristic is shown in Fig. 7 for two values of antenna resistance,  $R=7.15$  ohms, and  $R=3.15$  ohms, and variable capacity. The effect of increasing the antenna resistance is to make the maximum output

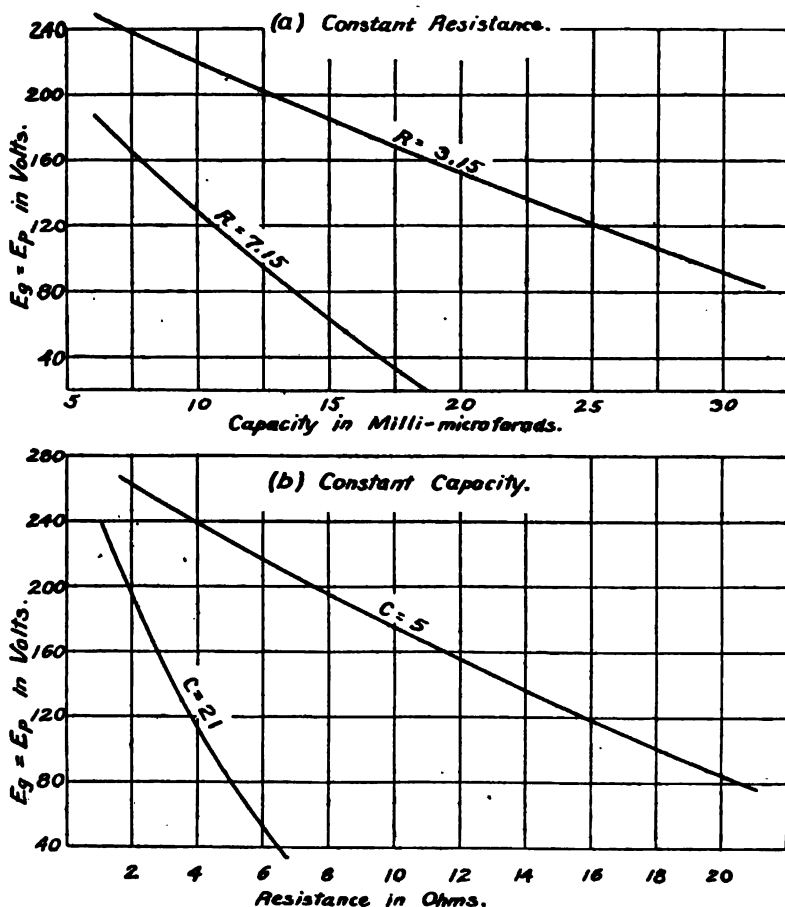


FIG. 6.—Voltage characteristics of output circuit

from the tube occur at lower capacity values. Upon Fig. 7 are shown, for purposes of comparison, the numerical values of  $I_a$ ,  $I_g$ ,  $I_c$ ,  $I_e$ . The harmonic constituents of plate and grid currents were calculated from the derived characteristic of Fig. 3 following the same method employed for the fundamental constituents.  $\kappa I_p$  and  $\kappa I_g$  were subtracted algebraically and the resulting  $\kappa I_e$  plotted as a function of  $C$  for one value of  $R$ ,  $R=3.15$  ohms, by virtue of the voltage characteristic, Fig. 6a.

The output currents for various capacity values follow immediately from the supply characteristic by substitution in equations (13) and (14). In Fig. 8 are shown theoretical curves, of output current, calculated in this manner. The points marked by circles show actual hot-wire ammeter readings, multiplied by  $\sqrt{2}$ , observed in a circuit having these constants, and supplied by the tube for which output characteristics shown on Fig. 4 had been obtained. The calculated and experimental results check quite closely, in view of the difficulties encountered in reproducing exactly the

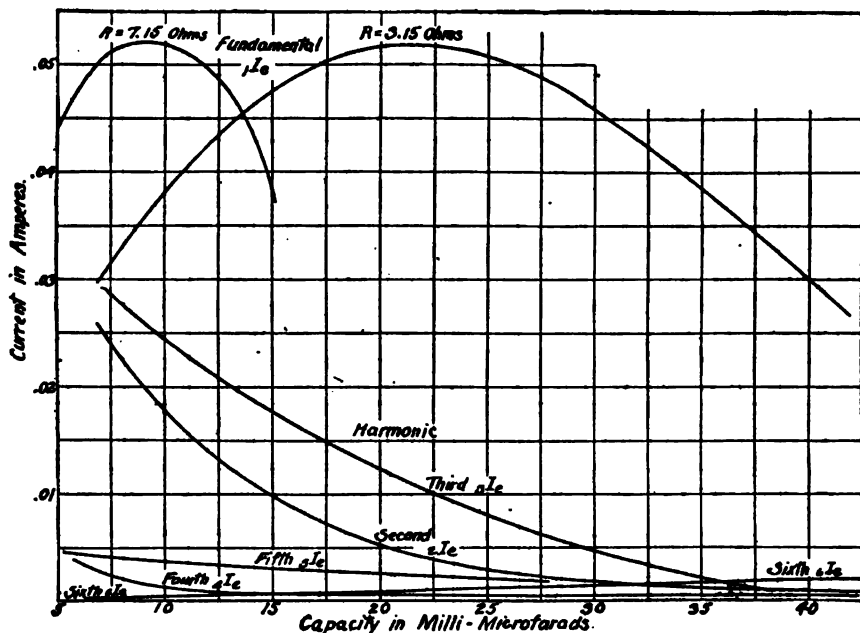


FIG. 7.—Supply current characteristics

operating condition of the tube from one set of measurements to the next.

It is a matter of experience that in any output circuit in which the ratio  $\frac{R}{L_a \omega} < 1$  the harmonics are practically insignificant in their effect upon a hot-wire ammeter. Consequently the readings of such an instrument can be taken as a true indication of the amplitude of the fundamental.

Upon Fig. 8 are shown calculated amplitude curves for the double and triple harmonics at  $R = 3.15$  ohms. The highest value reached by any harmonic is 3 per cent of the fundamental at

points well below maximum output. At maximum output all harmonics are entirely negligible.

Upon Fig. 9 are shown calculated curves for the double, triple, quadruple, and quintuple frequency harmonics, at a resistance of 3.15 ohms. These curves were calculated by substitution from Fig. 7 in equation (13). Measurements of the harmonics were made by the following method: A standard wave length circuit

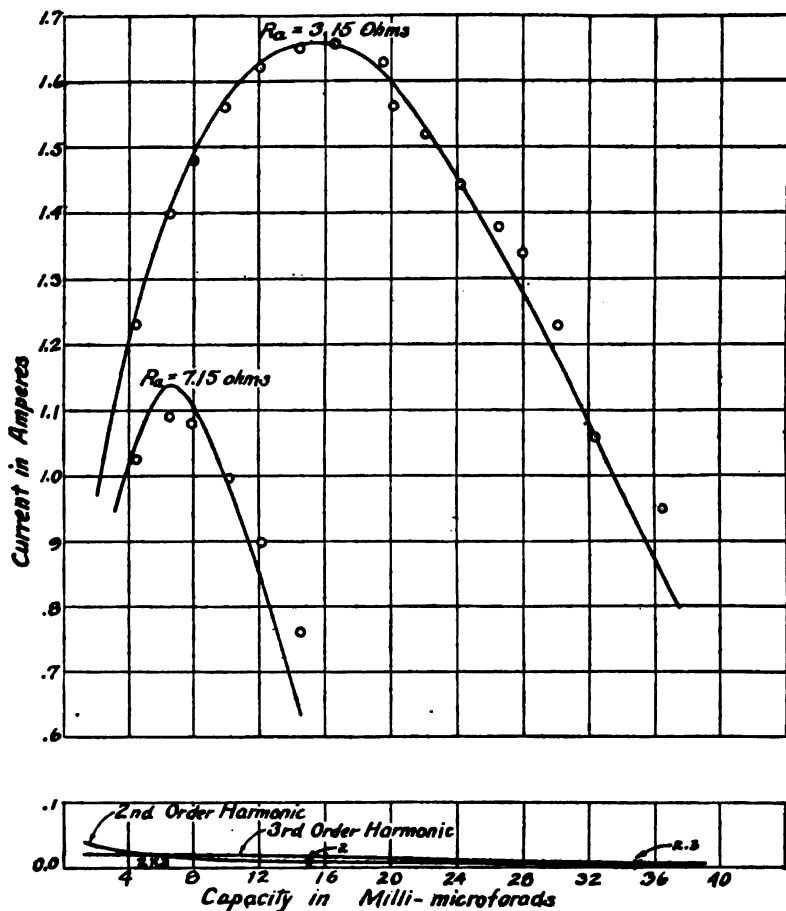


FIG. 8.—Output currents

with a 4-ohm vacuum thermoelement was coupled to a small wire loop connected in series with the output capacity. The wave meter was tuned to resonance with the various harmonic frequencies and the currents induced at these frequencies measured; then with the same coupling and a suitable noninductive resistance in series with the thermoelement the wave meter was tuned

to resonance with the fundamental. The resistance of the standard circuit being accurately known, the voltages induced in this circuit at the fundamental and at the harmonic frequencies could be computed. These voltages indicate the relative amplitudes of the harmonic constituents of the output current, provided that account is taken of the change in frequency from fundamental to harmonic. The relative amplitudes of the harmonics with respect to the fundamental being known, their absolute amplitudes could be calculated from the deflections of the hot-wire ammeter in the output circuit, assuming these to be due entirely to the fundamental. The double and triple harmonics are the

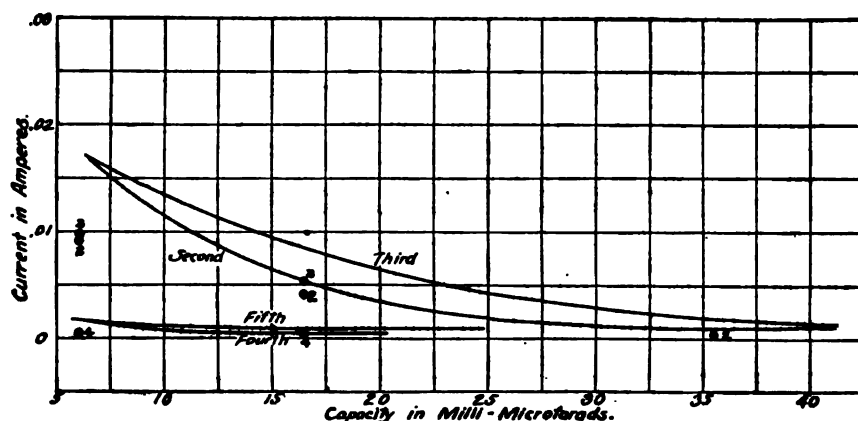


FIG. 9.—Harmonic constituents of output currents

only ones of any importance in the output circuit, owing to the extremely high impedance of this circuit to the higher multiples of the fundamental frequency.

Upon Figs. 10 and 11 are shown power and efficiency curves for the output circuit, giving the input on the tube and the output power as functions of the capacity for constant resistance, and of the resistance, for constant capacity. The calculated curves were obtained by multiplying  $I_s$  and  $E_p$  as obtained from Fig. 4, and expressing these products as functions of the constants of the output circuit by the use of the voltage characteristics (Fig. 6). This process is equivalent to taking the theoretical expression for  $I_s$ , equation (13), squaring, and multiplying by the resistance. The measured values of power were calculated from the hot-wire ammeter readings shown on Fig. 8.

It must not be inferred from the foregoing discussion that this analysis is recommended for use in toto as a method for testing

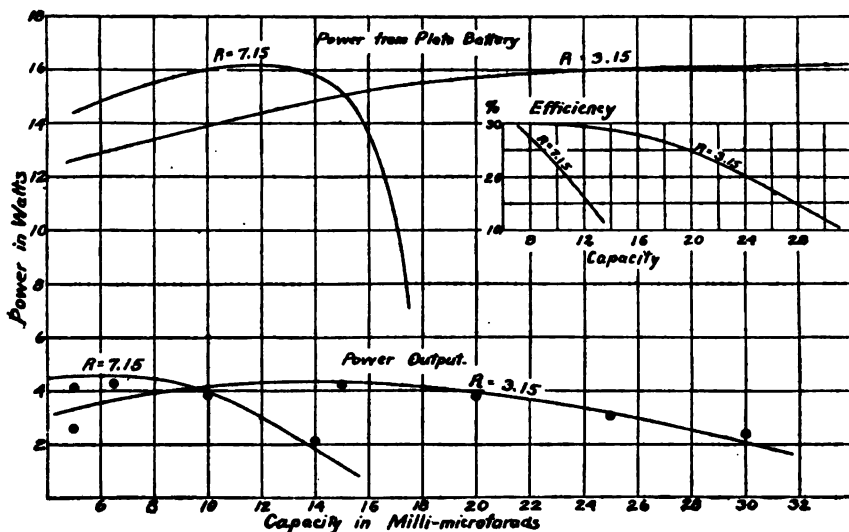


FIG. 10.—Power output—Constant resistance

and rating electron tubes. It is a cumbersome process to carry through the calculations from the derived characteristic of the

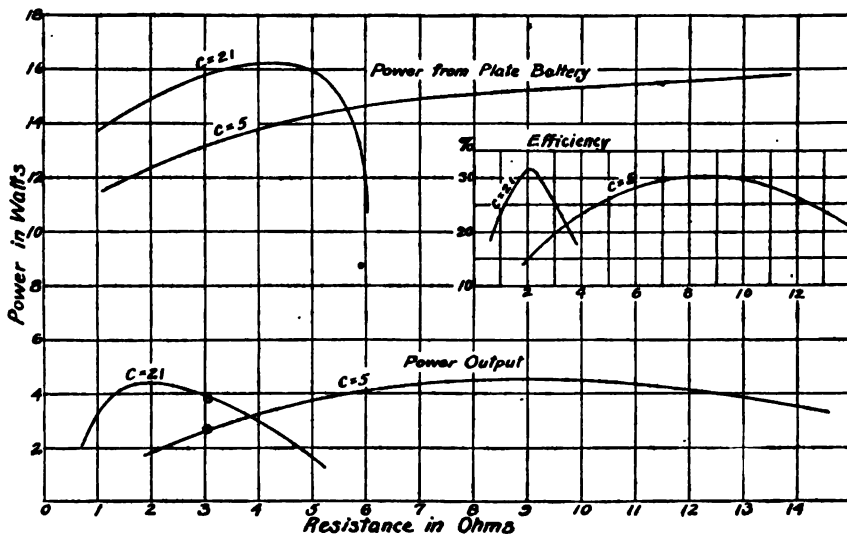


FIG. 11.—Power output—Constant capacity

tube to the output current as a function of the output resistance and capacity.

Experimental work is now in progress upon a method for obtaining by direct measurement the current characteristics of power tubes, as shown on Fig. 4. This will make unnecessary the use of harmonic analysis of the derived characteristics. The tube under test is excited by 60-cycle sinusoidal grid and plate voltages and mechanical resonance with this frequency is attained with a vibrating system which gives direct readings of the amplitudes of the fundamental constituents of the pulsating plate and grid currents. The power output from a tube can thus be predetermined as a function of  $n$  and of  $E_g$  for different operating conditions of filament emission and plate voltage. The results of such measurements for a variety of tubes will be given in a later paper.

The author desires to express appreciation of the assistance of H. A. Snow of this Bureau who made most of the measurements described in this paper.

WASHINGTON, July 11, 1919.





DEPARTMENT OF COMMERCE



# SCIENTIFIC PAPERS OF THE BUREAU OF STANDARDS

S. W. STRATTON, DIRECTOR

No. 356

## MICROSTRUCTURE OF IRON AND MILD STEEL AT HIGH TEMPERATURES

BY

HENRY S. RAWDON, Physicist

HOWARD SCOTT, Assistant Physicist

*Bureau of Standards*

ISSUED MARCH 15, 1920



PRICE, 10 CENTS

Sold only by the Superintendent of Documents, Government Printing Office  
Washington, D. C.

WASHINGTON  
GOVERNMENT PRINTING OFFICE

1920



# MICROSTRUCTURE OF IRON AND MILD STEEL AT HIGH TEMPERATURES

By Henry S. Rawdon and Howard Scott

## CONTENTS

	Page
I. Introduction.....	519
II. Method of revealing structural changes occurring at high temperatures..	521
1. Pure iron.....	521
2. Low-carbon steel.....	523
III. Nature and extent of surface changes upon heating.....	524
IV. Interpretation of results.....	526
V. Summary.....	527

## I. INTRODUCTION

The method of demonstrating the structure which exists in any particular metal or alloy at high temperatures by etching a polished sample while it is being heated at the desired temperature is quite familiar to metallographists. The usual method of procedure<sup>1</sup> is to heat the specimen previously polished for microscopic examination in a neutral atmosphere (hydrogen or nitrogen) to the desired temperature, then to admit the etching gas (chlorine, hydrochloric acid, or similar gas) for a few seconds, and after flushing out the etching gas with the neutral one, and finally to cool the specimen in the neutral atmosphere. The etch pattern produced by etching at any definite temperature is usually taken as a record of the microstructure which prevailed at that temperature. It has been pointed out frequently that changes in composition of the surface metal occur during the preliminary heating in the neutral atmosphere, so that the appearance produced by the etching at high temperature may not be truly representative of the condition of the interior of the specimens. To overcome this uncertainty the heating has at times been done in vacuo,<sup>2</sup> the etching gas admitted when the desired temperature was reached, and then pumped out; the specimen then cooled in vacuo.

<sup>1</sup> N. Gutowsky, *Über die Structur des Stählen bei hohen Temperaturen*, *Metallurgie*, 6, p. 743; 1909.  
H. Hanemann, *Etching at High Temperatures*, *Inter. Zeit. Metallographie*, 3, p. 176.

<sup>2</sup> N. Tschischewsky and N. Schulgin, *Jour. Iron and Steel Inst.*, 96, p. 189; 1917.

crystal, the boundaries of which can be faintly seen. Another network, outlining a second system of grains, is superimposed upon the twinned crystals. Fig. 1*b* shows similar features.

The network which delineates the straight-sided polyhedral twinned crystals is a record of the structure of the  $\gamma$  iron; that is, the form existing above the  $A_1$  transformation. The second network belongs to the crystal structure which prevails below this transformation, as is shown in specimens heated to a temperature below  $A_1$ . Only one network is developed in such a case; this is identical with the second pattern of specimens heated above  $A_1$ . The specimen shown in Fig. 2 illustrates this, and also shows that no characteristic crystal form corresponds to the so-called  $\beta$  range. The appearance is the same as that of specimens heated at a temperature well below  $A_1$  (Fig. 3), and also of samples polished and etched under ordinary conditions. This observation confirms that of Rosenhain and Humfrey<sup>6</sup> in this respect.

In Fig. 3 is shown the surface of a polished specimen heated to 700° C. The network outlining the arrangement of the crystals showed faintly even at this relatively low temperature.

The surface of freshly heated specimens often has a "matt finish" appearance, and when viewed at an oblique angle is seen to be considerably roughened. The volatilization which occurs at high temperature, as shown in Fig. 1*a*, accounts partly for the matt finish. It will be noted that the volatilization develops rather well-defined "etching pits" on the surface, by means of which the structural orientation within the twin crystals relative to the mother crystal is plainly shown. The roughened appearance is due largely to a buckling of the surface of the individual crystals. Fig. 4, which shows a section perpendicular to the polished surface which was exposed to the heat, demonstrates the distortion which occurs; the boundary—that is, the trace of the polished flat surface—originally rectilinear, now consists of a series of undulations. Specimens heated to a temperature a little below  $A_1$  show an irregular branching network within the grains themselves (Fig. 2*b*). This is often seen in pure iron after ordinary etching, for microscopic examination particularly, if the sample has been strongly heated previously; for example, specimens which have been heated several times for thermal analysis curves. Whether this bears any relation to the  $\beta$  change has not yet been determined.

<sup>6</sup> Loc. cit. See note 3.

a

b

**FIG. 1. —Microstructure of pure iron above the  $A_3$  transformation**

Both micrographs show the surface appearance of the same material, a specimen of which was heated for 30 minutes at  $950^\circ\text{C}$ . Two networks, indicative of two different crystalline arrangements, are to be seen. The one showing the twinned crystals is the structure prevailing above  $A_3$ ; the other, superimposed upon the first, corresponds to the structure at lower temperatures. Magnification, 500 diameters; "heat-etched"

a

b

FIG. 2.—*Microstructure of pure iron between the  $A_2$  and  $A_3$  transformations*

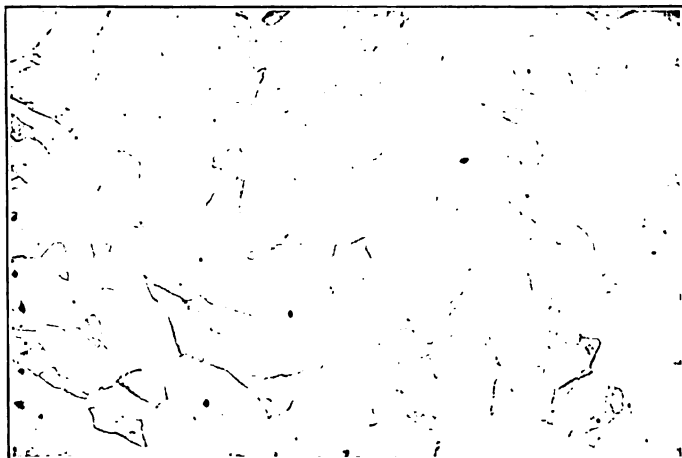
The polished specimen, represented by the two micrographs, was heated 30 minutes at 880° C, i. e., just below  $A_3$ . The appearance of the previously polished surface reveals the structure, which is of the same type as that prevailing at ordinary temperatures. The excessive volatilization at the margins of the grains has clearly developed the boundaries. Magnification, 500 diameters; "heat-etched"

FIG. 3.—*Microstructure of pure iron below the transformation temperatures*

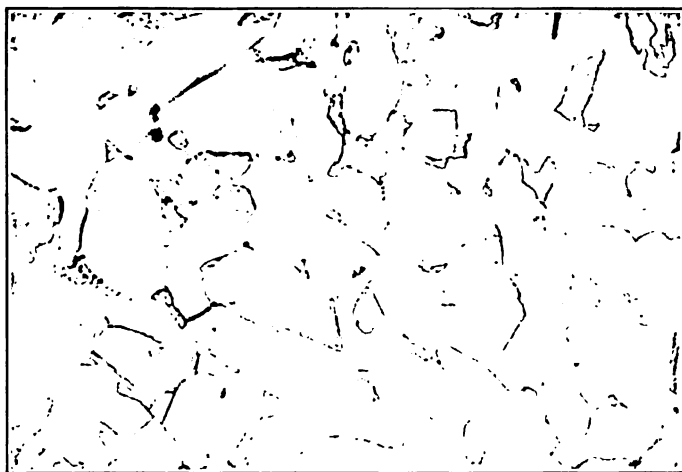
A polished specimen of the material was heated for 30 minutes at 700° C. The volatilization at the grain boundaries, though slight, has been sufficient to reveal the structure, which is of the same type as that existing between A<sub>2</sub> and A<sub>3</sub>. Magnification, 500 diameters; "heat-etched"

FIG. 4.—*Microstructure of pure iron at high temperatures*

The micrograph shows a section perpendicular to the polished and "heat-etched" surface of Fig. 1. A layer of electrolytic copper was deposited to preserve the edge during the polishing of the specimen. The originally rectilinear edge has been changed into a series of undulations by the volume changes at the transformation temperature. Magnification, 500 diameters; etching, 2 per cent alcoholic nitric acid



(a) The polished specimen was heat-etched by heating it for 30 minutes at  $700^{\circ}\text{C}$



(b) The polished specimen was distorted sufficiently to show slip-bands and then heat-etched as in (a). The slip-bands still persist

**FIG. 5.**—*Microstructure of low-carbon steel just below the  $A_1$  transformation. Magnification, 100 diameters*



(a) The material of Fig. 5a was slightly polished to remove the effects of heat-etching and etched with 2 per cent alcoholic nitric acid. The material shows the normal structure for this class of steel

(b) A specimen similar to Fig. 5a was etched with 2 per cent alcoholic nitric acid directly after being heat-etched. The surfaces etch and darken immediately

FIG. 6.—Microstructure of low-carbon steel just below the  $A_1$  transformation. Magnification, 100 diameters in both cases

(e) Magnification, 200 diameters. Both ferrite and pearlite are clearly shown

(b) Magnification, 500 diameters. The boundaries of the ferrite grains extend through the pearlite islands

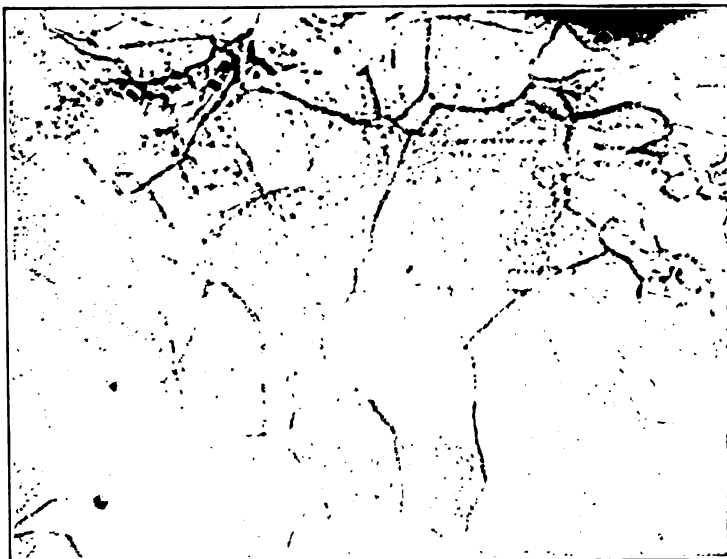
**FIG. 7.—Microstructure of low-carbon steel just above the  $A_1$  transformation**

The polished specimen was heat-etched by heating 30 minutes at  $760^{\circ}\text{C}$

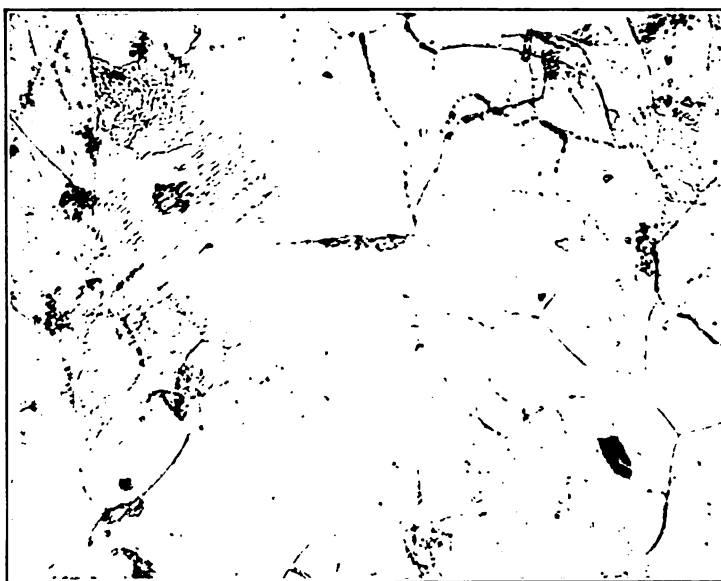
(a) The specimen of Fig. 7a was slightly polished and etched. The surface metal is pure ferrite

(b) Section of the specimen shown in (a), taken perpendicular to the heat-etched surface. A layer of electrolytic copper was deposited to protect the edge during polishing. The pearlite has been removed from the surface metal, by the heating, for a considerable depth

**FIG. 8.**—*Microstructure of low-carbon steel previously heated just above the  $A_1$  transformation. Etched with 2 per cent alcoholic nitric acid. Magnification, 100 diameters*



(a) The polished specimen was heat-etched by heating 30 minutes at 950° C. Two patterns corresponding to the  $\alpha$  and the  $\gamma$  forms (compare Fig. 2) are to be seen



(b) The polished specimen was etched with 2 per cent nitric acid before heating at 1000° C for 30 minutes. The original pearlite pattern shown by the first etching has persisted throughout the heating. Upon this two other patterns similar to those in (a) above, have been superimposed

FIG. 9.—Microstructure of low-carbon steel above the  $A_3$  transformation.  
Magnification, 500 diameters

(a) Heated for 30 minutes above the  $A_1$  transformation ( $760^\circ\text{C}$ )

(b) Heated for 30 minutes just below the  $A_2$  transformation ( $820^\circ\text{C}$ )

(c) Heated for 30 minutes above the  $A_1$  transformation ( $890^\circ\text{C}$ )

**FIG. 10.**—*Surface changes produced in low-carbon steel by heating in vacuo*

In each case a section perpendicular to a surface which had been heat-etched was taken. Magnification, 100 diameters; etching, 2 per cent alcoholic nitric acid.

(e) Carbonless surface layer.

(f) The average structure at the center of the specimen

FIG. 11.—*Surface changes produced in low-carbon steel by heating above the  $A_3$  transformation temperature*

A polished specimen was heated continuously for four hours above the  $A_3$  transformation temperature. The heat-etched surface was then protected with a deposit of electrolytic copper, and the specimen sectioned perpendicularly to this face. Magnification, 500 diameters; etching, 3 per cent alcoholic nitric acid

(a) Carbonless surface layer

(b) Average structure of the central portion

FIG. 12.—*Surface changes produced in low-carbon steel by heating above the  $A_3$  transformation temperature*

The specimen was used for a series of thermal curves and was heated four times above the  $A_3$  transformation temperature; the total period above this temperature was four hours. The specimen was treated as for Fig. 11, with which this figure should be compared. Magnification, 300 diameters; etching, 2 per cent alcoholic nitric acid

(a) The average surface condition is shown. The cementite envelopes disappear at some distance below the surface. In the original condition of the specimen they extended to the surface. Cementite has been removed from the surface

(b) In a few exceptional spots a thin white (probably ferrite) layer formed at the surface. Etching with hot sodium picrate showed that this layer was not cementite

FIG. 13.—*Surface changes produced in high-carbon steel by heating in vacuo above the  $A_3$  transformation temperature*

The specimen was prepared in a manner similar to those of Fig. 12. Magnification, 500 diameters; etching, 2 per cent alcoholic nitric acid



## 2. LOW-CARBON STEEL.

A synthetic low-carbon steel<sup>1</sup> of the following composition was used as representative of this class of material: Carbon, 0.18 per cent; silicon, 0.007 per cent. The steel has the following thermal characteristics:  $Ac_1$ , 738° C;  $Ac_2$ , 769° C;  $Ac_3$ , 840° C;  $Ar_3$ , 792° C;  $Ar_2$ , 769° C;  $Ar_1$ , 700° C. The specimens, which were first polished ready for microscopic examination, were heated in vacuo in the same manner as the pure iron; the sample was held in each case, approximately 30 minutes, at the maximum temperature. The specimens were heated to the following temperatures:

950° C.....	above $Ac_3$
760° C.....	above $Ac_1$
700° C.....	below $Ac_1$

Fig. 5 shows the appearance of a specimen heated to 700° C; that is, just below the transformation  $Ac_1$ . Even at this temperature the heat relief has been sufficient to clearly indicate the islands of pearlite. In Fig. 5b is shown the appearance of a specimen which, after polishing, was distorted enough to develop slip bands and then heated to 700° C. The slight roughening of the surface due to the slipping still persists at this temperature and shows that no marked volatilization has occurred at the surface.

Fig. 6a shows the specimen of Fig. 5a after it was polished slightly to remove the effects of the heat relief and then etched. The material has the usual appearance of low-carbon steel. When the specimen is etched directly after heating—that is, without any supplementary polishing—the surface darkens almost immediately and gives the appearance shown in Fig. 6b. A similarly pronounced darkening of ferrite upon etching is often observed when a specimen is finished on a polishing wheel which has been allowed to become quite free from water so that the surface heats considerably. Upon heating a polished specimen of this material above the  $Ac_1$  transformation the surface takes on the appearance shown in Fig. 7a, which is very similar to that produced by heating below  $Ac_1$ . The position of the preexisting pearlite islands is clearly indicated. It will be noted that the network which marks the boundaries of the ferrite crystals is now continuous through the pearlite areas instead of around them. This is best seen at a higher magnification as in Fig. 7b. When the surface is etched after heating—that is, without any polishing—the appearance is the same as is shown in Fig. 6b. However, when the surface is slightly

<sup>1</sup> An alloy of iron and carbon prepared according to the method given in Scientific Papers No. 266 was used.

polished and then etched, no darkening results, nor is there left any trace of the pattern developed by heat relief. The material which constitutes the surface is pure ferrite (Fig. 8a); all the pearlite has been removed to a considerable depth, as is shown in Fig. 8b, which shows a section of the specimen perpendicular to the polished face. The normal appearance of the material is shown in the lower portion of the micrograph. The boundary between the outer, or carbonless, metal and the inner normal material is very clearly defined. The change from the outer zone to the unchanged metal of the interior is very abrupt and not a gradual one.

In Fig. 9a is shown the pattern developed by heat relief on the polished surface by heating above the  $A_{c_1}$  transformation. The more clearly defined network corresponding to the  $\gamma$  condition is superimposed upon a less distinct one which shows the characteristic outlines of the  $\alpha$  crystals. In Fig. 9b this is more plainly seen. The polished specimen in this instance was etched to reveal its initial structure and then heated at  $1000^\circ\text{C}$  for 30 minutes; that is, well above the temperature of the  $A_{c_1}$  change. The roughening of the surface corresponding to the islands of pearlite, shown by the initial etching, still persists. Upon this pattern two others are superimposed; these show, respectively, the crystalline condition above  $A_{c_1}$  upon heating and below  $A_{c_1}$  on cooling. The twin crystal (Fig. 9b), which had its origin when the steel was in the  $\gamma$  state, is seen to cut through the preexisting islands of pearlite and to bear no relation to them. It should be borne in mind, however, that the carbide has been removed from the surface material, probably before the change to the  $\gamma$  state is brought about, as has been described above.

### III. NATURE AND EXTENT OF THE SURFACE CHANGES UPON HEATING

The magnitude of the change (apparently decarburization) which occurs in some samples (Fig. 8) makes the explanation offered by Howe<sup>8</sup> appear to be an inadequate one. In order to clearly show the nature of the change and to test out the explanation, a series of specimens of the low-carbon steel previously used were heated in vacuo for equal periods at the following temperatures:

760° C.....	above $A_{c_1}$ ,	for 30 minutes
820° C.....	just below $A_{c_1}$ ,	for 30 minutes
880° C.....	above $A_{c_1}$ ,	for 30 minutes

<sup>8</sup> Loc. cit. See note 4.

The specimens were cooled in the furnace at the same rate as the previous ones. In each case the carbonless layer varies considerably in thickness on the same specimen; the maximum thickness of this changed layer in specimens heated at the three temperatures given above is shown in Fig. 10. In the specimen heated at the lowest temperature, the decarburized layer is more pronounced than in those heated for the same period at higher temperatures. This is not to be attributed to a greater loss of carbon at the lower temperature, but rather to an increased rate of diffusion of carbide in iron at higher temperatures, by which any change at the surface due to loss of carbon is masked by a replenishment from the interior by diffusion.

In Fig. 11 is shown the condition at the surface and near the center of a specimen (the material is the low-carbon steel previously used) heated continuously for four hours above  $A_{c_1}$ ,  $990^{\circ}\text{C}$  was the maximum temperature. The structure of a sample of the same material used for a series of four thermal curves, and which was above the  $A_{c_1}$  temperature for a total of four hours, is shown in Fig. 12. The thickness of the changed surface layer of the sample heated intermittently is somewhat greater than that of the specimen heated continuously for four hours above the  $A_{c_1}$  transformation temperature. The carbon content of the interior, as estimated from the structure, is slightly less in the specimen heated continuously, however, than in second one. This apparently contradictory behavior of the specimen most strongly heated is to be interpreted as further evidence of the part played by diffusion in masking the change which occurs at the surface. By comparing Figs. 10a and 11a it will be noted that a much more pronounced change is produced in the surface metal for a short period at the lower temperature (30 minutes at  $760^{\circ}\text{C}$ ) than by prolonged heating at a higher one (240 minutes at  $990^{\circ}\text{C}$ ). Whether this difference in the rate of diffusion is one due entirely to temperature or partially to the allotropic condition of the iron,  $\alpha$  or  $\gamma$ , can only be conjectured.

In Fig. 13a, is shown the surface change induced in a high-carbon steel by heating four times in vacuo to a temperature above the  $A_{c_1}$  transformation ( $950^{\circ}\text{C}$ ). The steel was of the following composition: Carbon, 1.28 per cent; manganese, 0.23 per cent; phosphorus, 0.017 per cent; sulphur, 0.017 per cent; silicon, 0.23 per cent. The cementite grain envelopes do not extend entirely to the surface as they did originally, but gradually diminish in thick-

ness and disappear at some distance below the surface. In no case was an accumulation of cementite found, as Howe's explanation requires. In a few areas a very thin layer of ferrite was found to have formed, as is shown in Fig. 13b. The conclusion is evidently warranted that the change of structure of the surface metal heated in vacuo represents loss of carbon.

#### IV. INTERPRETATION OF RESULTS

The question may very properly be asked as to what extent the indications of the etchings, used to reveal the structure of steel at high temperature, are vitiated by the changes of composition which occur in the surface metal upon heating. The experimental results discussed in the previous sections show that no decarburization below the temperature of  $A_1$  transformation can be detected. This is due to the physical form in which the carbon exists. Not until the carbon (as carbide) is in the state of a solid solution in the iron—that is, above  $A_1$ —is there any appreciable change in the exposed surface metal. Below the  $A_1$  transformation the carbon occurs in the form of a definite crystalline compound, and the loss upon heating may be entirely neglected.

A very marked change, however, occurs upon heating a specimen just above the  $A_1$  transformation. The carbon passes from the form of crystalline cementite to a solution (of cementite) in the iron. In this form it quite readily volatilizes from the surface, so that a pronounced carbonless layer is soon formed in specimens (low-carbon steels) that are held for periods no greater than 30 minutes at this temperature. The method of heat etching, however, serves to record the structure both before and after the change has taken place. The pronounced differential expansion of pearlite and ferrite at the  $A_1$  transformation will account partially for this. The fact that at temperatures below  $A_1$  the structure is clearly revealed by heat etching, however, shows that this is not the sole cause, but that the slight general volatilization which occurs, together with the slight differences in the rate of thermal expansion of pearlitic steel and iron (ferrite) are sufficient to record clearly and definitely the structure of the metal. The volatilization of iron is pronounced enough at the crystal boundaries to clearly show them. Across the face of the crystals, however, there is very little loss, as is shown by the persistence of slip bands upon heating. That the ferrite is changed somewhat, however, is shown by its increased tendency toward oxidation.

Upon slight etching with nitric acid, a very pronounced oxide film readily forms, so that the ferrite is colored very dark.

Specimens which are heated to temperatures higher than the  $A_1$  transformation show a carbonless layer which becomes less pronounced as the temperature is increased. This is properly to be attributed to the increased rate of diffusion of carbide in iron, by which the change at the surface is masked. The results obtained by etching specimens at the higher temperatures (heat etching or otherwise) are more truly indicative, therefore, of the structure of the interior than those at lower temperatures; for example, just above  $A_1$ . That the loss of iron by volatilization across the face of the crystals is very slight, even at high temperatures, is shown by the persistence of the slight roughening due to preliminary etching throughout the entire period of heating. The loss by volatilization is of a magnitude sufficient to show the crystalline structure by the production of "etching pits;" at the crystal boundaries the loss is much greater. In addition the carbide is removed to a very appreciable depth on all the exposed faces of the specimen.

## V. SUMMARY

1. When polished metal specimens are heated in vacuo, a record of the structure which exists at the particular temperature used is inscribed on the polished surface of the specimen. This record consists of a slight roughening due to volatilization and to a slight buckling of the surface due to the volume change which forms part of the transformation. The terms "heat relief," "heat etching," and "vacuum etching" have been applied to this means for developing the microstructure.

2. By means of heat relief the structure of iron and steel at high temperatures is readily revealed. This is a much simpler method than high-temperature etching, often used. It appears probable that much of the effect usually attributed to etching at high temperature is due to the heating itself.

3. An appreciable change of composition and structure of the surface metal occurs in steel upon heating. This is very pronounced just above the  $A_1$  transformation, and becomes less so upon heating to higher temperatures due to the increased rate of diffusion of carbon (as carbide) in iron, with increase of temperature. The structure revealed on the surface by heat relief or by high-temperature etching is less representative of the interior, at

temperatures just above the  $A_1$  transformation than at any other temperatures.

4. The change in composition of the surface layer of steel heated in vacuo to high temperatures is to be explained as due to volatilization of the carbide. No appreciable change takes place until the carbide enters into solid solution in the iron, that is, above the  $A_1$  transformation.

5. The volatilization of iron from the surface, upon heating, is very slight. Polished specimens of iron and steel, etched before being heated, retain the slight roughening due to the etching even after pronounced heating. The volatilization of ferrite at the crystal boundaries is much more pronounced than across the face of the crystal.

WASHINGTON, July 14, 1919.

MAR 19 1920



DEPARTMENT OF COMMERCE

---

# SCIENTIFIC PAPERS OF THE BUREAU OF STANDARDS

S. W. STRATTON, DIRECTOR

---

No. 357

CONSTANTS OF RADIATION OF A UNIFORMLY  
HEATED INCLOSURE

BY

W. W. COBLENTZ, Physicist  
*Bureau of Standards*

---

ISSUED JANUARY 16, 1920



PRICE, 5 CENTS

Sold only by the Superintendent of Documents, Government Printing Office  
Washington, D. C.

---

WASHINGTON  
GOVERNMENT PRINTING OFFICE

1920





# CONSTANTS OF RADIATION OF A UNIFORMLY HEATED INCLOSURE

By W. W. Coblentz

## I. THE COEFFICIENT OF TOTAL RADIATION

In a previous paper<sup>1</sup> was given a value of the coefficient, or so-called Stefan-Boltzmann constant, of total radiation of a uniformly heated inclosure, or so-called black body. This value ( $\sigma = 5.72 \times 10^{-12}$  watt cm<sup>-2</sup> deg<sup>-4</sup>) was obtained by applying a correction, for reflection losses, to the data given in Table 6 of a previous publication.<sup>2</sup> This correction for losses by reflection was taken to be 1.2 per cent, irrespective of whether the surface of the receiver was covered with lampblack (soot) or electrolytically deposited platinum black. Subsequently, the data were recalculated (using the proper corrections for reflection of lampblack and of platinum black) and the results published elsewhere,<sup>3</sup> the intention being to give the details more fully in this Bulletin. This is the object of the present paper, which gives further experimental data on atmospheric absorption, and also a discussion of other data, recently published.

The data previously summarized<sup>4</sup> are based upon about 600 independent measurements, made with 10 receivers which, as already stated, were covered with either (1) a thin layer of lampblack or platinum black, smoked with soot, or (2) covered simply with an electrolytic deposit of platinum black.

The data obtained with receivers Nos. 8 and 9 are not included in the final value because, at the time the measurements were made, the apparatus was known to be defective, and hence the reliability of the results would be open to question.

To the data obtained with 10 receivers,<sup>5</sup> a correction of 1.2 per cent, for losses by reflection, were applied to measurements made with receivers covered with lampblack (soot), and a correction of 1.7 per cent to measurements made with receivers covered with platinum black. The reflection from a receiver covered with

<sup>1</sup> Bulletin, Bureau of Standards, 12, p. 553; 1916.

<sup>2</sup> Coblentz and Emerson, Bulletin, Bureau of Standards, 12, p. 549; 1916.

<sup>3</sup> Proc. Nat. Acad. Sci., 8, p. 504; 1917.

<sup>4</sup> Bulletin, Bureau of Standards, 12, p. 549; 1916 (Table 6).

<sup>5</sup> Erroneously stated to be nine receivers in Proc. Nat. Acad. Sci., 8, p. 504; 1917.

platinum black, then smoked, is 1.2 per cent. These corrections were determined by direct measurements upon some of the receivers, and by comparison of the surfaces of the other receivers with samples of lampblack whose reflection losses had been determined in a previous investigation.<sup>6</sup>

As mentioned in the first description of the apparatus used in making these measurements,<sup>7</sup> the edges of the slits over the sides of the receiver were beveled, and painted with lampblack on the beveled surface. This should absorb the radiations reflected in that direction from the receiver. Nevertheless, at this writing, it is an open question whether the loss by reflection is as large as it would be if no beveled edges were present. This might cause a slight over correction (say 0.1 per cent) of the data as now published, but it would be no greater than the variations in the reflectivity of the various surfaces from the mean value herein adopted.

The original data (from Table 6, loc. cit.), corrected for reflection as just described, are assembled in Table 1. It does not include a set of measurements made on an unblackened porcelain radiator, (Series CXLVIII to CLI). However, applying a correction (amounting to 1 per cent) for lack of blackness,<sup>8</sup> the observations are close to those obtained on a blackened radiator.

The value of the coefficient of total radiation, after applying the corrections just mentioned is

$$\sigma = (5.722 \pm 0.012) \times 10^{-12} \text{ watt cm}^{-2} \text{ deg}^{-4}.$$

No correction was made for atmospheric absorption, in view of the fact that the measurements had been made in the winter when the humidity was low. Furthermore, by means of phosphorous pentoxide, the water vapor had been removed from the apparatus, which was of quite air-tight construction.

Subsequent to this investigation, further consideration was given to the question of absorption by dry air.<sup>9</sup> The correction for absorption by dry air was determined by observing the transmission through a brass tube 6 cm in diameter and 51 cm long, the ends of which were covered with windows of clear rock salt. This tube was evacuated with an oil pump and then filled with air which had been passed through phosphorous pentoxide. It therefore contained only carbon dioxide, which may cause a small amount of absorption.

<sup>6</sup> Bulletin, Bureau of Standards, 9, p. 283; 1913.

<sup>7</sup> Bulletin, Bureau of Standards, 12, p. 507 (Fig. 2); 1916.

<sup>8</sup> Bulletin, Bureau of Standards, 12, p. 571; 1916.

<sup>9</sup> Loc. cit. See note 3.

TABLE 1.—Summary of the Dimensions of the Receivers and of the Slits, the Kind of Absorbing Surfaces, and the Results Obtained with Each Receiver

(Receivers 1, 3, and 5 are of manganin or "therio"; the others are of platinum)

Re- ceiver No.	Length between potential terminals	Width of strip	Width of slit	Serial number of test	Value of radi- ation con- stant $\times 10^{13}$	Ibld., cor- rected for reflec- tion	Remarks
1.....	mm 23.095	mm 2.545	mm 2.150	X to XIV (inc.).....	5.600	5.667	Repainted and smoked; alu- minum slits.
	22.985	.....	2.537	LXXXII.....	5.819	5.889	Repainted and smoked; brass slits.
2.....	24.354	3.584	3.192	IV to IX.....	5.67	5.756	Platinum black; aluminum slits.
3.....	24.910	5.035	4.990	XVI to XXV.....	5.50	5.566	Painted and smoked; alumi- num slits.
			5.000	LXXXII to LXXXI.....	5.607	5.674	Resmoked.
	21.620	.....	4.953	CXL to CXLIII.....	5.653	5.720	Repainted and smoked; brass slits.
5.....	18.561	5.667	5.640	XLVII to XLIX.....	5.736	5.804	Painted and smoked; brass slits.
			5.638	LXIII to LXVI.....	5.725	5.793	Repainted and smoked.
6.....	20.061	6.025	5.979	LII.....	5.533	5.627	Platinum black; brass slits.
			5.983	LIV to LXII.....	5.691	5.759	Platinum black; smoked.
7.....	24.659	7.965	7.952	LXXXIII to LXXXVIII.....	5.574	5.641	Platinum black; painted; smoked on front; brass slits.
			7.966	LXXXIX to XCVI.....	5.586	5.653	Repainted; smoked on both sides.
			7.964	XCVII to XCVIII.....	5.585	5.652	Front resmoked, thick layer.
			7.959	CXXIII to CXXVI.....	5.682	5.750	Paint removed; coated with platinum black; smoked on both sides.
10.....	19.947	6.8	6.721	CKV to CKX.....	5.726	5.822	Platinum black, excellent coat; brass slits.
				CXXI to CXXII.....	5.746	5.814	Platinum black; smoked.
11.....	22.389	6.5	6.481	CXLIV to CXLVII.....	5.663	5.758	Platinum black, best coat of all; brass slits.
				CXLVIII to CLI.....	5.576	.....	Unblackened radiator.
12.....	22.385	6.4	6.365	CLKVII to CLKX.....	5.673	5.741	Platinum black; smoked on both sides; brass slits.
			6.326	CLXXI to CLXXIV.....	5.625	5.692	Platinum black; resmoked; aluminum slits.
13.....	21.418	5.5	5.340	CLXIII to CLXVI.....	5.593	5.660	Platinum black; smoked on both sides; aluminum slits.
Mean value .....					5.722 ±0.012		

The transmission was determined by noting a series of galva-  
nometer deflections caused by black-body radiation (800° C)  
which was passed through the evacuated tube and focused upon  
a linear thermopile of bismuth-silver. Immediately thereafter a  
stopcock was opened and either dried or undried air was per-  
mitted to enter, under atmospheric pressure.

Using air containing 9.95 g of water per cubic meter, the absorption amounted to about 0.9 per cent.

Using dry air, the average value of the absorption (3 series of measurements) was about 0.09 per cent, which is the magnitude of the errors of observation. From this it is to be concluded that, in view of the fact that in the measurements of the radiation constant the column of dry air was less than 50 cm, if any correction is to be made to the aforementioned value of the radiation coefficient,  $\sigma$ , it can hardly be greater than 0.1 per cent.

## II. DISCUSSION OF OTHER DATA

Recently a new determination <sup>10</sup> of this radiation constant was brought to my attention, and in view of the fact that this paper appears to contain inaccurate statements concerning my own work, a few comments are permissible. For example, the statement is made that the only novelty in the apparatus employed by Coblenz and Emerson <sup>11</sup> was a thermopile with a continuous receiving surface; which is of secondary importance. As a matter of fact, the crucial part of the apparatus was a receiver with potential terminals attached thereto, at a sufficient distance from the ends to avoid the question of heat conduction to the electrodes. These potential wires, which were from 0.003 to 0.02 mm in diameter, accurately defined the length of the central part of the receiver which was utilized in the measurements. By exposing the whole length of the receiver to radiation, conduction losses did not enter the problem. The writer is not aware of any one having used a similar apparatus which compares with this receiver in nicety of construction, and reproducibility of results under given conditions.

The receiver used by Kahanowicz was placed at the center of a spherical mirror <sup>12</sup> with an opening in one side to admit radiation. In this manner the correction for reflection was eliminated. The shutter was close to the receiver. If its temperature was different from that of the water-cooled diaphragm, which was before the radiator, errors in the radiation measurements would occur. As mentioned in previous papers,<sup>13</sup> the shutter should be placed between the water-cooled diaphragm and the radiator, to avoid

<sup>10</sup> Kahanowicz, *Nuovo Cimento* (6), 18, p. 149, 1917; Naples.

<sup>11</sup> Bulletin, Bureau of Standards, 12, p. 506; 1916.

<sup>12</sup> Bulletin, Bureau of Standards, 12, p. 509; 1916. Use of hemispherical mirrors is discussed.

<sup>13</sup> Bulletin, Bureau of Standards, 12, p. 514; 1916.

a change in surroundings facing the receiver when the shutter is raised for making the radiation measurements.

The temperature range was from 260 to 530° C. The distance from the radiator to the receiver was 35 to 55 cm. A series of 28 measurements gave an average value of  $\sigma = 5.61 \times 10^{-12}$  watt  $\text{cm}^{-2}$   $\text{deg}^{-4}$ . Of this number 11 gave a value of  $\sigma = 5.7$ . Out of a series of 4 measurements made in December, 1916, with the distance  $d = 56$  cm, 3 gave a value of  $\sigma = 5.7$ .

No corrections were made for atmospheric absorption, which for the temperatures used is not negligible. In a previous paper<sup>14</sup> it was shown that on removing the moisture (vapor pressure of 10 to 12 mm) from a column of air 52 cm in length, the radiation constant was increased from  $\sigma = 5.41$  to 5.55, or about 2.6 per cent. For the spectral region transmitted by rock salt, to  $15\mu$ , the experimental data, just described, indicate an absorption of about 0.9 per cent, depending upon the vapor pressure. Other measurements mentioned in the paper just cited indicate an absorption of 2 to 3 per cent of the radiations emitted by a black body at 1000° C for the average humidity of Washington.

Dr. H. H. Kimball, of the U. S. Weather Bureau, very kindly sent me comparative data showing that the vapor pressures at Naples are considerably higher than at Washington. From these data it would appear that the corrections for atmospheric absorption must be at least 1 per cent. For the low temperatures at which the radiator was operated, a fair estimate of the correction to the radiation data obtained by Kahanowicz is 1.5 to 2 per cent, or a value of  $\sigma = 5.69$  to  $5.72 \times 10^{-12}$  watt  $\text{cm}^{-2}$   $\text{deg}^{-4}$ . In other words the Naples value of the coefficient of total radiation is comparable with other recent determinations<sup>15</sup> which indicate a value of  $\sigma = 5.7 \times 10^{-12}$  watt  $\text{cm}^{-2}$   $\text{deg}^{-4}$ .

### III. THE CONSTANT OF SPECTRAL RADIATION

During the past year a further examination was made of the accuracy of the factors used in converting the previously observed<sup>16</sup> prismatic spectral-energy data into the normal energy distribution. The graphical methods previously employed were checked, and similar factors were obtained by computation, using the first differential of the dispersion formula, which best repre-

<sup>14</sup> Bulletin, Bureau of Standards, 12, p. 576; 1916. See Table 3, Series CLXXX to CLXXXII.

<sup>15</sup> Millikan, Phys. Rev., 7, p. 379, 1916, quotes a value of  $\sigma = 5.67$ , by Westphal.

<sup>16</sup> Bulletin, Bureau of Standards, 10, p. 2; 1913.

sents the observed refractive indices of fluorite.<sup>17</sup> These refractive indices were obtained from consideration of all the available data, which in the region of 1 to  $2\mu$  are represented by the curve published by Langley and Abbot.<sup>18</sup> The best dispersion formula is that of Paschen.<sup>19</sup> However, owing to incompleteness of the formula, the graphical method is just as accurate as is the method of computation.

The conclusion arrived at is that the spectral radiation constant,  $C_2 = 14\,353$  micron degrees, determined some years ago,<sup>20</sup> remains unchanged. However, at this writing there is some doubt as to whether some of the corrections then applied should have been made, giving a value of  $C_2 = 14\,369$ . In view of the uncertainty of the temperature scale, and of the different experimental methods employed, the mean of the values of this constant, which have been used by Reichsanstalt and by this Bureau, viz,  $C_2 = 14\,325$ , is probably close to the true value. For example, from a consideration of related experimental data, as will be shown in a forthcoming paper,<sup>21</sup> the above determined value of  $\sigma = 5.72$  indicates a value of  $C_2 = 14\,320$ . The observations on the coefficient of total radiation were made at less than  $1000^\circ\text{C}$ , and hence do not require a correction to the temperature scale. Moreover, because of the difficulty in eliminating reradiation, the observed values of diffuse reflection, of long wave-length radiation, are higher than the true value.

#### IV. SUMMARY

The object of this paper is to give experimental data on atmospheric absorption as it affects the measurements of the radiation constants.

The paper gives also a recalculation of the coefficient of total radiation of a uniformly heated inclosure, taking into consideration all losses by reflection from the receivers, as well as losses by atmospheric absorption. The value of the coefficient of total radiation on recalculation is

$$\sigma = (5.722 \pm 0.012) \times 10^{-12} \text{ watt cm}^{-2} \text{ deg}^{-4},$$

which is the same as previously published.

<sup>17</sup> Bulletin, Bureau of Standards, 10, p. 39. In table 5, the value of the refractive indices at  $\lambda = 4.0\mu$ ,  $4.6\mu$ , and  $5.0\mu$  should be, respectively, 8, 7, and 8, instead of 3, 5, and 6, in the last decimal place, as previously published.

<sup>18</sup> *Annale, Astrophys. Obs.*, 1, p. 222, Pl. XXVIB.

<sup>19</sup> Paschen, *Ann. der Phys.*, 4, p. 299, 1901: Pl. II.

<sup>20</sup> Bulletin, Bureau of Standards, 18, p. 466: 1914.

<sup>21</sup> Bureau of Standards Scientific Paper, *Methods of Computing and Intercomparing Radiation Data*.

The effect of atmospheric absorption upon data obtained at Naples is discussed, and it is concluded that, if a correction is made for absorption by water vapor, the value of  $\sigma$ , obtained at that station, is of the order of  $\sigma = 5.7$ . This is about the average value of all observers when corrections are made for atmospheric absorption.

The present status of the constant of spectral radiation is discussed, and the conclusion arrived at is, that, in view of the uncertainty of the temperature scale, and of the different experimental methods used, the mean of the values of this constant, which have been used by Reichsanstalt and by this Bureau, viz,  $C_s = 14\,325$ , is probably close to the true value.

WASHINGTON, August 11, 1919.









# CONCERNING THE ANNEALING AND CHARACTERISTICS OF GLASS

By A. Q. Tool and J. Valasek

## CONTENTS

	Page
I. Introduction.....	537
II. Annealing temperature, and some characteristics in the annealing range....	539
1. Optical method.....	539
2. Measurements of retardation.....	542
3. Critical range.....	547
III. Annealing time.....	555
1. Measurement of the relaxation time by an applied load.....	557
2. Measurement of the relaxation time by an optical method.....	559
3. Application of relaxation time.....	561
IV. Cooling procedure.....	563
V. Conclusions.....	568
VI. Summary.....	569
VII. Bibliography.....	570

## I. INTRODUCTION

To anneal glass quickly and efficiently is one of the many problems met in its production. The purpose of annealing is to avoid or remove all stresses which might be permanent, and injurious after the glass is in use. The harmful effects produced by such stresses are the variations in the refractive index, which cause double refraction, and the tendency of the glass to warp or break.

The problems which arise in annealing glass for different uses may differ in particular cases but in general they are much the same. The actual annealing procedure is often varied materially, depending upon the degree of annealing required, on the nature of the glass, and the character of the pieces. Consequently, to plan the most efficient process, it is necessary to consider all the factors entering into the particular annealing problem. For this purpose, a thorough knowledge of the general nature of glass is important. Furthermore, it is desirable to develop and standardize a number of simple tests which will make it possible to determine the points at which changes in the annealing procedure

can be made to advantage. This paper is the result of an investigation concerning the characteristics of glass in the usual annealing range and some of the general problems met in annealing.

Three necessary factors enter into any process for annealing glass—the temperature at which it is annealed, the corresponding period of annealing, and the corresponding rate and mode of cooling. For brevity's sake these factors will be referred to as the “annealing temperature,” the “annealing time,” and the “cooling procedure.” The annealing temperature is the constant and uniform temperature at which any stresses that may exist in the glass are allowed to relax. The period during which the glass is held at this temperature is the annealing time. During this time, temperature uniformity and constancy are extremely important. The length of the annealing time is determined by the magnitude of the initial stresses, the chosen standard of annealing and the relaxation time. The cooling procedure is important since, if the cooling is not controlled properly, it will lead to reintroduction of permanent stresses while the glass is hardening, or to breakage, due to temporary stresses, after it has hardened sufficiently.

As intimated, the above factors may be varied considerably, but there is some definite treatment of any particular piece of glass which will give the desired results most quickly and efficiently. The range of temperature, however, within which it is practicable to anneal any particular type of glass is narrow. If the temperature is too low, the stresses will relax too slowly, consequently a much longer total time will be required to obtain the desired degree of annealing, although a higher initial cooling rate is permissible. If the temperature is too high, the danger of deforming the glass or changing its character is increased. The initial cooling, also, must be slow, and very accurately controlled to prevent the reintroduction of permanent stresses. The length of the annealing time and the subsequent rate of cooling depend on the annealing temperature selected, and on the degree of annealing desired.

For ordinary glassware in which the chief consideration is to remove danger of breakage, Twyman<sup>1</sup> considers that stresses as large as one-twentieth of the breaking stress are allowable. Where double refraction must be avoided, as in certain optical instruments, or where deformations due to slow relaxation of stresses are harmful, as in optical instruments or thermometers,

---

<sup>1</sup> F. Twyman, *Trans. Soc. Glass. Tech.*, 1; 1917.

the requirements are more exacting; but for these cases there seems to be a lack of reliable tests and specifications on the allowable magnitude of the stresses. In view of this uncertainty good practice would seem to demand that the stresses should be reduced to a minimum, especially for the best grade of instruments. The following measurements by Zschimmer and Schulz<sup>2</sup> give an approximate idea of what this minimum might be. They found that an especially well-annealed plate gave an average relative retardation of one-third millimicron per centimeter thickness. This plate was 24 cm in diameter and 3.9 cm thick, and was intended for a telescope lens. A normally annealed plate of approximately the same dimensions gave three times this retardation.

The stresses which correspond to this double refraction will be different for glasses of different compositions. In dealing with the ordinary small pieces, the stresses can be removed to such an extent that their effects are evident only with the most sensitive tests.

## II. ANNEALING TEMPERATURE, AND SOME CHARACTERISTICS IN THE ANNEALING RANGE

Various arbitrary methods have been suggested for the purpose of determining a suitable annealing temperature. The majority of these involve tests which determine at what temperature the rate of deformation of loaded rods reaches a certain standard value. In such determinations the dimensions of the rods and the manner of loading must be taken into account. There are also a number of optical methods all of which are quite similar. These involve observations on the rate at which the double refraction decreases at various temperatures, or determinations of the temperature at which it disappears in a reasonable time.

In the present investigation, the working range of temperature at which several kinds of glass should be annealed has been determined by a number of these methods. A discussion of some of the methods used and the results obtained follows.

### 1. OPTICAL METHOD

Results obtained by one of the optical methods are shown in Table 1. The annealing temperatures (column 7) determined by this method (which will be designated method I) indicate the maximum temperature at which the annealing should ordinarily take place. The "upper limits" (column 8) are temperatures that may be used to remove large stresses quickly, if this should

---

<sup>2</sup> Zschimmer u. Schulz, *Ann. d. Phys.*, 42, p. 345; 1913.

appear necessary, but it is considered inadvisable to hold the glass at this temperature for any length of time owing to the consequent deformation or possible changes in the character of the glass. In addition, as already stated, special precautions must be taken in the cooling procedure when such high annealing temperatures are employed.

TABLE 1.—Critical Ranges in Various Glasses

Number	Name <sup>a</sup>	Critical range in glass				Annealing range by optical method: Method I	
		On cooling		On heating		Annealing temperature $\pm 15^{\circ}\text{C}$	Upper limit $\pm 15^{\circ}\text{C}$
		$\frac{A'}{\pm 15^{\circ}\text{C}}$	$\frac{B'}{\pm 10^{\circ}\text{C}}$	$\frac{A}{\pm 10^{\circ}\text{C}}$	$\frac{B}{\pm 5^{\circ}\text{C}}$		
		$^{\circ}\text{C}$	$^{\circ}\text{C}$	$^{\circ}\text{C}$	$^{\circ}\text{C}$	$^{\circ}\text{C}$	$^{\circ}\text{C}$
B. S. 76	Dense flint .....	435	495	460	490	.....	.....
B.S. 110	Medium flint.....	405	480	455	485	460	510
B.S. 188	Light flint .....	445	525	485	525	485	510
B.S. 145	Barium flint.....	470	550	520	560	515	550
B.S. 20	Light crown .....	450	525	495	525	480	530
B. S. 94	Borosilicate crown .....	475	560	515	565	525	550
K. 266	Borosilicate crown .....	500	585	545	585	525	550
B.S. 87	Light barium crown .....	520	590	575	605	570	610
B.S. 124	Heavy barium crown .....	530	610	575	630	605	625
	Pyrex tubing .....	.....	.....	520	670	.....	.....
	Approximate formula $\text{B}_2\text{O}_3$ .....	.....	.....	240	285	.....	.....
	0.13 $\text{Na}_2\text{O}$ , 1 $\text{B}_2\text{O}_3$ .....	.....	.....	340	375	.....	.....
	0.28 $\text{Na}_2\text{O}$ , 1 $\text{B}_2\text{O}_3$ .....	.....	.....	415	445	.....	.....
	0.44 $\text{Na}_2\text{O}$ , 1 $\text{B}_2\text{O}_3$ .....	.....	.....	450	480	.....	.....

<sup>a</sup> For composition, see Williams and Rand, J. Am. Ceram. Soc. 2, p. 422.

The method by which these points were determined simply consisted of observing samples of the glass placed between crossed nicols and heated in an electric tube furnace. The samples were in the form of cylinders about 2 cm in diameter and 5 cm long, or prisms approximately 2 by 2 by 5 cm, and were polished on both ends. The glass was heated at a rate that was reduced to a constant value of about  $2^{\circ}\text{C}$  per minute when approaching the anticipated annealing range. A Pt—Pt,Rh thermocouple was used to determine the temperature. During heating the intensity of the restored light, which was partly, if not wholly, due to temperature gradients caused by the heating, was observed. The double refraction so produced remained quite constant during the constant rate of heating until the "annealing temperature" was reached. At this temperature a perceptible diminution in the intensity of the light began. This showed that the stresses were

already relaxing at a fairly rapid rate. As the temperature rose still higher the intensity decreased at a constantly increasing rate until it had practically vanished at the "upper limit." At this latter temperature any sudden change in the heating or cooling was observed to produce very little double refraction. This showed that the glass deformed very quickly relieving the stresses caused by changes in the temperature gradients.

The choice of the "annealing temperature" and the "upper limit" as fixed points in the annealing range is made, because these points can be reproduced to within a few degrees centigrade on reproducing the conditions, provided care is taken to insure that the thermocouple measures the actual temperature of the glass. The best arrangement for measuring the temperature in these tests is to place the couple in a small hole along the axis of the cylinder, but this precaution is unnecessary if low heating rates are employed and if there is a good thermal contact between the couple and the surface of the glass. When rapid heating is employed considerable discrepancies will be observed, arising from the difference in temperature between the center of the cylinder and the surface. On heating at a rate of  $20^{\circ}$  C per minute, this difference may be as large as  $20^{\circ}$ . The increase in the thermal expansivity in this range, as will be shown later, also becomes a disturbing factor when the rates are large.

One of the chief elements of arbitrariness in the choice of these temperatures, especially the lower one, lies in the fact that if the glass is badly strained, the relaxation of the large stresses is perceptible at a much lower temperature. If several rings are visible in the interference figure, the double refraction may begin to decrease perceptibly almost  $100^{\circ}$  C lower than if fairly well annealed glass were employed. Such temperatures are in most cases too low for annealing. Hence it is advisable to use well annealed or only slightly strained specimens in these tests. The greater part of the stresses will then be due to the temperature gradient produced by heating.

When the annealing temperature was chosen at or slightly below the point where these small stresses began to diminish perceptibly, as determined by method I, a number of experiments indicated that one or two hours were sufficient to anneal the glass to such an extent that only a very little evidence of double refraction remained: This annealing time does not include the time required for establishing temperature equilibrium nor for subsequent cooling.

## 2. MEASUREMENTS OF RETARDATION

The rapid disappearance of the double refraction as the upper limit was approached seemed to make a more careful investigation desirable. Consequently an apparatus for measuring the ellipticity of the polarized light was used instead of a simple analyzing nicol. This apparatus consisted of a Stokes<sup>3</sup> elliptic analyzer modified by the addition of a Brace<sup>4</sup> elliptic half shade and a Jellet split nicol. A detailed description of this modified analyzer and the methods of taking the observations<sup>5</sup> and making the various calculations<sup>6</sup> have been published elsewhere. In order to use this method it was necessary to employ monochromatic light, and to place diaphragms on the end surfaces of the cylinder. These diaphragms were so placed that their openings, 2 mm in diameter, were within 1 mm of the circumference of the cylinder and on that radius of the cylinder which made an angle of  $45^\circ$  with the plane of polarization. This was a position of maximum ellipticity. The plane polarized monochromatic light entering the cylinder was practically parallel. The emergent light was elliptically polarized and for all small effects it was found that, on proper adjustment, one of the axes of the ellipse always fell very nearly the  $45^\circ$  plane. The light was homogeneous enough to permit fairly accurate settings for relative retardations as large as one-half wave. For small retardations the measurements were accurate to one-thousandth of a wave length.

The observations necessary for the calculation of the retardation  $\delta$  are the complementary settings  $C$  and  $C'$  of the compensator and  $N$  and  $N'$  of the nicol for a matched field. When any rapid changes were taking place in the relative retardation while the glass was being heated or cooled, the observations were taken at intervals of one to three minutes. They were then plotted against time or temperature, as seemed most advantageous. The resulting curves were used for the calculation of the retardation at regular temperature or time intervals. A set of such observations, for example, was made on a cylinder of medium flint which had been comparatively well annealed. The cylinder was held at  $275^\circ\text{C}$  until its temperature was steady and uniform. It was then heated at a rate of  $7^\circ\text{C}$  per minute, the double refraction being measured until it had entirely disappeared at the high tem-

<sup>3</sup> G. Stokes, *Phil. Mag.* (4), 2, p. 420; 1857.

<sup>4</sup> D. B. Brace, *Phys. Rev.*, 18, p. 70; 1904.

<sup>5</sup> Tool, *Phys. Rev.*, 31, p. 1; 1910.

<sup>6</sup> L. B. Tuckerman jr, *Univ. of Nebr. Studies*, 9, No. 2; April, 1909.



peratures above the usual annealing range. Fig. 1 shows the form of the curves obtained when these observations were plotted. The relative retardations between the tangential and radial components which were computed from these curves are shown in Fig. 2. This relative retardation is indicated as positive when the radial component was retarded with respect to the tangential component.

The curve indicates that the double refraction shows a distinct rise to a maximum just before it begins to fall rapidly. It does

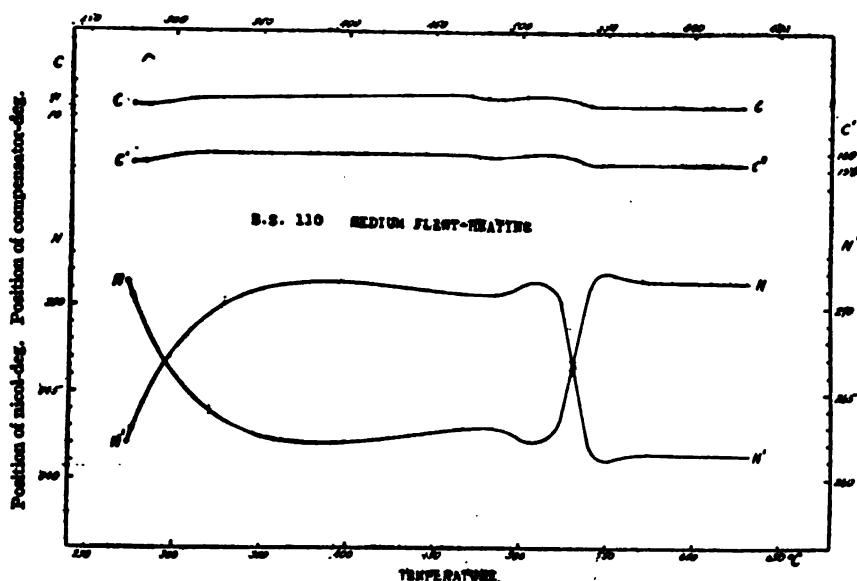


FIG. 1.—Nicol and compensator settings with elliptic analyzer

not, as might be expected, approach zero asymptotically, but crosses to negative values for a time, and then, after reaching a minimum, it gradually approaches zero again. This peculiar action at these temperatures is an indication of an interesting transformation that takes place near the annealing temperature range in glasses. Other manifestations of this effect lie in an apparent increased absorption of heat which has been observed in this laboratory,<sup>7</sup> as well as by M. So,<sup>8</sup> and in the increased thermal expansivity observed by C. G. Peters.<sup>9</sup> The form of this curve shows clearly that there is a rapid decrease in the ellipticity at these temperatures, and indicates that the cause of the

<sup>7</sup> Tool and Valasek, Meeting of Am. Phys. Soc., Baltimore; December, 1918.

<sup>8</sup> M. So., Proc. Tokyo Math. and Phys. Soc.; September, 1918.

<sup>9</sup> C. G. Peters, Meeting of Am. Phys. Soc., Baltimore; December, 1918.

definiteness of the "annealing temperature" and the "upper limit" of the annealing range, when the standardized method previously described is used, is to be found not only in the rapidly increasing mobility of the glass, but also in its changing thermal expansivity. In this connection it should be stated that a large difference in temperature between the center and the surface of the cylinder is necessary in order to obtain these curves with pronounced maxima and minima. Consequently, the surface temperatures at which the stresses become zero are much higher than if a slower rate of heating were used. Furthermore, the higher rate allows a shorter time for the stresses to relax in any given temperature interval. This also increases the measured temperature at which the double refraction disappears. Thus any

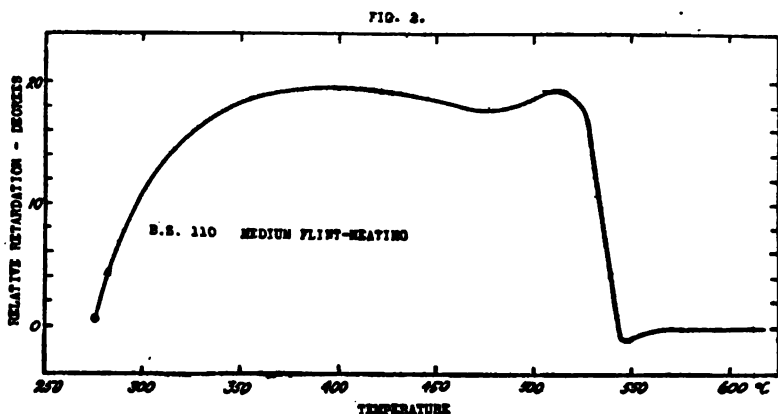


FIG. 2.—Relative retardation on heating

discrepancy between the temperatures for the disappearance of the double refraction as taken from the curve in Fig. 2 and the results by method I are accounted for.

The necessity for using large rates of heating and large differences in temperature in order to obtain curves showing a measurable maximum or minimum, is evident when the nature of this effect is considered. The explanation is clear when it is remembered that with rapid heating the outer surface of the cylinder reaches the temperature of increased rate of expansion (see Fig. 9) considerably ahead of the center. This increases the stresses and consequently the ellipticity of the transmitted light. When the center has reached this temperature, the surface is much hotter, and the stresses are, therefore, relaxing much more rapidly in the outer layers. This causes the stresses in the central portion to change from tension to compression. At the surface a re-

versal also takes place, but it is from compression to tension. A small temperature difference would not show this effect pronouncedly, but would merely change the slope of the ellipticity or retardation curve, without producing either a measurable maximum or a negative retardation. When such a procedure as that in method I is followed, this effect caused by the change in thermal expansivity, merely increases the sharpness of the disappearance of the restored light, and consequently the definiteness of the points determined.

In a similar manner the retardations were measured while cooling through this region. One of the resulting curves is shown in Fig. 3. The cooling started well above the "upper limit," Table 1, where the glass was soft enough to adjust itself to the temperature gradients due to cooling without showing double

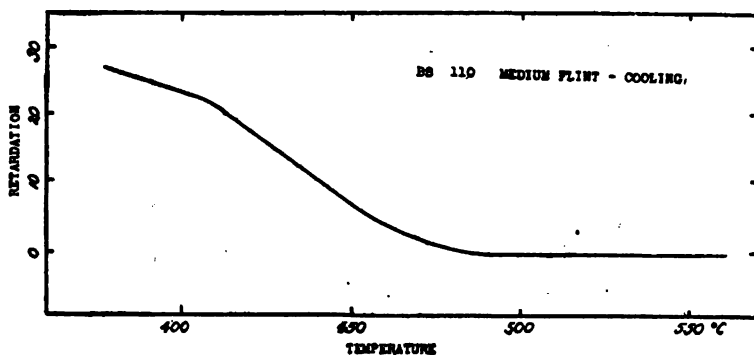


FIG. 3.—Relative retardation on cooling

refraction. An inspection of the curve shows that approximately at the "upper limit" the glass became double refracting, giving a positive retardation, the retardations rising first at an increasing rate, and then at a decreasing rate as the cooling proceeded. This decreasing rate is due partly to the decreased thermal expansivity and partly to the diminished rate of cooling at lower temperatures.

These positive retardations, which became evident while the glass (medium flint) was becoming rigid, were due to the differences in density that were incorporated in the glass at the high temperatures where the glass was soft. The temperature at which the retardation becomes evident coincides closely with that corresponding to the point *B'* on the cooling curve showing the apparent heat evolution for medium flint. (For the significance of the point *B'*, see p. 549, Table 1 and Figs. 6 and 7.) There is

also a suggestion of a discontinuity in the slope of the curve at a somewhat lower temperature which approximately corresponds to  $A'$ , the end of the apparent heat evolution. Between the temperature at which this change in slope of the retardation curve occurs and that at which the retardations first become evident, it would also appear that the slope of the curve is steeper than the small change in the cooling rate would warrant. Therefore it seems evident that the form of retardation curve obtained on cooling through this region is modified by the changes in the thermal expansivity and allied effects which accompany some molecular transformation which takes place in that temperature range where the glass ceases to deform readily under small stresses. As in the case of the curves obtained on

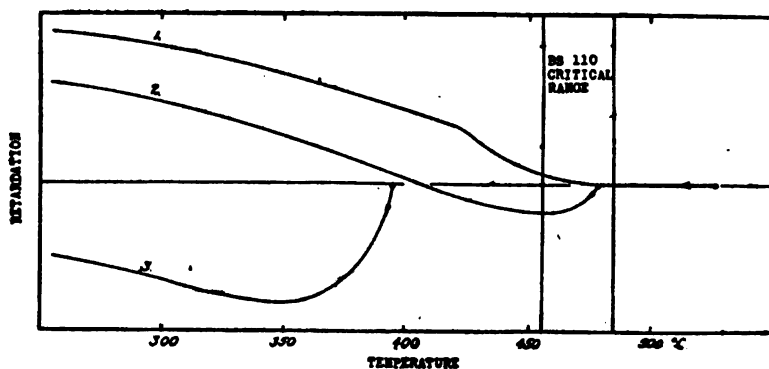


FIG. 4.—Relative retardation on cooling from various temperatures

heating, it would appear that the change in the thermal expansivity is the most potent factor producing the anomalous character of the curves for the retardation observed on cooling.

If similar determinations of the retardations evident on cooling are carried out when the starting point is below the "upper limit," there will be no initial stage in the curve where the double refraction remains practically zero. The retardations will, however, immediately become negative, as indicated in the curves 2 and 3, Fig. 4 (based on qualitative observations), then cross over to positive values at some point that depends on the starting temperature and on the cooling rate, and will remain permanently positive after temperature uniformity has been reached. For a well-annealed sample, and a starting temperature below that at which the glass loses its rigidity, this negative retardation will not change sign, and will become zero only when temperature uniformity is again established.

The initial negative retardations on these curves show that the glass is not soft enough to adjust itself wholly, in the time allowed, to the cooling gradients. The magnitude of the maximum negative retardation will, therefore, depend, for any one sample, on the distance of the starting point below the "upper limit" and on the rate of cooling. The magnitude of the positive retardation finally remaining is approximately the difference between this maximum negative retardation and the retardation which the same cooling rate would have produced in the glass at a temperature where it was quite rigid. The amount of permanent double refraction depends, therefore, on the plasticity or viscosity of the glass at the starting temperature and on the rate of cooling. This phase of the subject has been investigated by Zschimmer and Schulz,<sup>10</sup> who used a somewhat similar method to determine the residual double refraction for a certain mode of cooling. They found that the increment of retardation is inversely proportional to the difference between the starting temperature  $\theta$  and some other temperature  $\theta_0$  which appears to correspond closely to the "upper limit" of method I. If  $S$  denotes a quantity proportional to the retardation introduced by cooling from any temperature  $\theta$ , then their equation states that:

$$(S_0 + S) (\theta_0 - \theta) = C$$

where  $S_0$ ,  $\theta_0$ , and  $C$  are constants.

For temperatures near and above  $\theta_0$  the equation ceases to hold, and in the latter case the retardation obtained by cooling at a given rate remains constant. The curves in Figs. 2, 3, and 4, taken in conjunction with the data of Zschimmer and Schulz, show clearly the advisability of annealing at the lowest temperature possible without unnecessarily increasing the annealing time, and in all cases below the temperature  $\theta_0$ , which corresponds closely, as stated above, to the "upper limit" determined by method I.

### 3. CRITICAL RANGE

The peculiar manner of the disappearance of the stresses observed when studying the effect of rapid heating upon the results obtained by method I led to an investigation of the apparent heat absorption, and the thermal expansion in this range. To determine whether any heat effect accompanied the softening of the glass, a differential thermocouple method<sup>11, 12</sup> was used. (See diagram of

<sup>10</sup> Zschimmer u. Schulz, loc. cit.

<sup>11</sup> Burgess and Le Chatelier, *Measurements of High Temperatures*, 3 ed., p. 283.

<sup>12</sup> G. K. Burgess, this Bulletin, 8, p. 199; 1908.

apparatus, Fig. 5.) One of the junctions of a Pt,Rh—Pt—Pt,Rh differential couple was placed in a small piece of the glass under investigation and the other in a neutral body. A third wire of platinum leading down to the junction in the glass made it possible to determine the temperature of the glass as well as the difference in temperature between the two junctions of the differential couple. A number of neutral bodies were used, the most convenient being fine alundum, which was packed tightly about the junction. The other junction was introduced into the glass either by fusion or by placing it in a small hole drilled into the sample, or by packing finely powdered glass around it. The

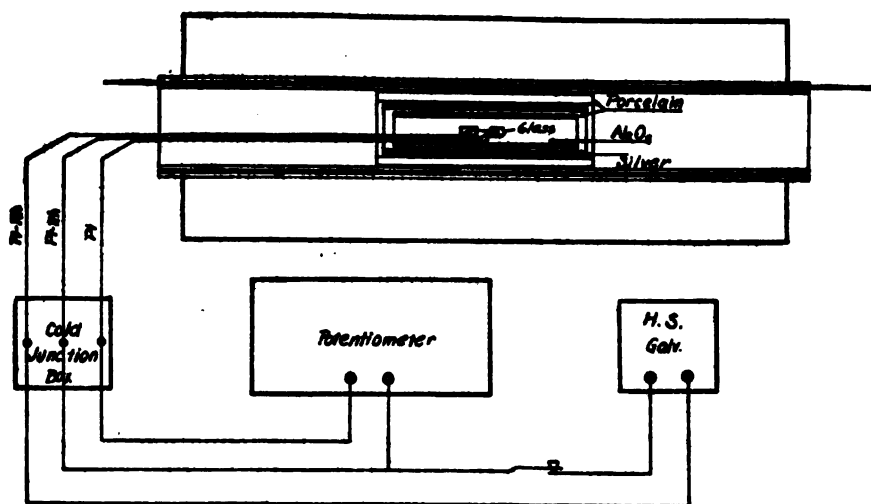


FIG. 5.—Diagram of apparatus for determining critical range

last method is by far the easiest to manipulate. The mass of glass used was varied from approximately 1 to 50 g and caused only minor variations in the result.

The glass and neutral body were usually packed in a small porcelain tube with fine alundum powder as the packing material. The porcelain container was then placed in a heavy silver tube which served to equalize the temperature and, consequently, to reduce the differential readings due merely to unequal heating. The silver tube with its contents was then heated in an electric tube furnace at a constant rate. After some trials in which rates varying from  $\frac{1}{2}$  to  $10^{\circ}$  per minute were tried, a uniform rate of  $4^{\circ}$  C per minute was adopted. A galvanometer deflection of 1 cm corresponded to approximately  $0.4^{\circ}$  C temperature difference. The temperature of the glass was determined in the usual way by

a thermocouple and a potentiometer. The galvanometer and potentiometer circuits were supplied with the necessary keys and switches so that readings on the two instruments could be taken without interference.

In the curves shown in Fig. 6 the galvanometer deflections are plotted against the temperature of the glass. The observations were made 4 to 8° apart, and the errors of observation are less than the width of the curves. In every case it will be seen that the glass shows an increased absorption of heat on heating, while on cooling there is evidence of a decrease in evolution of heat in passing through the same region. The temperature range covered by the phenomenon is twice as great for cooling as it is for heating, and moreover the limits on cooling are not so sharply defined. This is often the case with similar effects in other materials. These effects are not necessarily true endothermic or exothermic transformations as these terms are usually interpreted, but for the sake of brevity they will be referred to as heat absorptions and evolutions.

The temperatures at the beginning *A* and the maximum *B* on the curves for the heat absorption on heating and at the maximum *B'* and the end *A'* on the curves showing a heat evolution on cooling were determined as shown in Fig. 7. They are given for a number of glasses in Table I. This table shows that the temperature range within which a rapid softening of the glass occurs, as determined by method I, corresponds within reasonable limits to the range between *A* and *B*. It would appear, therefore, that the heat absorption and the rapid softening of the glass are allied phenomena, and that it should be possible to determine the annealing range by means of the heat absorption. Tests on a number of glasses in this laboratory support this view. Since in most cases it is advisable to carry out the whole process of annealing below the temperatures where the glass becomes too soft, it appears that the region of this heat absorption must be considered as defining the upper limit of the annealing range. The experimental errors in determining this region are in most instances much smaller than those in determining the annealing range by other methods. Considering both accuracy and convenience, it may be said to be one of the best methods for this purpose. In the case of certain opaque or colored glasses it is especially advantageous. This method for determining the annealing range will be referred to as method II.

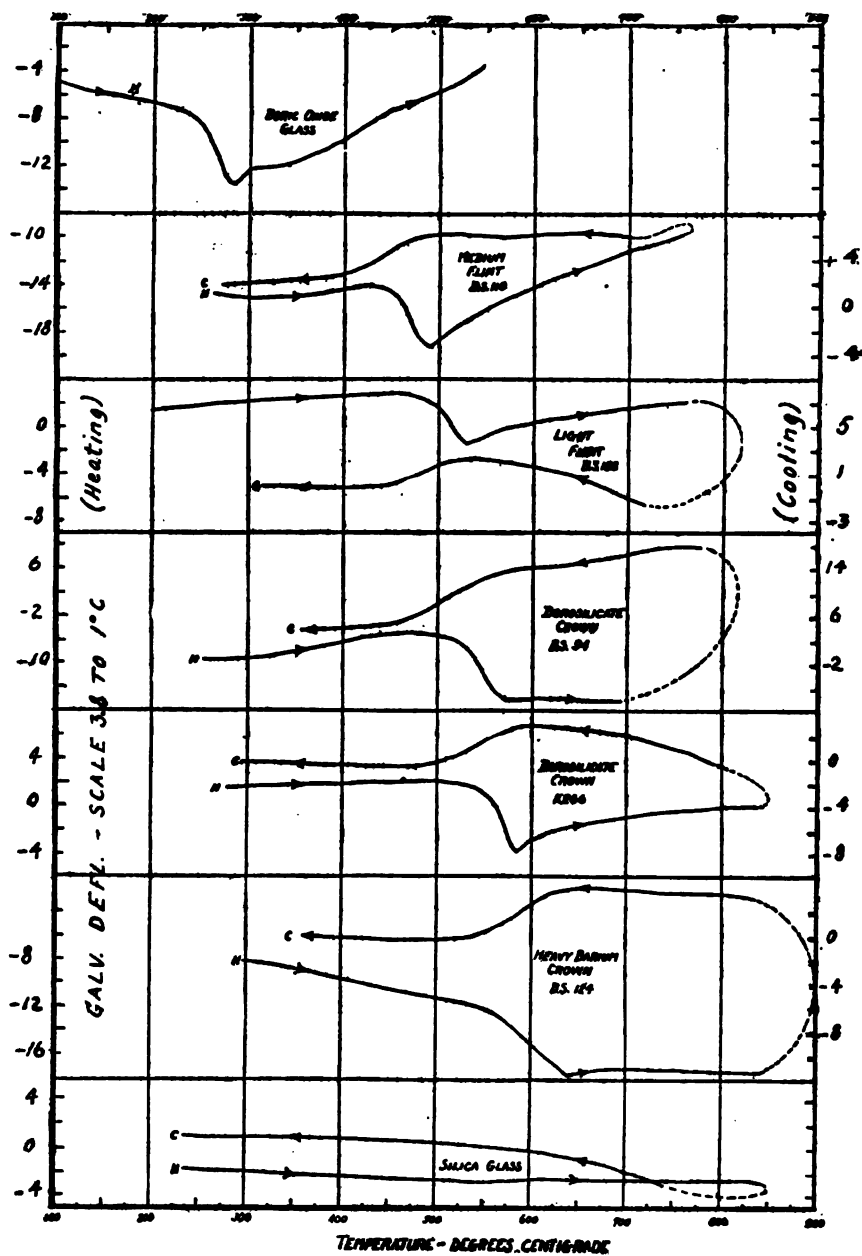


FIG. 6.—Critical range by differential thermocouple



The location of this heat effect was also determined by the use of the "inverse time" method of Osmond.<sup>12</sup> This method employs only one couple, and involves the measurement of the time that it takes the sample to rise through successive short and equal steps of temperature. The time interval is best measured on a chrono-

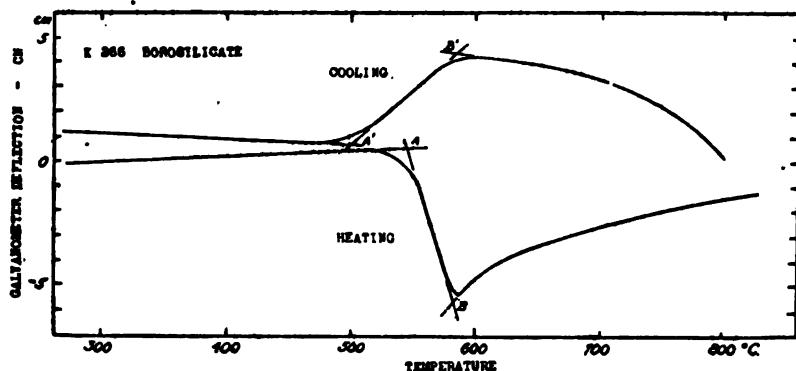


FIG. 7.—Determination of critical range from curves by differential thermocouple

graph but can be determined by a stop watch or, as tests have shown, even by an ordinary watch if great care is exercised. The temperature measurements must be accurate to within one-half degree centigrade. In the glass factory it would probably be easiest to prepare the sample by dipping the end of the thermo-

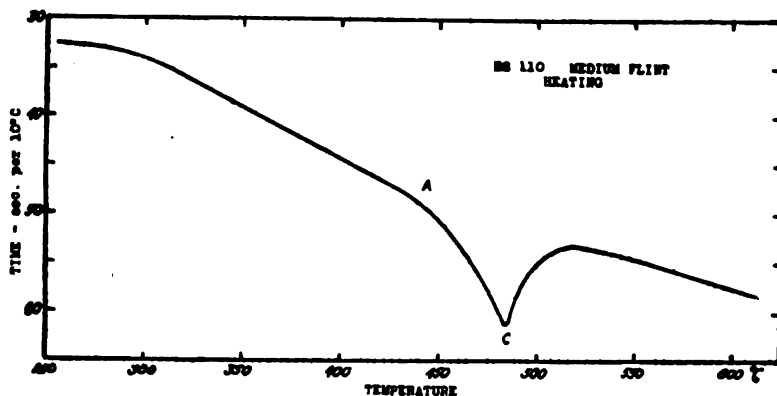


FIG. 8.—Critical range by inverse rate method

couple into the molten glass and taking out a very small amount. With the proper apparatus the location of this heat effect, and hence the approximate annealing temperature, could be determined before the pot had solidified. A base metal couple should be sufficient for this purpose. Fig. 8 shows a curve,

<sup>12</sup> Burgess, loc. cit.

obtained by this method, in which an iron-constantan thermocouple, a stop watch, and a Leeds and Northrup type K potentiometer were employed. The point *A* on this curve indicates the beginning of the effect on heating, and is identical with the same point obtained by the differential method. The cusp *C*, however, indicates the temperature at which the rate of heating is the least, and does not correspond to the point *B* on the differential curve in Fig. 7. The latter point indicates approximately the end of the effect.

Fig. 9 shows the close correspondence between the region of this heat absorption by the differential method and the increased

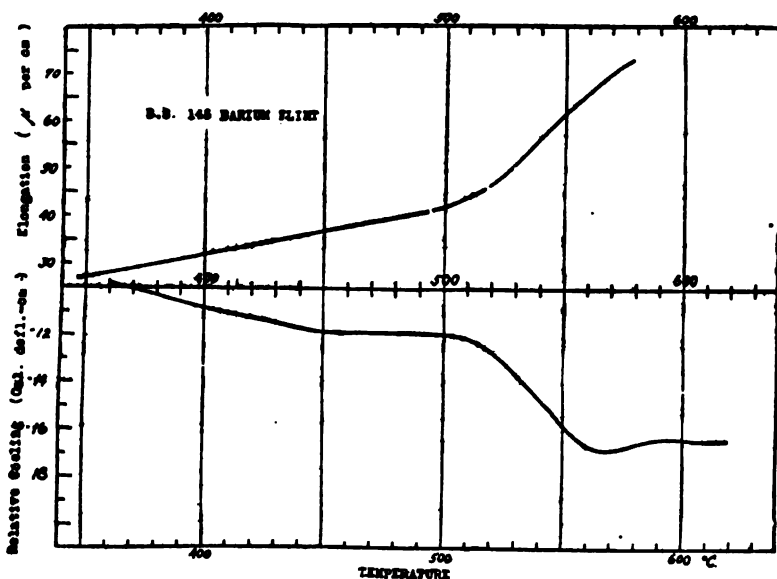


FIG. 9.—Comparison of thermal expansion and curves by differential thermocouple

thermal expansivity observed by C. G. Peters. The effects begin at substantially the same temperature. The curve for thermal expansion gives, therefore, as Peters has shown, another method of determining the highest advisable annealing temperature.

It was decided that the beginning of these effects should be considered as the upper limit of the annealing range. The advantage to be gained by the more rapid disappearance of the stresses at higher temperatures seems to be outweighed by the necessary precautions to be observed on cooling through this region without reintroducing additional strain. As already indicated, this difficulty is not due to the softness of the glass alone, but also to the marked changes in the thermal expansivity and other con-

stants, which accompany radical changes in the molecular groupings of the glass. In addition, such molecular changes may expedite certain deleterious effects, such as crystallization during the annealing and slow cooling.

The exact nature of these changes in the molecular groupings is not to be explained without a further and thorough investigation of the subject. It appears, however, that they are accompanied either by a small, but definite, absorption of heat on heating, and a corresponding, but less well-defined, evolution of heat on cooling; or, by a change in the thermal conductivity; or, some other property of such a character as to produce an apparent absorption or evolution of heat. The usual magnitude of the relative heating or cooling with respect to the neutral body amounted to 2 or 3° C. Although a number of experiments were carried out to determine the exact nature of this effect, its explanation has not been established positively. Neither has it been determined whether this heat absorption results merely from a change in the specific heat<sup>14</sup> or something which might be considered as a heat of chemical solution or reaction, or a latent heat of change in state.<sup>15</sup> The possibility of a change in the specific heat or conductivity caused by the relaxation of the internal stresses was considered, but no relation between the magnitudes of the stresses and the heat effect was found. Moreover, powdering the glass did not alter results.

M. So, whose observations corroborated those on the absorption while heating, apparently did not notice the corresponding effect on cooling. He ascribes the effect to a melting of some component in the glass. However, it may suggest the rapid change in properties which characterize a substance not too far removed from conditions which would admit of the coexistence of phases in equilibrium at a transformation point.

In order to determine whether the transformation was connected with the complex chemical composition of the usual glasses, some simple borax glasses were made up with proportions ranging from pure boric-acid glass to fused borax. The curves were quite similar to those obtained on the common glasses, but the absorption occurred in different regions. The temperature ranges for the absorption are given in Table 1 under the heading "Critical range."

It was considered that, even in stable glasses, the transformation might be associated with or followed by a slight crystalliza-

<sup>14</sup> W. P. White, *Am. Jour. Sci.*, 47; January, 1919.

<sup>15</sup> M. So, *loc. cit.*

tion. Usually such crystallization effects are too small to be observed easily. Consequently it seemed desirable to investigate a case where a marked crystallization does occur. Some observations were made, therefore, on the unstable sodium metasilicate glass made as described by Guertler.<sup>16</sup> According to Guertler this glass shows a large evolution of heat due to crystallization when it softens. The heating curves presented in Fig. 10 show

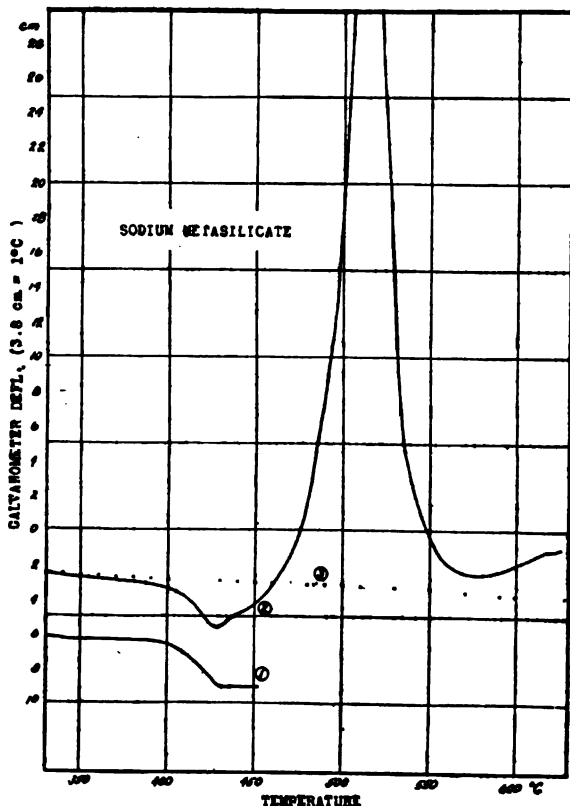


FIG. 10.—Heating curves on sodium metasilicate with differential thermocouple

that this exothermic transformation in sodium metasilicate glass occurs soon after but not coincident with the apparent endothermic effect on heating. Curves 1, 2, and 3 in this figure were taken in this sequence on the same sample. They show that the glass can be heated for a short time beyond the first transformation without changing its properties to any great extent, although the slight difference between curves 1 and 2 would lead one to infer that some crystallization had occurred during the first heat-

<sup>16</sup> Guertler, *Zeits. fur. Anorg. Chem.*, 40, p. 8268: 1904.

ing. On continued heating the glass became crystallized, giving the second curve, and when heated again gave the smooth curve shown as 3. This latter curve was continued until melting occurred, which was above  $1000^{\circ}\text{C}$ . It would appear, from curves 1 and 2, that for this glass at least there is no danger of crystallization when it is held for a short period of time at temperatures near and possibly even somewhat above the first or endothermic transformation. Further investigation showed that the presence of a few crystals caused crystallization to begin sooner than if a perfect glass had been used, but in no case did it occur until after the first transformation. A more thorough study of the tendency of the ordinary glasses to crystallize in this region seems desirable, since in practice this tendency has sometimes been found to interfere with the free choice of an annealing temperature.

Tests made on some of the optical glasses from this Bureau indicated that such glasses were too stable to show sufficient crystallization within the time available, hence no relation could be established between the tendency toward crystallization and the apparent endothermic transformations which they show when heated. Crystallization of the ordinary glasses seems to be greatly accelerated by impurities<sup>17 18</sup> or dissolved gases, as has been demonstrated. It appears that the most active substances in this respect are the chlorides and sulphates that occur as impurities in potash. The general composition of the glass and the temperatures used in its manufacture are other factors that affect the tendency toward devitrification. It has been demonstrated that the injurious effects of impure chemicals often can be ameliorated by the proper control of the melting temperature. It would therefore be of interest to determine whether these impurities affect the endothermic transformation on heating.

### III. ANNEALING TIME

The results outlined above all point to the desirability of as low an annealing temperature as is consistent with the efficient and rapid removal and prevention of permanent stresses. In order to employ such low "annealing temperatures" efficiently it is necessary to obtain some information concerning the "annealing time" required, and the rate of relaxation of the stresses at various temperatures. This leads to the consideration of methods for the determination of Maxwell's "relaxation time" for stresses

<sup>17</sup> Cauwood and Turner, *J. Soc. Glass Tech.*, 1, pp. 87-96; 1917.

<sup>18</sup> Fenner and Ferguson, *J. Am. Ceram. Soc.*, 1, pp. 468-76; 1918.

in viscous media. A number of such methods have been in use, and they are, perhaps, the best means available to determine the most satisfactory annealing time and temperature. These methods may be divided into two classes, of which the first to be considered deals with the rate of deformation of the glass under an external force, and the second, with the rate at which the glass loses its double refracting power. Of the first class, the methods commonly used consist of bending, twisting, or stretching strips or rods. Of these the latter two are to be considered the most satisfactory except in those cases where the preparation of the samples is difficult.

The methods of the second class vary only in the manner in which the double refraction is measured. When the stresses are large, this may be done by determining the rate of disappearance of the interference rings in a badly strained cylinder of glass. When they are small, the retardation may be measured by some such instrument as the Stokes analyzer described previously.

The theory and equations necessary for the determination of the relaxation time are discussed thoroughly in articles by Maxwell,<sup>19</sup> Zschimmer and Schulz,<sup>20</sup> and Twyman.<sup>21</sup>

Some of the discussions will be given here, merely that the symbols used may be clearly defined. Maxwell's equation on which all these measurements are based states that:

$$\frac{dF}{dt} = E \frac{dS}{dt} - \frac{F}{T}$$

where  $F$ ,  $S$ , and  $t$  are respectively the stress, strain, and the time, while  $E$  is the elastic coefficient involved and  $T$  is a constant called the "relaxation time."

According to the value of  $T$  and its variation with the magnitude of the stress, the body will show the properties of elasticity, plasticity, or viscosity. These terms are used by different authors in different senses, and even the same author is not always consistent. This uncertainty is, in a large measure, due to the present incomplete knowledge of the subject, but the following discussion may serve tentatively to distinguish between these terms.

When  $T$  is infinite the above equation represents the behavior of a perfectly elastic body. For a large number of the common rigid bodies this condition is approximated until very large forces, which are said to exceed the elastic limit and to approach the

<sup>19</sup> J. C. Maxwell, *Phil. Mag.* (4), 35, p. 129, 1868.

<sup>20</sup> Zschimmer and Schulz, *loc. cit.*

<sup>21</sup> F. Twyman, *loc. cit.*

limit of rupture, are applied. For many materials  $T$  ceases to be extremely large for comparatively small stresses. In other words, such materials have low elastic limits. Under stresses, whose magnitude lies between the elastic limit and the breaking stress, materials are plastic. Hence those materials with low, finite elastic limits are usually considered plastic bodies. For a plastic condition  $T$  the relaxation time generally varies with the stress. It may be practically constant, however, if the variations of the stresses are confined within certain limits. When the elastic limit is zero and  $T$  is independent of the stress, the material may be termed "viscous." In a truly viscous material  $T$  is independent of the stresses even when these are indefinitely small. In general, when  $T$  is extremely large, the material is elastic; when  $T$  is a function of the stress, the material is plastic; and when  $T$  is independent of the stresses, even when they become indefinitely small, the material is viscous. It is to be noted that this conception of "viscous" bodies does not identify "viscosity" with the "internal friction" which is characteristic of all substances.<sup>22</sup> Generally there is no sharp line of demarcation between the elastic, plastic, and viscous conditions, and they merge gradually into each other. Most solids, such as metals or glass, may exhibit any or all of these properties depending on the manner in which they are tested. For that reason they may be termed elastico-plastico-viscous materials. Certain theories concerning molecular aggregations and their action in solids are often helpful in explaining these characteristics and the various elastic aftereffects. A number of such theories have been advanced, one of which is the Maxwell-Butcher<sup>24</sup> theory. It has been employed by certain investigators as an aid in discussing the properties of glass.

#### 1. MEASUREMENT OF THE RELAXATION TIME BY AN APPLIED LOAD

When  $F$  in Maxwell's equation is constant as in the methods of the first class, which employ a glass body under a constant external load, the following solution is obtained:

$$ET = F / \frac{dS}{dt}$$

Here  $ET$  has the dimensions of a coefficient of viscosity. In the strip-bending experiment, for example,  $F$  and  $\frac{dS}{dt}$  may be de-

<sup>22</sup> Thomson and Tait, *Nat. Phil.*, 1, art. 741.

<sup>23</sup> Love, *Math., Theory Elast.*, Cambridge, 2 ed., p. 115.

<sup>24</sup> Butcher, *Proc. London Math. Soc.*, 8, p. 103; 1876.

terminated by observation and the value of  $ET$  calculated. It is not possible to determine  $T$  unless  $E$  is known, and this is an inherent weakness of this method when  $T$  is desired. The elastic coefficient is not very easily determined at the temperatures employed, and is usually assumed to be approximately the same as at ordinary temperatures, although probably it changes considerably in the critical range. When values for  $T$  (expressed in hours) are calculated for several temperatures on the assumption of some constant value for  $E$ , they will be found to satisfy the equation given by Twyman:

$$T_{\theta} = T_0 e^{\frac{\theta_0 - \theta}{k}}$$

In this,  $T_{\theta}$  and  $T_0$  are the relaxation times at temperatures  $\theta$  and  $\theta_0$ , while  $k$  is a constant depending on the nature of the glass. The constant  $k$  may be determined from observations on the variation of the rate of bending with the temperature.

The methods of this type used in this laboratory consisted of stretching thin rods or bending strips of glass. The former was used only occasionally to check the results obtained by bending. The latter method was very similar to that described by Twyman except that in most cases the strip rested on two supports instead of being clamped at one end. The method of support did not appear to affect the results. When the two supports were used, they consisted of small smooth porcelain tubes. The strips tested were approximately 50 mm. long, 4 to 10 mm. wide, and 1 to 2 mm. thick. The loads varied from 15 to 500 gms. and were always large enough to make the weight of the strip negligible in the calculations. The strip was heated in an electric tube furnace and observed with a long-focus micrometer microscope. The temperature of the strip could be determined within  $\pm 2^{\circ}$  C and held constant for a considerable length of time to within one-half of 1 degree. Observations on the rates of bending were taken at four or five points in an average range of  $40^{\circ}$  C without changing the load. The logarithms of the rates plotted against the corresponding temperatures fell on a straight line as required by Twyman's equation. The slope of this line determines  $k$ .

The bending method gave very consistent values for both  $ET$  and  $k$  when the observations were repeated. The values of  $k$  for the different glasses tested varied from 10 to 13. (See Table 2.) The average value was such that, roughly speaking,  $ET$  doubled for every  $8^{\circ}$  C drop in temperature. As the temperature was



increased  $k$  seemed to increase somewhat. It must also increase for lower temperatures since otherwise the glass would be more rigid at room temperature than the experiments of Zschimmer and Schulz would indicate.

TABLE 2

Name	Method	Range °C	$k$	$T_{100}^a$
				Hours
Borosilicate.....	Bend.....	535-585	11.4	.....
Do.....	do.....	555-590	11.5	2.1
Do.....	do.....	605-640	11.6	.....
Do.....	do.....	600-660	12.6	.....
Do.....	Optical.....	510-535	10.3	8.5
Light flint.....	Bend.....	475-530	12.3	.0094
Do.....	Stretch.....	500-545	11.9	.0114
Do.....	Optical.....	440-490	11.7	.067
Dense flint.....	Bend.....	485-530	10.2	.0059

<sup>a</sup>  $T_{100}$  extrapolated by Twyman's equation when necessary.

The values assumed for  $E$  were as follows:

Borosilicate -  $E = 7500 \text{ kg/mm}^2$

Light flint -  $E = 6500 \text{ kg/mm}^2$

Dense flint -  $E = 6000 \text{ kg/mm}^2$

Contrary to expectation the values obtained for  $ET$  by varying the load from 15 to 250 g were constant within the experimental error. Moreover the values for  $T$ , on assuming  $E$  to be the same as at room temperature, were about one-sixth as large as those obtained by the optical method for a retardation of 10 to 15°, or approximately 15 to 23 millimicrons. That this discrepancy could be due entirely to assuming a wrong value for  $E$  is extremely doubtful. A more plausible explanation lies in the fact that the bending experiments as they were carried out necessitated the use of higher temperatures and greater stresses than could be employed successfully in the more accurate measurements by the optical methods.

## 2. MEASUREMENT OF THE RELAXATION TIME BY AN OPTICAL METHOD

For applying the optical methods (that is, methods of the second class) Zschimmer and Schulz assumed that the deformation or  $S$  remained constant while the stresses causing double refraction relaxed. This assumption would appear to be inadequate, at least for bodies of limited dimensions under no external constraint. Solving Maxwell's equation on this assumption, however, gives

$$F = F_0 e^{-\frac{t}{T}}$$

$$\text{or } t = T \log_e \frac{F_0}{F}$$

If it is assumed that  $F$  is proportional to the retardation  $\delta$ , which Pockels<sup>28</sup> has shown to be the case for externally applied forces, then

$$T = t / \log_e \delta_0 / \delta$$

In these equations  $F_0$  and  $\delta_0$  are the initial stresses or retardations while  $F$  and  $\delta$  are the corresponding quantities after a time  $t$ . When these quantities are measured the relaxation time  $T$  may be computed, or if  $\log_e \delta$  is plotted against time, then  $T$  may be found from the slope of the resulting curve. If  $T$  is constant for all stresses, this curve should be a straight line. This was not found to be the case, however, when this method was used. In fact,  $T$  appeared to increase quite materially as the stresses and the resulting double refraction decreased. This was to be expected if the glass was plastic.

The retardations were measured with the Stokes analyzer while the strained cylinder of glass was being annealed at a constant temperature. The temperature could be kept constant within a few tenths of a degree for several hours. Some of the resulting observations are summarized in Table 2.

When  $T$  was determined for the same magnitude of retardation at different temperatures, it was found that Twyman's empirical equation connecting  $\theta$  and  $T$  was satisfied. Some of the computed values of the exponent  $k$  in this equation are also given in Table 2.

In order to obtain values for  $T$  when the retardations were large, some observations were made on the rates at which the rings in a badly strained cylinder disappeared. A very large variation of  $T$  with the magnitude of the double refraction was evident. When two or three rings were visible the value of  $T$  was the same as obtained by bending a strip. This would indicate that the difference in the magnitude of the stresses was a factor in causing the discrepancy between the two methods. It is possible, also, that the assumption of a constant strain is relatively a closer approximation for larger strains. However, the entire question of the distribution of the stresses, the magnitudes of the elastic coefficients involved, and of the manner in which glass deforms is unsettled. It is worthy of note in this connection that Zschimmer and Schulz using an optical method found that, at room temperatures, the average retardations in pieces with large strains would show a perceptible decrease after one month, while

---

<sup>28</sup> F. Pockels, *Ann. der Physik*, 7, p. 745; 1902.

the small average retardations in samples with less strain actually increased after the same period of time. If this same condition exists at higher temperatures, it might well cause the above described variation in  $T$  with the magnitude of the double refraction and the discrepancy in the results obtained for the relaxation time by the two methods.

The values in Table 2 are only a few collected from tests to determine the annealing time, and are given to illustrate the points discussed and to emphasize the necessity of a more thorough investigation of the manner in which the stresses relax while the glass is being annealed. For such an investigation the methods for determining  $T$  and  $k$  should be far more refined than is required for general testing. The determination of these constants over a wide range of temperatures is especially desirable. An interference method would undoubtedly be of advantage in determining the rate of deformation at low temperatures and under small loads.

### 3. APPLICATION OF RELAXATION TIME

Although the constancy of  $T$  and  $k$  must be questioned, in the case of the former when the force is varied, and of the latter when the temperature range is very large, still they are of great value in estimating the annealing time and determining a cooling procedure. If the initial stresses are to be reduced by holding at some constant annealing temperature until they are any fraction  $F/F_0$ , for example, one-tenth of their original value, then the time required to anneal will be:

$$t_1 = T \log_e F_0/F = 2.3 T$$

When due allowance is made for the variation of  $T$  with the stress, a very fair approximation to the annealing time can be obtained. Furthermore, the time required for the stresses to decrease to  $(\frac{1}{10})^n$  of their initial magnitude will be equal to  $n \times t_1$  hours. In order to obtain  $t_1$  for successive drops of  $10^\circ$  in the annealing temperature, it is necessary only to multiply by a constant derived from Twyman's equation. Thus

$$t_{(0-10)} = t_0 \times e^{\frac{10}{k}}$$

Assuming an average value of  $k = 11.3$  this would give the relation:

$$t_{(0-10)} = 2.4 t_0$$

In arranging the annealing schedules, for small articles at least, usually it was found desirable to choose an annealing tem-

perature somewhat below the beginning of the heat absorption. Schedules beginning at temperatures much higher or much lower were usually found to be less efficient. Some experiments on a piece of badly strained light flint illustrate this. The location of the beginning of the heat absorption was at  $485^{\circ}\text{C}$ . It was found that 10 days at  $430^{\circ}\text{C}$  were required to obtain the same reduction of stresses that could be obtained in one-half hour at  $485^{\circ}\text{C}$ . On the other hand, it could be cooled very rapidly from the lower temperature without reintroduction of permanent strain, while from  $485^{\circ}\text{C}$  the cooling rate during the first  $30$  or  $40^{\circ}$  required much more accurate control to obtain the same result. There is apparently some temperature, with the corresponding method of cooling, that gives the most efficient procedure. For small pieces this temperature appears to be  $10$  to  $20^{\circ}\text{C}$  below the critical range.

It is of the utmost importance that the temperature of the glass should be as uniform as possible, especially in the annealing range. The introduction of strains in homogeneous glass is due solely to temperature gradients. Whether these are due to rapid or unsymmetrical cooling, or to a lack of temperature uniformity while annealing, is immaterial. Stresses due to the latter cause may be larger and more harmful, inasmuch as they may be very irregularly distributed. The importance of temperature uniformity can not be overemphasized, since the lack of it is the chief source of difficulty in annealing glass. This is especially the case when fine annealing is attempted. Temperature control, such that there are no disturbing fluctuations in, or uncertainties concerning the actual temperature which the glass attains, is absolutely necessary to insure successful annealing. Unless these conditions are met, certain devices which are used to determine whether the temperatures which existed in a lehr or kiln have been satisfactory will give misleading indications. Such devices usually consist of a rod or tube of the glass to be annealed, supported horizontally but free to bend. The suitability of the temperature conditions which existed is determined from the amount this rod deformed during its passage through the lehr with the glass which was being annealed. Unless the temperature control and distribution were satisfactory, the indication derived from the amount of deformation will have no meaning, since a very unsatisfactory temperature condition might have produced the same bending. With proper pre-

cautions such devices may be of value, although examining the product itself in a reflection polariscope would be as easy and would give more reliable information.

#### IV. COOLING PROCEDURE

Certain generalizations concerning cooling can be made, but the process can not be completely defined without a knowledge of the conditions to be met. A different cooling procedure will have to be followed for every change in the kind of glass and in the size or shape of the article. In any case where all the conditions are known it is possible, however, to specify with considerable accuracy what should be a good cooling procedure. The efficiency of the procedure must be determined by the expense and time required to produce a satisfactory product.

As an example of a mode of cooling which proved very satisfactory from the standpoint of laboratory experience, the following experimental cooling procedure is given. The glass was light flint and the maximum size of the pieces was approximately 2 by 6 by 8 cm. The cooling followed an annealing period of about two hours, during which the glass was held at a constant uniform temperature of 475° C, or 10 to 15° below the critical range. After various trials it appeared that satisfactory results could be obtained by a cooling rate that had reached 5° C per hour at 460° C and which was increasing in such a way that it doubled for every 10° C drop thereafter until the natural cooling rate of the furnace was reached at approximately 420° C. This method of cooling is practically that suggested by Boys,<sup>26</sup> Twyman,<sup>27</sup> and English and Turner<sup>28</sup>. The previously mentioned measurements by Zschimmer and Schulz on the double refraction shown by annealed glass were the basis for considering the results satisfactory. The time consumed was also taken into account.

Doubtless the cooling rate could have been further increased at the lower temperatures since experiments on similar blocks showed that a much more rapid rate of cooling at 200° C did not introduce serious permanent double refraction. Increasing the rate must, however, in any case be discontinued after it becomes large enough to produce stresses approaching the elastic limit.

For large pieces of the same glass, the rate at any temperature must be much lower. In the case of the simpler types of solids

<sup>26</sup> Boys, *Nature*, 96, p. 150; 1916.

<sup>27</sup> Twyman, *loc. cit.*

<sup>28</sup> English and Turner, *J. Soc. Glass Tech.*, 2, p. 90; 1918.

such as the sphere, a statement of the relation between the rate of cooling and the size may be made when the cooling is approximately linear. Linear cooling means equal changes of surface temperature in equal time intervals. If the pieces are not very large and the rate of cooling is not changing rapidly, the method of cooling discussed above may be considered to be linear at any instant; that is, the temperature distribution inside the piece of glass approximates that of linear cooling. For linear cooling of a sphere the difference between the surface temperature and the mean temperature is proportional to the square of the radius. The tangential stresses at the surface, which are the largest stresses in the sphere, are proportional to this difference in temperature, and, consequently, to the square of the radius. The cases of the slab and cylinder are very similar, and it may be said that the maximum stresses present are roughly proportional to the square of the least dimension. If, then, the cooling may be considered linear in effect at any instant, the rate of cooling at any given temperature should be inversely proportional to the square of the least dimension.

In the case of very large pieces it may be necessary to reduce the annealing temperature, and correspondingly to increase the annealing time in order to shorten the extremely long period of cooling that otherwise would be necessary. Large blocks of glass for optical purposes naturally take a longer time to anneal because of the more rigid requirements as to double refraction.

The mode of cooling just discussed is based on the increasing rigidity of the glass as it cools. Above the critical range the glass may be considered to have changed from a plastic to a nearly viscous state, the elastic limit for a large part of the molecular aggregates being practically zero. As the cooling proceeds through the critical range the glass loses its viscous nature very rapidly, and below this range may be considered practically as a plastic body. It is in the temperature region where the glass is predominately plastic, but still viscous enough to allow the relaxation of small stresses, that annealing should take place. Unless the annealing temperature is chosen too low, all stresses, no matter how small, will disappear in a reasonable time as measurements on the double refraction will show. These stresses disappear completely, due to the fact that the glass still retains to a certain extent its viscous character.

At lower temperatures the relaxation time rapidly increases, and the glass becomes more and more rigid, losing much of its

plasticity and becoming like an elastic substance; accordingly when the glass is being cooled from its annealing temperature, the rate, which initially must be relatively low, may be increased as the glass cools without adding materially to the amount of permanent strain. The manner of increasing the cooling rate is based partly on the assumption that Twyman's relation still holds for a considerable distance below the critical range. Although the measurements by Zschimmer and Schulz would indicate that the glass in the cooling range grew rigid more slowly, with decreasing temperature, than this relation demands, still it appears that it adequately represents the conditions so far as the first 100° C of cooling is concerned.

In the preceding discussion of the annealing procedure it was found convenient to use certain concepts and methods of discussion which involve one of the various molecular theories devised to explain the continuous change of a body from a viscous fluid to an elastic solid. For discussing the behavior of glass the Maxwell-Butcher theory seemed especially convenient. According to this theory, metals and many other materials, including glasses, which are elastico-plastico-viscous, are composed of various types of aggregates, molecules or groups of molecules, which can be divided into two classes. Aggregates of the first class will deform under forces so small that they have no sensible magnitude, and those of the second class will require a finite force before disorganizing. The second class may again be separated into groups having different disorganization limits, or, in other words, different elastic limits. When the body consists chiefly of groups of the first class, it will behave as a viscous substance. When, however, groups of the second class predominate, the deformation will appear to be elastic for small loads applied for a short time, and plastic for loads exceeding the elastic limit. Now if the disintegration limits of any of the groups vary with the temperature, the elastic limit, the plasticity, and the viscosity will show variation. In the case of glass, as the temperature is raised the magnitude of the stresses necessary to cause the disintegration of many of the groups becomes small, and the glass becomes quite plastic. This is the condition that exists for some 50° C, or more, below and throughout the critical range. At higher temperatures the disintegration limits of many groups become practically zero, and these aggregates then belong to the first class. The glass then behaves much like a viscous fluid.

Whether the characteristics of the glass will be predominately elastic, plastic, or viscous will, accordingly, depend on the temperature, the magnitude of the load, and the time of its application. In the case of the plastico-viscous type of deformation, the relaxation time should under certain conditions be practically independent of the load. These considerations show that, in the bending experiment, a condition may well have existed that caused the relaxation time to remain independent of the load, since the manner of conducting these experiments necessitated the application of rather large stresses at relatively high temperatures in order to obtain measurable rates of bending. These stresses may easily have exceeded the majority of the disorganization limits at those temperatures. On the other hand, the measurements by the optical method were carried out at relatively low temperatures, and for small stresses. The glass was predominately plastic for these conditions, hence as the retardations decreased the relaxation time continually became larger. The two methods can hardly be expected to agree when employed under such different states of aggregation in the glass, and with forces of unlike magnitudes applied in a radically dissimilar manner. The optical method could not be employed in the critical range because the double refraction disappeared so rapidly that time was not available to take sufficient observations. It would appear, therefore, that this view concerning the character of such solids explains in part the discrepancy between the results as obtained by the two methods. Moreover, it is apparent that these characteristics must be taken into account if the cooling method chosen is to be efficient. As glass appears to be always slightly viscous, there always will be a slight residual strain after cooling.

Since the selection of the cooling procedure depends on the ultimate strains introduced, it is necessary to determine their magnitude, or rather the magnitude of the stresses which accompany them. For such a determination there is no really good method. Practically the only one available is the study of the double refraction. This method is unsatisfactory in the first place because no reliable investigations have been published which specify the allowable double refraction for any kind of optical glass, and secondly because the different kinds of glass show different amounts of double refraction under the same stress. There are, in fact, very heavy lead glasses that show no double refraction under stress, while still heavier glasses exhibit an effect opposite in sign to that of the common types. In most, if not all glasses, both com-



ponents of the light, resolved in and perpendicular to the direction of the pressure, are retarded. With the exceptions noted above, the electric component vibrating perpendicular to the direction of the pressure is retarded by the greater amount. Under tension both components are accelerated. Neuman,<sup>20</sup> Pockels,<sup>20</sup> Zschimmer, and Schulz,<sup>21</sup> and others<sup>22</sup> have investigated this subject quite thoroughly, both from theoretical and experimental standpoints. They have, also, discussed in some detail the relation these double refraction effects bear to the chemical composition. This aspect of the subject, however, is not well enough understood to be of any great aid in testing. Consequently such standards as have been established are purely arbitrary. It may be possible to establish more definite standards by specifying the relation between the double refraction due to permanent strain and that produced by a standard pressure on a standard specimen of the same glass. Only a careful investigation will show whether such a method is feasible. At present it is only possible to state that, in annealing glass for optical purposes, it is advisable to remove the stresses as completely as possible, and to bring about a symmetrical distribution of those stresses which cannot be removed in the time available. This latter can be accomplished only when the temperature distribution over the surface is uniform during annealing. It is not difficult to anneal small pieces so that the double refraction is imperceptible under ordinary methods of testing.

It is often of advantage to know something of the magnitude and distribution of the stresses in the body during cooling. The theory of these thermoelastic stresses has been thoroughly developed by Neuman,<sup>23</sup> Hopkinson,<sup>24</sup> Rayleigh,<sup>25</sup> and others.<sup>26</sup> They have also given the equations for the stresses in a number of cases under certain conditions of heat flow. These equations are quite interesting, and are in a number of cases important in testing. In the case of annealing, however, they do not give the distribution of stresses since they all assume that the stresses depend only on the existing temperature differences. In the actual process of annealing and cooling the stresses are continually relaxing at various rates through viscous and plastic flow, so that those present

<sup>20</sup> Neuman, *Pogg. Ann.*, 54, p. 440; 1841.

<sup>20</sup> F. Pockels, *Ann. d. Phys.*, 7, p. 745; 1902.

<sup>21</sup> Zschimmer and Schulz, *loc. cit.*

<sup>22</sup> Kerr, *Phil. Mag.* (5), 190, p. 322; 1888.

<sup>23</sup> F. E. Neuman, *Vorles. über d. Theorie d. Elast. d. fest Körper*, Leipzig; 1885.

<sup>24</sup> Hopkinson, *Mess. of Math.*, 8, p. 168; 1879.

<sup>25</sup> Rayleigh, *Phil. Mag.* (6), 1, p. 169; 1901.

<sup>26</sup> The publication in the near future of a collection of these formulas is contemplated.

at any time depend not only on the temperature distribution then present but on the whole previous history of the annealing. These equations do, however, lead to a better understanding of the manner in which the strains are produced in glass by different modes of cooling. They also make it possible to gain an approximate idea of the stresses during any process of heat treating.

## V. CONCLUSIONS

In summarizing the annealing procedure, it is evident that the first step is to determine a suitable "annealing temperature." This may be done by the use of method I, or still better, by determining the beginning of the critical range (method II). With the proper apparatus (described on p. 551) this latter determination is simple and preferable. If it is used, the annealing temperature should usually be chosen 10 or 20° C below the beginning of critical range.

The next step requires the determination of the "annealing time" corresponding to the chosen "annealing temperature." This is most easily done by studying the rate of deformation of loaded rods of glass. In this way the "relaxation time," and hence the "annealing time" for any degree of annealing, can be approximated in the manner discussed.

A study of the change of the relaxation time with temperature aids in determining the proper rate and mode of cooling. Since, for a certain temperature interval below the critical range, the relaxation time increases very rapidly with decreasing temperature, the rate of cooling, which initially must be very small, may be increased gradually to a certain maximum. This maximum and the rate at any given temperature depends on the size and other characteristics of the object to be annealed. A cooling procedure which appears satisfactory for small pieces is discussed under "cooling."

Since the rate of cooling must be reduced materially in annealing large pieces, consideration must be given to the fact that the slow cooling in the upper range allows the thermoelastic stresses to act for a much longer time. This makes it seem advisable to anneal at a lower temperature where the relaxation time is larger. In this case the annealing time must be increased according to Twyman's equation. For example, if the annealing temperature is reduced 20° C, the annealing time should be increased by a factor of at least 4 and possibly 8. The cooling may then begin at a much more rapid rate.

The procedure outlined here can serve at best only as a guide, since in actual practice the conditions are entirely different from those which exist in a laboratory. The chief causes of poor results in practice are without doubt the lack of temperature uniformity, fluctuations in the temperature during the annealing period, and too rapid or irregular cooling in the upper part of the cooling range. It is essential that the glass take on the required temperature for the required time while annealing, and that it does not merely pass through air heated to that temperature. In cooling, care must be taken that the heat flow is not chiefly through one part of the surface, especially when the body is somewhat extended.

## VI. SUMMARY

Certain methods for determining the annealing range were tested, and the "annealing temperatures" obtained are given for a number of optical glasses.

The critical temperature range for these glasses was determined. In this range there is an apparent absorption of heat on heating, and a corresponding evolution of heat on cooling. In this range there is, also, a marked change in a number of the properties of glass. For most optical glasses, at least, it was found advisable to anneal at a temperature somewhat below this range.

Some of the methods available for determining the relaxation time, and consequently the "annealing time," were tested. The manner in which the relaxation time varies with the temperature was investigated, also, and some results on representative glasses are given.

A cooling procedure which proved very satisfactory in the laboratory is discussed. Mention is also made of the factors which must be considered in cooling the glass and in testing the final product.

Acknowledgment is due to Dr. Paul D. Foote for initiating this investigation, and to C. O. Fairchild for suggestions in temperature measurement and control.

## VII. BIBLIOGRAPHY

## ANNEALING

Year	Author	Reference	Volume	Page
1891.....	Schott.....	<i>Zeits. f. Instk.</i> .....	11	334
1906.....	Dickinson.....	<i>Bull. Bur. Stand.</i> .....	2	189
1906.....	Hitchcock.....	<i>Proc. Eng. Soc. West Pa.</i> .....	22	357
1912.....	Zachimmer.....	<i>Zeits. f. Instk.</i> .....	33	303
1916.....	Boys.....	<i>Nature</i> .....	98	150
1917.....	Twyman.....	<i>Soc. Glass Tech., Tr. (1917)</i> .....	1	.....
1917.....	Parker & Dalladay.....	<i>Phil. Mag.</i> .....	33	276
1918.....	English & Turner.....	<i>J. Soc. Glass Tech.</i> .....	2	90
1919.....	Bellamy.....	<i>J. Am. Cer. Soc.</i> .....	2	313
1919.....		<i>Symposium on Pyrometry: Am. Soc. Mining Engineers; September, 1919.</i>		

## VISCOUS AND PLASTIC DEFORMATION

1868.....	Maxwell.....	<i>Phil. Mag. (4)</i> .....	35	129
1876.....	Butcher.....	<i>Proc. London Math. Soc.</i> .....	8	103
1892.....	Voigt.....	<i>Ann. d. Phys.</i> .....	47	671
1901.....	Reiger.....	<i>Phys. Zeits.</i> .....	2	213
1904.....	Trouton & Andrews.....	<i>Phil. Mag.</i> .....	7	347
1911.....	Bingham.....	<i>Am. Chem. Journ.</i> .....	45	264
1914.....	Guye.....	<i>Arch. d. Sci. Phys. et Nat.</i> .....	37	301

## DOUBLE REFRACTION

1843.....	Neumann.....	<i>Ab. d. Konig Ak. d. Wissen.</i> .....	.....	112
1850.....	Stokes.....	<i>Phil. Mag. (4)</i> .....	2	420
1880.....	Macé de l'Épinay.....	<i>Ann. chim et Phys.</i> .....	19	5
1888.....	Kerr.....	<i>Phil. Mag.</i> .....	26	321
1891.....	Schott.....	<i>Zeits. f. Instk.</i> .....	11	330
1903.....	Czapski.....	<i>Wied Ann.</i> .....	42	319
1904.....	Brace.....	<i>Phys. Review</i> .....	18	70
1908.....	König.....	<i>Ann d. Phys.</i> .....	4	1
1908.....	Wright.....	<i>Am. Jour. Sci.</i> .....	26	370
1909.....	Tuckerman.....	<i>Univ. of Nebr. Studies (No. 2)</i> .....	9	.....
1910.....	Tool.....	<i>Phys. Review</i> .....	31	1
1914.....	Wright.....	<i>Jour. Wash. Acad. Sci.</i> .....	4	594
1914.....	Filen.....	<i>Proc. Roy. Soc.</i> .....	A 89	587

## STRESSES

1879.....	Hopkinson.....	<i>Meas. of Math.</i> .....	8	168
1885.....	Neuman.....	<i>Theorie der Elasticität (Leipzig)</i> .....	.....	112
1894.....	Winkelman & Schott.....	<i>Ann. d. Phys.</i> .....	51	745
1901.....	Rayleigh.....	<i>Phil. Mag. (6)</i> .....	1	169
1914.....	Schulz.....	<i>Sprechsaal</i> .....	47	460, 478
1919.....	Williamson.....	<i>Proc. Wash. Acad. Sci.</i> .....	9	209

## NATURE AND CHARACTERISTICS OF GLASS

Year	Author	Reference	Volume	Page
1898.....	Reed.....	Ann. d Phys.....	65	707
1900.....	Hovestadt.....	Jenaer Glas, Jena.....		
1904.....	Guertler.....	Zeits. für Anorg. Chem.....	40	268
1905.....	Zachimmer.....	Zeits. für Elektrochem.....	11	628
1912.....	Kroll.....	Zeits. für Anorg. Chemie.....	77	1
1914.....	Breckbank.....	Trans. Am. Ceram. Soc.....	15	600
1915.....	Quincke.....	Ann. d. Phys.....	46	1025
1916.....	Langmuir.....	J. Am. Chem. Soc.....	38	2244
1917.....	Canwood and Turner.....	J. Soc. Glass Tech.....	1	87
1917.....	Tillotson.....	J. Ind. Eng. and Chem.....	9	987
1918.....	Tool and Valasek.....	Meet Am. Phys. Soc., Baltimore.....		
1918.....	Peters.....	do.....		
1918.....	Se.....	Proc. Tokyo Math. and Phys. Soc.....		
1918.....	Fenner and Ferguson.....	J. Am. Ceram. Soc.....	1	468
1918.....	Schulz.....	Verh d. Dent. Phys. Ges.....	20	24
1919.....	Bowen.....	J. Am. Ceram. Soc.....	2	261
1919.....	Williams and Rand.....	J. Am. Ceram. Soc.....	2	422

WASHINGTON, June 17, 1919.









# EFFLUX OF GASES THROUGH SMALL ORIFICES

By Edgar Buckingham and Junius David Edwards

## CONTENTS

	Page
1. Introduction.....	573
2. General outline of the investigation.....	574
3. Effusion apparatus and method of experimenting.....	577
4. Orifices.....	579
5. Gases.....	580
6. Method of representing the experimental results.....	582
7. Remarks on the accidental errors of the effusion rates.....	583
8. General equation for efflux of any fluid.....	584
9. Efflux of an ideal gas.....	586
10. Isentropic efflux of a gas.....	587
11. Application to the comparison of different gases.....	589
12. Adiabatic efflux of a viscous gas.....	592
13. Equation for the comparison of viscous gases.....	594
14. Method of comparing the foregoing theory with the observations.....	596
15. Results of the comparison.....	598
16. Efflux with addition of heat but without dissipation.....	600
17. Application to the comparison of nonviscous but thermally conducting gases.....	604
18. Allowance for the simultaneous action of viscosity and conductivity.....	605
19. Attempts to allow for turbulence.....	606
20. Results of the observations on orifice No. 31; values of $\beta'/\beta$ for hydrogen and carbon dioxide.....	607
21. Observations on orifice No. 28; values of $\beta'/\beta$ for methane and argon.....	608
22. Results of applying the theory to orifices Nos. 29 and 23A.....	609
23. Behavior of orifice No. 23B.....	611
24. Remarks on orifices Nos. 23A and 23B I, II, III, and IV.....	612
25. Concluding remarks.....	614

## 1. INTRODUCTION

In Bunsen's effusion method for determining the relative densities of gases, two gases are successively allowed to flow under a small pressure head through a very small hole in a thin plate. The denser the gas the slower is the rate of efflux or effusion, and if the conditions of pressure and temperature are the same for both gases, the times required for the escape of a given volume are approximately proportional to the square roots of the densities. Accordingly, the densities may be set proportional to the squares of the times, and the subsistence of this relation permits

of a simple experimental comparison of the densities by means of time measurements.

In general, the relation just mentioned is only roughly approximate and except with special precautions the effusion method is not at all satisfactory, errors of 30 or 40 per cent being possible. It has been used to a considerable extent in the natural gas industry, and in consequence of difficulties encountered in practice this Bureau was requested, in 1915, to investigate the subject and, if possible, suggest means for making the method more reliable. The work was undertaken by one of the present authors and the results obtained, in so far as they are of immediate interest to gas engineers, have already been published<sup>1</sup> and need not be further discussed from the purely practical point of view. The present paper deals with the more strictly scientific aspect of the investigation.

At the beginning of the experiments it was impossible to foresee the length to which the work would need to be carried, and the experimental accuracy aimed at in designing the apparatus to be used, while ample for the commercial ends then in view, was not so high as we could have desired when the work had gone on for some time and the complexities of the subject were better appreciated. Some improvements and refinements were, however, introduced as opportunity offered and the later measurements are more satisfactory than the earlier ones.

The chief fault to be found with the experimental data is that there are not more of them. It would be interesting, with our accumulated experience, to resume and extend the work, which was interrupted in the summer of 1917. This, however, is impossible and we therefore publish a description of the results of the investigation in the hope that in spite of their obvious incompleteness they may be of interest.

## 2. GENERAL OUTLINE OF THE INVESTIGATION

Preliminary experiments with a number of orifices and with several gases, the densities of which had been determined gravimetrically, gave rather surprising discrepancies and irregularities in the rates of effusion, and showed that the difficulties encountered in the commercial determination of specific gravities by the effusion method could not all be ascribed to faulty procedure or unsatisfactory manipulation, but represented inherent characteristics of the method itself. It soon became evident

<sup>1</sup> J. D. Edwards, Tech. Paper No. 94, Bur. of Standards; Met. Chem. Eng., 16, pp. 518-524, 1917.

that a systematic investigation would be required and that the experimental work must be planned and the results as obtained analyzed and interpreted in the light of such theoretical considerations as could be brought to bear. The first task was, therefore, to devise some sort of theory, making it very simple at first and adding to or modifying it as might be found necessary in order to fit the observed facts as the experiments proceeded.

The orifices being rather small, it seemed at first sight that it might be necessary to have recourse to the kinetic theory of gases. But since even the smallest diameter used is about 300 times the mean free path for hydrogen, under the working conditions, it appeared upon consideration that it would probably be sufficient to regard each gas as a continuum and to treat the orifices merely as small steam-turbine nozzles, keeping in mind that disturbing causes which are of negligible importance for nozzles and orifices of diameters of the order of 1 cm might well have appreciable effects for diameters 100 times smaller. The theory was therefore developed on this basis.

The general method was first to compare the experimental results obtained with the equations for adiabatic flow of an ideal gas through a frictionless orifice. It at once appeared that there was no agreement and that the flow was certainly not of this character. An allowance for the effect of viscosity was then introduced and a qualitative agreement between theory and observation was obtained, but it was evident that at least one more disturbing factor must be taken into account. Transmission of heat from the walls of the orifice to the jet of gas was next considered and a correction for this was tentatively introduced into the theoretical equations. The theory as thus modified seems to be adequate to representing the observed facts quantitatively, for most of the orifices on which much work was done, within the rather wide limits of error of the experiments.

For orifices with a very sharp entrance, and presumably, therefore, for orifices in very thin plates, it appears that the occurrence of contraction of the jet enters as an additional complication; while the effect of this has been recognized, we have not succeeded in representing it quantitatively in the equations. To do so would require a long series of accurate experiments which can not now be undertaken. We have, therefore, to rest satisfied with having devised a rational physical interpretation of the major portion of the observed facts, which appears to be sound so far as it goes, thus giving us some understanding of the phenomena

and enabling us to make qualitative predictions with respect to the relative behavior of gases of known physical properties flowing through small orifices with rounded entrances.

A great deal of time had to be spent in devising and testing various modifications of the theory, but only the final form of

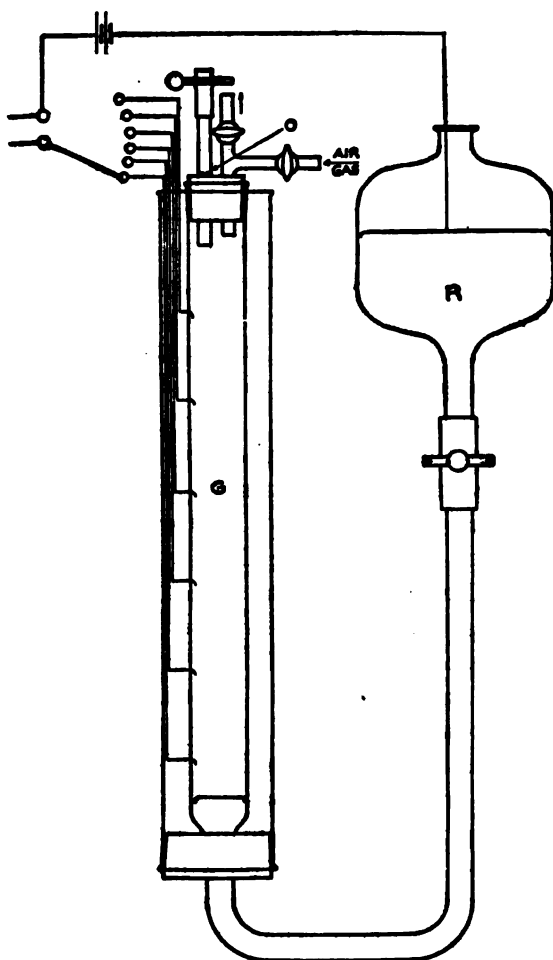


FIG. 1.—Effusion apparatus with automatic timing system

it need be discussed in any detail. The bare experimental results, if presented separately from the theory, would be difficult to grasp, and it seems that the best mode of exposition will be to develop the theory, comparing it step by step with the facts which it purports to represent. After describing the apparatus, the experimental procedure, and the materials, we shall pursue the plan just mentioned.

### 3. EFFUSION APPARATUS AND METHOD OF EXPERIMENTING

Apparatus No. I, which was used in most of the effusion experiments, is shown in outline in Fig. 1. It consisted of a vertical, cylindrical, glass gas chamber *G*, surrounded by a water jacket and connected through a glass tube to the mercury reservoir *R*. The rubber stopper which closed the upper end of the gas chamber carried, first, a glass tube in which the orifice was mounted and, second, an inlet tube through which the gas could be introduced under pressure.

During the course of a run, with the inlet tube closed and the orifice tube open, the gas in *G* was under an excess of pressure equal to the difference of level of the mercury in the two sides of the apparatus. As the gas escaped through the orifice, the mercury, falling in *R* and rising in *G*, swept the gas before it, and at the same time the excess pressure gradually decreased as the mercury surfaces in *R* and *G* approached the same level.

The internal diameter of *G* was about 22 mm and that of the tube connecting it with *R* was about 8.5 mm. A short length of heavy-walled rubber tubing was inserted at a break in this tube, so that the mercury reservoir could be cut off by a pinchcock when it was desired to evacuate the gas chamber. The connecting tube was not blown on to the lower end of *G*, as shown in the figure, but attached through a short rubber connector so that the connection could be broken at this point.

Six platinum contact points were sealed into the wall of *G* and insulated connecting wires were led from them up through the water jacket. When gas was escaping from the orifice during a run, the mercury rising and driving the gas before it made electrical contact with these points, one after the other, and the instants of contact were recorded automatically on a chronograph controlled by the master clock of the Bureau. The time interval between any two successive contacts could thus be determined to about 0.05 second.

The spacing of the six contact points determined five volume intervals. The volume of each was found by weighing the mercury required to fill it, the gas chamber *G* being disconnected for this purpose so that mercury could be run out at the bottom. The volumes of the intervals, counting from the bottom up, were found to have the values shown in Table 1.

TABLE 1.—Volumes for Apparatus No. I

Interval.....	1	2	3	4	5
Volume in cubic centimeters.....	18.59	17.85	17.45	17.06	13.23

The difference of the chronograph readings for the beginning and end of any interval gives the time required for the escape of a mass of gas which occupied the volume of that interval under the conditions of pressure and temperature prevailing within the apparatus. When the volume of the interval is divided by this time, the result is the mean rate of decrease of volume of the confined gas, in cubic centimeters per second, a quantity required in the computations as a measure of the rate of effusion.

For a given gas and a given orifice the rate of effusion depends on the excess of pressure within the container  $G$  over the barometric pressure of the outside atmosphere into which the gas escapes; in other words, on the difference of level of the mercury surfaces in  $R$  and  $G$ . With a given apparatus and a given volume of gas, this head  $\Delta p$  depends on the amount of mercury used. With apparatus No. I, as actually used, the heads of mercury at the instants of contact with the six points, counting from the bottom up, were as shown in Table 2:

TABLE 2.—Values of  $\Delta p$  for Apparatus No. I

Number of point.....	1	2	3	4	5	6
$\Delta p$ , millimeters.....	251	201	154	100	59	17

The loss of head due to the resistance of the connecting tube to the flow of mercury was estimated and found to be negligible.

The total pressure  $p_0$  within the gas chamber at any instant is the sum of the instantaneous values of the head  $\Delta p$  and the outside barometric pressure  $p$ , which was read from a standard barometer.

The temperature of the water in the jacket was always nearly the same as that of the room and did not vary more than a few tenths of 1 degree C during any one experiment, comprising several runs on air and several on one of the test gases. It was assumed to be the same as the temperature of the gas within  $G$ . The slight error in this assumption, due to the fact that the gas is expanding slowly, was computed and found to be quite negligible.

In addition to the apparatus just described, a second which we shall designate as apparatus No. II, was used in a few of the later

experiments. In its general design it was much like No. I and in was used in the same way, but it was larger, so that the times of effusion were longer and the errors in timing, therefore, less important. The water jacket, which had given rise to some insulation difficulties, was replaced by an oil jacket in which circulation and uniformity of temperature were maintained by means of an air lift in a vertical side tube which was joined to the jacket at top and bottom.

Apparatus No. II had nine contact points defining eight volume intervals. The volumes, measured as before by weighing mercury, were found to have the values shown in Table 3.

TABLE 3.—Volumes for Apparatus No. II

Number of interval.. Volume in cubic centimeters.....	1	2	3	4	5	6	7	8
	54.69	48.38	50.71	50.56	41.56	35.06	27.47	22.60

The heads of mercury at the instants of contact with the points were found to be as shown in Table 4:

TABLE 4.—Values of  $\Delta p$  for Apparatus No. II

Number of point... $\Delta p$ , millimeters.....	1	2	3	4	5	6	7	8	9
	266.9	223.1	184.2	143.6	103.1	69.9	42.2	19.8	1.5

A few experiments were also made with a third piece of apparatus. This was intended for use with very low heads and sulphuric acid of density 1.84 was used instead of mercury. There was only one interval and its volume was 189.4 cc. The heads at the beginning and end of this interval were 110 and 6 mm of  $H_2SO_4$ , equivalent to 14.9 and 0.81 mm of mercury.

#### 4. ORIFICES

The orifice plates were made from a stiff platinum-iridium alloy and were about 5 or 6 mm in diameter. The hole was pierced with a fine needle and then reamed out as desired. Any burr could be removed and the plate ground down by rubbing on fine emery paper, the appearance of the orifice during the finishing operation being observed under the microscope. The thickness of the plate was measured by a micrometer caliper and the diameter of the hole was deduced from a number of measurements under a micrometer microscope. When the plate was finished it was sealed into the end of a glass tube and another piece of tube was then sealed on, so that when the job was complete the orifice

plate formed a diaphragm across the middle of a continuous glass tube 8 or 10 cm long.

The dimensions of the orifices to which reference will be made in this paper are given in Table 5:

TABLE 5.—Dimensions of the Orifices in Millimeters

Number of orifice.....	23	28	29	31
Diameter of hole.....	0.070	0.069	0.055	0.067
Thickness of plate.....	.04	.10	.05	.10

Orifice No. 23 was used in two positions and will be referred to as 23A or 23B, depending on which face was uppermost.

It was not practicable to finish such small orifices with any great nicety, hence the holes were not quite round and their edges were more or less irregularly rounded off and neither perfectly smooth nor perfectly sharp.

## 5. GASES

Four samples of gas were used in addition to air which served as the standard. They were stored in steel cylinders at high pressure and drawn off as needed through pressure regulators which delivered them at a convenient rate for filling the apparatus. The gases were not pure, but to avoid circumlocution each gas will be designated by the name of its most important constituent and, when appropriate, denoted by the chemical symbol of that constituent. The gases may be described as follows:

*Hydrogen, H<sub>2</sub>.*—This was a commercial electrolytic gas. Its specific gravity referred to air, when determined gravimetrically at the beginning of the investigation, was found to be 0.08854, the value for pure hydrogen being 0.06951. Assuming the impurity to consist of oxygen, the oxygen content was about 1.8 per cent by volume.

After an interval of about one year, during which the gas had been kept in a steel cylinder under pressure, new effusion experiments indicated that the gas had become lighter. A new determination of the specific gravity was therefore made and the result was 0.08587, corresponding to an oxygen content of 1.6 per cent by volume.

*Methane, CH<sub>4</sub>.*—This was a sample of natural gas. It contained over 90 per cent of methane and its specific gravity was found to be 0.583, the value for pure methane being 0.554.

*Carbon Dioxide, CO<sub>2</sub>.*—This was a commercial gas of specific gravity 1.528; since the specific gravity of pure carbon dioxide is 1.529, this sample appears to have been fairly pure.



**Argon, Ar.**—This was a mixture of argon, oxygen, and nitrogen, obtained from liquid air. Its specific gravity was 1.167, and this, together with a volumetric determination of the oxygen content, showed that the composition, in volume per cent, was approximately

$$\text{Ar} = 33 \quad \text{O}_2 = 46 \quad \text{N}_2 = 21$$

The details of the method of gravimetric determination of gas density are given in Technologic Paper No. 94 of this Bureau.

In addition to the specific gravities of the gases, data on certain other physical properties were required for use in developing and testing the theory. The first of these was the specific heat ratio  $C_p/C_v = k$ . It was assumed that the value for air was  $k = 1.400$  and that the value for hydrogen was the same. The values for the other three gases were measured in terms of the value for air by means of a Kundt's tube, using the measured specific gravities in the computations. The precision of the Kundt's tube measurements was ample, the accuracy of  $k$  being limited by that of the gravimetric determinations of specific gravity. The values of  $k$  are given in Table 6.

It was also necessary to know the relative viscosities of the gases, although no high accuracy was required because the values were to be used only in computing corrections. The determinations were made by substituting, in apparatus No. I, a long fine glass capillary for the orifice tube, and comparing the rates of escape of air and of the gas in question under identical conditions of pressure and temperature. The values of the relative viscosity  $\mu'/\mu$  referred to air are given in Table 6. The quantities  $P$  and  $\beta'/\beta$  which are also included in Table 6 will be discussed later.

TABLE 6.—Physical Properties of the Gases

Specific gravity	Air	H <sub>2</sub>	CH <sub>4</sub>	CO <sub>2</sub>	Ar
$\rho'/\rho = \delta$	1.000	0.06954 (1916) .08587 (1917)	0.583	1.528	1.167
$C_p/C_v = k$	1.400	1.400	1.303	1.290	1.462
$(k-1)/k = \alpha$	$\frac{2}{7}$	$\frac{2}{7}$	.233	.225	.316
$\mu'/\mu$	1.000	.519	.618	.815	1.126
$\alpha' \mu'/\alpha \mu \sqrt{\delta} = P$	1.000	1.745	.660	.519	1.153
$\beta'/\beta$ (tentative)	1.00	1.69 (1916) 1.62 (1917)	.47	.46	1.10
$\beta'/\beta$ (as finally used)	1.00	1.50	.75	.40	1.04

The values for air are all given by definition or assumption.

## 6. METHOD OF REPRESENTING THE EXPERIMENTAL RESULTS

In order to compare the results obtained with different gases so as to get an insight into the relation of the errors of Bunsen's method to the physical properties of the gases, it seemed desirable to represent the results in such a way as to exhibit the fractional rather than the absolute errors and the following plan was adopted:

Let  $p$  = the outside or barometric pressure

Let  $p_0 = p + \Delta p$  = the pressure within the gas chamber, or the initial pressure as we shall call it.

Let  $r = p/p_0$ ; it will be called the pressure ratio. At the start of a run,  $\Delta p$  has its largest value and  $r$  its smallest, and as the run proceeds,  $\Delta p$  approaches zero and  $r$  increases toward unity.

Let  $\tau$  = the time in seconds required for the volume of gas within the apparatus to decrease by 1 cc, when the pressure ratio has a particular value  $r$  and the gas under experiment is air.

Let  $\tau'$  = the corresponding time for the test gas under identical conditions.

Let  $\delta$  = the specific gravity of the test gas, referred to air.

Then the relation on which the effusion method of determining specific gravity is based is that  $\delta = (\tau'/\tau)^2$ , approximately.

Let

$$\left(\frac{\tau'}{\tau}\right)^2 / \delta = R$$

If the effusion method gave correct results, we should have  $R = 1$ , and in practice the observed value of  $(R - 1)$  is the fractional error of a determination of specific gravity by this method.

In the experiments with apparatus No. I, which had five volume intervals, each experiment gave five mean values of  $\tau'/\tau$  and therefore of  $R$ , each corresponding to a certain mean value of  $r = p/p_0$ . With apparatus No. II each experiment gave eight instead of five values of  $R$ . What we have done is to plot the observed mean values of  $R$  as ordinates against the corresponding mean values of  $r$  as abscissas.

When the results of any one experiment are plotted in this way, the points lie along a more or less smooth curve, and by plotting the results of a number of supposedly identical experiments an idea may be formed of the accidental errors of the observations.

If Bunsen's method were correct in principle, the points would always be grouped indiscriminately about the straight line  $R = 1$ , and any grouping of points about a different curve indicates the presence of a systematic error in the method itself, upon which the accidental errors of experiment are superimposed. When all the results obtained with different gases but the same orifice are plotted together on one diagram, we have a convenient means of comparing the behavior of the gases.

If we can then build up a theory for predicting the behavior of the gases from a knowledge of their physical properties, and compute values of  $R$  in terms of  $r$ , we may plot theoretical curves  $R = f(r)$  for comparison with the observed values of  $R$ , and thus test the ability of the theory to represent the observed facts.

By examining plates 2 to 7, the reader may form an estimate of the accidental errors of the observations which are represented by the plotted points, all the points of any one series being denoted by the same symbol. The curves on these plates are drawn from the theory which will be discussed in detail later on.

The theory is based on the consideration of the steady flow of fluids, whereas in the experiments the rate of flow was not constant but continually decreasing. This change of rate was so slow that there is no doubt that at any instant it was sensibly the same as if the conditions had already been held constant for a long time; but the observations of the rates of efflux had to be made by means of a small number of contact points and gave, of course, only average rates over considerable ranges of variation of the pressure ratio  $r$ . Each value of  $r$  or of  $r'$  was obtained by dividing the observed time in seconds for the interval in question by the volume of the interval in cubic centimeters. The corresponding value of  $r$  was taken to be the geometric mean of the values at the beginning and end of the interval; it did not in any case differ more than 0.2 per cent from the arithmetic mean.

## 7. REMARKS ON THE ACCIDENTAL ERRORS OF THE EFFUSION RATES

Each experiment or "series" consisted of several runs on the test gas, preceded or followed by several runs on air under nearly identical conditions of temperature and barometric pressure. A "run" was made by filling the gas chamber with dry gas under pressure until the mercury level was somewhat below the lowest contact point, opening the orifice tube, and recording on the chronograph the times at which the mercury surface reached the

contact points as it rose and swept the gas before it through the orifice. The number of runs in each series was usually from five to eight with each of the two gases, and the values of  $\tau$  and  $\tau'$  for the series were means of the values for the separate runs.

It sometimes happened that separate runs which should have differed only by accidental errors in reading the chronograph sheets differed considerably more than this. It seems probable that these irregularities are to be attributed mainly to dust or condensed mercury catching on the edges of the orifice; for they were most frequent in the case of orifice No. 23, which had rougher edges than the other orifices and so was more adapted to catching and retaining small particles. Occasionally two series, each of which gave values of  $R = f(r)$  lying along a smooth curve, would differ considerably without there being, a priori, any evident reason for the difference. It seems likely that such differences were due to dust particles which may in one case have lodged in the orifice at the start and remained in the same position throughout the series.

Another sort of irregularity sometimes observed consisted in a delay of the time registered for one of the contacts, and resulted in too long a time for the preceding and too short a time for the following interval. This may have been due to a slight sticking of the rising mercury surface at the glass wall (the contact points being rather near the wall instead of in the middle of the gas chamber) or to irregularities in the action of the chronograph.

Any error in timing, whatever its source, would have more effect on the values of  $R$  computed from the time intervals if the time intervals were short—that is, the effusion rapid—than if they were long. Accordingly it was to be expected that the results would be much more irregular and scattering for hydrogen than for the other gases and this is what actually happened as may be seen from the plates.

### 8. GENERAL EQUATION FOR EFFLUX OF ANY FLUID

Let a fluid be flowing steadily along a channel with impermeable walls; the walls may be material or the channel may be merely a stream tube within the fluid, its boundary being an imaginary surface across which no fluid passes either in or out. Let us consider a portion of the channel or tube extending from an entrance section  $A_0$  to an exit section  $A$ ,  $A_0$  and  $A$  being drawn so as to be, at each point, normal to the mean direction of flow at that point. Let the sections be at the same level so that no

gravitational work is done by or on the fluid in its passage from  $A_0$  to  $A$ .

Let  $p_0$  and  $p$  be the pressures, and  $\theta_0$  and  $\theta$  the absolute temperatures in the fluid at the two sections. Let  $v_0$ ,  $\epsilon_0$ ,  $T_0$  be, respectively, the volume, internal energy, and kinetic energy of each gram of the fluid as it enters at  $A_0$ ; and let  $v$ ,  $\epsilon$ ,  $T$  be the corresponding values at  $A$ . Let  $Q$  be the quantity of heat added from outside the channel to each gram during its passage from  $A_0$  to  $A$ ;  $Q$  includes only heat which actually passes through the boundary of the channel and does not include heat developed within the fluid by viscous or other resistances.

The work per gram done on the fluid as it enters at  $A_0$  is  $p_0 v_0$ ; and the work done by it on the fluid ahead of it, as it issues at  $A$  is  $p v$ . We therefore have, by the first law of thermodynamics, the equation

$$(T + \epsilon) - (T_0 + \epsilon_0) = p_0 v_0 - p v + Q \quad (1)$$

We proceed to apply this equation to the case of a fluid escaping in a jet through a small orifice in the wall of a large container in which the fluid is at rest except for its slow general motion toward the orifice.

Let  $A$  be the minimum section of the jet; if the entrance to the orifice is sufficiently rounded off there is no contraction, and  $A$  is the minimum or throat area of the orifice. The symbols  $p$ ,  $\theta$ ,  $v$ ,  $\epsilon$ ,  $T$  now refer to conditions in the jet. If the jet speed is less than that of sound in the fluid,  $p$  is equal to the outside back pressure and this was the case in our experiments, the pressure ratio  $r$  being always greater than the critical ratio, which for air is about 0.53.

Let  $A_0$  be described within the container, normal to the direction of flow toward the orifice and far enough back along the stream that  $A_0$  is very large compared with  $A$  and the motion at  $A_0$  very slow compared with the speed at the jet. The kinetic energy  $T_0$  will then be negligible and  $p_0$ ,  $\theta_0$  will be the pressure and temperature of the nearly stationary fluid within the container.

By setting  $T_0 = 0$  in (1) we now obtain the equation

$$T = (\epsilon_0 + p_0 v_0) - (\epsilon + p v) + Q \quad (2)$$

No restrictions have been imposed on the properties of the fluid or the nature of the motion so that equation (2) is general.

## 9. EFFLUX OF AN IDEAL GAS

Let the fluid be an ideal gas<sup>2</sup>—that is, one for which the equations

$$pv = m\theta \qquad C_v = \text{const} \qquad (3)$$

are satisfied— $\theta$  being measured on the thermodynamic scale, and  $C_v$  denoting the specific heat at constant volume. In our experiments the range of temperature was less than 30° C, and the pressures were between 1 and 1.4 atmospheres. And while the gases used are by no means strictly ideal, they are so nearly ideal that over this small range of pressure and temperature equations (3) may be applied to them without sensible error.

It is easily shown by elementary thermodynamics that for the ideal gas defined by equations (3), the further equations

$$\epsilon = \theta C_v + \text{Const.} \qquad (4)$$

$$C_v + m = C_p \qquad (5)$$

are always satisfied,  $C_p$  denoting the specific heat at constant pressure. If we eliminate  $\epsilon$ ,  $\epsilon_0$ ,  $pv$ , and  $p_0 v_0$  from (2) by means of (4) and (3) and then apply (5), we obtain the equation

$$T = (\theta_0 - \theta)C_p + Q \qquad (6)$$

which is sensibly exact as applied to our experiments on efflux.

Let  $S$  be the mean speed of the jet at  $A$ , and let us set

$$T = \frac{1}{2}S^2 \qquad (7)$$

This amounts to assuming, first, that the kinetic energy of turbulence is negligible in comparison with that of the axial motion, and second, that the arithmetical mean speed taken over the section  $A$  is sensibly identical with the square-root-of-mean-square speed; that is, that the speed is nearly uniform all over the section. Both these assumptions are known to be legitimate for larger orifices and there is no reason to expect that they will lead us into any difficulties. We therefore adopt them and so, by means of (7), reduce equation (6) to the form

$$\frac{1}{2}S^2 = (\theta_0 - \theta)C_p + Q \qquad (8)$$

Subject to the assumption of equation (7), equation (8) is entirely general as applied to the efflux of an ideal gas. Any sort

<sup>2</sup> See Bull., Bur. Standards, 6, No. 3, p. 409, 1910; Scientific Paper No. 136.

of passive resistance will, of course, decrease the jet speed  $S$ ; but the dissipation of energy by the resistance heats the fluid and raises its final temperature  $\theta$ , so that  $(\theta_0 - \theta)$  is also decreased and equation (8) remains satisfied.

It frequently happens that the transmission of heat from the orifice to the jet of gas is so small as not to produce any sensible effect on the phenomena. The efflux is then sensibly adiabatic, and by setting  $Q = 0$  we have, for adiabatic efflux of an ideal gas,

$$\frac{1}{2}S^2 = (\theta_0 - \theta)C_p \quad (9)$$

If we were dealing with such ranges of pressure and temperature as occur at the valve of an air liquefier, it would not be legitimate to treat the gases used in our investigation as ideal; in fact, the possibility of liquefying gases by the Hampson-Linde method is due to their not being ideal.<sup>3</sup> But for our present purposes it is safe to treat the gases as ideal, and for simplicity we may as well drop the adjective ideal and, for the future, speak merely of "gases."

#### 10. ISENTROPIC EFFLUX OF A GAS

As a first attempt to formulate a theory, let us suppose that the efflux is adiabatic and that there are no passive resistances and therefore no development of heat within the fluid; that is, no dissipation. Then the gas expands isentropically from its initial pressure  $p_0$  to the back pressure  $p$ , which exists at the minimum section of the jet so long as the jet speed is less than the speed of the sound in the gas at  $p$ ,  $\theta$ . Hence, we may use the familiar equations for isentropic expansion of an ideal gas, namely:

$$p v^k = \text{const} \quad (10)$$

$$\theta v^{k-1} = \text{const} \quad (11)$$

$$\theta = \text{const} \times p^{\frac{k-1}{k}} \quad (12)$$

If, for convenience, we introduce the abbreviations

$$\frac{p}{p_0} = r \text{ and } \frac{k-1}{k} = a \quad (13)$$

we have by (12)

$$\frac{\theta}{\theta_0} = r^a \quad (14)$$

<sup>3</sup> See Bull., Bur. Standards, 6, No. 1, p. 225, 1909; Scientific Paper No. 223.

and equation (9) for adiabatic efflux of a gas may be written

$$\frac{1}{2} S^2 = \theta_0 C_p (1 - r^a) \quad (15)$$

From equation (5) together with the definitions of  $k$  and  $\alpha$ , we have the relation

$$C_p = \frac{m}{a} \quad (16)$$

Substituting in (15) and setting  $m \theta_0 = p_0 v_0$  we now have

$$\frac{1}{2} S^2 = p_0 v_0 \frac{1 - r^a}{a} \quad (17)$$

which is one form of the familiar equation of St. Venant. Since we are interested in the density  $\rho$  rather than its reciprocal, the specific volume  $v$ , we substitute  $v_0 = 1/\rho_0$  and write equation (17) in the form

$$\frac{1}{2} S^2 = \frac{p_0}{\rho_0} \frac{1 - r^a}{a} \quad (18)$$

This is not yet in shape for immediate use, because in the experiments on efflux the quantity measured is not the speed of the jet but the time required for a certain volume of gas at  $p_0, \theta_0$  to disappear from the container. We have, therefore, to eliminate  $S$ .

Let  $\tau$  be the observed time rate of disappearance of the gas, in seconds per cubic centimeter, and let  $V_0 = 1/\tau$ , so that  $V_0$  is the volume, measured in cubic centimeters at  $p_0, \theta_0$ , of the mass of gas which escapes from the orifice per second. Let  $V$  be the volume of this same mass of gas measured at  $p, v$ , the conditions which prevail in the jet at  $A$ . Then since the expansion is isentropic we have, by equations (10) and (13)

$$V = \frac{V_0}{r^{1-\alpha}} \quad (19)$$

But we have also, obviously, the equation

$$V = AS \quad (20)$$

and therefore by (19)

$$S = \frac{V_0}{A r^{1-\alpha}} \quad (21)$$



If we substitute this value of  $S$  in equation (18), replace  $V_0$  by  $1/\tau$ , and solve for  $\rho_0/\tau^2$ , the result is

$$\frac{\rho_0}{\tau^2} = 2A^2 p_0 \frac{r^{2-2\alpha}}{a} (1 - r^\alpha) \quad (22)$$

a relation which would subsist between the observed value of  $\tau$  and the other quantities involved, if the efflux were isentropic.

## 11. APPLICATION TO THE COMPARISON OF DIFFERENT GASES

Having made a run with the standard gas and determined  $\tau$  under the given conditions,  $p_0$ ,  $\theta_0$ ,  $\tau$ , let us repeat the experiment under the same conditions with a second gas and determine its time  $\tau'$ . The specific gravity of the second or test gas as indicated by the results of the efflux method is  $(\tau'/\tau)^2$ , while if  $\rho_0$  and  $\rho_0'$  are the densities of the gases at  $p_0$ ,  $\theta_0$ , the true value of the specific gravity of the test gas in terms of the standard is  $\delta = \rho_0'/\rho_0$ .

$$\text{Let} \quad \left(\frac{\tau'}{\tau}\right)^2 / \delta = R \quad (23)$$

When Bunsen's method gives a correct value,  $R = 1$ ; and  $(R - 1)$  is the fractional error in the specific gravity of the test gas as determined by this method. The value of  $R$  which would result from the observations if the efflux were isentropic for both gases shall be denoted by  $R_1$ .

Let equation (22) refer to isentropic efflux of the standard gas and let the corresponding equation for the test gas be

$$\frac{\rho_0'}{\tau'^2} = 2A'^2 p_0 \frac{r'^{2-2\alpha'}}{a'} (1 - r'^{\alpha'}) \quad (24)$$

The area  $A'$  is that of the minimum section of the jet of the test gas; and if the orifice is sharp edged so that a vena contracta is formed,  $A'$  may differ from  $A$ , even though the orifice be unchanged. For the present, however, we shall suppose the orifice to have a rounded entrance so as not to give rise to contraction, and we shall set  $A' = A$ .

If we divide equation (22) member for member by (24), set  $A' = A$ , utilize (23), and replace  $R$  by  $R_1$ , we have

$$R_1 = \frac{a'}{a} r'^{2(\alpha' - \alpha)} \frac{1 - r^\alpha}{1 - r'^{\alpha'}} \quad (25)$$

For two gases, for example, air and hydrogen, which have the same specific heat ratio,  $\alpha' = \alpha$  and  $R_1 = 1$  for all values of the pressure ratio  $r$ . For two such gases Bunsen's method would give a correct value of the relative density if the efflux were isentropic. But if  $\alpha' \neq \alpha$ ,  $R_1$  will differ from unity and Bunsen's method would not give a correct value of the relative density, even under ideal isentropic conditions.

In plate 1 curves of  $R_1 = f(r)$  are plotted from equation (25) using the known values of  $\alpha$  and  $\alpha'$  for the gases investigated,  $\alpha$  referring to air, which was treated as the standard. The separate points plotted are values of  $R = (\tau'/\tau)^2 + \delta$  computed from values of  $\tau$  and  $\tau'$  actually obtained in experiments on orifice No. 23A, series 2, 5, 9, and 21.

Upon comparing the observed values of  $R$  with the computed curves of  $R_1$  it appears that there are large systematic differences which increase as  $r$  approaches unity, that is, as the pressure difference and the jet speed approach zero. The departure of the observed values of  $R$  from the computed values of  $R_1$  is of the same general nature for all four gases though it is positive for hydrogen and argon, and negative for methane and carbon dioxide. It is evident that equation (25) does not represent the facts accurately and that the efflux is not isentropic, hence we must reexamine the assumptions that have been made, the principal ones being that there are no viscous resistances to flow and that there is no heat leakage to the escaping gas.

Since the orifices are of more or less irregular shapes, which moreover are not accurately known, it would be quite useless to attempt to attack the problem of computing the resistance by the ordinary methods of hydrodynamics, even if we were sure that the motion were strictly in stream lines and quite free from turbulence. Similarly with the question of heat transmission from the walls of the orifice to the gas—to treat this in detail by reference to the temperature gradients would require a complete knowledge of the motion of the gas, so that such a treatment is out of the question. Accordingly we are forced to do the best we can with very elementary physical reasoning, and our aim will be merely to develop equations containing empirical orifice constants, one for the viscous resistances and one for the effect of heat leakage, which shall be correct or at least satisfactory in their forms, so that when the values of the two orifices constants are suitably

chosen, the theoretical equations may represent the observed facts within the limits of experimental error.

Hitherto we have assumed that the only resistance that limited the speed of efflux of the gas was the kinetic or inertia resistance, due to its density and proportional to the square of the linear speed. On the other hand, viscous resistances, if present, would be proportional to the first power of the speed, and the disturbing effect of such resistances should therefore become more pronounced as the linear speed diminished; that is, as the pressure ratio  $r$  approached unity. This is just the character of the departures of the observed values of  $R$  from the computed values of  $R_1$ , hence it seems advisable to proceed next to a consideration of the probable effect of viscosity, and attempt to make an addition to our theory which shall allow for it while still assuming that the flow is adiabatic.

## 12. ADIABATIC EFFLUX OF A VISCOUS GAS

In consequence of the passive resistance due to viscosity, heat is developed within the gas during its passage from  $A_0$  to  $A$  or, as we say, there is a certain amount of "dissipation." We shall denote this quantity of heat or amount of dissipation, per gram of gas, by the letter  $D$ .

The major part of the dissipation will evidently occur close to or in the orifice where the gas has almost attained its lowest pressure, both because the gas has there nearly reached its greatest speed and because the reduction in cross section of the stream increases the transverse velocity gradients and the rate of shear. The final net result of the dissipation must, therefore, be nearly the same as if the gas first expanded isentropically to the back pressure  $p$  and the dissipation then all occurred at the constant pressure  $p$ , reducing the speed from the value attained in isentropic expansion and given by equation (18), and simultaneously raising the temperature from its lowest value by an amount  $D/C_p$ . Since we can do no better, we shall adopt this simplified view of the matter, which is certainly a fair approximation, and proceed as if the dissipation really did occur in this way.

The temperature after isentropic expansion being  $\theta_0 r^\alpha$ , by equation (14), the final temperature at  $A$  is now

$$\theta = \theta_0 r^\alpha + \frac{D}{C_p} \quad (26)$$

Substituting this value in equation (9), which is satisfied for adiabatic efflux regardless of dissipation, we have

$$\frac{1}{2}S^2 = \theta_0 C_p (1 - r^a) - D \quad (27)$$

or after eliminating  $\theta_0 C_p$  as before

$$\frac{1}{2}S^2 = \frac{p_0}{\rho_0} \frac{1 - r^a}{a} - D \quad (28)$$

We must next express  $D$  in terms of the other quantities, and to do this we first *assume* that for an orifice of given shape the value of  $D$  depends on and is determined by the diameter of the orifice  $a$ , the jet speed  $S$ , the viscosity of the gas  $\mu$ , and its initial density  $\rho_0$ . The subsistence of such a relation may be symbolized by writing

$$D = f(a, S, \mu, \rho_0) \quad (29)$$

and dimensional conditions require<sup>4</sup> that any relation involving these five quantities and no others have the form

$$D = S^2 \varphi \left( \frac{a \rho_0 S}{\mu} \right) \quad (30)$$

in which  $\varphi \left( \frac{a \rho_0 S}{\mu} \right)$  is an unknown function of the single dimensionless quantity  $(a \rho_0 S / \mu)$  and remains to be found by other than dimensional considerations.

The flow toward and into the orifice is convergent, and we know from observation that convergence tends to suppress turbulence and maintain stream line flow. We shall therefore *assume*, as a sufficient approximation to the true state of affairs, that there is no turbulence whatever. But in purely stream line motion the resistances and the dissipation are, other things being equal, directly proportional to the viscosity of the fluid; hence it follows from our assumption that  $\varphi \left( \frac{a \rho_0 S}{\mu} \right)$  must be directly proportional to  $\mu$ , and that equation (30) must have the form

$$D = B \frac{\mu S}{a \rho_0} \quad (31)$$

in which  $B$  is a dimensionless constant shape factor determined by the shape of the orifice and of the approach to it. By substitut-

<sup>4</sup> See Trans. Am. Soc. Mech. Engineers, 37, p. 263, 1915; or Phys. Rev., 4 p. 345, Oct. 1914.

ing this expression for  $D$  in equation (28) we obtain the equation

$$\frac{1}{2}S^2 = \frac{p_0}{\rho_0} \frac{1-r^a}{a} - \frac{B\mu S}{a\rho_0} \quad (32)$$

which serves as the starting point of our tentative theory of the effusion method of determining the relative densities of gases which are not free from viscosity.

To eliminate the jet speed  $S$  and replace it by the observed quantity  $\tau$  or its reciprocal  $V_0$ , we proceed as follows. If  $V$  is the volume, measured at  $p, \theta$ , of the gas which escapes per second; and  $V_0$  its volume at  $p_0, \theta_0$ , we have by (3)

$$\frac{V}{V_0} = \frac{p_0}{p} \frac{\theta}{\theta_0} = \frac{1}{r} \frac{\theta}{\theta_0} \quad (33)$$

whence by (26)

$$V = \frac{V_0}{r^{1-a}} \left[ 1 + \frac{D}{r^a \theta_0 C_p} \right] \quad (34)$$

We next eliminate  $\theta_0 C_p$  by means of (16) and (3), replace  $D$  by its value from (31), and combine with the equation  $V = AS$  which subsists as before. The result is

$$S = \frac{V_0}{Ar^{1-a}} \left[ 1 + \frac{B\mu a S}{ar^a p_0} \right] \quad (35)$$

an equation which may be used with (32) for eliminating  $S$ .

For convenience in the algebraic work we introduce the abbreviation

$$\frac{B}{Aa} = C \quad (36)$$

Since the orifices were so small that neither  $A$  nor  $a$  could be determined at all accurately, and since furthermore the value of  $B$  is entirely unknown,  $C$  is a purely empirical orifice constant.

We shall also use the further abbreviation

$$\frac{B}{Aa} \frac{a\mu V_0}{r p_0} = \frac{Ca\mu}{p\tau} = X \quad (37)$$

For a given orifice and a given back pressure,  $C/p$  is constant. In all our experiments  $p$  was nearly constant, being simply the barometric pressure of the outside atmosphere. For a given gas and a given temperature,  $a\mu$  is also constant so that  $X$  depends sensibly only on  $\tau$ , which varies with the pressure ratio  $r$ .

Upon eliminating  $S$  between (32) and (35) we now have the equation

$$\left\{ \frac{1}{A r^{1-\alpha} \tau (1-X)} \right\}^2 + \frac{2 p_0 r^\alpha X}{a \rho_0 (1-X)} = 2 \frac{p_0 (1-r^\alpha)}{\rho_0 a} \quad (38)$$

whence

$$\frac{\rho_0}{\tau^2} = 2 A^2 p_0 \frac{r^{2-2\alpha}}{a} [(1-r^\alpha) - (2-r^\alpha)X + X^2] \quad (39)$$

By comparing (39) with (22) which was deduced for isentropic efflux we see that the result of our considerations on the effects of viscosity has been to modify the isentropic equation by the addition of two correction terms which involve the viscosity of the gas. It is to be presumed that these terms are small enough that the second, containing  $X^2$ , will be negligible. Trial computations with values of  $C$  found from the experiments confirm this inference and show that for our purposes the  $X^2$  term may be ignored and equation (39) used in the simpler form

$$\frac{\rho_0}{\tau^2} = 2 A^2 p_0 \frac{r^{2-2\alpha}}{a} [(1-r^\alpha) - (2-r^\alpha)X] \quad (40)$$

### 13. EQUATIONS FOR THE COMPARISON OF VISCOUS GASES

Let the value of  $R$  which would be obtained from the observations, if the efflux of each of two gases were adiabatic but affected by their viscosities in the manner assumed in the foregoing section, be denoted by  $R_\mu$ . Let equation (40) refer to the standard gas, and a similar equation with the appropriate letters primed refer to the test gas. Then upon comparing the two equations and assuming as before that  $A' = A$ , we have

$$R_\mu = \frac{a'}{a} r^{2(\alpha'-\alpha)} \frac{(1-r^\alpha) - (2-r^\alpha)X}{(1-r^{\alpha'}) - (2-r^{\alpha'})X'} \quad (41)$$

and we now wish to find out whether this equation can be made to fit the observed facts by a suitable choice of the orifice constant  $C$ . The graphical comparison of theory with observation is the most enlightening and in order to use equation (41) for computing and drawing a curve  $R_\mu = f(r)$  we must first undertake some further transformations.

By equation (37) which defines  $X$  and  $X'$ , we have

$$X' = X \frac{a'}{a} \frac{\mu'}{\mu} \frac{\tau}{\tau'} \quad (42)$$

and by the definition of  $R$  in equation (23) we have for the present case of adiabatic efflux under the influence of viscosity

$$\frac{\tau}{\tau'} = \sqrt{\frac{\rho_0}{\rho'_0 R_\mu}} \quad (43)$$

so that by (42)

$$X' = X \frac{a'}{a} \frac{\mu'}{\mu} \sqrt{\frac{\rho_0}{\rho'_0}} \frac{1}{\sqrt{R_\mu}} \quad (44)$$

Let

$$\frac{a' \mu'}{a \mu} \sqrt{\frac{\rho_0}{\rho'_0}} = P \quad (45)$$

The quantity  $P$  is a dimensionless constant which expresses the value of a certain property of the test gas in terms of the corresponding property of the standard. Its value is known because the values of  $a'/a$ ,  $\mu'/\mu$  and  $\rho'_0/\rho_0$  have been measured for all the gases used, except that  $a'$  for hydrogen was assumed to be equal to  $a$  for air and was not measured. The value of  $\mu'/\mu$  was, to be sure, measured only for a single temperature; but since the viscosity of gases does not vary rapidly with temperature nor very differently for different gases, and since the whole temperature range in our work was small, a single constant value of  $\mu'/\mu$  may be used for each gas. The values used for  $P$  have been given in Table 6.

By equations (44) and (45) we now have

$$X' = \frac{P}{\sqrt{R_\mu}} X \quad (46)$$

whence by substitution in (41) we have

$$(1 - r^{a'})R_\mu - (2 - r^{a'})PX\sqrt{R_\mu} = \frac{a'}{a} r^{a'(a'-a)} [(1 - r^a) - (2 - r^a)X] \quad (47)$$

If we solve this for  $R_\mu$ , the result may be written in the form

$$R_\mu = L + 2G^2[1 + \sqrt{1 + L/G^2}] \quad (48)$$

where

$$\left. \begin{aligned} L &= \frac{a'}{a} r^{a'(a'-a)} \frac{(1 - r^a) - (2 - r^a)X}{1 - r^{a'}} \\ G &= \frac{2 - r^{a'}}{1 - r^{a'}} \frac{PX}{2} \\ X &= \frac{Ca\mu}{p} \frac{1}{\tau} \end{aligned} \right\} \quad (49)$$

Trial computations showed that the positive value of the radical in (48) was the proper one to use, so the negative sign is omitted.

#### 14. METHOD OF COMPARING THE FOREGOING THEORY WITH THE OBSERVATIONS

The value of  $R_\mu$  computed for any value of  $r$  from equations (48) and (49) depends upon: (a) The values of  $a$ ,  $a'$ ,  $\mu'/\mu$ , and  $\rho'/\rho_0$  which were determined experimentally; (b) the value selected for the orifice constant  $C$ ; and (c) the value of  $\tau$  observed for air at the given  $r$ .

The most obvious procedure for testing the agreement of the theory with the observations is as follows: For each of the volume intervals of the apparatus we may find the mean pressure ratio from the barometric pressure  $p$ , and the pressure differences ( $p_0 - p$ ) at the beginning and end of the interval, which have been measured once for all. We may next find the value of  $r$  corresponding to each of these values of  $r$  by dividing the air time for the interval by the known volume of the interval. We may then assume a value of  $C$  and compute from (48) the value of  $R_\mu$  which corresponds to each of the values of  $r$ . These computed values of  $R_\mu$  may then be compared with the observed values of  $R$ , the clearest way of doing this being to draw a curve  $R_\mu = f(r)$  from the computed values and plot the observed values of  $R$  as separate points. A similar process may be carried out for each of the other experiments on the orifice in question, with the same value of the orifice constant  $C$ . Finally, the whole may be repeated with various values of  $C$  until no further improvement can be obtained in the agreement between theory and observation.

Upon consideration of the cumbersome nature of the equations it is quite evident that the foregoing method would, in practice, be intolerably laborious and that a simpler one must be used. The procedure was therefore modified, the idea being, first, to work only at a few fixed values of  $r$  for which values of the various functions such as  $(1 - r^2)$  could be tabulated once for all; and second, to treat all the experiments on a single gas together and draw a single average curve  $R_\mu = f(r)$  for that gas instead of a separate curve for each experiment.

The separate experiments differed, first, in that the initial temperature  $\theta_0$  varied somewhat so that the air times  $\tau$  for any one interval could not be expected to be quite the same even



if  $\tau$  were the same; and second, in that the barometric back pressure also varied from one experiment to another with consequent small variations of  $\tau$ . Thus, for each of the volume intervals of the apparatus, the experiments on any one orifice gave a number of slightly differing values of  $\tau$  corresponding to slightly differing values of  $\theta_0$  and of  $r$ . The first step was to average these values and it was done as follows.

Considering one interval only, the values of  $V_0 = 1/\tau$  were found for all the runs with air made through the orifice in question. From each of these the value of  $V_0^2(295/\theta_0)$  was computed; this amounts to reducing the value of  $V_0^2$  observed at  $\theta_0$  to what would have been observed at  $22^\circ$  C on the assumption that the rate of efflux of air is proportional to the square root of the absolute temperature. The initial temperatures all fell between  $19^\circ$  and  $28^\circ$  with a mean of about  $22^\circ$ , and the reduction just mentioned was a short one. The reduction by setting  $V_0 \propto \sqrt{\theta_0}$  was adopted because equation (22), which is a first approximation to the truth gives  $V_0^2 \propto \theta_0$ , and equation (39) would not give a very different relation since it differs from (22) only by correction terms.

These values of  $V_0^2(295/\theta_0)$  were averaged and the corresponding values of  $\tau$  also averaged. The mean values of  $V_0^2(295/\theta_0)$  were plotted against the mean values of  $\tau$  and a curve drawn through the points; this curve was used for interpolation and was of a satisfactory shape for the purpose. Readings were now made at the round values of  $\tau$  which it had been decided to use in the computations, namely  $\tau = 0.75, 0.79, 0.82, 0.86, 0.90, 0.93, 0.96, 0.986$ . These were selected because while fairly evenly spaced they were not far from the means, so that in interpolating by means of the curve no great error could be introduced by the arbitrary shaping of the curve between the plotted points. The square root of the reciprocal of each interpolated value of  $V_0^2(295/\theta_0)$  was now extracted and used in the computation of  $R_\mu$  as if it were a value of the air time  $\tau$  actually observed at the standard pressure ratio  $r$ .

It remained to select a mean value of  $C' = Ca\mu/p$ ,  $a$  and  $\mu$  being constant, and  $p$  nearly so. This value, together with the values of  $\tau$  obtained as described above, and the known values of  $a$ ,  $a'$  etc., was used to compute values of  $R_\mu$  by means of equation (48). On the supposition that our theory is correct and that  $C'$  has been properly chosen, these computed values of  $R_\mu$  are

equal, as nearly as we can tell, to the values of  $R$  which would have been found from observations at  $r=0.75, 0.79$  etc., if: (a) the efflux had been strictly adiabatic; (b) the initial temperature had always been  $22^{\circ}\text{C}$ ; and (c) the barometric pressure had been the same during all the runs.

A curve  $R_{\mu}=f(r)$  was drawn through these computed points and the observed points were plotted separately. The effect of correcting the positions of the observed points to reduce them to  $22^{\circ}$  and a common mean value of  $p$  would have been small compared with the experimental uncertainties of their positions and no such reduction was undertaken. The graphical comparison is therefore finally between a curve computed for  $22^{\circ}$  and constant  $p$ , and observations made under various conditions differing a little from these but not more than would be covered by the observational errors.

## 15. RESULTS OF THE COMPARISON

The method of making the computations with a particular value of  $C'$  having now been described, the question remains whether, by repeating the computations and adjusting the value of  $C'$  by trial, a satisfactory agreement with the observed facts can be achieved. If it can, our theory may be regarded as satisfactory, for in any event the constant  $C'$  is purely empirical and can be found only by fitting the equations to the observations.

This question has to be answered in the negative: after all the laborious computations it was found that no possible value of  $C'$  would make equation (48) fit the observations within their experimental uncertainties, and the theory as so far developed could not be regarded as satisfactory. But on the other hand, it was found that while the theory was not entirely satisfactory, it was not very bad. For a suitably chosen value of  $C'$  would give computed curves which were fairly near to the observed points, so that the differences  $(R_{\text{obs}} - R_{\mu})$  were numerically very much smaller than the differences  $(R_{\text{obs}} - 1)$ . In other words, our allowance or correction for the effects of viscosity did account for the major part of the observed errors of the effusion method; and moreover, the residual errors which could not be accounted for in this way appeared to have a regular systematic run which was of the same nature for all the gases. It therefore seemed probable that the theory was correct in its main outlines and in attributing to viscosity an important part in causing the errors of

Bunsen's method, but that either the treatment of viscosity required to be somewhat modified or some further disturbing cause remained to be allowed for.

Several modifications of the above-described theory of the effect of viscosity were developed by modifying the assumptions, and trial computations were undertaken with the resulting equations. None of these slightly different forms of the theory seemed any better founded in physical common sense than the original one already described; none of them gave any better agreement with observations; and none of them was so easy to use. We therefore abandoned further attempts in this direction and proceeded to search for an additional correction, due to some other cause than viscosity, which if added to the correction already made should lead to a better agreement between the theory and the observed facts.

The most obvious possibility is that in addition to the retardation of efflux by viscosity, heat transmission from the orifice to the jet may also have a sensible effect on the rate of efflux, the phenomenon being appreciably different from an adiabatic expansion; so we turned our attention to this subject. Since it seemed quite hopeless to attempt to treat viscosity and heat transmission simultaneously and with due allowance for their interaction, a more rudimentary plan was followed. In view of the fact that the effects of both viscosity and the second disturbing cause, now assumed to be heat transmission, are of the nature of corrections—that is, relatively small, at least until  $r$  approaches unity—it was assumed that they might properly be treated separately as if each acted alone; and we therefore proceeded to develop a theory of the efflux of a nonviscous but thermally conducting gas, and to deduce an expression for the effect of heat transmission on the value of  $R$ .

This expression, like the one for  $R_v$ , contains an empirical orifice constant. After obtaining the expression, we make up a combined equation which purports to take account of the effects of both viscosity and heat transmission and contains therefore two empirical orifice constants. The theory must then be tested by adjusting the constants; if a pair of values can be found such that the computed values of  $R$  are in satisfactory agreement with the observed, the theory in this final shape may be regarded as satisfactory and as probably correct in its main outlines if not in all details.

We may now go on to consider effusion which is affected by heat transmission but is not retarded to any sensible extent by viscous resistances.

#### 16. EFFLUX WITH ADDITION OF HEAT BUT WITHOUT DISSIPATION

Since the rate of heat flow into the gas from the metal increases with the difference of temperature and with the intimacy of contact, it is evident that most of the heat transmission will occur in the orifice, after the gas has almost attained its lowest pressure. We shall therefore, assume as an approximation, that the effect of heat transmission on efflux is the same as if the gas expanded isentropically to the back pressure  $p$  and a quantity of heat  $Q$  per gram were then added to it at the constant pressure  $p$ , raising its temperature from the lowest point by the amount  $Q/C_p$ . This assumption is similar to one made in section 10 and it is unquestionably a fairly approximate representation of what actually occurs.

If  $\theta$  denotes the final temperature of the gas and  $\theta_1 = r^a \theta_0$  its temperature after isentropic expansion, we have by the foregoing assumption.

$$\theta = r^a \theta_0 + \frac{Q}{C_p} \quad (50)$$

Substituting this value of  $\theta$  in equation (8) and reducing, we have

$$\frac{1}{2} S^2 = \theta_0 C_p (1 - r^a) \quad (51)$$

$Q$  having disappeared. But (51) is identical with (15) which applies to isentropic efflux; whence it follows that addition of heat in the manner postulated above has no effect at all on the linear exit speed of the jet.

But though the speed of the gas at the section  $A$  is not affected, the temperature is raised, and the specific volume is increased in the same ratio, viz,

$$\frac{\theta}{\theta_1} = 1 + \frac{Q}{r^a \theta_0 C_p}$$

The time required for a given mass to escape will be increased in this ratio; hence if  $\tau_\lambda$  is the time observed under the present conditions, and  $\tau_1$  the time that would be observed if the efflux were isentropic, we have

$$\frac{\tau_\lambda}{\tau_1} = 1 + \frac{Q}{r^a \theta_0 C_p} \quad (52)$$

We have next to find an expression for  $Q$ , and we again have recourse to the principle of dimensional homogeneity in the convenient form of the  $\Pi$  theorem.<sup>6</sup> We assume that for an orifice of given shape,  $Q$  is determined by the diameter of the orifice, the speed of the jet, the difference of temperature between the jet and the orifice, and the properties of the gas. The most obviously important of these properties are the density  $\rho$ , specific heat  $C_p$ , and thermal conductivity  $\lambda$ . But we shall also, at the start, include the viscosity  $\mu$  as possibly affecting  $Q$  through its influence on the nature of the flow, although it seems likely that  $\mu$  will be of small importance, and we have already agreed to disregard dissipation. If we let  $\Delta$  represent the temperature difference, our assumption regarding  $Q$  is now symbolized by the equation

$$Q = f(a, S, \Delta, \rho, C_p, \lambda, \mu) \quad (53)$$

All the quantities except  $Q$  and  $a$  are to be regarded as mean values averaged over the time during which  $Q$  is being transmitted to the gas, but as an approximation we shall identify them with their values at the end of the isentropic expansion.

By applying the  $\Pi$  theorem, equation (53) may be thrown into the form

$$Q = \Delta C_p \varphi \left\{ \frac{\Delta C_p}{S^2}, \frac{\mu C_p}{\lambda}, \frac{\lambda}{aS\rho C_p} \right\} \quad (54)$$

and the next question is whether we have any information that will help us to make a rational guess at the form of the operator  $\varphi$ .

The greatest temperature drop in any of our experiments was less than  $26^\circ \text{C}$ ; hence it seems safe to assume that  $Q$  was sensibly proportional to  $\Delta$ . This assumption gives us a first simplification of (54) to the form

$$Q = \Delta C_p \varphi_1 \left\{ \frac{\mu C_p}{\lambda}, \frac{\lambda}{aS\rho C_p} \right\} \quad (55)$$

For the gases used in our work the relative values of  $\mu C_p/\lambda$  are approximately as follows:

Air	H <sub>2</sub>	CH <sub>4</sub>	CO <sub>2</sub>	Ar
$\mu C_p/\lambda = (1.00)$	0.93	1.28	1.10	1.01

In view of the great uncertainty in the values of  $C_p$  and  $\lambda$ , even for pure gases, and of the fact that we were obliged to rely upon

<sup>6</sup> See Trans. Am. Soc. Mech. Engineers, 87, p. 289; 1925.

a mixture rule for computing the foregoing values of  $\mu C_p/\lambda$ , it can not be said with certainty that the differences in the values are not illusory. Hence in the intercomparison of these gases we may as well treat  $\mu C_p/\lambda$  as a constant and so reduce equation (55) to the simpler form

$$Q = \Delta C_p \varphi_2 \left\{ \frac{\lambda}{a S \rho C_p} \right\} \quad (56)$$

The next point to be considered is whether or not we may regard the flow as stream line. If we may,  $Q$  will be proportional to the conductivity of the gas and (56) will be still further simplified to the form

$$Q = N \frac{\Delta \lambda}{a S \rho} \quad (57)$$

in which  $N$  is a dimensionless shape factor. We have already made this assumption in treating the effects of viscous resistance, and we shall also make it here, although the point will be touched upon again in section 19.

Substituting from (57) into (52), we now have

$$\frac{\tau_\lambda}{\tau_1} = 1 + \frac{N \Delta \lambda}{a S \rho r^a \theta_0 C_p} \quad (58)$$

The comparisons already made between our equations for adiabatic efflux of a viscous gas and the observed facts, showed that the remaining discrepancy which we are now attempting to account for by heat transmission is small, though greater than the uncertainties of the experiments. Hence the correction term in (58) is small and we may write

$$\left( \frac{\tau_\lambda}{\tau_1} \right)^2 = 1 + \frac{2 N \Delta \lambda}{a S \rho r^a \theta_0 C_p} \quad (59)$$

Let  $\rho_n$  be the density at a normal state  $p_n, \theta_n$ , so that

$$\rho = \rho_n \frac{p}{p_n} \frac{\theta_n}{r^a \theta_0} \quad (60)$$

Let  $\lambda_n$  be the value of  $\lambda$  at this same normal state, and let us assume that  $\lambda \propto \sqrt{\theta}$ , a rough approximation but better than entirely disregarding the variation of thermal conductivity with temperature. Then we have

$$\lambda = \lambda_n \sqrt{\frac{r^a \theta_0}{\theta_n}} \quad (61)$$

Substitute into (59) the values of  $\rho$  and  $\lambda$  from (60) and (61); also the values

$$\Delta = \theta_0(1 - r^2) \quad (62)$$

and

$$S = \sqrt{2\theta_0 C_p (1 - r^2)} \quad (63)$$

Let

$$\frac{\sqrt{2N} p_0 \theta_0}{a \theta_0^{1/2} p} = W \quad (64)$$

and

$$\frac{\lambda_0}{\rho_0 C_p^{1/2}} = \beta \quad (65)$$

Then after the substitutions and reduction we have

$$\left(\frac{r_2}{r_1}\right)^2 = 1 + W\beta\sqrt{r^2(1 - r^2)} \quad (66)$$

In the quantity  $W$  defined by equation (64) all the factors except  $\theta_0$  and  $p$  are constants, and  $\theta_0$  and  $p$  vary only slightly from one experiment to another. Under the circumstances it would be a waste of time to take any account of these relatively small variations, and we may therefore treat the quantity  $W$  as an orifice constant.

The quantity  $\beta$  defined by equation (65) measures a property of the gas in question, but its value is a priori, very uncertain indeed; for while the densities of our gases were measured, the values of the thermal conductivities and specific heats had to be obtained from Landolt and Börnstein's tables. The values of  $\lambda$  are only very roughly known even for the pure gases, so that the values of  $\beta$  which we could compute a priori had to be regarded as only tentative and subject to correction. The manner in which they were corrected will be described later.

Assuming for the instant that the orifice constant  $W$ , and the gas constant  $\beta$  are known, equation (66) shows us how the rate of efflux of a nonviscous but thermally conducting gas will be affected by heat transmission from the orifice, if the simplifying assumptions used in developing the theory have been reasonably good approximations to reality.

# 17. APPLICATION TO THE COMPARISON OF NONVISCOUS BUT THERMALLY CONDUCTING GASES

Let  $R_\lambda$  be the value which would be found in a comparison of two gases by the effusion method if the flow were affected by heat transmission but not by viscous resistances; and as before let  $R_1$  be the value for isentropic efflux. Then we have

$$\frac{R_\lambda}{R_1} = \left( \frac{\tau'_\lambda}{\tau_\lambda} + \frac{\tau_1'}{\tau_1} \right)^2 = \left( \frac{\tau'_\lambda}{\tau_1'} \right)^2 + \left( \frac{\tau_\lambda}{\tau_1} \right)^2 \quad (67)$$

Let equation (66) refer to the standard gas, and let us divide it, member for member, into the corresponding equation for the test gas. Then by equation (67) we shall have

$$\frac{R_\lambda}{R_1} = \frac{1 + W\beta' \sqrt{r^{a'}(1 - r^{a'})}}{1 + W\beta \sqrt{r^a(1 - r^a)}} \quad (68)$$

or very nearly

$$\frac{R_\lambda}{R_1} = 1 + W[\beta' \sqrt{r^{a'}(1 - r^{a'})} - \beta \sqrt{r^a(1 - r^a)}] \quad (69)$$

whence

$$R_\lambda - R_1 = R_1 W \beta \left[ \frac{\beta'}{\beta} \sqrt{r^{a'}(1 - r^{a'})} - \sqrt{r^a(1 - r^a)} \right] \quad (70)$$

Now in our experiments the value of  $R_1$  always remained within the limits 0.986 to 1.027. Hence it will be legitimate to set  $R_1 = 1$  in the second member of (70) because we know already that the correction we are trying to compute is small—in fact, not very much greater than the observational errors. Since  $\beta$  is a constant for the standard gas, if we let

$$W\beta = M \quad (71)$$

$M$  is an empirical orifice constant. And if we let

$$R_\lambda - R_1 = \Delta_\lambda \quad (72)$$

equation (70) may now be written

$$\Delta_\lambda = M \left[ \frac{\beta'}{\beta} \sqrt{r^{a'}(1 - r^{a'})} - \sqrt{r^a(1 - r^a)} \right] \quad (73)$$

Supposing all our hypotheses and approximations to be satisfactory and the values of  $M$  and of  $\beta'/\beta$  to be known, equation (73) would enable us to compute the amount  $\Delta_\lambda$  by which the



value of  $R$  found with conducting gases would exceed the value found if there were no conduction, viscous resistances being negligible in both cases.

# 18. ALLOWANCE FOR THE SIMULTANEOUS ACTION OF VISCOSITY AND CONDUCTIVITY

We have now devised a theory of the effect of viscosity alone on the results of Bunsen's method of determining relative density; and we have found it not adequate to representing the observed facts, though nearly so. We have then developed an equation for computing the effect of heat transmission acting alone. We shall now *assume* that when the gases are both viscous and conducting, as they all are in reality, the effects of viscosity and conduction are additive and may be computed by the equation

$$R = R_\mu + \Delta_\lambda \quad (74)$$

where by equations (48) and (49)

$$R_\mu = L + 2 G^2 [1 + \sqrt{1 + L/G^2}] \quad (75)$$

$$\left. \begin{aligned} L &= \frac{a'}{a} r^{2(a'-a)} \frac{(1-r^a) - (2-r^a) X}{1-r^{a'}} \\ G &= \frac{2-r^{a'}}{1-r^{a'}} \frac{PX}{2} \\ X &= \frac{Ca\mu}{p\tau} = \frac{C'}{\tau}; \end{aligned} \right\} \quad (76)$$

by equation (73)

$$\Delta_\lambda = M \left[ \frac{\beta'}{\beta} \sqrt{r^{a'} (1-r^{a'})} - \sqrt{r^a (1-r^a)} \right]; \quad (77)$$

and  $C'$  and  $M$  are empirical orifice constants. It remains to be seen whether these equations are, in fact, capable of representing the observations, and this must be investigated by means of trial computations.

The values of  $a$ ,  $a'$  and  $P$  have been discussed in sections 5 and 13, and the values of the air time  $\tau$  in section 12. The values of  $\beta'/\beta$  are known only very roughly and those of  $C'$  and  $M$  are altogether unknown. We therefore have set before us a rather complicated task of adjusting empirical constants, with no a priori certainty that a satisfactory adjustment is possible. The manner

in which the problem was attacked and the degree of success achieved will be treated in sections 19 to 22.

## 19. ATTEMPTS TO ALLOW FOR TURBULENCE

A number of preliminary computations appeared to show that the results of experiments on orifices 23A, 23B, 28, and 29 could not be represented by equations (74) to (77), if the values of  $\beta'/\beta$  given tentatively in Table 6 were used; but that if the values were arbitrarily changed to about the following

H <sub>2</sub>	CH <sub>4</sub>	CO <sub>2</sub>	Ar
$\beta'/\beta = 1.5$	0.75	0.37	1.13

values of  $C'$  and  $M$  could be found for each orifice which would make the theory agree pretty well with the facts. It was not clear from the results whether the theory of the conduction effect required modification or whether the tentative values of  $\beta'/\beta$  required correction.

Attempts were made to modify the theory of the heat transmission effect by allowing for the possibility of turbulence in the orifice. One such attempt was made in connection with equation (56). Instead of assuming that there was no turbulence and so passing directly from (56) to (57), it was assumed that

$$\varphi_2 \left\{ \frac{\lambda}{a S \rho C_p} \right\} = N \left\{ \frac{\lambda}{a S \rho C_p} \right\}^\epsilon \quad (78)$$

where  $\epsilon$  is a new constant dependent on the degree of turbulence of the motion. If there were no turbulence at all, we should set  $\epsilon = 1$  and get equation (57) as before. But if turbulence were present, the effect of the conductivity  $\lambda$  would be decreased while that of the specific heat  $C_p$  would be increased because of convection due to turbulence. Hence for turbulent motion we should have  $\epsilon < 1$ , and the greater the turbulence the more nearly  $\epsilon$  would approach zero, the physical meaning of this being that if the motion were very turbulent virtually the whole of the transfer of heat would occur by convection and not by conduction.

The result of adopting equation (78) was to give the equation

$$Q = N \Delta C_p^{1-\epsilon} \left\{ \frac{\lambda}{a S \rho} \right\}^\epsilon \quad (79)$$

instead of the simpler equation (57) to which it reduces when

$\epsilon = 1$ . The same process of reasoning as already described then led to an equation of the form

$$\frac{R_\lambda}{R_1} = 1 + W \left\{ \beta' r^{a'} \left[ \frac{3}{2} - 1 \right] (1 - r^{a'}) \left[ 1 - \frac{1}{2} \right] - \beta r^a \left[ \frac{3}{2} - 1 \right] (1 - r^a) \left[ 1 - \frac{1}{2} \right] \right\} \quad (80)$$

in place of equation (69) to which it reduces when  $\epsilon = 1$ . Equation (80) then permitted of our obtaining an expression for  $\Delta_\lambda$ , analogous to but far more complicated than that given by equations (73), and computations could then be made by equation (74).

Computations by this method with several values of  $\epsilon$  and with the tentative values of  $\beta'/\beta$  given in Table 6, left it doubtful whether any improvement had been attained to offset the increased difficulty of the computations.

## 20. RESULTS OF THE OBSERVATIONS ON ORIFICE NO. 31; VALUES OF $\beta'/\beta$ FOR HYDROGEN AND CARBON DIOXIDE

At this stage of the investigation the experiments were resumed. Improved apparatus (No. II) was constructed and calibrated, and greater accuracy of measurement ensured. A new orifice, No. 31, was also made, great care being taken to have its entrance smooth and trumpet-shaped on one side (31A) and sharp on the other (31B). With 31A, the entrance being smooth and rounded, it seemed safe to assume, first, that there would be little or no contraction, and, second, that the motion would be sensibly free from turbulence, so that if the rudimentary theory embodied in equations (74) to (77) were ever to be applicable, it would be to experiments made on this orifice.

For lack of time only two experiments were made with orifice 31A, one with hydrogen and one with carbon dioxide, but they appeared satisfactory as to experimental accuracy. Upon applying the theoretical equations to the experimental data the results were as follows.

(a) If the motion was assumed to be somewhat turbulent and the form of theory consequent on the assumption of equation (78) with  $\epsilon$  considerably less than unity was adopted, no satisfactory agreement between the theory and the observations could be obtained with any possible values of the orifice constants  $C'$  and  $M$  or any values of  $\beta'/\beta$  for hydrogen and carbon dioxide. It was clearly apparent that if  $\epsilon$  were sensibly different from unity the form of the heat transmission term  $\Delta_\lambda = f(r)$  was unsuitable. In other words, for this orifice, where we have every reason to

suppose that turbulence was absent, the equation developed on the assumption that turbulence was absent fits the facts better than the modification of it, which supposes that turbulence is present.

(b) By setting  $\epsilon = 1$ —that is, by assuming turbulence to be absent and using the theory as embodied in equations (74) to (77) and as first given—values of  $C'$  and  $M$  could be found which brought about an excellent agreement of the theory with the observations, if, but only if, at least one of the values of  $\beta'/\beta$  (for hydrogen and carbon dioxide) was arbitrarily changed from its original tentative value.

On the strength of these results, obtained from new and improved apparatus but consistent with all the previous observations, we decided to accept the theory as developed and to correct the values of  $\beta'/\beta$  arbitrarily by reference to the experiments, choosing such values, not greatly differing from the original tentative values computed a priori, as should if possible result in a satisfactory agreement between theory and observation.

After consideration of the above-mentioned experiments on orifice 31A the values

$$\begin{array}{cc} H, & CO, \\ \beta'/\beta = 1.5 & 0.4 \end{array}$$

instead of the original tentative values 1.69 or 1.62 and 0.46 were definitively adopted for use in all future computations on these two gases.

The constants  $C'$  and  $M$  of equations (76) and (77) were then adjusted by trial and the values

$$C' = 0.0075 \quad M = 0.23$$

adopted. The values of  $R = f(r)$  computed with these values from equation (74) are represented by the curves in plate 2, while the observed points are plotted separately.

## 21. OBSERVATIONS ON ORIFICE NO. 28; VALUES OF $\beta'/\beta$ FOR METHANE AND ARGON

It now remained to adopt values of  $\beta'/\beta$  for methane and argon which had not been used with orifice 31A. For this purpose reference was made to the experiments on orifice 28, because the experiments on this orifice appeared to be more consistent and therefore probably more accurate than those on 23A, 23B, and 29. They were also more numerous and had been made with three

separate pieces of apparatus, so that the average results were less likely to be subject to systematic errors due to peculiarities of the apparatus or errors in calibration.

We proceeded as follows. With the values of  $\beta'/\beta$  already adopted for hydrogen and carbon dioxide as suited to the experiments on orifice 31A, computations were undertaken by equations (74) to (77) and values of  $C'$  and  $M$  were determined as to give as satisfactory an agreement as possible between the observations on hydrogen and carbon dioxide and the computed curves  $R = f(r)$ . These values were

$$C' = 0.012 \quad M = 0.24$$

and the agreement between the computed curves and the observed points is to be seen by examining plate 3.

The values of  $C'$  and  $M$  having thus been determined without any attention to the observations on methane and argon, the computations were next made for the latter two gases with these same values of  $C'$  and  $M$  and with such values of  $\beta'/\beta$  for methane and argon as to make the computed curves of  $R = f(r)$  fit the observations as well as possible. The values finally adopted for all four gases were as follows:

Gas $H_2$	$CH_4$	$CO_2$	$Ar$
$\beta'/\beta = 1.50$	0.75	0.40	1.04

and these were used without further change in all the remaining computations. They differ considerably from the tentative values given in Table 6 but not by more than the uncertainties of those values.

The curves for methane and argon, computed with the foregoing values of  $\beta'/\beta$ , but with the values of  $C'$  and  $M$  determined by reference only to hydrogen and carbon dioxide, agree excellently with the observed points, the fit being on the whole decidedly better than for carbon dioxide and very much better than for hydrogen.

## 22. RESULTS OF APPLYING THE THEORY TO ORIFICES NOS. 29 AND 23A

The result so far is to show that if the values given above for  $\beta'/\beta$  are adopted, the theory embodied in equations (74) to (77) is capable of representing the observed facts for orifices 31A and 28, nearly or quite within the limits of the experimental errors, except at the largest values of  $r$ , where the values of  $(R-1)$  can no longer be regarded as small corrections, as demanded by the theory.

Satisfactory values of  $\beta'/\beta$  having thus been obtained, the theory was applied to the observations on the other orifices, without further attempt to improve the values of  $\beta'/\beta$ . The work consisted merely in finding by trial for each orifice, a suitable pair of values for the orifice constants  $C'$  and  $M$ .

*Orifice 29.*—The trial computations were all made with reference to hydrogen and carbon dioxide, no attention being paid to the observations on methane and argon. The values adopted were

$$C' = 0.013 \qquad M = 0.12$$

These were then used in computing the curves for methane and argon. The curves, together with the separate observed points, are shown on plate 4. As was found to be the case with orifice 28, the theory seems to fit the observations on methane and argon somewhat better than those on carbon dioxide and much better than it fits the observations on hydrogen.

*Orifice 23A.*—As before, the trial computations were all made with reference to hydrogen and carbon dioxide. One of the three series for carbon dioxide differed considerably from the other two and it was disregarded. This series had been ignored in our earlier computations as if under suspicion, but we have no note as to why this was done. The values found for the orifice constants were

$$C' = 0.01 \qquad M = 0.19$$

and these values, determined by reference to hydrogen and carbon dioxide, were used in the computations for methane and argon. The computed curves and the observed points are shown on plate 5.

In all the computations for orifices 31, 28, and 29 the values used for  $\tau$  were means found from all the air runs on each orifice as described in section 14. But during the experiments on orifice 23A, some change in the orifice occurred about April, 1916, after all the experiments except those on argon had been completed. This change manifested itself by a change in the values of the air time  $\tau$ , which decreased a little as if the orifice had been enlarged or a slight obstruction removed from it. We therefore used the means of the earlier values of  $\tau$  in the computations on hydrogen, methane, and carbon dioxide, but for argon we used the values of  $\tau$  obtained from the argon series only.

A change in the air time means a change in the orifice, and after this change the orifice might be expected to behave as a different orifice with other values of  $C'$  and  $M$ . In this instance, however, the change was slight and no attempt was made to determine a separate pair of values for the observations on argon. A more striking example of such a change occurred with orifice 23B, which was merely 23A turned the other side up so that the direction of flow through the orifice was reversed.

### 23. BEHAVIOR OF ORIFICE NO. 23B

A study of the air times for orifice 23B showed that during the period of the experiments, January 26 to May 24, 1916, this orifice underwent three changes—two rather small, but the third quite marked. The orifice was therefore treated as four separate orifices with different constants, the computations being carried out with values of  $\tau$  obtained from four separate mean curves of  $V_o^2(295/\theta_o) = f(\tau)$ .

I. Before February 27, 1916, two series were run with hydrogen, one with methane, and one with carbon dioxide. The results for hydrogen and carbon dioxide are not consistent; that is, no values of  $C'$  and  $M$  can be found which will make the theory agree well with the observations. On the other hand, by using the observations on hydrogen and methane a good agreement can be had by adopting the values

$$C' = 0.0087 \quad M = 0.05$$

The observations for carbon dioxide are then very far from the carbon-dioxide curve found from these constants, and they show a systematic divergence from the *shape* of the curve, which we suspect to be due to the formation of a vena contracta.

The computed curves and the observed points are shown on plate 6.

The first change in the orifice occurred between the foregoing and the next-mentioned experiments.

II. On May 3 and 4 two series were run with argon. The best values for representing these series are about

$$C' = 0.0079 \quad M = 0.07$$

and the resulting fit is only fair as may be seen from plate 7.

Between these and the next series a second change occurred, and

III. On May 17 one series was run with hydrogen. The constants

$$C' = 0.0079 \quad M = 0.03$$

give a computed curve which fits the observed points better than could have been expected. The curve and the points are shown on plate 7.

Between May 17 and May 24 a third and larger change occurred, and

IV. On May 24 one series was run with carbon dioxide. If the constants

$$C' = 0.075 \quad M = 0.07$$

are used, the agreement of the computed curve with the observed points is excellent. The curve and observed points are shown on plate 7 along with those for cases II and III.

#### 24. REMARKS ON ORIFICES NOS. 23A AND 23B, I, II, III, AND IV

A study of the behavior of orifice 23 is instructive in throwing light on some of the difficulties and sources of error in the effusion method of determining gas densities, and also in giving a probable qualitative interpretation of some of the divergences between theory and observation.

In the first place, examination under the microscope showed that this orifice was rather rough and irregular on both sides, and it appeared to have a burr on one side. In the second place, difficulties were encountered from the start, especially with position 23B, in getting consistent and reproducible results, whether with air or with one of the test gases. It seems highly probable that these difficulties and irregularities of behavior were due to the roughness of the edges of the orifice which would have a tendency to catch and hold, for a longer or shorter time, minute particles of dust which might be suspended in the gas. Large irregularities were observed on one occasion when there was reason to suspect that the gas had not been thoroughly dried, so that water droplets might have been formed. And although care was taken to have the gases dry and dust free, there was always the chance that mercury droplets might cling to the sides of the orifice. For the gas within the apparatus is presumably saturated with mercury vapor; and although the density of mercury vapor at room temperature is small, it nevertheless seems possible that the cool-



ing in the jet may have caused some condensation. At all events, the indications are that particles of some sort did catch on the edges of the orifice.

If the orifice were rougher on one side than on the other and especially if it had a burr on one side, it might be expected that these difficulties would be more pronounced when that was the entrance side. Furthermore, the presence of a rough or burred entrance would render the orifice more susceptible to mechanical changes than it would otherwise be. This describes the behavior of 23B as compared with 23A. The observations were more irregular, and more difficulty was found in getting reproducible results with 23B than with 23A; and while both showed the effect of mechanical changes, probably due in some way to handling, these changes were much more pronounced for 23B than for 23A. It looks therefore as if on the side B the entrance had been rough, possibly with a burr, while on the side A it had been smoother.

Now let us consider what further differences of behavior would probably be observed between two orifices of the same diameter and length, one of which had a burred or sharp-cornered entrance while the entrance of the other was smooth and well rounded.

In the first place, the sharp entrance might give rise to the formation of a vena contracta. If it did, the jet area  $A$  would be reduced and the discharge coefficient would be less than for the orifice with rounded entrance. This describes the behavior of 23B as compared with 23A: The discharge coefficient was smaller for 23B, that is, the air times were longer than for 23A.

In the second place, if the entrance is sharp, the high speed jet is in contact with the metal for a much shorter distance than if the entrance is rounded and there is no contraction. Hence, sharpness of entrance, while it reduces the discharge by causing contraction, will tend to decrease the effect of viscosity but more especially that of heat transmission. If 23B has, in fact, a sharper entrance than 23A, we should expect its values of  $C'$  and  $M$  to be lower than those for 23A. The values actually found were  
for 23A..... $C'=0.010$ ..... $M=0.19$   
for 23B (mean)..... $C'=0.0080$ ..... $M=0.054$   
which agrees with the above-mentioned suppositions.

It therefore appears, although it could not have been predicted with certainty from the appearance of the orifice under the microscope, that this orifice behaved as though it had a rounded entrance when used in the position 23A and a sharp or burred entrance when used in the position 23B.

## 25. CONCLUDING REMARKS

In developing the equations used for representing the experimental results, we assumed that at any given value of  $r$  the minimum section of the jet was the same for air as for the test gas, and the ratio  $A'/A$  of the two sections therefore disappeared from the equations for  $R$ .

This condition would be satisfied if there were no contraction at all, for then  $A'$  and  $A$  would be simply the smallest section of the orifice. But it would also be satisfied if there were contraction, provided the amount of contraction were the same for the different gases at any given  $r$ , even though the contraction might vary with  $r$ . If the efflux could be made dynamically similar during the comparison of two gases, we could ensure that the forms of the jets should be the same and the contraction coefficients equal; but in the sort of comparison made in using Bunsen's method the conditions of dynamical similarity are not fulfilled.

An investigation of the values of the discharge and contraction coefficients for these small orifices would be interesting, and some attempts in this direction were made; but the experimental data are not sufficient in either number or accuracy to justify a description of these attempts. All that can be said definitely is that the variations of the discharge coefficient with the diameter of the orifice are qualitatively in agreement with what is known about the flow of water and air through larger orifices up to 4.5 inches diameter.

Upon considering the general nature of the agreement of the computed curves with the observed points, it appears that for hydrogen there is a systematic divergence; and it seems quite possible that this is due to a difference in the form of the jets for hydrogen and air, a difference which itself changes with  $r$ . For at a given value of  $r$  jets of hydrogen and air are farther from dynamical similarity than, for instance, jets of methane and air which have more nearly the same density.


Certain early experiments with other somewhat larger orifices, which have not been discussed in this paper because the data were too few, gave points for carbon dioxide which seemed to diverge systematically from the computed curves in the same way as the carbon-dioxide points on plate 6 diverge from the curve there given, but to a more marked degree. Whether these divergences are really to be attributed to contraction and changed form of the jets can not be definitely stated, but if we were to pursue the

research farther, this is the direction in which we should first attempt to extend it.

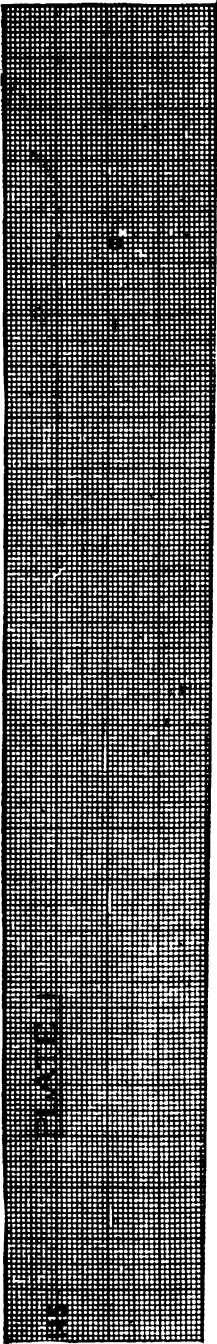
It may be noted that the observations at  $r=0.986$  and  $0.990$  (pls. 2, 3, 4) are a good way off from the curves, the observed value of  $(R-1)$  being numerically greater than the computed value as shown by the position of the curve. Upon remembering that to manage the problem at all we were obliged to treat the errors—that is, the values of  $(R-1)$  as small quantities—it does not appear surprising that the approximation ceases to be satisfactory when  $(R-1)$  is so large as it is for these points, where the pressure ratio  $r$  is approaching unity.

On the whole, it appears that the theory as given does represent the major part of the facts reasonably well, and that the physical ideas on which it was based are probably sound, so far as they go.

WASHINGTON, May 8, 1919.

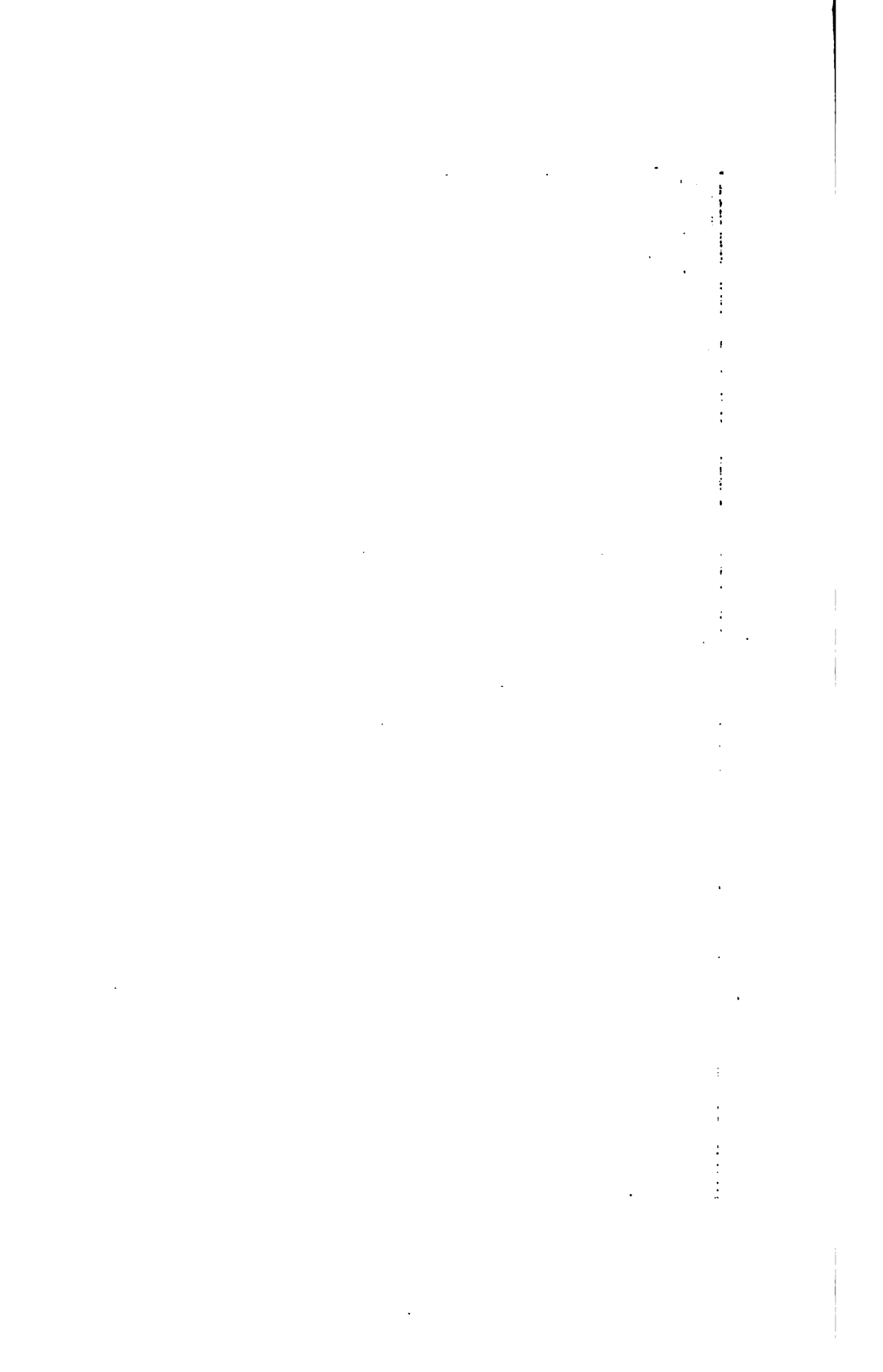






1900  
1910

85



UNIV. OF  
CALIFORNIA

70 7000  
ALABAMA





U.S. DEPT. OF  
COMMERCE

70 1000  
1000000 100





MAR 19 1920



DEPARTMENT OF COMMERCE

# SCIENTIFIC PAPERS OF THE BUREAU OF STANDARDS

S. W. STRATTON, DIRECTOR

No. 360

METHODS FOR COMPUTING AND INTERCOMPAR-  
ING RADIATION DATA

BY

W. W. COBLENTZ, Physicist  
*Bureau of Standards*

ISSUED JANUARY 31, 1920



PRICE 5 CENTS

Sold only by the Superintendent of Documents, Government Printing Office  
Washington, D. C.

WASHINGTON  
GOVERNMENT PRINTING OFFICE  
1920



# METHODS FOR COMPUTING AND INTERCOMPARING RADIATION DATA

By W. W. Coblenz

## I. INTRODUCTORY STATEMENT

This paper gives a simple method for computing spectral energy curves, using the Planck formula. In order to facilitate the computations, a table of values of  $\log (e^u - 1)$  is given. Such data do not appear to have been published heretofore. By means of this table, a table of logarithms, and a slide rule, one can compute a complete spectral energy curve in an hour.

The paper gives also a chart for intercomparing the thermal radiation constants, with similar data which may be obtained indirectly from theoretical considerations, using Planck's universal constant,  $h$ , and data obtained from ionization-potential, photoelectric, and X-ray work. Of course it is to be understood that whatever the true (theoretical) value of the constant,  $h$ , and the spectral radiation constant,  $c_2$ , may be, the value of  $c_2$ , as obtained from measurements on black-body radiators should be used in optical pyrometry and radiation work.

During the past few years the writer<sup>1</sup> has made frequent use of this table in computing spectral energy data and has found it sufficiently extensive for ordinary use. The chart is the outcome of numerous intercomparisons<sup>2</sup> of spectral radiation data with similar data resulting from photoelectric and other experiments, supplemented by the very complete computations and tabulations made by Dushman.<sup>3</sup>

## II. COMPUTATION OF SPECTRAL RADIATION DATA

The Planck radiation formula, as usually written, is

$$E_\lambda = c_1 \lambda^{-5} (e^{c_2/\lambda T} - 1)^{-1} \dots \dots \dots (1)$$

The function,  $e^u - 1$ , does not appear to have been tabulated heretofore. Some years ago a system of computation was

<sup>1</sup> Bulletin, Bureau of Standards, 12, p. 471, 1916.

<sup>2</sup> Coblenz, Phys. Rev., 32, p. 613, 1911 (On the Elementary Electrical Charge); also Bulletin, Bureau of Standards, 12, p. 553, 1916.

<sup>3</sup> Dushman, Gen. Elect. Rev., 18, p. 1167, 1915.

adopted whereby the value of  $\lambda$  was so chosen that the exponent  $u = c_2/\lambda T$  resulted in a number which is given in exponential tables<sup>4</sup> of  $e^u$ . This, of course, is possible, whatever values of  $c_2$  may be used. Hence, the present table is of permanent value. In view of the uncertainty of the exact value of  $c_2$ , the time does not yet seem ripe for tabulating  $E_\lambda$ , for different temperatures (say, in steps of  $50^\circ$ ) and wave lengths.

By the system of calculation herein employed, spectral intensity data may be quickly computed. For this purpose the value of  $\log c_1 = 5.00000$  is employed, the resulting values of  $E_\lambda$  being, of course, in arbitrary units. The Planck formula then becomes

$$\log E_\lambda = \log k - 5 \log \lambda \dots \dots \dots (2)$$

in which values of  $\log k = \log c_1 - \log (e^u - 1)$  are given in the fourth column of Table 1.

As already mentioned, the usefulness of the method lies in selecting the exponent

$$u = c_2/\lambda T \dots \dots \dots (3)$$

so that values of  $u$  may be taken from the table. The value of  $\lambda$  usually comes out some uneven number, but this is unimportant.

*Example.*—The following data are given as an illustration of the computation<sup>5</sup> of the isothermal spectral energy curve for  $T = 1596^\circ \text{K}$ , using  $c_2 = 14350$ .

Here

$$u = c_2/\lambda T = \frac{8.99}{\lambda}$$

From Table 1, for

$$u = 8.0, \lambda = 1.123\mu;$$

$$\log k = 1.52579$$

$$5 \log \lambda = .25190$$

$$\log E_\lambda = 1.27389$$

$$E_\lambda = 18.79 \text{ at } \lambda = 1.123\mu.$$

<sup>4</sup> Smithsonian Mathematical Tables, Hyperbolic Functions.

<sup>5</sup> Bulletin, Bureau of Standards, 18, p. 476, 1916.



TABLE 1

$u$	$e^u$	$\log_{10} [e^u - 1]$	$\frac{\log k}{5 - \log [e^u - 1]}$
0.10	1.10 517	I. 021 932	5.97 807
.15	1.16 183	I. 209 069	5.79 094
.20	1.22 140	I. 345 177	5.65 483
.25	1.28 403	I. 453 357	5.54 665
.30	1.34 986	I. 543 894	5.45 611
0.35	1.41 907	I. 622 286	5.37 772
.40	1.49 183	I. 691 815	5.30 819
.45	1.56 831	I. 754 586	5.24 542
.50	1.64 872	I. 812 057	5.18 795
.55	1.73 325	I. 865 254	5.13 475
0.60	1.82 212	I. 914 935	5.08 507
.65	1.91 554	I. 961 677	5.03 833
.70	2.01 375	0.005 926	4.99 407
.75	2.11 700	.048 053	4.95 195
.80	2.22 554	.088 317	4.91 169
0.85	2.33 965	.126 971	4.87 303
.90	2.45 960	.164 234	4.83 577
.95	2.58 571	.200 221	4.79 978
1.00	2.71 828	.235 099	4.76 491
.05	2.85 765	.268 964	4.73 104
1.10	3.00 417	.301 935	4.69 808
.15	3.15 819	.334 089	4.66 591
.20	3.32 012	.365 509	4.63 449
.25	3.49 034	.396 287	4.60 374
.30	3.66 930	.426 397	4.57 361
1.35	3.85 743	.455 976	4.54 403
.40	4.05 520	.485 039	4.51 497
.45	4.26 312	.513 633	4.48 637
.50	4.48 169	.541 789	4.45 822
.55	4.71 147	.569 546	4.43 046
1.60	4.95 303	.596 929	4.40 308
.65	5.20 698	.623 970	4.37 603
.70	5.47 395	.650 691	4.34 931
.75	5.75 460	.677 114	4.32 289
.80	6.04 965	.703 261	4.29 674

TABLE 1—Continued

$u$	$e^u$	$\log_{10} [e^u - 1]$	$\log k =$ $5 - \log [e^u - 1]$
1.83	6.23 399	.718 825	4.28 118
.85	6.35 982	.728 150	4.27 185
.90	6.68 589	.754 798	4.24 521
.93	6.88 951	.770 079	4.22 992
.95	7.02 869	.780 223	4.21 978
2.00	7.38 906	.805 437	4.19 456
.10	8.16 617	.855 287	4.14 471
.20	9.02 501	.904 446	4.09 555
.30	9.97 418	.952 995	4.04 701
.40	11.0 232	1.001 005	3.99 899
2.50	12.1 825	1.048 529	3.95 146
.60	13.4 637	1.095 647	3.90 435
.70	14.8 797	1.142 386	3.85 761
.80	16.4 446	1.188 779	3.81 122
.90	18.1 741	1.234 875	3.76 513
3.00	20.0 855	1.280 705	3.71 920
.10	22.1 980	1.326 293	3.67 371
.20	24.5 325	1.371 668	3.62 833
.30	27.1 126	1.416 851	3.58 315
.40	29.9 641	1.461 859	3.53 815
3.50	33.1 155	1.506 714	3.49 329
.60	36.5 982	1.551 428	3.44 867
.70	40.4 473	1.596 017	3.40 398
.80	44.7 012	1.640 493	3.35 951
.90	49.4 024	1.684 867	3.31 513
4.00	54.5 982	1.729 150	3.27 085
.10	60.3 403	1.773 349	3.22 664
.20	66.6 863	1.817 541	3.18 246
.30	73.6 998	1.861 532	3.13 846
.40	81.4 509	1.905 531	3.09 446
4.50	90.0 171	1.949 474	3.05 053
.60	99.4 843	1.993 367	3.00 663
.70	109. 947	2.037 215	2.96 278
.80	121. 510	2.081 023	2.91 898
.90	134. 290	2.124 798	2.87 520

TABLE 1—Continued

<i>u</i>	<i>e<sup>u</sup></i>	log <sub>10</sub> [ <i>e<sup>u</sup></i> − 1]	log <i>k</i> = 5 − log [ <i>e<sup>u</sup></i> − 1]
5.00	148. 413	2. 168 536	2. 83 146
. 10	164. 022	2. 212 246	2. 78 775
. 20	181. 272	2. 255 928	2. 74 407
. 30	200. 337	2. 299 588	2. 70 041
. 40	221. 406	2. 343 223	2. 65 678
5. 50	244. 692	2. 386 841	2. 61 316
. 75	314. 191	2. 495 809	2. 50 419
6. 00	403. 429	2. 604 689	2. 39 531
. 50	665. 142	2. 822 261	2. 17 774
7. 00	109 6. 63	3. 039 664	1. 96 034
7. 50	180 8. 04	3. 256 959	1. 74 304
8. 00	298 0. 95	3. 474 209	1. 52 579
8. 50	491 4. 77	3. 691 414	1. 30 859
9. 00	810 3. 08	3. 908 596	1. 09 140
9. 50	133 59. 7	4. 125 770	. 87 423
10. 0	220 26. 5	4. 342 926	. 65 707
11. 0	598 74. 1	4. 777 232	. 22 277
12. 0	162 755.	5. 211 532	1. 78 847
13. 0	442 413.	5. 645 828	1. 35 417
14. 0	1202 604.	6. 080 123	1. 91 988

It is of course to be understood that after computing these data they must be multiplied by a factor to superpose them upon the observed spectral energy curve. This, as well as the determination of the different values of *u*, is easily accomplished with a slide rule.

III. INTERCOMPARISON OF RADIATION AND OTHER DATA

From Planck's radiation theory we have the following relations:

$c_2 = c \, h \, k^{-1} = 4.9651 \, \lambda_m \, T \dots\dots\dots (4)$

$\sigma = \frac{ac}{4} = \frac{12\pi \times 1.0823 \, k^4}{c^2 \, h^3} \dots\dots\dots (5)$

$\lambda_m T = \frac{c \, h}{4.9651 \, k} \dots\dots\dots (6)$

$k = \frac{eR}{cF} \dots\dots\dots (7)$

In these equations  $h$  is Planck's universal constant or constant of action;  $k$  is the Boltzmann gas constant,  $k = 1.372 \times 10^{-18}$  erg. deg<sup>-1</sup>;  $c$  is the velocity of light,  $c = 2.9986 \times 10^{10}$  cm. sec.<sup>-1</sup>;  $F$

C,  
14 400  
14 300  
14 200  
14 100

FIG. 1.—Curves showing the relation between the radiation and other constants.

is the Faraday constant,  $F = 96500$  coulombs;  $R$  is the absolute gas constant,  $R = 831.5$  erg. deg<sup>-1</sup>; and  $e$  is the unit electric charge,  $e = 4.774 \times 10^{-10}$  e. s. u. From equation (7) it may be

noticed that a change in the value of  $e$  affects the value of  $c$ , directly, while the value of  $\sigma$  is affected by  $e^4$ .

The data computed from the above-mentioned constants and formulæ are illustrated in Fig. 1, from which it is an easy matter to compare experimental data. For example, the writer's <sup>6</sup> value of the coefficient of total radiation is  $\sigma = (5.72 \pm 0.012) \times 10^{-12}$  watt.  $\text{cm}^{-2}$ .  $\text{deg}^{-4}$ . This indicates a value of  $c_2 = 14\,320$  micron degrees and a value of  $h = 6.55 \times 10^{-27}$  erg sec. The value of  $h$ , determined by Blake and Duane <sup>7</sup> by X rays, is  $h = 6.555 \times 10^{-27}$  erg sec.; or an indicated value of  $c_2 = 14\,330$  micron degrees, which is close to experimental determinations of this constant.

Using the early determinations of  $c_2$  and  $\sigma$  by Lummer and Pringsheim, and by Kurlbaum, and the above-mentioned relations in his radiation theory, Planck <sup>8</sup> deduced a value of  $e = 4.69 \times 10^{-10}$  e. s. u. for the elementary charge of an electron. He calls attention to the fact that the value of this constant will depend upon the accuracy of the experimental determination of the constants of radiation, which in the meantime have been found quite different from the values used by him.

In the meantime the unit electric charge has been determined with high precision by Millikan,<sup>9</sup> and recent writers have been computing the radiation and other constants, using the value of  $e = 4.774 \times 10^{-10}$  e. s. u. As shown by the dotted,  $c_2$ ,  $\sigma$ -curve in Fig. 1, a change of about 0.1 per cent in  $e$  (using  $e = 4.777$  as found in earlier experiments—1912) has an appreciable effect upon, and happens to bring a closer agreement between, the writer's values of  $c_2$  and  $\sigma$ ; though no particular significance is to be attached to this fact.

In view of the fact that several writers<sup>10</sup> have expressed the opinion that the radiation constants  $c_2$  and  $\sigma$  could be derived more accurately from determinations of  $h$  by photoelectric and other data, it is important to emphasize that whatever the theoretical value of  $c_2$  may be, the value of  $c_2$  as determined on the best black bodies that can be constructed, using accepted experimental methods, is the one to be used in optical pyrometry and radiation work.

<sup>6</sup> Proc. Nat. Acad. Sci., 8, p. 504, 1917.

<sup>7</sup> Blake and Duane, Phys. Rev. (2), 10, p. 624, 1917.

<sup>8</sup> Planck, Vorlesungen ü Warmestrahlung, p. 163; 1906.

<sup>9</sup> Millikan, Proc., Nat. Acad. Sci., 8, p. 231; 1917.

<sup>10</sup> Millikan, Phys. Rev., (2) 7, p. 378; 1916. Dellinger, Bulletin, Bureau of Standards, 18, p. 543; 1916.

From a recent recalculation and intercomparison by Birge <sup>11</sup> of the data on  $c$ ,  $\sigma$ , and  $h$ , as determined by radiometric, photoelectric, X rays, and ionization potential measurements, it appears that the value of  $h$ , computed from radiometric data, compares favorably with that obtained by more direct measurement. The outstanding disagreement between all the observed and computed data appears to be of the order of 2 to 3 parts in 1000, whatever the method of experimentation. This is a very close agreement, considering the variety of the data and the difficulties involved in making the experiments. It seems to indicate something more than a fortuitous relation between properties of matter.

#### IV. SUMMARY

In this paper a simple method is given for computing spectral-energy curves, using the Planck formula. For this purpose a table of values of  $\log (e^u - 1)$  is given.

The paper gives also a chart for the intercomparison of thermal radiation constants with similar data, obtained indirectly from ionization potential, photoelectric, and X-ray measurements.

WASHINGTON, August 6, 1919.

---

<sup>11</sup> Birge, *Phys. Rev.*, (2) 14, p. 361; 1919.

12  
MAY 1920  
DEPARTMENT OF COMMERCE



# SCIENTIFIC PAPERS

OF THE

# BUREAU OF STANDARDS

S. W. STRATTON, DIRECTOR

No. 361

## MAGNETIC TESTING OF STRAIGHT RODS IN INTENSE FIELDS

BY

W. L. CHENEY, Assistant Physicist

*Bureau of Standards*

ISSUED FEBRUARY 21, 1920



PRICE, 5 CENTS

Sold only by the Superintendent of Documents, Government Printing Office  
Washington, D. C.

WASHINGTON  
GOVERNMENT PRINTING OFFICE

1920







FIG. 4.—*Photograph of the Du Bois electromagnet, showing specimen and test coils in place*

# MAGNETIC TESTING OF STRAIGHT RODS IN INTENSE FIELDS

By W. L. Cheney

## CONTENTS

	Page
I. Introductory.....	625
II. Historical.....	625
III. Apparatus.....	628
IV. Experimental method.....	629
1. Normal induction.....	629
2. Hysteresis values.....	630
V. Experimental results.....	632
1. Normal induction.....	632
2. Reluctivity and intensity of magnetization.....	634
VI. Summary.....	637

## I. INTRODUCTORY

The usual types of permeameter, for the measurement of the magnetic properties of iron and steel bars, do not permit the magnetizing force to be carried to very high values. The Burrows permeameter,<sup>1</sup> for example, is limited to  $H=300$  gauss. Frequently in the testing of the magnetic properties of fairly long straight rods, it is desirable to carry the magnetizing force considerably higher in order to determine the saturation intensity of magnetization. The majority of methods for doing this (vide infra) necessitate the use of very small specimens and, therefore, preclude the possibility of comparing results for low fields with similar results obtained with a standard permeameter. The solenoid method is not entirely satisfactory on account of the demagnetizing factor of the specimen.

In view of these facts, a method suitable for magnetic measurements of long straight bars of iron or steel in intense fields has been developed.

## II. HISTORICAL

Early experiments to ascertain the intensity of magnetization due to high magnetizing forces were made principally upon specimens either in the form of rings or toroids<sup>2</sup> or with a long

<sup>1</sup> Scientific Paper, No. 117, Bureau of Standards.  
150059°—20

<sup>2</sup> Rowland, Phil., Mag., 46 1873; 48, 1874.

rod in a solenoid.<sup>3</sup> The results obtained by these early experimenters have since been found not to be very accurate.

In 1887 Ewing and Low<sup>4</sup> developed the well-known "isthmus method" for testing the permeability of ferromagnetic materials under the influence of intense fields. A strong electromagnet was used because in the air space between the pole pieces there can be produced more easily a magnetic field of much greater intensity than in a magnetizing coil where the field is due to the direct action of the electric current. The specimen was in the form of a bobbin or isthmus and placed between the conical pole pieces of the electromagnet (Fig. 1). The magnetic induction in the isthmus was measured by means of a small test coil wound around it and connected in series with a ballistic gal-

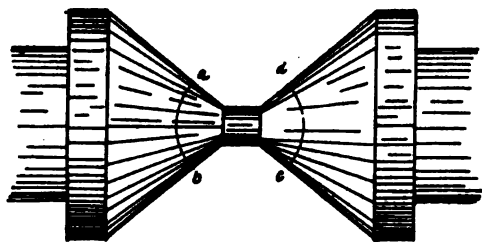


FIG. 1.—Illustrating the "isthmus" as used by Ewing and Low

vanometer. Upon suddenly rotating the specimen through  $180^\circ$  about an axis at right angles to the direction of the magnetic flux, the throw of the ballistic galvanometer (previously calibrated), indicated the induction in the specimen. To permit the

rotation, the tips of the pole pieces were bored through transversely by a circular hole *abcd*.

To determine the value of the magnetizing force ( $H$ ), a second coil surrounding the first was used. The difference in magnitude of the throws of the galvanometer caused by the two coils respectively is proportional to the flux through the air space between the two coils, and can be easily calculated when the difference in the area turns of the coils is known. When there is a uniform magnetic field between the pole pieces, the magnetic flux through the space included by the two coils is probably only a very little greater than the mean force within the metal itself, hence may be taken as a measure of the latter.

Du Bois<sup>5</sup> employed an optical method for determining the intensity of magnetization of iron in strong fields, having first examined the material in the weaker fields of a solenoid. Similar experiments were also carried out by Roessler.<sup>6</sup>

<sup>3</sup> Weber; 1884.

<sup>4</sup> Ewing, *Magnetic Induction in Iron and Other Metals*, pp. 136-158.

<sup>5</sup> Du Bois, *Phil. Mag.*, 20, p. 253, 1890.

<sup>6</sup> Roessler, *Elektrotech. Zeit.*, 14, 1893.

Du Bois and Jones<sup>7</sup> tested specimens between the conical pole pieces of an electromagnet of the Du Bois type. They measured ballistically the change in induction upon suddenly withdrawing the specimen, which formed a part of the isthmus, through a hole in one of the pole pieces.

Weiss<sup>8</sup> employed small ellipsoids of revolution and placed them symmetrically between the flat pole pieces of an electromagnet of great power. The ellipsoid was suddenly extracted from the field through a hole in the axis of one of the pole pieces while the change in flux was measured by a test coil outside the iron.

B. O. Peirce<sup>9</sup> studied the magnetic properties, particularly the reluctivity and permeability, of some specimens of very pure Norway iron. He used the isthmus method, having for his apparatus a massive yoke weighing about 300 kg, excited by a current through a coil of 2956 turns wound on spools, as shown in Figure 2. The specimens were of two forms. The first was a cylinder about 1.27 cm in diameter and about 15 cm long. Its ends were tapered to fit snugly into sockets in the conical ends of the pole pieces. The other form was much shorter, the exposed portion being constricted to a smaller diameter than the remainder of the specimen.

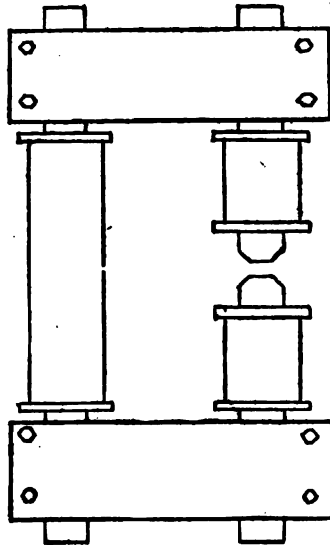


FIG. 2.—Showing the form of the yoke of B. O. Peirce

Instead of reversing the specimen in the magnetic field, as did Ewing and Low, Peirce reversed the magnetic field by reversing the current through the windings of the electromagnet. He found that this worked satisfactorily, provided he used a ballistic galvanometer whose period was appreciably greater than the time lag of the electromagnet. He employed the same method as Ewing and Low for determining  $B$  and  $H$ , the latter being measured by connecting two coils in opposition, so that the throw of the galvanometer was proportional to the flux in the annular space between them.

<sup>7</sup> Du Bois and Jones, *Elekt. Zeit.*, 17, p. 543; 1896. *Electrician*, 37, p. 595; 1896.

<sup>8</sup> P. Weiss, *Comptes Rendus*, 146, p. 1155; 1907.

<sup>9</sup> B. O. Peirce, *Am. Acad. Arts and Sci., Proc.*, 44, p. 354; 1909. *Am. Jour. of Sci.*, 27, p. 273, 1909; 28, p. 1, 1909.

In some of his subsequent experiments Peirce<sup>10</sup> used a large magnetizing solenoid to supplement his observations with the modified isthmus method.

Gumlich<sup>11</sup> employed the isthmus method for determining the intensity of magnetization of some very carefully prepared specimens of iron. He used an electromagnet of the Du Bois type and suddenly reversed the isthmus (specimens 28 mm long and 3 mm diameter), according to the method of Ewing and Low. Later, Gumlich<sup>12</sup> used a special yoke which proved satisfactory.

Hadfield and Hopkinson,<sup>13</sup> in a very extensive investigation of the magnetic properties of iron alloys, used a modified isthmus

method somewhat after the manner of Peirce, but used very much smaller specimens.

Further developments were made by Campbell and Dye,<sup>14</sup> the form of whose electromagnet is shown in Fig. 3. The specimens tested were either in the form of a rod 7 cm long and 0.5 cm in diameter, or an equivalent bundle of strips or wires. The specimen was fitted into thick, soft iron disks *E* and *F*, which formed the pole pieces. These disks did not touch the magnet poles but were separated from them by a small air gap. In the middle portion of the test specimen was a coil of 40 turns of wire used for measuring *B*, and three outer successively larger coaxial coils of 400 turns each used differentially to determine *H*. By using alternately one set of coils and then the other, the uniformity of the field between the poles of the electromagnet could be tested.

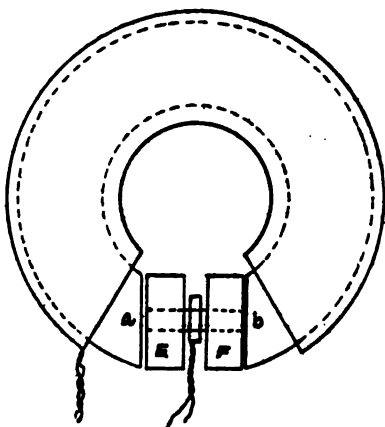


FIG. 3.—Illustrating the form of the electromagnet used by Campbell and Dye

method somewhat after the manner of Peirce, but used very much smaller specimens.

### III. APPARATUS

The apparatus used in the present investigation consists essentially of an electromagnet of the Du Bois type (Fig. 4) with flat pole pieces, separated by an air gap of approximately 2 cm and pierced coaxially so that a rod 6 mm in diameter and several

<sup>10</sup> B. O. Peirce, *Am. Acad. Arts and Sci., Proc.*, **49**, p. 227; 1913.

<sup>11</sup> E. Gumlich, *Elekt. Zeit.*, **30**, pp. 1065-1067; 1909.

<sup>12</sup> E. Gumlich, *Archiv. für Elektr.*, **2**, p. 461; 1913-1914.

<sup>13</sup> Hadfield and Hopkinson, *Inst. of Elec. Eng. Jour.*, **46**, p. 235; 1911.

<sup>14</sup> Campbell and Dye *Inst. of Elec. Eng. Jour.*, **54**, p. 35; 1915.

centimeters long can be extended through them and the electromagnet. Surrounding the specimen are three coaxial coils wound on brass forms each 1 cm long and having external diameters of 7 mm, 10.5 mm, and 13.2 mm, respectively. Each coil has 100 turns of No. 40 (B. & S. gage) enameled copper wire. To insure insulation from the brass form, the latter was first wrapped with a thin sheet of paper, and to secure a moisture-free coating of insulating material, the whole coil after winding was well shellacked and baked in an oven at 100° C for several hours. To measure the number of area turns of the coils, they were placed in the center of a solenoid and the throw of a ballistic galvanometer upon reversing a known magnetizing force inside the solenoid was compared with the throw observed when the current was reversed through the primary coil of a known mutual inductance.

Fig. 5 is a diagram of the circuits and connections. A Leeds and Northrup, type R, ballistic galvanometer, calibrated with the aid of a mutual inductance, is used. There are employed three sensitivities of the galvanometer, regulated by the parallel resistance  $R_p$  and the series resistances  $R'_{h_1}$  and  $R'_{h_2}$  for low values of  $H$ , as measured by inner and outer annuluses, respectively,  $R_{h_1}$  and  $R_{h_2}$  for high values of  $H$ , and  $R_b$  for  $B$ , making necessary five secondary circuits in series with the galvanometer.  $R_b$  is adjusted so that a reversal of 10 000 lines of induction per square centimeter gives a throw of 10 cm of the galvanometer;  $R_{h_1}$  and  $R_{h_2}$  so that a reversal of a magnetizing force of 1000 gaussess gives a deflection of 10 cm; and  $R_{h_1}'$  and  $R_{h_2}'$  so that a reversal of 200 gaussess gives a throw of 10 cm. In the latter case it is also necessary to increase the magnitude of  $R_p$ .

#### IV. EXPERIMENTAL METHOD

##### 1. NORMAL INDUCTION

To determine the value of the magnetic induction  $B$ , the inner coil is connected in series with the ballistic galvanometer. Upon suddenly reversing the current in the windings of the electromagnet the throw of the ballistic galvanometer is proportional to the induction in the specimen. To measure the magnetizing force  $H$ , the inner and middle coils are connected differentially, so that the throw of the galvanometer is proportional to the flux in the annular space between the coils. To check the uniformity of the field, the middle and outer coils are connected in a similar manner and the throw again observed. Observations obtained by the

two sets of coils seldom differ by more than 2 per cent and in most cases check much more closely.

By measuring  $B$  for successively increasing values of  $H$ , normal induction curves can be obtained.

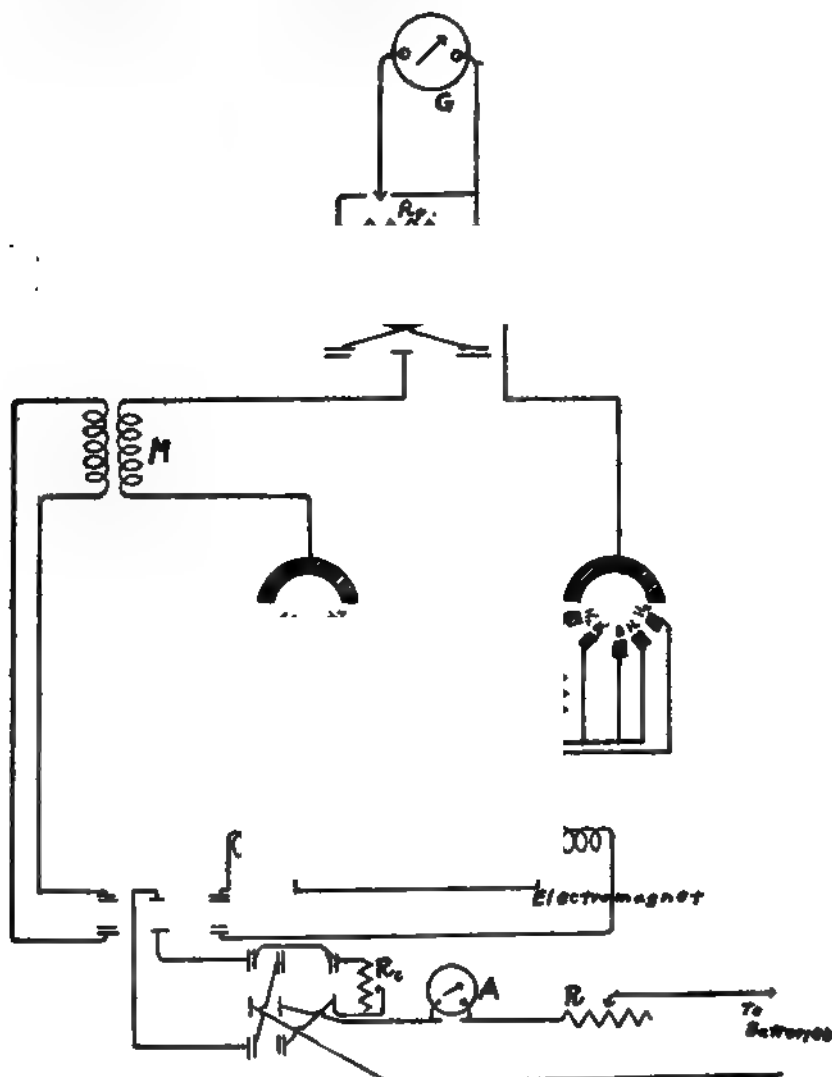


FIG. 5.—Diagram of electrical circuits and connections

## 2. HYSTERESIS VALUES

The part of the whole experiment which requires the greatest care and yields the least accurate results has to do with the measurement of the hysteresis constants, residual induction ( $B_r$ ) and the coercive force ( $H_o$ ).



Consider the hysteresis loop (Fig. 6) and suppose the induction is at the tip  $B_m$  for a given maximum magnetizing force  $H_m$ . By reversing the current in the windings of the electromagnet,  $B$  changes from  $B_m$  to  $-B_m$  and  $H$  changes from  $H_m$  to  $-H_m$ . Now, if instead of reversing the current, the circuit is suddenly broken,  $H$  is reduced to zero and  $B$  changes from  $B_m$  to  $B_r$  which can be located on the curve. In practice, however, the

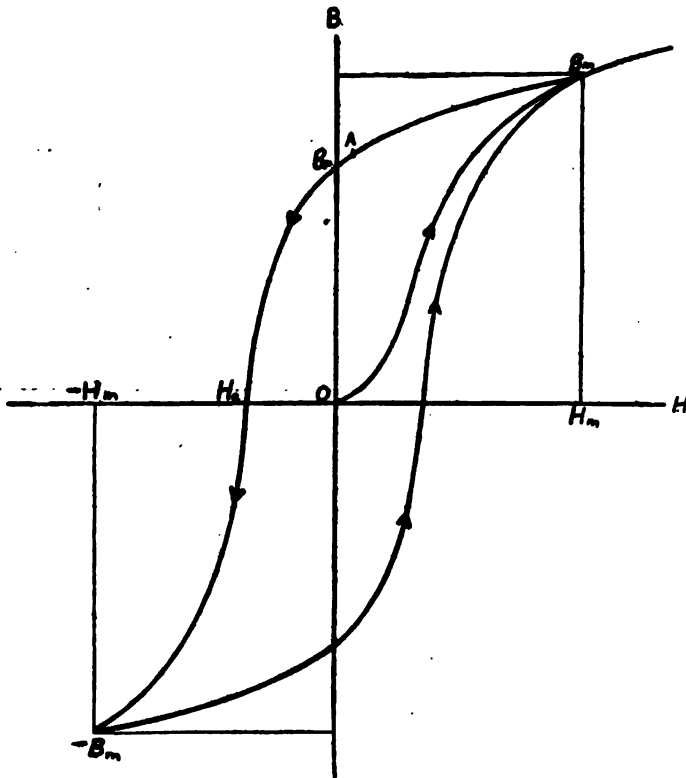


FIG. 6.—Characteristic hysteresis loop

point  $B_r$  is not quite reached on account of the small residual field in the electromagnet—but, rather, some point  $A$ . This point, however, does not differ very greatly from the true value of the residual induction, particularly in the case of hard materials, since the curve is quite flat in this region.

To determine the coercive force, the galvanometer is connected in series with the  $B$  coil. Resistance ( $R_0$ ) is added to the primary circuit simultaneously upon reversal of the current, so that instead of passing from  $B_m$  to  $-B_m$  the induction changes from  $B_m$  to

zero, and the magnetizing force from a large value  $H_m$  to a small negative value  $H_o$ . Now, on suddenly breaking the circuit,  $H$  changes from  $H_o$  to zero, from which the coercive force may be found, although it is difficult to determine very accurately owing to the small order of magnitude of the throw of the galvanometer, which is hardly sensitive enough for such small values as occur in the case of soft material. The galvanometer throw is increased considerably by connecting the inner and outer coils together in opposition (thus increasing the number of area turns in the annulus) by reducing  $R_h$  and by increasing  $R_p$ . Even then the values of

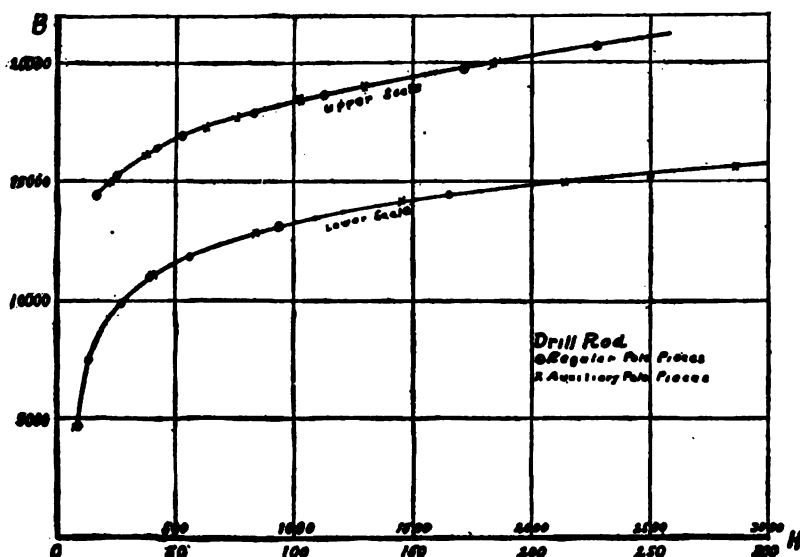


FIG. 7.—Showing the agreement of normal induction data for drill rod as obtained with regular pole pieces and with auxiliary pole pieces

$H_o$  for soft materials do not appear to be reliable. An investigation of this feature is being continued.

## V. EXPERIMENTAL RESULTS

### 1. NORMAL INDUCTION

It will be recalled that Campbell and Dye<sup>14</sup> used a short rod, placed in auxiliary pole pieces of the electromagnet. To compare the results obtained by their method with those obtained by the present method, two auxiliary pole pieces were prepared and introduced as in Fig. 3. After testing a specimen of drill

<sup>14</sup> Loc. cit.

rod, 6 cm long, the auxiliary pole pieces were removed and the air gap of the electromagnet adjusted so that 2 cm of each end of the specimen projected into the regular pole pieces. The normal induction curve was again observed. No difference could be found in the case of the two sets of observations as illustrated in Fig. 7.

A series of tests were made upon 12 rods 6 mm in diameter and 35 cm long. Four of these, Nos. 293-296, were of Norway

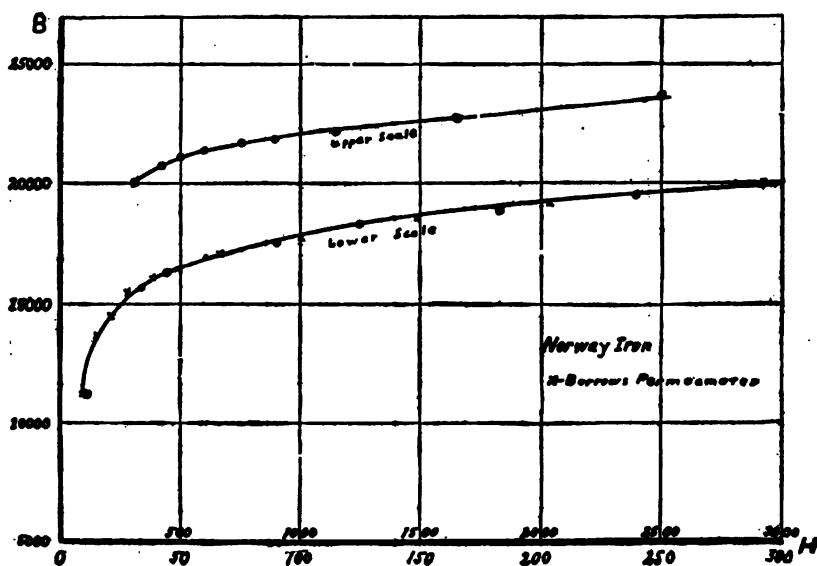


FIG. 8.—Normal induction curve for Norway iron

iron, four (297-300) were of Bessemer steel, while four (301-304) were of tool steel.

To check the accuracy of the results, these specimens were tested both in the Burrows permeameter and in the apparatus herein described. Figs. 8, 9, and 10 show typical  $B$ - $H$  curves obtained in this manner. An inspection of these curves reveals the unusually good agreement between the results obtained by the two types of apparatus. It is assumed, therefore, that the higher values of the induction, which can not be measured in the Burrows apparatus, are correct.

Fig. 11 shows the curves for normal induction and permeability for a specimen of unusually hard magnet steel known as "K S" magnet steel and prepared by Prof. Honda.

## 2. RELUCTIVITY AND INTENSITY OF MAGNETIZATION

The reluctivity ( $\rho$ ) is defined by the relationship

$$\rho = \frac{H}{B} = \frac{1}{\mu}$$

The magnetic induction ( $B$ ) increases indefinitely as the magnetizing force ( $H$ ) is increased, but it is found that if  $H$  be subtracted from the value of  $B$ ,  $B-H$  reaches a finite saturation value in intense fields.  $B-H$  may be considered as the induction carried by the molecules of the iron after allowance is made for

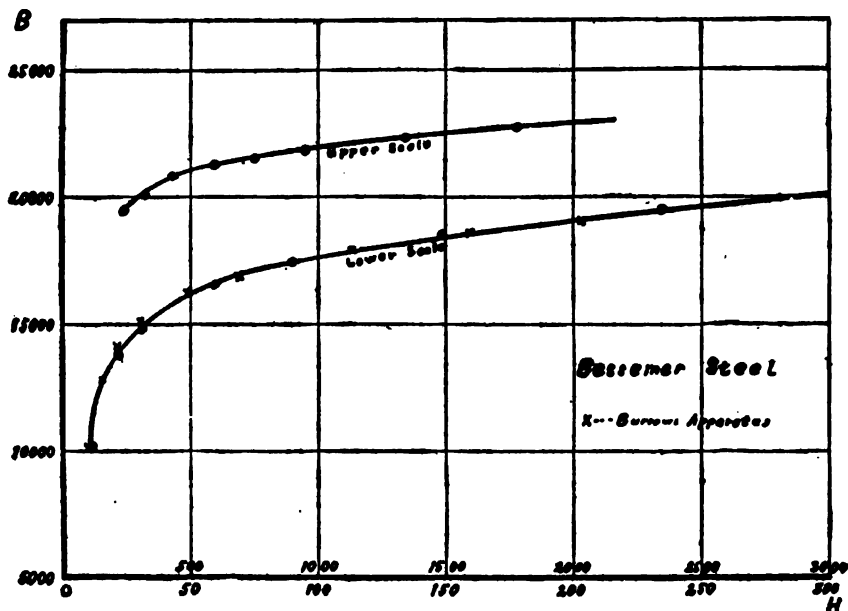


FIG. 9.—Normal induction curves for Bessemer steel

the flux in the space occupied by the material but independent of it. Replacing  $B$  by  $B-H$ ,

$$\rho_0 = \frac{H}{B-H}$$

and is called the "metallic reluctivity." Kennelly<sup>10</sup> has shown that  $\rho_0$  plotted against  $H$  as the independent variable gives a straight line (except near the origin) whose equation may be written as

$$\rho_0 = a + bH$$

From the usual equation

$$B = H + 4\pi I$$

<sup>10</sup> Kennelly, A. I. E. E., Proc., 8, p. 485; 1891.

the intensity of magnetization may be written

$$I = \frac{B-H}{4\pi}$$

and can be easily calculated for successively higher values of  $H$ . The reciprocal of the susceptibility ( $k$ ) is given by

$$\frac{1}{k} = \frac{H}{I} = \frac{4\pi H}{B-H} = 4\pi\rho_0.$$

Therefore, if  $\frac{1}{k}$  be plotted against  $H$  as the independent variable, the curves obtained will be precisely of the same shape as the

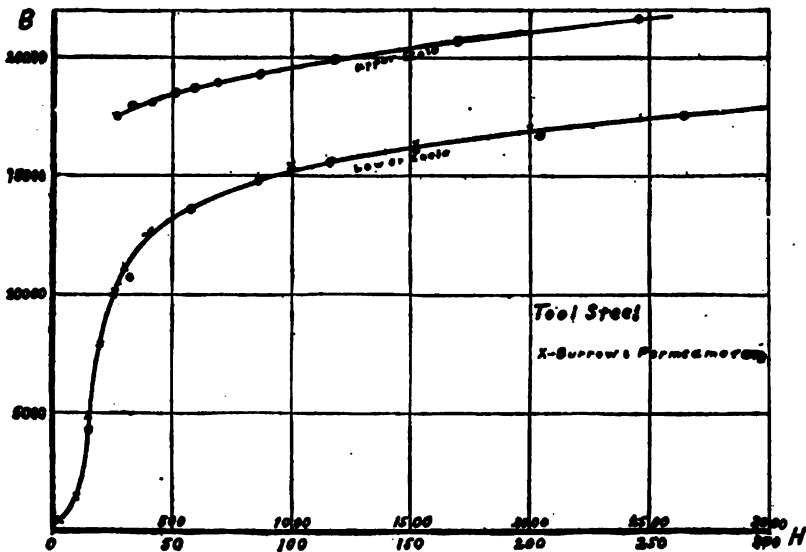


FIG. 10.—Normal induction curve for tool steel

$\rho_0$ - $H$  curves and such graphs are shown for five different materials in Fig. 12, the ordinates representing the reciprocal of the susceptibility, and the abscissæ the field strength.

Now, by calculating the reciprocal of the slope of these graphs, the value for the maximum value of the intensity of magnetization is determined. This has been done for a number of specimens and the results are incorporated in Table 1 together with observed values for  $H = 2000$ .

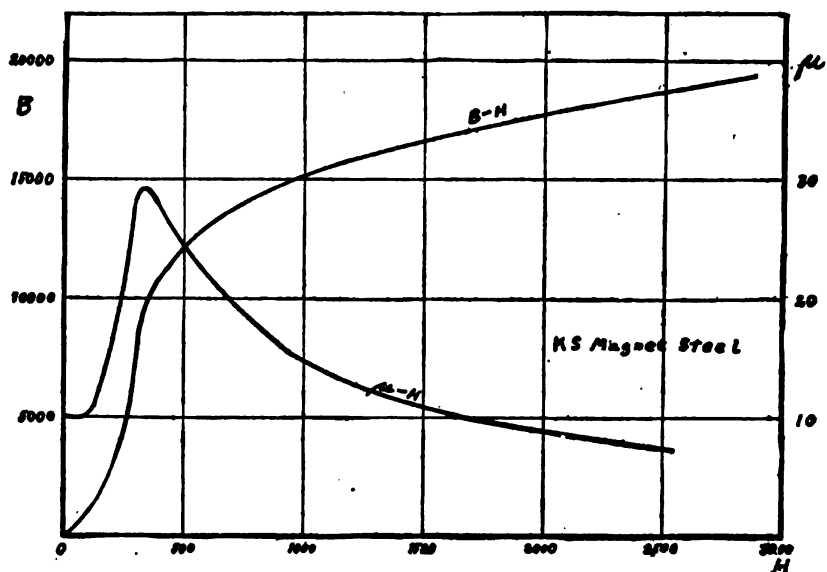


FIG. 11.—Normal induction and permeability for curves for "KS" magnet steel

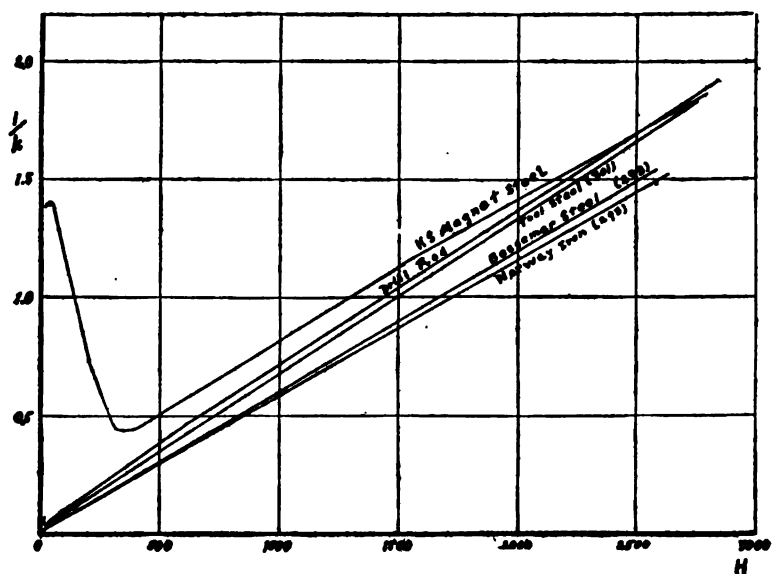


FIG. 12.—Showing the reciprocal of the susceptibility plotted against the magnetizing force

TABLE 1

Specimen No.	Material	$I_{\max}$ (calculated)	$I$ for $H=2000$	Specimen No.	Material	$I_{\max}$ (calculated)	$I$ for $H=2000$
293.....	Norway iron.....	1747	1725	301.....	Tool steel.....	1579	1490
294.....	do.....	1701	1686	302.....	do.....	1564	1525
295.....	do.....	1679	1672	303.....	do.....	1545	1515
296.....	do.....	1729	1723	304.....	do.....	1564	1530
297.....	Bessemer steel.....	1695	1665		K S magnet steel.....	1613	1412
298.....	do.....	1672	1672			1795	
299.....	do.....	1667	1652		Drill rod.....	1394	1465
300.....	do.....	1698	1665			1534	

In the case of the K S magnet steel and drill rod, the slope of the  $\frac{I}{k}$  curve changes, thus giving two values for  $I_{\max}$ . In the case of the former this change occurs in the neighborhood of  $H=1500$ , while for the latter it occurs near  $H=600$ . B. O. Peirce<sup>17</sup> has pointed out that the value of  $I_{\max}$  obtained from the lower portion of the curve is less than the saturation value, while  $I_{\max}$  calculated from the upper portion of the curve where the slope is different is somewhat larger than the saturation value. As pointed out by Steinmetz<sup>18</sup> this change in slope is indicative of the presence of two constituents of differing degrees of hardness, which reach the maximum intensity of magnetization for different values of  $H$ .

## VI. SUMMARY

1. A resume of previous methods of measuring high inductions is given.

2. A new modification of the isthmus method which is adapted to the testing of long straight specimens is described.

3. Data are given to illustrate the accuracy of the method as compared with standard methods.

4. Normal induction, intensity of magnetization, and reluctance data are discussed for various materials.

The writer is indebted to R. L. Sanford and Dr. C. Nusbaum for valuable suggestions throughout the course of the experiments.

WASHINGTON, August 29, 1919.

<sup>17</sup> B. O. Peirce, *Am. Acad. Arts and Sci., Proc.*, 49, pp. 217-246; 1913.

<sup>18</sup> Steinmetz, *Gen. Elec. Rev.*, 20, p. 135; 1917.





MAR 20 1920

DEPARTMENT OF COMMERCE



# SCIENTIFIC PAPERS

OF THE

# BUREAU OF STANDARDS

S. W. STRATTON, DIRECTOR

No. 362

## DISTRIBUTION OF ENERGY IN THE SPECTRUM OF AN ACETY- LENE FLAME

BY

W. W. COBLENTZ, Physicist  
*Bureau of Standards*

ISSUED FEBRUARY 12, 1920



PRICE, 5 CENTS

Sold only by the Superintendent of Documents, Government Printing Office  
Washington, D. C.

WASHINGTON  
GOVERNMENT PRINTING OFFICE

1920



# DISTRIBUTION OF ENERGY IN THE SPECTRUM OF AN ACETYLENE FLAME

By W. W. Coblentz

## CONTENTS

	Page
I. Introductory statement.....	639
II. Optical properties of the acetylene flame.....	640
III. Revision of data previously published.....	643
IV. Effect of this revision upon previous investigations.....	647
V. Summary.....	650

## I. INTRODUCTORY STATEMENT

The object of this paper is to give some new data on the distribution of energy in the infra-red spectrum of a cylindrical acetylene flame, and to revise some of the previously published spectral-energy data,<sup>1</sup> pertaining to the violet end of the visible spectrum, which are superseded by the present data.

The data previously published<sup>2</sup> seem to be the first attempt that has yet been made to supply the demand for quantitative radiometric measurements of spectral-energy distribution. Such data are of value in investigations involving spectrophotometry, color-matching, etc. However, for a source like the acetylene flame, which is weak in intensity in the violet, it is quite impossible to attain high accuracy in the radiation measurements. Nevertheless, in response to requests therefor the data were published, the papers indicating clearly the accuracy attainable and the variability<sup>3</sup> of the emissivity with thickness of the acetylene flame.

The acetylene flame does not appear to be a suitable standard of spectral radiation, in which high accuracy is desired. As indicated some time ago,<sup>4</sup> the proper procedure is to refer all spectral-energy specifications to a black body at a given temperature, the spectral-energy curve of which can be computed with greater accuracy than it can be observed in the violet end of the spectrum. In recent years great advances have been made in the construction of black bodies; in the establishment of a high

<sup>1</sup> B. S. Bulletin, 18, p. 355; 1916.

<sup>2</sup> B. S. Bulletin, 7 p. 253, 1911; 18, p. 355, 1916.

145824\*—20

<sup>3</sup> B. S. Bulletin, 18, p. 357; 1916.

<sup>4</sup> B. S. Bulletin, 6, p. 349; 1909.

temperature scale; in the determination of the radiation constants; and in the specification of the temperature of sources of high intensity (for example, the gas-filled tungsten lamp), in terms of the color temperature of a black body. Hence, it seems opportune to advocate the specification of spectral energy, colorimetric and other similar specifications in terms of a black body at a given temperature, the spectral-energy curve of which can be computed and checked radiometrically. In this manner experimenters will be using a uniform scale of spectral-energy distribution, whatever the actual energy distribution may be in the spectrum.

As will be discussed more fully on a subsequent page, until recently, when radiometric measurements were supplied to Priest,<sup>5</sup> there has been no real test of the accuracy of the radiometric measurements or of color matching in terms of these measurements. The energy curve for acetylene as obtained by color matching is high in the violet, but from  $0.5\mu$  to  $0.75\mu$  the two curves are in excellent agreement. This test indicated the possibility of the acetylene-energy data being too high in the violet, as previously surmised.<sup>6</sup>

Recently Hyde<sup>7</sup> and his collaborators, in an interlaboratory comparison, by color matching a tungsten lamp against the acetylene flame, placed the color temperature of the Eastman Kodak standard burner at  $2360^\circ\text{K}$ . From this test, also, it appears that the directly observed radiometric measurements may be too high in the region of  $0.4\mu$  to  $0.48\mu$ . However, as will be shown below, in the spectral region from  $0.5\mu$  to  $0.75\mu$  the observed data are in excellent agreement with those computed on the basis of color temperature.

## II. OPTICAL PROPERTIES OF THE ACETYLENE FLAME

As a result of the combustion of acetylene gas the emission spectrum of the acetylene flame is a composite of the radiation (1) from incandescent carbon particles, (2) from water vapor and (3) from carbon dioxide. The heated carbon dioxide gives bands of selective emission at  $2.7\mu$  and  $4.4\mu$ . The water vapor gives a somewhat continuous spectrum at  $1\mu$  to  $6\mu$  with bands of selective emission in the region of  $1.4\mu$  and  $1.85\mu$ . This is well illustrated

<sup>5</sup> Priest, *Phys. Rev.* (2), **10**, p. 808; 1917. (See Fig. 3.)

<sup>6</sup> B. S. Bulletin, **18**, p. 359; 1916.

<sup>7</sup> Hyde, Forsythe and Cady, *Phys. Rev.*, (2) **18**, p. 157; 1919.

in the emission spectrum of a bunsen acetylene flame published by Stewart.<sup>8</sup>

The emission spectrum of the incandescent carbon particles is supposed to be smooth and continuous (free from indentations or protuberances), with a maximum of emission at about  $1.28\mu$  to  $1.3\mu$ .

Observations of a flat flame, viewed flatwise, *F*, and edgewise,<sup>9</sup> *E*, also on a cylindrical flame, *C*, Fig. 1, do not show a marked difference in the position of the emission maximum. These data were obtained six years<sup>10</sup> ago but not published. The slope at

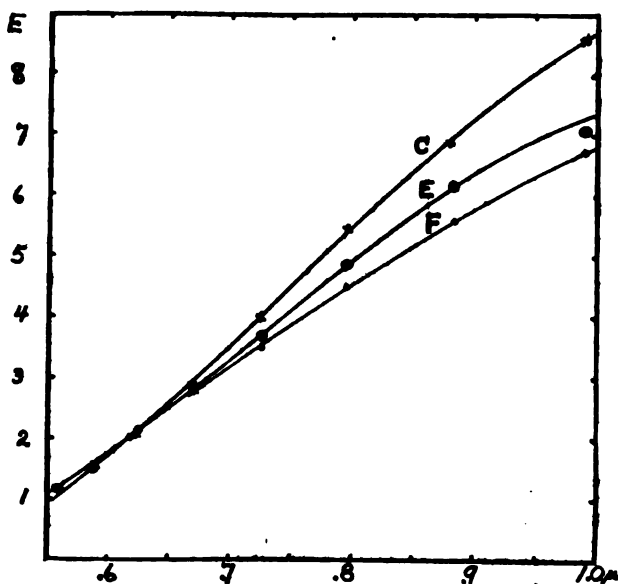


FIG. 1.—Spectral energy distribution of acetylene flame: *C*=cylindrical flame; also flat flame viewed flatwise, *F*, and edgewise, *E*.

$0.5\mu$  to  $0.8\mu$  of the spectral-energy curve of the cylindrical flame is much steeper than that of the flat flame, indicating a much lower black body color temperature, as observed experimentally.

With the assistance of H. Kahler, recently an examination was made of the emission of the Bray tip (Eastman Kodak Co. burner). The emission maximum was not quite smooth, owing to atmospheric absorption which produced a depression at  $1.4\mu$  in the spectral-energy curve. However, the maximum appears to be at  $1.28\mu$  to  $1.30\mu$ , corresponding to a black (gray) body temperature of  $2225$  to  $2250^\circ$  K.

<sup>8</sup> Stewart, *Phys. Rev.*, 18, p. 272; 1901.

<sup>9</sup> B. S. Bulletin, 7, p. 263; 1911.

<sup>10</sup> B. S. Bulletin, 9, p. 98; 1912, gives data on the emissivity of different parts of the flame.

Ångström<sup>11</sup> found that thin layers of soot, at room temperatures, decrease rapidly in absorption, from the visible to the infra-red, thus behaving like a turbid medium. However, incandescent carbon particles appear to have a maximum absorption in the visible spectrum.<sup>12</sup> Although the discovery of an absorption band may appear novel, the writer was recently informed by Dr. Ångström that some years ago this phenomenon was observed also in his laboratory.

Beyond  $1\mu$  the absorptivity of the flame is fairly constant. While no great reliance can be placed upon the absolute value of the absorptivity measurements of a cylindrical flame which is only 3 mm in diameter, recently measurements were made of the absorptivity of the cylindrical flame used in the visibility work. For wave lengths  $0.88\mu$  and  $1.2\mu$  the absorptivity was found to be practically the same, within the errors of observation, the value being about 2.2 per cent. This is not much greater than that of a flat flame, and it is probably to be expected in view of the fact that only the outer layer of gas of the (cylindrical) flame is incandescent.

From the constancy of the absorptivity data it appears that, within the limits of errors of observation, in the region of the spectrum from  $1\mu$  to  $1.5\mu$  the emission spectrum of the acetylene flame may be taken the same as that of a gray body. From the black body radiation constant,  $\lambda_m T = 2890$ , and the observed emission maximum of  $\lambda_m = 1.25\mu$  (to  $1.3\mu$ ) the black body temperature is about  $2300^\circ \text{K}$  (to  $2220^\circ \text{K}$ ).

This is somewhat lower than the observed black body color temperature for the visible spectrum, but it is to be expected from consideration of the absorptivity data. For, as we extend our observations toward the violet end of the spectrum, the absorptivity and hence the emissivity becomes higher and higher, and the slope is that of a black body at a higher temperature than obtains for the infra-red energy curve at  $1.3\mu$ .

If we multiply the spectral-energy curve of a black body at  $2300^\circ \text{K}$  by the observed absorptivities, the resulting spectral-energy curve has a slight maximum at  $0.65\mu$ , and the slope of the curve in the visible spectrum indicates a temperature higher than  $2300^\circ \text{K}$ , though not in exact agreement with the energy curve for the observed color temperature of  $2360^\circ \text{K}$ .

<sup>11</sup> Ångström, *Ann. der Phys.*, 36, p. 715; 1839.

<sup>12</sup> B. S. Bulletin, 7, p. 266; 1911. (See Fig. 9, p. 270.)

The direct radiometric observations do not show a distinct emission maximum in the visible spectrum, though spectrophotometric data are at hand<sup>13</sup> showing the possibility of such a condition. From the data at hand on emission and absorption it would appear that one should not expect to obtain a smooth spectral-energy curve in the visible spectrum of the acetylene flame, which can be superposed exactly upon the spectral-energy curve of a black body at a temperature corresponding with the color of the flame. The observed spectral-energy data of the acetylene flame given in Table 1 may, therefore, perhaps be nearer to the true curve than are the computed data. The observed spectral-energy curve of the gas-filled tungsten lamp on normal operation is practically a straight line from  $0.5\mu$  to  $0.7\mu$ , though the corresponding energy distribution for a black body color temperature shows some curvature.

TABLE 1.—Spectral Energy Distribution of a Cylindrical Acetylene Flame; Observed and Computed Using Wien's eq.,  $C_2=14350$  and  $T=2360^\circ\text{K}$ .

Wave length $\mu=0.001\text{ mm}$	$E_1$ ob- served 1911-1916	$E_1$ re- vised 1919	$E'$ com- puted	$100E'/$ $E_1$	Wave length $\mu=0.00\text{ mm}$	$E_1$ ob- served 1911-1916	$E_1$ re- vised 1919	$E'$ com- puted	$100E'/$ $E_1$
0.400 $\mu$	5.9	5	3.3	66	0.600 $\mu$	62.1	62.5	62.9	100.6
.425	8.2	7	5.5	79	.620	73.0	73.3	74.0	101.1
.440	10.0	8.5	7.6	89.4	.635	75.7	76.1	76.8	100.8
.450	11.5	10.0	9.25	92.5	.640	84.7	85.0	86.0	101.1
.460	13.0	11.8	11.2	94.9	.650	91.1	91.2	92.1	101.0
.475	16.0	15.0	14.6	97.4	.660	97.4	97.6	98.5	100.7
.500	21.9	20.9	21.0	100.5	.675	107.5	107.5	108.0	100.4
.520	27.9	27.5	27.3	99.3	.680	110.9	110.9	111.3	100.7
.525	29.5	29.2	29.2	100.0	.700	124.6	124.1	124.1	100.0
.540	35.0	34.6	34.6	100.0	.720	138.5	137.5	137.2	99.8
.550	38.9	38.9	38.8	99.8	.725	141.9	141.0	140.5	99.6
.560	42.9	42.9	43.1	100.4	.740	152.0	151.0	150.2	99.5
.575	49.8	49.8	49.9	100.2	.750	158.9	157.9	157.2	99.5
.580	52.2	52.2	52.4	100.3	a .750	163.7	163.0	157.2	96.5

a Bray tip.

### III. REVISION OF DATA PREVIOUSLY PUBLISHED

The numerical data, previously published,<sup>14</sup> on spectral-energy distribution of the acetylene flame, were based upon observations extending from  $0.45\mu$  to  $0.75\mu$  made with a mirror spectrometer and fluorite prism; also with a glass-lens spectrometer and flint-glass prism.

<sup>13</sup> Nichols and Merritt, *Phys. Rev.*, **80**, p. 328; 1910. See also B. S. Bulletin, **7**, p. 268 (Fig. 8), 1911, for ratios of emissivities which indicate such a maximum.

<sup>14</sup> B. S. Bulletin, **7**, p. 253, 1911; **12**, p. 355, 1916.

Hoping to overcome the difficulties in correcting for absorption, a spectrometer consisting of a quartz prism and two plano-convex quartz lenses was used in obtaining the spectral energy in the violet from  $0.4\mu$  to  $0.5\mu$ .

In one of the previous papers<sup>15</sup> an estimate is given of the accuracy attainable in making the observations. It is based upon the deviations of the observations from the mean value, and it is shown that, whereas in the red end of the spectrum an accuracy of 0.5 per cent is attainable (provided the flame stays constant), an accuracy of 10 per cent is hardly attainable in the violet where the intensity is low. Unfortunately, no mention is made of the difficulties and uncertainties in reducing these observed data from the prismatic into the normal spectrum. The slit-width factor is probably accurate to 1 per cent. The greatest uncertainty is the correction for spectral purity, also for absorption in the glass prism, or the silver mirrors, or both, in the violet end of the spectrum. Corrections<sup>16</sup> must be made also for diffuse light. Furthermore, when using the quartz spectrometer, the lenses not being achromatic, a correction was made for change in aperture with change in focal length for different parts of the spectrum. A recent examination of the original computations shows that the published data have probably been overcorrected (by 5 to 10 per cent in the violet) for change in aperture, so the utility of a chromatically uncorrected instrument for making radiometric measurements is questioned. For example, suppose that we have two spectral lines of widely different wave lengths (say red and blue) but of equal energy value as measured with achromatic apparatus. Using the simple quartz lens system, suppose that a red spectral line 10 mm high and 0.5 mm wide—that is, an image of a spectrometer slit—falls upon a thermopile receiver. It represents a certain amount of energy. Increasing the aperture of the objective telescope by decreasing the focal length (to measure the blue line) increases the energy flux per unit area—that is, energy density—but, the aperture of the collimating lens being unchanged, the total energy falling upon the thermopile remains the same as before.

The problem is not quite so simple as this in practice, seeing that we are dealing with a continuous spectrum. Moreover, in view of possible errors owing to the mechanical difficulties involved

<sup>15</sup> B. S. Bulletin, 7, p. 252; 1916.

<sup>16</sup> B. S. Bulletin, 14, p. 229, 1917, gives diffuse light tests of the acetylene flame as used in the visibility work.



in using a nonachromatic spectrometer, the revised data, obtained with the quartz lens spectrometer at  $0.4\mu$  to  $0.45\mu$  can not be given full weight. The revised data are given in Table 1. They represent a careful reading of the values, after redrawing the curve through the original spectral energy data a copy of which is given in Fig. 3 of the preceding paper on this subject. In many cases the differences between the old and the new readings are caused by lack of exactness in making up the previous table. For wave lengths less than  $0.5\mu$  the present data were obtained from measurements with a flint-glass prism and lens spectrometer; also from a recalculation of the original data obtained with the quartz-lens spectrometer, no correction being made for change in aperture. The uncertainty in the spectral purity factor at  $0.4\mu$  to  $0.45\mu$  amounts to several per cent. But, from  $0.46\mu$  (where the difference between the observed and computed curves amounts to only about 5 per cent) to  $0.75\mu$ , these two curves can be considered in exact agreement. At  $0.4\mu$  the observed data may be somewhat too high, owing to diffuse light. However, it will require more than a color-match test as compared with a radiometric match to show that the observed data at  $0.4\mu$  are entirely incorrect. Sometime ago it was shown<sup>17</sup> that, in two widely different sources of radiation (for example, a tungsten lamp and a Nernst glower) which are set to a color-match, the two spectral-energy curves intersect at an extremely small angle, thus giving the appearance of exact coincidence throughout that part of the spectrum to which the eye is the most sensitive. The measurements being comparative the various correction factors apply to both sources, and a higher accuracy is possible than can be obtained in determining absolute intensities.

Calculations made at the time the data were obtained six years ago, indicated that, for the region of  $0.45\mu$  to  $0.75\mu$  the spectral-energy distribution of the acetylene flame was that of a black body at about  $2100^{\circ}\text{C}$  ( $2370^{\circ}\text{K}$ ) though, at the time, no significance was attached to it.

Recently, from an interlaboratory color-match comparison of a tungsten lamp with the acetylene flames used in this laboratory and in the Eastman Kodak Laboratory, Hyde<sup>18</sup> obtained a color temperature of  $2360^{\circ}\text{K}$  for the Eastman Kodak type of lamp. He obtained a somewhat higher temperature for the burner used

<sup>17</sup> B. S. Bulletin, 7, p. 291 (Fig. 13), 1910.

<sup>18</sup> Hyde, Forsythe and Cady, *Phys. Rev.* (2), 18, p. 157; 1919.

by the writer. However, this was for a slit 10 cm in height instead of an 8 cm slit which was used in the spectral-energy measurements for the visibility data. In view of the fact that, within experimental errors of observation, the two types of burners had the same spectral-energy curves, their black body color temperatures may be taken at 2360° K.

In Table 1, column 2 gives the spectral-energy data previously published, and column 3 gives the revised data. Column 4 gives the spectral-energy distribution of a black body at 2360° K, kindly computed by H. Kahler and carefully superposed upon the observed data, using a scale which was sufficiently large to eliminate errors (estimated to be 0.5 per cent) in drawing the curves and reading off the data. Column 5 gives the ratios of the revised acetylene energy data to the computed data for 2360° K. If the two curves coincided exactly, these ratios would be 100. As shown in the table, between  $0.48\mu$  and  $0.75\mu$  the departure from exact coincidence is only from  $\pm 1$  to 2 per cent, which is within the experimental errors involved in observing the data and reducing them to a normal spectrum. But considering the data previously published, given in column 2 of Table 1, the greatest departure from coincidence of the observed and the computed curves in the spectral region of  $0.5\mu$  to  $0.75\mu$  is only from  $\pm 2$  to  $\pm 4$  per cent, instead of 8 per cent as stated by Hyde.

The color temperature data of Hyde, therefore, confirm the radiometric measurements in the region of  $0.48\mu$  to  $0.75\mu$ . This is the region in which the radiometric measurements are of importance in the writer's work on the visibility of radiation, and in which it was possible to make precise radiometric measurements.

Although the writer doubts the reliability of the color-match test in the extreme violet of the spectrum, where the eye is very insensitive and subject to great decrease in sensitivity with age, he concurs in the recommendation made by Hyde that the spectral-energy distribution of the acetylene flame (using a certain type of burner) in the visible spectrum is satisfactorily represented by the black body curve at 2360° K, as given in Table 1. A difference of 10° or even 50° K is hardly to be considered in view of the great divergence in burners, the effect of humidity, etc. Moreover, the color temperature varies greatly for different parts of the flame<sup>19</sup>—for example, 2368° K for the whole flame and 2448° K for one spot.

---

<sup>19</sup> Hyde, *Jour. Franklin Institute*, 188, p. 354; 1917.

#### IV. EFFECT OF THIS REVISION UPON PREVIOUS INVESTIGATIONS

As already stated, in order to test the accuracy of his new method of color matching, Priest<sup>20</sup> compared the writer's radiometrically determined spectral-energy curve of a 500-watt gas-filled tungsten lamp with that of the acetylene flame as modified by the quartz-nicol system used in making the color match. The curve for the acetylene flame is too high in the violet; but from  $0.5\mu$  to  $0.75\mu$  the two spectral-energy curves are in exact coincidence. Using the revised spectral-energy data of Table 1, brings them into a close agreement also in the region of  $0.45\mu$  to  $0.48\mu$ .

Some doubt has been expressed as to the accuracy of measuring the energy at the observing slit, in visibility work, instead of computing it from the color temperature of the source. In the latter case it is necessary to reduce the data to the prismatic distribution for the particular apparatus used; and there is no check on the actual energy distribution at the slit.

On the other hand, to measure the prismatic spectral energy distribution at the observing slit, reduce it to a normal spectrum, compute the temperature of the source and find it in agreement with the directly observed color temperature, as has just been found, constitutes a real test of the accuracy attained in the energy evaluation. It would be more logical to doubt the computed spectral energy distribution which has not been checked by direct radiometric observations.

As already stated, instead of a disagreement between the color temperature test and the spectral radiation measurements, the independent check by Hyde and his collaborators confirms the direct radiometric observations on the spectral-energy distribution of the acetylene flame, in the region of  $0.48\mu$  to  $0.75\mu$ , as used in the visibility of radiation work, and leaves the visibility data<sup>21</sup> unchanged in this part of the spectrum. If any correction is to be made it falls at  $0.60\mu$  to  $0.67\mu$  (see Table 1), being a decrease of 0.5 to 1 per cent in the visibility data.

As for the visibility data in the violet, they were obtained separately from the main part of the curve (from  $0.5\mu$  to  $0.7\mu$ ) using a much lower field illumination, which may account for the higher values as compared with other experimenters. In view of the great variability of visibility in the violet, especially with age,

<sup>20</sup> Priest, *Phys. Rev.* (2) 10, p. 208; 1917. (See Fig. 3.)

<sup>21</sup> B. S. Bulletin, 14, p. 168; 1917.

one can hardly establish an "average visibility curve" and hence no attempt is made to revise the data (in the violet) previously published. If the data on 125 observers previously published serve no other purpose, they are useful in demonstrating the extraordinary variability in sensibility of the eye,<sup>25</sup> and hence the futility of attempting to establish an "average eye without arbitrarily choosing the observers."

In a recent paper Ives<sup>26</sup> expresses the opinion that, in the writer's visibility work, the field brightness should have been somewhat higher (200 m. c.), in order to meet the requirements in photometry; and that, as a consequence of this low illumination, the visibility curve is shifted too far toward the red. It is therefore relevant to say, in reply to this criticism, that a field brightness of 50 m. c. was used on the sector disk, because it permitted observing over a wide range of the spectrum, and because the visibility curve for this illumination was found in agreement<sup>24</sup> with that obtained for an illumination of 350 to 780 m. c., as was previously observed by Nutting and others. At the time the visibility work was undertaken, Ives<sup>26</sup> specified an illumination of 25 m. c. on the disk, for flicker photometry, but no specifications were given for obtaining the visibility curve. His visibility<sup>26</sup> curves for 68 m. c. and 270 m. c. illumination on the disk appeared to be sufficiently close in agreement to conclude that the lower illumination was satisfactory, as was proved by the subsequent experiments just cited. However, it is conceivable that the average visibility curve of a large group of observers, whose eyes have not been subjected to years of hard usage, would be different for these same illuminations.

In the paper on visibility (*loc. cit.*) attention was called to the great number of red-sensitive subjects, whose observations shift the average visibility curve toward the red to a greater extent than would obtain if a smaller number of red-sensitive subjects had been used. The alleged shift of the visibility curve toward the red is no doubt owing in part to the relatively large number of red-sensitive subjects and the relatively low number of green-sensitive subjects found in the 125 persons tested by the writer,<sup>27</sup> rather than attributing it entirely to a low field illumination. On

<sup>25</sup> B. S. Bulletin, 14, p. 206; 1917. (See the composite curve, Fig. 13.)

<sup>26</sup> Ives, Jour. Franklin Inst., 188, p. 227; 1919.

<sup>24</sup> See Fig. 2, B. S. Bulletin, 14, p. 178; 1917.

<sup>25</sup> Ives, Trans. Illum. Eng. Soc., 10, p. 317; 1915.

<sup>26</sup> Ives, Phil. Mag. (6), 24, pp. 149, 352, 744, 845, 853; 1912.

<sup>27</sup> See Table 3, B. S. Bulletin, 14, p. 205; 1917.

the other hand in the group of 21 observers examined by Nutting,<sup>28</sup> there were as many green-sensitive as average subjects (4 of each group, see Table 3 *loc. cit.*), and there was one unusually blue-sensitive subject. These five subjects constitute almost one-fourth of the total number examined, and their observations tend to suppress the average visibility curve in the red. The average visibility curve of Nutting, which happens to meet Ives's requirements, is not shifted quite so far to the red as is the average visibility curve obtained by the writer.<sup>29</sup>

Nutting used an illumination of 350 m. c. on the sectorized disk; but did not use an illuminated surrounding field as was done by the writer and as specified by Ives. As originally published, the visibility curve obtained by Nutting was in error owing to improper energy evaluation of his Bray tip, acetylene flame. Subsequently the spectral-energy distribution of this burner was determined by the writer with the same spectrometer used in his visibility work and found in agreement with the herein described data. Using these spectral energy measurements, the corrected visibility curve of Nutting<sup>30</sup> is in close agreement with that obtained by the writer, except in the red end of the spectrum, where it is slightly lower, and happens to be in agreement with tests made on a physical photometer.<sup>31</sup>

Neither Nutting nor the writer attempted to obtain their visibility data for normal pupil illumination; though, by using 350 m. c. on the disk, the former had practically an artificial pupil illumination corresponding to 25 m. c. normal pupil as previously used by Ives. But this illumination (350 m. c. on the disk) was constant for all observers, whereas Ives found that the artificial pupil illumination varied greatly for various observers, the highest illumination on the disk being twice the lowest. Ives's criticism that the "curves are not coordinated with any accurately specified observing conditions nor method of choosing observers" applies to Nutting's as well as the writer's visibility curves, and hence, aside from the higher illumination used by Nutting, there is no reason for selecting either one simply because it happens to fit the tests of a physical photometer.

Evidently, where great refinement is required, the visibility curve of the so-called average eye should be based upon observations made by a selected group of observers, having closely normal

<sup>28</sup> Nutting, *Trans. Illum. Eng. Soc.*, 9, p. 663; 1914.

<sup>29</sup> See Fig. 14, *B. S. Bulletin*, 14, p. 216; 1917.

<sup>30</sup> *B. S. Bulletin*, *loc. cit.*, Fig. 14.

<sup>31</sup> Ives, *Jour. Franklin Inst.*, 188, p. 222; 1919.

color vision. Fortunately the writer's visibility data are classified as to normality of visibility<sup>23</sup> and the average value of the visibility curve of observers having closely normal color vision is easily obtained. The average visibility data of 29 observers, classified as normal in the previous paper, are given in column 3 of Table 2, along with the previously published data (column 2) on 125 observers. The total number of observers being so large, the effect of the observers having abnormal color vision is quite inappreciable upon the average visibility curve, except in the extreme red, as just mentioned.

TABLE 2.—Visibility of Radiation of a Group of 125 Observers and of Selected Group of 29 Observers Having Closely the Average Visibility

Wave length $\mu=0.001$ mm	Visibility of radiation		Wave length $\mu=0.001$ mm	Visibility of radiation	
	125 observers	29 observers		125 observers	29 observers
0.493 $\mu$	0.223	0.230	0.596 $\mu$	0.734	0.735
.502	.350	.357	.604	.636	.636
.512	.553	.559	.613	.517	.517
.523	.771	.778	.623	.390	.367
.534	.908	.908	.633	.267	.264
.546	.983	.987	.643	.165	.164
.552	.998	1.000	.654	.095	.093
.559	1.000	.998	.665	.046	.045
.573	.952	.955	.678	.0302	.0197
.580	.899	.900	.690	.0086	.0075
.587	.623	.624	.703	.0034	.0033

## V. SUMMARY

The object of this paper is to give some new data on the distribution of energy in the infra-red spectrum of a flat and of a cylindrical acetylene flame. The paper gives, also, a revision of previously published spectral-energy data pertaining to the violet end of the visible spectrum.

The optical properties of the flame are discussed, and it is shown that, owing to the high selective absorption of the flame in the visible spectrum, the apparent color temperature is higher than that obtained from a consideration of the maximum emission in the infra-red.

The radiometric, as well as the color-temperature measurements, indicate that in the visible spectrum, from 0.48 $\mu$  to 0.74 $\mu$  the spec-

<sup>23</sup> B. S. Bulletin, 14, pp. 182, 193; 1917.

tral-energy distribution of the central zone of the cylindrical acetylene flame is that of a black body at  $2360^{\circ}$  K.

It is shown that the revision of the spectral-energy data of the acetylene flame has no effect upon the previously published visibility data in the region of the spectrum from  $0.48\mu$  to  $0.75\mu$ . This is the part of the spectrum in which an attempt had been made to attain high accuracy in the visibility data. A table is given of the visibility of the average of 29 observers having closely normal color vision, as observed with a flicker photometer.

WASHINGTON, September 3, 1919.

NOTE.—The criticism recently made by Hyde<sup>23</sup> and his collaborators that the writer's data (particularly in the red) do not fit the black body energy distribution better than 7 to 8 per cent is inconsistent with their own observations. Using a spectral pyrometer, they find that at  $0.75\mu$  the observed emissivity is slightly (about 7 per cent) higher than that of a black body at  $2360^{\circ}$  K.

In other words, their data show, as was found by the writer<sup>24</sup> some years ago, that, in making a color match, the eye is not able to distinguish a difference in the spectral energy match amounting to perhaps 3 to 5 per cent in the extreme red end ( $0.75\mu$ ) of the visible spectrum. The supposed disagreement appears to be in our interpretation of the data, rather than in the experimental results themselves. For, if the emissivity is higher in the red, then the ratios must decrease as shown in column 10 of Table 1.

WASHINGTON, January 9, 1920.

---

<sup>23</sup> Hyde, Forsythe and Cady. *Phys. Rev.* (2), 14, p. 382; 1919.

<sup>24</sup> B. S. Bulletin, 6, p. 317; 1910.





MAR 20 1920

DEPARTMENT OF COMMERCE



# SCIENTIFIC PAPERS

OF THE

## BUREAU OF STANDARDS

S. W. STRATTON, DIRECTOR

No. 363

PREPARATION AND REFLECTIVE PROPERTIES  
OF SOME ALLOYS OF ALUMINUM WITH  
MAGNESIUM AND WITH ZINC

BY

R. G. WALTENBERG, Associate Physicist

W. W. COBLENTZ, Associate Physicist

*Bureau of Standards*

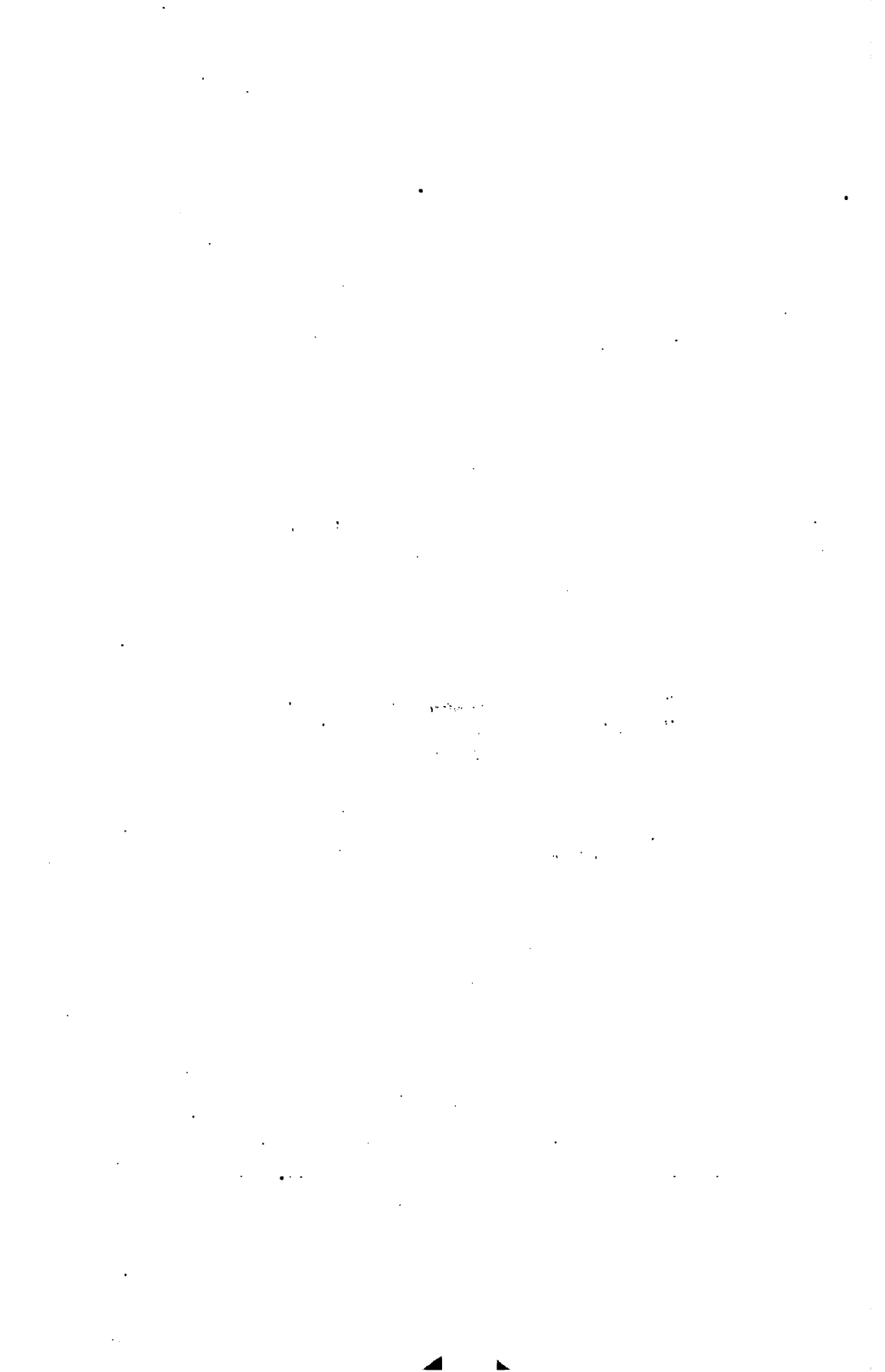
ISSUED FEBRUARY 12, 1920



PRICE, 5 CENTS

Sold only by the Superintendent of Documents, Government Printing Office,  
Washington, D. C.

WASHINGTON  
GOVERNMENT PRINTING OFFICE  
1920



# PREPARATION AND REFLECTIVE PROPERTIES OF SOME ALLOYS OF ALUMINUM WITH MAGNESIUM AND WITH ZINC

By R. G. Waltenberg and W. W. Coblentz

## CONTENTS

	Page
I. Introduction.....	653
II. Preparation and physical properties of these alloys.....	654
III. Reflectivity measurements.....	656
IV. Summary.....	657

## I. INTRODUCTION

During the past few years numerous requests for information regarding metals of high reflectivity have been received by this Bureau. A particularly urgent request was received for an alloy with high reflecting power throughout the spectrum. As some of the alloys of aluminum and magnesium give exceptional reflection in the ultra-violet it was thought desirable to make an investigation of the reflectivity of various alloys of these two metals.

L. Mach and V. Schumann <sup>1</sup> gave an account of the preparation of aluminum-magnesium alloys of various compositions with remarks on their optical properties. Hagen and Rubens <sup>2</sup> determined the reflectivity, in the ultra-violet, visible, and infra-red spectrum, of an alloy containing 69 per cent aluminum and 31 per cent magnesium, and it was shown to have an exceptionally high reflection in the ultra-violet. This alloy is known as Mach's magnalium.

An alloy for mirrors should be homogenous and uniform. It would not be expected that an alloy whose structure was made up of two or more constituents would have a higher reflectivity than either of its structural constituents, so that in a series of alloys of two or more metals we would expect the maximum or minimum reflection for any given wave length to occur for the composition at which a stable compound is formed, or in a range

<sup>1</sup> Mach and Schumann, Sitzunber., Wien Akad., 108 A, p. 135; 1899.

<sup>2</sup> Hagen and Rubens, Ann. d. Phys., 8, p. 16; 1902.

in which the metals form a solid solution. Aluminum and magnesium form solid solutions only at low percentages of either metal, but they form a compound,  $\text{Al}_2\text{Mg}_3$ , containing 46 per cent aluminum and 54 per cent magnesium,<sup>3</sup> and our efforts were confined largely to the preparation of mirrors of this compound.

Aluminum and zinc form a compound,<sup>4</sup>  $\text{Al}_2\text{Zn}_3$ , containing 78.3 per cent zinc and 21.7 per cent aluminum, and as both of these metals have rather high reflecting powers, a specimen of this compound was prepared and examined. The work of Rosenhain and Archbutt would indicate that, although this compound decomposes on slowly cooling, a chill-cast specimen would remain stable at room temperatures.

## II. PREPARATION AND PHYSICAL PROPERTIES OF THESE ALLOYS

The specimens for reflectivity determinations were prepared from the purest materials available. The aluminum contained 0.15 per cent iron, 0.12 per cent silicon, and 0.02 per cent copper. The magnesium contained 0.08 per cent iron and 0.03 per cent copper. The zinc contained less than 0.05 per cent impurities.

Small castings about 25 mm diameter and weighing 100 g were made of alloys containing aluminum with 15 per cent magnesium, which is a duplex alloy consisting of a solid solution and the eutectic, with 31 per cent magnesium, which is the eutectic of the solid solution and the compound, and with 54 per cent magnesium, which is the compound. A similar specimen of the aluminum-zinc compound containing 78.3 per cent zinc was prepared.

The alloys were made by melting the aluminum in an Acheson graphite crucible, and adding the magnesium or zinc to the molten aluminum, care being taken to keep the temperature of the molten material below 750° C (1380° F). The alloys were cast in a large graphite mold. Since it was not possible to get sound castings of the aluminum-magnesium compound, 54 per cent magnesium, in this manner, the specimens of this alloy were remelted in a vacuum, and cooled slowly. The preparation of this compound was simplified by the fact that on stirring the molten material an excess of either aluminum or magnesium would oxidize and leave the compound. This was confirmed by an examination with the microscope.

<sup>3</sup> Grube, *Zelt. Anorg. Chem.*, 45, p. 225, 1915; Schirmeister, *Metal u. Erz.*, 11, p. 522, 1914.

<sup>4</sup> W. Rosenhain and L. S. Archbutt, *Constitution of Alloys of Aluminum and Zinc*, *Phil. Trans. Royal Soc.*, 211, p. 315; 1911.

Plates of the  $Mg_2Al$ , 12 inches (30 cm) square and 1 inch (2.5 cm) thick were prepared by casting the alloy in an iron mold, placing this mold in a vacuum furnace, melting the  $Al_2Mg_3$  in vacuo, and cooling slowly. It was found necessary to cool this compound very slowly in order to relieve stresses in the casting. Some of the specimens burst into fragments after removal from a chill mold.

The compound of aluminum with magnesium,  $Mg_2Al$ , is very hard and brittle, and its resistance to the action of dilute acids and alkalis is much greater than any other magnalium which has come under our observation. A specimen of this compound was placed in 0.5 per cent NaOH for 90 minutes. The surface was not dulled appreciably, and no action could be detected with the microscope.

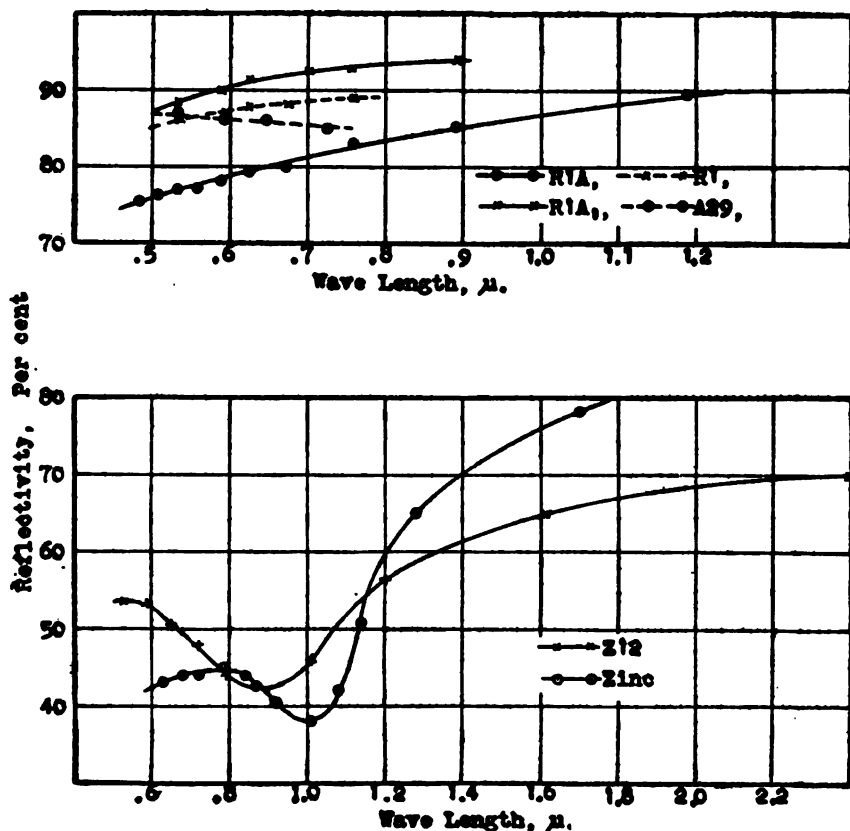


FIG. 1.—Reflecting power of zinc and of alloys of aluminum with zinc and with magnesium

On the other hand all the alloys made up, including the compound, seem to deteriorate on exposure to the air in the laboratory for a few weeks. The polished surfaces of the zinc-aluminum alloys

tarnished in a few days. The magnesium-aluminum alloys seem to be more stable, but in view of the difficulties in preparing optically perfect surfaces, these alloys do not seem to be as suitable for mirrors as are nickel-steel and stellite. The reflectivities of the latter are lower, but the surfaces promise to be more permanent.

### III. REFLECTIVITY MEASUREMENTS

The reflectivity measurements were made by means of a mirror spectrometer, a fluorite prism, and a vacuum thermopile described in previous publications.<sup>5</sup> The reflecting power of the sample, which had a plane surface, was determined by comparison with a silver mirror; and also by a new method in which the silver reflecting surface was replaced by the hypotenuse face of a right-angled glass prism. The reflectivity data are illustrated in Fig. 1, and summarized in Table 1, which gives also the identification numbers and the composition of the alloys.

TABLE 1

Sample marked—	Composition		Kind of polish	Reflection	
	Aluminum	Magnesium		0.5 $\mu$	0.7 $\mu$
				Per cent	Per cent
R-1-A.....	46	54	Wax.....	76	81
R-1-A <sub>1</sub> .....	46	54	Buffed.....	89	92
R-1.....	46	54	Wax.....	86	88
A-29.....	69	31	Buffed.....	87	86
A-27.....	85	15	do.....	74	73
		Zinc.			
Z-12.....	22	78	Wax.....	47	51
Z-12.....	22	78	Buffed.....	74	70

These data are instructive in showing the effect of polish upon the reflecting power. The best surface for reflecting is not obtained with the ordinary optical polishing methods, in which a pitch polisher and rouge are used. As illustrated in Fig. 1, at 0.7 $\mu$  the reflecting power of the magnesium compound was increased from 81 per cent (R-1-A) to 92 per cent (R-1-A<sub>1</sub>), by merely improving the polish by using alumina on broadcloth moistened with alcohol.

The sample of Mach's alloy, A-29, has a uniform reflectivity, of about 86 per cent, throughout the visible spectrum. This is in agreement with the observations of Hagen and Rubens (*loc. cit.*) who observed a uniform reflectivity of about 83 per cent.

<sup>5</sup> W. W. Coblentz and W. B. Emerson, The Reflecting Power of Tungsten and Stellite, Scientific Paper No. 308, U. S. Bureau of Standards; 1917.

The reflectivity curve of the alloy of aluminum and zinc,  $\text{Al}_2\text{Zn}_3$  (Zn 12 in Fig. 1) is unusual in that it has a wide minimum of reflectivity at  $0.9\mu$ , beyond which point the reflectivity increases gradually to 93 per cent at  $4\mu$ . This minimum is so novel that an examination of the reflectivity of pure zinc was made to determine whether there is a minimum in its reflectivity curve.

The bluish white color of a zinc mirror, and the unusually low reflectivity previously observed<sup>6</sup> at  $1\mu$ , indicate the possibility of a minimum of reflectivity in the region of  $0.8\mu$  to  $0.9\mu$ . An examination of the reflectivity of the zinc mirror previously used, disclosed a sharp reflectivity minimum at  $1\mu$ , as shown in Fig. 1. The surface of this mirror was not highly polished, which accounts for the low reflectivity throughout the spectrum. At  $2\mu$  the reflectivity was 85 per cent.<sup>7</sup>

But few metals are known which have a minimum reflectivity<sup>8</sup> in the infra-red, though, as is well known, copper and gold are excellent examples of metals having a reflectivity minimum in the visible spectrum.

As already stated, mirrors made of zinc-aluminum alloys tarnish rapidly, and hence are unsuitable for laboratory use.

#### IV. SUMMARY

This paper gives the manner of preparation and determination of the spectral reflective properties of some alloys of aluminum with magnesium and with zinc. All of these alloys tarnish in time, and hence are not suitable for mirrors where permanency is of prime importance. The compound of aluminum and magnesium,  $\text{Al}_2\text{Mg}_3$ , deteriorates less rapidly than any of the other alloys examined, and could be used in apparatus where a highly reflecting mirror is desired for a short time. A reflectivity of 92 per cent at  $0.7\mu$  was obtained with this compound.

The zinc-aluminum alloy has a minimum reflectivity at  $0.9\mu$ . An examination of the reflectivity of pure zinc disclosed a similar reflectivity minimum at  $1\mu$ .

WASHINGTON, August 19, 1919.

<sup>6</sup> W. W. Coblentz, *Radiometric Investigations of Infra-Red Absorption and Reflection Spectra*, Scientific Paper No. 45, U. S. Bureau of Standards; 1907.

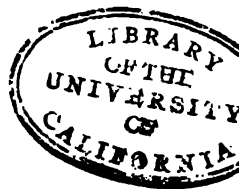
<sup>7</sup> These data were obtained with the assistance of H. Kahler, using a quartz prism which gives practically twice the dispersion of the fluorite prism used for obtaining the data on the alloy.

<sup>8</sup> See Coblentz and Emerson, loc. cit., for tungsten as a similar example.





MAR 20 1920



DEPARTMENT OF COMMERCE

---

# SCIENTIFIC PAPERS

OF THE

## BUREAU OF STANDARDS

S. W. STRATTON, DIRECTOR

---

No. 364

### RELATION OF VOLTAGE OF DRY CELLS TO HYDROGEN-ION CONCENTRATION

BY

H. D. HOLLER, Associate Chemist

L. M. RITCHIE, Assistant Chemist

*Bureau of Standards*

---

ISSUED FEBRUARY 24, 1920



PRICE, 5 CENTS

Sold only by the Superintendent of Documents, Government Printing Office  
Washington, D. C.

---

WASHINGTON  
GOVERNMENT PRINTING OFFICE

1920



# RELATION OF VOLTAGE OF DRY CELLS TO HYDROGEN-ION CONCENTRATION

By H. D. Holler and L. M. Ritchie

## CONTENTS

	Page
I. Introduction.....	659
II. Experimental work.....	660
1. Method of measurement.....	660
2. Preparation of electrodes.....	661
3. Preparation of solutions.....	662
III. Discussion of results.....	663
1. Hydrogen-ion concentrations.....	663
2. Potential of manganese-dioxide electrode.....	663
3. Effect of time.....	665
4. Relation of hydrogen-ion concentration and open-circuit voltage of dry cells.....	665
5. Relation of hydrogen-ion concentration and polarization of a dry cell.....	666
IV. Conclusions.....	668

## I. INTRODUCTION

In connection with the testing at the Bureau of Standards of materials to be used in the manufacture of dry cells, it became necessary to measure the potentials of some carbon-manganese-dioxide electrodes, such as are used in dry cells. It was originally planned to make a thorough study of the oxides of manganese in their rôle as depolarizers in dry cells, with particular attention to the shelf-life of the cell; but, since it was necessary to discontinue the work for a time, it was felt that the results thus far obtained would be useful to manufacturers of dry cells and might be suggestive to other workers in this field.

Several important papers have been published on the manganese-dioxide electrode. Tower<sup>1</sup> and Smith<sup>2</sup> studied the electrolytically prepared oxide as a means for measuring the hydrogen-ion concentration of organic acid salts. Thompson and Crocker<sup>3</sup> noted the effect of alkalis and acids upon the

<sup>1</sup> Tower, *Zeit. phys. Chem.*, 18, p. 17; 1895. Tower, *Zeit. phys. Chem.*, 33, p. 566; 1900.

<sup>2</sup> Smith, *Zeit. phys. Chem.*, 21, p. 93; 1896.

<sup>3</sup> Thompson and Crocker, *Trans. Am. Electrochem. Soc.*, 27, p. 155; 1915.

potential of electrodes prepared from a mixture of granulated carbon and pyrolusite.

Allmand<sup>4</sup> states that the reaction of manganese dioxide as a depolarizer may be represented by an equation such as



According to Nernst's equation, the electrode potential at 25° C would then be

$$\begin{aligned} E &= \text{constant} + 0.059 \log \frac{[\text{MnO}_2]}{[\text{Mn}_2\text{O}_3]^{1/2} [\text{OH}^-]} \\ &= \text{constant} - 0.059 \log [\text{OH}^-] = \text{constant} + 0.059 \log [\text{H}^+] \end{aligned}$$

in which the potential is a logarithmic function of the hydrogen-ion concentration.

No experimental data have been published to show whether this relation is true. While the authors previously mentioned recognized that a logarithmic relation exists and suggested equations representing it, they did not establish their conclusions by measurements with a hydrogen electrode. Moreover, no one has pointed out the significance of the hydrogen-ion concentration as explanatory of variations in the open-circuit voltage of dry cells and the part it plays in the polarization of a dry cell during discharge.

It is, therefore, the purpose of this paper to present experimental data showing (1) that the potential of a manganese-dioxide electrode prepared from certain ores is a logarithmic function of the hydrogen-ion concentration of the solution in contact with it; (2) that chemically prepared manganese dioxide does not show the logarithmic relation; (3) that the relation between the potential of the manganese-dioxide electrode and hydrogen-ion concentration serves as a partial explanation of variations in the open-circuit voltage and polarization of dry cells.

## II. EXPERIMENTAL WORK

1. METHOD OF MEASUREMENT.—The method used for measuring the potential of the carbon-manganese dioxide electrode in different solutions was briefly as follows:

The electrode was introduced into a 2-ounce bottle containing the solution of known hydrogen-ion concentration. Into this solution dipped a siphon containing a saturated solution of potassium chloride which led to a tenth-normal calomel electrode.

<sup>4</sup> Allmand, *Applied Electrochemistry*, p. 206; 1912.

This set-up is shown in Fig. 1. The electromotive force of this chain



was then measured with a potentiometer.

FIG. 1.—Set up for measuring the potentials of the carbon manganese dioxide electrode in different solutions of known hydrogen-ion concentration

2. PREPARATION OF ELECTRODES.—Because of the variety of manganese ores used at the present time in making dry cells, it was decided to select for this investigation several ores typical of those in use. For this purpose some of the manufacturers furnished\* a number of ores, of which three were selected for this work.

\* Acknowledgment is made of the courtesy of the Burgess Battery Co., and the National Carbon Co.; who furnished the samples of ores.

The materials selected were a Caucasian ore, which is considered to be the best material in all respects for dry cells; a Brazilian ore, which has been used since the importation of the Caucasian ore, was interrupted by the war in 1914; a domestic ore; and a chemically prepared oxide. The latter is used in large proportions mixed with the natural ores for making dry cells of small sizes, such as are used in flash lights.

For use in the electrodes the ores were ground and sifted. The portion of each ore which passed through a 65-mesh and was held back by an 80-mesh sieve was used. The chemically prepared oxide was a fine powder and was not sifted.

The electrodes were prepared from a mixture of two parts, by weight, of the ore or oxide, and one part of Acheson "D A G" graphite. The fineness of the graphite was such that 99 per cent passes through a 200-mesh sieve. This mixture was moistened with water sufficiently to permit molding into small cylinders 33 mm long and 12 mm in diameter, around a carbon rod 25 mm long and 5 mm in diameter. The electrodes were then wrapped in filter paper, tied with linen thread, and dried at 110° C. The dried electrodes were then ready for use. A copper wire was soldered to a brass cap on the carbon rod, which served as a lead to the potentiometer.

3. PREPARATION OF SOLUTIONS.—Solutions of constant and easily reproducible hydrogen-ion concentrations were necessary for this work. The simplest method of preparing such solutions is to add to a salt solution of known concentration a definite amount of its acid or base. Fortunately, ammonium chloride, which is used in large proportion in dry cells, is a very satisfactory salt for the purpose desired. The series of solutions used was, therefore, prepared in the following manner:

A solution containing 200 grams of ammonium chloride per kilogram of solution was prepared from the cp salt. To 100 cc portions of this solution, 1 cc, 5 cc, 10 cc, 50 cc, and 100 cc of tenth-normal hydrochloric acid or ammonium hydroxide were added. The hydrogen-ion concentration of each one of these solutions was determined by the bell type of hydrogen electrode suggested by Hildebrand<sup>6</sup> and measured against a tenth-normal calomel electrode.

---

<sup>6</sup>Jour. Am. Chem. Soc., 35, p. 864; 1913.

## III. DISCUSSION OF RESULTS

1. HYDROGEN-ION CONCENTRATIONS.—In Fig. 2, curve *V* represents the series of ammonium-chloride solutions the preparation of which was previously described. The zero ordinate represents the neutral 20 per cent ammonium-chloride solution. Additions of tenth-normal ammonium hydroxide to a volume of 100 cc of the salt solution are indicated from zero to the right, and similar additions of tenth-normal hydrochloric acid to 100 cc of the salt solution are indicated from zero to the left.

The range in hydrogen-ion concentration thus obtained is  $10^{-1}$  to  $10^{-8}$ . The uncertainty of the potential of the hydrogen electrode in ammoniacal solutions, due to loss of ammonia produced by passage of hydrogen, makes the alkaline part of the curve a little doubtful, but the error is believed to be small.

The alkalinity of the ammonia is considerably reduced by the presence of the ammonium chloride. Thus, in the solution prepared by adding 100 cc of tenth-normal ammonium hydroxide to 100 cc of 20 per cent ammonium-chloride we really have a twentieth-normal solution of ammonia containing 10 per cent of ammonium-chloride and with a hydrogen-ion concentration (curve *V*) of  $10^{-8}$ . The hydrogen electrode in twentieth-normal ammonia without the salt showed the hydrogen-ion concentration to be  $10^{-10}$ . That is, the presence of 10 per cent of the salt reduced the hydrogen-ion concentration by one hundredfold. Similar calculations were made by Blum,<sup>7</sup> using the ionization constants of ammonia and water.

2. POTENTIAL OF MANGANESE-DIOXIDE ELECTRODE.—The potentials of the three samples of ores and oxide are represented by the curves in Fig. 2, curve *I* for the Caucasian ore; curve *II* for the domestic ore; curve *III* for the Brazilian ore; and curve *IV* for the chemically prepared oxide.

In the case of the ores, although the parallelism is not exact, it appears that the potential is a logarithmic function of the hydrogen-ion concentration. Thus, while the potential of the hydrogen electrode in curve *V* decreases ( $-0.39$  to  $-0.79$ )  $0.40$  volt, the potential of the Caucasian ore decreases ( $+0.62$  to  $+0.15$ )  $0.47$  volt; the domestic ore ( $+0.67$  to  $+0.11$ )  $0.56$  volt; and the Brazilian ore ( $+0.64$  to  $+0.19$ )  $0.45$  volt. That is, for

<sup>7</sup> Blum—Bull. Bur. Stand., 18, p. 521; 1916.

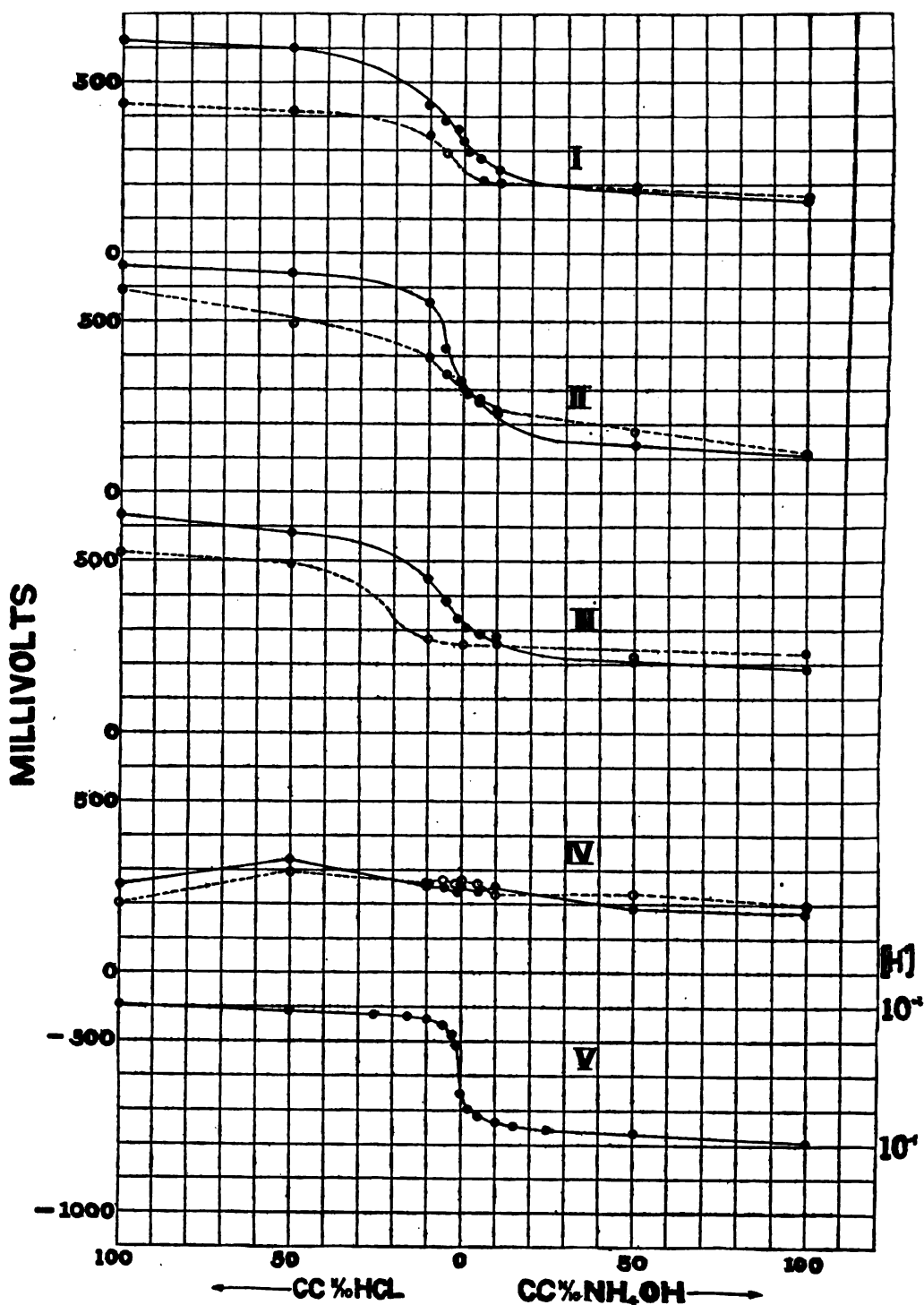


FIG. 2.—The potentials of different manganese ores and an oxide as measured in series of  $\text{NH}_4\text{Cl}$  solutions of known hydrogen-ion concentration are represented by above curves I, Caucasian ore; II, domestic ore; III, Brazilian ore; IV, chemically prepared oxide; V represents the curve of the series of  $\text{NH}_4\text{Cl}$  solutions used in this work, the hydrogen-ion concentration ranging from  $10^{-1}$  to  $10^{-6}$ .



each tenfold decrease in hydrogen-ion concentration, the potential of the Caucasian ore decreased  $\left(\frac{0.47}{7}\right)$  0.067 volt; the domestic ore  $\left(\frac{0.56}{7}\right)$  0.080 volt; and the Brazilian ore  $\left(\frac{0.45}{7}\right)$  0.064 volt.

The potential of the chemically prepared oxide appears to be independent of hydrogen-ion concentration, for which no explanation is offered. This difference from the ores was entirely unexpected and requires further study.

3. EFFECT OF TIME.—The increase in potential produced by increased acid concentration would suggest a simple means of increasing the voltage of a dry cell, and it has been said to have been used by dishonest makers to "boost" the voltage and "flash point" of their dry cells. It has the disadvantage, however, that the voltage drops from day to day. This is indicated by the dotted curves in Fig. 1, which represents, the potentials at the end of one week. Thus it is seen that the potential gradually decreased in acid solutions and increased slightly in alkaline solutions. These results would indicate that the shelf-life<sup>8</sup> of a cell containing acid would probably be short, entirely apart from the action of the acid solution upon the zinc.

4. RELATION OF HYDROGEN-ION CONCENTRATION AND OPEN-CIRCUIT VOLTAGE OF DRY CELLS.—Experiments showed that the potential of a zinc electrode in the solutions corresponding to curve V varies less than 0.02 volt; that is, the zinc potential is practically independent of the hydrogen-ion concentration of the solution. But since the potential of the carbon-manganese dioxide is dependent upon the hydrogen-ion concentration, the open-circuit voltage of the dry cell, containing a given ore, is, therefore, determined by the hydrogen-ion concentration of its electrolyte. It would be possible, then, to vary the open-circuit voltage, when the cell is new, by 0.4 or 0.5 volt by simply adding acid or alkali to it.

Measurements of the hydrogen-electrode potential in solutions containing 12.5 to 50 per cent of ammonium chloride and up to 40 per cent of zinc chloride gave values from 0.52 to 0.59 volt against the tenth-normal calomel electrode, corresponding to hydrogen-ion concentrations from  $10^{-3}$  to  $10^{-4.5}$ . Since the slope

<sup>8</sup> At the beginning of this investigation it was hoped that the change in potentials over a short period of time might serve as an indication of the probable shelf-life of a dry cell containing the ore or oxide tested. The results obtained, however, were not sufficient to justify the conclusion that it is possible to predict the shelf-life of an ore by such a method.

of the curves for the ores near the neutral point is much less than that for the hydrogen electrode, the variation in the open-circuit voltage, caused by differences in hydrogen-ion concentration of ammonium and zinc chlorides solutions, would be somewhat less than 0.07 volt.

5. RELATION OF HYDROGEN-ION CONCENTRATION AND POLARIZATION OF A DRY CELL.—There is no means of measuring the hydrogen-ion concentration of the electrolyte in a dry cell with a hydrogen electrode. From the previous discussion it appears that the potential of the manganese dioxide electrode gives about as true value of the hydrogen-ion concentration in a dry cell as it is possible to obtain.

While it is true that zinc chloride would reduce the alkalinity produced by ammonia formed during discharge of the cell, it is probable that the alkalinity would at least amount to that represented in curve V; that is,  $[10^{-8}]$ . Assuming this to be true, then, the decrease in hydrogen-ion concentration from that of the neutral ammonium-chloride solution to about  $10^{-8}$  would cause a drop of 0.17 volt in the voltage of a cell containing the Caucasian ore; 0.21 for the domestic ore; and 0.14 volt for the Brazilian ore. Roughly, then, a drop in voltage of at least 0.15 to 0.20 volt may be due to decreased hydrogen-ion concentration. At least a portion of the polarization of a dry cell is, therefore, probably due to the layer of electrolyte on the surface of the electrode becoming impoverished in hydrogen ions.

To determine the relative change in potentials of the electrodes of a dry cell, during discharge, a No. 6 cell was discharged continuously through a resistance of 10 ohms, and the potentials of the electrodes were measured at frequent intervals with a tenth-normal calomel electrode and a potentiometer (Fig. 3). It is noted that after the first 50 hours the potential of the zinc is very constant for the remaining 170 hours, while during the latter period of time the manganese dioxide electrode dropped 0.28 volt (from +0.04 to -0.24). From the previous discussion it is reasonable to assume that the reduced hydrogen-ion concentration is responsible for 0.15 or 0.20 volt of this drop. It, however, must not be forgotten that the chemical changes (reduction of the oxide) at the surface of the electrode during discharge would also lower the potential.

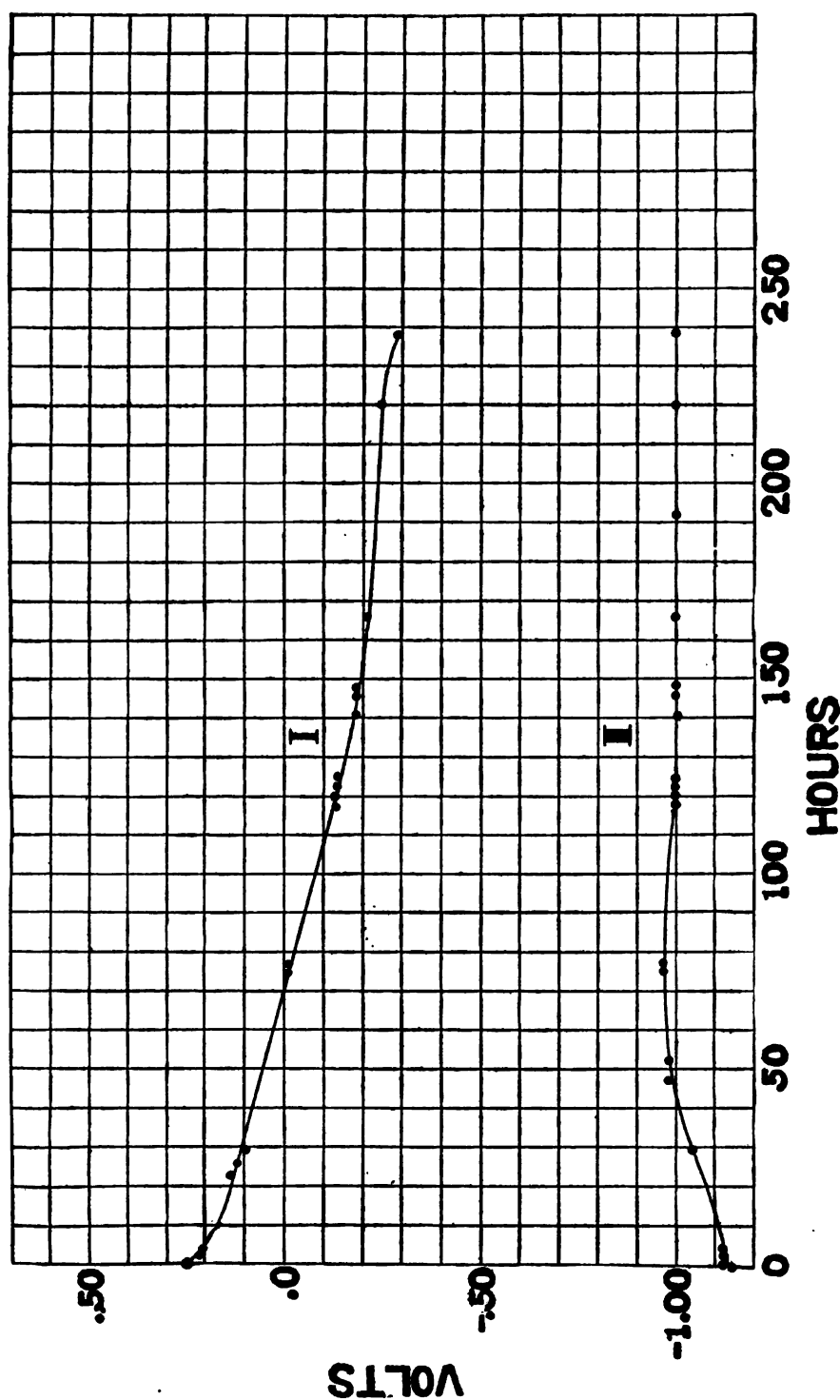


FIG. 3.—Relative change of the electrodes of a No. 6 dry cell when discharged through 10 ohms resistance and measured at frequent intervals of time with an N/10 calomel electrode and a potentiometer. Curve I represents the MnO<sub>2</sub> electrode and curve II the zinc electrode

#### IV. CONCLUSIONS

1. The potential of an electrode composed of a mixture of graphite and some manganese ores is a logarithmic function of the hydrogen-ion concentration of the solution in contact with the electrode.

2. The potential of similar electrodes containing a chemically prepared oxide instead of the natural ores is independent of the hydrogen-ion concentration.

3. The potential of the natural ores steadily decreased with time in acid solutions, indicating either a consumption of hydrogen ions or a reduction of the oxide or both.

4. The potential of the natural ores steadily but slowly increased in alkaline solutions, indicating either a consumption of hydroxyl ions or oxidation of the oxide or both.

5. Slight variations in the hydrogen-ion concentrations of solutions of ammonium chloride and zinc chloride are sufficient to account for variations of several hundredths of a volt in open-circuit voltages of dry cells containing the same ore.

6. At least a portion of the polarization of a dry cell during discharge may be explained as being due to a layer of electrolyte on the surface of the electrode impoverished in hydrogen ions.

The authors acknowledge the assistance of A. B. Goodall in making the drawings for this paper.

WASHINGTON, August 13, 1919.



DEG 2 1920

DEPARTMENT OF COMMERCE



# SCIENTIFIC PAPERS OF THE BUREAU OF STANDARDS

S. W. STRATTON, DIRECTOR

No. 365

## A NEW INTERFERENTIAL DILATOMETER

BY

IRWIN G. PRIEST, Physicist

*Bureau of Standards*

ISSUED FEBRUARY 28, 1920



PRICE, 5 CENTS

Sold only by the Superintendent of Documents, Government Printing Office  
Washington, D. C.

WASHINGTON  
GOVERNMENT PRINTING OFFICE

1920



# A NEW INTERFERENTIAL DILATOMETER

By Irwin G. Priest

## CONTENTS

	Page
I. Introduction.....	669
II. Description of instrument.....	670
III. Theory of method.....	670
IV. Measurements.....	673
V. Sensitiveness, accuracy, and range.....	674
VI. Applications and advantages.....	675
VII. Considerations of mechanical construction.....	677

## I. INTRODUCTION

Interferential measurements of displacement or change in length by use of the interference fringes due to two nearly parallel plane mirrors have heretofore been made almost, if not quite, exclusively by means of observations on the *displacement* of the fringes.<sup>1</sup> In 1912, the author designed a dilatometer to measure small changes in length by the *change in width* of interference fringes and thereby obtained a number of advantages in special cases. An instrument according to this design was later constructed in the Bureau of Standards optical shop.<sup>2</sup> Although a few preliminary tests of the use of this method in determining differential thermal expansions were made with improvised apparatus in 1912, and reported to the Bureau of Standards scientific staff,<sup>3</sup> no practical use was made of it for several years; and it was not thought worth while to publish anything concerning the new instrument or method until they had been thoroughly tried in practice. Such practical tests have now been made and, indeed, the instrument and method are now used regularly at the Bureau of Standards,<sup>4</sup> in tests of thermal expansion. Some account of its use in this field has been given to the Philosophical Society of Washington, and the American Physical Society,<sup>5</sup> but no adequate description of the instrument has yet been published.

<sup>1</sup> Fizeau, *Ann. de Chim. et de Phys.* (4), 2, pp. 146-151; 1864. Pulfrich, *Zeit. für Inst.*, 12, p. 365; 1893.

<sup>2</sup> By John Clacey.

<sup>3</sup> Irwin G. Priest and L. B. Olmstead, *Bur. Standards Scientific Staff Meeting*, Nov. 1, 1913. (Not published.)

<sup>4</sup> By C. G. Peters. See, for example, Souder and Peters, *An Investigation of the Physical Properties of Dental Materials*, forthcoming B. S. Tech. Paper.

<sup>5</sup> Priest and Peters, *Jour. Wash. Acad. of Sci.*, Aug. 19, 1917, p. 475. Peters and Priest, and Peters and Souder, *Am. Phy. Soc. New York Meeting*, Mar. 1, 1919.

A general familiarity with the literature of interferometry indicates that methods such as described in this paper have been used very little if at all, and it seems probable that the instrument to be described is the first of its kind to be constructed. While making the final revision of this paper, the author has noticed for the first time a suggestion by Pulfrich <sup>6</sup> that the number of fringes between two fixed lines on one mirror affords a very accurate measure of the angle between the two mirrors. This is, indeed, the essential feature of the method to be described, but it has apparently not met with much practical application heretofore. An examination of the subject in *Science Abstracts* and the *Fortschritte der Physik* has not disclosed any such applications of Pulfrich's important and valuable suggestion.

On account of the uniqueness of the design and the fact that the instrument now gives promise of being useful in attacking various problems in thermal expansion, elasticity, change in length due to magnetization, "critical points," shrinkage or expansion due to change in moisture content, etc., it now seems desirable to publish a definite description of this dilatometer and the theory of its use.

## II. DESCRIPTION OF INSTRUMENT

The instrument may, of course, assume somewhat varied mechanical forms. That perhaps best adapted to explanation is shown in Fig. 1, which is nearly the same, except for its exact dimensions and the shape of the sample, as the model actually constructed by Mr. Clacey, and now in practical use at the Bureau.

## III. THEORY OF METHOD

Referring to Fig. 1, the theory of the method may be explained as follows:

Let the apparatus be illuminated by monochromatic light from above. An observer looking down in the direction  $OO$  will see a system of interference fringes as shown in the Plan, Fig. 1, appearing to lie in the plane  $bb$  of the interferometer mirror; that is, the fringes and the reference lines on the mirror can be simultaneously focused by a suitable optical instrument. These fringes are due to the interference of the light reflected from the surfaces  $cc$  and  $bb$ , which inclose a wedge-shaped space regarded as "thick" (0.1 to 0.3 mm) compared to the wave length. They thus belong to the category of so-called "Fringes of thick

---

<sup>6</sup> *Zeit. für Instr.*, September, 1898, p. 566.



plates.<sup>7</sup> Such fringes were first described by Fizeau and are known as "Fizeau's curves of equal thickness."<sup>8</sup> They are the same as used in the Fizeau-Abbe dilatometer.<sup>9</sup>

Numerous elaborate treatments of such interference phenomena have been published<sup>10</sup>, but the reader not already familiar with them and desiring a brief elementary description and explanation is referred to textbooks by Lummer and Edser.<sup>11</sup>

If both the cover plate and the base plate are of glass or quartz they should not be silvered. If the base plate is of polished metal, the surface *cc* should be coated with a thin semitransparent film of some metal to improve the visibility of the fringes.

In Fig. 1, *aa* is the trace of a plane through the point of observation and perpendicular to the intersection of the mirror planes *cc* and *bb* produced; that is, also perpendicular to *SS*. The fringes which are nearly straight and indeed sometimes called "straight" fringes are, accurately speaking, curves convex toward the intersection of *cc* and *bb* and normal to *aa*.

If  $L_x$ , the length of the sample, is slightly greater (a few microns) than  $L_s$ , the perpendicular from *S* to the plane *b' b'* parallel to plane *bb*, the fringes will have the curvature qualitatively indicated in the figure. If  $L_x$  is slightly less than  $L_s$  the curvature will be reversed. If  $L_x$  is exactly equal to  $L_s$  the fringes become perfect circles ("Haidinger rings")<sup>12</sup> apparently at an infinite distance from the observer, in which case no measurements can be made by the method proposed. Measurements are made for the condition of a difference of a few microns in the lengths  $L_x$  and  $L_s$ . In this case small segments of the fringes near the axis *aa* are apparently straight and parallel to *ss* and *xx*. Let  $L_x$  be adjusted so that a few straight fringes (say 5 to 20) appear between the lines *ss* and *xx*. If, for any cause, the difference in the lengths  $L_s$  and  $L_x$  then changes, the number of fringes between *ss* and *xx* will change; and the change in  $L_s - L_x$  can be computed from this change in the number of fringes.

<sup>7</sup> Edser, *Light for Students*, p. 414.

<sup>8</sup> Müller-Pouillet, *Lehrbuch der Physik*, 10th ed., 2, book 3 (Optik), p. 747.

<sup>9</sup> Fizeau, *Ann. de Chim. et de Phys.* (4), 2, pp. 146-151; 1864. Pulfrich, *Zeit. für Instk.*, 12, p. 365; 1893.

<sup>10</sup> Michelson, *Phil. Mag.* (5), 12, p. 236; 1883. Feussner, *Winklemann's Handbuch der Physik*. Pockington, *Camb. Phil. Soc. Proc.*, 11, p. 105; 1901. Drew, *Phys. Rev.*, 15, p. 226; 1902. Bartsch, *Diss. Marburg*; 1910. Wetthauer, *Diss. Marburg*; 1911. Gehrecke and Janicki, *Ann. der Phys.* (4), 29, p. 431; 1912. Pahlen, *Ann. der Phys.* (4), 29, p. 1567; 1912. Janicki, *Ann. der Phys.* (4), 40, p. 493; 1913.

<sup>11</sup> Lummer, Müller-Pouillet *Lehrbuch*, loc. cit. Edser, *Light for Students*, pp. 416-418; 1907.

<sup>12</sup> Haidinger, *Pogg. Ann.*, 96, pp. 453-468; 1855. Also Rayleigh, *Phil. Mag.*, 12, p. 429; 1906.

The equation for this computation may be given in the following terms:

$\lambda \equiv$  wave length of light used.

$D \equiv$  perpendicular distance from  $X$ , bearing point of sample on plane  $cc$ , to knife-edge  $SS$ .

$d \equiv$  perpendicular distance between lines  $ss$  and  $xx$ .

$n_{x_1} \equiv$  order of interference at  $xx$  before the change in  $L_s - L_x$  to be measured.

$n_{s_1} \equiv$  order of interference at  $ss$  before the change in  $L_s - L_x$  to be measured.

$n_{x_2}$  and  $n_{s_2} \equiv$  analogous meanings after the change.

$\delta n_1 \equiv n_{x_1} - n_{s_1}$ .

$\delta n_2 \equiv n_{x_2} - n_{s_2}$ .

$L_s \equiv$  perpendicular distance from  $S$  to plane  $b'b'$  through base of sample and parallel to  $bb$ .

$L_x \equiv$  length of sample (perpendicular distance from  $X$  to plane  $b'b'$ ).

$L_{s_1} \equiv L_s$  before the change to be measured.  $L_{s_2} \equiv L_s$  after the change.

$L_{x_1} \equiv L_x$  before the change to be measured.  $L_{x_2} \equiv L_x$  after the change.

$\Delta L_s \equiv L_{s_2} - L_{s_1}$ .

$\Delta L_x \equiv L_{x_2} - L_{x_1}$ .

Then, in general,

$$\Delta L_x = \Delta L_s + \frac{\lambda \cdot D}{2d} (\delta n_2 - \delta n_1). \quad (1)$$

The derivation of the foregoing equation (1) is very simple, as may be shown with the aid of Fig. 1A, which shows in a very exaggerated way the angle between the mirrors  $cc$  and  $bb$  which are nearly but not quite parallel. Let  $t_s$ , perpendicular to  $bb$ , be the distance between  $cc$  and  $bb$  at reference line  $s$ . Let  $t_x$ , perpendicular to  $bb$ , be the distance between  $cc$  and  $bb$  at reference line  $x$ . From the proportion of sides in similar triangles,

$$\frac{L_x - L_s}{t_x - t_s} = \frac{D}{d} \quad (2)$$

It is also obvious that

$$t_x - t_s = \frac{\lambda \cdot \delta n}{2} \quad (3)$$

Substituting (3) in (2),

$$L_x - L_s = \frac{\lambda \cdot D \cdot \delta n}{2d} \quad (4)$$

Or, in the two particular cases,

$$L_{x1} = L_{s1} + \frac{\lambda \cdot D \cdot \delta n_1}{2d} \quad (5)$$

and

$$L_{x2} = L_{s2} + \frac{\lambda \cdot D \cdot \delta n_2}{2d} \quad (6)$$

From (5) and (6) and the definitions of  $\Delta L_x$  and  $\Delta L_s$  above,

$$\Delta L_x = \Delta L_s + \frac{\lambda \cdot D}{2d} (\delta n_2 - \delta n_1) \quad (1)$$

which is the equation to be derived.

#### IV. MEASUREMENTS

$\lambda$  is a known constant.  $D$ ,  $d$ ,  $\delta n_1$  and  $\delta n_2$  must be measured.

$d$  is readily determined by a traveling microscope or Fraunhofer micrometer.

$D$  is determined as follows: Lightly silver the surface  $cc$ . Place it on its bearings,  $S$  and  $X$  (Fig. 1), and slide it a few millimeters in a direction accurately parallel to  $SS$ , the sample being, meanwhile, held firmly in contact with the base plate in its V-notch as shown in the figure. The bearing points will leave fine traces in the silver film. The distance between these traces ( $=D$ ) may then be determined in the same way as  $d$ .

If samples are made of a constant standard diameter, the distance  $D$  becomes an instrument constant for all tests; and, indeed,  $\frac{\lambda \cdot D}{2d}$  becomes an instrument constant, say  $K$ , to be computed once for all, and we have

$$\Delta L_x = \Delta L_s + K(\delta n_2 - \delta n_1) \quad (7)$$

If it is desired to work with samples of various diameters, a graph or table of  $K$  as a function of the sample diameter will facilitate the computations.

It is, of course, not absolutely necessary that the sample be a cylinder. This has been chosen as, in many cases, the simplest form to prepare and as well adapted to facilitate the automatic adjustment of  $D$ . In special cases where some other form of sample must perforce be used, other methods of determining  $D$  will readily occur to users of the instrument.

$\delta n_1$  and  $\delta n_2$  are obtained as the direct result of observation by counting the whole number of fringes in each case between  $ss$  and

$xx$ , adding to this counted number the fractions of a fringe-width at  $ss$  and  $xx$ , and prefixing algebraic signs according to the following rule:

+ , if the center of curvature lies on the side  $xx$ .

- , if the center of curvature lies on the side  $ss$ .

The fractional parts may generally be estimated with an uncertainty of 0.1 to 0.2 by direct inspection; but more accurate measurements require suitable micrometric observation. The essential requirement for such micrometric observation may be met by an optical system forming a real image of the fringes and reference lines in a focal plane over which a filar micrometer observed by a low power ocular can be moved. Such apparatus can be readily improvised in any optical laboratory; but by far the best and most convenient method of measuring these fractions and observing the whole number of fringes is by means of the Pulfrich interferometer, exactly as constructed for use with the Fizeau method.<sup>13</sup> This instrument also provides means for monochromatic illumination. It was with this instrument that all measurements at the Bureau of Standards have been made.

If a value of  $L_x$  is required as in the computation of the expansion coefficient, it may be obtained by a mechanical contact micrometer.  $L_s$  may be obtained from  $L_x$  by equation (4).

## V. SENSITIVENESS, ACCURACY, AND RANGE

### SENSITIVENESS

By means of the Pulfrich instrument,  $\delta n_2 - \delta n_1$  may be determined as the mean of a small number of observations (say five) with an uncertainty, due to observational error, not greater than 0.01 or 0.02. The instrument constant  $K$  has the dimension of length. In the dilatometer which has actually been made  $K = 0.6$  micron. ( $D = 28.71$  mm.  $d = 14.00$  mm.  $\lambda = 0.5876$  micron.) The sensitiveness is, therefore, about 0.006 to 0.012 micron. It is possible to design an instrument of the same general type with a slightly but not much greater sensitiveness.

### ACCURACY

Besides the error of observation above noted, the accuracy is limited only by unavoidable variation in contacts during the course of measurements. The consistency of Mr. Peters' extensive

<sup>13</sup> Pulfrich, *Zeit. für Instk.*, p. 261; Sept., 1898.





measurements of thermal expansion of crystal quartz parallel and perpendicular to the axis, by this method and the Fizeau method, over an interval from about  $26^{\circ}\text{C}$  to  $55^{\circ}\text{C}$ , shows that the determinations of  $\Delta L_x$  are actually reliable to about 0.01 or 0.02 micron. In these particular circumstances, therefore, the accuracy is nearly as good as the sensitiveness. Within the limits of its applicability, this method is found to be at least as accurate as the Fizeau method, and is probably more reliable. The contact errors must be separately considered under the particular circumstances of each investigation.

The determination of  $K$  with sufficient accuracy to obtain in the computed result the full value of [the accuracy attained in the measurement of  $\delta n_2 - \delta n_1$  presents no difficulty. For small values of  $\delta n_2 - \delta n_1$ , it is evident that only a roughly approximate value of  $K$  is required. In practical work as contemplated,  $\delta n_2 - \delta n_1$  will never be greater than 40 and will be determined with an uncertainty of about 0.02 or one part in 2000. With the traveling microscope,  $D$  and  $d$  may be determined with about the same relative accuracy by careful observation.  $\lambda$  is, of course, already known with far greater accuracy than required.

$L_x$  may be obtained by a mechanical contact micrometer with the same relative accuracy with which  $\Delta L_x$  is determined by the interferential measurements.  $L_s$  may usually be taken as equal to  $L_x$  with sufficient accuracy.

#### RANGE

With the apparatus here described, the largest value of  $\Delta L_x - \Delta L_s$  which can well be measured is about 20 microns, in which case  $\delta n_1$  and  $\delta n_2$  are each about 20 and of opposite sign. It would be possible to increase the range slightly, but not very much.

#### VI. APPLICATIONS AND ADVANTAGES

The application of this dilatometer to the determination of relative thermal expansivity, particularly in case the differential expansion is small, is obvious, and, as has been mentioned, it is already being used for this purpose. The base plate may be made of any material of standard expansivity and the various samples determined relative to it.

It appears that the instrument might also be adapted to the measurement of small increments in length, due to other causes,

such as mechanical stress, magnetization, change in moisture content, etc.

The detailed methods will doubtless occur to those interested in such measurements; but it is well to point out in advance one important feature which might be overlooked. The absolute length of the sample is quite undetermined so far as the principle of the method is concerned. It is only necessary to construct the base plate with suitable distance between the planes  $bb$  and  $b'b'$  to accommodate the sample, the length of which may be fixed by other considerations. Thus, in magnetic tests it may be desirable to make this several centimeters instead of one.

The advantages of this method over the Fizeau method,<sup>14</sup> which has been so widely used in measurements of thermal expansivity, may be enumerated as follows:

1. Smallness and simplicity of sample. Only one small pin is required, whereas the Fizeau method requires *three similar pins*, a ring 3 to 4 cm in diameter with three bearing points for the base plate and cover plate, or a block with one *true plane* surface about 10 mm in diameter. This advantage is important on three separate considerations, viz, (a) economy of time and labor in preparing the sample; (b) economy of material, which is important in some cases; (c) the possibility of more minute study of homogeneity of material.

2. The correction for change of refractive index due to change in density of the air during the experiment is eliminated without evacuating the container. In the Fizeau method for thermal expansion, this is a very clumsy and troublesome although a small correction.<sup>15</sup>

3. The trouble of counting the passage of fringes, or obtaining their displacement by other tedious methods (observations on different wave lengths and solution of fraction puzzles)<sup>16</sup> is entirely eliminated.

4. The chance of errors due to variation in contacts is reduced.

5. The possibility of displacement of the reference lines due to "creeping" or accidental displacement of the cover plate in the Fizeau apparatus is eliminated.

---

<sup>14</sup> Fizeau, *Ann. de Chim. et de Phys.* (4), 2, p. 146; 1864.

<sup>15</sup> Pulfrich, *Zeit. für Instk.*, 13, p. 456. Priest, *Bulletin of the Bureau of Standards*, 9, p. 479.

<sup>16</sup> Pulfrich, *Zeit. für Instk.*, 13, pp. 369, 437, et seq.



## VII. CONSIDERATIONS OF MECHANICAL CONSTRUCTION: A TYPE OF SIMPLER CONSTRUCTION

The theory of the construction of the base plate shown in Fig. 1 is as follows:

1. A plate is made with plane and parallel surfaces, tested by Haidinger rings.<sup>17</sup>
2. All of one of these surfaces except a minute strip or edge forming the knife-edge  $S$  is then ground away as shown in the figure. The knife-edge  $S$  is thus, by construction, an element of the original surface, and so is parallel to the base  $b'' b''$ , the other original surface.
3. The surface  $bb$  is then ground and polished plane and parallel to  $b'' b''$  (by interference fringe tests) and about 0.2 to 0.3 mm below the original surface; and is thus, by construction, parallel to the knife-edge  $SS$ .
4. The recess to receive the sample is then ground into one side of the plate as shown leaving the surface  $b' b'$  plane and parallel to  $b'' b''$  with good mechanical but not optical accuracy. (The disturbing reflection from  $b'' b''$  which results from this construction may be eliminated by cementing a plate of black glass onto  $b'' b''$ .)

The construction was begun on this theory, but in the end it was found necessary, in order to save the piece, to slightly adjust the knife-edge. Indeed the middle portion of this edge has been cut away leaving only bearings near the ends to support the cover plate. There is no objection to this alteration.

This design is admittedly difficult to construct. The difficulty lies in the fact that the projecting knife-edge  $S$  interferes greatly with the normal polishing process of correcting the surface  $bb$  to an accurate true plane which is necessary. Although the piece which has actually been made is a credit to the optician, considering the difficulty of its construction, still the surface  $bb$  is not as perfectly true plane as could be desired.

This difficulty can, of course, be obviated by making the expansion standard (a block with its base in the plane  $b' b'$  and its apex at  $S$ , Fig. 1) separate from the base plate. Indeed, several pieces of apparatus of this type have been made and used at the Bureau of Standards, the expansion standard consisting of two similar but separate posts or pins having their position deter-

<sup>17</sup> Müller-Pouillet, *Lehrbuch der Physik*, 10th ed., 2, book 3 (Optik), articles 351-353.

mined by contact with the base plate and lower mirror, just as the position of the sample is determined. In some cases the plate between  $b'b'$  and  $b''b''$  has been made separate from the lower mirror plate (the part between  $bb$  and  $b'b'$ ). The standard posts need not even be of the same material as the mirror plate.

The only disadvantage of this design is that the chance of contact errors and accidental lateral displacement of the points of support with reference to the reference lines on the lower mirror is introduced. These posts could, however, be mechanically bound in place, but this procedure has not actually been tried. Light spring clips might suffice. In the case of glass or fused-quartz apparatus, the fusion method of Parker and Dalladay<sup>18</sup> might be used to secure the standard posts to the base plate.

The advisability of constructing special apparatus such as described in this paper will, of course, be determined by the extent of systematic work contemplated in any case. For a few experiments, it would not be worth while; but if large numbers of samples are to be examined, the special apparatus will soon "pay for itself" in convenience and economy of time. One of these standard instruments being ready, the preliminary adjustments for each separate determination will be simply:

1. Adjustment of diameter of sample to gage (mechanical caliper test) in order to give  $D$  its standard value.
2. Adjustment of length of sample,  $L_s$ , to give fringes of suitable width. (The parallelism of the fringes to the reference lines  $xx$  and  $ss$  is fixed by construction of the instrument.)

Extensive data on the use of this apparatus have been obtained by C. G. Peters at this Bureau (See Sec. V, 2, above) and it is expected that he will publish these in the near future. In the meantime, the author would express his appreciation of Mr. Peters' work in developing and perfecting the method.

WASHINGTON, June 21, 1919.

---

<sup>18</sup> *Phil. Mag.*, **32**, p. 276; March, 1917.



DEPARTMENT OF COMMERCE

# SCIENTIFIC PAPERS OF THE BUREAU OF STANDARDS

S. W. STRATTON, DIRECTOR

No. 366

## CONTRAST SENSIBILITY OF THE EYE

BY

ENOCH KARRER, Associate Physicist

E. P. T. TYNDALL, Assistant Physicist

*Bureau of Standards*

ISSUED MARCH 8, 1920



PRICE, 5 CENTS

Sold only by the Superintendent of Documents, Government Printing Office  
Washington, D. C.

WASHINGTON  
GOVERNMENT PRINTING OFFICE  
1920



# CONTRAST SENSIBILITY OF THE EYE

By Enoch Karrer and E. P. T. Tyndall

## CONTENTS

	Page
I. Introduction.....	679
II. General method.....	679
III. Apparatus.....	681
1. General description.....	681
2. Photometric measurements.....	683
3. Auxiliary screen.....	684
IV. Observing conditions.....	684
V. Data obtained.....	685
1. Results by first method.....	686
2. Results by second method.....	691
VI. Summary.....	692

## I. INTRODUCTION

The research reported in this paper was undertaken as part of the Bureau investigation of certain problems of searchlight illumination. One of the important aspects of searchlight illumination, such as the detecting of airplanes, is a matter of contrast, since the object illuminated by the search lamp must be seen in contrast to the diffused light in the path of the beam, or in contrast to other diffused light. The brightness of the path of the beam determines what the brightness of a target of any given size must be in order that it may be visible. This is a matter of the contrast sensibility of the eye, usually at low levels of illumination. To obtain data bearing upon this point, laboratory experiments were performed.

## II. GENERAL METHOD

The general method followed was to illuminate a screen to a known amount so that its brightness might be comparable with that of the path of the searchlight beam. Upon this screen was projected a rectangular beam whose horizontal width could be varied at will.

The aspect then was that of a rectangular strip of light upon a light background. The length of the strip was varied from nothing to a length which enabled the observer at 26.3 m from

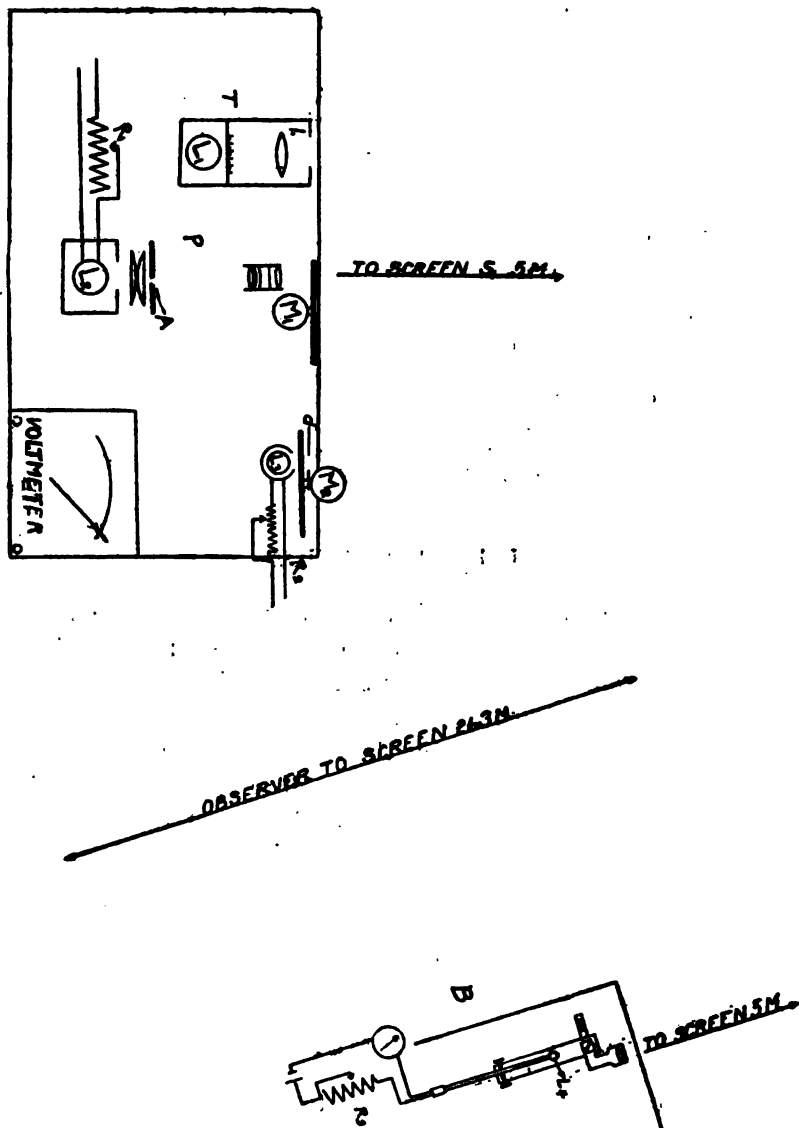


FIG. 1.—Disposition of apparatus for contrast sensibility

T, scale projector; P, lantern for projecting slit A;  $M_1$ ,  $M_2$ , sector disks;  $L_2$ , illumination for main screen B, photometer

the screen just to see the patch. This length, together with the brightness of the screen and the brightness of the strip, was recorded.

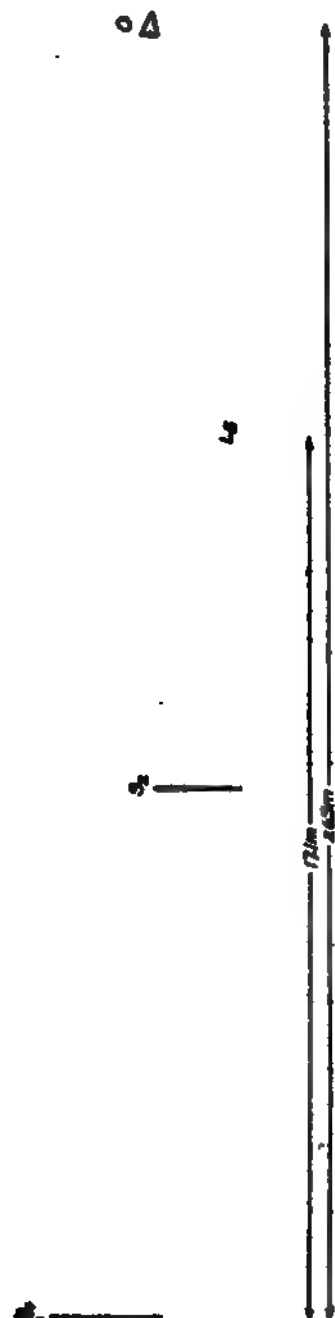
Two series of observations were made. In the first series the field illumination and strip illumination were varied by steps in the same ratio, so that a constant contrast between the two was maintained. In the second series the field brightness was kept constant, and the strip brightness was varied by steps thus giving a varying contrast.

### III. APPARATUS

#### 1. GENERAL DESCRIPTION

The disposition of apparatus for these experiments is depicted in Figs. 1 and 2. The screen was coated with a white diffusing paint of magnesium oxide in water having dissolved in it a slight amount of white library paste as a binder. This screen was illuminated by means of the locomotive headlight lamp  $L_1$ , Fig. 1, operated at 29 volts. By means of sectorized disks on the motor  $M$ , the intensity of the general illumination on the screen was regulated. The lamp,  $L_1$ , was inclosed by a metal cylinder with a suitable aperture. An additional black screen,  $d$ , was placed just beyond the disk. These precautions assured us that the screen received a negligible amount of illumination from the light-colored walls of the room. The screen was, furthermore, surrounded by a black-cloth border. The projection lantern by means of which the variable strip of light was projected upon the screen was equipped with a miniature signal lamp,  $L_2$ , operated at 6 volts. The two lamps,  $L_1$  and  $L_2$ , Fig. 1, were operated on storage batteries, and voltage was kept constant to 0.1 volt.

FIG. 1.—Relative position of screens and observer  
 $S_1$ , main screen;  $S_2$ , auxiliary screen on carriage;  $P$ , pulley;  $L_1$ , illumination for  $S_1$ ;  $O$ , observer



The lantern was provided with a bilateral slit, whose construction is shown in detail in Fig. 3. Its chief parts were two jaws,

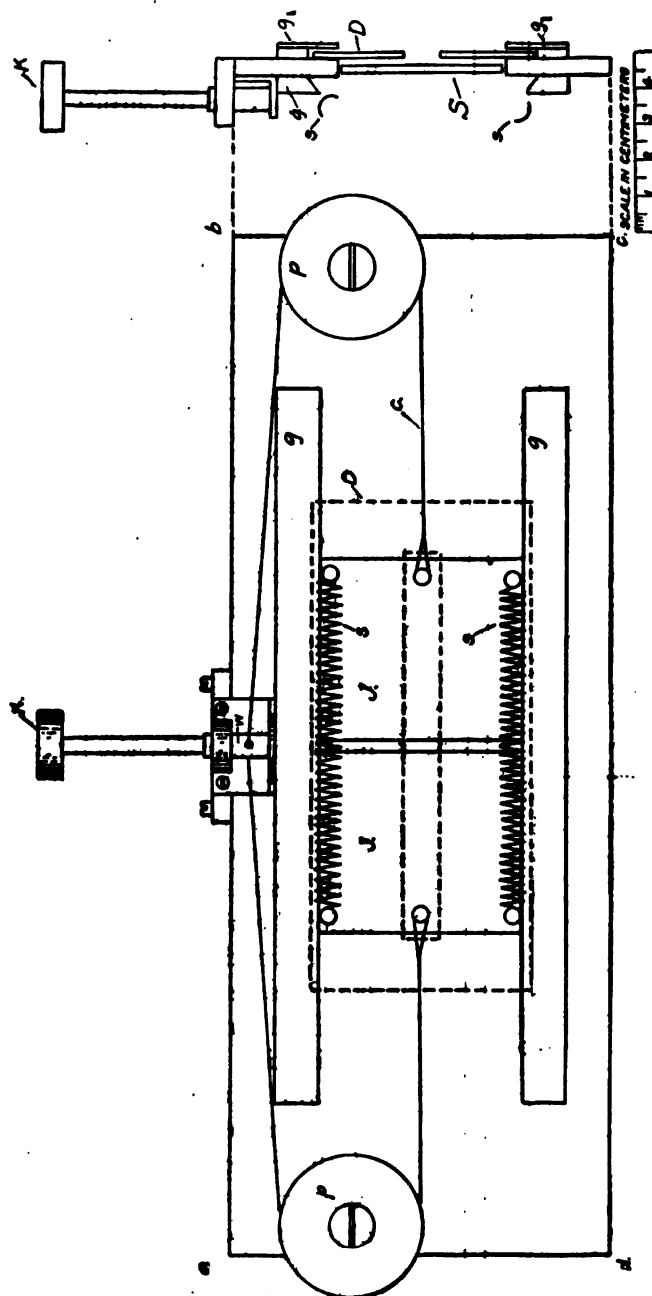


FIG. 3.—Adjustable slit for projection lantern

*J*, sliding jaws; *g*, guides; *s*, springs; *c*, cord; *p*, pulleys; *w*, winch; *K*, key; *D*, diaphragm; *s*, guides; *S*, equalization screws

*J*, smoothly displaceable horizontally in guides, *g*, under tension of two springs, *s*. The displacement of the jaws—that is, the



opening of the slit—was varied by means of a cord,  $c$ , attached to the jaws and passing over pulleys,  $p$ , to the winch,  $w$ , operated by the key,  $k$ . To limit the aperture vertically to a required height, a diaphragm,  $D$ , of any desired width could be inserted into guides,  $g$ . This simple slit mechanism when in good condition gave entire satisfaction for the purpose in hand. A second sector disk,  $M_1$ , Fig. 1, was placed before the projection lantern to control the brightness of the variable strip. To determine the length of a strip projected upon the screen a scale,  $T$ , Fig. 1, was projected alongside of the strip by means of the lens,  $l$ . When measurements of the length of the strip were made, the light from lamp,  $L_1$ , was eclipsed by means of a screen operated by a lever which simultaneously closed the circuit with lamp  $L_1$ , causing only the strip and the scale superimposed to be visible. All the manipulation of the sector disks, the variable slit, and the reading scale, as well as the recording, was done by one operator.

## 2. PHOTOMETRIC MEASUREMENTS

The brightness of the screen and of the strip were measured by means of a photometer (Macbeth) equipped with a lens, and calibrated to read in microlamberts. The lamp in the lantern and the lamp illuminating the screen, and that in the photometer were adjusted for a color match.<sup>1</sup> Measurements of the brightness of strip and screen were made twice in each night, viz, at the beginning and end of the observations. The calibration of the photometer was usually checked once during the night by comparison with a secondary standard. The screen was explored for uniformity of brightness over its entire area, and was found satisfactory over the portion of it that was actually used.

It was somewhat more difficult to obtain uniformity of brightness across the entire maximum length of the strip because of the slight obliquity of the projection. This was accomplished in the following manner: A photograph was taken of the screen illuminated by means of the projection lantern with the variable slit entirely extended, and the diaphragm,  $D$ , Fig. 3, removed. The size of the picture was made about the size of the aperture in the lantern. The negative was then cut down to fit into the slide, as shown by  $S$  in Fig. 3. The resultant distribution across the strip was very uniform. The exposure of the negative was short so that its absorption at the densest parts was probably no more

<sup>1</sup> It may be pointed out, however, that when the strip was very small a slight physiological color difference appeared.

than 15 per cent. This was necessary not only to economize the light but to avoid appreciable changes in the brightness when the strip length was varied. Within experimental errors the brightness of the center of the strip when entirely extended and when almost closed was the same.

### 3. AUXILIARY SCREEN

It has been stated above that the general illumination on the screen was cut off when the length of the strip was read. This was, of course, subjecting the eye of the observer to a variable and uncertain state of adaptation. To avoid this an auxiliary white diffusing screen was used upon which the eye of the observer was fixed whenever the illumination on the main screen was cut off or seriously changed, as during the time of adjusting the sectorized disks. The relative position of the screens and observer is shown in Fig. 2, where  $S_1$  is the main screen and  $S_2$  the auxiliary screen mounted upon a carriage which could be moved to or from the observer at  $O$ , until the brightness of it due to illumination from the lamp,  $L_2$ , Fig. 2, whose voltage was also controlled by the observer at  $O$ , was equal to the brightness of the screen  $S_1$ . The lamp,  $L_2$ , was turned out by the observer during the time that he was observing the strip upon the screen.

### IV. OBSERVING CONDITIONS

The observer was seated in a room at a distance of 26.3 m from the screen and test strip. This room could be darkened but was not entirely light-tight. Skylight and moonlight were always present to a very small extent. However, since the observations were, perforce, made after nightfall and before dawn, the effects of the small amount of stray light from external sources were, undoubtedly, smaller than the corresponding effect of the light from the lamp,  $L_2$ , and from the two screens, for there was some general illumination in the observer's room at all times from both of the screens. The walls of this room as well as the walls of the adjoining room containing the auxiliary screen and lamp were all of very light tint.

It is of interest to point out that additional illumination other than from the main screen entering the observer's eye, did not necessarily decrease the sensibility. It was noticed, for example, that when the auxiliary screen was illuminated while the strip was observed, the strip became more visible. This phenomenon

is similar to that observed by Nutting, that when the field was stopped down with black the threshold was raised.<sup>2</sup>

The observer used his right eye only, having the natural pupil. The left eye was covered by a dark card over the left spectacle lens in case of one observer (E.K.) who wore glasses. A similar method sufficed for the second observer (E.P.T.T.) by the use of a spectacle frame without glasses. Both observers have had considerable experience in photometric measurements. Before the subject began to observe he remained under the test conditions from 10 to 15 minutes with the eye exposed to the screen of the brightness desired to begin the observations. To keep the observer alert, particularly at the lower contrasts and at low field illumination, "blank" settings were made as follows: The slit was entirely closed as when starting all observations; then it was announced to the observer that he look for the strip as customarily. The slit, however, was not opened, so that any strip seen by the observer was imaginary. Such checking was made at the pleasure of the operator at irregular intervals. When several imaginary strips were reported for any condition of the brightness or contrast and of the physiological condition of the observer, the observations were discontinued and resumed on some succeeding day, if it was desired to extend or repeat the observations.

The amount of the surface of the screen and the maximum length of the test strip seen by the observer were limited by intervening doorways. The maximum length of strip was about 125 cm. The area of screen actually used was approximately 125 by 125 cm.

The rooms in which these experiments were made were not available for this purpose during the daytime. As a consequence the observations were usually made after the observers had been performing other active duties for 8 or 10 hours previously. The disposition to manifest fatigue, at times very markedly as noted below, was, undoubtedly, due to this fact.

## V. DATA OBTAINED

The two methods by which the two series of observations previously mentioned were obtained are as follows:

1. The illumination on the screen (this will be referred to as the field brightness) is kept constant, while the illumination on the strip (strip brightness) is varied by known amounts by means

---

<sup>2</sup> Trans. Ill. Eng. Soc. 11, p. 1; 1916.

of sectored disks. By this method a relation is directly obtained between the length of strip and contrast between the field and strip for any desired field brightness.

2. The relative brightness of the field and strip is fixed, and the brightness of both is reduced in known steps by sectored disks. A relation is thus obtained directly between the length of strip and the field brightness for any desired contrast between field and strip.

Both of these methods differ materially from the method by which Reeves<sup>3</sup> obtained his excellent results, and also differ from that of Koenig.<sup>4</sup>

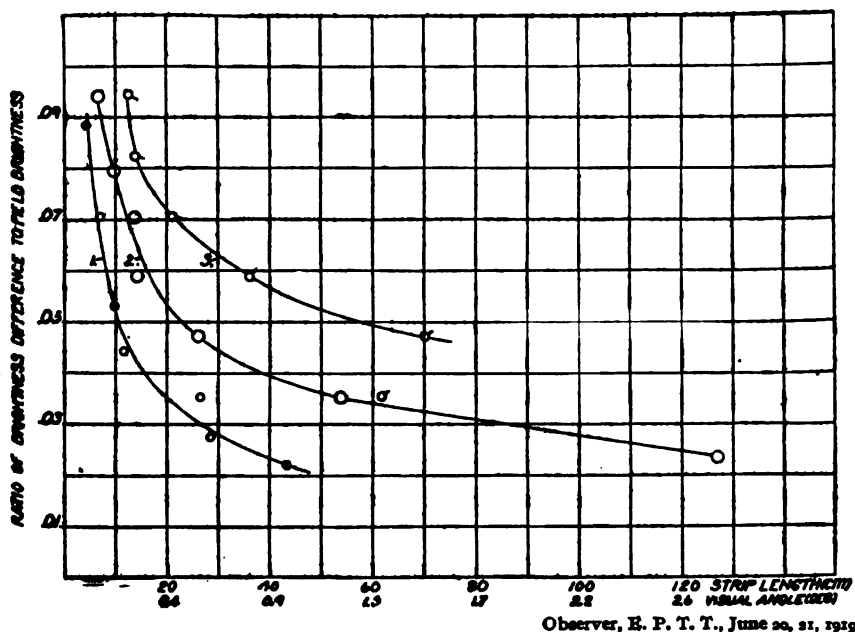


FIG. 4.—Relation between strip length (visual angle) and ratio of brightness difference to field brightness

Average of decreasing and increasing brightness difference: 1, F. B. = 457 microlamberts; 2, F. B. = 350 microlamberts; 3, F. B. = 160 microlamberts

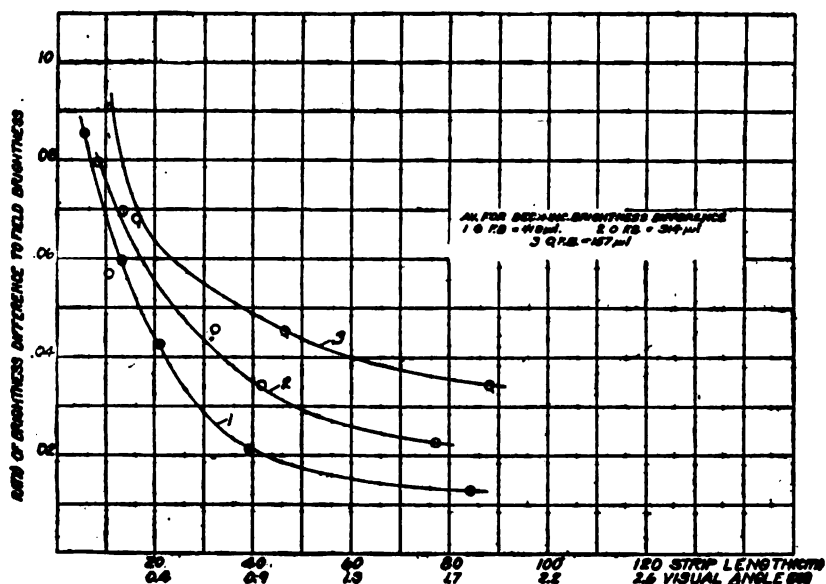
### 1. RESULTS BY FIRST METHOD

The data obtained by the first method for each of the two observers are given in curves of Figs. 4 and 5 where the strip length is indicated along the axis of abscissae in centimeters, and in terms of the angle which this length subtended at the observer's

<sup>3</sup> J. Opt. Soc. Amer., 1, p. 148; 1917.

<sup>4</sup> Physiological Optics, p. 135. The results of Blanchard should also be noted, obtained by a similar photometric method and confirming the results of Koenig, when the intensity unit of the latter are properly evaluated. These are reported by Nutting in Trans. Ill. Eng. Soc., 11, p. 939, 1916; and in J. Frankl. Inst., 188, p. 387; 1917.

eye. The contrast condition is indicated along the axis of ordinates in terms of the Fechner fraction; that is, the ratio of difference between strip brightness and field brightness to the field brightness. A series of observations, Fig. 4, for three different values of the field brightness, viz, 427, 320, and 160 microlamberts ( $\mu$ l) were made by one observer (E. P. T. T.). Similar observations, Fig. 5, were made by the second observer (E. K.) with field brightness of 418, 314, and 157  $\mu$ l. For each value of the field brightness, observations were made both on decreasing and increasing the strip illumination. The curves of Figs. 4 and 5 are the average

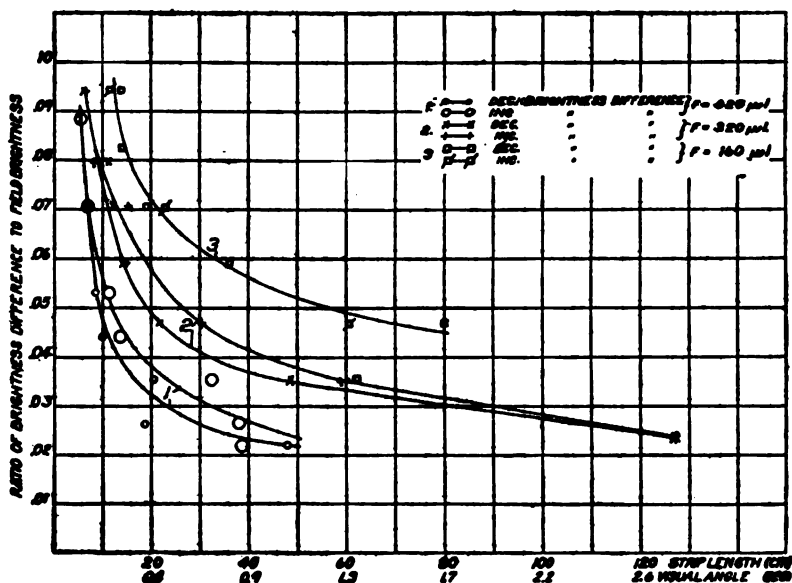


E. K., June 24, 25, 1929

FIG. 5.—Relation between strip length (visual angle) and ratio of brightness difference to field brightness

curves. The values of the strip length obtained on decreasing the strip illumination usually were smaller at any given contrast than those obtained on increasing the illumination. At times this "lag" was very marked. It was related to the general physiological condition of the observer as well as to the immediate condition of the eye due to prolonged functioning. These differences are the fatigue effects referred to previously. The time required to make a complete series of observations both for decreasing and for increasing the strip illumination for a given field brightness was approximately 1.25 hours.

It is of interest to record some typical cases of this fatigue, as those in Fig. 6 for one observer (E. P. T. T.); and in Fig. 7 for the second observer (E. K.). For the latter is given one extreme case of this fatigue for a field brightness of  $418\mu\text{l}$ . A second series of curves is given in Fig. 8 for one observer (E. K.) picturing the data taken at an earlier date. The field brightness was 432, 324, and  $162\mu\text{l}$ . These curves are of the same general nature as those given in Fig. 5 above, and lie fairly consistently with them. In all respects the external conditions were approximately the

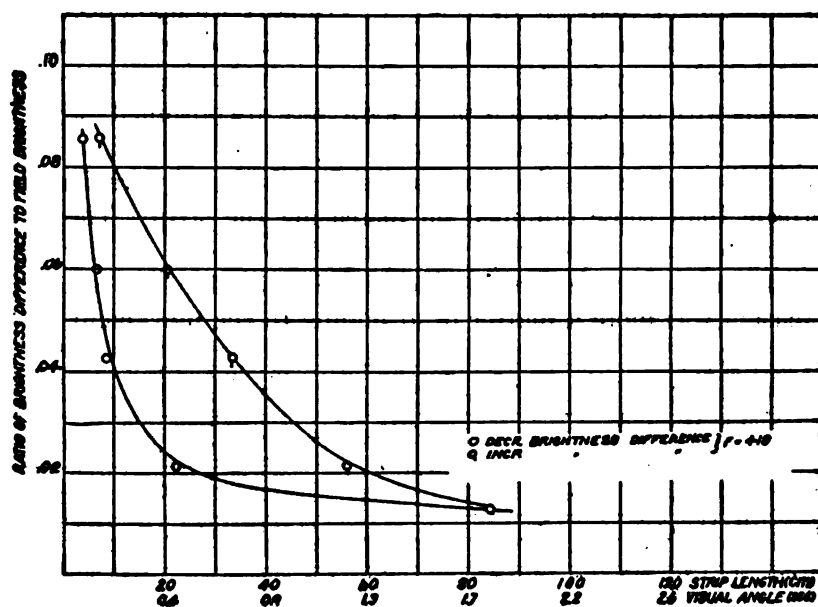


Observer, E. P. T. T., June 20, 21, 1929

FIG. 6.—Relation between strip length (visual angle) and ratio of brightness difference to field brightness

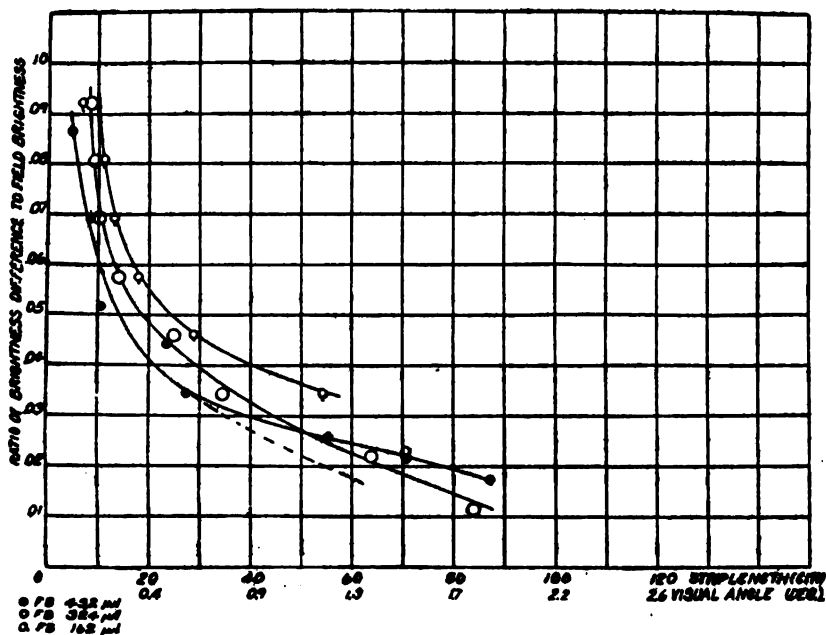
same in the two cases. The crossing of the two curves for the higher field brightness is a result of fatigue and lack of control of the factor of time. When fatigued the eye required a longer time to distinguish the test strip.

In both methods six observations and frequently more were made for each setting of the sector disk. The time between two adjustments of the strip was approximately uniform. The slit was opened at a rate such that the motion of the boundary of the strip of light was imperceptible to the observer. In this connection it may be noted that, in the beginning of the experiments upon the contrast sensibility, it was attempted to record obser-



Observer, E. K., June 24, 25, 1919

FIG. 7.—Relation between strip length (visual angle) and ratio of brightness difference to field brightness



Observer, E. K., June 21, 22, 1919

FIG. 8.—Relation between strip length (visual angle) and ratio of brightness difference to field brightness

vations of the strip length when just visible, both upon decreasing and upon increasing it. The strip length for the former condition was usually very much less than that for the latter. Such observations with decreasing length of strip were discontinued, however, for the following reasons:

1. The results obtained on decreasing the strip were far more erratic than those obtained on increasing the strip. The latter could be quite satisfactorily duplicated from day to day when conditions were the same. The visibility of the strip while decreasing was more a matter of attending to the movement of the

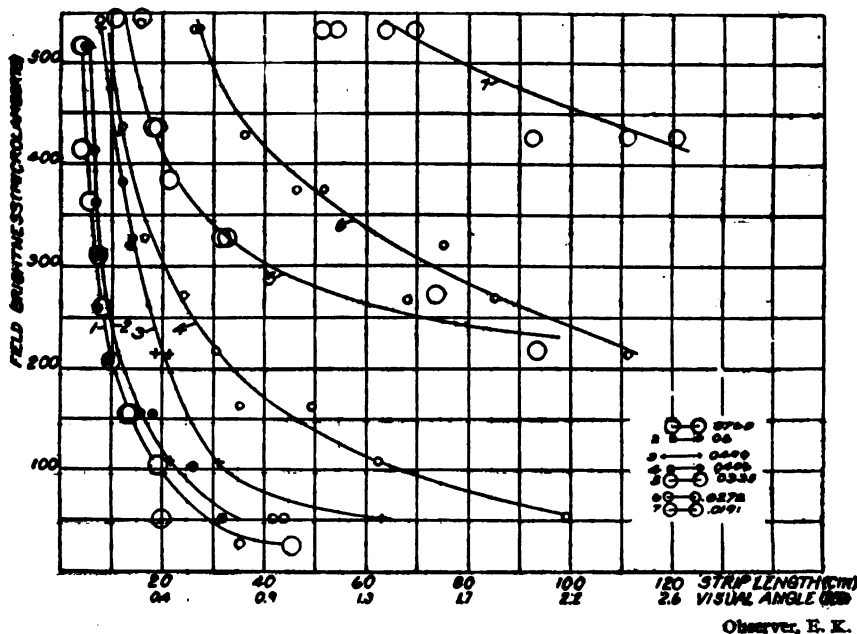


FIG. 9.—Relation between field brightness and strip length (visual angle) ratio between brightness difference and field brightness

terminal boundaries of the strip even when such movement was slow.

2. The time required was approximately doubled so that greater fatigue effects were introduced into the observations that were reliable.

3. Much longer time than could be devoted to these experiments would have been demanded in order to obtain satisfactory results with the strip decreasing.

The curves of Figs. 4 and 5 are similar, and are somewhat suggestive of hyperboles, but by test are shown not to be such. These curves are typical of curves that are obtained under ap-



proximately the same external conditions. These data should not be generally applied, but similar curves obtained for a large number of observers would be applicable. The necessity of a large number of observers is to eliminate not only differences between individuals but also to eliminate the variations for each individual that depend upon the physiological conditions of the eye.

## 2. RESULTS BY SECOND METHOD

The data obtained by the second method are somewhat more extensive. These are represented by the curves of Figs. 9 and 10. Ordinates are values of field brightness, in microlamberts;

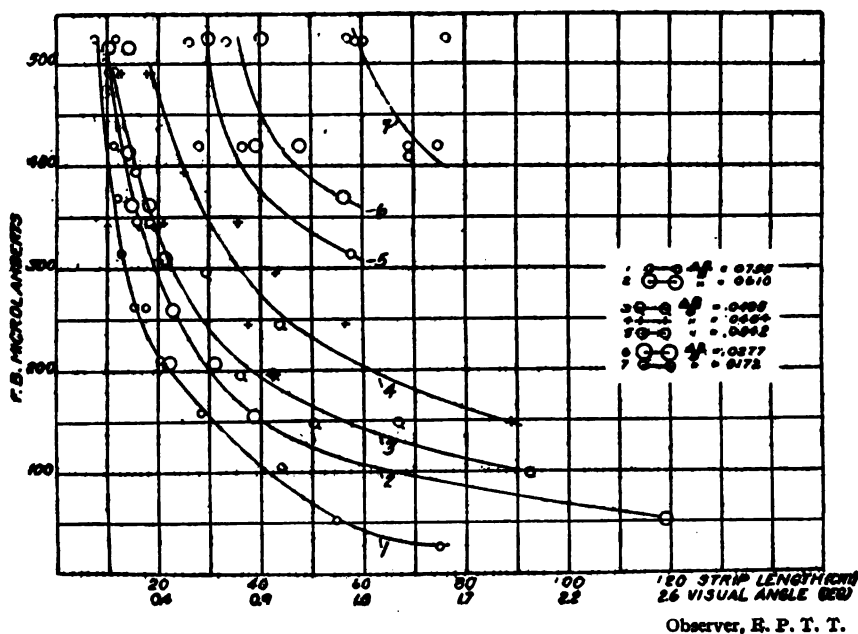


FIG. 10.—Relation between field brightness and strip length

abscissas are lengths of the strip in centimeters with the equivalent visual angle subtended at the eye of the observer. The relation is given between the visual angles and field brightness, for ratios of difference in brightness to field brightness of 0.0762 to 0.0191 for one observer, Fig. 9, and from 0.0755 to 0.0172 for the second observer, Fig. 10. The curves for the two observers are very similar. The exact location of the individual curves may change with the physiological condition of the observer, but they are always of the same type. Under favorable conditions the curves could be very closely duplicated at different times. The data in the curves were obtained in an interval of 10 nights.

Several of the curves are repetitions of curves originally obtained that were obviously out of proper place for reasons of fatigue.

The curves giving the relationship between the visual angle and brightness or contrast show that, under certain conditions, a very small change in the size of the target demands a very great change in contrast or field brightness. This relationship is such as to suggest the possibility of adapting it to the measurement of distances.

The data given in the curves were obtained with a strip whose width was fixed (19.5 cm). Only a few observations were made with a strip of 8.5 cm wide. These indicated that; first, for a field brightness of 533 $\mu$ l where the lengths of the strips are relatively small, the area just visible was greater for the narrow strip than for the wider; second, for field brightness of 200 $\mu$ l the reverse was the case; third, for intermediate brightness, areas for the two strips of different widths were very approximately equal. When making any application of the data the square root of the area may be used to obtain approximately the minimum visual angle, if it is assumed that the area just visible is independent of the shape of the target.

To see whether the effect of the introduction of a color contrast is very marked, one set of observations was made when a deep blue glass was placed before the lamp illuminating the field. The field brightness was approximately 90 $\mu$ l. There was a very great color difference during the measurement of the field brightness when the glass was present. The glass was then displaced by a sector disk of approximately the same transmission. The length of the strip was decidedly shorter for the former condition. Time did not permit pursuit in this direction with greater refinement and detail.

## VI. SUMMARY

1. Data on the contrast sensibility of the eye is fundamental in searchlight and similar illumination.
2. The relations between visual angle, contrast, and field brightness for two observers are represented in groups of curves which lie consistently with each other.
3. For practical applications mean values obtained from a large number of observers should be employed.

WASHINGTON, August 4, 1919.





DEPARTMENT OF COMMERCE

---

# SCIENTIFIC PAPERS

OF THE

# BUREAU OF STANDARDS

S. W. STRATTON, DIRECTOR

---

No. 367

## TURBIDITY STANDARD OF WATER ANALYSIS

BY

P. V. WELLS, Associate Physicist  
*Bureau of Standards*

---

ISSUED MARCH 17, 1920



PRICE, 10 CENTS

Sold only by the Superintendent of Documents, Government Printing Office  
Washington, D. C.

---

WASHINGTON  
GOVERNMENT PRINTING OFFICE

1920



# TURBIDITY STANDARD OF WATER ANALYSIS

By P. V. Wells

## CONTENTS

	Page
I. Introduction.....	693
II. Properties of turbid media.....	694
III. Optics of turbid media.....	695
IV. Turbidimetry of water.....	697
V. Turbidity standard of water analysis.....	704
VI. Description of turbidimeter.....	709
VII. Preliminary experimental studies.....	713
VIII. Intercomparison of standards from water laboratories.....	718
IX. Conclusion.....	721

## I. INTRODUCTION

In practical water analysis the amount of suspended matter has been roughly estimated by the turbidity of the water. In order to render it possible for different laboratories to compare their results the water analysts of the country have adopted a standard of turbidity. This standard, however, has long been considered by them as unsatisfactory, and so it was thought advisable to investigate the subject with the hope of finding some way by which it could be improved. The cooperation of the Bureau was invited by the joint committee on standard methods of the American Public Health Association, the American Chemical Society, and the American Water Works Association.

As a first step in this investigation the methods of measuring turbidity were studied, and a turbidimeter was designed, constructed, and tested. Requests were then sent out to a list of about 30 representative State and municipal water laboratories for samples of their standard turbidity, and these were intercompared with the turbidimeter. At this point the work was discontinued and parts of the apparatus were used on urgent military problems. The present paper discusses some of the properties of turbid liquids bearing on a standard of turbidity, and describes the methods and results of the intercomparison.

## II. PROPERTIES OF TURBID LIQUIDS

The word *turbid* is derived from the Latin verb *turbare*, to disturb. The same meaning is attached to the French *troublé*, and to the German *trübe*. Hence a turbid medium is one having the mud stirred up. In the scientific sense any medium containing small particles in suspension is turbid. While the original meaning of the word has no direct reference to the eye, turbidity has become associated with the appearance of a turbid medium. The small particles either reflect or scatter light in all directions, making their presence strikingly evident.

The particles may be of any size, from  $10^{-8}$  cm, which can just be seen individually with the unaided eye, to  $10^{-5}$  cm, or molecular dimensions. The smaller particles are in incessant Brownian motion. The smaller the particle, the greater is the violence of this motion, so that small particles are continually coming into contact and coalescing. When they have thus grown into relatively large agglomerates they settle to the bottom of the vessel unless the liquid is stirred mechanically or by convection currents.

When material is dispersed into small particles it presents an enormous surface, so that there may be a relatively large amount of energy represented in the surface layers. Surface phenomena would thus be expected to play an important part in determining the equilibrium. In such cases the conditions of thermodynamic equilibrium in dispersed systems require, according to Tolman,<sup>1</sup> that the particles shall all be of the same size, and for permanent stability the surface tension between the particles and the liquid must be zero. It is obvious from this that many of the ordinary suspensions of solids in liquids, such as silica and clay suspensions, can not be considered as systems in thermodynamic equilibrium, and in fact it is well known that such suspensions rapidly settle out unless kept well stirred. Very little is known regarding the amount of absorption of the liquid by the dispersed phase, but the relatively large surface would make such an effect important if it existed. In order to have an appreciable concentration represented in the particles enormous numbers must be present, because each one is so very small. Thus, for particles of silica of density 2.6, and diameter  $10^{-5}$  cm, over  $10^8$  or 100 000 000 particles per cubic centimeter must be present to produce a concentration of  $10^{-6}$ , 1 mg per liter, or as it is commonly expressed, 1 part per million. It is not surprising that particles crowded together so

---

<sup>1</sup> R. C. Tolman, Jour. Am. Chem. Soc., 85, pp. 317-333; 1913.



closely coagulate unless forces are constantly at work to keep them separated.

### III. OPTICS OF TURBID MEDIA

When a turbid medium is illuminated by a beam of light, each particle acts as a secondary source of light. The resultant intensity of the light thus dispersed by the particles in any given direction can be obtained only as the result of an exceedingly complicated calculation, depending on the number, size, shape, and distribution of the particles. Since light is considered to be an electromagnetic wave disturbance, the electrical constants of the particles and of the medium must also be taken into account. From general considerations it is obvious that the phenomena, when the particles are larger than the wave length of the incident light, depend almost entirely upon reflection at the surface of the particles; but when the particles are small compared with the wave length the volume of the disturbing particle is of chief importance, and the phenomenon is then called scattering.

The simplest case is that of a single particle of infinitesimal size compared with the wave length of light. The particle then acts as an electric oscillator, performing forced vibrations in the direction of the impressed force with a certain amplitude,  $a$ . The oscillator, therefore, sends out scattered waves in all directions, the vibrations being, of course, in every case perpendicular to the direction of the light, since light waves are transverse. But the component of  $a$  normal to a line making an angle  $\theta$  with the vibration is  $a' = a \sin \theta$ , so that the scattered intensity in this direction, measured by the square of the amplitude, is

$$I_s = ka'^2 = ka^2 \sin^2 \theta \quad (1)$$

Here the incident light is regarded as plane polarized. By (1) the scattered intensity vanishes when  $\theta = 0$ , that is normally to the incident ray, and in the direction of the incident vibration, in agreement with Tyndall's<sup>2</sup> experiment.

If the light is unpolarized it is more convenient to consider, not the direction of vibration, but the direction of light propagation. If unpolarized light is incident along the axis of  $y$ , the incident vibration may be regarded as compounded of two vibrations of equal amplitude in the directions of the axes of  $x$  and  $z$ . If the particle is situated at the origin of coordinates, two vibrations of equal amplitude— $a$  along  $x$  and  $z$ —spread out in all

<sup>2</sup> J. Tyndall, *Cont. to Molecular Physics*, Appleton, N. Y., p. 431, 1897; also *Proc. R. S.*, 106, 1869.

directions from the origin as from a source. The components of these vibrations perpendicular to a direction  $r$ , defined by the angles  $\alpha$ ,  $\beta$ ,  $\gamma$ , with the axes of  $x$ ,  $y$ ,  $z$ , are, respectively,  $a \sin \alpha$  and  $a \sin \gamma$ . The resultant intensity  $I_s$ , of the scattered light along  $r$ , is

$$I_s = ka^2 (\sin^2 \alpha + \sin^2 \gamma) \quad (2)$$

but from geometry  $\cos^2 \alpha + \cos^2 \beta + \cos^2 \gamma = 1$ , and hence

$$I_s = k a^2 (1 + \cos^2 \beta) \quad (3)$$

This gives the variation of the scattered intensity with the angle between the directions of the incident and scattered light. The intensity is a maximum in the direction of the incident light, decreasing to one-half normally, and zero in the opposite direction.

The amplitude of the vibration in the scattered light, on either the elastic solid theory or the electromagnetic theory of light, is proportional to the volume,  $V$ , of the small disturbing particle. At a distance  $r$  from the particle the amplitude must be inversely proportional to  $r$ , so that in order to be dimensionally correct, the ratio of the amplitudes  $a$  of the scattered light and  $a_0$  of the incident light of wave length  $\lambda$  must be

$$\frac{a}{a_0} = k \frac{V}{\lambda^2 r} \quad (4)$$

These simple considerations may help to explain Rayleigh's expression for the intensity  $I_s$  of the light scattered from  $N$  particles each of volume  $V$ , the incident intensity being  $I_0$  and the wave length  $\lambda$ . This is<sup>3</sup>

$$\frac{I_s}{I_0} = \frac{n'^2 - n^2}{n^2} \frac{NV^2}{\lambda^4 r^2} (1 + \cos^2 \beta) \quad (5)$$

Here  $n$  is the refractive index of the medium,  $n'$  that of the particles. The particles are supposed to be contained in such a small volume that the distance  $r$  and the angle  $\beta$  between the scattered and incident beams are the same for all the particles. For particles of different size, all small compared with the wave length, a summation must be made, requiring the size distribution of the particles. When the particles are not small compared with the wave length, terms of higher order must be included, and again the expression becomes complicated.

No account is taken in (5) of secondary scattering. All of the light scattered by the particles is supposed to reach the eye with-

<sup>3</sup> Lord Rayleigh, *Sci. Papers*, 1, pp. 87-110, Camb. Univ. Press; 1899.

out loss. When the medium is densely filled with particles, this factor may become of first importance. The fractional decrease of the intensity  $I$  in traversing a thickness,  $dx$ , of the turbid medium is

$$\frac{dI}{I} = -\frac{h}{\lambda^4} dx \quad (6)$$

where  $h$  is a constant independent of  $\lambda$ .

Integrating

$$I_x = I_0 e^{-\frac{hx}{\lambda^4}} \quad (7)$$

where  $I_0$  is the intensity of the light when  $x=0$  and  $I_x$  is the intensity after traversing a thickness  $x$ .

The most striking characteristic of equations (5) and (7) is the occurrence of the factor  $1/\lambda^4$ , indicating that the scattered light increases rapidly as the wave length decreases. The scattered light is, therefore, much bluer than the incident light, while the blue is correspondingly absent in the transmitted portion, which contains a relatively large fraction of the red light. This was used by Rayleigh to explain the blue color of the sky, as well as the red colors of the sunset. The blue color may be used as a test of the size of the particles of any turbid medium. Thus the fine blue smoke from the end of a cigar is an indication that the smoke particles are much smaller than the wave length of light. Tyndall's test of complete polarization at right angles to the incident beam is still more sensitive.

Strutt<sup>4</sup> has recently observed the light scattered by the molecules of gases, and finds that it is not completely polarized, as demanded by the simple theory. He considers this to be due to the departure of the molecules from spherical symmetry. It is not necessary here to go into the large amount of research, both theoretical and experimental, that has been done on the optics of turbid media. Enough has already been given to show that these phenomena are very complicated.

#### IV. TURBIDIMETRY OF WATER

Natural waters are almost always found to have foreign matter in suspension. The suspended matter is usually silt and clay abraded from the soil over which the water flows, and prevented from settling by convection currents. Organic material is also found, sometimes in large quantities. This is usually of microscopic size, and is different from the mineral ingredients both in

<sup>4</sup>R. J. Strutt, *Proc. Roy. Soc.*, 96, pp. 155-176; 1922.

density and color. It is obviously impossible to completely describe the important properties of suspended matter composed of particles of widely different sizes and materials by means of a single quantity. Turbidity is, therefore, usually defined as the mass of suspended matter per unit volume. In absolute cgs units turbidity is expressed in grams per cubic centimeter, while in technical water analysis it is usually expressed in parts (by weight) per million. The density and size of the suspended particles are thus ignored.

When the particles are large it is not difficult to remove them from the liquid by filtering, washing, and drying, and then the mass can be determined directly by weighing. When the particles are smaller than the pores of the filter they must be increased in size by some method of coagulation. If there are no non-volatile substances in solution, it is not necessary to filter, for the volatile constituents can be removed by evaporating the medium to dryness directly. But these methods are limited by the precision of the balance.

It is possible to detect, optically, the presence of suspended matter when the gravimetric method fails, completely. In fact, it is difficult to obtain liquids which are optically clear, except in a few special cases. This is particularly true of water. Optical methods of measuring turbidity are, therefore, especially valuable in the analysis of waters containing very small traces of suspended matter.

The optical methods of measuring turbidity fall into two classes, (1) those in which the measured quantity is the thickness of the turbid medium required to cause some standard object to disappear, and (2) those in which the quantity measured is the intensity of the light, either reflected or scattered by the turbid medium. These may be briefly called (1) disappearance and (2) intensity methods, respectively.

Disappearance methods have arisen from the demands of measurements in the field. Thus the platinum-wire method, now used as the standard for water analysis, as originally designed by Hazen,<sup>5</sup> was simply a pin stuck into a piece of wood and lowered into sewage until it vanished. In its present form it is designed for the field assay of water.<sup>6</sup> Similarly for over a hundred years the oceanographer has lowered circular disks of canvas into the sea to

<sup>5</sup> Hazen, A., *Filtration of Public Water Supplies*, 3d ed., Wiley & Sons, New York.

<sup>6</sup> See Leighton, M. O., *Field Assay of Water*, U. S. Geol. Surv., Water Supply and Irrigation Paper No. 151, Washington, D. C.; 1905.

measure the depth at which they disappeared. This method is an obvious outgrowth of the simple observation of objects beneath the surface of the sea, which in clear tropical waters are sometimes visible to a depth of over 80 fathoms. The determining factors in field methods are simplicity, speed, and ease of carrying, not precision and reliability. But even in field methods the desire for simplicity decreases with familiarity, and the faults become increasingly evident, so that the tendency is ever toward increasing precision, which usually involves more complicated apparatus. This is illustrated by the development of the candle and electric turbidimeters for field work.

The earliest form of laboratory apparatus using the disappearance principle was the diaphanometer designed by Horning<sup>7</sup> in 1876. This instrument was improved by Parmelee and Ellms,<sup>8</sup> Jackson, Leighton<sup>9</sup>, and Weaver<sup>10</sup>, and is used in the chemical laboratory for rapid work. It usually consists of a cylindrical glass Nessler tube, sealed and polished flat on the bottom. The turbid liquid is poured into this until the test object just disappears from view. Jackson and Leighton used for a test object a slit, 0.5 mm. wide, in the form of a cross illuminated from below by an electric lamp, but I am informed by Mr. Weaver that the incandescent filament of a carbon lamp gives a sharper and more reproducible end point. The depth of the liquid is then measured. In order to exclude the stray light, the turbidity tube is inclosed in a metal casing, which in the Smith<sup>11</sup> form is perforated with a slit parallel to its axis and graduated so that the depth can be read directly in parts per million. The electric bulb is also inclosed in a light-tight metal chamber.

The theory of the disappearance method is very complicated, but it is found empirically that for particles of a given size the concentration,  $C$ , is related to the depth  $z$  over small ranges by an expression of the form

$$C = kz^{-\alpha} \quad (8)$$

where  $k$  and  $\alpha$  are constants.

This equation will be considered later in connection with the turbidity standard of water analysis. From the optics of the question it is evident that regardless of loss of definition the test

<sup>7</sup> Horning, G., *Engineering News*, 35-36, p. 219; 1896.

<sup>8</sup> Parmelee, C. L., and Ellms, J. S., *Technology Quarterly*, 12, pp. 145-164; 1899.

<sup>9</sup> Loc. cit. See note 6.

<sup>10</sup> R. S. McBride and E. R. Weaver, Bureau of Standards Tech. Paper No. 20, p. 36; 1913.

<sup>11</sup> O. M. Smith, U. S. Patent Nos. 1, 232, 989, 10, July, 1917.

object disappears when its brightness is just equal to the brightness of the turbid medium. Now its brightness depends upon (1) its illumination, (2) its reflection coefficient, and (3) the fraction of this reflected light transmitted through the medium to the eye. Similarly the brightness of the turbid medium depends upon the integrated effect of a host of particles, each of whose differential contributions to the brightness depends upon (1) its illumination, (2) its coefficient of reflection, or of scattering if the particle is smaller than the wave length of the light, and (3) the loss in transmission to the eye. The particles situated between the test object and the eye contribute light which is superposed on the image of the object itself. In addition to these brightness effects the definition of the image of the test object is impaired by the blur circles of images of particles out of focus, and by diffraction of the rays from the test object around the edges of the particles. Disappearance methods thus involve an estimation by the eye of brightness contrast and definition. The factors producing this criterion all vary as we pass from one disappearance method to another, so that each must be considered separately.

In the laboratory form of turbidimeter described above, the controlling factors are simplest and most nearly constant. This is the reason for its precision and reliability. The test object is an incandescent carbon filament. The fraction of the light reaching the eye is given by a decreasing exponential function as in equation (7). The illumination of the suspended particles comes from the slit which is used as the test object, or from other particles by secondary scattering. The brightness of the turbid medium is thus an integrated effect of all the particles. Since the brightness, both of the filament and of the medium, is proportional to the intensity of the source, changes in the voltage of the lamp only influence the color effect. For particles small enough to obey Rayleigh's law the source appears redder than the medium, but for large particles this is not troublesome as the reflected light is practically the same for all colors.

Intensity methods have been developed to meet the needs of the laboratory in measuring small turbidities. Here simplicity is not the prime requisite, and the attempt is made to obtain the utmost precision and reliability. The growth of such instruments is quite recent, with the exception of the nephelometer of Richards,<sup>12</sup> which appeared in its first form in 1894. It is designed

---

<sup>12</sup> R. W. Richards and R. C. Wells, *Am. Chem. Jour.*, 81, pp. 235-243; 1904.

for the photometric comparison of two turbid liquids of nearly equal physical properties with high precision. In research on the optics of turbid media many experimenters have used apparatus for measuring the intensity of light scattered by a turbid medium.<sup>13</sup>

In 1914 Mecklenburg and Valentiner<sup>14</sup> described a tyndall-meter by which the light scattered by a turbid medium perpendicularly to the incident beam can be measured. Recently Tolman<sup>15</sup> has designed an instrument for measuring the turbidity of smokes as well as of liquids.

Intensity methods possess great advantages over disappearance methods in sensitiveness. They are thus particularly adapted to the measurement of exceedingly small traces of turbidity. The sensitiveness is due to the fact that the eye never views the source of illumination directly, but only the light scattered by the particles, against a perfectly black background. It is what is known to the microscopist as dark-ground illumination, the principle underlying the design of the ultramicroscope. A source of great intensity is used to illuminate the particles, and the brightness of the turbid medium in a given direction is measured photometrically. For simplicity the direction usually chosen is that perpendicular to the incident beam. If the medium is perfectly clear, the field is absolutely black, in spite of the fact that a powerful beam of light is passing through the medium.

It is obvious that the slightest amount of stray light may upset the measurement completely, so that great care must be taken that the background be absolutely black, and that any glass surfaces in the field be either perfectly polished, free from scratches, or be in such a position that the powerful beam does not shine directly or indirectly upon them. Scrupulous cleanliness is also required in the cell containing the turbid medium to insure that the turbidity is due, not to the cell, but to the medium itself.

The brightness of the turbid medium is a complicated function of the concentration of the dispersed phase. For particles of one substance and one size, small compared with the wave length of the light employed, the brightness  $B$  of a thin section of the medium would be expected to be, from Rayleigh's expression (5)

$$\frac{B}{B_0} = \frac{kd^2Cx}{\lambda^4} \quad (9)$$

<sup>13</sup> See for instance papers by Rayleigh (1871), Abney (1886), Hurlon (1891), Lampa (1891), Barnes (1902), Ehrenhaft (1903), Müller (1907), Bence (1909), Herzheimer (1912), and Keen and Porter (1914).

<sup>14</sup> W. Mecklenburg and S. Valentiner *Zeitschrift für Instrumentenkunde*; July, 1914.

<sup>15</sup> R. C. Tolman, *Jour. Am. Chem. Soc.*, 41.

where  $B_0$  is the brightness of a comparison field illuminated by the same source,  $C$  the concentration (mass per unit volume),  $d$  the uniform diameter of the particles,  $x$  the thickness of the section in the direction viewed,  $\lambda$  the wave length of light employed, and  $k$  a constant. On the other hand, for particles larger than the wave length of light the brightness would be expected to be proportional to the total surface of the particles, and to be dependent on the color only as the reflection coefficient varies with  $\lambda$ . Thus for large particles

$$\frac{B}{B_0} = \frac{kCx}{d} \quad (10)$$

In ordinary suspensions particles of many different sizes are usually found. The brightness of such a turbid medium depends upon the size distribution of the particles and may be much more complicated than either (9) or (10). Moreover, the effect of secondary scattering and reflection, and of absorption, have been entirely ignored in both (9) and (10). For particles of certain substances and of sizes not negligibly small compared with the wave length, the light scattered shows marked color effects, usually ascribed to resonance phenomena<sup>16</sup>. It is evident from these considerations that the brightness of a turbid medium can not be taken as a measure of the concentration except in very special cases, for it varies rapidly with the size of the suspended particles.

The occurrence of many variables in the expression for the brightness of the turbid medium does not impair its use for the comparison of turbid media similar in all respects and only slightly different in concentration. It was for just such purposes that Richards and Wells used the nephelometer. Two samples of known concentration are successively compared with the unknown, the concentration of which is obtained by interpolation. Over such small ranges the other variables may be regarded as sensibly constant.

Both classes of optical methods, (1) the disappearance and (2) the intensity methods, are dependent upon the sensitiveness of the eye. Both involve the photometric comparison of the brightnesses of two adjacent objects, but this is complicated in disappearance methods by the estimation of definition. Under the best conditions, namely, (1) sufficient illumination, (2) exact juxtaposition of the two fields, and (3) perfect color match, the photometer is

<sup>16</sup> See Wood's *Physical Optics*, 2d ed., Macmillan, p. 635; 1914.



capable of a precision of better than one-half of 1 per cent. Very slight departures from ideal conditions reduce the precision rapidly to not better than 1 per cent.

In turbidimetry the photometric conditions are often far from ideal. With media of slight turbidity the illumination is below that at which the eye is most sensitive, with disappearance methods and also with intensity methods unless a powerful beam of light is used. The selective action of the turbid medium produces a color which varies with the sample measured. Of course, this does not affect the nephelometer, which merely compares two similar samples, but tyndallmeters suffer from this variable color difference between the photometric fields. If monochromatic light is used the loss in intensity seriously affects the sensitiveness.

In passing it may be useful to note that for the purposes of chemical analysis the turbidimeter is of wide utility, wherever it is desired to measure quickly fine precipitates which do not coalesce and settle rapidly. For high turbidities the disappearance method is very serviceable, because of its simplicity and precision. For extremely small turbidities it is necessary to use an intensity method.

In routine water analysis the turbidity is ordinarily estimated by comparison of the sample with the standard under similar conditions. The instructions given in *Standard Methods of Water Analysis*, 1917, page 5, are as follows: "Comparison with the standards shall be made by viewing both standard and sample sidewise toward the light by looking at some object and noting the distinctness with which the margins of the object can be seen." The method is thus essentially a distinctness test, similar in principle to the disappearance methods. The sample and the standard must be in similar bottles or tubes and they must be under the same illumination.

In testing this method the cylindrical shape of the bottles and tubes was found unsatisfactory for distinctness judgments. Cells with parallel flat faces were preferable. But if care was taken to have uniform illumination, and the samples were viewed against a black screen with the eye properly protected from the direct light, satisfactory results were obtained without using any distinctness test. Turbidity differences of 15 per cent were almost certain of detection, but some errors were made in comparing turbidities differing by 10 per cent. For the purposes intended the method seems to be quite satisfactory. Its accuracy can not be greater

than that of the standards used for comparison. For turbidities differing much in color the distinctness test is preferable and the precision is much less.

## V. TURBIDITY STANDARD OF WATER ANALYSIS

As the result of a comparative study of the methods in use for measuring the turbidity of water, Whipple and Jackson<sup>17</sup> recommended as the standard of turbidity water containing a definite amount of powdered silica obtained from diatomaceous earth. This recommendation has been followed and now constitutes the turbidity standard of water analysis. The complete specifications for this standard are given in *Standard Methods of Water Analysis*, third edition, published by the American Public Health Association, Boston, 1917, pages 4 to 9. The first paragraph is as follows:

The standard of turbidity shall be that adopted by the United States Geological Survey, namely, a water which contains 100 parts per million of silica in such a state of fineness that a bright platinum wire 1 mm in diameter can just be seen when the center of the wire is 100 mm below the surface of the water and the eye of the observer is 1.2 meters above the wire, the observation being made in the middle of the day, in the open air, but not in sunlight, and in a vessel so large that the sides do not shut out the light so as to influence the results. The turbidity of such water is arbitrarily fixed at 100 parts per million.

Comparison standards are obtained by dilution of a stock suspension containing 1000 parts per 1 000 000 by weight of silica. Comparison with these standards is made by noting the distinctness of objects seen through the samples. The platinum-wire methods for regulating the fineness depends upon the fact that for the particles used the vanishing depth increases with the size of particle. The particles required to give the proper reading are of the same size as clay, which is the most important ingredient of turbid waters from the standpoint of filtration.

Any standard may be judged from three points of view, namely, (1) accuracy, (2) convenience, and (3) range of application. The primary requisite of a standard, no matter what its convenience or range of application, is sufficient accuracy for its reliable use. It must be constant, permanent, and reproducible. Given these, the less important qualities of convenience and range of application must be considered.

The present standard of turbidity for water analysis is prepared according to specification in each local laboratory, introducing an unnecessary lack of uniformity. The regulation of the fineness

<sup>17</sup> Whipple, G. C., and Jackson, D. C., *Technology Quarterly*, 18, pp. 274-294; 1900.

by the platinum-wire method is relatively difficult of performance, and depends upon meteorological conditions which are not constant. Laboratories are, therefore, deterred from reproducing the stock suspension frequently; but unfortunately the silica suspension is not in stable equilibrium, the particles coagulate slowly, so that the standards decrease in turbidity on standing. It is appropriate and simple in use, so that as regards convenience there is little to be desired. The range of application of the turbidity standard is, unfortunately, limited, but this is unavoidable, as it is due to the complex nature of dispersoids in general, and particularly to the wide variety of turbid waters which must be utilized for water supplies. When it is considered that moving water carries in suspension objects of weight increasing with the sixth power of the velocity of the current, it is not surprising that natural waters contain particles of widely different sizes. But the same law is just as efficient in allowing the larger particles to settle out in reservoirs where the water is still, leaving in suspension only some of the finer silt, the clay, and organic material. This varies widely in color, according to the nature of the suspended matter, and colored samples are not easily compared with the bluish-white standard silica suspensions, even when the criterion used is the distinctness of objects seen through the sample. This limitation has caused the rejection of the standard in some localities.

The use of the platinum-wire method as a means of regulating the fineness of the standard is the least satisfactory part of the specification, from the standpoint of accuracy. The rate of change of the vanishing depth with the size of particle is rather small, as is the precision of the reading itself, so that the standard may vary considerably from uniformity in size of particle. The law of the instrument is rather complicated and seems to be entirely empirical. The relation between the concentration,  $C$ , and the vanishing depth,  $z$ , is best represented by the equation

$$C = kz^{-a} \quad (8)$$

but this holds only for small ranges. If this be fitted to the smoothed data for the turbidity rod of 1902,<sup>18</sup> the formula (8) is found to hold within 1 per cent over the ranges and with the constants given in Table 1. The concentration is in parts per million by weight, the depth in millimeters.

---

<sup>18</sup> See Standard Methods of Water Analysis, 1917 ed., p. 6.

TABLE 1

Valid range of $C$ (parts per 1 000 000)	$\alpha$	Constants $k$
7-100	1.11	$1.67 \times 10^4$
100-200	1.25	$3.95 \times 10^4$
200-400	1.44	$6.67 \times 10^4$
400-800	1.67	$1.56 \times 10^5$
800-3000	2.01	$4.42 \times 10^5$

But if the formula be fitted to the points 10 and 3000 parts per million, the constants are  $\alpha = 1.36$  and  $k = 8.51 \times 10^4$ , and while it fits at the ends, it is in error 66 per cent at 100 parts per million. The simpler formula .

$$C = \frac{7850}{z-9} \quad (11)$$

fitted in the same manner is in error by only 14 per cent at 100 parts per million. This formula is less satisfactory theoretically, for it indicates that  $C$  is infinite when  $z = 9$ , instead of the proper value of  $C$ , about 4300. Moreover, if fitted to the ranges 7 to 100 and 800 to 3000 parts per million, deviations from the observed values of 5 and 12 per cent are found while equation (8) fits to 1 per cent over these ranges. Neither formula is good enough for practical use over the whole range. For turbidities below 100 parts per million the concentration is roughly proportional inversely to the vanishing depth, while for turbidities above 800 parts per million it is nearly inversely proportional to the square of the vanishing depth. Between 100 and 800 parts per million there is a transition in  $\alpha$ , the exponent of  $z$ . A knowledge of the size of particles used in obtaining the data upon which this calibration is based might be of interest in this connection.

A few experiments were made in order to become familiar with the platinum-wire method. A piece of platinum wire, 1 mm in diameter (within less than 1 per cent), and 25 mm long was sealed into the side of a glass tube within which was inserted a millimeter scale. The silica suspension was placed in a liter graduate 6 cm in diameter and 40 cm deep. This was immersed in a large glass vat, 30 cm in diameter, 60 cm deep, until the level in the vat was 3 mm below that of the liquid in the graduate. The turbidity rod was clamped in a telescope stand and adjusted vertically by the eye. Thus the observer could lower the rod by means of a rack and pinion smoothly at any desired slowness,

and could hold it indefinitely at a given point without muscular effort. The turbidity vat was placed directly below a skylight in an attic room which gave diffuse light simulating a cloud. The turbidity of the liquid in the vat was roughly equal to that in the liter graduate.

The results of the first day with four observers, all experienced in physical measurements, are summarized in Table 2. In the first column is given the serial number of the observer, in the second the number of depth observations taken by him, in the third the mean of his vanishing depth readings,  $z$ ; in the fourth the average deviation of his individual observations from his mean, and in the last column the deviations of the means of the single observers from the weighted mean of all the means.

TABLE 2

Jan. 9, 1914 (observer)	Number of observations	Mean vanishing depth $z$ (mm)	Average deviation, single observations	Deviations from weighted mean
1.....	13	46.22	1.23	1.17
2.....	14	46.13	1.32	1.08
3.....	22	43.66	1.75	1.39
4.....	7	45.21	1.39	.16
Total and average.....	56	45.05	1.42	.95

NOTE.—Weighted mean  $45.05 \pm 0.95 = 2.1$  per cent; maximum difference = 2.56 = 5.7 per cent.

TABLE 3

Jan. 10, 1914 (observer)	Number of observations	Mean vanishing depth	Average deviation, single observations	Deviations from weighted mean
1.....	9	46.03	1.77	2.37
1.....	6	46.49	1.07	1.91
1.....	2	51.60	1.10	3.20
1.....	4	53.58	1.25	5.18
4.....	14	47.68	2.03	.73
1.....	5	51.56	.80	3.16
Total and average.....	40	48.40	1.34	2.76

NOTE.—Weighted mean  $48.40 \pm 2.76 = 5.7$  per cent; maximum difference = 7.55 = 15.6 per cent.

These results show no systematic differences between the four observers, who consistently reproduced their single observations to 3 per cent, and agreed in their mean results to 2 per cent, the maximum difference being less than 6 per cent. The sun appeared bright through a uniform mist, and remained the

same from 11.30 a. m. to 2.30 p. m. during the observations. There was indication that the longer the time occupied in making an observation, the greater the vanishing depth obtained.

The results of the next day, given in Table 3, were not so favorable.

An increase in the reading seemed to occur with practice; but the results with an observer (5) skilled in estimating the brightness of faint stars showed the most disconcerting disagreement. These are given in Table 4.

TABLE 4

Jan. 13, 1914 (observer)	Number of observations	Mean vanishing depth	Average deviation, single observation	Deviation from weighted mean
1.....	6	53.98	1.0	7.87
1.....	5	56.46	1.6	5.39
5.....	6	74.22	6.2	12.37
Total and average.....	17	61.55	2.9	8.54

NOTE.—Weighted mean  $61.55 \pm 8.54 = 13.9$  per cent; maximum difference  $= 20.24 = 32.7$  per cent.

The observer (5) took great care, despite the discrepancy in his single observations. There is no reason to suppose that his interpretation of the criterion might not be duplicated by other observers preparing the standard according to specifications.

The experiments were performed merely to become familiar with the procedure of the platinum-wire method. A critical study of the method would require an extended experimental investigation. Nevertheless, the results agree with those of other observers.

The choice of platinum wire 1 mm thick as the test object, the eye being placed at a distance of 1.2 m, produces an image so small that it can hardly be resolved by the eye. The limit of resolution is usually taken as 1 minute of arc. The bright line on the wire due to reflection probably does not subtend at the eye an arc of more than 3 minutes, but the effect of irradiation tends to obliterate a fine, dark line on a brighter background. Thus, a strip of black paper 1 mm wide on a sheet of white paper disappeared at about 15 m, while a strip of the same white paper 1 mm wide on a sheet of the same black paper disappeared at nearly 30 m under the same conditions. This effect, combined with the light superposed on the image from the turbid medium between the wire and the eye, sufficiently explain the failure of

the wire to reappear as a dark line in a brighter field when lowered below the critical depth, regardless of any loss of definition. But whether the criterion of disappearance is a matching of brightness, is simply a loss of definition, or is a combination of both remains an open question.

The turbidity standard of water analysis is regarded as unsatisfactory by many water analysts. Some consider it inaccurate, others inconvenient, and others find it inapplicable to particular water supplies. The question of accuracy obviously should be considered first. Our preliminary study of the problem indicates (1) that the theory is very complicated, (2) that the standards would not be expected to be permanent for any length of time, and (3) that the preparation of the standard by means of the platinum-wire method at each laboratory would be expected to lead to considerable lack of uniformity. An intercomparison of the laboratory standards was, therefore, undertaken to determine the accuracy of the present standards in actual use.

## VI. DESCRIPTION OF TURBIDIMETER

The superiority of intensity methods of measuring turbidity, both from the theoretical aspect and in the criterion which forms the basis of the measurement, led to the adoption of this principle in the design of a turbidimeter for the experimental investigation. After a few experiments and a preliminary instrument<sup>19</sup> had been studied it became evident that no one instrument is satisfactory for use over a wide range of turbidities. For turbidities above  $10^{-5}$  g per cubic centimeter (10 parts per 1 000 000 by weight), sensitiveness is not the primary consideration, and such requisites as simplicity, convenience, and size may be included. Below  $10^{-5}$  (10 parts per 1 000 000) strict attention to sensitiveness must be given. The final design<sup>20</sup> adopted is shown in the photographs, Figs. 1 and 2. The instrument was constructed in the Bureau instrument shop by H. C. Wunder.

The essential purposes of the design—great sensitiveness, combined with as wide a range as possible—required a variable thickness of cell and the measurement of the light scattered by the sample at a small angle from the incident beam. It was also advisable to have this angle variable, in order to be able to compare the scattered light from the sample with the reflected

<sup>19</sup> This instrument was described in a paper presented to the Physical Society, Apr. 24, 1914. See *Phys. Rev.*, 4, p. 396; 1914.

<sup>20</sup> A much simpler instrument would have sufficed for the present investigation, but further research was contemplated which led to this design.

light from an opaque surface. The instrument was not inclosed, in order to give greater freedom for experiments, and also because stray light could thus be better controlled.

The source of light used was a 108-watt concentrated filament locomotive-headlight lamp of high efficiency, taking 5.5 volts. The rays from the lamp were made parallel by a cemented triplet lens 5 cm in diameter and 12 cm in focal length. The parallel beam thus produced passed through a plate-glass reflector and was incident at a slight angle, usually  $20^\circ$  from the normal to the face of the cell containing the turbid sample. The intensity of the scattered light was measured with a Martens polarization photometer placed in such a position that the axial ray of one field passed through the middle of the cell containing the sample and normally to its face. In the comparison field of the photometer was a diffusing screen of ground opal glass. This was illuminated by the reflected portion of the parallel beam from the plate-glass reflector, after passing through total reflecting prisms to provide for the rotation of the photometer about a vertical axis.

The cell containing the turbid sample was made so that it could be chemically cleaned. A cylindrical hole about 5 cm in diameter was bored through a sheet of plate glass of the desired thickness. Thin sheets of plate glass were held by compression against the bored plate, forming a cell of glass. The pressure was produced by two plates of brass with four long bolts. The glass pieces could thus be removed, taken apart, and soaked in hot cleaning solution, washed, dried, and put together with the cell walls, and especially the faces, spotlessly clean. A series of these cells was made of thicknesses varying from 2 to 38 mm to determine the variation in the reading with the thickness. The lamp house and collimating lens, mounted on a single sliding base, could be moved away from the photometer to make room for long cells for gases. The cells were mounted on a plate supported by three adjusting screws, and were placed against an adjustable stop so that they could be replaced quickly and accurately in the same position.

The lamp was mounted on an adjustable base so that new lamps could be easily inserted in precisely the proper position, namely, so that the filament was in the optical axis of the system. It was inclosed in a ventilated light-tight lamp house. The stray light from the opening toward the lens was absorbed by sheets of black cardboard properly placed.

The photometer was mounted on an arm, so that it could be rotated about a vertical axis. In this way the optical axis of the



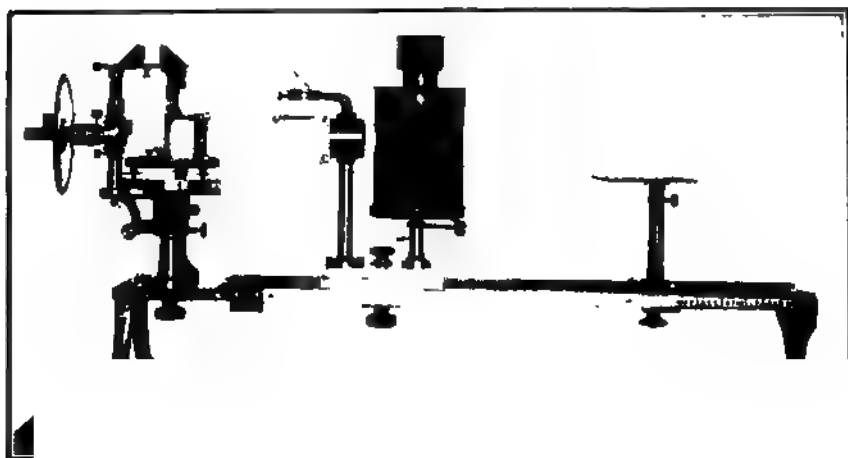


FIG. 1.—Instrument as used for measuring intensity of scattered light at angle of  $20^{\circ}$

FIG. 2.—Instrument as used for measuring light reflected from a standard magnesia surface



photometer could be set at any desired angle with the axis of the parallel incident beam. An inclosed circle, graduated in degrees, was provided for measuring this angle. Fig. 1 shows the instrument adjusted for measuring the light scattered at an angle of  $20^\circ$  by the turbid sample in a cell 38 mm thick, the face of which was normal to the optical axis of the photometer. Fig. 2, on the other hand, shows the instrument adjusted for measuring the light reflected by a standard magnesia surface normally, the parallel beam being incident at an angle of  $45^\circ$ . The surface here is also normal to the photometer axis. A sectored disk is also shown in this figure, which was used for reducing the intensity of the incident beam to bring the brightness of the magnesia surface within the range of the photometer.

The Martens polarization photometer is an instrument of high precision, which on account of its convenient size, and design, is very useful in the optical laboratory. It is not as popular in technical photometry, because there the polarization of the light is not of interest, and this instrument measures the component in one plane. The two fields measured by the photometer are each about  $5^\circ$ , with their axes about  $10^\circ$  apart. These fields are brought into precise juxtaposition by means of a biprism and their brightness adjusted to equality by means of a combination of a Wollaston prism as a polarizer and a Nicol prism as an analyzer. A circle graduated in degrees measures the angle between the principal planes of the prisms. The law of the instrument is

$$R = k \tan^2 \omega \quad (12)$$

where  $R = A_v/B$  is the ratio of the component of the brightness of one field ( $A_v$ ) in the vertical plane to the component of the brightness of the other field ( $B$ ) in the horizontal plane. The angle  $\omega$  is that between the principal planes, and is given by  $\omega = \alpha + \delta$ , where  $\alpha$  is the observed angle and  $\delta$  is the displacement of the index on the scale. When properly adjusted  $\delta$  should be zero. The constant  $k$  should equal unity if the transmission of the optical system of the photometer is the same for both beams. It was found that  $k$  was equal to 1 within 0.1 per cent. The zero reading  $\delta$  could be reduced to  $0.1^\circ$  (less than 0.2 per cent), but it was tedious to adjust it more closely with the coarse adjustment provided. It was eliminated very easily by taking the mean of the readings in two adjacent quadrants. A careful study of the instrument has shown it to have a precision under the best conditions of better than 0.5 per cent.

Of course, this is not required in turbidimetry, where the precision is limited by other than photometric factors.

The photometer readings are most accurate when comparing two fields of equal brightness. When the brightness ratio exceeds 300 or is less than 0.03, the stray light in the photometer appreciably affects the reading. The range of the photometer was then extended by using a sectored disk. This was made adjustable to any transmission up to 35 per cent. The circle was graduated to read directly in per cent transmission, and could be set easily with a precision equal to its accuracy. The edges of the sectors were made of steel, accurately ground straight, and adjustable to fit each other exactly when shut. The index on the divided circle was set on zero when the edges were in contact, eliminating any correction. The whole disk was made symmetrical about the axis to avoid any strains due to centrifugal action. It was mounted directly on the shaft of a 0.01-horsepower 110-volt direct-current series motor, and rotated with a speed which averaged about 1670 rpm. There were thus about 56 flashes per second, which is much above flicker speed. Yet at perfect match it was often possible to detect a slight flickering just at the dividing line between the two fields, which disappeared when the fields were not matched. The sectored disk was carefully investigated on the precision circular dividing engine of the Bureau, especially with regard to eccentricity of the graduated circle and the axis of rotation, and also with regard to the accuracy of the edges. In no case was an error in one sector of more than five minutes of arc detected, and the average was about two minutes. But  $5' = 0.083^\circ$ , so that the minimum angle which could be used with a precision of 1 per cent was  $8.3^\circ$ , which corresponded to a transmission of 4.6 per cent. The sectored disk was thus accurate much beyond what was required in this work when used at transmissions above 5 per cent. Actually it was never used below 8 per cent.

The most important optical consideration in any turbidimeter is stray light. This introduces constant errors which may become very serious with small turbidities. Stray light may come from three main sources, (1) reflections from the walls of the instrument, (2) reflections from the cell walls, and (3) imperfections on the cell faces. Reflections from the walls of the instrument were completely eliminated by having no walls visible in the field of the photometer. Black silk velvet was placed at a distance opposite the photometer field, giving an absolutely black field.

Diaphragms were used to cut off the incident light from the cell walls. The scattered light from the turbid medium was reflected by the walls back into the medium again, causing a slight increase in the illumination of the particles. This must have been a second order effect, and was probably negligible. The most important stray light was that coming from scratches and particles on the cell faces. When the incident beam illuminated these faces a constant amount of stray light was produced directly in the field of the instrument and changed the zero reading. It was corrected by taking the zero reading with optically clear water. Doubly distilled water was used, which always contained plenty of turbidity, and this masked the zero reading due to the cell faces themselves. With air in the cell, the conditions were not exactly comparable, but this gave a fairly good idea of the amount of stray light from the faces themselves. The zero reading was reduced to a minimum by using carefully polished, scratch-free, optically clean glass faces.

## VII. PRELIMINARY EXPERIMENTAL STUDIES

In order to test the turbidimeter, it was necessary to have standards which remained constant. Three such standards were used, designated  $U_{10}$ ,  $U_{11}$ , and  $U_{12}$ .  $U_{10}$  was a piece of opal glass faced with clear glass, to which it was fused. The clear-glass faces were carefully polished optically flat by the Bureau optician, J. Clacey. In order to reduce the brightness of this, a plate of neutral-tint smoke glass was used. The whole was properly mounted so that it could be placed in a given position and adjusted in the same way as the turbidity cells.  $U_{11}$  and  $U_{12}$  were also pieces of opal glass, but instead of clear glass both faces were carefully ground with fine emery powder, producing uniform diffusing white-glass surfaces. The polished surfaces of  $U_{10}$  permitted of thorough cleaning and precise adjustment of its faces, while the diffusing surfaces of  $U_{11}$  and  $U_{12}$  were less sensitive to changes of direction and parallelism of the incident beam. They were also found not to change when the surfaces were washed with soap and water.

It is not necessary here to describe in detail the tests made with these constant standards to determine the causes of the variations in the readings, the reproducibility of the adjustments and of various parts of the apparatus, and the final methods adopted for keeping the instrument in adjustment. The most

important causes of variation were those due to the source of light and those due to cleaning the various optical surfaces. A telescope focussed for parallel rays was used for adjusting the filament of the source to the principal focus of the collimating lens. The optical axes of the system were adjusted by reflection methods. It was found that no single adjustment determined the precision of the instrument. Table 5 below gives all the readings obtained during a period of two months upon the three standards  $U_{10}$ ,  $U_{11}$ , and  $U_{12}$  to discover a secular change in the standards or the instrument. The readings are referred to their mean values for comparison. Each reading is the mean of 10 observations. During the interval all the adjustments were remade, the optical surfaces cleaned, and a new lamp inserted and readjusted.

TABLE 5.—Constancy of Instrument

Data	$U_{10}$	$U_{11}$	$U_{12}$
Readings	1.07	1.03	1.04
	.95	.97	.98
	.96	.97	.96
	.96	.99	.99
	.98	.97	.98
	1.07	1.07	1.06
	1.03	1.04	1.03
	.96	.96	.96
Mean .....	1.00	1.00	1.00
Average deviation (per cent) ..	4.8	3.5	3.3
Maximum difference (per cent) .....	12.0	11.0	10.0

The variations are due obviously to erratic changes in adjustment. No secular change in the standards is noticeable. The variations in  $U_{11}$  and  $U_{12}$  are less than those in  $U_{10}$ , probably because they were less sensitive to adjustment due to their diffusing surfaces. The standard  $U_{10}$  was used over a much longer period—seven months, including the readings in Table 5. The average deviations of a single reading from the mean of all (22 readings) was 4.3 per cent, and Table 5 itself includes the highest and lowest readings of the whole series. In fact, if the readings of the first five months only were considered, the average deviation was 2.2 per cent, and the maximum difference is 9 per cent. When the instrument was kept fixed in adjustment the readings were more nearly constant.

A few experiments were made upon silica suspensions to determine the errors involved with liquid standards. The magnitude of the zero reading due to stray light from the cell faces was found to vary considerably, unless great care was taken to wash the cells as well as the cell faces perfectly clean. With proper precautions the zero reading could be kept below that due to a turbidity of  $10^{-8}$  (0.01 parts per 1 000 000), and with ordinary technique it was below  $10^{-7}$  (0.1 parts per 1 000 000), so that without correction it would introduce an error of less than 1 per cent in turbidities greater than  $10^{-5}$  (10 parts per 1 000 000).

A considerable error may be introduced in the process of filling and washing the turbidity cells, to avoid which a definite procedure must be followed. Washing the cells three times with doubly distilled water, and then once with the sample, was found to give results better than 2 per cent in most cases.

When much time is consumed in making the observations, as is usually necessary in photometric work, an error is introduced due to the settling of coarser particles of the suspension. A rough time run was taken to determine the rate of settling with a standard suspension of  $10^{-4}$  (100 parts per million) concentration. The fractional rate of settling is given by  $s = 1 - S$ , where  $S$  is the fraction remaining in suspension after unit time. Thus, if  $R_0$  is the original reading, and  $R$  the reading after  $t$  minutes,

$$R = R_0 S^t \quad (13)$$

The results are given in Table 6.

TABLE 6.—Rate of Settling

Time (p. m.)	Reading $R$	Log $R$	Log $S$	$S$	$s$ per cent per minute
1.40.....	12.95	1.1123	0.9953	0.989	1.1
1.45.....	12.27	1.0888			
1.50.....	11.99	1.0788	.9980	.995	.5
2.00.....	9.05	.9566	.9983	.996	.4

It is seen that for the first five minutes the reading decreases at the rate of about 1 per cent per minute, after which time a steady rate of about one-half of 1 per cent per minute is reached. The time element is uncertain because the readings themselves require about five minutes for a series of 10 photometric observations. The results show that care must always be taken to shake the standard suspension well immediately before the observations.

Here a difficulty is encountered, for shaking produces bubbles which increase the reading.

The most important factor in the calibration of any turbidimeter is the determination of the relation between the reading and the concentration, for every type of suspension which is to be used. The simplest method of obtaining the concentration as a function of the reading is to dilute the suspension by known amounts and obtain the readings for the successive dilutions. The resulting function may be called the law of dilution. It is assumed in this procedure that the constitution of the suspension does not change on dilution, but the particles may break up or in some way change in size, involving in itself a change of reading.

TABLE 7.—Law of Dilution

Concentration $C$		Reading $R$	Obs.—Calc. $\frac{\Delta C}{C}$ , per cent
Grams per cubic centimeter	Parts per million		
$5.00 \times 10^{-4}$	50.0	103.0	+11.9
2.92	29.2	74.1	+ 3.5
1.70	17.0	49.0	— 2.8
$9.90 \times 10^{-5}$	9.90	31.5	— 5.7
5.76	5.76	19.4	— 5.4
3.36	3.36	11.9	— 3.8
1.96	1.96	7.18	0.0
1.14	1.14	4.37	+ 2.1
$6.64 \times 10^{-7}$	.664	2.63	+ 6.9
3.87	.387	1.69	+ 3.0
2.26	.226	1.01	+ 7.6
1.31	.131	.636	+ 5.7
$7.66 \times 10^{-8}$	.0766	.394	+ 7.4
4.46	.0446	.283	—10.4
2.60	.0260	.194	—22.5
Mean...	.....	.....	6.6

A given thickness of cell is appropriate only for a definite range of turbidities, and for each cell thickness the constants in the law of dilution are different. The 38 mm cell was found to be suitable for silica suspensions of concentrations ranging from  $5 \times 10^{-5}$  (50 parts per 1 000 000) to  $3 \times 10^{-8}$  (0.03 parts per 1 000 000), and over this range the law of dilution was obtained. A suspension containing  $5 \times 10^{-5}$  (50 parts per million) of silica was first read. Twenty-five cubic centimeters were removed with a pipette and replaced by doubly distilled water, and as the



total volume was 60 cm<sup>3</sup>, the concentration was reduced by a factor of seven-twelfths at each dilution. The data obtained in one run are given in Table 7.

The observed reading is corrected for the displacement of the photometer scale ( $\delta = +0.14^\circ$ ) and for the zero reading with doubly distilled water, which averaged  $1.7 \times 10^{-8}$  (0.017 parts

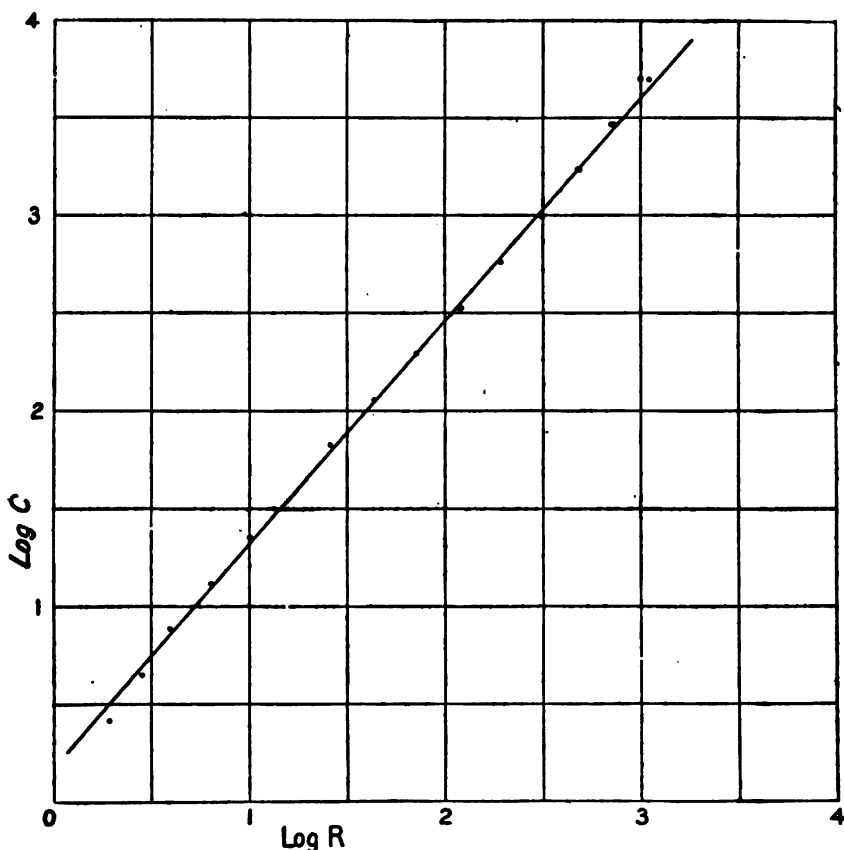


FIG. 3.—Shows relation between concentration ( $C$ ) and turbidimeter readings ( $R$ )

per million). The data are fitted fairly well by the formula

$$C = k R^{\alpha} \quad (14)$$

in which  $C$  is the concentration,  $R$  the corrected turbidimeter reading, and  $k$  and  $\alpha$  constants. The data are plotted logarithmically in Fig. 3, giving the value  $\alpha = 1.194$ , the observed values of  $C$  differing from the calculated on the average by 6.6 per cent. In reality the law is much more complicated, as is shown by the systematic deviations in the last column of Table 7.

The results of a trial run made on the previous day check fairly well, as is shown in Table 8, the average difference between the readings being 2.2 per cent. They are also plotted in Fig. 3.

TABLE 8.—Reproducibility of Dilution

Log R		$\Delta$ (log R) difference
Run 1	Run 2	
2.997	3.015	+0.018
2.855	2.870	+ .015
2.678	2.690	+ .012
2.497	2.499	+ .002
2.286	2.288	+ .002
2.082	2.075	— .007
Mean.....	.....	.0093

Mean  $\Delta R = 2.2$  per cent.

## VIII. INTERCOMPARISON OF STANDARDS FROM WATER LABORATORIES

A list of about 30 representative water laboratories was kindly furnished by Dr. E. B. Phelps, of the committee on standard methods. Reagent bottles of 500 cm<sup>3</sup> capacity were washed and cleaned with hot cleaning solution ( $K_2Cr_2O_7$  and  $H_2SO_4$ ), which was left in the bottles two days, being shaken at intervals. They were then rinsed thoroughly and left to soak for about a week filled with distilled water. These were sent to the laboratories and 22 samples of standard turbidity containing  $10^{-4}$  (100 parts per million) of silica were thus obtained.

The turbidimeter was kept fixed in adjustment throughout the whole intercomparison. Reference standards  $U_{11}$  and  $U_{12}$  were read at intervals to insure that the adjustment did not change. The readings referred to their means are given in Table 9.

TABLE 9.—Constancy During Intercomparison

Data	$U_{11}$	$U_{12}$
Readings .....	1.00	1.00
	1.03	1.00
	.97	1.02
	1.00	.98
Mean .....	1.00	1.00
Average deviation (per cent)....	1.5	1.0
Maximum difference (per cent)....	6.0	4.0

The variations are evidently accidental, and not due to changes in adjustment.

A definite procedure was followed in reading the turbidity standards. In each case the cell was washed three times with doubly distilled water and emptied with a vacuum siphon with a fine tip to suck the liquid from the corners. The third washing was read, giving the readings in Table 10 marked D. D. H<sub>2</sub>O. The standard sample was then carefully shaken and the cell washed once with it. The second filling was read, with and

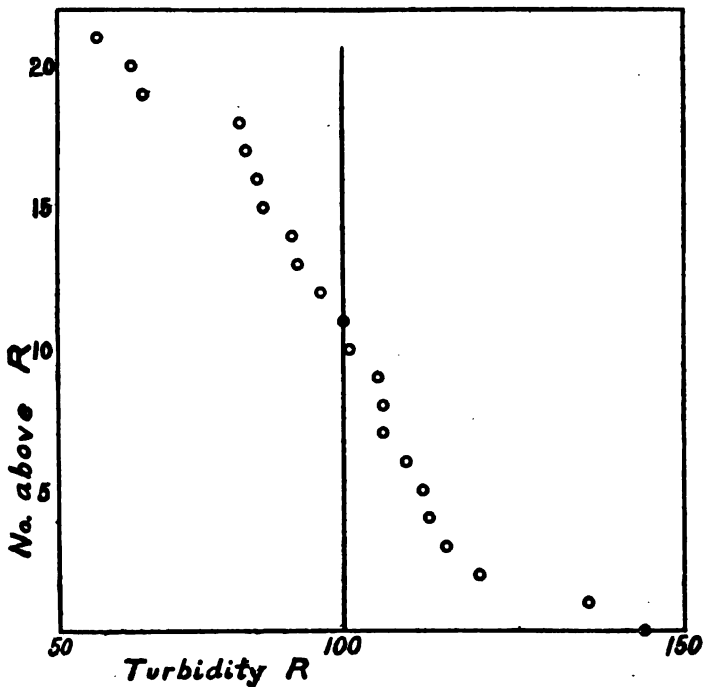


FIG. 4.—Shows the lack of uniformity in standards of turbidity used in practice

without a green filter over the eyepiece to eliminate small color differences. Five samples were remeasured several times and were found to check in every case except one to better than 3 per cent, averaging 1.3 per cent. One reading was higher than the mean of three by 10 per cent, probably due to an error in washing and filling, as the sample was low and the reading was taken immediately after a high sample. Readings were taken with and without a green filter over the eyepiece, five observations each, and the means are given in the second and third columns of Table 10. The readings referred to the mean of all

which is fixed at 100, as the standards were supposed to be 100 parts per million by weight. In the last column are given the differences between the readings without and with the green filter. The average difference is 3 per cent, the maximum 10 per cent. These differences may be due to color variations among the samples, but the average reading with the green filter was 10.64, with no filter 10.56, a difference of 0.8 per cent.

TABLE 10.—Intercomparison of Standards

Doubly-distilled water (D. D. H <sub>2</sub> O)	No filter	Green filter	Difference
0.9.....	107	106	+ 1
.3.....	100	97	+ 3
.3.....	86	89	- 3
.9.....	118	118	0
.6.....	85	83	+ 2
1.1.....	115	119	- 4
.9.....	114	108	+ 6
.8.....	82	81	+ 1
.7.....	83	85	- 2
.5.....	153	162	- 9
.8.....	143	146	- 4
.5.....	57	56	+ 1
1.1.....	107	97	+10
1.1.....	91	89	+ 2
.5.....	111	112	- 1
.6.....	124	126	- 2
.7.....	65	64	+ 1
.8.....	106	113	- 7
.8.....	92	90	+ 2
.6.....	63	62	+ 1
.7.....	101	103	- 2
.8.....	96	94	+ 2
Mean.....	100	100	....
Average deviation (per cent).....	18	19	3
Maximum difference (per cent).....	96	107	10

The readings without filter are presented graphically in Fig. 4, which is a Galton ogive curve, or "direct plot." The abscissas are the readings *R*, ordinates, the number of readings above *R*; each reading thus being given an equal ordinate spacing, and arranged in order of magnitude.

The results show a rather serious lack of uniformity in the turbidity standard actually in use. It was at first suspected that this was due to variations in the methods of preparation, such as the use of diatomaceous earth, local clays, the candle turbidimeter, etc., but a study of the results indicates that they are due to chance irregularities, not to systematic differences of

method. The lowest three and the highest two readings fall apart from the rest, and are perhaps exceptional, but omitting these five, the variation in average deviation = 11 per cent and maximum difference = 42 per cent. It is interesting to note that both the highest and lowest results are from the same city.

## IX. CONCLUSION

The foregoing study of the present standard of turbidity in water analysis has shown it to be inaccurate, the variations from the average amounting in some cases to over 50 per cent. This could be eliminated largely by the simple expedient of having all these standards prepared by the Bureau of Standards, without changing the specifications at all. But if the standards were thus centrally prepared, it would not be necessary to use the platinum-wire method for regulating the size of the particles. Simplicity could be sacrificed for precision in preparing the standard. This would require no change in the routine laboratory comparison of the unknown with the standard. Regardless of the questions of convenience and range, there seems to be no reason why the standard should not be made precise to at least 10 per cent.

There is a possibility that standard samples of dry powdered silica can be prepared sufficiently uniform in size of particle to use directly. In this case certified samples can be furnished the water laboratories, where it would be necessary only to suspend the appropriate amount in distilled water. This question is now being investigated.

The constant advice and encouragement of W. F. Wells, who first brought the problem of turbidity standardization to the attention of the author; the assistance of Prof. E. B. Phelps in furnishing a list of representative water laboratories; and the cooperation of the water laboratories in furnishing samples of their standard turbidity and in giving their opinions respecting the standard, are acknowledged.

WASHINGTON, April 25, 1919.



MAR 20 1920



DEPARTMENT OF COMMERCE

---

# SCIENTIFIC PAPERS OF THE BUREAU OF STANDARDS

S. W. STRATTON, DIRECTOR

---

No. 368

## IONIZATION AND RESONANCE POTENTIALS FOR ELECTRONS IN VAPORS OF LEAD AND CALCIUM

BY

F. L. MOHLER, Associate Physicist  
PAUL D. FOOTE, Physicist  
H. F. STIMSON, Associate Physicist

*Bureau of Standards*

---

ISSUED FEBRUARY 26, 1920



PRICE, 5 CENTS

Sold by the Superintendent of Documents, Government Printing Office,  
Washington, D. C.

---

WASHINGTON  
GOVERNMENT PRINTING OFFICE  
1920





# IONIZATION AND RESONANCE POTENTIALS FOR ELECTRONS IN VAPORS OF LEAD AND CALCIUM

By F. L. Mohler, Paul D. Foote, and H. F. Stimson

## CONTENTS

	Page
I. Introduction.....	723
II. Apparatus.....	725
III. Observations.....	726
IV. Discussion of results with lead.....	729
V. Discussion of results with calcium.....	731
VI. Summary.....	736

## I. INTRODUCTION

Previous papers<sup>1</sup> have discussed measurements made in this laboratory of ionization and resonance potentials of a number of metals.

A continuation of this work has led to satisfactory results for lead and calcium.

The method of measurement employed has been described in detail elsewhere. The metal is boiled at low pressure in a vacuum tube containing a Wehnelt cathode surrounded by a cylindrical grid and plate. Between the cathode and grid is placed a variable potential to accelerate the electron current from the cathode, while a small retarding field is fixed between the grid and plate. Measurement of the total current, leaving the cathode as the accelerating potential is increased, shows a sudden increase in the current when the ionization point is reached on account of the direct effect of ionization and the indirect effect of positive charges on the electric field. The "partial current" reaching the plate against a small retarding field decreases when the electrons near the grid lose nearly all their velocity by inelastic impact with vapor molecules. The curve of "partial current" versus accelerating potential shows a series of drops in the current at equal voltage intervals. This interval is equal to the resonance potential, and the distance of the first drop from the origin is the resonance potential, minus the initial velocity in volts, of electrons leaving the cathode. The initial velocity correction added to the applied potential at the ionization point gives the ionization potential.

<sup>1</sup> Tate and Foote, *Phil. Mag.*, **36**, p. 64; 1918. Bur. Stds. Sci. Pap. 317. Foote and Mohler, *Phil. Mag.*, **37**, p. 33; 1919. Jour. Wash. Acad. Sci., **8**, p. 513; 1918. Foote and Rogaley and Mohler, *Phys. Rev.*, **12**, p. 59; 1919.

This interpretation of the partial-current curves is based on two assumptions:

(a) That, when the velocity of an electron is less than that corresponding to the resonance potential, collisions are elastic.

(b) That, when equal to or greater than the resonance potential, the velocity lost at collision is equal to the resonance potential.

The first assumption is almost certainly justified, although no direct measurements of velocity lost by collision with metal molecules have been made. The second assumption seems to agree with all experimental results, but the evidence available does not exclude other hypotheses.

If the transfer of energy from an electron in passing through an atom is analogous to mechanical resonance phenomena, an electron with velocity equal to or twice or three times the resonance velocity will lose some kinetic energy in passing through, thus giving rise to the successive inflections in the current curve. These inflections in this case would be much more marked if the retarding field between the grid and the plate were nearly as large as the accelerating field between the cathode and grid, for most of the electrons would lose only a small part of their velocity. Experiment, however, shows that the partial-current curve is not noticeably changed by increasing the retarding field above a fraction of a volt.

An entirely different hypothesis to explain the decrease in the partial current at the resonance potential is that radiation at this voltage causes a photo-electric current between the plate and grid opposite in direction to the original electron current. The experiments of Davis and Goucher<sup>2</sup> with mercury vapor prove that such a current exists and increases by steps equal to the resonance potential. However, experiments in this laboratory with an ionization chamber of the type used by Davis and Goucher show that when the partial current gives strong inflection and full scale deflection on a shunted galvanometer the photo-electric current is immeasurably small. The effect is probably of negligible importance in all our experiments.

Another possible explanation of the inflections suggested by the work of Akesson<sup>3</sup> is that electrons with velocity several times the resonance potential may lose several "quanta" of energy at one collision. Akesson's conclusions are based on experiments with nonmetallic gases, and the authors doubt whether he has conclusively proven this important point. A quantitative study

<sup>2</sup> Phys. Rev., 10, p. 101; 1917.

<sup>3</sup> Lunds Universitets Årsskrift, NF, Afd., 2 Bd, 12, Nr 11.

of partial and total currents in a metallic vapor at various known pressures may answer this and other important questions definitely. The changes observed in partial-current curves as the vapor density is increased indicate that Akesson's assumption is not necessary to explain the facts; but no crucial test has yet been made.

## II. APPARATUS

The difficulties in experiments with calcium and lead arise largely from the high temperature necessary for vaporization. The lead was heated to about 1050° C and the calcium to about 950° C; but the latter metal is more difficult to handle on account of the chemical action of its vapor on quartz or porcelain.

The vacuum tubes were about 3 cm in diameter and 35 cm long, closed at the bottom, and with a brass plate which supported the electrodes sealed in the top. The grid was a cylinder of iron gauze about half the diameter of the tube, the outer electrode usually a short cylinder of thin sheet steel of nearly the diameter of the tube. These were supported by iron rods sealed in the top plate while the cathode was suspended from a ground glass joint.

A successful experiment with calcium was made with a fused quartz tube and electrodes as described above, but the condensed calcium stuck to the quartz and broke it when the tube cooled. Further experiments were made with a tube of glazed porcelain, and an inner protecting tube of thin steel fitting the porcelain tube snugly and reaching nearly to the top. This tube served as the outer electrode, and at the same time protected the porcelain from the hot calcium. Porcelain tubes with outer electrodes of the type first described were satisfactory for lead.

The greatest difficulty at high temperature is the large electric leak due to emission of electricity from the plate and grid. The only remedy is to employ relatively large electron currents. With calcium we used a hot wire cathode consisting of a loop of molybdenum wire coated with calcium oxide. This was welded to slightly larger tungsten leads run through pyrex-glass insulating tubes to avoid short-circuiting by condensing calcium. A similar electron source was tried in lead, but an equipotential surface gave much better results. A tube of sheet steel 6 mm in diameter coated with calcium oxide served as the surface. This fitted over a thin-walled porcelain tube in which a heating coil of molybdenum was mounted.

Current was measured on a shunted galvanometer with sensibility ranging from  $10^{-8}$  to  $10^{-6}$  amperes per mm.

The lower part of the containing tube was heated in a tube resistance furnace wound with chromel wire, while its top was water cooled. The space between the ionization chamber and furnace tube was filled with sand to make the rate of cooling small when the heating circuit was broken, as was necessary while observations were being taken. Temperature was measured by a thermocouple in the sand.

The vacuum was maintained by glass mercury-vapor pumps of the type designed by one of the authors.<sup>4</sup> With lead in the vacuum tube at 1000° C the gas pressure was never less than 0.002 mm, but with calcium very high vacua were easily obtained. Gas was rapidly evolved until a temperature of about 600° C was reached, but above this point the gas was absorbed by the calcium and the pressure dropped quickly to less than 0.0001 mm.

### III. OBSERVATIONS.

Fig. 1 gives some of the curves of partial and total current versus accelerating potential in lead vapor. Curves 4, 14, 20, 26 are total current, and curves 1, 3, 10, 19, 23 partial current reaching the outer electrodes. In Table 1 are given the results from 19 partial-current curves and 12 total-current curves.

The results from all the curves in which the inflections were sharp enough for measurement are tabulated, and the curves in the figure are typical. The total current showed ionization when the temperature reached 900° C, but most of the data were obtained in the range 950 to 1050° C. Through a window in the top plate of the vacuum tube it was possible to observe the arc at potentials above the ionization point. The arc was blue in color, due, probably, to the line  $\lambda = 4058 \text{ \AA}$ .

Fig. 2 gives typical curves of total and partial current in calcium vapor. Curves 8, 18, and 22 are total current, and curves 1, 3, 9, 14, and 15 partial current. In Table 2 the points of inflection in 11 total-current curves and 11 partial-current curves are given.

Some vaporization was visible at 600° C, and the ionization point showed at 700° C. The curves were obtained between 800 and 900° C. The pressure was very low except in the case of curve 9, when the pump was stopped and a pressure of 0.02 mm was reached. The similarity of this curve to the others shows that when the metal is vaporizing rapidly traces of gas do not affect the results. The gas is cleaned out of the hot part of the tube by the current of vapor to an extent far in excess of the indicated gas pressure.

<sup>4</sup> Wash. Acad. of Sci. Jour., 7, p. 477; 1917.

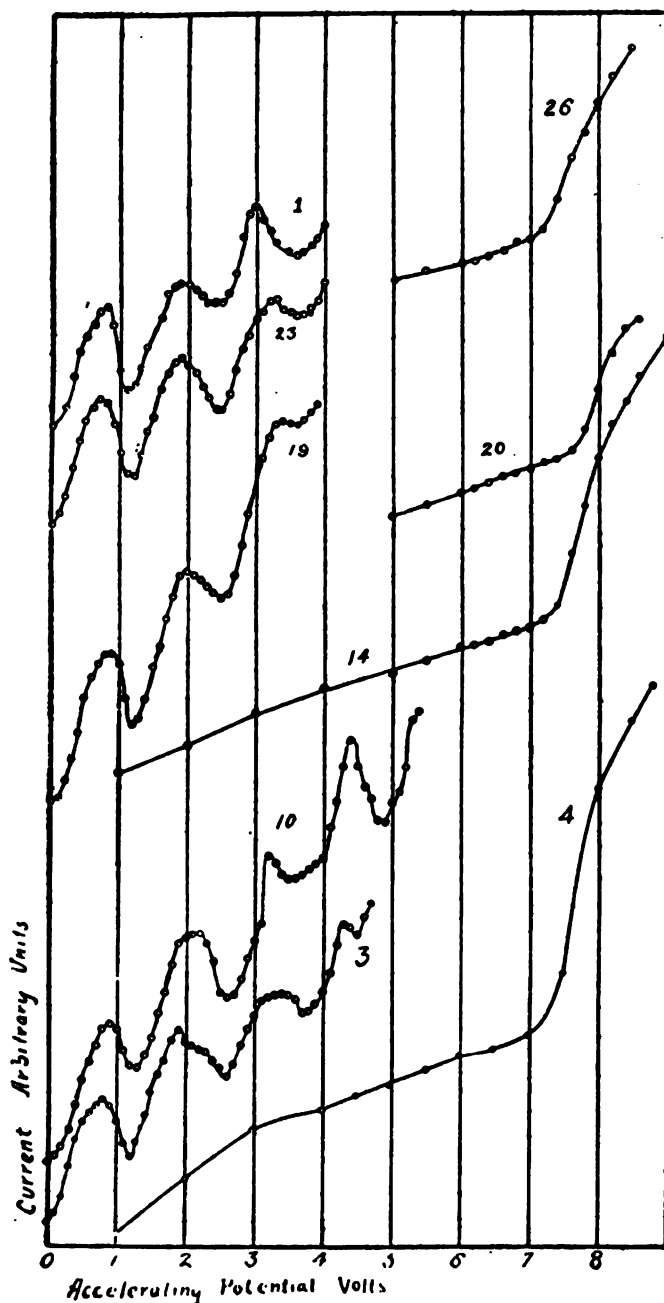


FIG. 1.—*Electron currents in lead vapor*

Curves 4, 14, 20, and 26 "total current"; curves 1, 3, 10, 19, and 23 "partial current."

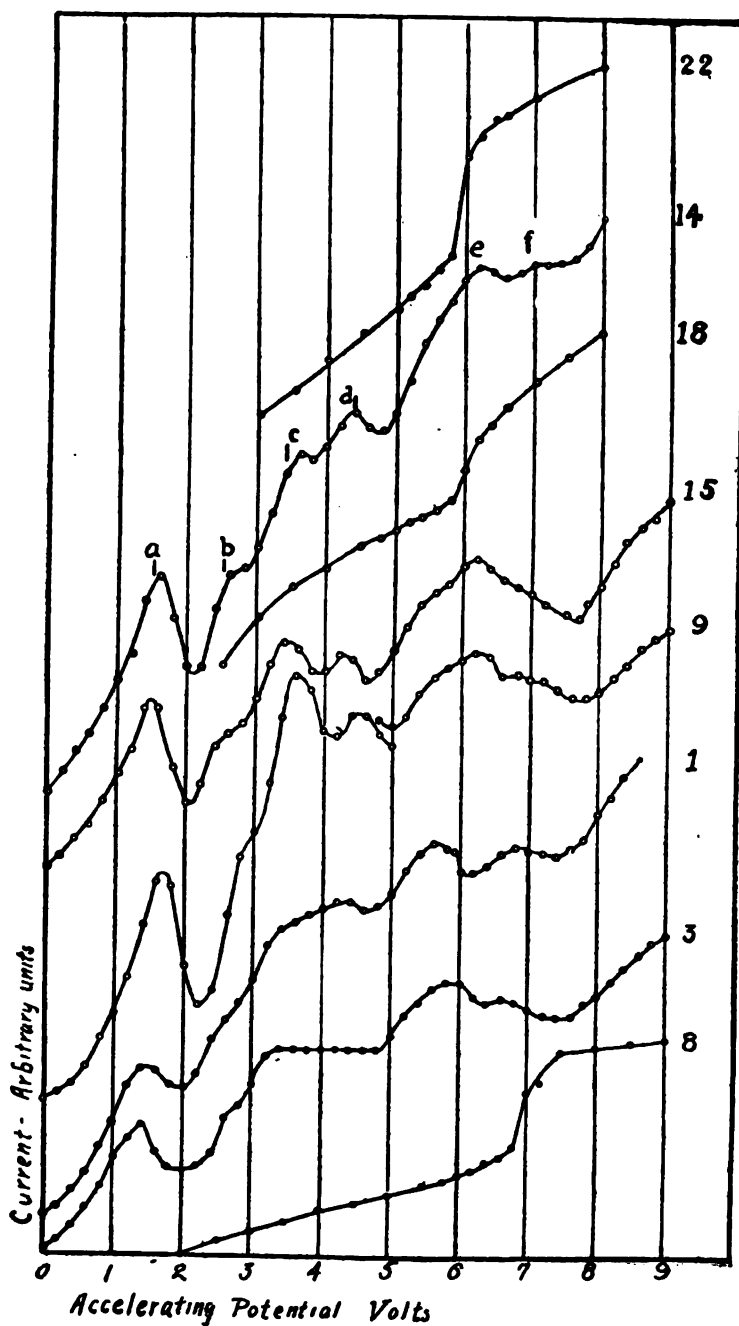


FIG. 2.—Electron currents in calcium vapor

Curves 8, 18, and 22 "total current"; curves 1, 3, 9, 14, and 15 "partial current".

As already noted, the current in lead was obtained from an equipotential source, while in calcium an incandescent wire was used. The current from a hot wire does not approach saturation in this range of voltage, while with an equipotential source saturation is approached with a few volts. This is the chief advantage of an equipotential surface when inelastic impact occurs at a low voltage. The difference in type of the two sets of curves is in part explained by this fact.

#### IV. DISCUSSION OF RESULTS WITH LEAD

The points of inflection in the current-voltage curves for lead shown in Table 1 give a mean value of 1.26 volts for the resonance potential and 7.93 volts for the ionization potential. The initial velocity correction to be added to the applied potential to give the ionization potential is taken in each case from the preceding or following partial-current curve, as varying conditions change this correction noticeably during the observations.

No series relations have been found as yet in the lead spectrum, nor is there anything known of fundamental frequencies in any of the metals in this column of the periodic table. In metals previously studied the quantum relation  $Ve = h\nu$  has been found to hold where  $V$  is the resonance or ionization potential,  $\nu$  a fundamental frequency in the spectrum,  $e$  the electron charge, and  $h$  Planck's constant of action. Taking  $e = 4.774 \times 10^{-10}$ ,  $h = 6.547 \times 10^{-27}$ , and the velocity of light  $= 2.999 \times 10^{10}$ ,

$$\lambda = 12334/V$$

when  $V$  is measured in volts and  $\lambda$  in Angstrom units.

The value of  $V$ , corresponding to the resonance potential, is the frequency of a prominent spectrum line, the first line of a principal series or combination series in the metals so far studied. The limiting frequency of this series gives the value of  $\nu$ , corresponding to the observed ionization potential, except in the case of thallium.

The resonance potential  $V = 1.26$  volts makes  $\lambda = 9800 \text{ \AA}$ , with a possible error of  $800 \text{ \AA}$  or  $0.1$  volt. The single-line spectrum of lead, if such exists, should be in this region. Thermopile measurements of the lead spectrum by Randall\* show an isolated group of strong lines near this point and the shortest wave-length line of the group  $\lambda = 10\ 291$  agrees with our prediction within experimental error.

\* *Astro. Phys. Jour.*, **34**, p. 1; 1911.

TABLE 1.—Resonance and Ionization Potentials in Lead

Curve	Applied potentials					Resonance potential			Initial velocity	Ionization potential
	At resonance				At ionization					
	a	b	c	d		b-a	c-b	d-c		
1.....	0.4	1.65	2.9			1.25	1.25		0.86	
2.....					6.8					7.66
3.....	.4	1.7	3.1	4.2		1.3	1.4	1.1	.86	
4.....					6.8					7.66
5.....	.7	1.9	3.3			1.2	1.4		.56	
6.....					7.4					7.96
7.....	.7	2.0				1.3			.56	
8.....	.6	1.9				1.3			.66	
9.....					7.6					8.26
10.....	.6	1.85	3.2	4.4		1.25	1.35	1.2	.66	
11.....					7.2					8.01
12.....	.45	1.8	3.05			1.35	1.25		.81	
13.....	.45	1.6	2.8	4.1		1.15	1.2	1.3	.81	
14.....					7.2					7.99
15.....	.5	1.6				1.1			.76	
16.....	.5	1.9	3.2			1.4	1.3		.76	
17.....					7.2					7.96
18.....	.5	1.8	3.0			1.3	1.2		.76	
19.....	.5	1.8	3.2			1.3	1.4		.76	
20.....					7.4					8.16
21.....	.4	1.6	2.7			1.2	1.1		.86	
22.....	.4	1.5	2.7	4.0		1.1	1.2	1.3	.86	
23.....	.5	1.6	3.0	4.3		1.1	1.4	1.3	.76	
24.....					7.2					7.96
25.....	.4	1.6	2.9	4.2		1.2	1.3	1.3	.86	
26.....					6.7					7.66
27.....	.2	1.35	2.8	4.0		1.15	1.45	1.2	1.06	
28.....					6.8					7.86
29.....	.1	1.3	2.6			1.2	1.3		1.16	
30.....					7.0					8.16
31.....	.1	1.3	2.6	3.9		1.2	1.3	1.3	1.16	

Mean resonance potential, 1.56 volts.

Mean ionization potential, 7.93 volts.

The ionization potential corresponds to  $\lambda = 1550$ . This may be the limit of a series of which  $\lambda = 10'291$  is the first line; but it is noticeable that the frequency ratio between the first line and limit of such a series would be much greater than in the usual type. In nearly all known series the ratio of frequencies is between 2 and 3 while this is nearly 7. In the case of thallium alone we found that ionization was not determined by the limit of a principal series; but our results have shown that there is little basis for reasoning by analogy when we are dealing with metals in different columns of the periodic table. If  $\lambda = 10'291$  is the single-line spectrum, we are able to compute an accurate value for the resonance potential. The above data thus give  $V = 1.198$  volts.



# V. DISCUSSION OF RESULTS WITH CALCIUM

In Table 2 is presented a summary analysis of the curves obtained with calcium vapor. The tabulation of these inflectional points in the partial-current curves appears to indicate a resonance potential of about 1 volt, but inspection of the curves on Fig. 2 shows that strong inflections occur at 2-volt intervals with less marked, intermediate inflections. Such curves may be explained by the existence of 2 resonance potentials.

TABLE 2.—Resonance and Ionization Potentials in Calcium

Curve	Applied potentials at resonance						At ionization	Resonance potentials		Initial velocity	Ionization potential
	a	b	c	d	e	f		First c-a	Second d-a		
1.....	1.4	2.4	3.2	4.2	5.2	6.8	.....	1.8	2.8	0.5	.....
2.....	.....	.....	.....	.....	.....	.....	5.5	.....	.....	.....	6.0
3.....	1.4	2.6	3.2	.....	5.2	6.6	.....	1.8	.....	.5	.....
4.....	.....	.....	.....	.....	.....	.....	5.6	.....	.....	.....	6.1
5.....	.....	.....	.....	.....	.....	.....	5.5	.....	.....	.....	6.0
6.....	1.6	.....	3.2	4.4	5.6	6.6	.....	1.6	2.8	.3	.....
7.....	1.4	2.6	3.6	4.6	.....	.....	.....	2.2	3.2	.5	.....
8.....	.....	.....	.....	.....	.....	.....	6.0	.....	.....	.....	6.6
9.....	1.5	2.8	3.5	4.4	5.5	6.8	.....	2.0	2.9	.4	.....
10.....	.....	.....	.....	.....	.....	.....	5.5	.....	.....	.....	5.9
11.....	.....	.....	.....	.....	.....	.....	5.8	.....	.....	.....	6.2
12.....	1.6	2.6	3.6	4.2	5.6	6.2	.....	2.0	2.6	.3	.....
13.....	1.4	2.4	3.3	4.2	.....	.....	.....	1.9	2.8	.5	.....
14.....	1.5	2.5	3.4	4.4	5.8	6.8	.....	1.9	2.9	.4	.....
15.....	1.4	2.4	3.3	4.2	5.4	6.2	.....	1.9	2.8	.5	.....
16.....	.....	.....	.....	.....	.....	.....	5.6	.....	.....	.....	6.1
17.....	1.4	2.4	3.3	4.3	5.4	6.6	.....	1.9	2.9	.5	.....
18.....	.....	.....	.....	.....	.....	.....	5.4	.....	.....	.....	5.9
19.....	.....	.....	.....	.....	.....	.....	5.4	.....	.....	.....	5.9
20.....	1.5	2.4	3.4	4.3	5.4	6.5	.....	1.9	2.8	.4	.....
21.....	.....	.....	.....	.....	.....	.....	5.3	.....	.....	.....	5.7
22.....	.....	.....	.....	.....	.....	.....	5.4	.....	.....	.....	5.8

Mean resonance potentials, 1.90 volts and 2.85 volts.

Mean ionization potential, 6.01 volts.

In order to illustrate this fact, we shall anticipate our results to the extent of postulating that two types of inelastic impact without ionization may take place in calcium vapor, type 1, in which the colliding electron loses 1.877 volts velocity, and type 2, in which 2.918 volts velocity is lost. Collisions of type 1 are somewhat more probable than those of type 2. Up to a maximum loss in velocity of 7 volts the following table represents the possible permutations with these two types of collision. The corresponding total loss in velocity after each successive collision is given in columns 2 to 4.

TABLE 3.—Velocity Losses in Calcium

Type of collision	First impact	Second impact	Third impact
	Volts	Volts	Volts
(1) (1) (1).....	1.877	3.754	5.631
(1) (2) (1).....	1.877	4.795	6.672
(2) (1) (1).....	2.918	4.795	6.672
(1) (1) (2).....	1.877	3.754	6.672
(1) (2).....	1.877	4.795	.....
(2) (1).....	2.918	4.795	.....
(2) (2).....	2.918	5.836	.....

Since collisions of type 1 are more probable, we should expect that the velocity losses of 1.88 volts would show prominently on the partial-current curves. A loss of 2.92 volts resulting from the less probable collision of type 2 should appear less prominently. Similarly, two collisions of type 1 are more probable than two of type 2 or one of each type, and hence the point 3.75 should be more pronounced than the point 4.80. From 5.6 to 5.8 the effects of two collisions of type 2 and of three collisions of type 1 are superposed, and above this point two collisions of type 1 and one of type 2 causes an inflection in the curve at 6.67 volts. As the velocity is still further increased the various permutations overlap and the true inflectional points are obscured. The prominence attained by different portions of the curves depends upon the vapor density, since with very attenuated vapor the probability of two or more collisions of any type may be exceedingly small. The curves of Fig. 2 confirm the above deductions.

If the average values of the successive points *a*, *b*, *c*, etc., of Table 2 are corrected by the average initial potential, we obtain a composite curve which may be compared with the values to be expected from Table 2 on the basis of the above assumption as follows:

TABLE 4.—Velocity Losses in Calcium

	Observed	Theoretical		Observed	Theoretical
	Volts	Volts		Volts	Volts
a.....	1.88	1.88	d.....	4.74	4.80
b.....	2.93	2.92	e.....	5.84	5.6 to 5.8
c.....	3.78	3.75	f.....	6.9	6.67

Most of the curves given show six points of inflection, but point *b* is always very faint and points *e* and *f* vary both in position and distinctness. As the latter points are above the ionization potential, this gives rise to an effect varying with the vapor pressure which makes current readings unreliable. For these

reasons the two resonance potentials and initial velocity-corrections were computed from the points *a*, *c*, and *d*. Thus, in curve 14, *a* is at 1.5 volts; *c* at 3.4; and *d* at 4.4, giving the first resonance potential, *c-a*, 1.9 volts; the second, *d-a*, 2.9 volts; and the initial velocity, 0.4 volt.

Computed in this manner the mean values from the data in Table 2 are principal resonance potential 1.90 volts, secondary resonance potential 2.85 volts, ionization potential 6.01 volts.

The occurrence of two resonance potentials has been suspected in the case of other metals, notably zinc and magnesium; but this is the first instance in which the phenomena were unmistakable. It suggests the possibility that in all metals there may be many potentials of inelastic impact of which the observed potential is the most probable.

The chief purpose of the authors in making these measurements in calcium vapor was to find the frequencies of the spectrum which correspond to the resonance and ionization potentials in the quantum relation  $Ve = h\nu$  or  $V = \frac{12334}{\lambda}$ . Previous work

shows that spectral relations are similar among metals in the same group of the periodic table. Spectra of elements in the second column are characterized by three groups of series; single line, doublet and triplet series, and combination series lines, of which combinations of single line and triplet terms are prominent. The frequency of the combination line  $1.5 S - 2p$ , has been shown to give the resonance potential and the frequency  $1.5 S$  the ionization potential in the case of all these metals previously studied—namely, zinc, cadmium, mercury, and magnesium. The first line of the principal series of single lines  $1.5 S - 2 P$  is, however, predominant in the spectra of magnesium, calcium, strontium, and barium and strong in all the metals of this group.

The limit of the principal series of single lines  $1.5 S$  in the calcium spectrum is computed by F. A. Saunders\* to be  $\nu = 49304.8$ ,  $\lambda = 2027.56$ . As this is based on better data, it is to be preferred to the number deduced by Lorensen. This gives  $V = 6.081$  volts in close agreement with the observed value  $V = 6.01$  volts.

The line  $1.5 S - 2p$ , has not been correctly identified in any published work. Using Saunders's value of  $1.5 S$  and Dunz's value of  $2p$ ,  $\nu = 34089.47$ ,  $1.5 S - 2p = 15215.33$ . There is a calcium line at  $\lambda = 6572.78$ .  $\frac{1}{\lambda} = 15210.3$  in vacuum. This agreement is

\* Data furnished by Dr. Saunders.

good, for the limiting frequency  $1.5 S$  is difficult to determine, as is shown by the various results of different authorities. Physical properties of this line make its identification almost certain, although it is apparently insignificant in arc or spark spectra. The wave length  $\lambda = 6572.78$  corresponds to  $V = 1.877$  volts, while the observed value is  $V = 1.90$  volts.

The first line of the principal series  $1.5 S - 2 P$  is  $\lambda = 4226.73$ , giving  $V = 2.918$  in good agreement with the observed secondary resonance potential  $V = 2.85$  volts.

These results add importance to the study of the relative intensity of the lines  $1.5 S - 2p_2$  and  $1.5 S - 2 P$  in spectra of metals of this group under different modes of excitation. Following the discovery by Franck and Hertz<sup>7</sup> that mercury vapor, when bombarded by electrons with velocity equal to the resonance potential, emitted the line  $1.5 S - 2p_2$  ( $\lambda = 2537$ ) alone or at least predominantly. McLennan<sup>8</sup> made similar observations on low voltage arcs in cadmium, zinc, and magnesium. In cadmium and zinc the results were analogous to mercury, but in magnesium the line  $1.5 S - 2 P$  alone was observed below the ionization potential. He concluded that the frequency  $1.5 S - 2p_2$  was fundamental in zinc, cadmium, and mercury, and  $1.5 S - 2 P$  in magnesium, calcium, strontium, and barium.

Davis and Goucher,<sup>9</sup> by their ingenious method of detecting the appearance of different types of radiation from the photo-electric effect, showed that in mercury vapor radiation occurred with 4.9 volts accelerating potential corresponding to  $\lambda = 2537$  and increased at 6.7 volts corresponding to the first line of the principal series  $\lambda = 1849$ .

Later McLennan and Ireton<sup>10</sup> showed by spectroscopic methods that in zinc and cadmium the first line of the principal series appeared at potentials corresponding to their respective frequencies.

The Davis and Goucher experiment is entirely different in principle from the method used by Franck and Hertz to detect the potential of inelastic impact in mercury and used by us in our work. The curves obtained by Franck and Hertz<sup>11</sup> are beautifully regular and show only one resonance potential.

Our measurements show that the frequency  $1.5 S - 2p_2$  is of predominant importance in determining inelastic impact in all

<sup>7</sup> Verh. der Deut. Phys. Ges., 16, p. 512; 1914.

<sup>8</sup> Proc. Roy. Soc., 91, p. 485; 92, p. 307; 92, p. 574; 1915-16.

<sup>9</sup> Phys. Rev., 10, p. 101; 1917.

<sup>10</sup> Phil. Mag., 36, p. 461; 1918.

<sup>11</sup> Verh. der Deut. Phys. Ges., 16, p. 457; 1914.

the metals of this group which we have studied, although the frequency  $1.5S - 2P$  is also effective in calcium, and possibly magnesium. The relation between low-voltage arc lines and potentials of inelastic collision is evidently complicated.

McLennan has made no observations of the low-voltage arc in calcium. An experiment performed in this laboratory by Dr. Meggers and one of the authors indicates that the line  $1.5S - 2P$  ( $\lambda = 4227$ ) does appear below the ionization potential.

The evidence is based on a purely accidental result of a spectroscopic study of low-voltage arcs in caesium vapor. Several photographs of the arc spectrum, with an applied potential of 2.2 volts, showed a line which in all probability was the 4227 line of calcium. As the dispersion was very small, the evidence is not certain, but the caesium was made by heating caesium chloride in calcium so the occurrence of calcium or calcium chloride was not unlikely. The fact that the line appeared with an applied voltage less than the secondary resonance potential, 3 volts, may not be important, for the actual potential may have been as much as 1 volt higher than the applied potential.

Interesting light on these fundamental frequencies in the spectra of calcium and magnesium is given by the work of A. S. King<sup>12</sup> on spectra in the vacuum tube furnace at different temperatures. The contention of Hemsalech<sup>13</sup> that spectra observed in tube furnaces are at least in part low-voltage arcs may be significant, for if this is true low-temperature spectra are low-voltage spectra.

In the calcium spectrum at high temperature the line  $\lambda = 4227$  is predominant and  $\lambda = 6573$  quite faint, while at low temperature  $\lambda = 4227$ , though still the brightest line, has lost considerably in relative brightness, and  $\lambda = 6573$  has increased until it is second only to  $\lambda = 4227$ . Magnesium shows the same phenomena. The wave length  $\lambda = 2852$ , which is the first line of the principal series, is predominant at high temperature, while  $1.5S - 2p$ , ( $\lambda = 4571$ ) is faint; but at low temperature in this case  $\lambda = 4571$  is the brightest line in the spectrum and  $\lambda = 2852$  has entirely disappeared.

Whether tube-furnace spectra are due to thermal emission or low-voltage arcs, the change in the spectra as the temperature is varied offers a means of differentiating the fundamental frequencies in other elements.

From the combined results of experiments on the metals of the second group of the periodic table the following conclusions can

<sup>12</sup> *Astrophys. Jour.*, 48, p. 13; 1918.

<sup>13</sup> *Phil. Mag.*, 26, p. 282; 1918.

be drawn: Inelastic collision in all these metals occurs at a potential corresponding to the spectral frequency  $1.5S-2p$ . In calcium, and probably in some other metals of the group, there is a second resonance potential given by the line  $1.5S-2P$ . The ionization potential is in all cases determined by the frequency  $1.5S$ . Arcs with voltage less than the ionization potential in zinc, cadmium, and mercury show the line  $1.5S-2p$ , predominantly, while magnesium, and probably all the alkali earth metals, shows  $1.5S-2P$  predominantly. The line  $1.5S-2P$  probably appears in spectra of all metals in this group below the ionization potential.

The evidence of the proportionality between potentials of inelastic collision and spectral frequency is now so extensive as to be beyond question. However, the assumption that all electron collisions of one type give rise to one spectral line does not seem to explain the relative intensity of the two lines  $1.5S-2P$  and  $1.5S-2p$ , below the ionization potential. The tube-furnace spectra, for instance, show at least that the two emission centers are affected differently by a change in physical condition, whether it is the temperature or the electric field that plays the important part.

## VI. SUMMARY

The resonance and ionization potentials in lead vapor are at 1.26 and 7.93 volts, respectively. The line  $\lambda = 10\,291$  is probably related by the quantum equation to the resonance potential. This gives a theoretical value of 1.198 volts for the resonance potential.

Measurements in calcium vapor show two resonance potentials, 1.90 volts and 2.85 volts, the former of which is most pronounced. The observed value of the ionization potential is 6.01 volts.

The first resonance potential is determined by the frequency  $1.5S-2p$ , ( $\lambda = 6572.78$ ). The theoretical value is 1.877 volts.

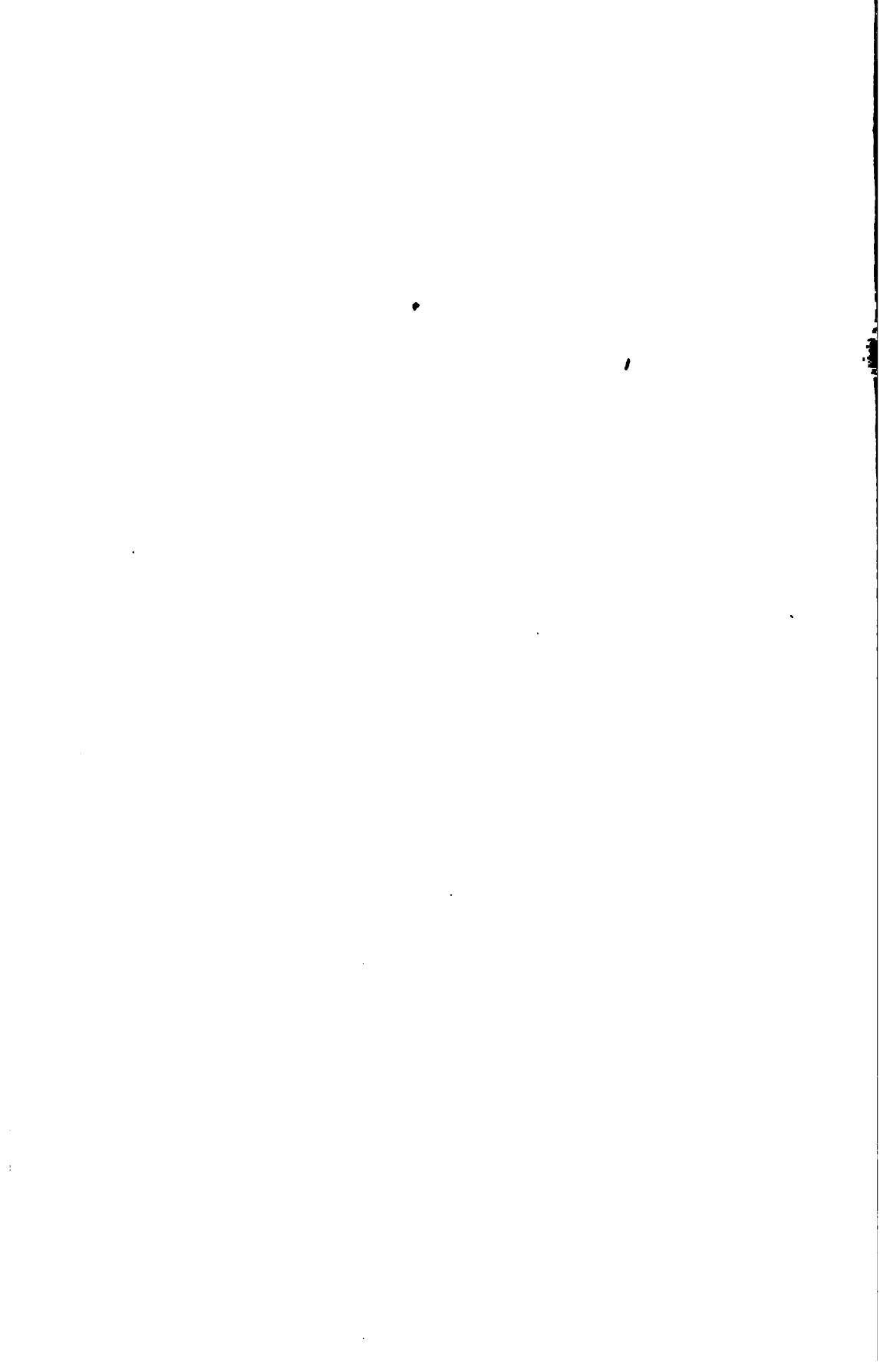
The second resonance potential is related to the first line of the principal series,  $1.5S-2P$  ( $\lambda = 4226.73$ ), giving the theoretical value 2.918 volts.

The limit of the principal series,  $1.5S$  ( $\lambda = 2027.56$ ), corresponds to the value 6.081 volts for the ionization potential.

The spectral relations of the first resonance potential and ionization potential are analogous to those previously found in other metals of this group in the periodic table.

WASHINGTON, October 1, 1919.









BR

BR

BR



